FAA CENTER OF EXCELLENCE FOR ALTERNATIVE JET FUELS & ENVIRONMENT

Annual Technical Report

2019

For the period

October 1, 2018 – September 30, 2019

Boston University
Georgia Institute of Technology
Massachusetts Institute of Technology
Missouri University of Science and Technology
Oregon State University
Pennsylvania State University
Purdue University
Stanford University
University of Dayton
University of Hawaii
University of Illinois
University of North Carolina
University of Pennsylvania
University of Tennessee
University of Washington
Washington State University

This work was funded by the US Federal Aviation Administration (FAA) Office of Environment and Energy as a part of ASCENT Project AJFE under FAA Award Number 13-C. Any opinions, findings, and conclusions or recommendations expressed in this material are those of the authors and do not necessarily reflect the views of the FAA or other ASCENT Sponsors.

Table of Contents

Overview

This report covers the period October 1, 2018 through September 30, 2019. The Center was established by the authority of FAA solicitation 13-C-AJFE-Solicitation. During that time the ASCENT team launched a new website, which can be viewed at ascent.aero. The next meeting will be held virtually March 31 - April 1, 2020.

Over the last year, the ASCENT team has made great strides in research, outreach, and education. The team's success includes the following:

- **30 active research projects.**

The projects are divided into five categories: tools, operations, noise, emissions, and alternative fuels. See the project category descriptions for more detail on each category and a summary of the projects. Funding for these projects comes from the FAA in partnership with Transport Canada.

- **166 publications, reports, and presentations by the ASCENT team.**

Each project report includes a list of publications, reports, and presentations. A comprehensive list of the publications, reports, and presentations for all projects is available in the publications index on page 546.

- **236 students participated in aviation research with the ASCENT team.**

Each project report includes the names and roles of the graduate and undergraduate students in the investigator's research. Students are selected by the investigators to participate in this research.

- **76 industry partners involved in ASCENT.**

ASCENT's industry partners play an important role in the Center. The members of the ASCENT Advisory Board provide insight into the view of stakeholders, provide advice on the activities and priorities of the Center's co-directors, and ensure research will have practical application. The committee does not influence FAA policy. Industry partners also play a direct role in some of the research projects, providing matching funds, resources and expertise to the project investigators.

Leadership

Dr. Michael Wolcott
Center Director and Technical Lead for Alternative Jet Fuels Research
Washington State University
(509) 335-6392
wolcott@wsu.edu

Dr. R. John Hansman
Center Co-Director and Technical Lead for Environmental Research
Massachusetts Institute of Technology
(617) 253-2271
rjhans@mit.edu

Dr. John Holladay
Federal Research Laboratories and Agency Liaison
john.holladay@pnnl.gov

Dr. James Hileman
Chief Scientific and Technical Advisor for Environment and Energy
Office of Environment and Energy
Federal Aviation Administration
james.hileman@faa.gov

Research Topics

Research projects within ASCENT are divided into five categories: tools, operations, noise, emissions, and alternative fuels.

Tools

The aviation system operation involves complex interactions between many different components when aircraft are on the ground, taking off, in the air, and when landing. Aviation system operations also require the understanding of how to optimize aviation activities, which is best done by implementing advanced modeling tools.

The Federal Aviation Administration's suite of modeling tools have been developed to characterize and quantify the interdependences of aviation-related noise and emissions, impacts on human health and welfare, and the costs and market impacts to industry and consumers under varying policies, technologies, operations and market scenarios.

The ASCENT researchers are further developing and expanding the capabilities of these modeling tools in a variety of ways, from improving the way basic physical properties are represented and effectively modeled to how new technologies will enter the aircraft fleet and identifying the benefits of such technologies.

Projects include:

- 010 - Aircraft Technology Modeling and Assessment
- 011 - (COMPLETE) - Rapid Fleet-wide Environmental Assessment Capability
- 012 - (COMPLETE) - Aircraft Design and Performance Assessment Tool Enhancement
- 035 - (COMPLETE) - Airline Flight Data Examination to Improve flight Performance Modeling
- 036 - (COMPLETE) - Parametric Uncertainty Assessment for AEDT2b
- 037 – CLEEN II Technology Modeling and Assessment
- 040 - (COMPLETE) - Quantifying Uncertainties in Predicting Aircraft Noise in Real-world Situations
- 043 - Noise Power Distance Re-Evaluation (NPD+C) to Include Airframe Noise in AEDT
- 045 – Takeoff/Climb Analysis to Support AEDT APM Development
- 046 – Surface Analysis to Support AEDT APM Development

Operations

Aviation operations result in fuel burn, emissions, and noise impacts. The nature and scale of these effects depends on a number of related factors, including:

- Aircraft flight paths and profiles,
- Schedule and frequency of operations, and
- Aircraft fleet mix.

ASCENT research focuses on identifying and accelerating the implementation of operational concepts that will reduce aviation environmental impacts and/or improve energy efficiency while maintaining the efficiency of the National Airspace System. The research spans multiple phases of flights and targets all environmental impact areas.

Projects include:

- 006 - (COMPLETE) - Rotorcraft Noise Abatement Operating Conditions Modeling
- 015 - (COMPLETE) - Cruise Altitude and Speed Optimization
- 016 - (COMPLETE) - Airport Surface Movement Optimization
- 023 - Analytical Approach for Quantifying Noise from Advanced Operational Procedures
- 038 - Rotorcraft Noise Abatement Procedures Development
- 044 - Aircraft Noise Abatement Procedure Modeling and Validation

Noise

ASCENT researchers work to understand all aspects of the aircraft operations that contribute to aviation's noise impact. They are working on understanding how aircraft and rotorcraft performance and operation affect noise generation and how they could be modified for mitigation measures. Research is also under way to look how noise propagates from the source to the ground and how it affects human health, wellbeing, and quality of life. This research will improve the modeling tools used

to estimate the noise impacts from aviation operations and provide data to inform policy development as well as public engagement and education.

Projects include:

- 003 - Cardiovascular Disease and Aircraft Noise Exposure
- 004 - (COMPLETE) - Estimate of Noise Level Reduction
- 005 - (COMPLETE) - Noise Emission and Propagation Modeling
- 007 - (COMPLETE) - Civil, Supersonic Over Flight, Sonic Boom (Noise) Standards Development
- 008 - Noise Outreach
- 017 - Pilot Study on Aircraft Noise and Sleep Disturbance
- 040 – Quantifying Uncertainties in Predicting Aircraft Noise in Real-world Situations
- 041 – Identification of Noise Acceptance Onset for Noise Certification Standards of Supersonic Airplane
- 042 – Acoustical Mode of Mach Cut-off

Emissions

The demand for passenger and cargo air transportation has grown rapidly over the last several decades. According to the International Air Transport Association (IATA), in 2016 there were 3.8 billion air travelers, a number it predicts will rise to 7.2 billion passengers by 2035—a near doubling of current levels. This staggering growth is accompanied by airport expansions and increases in emissions from aircraft, ground services equipment, and vehicle traffic on and near airports. The increases in these activity-based emissions impact the air quality around airports, cumulatively contribute to global climate change, and can negatively affect human health.

ASCENT researchers are analyzing data and improving predictive models to understand the effects of aircraft and ground vehicle emissions, create and refine emission-based analytical techniques at both airport-specific and global scales, and assess how policy changes affect emissions and its impacts.

Projects include:

- 002 - Ambient Conditions Corrections for Non-Volatile PM Emissions Measurements
- 013 - (COMPLETE) - Micro-Physical Modeling & Analysis of ACCESS 2 Aviation Exhaust Observations
- 014 - (COMPLETE) - Analysis to Support the Development of an Aircraft CO2 Standard
- 018 - Community Measurement of Aviation Emission Contribution of Ambient Air Quality
- 019 - Development of Improved Aviation Emissions Dispersion Capabilities for AEDT
- 020 - (COMPLETE) - Development of NAS wide and Global Rapid Aviation Air Quality
- 021 - (COMPLETE) - Improving Climate Policy Analysis Tools
- 022 - Evaluation of FAA Climate Tools
- 024 - (COMPLETE) - Emissions Data Analysis for CLEEN, ACCESS, and Other Recent Tests
- 039 - Naphthalene Removal Assessment
- 047 - Clean Sheet Supersonic Aircraft Engine Design and Performance
- 048 - Analysis to Support the Development of an Engine nvPM Emissions Standard

Alternative Fuels

The development of alternative jet fuels (AJFs) -- or sustainable aviation fuels (SAF) -- is of great interest to an array of aviation stakeholders, including aircraft and engine manufacturers and airlines. Alternative fuels that are produced from bio-based materials provide sustainable jet fuel alternatives that not only help alleviate environmental impacts from aviation emissions but can also create jobs in rural areas and lessen our reliance on foreign petroleum supplies.

Effective research and development, co-funded by the federal government and industry, enables SAF development by reducing the costs of producing renewable fuel. ASCENT research provides the scientific expertise and data to evaluate the environmental benefits associated with these sustainable fuels. ASCENT's collaborative R&D activities focuses on evaluating promising sustainable aviation fuel pathways to ensure environmental and social benefits, reduce technical uncertainties, inform aviation emission policies, and promote private sector investment in production.

Projects include:

- 001 - Alternative Jet Fuel Supply Chain Analysis
- 025 - National Jet Fuels Combustion Program – Area #1: Chemical Kinetics Combustion Experiments

- 026 -(COMPLETE) - National Jet Fuels Combustion Program – Area #2: Chemical Kinetics Model Development and Evaluation
- 027 - National Jet Fuels Combustion Program – Area #3: Advanced Combustion Tests
- 028 - National Jet Fuels Combustion Program – Area #4: Combustion Model Development and Evaluation
- 029 - National Jet Fuels Combustion Program – Area #5: Atomization Tests and Models
- 030 - National Jet Fuels Combustion Program – Area #6: Referee Swirl-Stabilized Combustor Evaluation/Support
- 031 - Alternative Jet Fuels Test and Evaluation
- 032 – (COMPLETE) - Worldwide LCA of GHG Emissions from Petroleum Jet
- 033 - Alternative Fuels Test Database Library
- 034 - National Jet Fuels Combustion Program – Area #7: Overall Program Integration and Analysis

Project 001(A) Alternative Jet Fuel Supply Chain Analysis

Washington State University

Project Lead Investigator

Michael P. Wolcott
Regents Professor
Department of Civil & Environmental Engineering
Washington State University
PO Box 642910
Pullman, WA 99164-2910
509-335-6392
wolcott@wsu.edu

University Participants

Washington State University

- PI(s): Michael P. Wolcott, Regents Professor; Christina Sanders, Acting Director, DGSS; Manuel Garcia-Perez, Associate Professor; Xiao Zhang, Associate Professor; and Ji Yun Lee, Assistant Professor
- FAA Award Number: 13-C-AJFE-WaSU-016
- Period of Performance: August 1, 2018 to September 30, 2019
- Task(s):
    1. WSU 1. Design cases. Garcia-Perez, Zhang
    2. WSU 2. Evaluate the most promising biorefinery concepts for alternative jet fuel (AJF) production. Garcia-Perez, Zhang
    3. WSU 3. Supplement and maintain the current inventory of biorefinery infrastructures that are useful for the production of AJF, as identified in the conversion design cases. Wolcott
    4. WSU 4. Perform a community social asset assessment. Gaffney
    5. WSU 5. Refine and deploy facility siting tools to determine regional demand and to identify potential conversion sites to be used in regional analyses. Wolcott
    6. WSU 6. Perform a refinery-to-wing stakeholder assessment. Gaffney
    7. WSU 7. Conduct a supply chain analysis. Wolcott, Garcia-Perez
    8. WSU 8. Provide analytical support for regional CAAFI and USDA jet fuel projects. Wolcott

Project Funding Level

$510,918 FAA funding and $510,918 matching funds. State-committed graduate school contributions for four PhD students. Faculty time for Michael Wolcott, Manuel Garcia-Perez, and Xiao Zhang contributes to the cost share.

Investigation Team

- Michael Wolcott, WSU, Project Director/PI
- Christina Sanders, WSU, Co-Project Director/Co-PI
- Season Hoard, WSU, Co-Project Director/Co-PI
- Manuel Garcia-Perez, WSU, Co-Project Director/Co-PI
- Xiao Zhang, WSU, Co-Project Director/Co-PI
- Ji Yun Lee, WSU, Co-Project Director/Co-PI
- Michael Gaffney, WSU, Faculty
- Kristin Brandt, WSU, Staff Engineer
- Scott Geleynse, WSU, Post-Doctoral Researcher
- Dane Camenzind, WSU, Staff Engineer
- Lina Pilar Martinez Valencia, WSU, Graduate Student

- Tanzil Abid Hossain, WSU, Graduate Student
- Anamaria Paiva, WSU, Graduate Student
- Daniel Mueller, WSU, Graduate Student
- Kelly Nguyen, WSU, Graduate Student
- Jie Zhao, WSU, Graduate Student
- Fangjiao Ma, WSU, Graduate Student

Collaborating Researchers

- Burton English, University of Tennessee
- Kristin C. Lewis, Volpe

Project Overview

As part of an effort to realize an "aviation system in which air traffic will move safely, swiftly, efficiently, and seamlessly around the globe," the FAA has set a series of goals and supporting outcomes, strategies, and performance metrics (Hileman et al., 2013). The goal entitled "Sustaining our Future" outlines a number of strategies that are collectively aimed at reducing the environmental and energy impacts of the aviation system. To achieve this goal, the FAA set an aspirational goal for the aviation industry to utilize 1 billion gallons of AJF by the year 2018. This goal was created from an economic, emission, and overall feasibility perspective (Richard, 2010; Staples et al., 2014).

Current approaches to supply chain analysis for AJF optimize the feedstock-to-refinery and refinery-to-wing transportation logistics (Bond et al., 2014). One of the greatest barriers to large-scale AJF production is the high capital of greenfield facilities, which translates to risk in the investment community (Huber et al., 2007). The cost of cellulosic ethanol plants ranges from $10 to $13 per gallon capacity (Hileman and Stratton, 2014); moreover, the additional processing steps required to convert the intermediate to a drop-in AJF could increase this cost to over $25 per gallon capacity (Hileman, 2014).

Motivated by the realities of converting these initial commercialization efforts into second-generation AJF, researchers have considered alternate conversion scenarios, including the transitioning of existing facilities (Brown, 2013). Currently, Gevo is employing retrofit strategies for corn ethanol plants to produce isobutanol, a potential intermediate for the alcohol-to-jet (ATJ) process of producing iso-paraffinic kerosene (Pearlson, 2011; Pearlson et al., 2013). Research on approaches for achieving the aspirational FAA goal of AJF consumption has relied upon "switching" scenarios, in which the existing and planned capacity are used to produce drop-in fuel (Malina, 2012). These approaches require the identification of existing industrial assets that can be targeted for future AJF production. Thus, siting becomes not only an exercise for optimizing feedstock transportation, but a necessary task for aligning this critical factor with the existing infrastructure, markets within regions, and the appropriate social capital for developing this new industry (Henrich et al., 2007; Seber et al., 2014).

Thus far, all published AJF supply chain analyses have been limited to stand-alone jet fuel production technologies that do not generate bio-products. Hence, the potential techno-economic and environmental benefits of using existing industrial infrastructure and the production of coproducts with respect to the development of jet fuel production scenarios must be considered in future studies.

Design cases of stand-alone AJF production facilities will be used in supply chain evaluations. Social asset modeling is not well developed, and efforts are likely hampered by difficulties in quantifying social assets when compared to improved environmental performance or reductions in AJF costs, which may be better observed by optimizing economic and environmental constraints. However, the community characteristics of a potential site must be considered when determining preferred locations for a new biorefinery. Community resistance or enthusiasm for the AJF industry can strongly influence the success or failure of a facility (Martinkus et al., 2014). Thus, community social asset modeling efforts conducted within this project, such as those based on the Community Asset and Attribute Model (CAAM), will inform disciplinary applications and advances. Clearly, social factors can have a significant effect – positive or negative – on project adoption and implementation, particularly in high technology or energy-related projects (Lewis et al., 2012; Martinkus et al., 2012). The consideration of social factors in site selection and implementation decisions can maximize positive social support and minimize opposition and social negatives, which can significantly promote the success of a project. In this regard, the CAAM originally piloted in the NARA project was designed to provide a quantitative rating of select social factors at the county level (Martinkus et al., 2014).

Focusing on regional supply chains, this research aims to identify the key barriers that must be overcome to produce 1 billion gallons of AJF. We will address this overall goal by developing tools to support the AJF supply chain assessment performed at the Volpe Center. Our effort will provide facility siting analyses that assess conversion design cases combined with regional supply chain assets and social capacity assessments for communities to act collectively toward development goals. Finally, a refinery-to-wing stakeholder assessment will support modeling and accounting of AJF distribution for downstream fuel logistics.

References

Bond, J.Q., Upadhye, A.A., Olcay, H., Tompsett, G.A., Jae, J., Xing, R., Alonso, D.M., Wang, D., Zhang, T., Kumar, R., Foster, A., Sen, S.M., Maravalias, C.T., 13, R., Barret, S.R., Lobo, R., Wayman, C.E., Dumesic, J.A., & Huber, G.W. (2014). Production of renewable jet fuel range alkanes and commodity chemicals from integrated catalytic processing of biomass. Energy Environ. Sci, 7:1500.

Brown, N. (2013). FAA Alternative Jet Fuel Activities. Overview. Presented to: CLEEN Consortium, November 20, 2013.

Henrich, E. (2007). The status of FZK concept of biomass gasification. 2nd European Summer School on Renewable Motor Fuels. Warsaw, Poland 29-31, August 2007.

Hileman, J.I., De la Rosa-Blanco, E., Bonnefoy, P.A., & Carter, N.A. (2013). The carbón dioxide challenge facing aviation. Progress in Aerospace Sciences. 63:84-95.

Hileman, J. I., & Stratton, R. W. (2014). "Alternative jet fuel feasibility." Transport Policy, 34:52-62.

Hileman, J. (2013). Overview of FAA alternative jet fuel activities. Presentation to the Biomass R&D Technical Advisory Committee, Washington DC, August 14, 2013.

Huber, G.W. & Corma, A. (2007). Synergies between bio- and oil refineries for the production of fuels from biomass. Angewandte Chemie. 46(38):7184-7201.

Lewis, K., Mitra, S., Xu, S., Tripp, L., Lau, M., Epstein, A., Fleming, G., & Roof, C. (2012). Alternative jet fuel scenario analysis report. No. DOT/FAA/AEE/2011-05. (http://ntl.bts.gov/lib/46000/46500/46597/DOT-VNTSC-FAA-12-01.pdf) (Retrieved on 2014-07)

Malina, R. (2012). HEFA and F-T jet fuel cost analyses. Laboratory for Aviation and the Environment. MIT, Nov 27, 2012.

Martinkus, N., Kulkarni, A., Lovrich, N., Smith, P., Shi, W., Pierce, J., & Brown, S. (2012). An Innovative Approach to Identify Regional Bioenergy Infrastructure Sites. Proceedings of the 55th International Convention of Society of Wood Science and Technology, Beijing, China.

Martinkus, N., Shi, W., Lovrich, N., Pierce, J., Smith, P., & Wolcott, M. (2014). Integrating biogeophysical and social assets into biomass-to-alternative jet fuel supply chain siting decisions. Biomass and Bioenergy, 66:410-418.

Pearlson, M.N. (2011). A techno-economic and environmental assessment of hydroprocessed renewable distillate fuels. MSc Thesis in Technology and Policy, MIT.

Pearlson, M., Wollersheim, C., & Hileman, J. (2013). A techno-economic review of hydroprocessed renewable esters and fatty acids for het fuel production. Alternative jet fuels, Bioproducts and Biorefining, 7(1):89-96.

Richard, T.L. (2010). Challenges in scaling up alternative jet fuels infrastructure. Science, 329:793.

Seber, G., Malina, R., Pearlson, M.N., Olcay, H., Hileman, J.I., & Barret, S.R.H. (2014). Environmental and economic assessment of producing hydroprocessed jet and diesel fuel from waste oil and tallow. Biomass and Bioenergy 67:108-118.

Staples, M.D., Malina, R., Olcay, H., Pearlson, M.N., Hileman, J.I., Boies, A., & Barrett, S.R.H. (2014). Lifecycle greenhouse gas footprint and minimum selling price of renewable diesel and jet fuel from fermentation and advanced fermentation technologies. Energy & Environmental Science, 7:1545.

Task 1 - Design Cases

Washington State University

Objective(s)

In previous years, our team has worked towards completing the reviews and final reports of design cases for six stand-alone AJF technologies (Table 1) and four relevant industries (sugarcane, pulp and paper, corn ethanol, and petroleum refineries). The updated statuses of each stand-alone AJF techno-economic analysis (TEA) and report are shown in Table 1. The results from pyrolysis and ATJ pathways have been published in peer-reviewed journals, while the work conducted from October 1, 2018 to September 30, 2019 has focused on the following tasks:

1. Conduct a detailed analysis of a “catalytic hydrothermolysis pathway for jet fuel production”
2. Conduct a detailed analysis of a new AJF pathway for hydrothermal liquefaction processing

3. Conduct TEA analyses on the integration of lignin coproduct technologies in the ATJ pathway to determine the potential for reducing fuel costs
4. Develop a new case report, focusing on a technology review and an evaluation of lipid conversion processes (HEFA, CH, SBI, Forge, Tyton, decarboxylation) and new technologies for the production of alternative lipids (HTL and sugar-to-lipid)
5. Prepare manuscripts for publication

Table 1. Evaluated stand-alone AJF technologies.

	Literature review and design report date	Publications	TEA model
Pyrolysis	Literature review based on a design report, 138 pages (2017)	Energy fuel 33:4683, 2019; Fuel process technology 195:106140, 2019	Standardized TEA complete.
Alcohol-to-jet (ATJ)	Literature review based on a design report, 28 pages (2015)	ChemSusChem 11:3728, 2018	A core ATJ model, from ethanol and butanol to final fuel, was developed and analyzed. This manuscript was reviewed by LanzaTech and Gevo. Standardized TEA.
Synthetic kerosene and synthetic aromatic kerosene (SK-SKA)	Literature review based on a design report, 36 pages (2015)	Due to a lack of further development (Sasol process), this activity is on hold	N/A
Direct sugar-to-hydrocarbon (DSHC)	Literature review based on a design report, 88 pages (2017)	Manuscript in preparation, which includes a DSHC summary (draft to be completed in 2020)	Standardized TEA in progress.
Virent BioForming process	Literature review based on a design report, 46 pages (2015)	Manuscript in preparation	Standardized TEA complete.
Catalytic hydrothermolysis (CH)	Literature review based on a design report, 35 pages (2018)	Manuscript completed, under internal review	CH based on the ARA process. Four feedstocks were analyzed (soybean oil, carinata, yellow grease, and brown grease). This manuscript was reviewed by Agrisoma.
Gasification Fischer Tropsch (GFT)	No literature review conducted		A GFT techno-economic model was completed. Standardized TEA.
Microchannel gasification Fischer Tropsch (microGFT)	No literature review conducted		A standardized GFT techno-economic model was completed.
Hydroprocessed esters and fatty acids (HEFA)	No literature review conducted		A standardized HEFA techno-economic model is now available.

Research Approach

Background

We have conducted a detailed literature review and prepared design case reports on six AJF pathways, including pyrolysis, ATJ, synthetic kerosene and synthetic aromatic kerosene, direct sugar-to-hydrocarbon (DSHC), Virent BioForming, and catalytic hydrothermolysis (CH). We have also collected data from the literature to conduct techno-economic analyses for these pathways. The results from these design cases are being applied in the development of supply chains and the

identification of synergisms that may eventually lead to the construction of integrated AJF production systems that take advantage of the infrastructure in a given region. An analysis of the locations of existing infrastructure demonstrated that the United States can be divided into regions based on the dominant biomass. Thus, we believe that the generation of advanced biorefinery concepts focused on petroleum refineries, pulp and paper mills, sugarcane mills, and corn ethanol mills is a viable approach for evaluating the synergism among AJF pathways, existing infrastructure, and coproducts. We can then compare the biorefinery concepts developed for each technology to identify the most promising approach, which will then be used in supply chain analyses.

Stand-alone design case reports were generated by conducting reviews of relevant research in the academic literature and public information provided by commercial entities developing the corresponding technology. The published papers have been subjected to an industrial expert review, and the reports provide details regarding the processes involved in each conversion pathway and outline the technology readiness and particular barriers to implementation. Publicly available information regarding the commercial processes and research literature will provide a foundation of information to be used in modeling efforts. Where detailed process engineering information is lacking, new models will be built to estimate the parameters needed to complete assessments such as techno-economic modeling, lifecycle analysis, and supply chain modeling. Aspen Plus is primarily used to generate process models and details, including mass balances, energy balances, energy requirements, and equipment size and cost. These results will also provide the basis for a comparative analysis between design cases, which will identify the key advantages and markets for each technology.

Each design case has the following components:

1. Feedstock requirements
2. Companies developing/commercializing the technology
3. Current location of units in the United States and worldwide
4. Block and flow diagram of the technology
5. Unit operations and process conditions (reactor type, separation unit type, catalysts, product yield, jet fuel yield)
6. Properties of the produced jet fuel
7. Identification of potential intermediates
8. Current and potential uses of wastes and effluents
9. Developed coproducts
10. Potential ways to coprocess intermediates, wastes, and coproducts using existing infrastructure (petroleum refineries, pulp and paper mills, etc.)
11. Preliminary TEA
12. Technological challenges and gaps

We have submitted technical reports and supplementary Microsoft Excel files with mass and energy balances and TEAs for the pathways listed below. All files are available on shared drives for the Project 01 team members. Where indicated, the TEAs are still undergoing internal review.

- Pyrolysis-bio-oil hydro-treatment concept (hydro-treated depolymerized cellulosic jet)
- Synthetic kerosene and synthetic aromatic kerosene
- ATJ- A manuscript with information regarding the mass and energy balances and the TEA was recently published (an internal review of the DSHC TEA is in progress).
- Gasification Fischer Tropsch (GFT)- Two design cases have been prepared for biomass gasification. The first case focuses on microreactors, and the second design case is applicable to technology based on large standard reactors (reviews on the TEAs for GFT and microGFT have been completed).
- HEFA mass and energy balances and TEA- A stochastic TEA was created in MATLAB and was confirmed to match the completed, deterministic TEA when assumptions and costs match (deterministic TEA review completed).
- TEA of CH pathway for jet fuel production

We are currently preparing a manuscript comparing the economic and environmental performance of the AJF technologies discussed above. This manuscript will also present a strategic analysis of the yield increases needed to achieve an MSP comparable to those of current commercial fuels. Over the last year, we also made progress in design cases for existing industries that could be used to reduce the production cost of AJFs.

A paper detailing the impact of coproducts on the financial viability of the ATJ process has been submitted to *BioFPR* and is currently under review.

A preliminary technical report containing information on the mass and energy balances and the TEA of the petroleum refinery is being developed for the corn ethanol and sugarcane design cases. Major progress has been made on the analysis of corn ethanol and sugarcane biorefineries for jet fuel production. Two papers in this area are under internal review.

We are working with the Pacific Northwest National Laboratory (PNNL) to complete a case design report on HTL for AJF conversion. This work involves the collection of primary data, the establishment of process flow diagrams for several feedstocks including municipal wastewater (primary and secondary sludge), algae, and tall oil, and a detailed TEA. We have discussed the draft report with PNNL. We will also work with PNNL to identify methods for improving the HTL conversion efficiency.

A summary report on several lipid conversion pathways, including SBI, Forge, Tyton, decarboxylation, and coprocessing, has been prepared. We have also revised the design case for CH and have prepared a manuscript entitled "Techno-economic analysis of the CH pathway for jet fuel production." This manuscript reviews the technological development and commercialization of the CH pathway and assesses the advantages of the CH pathway in utilizing a wider range of feedstock, including edible and inedible vegetable oils and fats, oils, and greases (FOGs), and generating a broader mix of hydrocarbons. Potential cost savings for the use of low-cost feedstock such as FOGs have been assessed, with a consideration of the added costs for preconditioning and feedstock availability. A draft manuscript has been reviewed by Agrisoma. We plan to revise and submit the manuscript in 2020.

Milestone(s)

An Excel file with TEAs for all AJF technologies has been completed, and design cases for the corn ethanol and sugarcane industries are still being reviewed by the standardization team. A detailed analysis entitled "Catalytic hydrothermolysis pathway for jet fuel production" has been completed, and a design case report entitled "Jet Fuel Design Case: Hydrothermal liquefaction case design report" has been completed. A summary report entitled "Lipid and Bio-processing Technologies: Process Intensification and Continuous Flow-Through Reaction (PICFTR), Lipid-to-Hydrocarbon (LTH), TYTON, Decarboxylation and Co-processing" has been produced, and manuscripts have been prepared for publication.

Major Accomplishments

A manuscript entitled "Comparison of Techno-economic and Environmental Performance of Alternative Jet Fuel Production Technologies" has been prepared and reviewed. Another manuscript entitled "Economic Analysis of Catalytic Hydrothermolysis Pathway for Jet Fuel Production" has been prepared and sent to Agrisoma and our internal team for review. The revised manuscript will be submitted for FAA review. We have also updated the "Lipid-to-Biofuel Conversion Pathways" manuscript in preparation for its publication. In addition, we are drafting a manuscript entitled "Oleaginous yeast/fungi for jet fuel production" with PNNL scientists and are updating the "Hydrothermal liquefaction case design report" manuscript as preparation for publication. We intend to submit these manuscripts to the FAA for review within the next four months. We have also initiated the construction of a TEA for lignin extraction and utilization in a biorefinery process (National Renewable Energy Laboratory [NREL] biochemical conversion, https://www.nrel.gov/docs/fy19osti/71949.pdf).

Data generated from the design cases have been made available to A01 partners to assist with supply chain analysis and techno-economic modeling by improving the conversion and cost figure database values. Evaluations of the effects of process variations on the chemical properties of the generated products are being used to provide insight into the challenges that will be faced when AJFs are blended into commercial jet fuel.

Publications

Peer-reviewed journal publications

Pires, A.P.P., Arauzo, J., Fonts, I., Domine, M.E., Fernanzed, Arroyo, A., Garcia-Perez, M.E., Montoya, J., Chejne, F., Pfromm, P., & Garcia-Perez, M. (2019). Challenges and opportunities for bio-oil refining: A review. Energy & Fuels, 33(6):4683-4720.

Yinglei Han, Mortaza Gholizadeh, Chi-Cong Tran, Serge Kaliaguine, Chun-Zhu Li, Mariefel Olarte, Manuel Garcia-Perez. (2019). Hydrotreatment of pyrolysis bio-oil: A review. Fuel Processing Technology, 195:106140.

Outreach Efforts

During the preparation of design case reports, we have closely interacted with industrial companies, including Gevo, LanzaTech, and Agrisoma. These companies have also helped us review reports and draft manuscripts.

Awards
None.

Student Involvement
Several graduate students (Senthil Subramaniam, Sudha Eswaran, Kelly Nguyen, Tanzil Hossain, Anamaria Paiva, Lina Martinez) and one undergraduate student (Kitana Kaiphanliam) participated in the creation, editing, and updating of the design cases for stand-alone AJF technologies, relevant existing infrastructure, and lignin coproducts.

Plans for Next Period
We intend to complete the manuscript submission process (3–4 papers), complete the lignin coproduct analyses, and prepare additional manuscripts based on the AJF analyses.

Task 2 - Evaluation of the Most Promising Biorefinery Concepts for AJF Production
Washington State University

Objective(s)
Continuation from previous years
During this upcoming year, we will complete our evaluation of biorefinery scenarios for AJF production using corn ethanol, sugarcane, pulp and paper mills, and petroleum refineries. Over the past year, we advanced our analyses for corn ethanol and pulp and paper mills, and in the coming year, we aim to complete our analyses for sugarcane and petroleum refineries.

We will conduct detailed TEA analyses on the integration of lignin coproduct technologies and the ATJ pathway to determine the potential for reducing fuel costs.

Research Approach
Background
In this task, we will utilize the design cases for existing infrastructure, AJF production technology, and identified coproducts to generate new biorefinery concepts for petroleum refineries, pulp and paper mills, sugarcane mills, and corn ethanol mills. The results from this effort will allow us to identify and select the most commercially feasible biorefinery concepts. Major technical gaps/barriers toward the commercialization of each biorefinery concept will also be determined from the results of this study.

The integration of process technologies will be assessed using an approach similar to that for the stand-alone design cases. The integration concepts will be developed by pairing stand-alone cases with these concepts to evaluate the economic and environmental advantages of the integration approaches. Over this period, we have conducted detailed analyses of ATJ conversion and integration with pulp mill operations. We have also investigated the potential contribution of lignin coproducts to the overall process economy.

A dry grind corn ethanol mill (DGCEM) with a capacity of 80 million gallons of ethanol per year was studied in order to evaluate potential biorefinery scenarios for AJF production. Five AJF technologies were studied: Virent's BioForming, Gevo ATJ, DSHC, fast pyrolysis, and GFT. A standardized methodology was adopted to compare DGCEM and AJF technologies in 12 integration scenarios in terms of the minimum fuel selling price and greenhouse gas emission. We are currently conducting similar analyses for petroleum refineries and are comparing sugarcane biorefinery concepts for aviation fuel production.

We will complete a manuscript on the integration of ATJ technologies in pulp mill infrastructure during this coming year. We will then apply this methodology to analyze another advanced fermentation technology (DSHC by Amyris) for use in a pulp mill during the next year. We will also expand the lignin coproduct analysis to all other AJF pathways.

Major Accomplishments
Building upon the ATJ pathway analyses, we have analyzed the integration of the ATJ process in a pulp mill infrastructure. A manuscript entitled "Pulp Mill Integration with Alcohol-to-Jet Conversion Technology" has been submitted to *Fuel Processing*

Technology. Following the reviewer's input, a revised manuscript has been submitted. Economic models and life cycle assessments have been applied to select the most promising biorefinery concepts for corn ethanol, sugarcane, and pulp and paper, and manuscripts on jet fuel production using corn ethanol, sugarcane, and pulp and paper biorefineries will be submitted shortly. We are currently working on methods for utilizing petroleum refineries as part of biorefineries.

Publications

Written reports under peer review

Impact of co-product selection on techno-economic analyses of alternative jet fuel produced with forest harvest residuals. (2019). In revision, BioFPR.

Pulp Mill Integration with Alcohol-to-Jet Conversion Technology. (2019). In revision, Fuel Process Technology.

Outreach Efforts

Scott Geleynse, Xiao Zhang. Techno-Economic Assessment of Pulp Mill Infrastructure Integration with the Alcohol-to-Jet Pathway for Aviation Fuel Production. International Bioenergy & Bioproducts Conference, October 30, 2018

Awards

None.

Student Involvement

Graduate students (Senthil Subramaniam, Kelly Nguyen, Abid Tanzil Hossain, Lina Martinez Valencia, and Anamaria Paiva) have received training in this project. An undergraduate student, Kitana Kaiphanliam, funded under a National Science Foundation Research Experience for Undergraduates (NSF-REU) grant, assisted in building techno-economic models for coproduct production scenarios.

Plans for Next Period

During the next period, Dr. Garcia-Perez's team will focus on potential cost reductions that can be achieved by integrating AJFs with a petroleum refinery.

Task 3 - Supplement and Maintain the Current Inventory of Biorefinery Infrastructures that are Useful for AJF Production, as Identified in the Conversion Design Cases

Washington State University

Objective

This task requires an annual evaluation of the database to add or eliminate new and closed facilities in each category such that the geospatially specific assets are current.

Research Approach

The use of existing infrastructure assets is a key component of retrofit approaches for advances in this industry. To differentiate between the relative value of different options, the specific assets must be valued with respect to their potential use within a conversion pathway. Regional databases of industrial assets that might be utilized by a developing AJF industry have been assessed on a national level. These baseline databases are compiled from a variety of sources, including industry associations, universities, and news outlets. These databases will be expanded, refined, and validated as the conversion design cases articulate additional needs for the regional analyses.

Milestone(s)

National databases have been compiled, geolocated, validated, and shared for biodiesel, corn ethanol, energy pellet, pulp and paper, and sugar mill production. We are evaluating the database to add or eliminate new and closed facilities in each category to ensure that the geospatially specific assets are current.

Geospatially specific facility databases, waste feedstock estimates, and forest residual inventories have been developed and prepared in conjunction with the Volpe Center. FTOT analyses of specific scenarios are compared to similar analyses reported by the NREL Biomass Scenario Model to assess the adoption of AJF technologies and to determine potential national targets.

Major Accomplishments

National databases have been compiled, validated, and shared with the A01 teams. All of the metadata are available for use in the regional analyses.

Publications

Peer-reviewed journal publications

Lewis, K. C., Newest, E. K., Peterson, S. O., Pearlson, M. N., Lawless, E.A., Brandt, K., Camenzind, D., Wolcott, M. P., English, B. C., Latta, G. S., Malwitz, A., Hileman, J. I., Brown, N. L., Haq, Z. (2019). US alternative jet fuel deployment scenario analyses identifying key drivers and geospatial patterns for the first billion gallons. Biofuels, Bioproducts and Biorefining, 13(3):471-485. Doi:10.1002/bbb.1951

Outreach Efforts

N/A

Awards

None; these are shared assets for later analyses.

Student Involvement

Dane Camenzind, a Master's student in Civil Engineering, validated the operating status of previously identified production facilities, compiled and geolocated MSW incinerators and landfill gas-to-energy facilities, and assisted in assembling and updating all county-level feedstock information. Dane Camenzind graduated in September 2019 and is currently working for WSU as an operations research engineer.

Plans for Next Period

N/A

Task 4 - Continue Work on Social Asset Decision Tools Developed in Phase 1 for Plant Siting (CAAM), Including Additional Validation and Incorporation of Multi-decision-making Tools.
Extend Applications to Another U.S. Region in Coordination with Other Team Members (Inland Northwest, Appalachian Region). Prepare for National Extension and Replication in Select Countries.

Washington State University

Objective(s)

Expand and refine social asset decision tools for biorefinery plant siting (CAAM) through the addition of political capital. Prepare for national extension and replication for Canada and select E.U. countries.

Research Approach

Based on key measures of social, cultural, human, and political capitals, WSU has developed and finalized CAAM. The first tool was initially applied to the NARA region in the Pacific Northwest, and a refined tool that added more complete measures of social, cultural, and human capital was deployed in two sub-regions of NARA. An initial measure of political capital has now been added to the CAAM, which can be used across the continental United States. The refined CAAM (excluding political capital) has been used to assess social capacity for biorefinery siting in two separate studies, including the retrofitting of paper mill facilities in the Pacific Northwest. Ground-truthing analysis was used to assess the role of social, cultural, and

human capitals in the success or failure of AJF-related projects in both the NARA and BANR regions. This ground-truthing analysis supported the role of CAAM measures of project success and highlighted opportunities for further improving the CAAM. The final CAAM includes measurements of political capital, and the manner in which capital is measured varies for each capital type. We have also completed a strategic application model that combines the final CAAM and supplementary data, providing strategic community engagement recommendations to increase the likelihood of project success. The strategic application model was validated with case studies of biorefineries in the Pacific Northwest, and a manuscript describing this validation was submitted to the *Community Development Journal*. Additional efforts are currently underway to validate the final CAAM and to implement strategic applications that involve the BANR region and the Inland Northwest.

Milestone(s)

The CAAM model has been tested and is available for use. The CAAM dataset and a codebook for its use are available for incorporation in regional projects.

Major Accomplishments

A strategic application model has been created using completed CAAM measures and supplementary data to provide engagement recommendations for improving the likelihood of success when making initial contacts with communities. A paper explaining the development of the final model and strategic application recommendations for three case studies of refineries in the Pacific Northwest was submitted to the *Community Development Journal* and is currently being revised for resubmission. We presented this paper at the Pacific Northwest Political Science Conference in November 2018. Significant research collaborations have been organized to further test the CAAM's effectiveness, including areas beyond aviation AJF and refinery site selection (namely, climate change resiliency and community vulnerability to climate change). We are currently working on an additional manuscript for BANR on an application of the CAAM in Colorado and Wyoming.

Publications

Written report under peer review

Mueller, D., Hoard, S., Roemer, K., Rijkhoff, S., Sanders, C. "Quantifying the Community Capitals Framework: Strategic Application of the Community Assets and Attributes Model." In revision, Community Development.

Outreach Efforts

Boglioli, M., Strauss, S., Hoard, S., Mueller, D., Budowle, R., Beeton, T. & Jensen-Ryan, D. Searching for culture in 'cultural capital': The case for a mixed-methods approach to production facility siting. CSU Energy.

Gaffney, M., Sanders, C., Hoard, S. & Mueller, D. Community capitals: Strategic application of the CAAM. Commercial Aviation Alternative Fuels Initiative (CAAFI) Annual Meeting. Washington DC.

Mueller, D., Hoard, S., Roemer, K., Rijkhoff, S. & Sanders, C. Quantifying the community capitals framework: Strategic application of the community assets and attributes model. Pacific Northwest Political Science Association. Bend, OR.

Mueller, D., Hoard, S., Roemer, K., Sanders, C., & Rijkhoff, S.A.M. Quantifying the community capitals framework: Strategic application of the community assets and attributes model, WSU Academic Showcase, Pullman, WA.

Mueller, D., Hoard, S., Sanders, C., & Gaffney, M. From field to flight: Using community capitals to predict sustainable aviation biofuel scale-up, WSU Academic Showcase, Pullman, WA.

Awards

None

Student Involvement

Daniel Mueller graduated with a PhD in political science at WSU in May 2019 and continued as a research assistant on this project until August 2019.

Plans for Next Period

The final CAAM and strategic application will be validated in the Inland Northwest and BANR regions. This approach will include the incorporation of multi-method decision-making tools and appropriate weighting of the capital types based on their correlations.

Task 5 - Refine and Deploy Facility Siting Tools to Determine Regional Demand and Potential Conversion Sites to be Used in Regional Analyses

Washington State University

Objective

Develop readiness level tools for regional projects.

Research Approach

Developed under the NARA project and refined for ASCENT applications, the CAAM provides county-level data collected from national datasets to conduct a preliminary assessment of community characteristics for four (cultural, social, human, and political) of the seven "Community Capitals" developed by Emery and Flora (2006).

To improve facility siting tools, prior CAAM models (focusing on three assets: social, cultural, and human capital) were added to economic assets to assess the suitability of communities in the Pacific Northwest for biorefineries. Expanding on these analyses, our CAAM measures have been added to a decision support tool to assess the repurpose potential of pulp mills in the Pacific Northwest for biorefineries. An additional manuscript has been written on the effectiveness of this tool and will be submitted for review. These approaches have been utilized for cellulosic ATJ supply chains in the Pacific Northwest, and we will demonstrate the application of this tool in supply chain siting analyses for AJF production using HEFA conversion technology and FOGs as feedstock in the Inland Northwest.

Concepts from the decision support tool have been applied to inform a new siting tool that uses general types of geospatial data to find and rank candidates for supply chain optimization. These candidates can then be further analyzed or used in a supply chain optimization model that will select one or multiple candidates.

Milestone(s)

The CAAM has been updated with four capitals, and readiness level tools for regional projects have been developed.

Major Accomplishments

During this reporting period, a manuscript combining the CAAM with economic and environmental indicators to assess site selection in Western Oregon and Western Washington was submitted to *Biomass and Bioenergy*, which recommended a revision and resubmission.

Publications

Peer-reviewed journal publications

Martinkus, N., Latta, G., Rijkhoff, S.A.M., Mueller, D., Hoard, S., Sasatani, D., Pierobon, F., & Wolcott, M. (2019). A multi-criteria decision support tool for biorefinery siting: Using economic, environmental, and social metrics for a refined siting analysis, Biomass and Bioenergy, 128, 105330.

Outreach Efforts

N/A

Awards

None.

Student Involvement

Daniel Mueller completed his PhD in political science at WSU in May 2019 and continued as a research assistant on this project until August 2019.

Plans for Next Period
During the upcoming year, the latest iteration of the CAAM will be applied for the Inland Northwest and BANR regions.

Task 6 - Refinery-to-Wing Stakeholder
Washington State University
This is a shared task led by Penn State University. The report is provided in Award No. 13-C-AJFE-PSU-002.

Objective(s)
We will extend the stakeholder assessment to a limited sample of informed stakeholders in the remaining sections of the country to provide insight into market and industry dynamics, with the aim of optimizing successful outcomes.

Research Approach
The team collected primary data via surveys to better understand the awareness, opinions, and perspectives of key aviation fuel supply chain stakeholders regarding the potential impacts and key factors for an economically viable biojet fuel production industry in the United States. These aviation fuel supply chain stakeholders include airport management, FBOs, aviation fuel handlers, relevant airlines, and CAAFI personnel. Data were collected to assess the opinions, awareness, and perceptions of aviation fuel supply chain stakeholders regarding factors impacting the adoption and diffusion of AJF. A national survey of aviation management and FBOs was distributed to several hundred stakeholders across the United States and was completed in the summer of 2019.

Milestone(s)
A manuscript on perceptions in the Pacific Northwest was published by the *International Journal of Aviation Management* in 2018, and a national survey has been completed. Due to low response rates, the national data are being assessed for appropriate analysis for potential manuscripts.

Major Accomplishments
Data collection for the national survey has been completed, and the data are currently being assessed for potential analysis and manuscripts.

Publications
Peer-reviewed journal publications
Mueller, D., Hoard, S., Smith, P. M., Sanders, C., & Gaffney, M. (2018). Airport management perspectives on aviation biofuels: Drivers, barriers, and policy requirements in the U.S. pacific northwest. International Journal of Aviation Management. https://doi.org/10.1504/IJAM.2019.098380

Outreach Efforts
N/A

Awards
None.

Student Involvement
Daniel Mueller completed his PhD in political science at WSU in May 2019 and continued as a research assistant on this project until August 2019.

Plans for Next Period
The team will begin drafting a manuscript based on the national survey results.

Task 7 - Supply Chain Analysis

Washington State University-Volpe

Objective(s)

Washington State University and Volpe have each developed modeling tools that apply trans-shipment optimization to model the geospatial layout of developing supply chains. A comparison of these tools would be useful to identify the strengths and weaknesses of each.

We plan to develop a framework for assessing the resilience of a sustainable aviation fuel (SAF) supply chain subjected to multiple uncertain hazards and conditions and will prepare for the application of the proposed framework to hypothetical SAF supply chains in the Pacific Northwest region.

Research Approach

Focusing on the use of woody-biomass-to-jet-fuel conversion via fast pyrolysis and the upgrading of a supply chain centered in the Northern Rockies, a series of comparison studies was conducted using optimization tools from Volpe and Washington State University. Each modeling approach was required to determine sites for new pyrolysis depots and upgrading refineries. Forest production data were provided by the LURA model from the University of Idaho. Pyrolysis depot locations were selected by candidate generation tools included in each approach, and existing petroleum refineries were used as candidates for upgrading refineries. Cities, ports, and airport hubs throughout the U.S. West Coast and Rocky Mountain regions were used as markets for road transportation fuel, bunker fuel, and jet fuel.

Resiliency

A supply chain can be exposed to multiple unpredictable events and conditions over the medium- to long-term horizon. These events and conditions include natural (e.g., earthquakes, hurricanes, floods, wildfires, tsunamis) and man-made (e.g., terrorist attacks, cyber-attacks, industrial accidents) hazards, climate change, technology development, evolving customer preferences, dynamic changes in government regulation and political circumstances, etc., which may have negative or positive impacts on supply chain performance. Although supply chain resilience assessments should address the combined effects of multiple negative and positive events and conditions, most existing studies have focused on negative consequences induced by a single type of natural hazard, which often leads to the under- or overestimation of potential risks. Moreover, previous studies have assessed supply chain resilience in a more qualitative manner, utilizing either conceptual or empirical analysis. To address these deficiencies in the existing literature, the proposed framework quantitatively assesses the effect of both negative and positive events and conditions on the performance of a supply chain and supports resilience-enhancing strategies that minimize negative impacts while capitalizing on opportunities. Furthermore, in contrast to conventional resilience assessments, which focus on a single type of hazard and provide a snapshot of the resilience index immediately following a hazardous event, the proposed resilience assessment considers the medium- to long-term performance of a supply chain, thereby providing the resilience index as a function of time over the planning horizon. In this way, the time-dependent performance-based supply chain resilience index enables the quantification of multiple dimensions of resilience.

In this task, we have developed a multi-dimensional resilience assessment framework for a supply chain system subjected to multiple uncertain hazards and conditions. The framework consists of three stages: risk identification, hybrid risk assessment, and resilience assessment.

1. Risk identification: In the first stage of the framework, potential events and conditions that may affect supply chain performance are identified and categorized based on their characteristics. In this study, eight risk categories are identified: natural hazards, man-made hazards, government assistance, market, supply, technology, finance, and human/organizational behavior. Because most risk factors classified into the abovementioned categories are site- and problem-specific, each supply chain is subjected to a distinct combination of risk factors.
2. Hybrid risk assessment: Each risk factor has unique properties, and its effect on supply chain performance should be assessed using an appropriate risk assessment methodology. For example, while quantitative risk assessment has emerged as a widely accepted tool for quantifying uncertainties and managing risks associated with natural hazards, a purely probability-based approach to uncertainty and risk analysis can be problematic when dealing with low-probability, high-consequence man-made hazards. The knowledge and information needed to characterize such hazards are invariably limited. Additionally, changes in market demand and capacity are often forecasted based on prior knowledge and historical data. As such, each risk factor is incorporated by using an appropriate methodology based on its characteristics, and the realizations of all risk factors are layered to generate a single scenario over the

projection horizon. The scenario generation process is repeated until a sufficiently large set of plausible future scenarios is generated. At each time step for each scenario, the combined effects of multiple hazards and conditions on supply chain performance are assessed using supply chain analysis.

3. Resilience assessment: At each time step for each scenario, the performance of each node and link in a supply chain is adjusted, and the optimal routes are recalculated to maximize the system performance, based on the given conditions. In this study, the resilience of a supply chain, which is expressed as a function of time over the planning horizon, has three dimensions: (a) nonhazardous-event-induced resilience, reflecting the adaptability of a system; (b) hazardous-event-induced resilience, primarily indicating the robustness, rapidity, and resourcefulness of a system; and (c) opportunity-induced resilience, representing the redundancy of a system. Because each scenario has different values for the three dimensions of resilience, the expected values of each dimension are calculated over the entire set of plausible scenarios and then combined to compute a single resilience index. The main advantages of the proposed resilience index are as follows: (a) it can consider multiple types of uncertain hazards and conditions and can better address the associated uncertainties by considering a large set of scenarios, (b) it enables supply chain managers to assess the relative effect of each risk factor on the overall resilience to facilitate effective budget/resource allocation, and (c) it captures both opportunities and disruptions affecting the performance of a supply chain, which allows supply chain managers to design resilience-enhancing strategies that reduce negative impacts while taking advantage of opportunities in the decision-making stage.

To examine the feasibility and practicability of the proposed framework, the team has prepared to apply the framework to hypothetical oilseed-to-AJF supply chains in the PNW region. Some of the supply chains are adopted from the Master's thesis of Dane Camenzind, in which the locations of three oilseed crushers are determined using the many-step trans-shipment solver (MASTRS). The team has identified four risk factors, including earthquakes, drought conditions induced by climate change, intelligent attacks on airports, and increasing HEFA conversion rates. During the upcoming year, our team will compute a resilience index for each supply chain to determine which supply chain is the most resilient to current and future changes and conditions.

Milestone(s)

The proposed multi-dimensional resilience assessment framework provides two novel contributions. First, hybrid risk assessment can address uncertainties associated with each risk factor and can uniquely combine all risk factors to generate a set of plausible scenarios. Second, this new resilience index has three dimensions of resilience corresponding to multiple attributes (i.e., adaptability, robustness, rapidity, resourcefulness, and redundancy) of a supply chain in response to current and future events and conditions.

Major Accomplishments

The WSU MASTRS and Volpe FTOT were compared for siting analyses in the BANR region. Similar and differing modeling assumptions were identified, and the appropriate model for a given objective was determined.

The team has developed a theoretical framework for multi-dimensional resilience assessment. As part of this development, we also investigated stochasticity in various input parameters for TEA, which was incorporated in the analysis. The team has prepared case studies to apply the proposed framework to potential oilseed-to-AJF supply chains in the PNW region. The team has also been working on a journal paper primarily focused on the development of a multi-dimensional resilience assessment framework and plans to submit this paper in February 2020.

Publications

N/A

Outreach Efforts

N/A

Awards

None.

Student Involvement

Dane Camenzind, MS Environmental Engineering, Washington State University – graduated in September 2019; currently employed by WSU as an operations research engineer
Jie Zhao, PhD candidate, Civil Engineering, Washington State University
Fangjiao Ma, PhD candidate, Civil Engineering, Washington State University

Plans for Next Period

We will utilize regional supply chain tools to assess forest residuals for AJFs using pyrolysis methods, as described in Task 8 below.

The team will submit a manuscript on a multi-dimensional resilience assessment framework in February 2020. We will continue working on case studies to demonstrate how the proposed framework enables comparisons between alternative supply chain designs based on their resilience indices and how the framework supports the most resilient design under given conditions and constraints. The case studies will require an extensive utilization of either MASTRS or FTOT in a continuous reoptimization process, a thorough investigation of the total cost function, and more practical applications to decision-making problems.

Task 8 - Analytical Support for Regional CAAFI and USDA Jet Fuel Project

Washington State University

Objective(s)

We will develop a readiness level tool to assess the status of regional AJF production projects and will use supply chain and stand-alone design cases to support the USDA BANR project in TEA and supply chain analysis. This regional CAP project focuses on the use of softwood forest salvage feedstock for fuels via a catalyzed pyrolysis conversion pathway.

Research Approach

We will develop readiness level tools for regional projects to assess the status of developing fuel projects and to identify critical missing components. This tool will be similar in form to the CAAFI Feedstock and Fuel Readiness Levels and will be used to assist CAAFI in understanding the stage of development for projects of interest and to assess critical gaps. In addition, we will assist the regional USDA BANR team in deploying TEA and supply chain analysis for their project. This effort will be focused on the use of softwood forest salvage feedstock in a thermochemical conversion process to produce fuels and coproducts.

Milestone(s)

We are progressing on the use of supply chain and stand-alone design cases to support the USDA BANR project in TEA and supply chain analysis. Additionally, we have supported the BANR team in creating TEAs for the technologies under consideration.

Major Accomplishments

We have collaborated with the USDA BANR project and attended their annual meeting to coordinate analysis. We currently await their completion of dead wood estimates to complete the supply chain analysis. Moreover, analyses with previous forest residue data have been successfully modeled.

Publications

N/A

Outreach Efforts

N/A

Awards

None.

Student Involvement

Dane Camenzind, M.S. Environmental Engineering, Washington State University - graduated in September 2019; currently employed by WSU as an operations research engineer
Lina Martinez, PhD candidate, Biosystems Engineering, Washington State University

Plans for Next Period

Analysis of the BANR region is underway and will be completed within the project year.

Project 001(B) Alternative Jet Fuel Supply Chain Analysis

University of Hawaii

Project Lead Investigator

University of Hawaii Lead
Scott Q. Turn
Researcher
Hawaii Natural Energy Institute
University of Hawaii
1680 East-West Rd., POST 109; Honolulu, HI 96822
(808)-956-2346
sturn@hawaii.edu

University Participants

University of Hawaii

- PI: Scott Q. Turn, Researcher
- FAA Award Number: 13-C-AJFE-UH, Amendment 005
- Period of Performance: October 1, 2015 to July 1, 2020
- Task(s):
    1. Informing regional supply chains
    2. Identification of supply chain barriers in the Hawaiian Islands

University of Hawaii

- PI: Scott Q. Turn, Researcher
- FAA Award Number: 13-C-AJFE-UH, Amendment 007
- Period of Performance: October 1, 2016 to July 1, 2020
- Task(s):
    1. Informing regional supply chains
    2. Support of Indonesian alternative jet fuel supply initiatives

University of Hawaii

- PI: Scott Q. Turn, Researcher
- FAA Award Number: 13-C-AJFE-UH, Amendment 008
- Period of Performance: August 1, 2017 to July 1, 2020
- Task(s):
    1. National lipid supply availability analysis
    2. Hawaii regional project

University of Hawaii

- PI: Scott Q. Turn, Researcher
- FAA Award Number: 13-C-AJFE-UH, Amendment 011
- Period of Performance: May 31, 2019 to July 1, 2020
- Task:
    1. Hawaii regional project

Project Funding Level

Under **FAA Award Number 13-C-AJFE-UH, Amendment 005**, the Alternative Jet Fuel Supply Chain Analysis-Tropical Region Analysis project received $75,000 in funding from the FAA and cost share funding of $75,000 from the State of Hawaii.

Under **FAA Award Number 13-C-AJFE-UH, Amendment 007**, the Alternative Jet Fuel Supply Chain Analysis-Tropical Region Analysis project received $100,000 in funding from the FAA and cost share funding of $75,000 from the State of Hawaii and $25,000 of in-kind cost match in the form of salary support for Scott Turn from the University of Hawaii.

Under **FAA Award Number 13-C-AJFE-UH, Amendment 008**, the Alternative Jet Fuel Supply Chain Analysis-Tropical Region Analysis project received $125,000 in funding from the FAA and cost share funding of $125,000 from the State of Hawaii.

Under **FAA Award Number 13-C-AJFE-UH, Amendment 011**, the Alternative Jet Fuel Supply Chain Analysis-Tropical Region Analysis project received $200,000 in funding from the FAA and cost share funding of $200,000 from the State of Hawaii.

Investigation Team

Lead
Scott Turn, University of Hawaii, PI

Other Lead Personnel
Tim Rials, professor, and Burt English, professor (UT Co-PIs)
Manuel Garcia-Perez, profesor (WSU Co-PI)
Kristin Lewis, principal technical advisor (Volpe PI)
Michael Wolcott, professor (WSU PI)

UH Investigation Team
Under **FAA Award Number 13-C-AJFE-UH, Amendment 005**, Task 1 and Task 2 include
Dr. Scott Turn, researcher, Hawaii Natural Energy Institute, UH
Dr. Trevor Morgan, assistant researcher, Hawaii Natural Energy Institute, UH
Dr. Richard Ogoshi, assistant researcher, Department of Tropical Plant and Soil Sciences, UH
Dr. Adel H. Youkhana, junior researcher, Department of Tropical Plant and Soil Sciences, UH

Under **FAA Award Number 13-C-AJFE-UH, Amendment 007**, Task 1 and Task 2 include
Dr. Scott Turn, researcher, Hawaii Natural Energy Institute, UH
Dr. Trevor Morgan, assistant researcher, Hawaii Natural Energy Institute, UH
Dr. Richard Ogoshi, assistant researcher, Department of Tropical Plant and Soil Sciences, UH
Dr. Adel H. Youkhana, junior researcher, Department of Tropical Plant and Soil Sciences, UH
Dr. Curtis Daehler, professor, Department of Botany, UH
Ms. Sharon Chan, junior researcher, Hawaii Natural Energy Institute, UH

Under **FAA Award Number 13-C-AJFE-UH, Amendment 008**, Task 1 and Task 2 include
Dr. Scott Turn, researcher, Hawaii Natural Energy Institute, UH
Dr. Trevor Morgan, assistant researcher, Hawaii Natural Energy Institute, UH
Dr. Jinxia Fu, assistant researcher, Hawaii Natural Energy Institute, UH
Dr. Quang Vu Bach, postdoctoral fellow, Hawaii Natural Energy Institute, UH
Ms. Sabrina Summers, undergraduate student, Bioengineering Department, UH
Ms. Sarah Weber, undergraduate student, Molecular Biosciences and Biotechnology, UH
Mr. Taha Elwir, undergraduate student, Chemistry Department, UH

Under **FAA Award Number 13-C-AJFE-UH, Amendment 011**, Task 1 includes
Dr. Scott Turn, researcher, Hawaii Natural Energy Institute, UH
Dr. Quang Vu Bach, postdoctoral fellow, Hawaii Natural Energy Institute, UH

Project Overview

Under **FAA Award Number 13-C-AJFE-UH, Amendment 005**, the research effort has two objectives. The first objective is to develop information on regional supply chains for use in creating scenarios of future alternative jet fuel (AJF) production in tropical regions. Outputs from this project may be used as inputs to regional supply chain analyses being developed by the FAA and Volpe Center. The second objective is to identify the key barriers in regional supply chains that must be overcome to produce significant quantities of AJF in the Hawaiian Islands and similar tropical regions.

The **FAA Award Number 13-C-AJFE-UH, Amendment 005** project goals are to

- Review and summarize
  - the available literature on biomass feedstocks for the tropics,
  - the available literature on pretreatment and conversion technologies for tropical biomass feedstocks, and
  - the available literature on geographic information systems (GIS) data sets available for assessment of AJF production systems in the tropics.
- Identify AJF supply chain barriers in the Hawaiian Islands.

Under **FAA Award Number 13-C-AJFE-UH, Amendment 007**, the research effort has two objectives. The first objective is to develop information on regional supply chains for use in creating scenarios of future AJF production in tropical regions. Outputs from this project may be used as inputs to regional supply chain analyses being developed by the FAA and Volpe Center. Included in this objective is the development of fundamental property data for tropical biomass resources to support supply chain analysis. The second objective is to support the memorandum of understanding between the FAA and Indonesian Directorate General of Civil Aviation (DGCA) to promote development and use of sustainable, alternative aviation fuels.

The **FAA Award Number 13-C-AJFE-UH, Amendment 007** project goals are to

- Support the Volpe Center and Commercial Aviation Alternative Fuels Initiative (CAAFI) Farm to Fly 2.0 supply chain analysis
- Use GIS-based estimates of fiber crop production potential to develop preliminary technical production estimates of jet fuel in Hawaii
- Develop fundamental property data for tropical biomass resources
- Transmit data and analysis results to other ASCENT Project 1 researchers to support improvement of existing tools and best practices
- Support Indonesian AJF supply initiatives

Under **FAA Award Number 13-C-AJFE-UH, Amendment 008**, the research effort has two objectives. The first objective is to support a national lipid supply availability analysis that will inform industry development and guide policy. The second objective is to conduct a targeted supply chain analysis for AJF production facility based on the Hawaii regional project.

The **FAA Award Number 13-C-AJFE-UH, Amendment 008** project goals are to

- Support ASCENT partners conducting the national lipid supply availability analysis by contributing information on tropical oilseed availability
- Evaluate supply chains for targeted waste streams and purpose-grown crops in Hawaii to a location in the principal industrial park on the island of Oahu

Under **FAA Award Number 13-C-AJFE-UH, Amendment 011**, the main objective of the research effort is to conduct bench-scale testing of tropical feedstocks for use in targeted supply chain analysis for AJF production facility based on the Hawaii regional project initiated under Amendment 008.

The **FAA Award Number 13-C-AJFE-UH, Amendment 011** project goals are to

- Survey bench-scale systems available for relevant sustainable aviation fuel (SAF) conversion technology options
- Down select from the available bench-scale systems to no more than two systems capable of conducting feedstock testing and quantify product yields and contaminant concentrations
- Conduct bench-scale feedstock tests and quantify product yields and quality and contaminant concentrations

Task 0.1 - Informing Regional Supply Chains

University of Hawaii

Objective(s)

This task included two activities: (1) a review of the archival literature on existing tropical crops and potential new crops that could provide feedstocks for AJF production, and (2) a review of relevant pretreatment and conversion technology options and experience with feedstocks identified in (1).

Research Approach

Activity 1. The archival literature will be reviewed to construct an updated database of relevant citations for tropical crops; new potential energy crops will be identified and added to the database. Available information on agronomic practices, crop rotations, and harvest techniques will be included. The database will be shared with and serve as a resource for the Project 1 team and Volpe Center analyses of regional supply chains.

Activity 2. A database of relevant pretreatment and conversion technology options and experience with potential tropical feedstock materials will be assembled from the archival literature and from existing Project 1 team shared resources. Of particular interest are inventories of material and energy flows associated with the pretreatment and conversion unit operations fundamental to the design of sustainable systems and the underlying analysis. Pairings of pretreatment and conversion technology options provide the starting point for evaluation of tropical biorefineries that can be integrated into ASCENT Project 1 team and Volpe Center activities.

Milestone(s)

Task 1, Activity 1: Identify target list of databases to search for relevant literature
Task 1, Activity 1: Interim report summarizing progress on literature search
Task 1, Activity 2: Identify target list of databases to search for relevant literature
Task 1, Activity 2: Interim report summarizing progress on literature search

Major Accomplishments

This work is completed. A report was produced for each of the two activities, and the two reports were combined to form a manuscript published in the journal *Energy & Fuels*.

Publications

Peer-reviewed journal publication

Morgan, T.M., Youkhana, A., Ogoshi, R., Turn, S., & Garcia-Perez, M. (2019). Review of biomass resources and conversion technologies for alternative jet fuel production in Hawai'i and tropical regions. *Energy & Fuels*, 2699-2762.

Outreach Efforts

On February 21, 2018, the PI participated in a ThinkTech Hawaii broadcast focused on AJFs with collaborators from WSU and CAAFI (https://www.youtube.com/watch?v=Ci4oWITPRKQ&feature=youtu.be).

Awards

None

Student Involvement

None

Plans for Next Period

N/A

Task 0.2 - Identification of Supply Chain Barriers in the Hawaiian Islands

University of Hawaii

Objective

Identify the key barriers in regional supply chains that must be overcome to produce significant quantities of AJF in the Hawaiian Islands and similar tropical regions.

Research Approach

UH developed the Hawaii Bioenergy Master Plan for the State of Hawaii (https://www.hnei.hawaii.edu/sites/www.hnei.hawaii.edu/files/Hawaii%20Bioenergy%20Master%20Plan.pdf), which was completed in 2009. In that plan, UH was tasked with determining whether Hawaii had the capability to produce 20% of land transportation fuels and 20% of electricity from bio-based resources. To this end, the plan included assessments of (1) land and water resources that could support biomass feedstock production, (2) potential biomass resources and their availabilities, (3) technology requirements, (4) infrastructure requirements to support logistics, (5) economic impacts, (6) environmental impacts, (7) availability of human capital, (8) permitting requirements, and (9) limitations to developing complete value chains for biomass-based energy systems. In keeping with the stakeholder-driven development of the Hawaii Bioenergy Master Plan, barriers to development of regional supply chains for ASCENT will be identified by interacting with key stakeholder groups. Green Initiative for Fuels Transition Pacific (GIFTPAC) meetings are held quarterly and attended by biofuel development interests in Hawaii, including representatives of large landowners, producers of first-generation biofuels, petroleum refiners, electric utilities, the State Energy Office, U.S. Pacific Command, biofuel entrepreneurs, county government officials, and the University of Hawaii. Additional stakeholders are invited as necessary to fill information and value chain gaps. These meetings are excellent opportunities to receive stakeholder input, identify barriers to supply chain development, and organize data collection efforts that span supply chain participants.

Milestone(s)

Task 2: Introduce activities at next regularly scheduled GIFTPAC meeting after contract executed
Task 2: Prepare interim report outlining two tropical supply chain scenarios developed in consultation with Project 1 team and with input from GIFTPAC participants

Major Accomplishments

This task is completed. A stakeholder meeting was held and documented in a report submitted to the FAA. The stakeholders identified barriers to AJF production in Hawaii and ranked the barriers in order of importance as indicated below:

- Economic constraints (e.g., high costs of entry for production factors such as land) throughout the whole production chain
- Issues associated with access to capital, including high initial risks and uncertain return on investment
- Insufficient government support in the form of incentives and favorable policies to encourage long-term private investment
- Cost, availability, and competition for water
- AJF production technologies (emerging but have not yet demonstrated full commercial viability)
- Insufficient or inadequate infrastructure (e.g., harbors, roads, fuel distribution infrastructure, irrigation systems) to support the whole production chain

Several of the barriers are held in common with other locations in the continental United States but those related to water and infrastructure are unique characteristics of an island state.

Publications

N/A

Outreach Efforts

This activity engaged stakeholders to identify barriers to AJF production in Hawaii. Preparation included reviewing stakeholder lists from previous activities. Facilitators appropriate to the stakeholder group were retained. The stakeholder

meeting included a presentation about the scope and goals of the larger ASCENT program and other aspects of the UH ASCENT project.

Awards
None

Student Involvement
None

Plans for Next Period
This task is complete but stakeholder outreach activities will continue under other tasks outlined below.

Task 0.3 - Informing Regional Supply Chains
University of Hawaii

Objective(s)
Building on FY16 activities, additional supporting analysis will be conducted for proposed supply chains in Hawaii, including

0.3.1 Support Volpe Center and CAAFI Farm to Fly 2.0 supply chain analysis
0.3.2 Use GIS-based estimates of fiber crop production potential to develop preliminary technical production estimates of jet fuel in Hawaii
0.3.3 Develop fundamental property data for tropical biomass resources
0.3.4 Transmit data and analysis results to support improvement of existing tools (e.g., POLYSYS; https://bioenergykdf.net/content/polysys)

Research Approach
Activity 0.3.2 has been conducted using GIS data to identify areas suitable for purpose-grown crop production of feedstocks for AJF production in Hawaii. The approach has been to use GIS layers for land capability class (LCC), slope, and zoning as preliminary screens for suitability. Lands are classified by the Natural Resources Conservation Service (NRCS) with ratings from 1 to 6. LCCs from 1 to 3 are generally suitable for agricultural production; LCC of 4 can be productive with proper management; and LCCs of 5 or 6 can support less intensive production and could be suitable for forestry. The slopes of terrains affect aspects of production, including mechanization and erodibility. An elevation GIS layer was used to derive a slope layer. Zoning layers were acquired from state and county GIS offices. Only agricultural zoning was deemed suitable for this analysis.

The EcoCrop model was used to develop yield models for the crops selected in Task 0.1 based on the annual rainfall and mean minimum monthly temperature data. EcoCrop includes model parameters on sugarcane, bana grass, 5 species of eucalyptus, gliricidia, leucaena, pongamia, jatropha, and sorghum. The parameters for sugarcane have been used to provide a base case assessment for comparison with historical sugarcane acreage and yield. Using sensitivity analysis, the model can be tuned to account for the differences between parameters developed from global sugar production and a century of production experience in Hawaii that was refined through plant breeding to adapt sugarcane varieties to a wide variety of agro-ecosystems. Model results across all of the potential feedstocks have been used to identify land-use patterns that would match plants with environmental conditions toward maximizing productivity in support of AJF production.

Pongamia (*Millettia pinnata*) will be the initial focus of Activity 0.3.3. Pongamia is an oilseed-bearing, leguminous tree that has production potential in Hawaii and Florida. The tree produces pods containing oil-bearing seeds. Pods, oilseed cake, and oil will be evaluated from a number of trees growing on the island of Oahu. Fundamental measurements of chemical composition will be conducted and reported. Development of coproducts from the pods and oilseed cake will be explored.

Milestone(s)
- Identify target opportunities to augment POLYSYS, Alternative Fuel Transportation Optimization Tool (AFTOT; https://trid.trb.org/view/1376122), and conversion modules

- Review previously developed GIS information layers for tropical fiber crops and identify updating requirements
- Conduct preliminary estimates of AJF technical potential in Hawaii based on previously developed GIS information layers

Major Accomplishments

The GIS-based analysis of AJF production potential is ongoing. The assessment of potential lands meeting requirements for LCC, slope, and land-use zoning is complete. The EcoCrop model is being implemented to predict yield as a function of minimum mean monthly temperature and annual rainfall. This will allow prescription of potential AJF feedstock crops on land areas capable of supporting their production under both rain-fed and irrigated conditions. This analysis will provide information necessary in determining cropping patterns and assessing transport costs to processing facility locations. The EcoCrop model's prediction of sugarcane potential was determined and the results were compared with historic sugarcane acreage, both rain-fed and irrigated. EcoCrop's upper and lower values for temperature and rainfall that support optimal sugarcane production were varied to calibrate the prediction against historic acreage. The difference between the EcoCrop values and those representative of Hawaii conditions can be attributed to improvements due to plant breeding and unique combinations of environmental conditions. An example of the latter is the relatively young volcanic soils present in high-rainfall areas on the island of Hawaii that allow for high drainage rates and accommodate sugar production.

Calibration of the EcoCrop model using historic sugarcane planted acreages was completed in 2018. This effort used a confusion matrix approach to validation (resulting in a kappa value >0.4) and demonstrated that mean annual temperature was a better indicator of environmental capability than the minimum mean monthly temperature recommended by the EcoCrop developers. This effort highlights the need to adapt models to local conditions. Model predictions for suitable cropping are being compared with current land uses to provide another indicator of agreement.

The GIS analysis of SAF feedstock production potential has been completed to include statewide working maps for each of the species summarized in a draft report currently undergoing internal review. This report will serve as the basis for a publication targeted for *Biomass & Bioenergy* or similar journal.

Dr. Curtis Daehler (University of Hawaii, Department of Botany) completed a report assessing the invasiveness of pongamia. Retrospective analyses show that predictive weed risk assessment systems correctly identify many major pest plants, but such predictions are not 100% accurate. The purpose of this study was to make field observations of pongamia planted around Oahu to look for direct evidence that pongamia is escaping from plantings and becoming an invasive weed. Seven field sites were visited in varying environments across Oahu. Although some pongamia seedlings were found in the vicinity of some pongamia plantings, particularly in wetter, partly shaded environments, almost all observed seedlings were restricted to areas directly beneath the canopy of mother trees. This finding suggests a lack of effective seed dispersal away from pongamia plantings. Based on its current behavior in the field, pongamia is not invasive or established outside of cultivation on Oahu. Because of its limited seed dispersal and low rates of seedling establishment beyond the canopy, the risk of pongamia becoming invasive can be mitigated through monitoring and targeted control of any rare escapes in the vicinity of plantings. Seeds and seed pods are water dispersed, so future risks of pongamia escape and unwanted spread would be minimized by avoiding planting at sites near flowing water, near areas exposed to tides, or on or near steep slopes. Vegetative spread by root suckers was not observed around plantings on Oahu but, based on reports from elsewhere, monitoring for vegetative spread around plantations is recommended; unwanted vegetative spread might become a concern in the future that could be addressed with localized mechanical or chemical control.

Pods, oilseed cake, and oil were evaluated from a number of trees growing on the island of Oahu. Fundamental measurements of chemical composition were made for seeds, pods, extracted oil, and post-extraction seed material. Measured values included C, H, N, and S elemental composition; energy content; volatile matter, fixed carbon and ash content; and trace element composition. Oils were characterized for peroxide value, iodine value, fatty acid profile, free fatty acid content, flash point, density, viscosity, and phase transition temperatures. Chemical composition and fuel properties of the oilseed cake and the pod material have been characterized. Pods have been evaluated as feedstock for a torrefaction process that can produce a coal substitute. A manuscript summarizing the results of this effort has been drafted. TerViva, a company pursuing pongamia commercialization, has provided material from orchards on Oahu. Permission has been requested to include data from analysis of their pongamia samples in the manuscript. Their reply will determine whether the manuscript is submitted with the current data set or expanded to include TerViva samples.

Publications

Written report

Fu, F., Summers, S., Morgan, T.J., Turn, S.Q., & Kusch, W. Fuel properties of *Millettia pinnata* seeds and pods grown in Hawaii. Draft manuscript.

Outreach Efforts

Outreach in this task has focused on interactions with TerViva, a startup company that has identified pongamia germplasm production and marketing as the central focus of their business plan.

Awards

None.

Student Involvement

Three undergraduate students are involved in the project, with primary responsibility for processing and analyzing samples of biomass materials selected for evaluation as potential AJF feedstocks. The pongamia torrefaction work was the focus of an Undergraduate Research Opportunity Program project for Sabrina Summers, a bioengineering and chemistry double major. The results of her work were presented at the fall 2019 American Chemical Society meeting in San Diego, California.

Plans for Next Period

The report summarizing the analysis of the GIS analysis of SAF feedstock production potential will be completed and published as a manuscript in *Biomass & Bioenergy* or similar journal.

Statewide working maps for each of the feedstock species will be used as the basis for discussions with targeted stakeholder groups including landowners and NRCS staff. Funding for planting and evaluating the more promising feedstock plants on University of Hawaii experiment station land will be pursued.

The current manuscript summarizing fuel properties of pongamia seed, pod, and oilseeds will be finalized and published.

Analysis of coproduct development based on pongamia oilseeds and husks will be continued.

Task 0.4 - Support of Indonesian Alternative Jet Fuel Supply Initiatives

University of Hawaii

Objective

This task supports the memorandum of understanding between the FAA and the Indonesian DGCA to promote development and use of sustainable, alternative aviation fuels. Under the coordination of the FAA, efforts to establish points of contact and coordinate with Indonesian counterparts are ongoing.

Research Approach

This task will support the memorandum of understanding between the FAA and Indonesian DGCA to promote development and use of sustainable, alternative aviation fuels. This will begin with working with the FAA to establish points of contact to coordinate efforts with Indonesian counterparts. The Indonesian Aviation Biofuels and Renewable Energy Task Force (ABRETF) membership includes Universitas Indonesia, Institut Teknologi Bandung, and Universitas Padjadjaran. A prioritized list of tasks will be developed in consultation with Indonesian counterparts, and data required to inform sustainability and supply analyses and potential sources of information will be identified. This could include data collection on Indonesian jet fuel use and resources for AJF production, airport locations, and annual and monthly jet fuel consumption patterns. Characterization of sustainable biomass resources with potential for use in producing AJF supplies could include developing preliminary GIS mapping information of their locations and distributions and preliminary estimates of their technical potentials.

Milestone(s)

- Identify points of contact at Indonesian universities participating in ABRETF

- Identify research needs and develop project plan
- Develop data on potential project

Major Accomplishments

The PI traveled to Jakarta in the first week of August 2017 and met with the following individuals:

- Cesar Velarde Catolfi-Salvoni (International Civil Aviation Organization)
- Dr. Wendy Aritenang (International Civil Aviation Organization)
- Dr. Ridwan Rachmat (head of Research Collaboration, Indonesian Agency for Agricultural Research and Development)
- Sylvia Ayu Bethari (head of Aviation Fuel Physical & Chemical Laboratory, Research and Development Centre for Oil and Gas Technology)
- Dr. Ina Winarni (Forest Product Research and Development Center, Ministry of Environment and Forestry)
- Dr. SD Sumbogo Murti (Center of Technology Energy Resources and Chemical Industry, Agency for the Assessment and Application of Technology)

The activities of the tropical supply chain analysis effort were presented to the group, followed by a general discussion. The conclusion from this introductory meeting was that the Indonesian counterparts would seek agreement on how to move forward with future cooperation.

The PI traveled to Jakarta and met with Dr. Wendy Aritenang of the International Civilian Aviation Organization Jakarta office. The same trip included meetings with renewable energy researchers at Universitas Indonesia. Following the meeting, Dr. Aritenang suggested points of contact for future engagement: Frisda Panjaitan from the Palm Oil Research Institute and three researchers from the Bandung Institute of Technology: Tatang Soerawidjaja, Tirto Prakoso Brodjonegoro, and Imam Reksowardojo.

Publications

N/A

Outreach Efforts

Outreach efforts by the PI are described in the Major Accomplishments section above.

Awards

None

Student Involvement

None

Plans for Next Period

The PI will continue to develop the cooperative research agenda between UH and Indonesian universities through continued dialog with FAA, International Civil Aviation Organization, and the Indonesian DGCA. Travel to Southeast Asia for other projects is anticipated in 2020, and meetings with the researchers at Indonesian institutions suggested by Dr. Aritenang will be pursued.

Task 2.2 - National Lipid Supply Availability Analysis

University of Hawaii

Objective

Activities under this task will support ASCENT partners working on a national lipid supply availability analysis by sharing data on tropical oilseed availability developed under previous years' activities.

Research Approach
Activities under this task will support ASCENT partners working on a national lipid supply availability analysis by sharing data on tropical oilseed availability developed under previous years' activities. This support will include estimates of pongamia production capability in the state, in addition to assessments of waste cooking oil and tallow.

Milestone(s)
Milestones will coincide with the schedule of the lead institution (WSU) for the national lipid supply analysis.

Major Accomplishments
Additional seeds and pods were collected from the pongamia tree on the University of Hawaii campus, Foster Botanical Garden, and the Ke'ehi Lagoon Beach Park. Large quantities (tens of kilograms) of material were acquired from TerViva's plantings on Oahu's north shore for use in oil evaluation. Two oilseed presses were acquired, and safety documents were developed. Pods, oilseed cake, and oil were evaluated from a number of trees growing on the island of Oahu. Fundamental measurements of chemical composition were made for seeds, pods, extracted oil, and post-extraction seed material. Measured values included C, H, N, and S elemental composition; energy content; volatile matter, fixed carbon, and ash contents; and trace element composition. Oils were characterized for peroxide value, iodine value, fatty acid profile, free fatty acid content, flash point, density, viscosity, and phase transition temperatures. Development of coproducts from the pods and oilseed cake will be explored.

Publications
N/A

Outreach Efforts
Data were presented at the April 2019 ASCENT review meeting in Atlanta, Georgia.

Awards
None

Student Involvement
Three undergraduate students—Sabrina Summers, Sarah Weber, and Taha Elwir—are involved in the project, with primary responsibility for processing and analyzing samples of biomass materials selected for evaluation as potential AJF feedstocks.

Plans for Next Period
Estimates of suitable oilseed crop area in Hawaii will be completed based on the recently completed GIS mapping tools. Waste oil supply estimates were not completed in the 2019 reporting period but will be assessed in 2020. Information will be provided to the lead institution (WSU).

Task 3.2 - Hawaii Regional Project
University of Hawaii

Objective(s)
A supply chain based on fiber feedstocks transported to a conversion facility located at Campbell Industrial Park (CIP) on Oahu will be evaluated (Figure 1). CIP is the current site of two oil refineries. Construction and demolition (C&D) wood waste from PVT Landfill could be the primary source of feedstock. Other sources will be evaluated from elsewhere on Oahu and from outer islands, including municipal solid waste (MSW) stream from outer islands and mining of current stocks of waste-in-place. Waste streams and purpose-grown crops form the basis for a hub-and-spoke supply system with the hub located on Oahu. Pipelines for jet fuel transport are in place from CIP to Daniel K. Inouye International Airport and adjacent Joint Base Pearl Harbor/Hickam. Other coproduct off-takers for alternative diesel fuel include Hawaiian Electric Co. and several military bases, including Schofield Barracks (~50 MW alternative fuel-capable power plant under development) and Kaneohe Marine Corp Base. Hawaii Gas (a local gas utility) is also seeking alternative sources of methane if methane or feedstock suitable for methane production is available as a coproduct. Hawaii Gas currently off-takes feedstock (naphtha) from refinery.

Figure 1. Possible locations of value chain participants for fiber-based alternative jet fuel production facility located at Campbell Industrial Park, Oahu.

Research Approach

Task 3.2.G1. Analysis of feedstock-conversion pathway efficiency, product slate (including coproducts), maturation
Building on activities from previous years, additional supporting analysis will be conducted for proposed supply chains in Hawaii, as follows:

- 3.2.G1.1 Assess feedstock suitability for conversion processes (e.g., characterization, conversion efficiencies, contaminants). [UH and WSU (Manuel Garcia-Perez)]
- 3.2.G1.2 Acquire data on feedstock size reduction, particle size of materials, bulk densities. [UH, WSU (Manuel Garcia-Perez)]
- 3.2.G1.3 Evaluate coproducts at every step of the supply chain. [A01 team]

Task 3.2.G2. Scoping of techno-economic analysis (TEA) issues
This task will determine the current TEA status of targeted AJF production technologies that use fiber feedstocks as production inputs. [UH, WSU (Manuel Garcia-Perez), Purdue (Wally Tyner)]

Task 3.2.G3. Screening-level greenhouse gas (GHG) life-cycle assessment (LCA)
This task will conduct screening-level GHG LCA on the proposed target supply chains and AJF conversion technologies.

Subtasks:

3.2.G3.1 Assess Massachusetts Institute of Technology (MIT) waste-based GHG LCA tools in context of Hawaii application. [MIT (Mark Staples)]

3.2.G3.2 Assess requirements to link previously completed eucalyptus energy and GHG analysis to the edge of the plantation with available GHG LCA information for conversion technology options. [MIT (Mark Staples), UH]

3.2.G3.3 Identify and fill information/data gaps.

Task 3.2.G4. Identification of supply chain participants/partners

Subtasks:

3.2.G4.1 Define C&D landfill case.

3.2.G4.2 Identify eucalyptus in existing plantations: landowners, leaseholder/feedstock producer, harvesting contractor, trucking, etc. [UH]

3.2.G4.3 Define other feedstock systems as identified. [A01 Team]

Task 3.2.G5. Develop appropriate stakeholder engagement plan

Subtasks:

3.2.G5.1 Review stakeholder engagement methods and plans from past work to establish baseline methods. [UH, WSU (Season Hoard)]

3.2.G5.2 Identify and update engagement strategies based on updated Community Social Asset Modeling (CSAM) /Outreach support tool. [UH, WSU (Season Hoard)]

Task 3.2.G6. Identify and engage stakeholders

Subtasks:

3.2.G6.1 Identify stakeholders along the value chain and create database based on value chain location. [UH]

3.2.G6.2 Conduct stakeholder meeting using instruments developed in Task 3.2.G5. [UH, WSU (Season Hoard)]

3.2.G6.3 Analyze stakeholder response and feedback to process. [UH, WSU (Season Hoard)]

Task 3.2.G7. Acquire transportation network and other regional data needed for Freight and Fuel Transportation Optimization Tool (FTOT) and other modeling efforts

Subtasks:

3.2.G7.1 Acquire necessary data to evaluate harbor capacities and current usage. [UH, Volpe (Kristin Lewis), WSU (Mike Wolcott)]

3.2.G7.2 Acquire data on interisland transport practices. [UH, Volpe (Kristin Lewis), WSU (Mike Wolcott)]

Task 3.2.G8. Evaluate infrastructure availability

Subtasks:

3.2.G8.1 Evaluate interisland shipping options and applicable regulation. [UH, Volpe (Kristin Lewis), WSU (Mike Wolcott)]

3.2.G8.2 Evaluate transport or conveyance options from conversion location to end user and applicable regulation. [UH, Volpe (Kristin Lewis), WSU (Mike Wolcott)]

Task 3.2.G9. Evaluate feedstock availability

Subtasks:

3.2.G9.1 Refine/ground truth prior evaluations of options for purpose-grown feedstock supply. [UH]

3.2.G9.2 Conduct projections of C&D waste supply moving forward and mining of waste-in-place on Oahu, MSW and mining of waste-in-place on other islands. [UH]

Task 3.2.G10. Develop regional proposal

This task will use the information collected in Tasks 3.2.G1 through 3.2.G9 to develop a regional project proposal.

Milestone

One milestone is associated with each of the subtask activities identified in the Research Approach section above.

Major Accomplishments

Characteristics of the feedstock generated at the landfill is the first piece of information needed to provide a basis for the ensuing analysis. The feedstock received at the landfill is an inhomogeneous mixture of C&D. PVT Land Company is

currently also mining waste-in-place from the existing landfill and processing it to produce a feedstock stream. Both sources of waste (material arriving in trucks and mined waste-in-place) produce feedstock with potentially variable fuel properties. ASTM sampling methods for refuse-derived fuels have been reviewed and adapted to the current circumstances. PVT Land Company and the University of Hawaii signed an agreement allowing UH personnel to locate equipment at the landfill, to obtain samples from the feedstock processing line, and to preprocess the samples to a particle size suitable for further work in a laboratory environment.

PVT Land Company operates a sorting line to remove recyclable and noncombustible material from the incoming C&D waste stream. The result is a product that may serve as feedstock for SAF production. Over a period of eight months, 12 samples of C&D waste were collected from the outlet of the sorting line where material drops from a conveyor into a reclaim pit. Sample sizes ranged from 35 to 50 kg. Samples were sorted to quantitatively separate noncombustible from combustible materials. The combustible fraction was size reduced and subdivided to produce ~500-g subsamples for analysis. The following sets of analyses (each replicated three times) were conducted for all samples:

- Ultimate analysis: major element, C, H, N, S, and O
- Proximate analysis (volatile matter, fixed carbon, and ash)
- Energy content as higher heating value
- Minor elements spanning the range of atomic weights from fluorine (F) to uranium (U) using X-ray fluorescence (XRF)

Ash deformation temperatures in oxidizing and reducing environments and inductively coupled plasma (ICP) analysis for metals were performed on selected samples. ICP and XRF results were compared. A summary of the data has been completed.

The element ratios calculated from these analyses were used as inputs to the software tool FactSage to predict the thermochemical equilibrium composition under steam and oxygen gasification reactor conditions. Gasification is anticipated to be the main unit operation used to convert C&D waste to synthesis gas for the Fischer–Tropsch process or to hydrogen-rich gas that can be used as a petroleum refinery input or for hydrotreating SAF intermediate products. The equilibrium analysis results provide a starting point for TEA data needs discussion by providing estimates of contaminants present in the raw product gas from the gasification process. These estimates can be used to identify contaminant removal unit operations that improve the raw gas quality to meet synthesis gas or hydrogen end-use specifications.

Preliminary discussions were held with Manuel Garcia-Perez (WSU) on using the sample analysis data and thermochemical equilibrium analysis results to inform the TEA for this regional project.

Based on GHG analysis previously conducted by ASCENT collaborators (Mark Staples), schematics for conducting inventory analysis were drafted. These will be used to drive discussions on GHG analysis of C&D-based SAF systems with landfill operators moving forward.

Publications

N/A

Outreach Efforts

Data were presented at the April 2019 ASCENT review meeting in Atlanta, Georgia.

Results of the fuel sampling, analyses, and equilibrium analyses were presented at the October 2019 *Thermochemical Biomass 2019* conference, in Chicago, Illinois.

Awards

None

Student Involvement

Three undergraduate students—Sabrina Summers, Sarah Weber, and Taha Elwir—have been involved in sample preparation and in operating the laboratory analytical equipment used for sample analysis.

Plans for Next Period

During the next period, activities will focus on completing subtasks identified in the Research Approach section above. The table below includes plans for each task moving forward.

Table 1. Summary of tasks for construction and demolition waste regional project

Task Identifier	Task Title	Activity Moving Forward
3.2.G1	Analysis of feedstock-conversion pathway efficiency, product slate (including coproducts), maturation	Based on the level of effort and results from 2019 activities, further physical work on this subtask will be only be conducted as specific needs are identified. Manuscripts will be prepared based on 2019 task activities and results.
3.2.G2	Scoping of techno-economic analysis (TEA) issues	Preliminary discussions on applying the TEA tools of ASCENT collaborators (Manuel Garcia-Perez) to the construction and demolition (C&D) data set will be continued to identify additional data requirements.
3.2.G3	Screening-level greenhouse gas (GHG) life-cycle assessment (LCA)	Data requests to support the inventory analysis of the C&D production operations will be sent to the host facility. Responses will be used to advance the GHG analysis of the project.
3.2.G4	Identification of supply chain participants/partners	The anchor supply chain participants have been identified, but potential participants needed to complete the supply chain will be identified. This activity will be continued.
3.2.G5	Develop appropriate stakeholder engagement plan	Based on the supply chain participants and the stakeholders identified in Task 3.2.G6, a stakeholder engagement plan will be drafted in cooperation with Season Hoard. This activity will be continued.
3.2.G6	Identify and engage stakeholders	Stakeholder lists from previous biomass energy planning efforts in Hawaii will be reviewed and revised as needed. Stakeholder engagement will ensue as Tasks 3.2.G1 to G4 results are developed. This activity will be continued.
3.2.G7	Acquire transportation network and other regional data needed for Freight and Fuel Transportation Optimization Tool (FTOT) and other modeling efforts	In consultation with ASCENT partners Kristin Lewis and Mike Wolcott, contacts from the State of Hawaii, Department of Transportation, Harbors Division, will be engaged to initiate data collection on pipeline use and interisland barge movement of fuels. This activity will be continued.
3.2.G8	Evaluate infrastructure availability	Based on information and data developed in Task 3.2.G7, availability of existing infrastructure and options to target infrastructure expansion will be developed. This activity will be continued.
3.2.G9	Evaluate feedstock availability	Refinement and ground-truthing of purpose-grown crops will be approached by identifying existing plantings of candidate crops in botanical gardens and experiment stations and assessing them in their environment. Opportunities to establish additional plantings will be identified. After reviewing solid waste management plans, meetings will be held with the Solid Waste Divisions in each county to explore options for waste diversion opportunities. This activity will be continued.

Task 4 - Hawaii Regional Project

University of Hawaii

Objective

This task builds upon the results from the previous years' work under the Hawaii regional project. The focus is the data and analysis necessary to plan a project that uses C&D waste as feedstock for SAF production. Using previous years' C&D feedstock characterization data and thermochemical equilibrium analysis, the Task 4 objective is to conduct bench-scale gasification tests and quantify the product gas yield and composition and contaminant concentrations. These results will be compared with equilibrium prediction, used to identify contaminants that must be addressed prior to end use, and provide the basis for contaminant control system design.

Research Approach

Task 4.G1. Analysis of feedstock-conversion pathway efficiency, product slate (including coproducts), maturation

Building on activities from previous years, additional supporting analysis will be conducted for proposed supply chains in Hawaii, as follows:

- 4.G1.1 Conduct bench-scale testing of feedstocks to measure product yields, identify contaminants, and investigate element partitioning between product phases (e.g., characterization, conversion efficiencies, contaminants). [UH and WSU (Manuel Garcia-Perez)]
- 4.G1.2 Evaluate potential coproducts from bench-scale test products. [A01 team]
- 4.G1.3 Evaluate coproducts at every step of the supply chain. [A01 team]

Task 4.G2. Scoping of TEA issues

This task will determine the current TEA status of targeted AJF production technologies that use fiber feedstocks as production inputs based on the results of Task 4.G1.1. [UH, WSU (Manuel Garcia-Perez)]

Task 4.G3. Screening-level GHG LCA

This task will conduct preliminary GHG LCA on the proposed target supply chains and AJF conversion technologies based on the results of Task 4.G1.1. Subtasks are outlined below.

- 4.G3.1 With appropriate modifications, apply MIT waste-based GHG LCA tools in context of Hawaii application based on the results of Task 4.G1.1. [MIT (Mark Staples)]
- 4.G3.2 Link previously completed eucalyptus energy and GHG analysis to the edge of the plantation with available GHG LCA information for conversion technology options explored in Task 4.G1.1. [MIT (Mark Staples), UH]
- 4.G3.3 Identify and fill information/data gaps.

Task 4.G4. Identification of supply chain participants/partners

This task will identify and assess technology providers that could support regional project development based on the results of 4.G1.1.

- 4.G4.1 Create evaluation rubric for technology providers. [UH, WSU (Manuel Garcia-Perez)]
- 4.G4.2 Identify and assess technology providers that could support regional project development based on the results of 4.G1.1 using the evaluation rubric. [UH, WSU (Manuel Garcia-Perez)]
- 4.G4.3 Assess technology providers' capabilities to conduct process development unit-scale testing of feedstocks.
- 4.G4.4 Identify and fill information/data gaps. [A01 Team]

Task 4.G5. Continue stakeholder engagement

Subtasks:

- 4.G5.1 Engage stakeholders to identify impacts of information developed from the results of 4.G1.1. [UH, WSU (Season Hoard)]
- 4.G5.2 Identify and update engagement strategies based on updated information generated in 4.G1.1 and 4.G5.1. [UH, WSU (Season Hoard)]

Task 4.G6. Update infrastructure requirements

Update interisland shipping options and applicable regulation based on results of 4.G1.1. [UH, Volpe (Kristin Lewis), WSU (Mike Wolcott)]

Task 4.G7. Assess preliminary supply chain economics

4.G7.1 Assemble preliminary economic model to evaluate regional project. [UH, UTK, Purdue, WSU, PSU]
4.G7.2 Assess growth in job creation and economic benefits that will result from regional project. [UH, UTK, Purdue, WSU, PSU]
4.G7.3 Initiate effort to model risk associated with the regional project. [UH, PSU].
4.G7.4 Identify and fill information/data gaps. [UH, UTK, Purdue, WSU]

Task 4.G8. Refine regional proposal

This task will use the information collected in previous years and Tasks 4.G1 through 4.G7 to update the regional project proposal.

Milestone

One milestone is associated with each of the subtask activities identified in the Research Approach section above.

Major Accomplishments

Funding for this task was received recently and the task is in the planning stage.

Publications

N/A

Outreach Efforts

N/A

Awards

None

Student Involvement

None

Plans for Next Period

During the next period, activities will begin on subtasks identified in the Task 4 Research Approach section above. As this task is largely being initiated, the primary focus will be planning and then conducting the bench-scale gasification tests outlined in subtask 4.G1.1. The initial focus will be to identify and compare companies/universities/national labs that have facilities that can conduct the bench-scale testing and the capacity to make the relevant contaminant measurements. Depending on the size of the unit identified in the selection process, sufficient feedstock will be acquired and prepared to conduct all tests from a single batch. Results of these tests will be used to inform later subtasks.

Project 001(C) Alternative Jet Fuel Supply Chain Analysis

Purdue University

Project Lead Investigator: October 1, 2018–August 15, 2019

Wallace E. Tyner
James and Lois Ackerman Professor
Department of Agricultural Economics
Purdue University
403 West State Street
West Lafayette, IN 47907-2056
765-494-0199
wtyner@purdue.edu

Project Lead Investigator: August 16, 2019–September 30, 2019

Farzad Taheripour
Research Associate Professor
Department of Agricultural Economics
Purdue University
403 West State Street
West Lafayette, IN 47907-2056
765-494-4612
tfarzad@purdue.edu

University Participants: October 1, 2018–August 15, 2019

Purdue University

- PI: Wallace E. Tyner, James and Lois Ackerman Professor
- FAA Award Number: 13-C-AJFE-PU
- Period of Performance: July 14, 2014 to August 15, 2019
- Task(s):
  1. **Lead: Tyner; supported by graduate students** – Develop stochastic techno-economic models for relevant pathways and identify key stochastic variables to be modeled for assessing risk in conversion pathways. This work will lead to a capability to compare pathways and their expected economic cost, plus the inherent uncertainty in each pathway.
  2. **Lead: Tyner; supported by Taheripour, Sajedinia, and Malina (Hasselt University)** – Life-cycle analysis (LCA) of alternative jet fuel pathways, in coordination with the International Civil Aviation Organization (ICAO) Committee on Aviation Environmental Protection (CAEP) Alternative Fuels Task Force (AFTF) and Fuels Task Group (FTG). Work with the CAEP/AFTF/FTG LCA group on issues such as system boundaries, induced land-use change (ILUC), LCA methodology, and pathway greenhouse gas (GHG) emissions assessment.
  3. **Lead: Tyner; supported by Taheripour, and Sajedinia** – Develop estimates of emissions associated with land-use change for alternative jet fuels for the ICAO AFTF. This task is closely related to Task #2,
  4. **Lead: Tyner** – **P**rovide support for the other ASCENT universities on analysis of aviation biofuel policy.
  5. **Lead: Tyner** – Provide support for the Farm to Fly initiative as needed.

University Participants: August 16, 2019–September 30, 2019

Purdue University

- PI: Farzad Taheripour, Research Associate Professor
- FAA Award Number: 13-C-AJFE-PU
- Period of Performance: July 14, 2014 to September 30, 2019
- Task(s):

1. **Lead: Farzad Taheripour; supported by Chepeliev and graduate student** – Develop stochastic techno-economic models for relevant pathways and identify key stochastic variables to be modeled for assessing risk in conversion pathways. This work will lead to a capability to compare pathways and their expected economic cost, plus the inherent uncertainty in each pathway.
2. **Lead: Taheripour; supported by Sajedinia, Aguiar, and Malina (Hasselt University)** – LCA of alternative jet fuel pathways, in coordination with ICAO CAEP/FTG. Work with the CAEP/FTG LCA group on issues such as system boundaries, ILUC, LCA methodology, and pathway GHG emissions assessment.
3. **Lead**: **Taheripour; supported by Sajedinia and Aguiar** – Develop estimates of emissions associated with land-use change for alternative jet fuels for the ICAO AFTF. This task is closely related to Task #2,
4. **Lead: Taheripour** - Provide support for the other ASCENT universities on analysis of alternative jet fuel policy.

Project Funding Level

- Amendment 3: $250,000
- Amendment 6: $110,000
- Amendment 10: $230,000
- Amendment 15: $373,750
- Amendment 19: $400,000
- Amendment 29: $400,000

Current cost sharing for this project year was from Oliver Wyman.

Investigation Team

Wallace E. Tyner: PI until August 15, 2019, James and Lois Ackerman Professor, Purdue University
Farzad Taheripour: PI since August 16, 2019, Research Associate Professor, Purdue University; involved in several aspects of the project, particularly LCA and land-use change
Xin Zhao: PhD student, Purdue University (graduated and left Purdue); stochastic techno-economic analysis (TEA) and Global Trade Analysis Project (GTAP) ILUC analysis
EhsanReza Sajedinia: PhD student, Purdue University; stochastic TEA and GTAP ILUC analysis
Jeremiah Stevens: MS student, Purdue University (graduated December 2019 and will continue to work for the project as a consultant); stochastic TEA
Maksym Chepeliev: PhD Research Associate, GTAP Center, Purdue University (collaborates part time in the project)
Angel H. Aguiar: PhD Research Associate, GTAP Center, Purdue University (collaborates part time in the project)
Note: Wallace E. Tyner passed away August 17, 2019

Project Overview

This project has five main components. First is the advancement of stochastic TEA for aviation biofuel pathways. Second is LCA and production-potential analysis of alternative jet fuel pathways in coordination with ICAO/AFTF/FTG. The third component also involves working with ICAO/AFTF/FTG, specifically on estimating the emissions associated with land-use change for alternative jet fuels. The fourth component is to provide support for the policy subgroup in AFTF/FTG and to bridge the existing TEA for alternative jet fuels with partial and general equilibrium economic models to develop alternative scenarios for including alternative jet fuels in the mixed fuel used by the industry and to provide policy guidelines to facilitate expansion of the use of sustainable aviation fuels. The fifth component is providing support for Farm to Fly 2.0, a collaboration between government and industry to enable commercially viable, sustainable alternative jet fuel supply chains in the United States at the state and regional levels that are able to support the goals of an alternative jet fuel production capacity of 1 billion gallons and use by 2019. To support this effort, Purdue provides necessary analytical support in this process.

Task 1 - Develop Stochastic Technoeconomic Models for Relevant Pathways and Identify Key Stochastic Variables for Assessing Risk in Conversion Pathways

Purdue University

Objective(s)
Develop stochastic techno-economic models for relevant pathways and identify key stochastic variables to be modeled for assessing risk in conversion pathways. This work will lead to a capability of comparing pathways and their expected economic cost, plus the inherent uncertainty in each pathway.

Research Approach
For each fuel pathway being evaluated, we developed a stochastic model covering the entire pathway, to allow for use in both TEA and LCA. Over this period, we evaluated alcohol-to-jet and catalytic hydrothermolysis processes. We have also developed some new approaches to stochastic TEA.

Milestone(s)
We developed a new a stochastic TEA for a plant designed to use catalytic hydrothermolysis technology to produce renewable diesel fuel, renewable jet fuel, and renewable naphtha from pennycress oilseed. Beyond the standard stochastic practices, this TEA takes uncertainty in biofuel policies into account and highlights the existing policies that can be altered to support production of alternative jet fuels. This research shows that with proper policies in place, producing alternative jet fuels could be commercially viable in the near future. This research has been fully and successfully conducted, and we continue to publish the related results.

Beyond the TEAs, we are now collecting and reviewing the existing TEAs on alternative jet fuels to summarize and synthesize their findings, advantages, and limitations. The results of this work will help us bridge the TEA approach with a modeling framework that aims to develop a supply schedule for alternative jet fuels. We developed a template to collect information from the existing TEAs, and we are in the process of filling in this template. We collected data from the literature and the ASCENT experiments and are awaiting information from the MIT TEA cases.

Major Accomplishments
See the Publications section below.

Publications
Written Reports
Two papers are under development from the TEA of pennycress to jet fuel:

1. Stevens, J., Taheripour, F., & Tyner, W.E. A stochastic techno-economic analysis of aviation biofuel production from pennycress oilseed.
2. Stevens, J., Taheripour, F., & Tyner, W.E. Policy recommendations to expand production of aviation biofuels: lessons from a TEA.

Outreach Efforts
Tyner attended a meeting of the Civil Aviation Alternative Fuels Initiative (CAAFI) and made presentations on the economic availability of feedstock for alternative jet fuels. The meeting was in Washington, DC on December 3–7, 2018.

Awards
None.

Student Involvement
Jeremiah Stevens: MS student, Purdue University; graduated in December 2019 and will collaborate with the project until August 2020

Plans for Next Period
We plan to continue the work on the case of producing alternative jet fuels from pennycress oilseed for the following reasons, with the aim of publishing the results of this research. We will repeat the new stochastic TEA method in analysis of the case of carinata to determine the sensitivity of this approach with respect to feedstock. We will study the existing TEAs to summarize and synthesize their findings, advantages, and limitations, and will use them to develop an aviation supply function. Finally, the review of the existing TEAs will help us determine the gaps in this research area and define priorities for future research in this field.

Task 2 - LCA of Alternative Jet Fuel Pathways in Coordination with ICAO-AFTF-FTG

Purdue University

Objective(s)

- Provide required data and analysis to support the low-land-use-change risk practices adopted in CAEP
- Provide required data and analysis to support the core LCA group with respect to ILUC for coprocessing of esters and fatty acids in petroleum refineries and other tasks as needed

Research Approach

There are many varied assignments and components in this task. For LCA, working with other team members, we use standard approaches for consequential LCA. For system boundaries, we have investigated the consequences of different approaches to defining system boundaries. For estimating ILUC, we use the GTAP-BIO model and have modified it to improve land allocation and represent more jet fuel pathways. We have developed new data sets to rank countries according to their likely ILUC potentials. We have collaborated with the Technology, Policy, and Production (TPP) subgroup as well.

- Tyner was co-chair of the AFTF/FTG ILUC group.
- Tyner was working with Dr. Brad Saville on low risk for ILUC.
- Tyner was working with the TPP and other subcrops.
- Taheripour will co-chair the FTG ILUC group.
- Taheripour will work with Dr. Brad Saville on low risk for ILUC.
- Taheripour will work with other FTG/TPP and other subgroups

Milestone(s)

Tyner participated in the FTG1 meetings in Montreal in May 2019. Taheripour, Chepeliev, and Aguiar participated in the FTG2 meeting in Montreal in September 2019. Tyner and Taheripour have been involved in many tasks and document-preparation activities for the meetings. They responded to other subgroups' requests for help and collaboration. They led the efforts on ILUC modeling efforts and the ILUC-related tasks associated with other subgroups. We developed a framework to examine regional ILUC and to rank countries according their land-use-change determinants. We collected data on land-use-change determinants and developed a primary analysis.

Major Accomplishments

Helped design the next-step properties of the TPP subgroups.

Publications

See the list for Task #3.

Outreach Efforts

Taheripour attended the CRC meeting and made a presentation on regional land-use-change values. The meeting was in Argonne National Laboratory, Lemont, IL on October 15–17, 2019.
Taheripour attended the ASCENT Advisory Group Meeting and made a presentation on limiting deforestation from palm oil in Malaysia and Indonesia. The meeting was in Washington, DC on October 22–23, 2019.

Awards

None.

Student Involvement

EhsanReza Sajedinia: PhD student, Purdue University.

Plans for Next Period

- We will continue to support TPP, LCA, and other subgroups,
- See Plans for Next Period for Task 3.

Task 3 - Develop Estimates of Emissions Associated With Land-Use Change for Alternative Jet Fuels for the ICAO Alternative Fuels Task Force

Purdue University

Objective(s)

- Compute ILUC emissions of alternative jet fuels for use in CORSIA
- Improve the GTA-BIO model and its database and make proper modifications in the AEZ-EF emissions model
- Define and implement a method to determine regional ILUC values and rank countries according to their land-use-change determinants.

Research Approach

We modify, update, and use the GTAP-BIO model to produce estimates of ILUC for AFTF/FTG. We also collaborate with IIASA and Hugo Valin to evaluate the outcomes of GTAP-BIO and GLOBIOM models. We collect data and develop new approaches to assess issues related to ILUC emissions due to production of alternative jet fuels.

Milestone(s)

We added several new pathways to the GTAP-BIO model. We examined new regional ILUC values. We developed primary analyses to rank countries according to their land-use-change determinants.

Major Accomplishments

Most of the accomplishments under this task are in the form of work progress of ICAO/CAEP/AFTF. Some of the working papers and information papers that we have produced over this period are listed in this section and in the overall publication list at the end of this report.

Publications

Written Reports

Several working papers and information papers have been produced for the AFTF/FTG work. Below, we present only a few items produced in recent months, since August 15, 2019. We have not included reports submitted by late professor Wallace E. Tyner from October 2018 to August 15, 2019.

- CAEP/12-FTG/02-IP/03: Land Use Change Emission Accounting in GLOBIOM and GTAP-BIO. Montreal, September 2019.
- CAEP/12-FTG/02-WP/08: Progress Report from the ILUC Subgroup. Montreal, September 2019.
- CAEP/12-FTG/02-WP/15: ILUC Permanence. Montreal, September 2019.
- CAEP/12-FTG/02-WP/09: Potential Methodology for the Fuel Production Evaluation Task. Montreal, September 2019.
- CAEP/-SG/20191-WP/09: Progress on Development of LCA Values. Johannesburg, December 2019.
- Comments on: CAEP-SG/20194-WP Indonesia Observations on Result of LCA. Johannesburg, December 2019.

In addition to the above reports, the following papers are already published or in press:

- Taheripour, F., & Tyner, W. (in press). US biofuel production and policy: Implications for land use changes in Malaysia and Indonesia. *Biotechnology for Biofuels*.
- Taheripour, F., Zhao, X., Horridge, M., Farrokhi, F., & Tyner, W. (in press). Modeling land use in computable general equilibrium models: preserving physical area of land. *Journal of Global Economic Analyses*.
- Zhao, X., van der Mensbrugghe, D., Keeney, R., & Tyner, W. (2020). Improving the way land use change is handled in economic models. *Economic Modeling*, 84,13-26. https://doi.org/10.1016/j.econmod.2019.03.003

Taheripour also published the following related paper with no reference to FAA support:

- Taheripour, F., Hertel, T., & RamanKutty, N. (2019). Market-mediated responses confound policies to limit deforestation from oil palm expansion in Malaysia and Indonesia. *PNAS*, 1903476116.

Outreach Efforts

Tyner attended a CAAFI meeting and made presentations on ILUC values for alternative jet fuels. The meeting was in Washington, DC on December 3–7, 2018.

Taheripour attended several meetings to present the research outcomes on ILUC values, including the following:

- National Biodiesel Conference & Expo, San Diego, California, January 21–24, 2019
- GTAP 22nd Annual Conference on Global Economic Analysis, University of Warsaw, Warsaw, Poland, June 2019
- 2019 AAEA Annual Meeting, Atlanta, July 2019

Awards
None.

Student Involvement
EhsanReza Sajedinia: PhD student, Purdue University

Plans for Next Period
We will continue working with ICAO on ILUC emission estimates including the following highlights:

- The current model uses a database representing the world economy in 2011. We plan to update this database to 2014. This is a major task and new development.
- We will work to develop regional ILUC values.
- We are in the process of developing a method to rank countries according to their land-use-change-determinant factors.
- We are now working on values for direct land-use change.

Task 4 - Provide Support for the Other ASCENT Universities on Alternative Jet Fuel Policy Analysis
Purdue University

Objective
Provide support for the other ASCENT universities on alternative jet fuel policy analysis.

Research Approach
We are developing spreadsheet models of various pathways incorporating risk analysis. The output of the risk analysis is the distribution of net present value, the internal rate of return, and the probability that the investment will lose money. Being able to provide a distribution of financial outputs is immensely valuable to private-sector investors and other parties. The analysis outputs can also be used to help target future research to areas in which the research outcomes could be expected to have high payoff. We have been working with WSU on stochastic TEA and expect in the next year to work with WSU, PSU, and universities in Hawaii and Tennessee on stochastic TEA and risk analysis. More recently, we made several efforts to harmonize the TEA across the active research groups on TEA for alternative jet fuels, including their components and underlying assumptions. We have developed a new approach to take uncertainty in biofuel policies into account.

Any of the stochastic TEAs can be used with policy overlays to conduct evaluations of alternative policy options. The stochastic models can also be used to examine the effects of alternative feedstock contracting mechanisms for feedstocks without effective hedging alternatives available, such as the cellulosic feedstocks or new lipids such as those from pennycress oilseed. We have worked with the ICAO/AFTF policy subgroup to develop such policy case studies.

Milestone(s)
See Task 1.

Major Accomplishments
See Task 1.

Publications
N/A

Outreach Efforts
N/A

Awards
None.

Student Involvement
Jeremiah Stevens: MS student, Purdue University; graduated in December 2019 and will collaborate with the project until August 2020

Plans for Next Period
In collaboration with ASCENT, we are collecting and reviewing the exiting TEAs on alternative jet fuels and their feedstocks. This effort will help us evaluate what we have learned to date and what we need to accomplish in the future. It also will help us develop a supply schedule for alternative jet fuels by feedstock and conversion technology, and to define and outline alternative policies that can be used to encourage expansion of alternative jet fuels.

Task 5 - Provide Support for the Farm to Fly Initiative as Needed
Purdue University

Objective
Provide support for the Farm to Fly initiative as needed.

Research Approach
This activity is a general support for other initiatives. Our main role is to consult with researchers involved in other projects and activities and provide assistance as needed.

Milestone(s)
There has been little activity under this task in this reporting period.

Major Accomplishments
N/A

Publications
N/A

Outreach Efforts
N/A

Awards
None.

Student Involvement
None.

Plans for Next Period
We will continue to be available to support other projects and universities as needed in regional and national analysis related to Farm to Fly.

Project 001(D) Alternative Jet Fuel Supply Chain Analysis

The Pennsylvania State University

Project Lead Investigator

Saurabh Bansal
Associate Professor of Supply Chain Management
Department of Supply Chain and Information Systems
The Pennsylvania State University (PSU)
405 Business
University Park, PA 16802
814.863.3727
Sub32@psu.edu

University Participants

The Pennsylvania State University PI(s)

- Saurabh Bansal, Associate Professor of Supply Chain Management
- Lara Fowler, Senior Lecturer, Law School; Assistant Director, Penn State Institutes of Energy and the Environment
- Ekrem Korkut, Law School,
- Gaby Gilbeau (through August 2019), Staff Attorney

The Washington State University

- Kristin Brandt, Staff Engineer

University of Tennessee

- Tim Rials, Associate Dean AgResearch
- Burt English, Professor of Agricultural and Resource Economics

Project Funding Level

FAA Funding: $200,000
Matching, PSU: $200,000
Total Funding: $400,000

Investigation Team

1.3.1 **(Lead: Bansal;** supported by Brandt and English): risk-reward profit sharing modeling for first facilities

1.3.2 **(Lead: Bansal; supported by Brandt and English):** additional quantification of risk and uncertainties in supply chains (foundational part of task above)

1.3.3 **(Lead: Bansal; supported by Brandt and English):** supply chain risk analysis tools for farmer adoption

1.4.1 **(Lead: Fowler; supported by Korkut):** national survey of current and proposed state and federal programs that monetize ecosystem services

1.4.3 **(Lead: Fowler; supported by Korkut):** support in stakeholder engagement efforts

Project Overview

The project focuses on developing a qualitative and quantitative understanding of factors that can help the establishments of biofuel supply chains aimed at supplying alternative jet fuels. Efforts have been made in the past to establish these supply chains. However, many of these efforts have been unsuccessful because of a lack of clarity regarding what incentives stakeholders would require to engage in these supply chains and devote their resources to invest in the facilities required for these supply chains. To this end, the project has two goals:

1. Develop pro forma cash flows that represent the financial status of various participants in biofuel supply chains for alternative jet fuels, and
2. Understand the policy landscape that exists in various parts of the United States to encourage these supply chains and identify further policy initiatives that may be needed.

Task 1.3.1 - Risk-Reward Profit Sharing Modeling for First Facilities

Pennsylvania State University

Objective

Develop a transparent risk-sharing tool to provide all partners with an understanding of the cash flows and risks faced by all supply chain partners.

Research Approach

We first collected a large number of risk sharing tools that have been proposed in the supply chain literature. Subsequently, we narrowed the list down to 9–12 mechanisms. We created an Excel-based framework in which the cash flows of all supply chain partners are modeled by using the numbers from the techno-economic analyses developed by WSU. This framework incorporates the risk sharing mechanisms.

Milestone

We developed the Excel models for four realistic configurations by using data from techno-economic analysis models from WSU.

Major Accomplishments

We developed an Excel-based framework showing the cash flows of four key stakeholders of alternative jet fuel supply chains: farmers, preprocessors, refineries, and airlines. The framework shows various risk sharing contracts that each of the stakeholders can extend to others, as well as the financial burden or opportunity associated with these mechanisms. The framework also shows the government's financial burden of supporting these mechanisms. The framework is developed for four levels of refinery capacities. Overall, this framework can be used as a decision support tool by various stakeholders to determine whether to engage in alternative jet biofuel supply chains and negotiate with each other.

Publications

We anticipate publishing a paper based on combined work from the last year and the coming year.

Outreach Efforts

The tool has been discussed at three avenues at the ASCENT enterprise.

Awards

None.

Student Involvement

None.

Plans for Next Period

We intend to run some focus group and laboratory studies to quantify the expected benefit from the tool. We recently ran a pilot study with undergraduate students, but it did not work well. Undergraduate students may not be an optimal study

population, because they may not have the training to understand complex Excel cash flows. We will re-run the study with MBA students in spring 2020.

Task 1.3.2 - Additional Quantification of Risk and Uncertainties in Supply Chains (Foundational Part of Task Above)

Pennsylvania State University

Objective

Develop methods to rely on expert judgments to quantify uncertainties associated with biofuel supply chains.

Research Approach

We developed a new econometric approach to quantify probability distributions of uncertain quantities such as yield or demand when a panel of experts provides judgments regarding the most likely values. This approach exploits the well-known theory of generalized least squares in statistics, for the context in which historical data are available to calibrate expert judgments or when these data are not available.

Milestone(s)

We have described the method in two manuscripts provided as attachments with the annual report. In the first manuscript, we develop a two-stage procedure to calibrate expert judgements for the distribution of biofuel uncertainties, such as the uncertain yield of new varieties of oil seeds, demand, or selling price. In the first step of the procedure, we calibrate the expert judgements by using historical data. Specifically, we use prior judgments provided by experts and compare them with actual realizations (such as predicted yield versus actual yield) to determine the frequency with which each expert over- or underestimated the uncertainty, e.g., expert 1 underestimated the yield 60% of the time, but expert 2 underestimated the yield 90% of the time. In the second step, we use this information to determine the optimal way to aggregate the experts' judgments to determine the mean and standard deviation of the probability distributions. In the second manuscript, we develop a new optimization protocol to determine the optimal acreage for growing specific crops, by taking into account the estimated mean and standard deviation as well as incorporating the variability in these estimates.

Major Accomplishments

Theoretical development and a numerical study have demonstrated the promise of this approach.

Publications

One paper has been accepted pending editorial changes. The second paper is finished.

Outreach Efforts

N/A

Awards

None.

Student Involvement

None.

Plans for Next Period

The second paper will be finalized during the period. Any revisions required for the first paper will also be made in the next 1-2 years.

Task 1.3.3 – Supply Chain Risk Analysis Tools for Farmer Adoption

Pennsylvania State University

Objective(s)

Understand farmers' risk preferences over a long duration and how these preferences affect their decisions to grow crops that can support alternative jet fuel supply chains.

Research Approach

We surveyed farmers to understand their risk preferences over extended durations. Specifically, we showed them sample yield ranges over extended periods and asked them to estimate the lowest equivalent guaranteed yield that they would be willing to accept given the uncertain yields. We used these responses for statistical analyses.

Milestone(s)

We have completed the survey and finished a manuscript based on the survey.

Major Accomplishments

We compiled data from 43 farmers in central Pennsylvania regarding their preferences given the uncertain yields from their land. The results quantify the loss of value that farmers attribute to an uncertain yield. The reported results are for both 1-year and 10-year horizons. For the 10-year horizon, we also report results with an initial yield buildup, as is the case with most biofuel crops. The key takeaways from this study are that: (a) farmers' valuation of a new crop decreases acutely as the uncertainty in yield increases, and (b) the initial build-up period of low yields can be a large deterrent to farmers' adopting new crops for the purpose of supporting biofuels.

Publications

The second paper is finished and has been submitted to sponsors.

Outreach Efforts

N/A

Awards

None.

Student Involvement

None.

Plans for Next Period

We plan on submitting a journal article based on the paper during the coming year.

Task 1.4.1 - National Survey of Current and Proposed State and Federal Programs that Monetize Ecosystem Services

Pennsylvania State University

Objective(s)

Conduct a survey and summarize current and proposed state and federal programs to monetize economic systems.

Research Approach

This task builds on and continues the work done under ASCENT Project 01, Task 8.1, which focused on the biomass and water quality benefits to the Chesapeake Bay watershed. Under this task, we examined the biofuel law and policy landscape of the Pacific Northwest and Southeast regions, as well as the state of Hawaii. We also researched federal biofuel law and policy. We have had a change in personnel working on this project. Lara Fowler remains the lead; however, Gaby Gilbeau left the project in August 2018, and Ekrem Korkut joined the project during the fall of 2018.

Milestone(s)

We have captured this research in three region-specific white papers describing the biofuel law and policy incentives, and the ecosystem service drivers for the subregions:

- Project 01A, Tasks 3.1, the Pacific Northwest
- Project 01B, Task 3.2, Hawaii
- Project 01E, the Southeast

Copies of these documents are available online:

- Western U.S. policy paper (with a focus on Washington State): https://psu.box.com/s/l9ektkcr8lk10gjqu93l4jmm9djmnmhf
- Southeast policy paper (with a focus on Tennessee): https://psu.box.com/s/iyeowdfo0447t4ya8dl5md2zu5un48u6
- Hawaii policy paper: https://psu.box.com/s/92a7tl19tpphg69t4ff12t9d4rdshgq1

Major Accomplishments

We have captured this research in three regional white papers describing the biofuel law and policy incentives. In addition, we have researched and are nearly finished with drafting a document summarizing aviation and biofuel at the national level in the United States. We are starting to examine legal and policy drivers from other parts of the world.

Publications

The white papers have been sent to ASCENT leads for review and comment.

After these papers are reviewed for circulation, we anticipate circulating them to ASCENT team members and seeking publication.

Outreach Efforts

An economic model to motivate land use conversion has been demonstrated at Civil Aviation Alternative Fuels Initiative meetings in previous years (that aspect of this task is no longer ongoing). For the law and policy dynamics, Lara Fowler and Gaby Gilbeau (formerly on the project team) provided a presentation to the ASCENT team on March 25, 2019, giving an update on national and regional legal changes.

Awards

None.

Student Involvement

During summer 2019, PSU hosted a Drawdown Scholars Research Experience for Undergraduates focused on reducing greenhouse gas emissions. As part of this project, Lara Fowler and Ekrem Korkut worked with undergraduate scholars who had questions associated with biofuel law and policy, including providing them with the white papers and engaging in discussions.

Starting in the fall of 2019, Ekrem Korkut transitioned from a research assistant to a full-time student at the Penn State School of International Affairs. He has continued to work on the ASCENT project as a part-time research assistant.

Plans for Next Period

Future research will expand on these regional and national overviews to explore law and policy drivers at the national level. This work will continue to expand to a variety of environmental service and credit trading markets and will help support work identified by other ASCENT team members.

Task 1.4.3 - Help Support Stakeholder Engagement Efforts

Pennsylvania State University

Objective

Facilitate dialogue among producers, industry, government, and other affected stakeholders.

Research Approach

Our work under this objective focused on stakeholder engagement and facilitation of effective dialogue to help bridge the gaps among producers, industry, government, and other affected stakeholders. This role supports other team members' needs.

Milestone

These efforts supported the stakeholder engagement efforts led by other teams, including but not limited to the regional partners identified in ASCENT Project 01, Tasks 3.1, 3.2, and 3.3.

Major Accomplishments

While we held initial conversations with partners in Tennessee, the process was delayed because of constraints for the Tennessee partners. We have continued to participate in discussions and calls related to potential stakeholder engagement needs.

Publications

N/A

Outreach Efforts

N/A

Awards

None.

Student Involvement

None.

Plans for Next Period

Future work under this objective will include presenting to the project partners on facilitation skills and tactics. Additional support for regional projects will be offered as needed for facilitation and stakeholder engagement sessions as the regional projects move to the deployment stage.

Project 001(E) Alternative Jet Fuel Supply Chain Analysis

University of Tennessee

Project Lead Investigator

Timothy Rials
Professor and Director
Center for Renewable Carbon
University of Tennessee
2506 Jacob Dr. Knoxville, TN 37996
865-946-1130
trials@utk.edu

University Participants

University of Tennessee

- PI: Burton English, Professor
- FAA Award Number: 11712069
- Period of Performance: October 1, 2018 to September 30, 2019
- Task(s):
  - Task 1.1: Assess and inventory regional forest and agricultural biomass feedstock options
  - Task 1.2: Delineate the sustainability impacts associated with various feedstock choices including land-use effects
  - Task 3: Lay the groundwork for regional deployment and production of lipids and/or biomass in Tennessee and the Southeast United States
  - Task 4: Support biorefinery infrastructure and siting

Project Funding Level

Total 4-year funding/this year's funding
Total Estimated Project Funding: $664,056/$260,000
Total Federal and Non-Federal Funds: $1,328,112/$450,000
Faculty salary was provided by The University of Tennessee, Institute of Agriculture, in support of the project.

Investigation Team

- Tim Rials, Project Director/Principal Investigator (PD/PI)
- Burton English, Co-Principal Investigator (Co-PD/PI)
- Chris Clark, Faculty
- R. Jamey Menard (Tasks 1 and 3), Other Professional
- Brad Wilson (Task 3), Other Professional (geographic information system)
- Kim Jensen, Faculty
- David Hughes, Faculty
- Jim Larson, Faculty
- Edward Yu, Faculty
- Evan Markel (Task 1.1), Graduate Student
- Katryn Pasaribu (Task 1.1), Graduate Student
- Umama Rahman (Task 1.1), Master's Graduate Student
- Bijay Sharma (Task 1.1), Graduate Student
- McKenzie Thomas (Task 3), Master's Graduate Student
- Latif Patwary (Task 1.2), Master's Graduate Student
- Alan Robertson (Tasks 1 and 3), Master's Graduate Student

- Gill MacKenzie (Task 3), Master's Graduate Student

Project Overview

The University of Tennessee will lead the feedstock production (Task 1) component of the project. This component targets the need to assess and inventory regional forest and agricultural biomass feedstock options and delineate the sustainability impacts associated with various feedstock choices, including land-use effects. The University of Tennessee will lead the analysis of national lipid supply availability by using the Policy Analysis System (POLYSYS) model to develop information on the potential impacts and feasibility of using lipids to supply aviation fuel. The team at the University of Tennessee will facilitate regional deployment and production of jet fuel by laying the groundwork and developing a regional proposal for deployment. The team also supports activities in Task 3 by providing information and insights regarding feedstocks, along with potential regional demand centers for aviation fuels and coproducts, and information on current supply chain infrastructure, as required.

Additionally, the University of Tennessee hosted a workshop on sustainable aviation fuels (SAFs). The meeting was held April 24–25, 2019, in Knoxville, Tennessee. More than 50 invited leaders from the region met to discuss critical barriers to increasing the availability of SAF in the Southeast. The group included individuals experienced in the different unit operations that make up the biofuel supply chain, and brought industry, university, and government perspectives to the dialogue.

Major goals included the following:

1. Developing a rotation based oil seed crop scenario and evaluate potential with POLYSYS
2. Developing a database on infrastructure and needs for the Southeast
3. Organizing and convening for a workshop on the alternative jet fuel supply chain for southeastern stakeholders
4. Initiatiang an aviation fuel supply chain study in the Southeast
5. Continuing with sustainability work for both goals 1 and 4

Task 1.1 - Assess and Inventory Regional Forest and Agricultural Biomass Feedstock Options

University of Tennessee

Objective(s)

Because the markets for lignocellulosic biomass (LCB) feedstock, i.e., grasses, short-rotation woody crops, and agricultural residues, are currently not well established, evaluating the feasibility of supplying those LCB feedstocks is important. The opportunity cost of converting the current agricultural lands to LCB feedstock production will be estimated. In addition, the production, harvest, storage, and transportation costs of the feedstocks are included in the assessment. A variety of potential crop and biomass sources will be considered in the feedstock path, including:

- **Oilseed crops:**
  - Mustard/Crambe (*Sinapsis alba/Crambe abyssinicia*)
  - Pennycress (*Thlaspi arvense*)
  - Rapeseed/Canola (*Brassica napus/B. campestris*)
  - Safflower (*Carthamus tinctorius*)
  - Sunflower (*Helianthus spp.*)
  - Soybean (*Glycine max*)
  - Camelina (*Camelina sativa*)
  - Carinata
- **Perennial grasses**:
  - Switchgrass (*Panicum virgatum*)
  - Miscanthus (*Miscanthus sinensis*)
  - Energy cane (*Saccharum complex*)
- **Short-rotation woody crops**:
  - Poplar (*Populus species*)
  - Willow (*Salix species*)
  - Loblolly pine (*Pinus taeda*)
  - Sweetgum (*Liquidambar styraciflua*)

    - Sycamore (*Plantanus occidentalis*)
- **Agricultural residue**:
    - Wheat straw
    - Corn stover
- **Forest residue**:
    - Logging and processing residue

POLYSYS will be used to estimate and assess the supply and availability of these feedstock options at the regional and national levels. This U.S. agricultural sector model forecasts changes in commodity prices and net farm income over time.

County-level estimates of all live total woody biomass, as well as the average annual growth, removal, and mortality, will be obtained from the Forest Inventory and Analysis (FIA) Database. Mill residue data will be obtained from the U.S. Forest Service FIA Timber Product Output data. The ForSEAM model will be used to estimate and predict logging residues. ForSEAM uses U.S. Forest Service FIA data to project timber supply on the basis of the United States Forest Products Model (USFPM) demand projections. Specific tasks related to this objective are outlined below. These supply curves will be placed in POLYSYS, and estimates into the future will be made.

1. Complete the economic viability analysis on switchgrass, short-rotation woody crops, crop residues, forest residues, and cover crops to assist the team with Theme 1.3
2. Assist in modeling of risk-reward profit sharing by providing information from past work on cellulosic supply chains to Pennsylvania State University (PSU)
3. Assist PSU in the National Survey of current and proposed programs that incentivize ecosystem services
4. Finish environmental impact analysis for the aforementioned crops, examining soil, water, greenhouse gas (GHG) emissions and sequestration, and direct land-use change

Research Approach

1. Using an existing model, POLYSYS, the price for a commodity or annual demand for feedstock was exogenously determined and placed into the model. For this year, no analysis was conducted for a model cover crop. Instead, additional work was pursued on last year's model runs by using carinata as a feedstock. The camelina work captured in a thesis will be further developed as a journal article on the findings of the POLYSYS camelina feedstock analysis.
2. The carinata budget developed last year was revisited by using new information received from Florida.
3. The cover crop carinata was added to the list of potential feedstock candidates; we are in the process of developing a fact sheet for this crop.
4. Logging residues in the Southeast United States were examined. ForSEAM output generated for the Billion Ton Study was downscaled to BioFLAME hexagon-shaped supply regions of 5 square miles, and these hardwood and softwood potential feedstock availability streams are being readied for placement in ASCENT 1's Database. Note: These were initially developed at the POLYSYS region level and downscaled with Cropscape.
5. Using internal funds, trial plots were established for the oilseed cover crops pennycress, camelina, carinata, and canola. This procedure was performed to validate the yield estimates that we are using for Tennessee cropping systems.

New Findings

- Carinata has the potential to supply both oil and biomass to the biofuel market in the southern United States. We currently do not know how far north carinata could be grown.

Milestone(s)

- We generated data that have been passed on to the ASCENT 01 database for camelina feedstock.
- The camelina pathway analysis was completed, and an article is being written.

Major Accomplishments

- We provided information to Purdue regarding the pennycress potential (yield and costs) around northeast Indiana and Sioux City, Iowa.
- We ensured that the crushing facility spreadsheet matched ASCENT's current financial assumptions.

Publications
None.

Outreach Efforts
The results have been disseminated to academia through professional conferences. A poster was presented at the Southern Agricultural Economics Association annual meeting. A selected paper was presented at the 2019 Southern Agricultural Economics Association Annual Meeting in Alabama, in February, 2019, which was based mainly on the pro forma financial analysis of the crushing facility for pennycress. A manuscript based on this presentation was submitted to a journal for peer review during the spring/summer of 2019.

English, B.C., Menard, J. R., Trejo-Pech, C., Rahmann, U., & Edward Yu, T. (2018). Initial steps to laying the groundwork for a renewable aviation fuel industry in Tennessee: Economic feasibility and economic impact analysis. Poster presented at the CAAFI annual meeting, Washington, D.C.

English, B.C. & Rials, T. (2018). Feedstock viability and potential economic impacts. Paper presented at the CAAFI annual meeting, Washington, D.C.

Sharma, B. P., Edward Yu, T., English, B.C., & Boyer, C.N. (2018). Welfare analysis of carbon credits to the sustainable aviation fuel sector: A game-theoretic perspective. Poster presented at the CAAFI annual meeting, Washington, D.C.

Trejo-Pech, C.O., Larson, J., English, B., & Yu, T.E. (2019). Return and risk profile of a potential Pennycress processing facility for the aviation industry. Southern Agricultural Economics Association, 51st Annual Meeting Program, Birmingham, AL.

Awards
None.

Student Involvement
In the near future, the pro forma financial analysis spreadsheet will be used either for teaching purposes in a graduate class in agribusiness finance at the University of Tennessee or as a guide or template for graduate students completing capital budgeting analysis for similar crops.

A Master's degree student, Alan Robertson, is working on this project. He has gathered information on carinata and developed an analysis examining this crop as a cover crop feedstock. He will be conducting a feasibility analysis using carinata as a potential feedstock for SAF needs at the Memphis airport. A previous PhD student, Bijay Sharma, currently working at the University of Illinois as a postdoctoral student, worked on completing journal articles reflecting risk.

Plans for Next Period
- Complete cover crop analysis for feedstock costs and yields.
- Develop POLYSYS analysis for camelina, carinata, and winter rye.
- The information gained is available online[1].

[1] https://app.box.com/folder/2689605965

Task 1.2 - Delineate the Sustainability Impacts Associated with Various Feedstock Choices, Including Land-Use Effects

University of Tennessee

Objective(s)

Environmental Sustainability – Regarding environmental sustainability, the impacts associated with LCB feedstock production, such as GHG flux and soil erosion, are estimated on the basis of local geographic characteristics. The GHG flux related to land-use change and LCB feedstock production is analyzed with the POLYSYS model. Different agricultural land-use systems have varying effects on soil erosion or soil loss. The effect of different LCB feedstock production on soil erosion is simulated with the Universal Soil Loss Equation and the 1997 National Resources Inventory database.

Economic/Social Sustainability – The input-output analysis provides estimates of output, employment, and income multipliers, which measure the response of the economy to changes in demand or production. The economic multipliers measure the indirect and induced effects of a change in final demand (direct effects) for a particular industry (for example, the introduction of biorefineries and preprocessing facilities in a region). The indirect effects are the secondary effects or production changes when input demands change because of the effects of the directly affected industry (for example, the construction sector, agriculture producers, and transportation sectors). The induced effects represent the response by all local industries caused by changes in expenditures by households and interinstitutional transfers generated from the direct and indirect effects of the change in final demand. Projections of changes in jobs (job creation), economic activity, taxes, and gross regional domestic product are estimated, providing information on what might be expected if an industry developed within the region. The FT-SPK and ATJ-SPK multipliers have been estimated for the entire 48 contiguous states, and maps have been developed that will allow for estimation of the economic impacts of the direct investment and operating transactions to be reflected in the economic impacts of a given area within the country. The model regions are the 187 Bureau of Economic Analysis regions in the country. This process was completed, and information is available for total industry output, value added, and employment.

Research Approach

Develop impact analysis for economic and environmental parameters

Input-output analysis

By using the revised ASCENT techno-economic analyses (TEAs) developed by Washington State University (WSU), the economic impact information is being revised. We received seven ASCENT conversion technologies and have placed investment and operating costs into IMPLAN industries by using NACS conversion tables. We have completed a crush facility spreadsheet and used it in an oilseed cover crop analysis.

Environmental parameters

We have not made additional progress, but we have made presentations and have two journal articles in review examining welfare analysis linked to carbon credits, by using feedstock locations in Tennessee and airport SAF potential demands. The work is not completed yet.

Consumer preferences

Marketing coproducts could significantly improve the cost effectiveness of biofuel production. We conducted two surveys that examined potential coproducts of a biofuel pathway including biochar and cellulose. We administered a survey through Qualtrics to Tennessee respondents 18 years of age or older in late August 2018. The survey contained several sections, including questions about the level of influence of environmental attributes on purchase decisions for disposable dinnerware; expenditure patterns for disposable dinnerware; demographics including age, education, gender, and household income; and attitudes toward the environment. The purposes of this study are to provide estimates of consumers' preferences for environmental attributes in disposable dinnerware; the probabilities of preferring particular attributes; and the influence of demographics, expenditure patterns, and environmental attitudes on these preferences for environmental attributes in disposable dinnerware.

- The results from this study suggest that consumers are interested in disposable dinnerware with environmental attributes. In particular "no plastic" and "recyclable" are the two attributes most often selected. Results from this study also suggest that consumers view products made from cellulose from crop byproducts similarly to those made from dedicated crops. Interestingly, "no trees" was least often selected, despite its use in labels on some alternative

fiber products in the marketplace. This result may suggest that consumers believe that trees can be grown in a sustainable manner for their cellulose and/or may suggest that consumers might potentially be willing to purchase disposable dinnerware that is blended from tree cellulose along with other cellulose sources (for example, bamboo, bagasse, or wheat straw). However, determining the motivations underlying the responses with regard to how people view growing or harvesting trees for cellulose in disposable dinnerware is beyond the scope of this study.

- Certain market segments have stronger views about environmental attributes in disposable dinnerware (e.g., those with males, in urban areas, with children in the household, with higher income, and with stronger environmental concerns). In addition, prior purchase of alternative fiber products had a positive effect on the environment as well as the probability of choosing a greater number of environmental attributes. This result suggests that consumers who have tried these products before may be repeat customers.
- This study region was limited to Tennessee. To effectively market these emerging products, a national study should be conducted. Furthermore, the study did not include price effects. Additional research might integrate prices along with attributes in a conjoint analysis for a disposable dinnerware product.

Another coproduct, biochar, can serve as an effective soil amendment. Markets for soil amendments with biochar are emerging, but consumer willingness to pay (WTP) is uncertain. This study uses results from a survey of 577 Tennessee home gardeners to estimate the WTP for a potting mix consisting of 25% biochar. The estimated WTP for an 8-quart bag was $8.52, compared with $4.99 for a bag with no biochar. Consumer demographics and attitudes toward both the environment and biofuel production were associated with WTP for the biochar-supplemented potting mix. The results also suggested that the Tennessee gardeners most likely to purchase the biochar mix are younger, spend a higher percentage of their income (up to 2.44%) on gardening supplies, purchase greater amounts of potting mix in a year, and usually purchase this potting mix at garden centers. The results suggest the following:

- Garden centers appear to be a prime retail outlet for biochar-supplemented potting mix.
- Positive correlations between WTP for the biochar mix and the use of organic gardening practices, as well as respondents' views on the importance of biofuels for meeting our nation's future energy needs and the need to take action to combat climate change, suggest that more environmentally concerned gardeners are likely to constitute a target market for biochar-blended potting mix.
- The most common reason for unwillingness to pay a premium for biochar-supplemented potting mix was an inability to afford the biochar mix.
- However, the second most commonly cited reason was that the respondents did not pay much attention to labels on potting mix bags. Thus, differentiating potting mixes supplemented with biochar from conventional potting mixes may pose a hurdle to marketing biochar mixes at higher prices.
- Hence, coupling labeling measures with media messaging (such as on gardening-related television shows and in gardening magazines) highlighting the performance and environmental benefits of blending biochar with potting mix might help to market biochar potting mix blends.

Major Accomplishments

- Completed biochar analysis and estimated demand in Tennessee for biochar-supplemented potting mix
- Obtained ASCENT TEAs and determined the linkage between input and equipment requirements and IMPLAN industrial sectors
- Submitted two journal articles examining the impacts of carbon emissions and credits and the effects on industry feasibility

Publications

Peer-Reviewed Journal Publications

Sharma, B. P., Yu, T.E., English, B.C., Boyer, C., & Larson, J.A. (2019). Impact of government subsidies on a cellulosic biofuel sector with diverse risk preferences toward feedstock uncertainty. (In review). Submitted to Energy Policy.

Sharma, B. P., Yu, T.E., English, B.C., Boyer, C., & Larson, J.A. (2019). Stochastic optimization of cellulosic biofuel supply chain under feedstock yield uncertainty. Energy Procedia, 158: 1009-1014.

Yu, E., Sharma, B.P., English, B.C., & Boyer, C.N. (2019). Economic and environmental analysis of a sustainable jet fuel sector: A game-theoretic perspective. (In review). Submitted to Energy Economics.

Outreach Efforts

Gill, M., Jensen, M., Upendram, S., Labbe, N., & English, B.C. Consumers' willingness to pay for disposable dinnerware molded from wheat straw. Western Agricultural Economics Association Annual Meeting, Coeur d'Alene, Idaho

Gill, M., Jensen, M., Upendram, S., English, B., Labbe, N., Jackson, S., & Lambert, D. (2019). Consumer preferences for environmental attributes in disposable dinnerware. Applied and Agricultural Economics Association, poster presentation, Atlanta, Georgia

Sharma, Bijay P., Yu, T.E., English, B.C., & Boyer, C.N. (2018). Welfare analysis of carbon credits to the sustainable aviation fuel sector: a game-theoretic perspective. CAAFI annual meeting, poster presentation, Washington, DC.

Thomas, M., Jensen, K.L., Clark, C.D., Lambert, D., English, B.C., & Walker, F.R. (2019). Tennessee home gardener preferences for environmental attributes in gardening supplies: a multiple indicators multiple causation analysis. SNA

Yejun, C., Lambert, D., Jensen, K., Clark, C., English, B., & Thomas, M. (2019). Consumer preferences for potting mix product with biochar under the IIA assumption. Western Agricultural Economics Association Annual Meeting, Coeur d'Alene, Idaho

Awards

None.

Student Involvement

Gill MacKenzie, MS student at University of Tennessee
McKenzie Thomas, MS student at University of Tennessee
BiJay Sharma, PhD, postdoctoral associate at University of Illinois

Plans for Next Period

N/A

Task 2 - Support the Lipid-Focused Comprehensive Analyses in ASCENT Project 1 Strategy

University of Tennessee

Objectives

Task 2.1 – Provide national analysis for lipid-based feedstocks

Task 2.2 - Complete supply potential analysis for each lipid fuel pathway, incorporating supply chain costs, preprocessing and conversion facility costs for selected fuel pathways, including social capital and environmental tradeoff components (WSU, PSU)

Task 2.3 - Continue to conduct analysis on new lipid feedstocks, and achieve a one-month turnaround on national analysis, with documentation to follow (this also contributes to Task 2.2)

Research Approach

Same as in Task 1, focused on oilseed analysis.

1. The carinata budget developed last year was revisited by using new information received from Florida.
2. The cover crop carinata was added to the list of potential feedstock candidates; we are in the process of developing a fact sheet for this crop.

Milestone

Initiated a thesis with a chapter focused on carinata.

Major Accomplishments

- The carinata budget has been revised and is under review.

- The Southeast Partnership for Advanced Renewables from Carinata and oilseed U.S. Department of Agriculture projects have been contacted; information has been transferred and compared to our assumptions.

Publications
N/A

Outreach Efforts
N/A

Awards
None.

Student Involvement
None.

Plans for Next Period
Incorporate camelina study, national pennycress study, and carinata analysis into POLYSYS.

Task 3 - Lay the Groundwork for Regional Deployment and Production of Lipids and/or Biomass in Tennessee and the Southeast United States
University of Tennessee

Objective(s)
The University of Tennessee will lead the process of laying the groundwork for supply chain analysis of lipids and/or biomass in Tennessee and the Southeast United States in the following:

- Identifying two potentially viable supply chains to support a specific airport and end user in the Southeast United States, and providing a proposal for a specific (tactical) deployment project
- Delineating sustainability impacts associated with different feedstock choices
- Assessing viable conversion technologies
- Identifying stakeholders and partners
- Convening a workshop for southeastern stakeholders
- Initiating a stochastic analysis of the system
- Evaluating markets for potential coproducts for Task 3 groundwork and deployment projects
- Assisting in the development of social capital spatial analysis to be incorporated in regional analysis

Research Approach
We used similar techniques to those in in Task 1 but focused on the Southeast. We will develop a budget or use information from the modeling efforts in the 2016 Billion Ton Study analysis. We will use BioFLAME, a geographic information system model that has 5-square-mile hexagons defined as supply regions. Information supplied by ForSEAM will be used on logging residue locations through downscaling its estimates from agricultural statistical districts to the supply regions by using the National Agricultural Statistics Service crop supply layer as a means to achieve this goal. The analysis will be run to find where a sufficient supply might be available to provide a sustainable logging residue feedstock.

In examining potential coproduct markets, the research seeks to use the contingent valuation method to determine whether home gardeners would pay a premium for potting mix containing 25% biochar. The method used follows a random utility framework (McFadden, 1974). Responses are structured as a binary variable: respondents choosing the base product being are counted as zeros, and those who choose the 25% biochar product are counted as ones. Respondents are also given the option to select neither product. In the contingent valuation approach used, the prices of the base and biochar-potting mix products are provided to respondents, who may select either or neither product (Hanemann, 1984). The probability of choosing the biochar product is then a function of price, demographics, expenditure patterns, and attitudes. The model is estimated as a logit model, and WTP is calculated by using the estimates.

Additionally, The University of Tennessee Institute of Agriculture convened a workshop in Knoxville, Tennessee on April 24–25, 2019 to address approaches to making SAFs widely available in the Southeast. The invited participants were led through a facilitated brainstorming session to identify barriers restricting progress toward this goal. The group brought to the discussion extensive experience from different operations in the supply chain (from agriculture to airlines), as well as different perspectives from government, academia, and industry. After reviewing the workshop materials, it was decided that analysis was needed on two feedstocks: oilseed cover crop (such as pennycress, camelina, or carinata) and logging or forest residues.

1. Forest and logging residue:
    - From a different project, logging residues were explored, and facility locations were developed for Alabama.
    - The pathway selected for analysis was logging residues delivered directly to ASCENT's fast pyrolysis biorefinery in chipped form.
    - Last year, we found that biorefineries requiring 545,000–720,000 dry tons cannot be located in the Southeast, on the basis of the assumption of a maximum feedstock transportation distance of 70 miles, which was increased to 200 miles; at 150 miles, a capacity of 720,000 dry tons could be located. In a project funded by the Bioenergy Technologies Office, larger facilities were found to be able to be located within less distance if a blended feedstock was used.
    - If collection points were added where preprocessing could be achieved, then five biorefineries could be established at 720,000 dry tons of logging residues/year, if the maximum driving distance was increased to 150 miles.
    - Transportation costs could be reduced if logging residues were blended with a dedicated energy crop such as switchgrass (Figure 1).
2. Completed conversion facility economic feasibility analysis for pennycress/hydroprocessed ester and fatty acid (HEFA) pathway for Nashville airport.
3. Delivered pennycress and crush facility spreadsheets to WSU, Purdue, and PSU for use in other projects and for posting on the ASCENT website.

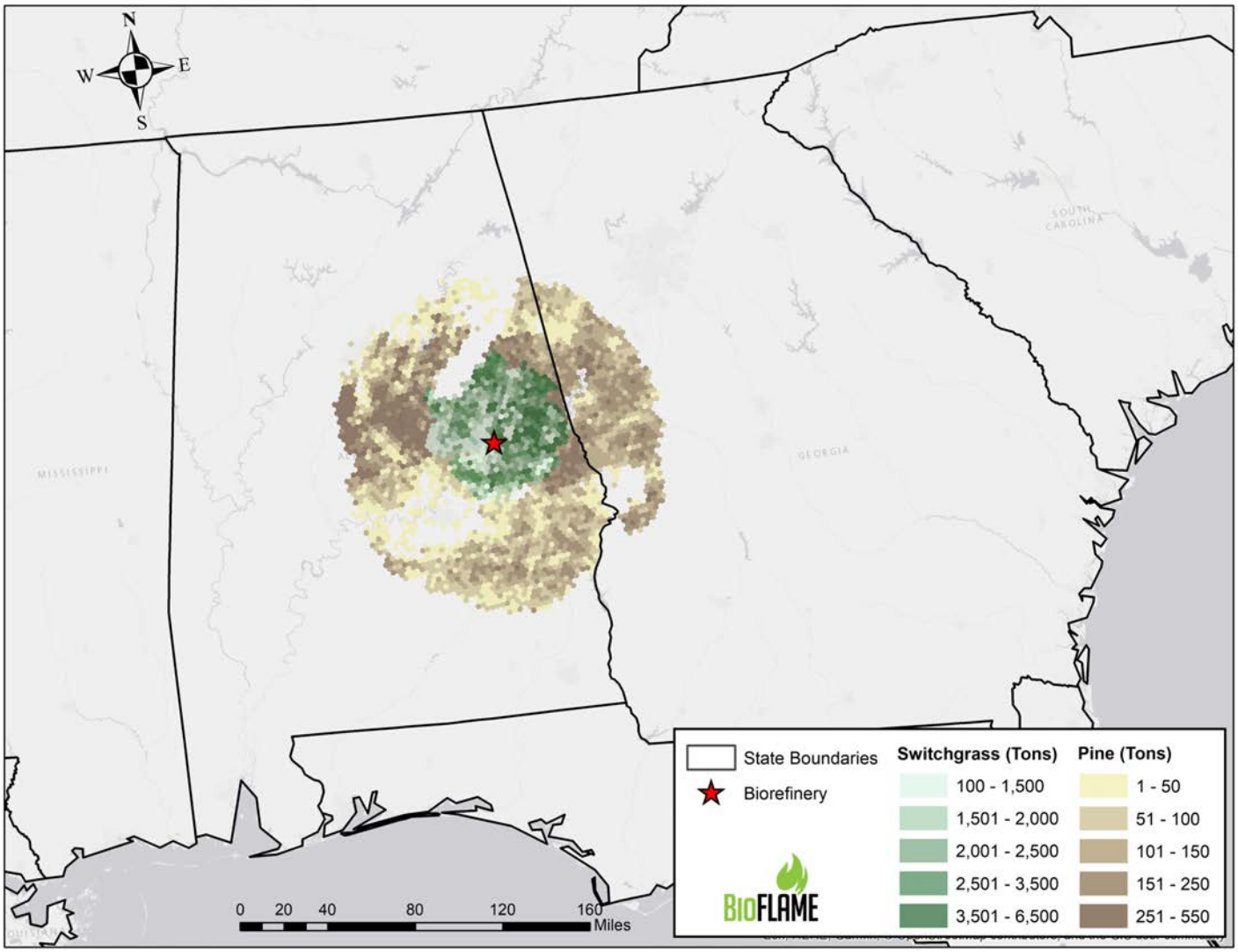

Figure 1. Using a 50–50% blend of pine logging residues with switchgrass a biorefinery reduces transportation needs.

4. Published a Nashville/pennycress article:
    - Use of ASCENT HEFA technology, the crushing facility cash flow spreadsheet, and pennycress as a cover crop feedstock yielded the following findings:
        - Three crush facilities would be required to supply the ASCENT HEFA TEA-based biorefinery.
        - Two of the three would be located in west Tennessee, and one would be located northwest of Nashville.
        - The biorefinery would be located near Nashville, transporting SAF (36 million gallons or 40% of current aviation fuel use) to the airport fuel depot via truck and transporting alternative coproducts to a blending facility (Figure 2).
        - Farmers can produce pennycress within a corn/soybean rotation as a cover crop following corn at a break-even cost of 8.1 cents/pound delivered; the crushing facility, under the assumption of a 12.5% return on investment, can afford to pay 10.5 cents/pound of pennycress seed. If 10.5 cents/pound is paid, the delivery cost to the biorefinery is estimated at $1.09/gallon of unrefined oil, and if

break-even costs are covered, the cost of producing and transporting the oil to the biorefinery is estimated to be $0.80 per gallon.

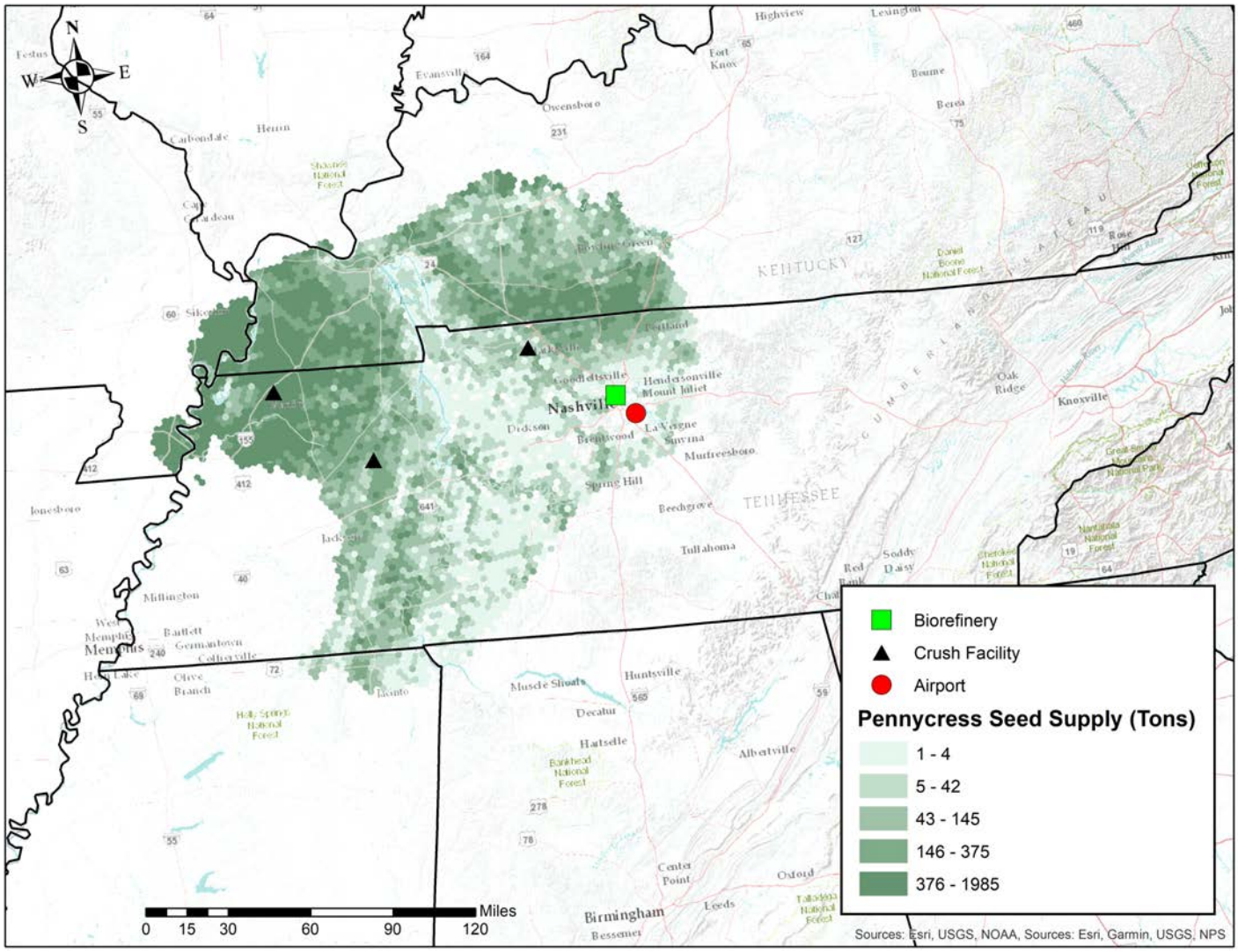

Figure 2. Locations of biorefineries and crush plants to supply nearly 40 million gallons of renewable aviation fuel to the Nashville Airport fuel depot.

5. Identified a number of challenges during the "Sustainable Aviation in the Southeast: Moving from Strategic to Tactical" workshop; pinpointed the following six initial areas hindering broader development of the region's SAF capacity:
    - Create a favorable policy environment: The average carbon intensity of fuels sold in California has declined almost 5% since 2010, thus resulting in a reduction of more than 38 million tons of carbon. A direct result of the low-carbon fuel standard, this finding highlights the potential for well-crafted policy to accelerate regional development.
    - Define sustainability criteria: The fundamental premise of biofuel systems is sustainable production; however, uncertainty exists in the methods and tools available to fully assess specific pathways. Progress is

needed to foster confidence in perceived benefits and to facilitate monetization of ecosystem services (e.g., water quality and carbon sequestration).

- Establish feedstock standards: The Southeast is characterized by a highly fragmented landscape, thus increasing the likelihood of feedstock being produced with an array of crops and biomass sources. This scenario reduces risk and introduces the strategic advantage of blended formulations; however, guidelines are needed to establish required feedstock properties to meet performance targets.
- Increase feedstock readiness level: One opportunity for our rural economy to benefit includes the demand for new, purpose-grown crops on the landscape. Improved management, innovative equipment, and intermediate processing facilities are necessary to advance the feedstock readiness level.
- Expand education programs: The state of the art of SAFs is rapidly progressing. Acceptance of innovative fuel products will require versatile new outreach programs to inform individuals involved in different supply chain operations, as well the flying public.
- Design coproduct strategies: Less than 50 percent of crop biomass is currently used in fuel production. Integrated conversion technologies are needed that fully utilize the individual components of the different biomass sources. Introduction of these new processes will require guidance to identify markets that align demand with potential supply.

Milestone(s)

1. Completed conversion facility economic impact analysis for the HEFA pathway
2. Convened a southeastern stakeholder workshop to collect supply chain input

Major Accomplishments

Completed cover crop analysis for Nashville airport.

Publications

Markel, E., English, B.C., Hellwinckel, C.M., & Menard, J.R. (2019). Potential for Pennycress to support a renewable jet fuel industry. Ecology, Pollution and Environmental Science, SciEnvironm 1:121.

Sharma, B. P., Yu, T.E., English, B.C., Boyer, C., & Larson, J.A. (2019). Stochastic optimization of cellulosic biofuel supply chain under feedstock yield uncertainty. Energy Procedia, 158: 1009-1014.

Trejo-Pech, C., Larson, J.A., English, B.C., & Yu, T.E. (2019). Cost and profitability analysis of a prospective Pennycress to sustainable aviation fuel supply chain in southern USA. Energies, 12, no. 16: 3055.

Outreach Efforts

N/A

Awards

None.

Student Involvement

None.

Plans for Next Period

- Continue to work on logging residues and their potential for meeting SAF needs in the Southeast
- Work on carinata and its potential in meeting the SAF needs at Memphis
- Work on feedstock sustainability issues

To maintain the momentum established during the workshop, six of the top barriers were selected as near-term targets for the alliance to address. The barriers, along with individuals who expressed interest in supporting the effort, are summarized below. The individual teams will work to better define the barriers and develop strategic approaches to reduce the challenges that they present. Regular web meetings will be hosted to facilitate the discussion.

Addressing the Need for Consistent Policy

- Rodney Hadley
- Valerie Thomas
- Charles Etter
- Dave Meyer
- Nate Brown

Addressing Poorly Understood Sustainability Criteria

- Rodney Hadley
- Valerie Thomas
- Jesse Nikkel
- Dave Meyer
- Tim Theiss

Advancing the Need for Outreach and Education

- Rodney Hadley
- Charles Etter
- Christina Sanders

Lack of Co-Product Strategy

- Gerald Tuskan
- Niki Labbé
- Nour Abdoulmoumine
- Dave Lanning
- Richard Molsbee
- Phil Weathers

Addressing Low Feedstock Readiness Level

- Burt English
- Niki Labbé
- Nour Abdoulmoumine
- Dave Meyer
- Dave Lanning
- Randy Rousseau
- Gerald Tuskan

Task 4 - Support Biorefinery Infrastructure and Siting

Washington State University

Objective(s)

The University of Tennessee team will play a supporting role in this task. Several models are available to contribute to the effort, including BioSAT (which is currently available for the 33 eastern states) and BioFLAME (whose geographic scope we hope to expand from its current Southeast U.S. regional focus to the contiguous 48 states).

Research Approach

- Provide feedstock information (location, price, and quantity) to the ASCENT Database
- Contact WSU for ASCENT conversion technologies
- Provide pennycress feedstock information to VOLPE and save it to shared folders available to all ASCENT Project 001 researchers
- Work with WSU on developing a TEA for the crush facility

Milestone(s)

- WSU provided additional TEAs for economic indicator development.
- Economic indicators were developed for those additional technologies, and existing indicators are being updated with the latest IMPLAN data.

Major Accomplishments

We reviewed current financial assumptions developed by Purdue and WSU and used them in our ASCENT analyses.

Publications

N/A

Outreach Efforts

N/A

Awards

None.

Student Involvement

None.

Plans for Next Period

- Complete the TEA for the crush facility and compare solvent-based and mechanical-based crush facilities
- Develop risk analysis around the oilseed pathway for Nashville
- Survey producers in a seven-state area regarding willingness to grow oilseed cover crops
- Explore oilseed/cover crop potential around the Memphis airport
- In June, collect information on oilseed plots and confirm current yield estimates used in the analysis

Project 001(F) Alternative Jet Fuel Supply Chain Analysis

Massachusetts Institute of Technology

Project Lead Investigator

PI: Steven R. H. Barrett
Raymond L. Bisplinghoff Professor of Aeronautics and Astronautics
Director, Laboratory for Aviation and the Environment
Massachusetts Institute of Technology
77 Massachusetts Ave, Building 33-322, Cambridge, MA 02139
+1 (617) 253-2727
sbarrett@mit.edu

Co-PI: Dr. Mark D. Staples
Research Scientist
Laboratory for Aviation and the Environment
Massachusetts Institute of Technology
77 Massachusetts Ave, Building 33-322, Cambridge, MA 02139
+1 (617) 253-7422
mstaples@mit.edu

University Participants

Massachusetts Institute of Technology

- P.I.: Professor Steven R. H. Barrett
- FAA award number: 13-C-AJFE-MIT, amendment nos. 003, 012, 016, 028, 033, 040, 048, and 055
- Period of Performance: August 1, 2014 to April 30, 2020 (via no-cost extension)
- Tasks (tasks listed here are for the reporting period, October 1, 2018 to September 31, 2019):
    1. Support U.S. participation in the International Civil Aviation Organization (ICAO) Committee on Aviation Environmental Protection (CAEP) by calculating default core life-cycle greenhouse gas (GHG) emissions associated with alternative jet fuel (AJF) use under the Carbon Offsetting and Reduction Scheme for International Aviation (CORSIA);
    2. Support U.S. participation in ICAO CAEP by providing guidance on the economic impacts of potential policies on AJF financial viability;
    3. Support U.S. participation in ICAO CAEP by developing tools and resources to assess the ramp-up of AJF production under CORSIA;
    4. Carry out environmental and economic assessment of co-processing of renewable lipids in petroleum refineries;
    5. Support coordination across all A01 universities' work on AJF supply-chain analyses.

Hasselt University (subaward from MIT)

- P.I.: Robert Malina
- Period of Performance: August 1, 2014 to April 30, 2020 (via no-cost extension)
- Tasks (relevant only to the reporting period, October 1, 2018 to September 31, 2019):
    1. Support U.S. participation in ICAO CAEP by calculating default core life-cycle GHG emissions associated with AJF use under CORSIA;
    2. Support U.S. participation in ICAO by providing guidance to CAEP on the economic effects of potential policies on AJF financial viability;
    3. Support U.S. participation in ICAO by developing tools and resources to assess the ramp-up of AJF production under CORSIA.

Project Funding Level

$2,235,000 FAA funding and $2,235,000 matching funds. Sources of match are approximately $388,000 from Massachusetts Institute of Technology (MIT), plus third-party in-kind contributions of $809,000 from Byogy Renewables, Inc. and $1,038,000 from Oliver Wyman Group.

Investigation Team

Principal Investigator: Prof. Steven Barrett (MIT) (all MIT tasks)
Co-Principal Investigator: Dr. Mark Staples (MIT) (all MIT tasks)
Co-Investigators: Dr. Raymond Speth (MIT, Tasks 1 and 4) and Dr. Florian Allroggen (MIT, Tasks 2 and 4))
Graduate Research Assistants: Juju Wang (MIT, Tasks 1, 2, and 5), Uyiosa Oriakhi (MIT, Tasks 1 and 4), and Tae Joong Park (MIT, Task 4)

Part of the research will be conducted through a subaward with Hasselt University (Belgium), led by Prof. Robert Malina, and Hasselt University post-doctoral researcher Hakan Olcay.

Project Overview

The overall objectives of ASCENT Project 1 for the reporting period were to derive information on regional supply chains for creating scenarios for future AJF production, to identify the key supply-chain-related obstacles that must be overcome for commercial-scale production of AJF in the near term, and to achieve large-scale replacement of conventional jet fuel with AJF in the longer term.

According to these overall objectives, MIT's work under ASCENT Project 1 during the assessment year (AY) 2018–2019 (from October 1, 2018 to September 31,2019) focused on the following: (a) participation in ICAO CAEP to calculate default LCA GHG-emission values associated with AJF use under CORSIA; providing quantitative guidance to CAEP on (b) the economic impacts of potential AJF policies and (c) the effect of policy options, including CORSIA, on AJF production ramp-up; (d) quantification of the life-cycle GHG emissions and costs of production of AJF from the co-processing of renewable lipids with petroleum; and (5) providing support for coordination of the A01 team.

Task 1- Default Core LCA Emission Value Calculation, Documentation, and LCA Methodology Development for Use under CORSIA

Massachusetts Institute of Technology and Hasselt University

Objective

The overall objective of this task is to provide support to the FAA in its engagement with the ICAO CAEP Alternative Fuels Task Force (AFTF) (during CAEP/11) and the Fuels Task Group (FTG) (during CAEP/12). The specific focus of the work during this period was to develop the method for appropriate accounting of AJF life-cycle GHG emissions under CORSIA, apply the methods to calculate AJF default core LCA emission values for use under CORSIA, and document this work for communication to the relevant stakeholders.

Research Approach

Introduction

In this reporting period, progress has been made on the work of the CLCA Task Groups of AFTF (CAEP/11) and FTG (CAEP/12). The MIT ASCENT Project 1 team (including a subaward to Hasselt University) has been key in this progress. In particular, the MIT ASCENT team had a leading role on the following tasks: (a) calculating the default core life-cycle emission value for four additional feedstock-to-fuel AJF pathways; (b) writing a technical report documenting the default core LCA analysis performed by AFTF during CAEP/11; (c) developing the reporting requirements for airlines wishing to use "actual" LCA values under CORSIA; (d) defining categories for feedstock classification under CORSIA; and (e) continued development of methods to account for avoided landfill emission credits (LECs) and recycling emission credits (RECs) associated with municipal solid waste (MSW)-derived fuel under CORSIA.

Default core LCA-value calculation

During the reporting period, the MIT ASCENT 1 team performed core LCA analyses for four additional feedstock-to-fuel pathways for inclusion with default values under CORSIA. The analysis procedure and results for each of these pathways are summarized below and documented in detail in CAEP/11-WP/44.

Corn-grain iso-butanol (iBuOH) ATJ

Two independent analyses were compared for this pathway to determine an appropriate default core LCA value: one performed by MIT and the other performed by the European Union Joint Research Centre (JRC). The LCA values from MIT and JRC are compared in Table 1. The presented values reflect initial reconciliation of inconsistencies in the results.

Table 1. Comparison of default core LCA values for corn-grain iBuOH ATJ from MIT and JRC

Conversion technology	Data source	Model	Cultivation	Feedstock transp.	Fermentation and upgrading	Jet fuel transp	Total emissions [gCO_{2e}/MJ]	Midpoint value [gCO_{2e}/MJ]
Corn grain iBuOH ATJ	MIT	GREET	15.9	0.9	38.8	0.4	56.0	55.8
	JRC	E3db	22.5	0.6	32.1	0.3	55.5	

The remaining differences in the LCA data presented here stem from differences in the underlying life-cycle inventories used: E3db assumes a corn-grain yield of 7.1 t/ha, as opposed to a yield of 10.4 t/ha in the Greenhouse Gases, Regulated Emissions, and Energy use in Transportation (GREET) 2017 data; a distiller's dried grains with solubles yield of 0.31 $kg/kg_{corn\ grain}$ in E3db versus 0.28 $kg/kg_{corn\ grain}$ in GREET 2017; and differing feedstock and fuel transportation distances and energy intensities leading to small differences in transportation emissions. Despite the remaining differences, the results from the two models are within the 8.9 grams of carbon dioxide equivalent per megajoule of jet fuel produced (gCO_2e/MJ) definition of a pathway for CORSIA. Therefore, the default core LCA value for the corn-grain iBuOH ATJ pathway was determined to be 55.8 gCO_2e/MJ.

Herbaceous lignocellulosic iBuOH ATJ

Three separate analyses were compared for this pathway to determine an appropriate default core LCA value. MIT modeled the switchgrass (*Panicum virgatum*) and miscanthus (*Miscanthus sinensis*) iBuOH ATJ pathways, and JRC independently modeled the switchgrass iBuOH ATJ pathway. The LCA values from the MIT and JRC analyses, which reflect an initial reconciliation of inconsistencies in results, are compared in Table 2. These results are within the 8.9 gCO_2e/MJ definition of a pathway for CORSIA. Therefore, the default core LCA value for the herbaceous lignocellulosic iBuOH ATJ pathway was determined to be 43.4 gCO_2e/MJ.

Table 2. Comparison of default core LCA results for herbaceous lignocellulosic iBuOH AJT from MIT and JRC

Conversion technology	Data source	Model	Cultivation	Feedstock transp.	Fermentation and upgrading	Jet fuel transp	Total emissions [gCO_{2e}/MJ]	Midpoint value [gCO_{2e}/MJ]
Miscanthus iBuOH ATJ	MIT	GREET	12.5	1.4	27.7	0.4	42.1	43.4
Switchgrass iBuOH ATJ	MIT	GREET	14.9	2.1	27.0	0.4	44.5	
	JRC	E3db	9.9	3.1	31.4	0.3	44.7	

Molasses iBuOH ATJ

Molasses iBuOH ATJ was included as one of the new pathways, as agreed upon by the CAEP Steering Group in March 2018, for which the default core LCA value needed to be calculated by AFTF. This pathway is based on, and consistent with, the sugarcane (*Saccharum officinarum*) iBuOH ATJ pathway, for which default core LCA values had already been agreed upon by AFTF: the fuel production is from sugar-derived iBuOH, which is subsequently converted to drop-in fuel via dehydration,

oligomerization, and hydrotreating. Data from both MIT and JRC were compared for this pathway. The results for the MIT analysis on the molasses iBuOH AJT pathway are shown below in Table 3 and are compared with the data proposed by JRC. These data are within the definition of a pathway of 8.9 gCO_2e/MJ for CORSIA, and therefore the default core LCA value for the molasses iBuOH ATJ pathway was determined to be 27.0 gCO_2e/MJ.

Table 3. Summary of core LCA results for the molasses iBuOH ATJ pathway

Conversion technology	Data source	Model	Cultivation	Feedstock transp.	Fermentation and upgrading	Jet fuel transp	Total emissions [gCO_{2e}/MJ]	Midpoint value [gCO_{2e}/MJ]
Molasses iBuOH ATJ	JRC	E3db	17.7	1.6	7.7	0.3	27.3	27.0
	MIT	GREET	17.8	2.1	6.4	0.3	26.6	

Sugarbeet synthesized iso-parrafin (SIP)

The sugarbeet SIP pathway was modeled in a manner consistent with the sugarcane SIP pathway, as approved by CAEP SG in June 2018. Both processes are based on the fermentation of sugars to hydrocarbon intermediates and subsequent hydrotreating to drop-in jet fuel. The results for the JRC and MIT analyses of the sugarbeet SIP pathway are shown below in Table 4. Several factors contribute to the remaining discrepancy between the data: the two analyses rely on differing data sources for sugarbeet cultivation; MIT assumes a lower sugar yield from sugarbeet, resulting in a 21%-lower energetic yield of farnesene per unit feedstock; and assumptions differ regarding the biogas yield from sugarbeet pulp and electricity and heat co-generation efficiencies.

Despite the differing assumptions, these data are within the definition of a pathway of 8.9 gCO_2e/MJ for CORSIA, and therefore the default core LCA value for the sugarbeet SIP pathway was determined to be 32.4 gCO_2e/MJ.

Table 4. Default core LCA results for sugarbeet SIP

Conversion technology	Data source	Model	Cultivation	Feedstock transp.	SIP production	Jet fuel transp	Total emissions [gCO_{2e}/MJ]	Midpoint value [gCO_{2e}/MJ]
SIP from sugarbeet	JRC	E3db	11.0	0.9	16.6	0.3	28.8	32.4
	MIT	GREET	23.4	1.4	10.8	0.4	36.0	

Summary

During this reporting period, the MIT ASCENT 1 team led the default core LCA analysis for four additional pathways (results summarized in Table 5).

Table 5. Pathway (column 1), data source (column 2), model (column 3), core LCA modeling results (column 4), default core LCA values agreed upon in this reporting period (column 5).

Conversion technology	Data source	Model	Core LCA results [gCO2e/MJ]	Proposed default core LCA value [gCO_{2e}/MJ]
Corn grain iBuOH ATJ	MIT	GREET	56.0	55.8
	JRC	E3db	55.5	
Herbaceous lignocellulosic iBuOH ATJ	MIT	GREET	42.1	43.4
	MIT	GREET	44.5	
	JRC	E3db	44.7	
Molasses iBuOH ATJ	JRC	E3db	27.3	27.0
	MIT	GREET	26.6	
Sugarbeet SIP	JRC	E3db	28.8	32.4
	MIT	GREET	36.0	

Technical report of the default core LCA calculation for CORSIA

To document the default core LCA calculations that occurred during the CAEP/11 cycle, MIT wrote a technical report, which is included as an appendix to Working Paper (WP) 45 from the February 2019 CAEP/11 meeting. This report is publicly available on the ICAO website and will also be available as part of the CAEP/11 report (ICAO Document 10126, 2019).

The purpose of this report is to present the methodology and calculation of default core LCA values for different sustainable alternative fuels (SAF), which can be used to reduce aircraft operators' offsetting obligations under CORSIA.

Methods

Chapter 1 of the report explains the methodology and steps agreed upon by AFTF to calculate default core LCA values to be used under CORSIA. This process includes an attributional approach using energy-based allocation, encompassing the following life-cycle stages:

- feedstock cultivation;
- feedstock harvesting, collection, and recovery;
- feedstock processing and extraction;
- feedstock transportation to processing and fuel-production facilities;
- feedstock-to-fuel conversion processes;
- fuel transportation and distribution; and
- fuel combustion in an aircraft engine.

Waste, residue, and by-product feedstocks are assumed to incur zero GHG emissions during the feedstock-production step of the life cycle; however, emissions generated during their collection, recovery, and extraction, as well as the processing of wastes, residues, and by-products are included.

Emissions are quantified in terms of 100-year global-warming potential (GWP) carbon dioxide equivalent (CO_2e) emissions of CO_2, CH_4 and N_2O from well-to-pump activities, and CO_2 emissions from pump-to-wake fuel combustion. The 100-year GWP was calculated by using the CO_2e values for CH_4 and N_2O from the Intergovernmental Panel on Climate Change (IPCC-AR5) (28 and 265, respectively) (Intergovernmental Panel on Climate Change (IPCC), 2014). Biogenic CO_2 emissions from fuel production or combustion are not included in the calculation, per the IPCC Fifth Assessment Report 100-year global warming potentials (IPCC, 2014). The functional unit selected for the LCA results is gCO_2e/MJ_{jet}, considering combustion in an aircraft

engine using the lower heating value for characterizing fuel energy content. A single global value is used to represent life-cycle emissions from petroleum-derived jet fuel and aviation gasoline: 89.0 gCO_2e/MJ and 95.0 gCO_2e/MJ, respectively.

Each pathway evaluation has been led by a single institution and verified by the other institution. The results of the calculations often diverged, as a result of differences in feedstock yields, process inputs, and other parametric assumptions. Therefore, a procedure was implemented to reach agreement on a single default core LCA value. A threshold equal to 10% of the jet-fuel baseline (i.e., 8.9 gCO_2e/MJ) was defined; if the difference between two analyses for the same pathway fell within this threshold, the midpoint between the results was taken as the default value. If the difference between two analyses was greater than 8.9 gCO_2e/MJ, harmonization of the parametric assumptions was undertaken, or the pathway was split into two to better represent physically different systems.

Analysis

Chapters 2–5 of the technical report document the data sources and results for 26 unique feedstock-to-fuel SAF pathways for which default core LCA values were calculated. The pathways are summarized in Table 6. Because feedstock type influences the results, we highlight classifications for each specific case. A color code is used to describe the feedstock classification: green for residues, wastes, and by-products [R,W,B]; orange for co-products [C]; and blue for main products [M].

Table 6. List of pathways included in the CAEP/11 technical report

Conversion process	Feedstock	Type of feedstock
Fisher-Tropsch (FT)	Agricultural residues	[R]
	Forestry residues	[R]
	Short-rotation woody crops	[M]
	Herbaceous energy crops	[M]
	MSW, 0% NBC	[W]
	MSW, NBC as % of total C	[W]
Hydro-processed esters and fatty acids (HEFA)	Tallow	[B]
	Used cooking oil	[W]
	Palm fatty acid distillate	[B]
	Corn oil	[B]
	Soybean	[M]
	Rapeseed/canola	[M]
	Camelina	[M]
	Palm oil - closed pond	[M]
	Palm oil - open pond	[M]
	Brassica carinata	[M]
Synthesized Iso-Paraffins (SIP)	Sugarcane	[M]
	Sugarbeet	[M]
Iso-butanol Alcohol-to-jet (ATJ)	Sugarcane	[M]
	Agricultural residues	[R]
	Forestry residues	[R]
	Corn grain	[M]
	Herbaceous energy crops	[M]
	Molasses	[C]
Ethanol Alcohol-to-jet (ATJ)	Sugarcane	[M]
	Corn grain	[M]

For a detailed review of the pathway-specific data and analysis associated with each of these pathways, please refer to CAEP/11 WP45, the CAEP/11 report, or the version of the technical report to be posted on the ICAO website[1].

[1] https://www.icao.int/environmental-protection/CORSIA/Documents/CORSIA%20Supporting%20Document_CORSIA%20Eligible%20Fuels_LCA%20Methodology.pdf

Results

Chapter 6 of the technical report documents all default core LCA values for CORSIA calculated during CAEP/11. These results are summarized in Table 7.

Table 7. Summary of default core LCA values calculated during CAEP/11

Conversion process	Feedstock	Default core LCA value [gCO_2e/MJ]
Fisher-Tropsch (FT)	Agricultural residues	7.7
	Forestry residues	8.3
	MSW, 0% NBC	5.2
	MSW, NBC as % of total C	NBC*170.5+5.2
	Short-rotation woody crops	12.2
	Herbaceous energy crops	10.4
Hydro-processed esters and fatty acids (HEFA)	Tallow	22.5
	Used cooking oil	13.9
	Palm fatty acid distillate	20.7
	Corn oil	17.2
	Soybean	40.4
	Rapeseed/canola	47.4
	Camelina	42
	Palm oil - closed pond	37.4
	Palm oil - open pond	60
	Brassica carinata	34.4
Synthesized Iso-Paraffins (SIP)	Sugarcane	32.8
	Sugarbeet	32.4
Iso-butanol alcohol-to-jet (ATJ)	Sugarcane	24.0
	Agricultural residues	29.3
	Forestry residues	23.8
	Corn grain	55.8
	Herbaceous energy crops	43.4
	Molasses	27.0
Ethanol Alcohol-to-jet (ATJ)	Sugarcane	24.1
	Corn grain	65.7

Reporting requirements for 'actual' core LCA values

CORSIA allows airlines to use an actual LCA value if the producer of the fuel can demonstrate, with certification from a sustainability certification scheme (SCS), that their fuel has an LCA value differing from the default core LCA value (a so-called "actual" core LCA value). Under the leadership of the MIT ASCENT 1 team, AFTF agreed to a set of reporting requirements, including chain-of-custody aspects, needed for use of actual LCA values. The details of these requirements are given in CAEP/11-WP/44.

In summary, the use of actual core LCA values under CORSIA requires the economic operator (i.e., the fuel producer or airline) to document all relevant data in a technical report. The report is verified by an accreditation body and is made available on request to the certifying SCS, which then passes it on to ICAO on request. The relevant data include the following:

- GHG emissions by life-cycle step within the scope of certification, subdivided into GHG-emission species and aggregated in CO_2e;
- LCA inventory data by life-cycle step, including all energy and material balances;
- emission factors for calculating GHG emissions associated with energy and material inputs, including sources;
- all relevant feedstock characteristics (e.g., agricultural yield, lower heating value, and moisture content);
- quantities for all final and intermediate products, per total energy yield; and
- in the case of MSW feedstock, all relevant data required for the calculation of LEC and REC according to the MSW-crediting method agreed upon by AFTF.

The SCS is also required to report evidence that the economic operator has accurately followed the method agreed to under CORSIA, using the most recent and scientifically rigorous data available, and that the LCA calculation is complete, accurate,

and transparent. The chain-of-custody system used should also be reported, and all data are to be recorded and reported to ICAO upon request in a format conducive to recalculation and verification.

The agreed-upon reporting method also requires each economic actor along the supply chain to implement a robust, transparent system to track the flow of data. Tracking should occur each time the feedstock or fuel passes through an internal processing step or changes ownership along the supply chain, and the SCS is required to implement procedures enabling verification that the economic operator used an appropriate chain-of-custody system.

Feedstock classification

Under the leadership of the MIT ASCENT 1 team, AFTF was able to reach agreement on a classification of feedstock types to be used under CORSIA. The three broad categories of feedstock include the following:

- Primary and co-products are the main products of a production process. These products have economic value and elastic supply (i.e., evidence of a causal link between feedstock prices and the quantity of feedstock being produced);
- By-products are secondary products with inelastic supply and some economic value.
- Wastes and residues are secondary products with inelastic supply and little to no economic value.

Using these definitions, AFTF further agreed to a set of feedstock definitions in an open positive list of by-products, residues, and waste feedstocks (summarized in Table 8). In addition, AFTF agreed upon a procedure for adding materials to this list (summarized in Figure 1). This work is discussed in detail in CAEP/11-WP/44.

Table 8. Positive list of materials classified as residues, wastes, or by-products

Residues
Agricultural residues:
- Bagasse
- Cobs
- Stover
- Husks
- Manure
- Nut shells
- Stalks
- Straw
Forestry residues:
- Bark
- Branches
- Cutter shavings
- Leaves
- Needles
- Pre- commercial thinnings
- Slash
- Tree tops
Processing residues:
- Crude glycerine
- Forestry processing residues
- Empty palm fruit bunches
- Palm oil mill effluent
- Sewage sludge
- Crude Tall Oil
- Tall oil pitch
Wastes
- Municipal solid waste
- Used cooking oil
By-products
- Palm Fatty Acid Distillate
- Tallow
- Technical corn oil

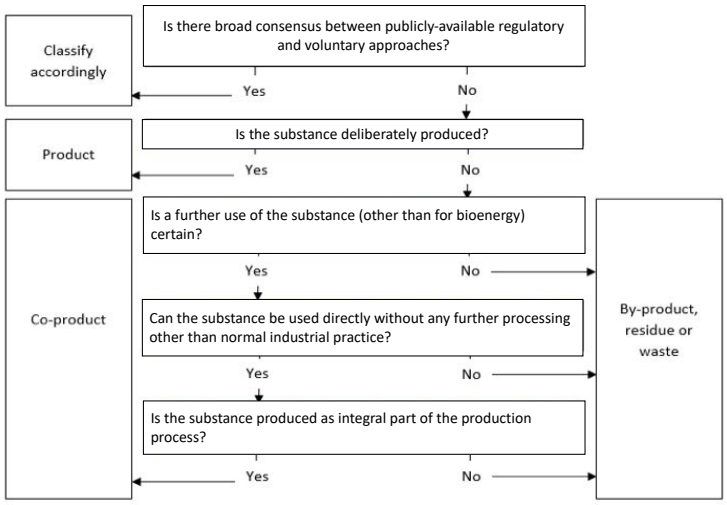

Figure 1. Guidance for inclusion of additional materials in the positive list

Method development for MSW-emission crediting

During this reporting period, the MIT ASCENT 1 team led an AFTF task group on emissions crediting. This small group addressed the following items relevant to MSW-emission credits:

- determining whether MSW-emission credits are consistent with the CAEP/10 LCA methodology;
- refining the LEC and REC methodologies previously agreed upon by AFTF; and
- evaluating the risk of double-counting emission credits, and assessing options to avoid or mitigate the risk.

This work is discussed in greater detail in CAEP/11-WP/46.

Consistency of MSW-emission credits with CAEP/10 LCA methods

The small group determined that emission credits are not consistent with the CAEP/10 LCA methodology, because AFTF had previously agreed on a process-based LCA approach for core LCA-value calculation. Emission credits imply a consequential approach distinct from the attributional approach otherwise adopted by AFTF for core LCA calculations.

To enable the inclusion of emission credits under CORSIA, the emissions-credit small group, under the leadership of the MIT ASCENT 1 team, developed rules for exceptional cases in which emission credits may be assigned to a SAF. Amended text was drafted for paragraph 12 of the CORSIA Implementation Elements (CAEP-SG/20183-WP/14) to allow for the inclusion of emission credits in these exceptional cases. This text, as currently written, strictly limits emission credits to the cases of LEC and REC calculated with the AFTF-approved methods and prohibits the issue of double issuance of emission credits.

Refinement of LEC and REC methods

During this reporting period, the emission-crediting small group (led by the MIT ASCENT 1 team) further developed the LEC and REC methods previously agreed upon by AFTF.

Specifically, the group compared the method developed by AFTF with the United Nations Framework Convention on Climate Change (UNFCCC) (UNFCC, 2018) Clean Development Mechanism (CDM) approach for crediting avoided landfilling emissions. One key reason for differences between the methods is the fundamentally different purposes of the two schemes: the CDM methodology credits ongoing behavior for a specific project, estimating avoided emissions on an annual basis, whereas the AFTF LEC methodology quantifies the emissions avoided over 100 years. The AFTF method follows diversion of MSW feedstock from a landfill and attributes it to the fuel produced from that MSW on a life-cycle basis for a unit of fuel. Other differences arise from technical details: CDM does not account for biogenic CO_2 emitted from, and sequestered in, landfills. The AFTF methodology provides guidance on estimating landfill gas collection to improve accuracy. Furthermore, the CDM includes an "uncertainty factor," which cannot be directly applied to the AFTF method. Although the CDM method could be applied to calculate LEC instead of the approach proposed by AFTF, doing so would result in a time series of LEC emission

credits, some of which could be claimed only in the years following SAF combustion. Adding this temporal index would add substantial complexity in the accounting of SAF to reduce offsetting obligations under CORSIA, including that the time series of reductions would extend past the end of CORSIA in 2035. Therefore, the emission-crediting small group proposed that AFTF continue to use the original methodological approach.

The REC methodology was also determined to need to cover only plastics and metals. This approach is appropriate because commercial operators indicated to AFTF that only plastics and metals are currently recovered, because other materials are more difficult and less lucrative to separate. Furthermore, a case study performed by the small group indicated that, even if glass were recovered, it would compose less than 3% of the total REC.

AFTF agreed on the LEC and REC methods proposed by the small group but noted that the methods should be revisited as more real-world data are collected.

Double-counting, and options to avoid and mitigate the risk of double-counting

Double-counting could occur if activities generating emission credits under CORSIA were to also result in fewer emissions being reported in another scheme, such as UNFCCC. For example, MSW-derived SAF might result in avoided landfill emissions, thus leading to a LEC. However, the state where the landfill is located might also report fewer emissions from the solid-waste-disposal sector to UNFCCC.

During this reporting period, the MIT ASCENT 1 team used the results of the CAEP/10 Fuel Production Assessment (CAEP/10-WP/44) to show that, even under conservative assumptions, the potential magnitude of double-counting of emission reductions under CORSIA is <5% of the projected international aviation CO_2 emissions in 2050. Notably, this calculation does not indicate the risk or likelihood of double-counting but instead indicates the potential magnitude of the phenomenon.

Several approaches to mitigate the risk of LEC/REC double-counting were evaluated by the small group. These included requiring adjustments to national inventories to account for LEC/REC credits claimed under CORSIA (which would avoid double-counting in principle but might be difficult to implement in practice); limiting the total life-cycle emissions value (LSf) value to ≥ 0 gCO_2e/MJ (which would decrease the risk of double-counting to a maximum of 2.6% of the 2050 international aviation CO_2, compared with 4.4% when LSf is allowed to be negative); and defining GHG-reporting requirements for the SCS, to allow national authorities to check for inconsistencies and make the corresponding adjustments noted above. The second of these options to mitigate the risk of double-counting, namely requiring LSf ≥ 0 gCO2e/MJ, was discussed in greater detail by AFTF, and the experts agreed that this practice could serve as an interim measure for mitigating double-counting.

Milestones

The work described above on this task represents the achievement of MS 1 as defined in the AY 2018/2019 Grant Proposal. The culmination of AFTF work on core LCA default-value calculations and emission crediting during CAEP/11 was presented to the Steering Group in February 2019. The MIT ASCENT 1 team wrote WPs 44, 45, and 46, which were presented by the FAA at this meeting, and prepared slide decks to communicate this information. In addition, the status of this work was reviewed at the first meeting of FTG for CAEP/12, during which the MIT ASCENT 1 team facilitated the drafting of a work program to continue to calculate default core LCA values for use in CORSIA during CAEP/12.

Major Accomplishments

The major accomplishments during this period of performance were the calculation of four additional default core LCA values and the writing of a comprehensive technical report documenting the calculation of default core LCA values, undertaken by AFTF during CAEP/11 for use under CORSIA. Furthermore, the MIT ASCENT 1 team led the development and agreement on methods to quantify avoided emissions from landfilling and recycling (LEC and REC), associated with MSW-derived SAFs under CORSIA. This work should enable the inclusion and use of AJF under CORSIA as soon as the policy goes into effect.

Publications

Peer-reviewed journal publications

N/A

Written reports

CAEP/11-WP/44, Core LCA values and methods, February 2019, Montreal, Canada.

CAEP/11-WP/45, Technical report outlining the methodology and calculation of default core life cycle emissions values for sustainable alternative fuels under CORSIA, February 2019, Montreal, Canada.

CAEP/11-WP/46, Emission credits from the production of CORSIA eligible fuels, February 2019, Montreal, Canada.

Outreach Efforts

Progress on these tasks was communicated during weekly briefing calls with the FAA and other U.S. delegation members to AFTF/FTG, numerous AFTF teleconferences between in-person meetings, and the first in-person meeting of FTG in May 2019. In addition, MIT presented its work under Project 1 to ASCENT at the biannual meetings in October 2018 (Alexandria, VA) and April 2019 (Atlanta, GA), in the form of a poster and presentation, respectively.

Awards

None.

Student Involvement

During the reporting period of AY 2018/2019, the MIT graduate students involved in this task were Juju Wang (graduated in the summer of 2019) and Uyiosa Oriakhi.

Plans for Next Period

In the coming year, the MIT ASCENT Project 1 team will continue its work in FTG. Default core LCA values will be calculated and proposed for additional pathways. Prof. Robert Malina from Hasselt University will continue to lead the core LCA Task Group. The work of the core LCA Task Group during CAEP/12 will be summarized in a series of working and information papers presented to FTG, and MIT will take a lead role in drafting papers.

References

CAEP/10-WP/44. (2016). Short-term and long-term alternative jet fuel production and associated GHG emissions reductions. Committee on Aviation Environmental Protection (CAEP). Montreal, Canada.

CAEP/11-WP/45. (2019). Technical report outlining the methodology and calculation of default core life cycle emissions values for sustainable alternative fuels under CORSIA. Montreal, Canada.

ICAO Document 10126. (2019). Report of the Eleventh Meeting of the Committee on Aviation Environmental Protection.

Intergovernmental Panel on Climate Change (IPCC). (2014). Climate Change 2014. Synthesis Report. https://www.ipcc.ch/pdf/assessment-report/ar5/syr/SYR_AR5_FINAL_full.pdf

United Nations Framework Convention on Climate Change (UNFCCC). (2018). AMS-III.G.: Landfill methane recovery – Version 9.0, Clean Development Mechanism. Valid from November 2014. The tool to estimate emissions from the solid waste disposal site is available at https://cdm.unfccc.int/methodologies/PAmethodologies/tools/am-tool-04-v8.0.pdf/history_view

Task 2 - Provide Guidance to CAEP on the Economic Impact of Potential Policies on AJF Financial Viability

Massachusetts Institute of Technology and Hasselt University

Objective

For AY 2018–2019 Task 2, the objective of the funded work was to quantify the impact of different policy options on the economic viability of AJF production, referred to as SAF in the ICAO context. This analysis was used to inform the work of the Policy Guidance Task Group of AFTF, by providing quantitative evidence of the effectiveness of policies that CAEP member states may be considering for supporting the deployment of AJF technologies. The analysis leverages techno-economic work and models that MIT developed previously, including the beginning of this modeling work with the Policy Guidance Task group of AFTF during AY 2017–2018. During AY 2018–2019, the stochastic techno-economic analysis (TEA) policy analysis work of AFTF was concluded for the CAEP/11 cycle.

Research Approach

Introduction

During CAEP/11, the Policy Task Group was tasked with "assessing specific industrial case studies in different world regions to extract lessons learned." Technical experts from MIT, Purdue University, and Hasselt University volunteered to lead this analysis, by performing stochastic TEA of different SAF production pathways and quantifying the impact of potential policies on their economic viability.

The purpose of the stochastic TEA presented here is to assess the impact of policies being considered by some CAEP member states to support the deployment of SAF production technologies. The results quantify the impact of policies on the economic viability of SAF production in terms of two metrics: net present value (NPV) and minimum selling price (MSP). This work took place over the entire CAEP/11 cycle; however, it was concluded and documented in a CAEP WP during the reporting period, which was presented to the CAEP Steering Group in February 2019.

Methods

Six different SAF production pathways were selected as case studies for the stochastic TEA, as shown in Table 9. These were chosen by consensus among the Policy Task Group members to reflect SAF pathways that are close to commercialization in different world regions.

Table 9. Case studies selected for stochastic TEA policy assessment

Process	Feedstock	Region	Company example
Micro FT	Forest residues	North America	Velocys
SIP	Sugarcane	South America	Total-Amyris
HEFA	Waste tallow and yellow grease	North America/ Europe	Altair/Neste
HEFA	Palm oil/palm fatty acid distillates (PFAD)	Asia and Pacific	Pertamina
FT	Municipal solid waste	North America	Fulcrum
ATJ via iBuOH	Corn	North America	Gevo

For evaluation of economic viability, the stochastic TEA model described in Bann et al. (2017) was adapted to reflect the case studies described above. The model builds on a number of previously published studies and modeling efforts (Martinkus et al., 2017; McGarvey and Tyner, 2018; Pearlson et al., 2013; Suresh et al., 2018). The model and assumptions are described in greater detail in Sections 1 and 2 of Appendix A to CAEP/11-WP/50. The results shown here should be considered preliminary, because additional robustness checks are still required before they can be finalized.

Four different policy types were considered in this analysis: input subsidy, modeled as a percentage reduction in the feedstock cost seen by the SAF producer; capital grant, which decreases the fixed capital investment of a new SAF production facility; output-based incentive, which increases the price received by the SAF producer for fuel products; and GHG-emission-reduction-defined incentive, modeled as a revenue stream received by the SAF producer equal to the product of the fuel volume, the life-cycle emission reduction relative to petroleum-derived jet fuel, and the assumed value of emission offsets. These policy types are summarized in Table 10, and the life-cycle emission values used to determine the GHG-emission-reduction-defined incentive are given in Table 11.

Table 10. Policy type to be considered in stochastic TEA policy assessment

Policy type	Implementation in stochastic TEA model
Input subsidy	Reduce feedstock costs seen by fuel producer by subsidy amount
Capital grant	Reduce initial capital cost by grant amount
Output-based incentives	Increase prices received by fuel producer for products by incentive amount
GHG-emission-reduction-defined incentive	Increase prices received by fuel producer for products, as a function of GHG reduction from petroleum fuels

Table 11. LCA values used for GHG-emission-reduction policy

Pathway	GHG emissions (gCO_2e/MJ)
Micro FT (wood residue)	8.3
SIP (sugarcane)	50.6
HEFA (FOG)	22.5
HEFA (palm oil/palm fatty acid distillates)	20.7
FT (MSW)	40
ATJ via iBuOH (corn)	75**

**This will depend on the calculation of a land-use-change emission factor, which remains to be determined.

In addition to the baseline no-policy results, NPV and MSP distributions were generated under these policies for three cases: an equivalent total cost analysis, quantifying the impact of the four policy types at the same total policy cost; a break-even analysis, which identifies the magnitude of each individual policy required to achieve an NPV of zero for each SAF pathway; and specific policy cases reflecting policies similar to those currently existing in the real world.

Preliminary results

The preliminary results of this analysis indicate that, in the baseline no-policy case, the mean MSPs of all six SAF pathways are greater than the current market price for conventional jet fuel of approximately 0.55 USD/L (IATA jet-fuel price monitor, accessed November 2018). The lowest mean MSP is 0.67 USD/L for MSW Fischer–Tropsch (FT) fuel, and the greatest is 1.52 USD/L for wood-residue FT. The baseline results for MSP and NPV are presented in Figure 2 and Figure 3 below. The results show the reference point when no policies have been implemented. The red line shows the median value, the boxes are marked at the 25th and 75th percentiles, and the whiskers extend to the furthest data points not considered outliers. The current selling price of jet fuel of 0.55 USD/L is shown as a blue vertical line.

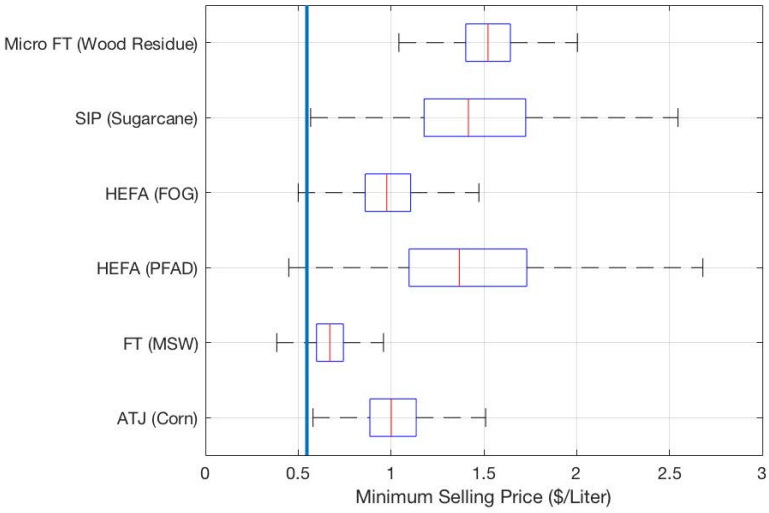

Figure 2. MSPs for the six modeled case studies

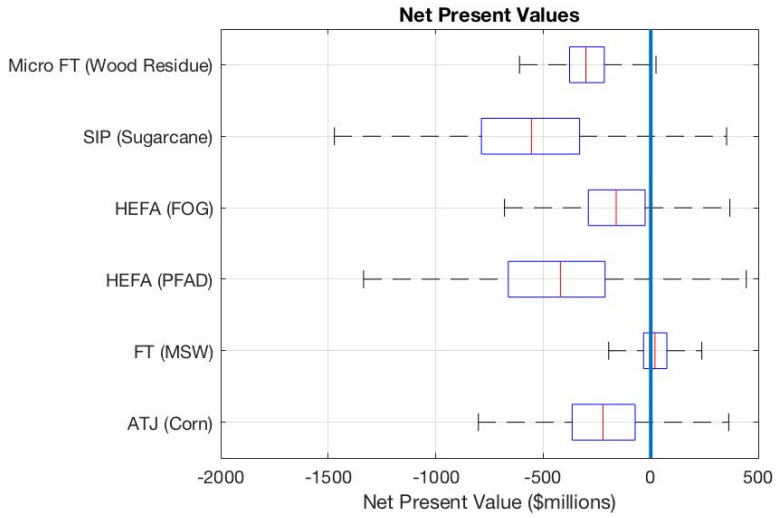

Figure 3. NPVs for the six modeled case studies

The preliminary results of the equivalent policy cost analysis indicate that different policies have different impacts on the mean and variance of SAF MSPs. For example, the capital-grant policy is found to be most effective at reducing the mean MSP at a given total policy cost, because the capital grant decreases the equity and debt required to build the SAF facility, and these benefits are not taxed in the discounted cash-flow model. In contrast, the feedstock input subsidy is shown to be more effective at reducing variance (and therefore risk) in the MSP results at an equivalent total policy cost, because variability in feedstock costs is a significant contributor to uncertainty in MSP. Because the feedstock input-subsidy policy is implemented as a percentage of total feedstock cost, the variability in feedstock costs (and the resultant uncertainty in MSP) is borne in part by the policy.

These findings indicate that policy-makers may wish to select different policy mechanisms depending on their objectives. For example, if reducing the average fuel cost of SAF is the primary policy objective, a capital grant may be a more appropriate policy. In contrast, if reducing fuel price uncertainty is the primary policy objective, a feedstock input subsidy may be a more appropriate policy. The equivalent total policy cost results are discussed in greater detail in Sections 5 and 9 of Appendix A in CAEP/11-WP/50. Example preliminary results for the equivalent policy cost analysis, as applied to the hydroprocessed ester and fatty acid (HEFA) fat, oil, and grease (FOG) pathway, are shown in Table 12.

Table 12. Policy cases for each of the four policy types, and the resulting total policy costs and effects on fuel MSP for the HEFA FOG pathway (mean values with standard deviation in brackets)

HEFA (FOG)			
Policy type	**Output subsidy**		
Policy	0.10 $/L output subsidy	0.25 $/L output subsidy	0.50 $/L output subsidy
Total policy cost ($ million) [standard deviation]	77 [3]	192 [8]	384 [15]
MSP ($/L) [standard deviation]	0.89 [0.19]	0.74 [0.19]	0.49 [0.19]
Policy type	**Input subsidy**		
Policy	14% subsidy on feedstock costs	36% subsidy on feedstock costs	71% subsidy on feedstock costs
Total policy cost ($ million) [standard deviation]	77 [19]	194 [50]	388 [102]
MSP ($/L) [standard deviation]	0.90 [0.16]	0.75 [0.13]	0.50 [0.07]
Policy type	**Capital grant**		
Policy	$77 million capital grant	$192 million capital grant*	$384 million capital grant*
Total policy cost ($ million) [standard deviation]	74 [4]	79 [9]	79 [10]
MSP ($/L) [standard deviation]	0.88 [0.19]	0.87 [0.19]	0.87 [0.19]
Policy type	**GHG-emission reduction policy**		
Policy	CO_2-reduction credit of 46 USD/t	CO_2-reduction credit of 114 USD/t	CO_2-reduction credit of 228 USD/t
Total policy cost ($ million) [standard deviation]	77 [3]	192 [8]	384 [15]
MSP ($/L) [standard deviation]	0.89 [0.19]	0.74 [0.19]	0.49 [0.19]

*The size of the capital grant in these cases is limited by total estimated CapEx: we have not considered capital grants that exceed total CapEx. For example, although the actual equivalent-cost policy to a 0.25 USD/L output subsidy would be a $192 million capital grant, in practice the total capital-grant policy cost is a mean of $79 million in this case. This is the mean estimated total CapEx of the facility, and the capital grant has not been allowed to exceed total CapEx.

The preliminary results of the break-even analysis demonstrate that each of the individual policies could be large enough to achieve an NPV of zero, with the exception of the capital grant, which was limited to being no greater than the total fixed capital investment. The magnitude of the median input subsidy required for breaking even ranges from 39% of feedstock costs for the corn-grain iBuOH ATJ pathway to 207% of feedstock costs for the wood-residue FT pathway, depending on the SAF pathway being considered. The magnitude of the output-based incentive for an NPV of zero ranges from 0.05 USD/L for the MSW FT pathway to 0.77 USD/L for the sugarcane SIP pathway. The magnitude of a GHG-based reduction incentive

(applied to all fuel products) required for an NPV of zero ranges from 106 USD/t_{CO2e} for the HEFA FOG pathway to 658 USD/t_{CO2e} for the corn iBuOH ATJ pathway. These results depend on the SAF-production pathway being considered. Example preliminary results for the break-even GHG-emission-reduction-incentive policy are shown in Figure 4.

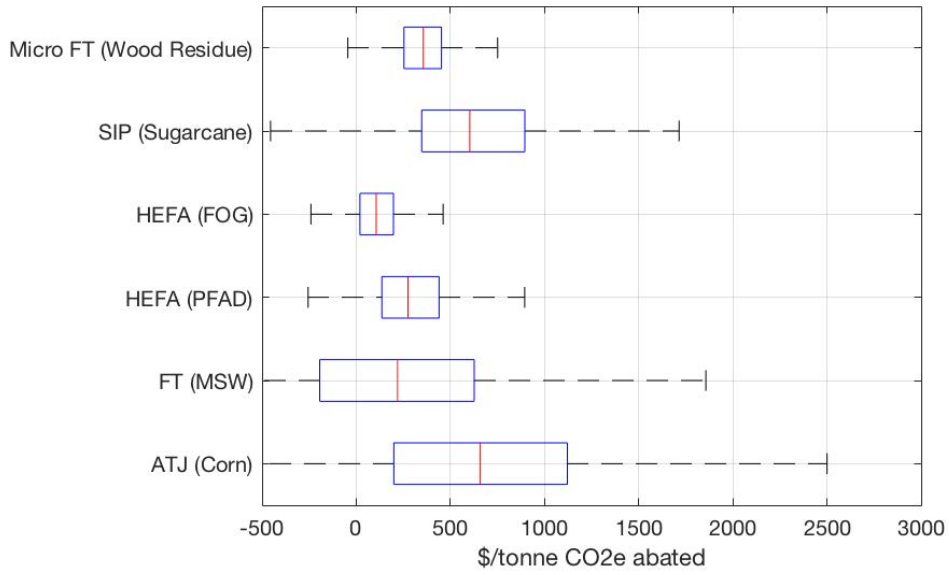

Figure 4. Break-even GHG-emission-reduction-incentive policy applied to all fuels for all pathways

Notably, in the breakeven analyses described above, each policy was considered in isolation. In practice, however, a combination of policy mechanisms from various or overlapping jurisdictions may be necessary to reach economic viability of SAF technologies. Therefore, we also considered a number of policies indicative of renewable-fuel incentives that exist in the real world and may be combined to improve the economic viability of SAF production.

The cases that we considered to be more representative of real-world policies are as follows:

- 27% feedstock cost subsidy (similar to existing feedstock subsidies in the Indonesian context)
- $5 million capital grant (similar to grants awarded by the U.S. Department of Energy and Bioenergy Technologies Office (U.S. DOE and U.S. BETO))
- GHG-reduction credit of 20 USD/t_{CO2e}, ramping up to 40 USD/t_{CO2e} by 2035 (equivalent to the high-range values used by GMTF in the CORSIA cost–benefit analysis)
- Output subsidy of 0.25 USD/L (similar to historical highs for renewable identification number (RIN) prices under the U.S. Renewable Fuels Standard (U.S. Environmental Protection Agency, 2015))

The preliminary results of these cases are presented in Section 7 of Appendix A of CAEP/11-WP/50 and are summarized in Table 13.

Table 13. Real-world policy effects on SAF MSP

Policy case	No policy	27% feedstock cost subsidy	$5 million capital grant	20 USD/tonne$_{CO2}$ reduction credit (40 USD/tonne$_{CO2}$ by 2035)	0.25 USD/L output subsidy	All four policies
Units	**MSP [$/L]**	**ΔMSP [$/L]**	**ΔMSP [$/L]**	**ΔMSP [$/L]**	**ΔMSP [$/L]**	**ΔMSP [$/L]**
Pathway						
Micro FT (wood residue)	1.53	−0.12	−0.01	−0.01	−0.46	−0.60
SIP (sugarcane)	1.49	−0.29	−0.01	−0.03	−0.22	−0.55
HEFA (FOG)	1.00	−0.19	−0.01	−0.01	−0.27	−0.48
HEFA (palm oil/palm fatty acid distillates)	1.46	−0.33	−0.01	−0.02	−0.24	−0.60
FT (MSW)	1.05	0.00	−0.01	−0.00	−0.30	−0.32
ATJ (corn)	1.02	−0.23	−0.01	−0.21	−0.01	−0.46

The preliminary results of this analysis demonstrate that the impact of each policy on the MSP is roughly linear with magnitude, and furthermore that the impacts of each policy type on MSP are independent and can be added together. Therefore, these results are useful to approximate the impacts of any combination of the four policies considered, at different magnitudes from those explicitly quantified here. This is demonstrated in the final column of Table 13: the reduction in MSP when all four policies are considered simultaneously is equal to the sum of the reduction in MSP from each of the individual policies.

Milestone

This analysis was completed and documented in CAEP/11-WP/50 and presented by the FAA to CAEP Steering Group in February 2019. It is also documented in an MIT Master's degree thesis submitted in August 2019. This represents completion of Milestone 2 in the AY 2018/2019 Grant Proposal Narrative.

Major Accomplishments

The MIT ASCENT 1 team drafted and submitted a WP to CAEP, documenting this policy analysis work and concluding the objectives of the Policy Task Group of AFTF during CAEP/11. This work also culminated in the drafting of an MIT Master's thesis, to be submitted in August 2019, and an associated journal publication.

Publications

Peer-reviewed journal publications

Z.J. Wang, M.D. Staples, W.E. Tyner, X. Zhao, R. Malina, S.R.H. Barrett. "Quantitative policy analysis for aviation biofuel production technologies" (*in preparation*)

Written reports

CAEP/11-WP/50, Summary of the work of the policy task group, February 2019, Montreal, Canada.

Outreach Efforts

Progress on these tasks was communicated during weekly briefing calls with the FAA and other U.S. delegation members to AFTF/FTG, numerous AFTF teleconferences between in-person meetings, and the first in-person meeting of FTG in May 2019. In addition, MIT presented its work under Project 1 to ASCENT at the biannual meetings in October 2018 (Alexandria, VA) and April 2019 (Atlanta, GA), in the form of a poster and presentation, respectively. Juju Wang presented the TEA analysis at the ICAO SAF stocktaking event in April 2019.

Awards

None.

Student Involvement

Juju Wang, Master's degree student at MIT's Department of Aeronautics and Astronautics performed most of the analysis, constituting her master's thesis. She graduated in August 2019.

Plans for Next Period

The work is being prepared for submission to a peer-reviewed journal. The complete work, in the form of a Master's degree thesis, will be available on the website of the Lab for Aviation and the Environment at MIT in the fall of 2019. In addition, the models and analysis described here were shared in June 2019 with other ASCENT researchers (from Purdue and Hasselt Universities) to continue to build on this work.

References

Bann, S.J., Malina, R., Staples, M.D., Suresh, P., Pearlson, M., Tyner, W.E., Hileman, J.I., Barrett, S.R.H. (2017). The costs of production of alternative jet fuel: A harmonized stochastic assessment. Bioresource Technology, Volume 227. (http://www.sciencedirect.com/science/article/pii/S0960852416316911)

Martinkus, N., Latta, G., Morgan, T. & Wolcott, M. (2017). A comparison of methodologies for estimating delivered forest residue volume and cost to a wood-based biorefinery. Biomass and Bioenergy, 106: 83-94. doi:10.1016/j.biombioe.2017.08.023 (https://www.sciencedirect.com/science/article/pii/S0961953417302672)

McGarvey, E., Tyner, W.E. (2018). A stochastic techno-economic analysis of the catalytic hydrothermolysis aviation biofuel technology. Biofuels, Bioprod. Biorefin. https://doi.org/10.1002/bbb.1863

Pearlson, M., Wollersheim, C., Hileman, J. (2013). A techno-economic review of hydroprocessed renewable esters and fatty acids for jet fuel production. Biofuels, Bioprod. Biorefin. 7, 89–96. http://dx.doi.org/10.1002/bbb.1378.

Suresh, P., R. Malina, M.D. Staples, S. Lizin, H. Olcay, D. Blazy, M.N. Pearlsonm S.R.H. Barrett, Life cycle greenhouse gas emissions and costs of production of diesel and jet fuel from municipal solid waste. (2018). Environmental Science & Technology, Volume 52. DOI: 10.1021/acs.est.7b04277

U.S. Environmental Protection Agency, 2015. A preliminary assessment of RIN Market Dynamics, RIN Prices, and their effects.

Task 3 - Develop Tools and Resources to Assess AJF Production Ramp-up under CORSIA

Massachusetts Institute of Technology and Hasselt University

Objective

The objective of this task is to develop tools and resources to assess AJF-production ramp-up under various policy options, including CORSIA offsets. This work will be used by the Technology, Production and Policy Task Group of ICAO CAEP FTG during CAEP/12.

Research Approach

At the CAEP Steering Group meeting in February 2019, a work program for FTG was agreed upon by the FTG Rapporteurs and the Secretariat. This is summarized in CAEP/12-FTG/01-WP/02 and includes Task S.09, the fuel-production evaluation. The objective of S.09 is to use data on the current offtake of CORSIA-eligible AJF, existing stochastic TEA models (as described in Section 2), and information from the CAEP/10 AFTF Fuel Production Assessment to assess AJF availability through the year 2035 on the basis of the range of estimated offset prices developed by GMTF.

When drafting the Grant Proposal Narrative for AY 2018/2019, the MIT ASCENT Project 1 team anticipated that this task would focus on the further development and use of a systems dynamics model described by Staples (2017). The strength of a dynamic modeling approach is that it captures systemic feedback occurring over time, such as learning by doing with nascent technologies, and non-linearities in land-use-change emissions due to feedstock demands. However, after the CAEP/12 work program was decided upon, it became clear that greater focus would be placed on the relationship between CORSIA offsets (and other policy incentives) and the availability of AJF volumes. This focus requires detailed economic modeling of the relationship between policy levers and AJF availability, to which a systems dynamics approach is not especially well suited.

Therefore, in preparation for the first meeting of FTG in May 2019, the MIT ASCENT 1 team reviewed and summarized the existing capabilities within AFTF/FTG that would be best suited to carrying out the Task S.09 fuel production evaluation for ICAO CAEP. This review resulted in a proposed plan for execution of this task, as documented in CAEP/12-FTG/01-WP/06 and agreed to by FTG, which uses the following tools and resources:

- Short-term AJF projection estimates developed and maintained by AFTF over the previous two CAEP cycles. This is a database of commercial AJF-production projects in various stages of development. The database will be a valuable resource in estimating the volumes of AJF in the near term as well as the feedstocks from which this fuel will be produced and can serve as a starting point for projections through 2035.

- Data from the CAEP/10 Fuel Production Assessment (FPA), which estimated the potential volume of AJF available through 2050, and the associated reduction in international aviation GHG emissions. The methods used for the FPA require several adaptations. First, the time scale of the CAEP/12 AJF availability analysis is 2035, as compared with the 2050 focus of CAEP/10 FPA. In addition, the nearer-term scope of this analysis would benefit from a narrower feedstock scope, to collect more detailed data on feedstocks likely to be commercialized by 2035. Specifically, the task could emphasize high-resolution data on waste and residue feedstocks, including (but not necessarily limited to) waste FOGs; agricultural residues; forestry residues; and MSW. The availability of these feedstocks as a function of price would be required to eventually estimate the impacts of CORSIA offset prices on AJF availability and economic viability.

- The stochastic TEA models described in Task 2 can be used to evaluate the economic viability of AJF production as a function of feedstock costs, under different CORSIA offset prices. The monetary value of CORSIA for fuel producers can be estimated by combining core LCA and ILUC values from the other task groups of CAEP/11 AFTF and FTG, together with CORSIA offsets estimates from GMTF.

The CAEP/10 FPA was performed at a global scale, and the analysis was led primarily by experts from the United States. However, this CAEP/12 task requires much higher-resolution feedstock data, including feedstock availability as a function of price. Therefore, the MIT ASCENT 1 team focused on world regions in which it has particular expertise, namely the United States and Europe.

Milestone

At the first meeting of the Fuels Task Group (FTG) of ICAO CAEP in May 2019, the MIT ASCENT 1 team presented a summary of tools and resources that can be used for fuel production evaluation and policy guidance to FTG during CAEP/12, as documented in CAEP/12-FTG/01-WP/06. This achievement represents the completion of Milestone 3 in the Grant Proposal Narrative for AY 2018/2019.

Major Accomplishments

The MIT ASCENT 1 team submitted and presented a WP to FTG, documenting the tools and resources available to accomplish Task S.09 fuel production evaluation for the CAEP/12 cycle.

Publications

Peer-reviewed journal publications

T.R. Galligan, M.D. Staples, R.L. Speth, S.R.H. Barrett. "Life cycle greenhouse gas emission reduction potential of aviation biofuels in the US" (*in preparation*)

Written reports

CAEP/12-FTG/01-WP/06, Discussion on the CAEP/12 workplan for the technology and production subgroup, May 2019, Montreal, Canada.

Awards

None.

Student Involvement

None.

Plans for Next Period

In the following period, the MIT team plans to support the development of methods to quantify the impacts of policy and incentives for global AJF production.

References

CAEP/12-FTG/01-WP/02, Work programme, structure and administration. (2019). Montreal, Canada.

CAEP/12-FTG/01-WP/06, Discussion on the CAEP/12 workplan for the technology and production subgroup. (2019). Montreal, Canada.

Staples, M. (2017). Bioenergy and its use to mitigate the climate impact of aviation. PhD Thesis submitted to the Massachusetts Institute of Technology.

Task 4 - Environmental and Economic Assessment of Co-processing Renewable Lipids in Petroleum Refineries

Massachusetts Institute of Technology

Objective

The objective of this task was to carry out an environmental and economic assessment of co-processing of renewable lipids in petroleum refineries. Recently, ASTM approved the addition of as much as 5% v/v lipid feedstock to petroleum-refining units, thus making this pathway important for use under CORSIA.

Research Approach

Introduction

Previous studies have considered the possibility of integrating bio-oils into the hydro-treating (Huber & Corma, 2007; Talmadge et al., 2014; Wang et al., 2012) or fluid catalytic cracking (FCC) (Bianchi et al., 2016; Graca et al., 2009; Schuurman et al., 2013) units at petroleum refineries. However, to date, no bottom-up assessment of the environmental and economic implications of lipid co-processing for AJF production has been performed.

Therefore, the approach taken to accomplish this task was to review the literature for the availability of empirical data on co-processing of biogenic feedstocks in petroleum refineries. The next step was to use the empirical data to quantify the effect of co-processing on life-cycle GHG emissions and production costs.

Methods

A review of the literature on co-processing highlighted several areas for which careful consideration will be required (Bezergianni et al., 2018). For example, in the peer-reviewed literature "co-processing of biogenic feedstocks" refers to both lipid (e.g., vegetable oils, used cooking oil, and waste grease) and bio-oil feedstocks (e.g., pyrolysis oils, or oils from other thermo-chemical processes). Furthermore, these feedstocks may be handled in either the hydro-treater or the fluid catalytic cracking (FCC) units of petroleum refineries. The simplest case is that of hydro-treating (which has less complex reaction kinetics than FCC) of vegetable oils (which are a homogenous, well-characterized feedstock). Therefore, we decided to begin the LCA and TEA analysis of the effects of co-processing there and to build up to more complicated cases.

Several methodological decisions must be considered for the LCA of co-processing. These are best discussed by using a simple example, illustrated in Figure 5. The Δ values indicate the changes in the mass and energy balances of the hydro-treater, from a business-as-usual (BAU) case (in which all Δ values equal 0), because of co-processing.

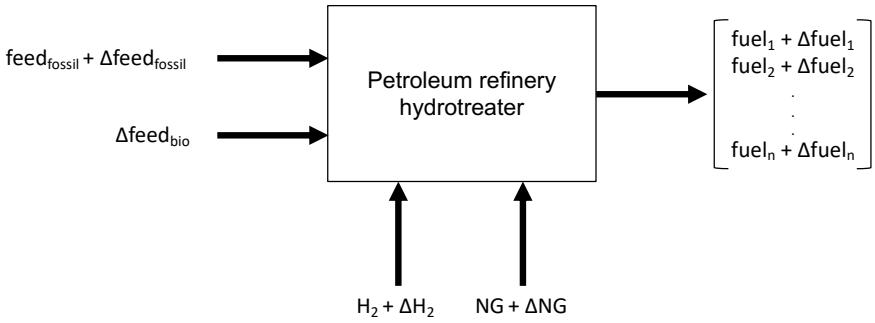

Figure 5. Example of co-processing mass and energy balance

The first methodological challenge is determining which fuel products (fuel$_1$ to fuel$_n$) will ultimately contain the carbon from the biogenic feedstock (feed$_{bio}$), and in what quantity. One means of accomplishing this task is the use of carbon-14 dating to determine the organic fraction of carbon in each fuel cut; however, ongoing testing may be required for each facility performing co-processing. Alternatively, a proportional approach may be used, in which the percentage of biogenic carbon in all fuel products is assumed to be equal to the percentage of biogenic carbon in the sum of the fossil and biogenic feedstock inputs.

A second challenge is deciding how to account for the change in life-cycle emissions due to co-processing. One option is to assume that the life-cycle emissions of all fuel products are affected in equal proportion by co-processing, relative to the BAU case. A second option is assuming that all changes in life-cycle emissions accrue to the biogenic fraction of fuel products (determined by either carbon-14 dating or a proportional approach), with the life-cycle emissions of the fossil fraction remaining the same as in the BAU case.

To illustrate the effects of these methodological decisions, the MIT ASCENT Project 1 team performed first-order analysis on the effects of co-processing on life-cycle emissions and the costs of production inputs. This analysis was based on empirical data from two peer-reviewed studies: Garrain et al. (2014), which considers soybean oil co-processed with mineral diesel in a hydro-treater, and Bezergianni et al. (2014), which considers waste cooking oil (WCO) co-processed with heavy atmospheric gas oil (HAGO) in a hydrotreater. For this analysis, a proportional approach was considered for determining the fate of biogenic carbon, owing to a lack of carbon-14 dating data.

For each data source, two methodological approaches were used. For method 1, the emission impact of co-processing (relative to a BAU case) is attributed to the entire product slate. For method 2, the emission impact is attributed only to the biogenic fraction of the fuel product, with the emissions of the fossil fraction remaining constant. The empirical mass and energy balances from that paper are used to determine the variable quantities referenced in Figure 1. The analysis assumes the BAU life-cycle emissions of the fuel products to be 89.0 gCO_2e/MJ (consistent with the CORSIA baseline) and uses life-cycle emission factors for gaseous hydrogen, natural gas as a stationary fuel in an industrial boiler, soybean oil as a biofuel feedstock, and conventional crude oil from GREET 2018 to calculate the effects on life-cycle emissions (Greenhouse Gases, Regulated Emissions, and Energy use in Transportation (GREET) Model, 2018). Two scenarios were considered: in the first scenario, life-cycle emissions were assumed to be spread across the entire fuel-product slate; and in the second scenario, the life-cycle emission impact on the biogenic fraction was calculated by assuming constant life-cycle emissions for the fossil fraction of 89.0 gCO_2e/MJ.

Unit costs for West Texas Intermediate crude oil, soybean oil, natural gas, hydrogen, and gate prices for U.S. Gulf Coast diesel were used to estimate the effects of co-processing on unit production input cost, relative to a BAU case (Energy Information Agency (EIA), 2019a; Energy Information Agency (EIA), 2019b; Macrotrends, 2019).

Results

LCA results

Under LCA method 1 (spreading emission impacts over the entire product slate), the data from both studies showed relatively moderate reductions in life-cycle emissions relative to the 89.0 gCO_2e/MJ baseline. With the data from Garrain et al. (2014),

the greatest reduction in life-cycle emissions is 1.5 gCO_2e/MJ with a 12.2% soy oil/mineral diesel blend (v/v%). With the data from Bezergianni et al. (2014), the greatest reduction in life-cycle emissions is 14.4 gCO_2e/MJ with a 30% WCO/HAGO blend (v/v%).

Under LCA method 2 (in which emission impacts are attributed only to the biogenic fraction), the data from both studies showed larger emission reductions relative to the 89.0 gCO_2e/MJ baseline, but only for a (relatively small) fraction of the fuel product proportional to the volumetric fraction of biogenic feedstock. With the data from Garrain et al. (2014), the greatest reduction in life-cycle emissions is 16.7 gCO_2e/MJ with a 12.2% soy oil/mineral diesel blend (v/v%). With the data from Bezergianni et al. (2014), the greatest reduction in life cycle emissions is 58.6 gCO_2e/MJ with a 30% WCO/HAGO blend (v/v%).

Several aspects should be noted to properly contextualize these results. First, the ASTM standard currently limits biogenic co-processing to 5% by volume of input feedstock. Therefore, the greatest emission reductions shown here could not be achieved for commercial jet-fuel production, given the current standard. Furthermore, much smaller life-cycle-emission reductions are observed from Garrain et al. (2014) because those data show a negative effect of co-processing on total product yield, and therefore more petroleum feedstock is required per unit of fuel product. This phenomenon is not present in the Bezergianni et al. (2014) data.

The results of this analysis illustrate the potential effects of methodological decisions regarding the LCA of biogenic feedstock co-processing and identify key areas for further analysis. In particular, the results highlight the importance of the effects of co-processing on total fuel yield as a key determinant of life-cycle emissions. Further empirical data are required to clarify these effects.

TEA results

The MIT ASCENT Project 1 team also performed a first-order approximation of the effects of co-processing on process input costs per unit output. With the data from Garrain et al. (2014), each 1% increase in v/v% fraction of biogenic co-processing results an approximate 2% increase in process input costs (in terms of petroleum and biogenic feedstocks, hydrogen, and natural gas). With the Bezergianni et al. (2014) data, each 1% increase in v/v% fraction of biogenic co-processing results in an approximate 0.8% increase in process input costs.

Similarly to the LCA analysis, in this analysis, the primary cause of the discrepancy between data sources is the effect of biogenic co-processing on overall fuel yield: the data from Garrain et al. (2014) show a negative correlation between the biogenic co-processing fraction and overall product yield, whereas the data from Bezergianni et al. (2014) do not show this relationship. The greater effect on process input costs with the Garrain et al. (2014) data than the Bezergianni et al. (2014) data is primarily due to the increased requirement for petroleum feedstock per unit product.

Notably, that this analysis accounts for only the effects of co-processing on variable operating costs, namely the cost of process inputs. As a result of this simplification, for example, the baseline process input costs for the Garrain et al. (2014) data constitute 0.36 $\$/kg_{product}$, whereas the current market price for U.S. Gulf Coast diesel is 0.66 \$/kg. The 0.30 \$/kg difference between the two is due to factors beyond the scope of this screening-level analysis, such as refinery capital and fixed operating costs, taxes, and profit margins.

Milestone

This analysis was documented in CAEP/12-FTG/01-WP/08 presented at the first meeting of ICAO CAEP FTG, in May 2019 in Montreal, Canada. In addition, the data, analysis, and slides summarizing the findings were shared with the FAA and other members of the ASCENT Project 1 team involved in FTG in June 2019. This represents completion of Milestone 5 in the Grant Proposal Narrative for AY 2018/2019.

Major Accomplishments

The major accomplishments from this task include the first-order assessment of the environmental and economic characteristics of co-processing of biogenic lipid feedstocks in a petroleum refinery. These accomplishments resulted in the writing and presentation of CAEP/12-FTG/01-WP/08 at the first meeting of FTG. In addition, the literature review and analysis performed to date, and shared with the FAA and other ASCENT Project 1 team members, will form the basis for further analysis during the CAEP/12 cycle.

Publications

Peer-reviewed journal publications
N/A

Written reports
CAEP/12-FTG/01-WP/08, Discussion on the CAEP/12 workplan for the core LCA subgroup, May 2019, Montreal, Canada.

Outreach Efforts

The work to-date was presented in a working paper at the first meeting of FTG, in May 2019 in Montreal, Canada.

Awards

None.

Student Involvement

The MIT graduate students involved in this task were Uyiosa Oriakhi and Tae Joong Park.

Plans for Next Period

Co-processed AJF fuels will be included under CORSIA during the CAEP/12 cycle. Therefore, a robust LCA method for quantifying their life-cycle emissions should be developed for this purpose. The analysis and resources developed under this task can be leveraged in the next period to contribute to this task in the context of FTG.

References

Bezergianni, S., A. Dimitriadis, O. Kikhtyanin, D. Kubicka. (2018). Refinery co-processing of renewable feeds, Progress in Energy and Combustion Science. 68, DOI: 10.1016/j.pecs.2018.04.002

Bianchi, D; Perego, C; Capuano, F. (2016). Biomass Transformation by Thermo- and Biochemical Processes to Diesel Fuel Intermediates. in Chemicals and Fuels from Bio-Based Building Blocks, F. Cavani, S. Albonetti, F. Basile, and A. Gandini, Eds. Wiley-VCH Verlag GmbH & Co. KGaA.

Energy Information Agency (EIA), US Government, 2019a. *Petroleum & other liquids – Spot prices*, https://www.eia.gov/dnav/pet/pet_pri_spt_s1_d.htm, Accessed 05/06/2019

Energy Information Agency (EIA), US Government, 2019b. *United States natural gas industrial price,* https://www.eia.gov/dnav/ng/hist/n3035us3m.htm, Accessed 05/06/2019

Garrain, D., I. Herrara, Y. Lechon and C. Lago. (2014). Well-to-Tank environmental analysis of a renewable diesel fuel from vegetable oil through co-processing in a hydrotreatment unit, Biomass and Bioenergy. 63, DOI: 10.1016/j.biombioe.2014.01.035

Graça, I; Ramoa Ribeiro, F; Cerqueira, HS; Lam, YL; de Almeida, MBB. (2009). Catalytic cracking of mixtures of model bio-oil compounds and gasoil, Applied Catalysis B: Environmental, vol. 90, no. 3, pp. 556–563.

Greenhouse Gases, Regulated Emissions, and Energy use in Transportation (GREET) Model. (2018). http://greet.es.anl.gov/

Huber, GW; Corma, A. (2007). Synergies between bio- and oil refineries for the production of fuels from biomass. Angew. Chem. Int. Ed. Engl., vol. 46, no. 38, pp. 7184–7201.

Macrotrends. (2019). *Soybean oil prices – 45 year historical chart*, https://www.macrotrends.net/2538/soybean-oil-prices-historical-chart-data

Schuurman, Y; Fogassy, G; Mirodatos, C. (2013). Chapter 10 - Tomorrow's Biofuels: Hybrid Biogasoline by Co-processing in FCC Units, in The Role of Catalysis for the Sustainable Production of Bio-fuels and Bio-chemicals, K. S. Triantafyllidis, A. A. Lappas, and M. Stöcker, Eds. Amsterdam: Elsevier, pp. 321–349.

Talmadge, MS; Baldwin, RM; Biddy, MJ; McCormick, RL; Beckham, GT; Ferguson, GA; Czernik, S; Magrini-Bair, KA; Foust, TD;Metelski, PD; Hetrick, C; Nimlos, MR. (2014). A perspective on oxygenated species in the refinery integration of pyrolysis oil, Green Chemistry, Vol. 16, no. 2, pp. 407–453.

Wang, C; Tian, Z; Wang, L; Xu, R; Liu, Q; Qu, W; Ma, H; Wang, B. (2012). One-step hydrotreatment of vegetable oil to produce high quality diesel-range alkanes, in ChemSusChem, Vol. 5, no. 10, pp. 1974–1983.

Task 5 - Support Coordination of all A01 Universities' Work on AJF Supply-chain Analyses

Massachusetts Institute of Technology

Objective

The objective of this task is to provide support for coordination of all ASCENT Project 1 Universities' work on AJF supply-chain analysis. The sharing of method and results decreases the replication of ASCENT Project 1 Universities' work on similar topics.

Research Approach

The MIT ASCENT Project 1 team performed several functions to accomplish this task.

- Participated in the bi-weekly ASCENT Project 1 coordination teleconferences, which were used as a venue to discuss progress on various grant tasks and learn about the activities of other ASCENT Universities.
- Presented twice at the CAAFI bi-annual general meeting in December 2018 in Washington, DC. One presentation focused on core LCA analysis performed in the context of ICAO CAEP, and the other summarized an analysis to quantify the potential for AJF production in the United States. In addition, the stochastic TEA work performed by the MIT ASCENT Project 1 team was presented in a CAAFI webinar in January 2019.
- Shared a model and code with collaborators at Volpe via Dropbox, as explained during a teleconference on May 31, 2019. This model and code quantify the availability of biomass feedstocks in the United States, and the Volpe team is planning to incorporate these data into the AFTOT model.

Milestone

The MIT ASCENT Project 1 team presented two facets of its work at the CAAFI bi-annual general meeting, in December 2018 in Washington, DC. This represents completion of Milestone 6 in the AY 2018/2019 Grant Proposal Narrative.

Major Accomplishments

The major accomplishments associated with this task include participation in bi-weekly ASCENT Project 1 coordination teleconferences; presentation at the CAAFI BGM in December 2018, and in a CAAFI webinar in January 2019; and sharing of a model and code, which quantify the availability of various bio-energy feedstocks in the contiguous United States, with Volpe team members.

Publications

N/A

Outreach Efforts

Staples, M. Long-term CO_2 emissions reduction potential of aviation biofuels in the US, Presentation at the CAAFI BGM, Washington DC, December 5, 2018.

Staples, M. Life cycle GHG emissions modeling for international policy, Presentation at the CAAFI BGM, Washington DC, December 5, 2018.

Wang, J. Harmonized stochastic techno-economic assessment and policy analysis for alternative fuels, Presentation for the CAAFI SOAP-Jet webinar, January 17, 2019.

Awards

None.

Student Involvement

The MIT graduate student involved in this task was Juju Wang (graduated in the summer of 2019), funded under ASCENT Project 1.

Plans for Next Period

Continued engagement in bi-weekly teleconferences and other events to disseminate MIT's ASCENT Project 1 work.

Project 002 Ambient Conditions Corrections for Non-volatile PM Emissions Measurements

Missouri University of Science and Technology, Aerodyne Research Inc., and Honeywell

Project Lead Investigator

Philip D. Whitefield
Chancellor's Professor of Chemistry
Missouri University of Science and Technology
400 W 11th Street, Rolla, MO 65409
573-341-4420
pwhite@mst.edu

University Participants

Missouri University of Science and Technology

- PI: Philip D. Whitefield, Chancellor's Professor of Chemistry
- FAA Award Number: 13-C-AJFE-MST Amendments: 002, 003, 005, 008, 010, and 012
- Period of Performance: September 18, 2014, to February 28, 2021
- Tasks:
  - Task 1 - Engine-to-engine variability at Honeywell
  - Task 2 - Ground-based non-volatile particulate matter (nvPM) emissions from an IAE V2527-A5 engine burning four different fuel types
  - Task 3 - Re-examination of engine-to-engine particulate matter (PM) emissions' variability using an Aerospace Recommended Practice (ARP) reference sampling and measurement system

Project Funding Level

PROJECT	FUNDING	MATCHING	SOURCE
13-C-AJFE-MST-002	$1,288,836.34	$1,288,836.34	EMPA LETTER
	$284,613.66	$284,613.66	TRANSPORT CANADA
13-C-AJFE-MST-003	$500,000.00	$500,000.00	EMPA LETTER
13-C-AJFE-MST 005	$500,000.00	$500,000.00	EMPA LETTER
13-C-AJFE-MST-008	$579,234.00	$579,234.00	EMPA LETTER
13-C-AJFE-MST-010	$725,500.00	$725,500.00	EMPA LETTER
13-C-AJFE-MST-012	$1,217,221.00	$1,217,221.00	EMPA LETTER

Investigation Team

- Professor Philip Whitefield, Missouri University of Science and Technology
- Dr. Wenyan Liu, research chemist, Missouri University of Science and Technology
- Steven Achterberg, research technician, Missouri University of Science and Technology
- Max Trueblood, research technician, Missouri University of Science and Technology
- Dr. Richard Miake-Lye, subcontractor, Aerodyne Research Inc.
- Dr. Zenhong Yu, subcontractor, Aerodyne Research Inc.
- Rudy Dudebout, subcontractor, Honeywell Aerospace

- Paul Yankowich, subcontractor, Honeywell Aerospace

Project Overview

The International Civil Aviation Organization (ICAO) has approved publication of the revised ICAO Annex 16 Vol. II specifying a standardized sampling system for the measurement of non-volatile particulate matter (nvPM) from aircraft engines for use in certification. The Missouri University of Science and Technology (MS&T) owns and operates the ICAO Annex 16 Vol. II compliant North American mobile reference system (NARS) to measure nvPM emissions from the exhaust of aircraft engines. The work under this project exploits the use of the NARS to address issues associated with ambient condition corrections, engine-to-engine variability, and fuel formulation sensitivity. During this reporting period, work has been performed on three major tasks:

Task 1
Testing has taken place at Honeywell as part of a series of measurements to acquire certification-like data on a set of engines identified by ICAO Committee on Aviation Environmental Protection (CAEP) Working Group 3 (Emissions Technical) Particulate Matter Task Group (CAEP/WG3/PMTG) to be representative of the commercial fleet for entry into the nvPM values database. The engine-to-engine variability of nvPM emissions data from a sample of a large number of engines is required in order to assess the characteristic variability of these engines, which is critical in establishing a regulatory limit for nvPM number- and mass-based emissions. The measurement activity in this task has been undertaken by Honeywell personnel under subcontract to MS&T. Technical oversight was provided by the MS&T team.

Task 2
The NARS and its ancillary equipment have been used to characterize ground-based nvPM emissions from an IAE V2527-A5 engine burning four different fuel types. This work was conducted as part of the NASA/DLR Multidisciplinary Airborne Experiment (ND-MAX) campaign.

Task 3
The NARS and its ancillary equipment are being prepared to quantify the impact of changing conditions on nvPM emissions from a combustor rig and to develop methods for the use of inventory modeling.

Task 1 - Engine-to-Engine Variability at Honeywell

Missouri University of Science and Technology

Objective

The objective of this effort is to gather emissions data from at least 20 Honeywell commercial propulsion engines of the same type to assess engine-to-engine variability and derive characteristic nvPM emissions.

Research Approach

In support of the anticipated 2019 ICAO/FAA Part 34 certification standard, Honeywell has measured engine-to-engine variability of nvPM emissions data from a sample of 20 Honeywell engines to assess the characteristic variability of these engines. The FAA proposed work included the following items:

1. Obtain nvPM mass and number emissions from 20 turbofan engines, which contain the same model and type as the standardized draft ICAO Annex 16 Appendix 7 compliant nvPM measurement system, along with ICAO Annex 16 compliant gaseous emissions (possibly obtained during green runs).
2. Use a single-point probe positioned at a spot in the exhaust stream that is representative of the average emissions in the exit plane. A certification-type probe is preferable if the added cost is not prohibitive.
3. Vary the rated thrust from idle to 100% in 10-percentage-unit increments. After the engine stabilizes at each thrust point, hold the throttle at that thrust point for approximately 3 min so that nvPM and gaseous emissions can be acquired.
4. Use limited release non-disclosure agreement as needed. Ensure that the nvPM and gaseous emissions data are available from the 20 engines for analysis to derive characteristic nvPM mass and number emissions indices (EI) or any other emissions metric as needed.

Milestone(s)

A final test report has been submitted by Honeywell to MS&T. It presents the results of a 25-engine test campaign to sample

nvPM from production engines of the same model type. The sampling systems and analysis procedures used for this test campaign conform to the guidance set forth in SAE AIR6241 and the draft Appendix 7 to ICAO Annex 16. This work has directly informed CAEP/11 LTO nvPM Mass and Number Standards Development, permitting the development of characteristic coefficients for emissions as a function of number of engines tested.

Major Accomplishments

1. Total variation, including measurement system uncertainty, ambient condition variation, fuel variation, and engine-to-engine variation, has been assessed on one measurement train with two mass measurement systems (MMS).
2. The highest standard deviation was noted at 30% power, with standard deviation equal to 93% of average.
3. The lowest standard deviation was noted at 100% power, with standard deviation equal to 16% of average.
4. Modal standard deviation was higher at lower mean values.
5. Generally, lower variation was noted in number measurement.
6. Similar variation was noted between system loss-corrected and only thermophoretic loss-corrected data.
7. Excellent agreement was demonstrated between the laser induced incandescence instrument (LII) and micro soot sensor (MSS) (see Figure 2).
8. Fuel correction reduced variation by <1%.
9. No significant correlation was found for landing and take-off cycle (LTO) mass or number with ambient temperature or humidity.
10. Standard deviation divided by average for 21-engine testing with fuel correction (see Figure 1):
    - LTO mass standard deviation of mean (combined LII + MSS) = 20.4%.
    - LTO number standard deviation of mean = 11.0%.

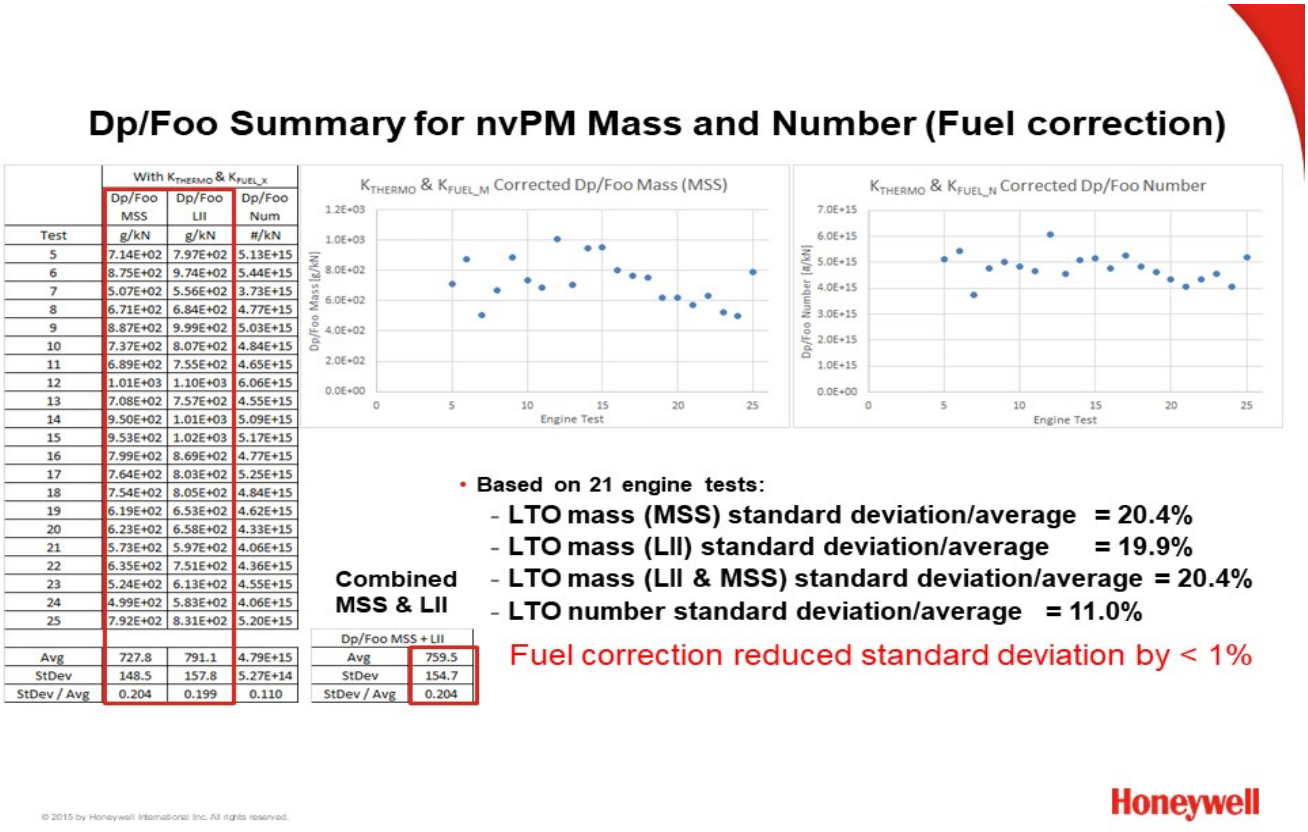

Figure 1. Summary of engine-to-engine variability data of 25 tests. nvPM, non-volatile particulate matter; LTO, landing and take-off cycle; LII, laser induced incandescence instrument; MSS, micro soot sensor; Dp/Foo, mass, in grams (Dp), of any pollutant emitted during the reference LTO cycle, divided by the rated output (Foo) of the engine.

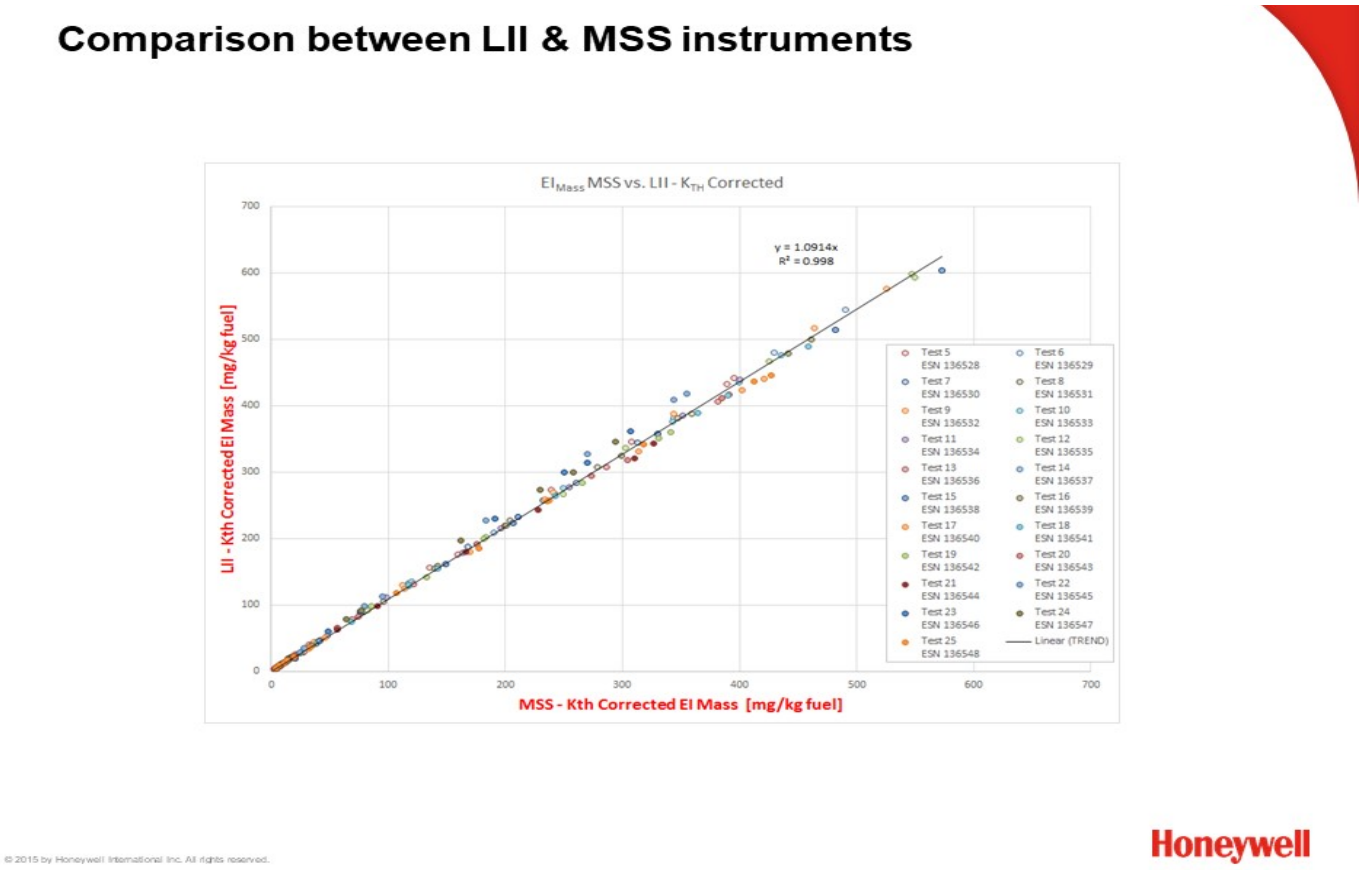

Figure 2. Comparison between micro soot sensor (MSS) and laser induced incandescence instrument (LII) data.

Publications
N/A

Outreach Efforts
This work was reported at the ASCENT advisory board meetings held in Cambridge, MA, in April 2018.
Data were provided to the ICAO CAEP/WG3/PMTG in paper CAEP11-WG3-PMTG7-IP01.

Awards
None.

Student Involvement
No graduate students were employed in this task; however, four undergraduate research assistants (Christian Hurst, Nicholas Altese, Davis Strassner, and Susan Donaldson) were employed in pre- and post-test activities, including individual component testing and calibration and data reduction and interpretation. Hurst, Altese, and Donaldson have not graduated; Strassner has graduated (current status unknown).

Plans for Next Period
With completion of the engine testing described above, additional scope is proposed in the form of a series of new tasks for MS&T and Honeywell to perform combustor rig testing with alternate fuels to establish nvPM ambient corrections designed specifically to address a set of FAA objectives (see Task 3 below):

- Set up a rich-quench-lean (RQL) full annular combustor rig and standardized nvPM measurement system

- Vary combustor inlet air conditions (range of ambient conditions on the ground and at altitude) and measure nvPM emissions
- Use probe designs that minimize losses and sample representatively
- Develop isokinetic sampling techniques such that particles are not over- or under-sampled
- Perform rig testing using Jet A fuel and three alternative fuels
- Analyze data to inform performance-based nvPM emissions modeling for all altitudes

Because the nvPM emissions from aircraft engines are affected by changing inlet conditions, a combustor rig test provides the most flexibility to quantify the impact of changing ambient or altitude conditions on nvPM mass and number emissions and to develop correlations for use in inventory modeling or for regulatory purposes.

Task 2 - Ground-Based non-volatile Particulate Matter (nvPM) Emissions from an IAE V2527-A5 Engine Burning Four Different Fuel Types

Missouri University of Science and Technology

Objective(s)

1. Measure engine emissions from four different fuel types on the ground using NARS and its ancillary equipment and compare it with the NASA measurement system and, where appropriate, quantify differences. Specifically, the research team will
    a. Deploy to Europe
    b. Make measurements and analyze data
2. Contribute to planning the emissions measurements at various altitudes and evaluate cruise nvPM models

Research Approach

In this task, MS&T and subcontractor Aerodyne Research Inc. have used the NARS to measure engine emissions from four different fuel types on the ground and compared the resulting data with that acquired by other ground-based and airborne NASA/DLR measurement systems. The NARS was used to conduct the following tasks:

Task A: Contribute to planning emissions measurements at various altitudes and evaluate cruise nvPM models

In this task, the primary objective of the MS&T team was to work closely with the ND-MAX PIs to plan the logistics and test matrices of the proposed emission measurements at ground level and altitude, including an inter-comparison of the NARS data with that acquired with the NASA/DLR-deployed nvPM measurement systems. The secondary objective of this task will be to evaluate models predicting cruise nvPM emissions by comparing the model results with in situ and ground-based measurements.

Task B: The NARS and ancillary equipment were prepared for deployment to test site in Germany

In this task, the NARS subsystems were laboratory tested at MS&T and Aerodyne to ensure they met operational specifications as defined in SAE AIR6241/SAE ARP 6320. On completion of laboratory testing, the NARS and ancillary equipment were packaged and shipped to the test site in Germany.

Task C: Deployment was undertaken to set up the NARS at an airfield in Germany

In this task, the MS&T team deployed to the test site in Germany, set up the NARS and ancillary equipment, and undertook subsystem check-out procedures in preparation for emissions testing.

Task D: Ground-based emissions measurements on four different aviation fuels were acquired

In this task, the MS&T team used the NARS and ancillary equipment to characterize the nvPM component of emissions from four fuels to be defined by the test matrix established in the work described in task A.

Task E: Tear-down and ship NARS and ancillary equipment to MS&T

In this task, the MS&T team tore down the NARS and ancillary equipment and packaged it for return shipment to the United States.

Task F: Reduce, analyze, and report nvPM data
In this task, the raw emissions data acquired during task D were reduced and analyzed using the methods described in AIR6241/ARP 6320. These data have been reported to the FAA and shared with ND-MAX participants.

Milestone(s)
The airborne and ground-based phases of the ND-MAX campaign have been successfully executed. Data analysis and interpretation are underway.

Major Accomplishments
- We measured the emissions from four different fuels—two conventional sources of Jet A-1 and two specifically designed sustainable alternative jet fuels (SAJFs) blended to 50% with each of the conventional fuels. The SAJFs were designed to have naphthalene contents that differed by an order of magnitude.
- The two SAJFs yielded substantial reductions in soot emissions compared with the two unblended conventional Jet A-1 fuels. The percentage reductions decreased with fuel flow rate (%N1). See Figure 3.
- The PM emissions were observed to decrease with increasing fuel hydrogen content. See Figure 4.
- Organic PM emissions were found to be insensitive to fuel type and had a distinct mode at 268 nm. Compositional analysis revealed the organic PM to be due to vented lubrication oil and not a product of combustor emissions. See Figures 5 and 6.
- H% serves as a useful proxy for EI of SAJF fuels.
- Black carbon or "nvPM" instruments generally perform consistently for SAJF fuels compared with traditional fuels. Filter-based instruments require source-specific calibrations when sources produce particles of a different composition or size, compared with the calibration of those instruments. The calibration factors of such instruments must not be treated as universal constants.

Publications
N/A

Outreach Efforts
Presentations on the data analysis and interpretation to date have been made at
- ASCENT advisory board meetings Washington, DC, in October 2018
- Aviation Emissions Characterization (AEC) Roadmap Meeting held in Washington, DC, in May 2019
- American Geophysical Union (AGU) Fall Meeting in session A33K: Improving the Science of Emissions through Inventories, Observations and Models III, 12 December 2018, Washington, DC

Awards
NASA Group Achievement Award to ND-MAX.

Student Involvement
No graduate students were employed in this task; however, four undergraduate research assistants (Christian Hurst, Nicholas Altese, Davis Strassner, and Susan Donaldson) were employed in pre- and post-test activities, including individual component testing and calibration and data reduction and interpretation. Hurst, Altese, and Donaldson have not graduated; Strassner has graduated (current status unknown).

Plans for Next Period
Continue with instrument inter-comparisons especially between other ground-based systems and their in-flight equivalents. Present papers at American Association of Aerosol Research Meeting October 2019.

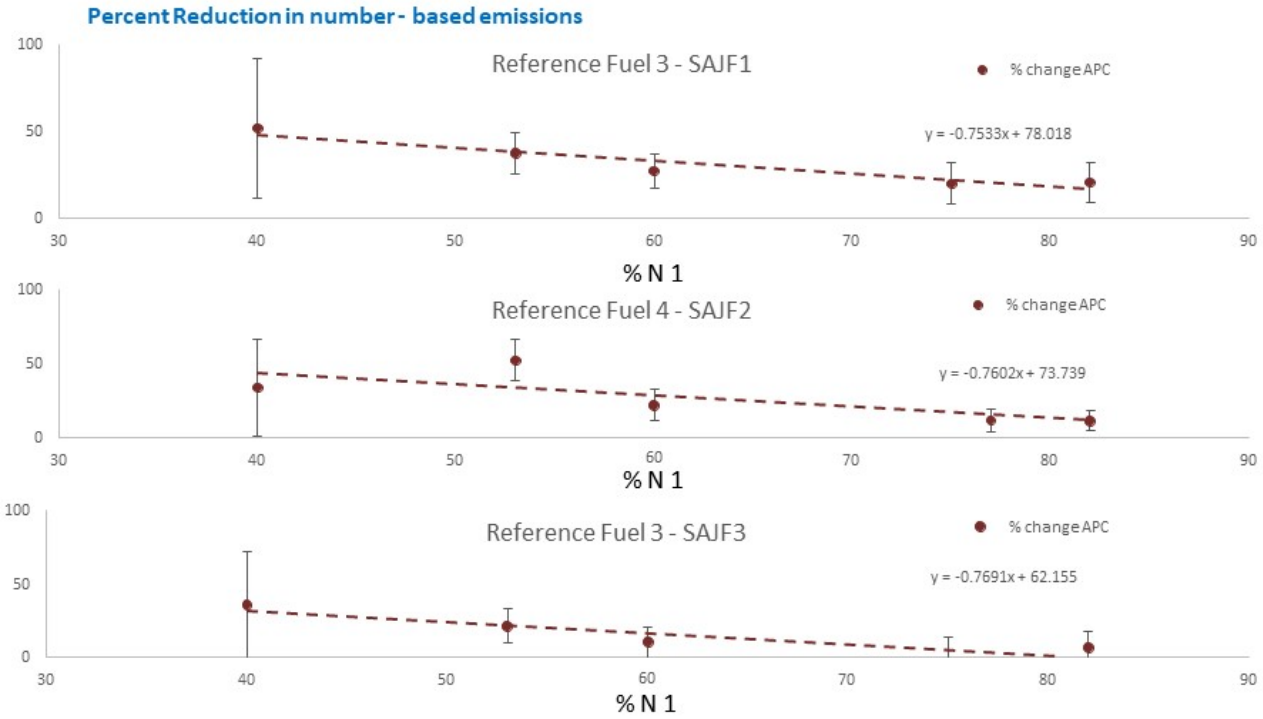

Figure 3. Example data of measured percentage reductions in particulate matter (PM) number-based emissions comparing blend emissions and reference fuel emissions. N1, rotational speed of the low-pressure compressor in a jet engine; APC, AVL particle counter (AVL, Graz, Austria).

Emissions Variation with Fuel Hydrogen Content

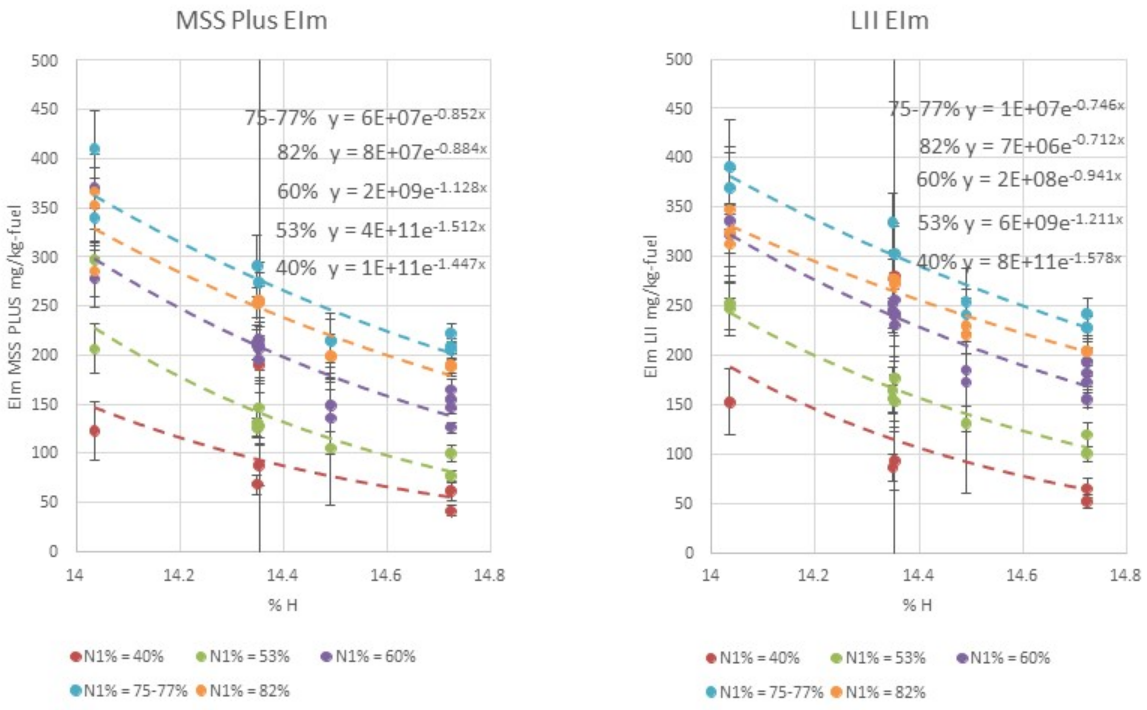

Figure 4. Example emission index values for the mass-based emission index (EI_m) as a function of fuel hydrogen content (% H) using the micro soot sensor (MSS) and laser induced incandescence instrument (LII) mass measurement techniques.

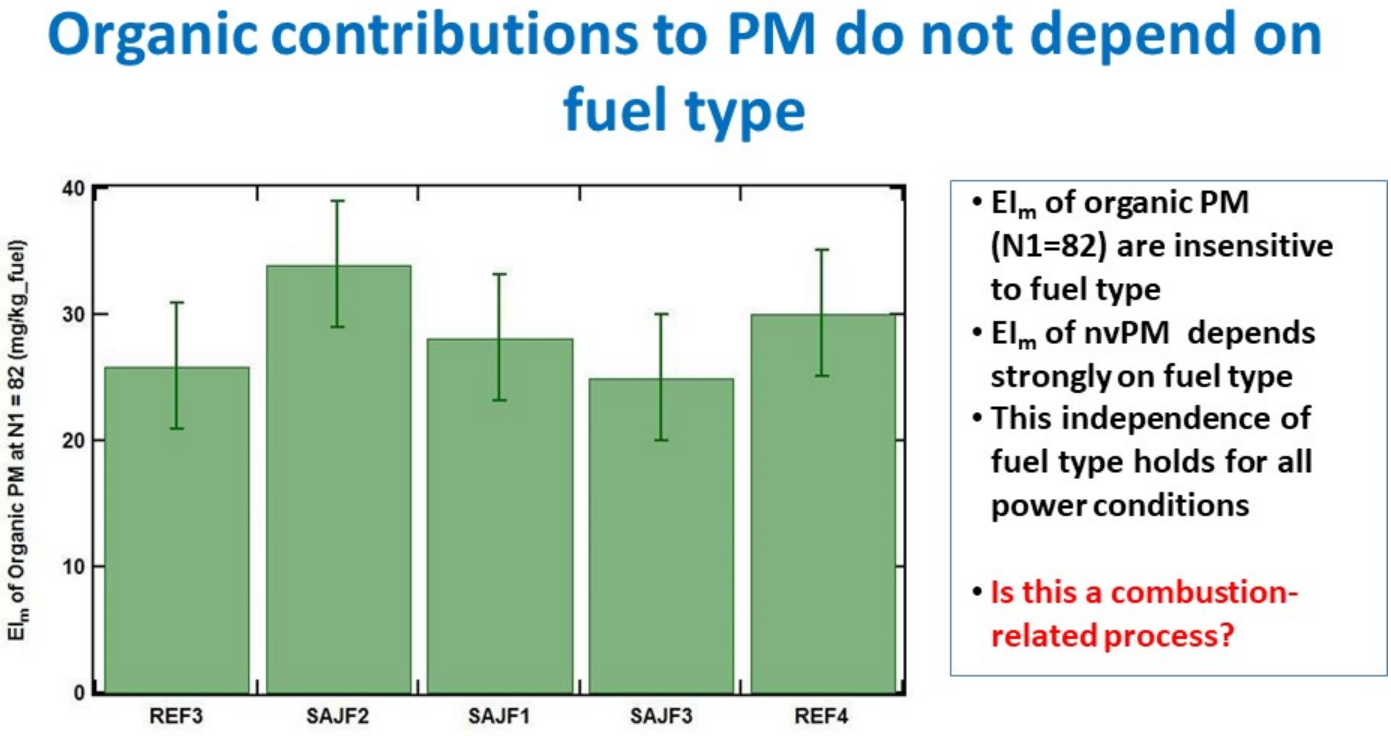

Figure 5. Data revealing that the mass-based emission index (EI_m) values for organic particulate matter (PM) are insensitive to fuel type. SAJF, sustainable alternative jet fuel; nvPM, non-volatile PM.

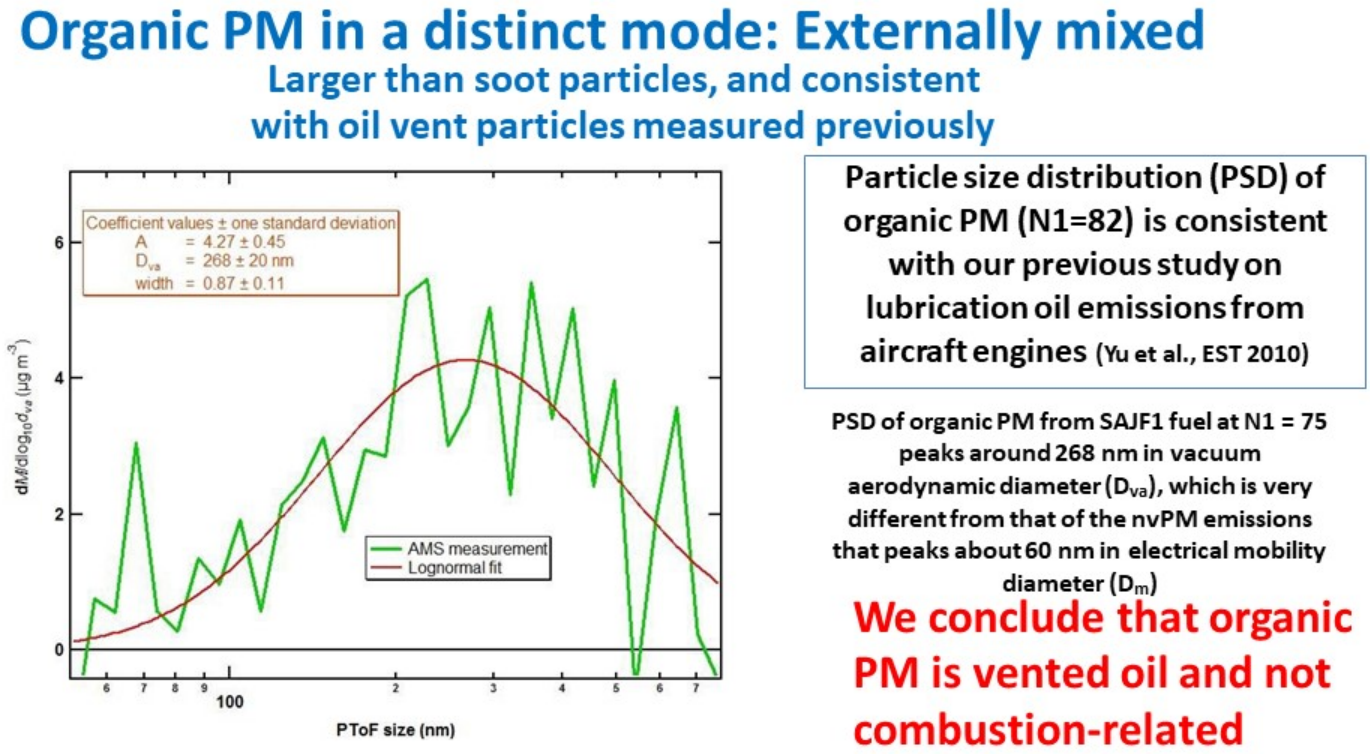

Figure 6. Size distribution data for organic particulate matter (PM) revealing that organic PM is vented oil. SAJF, sustainable alternative jet fuel.

Task 3 - Re-Examination of Engine-to-Engine Particulate Matter (PM) Emissions Variability Using an Aerospace Recommended Practice (ARP) Reference Sampling and Measurement System

Missouri University of Science and Technology

Objective(s)

nvPM emissions from aircraft engines are affected by changing inlet conditions. A combustor rig test provides the most flexibility to quantify the impact of changing conditions on nvPM emissions and to develop methods for use in inventory modeling. The MS&T/Aerodyne team will work with Honeywell to conduct combustor rig tests, collect nvPM mass and number emissions data, and analyze data to determine nvPM ambient corrections.

Research Approach

- Define and assemble a standardized nvPM measurement system that will include the same MMS that was used to sample nvPM from 25 Honeywell HTF7350 production engines in 2017
- Design and fabricate nvPM emissions rakes and combustor rig adaptive hardware required to enable nvPM and gaseous emissions data to be acquired from Honeywell's existing HTF7000 Combustor Test Rig
- Perform four combustor rig tests with Jet A and three alternative fuels
- Vary combustor test conditions (derived from engine cycle performance analysis, covering a range of engine ambient inlet conditions on the ground and at altitude) and measure nvPM emissions
- Analyze data to inform performance-based nvPM emissions modeling for all altitudes

Milestone

The funding for the Honeywell and Aerodyne subawards is in place and work is underway to prepare for testing at Honeywell's combustor rig facilities in Phoenix, AZ.

Major Accomplishments

- Honeywell and the MS&T/Aerodyne team have assembled two standardized nvPM emissions measurement systems. Key components are in the process of being recalibrated.
- Honeywell has completed design and fabrication of rakes and adaptive rig hardware required to enable nvPM emissions measurements in the HTF7000 Combustor Test Rig.

Publications

N/A

Outreach Efforts

Presentations on the project plan to date have been made at

- ASCENT advisory board meetings held in Alexandria, VA, in October 2018
- AEC Roadmap Meeting held in Washington, DC, in May 2019

Awards

None.

Student Involvement

No graduate students were employed in this task; however, four undergraduate research assistants (Christian Hurst, Nicholas Altese, Davis Strassner, and Susan Donaldson) were employed in pre- and post-test activities, including individual component testing and calibration and data reduction and interpretation. Hurst, Altese, and Donaldson have not graduated; Strassner has graduated (current status unknown).

Plans for Next Period

- Conduct performance analysis to define the rig test matrix
- Complete pre-test setup and shakedown of nvPM combustor rig measurement system with rig in test cell
- Conduct initial rig test with Jet A, following system shakedown and availability of test cell

Project 003 Cardiovascular Disease and Aircraft Noise Exposure

Boston University

Project Lead Investigator

Junenette L. Peters
Assistant Professor
Department of Environmental Health
Boston University School of Public Health
715 Albany St., T4W
Boston, MA 02118
617-358-2552
petersj@bu.edu

University Participants

Boston University (BU)

- PI(s): Prof. Jonathan Levy (University PI), Prof. Junenette Peters (Project PI)
- FAA Award Number: 13-C-AJFE-BU-016
- Period of Performance: June 14, 2019 to September 30, 2019

Massachusetts Institute of Technology (MIT)

- Sub-PI and Co-I: Prof. R. John Hansman, Dr. Florian Allroggen

Tasks (Performance Period)

Related to 2018 FAA Reauthorization, Section 189, Tasks 1-3

1. Generate preliminary results from analyses of aircraft noise (day-night average sound level [DNL] and equivalent sound level [Leq] Night) and hypertension
2. Generate preliminary results of supporting analyses
    a. Trends of aircraft noise exposure
    b. Sociodemographic patterning of aircraft noise exposure
3. Assess suitability of existing cohort data on sleep quality and potential approaches for noise-sleep analysis

Related to 2018 FAA Reauthorization, Section 189, Task 4

4. Review existing scientific literature to identify potential economic impacts of aviation

Project Funding Level

Total Funding (3-year funding): $1,729,286
Matching: $1,729,286
Source of Matching: Nonfederal donors to the Nurses' Health Study (NHS), Health Professional Follow-up Study (HPFS), and Women's Health Initiative (WHI) cohorts

Investigation Team

Junenette Peters, PI, Boston University
Dr. Peters is responsible for directing all aspects of the proposed study, including study coordination, design and analysis plans, and co-investigator meetings.

Jonathan Levy, Boston University
Dr. Levy will participate in noise exposure assessment and provide expertise in the area of predictive modeling and air pollution.

Francine Laden, Jaime Hart, and Susan Redline, Harvard Medical School/Brigham and Women's Hospital
Dr. Laden is our NHS and HPFS sponsor for this ancillary study. Dr. Hart will assign aircraft noise exposures to the geocoded address history coordinates of each cohort member. Dr. Laden and Dr. Hart will also assist in documenting data from the NHS and HPFS based on their previous experience in air pollution and chronic disease outcome research in these cohorts and in appropriate analyses of hypertension and cardiovascular outcomes. Dr. Redline will lead efforts related to noise and sleep disturbance in the NHS and WHI.

John Hansman and Florian Allroggen, Massachusetts Institute of Technology
Dr. Hansman will participate in the economic impact assessment and will provide expertise on analytical approaches for quantifying noise. Dr. Allroggen will perform an economic impact assessment based on his expertise in analyzing the societal costs and benefits of aviation.

Project Overview

Exposure to aircraft noise is considered the most significant perceived environmental impact of aviation in communities surrounding airports (Wolfe et al., 2014). Exposure to aircraft noise has been associated with physiological responses and psychological reactions (Bluhm & Eriksson, 2011; Hatfield et al., 2001), including sleep disturbances, sleep-disordered breathing, nervousness, and annoyance (Hatfield et al., 2001; Rosenlund et al., 2001). Recent literature, primarily from European studies, provides evidence of a relationship between aircraft noise and self-reported hypertension (Rosenlund et al., 2001), increased blood pressure (Evrard et al., 2017; Haralabidis et al., 2008; Haralabidis et al., 2011; Jarup et al., 2008; Matsui et al., 2004), antihypertensive medication use (Bluhm & Eriksson, 2011; Floud et al., 2011; Franssen et al., 2004; Greiser et al., 2007) and incidence of hypertension (Dimakopoulou et al., 2017; Eriksson et al., 2010). However, the extent to which aircraft noise exposure increases the risk of adverse health outcomes is not well understood. Impacts related to annoyance have been empirically studied using the stated preference approach (Bristow et al., 2015) and the revealed preference approach, which often relies on analyses of house prices (Almer et al., 2017; Kopsch, 2016; Wadud, 2013). Although the impacts of aircraft noise on individuals are well understood, little evidence has been presented on the impact of aircraft noise exposure on companies located beneath flight paths. Section 189 of the 2018 FAA Authorization has called for a study on the potential health and economic impacts attributable to aircraft overflight noise.

The goal of this ongoing project is to examine the potential health impacts attributable to noise exposure resulting from aircraft flights, and this project will leverage ongoing work within ASCENT to respond to Section 189. This study aims to assess the potential association between aircraft noise exposure and outcomes such as sleep disturbance and elevated blood pressure. The study will leverage existing collaborations with well-recognized and respected studies that have followed over 250,000 participants through the course of their lives to understand factors that affect health. These studies include the NHS and HPFS. Furthermore, this work is aligned with an ongoing National Institutes of Health (NIH)-funded effort to examine these associations in the WHI. The research team will leverage aircraft noise data for 90 U.S. airports from 1995–2015, as generated using the Aviation Environmental Design Tool (AEDT); these data will then be linked to demographic, lifestyle, and health data for the participants of long-term health studies. These studies provide considerable geographic coverage of the United States, including all of the geographic areas specified in Section 189.

This work will also respond to the aspect of Section 189 calling for the study of economic harm or benefits for businesses located underneath regular flight paths. The study will involve a first-of-its-kind empirical assessment of the economic impacts on businesses located beneath flight paths at selected U.S. airports. Such impacts are expected to be driven by (a) potential positive economic impacts related to the airport and its connectivity and (b) environmental impacts such as noise, which may reduce the revenue and productivity of businesses beneath flight paths. The team will evaluate whether such impacts can be empirically identified while considering economic outcome metrics such as the gross domestic product (GDP), employment, and revenue.

The overall aims for the three-year project are as follows:

- Perform Tasks 1–3 [*Sec. 189. (b)(1–3)*]: Potential health impacts attributable to aircraft overflight noise
    - Investigate the relationship between aircraft noise exposure and the incidence of hypertension in the NHS and HPFS, accounting for other individual- and area-level risk factors
    - Investigate the relationship between aircraft noise exposure and the incidence of cardiovascular disease (CVD) in the NHS and HPFS cohorts and determine whether sufficient data exist to prove a causal relationship

    - Determine whether a relationship exists between annual average aircraft noise exposure and general sleep length and quality in the NHS and the Growing Up Today Study (GUTS) and report whether sufficient data exist to prove a causal relationship
    - Evaluate the potential relationship between residing under a flight path and measures of disturbed sleep in the WHI WHISPER sub-study
- Perform Task 4 [*Sec. 189. (b)(5)*]: Potential economic impacts attributable to aircraft overflight noise
    - Model noise exposure before and after the introduction of area navigation (RNAV) procedures on the basis of FAA flight trajectory data
    - Combine noise data with yearly county-level data from the Bureau of Economic Analysis (BEA) (e.g., GDP, employment) and with city-level statistics for the years 2007, 2012, and 2017 from the Economic Census (e.g., revenue, employment)
    - Compare economic outcomes using state-of-the-art econometric approaches while controlling for regional and national economic trends
    - Evaluate whether the spatial resolution of the available data can significantly impact the study results.

Task 1- Generate Preliminary Results from Analyses of Aircraft Noise and Hypertension

Boston University

Objective

To generate preliminary results from analyses of aircraft noise (DNL and Leq Night) and hypertension.

Research Approach

We will intersect modeled noise exposure surfaces for 1995, 2000, 2005, 2010, and 2015 with geocoded addresses of the participants over the follow-up period. We will select a large set of a priori variables to be examined as confounders and/or effect modifiers and will use time-varying Cox proportional hazards models to estimate hypertension or CVD risks associated with time-varying aircraft noise exposure, while adjusting for both fixed and time-varying covariates. We will also perform a sensitivity analysis to address potential biases.

Milestone

Generate results from analyses of aircraft noise (DNL and Leq Night) and hypertension – January 2020.

Major Accomplishments

- Intersected modeled exposure surfaces for DNL with the participants' geocoded addresses over the follow-up period
- Determined the number of people free of hypertension at baseline
- Determined noise exposure distribution of those without hypertension at baseline in two cohorts (NHS and NHS II) for the follow-up period (Table 1)
- Selected a large set of a priori variables, including age, alcohol use (g/day), body mass index (BMI), calendar year, comorbidities (diabetes, hearing loss, hypercholesterolemia), smoking status, diet (dietary approaches to stop hypertension [DASH] score), hearing problems, family history of hypertension, individual-level socioeconomic status (SES) variables (educational attainment, marital status, and partner's educational attainment), medication use (current statin and non-narcotic analgesic drug use), menopausal status, physical activity (metabolic equivalent hours per week), and race, as well as region, latitude, area-level SES variables (census-tract median income and house value), and air pollution ($PM_{2.5}$ and $PM_{2.5-10}$).
- Used time-varying Cox proportional hazards models to estimate hypertension risks associated with time-varying aircraft noise exposure, while adjusting for both fixed and time-varying covariates
    - Performed analysis for each cohort separately (Figures 1 and 2 for NHS and NHS II, respectively)
    - Performed meta-analysis to combine the results found for each cohort – NHS and NHS II (Figure 3)
    - Performed the following sensitivity analyses (assessing the sensitivity of each primary analysis to underlying issues)
        - Restricted participants to those living close to one of the 90 modeled airports (≥45 dB) to address potential exposure errors, for example, to exclude those living near an airport that is not included in

the 90 airports and to minimize the impact of potential differences in populations living close to airports versus those living farther away

- Analyzed the potential effect of noise abatement programs for DNLs higher than 65 dB to address possible exposure errors related to noise abatement programs among those with noise exposure above the FAA threshold (>65 dB).
- Adjusted for air pollution and area-level SES, which is available for only a portion of the time period.

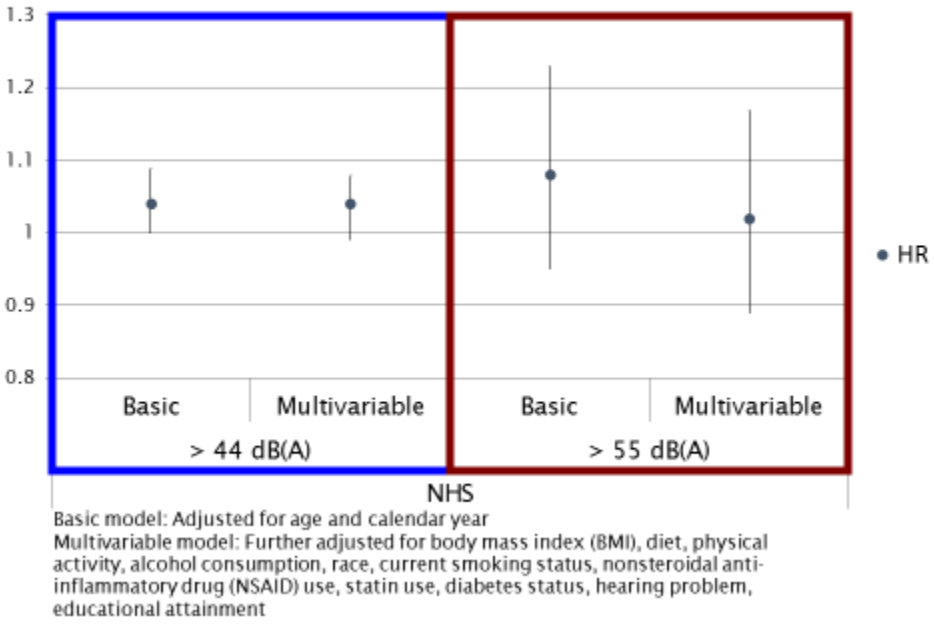

Figure 1. Hazard ratios (95% confidence intervals [CIs]) for hypertension associated with aircraft noise in the NHS, comparing results for >44 dB with those for ≤44 dB and comparing results for >55 dB with those for ≤55 dB.

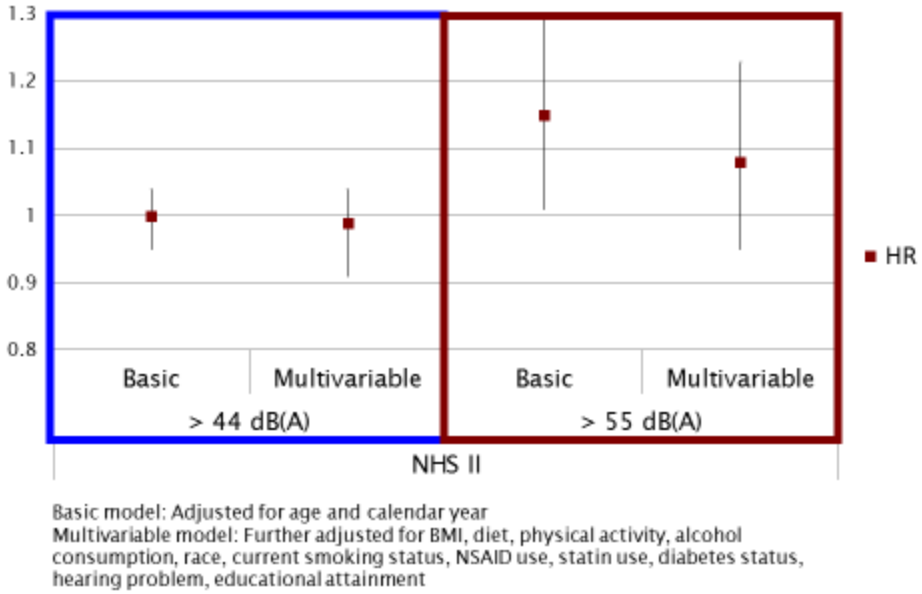

Figure 2. Hazard ratios (95% CIs) for hypertension associated with aircraft noise in NHS II, comparing results for >44 dB with those for ≤44 dB and comparing results for >55 dB with those for ≤55 dB.

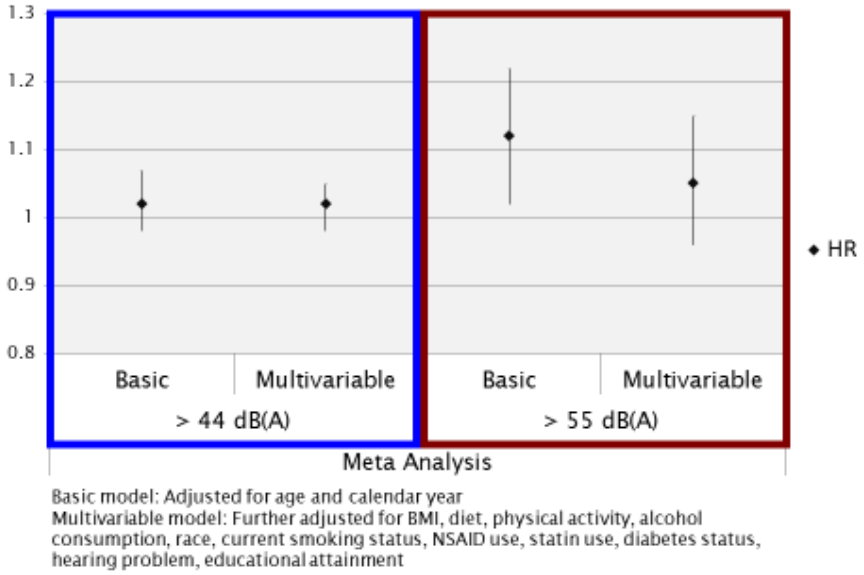

Figure 3. Hazard ratios (95% CIs) for hypertension associated with aircraft noise in a meta-analysis (combined results for NHS and NHS II), comparing results for >44 dB with those for ≤44 dB and comparing results for >55 dB with those for ≤55 dB.

The results indicate an increased risk for incident hypertension associated with higher aircraft noise exposure in both NHS and NHS II (Figures 1 and 2). A meta-analysis across both cohorts (Figure 3) gave a hazard ratio (HR) of 1.02 (95% CI: 0.98, 1.07) and 1.08 (95% CI: 0.98, 1.18) for the multivariable model with cut-points of 45 and 55 dB, respectively. The HRs were relatively stable across the sensitivity analyses.

Task 2 - Generate Preliminary Results from Supporting Analyses: (a) Trends in Aircraft Noise Exposure and (b) Sociodemographic Patterning of Aircraft Noise Exposure

Boston University

Objective

To understand changes in exposure that will facilitate our interpretation of time-varying exposure measures in noise-health analyses and to understand sociodemographic patterning of noise exposure that may confound or modify potential associations of noise and health.

Research Approach

For (a, Noise Trend), we will overlay noise contours for 2000, 2005, 2010, and 2015 and census block data from the U.S. Census Bureau and American Community Surveys for 2000, 2010, and 2015 in a geographic information system to estimate population changes within noise levels. We will utilize linear fixed-effects models to estimate changes in the sizes of exposure areas based on U.S. census regions/divisions with DNL values ≥65 dB or ≥55 dB. For (b, Sociodemographic Patterning), we will describe the characteristics of populations exposed to aviation noise by race/ethnicity and income/education using the U.S. Census Bureau and American Community Survey for 2010 and will perform univariate and multivariable hierarchical analyses.

Milestone

Perform supporting analyses characterizing aircraft noise trends and sociodemographic patterns of exposure to aviation noise - N/A.

Major Accomplishments

- Overlaid noise contours for 2000, 2005, 2010, and 2015 and census block data from the U.S. Census Bureau and American Community Surveys for 2000, 2010, and 2015
- Excluded areal hydrography (water bodies) using the Census Bureau's Topologically Integrated Geographic Encoding and Referencing (TIGER) data set and national, state, and local parks using ESRI and TomTom
- Determined the exposure area and number of people exposed to aircraft noise using data over time (2000–2015); preliminary results are presented in Figure 4
- Determined and implemented an optimal approach for assigning the exposed and unexposed census blocks
- Determined social patterning of aircraft noise exposure by race/ethnicity and income/education for 2010 using univariate and multivariable analysis; preliminary results are presented in Figure 5

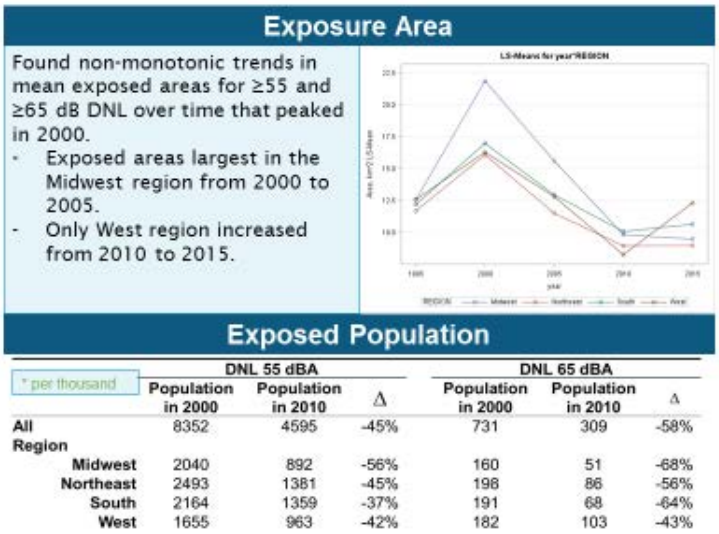

* per thousand	DNL 55 dBA Population in 2000	DNL 55 dBA Population in 2010	DNL 55 dBA Δ	DNL 65 dBA Population in 2000	DNL 65 dBA Population in 2010	DNL 65 dBA Δ
All Region	8352	4595	-45%	731	309	-58%
Midwest	2040	892	-56%	160	51	-68%
Northeast	2493	1381	-45%	198	86	-56%
South	2164	1359	-37%	191	68	-64%
West	1655	963	-42%	182	103	-43%

Figure 4. Preliminary results for noise trends based on exposure area and number of people exposed.

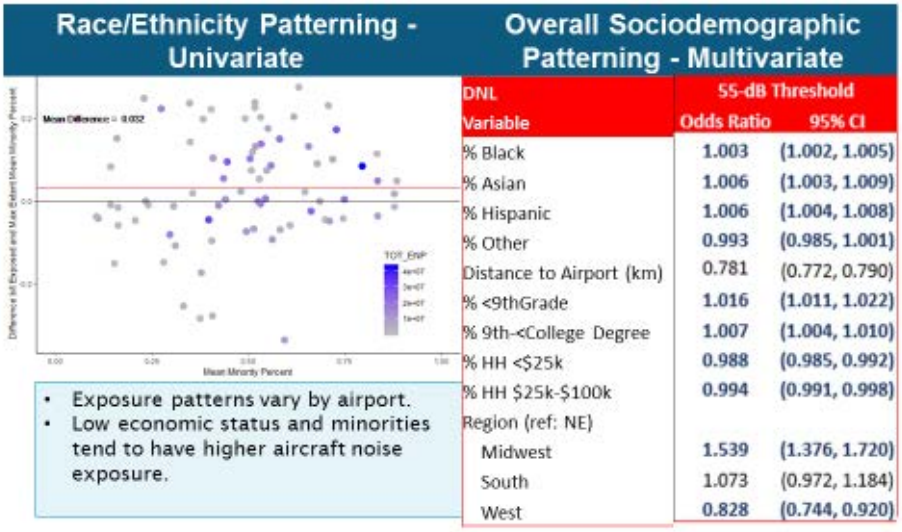

DNL Variable	55-dB Threshold Odds Ratio	95% CI
% Black	1.003	(1.002, 1.005)
% Asian	1.006	(1.003, 1.009)
% Hispanic	1.006	(1.004, 1.008)
% Other	0.993	(0.985, 1.001)
Distance to Airport (km)	0.781	(0.772, 0.790)
% <9thGrade	1.016	(1.011, 1.022)
% 9th-<College Degree	1.007	(1.004, 1.010)
% HH <$25k	0.988	(0.985, 0.992)
% HH $25k-$100k	0.994	(0.991, 0.998)
Region (ref: NE)		
Midwest	1.539	(1.376, 1.720)
South	1.073	(0.972, 1.184)
West	0.828	(0.744, 0.920)

Figure 5. Preliminary results for sociodemographic patterning in aircraft noise exposure based on univariate analysis for race/ethnicity and multivariable analysis.

Task 3 - Assess Suitability of Data on Sleep Quality and Potential Approaches for Noise-Sleep Analysis

Boston University

Objective

To identify sleep measures that may be used to evaluate potential associations between noise and sleep outcomes.

Research Approach

We will review the available measures of sleep quality for the NHS to determine their timing and frequency and their relationship to the timing of the noise exposure data. We will also determine which measures, if any, are relevant to the average exposure measures.

Milestone

Assess potential analysis approaches and suitability of sleep quality data from the NHS – January 2020.

Major Accomplishments

A BWH Research Fellow in sleep medicine with experience with the NHS has joined our team, been approved to work on the project by the Institutional Review Board, and met with team members to establish a timeline for this project. This task in on track to be completed on schedule.

Task 4 - Review Existing Scientific Literature to Identify Potential Economic Impacts of Aviation

Massachusetts Institute of Technology

Objective

To evaluate the literature to structure potential pathways through which the aviation sector can impact economic activity.

Research Approach

We will analyze the literature to structure the potential pathways through which the aviation sector can impact economic activity.

Milestone

Assess potential empirical approaches, data sources, and economic outcomes to be analyzed – December 2019.

Major Accomplishments

We have compiled a preliminary review of studies that analyze the economic impacts of the aviation sector in the United States. Preliminary results from the literature review, including potential empirical approaches and economic outcomes, are shown in Figure 6.

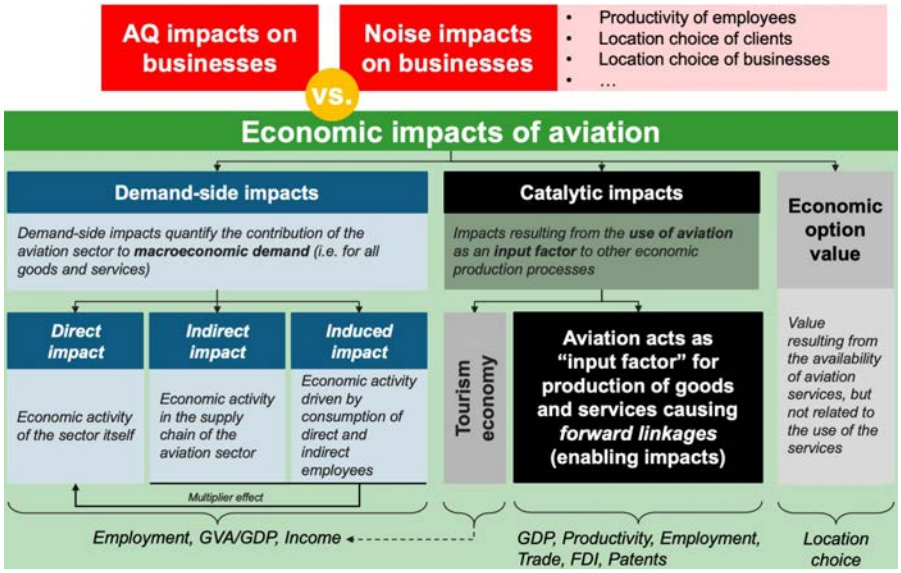

Figure 6. Preliminary structure outlining the economic impacts of the aviation sector.

The results show that the aviation sector can increase economic activity through three major pathways:

1. **Demand-side impacts:** The aviation sector can increase economic activity through its impact on macroeconomic demand. These impacts can be justified on the basis of Keynesian demand-side economics, including direct impacts in the sector, indirect impacts in the supply chain of the aviation sector, and induced impacts caused by increased demand due to income associated with direct and indirect impacts. Notably, these demand-side impacts can only be fully allocated to the aviation sector under the assumption of an underutilization of resources (e.g., labor) and production capacity.
2. **Catalytic impacts:** These impacts exist if the use of aviation services constitutes a benefit to an economic system. Such effects can include the establishment of a tourism economy that relies on air transport connections, potential forward linkages, and enabling effects (Lakshmanan, 2011). The latter impacts, which are often considered to increase the productivity of economic systems, have been demonstrated as significant in empirical studies, including, for example, reports by Brueckner (2003), Allroggen and Malina (2014), and Campante and Yanagizawa-Drott (2018).
3. **Economic option value of aviation:** This value can be observed if companies move closer to airports or other hotspots of the aviation industry, without currently being a regular user of air transportation or interacting with the air transport industry. While these effects do not immediately result in global economic benefits, they can benefit regions in the proximity of airports or other hotspots of the aviation industry.

Publications

N/A

Outreach Efforts

An outline of this project, preliminary results on the health impacts of aviation, and a first approach towards structuring the economic impacts of aviation were presented at the Fall 2019 ASCENT Advisory Committee Meeting.

Awards

None.

Student Involvement

The dissertation of Chloe Kim (doctoral candidate, BU) includes the development and implementation of statistical analyses on the noise and hypertension risk. Chloe Kim graduated in the fall of 2019 and is currently working for the Environmental Science, Policy, and Research Institute.

The dissertation of Daniel Nguyen (doctoral candidate, BU) includes a characterization of the temporal trends in aviation noise surrounding U.S. airports.

The research rotation of Stephanie Grady (doctoral student, BU) includes the development of statistical analyses on noise and cardiovascular event risk.

Carson Bullock (master's student, MIT) is supporting the literature review.

Plans for Next Period

(October 1, 2019 to September 30, 2020)

Related to 2018 FAA Reauthorization, Section 189, Tasks 1–3

- Assign noise exposure estimates to participants for Leq Day and Leq Night metrics and explore the value of assigning estimates for Time Above metrics
- Complete models estimating the risk of hypertension associated with aircraft noise exposure and finalize a manuscript for publication in a peer-reviewed journal
    - Perform analysis using Leq Night for NHS and NHS II
    - Perform a meta-analysis combining Leq Night results for the two cohorts
    - Update current draft of the manuscript
    - Submit manuscript for FAA review and to a professional journal
- Replicate noise and hypertension results in an all-male HPFS cohort
- Develop and execute models for estimating the risk of CVD events associated with aircraft noise exposure
- Develop a plan for analyzing the relationship between noise and sleep
- Develop abstracts for presentations at professional conferences

Related to 2018 FAA Reauthorization, Section 189, Task 4

- Finalize an overview of the literature analyzing the economic impacts of aviation
- Outline the empirical approach (including experimental design), potential data sources (including the airport sample), and economic outcomes to be analyzed
- Collect data on airport samples, experimental settings, and noise contours
- Perform empirical implementation and preliminary analysis using county-level BEA data

References

Allroggen F. & Malina, R. (2014). Do the regional growth effects of air transport differ among airports? Journal of Air Transport Management. 37:1-4.

Brueckner, J.K. (2003). Airline traffic and urban economic development. Urban Studies. 40(8):1455-1469.

Campante, F. & Yanagizawa-Drott, D. (2018). Long-range growth: Economic development in the global network of air links. Quarterly Journal of Economics. 133(3):1395-1458.

Lakshmanan, T.R. (2011). The broader economic consequences of transport infrastructure investments. Journal of Transport Geography. 19(1):1-12.

Project Overview References

Almer, C., Boes, S., & Nuesch, S. (2017). Adjustments in the housing market after an environmental shock: Evidence from a large-scale change in aircraft noise exposure. Oxford Economic Papers. 69(4):918-938.

Bluhm, G. & Eriksson, C. (2011). Cardiovascular effects of environmental noise: Research in Sweden. Noise and Health. 13(52):212-216.

Bristow, A.L., Wardman, M., & Chintakayala, V.P.K. (2015). International meta-analysis of stated preference studies of transportation noise nuisance. Transportation. 42(1):71-100.

Dimakopoulou, K., Koutentakis, K., Papageorgiou, I., Kasdagli, M.I., Haralabidis, A.S., Sourtzi, P., Samoli, E., Houthuijs, D., Swart, W., Hansell, A.L., & Katsouyanni K. (2017). Is aircraft noise exposure associated with cardiovascular disease and hypertension? Results from a cohort study in Athens, Greece. Occupational and Environmental Medicine. 74(11):830-837.

Eriksson, C., Bluhm, G., Hilding, A., Ostenson, C.G., & Pershagen, G. (2010). Aircraft noise and incidence of hypertension--gender specific effects. Environmental Research. 110(8):764-772.

Evrard, A.S., Lefevre, M., Champelovier, P., Lambert, J., & Laumon, B. (2017). Does aircraft noise exposure increase the risk of hypertension in the population living near airports in France? Occupational and Environmental Medicine. 74(2):123-129.

Floud, S., Vigna-Taglianti, F., Hansell, A., Blangiardo, M., Houthuijs, D., Breugelmans, O., Cadum, E., Babisch, W., Selander, J., Pershagen, G., Antoniotti, M.C., Pisani, S., Dimakopoulou, K., Haralabidis, A.S., Velonakis, V., Jarup, L.; HYENA Study Team. (2011). Medication use in relation to noise from aircraft and road traffic in six European countries: Results of the HYENA study. Occupational and Environmental Medicine. 68(7):518-524.

Franssen, E.A., van Wiechen, C.M., Nagelkerke, N.J., & Lebret, E. (2004). Aircraft noise around a large international airport and its impact on general health and medication use. Occupational and Environmental Medicine. 61(5):405-413.

Greiser, E., Janhsen, K., & Greiser, C. (2007). Air traffic noise increases prescriptions of cardiovascular drugs in the vicinity of a major airport. Epidemiology. 18(5):S33-S33.

Haralabidis, A.S., Dimakopoulou, K., Vigna-Taglianti, F., Giampaolo, M., Borgini, A., Dudley, M.L., Pershagen, G., Bluhm, G., Houthuijs, D., Babisch, W., Velonakis, M., Katsouyanni, K., Jarup, L.; HYENA Consortium. (2008). Acute effects of night-time noise exposure on blood pressure in populations living near airports. European Heart Journal. 29(5):658-664.

Haralabidis, A.S., Dimakopoulou, K., Velonaki, V, Barbaglia, G., Mussin, M., Giampaolo, M., Selander, J., Pershagen, G., Dudley, M.L., Babisch, W., Swart, W., Katsouyanni, K., Jarup, L.; HYENA Consortium. (2011). Can exposure to noise affect the 24 h blood pressure profile? Results from the HYENA study. Journal of Epidemiology and Community Health. 65(6):535-541.

Hatfield, J., Job, R., Carter, N.L., Peploe, P., Taylor, R., & Morrell, S. (2001). The influence of psychological factors on self-reported physiological effects of noise. Noise and Health. 3(10):1-13.

Jarup, L., Babisch, W., Houthuijs, D., Pershagen, G., Katsouyanni, K., Cadum, E., Dudley, M.L., Savigny, P., Seiffert, I., Swart, W., Breugelmans, O., Bluhm, G., Selander, J., Haralabidis, A., Dimakopoulou, K., Sourtzi, P., Velonakis, M., Vigna-Taglianti, F.; HYENA Study Team. (2008). Hypertension and exposure to noise near airports: The HYENA study. Environmental Health Perspectives. 116(3):329-333.

Kopsch, F. (2016). The cost of aircraft noise - does it differ from road noise? A meta-analysis. Journal of Air Transport Management. 57:138-142.

Matsui, T., Uehara, T., Miyakita, T., Hiramatsu, K., Yasutaka, O., & Yamamoto, T. (2004). The Okinawa study: Effects of chronic aircraft noise on blood pressure and some other physiological indices. Journal of Sound and Vibration. 277:469-470.

Rosenlund, M., Berglind, N., Pershagen, G., Jarup, L., & Bluhm, G. (2001). Increased prevalence of hypertension in a population exposed to aircraft noise. Occupational and Environmental Medicine. 58(12):769-773.

Wolfe, P.J., Yim, S.H.L., Lee, G., Ashok, A., Barrett, S.R.H., & Waitz, I.A. (2014). Near-airport distribution of the environmental costs of aviation. Transport Policy. 34:102-108.

Project 008 Noise Outreach

The Pennsylvania State University

Project Lead Investigator

Kathleen Hodgdon
Research Associate
Applied Research Laboratory
The Pennsylvania State University
State College PA 16804-0030
Phone: 814-865-2447
Email: kkh2@psu.edu

University Participants

The Pennsylvania State University

- P.I.: Kathleen Hodgdon, Research Associate
- FAA Award No.:13-C-AJFE-PSU Amendment 48
- Period of Performance: March 29, 2019 to March 28, 2020
- Task(s):
  1. Stakeholders Interactions
  2. Content Development
  3. Site Navigation and Infrastructure Enhancement

Project Funding Level

This project supports the Outreach efforts at Pennsylvania State University with $30,000 of FAA funds. Matching funds are anticipated to satisfy cost share on all tasks. This report covers period from October 1, 2018 through September 30, 2019. Incremental funding for 2018 – 2019 was not received until July 2019, so the activity period was shortened to July 2019 to September 2019.

Investigation Team

P.I.: Kathleen Hodgdon Research Associate

Advisory Committee Members

Gulfstream Aerospace Corporation	Robbie Cowart
Port of Portland Sr. Noise Analyst	Jason Schwartz
Volpe National Transportation System Center	Juliet Page

Project Overview

The NoiseQuest website is designed to support noise mitigation through information. NoiseQuest, located at www.noisequest.psu.edu, is an international resource that is designed to implement global education on aviation noise topics. The site presents aviation noise information that provides centralized web based educational outreach for all communities. This supports Outreach efforts for airports that are too small to have their own outreach programs, and provides additional outreach for airports with existing programs.

The site had been relocated to a new server to protect site integrity. The site was further reconfigured and tested after the move was completed. The content was reviewed as part of that effort.

Task 8.1- Stakeholders Interactions

Pennsylvania State University

Objective

The Outreach project seeks to improve airport and community interactions by providing information and education on aviation noise topics. The team interacted with stakeholders on Outreach topics.

Research Approach

Interactive outreach with stakeholders was conducted. The site user statistics were monitored to better inform the site development.

Milestones

Communications were held with aviation stakeholders via email and phone.

Major Accomplishments

We continue to interact with airport noise managers and community groups to identify topics of interest, successful implementations of outreach, or other approaches taken to resolve aviation noise issues. We continue to monitor our site statistics to gain insights on site usage (see Appendix A for Site Statistics).

Publications

Website contents are published at www.noisequest.psu.edu.

The website has also been utilized by reporters for aviation noise information. In this period of performance, Alex Davies, a transportation reporter from *Wired* magazine, used NoiseQuest for Outreach information and interviewed Professor Hodgdon for comments on aviation noise impact and mitigation. The article was published on 9/26/19 and can be found at: https://www.wired.com/story/teaching-pilots-new-trick-landing-quietly/. The article reported on changes in landing procedures that were evaluated in September 2019 by the German Aerospace Center. In addition to NoiseQuest, Professor Hodgdon referred Mr. Davies to the FAA website, the PARTNER website and the ASCENT website for additional references and information on aviation noise mitigation. Within the article he cited Professor Hodgdon and included a link to a research publication that was listed on the ASCENT site under ASCENT Project 17 "Pilot Study on Aircraft Noise and Sleep Disturbance". The article included a link to a research article entitled "Aviation noise impacts: state of the science in Noise and Health, which is also available on the ASCENT site. (Basner, M., Clark, C., Hansell, A., Hileman, J.I., Janssen, S., Shepherd, K., and Sparrow, V. 2017. Aviation noise impacts: state of the science. Noise and Health 19(87):41-50.).

Outreach Efforts

We interacted with airport noise managers and stakeholders from across the country.

Awards

None.

Student Involvement

None during July 2019 to September 2019.

Plans for Next Period

We will continue to monitor site statistics to determine site usage patterns. To promote greater site usage, we will work to get additional stakeholders to link to NoiseQuest and to provide recommendations for content.

Task 8.2- Content Development

Pennsylvania State University

Objective

This task focuses on identifying and developing content that addresses aviation noise impact and outreach education.

Research Approach

The Outreach team seeks to identify content that presents updates on aviation noise research, addresses noise issues, or meets the educational outreach needs of aviation stakeholders on specific topics.

Milestones

The team maintained existing site areas and added new content.

Major Accomplishments

The content organization was reviewed and updated as part of the site restructuring to enhance accessibility across all platforms. Featured content on AEDT, NextGen and Performance-Based Navigation was updated.

Publications

Site developed at www.noisequest.psu.edu

Outreach Efforts

We developed the Outreach content by reaching out to stakeholders for content ideas and development.

Awards

None.

Student Involvement

None.

Plans for Next Period

Content is currently in development. The plans for the future included generating enhanced content to further engage the public. New content topics will be identified and relevant features added to the site. Further topics will be identified based on stakeholder engagement.

Task 8.3- Site Navigation and Architecture Redesign and Development

Pennsylvania State University

Objective

Efforts under this task maintain the site architecture.

Research Approach

This effort includes website management including backups, updates, and infrastructure enhancement. The effort assures that the information on NoiseQuest is presented in an easily navigated, user-friendly format.

Milestones

Review of the site was completed and updates and new content was posted to the site.

Major Accomplishments

The site was reworked, with changes to the navigation features. To monitor usage of the entire site, website statistics can be viewed using Google Analytics. Changes were made to navigational aspects of the site to facilitate the ease of use across multiple platforms.

Publications
None.

Outreach Efforts
The team works to ensure that the changes resulted in clarity and ease of navigation across multiple platforms. These actions were taken to increase the mobile user base.

Awards
None.

Student Involvement
None.

Plans for Next Period
The site is now device agnostic and user-friendly on all platforms. The team will continue website management which includes backups, updates, and infrastructure enhancement as warranted.

Appendix A. NoiseQuest Statistics Usage in 2019

Table 1. NoiseQuest Usage by Country and Device

Country	Device Category	Users	Sessions	Pages/ Session
		38,672 **% of Total: 100.00%**	**43,660** **% of Total: 100.00%**	1.47 Avg. for View: 1.47
United States	desktop	10,305 (26.75%)	11,503 (26.35%)	1.81
United States	mobile	7,697 (19.98%)	8,733 (20.00%)	1.35
India	mobile	3,949 (10.25%)	4,543 (10.41%)	1.20
India	desktop	1,442 (3.74%)	1,586 (3.63%)	1.23
United Kingdom	mobile	1,392 (3.61%)	1,526 (3.50%)	1.26
United Kingdom	desktop	1,216 (3.16%)	1,321 (3.03%)	1.46
United States	tablet	978 (2.54%)	1,188 (2.72%)	1.78
Philippines	desktop	750 (1.95%)	864 (1.98%)	1.29
Canada	desktop	624 (1.62%)	664 (1.52%)	1.51
Philippines	mobile	516 (1.34%)	655 (1.50%)	1.27

Table 2. NoiseQuest Usage by Page

Rank	Page	Pageviews	% Pageviews
		64,127	100%
1.	/noisebasics-basics.html	14,003	21.84%
2.	/nationalairspace-typesofairports.html	12,016	18.74%
3.	/communitytools-faq.html	8,656	13.50%
4.	/	4,423	6.90%
5.	/communitytools-glossary.html	2,627	4.10%
6.	/noiseeffects-reducingnoise.html	2,260	3.52%
7.	/nqexplorer.html	1,538	2.40%
8.	/sourcesofnoise-military.html	1,299	2.03%
9.	/communitytools-homebuyers.html	1,294	2.02%
10.	/noisebasics-noisemodels.html	1094	1.71%

Table 3. NoiseQuest Usage by Country

Rank	Country	Users	% Users
1.	United States	19,042	49.36%
2.	India	5,437	14.09%
3.	United Kingdom	2,932	7.60%
4.	Philippines	1,287	3.34%
5.	Canada	1,121	2.91%
6.	Australia	916	2.37%
7.	Malaysia	537	1.39%
8.	Nigeria	478	1.24%
9.	Pakistan	462	1.20%
10.	Singapore	377	0.98%

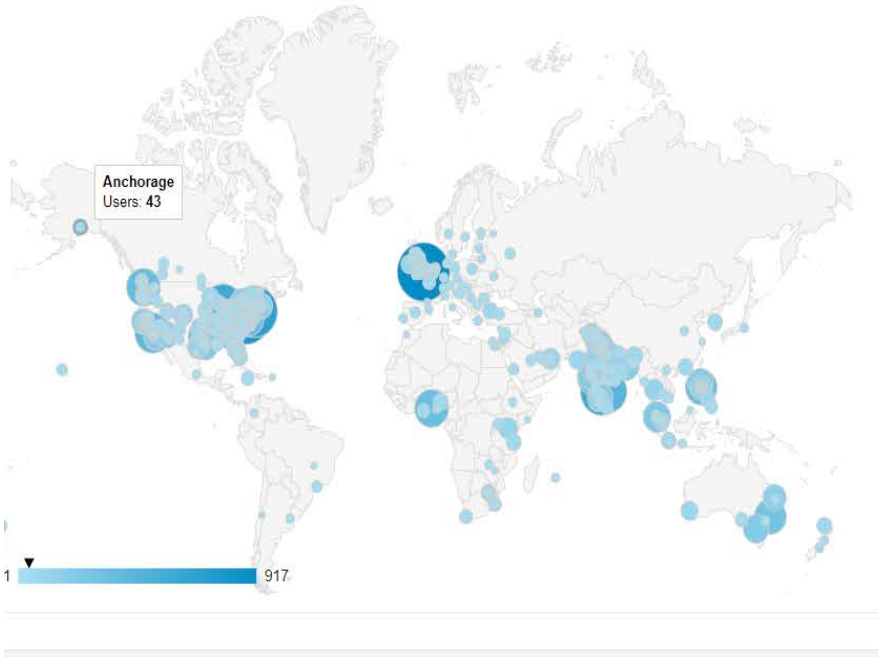

Figure 1. Global NoiseQuest Users by City. Example: 43 Users in Anchorage during 2019.

Project 010 Aircraft Technology Modeling and Assessment

Georgia Institute of Technology and Purdue University

Project Lead Investigators

Dimitri Mavris (PI)
Regents Professor
School of Aerospace Engineering
Georgia Institute of Technology
Mail Stop 0150
Atlanta, GA 30332-0150
Phone: 404-894-1557
E-mail: dimitri.mavrisatae.gatech.edu

William Crossley (PI)
Professor
School of Aeronautics and Astronautics
Purdue University
701 W. Stadium Ave
West Lafayette, IN 47907-2045
Phone: 765-496-2872
E-mail: crossleyatpurdue.edu

Jimmy Tai (Co-PI)
Senior Research Engineer
School of Aerospace Engineering
Georgia Institute of Technology
Mail Stop 0150
Atlanta, GA 30332-0150
Phone: 404-894-0197
E-mail: jimmy.taiatae.gatech.edu

Daniel DeLaurentis (Co-PI)
Professor
School of Aeronautics and Astronautics
Purdue University
701 W. Stadium Ave
West Lafayette, IN 47907-2045
Phone: 765-494-0694
E-mail: ddelaureatpurdue.edu

University Participants

Georgia Institute of Technology

- P.I.(s): Dr. Dimitri Mavris (PI), Dr. Jimmy Tai (Co-PI)
- FAA Award Numbers: 13-C-AJFE-GIT-006, -012, -022, -031, -041
- Period of Performance: September 1, 2018 to August 31, 2019
- Task(s): 1-5

Purdue University
- P.I.(s): Dr. William A. Crossley (PI), Dr. Daniel DeLaurentis (Co-PI),
- FAA Award Numbers: 13-C-AJFE-PU-004, -008, -013, -018, -026, -032
- Period of Performance: September 1, 2018 to August 31, 2019
- Task(s): 1, 2, 4, 5

Project Funding Level

The project was funded at the following levels: Georgia Institute of Technology ($650,000); Purdue University ($114,185). Cost share details are below:

The Georgia Institute of Technology has agreed to a total of $650,000 in matching funds. This total includes salaries for the project director, research engineers, and graduate research assistants, as well as computing, financial, and administrative support, including meeting arrangements. The institute has also agreed to provide tuition remission for the students, paid for by state funds.

Purdue University provides matching support through salary support of the faculty PIs and through salary support and tuition and fee waivers for one of the graduate research assistants working on this project.

Investigation Team

Georgia Institute of Technology
- PI: Dimitri Mavris
- Co-Investigator: Jimmy Tai (Task 5)
- Fleet Modeling Technical Leads: Holger Pfaender and Mohammed Hassan (Tasks 1, 2, 3, 4)
- Graduate Students: Thomas Dussage, Taylor Fazzini, Rick Hong, Nikhil Iyengar, Barbara Sampaio, Kevyn Tran, Edan Baltman

Purdue University
- PI: William Crossley (Tasks 1, 2, 4 and 5)
- Co-Investigator: Daniel DeLaurentis (Tasks 1, 2, 4 and 5)
- Graduate Students: Samarth Jain, Kolawole Ogunsina, Hsun Chao

Project Overview

Georgia Institute of Technology (Georgia Tech) and Purdue partnered to investigate the future demand for supersonic air travel and the environmental impact of supersonic transports (SSTs). In the context of this research, environmental impacts include direct CO_2 emissions and fuel consumption. The research was conducted as a collaborative effort to leverage capabilities and knowledge available from the multiple entities that make up the ASCENT university partners and advisory committee. The primary objective of this research project was to support the Federal Aviation Administration (FAA) in modeling and assessing the potential future evolution of the next-generation supersonic aircraft fleet. Research under this project consisted of five integrated focus areas: (a) establishing fleet assumptions and performing demand assessment; (b) performing preliminary SST environmental impact prediction; (c) testing the ability of the current Aviation Environmental Design Tool (AEDT) to analyze existing supersonic models; (d) performing vehicle and fleet assessments of potential future supersonic aircraft; and (e) modeling SSTs by using an Environmental Design Space (EDS) derivative modeling and simulation environment named Framework for Advanced Supersonic Transport (FASST).

To develop suitable assumptions for the fleet-level analysis incorporating new supersonic vehicles, it is necessary to forecast the future demand for supersonic air travel. Georgia Tech followed a two-step approach that first examines historical data to identify current premium demand (business and first class) and then estimates how such demand would scale for supersonic travel. This approach was applied globally. The first step was to develop a supersonic routing tool able to correctly find optimum ground tracks that avoid exposing land to sonic booms, while enabling evaluation of the possible time savings as well as estimation of the increased cost. For the second step, cost data documented by Airlines for America (A4A) were utilized and then scaled to estimate the cost of a supersonic airliner. Together, the two steps provided a better understanding of the potential demand for future commercial supersonic travel from both a passenger and an airline perspective.

In an independent but complementary approach to consider demand and routes for supersonic aircraft, the Purdue team developed a ticket pricing model for possible future supersonic aircraft that relies upon current as-offered fares for business class and above, for routes that could have passenger demand for supersonic aircraft. Via an approach considering the size of the potential demand at fares business class and above on a city-pair route, the distance of that city-pair route, an adjustment to allow for the shortest trip time by increasing the overwater distance of the route, and the range capability of a simplistically modeled medium SST (55-passenger capacity) to fly that route, the Purdue team identified 205 potential routes that could see supersonic aircraft service in a network of routes with at least one end in the United States. Of these 205 potential routes, 193 are direct routes, and 12 are routes with fuel stops. By providing these potential routes to the Fleet-Level Environmental Evaluation Tool (FLEET) simulation, the allocation problem in FLEET then determines how many supersonic aircraft would operate on these routes, giving a prediction of which routes would see supersonic aircraft use and the number of supersonic flights operated on those routes at dates in the future.

To provide a preliminary estimate for the performance of supersonic vehicles, the Georgia Tech team started by establishing a reference performance for a subsonic vehicle. Quantitative estimates of the impact of supersonic vehicles on the various key environmental indicators (KEIs), especially fuel efficiency, were then derived on the basis of literature review, future performance targets set by the National Aeronautics and Space Administration (NASA), and engineering judgement. For an appropriate estimation, performance parameters such as cruise lift-to-drag (L/D) ratio and engine thrust specific fuel consumption (TSFC) values were required. Those values could be determined from preliminary constraint, mission, and utilization analyses conducted on the basis of the vehicle's design mission requirements. Georgia Tech developed this rapid interactive tool to inform design decisions for vehicles developed in Task 5 and for assessing publicly announced vehicle capabilities. In addition, to facilitate environmental impact prediction for supersonic aircraft, modeling capabilities and potential gaps in existing tools must be identified. Georgia Tech identified existing supersonic aircraft models in the AEDT vehicle database, including the Concorde and some military aircraft. These models were reviewed to determine how they were modeled. The team developed a white paper outlining improvements necessary to accommodate supersonic vehicles in future AEDT versions.

One of the accomplishments of the project during the performance period is the preliminary development of the FASST, a modeling and simulation environment based on the architecture of EDS developed specifically for SSTs. Two supersonic vehicles, a business jet and medium SST, have been modeled in the preliminary version of FASST. The business jet SST is designed to carry 8 to 12 passengers for 4,000 nmi cruising at Mach 1.4. The medium SST is designed to carry 55 passengers for 4,500-nmi cruising at Mach 2.2. Currently, the engine design for the business jet SST is a derivative design using the core of a notional CFM56-7B27 engine, and the engine design for the medium SST is a clean sheet design.

Georgia Tech and Purdue exercised their respective fleet analysis tools—the Global and Regional Environmental Analysis Tool (GREAT) and Fleet-Level Environmental Evaluation Tool (FLEET)—and produced estimates of the fleet-level impact of a potential fleet of supersonic aircraft operating in the future. The SSTs required for these fleet-level analyses are provided by the vehicle modeling tasks with FASST, a derivative framework from EDS. The outcome of this study provides a glimpse into the future potential state of supersonic air travel by using physics-based models of supersonic vehicle performance. Future work should build on current estimates to conduct more detailed analyses of vehicle and fleet performance.

Table of Acronyms and Symbols

α	T/T_{SL}, installed full-throttle thrust lapse
A4A	Airlines for America
A_C	Inlet capture area
ADP	Aerodynamic design point
AEDT	Aviation Environmental Design Tool
ANP	Aircraft noise performance
A_O	Reference inlet area
APU	Auxiliary power unit
β	W/W_{TO}, ratio of instantaneous weight to takeoff weight or side slip angle
BADA	Base of Aircraft Data
BFFM	Boeing Fuel Flow Method
BPR	Bypass ratio
BTS	Bureau of Transportation Statistics
CAEP	Committee on Aviation Environmental Protection
CART3D	NASA Inviscid Computational Fluid Dynamics Program
CAS	Calibrated airspeed
C_{D_O}	Profile drag
C_{D_R}	Additional drag caused by flaps, ground friction, etc.
CG	Center of gravity
C_L	Lift coefficient
CLEEN	Continuous lower energy, emissions, and noise
CMPGEN	NASA Program for Compressor Map Generation
CO_2	Carbon dioxide
d	Distance between center of inoperative engine and aircraft longitudinal axis
Δt	Total segment flight time
ΔT	Change in temperature from standard atmospheric temperature
ΔX	Distance between CG of vehicle and aerodynamic center of tail
Δz_e	Total change in segment energy height
D	Drag
DNL	Day-night level
EDS	Environmental Design Space
EEDB	Engine Emissions Databank
EI	Emissions index
EIS	Entry into service
EPNdB	Effective perceived noise in decibels
ϕ	Cooling effectiveness
FAA	Federal Aviation Administration
FASST	Framework for Advanced Supersonic Transport
FLEET	Fleet-Level Environmental Evaluation Tool
FLOPS	Flight Optimization System
FPR	Fan pressure ratio
GRA	Graduate research assistant
GREAT	Global and Regional Environmental Analysis Tool
HPC	High-pressure compressor
HPCPR	High-pressure-compressor pressure ratio
HPT	High-pressure turbine
ICAO	International Civil Aviation Organization
IDEA	Interactive Dynamic Environmental Analysis
IGV	Inlet guide vanes
ISA	International standard atmosphere
K_1	Coefficients of parabolic lift-drag polar
K_2	Coefficients of parabolic lift-drag polar
KEI	Key environmental indicators
JFK	John F. Kennedy International Airport code

LAX	Los Angeles International Airport code
L/D	Lift-to-drag ratio
LPC	Low-pressure compressor
LPCPR	Low-pressure-compressor pressure ratio
LPT	Low-pressure turbine
LSA	Large single aisle
LTA	Large twin aisle
LTO	Landing and takeoff
M	Mach number
MDP	Multi-design point
MFTF	Mixed flow turbofan
MTOM	Maximum takeoff mass
MTOW	Maximum takeoff weight
n	Load factor or number of flight segments
NASA	National Aeronautics and Space Administration
NOx	Nitrogen oxide
NPD	Noise power distance
NPR	Nozzle pressure ratio
NPSS	Numerical Propulsion System Simulation
OGV	Outlet guide vanes
OpenVSP	Open Vehicle Sketch Pad
OPR	Overall pressure ratio
PACI	Passenger Airline Cost Index
PCBOOM	NASA PC Software for Predicting Sonic Boom on the Ground
PDEW	Passengers daily each way
PI	Principal investigator
PIPSI	Performance of Installed Propulsion System Interactive
PLdB	Sound pressure level in dB
P_s	Weight specific excess power
q	Dynamic pressure
ρ	Air density
R	Rolling resistance force
$R_{C,max}$	Maximum cruise range for supersonic vehicles
RJ	Regional jet
S	Wing area
S_C	Cruise range
SA	Single aisle (includes both SSA and LSA classes)
SEL	Single event level
SFTF	Separate flow turbofan
SLS	Sea level static
SSA	Small single aisle
SST	Supersonic transport
STA	Small twin aisle
S_{tail}	Tail area
T	Thrust
$T3$	Compressor exit temperature
$T41$	Turbine rotor entrance temperature
t_{cool}	Cooled temperature
$t_{C,sub}$	Cruise time for subsonic vehicle
$t_{C,sup}$	Cruise time for supersonic vehicle
t_{gas}	Gas temperature
TO	Takeoff
t_{metal}	Metal temperature
TOC	Top of climb
TSFC	Thrust specific fuel consumption
T_{SL}	Thrust at sea level
$t_{total,sub}$	Total subsonic flight time
$t_{total,sup}$	Total supersonic flight time

V	Velocity
V_C	Cruise speed
$V_{C,sub}$	Subsonic cruise speed
$V_{C,sup}$	Supersonic cruise speed
V_{SR1}	Reference stall speed
VLA	Very large aircraft
VTTS	Value of travel time savings
WATE	Weight approximation for turbine engines
W_E	Empty weight
W_F	Fuel weight
W_f	Weight of aircraft at the end of a mission segment
W_i	Weight of aircraft at the beginning of a mission segment
W_P	Payload weight
W_{TO}	Takeoff weight
x	Percentage of flight over water

Project Overview

Georgia Tech and Purdue partnered to investigate the effects of supersonic aircraft on future environmental impacts of aviation. Impacts assessed at the fleet level include direct CO_2 emissions and fuel consumption. The research was conducted as a collaborative effort to leverage capabilities and knowledge available from the multiple entities that make up the ASCENT university partners and advisory committee.

The primary objective of this research project was to support the FAA in modeling and assessing the potential future evolution of the next-generation supersonic aircraft fleet. Research under this project consisted of four integrated focus areas: (1) Developing a set of harmonized fleet assumptions for use in future fleet assessments; (2) modeling the environmental impact of supersonic vehicles expected to enter the fleet through 2050; (3) analyzing supersonic vehicle performance by using AEDT, and (4) performing vehicle- and fleet-level assessments based on input from the FAA and the results of (1) and (2) and EDS vehicle modeling (5) results.

Because of extensive experience in assessing the FAA Continuous Lower Energy, Emissions, and Noise project (CLEEN I), Georgia Tech was selected as the lead for all four objectives described above. Purdue supported the objectives shown in Table 1, which lists the high-level division of responsibilities.

Table 1. University contributions.

Objectives		Georgia Tech	Purdue
1	Fleet Assumptions & Demand Assessment	Identify supersonic demand drivers and supporting airports, and project demand for all scenarios Expand to international airports	Estimate latent demand and flight schedules for supersonic aircraft
2	Preliminary Vehicle Environmental Impact Prediction	Develop estimates of KEIs for supersonic aircraft relative to current-technology subsonic aircraft, Develop estimates of likely operating altitudes	Support with expert knowledge
3	AEDT Vehicle Definition	Test the ability of the current version of AEDT to analyze existing supersonic models Work with AEDT developers to understand the required modifications to support supersonic vehicles	N/A
4	Vehicle and Fleet Assessments	Apply GREAT to estimate the impact of SSTs in terms of fuel burn, water vapor, and landing and takeoff nitrogen oxide for a combination of vehicles and scenarios	Apply FLEET to estimate the impact of SSTs in terms of fuel burn, water vapor, and landing and takeoff nitrogen oxide
5	EDS Vehicle Modeling	Create two EDS supersonic vehicle models with boom signatures	Support with expert knowledge

Georgia Tech led the process of conducting a literature review on potential future demand for supersonic travel for fleet and technology evolution and evaluation. The focus this year was on expanding the analysis to international airports. This work was performed under Objective 1, and the outcome was used to support Objective 4. Under Objective 2, Georgia Tech developed conceptual design tools to estimate the environmental impact of supersonic vehicles compared with subsonic ones. In addition, Georgia Tech used AEDT to analyze supersonic aircraft performance under Objective 3. Georgia Tech also produced results for multiple scenarios to assess the fleet-level impacts of supersonic vehicles under Objective 4. Under Objective 5, two vehicle models were developed.

Purdue applied their FLEET tool under Objective 4, using a subset of the fleet assumptions defined in Objective 1 and preliminary vehicle impact estimates from Objective 2. This activity demonstrated the capabilities of FLEET for assessment of fleet-level environmental impacts as a result of new aircraft technologies and distinct operational scenarios.

Milestone(s)

Georgia Tech had four milestones for this year of performance:

1. Updated projected supersonic demand for the A10 scenarios
2. Development of KEIs for the list of current and future subsonic aircraft by type and size class
3. Updated fleet-level environmental impacts for each scenario in Aviation Portfolio Management Tool (APMT)-compatible format
4. FASST SST descriptions and characteristics in PowerPoint format

For Purdue, the proposal covering this year of performance listed two milestones:

1. Complete modeling of the chosen contractor's technologies
2. Updated fleet assessment

The Purdue team is using its in-house simplistic "back of the envelope" representation of the A10 notional medium SST aircraft; the representation of this in FLEET matches that of the earliest proposed supersonic aircraft, one that will fly at Mach 2.2 but only during overwater portions of flight. The team identified 205 potential "supersonic-eligible" routes, including 193 nonstop routes and 12 routes with fuel stops.

The Purdue team has also incorporated the supersonic aircraft model and performed initial fleet-level assessments for the single Current Trends Best Guess (CTBG) scenario. The FLEET allocation results indicate routes where supersonic aircraft might be used and the number of operations.

Major Accomplishments

The following were the major tasks completed under ASCENT Project 10 during the period of performance:

Fleet assumptions and demand assessment

The Georgia Tech team expanded the preliminary estimates of potential markets and routes for supersonic aircraft to a global set of routes. This was also supplemented by the development of a supersonic routing tool. This tool allows for more accurate route data, such as potential time savings, to be computed to supplement existing market and demand data as well as analysis of ticket price.

The Purdue team developed a "back of the envelope" representation of the A10 notional medium SST aircraft on the basis of the Breguet range equation with L/D ratios and specific fuel consumption values deemed reasonable for a near-future supersonic aircraft. Using the supersonic aircraft's range characteristics and the estimated block time savings possible, the team identified "supersonic-eligible" routes including both nonstop routes and routes with one fuel stop.

Preliminary vehicle environmental impact prediction

Georgia Tech finalized the development of a parametric constraint and sizing environment allowing users to explore aircraft sizing and performance constraints. This was used to inform constraints and parameters for Task 5 as well as to estimate preliminary environmental performance metrics for several potential future concept aircraft.

AEDT vehicle definition

Georgia Tech investigated and identified the existing gaps in modeling supersonic aircraft in AEDT. The result was a white paper on the modeling requirements and potentially required changes to the AEDT code and the associated modeling standards to improve and enable modeling of specific aspects of supersonic aircraft and their environmental impacts. This white paper was used to develop a plan for model improvements to develop the capability of future versions of AEDT to correctly model supersonic aircraft.

Vehicle and fleet assessments

Georgia Tech used the GREAT and Interactive Dynamic Environmental Analysis (IDEA) models to simulate the impact of potential supersonic vehicles on the fleet-level performance. This was used to identify the potential routes for the route optimization algorithm, which culminated in actual realized demand for the possible time savings on overland-restricted routes.

The Purdue team has updated problem formulation in FLEET from the previous year to predict which of the potential supersonic routes lead to profitable supersonic aircraft operations, the number of round trips operated by supersonic aircraft

on those routes, and how the airline then satisfies the rest of its passenger demand with the subsonic aircraft in its fleet for a representative day over a sequence of many years.

EDS vehicle modeling
Although EDS was developed for subsonic vehicles, its structure is still relevant and useful to adapt for the design of supersonic vehicles. One of the major accomplishments during this period of performance is the development of the supersonic version of EDS called FASST. Beyond architecting of the structure of FASST, another accomplishment is the development of a preliminary model of a medium-sized SST by using FASST. The preliminary medium SST carries 55 passengers with a range of 4,500 nmi cruising at Mach 2.2.

Task 1 - Fleet-Level Assumption Setting and Demand Assessment

Georgia Institute of Technology and Purdue University

Objective(s)

This task focused on identifying and predicting significant drivers of commercial supersonic travel demand. For this year, focus was on U.S. operations. Using scenarios from prior ASCENT Project 10 work, Georgia Tech was to identify drivers of supersonic demand to and from the United States, including domestic operations and international flight connections arriving to or departing from U.S. airports. In parallel, Purdue was to predict the latent demand for supersonic travel by using the same ASCENT 10 scenarios to bound the potential future demand. Georgia Tech was to identify specific airports globally that are likely to support supersonic operations under the various previously defined scenarios. Georgia Tech was to pass this information to Purdue to generate flight schedules (number of operations) for each identified airport. This information would then be used in Task 4 to estimate the impact of supersonic travel.

Research Approach (Georgia Tech)

To investigate demand for commercial supersonic travel, Georgia Tech followed a two-step approach that first examines historical data to identify current premium demand (business and first class) and then estimates how such demand would scale for supersonic travel. The first step relied heavily on data derived from the Bureau of Transportation Statistics (BTS) databases, especially the Airline Origin and Destination Survey (DB1B) database, which provided information on passenger itineraries on the basis of a 10% sampling of airline tickets from reporting carriers. For the second step, cost data documented by A4A were utilized. The A4A Passenger Airline Cost Index (PACI) was used to establish a baseline airline cost structure based on current operating costs. That structure was then scaled to estimate that of a supersonic airliner. Together, the two steps provided a better understanding of potential demand for future commercial supersonic travel from both a passenger and an airline perspective.

Current demand for premium seats
In gauging the demand for commercial supersonic travel, Georgia Tech attempted to identify current demand for premium seats. This is because supersonic travel, especially in the near term, is expected to cost more than subsonic travel (owing to the increased time savings and increased associated costs). The historical performance of the Concorde also supports that assumption. As a result, identifying current premium passengers became a priority. The 2016 BTS DB1B database provided important information for beginning this process. The database not only includes basic travel information such as origin, destination, and miles flown, but also includes important information such as number of passengers, fare class, and fare per mile. Premium passengers were identified as those who flew in the business and first classes (i.e., BTS DB1B fare classes C: unrestricted business class, D: restricted business class, F: unrestricted first class and G: restricted first class). However, there were some limitations in using the DB1B database. First, the data provided represent only a 10% sample of actual demand and are not a full representation of the flying public. It was assumed that the sample was large enough to be representative of total demand. Second, the DB1B database is restricted to U.S. domestic flights and does not include any information regarding international travel. This was a major limitation, because most supersonic operations, especially in the near term, are expected to be transoceanic (for the United States, this means most international travel across the Atlantic and Pacific oceans). The Georgia Tech team inquired about a more inclusive dataset from the BTS; however, access to such a dataset is restricted because of proprietary concerns. To overcome this limitation, the team relied on an additional inventory of global flights to which it has access. The inventory provides information on all flights in 2015, including the number of seats and number of operations, but, unlike the DB1B database, it does not specify the fare class or number of passengers. Assumptions regarding passenger load factor and premium passenger share were necessary to conduct a preliminary demand assessment. Results for U.S. domestic (using the 2016 BTS DB1B database) and global international (using the 2015 inventory) demand for premium seats are presented below.

For domestic demand, the cumulative average daily premium passengers were aggregated by fare paid, by using the DB1B data. This process was done by first filtering out all non-premium passengers (BTS DB1B fare classes U: unknown, X: restricted coach class and Y: unrestricted coach class), multiplying the number of passengers by 10 (because the DB1B is a 10% sample of total passengers), and then finally dividing by 365 (because the DB1B is annual). The *x* axis in Figure 1 represents the fare per mile in 2016 US dollars (calculated by dividing the total fare by trip distance). The *y* axis represents the cumulative average daily passengers who paid a certain fare per mile or higher. For example, the plot shows that approximately nine daily passengers paid three dollars per mile or higher in 2016 (orange square). The general trend is plotted in blue. Overall, the trend is sensible, because it suggests that demand decreases as price increases. For current subsonic operations, the average fare per mile is estimated to be on the order of 20 cents (shown in green on the plot). In addition, future supersonic operations are estimated to target an average fare per mile of 100 cents (shown in red on the plot). This result suggests that, at least for 2016 operations, supersonic airlines can capture a daily demand of approximately 100 premium passengers (red dotted line).

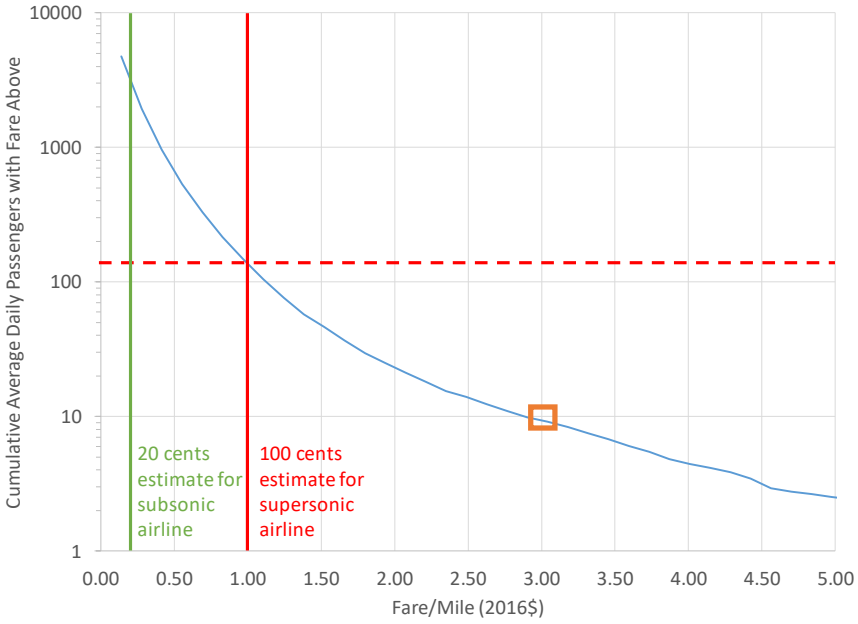

Figure 1. Demand curve estimation.

For international demand, the premium passengers daily each way (PDEW) was plotted against flight distance for all flights (Figure 2). This process was done by utilizing appropriate assumptions for passenger load factor and premium seat share to determine the number of premium passengers (because the inventory includes only the number of seats) and then dividing by 365 to compute the PDEW. Results from domestic demand analysis were used as a reference to estimate international demand. It is estimated that the international demand for supersonic travel would target routes with PDEW values greater than 55 (area above the horizontal orange line). This would provide enough demand to fill a single 55-seat plane with a single flight per day. Furthermore, this shows the potential size of the market, and it is therefore advisable to target markets that are large enough to support a high load factor without having to capture all of the existing potential demand, because that would be unrealistic. Supersonic flights, especially in the near term, are estimated to be long-haul flights of distances greater than 1,500 nmi (area to the right of the vertical orange line). Hence, it is estimated that international supersonic demand would be for routes that lie within the shaded orange area. These routes are plotted on the map shown in Figure 3. The thickness of the lines in the map corresponds to PDEW (thicker lines indicate routes with higher PDEW).

Potential airline market for supersonic travel

After analyzing the potential demand from a passenger perspective, the Georgia Tech team investigated the market for supersonic travel from an airline perspective. A4A data for airline operating costs were used to establish a baseline airline

cost structure representative of subsonic operations. Specifically, PACI data for the fourth quarter of 2016 were used to establish the structure shown in Figure 4.

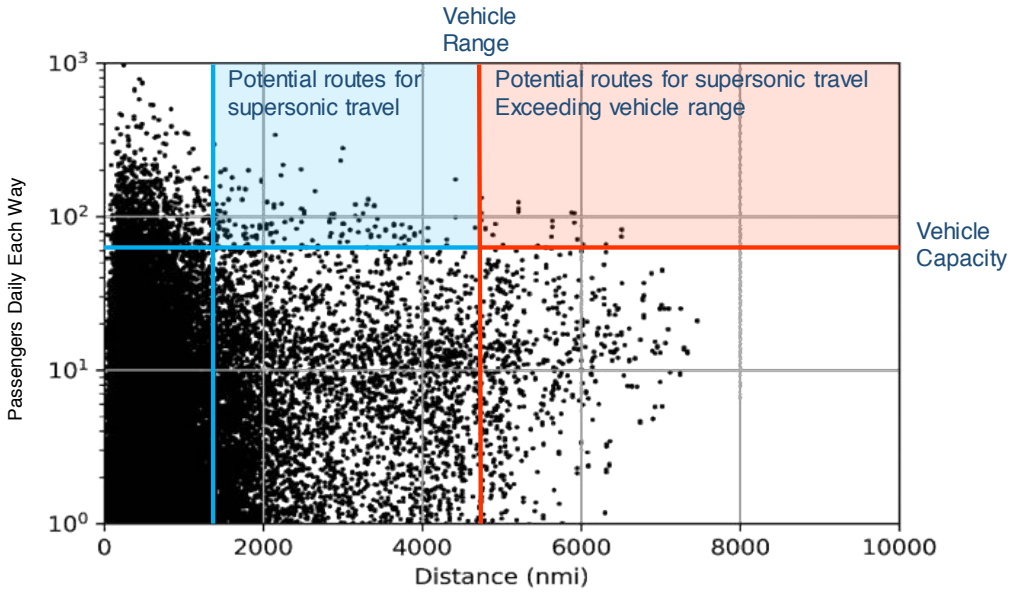

Figure 2. Market selection.

Figure 3. Selected routes.

As shown in Figure 4, "labor" and "fuel" costs account for approximately 50% of all airline operating costs. Other major contributors include "aircraft rents and ownership" and "professional services." This baseline structure was assumed to be representative of that for a currently operational reference subsonic aircraft with certain specifications. To estimate a similar

cost structure representative of operating costs for a concept supersonic aircraft, the specifications of the latter needed to be estimated relative to those of the reference aircraft. Engineering judgement was used, along with some feedback input based on the results of Task 2, to define the specifications of the concept supersonic vehicle. With these specifications, and by normalizing the cost structure by flight hour, the baseline airline structure could be adjusted to reflect the differences in various component costs (e.g., fuel and maintenance).

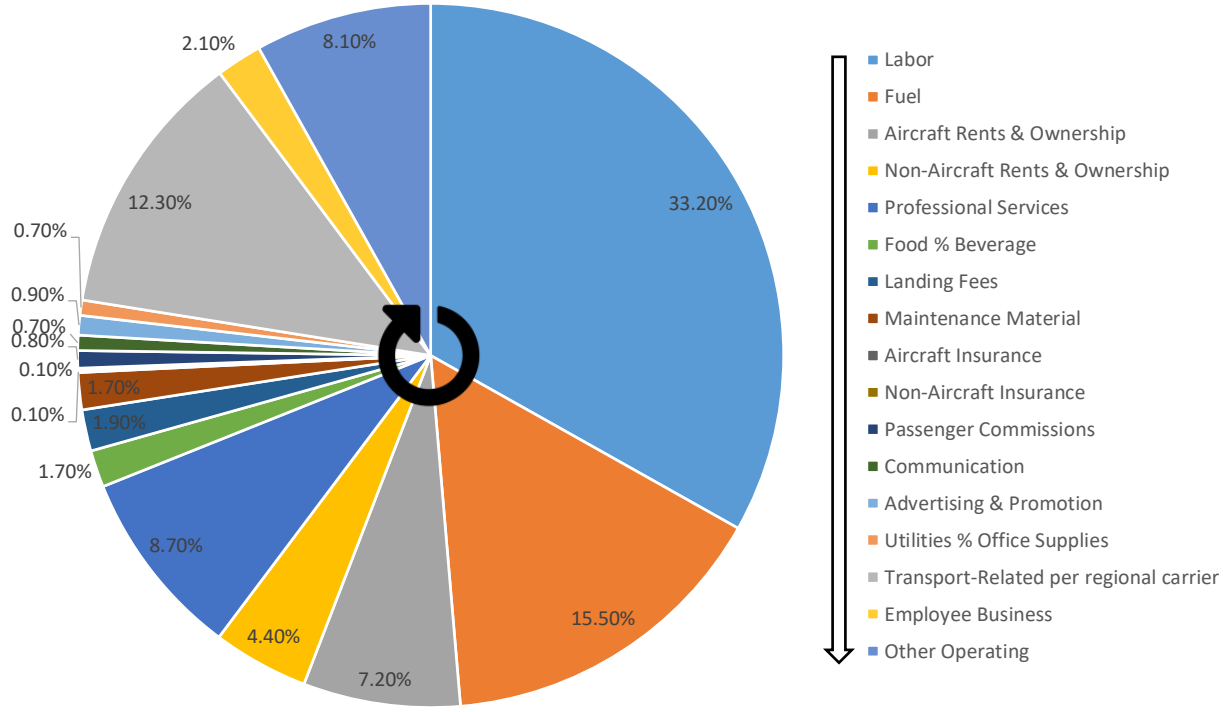

Figure 4. Commercial-airline cost index.

An important parameter that was estimated with this procedure was the required yield per seat mile (i.e., the average fare per seat mile). If airline profit margins are assumed to remain the same as those for subsonic operations, yield directly correlates with operating costs. The operating cost was estimated for different utilization and fuel consumption scaling values in Figure 5, which shows the resulting trends. Generally, the more fuel that is consumed, the higher the required yield should be to maintain the same profit margins. Alternatively, higher utilization allows for lower required yield values. For the concept supersonic aircraft characteristics assumed (fuel consumption 8 times that of subsonic aircraft and utilization of 1,000 hr per year), it was found that required yield would need to be almost 4.5 times that of subsonic operations for airlines to maintain the same profit margins (red square). Consequently, on average, airlines would need to charge passengers of supersonic flights 4.5 times more than passengers of subsonic flights. These adjustments are shown in Table 2.

Table 2. Relative cost index adjustments.

	Reference Subsonic Aircraft	Concept Supersonic Aircraft
Number of Seats	180	100
Load Factor	0.8	0.8
Block Speed (miles per hour)	500	1,350
Utilization (hours per year)	4,500	1,000
Fuel Consumption (relative per block hour)	1.0	8.0
Maintenance Costs (relative)	1.0	3.0
Acquisition Costs (relative)	1.0	2.0

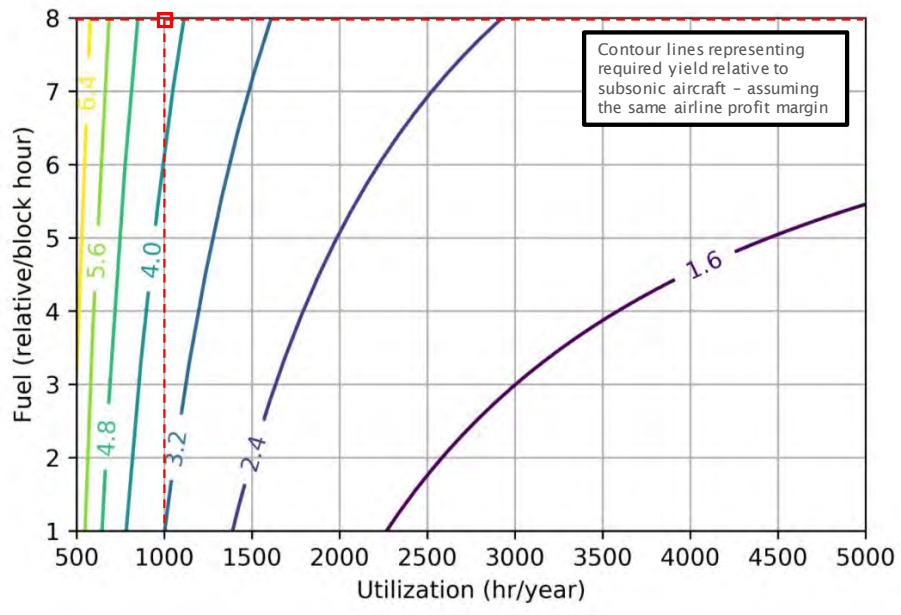

Figure 5. Relative required yield as a function of fuel multiplier and utilization.

As is quickly evident, the key determinant of the demand for SSTs is the value of travel time savings (VTTS). In a constrained scenario in which supersonic aircraft cannot fly supersonically over land to avoid exposing the land to sonic booms, the potential time savings is substantially constrained, and the cost is it increased because of potentially increased fuel burn of the aircraft operating under suboptimal conditions. The overall process approach is shown in Figure 6.

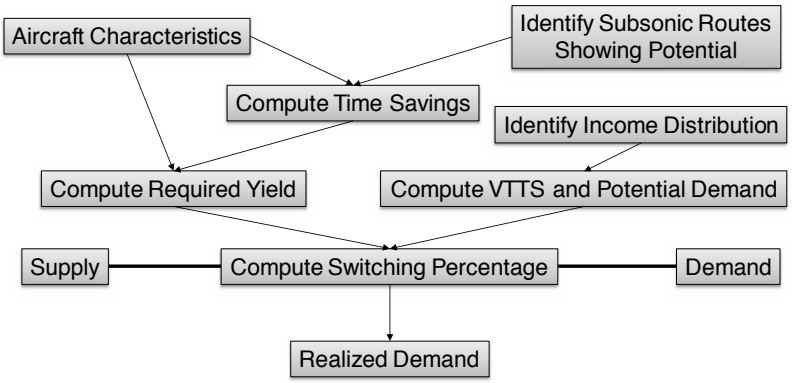

Figure 6. Process overview.

The steps are to start with the aircraft characteristics such as seat capacity and cruise Mach number or speeds. This process aids in identifying possible routes for a subsonic network that could show potential in supporting a premium supersonic service. After these routes have been identified, the estimated time savings can be computed; this can range from a simplistic speed differential—assuming that supersonic flight is permissible anywhere—to more sophisticated scenarios, as explained below with a routing algorithm that takes into account constraints such as no supersonic flight over land.

After the time savings are known, the required yield, or more simply an approximate ticket price, can be computed on the basis of the airline cost structure and estimates of the various operating cost factors and how they could be different for a new SST aircraft. The required yield and the time savings can then be used to compute the VTTS, which is the worth of an

hour of travel-time reduction. By using income distributions, a distribution of travel-time savings can be derived. This, along with a distribution of travel frequency, was then used to estimate the switching percentage, which is the fraction of passengers who would be willing to pay extra to save the specific amount of time at the premium prices that could be offered by a supersonic aircraft. This percentage applied to the existing or estimated future airline demand then yields the realizable demand for each route.

To identify the potential time savings for a given route in a constrained scenario, it becomes quickly evident that the geography of the origin and destination airport determines the specifics. In many cases—except direct overwater-only routes—the "best" route will potentially markedly deviate from the minimum-distance great circle ground track. Additionally, the question of what is "best" or optimum arises. Ideally this could be defined as the minimum time subject to attempting to minimize the subsonic portions over land, while minimizing the deviation from the great circle track. However, other considerations can be included, such as the consideration that the acceleration from subsonic to supersonic speeds can be quite costly in terms of fuel consumed, depending on the aircraft design.

The team first developed an algorithm based on the great circle track, splitting it into a number of control points, which then can be moved to optimize the ground track. An example for London Heathrow to New York John F. Kennedy International Airport (JFK) is shown in Figure 7. In this case, the track was divided to insert 10 movable control points perpendicular to the great circle track. This example also shows that the aircraft also must respect a stand-off buffer distance from the actual coast lines, because of the characteristics of the sonic boom propagation. The actual distance required depends highly on the shape, speed, and weight of the plane during its flight. Additionally, maneuvering, such as turning, accelerating, or decelerating, will also significantly affect the actual required stand-off distance. The typical value should probably be based on the lateral side stand-off distance, owing to the width of the boom carpet in steady level flight at cruise altitude and Mach number.

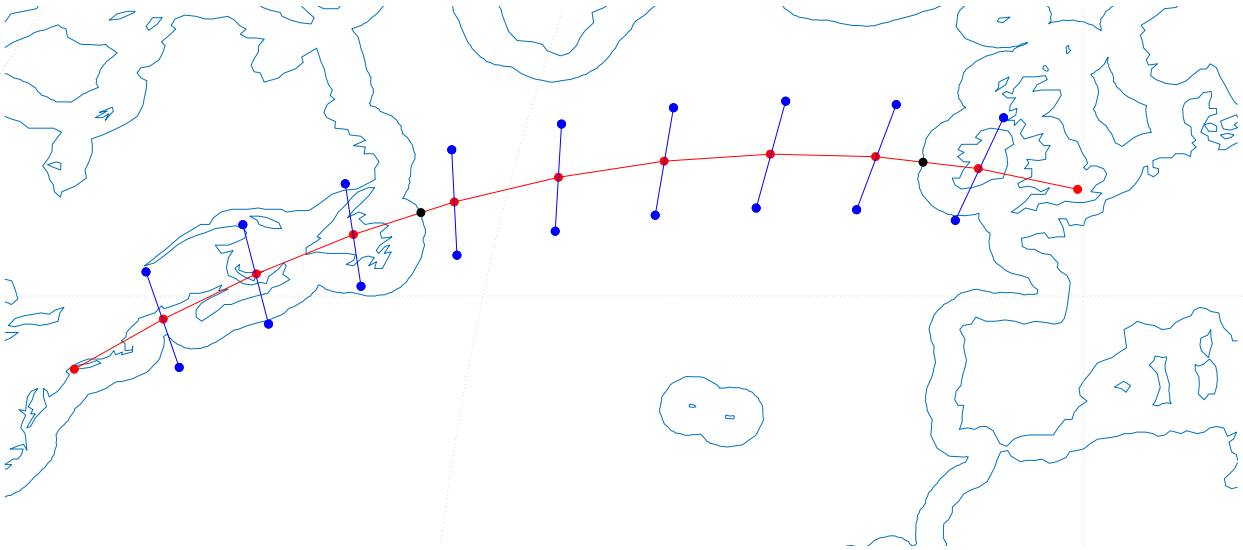

Figure 7. Example route stretching algorithm.

After experimenting with this approach, the team found that it is computationally very expensive. The shape of the land between routes in many cases is very non-uniform, and a simple optimization scheme often becomes stuck at a local minimum. Use of global optimization scheme that has a good chance of finding the global optimum is required. However, many runs of the optimizer are necessary to achieve this. Furthermore, the optimization space increases exponentially with the number of control points, yet some routes, especially long ones, require many additional points and still leave no possibility of fine control of the track to avoid obvious peninsulas and other land. Finally, the movement of the control points as described does not allow for departures or arrivals from the wrong way or the opposite direction, as can sometimes be necessary to depart or approach an airport from the ocean or water side and to avoid flying over land.

To alleviate these issues, the team switched to a more flexible algorithm based on the A-star algorithm, a derivative of Dijkstra's algorithm for finding the shortest path. It includes an optimistic heuristic estimate of the cost to the goal and thereby improves the time to convergence while still ensuring an optimum solution.

The implementation depends on a grid-based decomposition of the geography and land and ocean between the departure airport and arrival airport as well as ample space to accommodate deviations from the shorted great circle path. The possible choices for the algorithm are therefore the eight possible directions: four straight and four diagonal. In addition, instead of forcing the algorithm to assume supersonic flight when not over land or the buffer zone, the choice of subsonic or supersonic flight is also presented. This leaves the algorithm with 16 potential choices to investigate for each grid cell. The cost and heuristic functions implemented are purely time or fuel based or a mix of both, defined with a scaling parameter. This parameter is not a realistic choice that an airline would perform, such as a cost-index-based optimization. However, it can be used to explore the solution space, and then after the actual cost and time savings are known, the best solution can be chosen.

The algorithm also depends on the distances used to compute the cost and heuristic functions to behave like Euclidean distance computations. Thus, the geospatial coordinate system must be projected onto a flat plane with the distances closely aligned with a Cartesian coordinate system. Because this is not possible to achieve for the entire globe at the same time, the algorithm performs this projection in a truncated coordinate space to ensure a minimum amount of distortion. Some examples of the ground tracks as well as the resulting speed change profiles are shown in Figure 8 and Figure 9. These can then be used to compute actual aircraft performance to arrive at the potential time savings and the amount of fuel used.

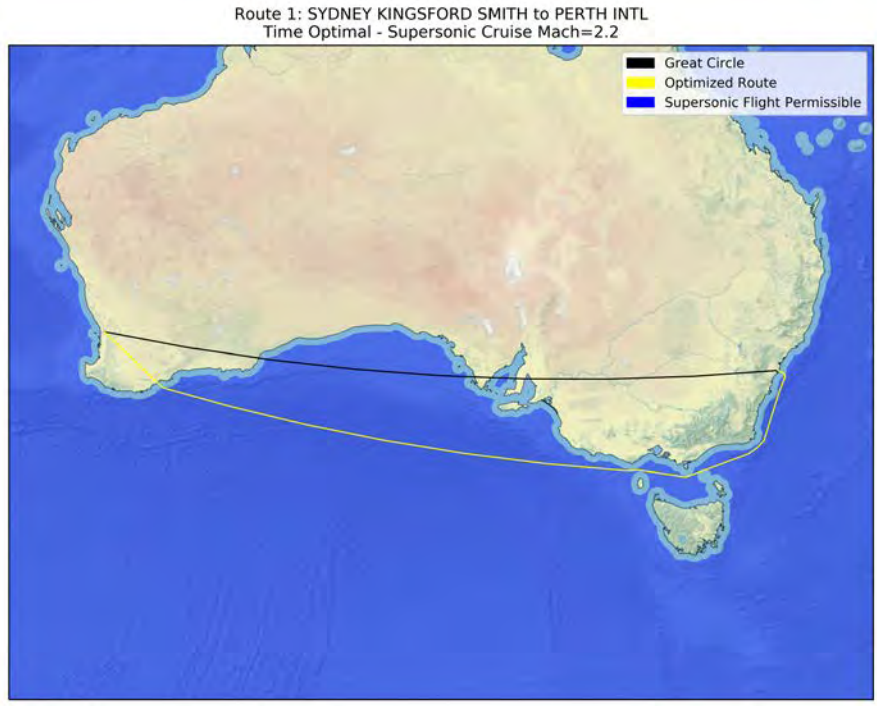

Figure 8. Example single acceleration route.

As these results show, there are quite a few routes in which more than a single acceleration to supersonic may be necessary to avoid exposing land to a sonic boom or otherwise flying excessive distances around land masses, such as India, as shown in the second example. The specific routes in the more complex cases highly depend on the aircraft properties, such as the cost of accelerating to supersonic speed, and the supersonic and subsonic efficiency of the aircraft. Consequently, the routes in many cases must be re-optimized for different aircraft. The results shown here are for the Georgia Tech medium SST described in Task 5.

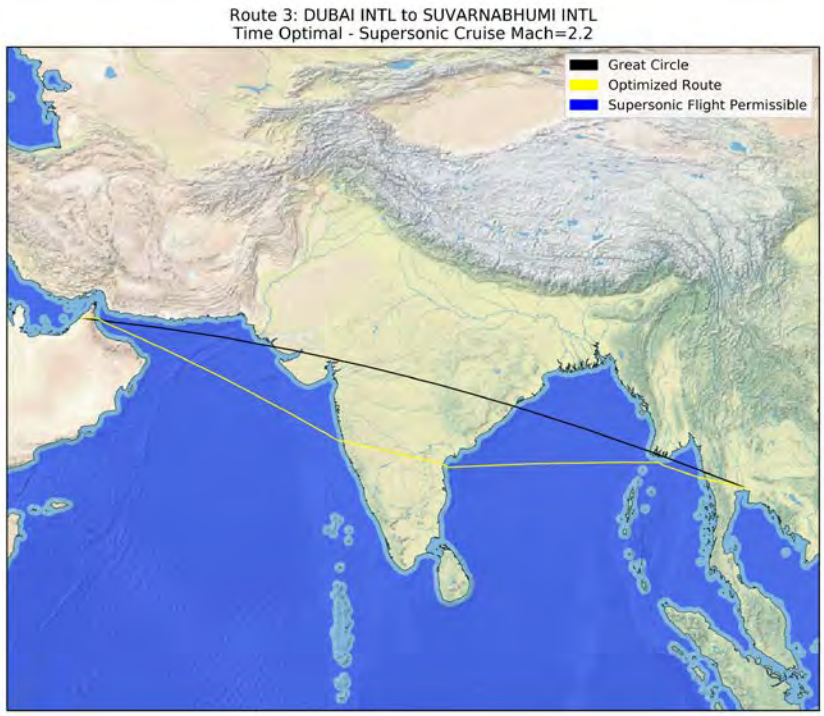

Figure 9. Example two-acceleration route

Figure 10. Realizable time savings.

These data can then be accumulated to show the realizable time savings as compared with an ideal unrestricted time savings for a given cruise Mach number or speed, as shown in Figure 10. This, together with the cost escalation, is then used to derive a VTTS value per route than an airline could deliver. To assess what percentage of passengers would switch to this potential supersonic service at the given VTTS, the team used an income distribution to derive the fraction of travelers given

certain values of the VTTS. This distribution was then used to compute the switching percentage for a given route, which then resulted in the final demand estimates and, together with the fuel burn results, was used to estimate the environmental consequences for Task 4.

Research Approach (Purdue)

FLEET Supersonic Simulation Requirements

Current supersonic aircraft model

The Purdue team has developed a "back of the envelope" representation of the A10 notional medium SST aircraft. The aircraft has a 55-seat configuration with a maximum design range of 4,500 nmi, according to a relatively simplistic approach to predict size and performance. The passenger capacity is chosen on the basis of the Boom Overture concept, because of the forthright presentation of the company's desire for this aircraft to be the first supersonic passenger-carrying entrant since the Concorde; this simply provides a convenient starting point. The supersonic aircraft modeled in FLEET makes no attempt at sonic boom reduction, so that it flies over water at a supersonic cruising speed of Mach 2.2 and flies over land at a subsonic cruising speed of Mach 0.95. The simplistic sizing and performance analysis uses the Breguet range equation to calculate the fuel burn and block time (total flight time, considering departure from gate at the origin airport to arrival at the destination gate) for routes of different lengths and different percentages of overwater flight. In the current model, the aircraft cost and performance modeling are accomplished by using multipliers to modify the cost and performance parameter outputs of already existing subsonic aircraft to mimic the operation of a supersonic aircraft.

For simplicity, the "back of the envelope" supersonic aircraft modeling uses the following simplifying abstractions:

- The overland segment is assumed to be equally split at each end of the overwater segment. For example, for a mission of 3,000 nmi with 75% of the flight over water, the overland portion of the flight is split into 375-nmi segments at the beginning and the end of the 2,250-nmi overwater segment, so that the total overland flight segment for the mission is 750 nmi. In reality, the overland segment is dependent on the airport pair and route (e.g., for one airport pair, the origin might be close to the ocean, and the destination might be further inland; the return flight on this pair would have the opposite); consequently, a higher resolution representation of the routes would lead to different fuel burn characteristics for each direction on each route.
- There is no range credit for the climb and acceleration segments from 35,000 ft at $M = 0.95$ to 55,000 ft at $M = 2.2$ for the supersonic aircraft. There is a simple estimate for fuel burn for these accelerations.
- There is no range credit for the decent and deceleration from supersonic to subsonic speeds. In addition, no fuel burn is considered for this descent segment.

On the basis of the team's engineering judgement, the L/D ratio for sizing the supersonic aircraft changes for supersonic ($M = 2.2$) and subsonic ($M = 0.95$) flight regimes, varying from a value of 8.0 at $M = 2.2$ to a value of 13.0 at $M = 0.95$. These values are meant to be a bit better than those of the Concorde to reflect improved aerodynamic design. The fuel burn estimates also vary for the two flight regimes. Again, guided by information for the Concorde, we determined the specific fuel consumption (SFC) value of the notional 55-passenger SST aircraft to be 1.0338 (1/hr) at $M = 2.2$. The subsonic flight regime's fuel burn is estimated by using the product of the supersonic flight regime's SFC value and the Concorde's ratio of subsonic flight to supersonic flight SFC, thus leading to a SFC value of 1.2025 (1/hr) at $M = 0.95$.

The simple sizing and performance assessment allows for estimation of the supersonic aircraft maximum range as a function of the route's overwater percentage. Figure 11 shows the supersonic aircraft maximum range capability as a function of the percentage of flight over water. The supersonic aircraft has an all-supersonic (100% overwater flight) range capability of 4,500 nmi. The range capability decreases with an increasing percentage of overwater flight because the supersonic aircraft must fly further at subsonic speeds, which is less efficient in the current model of the supersonic aircraft, thus leading to increased fuel burn and a reduced aircraft range. The supersonic aircraft modeled here shows a maximum range of 2,790.5 nmi when flying completely over land.

In the FLEET simulations run out to the year 2050, two generations of supersonic aircraft are considered with entry into service (EIS) dates of 2025 (generation 1) and 2038 (generation 2). The generation 2 supersonic aircraft shows improved fuel burn only with no change in the aircraft noise or sonic boom characteristics. The fuel burn multiplier and SFC values described above refer to the generation 1 supersonic aircraft. For modeling the second generation of the notional 55-passenger SST aircraft, the Purdue team implemented SFC values of 0.9019 (1/hr) at $M = 2.2$ and 1.0491 (1/hr) at $M = 0.95$, while keeping all the other design parameters unaltered.

Supersonic aircraft block time

In this current work, the supersonic aircraft is expected to fly supersonically over water only, so the block time for the current simplistic A10 notional medium SST aircraft is computed according to how much of the flight is over water. The simplistic model presumes that the supersonic aircraft cruises at Mach 2.2 over water and Mach 0.95 over land; hence, the total block time considers the time contributions for both its overwater and overland flight subsegments. For the overland flight (subsonic flight segment), the block time of the supersonic aircraft is equivalent to the block time of class 5 subsonic aircraft already existing in FLEET. The percentage of overwater flight for the supersonic aircraft is calculated by using the overwater calculations detailed in the next section. The modified block time equation is shown below.

$$Blocktime_{sup} = \left[Blocktime_{sub\_class5}^{min\_time\_route} \times (1 - \%_{overwater})\right] + \left[\%_{overwater} \times \frac{min\_time\_distance}{Sup\_cruise\_spd}\right]$$

Here, $Blocktime_{sub\_class5}^{min\_time\_route}$ represents the block time of subsonic class 5 aircraft on the minimum-time route identified by using the supersonic route path adjustment strategy and overwater calculation for supersonic aircraft operation, described below.

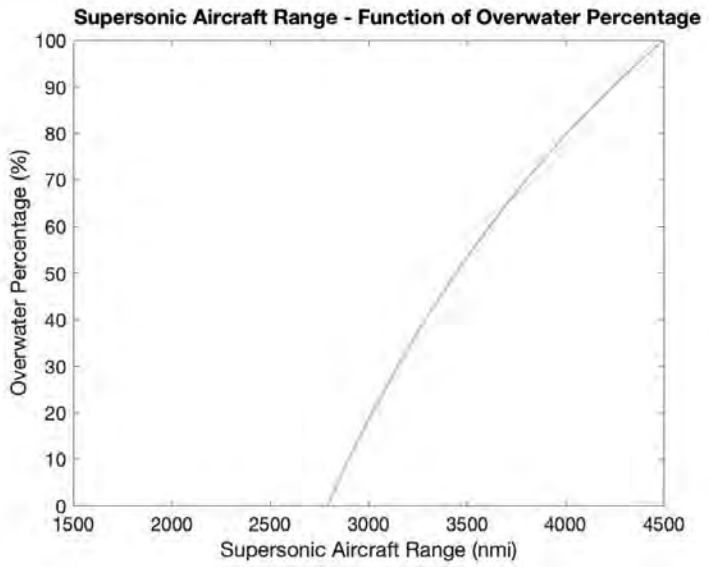

Figure 11. Supersonic aircraft maximum range capability as a function of the percentage of overwater flight.

Supersonic aircraft cost model

Because no commercial supersonic aircraft are currently in production or service, the team used some rational assumptions to model aspects of the supersonic aircraft cost as a starting point to run FLEET simulations. The assumptions used for supersonic aircraft cost modeling in FLEET are as follows:

- The 55-seat supersonic aircraft acquisition cost equals that of a very large commercial subsonic aircraft (a “class 6" aircraft in FLEET with 400+ seats).
- One hundred percent of the supersonic aircraft acquisition cost is amortized over a 15-year period, as reflected in the total operating cost of the supersonic aircraft.
- Fuel costs per gallon are the same for supersonic and subsonic aircraft.
- Yearly maintenance costs used to inform aircraft retirement decisions follow the same Boeing maturity curve as that of the subsonic aircraft. This curve predicts maintenance cost as the aircraft ages up to 40 years from EIS. Using this may be problematic, given that the operating conditions, particularly the in-flight heating and subsequent cooling and the cruise operating throttle settings of the engines, differ between supersonic and subsonic aircraft.
- The aircraft’s age-based fuel economy follows the Airbus trends that are also used for subsonic aircraft. Consequently, fuel consumption is increased each year of service to reach a 10% increase over the original fuel consumption after 40 years from EIS.

- Crew costs for the 55-seat supersonic aircraft have a higher hourly rate similar to those for large subsonic aircraft, thus reflecting the "premier" status that the supersonic aircraft crews might have. The operating cost per flight also reflects the faster speed (shorter block hour flights) of the supersonic aircraft. Using the aforementioned updated block time calculations, the crew cost for the simplistic supersonic aircraft is modeled with the equation below.

$$Crewcost_{sup} = Crewcost_{sub\_class5}^{\min\ \_time\_route} \times \frac{SeatCap_{sup}}{SeatCap_{sub\_class5}} \times \frac{Blocktime_{sup}}{Blocktime_{sub\_class5}^{min\ \_time\_route}}$$

  As with the previous case, $Blocktime_{sub\_class5}^{min\ \_time\_route}$ and $Crewcost_{sub\_class5}^{min\ \_time\_route}$ represent the block time and crew cost of subsonic class 5 aircraft on the minimum-time route identified by using the supersonic route path adjustment strategy and overwater calculation for supersonic aircraft operation, respectively.

Table 3 summarizes the multipliers used for developing the cost model for the simplistic A10 notional medium SST aircraft in FLEET.

Table 3. Cost parameters used for developing the simplistic "back-of-the-envelope" supersonic aircraft model in FLEET.

Cost Parameters of Simplistic Supersonic Aircraft	Multipliers/Modeling Characteristics
Crew Cost	Block time calculations and subsonic class 5 aircraft
Maintenance Hours	1.5 times that of subsonic class 5 aircraft
Insurance	Subsonic class 5 aircraft Insurance
Indirect Operating Cost	Subsonic class 5 aircraft
Acquisition Cost	Subsonic class 6 aircraft

Supersonic ticket price model using offered ticket prices for business class or above in 2018

One of the first steps in determining ticket prices for supersonic flights is identifying the potential routes where the supersonic aircraft might operate and then using available pricing information about those routes. Given that the Boom Overture concept is a possible first supersonic passenger-carrying entrant that does not make an attempt at low-boom flight, the initial supersonic aircraft are most likely to operate on over-ocean routes, where they can fly supersonically over the water. Consequently, primarily international routes will be "supersonic eligible." According to the discussion from Boom's website that indicates that their aircraft could operate with a ticket price similar to those of current business class tickets, the Purdue team assumes that the supersonic ticket price would be similar to the current business class ticket prices. Because data on the historical ticket prices paid for international routes are difficult to obtain, the presented work is dependent on the current (2018) offered pricing data for tickets business class or above to model supersonic ticket prices for FLEET simulations. The offered ticket price data for business class or above are procured through matrix.itasoftware.com as round-trip data for a subset of 26 supersonic-eligible transatlantic origin-destination pairs (and destination-origin pairs) for February 9, 2018, and the median of the ticket price data for every route is selected as the current offered ticket fare for business class or above.

Using the offered ticket fares for business class or above, this work builds a range-dependent delta-yield model, wherein delta-yield is the mark-up or profit per passenger-nautical mile ($/pax-nmi). The model builds a simplistic linear fit for ticket delta-yield with respect to the range elasticity. This simplistic model attempts to account for the passenger's willingness to pay more for increased time savings when flying longer distances in a supersonic aircraft. The supersonic ticket fare is hence equal to the sum of the supersonic aircraft operating cost per passenger and a margin term, expressed as the following equation:

$$Fare_{SST,\,route\,i} = \left(D\ yield_{per\ nmi} * range_{route\,i}\right) + \frac{CostofSST_{route\,i}}{55\ pax}$$

The operating cost of the aircraft (represented by the term *CostofSST*) includes the non-fuel direct operating cost (maintenance cost, crew cost, servicing cost, indirect operating cost, insurance cost, and amortized acquisition cost) and the fuel cost for operating the supersonic aircraft on a specific route.

Supersonic aircraft production and aircraft available in FLEET

The Purdue team assumes that the supersonic aircraft production follows the trend of Boeing 787 deliveries over the last decade. The available Boeing 787 annual aircraft delivery data from first delivery until 2018 provides the absolute supersonic aircraft production numbers for eight years (2011–2018), followed by extrapolation of the lower-slope production rates for years beyond the eighth year of production. There are two reasons for selecting the Boeing 787 production curve as a baseline for the simplistic supersonic aircraft. First, the Boeing 787 is a recent high-technology introduction aircraft, and given that the commercial supersonic aircraft are also expected to be high technology (owing to the addition of supersonic cruising abilities in the commercial sector), this assumption does not seem unfair. Second, because the deliveries of the Boeing 787 began in 2011, this assumption provides a historical basis for predicting supersonic aircraft deliveries from their initial delivery. Then, to use this as a guide for supersonic aircraft availability in the FLEET simulations, the total production must be scaled to reflect the number of aircraft available to the airline model that reflects U.S. flag carrier airlines on a U.S.-touching route network. On the basis of the Boeing Market Outlook, the share of future aircraft deliveries to North America is approximately 40% of the total aircraft production. In Figure 12, the red dotted line depicts the Boeing 787 production/delivery curve (which provides a model of the total number of supersonic aircraft delivered worldwide), and the black solid line depicts the number of supersonic aircraft delivered to FLEET's airline each year.

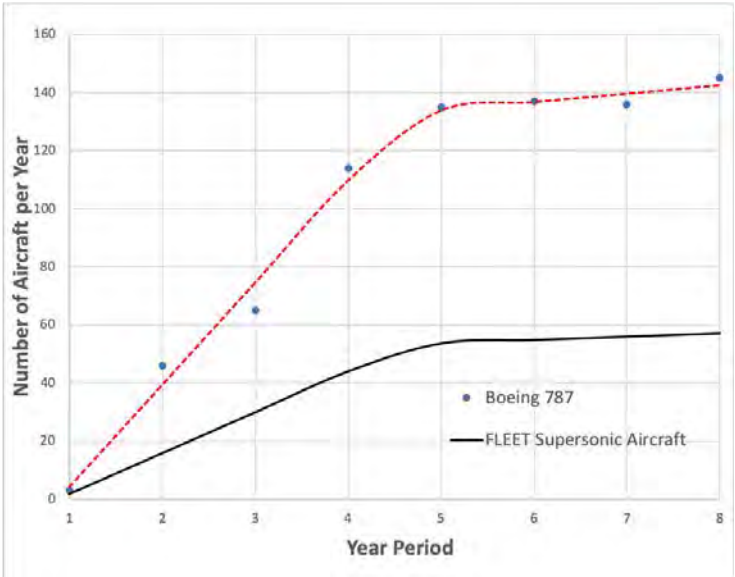

Figure 12. Supersonic aircraft production curve in FLEET.

Characterizing supersonic passenger demand

To estimate the supersonic passenger demand, the team starts from the discussion on Boom Supersonic Corporation's website regarding passengers paying same fares for supersonic flights as today's business class. Henceforth, this work assumes that the potential supersonic passengers are the current passengers who pay fares business class or above. In FLEET, the travel demand is split such that supersonic (business class or above) demand is a fixed percentage (5%) of the total travel demand, and the remaining demand is subsonic. As a starting point to estimate the number of potential paying passengers at the level of business class or above, the team considered typical aircraft currently flying transoceanic routes. Those aircraft have enough seats in business and above cabins that are approximately 10% of the total seat capacity, albeit with fairly substantial variation. Using this starting point, the team assumes that 50% of the daily business class or above passengers in the historical data (or 5% of the total demand are willing to pay the supersonic fare, and this 5% of total passenger demand on a route becomes the supersonic passenger demand on that route. This is a coarse approximation, in which half the passengers flying in business class or above cabins are paying that business class or above fare, whereas the other half are using upgrades or similar. A direct comparison with the BTS database is not possible for the 5% supersonic demand assumption, because the DB1B Coupon database sample consists of ticket prices paid only for domestic routes. However, an indirect comparison indicates that for all domestic routes in the DB1B for 2016, 4.82% of the reported tickets

were business class or above; among domestic flights between 2350 nmi and 4500 nmi, 6.89% of the reported tickets were business class or above. This finding supports that the 5% assumption is not unrealistic.

Identifying potential supersonic routes

This work considers both nonstop (direct) and with-fuel-stop (indirect) potential supersonic routes. The Purdue team identifies potential supersonic routes from FLEET's existing route network of 1940 routes, using a set of route filters based on the supersonic aircraft's maximum design range (differentiating between routes that require a fuel stop and those that do not require one), the aircraft maximum range capability for different percentages of supersonic and subsonic flight segments, and the block time savings incurred when flying supersonic aircraft compared to subsonic aircraft. To calculate the minimum-time flight path for a supersonic route, the team uses a very simple supersonic route path adjustment strategy that gives the block time, percentage of flight path over water, updated departure heading for the route, and minimum-time route distance as outputs.

Supersonic route path adjustment

This subsection details the supersonic route path adjustment method developed to estimate the overwater portions of flights for the supersonic-eligible routes. These percentages of overwater-flight calculations form the second component for determining the route-specific range capability of supersonic aircraft (shown in Figure 13). Because the current work considers that the supersonic aircraft can operate over Mach 1.0 only when flying over water, this method includes adjusting the supersonic-eligible route path from its great circle path to allow the aircraft to operate at supersonic speeds for the longest overwater route segment possible. The rerouting facilitates the identification of the supersonic-eligible route path along which minimum flight time is possible (by using supersonic speeds over water and subsonic speeds over land).

The overwater-portion calculations with rerouting technique have the following characteristics:

1. These calculations consider the longest route portion over water without any land portions. The great circle distance is based on the longitudes and latitudes of airports on a spherical earth model.
2. In case small islands might lie under the flight path (in the great circle path or during path rerouting), the algorithm checks whether the sum of path lengths before and after the island is greater than 40% of the total flight path. If so, then the small island is ignored, because the assumption that an aircraft can avoid the island by flying around it is made (and the interest is in the longest overwater route segment).
3. The rerouting technique finds 14 alternate flight path deviations above and below the great circle path. For generating the alternate flight path, the coordinates of the midpoint of the great circle path are determined, followed by incrementing (or decrementing) the midpoint latitude by 1° for each alternate flight path, ultimately changing the departure heading of the aircraft. The 14 alternate routes generated in this study correspond to incremental deviations in departure heading to a maximum of +7° and −7° from the great circle path. This is very simplistic for computational efficiency, but the approach does recognize that the supersonic aircraft might fly a longer distance so that the overwater portion of the flight minimizes block time. Higher-resolution flight paths would probably be adopted in actual operations, but the optimal path determination problem was deemed too computationally expensive for the current study.
4. Among the great circle path and all the alternate flight paths generated for a route, the minimum-time flight path is selected for the supersonic aircraft. The flight time is determined by using different flight speeds for overwater and overland flight operation. The minimum-time flight path is hence optimal because of the discrete departure deviations. The flight time for every route is calculated by using a supersonic flight speed of Mach 2.2 (at 55,000 ft) for the longest overwater segment and subsonic flight speed of Mach 0.95 (at 35,000 ft) for the remaining segments. These simplistic calculations are performed with the following equation:

$$t_{flight} = \frac{P_{overwater}/100}{vel_{sup}} + \frac{1 - (P_{overwater}/100)}{vel_{sub}}$$

where t_{flight} denotes the flight time, $P_{overwater}$ is the percentage of overwater flight, vel_{sup} is the supersonic aircraft speed (Mach 2.2 at 55,000 ft), and vel_{sub} is the subsonic aircraft speed (Mach 0.95 at 35,000 ft).

For example, considering the New York–John F. Kennedy (JFK) to Tokyo–Narita (NRT) route shown in Figure 13, the overwater-portion calculation technique indicates a minimum-time flight path (denoted by red dotted line) with a deviation from the great circle flight path (denoted by solid red line). In this case, the minimum-time flight path also has the longest segment over water among all the route path deviations generated by the technique.

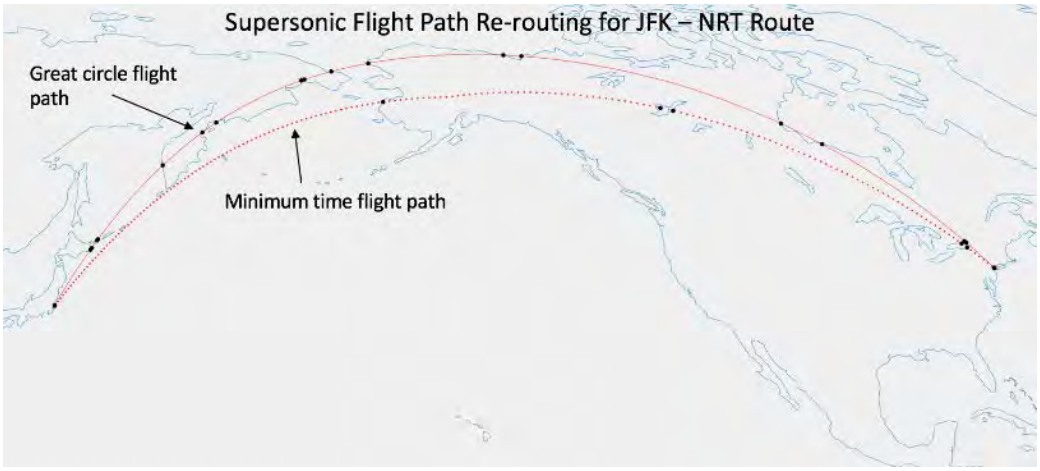

Figure 13. Demonstration of supersonic flight path rerouting for the JFK–NRT route to find the minimum-time flight path.

Nonstop supersonic-eligible routes

The following route filters are used to identify the nonstop potential supersonic routes:

1. Routes with a minimum-time route distance less than or equal to 4,500 nmi.
2. Routes satisfying the supersonic aircraft's range capability as a function of overwater flight percentage.
3. Routes with block time savings of 1 hr or more when flying supersonic aircraft. These time savings reflect a passenger's willingness to pay for flying supersonic. The team believes that only routes that show a potential time savings of more than 60 min will attract passengers; airlines would want to operate their supersonic aircraft on these routes only for maximizing their profit. A more rigorous passenger choice model might provide a better approach to this filter.

These filters lead to the identification of 193 nonstop potential supersonic routes in the FLEET network. Of these 193 routes, with the fairly simple route path adjustment, 137 routes have at least a 75% overwater flight segment, 33 routes have overwater flight segments between 50% and 75%, and the remaining 23 routes have overwater flight segments less than 50%.

Supersonic-eligible routes with fuel stops

For this work, only airports currently in the FLEET network are considered for potential fuel stops; there are two transpacific potential fuel-stop airports—Honolulu, Hawaii, USA (HNL) and Anchorage, Alaska, USA (ANC)—and four transatlantic potential fuel-stop airports—Shannon, Ireland (SNN); Keflavik, Iceland (KEF); Oslo, Norway (OSL); and San Juan, Puerto Rico (SJU). The team recognizes the existence of a number of other potential fuel-stop airports in the Pacific and the Atlantic; however, these airports do not have enough U.S. flag carrier service to appear in the BTS database and are not in the FLEET network. For routes with fuel stops, this work assumes that the fuel stops are just technical stops; hence, there is no boarding of any new passengers from the fuel-stop airport into the flight or debarkation of any existing passengers from the flight. The fuel stop adds 60 min to the block time of the supersonic aircraft flying on the with-fuel-stop route (including time for descent, landing, taxi, refueling, taxi, takeoff, and climb). The 60-min duration is an educated guess made by the team and could easily be varied in future studies; more information about the future supersonic aircraft design could improve this fuel-stop time estimate. The supersonic route path adjustment method for with-fuel-stop routes optimizes the heading deviation for each "hop" of the flight, i.e., from origin to fuel stop (first "hop") and then from fuel stop to destination (second "hop"), while also selecting the optimum fuel-stop airport that minimizes the overall block time. Figure 14 shows the route adjustment approach for routes with fuel stops, using the DFW–HNL–NRT route as an example. The following route filters are used to identify the with-fuel stop potential supersonic routes:

1. Routes with minimum-time route distance less than or equal to 9,000 nmi. This work does not consider more than one fuel stop on a route.
2. Routes satisfying supersonic aircraft range capability as a function of overwater flight percentage. This step is implemented for each "hop" of the flight. The route heading deviation is also adjusted for each "hop."
3. Routes with block time savings of 1 hr or more when flying supersonic aircraft. This block time savings includes additional 60 min gained in block time due to the technical stop.

These filters lead to identification of 12 additional potential supersonic routes with a fuel stop in the FLEET network. All 12 potential routes with fuel stops indicate a block time savings of more than 2 hr over the nonstop subsonic flight.

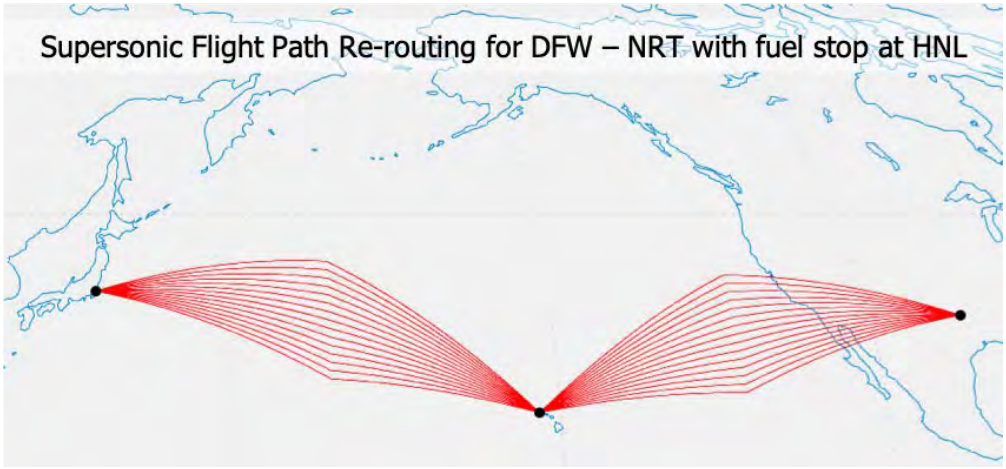

Figure 14. Demonstration of supersonic flight path rerouting for the DFW–HNL–NRT route to find the minimum flight time path.

Supersonic-eligible route network in FLEET

The network of supersonic-eligible routes in FLEET consists of a total of 205 potential supersonic routes, of which 193 are nonstop routes, and 12 are with-fuel-stop routes. Figure 15 depicts the entire potential supersonic route network for FLEET on a world map. The routes in gray are those without fuel stops, and the routes in red are those with fuel stops. Table 4 provides details about potential supersonic routes with maximum and minimum percentages of flight over water and block time savings.

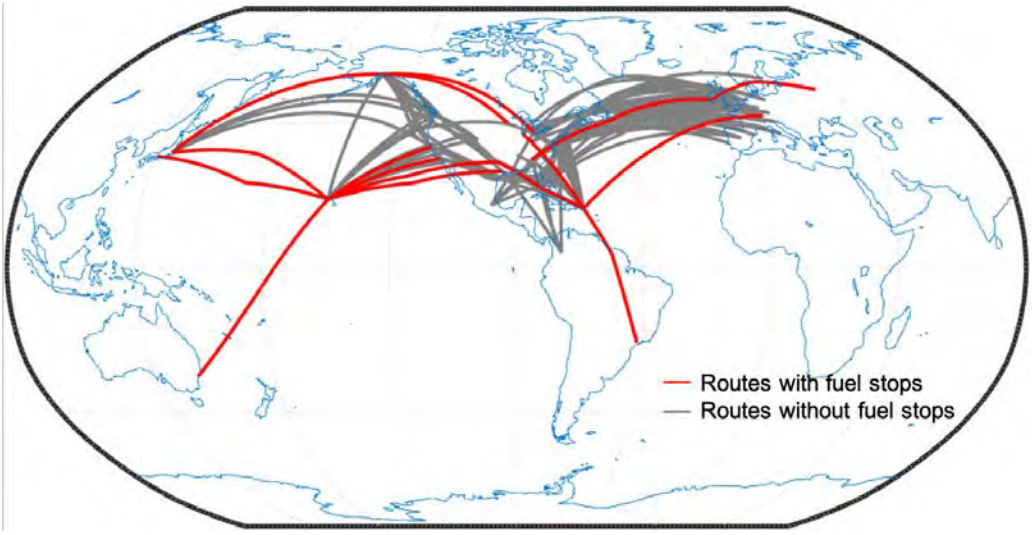

Figure 15. 205 Potential U.S.-touching supersonic routes in FLEET.

The current allocation problem setup in FLEET uses the 205 potential supersonic routes as an input. FLEET chooses which routes to allocate the supersonic aircraft on, according to the route profitability, which is specific for each year of the simulation. As with all routes in FLEET, the aircraft will travel a round trip on the route, so the Amsterdam Schiphol (AMS)-

to-JFK route also covers flights from JFK to AMS. Table 4 provides information about a few of the routes for potential supersonic service.

Table 4. Details about selected potential supersonic routes in FLEET.

	Parameter	Airport A	Airport B	Great Circle Distance [nmi]	% Over-water	Min Time Distance [nmi]	Block Time [in hours]		Time Savings [in hours]
							Subsonic	Supersonic	
Nonstop routes	Max % overwater	EWR	SJU	1400.98	**99.63**	1400.98	2.90	1.17	1.73
	Min % overwater	MIA	SEA	2364.89	**18.37**	2414.53	4.90	3.87	1.03
	Max time savings	NRT	SJC	4468.74	98.92	4468.80	9.26	3.60	**5.66**
	Min time savings	EWR	FLL	927.18	85.71	980.67	1.92	0.92	**1.00**
Fuel stop routes	Max % overwater	SFO	SYD	6452.35	**99.26**	6494.80	13.35	6.19	7.16
	Max time savings	LAX	SYD	6512.48	99.22	6639.63	13.48	6.31	**7.17**

Task 2 - Preliminary Vehicle-Level Environmental Impact Prediction

Georgia Institute of Technology

Objective

This task focused on providing a preliminary estimate of the environmental impact of supersonic travel. The likely performance of supersonic aircraft relative to existing subsonic transports for which performance is known was to be identified. This relative estimation was performed for a number of KEIs including fuel burn, emissions, water vapor, likely cruise altitudes, and noise. KEI information was to be compiled for three supersonic aircraft types:

1. Type 1: aircraft that operate at supersonic speeds in unrestricted areas and subsonic speeds over other areas.
2. Type 2: same aircraft as type 1, except that they also have technology to fly at Mach cut-off speeds over prohibited areas. Mach cut-off is a phenomenon that takes advantage of atmospheric characteristics to prevent sonic booms from propagating to the ground (typically works from Mach 1.1 to 1.15).
3. Type 3: aircraft specifically designed to produce very low sonic boom levels during all phases of supersonic flight.

Quantitative estimates for each KEI were to be generated through an extensive literature search of previously developed concepts and active projects in industry and government, by using sources such as NASA contractor reports, journal and conference publications, and press releases pertaining to concepts under active development. Georgia Tech was to estimate fuel burn, noise, water vapor, and emissions as a function of vehicle size, mission, and passenger capability, by using publicly available resources. These estimates were to be compared to those for baseline aircraft in the subsonic transport category, with the goal of establishing an equivalency in each of the KEI metrics.

Research Approach

To provide a preliminary estimate for the performance of supersonic vehicles, the Georgia Tech team started by establishing a reference performance for a subsonic vehicle. Quantitative estimates of the impact of supersonic vehicles on the various KEIs, especially fuel efficiency, were then derived through literature review, future performance targets set by NASA, and engineering judgement. The subsonic vehicle selected as a reference was the Boeing 737-800. This aircraft was chosen because of its similar payload-range capabilities to those of both the Concorde and future supersonic vehicles. The KEIs selected were primarily fuel burn, CO_2 emissions, nitrogen oxide (NOx) emissions, and noise. The first two KEIs correlate with each other to a great extent. For NOx, a distinction was made between emissions released during cruise and emissions released in the vicinity of airports at low altitudes during landing and takeoff (LTO). Similarly, for noise, a distinction was made between airport noise and sonic boom noise. The latter is a characteristic of only supersonic vehicles, because it is produced only in regimes of supersonic flow. As for targeted performance, NASA goals for supersonic vehicles were used as

a reference. NASA set vehicle performance goals for the midterm (business jet size) and far term (airliner size). Table 5 summarizes the findings.

The historical values in the table were derived from various sources. For the Concorde, flight manuals were utilized to determine fuel efficiency in terms of pounds of fuel per seat per nautical mile. Values for cruise NOx emissions and sonic boom noise were determined through a literature search. As for LTO NOx emissions, the value was determined by using the International Civil Aviation Organization (ICAO) engine databank. Finally, airport noise was determined according to the maximum takeoff mass relative to stage 3 certification standards. Notably, the Concorde did not need to meet any noise certification standards. Nevertheless, the noise margin (relative to that of Stage 3) was calculated for reference. For the Boeing 737-800, similar sources were utilized to gather the required information.

Table 5. Comparison of environmental metrics for subsonic and supersonic aircraft.

	1976 Concorde	1998 Boeing 737-800	Current Tech. Estimate	2025 NASA N+2	2035 NASA N+3	2035+ NASA N+3 Stretch
Fuel Efficiency (lb/seat/nmi)	0.53	0.10		0.30	0.29	0.22
Cruise NOx Emissions (g/kg of fuel)	23.3	-		<10.0	<5.0	<5.0
LTO NOx Emissions (g)	29,995	8,466		-	-	-
Cumulative Airport Noise Margin Stage 3 (EPNdB)	- 43.2	+ 13.0		-	20	30
Sonic Boom Noise (PLdB)	105	N/A		N/A	70-80	65-75
	Historical Performance		Supersonic		Targeted Performance	

After values for the Concorde and the Boeing 737-800 were gathered, preliminary estimates for current technology supersonic vehicles (types 1/2/3) needed to be established. However, for an appropriate estimation, performance parameters such as cruise L/D ratio and engine TSFC values were required. Those values could be determined from preliminary constraint, mission, and utilization analyses conducted according to the vehicle's design mission requirements.

Constraint and mission analysis

Preliminary constraint and mission analyses can be conducted on the basis of aircraft mission requirements. A constraint analysis translates a design's performance requirements into constraints on a thrust loading versus wing loading plot. It results in the definition of a feasible design space within which a design point may be selected. Alternatively, a mission analysis flies the chosen design through a mission to determine parameters such as aircraft takeoff weight, thrust requirement, and wing area. Both analyses followed the methods outlined by Mattingly et al. in the "Aircraft Engine Design" book. Mission requirements for supersonic vehicles considered in the analyses were as follows:

1. Takeoff ground roll (constraint and mission analyses)
2. Initial climb with one engine Inoperative (constraint analysis)
3. Accelerated climb (mission analysis)
4. Constant-speed climb: subsonic (constraint and mission analyses)
5. Transonic acceleration (constraint and mission analyses)
6. Constant-speed climb: supersonic (constraint and mission analyses)
7. Supersonic cruise (constraint and mission analyses)
8. Deceleration and descent (mission analysis)
9. Landing ground roll (constraint analysis)

For constraint analysis, the goal is to establish a relationship between the aircraft's thrust loading (defined as the ratio between sea level thrust and takeoff weight) and wing loading (defined as the ratio between takeoff weight and wing area) for every mission requirement. This relationship typically has the following form:

$$\frac{T_{\mathrm{SL}}}{W_{\mathrm{TO}}} = \frac{\beta}{\alpha}\left\{\frac{qS}{\beta W_{\mathrm{TO}}}\left[K_1\left(\frac{n\beta W_{\mathrm{TO}}}{qS}\right)^2 + K_2\left(\frac{n\beta W_{\mathrm{TO}}}{qS}\right) + C_{\mathrm{D_0}} + C_{\mathrm{D_R}}\right] + \frac{P_{\mathrm{S}}}{V}\right\}$$

T_{SL} is sea level thrust; W_{TO} is takeoff weight; S is wing area; n is load factor; $\alpha = T/T_{\mathrm{SL}}$ is the installed full-throttle thrust lapse; $\beta = W/W_{TO}$ is the ratio of instantaneous weight to takeoff weight; q is dynamic pressure; K_1 and K_2 are the coefficients of the parabolic lift-drag polar, $C_{\mathrm{D_0}}$ is profile drag; $C_{\mathrm{D_R}}$ represents additional drag caused by, for example, flaps or ground friction; P_{S} is the weight specific excess power; and V is velocity. When relationships for all mission requirements are plotted together on a thrust loading versus wing loading plot, a design space is defined in which any point selected is a feasible design that meets all requirements. An example plot is shown in Figure 16.

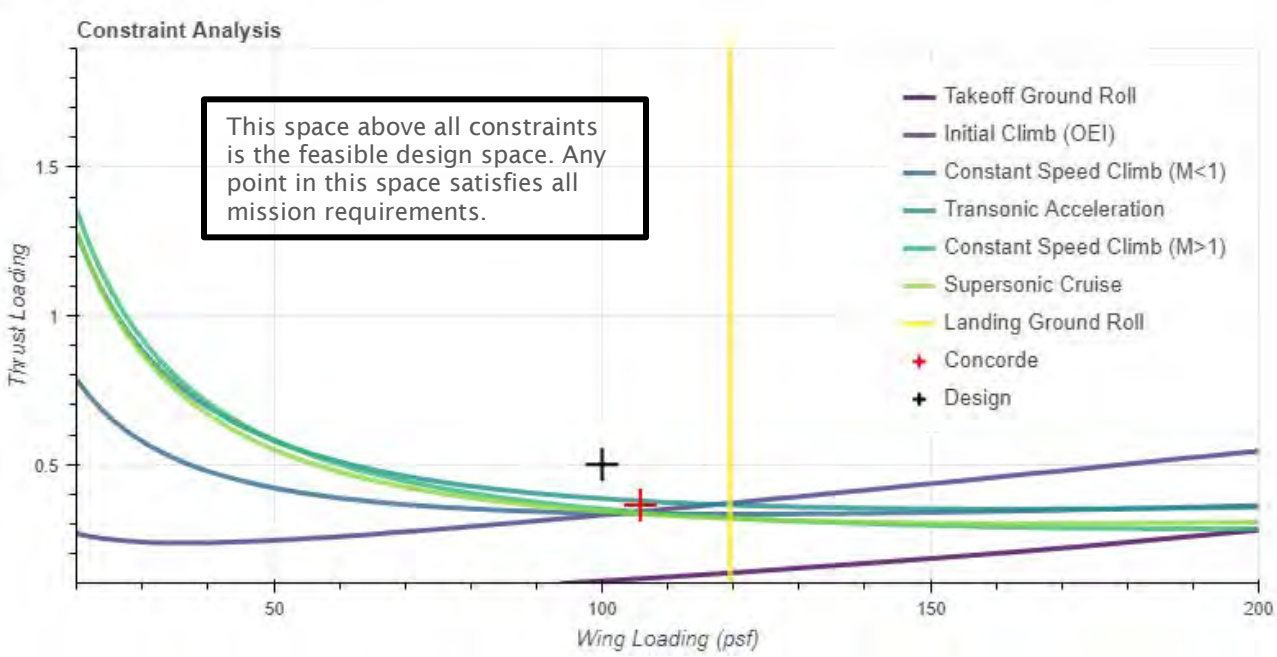

Figure 16. Constraint plot.

For mission analysis, the goal is to use the results of constraint analysis (mainly the selected design point in terms of thrust loading and wing loading) and calculate takeoff weight, sea level thrust, and wing area. This is done by determining the aircraft's fuel consumption throughout the different segments of a design mission:

$$\frac{W_{\mathrm{f}}}{W_{\mathrm{i}}} \approx \begin{cases} \exp\left\{-\dfrac{\mathrm{TSFC}\cdot(D+R)}{W}\Delta t\right\}, & \text{if } P_{\mathrm{S}} = 0 \\ \exp\left\{-\dfrac{\mathrm{TSFC}\cdot T}{V\cdot(T-(D+R))}\Delta z_e\right\}, & \text{if } P_{\mathrm{S}} > 0 \end{cases}$$

where $W_{\mathrm{f}}/W_{\mathrm{i}}$ is the ratio of aircraft final weight at the end of the segment to its initial weight at the beginning of that segment, TSFC is the thrust specific fuel consumption, $[T; W; (D+R)]$ are the instantaneous thrust, weight, drag, and rolling resistance forces, respectively, V is velocity, Δt is the total segment flight time, and Δz_e is the total change in segment energy height. For segments of the first type ($P_{\mathrm{S}} = 0$), all thrust work is dissipated, thus resulting in no speed and/or altitude

variation. Examples include constant-speed cruise, best cruise Mach number and altitude, and loiter. For segments of the second type ($P_S > 0$), some thrust work is converted to mechanical energy to vary speed and/or altitude. Examples include constant-speed climb, takeoff acceleration, and horizontal acceleration. An example plot of the progression in aircraft weight due to fuel consumption throughout the design mission is shown in Figure 17.

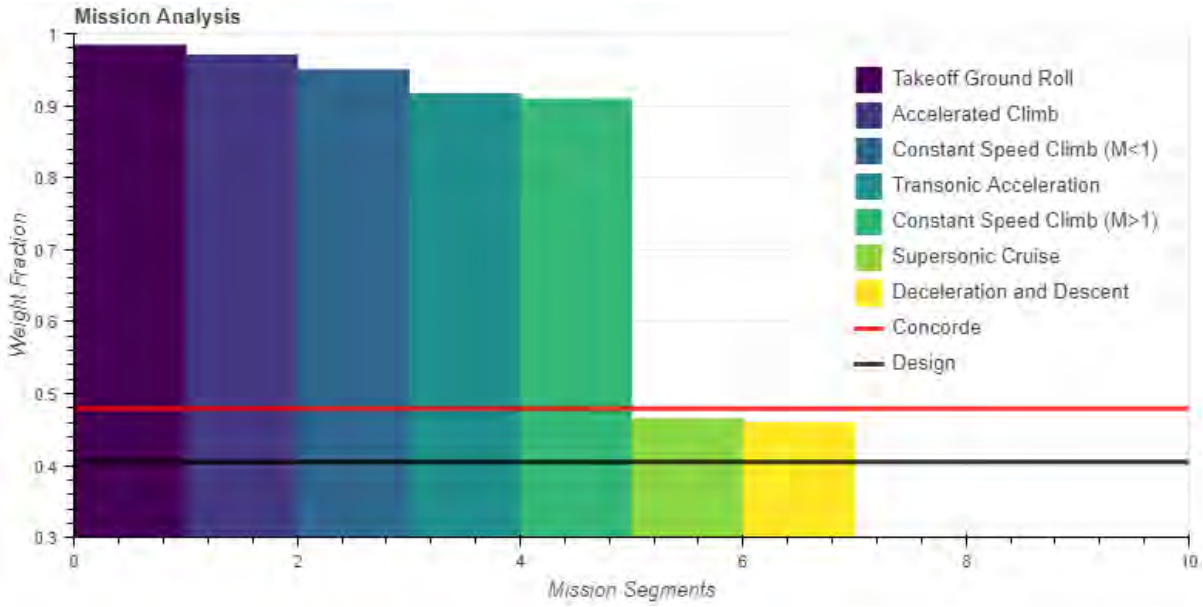

Figure 17. Weight fraction analysis.

The ratio of aircraft fuel weight to takeoff weight can be determined by using the fuel consumption relations of the different mission segments and accordingly, aircraft takeoff weight can be determined:

$$\frac{W_F}{W_{TO}} = 1 - \prod_{k=1}^{n} \left[\frac{W_f}{W_i}\right]_k \quad ; \quad W_{TO} = W_P \Big/ \left(1 - \frac{W_E}{W_{TO}} - \frac{W_F}{W_{TO}}\right)$$

where n is the total number of mission segments, W_P is the payload weight, and W_E/W_{TO} is the ratio of aircraft empty weight to takeoff weight (typically estimated by using empirical relations). After the aircraft takeoff weight is known, sea level thrust and wing area can be determined by using the design point value in terms of thrust loading and wing loading.

Constraint and mission analyses were integrated in the form of an interactive dashboard allowing users to parametrically vary mission requirements and the underlying assumptions (Figure 18). It was created with Bokeh, an interactive library that enables creation of web frontend visualizations without requiring a large amount of HTML or JavaScript development. A screenshot of the dashboard is shown below. Concorde design point and weights are embedded for reference.

With publicly available Concorde data (such as cruise L/D ratio and TSFC), the underlying models of the dashboard were calibrated such that the design point and weights of the Concorde were matched (refer to the snapshot in Figure 19).

Next, by using the calibrated models, and appropriate assumptions to account for efficiency gains in terms of aerodynamics (drag polar), propulsion (TSFC) and structures (empty weight fraction), we conducted a preliminary assessment of two concept supersonic vehicles. The first vehicle represents a 10–12-passenger business jet, and the second represents a 50–60-passenger airliner. The two snapshots in Figure 20 and Figure 21 show the results for both vehicles, respectively.

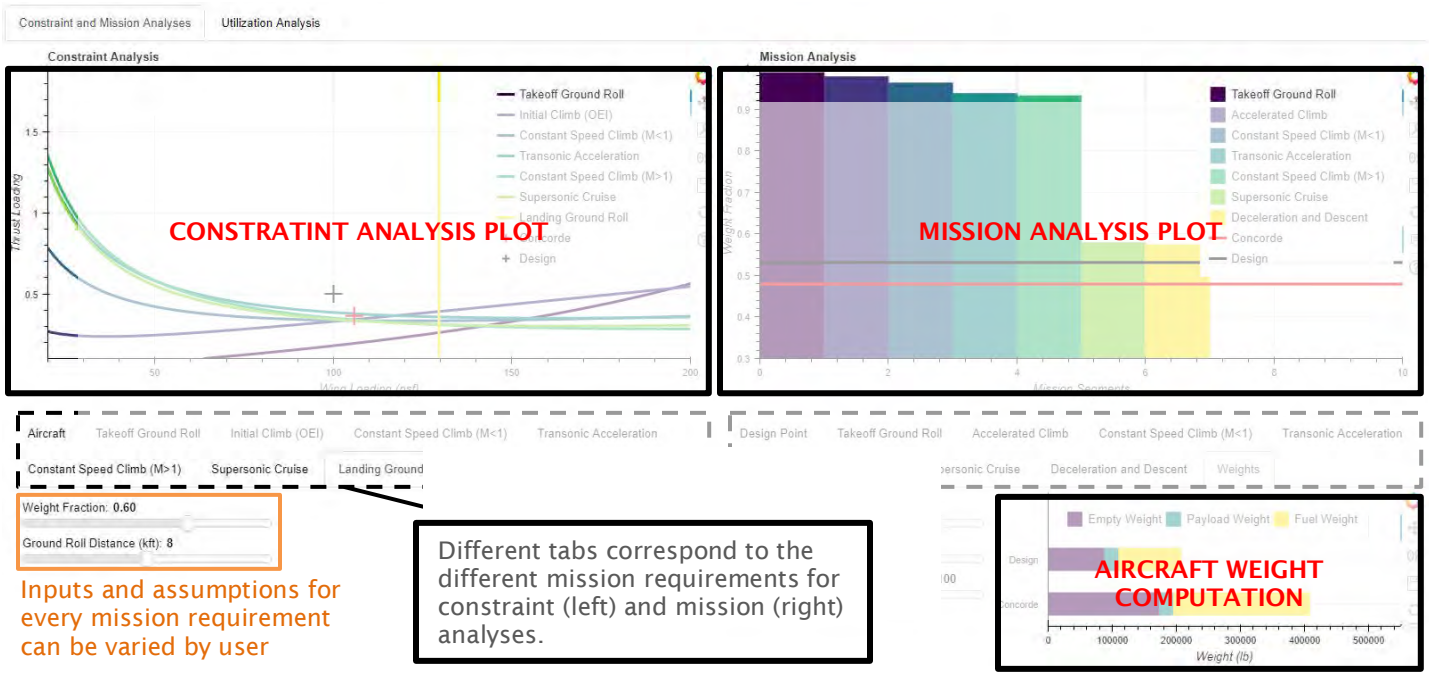

Figure 18. Synthesis and sizing overview.

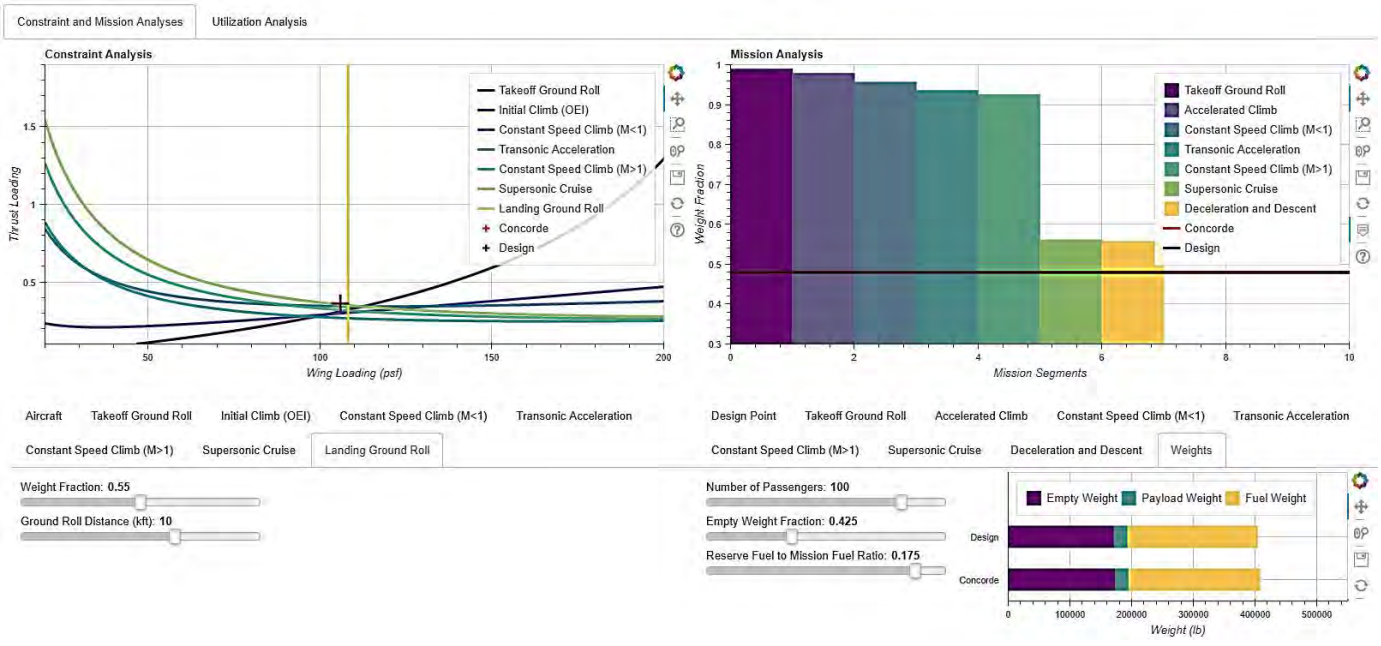

Figure 19. Matching Concorde design.

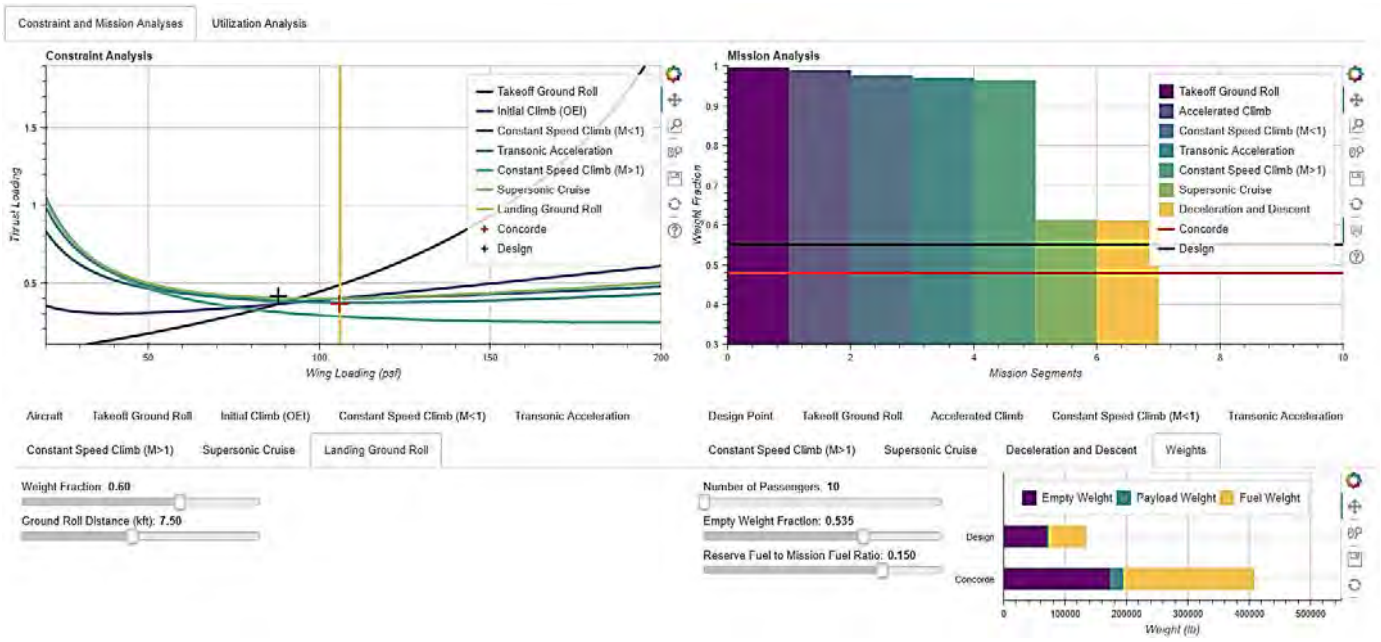

Figure 20. Exploring design of a supersonic business jet.

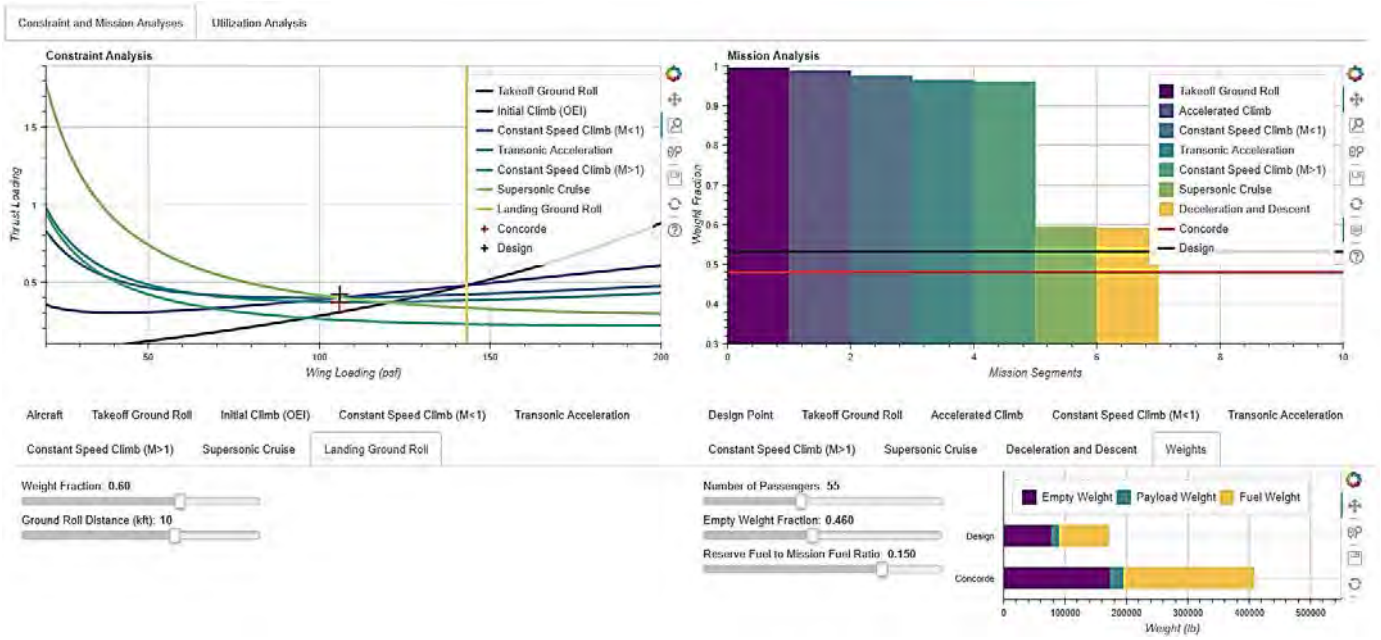

Figure 21. Exploring design of a 55-seat supersonic airliner.

Aircraft utilization

Aircraft utilization can be analyzed by using general flight and aircraft characteristics. The goal of a utilization analysis is to gauge the potential productivity of an aircraft. For supersonic vehicles, productivity is assessed in terms of the potential time savings per flight (relative to a subsonic vehicle) and the maximum aircraft utilization possible within a 24-hr period. Similarly

to constraint and mission analyses, utilization analysis was integrated in an interactive dashboard allowing users to parametrically vary flight and aircraft characteristics. A screenshot of the dashboard is shown in Figure 22.

Total flight time is broken into four components: time to takeoff and climb, time to descend and land, cruise time, and turnaround time (in cases in which the flight range exceeds the maximum design range). The first two are user inputs and are assumed to be the same for both subsonic and supersonic vehicles. The cruise time for the subsonic vehicle is simply computed as the cruise range divided by the cruise speed (which is derived from the user-input Mach number and cruising altitude). However, for supersonic vehicles, cruise time also depends on the percentage of flight over water, because supersonic vehicles may be restricted to fly at subsonic speeds over land. Therefore, the percentage of flight over water along with the subsonic cruise settings (for portions of the flight over land) have been embedded in the dashboard as inputs that the user may vary, as shown in orange in Figure 23 (note: to simulate unrestricted operations, the percentage over water should be set to 100).

Cruise flight time is hence calculated as:

$$t_{\mathrm{C,sub}} = S_{\mathrm{C}}/V_{\mathrm{C}}$$
$$t_{\mathrm{C,sup}} = x \cdot \left(S_{\mathrm{C}}/V_{\mathrm{C,sup}}\right) + (1-x) \cdot \left(S_{\mathrm{C}}/V_{\mathrm{C,sub}}\right)$$

where $[t_{\mathrm{C,sub}}; t_{\mathrm{C,sup}}]$ are cruise times for the subsonic vehicle and supersonic vehicle, respectively, $[V_{\mathrm{C}}; V_{\mathrm{C,sub}}; V_{\mathrm{C,sup}}]$ are the cruise speeds for the subsonic vehicle, supersonic vehicle flying subsonically, and supersonic vehicle flying supersonically, respectively, x is the percentage of flight over water, S_{C} is the cruise range, and $R_{\mathrm{C,max}}$ is the maximum cruise range of the supersonic vehicle. For flights that exceed the maximum cruise range of the supersonic vehicle, it is necessary for the vehicle to descend and land, refuel and turn around, and then take off and climb back to cruising altitude. Therefore, for every stop that the vehicle must make, the total flight time is increased by these additional components. The time to turn around is also a user input (shown in green in Figure 23).

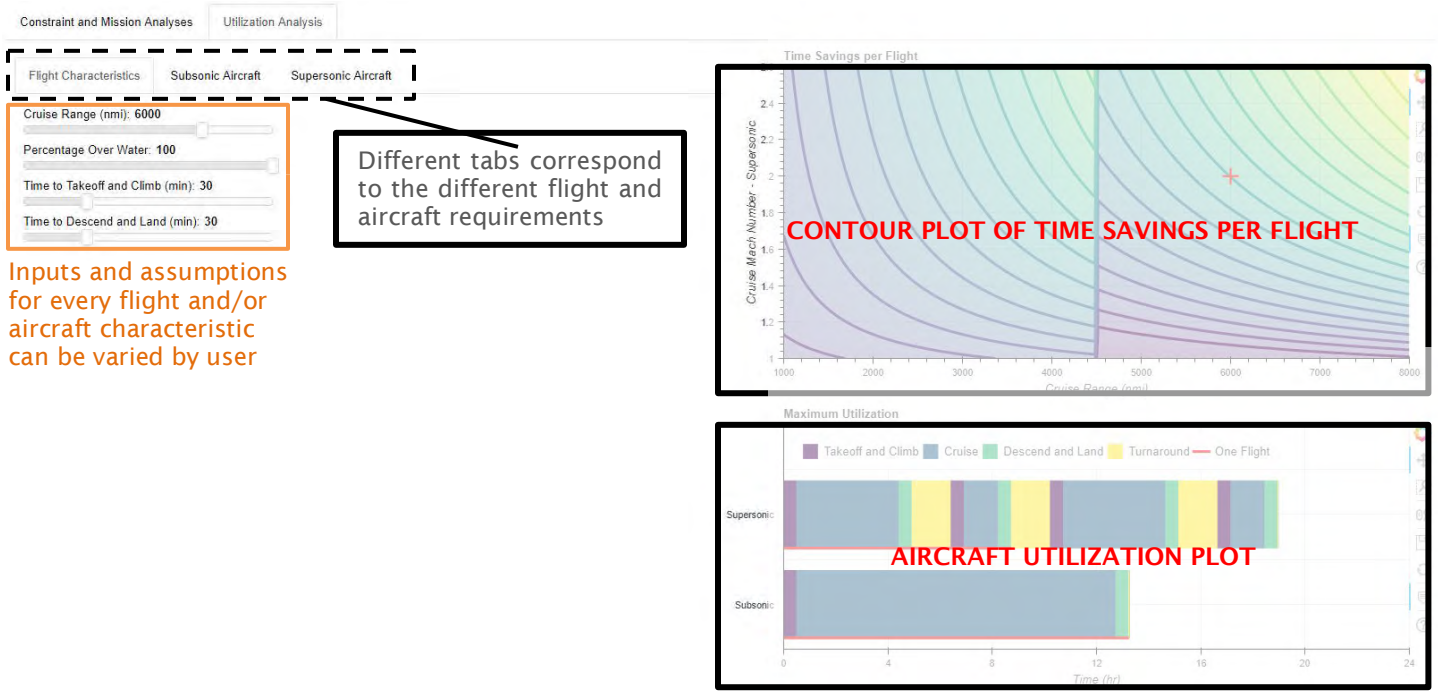

Figure 22. Exploring mission frequency and utilization.

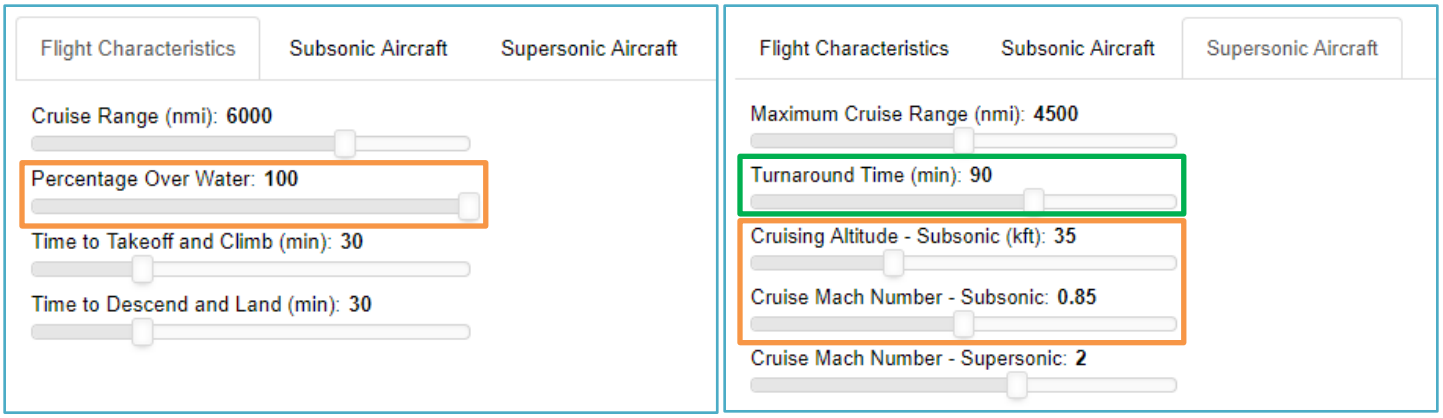

Figure 23. Airline operation assumptions.

On the basis of the previous assumptions, a contour plot of time savings per flight ($t_{\text{total,sub}} - t_{\text{total,sup}}$) can be constructed as a function of the cruise Mach number of the supersonic vehicle and cruise range. Figure 24 and Figure 25 show two example cases (100% over water for both). In the first example, the cruise Mach number and cruise range are set to 2.0 and 6,000 nmi, respectively (shown as the red cross in the figure), whereas the maximum range of the supersonic vehicle is set to 4,500 nmi. This is the reason why a vertical distortion in the contour lines appears at 4,500 nmi; additional time is required to make a refueling stop for any range beyond that value. In this example, the total time savings was 4.5 hr. In the second example, the cruise Mach number and cruise range are set to be 2.0 and 7,000 nmi, respectively (again shown as the red cross in the figure), whereas the maximum range of the supersonic vehicle is set at 3,000 nmi. In this case, two vertical distortions appear in the contour lines because one refueling stop would be required for any range between 3,000 nmi and 6,000 nmi, and another stop would be required for any range greater than 6,000 nmi. In this example, the total time savings was 3.2 hr.

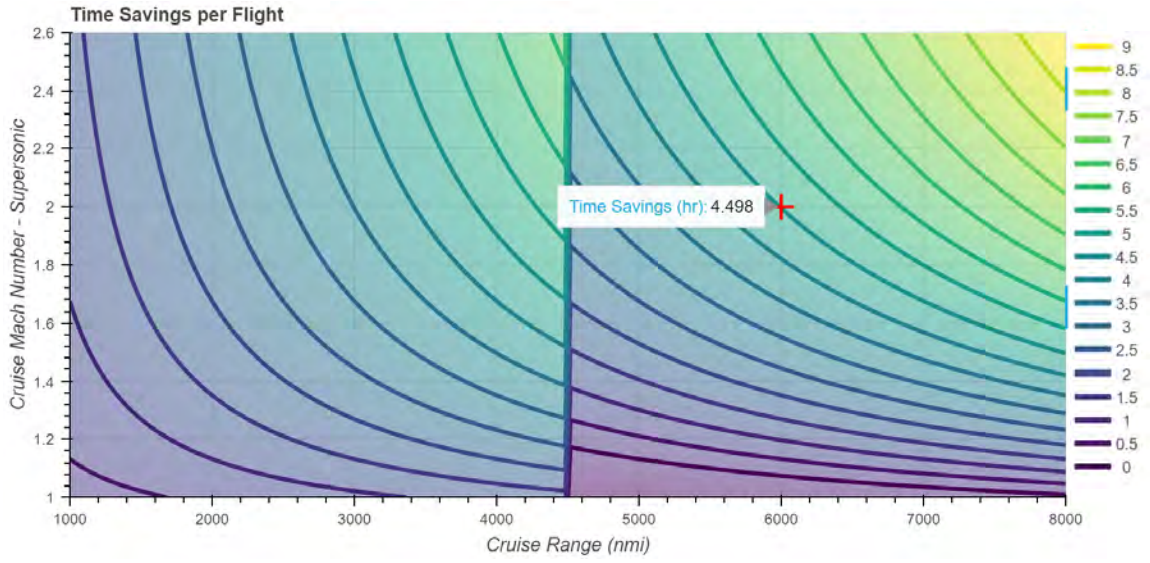

Figure 24. Time savings for Mach 2.0 and 4,500-nmi maximum range.

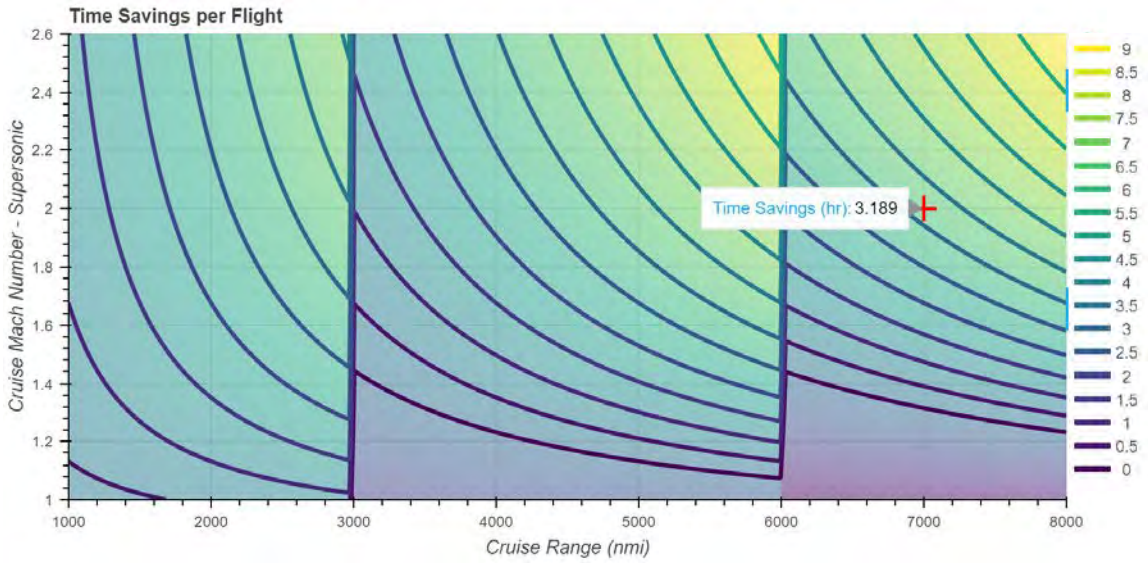

Figure 25. Time savings for Mach 2.0 and 3000-nmi maximum range.

Aircraft utilization within a 24-hr period for both subsonic and supersonic vehicles can also be determined by using the user-input flight and aircraft characteristics. On the basis of the total flight time per trip, and taking into account the turnaround time on the ground, the maximum utilization can be determined. Aircraft utilization corresponding to the two example cases is shown in the figures below. As shown in Figure 26 and Figure 27, a supersonic return flight is possible in the first case with an overall utilization of approximately 19 hr (including turnaround time). In the second case, however, the supersonic aircraft requires two refueling stops to accomplish its mission in approximately 12 hr, and there is no time left to turn around and complete a return flight.

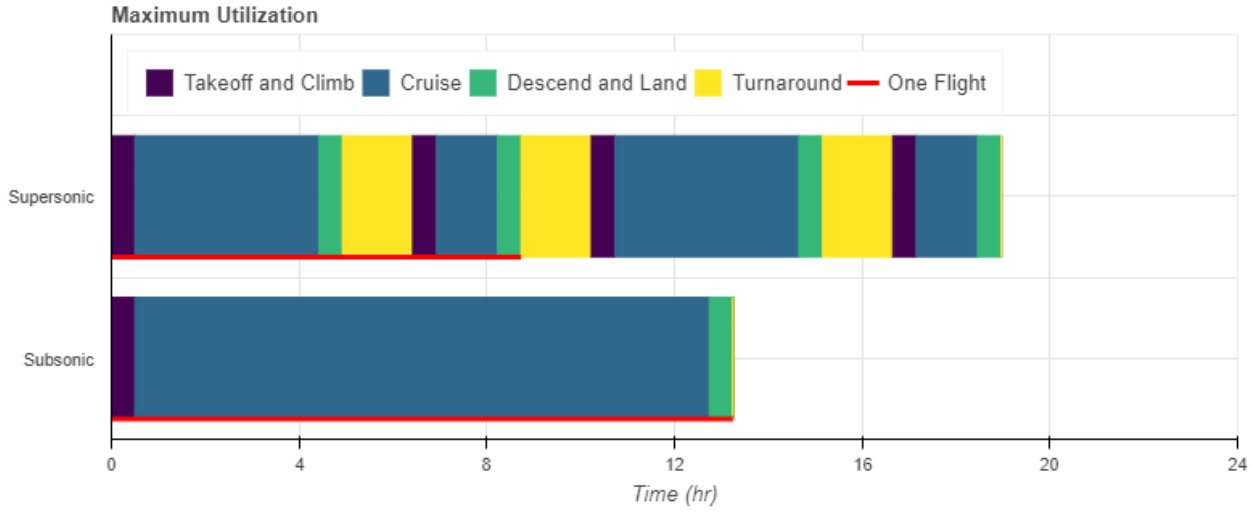

Figure 26. Utilization for supersonic vs. subsonic Mach 1.4.

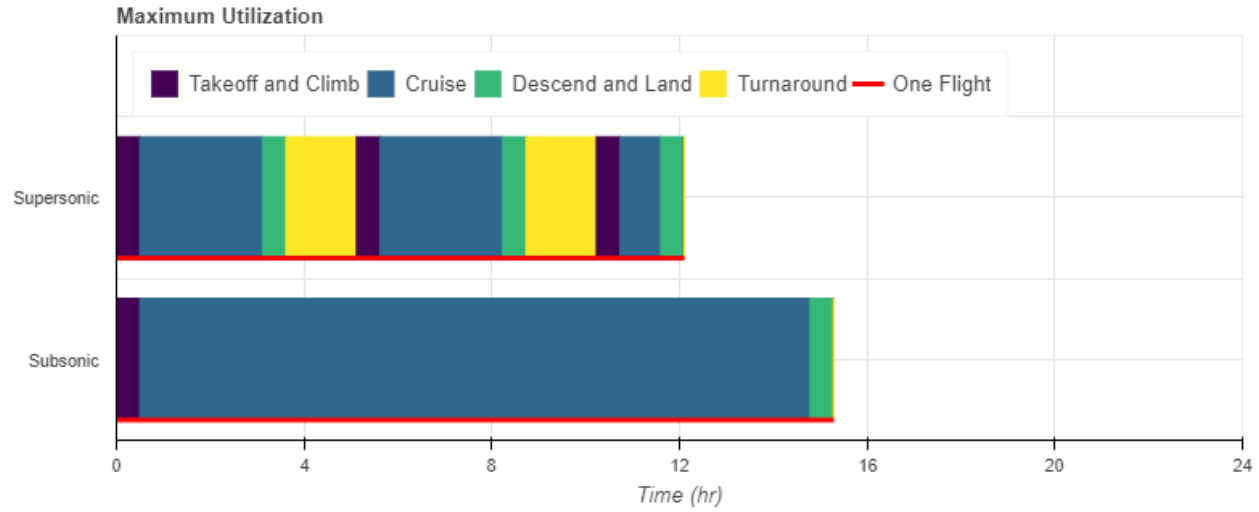

Figure 27. Utilization for supersonic vs. subsonic Mach 2.2.

A utilization analysis was conducted for the two concept supersonic vehicles assessed by using constraint and mission analyses. For the 10–12-passenger business jet, with a cruise Mach number of 1.4 and a maximum range of 4,000 nmi, a design range equal to its maximum provides aircraft utilization of approximately 21 hr (assuming 100% over water). The supersonic business jet provided 3.1 hr of time savings per flight relative to the subsonic vehicle. It was able to complete three flights within a 24-hr period, as compared with just two for the subsonic vehicle. Similarly, for the 50–60-passenger airliner, with a cruise Mach number of 2.2 and maximum range of 4,500 nmi, a design range equal to its maximum provides aircraft utilization of approximately 22.5 hr (assuming 100% over water). The supersonic airliner provided 5.6 hr of time savings per flight relative to the subsonic vehicle. It was able to complete four flights (two round trips) within a 24-hr period, as compared with just two (one round trip) for the subsonic vehicle. The utilization plots for the two concept vehicles are shown in the figures below. The results show that, for their respective design mission ranges, the two concept supersonic vehicles offer high productivity from a utilization standpoint. Both vehicles are able to perform more flights and result in higher utilization within 24 hr than their subsonic references (Figure 28 and Figure 29).

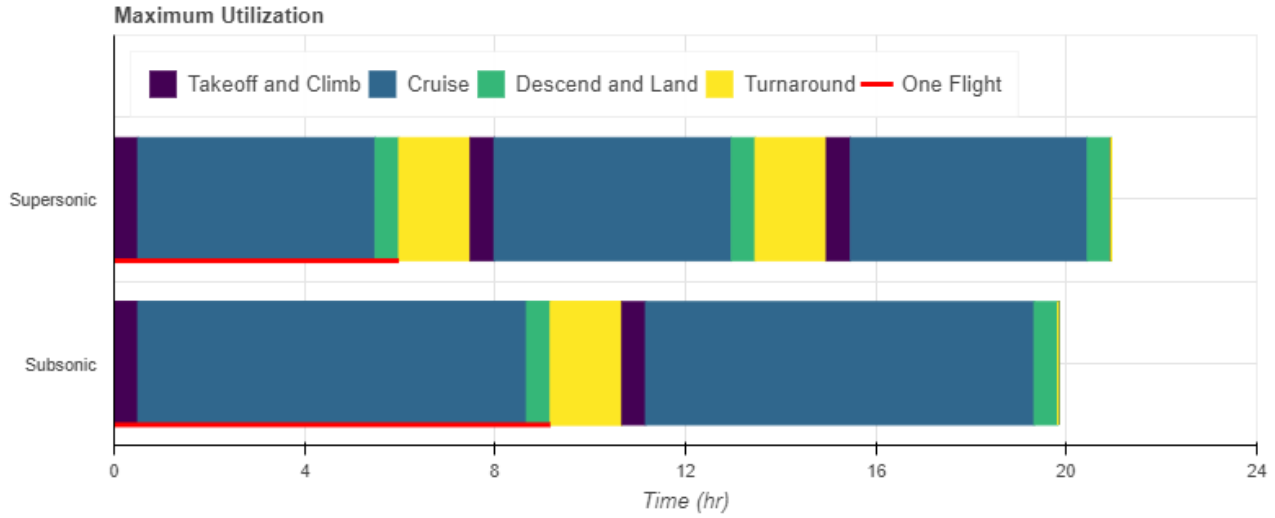

Figure 28. Utilization for supersonic vs. subsonic Mach 1.4.

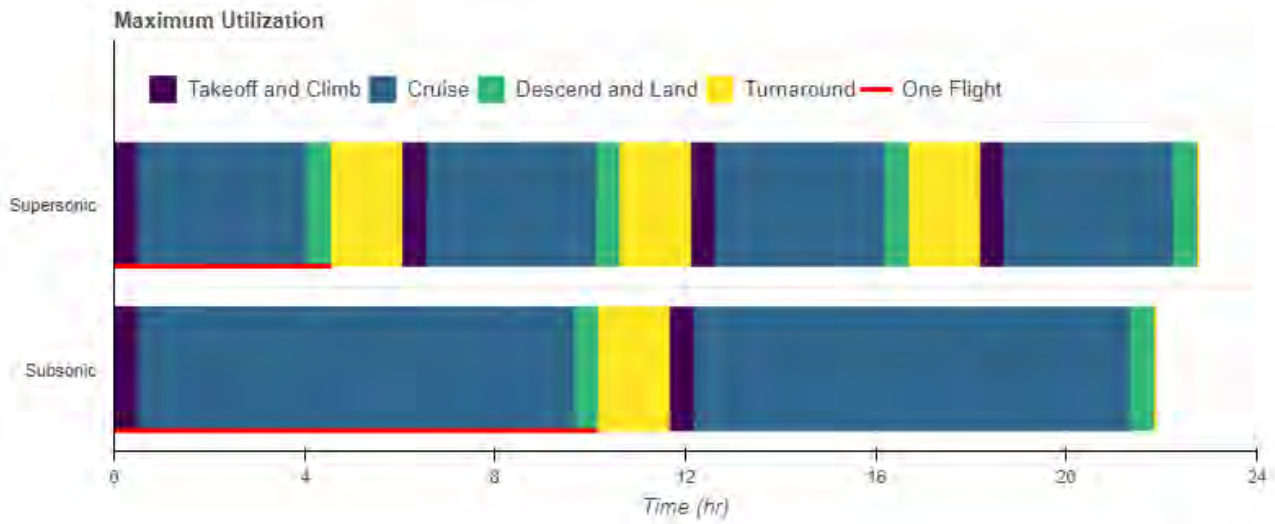

Figure 29. Utilization for supersonic vs. subsonic Mach 2.2.

Preliminary estimates
For the two concept supersonic vehicles considered in the previous constraint, mission and utilization analyses, a preliminary estimate of fuel efficiency can be determined by using the number of passengers, design range, and block fuel. For the supersonic business jet, the fuel efficiency was computed to be 1.275 lb/seat/nmi. This value is more than twice that of the Concorde. However, that finding was expected, given the low number of seats. Alternatively, for the supersonic airliner, the fuel efficiency was computed to be 0.275 lb/seat/nmi. This value is almost half that of the Concorde and is in perfect alignment with the NASA near- and midterm goals. Results for fuel efficiency are summarized in Table 6.

Preliminary estimates for the other KEIs, such as cruise NOx emissions and airport noise, remain to be investigated. The bulk of the effort for Task 2 was dedicated to the construction of the interactive and parametric conceptual design tools (dashboard), and the analysis of fuel efficiency. The developed tools will be utilized in a similar manner to assess the remaining KEIs in future work.

Table 6. Summary of characteristics for two supersonic aircraft concepts.

	Supersonic Business Jet	Supersonic Airliner
Number of Seats	10	55
Design Range (nautical miles)	4,000	4,500
Block Fuel (pounds)	51,000	68,000
Fuel Efficiency (pounds per seat per nautical mile)	1.275	0.275

This tool was also used to assess and inform specific phases of flight and constraints for the aircraft developed in Task 5 as well as other publicly reported aircraft data and capabilities on an ad hoc basis.

Task 3 - Investigation of the Ability of AEDT to Analyze Supersonic Vehicles

Georgia Institute of Technology

Objective

This task focused on identifying the modeling capabilities and potential gaps in the tools used for aircraft environmental predictions. Georgia Tech was to identify existing models of supersonic aircraft in the AEDT vehicle database, including the Concorde and some military aircraft. AEDT studies were to be created on some routes of interest to generate single-flight results for these vehicles, and their modeled KEIs were to be documented. Additionally, Georgia Tech was to update and

attempt to import and generate the same information for AEDT vehicle coefficients for a 100-passenger supersonic aircraft that was previously developed for the NASA Research Announcement "Integration of Advanced Vehicle Concepts into the NAS." In this process, any potential errors or gaps in the capability were to be documented. To identify potential modeling gaps, we identified coefficients in the AEDT vehicle modeling definitions pertaining to the specifics and peculiarities of those vehicles. An existing known subsonic aircraft with general characteristics close to those of the vehicles under study was to be duplicated, and coefficients used in certain aspects of modeling and phases of flight were to be adjusted to possible values for that particular supersonic aircraft. The resulting definition of this adjusted vehicle were to be run through AEDT to identify potential errors or gaps in modeling capability. This was to be documented along with potential solutions for addressing the particular requirements of modeling supersonic aircraft.

Research Approach

To facilitate environmental impact prediction of supersonic aircraft, the modeling capabilities and potential gaps in the tools used for these predictions must be identified. As part of this task, Georgia Tech researchers identified existing models of supersonic aircraft in the AEDT vehicle database, including the Concorde and some military aircraft. These models were then reviewed regarding how these aircraft were modeled. The next step will be to create AEDT studies on some routes of interest to generate single-flight results for these vehicles and document the modeled KEI information for these aircraft types. To identify potential modeling gaps, the Georgia Tech researchers identified coefficients in the AEDT vehicle modeling definitions that pertain to the specifics and peculiarities of those vehicles.

Supersonic vehicles in AEDT

The first step of the task was to test one of the current supersonic models in the AEDT database. The primary civilian aircraft in AEDT's fleet database is the Concorde.

For this test, a study was created in AEDT to plot the noise contour generated by a takeoff of the Concorde at JFK. The first step is selecting the adequate equipment, which is the CONCORDE/OLY593 in the AEDT database (Table 7).

To test the Concorde noise estimates in AEDT, an airport must be selected in AEDT. JFK, with default layout, is chosen for this purpose. The operation must be defined for the aircraft; here, takeoff is chosen, for the north-east track. An annualization for this operation is then defined (i.e., the frequency of such an operation). The idea is to plot the contours for a single flight and not repeat the operation over time. Of note, historically, the takeoffs and landings performed by the Concorde at JFK were not straight but instead attempted to minimize time over land because of noise concerns. Next, a receptor grid must be generated. A 120 × 120 receptor grid, spaced out by 1.5 nautical miles each, was chosen. The grid must be centered on the airport and sufficiently large to allow the noise contours to be closed; otherwise, they will not be plotted by AEDT.

Table 7. Default configuration of the Concorde in AEDT.

Parameters	Value
Maximum gross landing weight (lb)	245,000
Maximum landing distance (ft)	10,600
Maximum gross takeoff weight (lb)	400,000
Number of engines	4
Maximum SLS thrust (lbs/engine)	38,100
Maximum operating speed (knots)	500
Maximum operating Mach number	1.2
Maximum operating altitude (ft)	41,000
Wing surface area	181.2

In this case, the most relevant metric for noise of an aircraft c was the single event level (SEL), which is the most appropriate for a noise metric for a single flight, because it is the metric that is used in aggregated form in the day-night level (DNL) for regulatory purposes. With these parameters, the simulation on AEDT gives the following noise contours shown in Figure 30. Notably, this is for a specific straight departure from JFK only. This does not in any way represent the departures that the Concorde performed in the past, in which, to minimize noise exposure over land, the actual tracks were heavily biased to be over water. Furthermore, this straight path does not follow any currently used tracks at JFK or in the New York airspace.

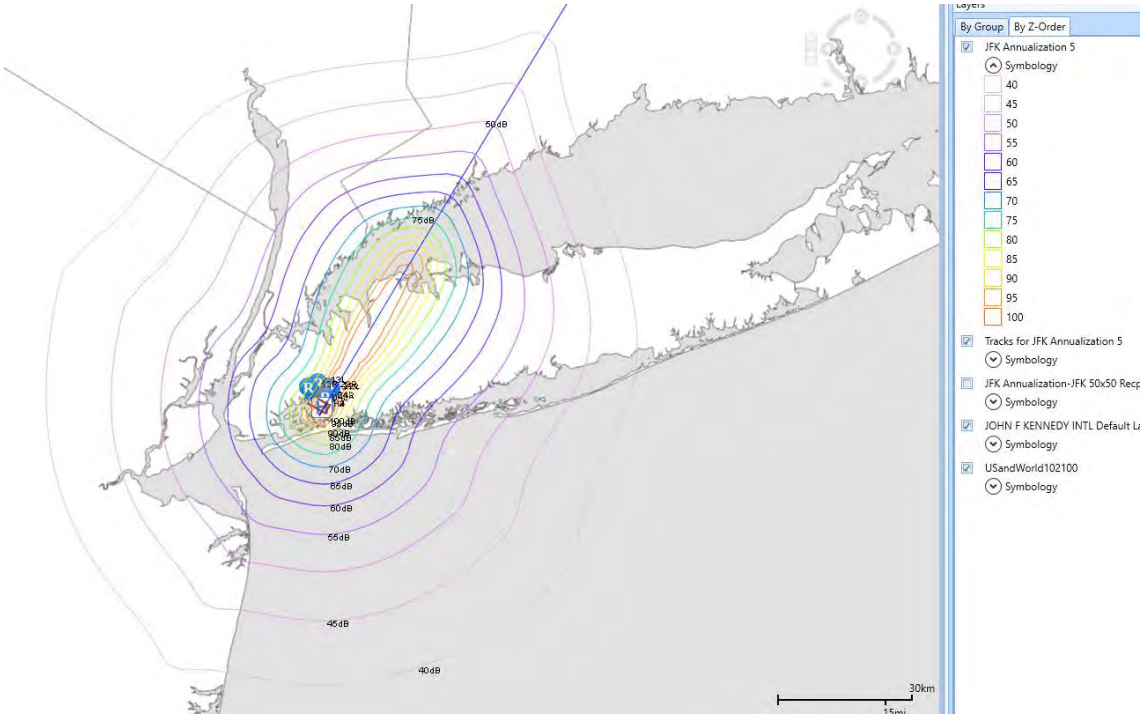

Figure 30. Noise contours for Concorde takeoff at JFK.

A simulation for several flights of the Concorde was performed through the AEDT tester developed by the Aerospace Systems Design Laboratory. The tester takes all the flight combinations from the AEDT database and performs the calculation for the flights suitable for the chosen aircraft.

AEDT model of the Concorde

Aircraft Noise Performance (ANP) model

The ANP model data contain a Concorde model. This is not surprising, given that the Concorde was one of the first aircraft to undergo noise certification, thus providing the necessary data to create the ANP model. The model has several interesting features, probably as a result of the age of the model data. First, only STANDARD procedures but no ICAO procedures are included, even though the Concorde did use noise-abatement procedures. Another feature of the ANP model is that it includes a standard climb power thrust curve and a reheat thrust curve, both of which are used in the procedures. However, it does not include alternate thrust curves for temperature variations, as found in most current ANP models.

In the noise model for the Concorde, there are only three thrust settings for which noise curves exist. Additionally, the highest departure thrust noise curve is at 32 klbf thrust per engine, whereas the Concorde produced close to 38 klbf per engine with reheat. Consequently, if the thrust exceeds the value of the highest thrust noise curve, the noise values will be extrapolated. In this case, even at 32-klbf thrust, the noise at a 200-ft distance is 138 db Single Event Level (SEL), which is without reheat. Extrapolation would push the noise close to 140 dB. The spectral classes being used in the noise modeling for atmospheric adjustments are 106 and 206, which are the low-bypass relative frequency loudness adjustments.

BADA 3

The Base of Aircraft Data (BADA) model database is used in AEDT for aircraft modeling over 10,000 ft above field elevation and especially during cruise phases. Because this model and database are relatively new, having been introduced after the retirement of the Concorde, they do not contain a Concorde model. The AEDT fleet database default substitution model is the FGTL (generic heavy fighter) model, which is based on the Rockwell B1 Lancer, using a cruise Mach of 0.8. This substitution is probably based on the closeness in the MTOW (180,000 kg vs. 186,000 kg) and the same number of engines with similar SLS thrust. The resulting mission fuel burn, compared with reference values from the flight manual, is shown in Figure 31.

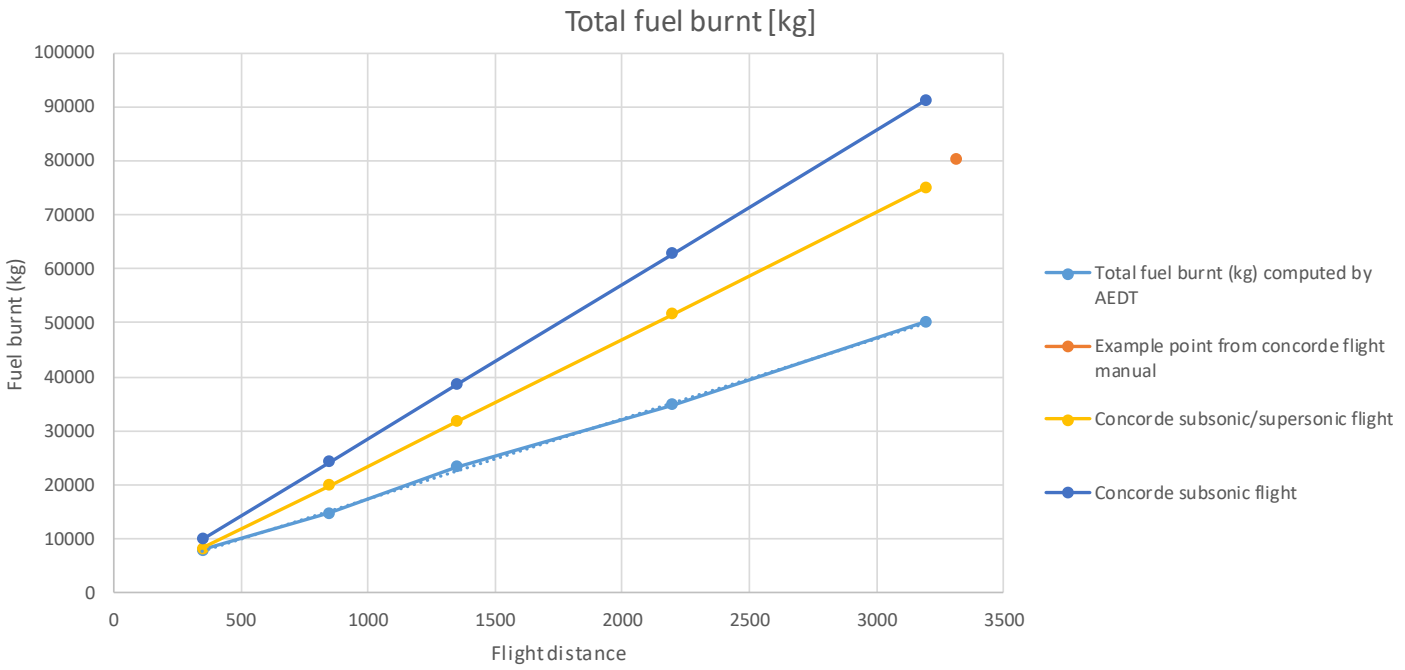

Figure 31. Concorde fuel burn estimates based on flight distance

Engine Emissions Databank (EEDB)

The latest versions of the EEDB do not contain any information of the Olympus engines. However, the AEDT fleet database does contain an entry, which is marked "EDMS 4.5 – Rolls Royce." Therefore, the Georgia Tech research team presumed that the engine at one point existed in the EEDB and was eventually removed after the retirement of the Concorde. Of note, the data do not include thrust information, and it is therefore not possible to conclude whether the data do or do not include reheat information. Additionally, the entry contains four values for fuel flow and each emissions species. This, however, does not match the expected five sets of values for the certification of supersonic engines. Additionally, the thrust levels for each sets of points are defined considerably differently and also depend on the presence of reheat capability. Therefore, what the values represent is unclear. These values might possibly be assumed to represent subsonic engine equivalents that are designed to match the definition of the four subsonic point values. This is consistent with how AEDT will interpret these values.

Modeling by phase of flight

ANP model

The current way of modeling takeoff and landing performance under 10,000-ft field elevation is to use the ANP models and the modeling methods described in ICAE Doc 9911 and previously described in SAE 1845, as well as the INM Manual. Because the modeling is derived from also modeling military aircraft, it does include provisions for aircraft whose performance characteristics are somewhat similar to those of high-speed military aircraft, at least in takeoff and landing characteristics. Specifically, these characteristics include possible use of reheat, aerodynamic optimization for high speed, and aircraft configuration changes.

The possible use of reheat is addressed in a later section. The aircraft shape optimization for high efficiency at supersonic Mach numbers usually requires a substantial trade-off in efficiency at low-speed flight. Therefore, many supersonic aircraft struggle to produce enough lift at low speeds to sustain flight. Consequently, in addition to very high angles of attack and deployable surfaces, increased speeds are often necessary at takeoff, such as V_1, V_R, and V_2, in addition to higher speeds at low altitudes, potentially in excess of 250 knots under 10,000 ft. Additionally, higher landing speeds can also be necessary. Thus, the default reference speeds used in the performance modeling, but especially in the source noise modeling and data, are potentially too low. The effects of this are currently being investigated in ASCENT Projects 43 and 45. Aerodynamic

configurations such as additional moveable surfaces and other features that change the configuration and aerodynamics of the aircraft are implementable by defining these as additional entries into the FLAPS table and using them in the corresponding procedure steps. Consequently, the manufacturer must supply this information so that it can be used during modeling.

BADA

BADA is currently used for modeling the aircraft performance over 10,000 ft above field elevation. It also includes only a single thrust and fuel curve, which might not be adequate to model the aircraft engine performance over a wide variety of Mach numbers and inlet and nozzle configurations, especially in a linear fashion, as is currently the standard in version 3. Although the model does not explicitly cover supersonic flight, it could potentially be adapted to allow this, given additional configuration data. The current implemented version explicitly forbids Mach numbers greater than 1.0. Additionally, BADA 3 currently provisions only a single cruise configuration. This would need to be expanded to account for the differences in subsonic and supersonic configurations of the aircraft.

The climb procedure over 10,000 ft, by default, uses a defined energy share (share of potential energy contribution to altitude vs. speed increases), while following a constant calibrated airspeed (CAS). This is continued until a transition altitude, wherein the climb CAS speed equals the climb Mach number. The climb to the initial cruise altitude then continues at that constant Mach number. This mimics a relatively standard way in which conventional subsonic passenger aircraft are flown.

For supersonic aircraft, however, in the aircraft procedure coefficients, a second segment climb and cruise speed and Mach number can be specified such that the transition altitude occurs at a projected altitude at which the transition from subsonic to supersonic flight is expected to occur. This was tested on the 100-seat airliner model created for NASA in a previous project (Blake et al., 2010). The result is that the current version of AEDT will handle the transition to supersonic cruise as long as the drag polar for cruise as well as the TSFC curves are designed to match cruise conditions correctly. The transition itself is not handled very well. It tends to consist of a very brief jump from subsonic to supersonic that completely misses the drag rise as well as the fuel burn and associated emissions caused by the transition. This can cause an additional modeling error on the order of a few percent of mission block fuel. However, given that the system was never designed for modeling these conditions, as well as the lack of any other modeling standards, it is probably acceptable for the short-term future.

Figure 32 shows that this is too simplistic for a supersonic passenger aircraft, at least in the way the Concorde was supposed to be flown. Specifically, there are different procedures depending on whether a subsonic cruise or a supersonic cruise will be performed and whether the climb to supersonic cruise must be delayed for overland noise rules. Additionally, the transition from subsonic flight to supersonic flight typically must be achieved as quickly as possible to minimize time in very high drag conditions while not violating flight envelope and center of gravity constraints. The current number of coefficients present in the BADA procedure definition is insufficient to describe the specific details, especially if this is materially different between potential future supersonic aircraft.

Noise modeling

The current state of noise modeling in AEDT is entirely limited to the use of noise-power-distance (NPD) curves, which describe the aircraft noise signature as a function of the engine thrust (power) and distance of the observer. The distance data are limited from 200 ft to 25,000 ft but can be extrapolated if required by using a linear method. This method is probably sufficient to properly capture the noise generated by a supersonic aircraft near and around airports but is not suited to propagating the boom noise created by the shock waves from high altitudes, nor does it capture any potential focusing or dissipating effects due to trajectory or atmospheric effects. However, there are a few research codes (such as PCBOOM), that currently allow for calculation of the boom effects on the ground. These methods and the required data will need be integrated in AEDT, if such functionality is desired.

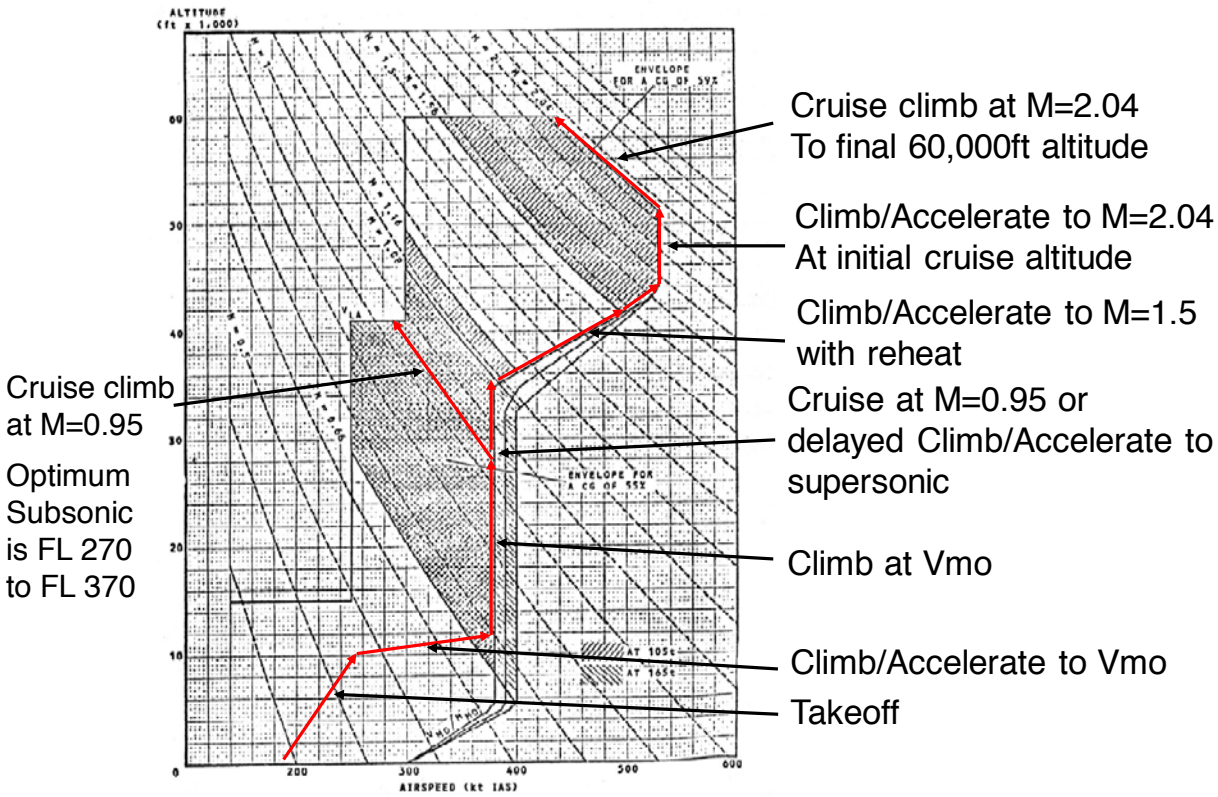

Figure 32. Concorde operational envelope (altitude in feet versus indicated airspeed in knots) with standard climb to cruise procedure shown (The Concorde Flying Manual Volume II, 1976).

Emissions modeling

AEDT uses the Fuel Flow Method version 2 (Dubois & Paynter, 2006) to use the ground test data obtained during engine certification and published in the ICAO EEDB. This method uses four defined throttle settings with fuel flow end emissions index (EI) values to interpolate the values over the entire flight envelope. It also adjusts the equivalent combustor inlet conditions from the SLS data to the appropriate conditions at any altitude. The altitude adjustment is based on adjusting the changes in free stream conditions to equivalent changes in combustor inlet conditions by using isentropic relations. Therefore, an aircraft in supersonic flight will violate this assumption because of the shocks produced by the nose and the inlet compression shocks during supersonic flight. Supersonic inlets tend to have a number of moving surfaces to optimally adjust to the required conditions and to allow the engine to operate normally and effectively during a wide range of Mach numbers. Consequently, the required conditions heavily depend on the specifics of the situation and the inlet configuration required. However, because an objective of the inlet is to slow the free stream to acceptable subsonic conditions at the face of the engine inlet at all times and to minimize losses as much as possible, an additional inlet correction factor could potentially be assigned according to inlet total pressure recovery. This correction factor could take the form of an ideal number based on Mach number or actual inlet performance, if available. The current combustor correction coefficients, which are based on a 1990s-era CFM56 empirical correlation, might possibly need to be updated similarly to the required updates for modern staged-combustion engines.

The nozzle performance is an additional potential issue. Supersonic aircraft will require a much more complex nozzle than that in a simple subsonic converging exit. The Concorde utilized a secondary set of nozzles on each engine designed to improve subsonic performance. The current modeling method adjusts for installed effects with simple fixed multipliers from the ground test data. How these multipliers will need to be adjusted is unclear, because of the much larger installed effects that an integrated engine of a supersonic aircraft will present. Another potential issue is that the adjustments for speed and altitude effects relative to the static ground tests will probably need to be adjusted. The specifics will depend on how and

which equipment will be included in the ground tests. Unlike the military-aircraft noise modeling that lends itself to adoption to supersonic passenger aircraft, there is no emissions certification requirement for military aircraft.

Reheat
The Concorde made use of reheat during takeoff to meet certification requirements in the case of engine failure but would terminate reheat below 1,000 ft if all engines continued to operate nominally. Additionally, the Concorde made use of reheat to minimize the time spent in the region of transonic drag rise during the climb to supersonic cruise.

Modern supersonic aircraft are not expected to require or include reheat, because of better engine thrust and efficiency, and the potential fuel penalty for not using reheat either being completely eliminated or small enough to outweigh a host of other issues, such as maintenance cost and regulatory complexity. The capability of properly representing reheat beyond the current capabilities is unlikely to be required in the future.

Potential areas for improvement
This work identified the following key issues that will need to be addressed for improving the modeling of supersonic aircraft in AEDT:

- Transition from subsonic to supersonic
- Supersonic cruise
- Emissions modeling
- Noise modeling
- Boom modeling

A key element in modeling a supersonic aircraft is to be able to model the transition from subsonic flight to supersonic flight. This involves crossing the highest drag regime of flight and contributes a substantial amount of the fuel burn and emissions. As investigated, this transition can currently be approximated by a sudden jump, but such a jump neglects this portion of flight almost completely. This will require modeling either through a generic transonic drag rise approximation or additional aircraft specific coefficients.

The modeling of supersonic cruise currently does work but can be improved. The atmosphere model that is used may potentially need to include more sophisticated data about the actual altitudes of the atmospheric layers. Additionally, an aircraft model is currently limited to either subsonic or supersonic flight but cannot accommodate both. This is potentially necessary because supersonic cruise is currently prohibited over land, and the model must be able to accommodate that.

After performance modeling, emissions modeling is another area for improvements. Specifically, the current full flight emissions modeling method—the Boeing Fuel Flow Method (BFFM)—is used because it avoids requiring detailed engine performance parameters. It relies on first-principles physics relations for atmospheric and engine cycle approximations and empirical fits for combustor properties. This needs to be updated to accommodate the cycle differences and the differences in operating conditions at altitude.

Finally, the modeling of aircraft noise needs to be addressed. The airport noise is not specifically different for supersonic aircraft but will be dominated by jet noise, owing to the potentially high exhaust speeds required for supersonic cruise. This will potentially require the de-rating for takeoff to meet stringent noise limits. This will need to be addressed, potentially in a similar way to handling of subsonic de-rating in AEDT. Integrating supersonic boom modeling with AEDT will become necessary. This could be accomplished either through the validation and integration with existing tools, such as PCBOOM and others, or alternatively direct integration of modeling methods or code into AEDT. Some work is required before AEDT will be able to model supersonic aircraft with good fidelity, but the issues have been identified.

Task 4 - Fleet-Level Environmental Assessments

Georgia Institute of Technology and Purdue University

Objective

This task was to quantify the fleet-level impact of supersonic aircraft. Georgia Tech was to use the GREAT fleet-prediction tool to perform a preliminary assessment of the impact of supersonic aircraft by using a subset of scenarios from prior

ASCENT 10 work and for a subset of the KEIs and aircraft types evaluated in Task 2. Similarly, Purdue was to utilize their FLEET capability to analyze this impact.

Research Approach (Georgia Tech)

To prepare modeling of supersonic aircraft, several changes to the modeling toolchain were necessary. First, the models developed in prior iterations—GREAT and the IDEA Tool—needed to be updated. In GREAT and IDEA, the current subsonic fleet is divided into seat classes to track the different sizes as well as the payload-range capabilities of the current fleet of aircraft in operation. To model a supersonic fleet, the team decided to add a new seat class, SST, to track these new aircraft separately. However, that means that, for now, there is only a single type of supersonic aircraft being tracked: a 55-seat commercial jet with a maximum range of approximately 4500 nmi, to mimic one of the potential new market entrants that could enter service in the next few years. For now, it was decided to set the earliest EIS to 2025.

The model was also altered in two ways to model the potential number of supersonic flights. First, it is now possible to simply specify a fraction of the fleet that would be switched or replaced by supersonic flights. Notably, this can be specified for all modeled regions: domestic, Atlantic, Pacific, Latin American, and other regions. Therefore, the implications of switching a certain number of passengers or flights in those regions can now be investigated. This is especially important with regard to investigating the potential for allowing or disallowing overland supersonic flights, because, most domestic flights are almost 100% overland flights in the United States. This also has an effect on the missions and markets in which a potential supersonic aircraft would be used.

The second method added to the models builds on this capability by partially reusing the logic of converting production numbers into potential replacement aircraft and therefore the ability to replace a certain share of the projected operations. This allows the user to specify aircraft production rates. The produced aircraft are then inserted into the fleet to be used to replace existing aircraft. This process also necessitates assuming a productivity per aircraft. This productivity refers to how many passengers and miles it will be used in service and is normally a function of primarily utilization, because subsonic fleet block times and speeds (the gate-to-gate time and average speed based on this time) have been relatively constant over the past decades. However, supersonic aircraft by definition have much higher block speeds and therefore would theoretically be capable of flying many more missions than subsonic aircraft. However, according to the analysis in Task 2, keeping a high utilization seems likely to become a major challenge, and consequently supersonic aircraft may be unlikely to yield increased productivity. Therefore, at present, the assumptions were set to have an increased block speed with a lower utilization and thus only a small change in the number of flights possible in a given time period per aircraft in the supersonic fleet. An example of the production assumption based on a study from the Boyd Consulting Group (Bachman, 2016) estimating a potential 10-year demand of up to 1,300 supersonic airliners is shown in Figure 33. This number of aircraft with the assumed productivity would be able to capture approximately 5% of the market. For the purposes of this investigation, the manufacturer was assumed to face a 4-year production ramp-up to the targeted production rate of 11 aircraft per month. The result is shown as a share of the overall fleet. The curve bends down substantially, because of the large increases in the conventional fleet forecasts in the coming decades, such that a constant production rate yields a diminishing share of the overall fleet.

The standard fleet turnover model applicable to all seat classes was also used. Consequently, the models have the capability to replace aircraft within their seat class with potential improved future aircraft with similar capabilities. At present, it was assumed that a supersonic aircraft would be operated more similarly to current wide-body aircraft in terms of time of ownership and the underlying financing and leasing durations and the expected useful economic life.

Using these production rate assumptions along with the vehicle specific performance estimates from Task 2 allows for the fleet analysis to be run. The scenarios developed for the subsonic projections of commercial-aviation environmental impact can be used as a basis for analyzing the effect of a potential supersonic fleet. Notably, the supersonic specific assumptions in terms of market share, production rate, passenger demand, and aircraft technology can be varied. This can serve as a guide as to the potential variability of these assumptions, as was done in this phase of the work. However, those assumptions may plausibly not be wholly independent of the assumptions developed for the subsonic-only scenarios. For example, engine and aircraft technology for both subsonic and supersonic vehicles could plausibly develop at least partly in tandem. Moreover, passenger demand for air travel is expected to affect both subsonic and supersonic travel together and not be completely decoupled, except in some very specific cases.

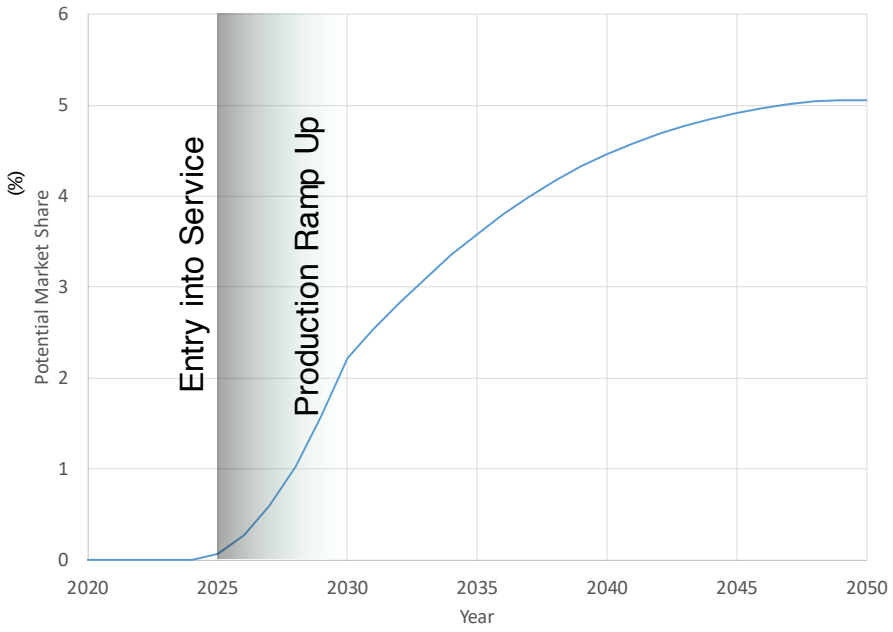

Figure 33. Percentage potential market share of a supersonic fleet.

The results presented here should be taken as a guide to the range of variability in the results instead of wholly consistent scenarios of the future. An example is in Figure 34, which shows the relative CO_2 emissions trajectories for the CTBG scenario as well as the same scenario but instead with a large fleet of operational supersonic commercial aircraft starting in 2025, with the production rate assumptions explained before.

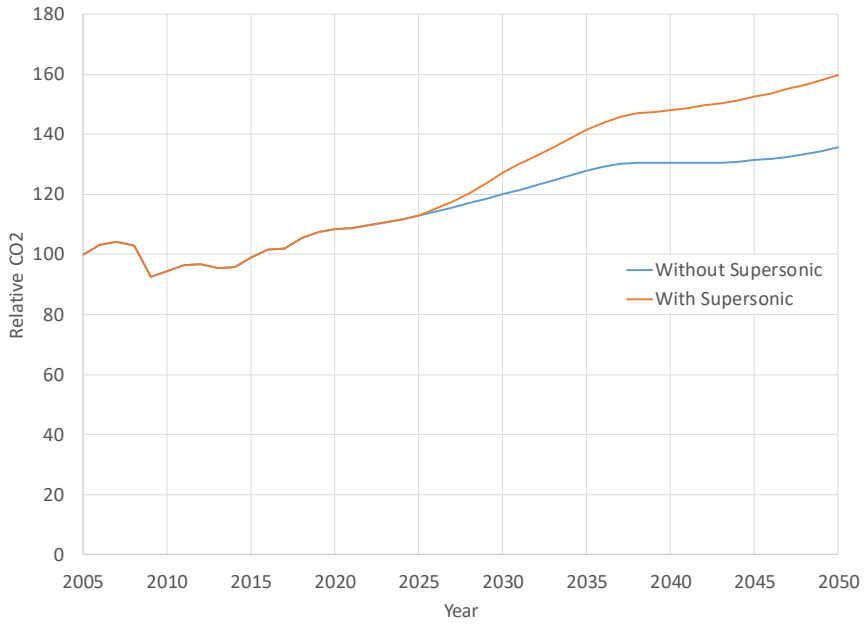

Figure 34. CTBG scenario's effects of including a large supersonic fleet (**Figure 33**).

Similar results were produced for most of the subsonic scenarios with and without supersonic aircraft being introduced. Additional metrics such as specific fleet makeup as well as passenger demand and airline operating cost structure were generated in addition to the fuel burn and CO_2 emissions results. To summarize the results of these runs, the Georgia Tech researchers aggregated them as ranges of the fleet-wide delta in CO_2 emissions in 2050, that is, the emissions with a supersonic fleet minus the emissions without a supersonic fleet. The results show the potential size of the resulting additional emissions that a fleet of supersonic airliners could potentially produce (Figure 35). The primary drivers of assumptions for the supersonic fleet are summarized in the three rows shown. The first row shows the impact of the market-size assumption, which could range from a very limited adoption of approximately 12 aircraft that fly only one to two round trips per day to the potential switch of the entire market of passengers paying for premium tickets in business class, first class, and above. A large fleet of supersonic airliners would be required, which, at a multiple of fuel burn and therefore emissions, would drive a substantial increase in emissions. The second row shows the impact of vehicle technologies on the 2050 emissions. The worst case would be a significant fleet of current-technology-only aircraft, with estimates as developed in Task 2, and the best case based on the aggressive mid- and far-term technology goals defined by NASA's supersonic vehicle project. The third row attempts to show the interaction between the primary subsonic aviation growth rates and the resultant supersonic demand. This is in effect a scaling occurring because of the overall increase or decrease—or better, high growth or low growth—of aviation travel as a whole, of which supersonic airliners are expected to capture only a small portion. Nonetheless, the results show substantial variation depending on the underlying assumptions provided by those specific scenarios.

Additionally, these ranges represent only a one-at-a-time sensitivity. There are potentially significant interactions that could take place, including not only interactions among the scenario assumptions for subsonic and supersonic demand, technology, operations, etc., but also the interactions among the supersonic market adoption rate, aviation growth, and vehicle technology. This was not studied at this stage of the project, but we envision such studies after better vehicle performance and demand estimates have been developed.

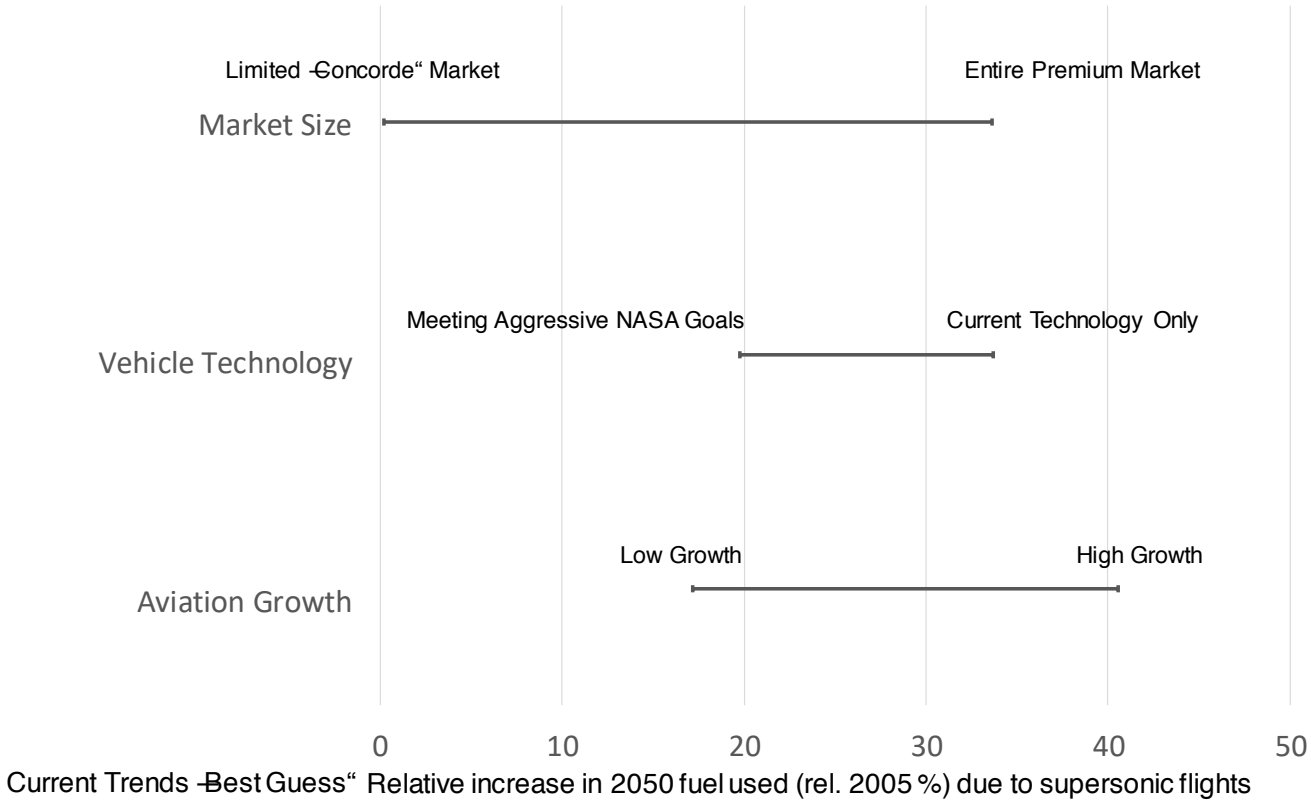

Figure 35. Range of results due to possible assumptions for supersonic aircraft.

Research Approach (Purdue)

Incorporating supersonic aircraft in the FLEET allocation problem

For the work presented here, the allocation of the airline's supersonic aircraft occurs before the allocation of the airline's subsonic aircraft. This approach allows for the characterization of a subset of total passenger demand as the passengers who would be willing to pay for the supersonic fare, and it currently assumes that the supersonic fare will be similar to the as-offered fares for business class or above available in 2018. Because these passengers would be willing to pay more for the higher-speed and shorter-time trips, this subset of demand is identified on all of the potential supersonic routes, and an allocation problem determines how many supersonic aircraft round trips operate on which of the potential routes to maximize the profit from the supersonic aircraft in the airline's fleet. Then, for any routes that have potential supersonic demand but do not receive supersonic aircraft service, and for any routes that have supersonic aircraft service but do not have enough round trips to serve all the supersonic passenger demand, the unserved supersonic passenger demand is recombined with the subsonic passenger demand. The subsonic allocation problem then determines the number of round trips operated by each subsonic aircraft type on all of the routes in the network to serve the recombined passenger demand. Figure 36. **SEQUENTIAL AIRCRAFT ALLOCATION APPROACH IN FLEET** depicts the subsonic and supersonic aircraft sequential allocation approach in a flowchart.

The team acknowledges that a simultaneous allocation approach in which the airline would allocate the supersonic and subsonic aircraft at the same time (to satisfy both supersonic and subsonic flight demands) could have some useful advantages. Such an approach could provide insights about passengers' travelling preferences via supersonic and subsonic aircraft while allowing for the enforcement of noise and/or airport capacity constraints in FLEET, if those are desired in the simulation. However, the simultaneous approach is difficult to implement in FLEET, because it requires some restructuring of the allocation problem, thus leading the team to use the sequential allocation approach for the current work.

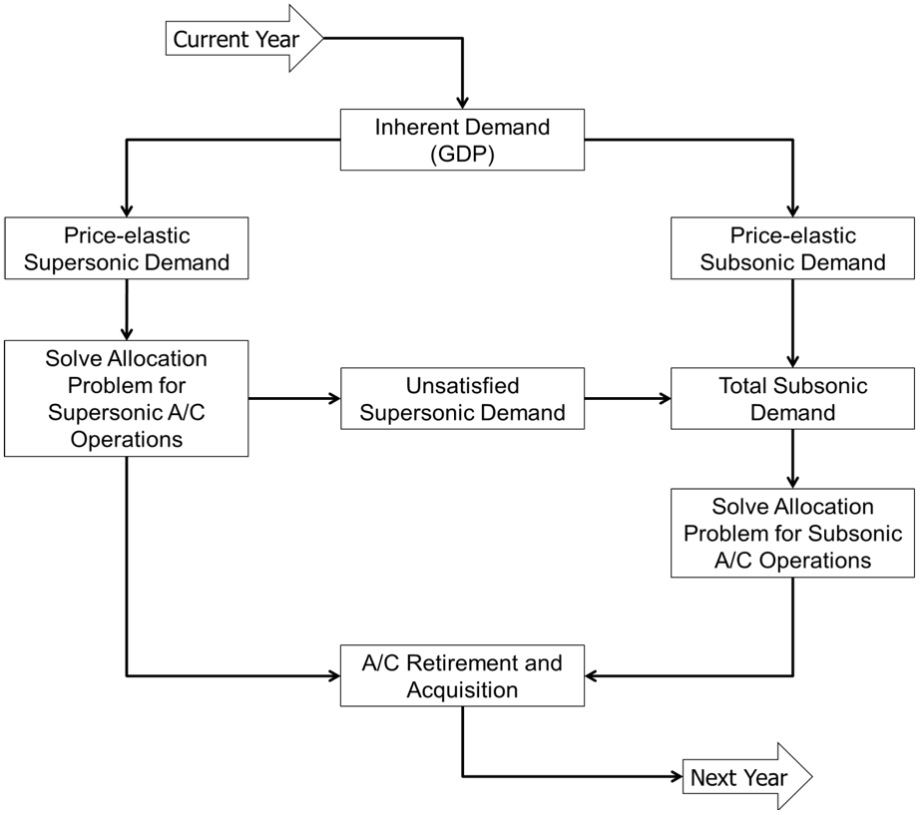

Figure 36. Sequential aircraft allocation approach in FLEET

In each simulation year, FLEET predicts the inherent growth in airline passenger demand due to the economic growth described in the scenario and then includes the effects of price-demand elasticity to account for the influence of airline ticket price changes from the previous year on passenger demand. For instance, if a new aircraft is introduced that is far more fuel efficient than its predecessors, some of the cost savings associated with that fuel reduction leads to a lower ticket price. That would drive the passenger demand up, separately from the inherent economic demand driver. After the sequential allocation problems are complete, the model can make assessments on the need for more aircraft to meet future demand and the future profitability of retiring a currently operating aircraft in favor of a newer model in the following year.

Allocation problem update

The previous FLEET simulation results included allocation of supersonic and subsonic aircraft over a 3-day period on the basis of a one-way allocation problem formulation. This caused the number of one-way daily flights in FLEET simulations to be in fractions (instead of integers). The Purdue team updated FLEET's allocation problem from a 3-day period to a 1-day period, while changing FLEET's problem formulation from a one-way formulation to a round-trip formulation. With the current updated problem formulation, the FLEET simulation results yield integer numbers of daily round-trip flights for both supersonic and subsonic aircraft allocations. The following expressions and equations describe FLEET's updated 1-day round-trip allocation problem setup.

Objective function:

$$\sum_{k=1}^{K}\sum_{j=1}^{J} pax_{k,j}price_{k,j} - \sum_{k=1}^{K}\sum_{j=1}^{J} X_{k,j}C_{k,j} \qquad \text{EQUATION 1}$$

Constraint functions:

$$\sum_{k=1}^{K} 2X_{k,j}\left(BH_{k,j} + MH_{k,j} + t\right) \leq 24 fleet_k \qquad \textbf{EQUATION 2}$$

$$\sum_{k=1}^{K} 2X_{k,j}\left(BH_{k,j} + MH_{k,j} + t\right) \leq 24 * 3\, fleet_k \qquad \textbf{EQUATION 3}$$

$$\sum_{k=1}^{K} pax_{k,j} \leq dem_j \qquad \textbf{EQUATION 4}$$

$$\sum_{k=1}^{K} pax_{sub,j} \geq 0.9 * subdem_j \qquad \textbf{EQUATION 5}$$

$$pax_{k,j} \leq cap_k X_{k,j} \qquad \textbf{EQUATION 6}$$

Equation 1 shows the profit-maximizing objective function of FLEET's sequential allocation problem. $pax_{k,j}$ is the number of passengers moved one way by using aircraft *k* on route *j* today. This assumes symmetricity in the number of passengers moved between origin-destination pairs A–B and B–A. $price_{k,j}$ is the round-trip ticket price for a passenger on aircraft type *k* flying route *j*. This work uses round-trip price because it matches most common fare paid by passengers (DB1B itinerary fare and the as-offered ticket prices for business and above in the current supersonic work). This step means that one passenger ($pax_{k,j}$) pays half of the round-trip price today. $X_{k,j}$ is the number of round trips that aircraft *k* provides on route *j*. A round trip is one flight from airport A to airport B and back from airport B to airport A. It can be only an integer. Finally, $C_{k,j}$ is the round-trip direct operating cost of aircraft *k* on route *j*.

Equation 2 constrains the total operation hours of subsonic aircraft and supersonic aircraft to 24 hr. This constraint signifies the update in FLEET's problem formulation from a 3-day to 1-day allocation. Equation 3 represents the previous 3-day-allocation version of this constraint with the total operation hours of subsonic aircraft and supersonic aircraft limited to 72 hr. The operating hours include block hours ($BH_{k,j}$), maintenance hours ($MH_{k,j}$), and aircraft turnover time (t) for both subsonic and supersonic aircraft. $fleet_k$ represents the number of subsonic and supersonic aircraft type k in the airline's fleet.

Equation 4 signifies the maximum demand constraint, which ensures that the demand served by the airline in FLEET does not exceed the demand value dem_j. Equation 5 ensures that the airline can satisfy all subsonic flight demand at a minimum of 90% of the total subsonic demand. Earlier, this constraint was set to a minimum of 20% subsonic demand satisfaction, thus leading to a faster computational runtime but comparatively reduced demand satisfaction. Currently, in practice, very high percentages of the available demand are satisfied (95% and above).

Finally, Equation 6 ensures that the carried passengers (for both supersonic and subsonic flights) are fewer than the total available seats for a specific flight k, where cap_k is the aircraft k seat capacity.

Preliminary simulation results

The FLEET simulation is run from years 2005 to 2050 with the supersonic aircraft introduced in 2025 (generation 1) and 2038 (generation 2). In FLEET simulations, the aircraft are available to the airline to use 1 year after the EIS date (i.e., the aircraft was first available during the EIS year, but the representative day when that aircraft was part of regular service is the year following the EIS). Hence, the first-generation supersonic aircraft becomes available for allocation by the airline for a representative day in 2026. Similarly, the second-generation supersonic aircraft becomes available for allocation in 2039.

Because FLEET models the behavior of a profit-seeking airline, the FLEET allocation problem decides which routes to operate the supersonic aircraft on while maximizing its profit over the whole network. This essentially allows FLEET to choose the routes for supersonic aircraft operation from the 205 supersonic-eligible routes presented in the previous section. This process ensures that the FLEET airline has the freedom to operate supersonic aircraft on profitable routes only, mimicking the behavior of an actual profit-seeking airline.

The simulation results presented here are based on Purdue's back-of-the-envelope representation of the A10 notional medium SST aircraft, Purdue's simple supersonic route path adjustment strategy, and the sequential aircraft allocation approach; i.e., supersonic aircraft allocation is performed before the subsonic aircraft allocation, and consequently FLEET is accommodating the premium passengers first. These results might change when higher-fidelity supersonic aircraft models along with detailed routing path data are implemented in the FLEET simulations. However, the current set of results (with the placeholder supersonic aircraft and simplistic routing path models) demonstrate the ability of FLEET to indicate the routes where supersonic aircraft might be used and the number of daily operations on those supersonic routes. Further, the results demonstrate the possible changes in the subsonic fleet allocations due to the introduction of supersonic aircraft on select routes. This work considers only the previously developed CTBG scenario, utilizing the previously obtained subsonic-only CTBG results for comparing and analyzing the supersonic FLEET CTBG allocation and fleet fuel burn results.

The FLEET setup for the CTBG scenario is defined as follows:

- The network consists of 169 airports including U.S. domestic routes and international routes that have either their origin or destination in the United States.
- The annual gross domestic product (GDP) grows at a constant value of 4.3% in Asia, 4.2% in Latin America, 2.4% in Europe, and 2.8% for airports in the United States.
- The annual population growth rate is a constant value of 1.1% in Asia, 1.26% in Latin America, 0% in Europe, and 0.58% in the United States.
- Jet fuel prices grow according to the Energy Information Administration (EIA) reference fuel price (Annual Energy Outlook 2011, 2011) case and are adjusted to meet the ASCENT survey fuel price, $77.08/bbl, by 2050.
- Carbon emission prices grow linearly from $0/MT in 2020 to $21/MT by 2050.

The set of subsonic aircraft utilized in the CTBG scenario for the current work is listed in Table 8. The aircraft denoted "GT Gen1 DD" are the Generation 1 aircraft modeled by Georgia Tech with a "direct drive" engine. The Generation 2 aircraft are labeled "GT Gen2 DD." These include aircraft belonging to the following classes: regional jet (RJ), single aisle (SA), small twin aisle (STA), large twin aisle (LTA), and very large aircraft (VLA). According to the amount and speed of technology incorporated into aircraft, in each of the scenarios, the new-in-class and best-in-class aircraft models will vary. Given the observation that new orders for 50-seat regional jet aircraft have diminished to zero, there are no small regional jet (SRJ) aircraft in the new- and future-in-class technology ages.

Table 8. Subsonic aircraft types used in simulation.

Subsonic Aircraft Types in Study				
	Representative in Class	Best in Class	New in Class	Future in Class
Class 1 (SRJ)	Canadair RJ200/RJ440	Embraer ERJ145		
Class 2 (RJ)	Canadair RJ700	Canadair RJ900	GT Gen1 DD RJ (2020)	GT Gen2 DD RJ (2030)
Class 3 (SA)	Boeing 737-300	Boeing 737-700	GT Gen1 DD SA (2017)	GT Gen2 DD SA (2035)
Class 4 (STA)	Boeing 757-200	Boeing 737-800	GT Gen1 DD STA (2025)	GT Gen2 DD STA (2040)
Class 5 (LTA)	Boeing 767-300ER	Airbus A330-200	GT Gen1 DD LTA (2020)	GT Gen2 DD LTA (2030)
Class 6 (VLA)	Boeing 747-400	Boeing 777-200LR	GT Gen1 DD VLA (2025)	GT Gen2 DD VLA (2040)

With the current modeling, the 2050 fleet fuel burn with supersonic aircraft is higher than the subsonic-only fuel burn. Figure 37 shows the normalized fuel burn for both supersonic- and subsonic-only runs. The supersonic run refers to the case in which both supersonic and subsonic aircraft are available for allocation in an airline fleet, whereas the subsonic-only run refers to the case in which only subsonic aircraft are available for allocation in an airline fleet (no supersonic aircraft are introduced in this case). The Purdue team noted that the introduction and allocation of the supersonic aircraft changes the use, retirement, and acquisition of the subsonic aircraft. That is, the airline modifies its subsonic fleet allocation to accommodate the new class of aircraft, i.e., supersonic aircraft, to maximize its overall profit. The change in the usage of the subsonic fleet can be seen by comparing the two charts in Figure 38 and Figure 39. In the first figure, the first six layers from the bottom in both charts indicate the fuel burn from the six classes of subsonic aircraft in FLEET, and the topmost layer in the upper chart indicates fuel burn from the supersonic aircraft in FLEET. Analysis of the two charts reveals that the pattern of the six common color layers in the two charts changes after 2025, indicating a change in the fuel burn (and the allocation) of the subsonic fleet after the introduction of the supersonic aircraft.

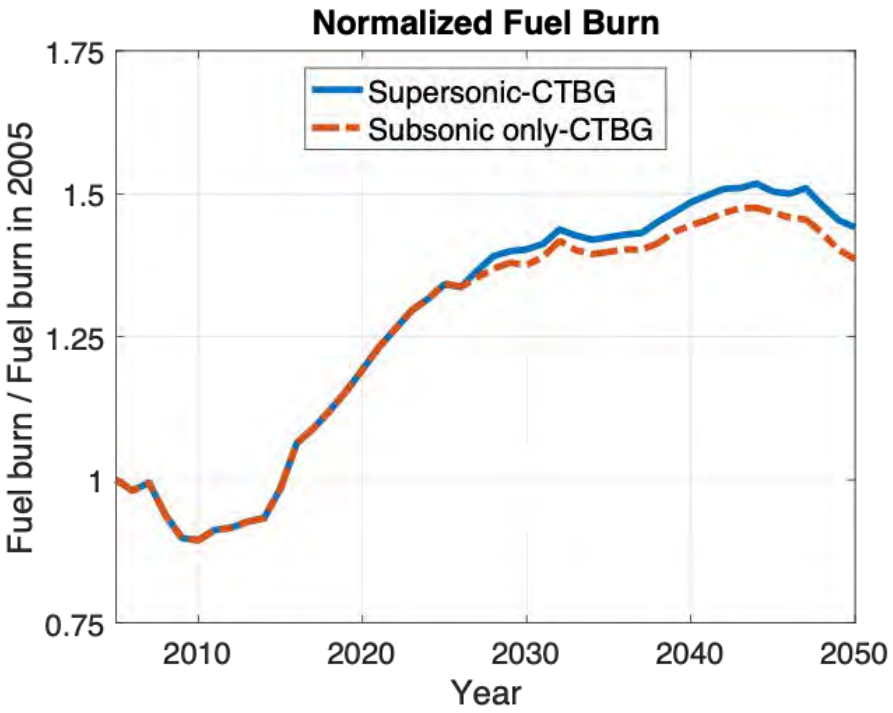

Figure 37. Normalized fuel burn from FLEET simulation.

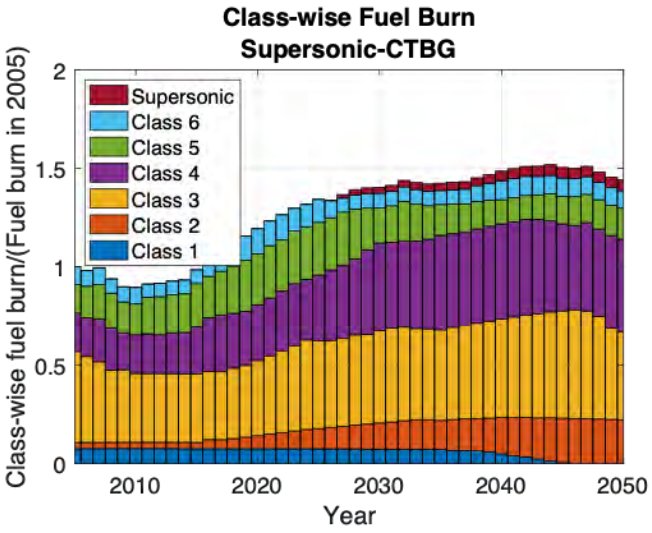

Figure 38. Class-wise fuel burn for supersonic case.

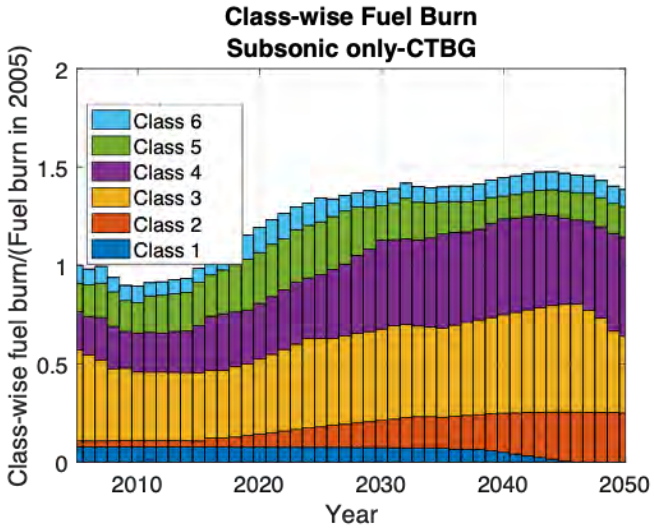

Figure 39. Class-wise fuel burn for subsonic-only case.

FLEET simulation results include details about the daily round-trip supersonic and subsonic aircraft allocations and the number of daily round-trip passengers carried on every route by each aircraft type each year. These data are used to generate different sets of output tables that provide yearly information about which routes the airlines chose to operate their supersonic aircraft on, and how the airline changed its subsonic aircraft allocation on those routes (and even on the non-supersonic-eligible routes in the FLEET network).

Table 9 depicts a partial output of FLEET aircraft allocations on potential supersonic routes for the year 2038. Here, 2038 is selected as the year of interest because the second generation of supersonic aircraft will become available to the airline in the next year in the simulation (i.e., only one type of supersonic aircraft is available for simulation in 2038). From this output, it is clear that the introduction of supersonic aircraft influences the subsonic aircraft allocation on both supersonic and non-supersonic routes. The results show allocation of five daily round trips on the LAX–HNL route compared with only two daily round trips on the JFK–LHR route (despite the latter route's greater popularity for SST, as evidenced by British Airways flying its Concorde on this route for several years). This anomaly in FLEET simulation results arises because FLEET represents demand carried by U.S flag carriers only. Hence, the LAX–HNL route has more demand in FLEET than the JFK–LHR route, thus explaining why there are more supersonic aircraft round trips on the former route. Future work will include estimating the overall demand on international routes by using the ratio of U.S. flag carriers and non-U.S. flag carriers on the route. The FLEET airline serves a total of 51 routes with supersonic aircraft in the year 2038 and a total of 73 routes with supersonic aircraft in the year 2050.

Table 9. FLEET aircraft allocations on selected supersonic routes in 2038.

Route Information		FLEET Allocation Information			Number of Daily Roundtrips for different A/C Size and Generation						
Airport A	Airport B	Allocation Model	Fuel Stop	Distance Flown (nmi)	Future-in-Class 3	Best-in-Class 4	New-in-Class 4	New-in-Class 5	Future-in-Class 5	New-in-Class 6	Best-in-Class Supersonic
JFK	LHR	*Supersonic*		3093.34	0	0	12	0	0	1	2
		Subsonic-only		2991.45	0	0	12	0	0	1	
LAX	HNL	*Supersonic*		2227.44	0	1	26	2	0	0	5
		Subsonic-only		2217.99	0	0	28	2	0	0	
DFW	NRT	*Supersonic*	HNL	6620.84	0	0	6	0	0	0	1
		Subsonic-only		5573.4	0	0	0	1	3	1	

Table 10 depicts the change in subsonic aircraft allocation when supersonic aircraft are made available for allocation to an airline fleet. This specific example shows the subsonic aircraft allocation on a non-supersonic-eligible route, EWR–LAS, for

supersonic- and subsonic-only cases. As shown in the allocation chart, even though supersonic aircraft service is not available on this route, the subsonic aircraft allocation is different in the two cases. When the airline has supersonic aircraft available to use elsewhere in the route network, the allocation problem selects one future-in-class class 3 (single-aisle) aircraft round trip and 11 new-in-class class 4 (small twin-aisle) aircraft round trips to satisfy passenger demand on the EWR–LAS route. When executing FLEET with no supersonic aircraft available for service anywhere (i.e., the airline's fleet is entirely subsonic aircraft), the allocation problem selects two new-in-class class 3 aircraft round trips, two best-in-class class 4 aircraft round trips, and nine new-in-class class 4 aircraft round trips to meet the EWR–LAS demand. Therefore, the total number of round trips per day differs: 12 when supersonic aircraft are available for use on other routes, and 13 when the airline has no supersonic aircraft. In addition, the subsonic aircraft used for round trips on the EWR–LAS route have newer technology (future-in-class aircraft have newer technology than new-in-class aircraft, and new-in-class aircraft have newer technology than best-in-class aircraft) when supersonic aircraft are available to use elsewhere in the network, relative to the technology when the airline has no supersonic aircraft. Therefore, given FLEET's current modeling techniques, the introduction of supersonic aircraft in an airline fleet affects the utilization of the subsonic fleet.

Table 10. FLEET Aircraft allocations on selected supersonic-ineligible route in 2038.

Route Information		FLEET Allocation Information		Number of Daily Roundtrips for different A/C Size and Generation				
Airport A	Airport B	Allocation Model	Distance Flown (nmi)	New-in-Class 3	Future-in-Class 3	Best-in-Class 4	New-in-Class 4	Best-in-Class Supersonic
EWR	LAS	*Supersonic*	1930.89	0	1	0	11	N/A
		Subsonic-only	1930.89	2	0	2	9	N/A

Sensitivity study of supersonic aircraft acquisition cost

The Purdue team performed a sensitivity study of the CTBG scenario to demonstrate the responsiveness (measured by fuel burn and number of supersonic routes with enplanements) of the FLEET airline to different cases of supersonic aircraft acquisition costs.

The Purdue team defined three different study cases: "lower than nominal," "nominal," and "higher than nominal." The lower-than-nominal case represents a CTBG scenario in which the available notional medium placeholder SST has an acquisition cost that is 80% of the acquisition cost of the subsonic class 6 aircraft, whereas the nominal and higher-than-nominal cases represent CTBG scenarios in which the available notional medium placeholder SST aircraft have acquisition costs 100% and 120% of the acquisition cost of the subsonic class 6 aircraft, respectively. For all three sensitivity study cases, the ticket price for supersonic passengers is unaffected by variations in supersonic aircraft cost and thus is fixed to the ticket price for the CTBG scenario in which the supersonic aircraft acquisition cost is nominal.

Figure 40 shows the fuel burn from allocated supersonic aircraft, normalized to the total airline fuel burn in 2005, for all three sensitivity study cases during the FLEET simulation period from 2005 to 2050. From normalized fuel burn trends for the three study cases shown in Figure 40, the CTBG scenario with lower-than-nominal medium SST acquisition cost consistently yielded the most fuel burn throughout the simulation period, as achieved by the FLEET airline serving more supersonic-eligible routes and using more first-generation supersonic aircraft than in the CTBG scenarios with nominal and higher-than-nominal medium SST acquisition costs.

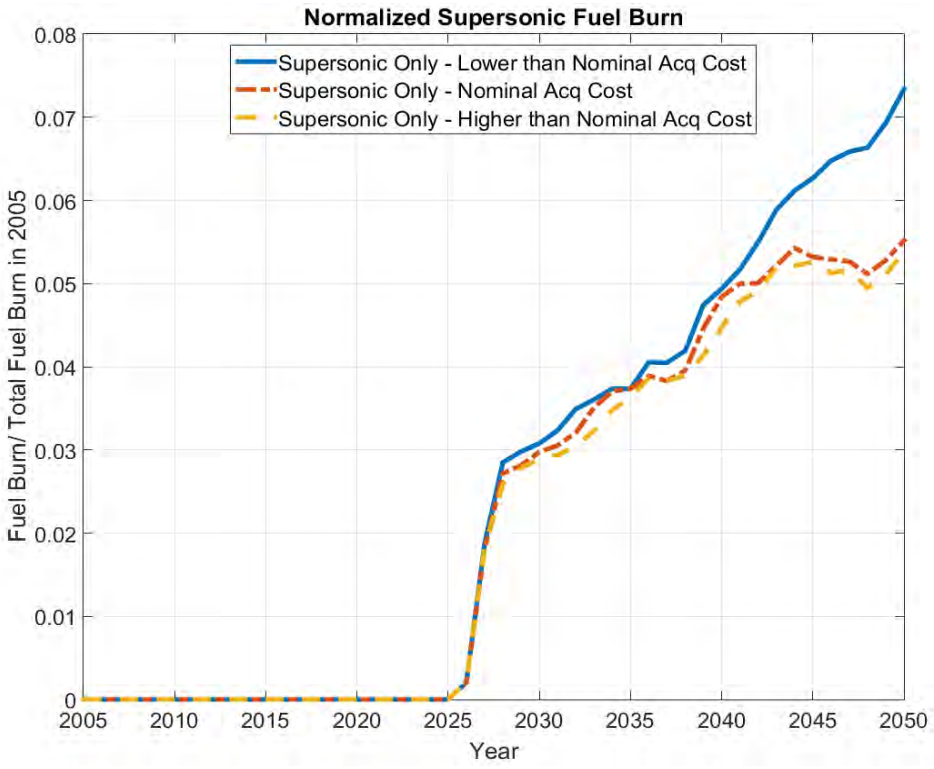

Figure 40. Normalized supersonic fuel burn for SST acquisition cost sensitivity study.

Task 5 - EDS Vehicle Modeling

Georgia Institute of Technology

Objective

The top-level objective of this task is to model the supersonic vehicles needed to support the CAEP Exploratory study. However, during the period of performance, emphasis is placed on the business jet and medium SST classes.

Research Approach

To model the business jet and medium SST classes, the Georgia Tech researchers will utilize a well-established modeling environment for subsonic vehicles, EDS, as a starting point. The approach is to use the infrastructure of EDS and develop a modeling and simulation environment for SSTs called FASST. The infrastructure of EDS is to be modified to that depicted in Figure 41 to accommodate supersonic aircraft with the exception of the step labeled “configuration exploration.” The overall approach starts with defining the requirements and design mission and then proceeding to configuration exploration.

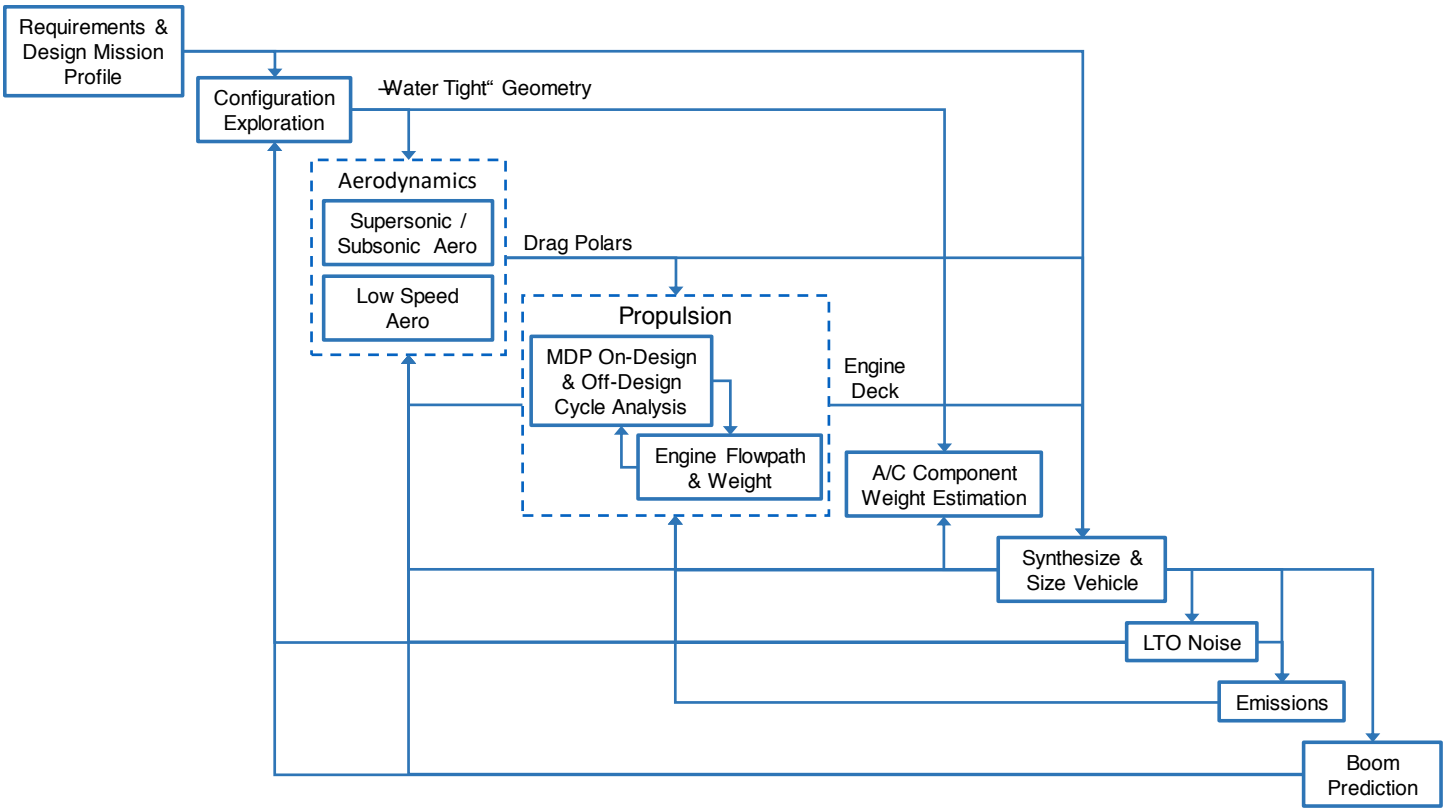

Figure 41. FASST overall architecture.

The configuration exploration step is partially done offline, in a brainstorming exercise in which likely candidates are developed with OpenVSP (NASA's open source parametric geometry tool) and run through CART3D (NASA's inviscid computational fluid dynamics tool) to examine the wave drag characteristics, make a configuration selection, and proceed to aerodynamic shaping to maximize the L/D ratio for the cruise condition. After the aerodynamic shaping is completed, a set of supersonic and subsonic drag polars is generated. The supersonic drag polars are generated in CART3D by sweeping vehicle angles of attack for multiple supersonic Mach numbers. The subsonic drag polars (i.e., Mach 0.3–0.8) are generated with the set of tools depicted in Figure 42. The subsonic aerodynamic module uses three empirically based aerodynamic codes from NASA to calculate lift and specific components of drag. OpenVSP's Parasite Drag Tool, based on turbulent flat plate theory and form factor corrections, is used to compute parasite drag. Then, either AERO2S (NASA's low-fidelity subsonic induced drag estimation tool) or WINDES (NASA's low-fidelity supersonic induced drag estimation tool) is used to compute drag due to lift depending on the flight regime. Both of these codes are based on linearized aerodynamics assumptions with empirical data corrections to estimate lift and drag. The subsonic aerodynamic module computes the drag polar for a given Mach number, angle of attack, and aircraft geometric information. The last element of the aerodynamic module for FASST is the landing and takeoff (LTO) drag polars. Unfortunately, no low-fidelity methods are available to estimate the LTO aerodynamic performance; therefore, the Georgia Tech researchers are investigating the process and computational resources needed to generate a set of LTO drag polars by using computational fluid dynamics models based on the Reynolds-averaged Navier–Stokes equations (CFD-RANS). After the process of generating a single set of LTO drag polars (as a function of aircraft angle of attack and flap deflections), the next step is to investigate a method to generate parametric LTO drag polars as a function of wing geometry. The propulsion module for FASST is the same as that of EDS, which is the Numerical Propulsion System Simulation (NPSS) using the Multi-Design Point (MDP) algorithm for on-design cycle analysis. The propulsion module also has a very different off-design power management algorithm form that of EDS. The aircraft component weight estimation is part of the vehicle synthesis process, which is performed with NASA's Flight Optimization System (FLOPS).

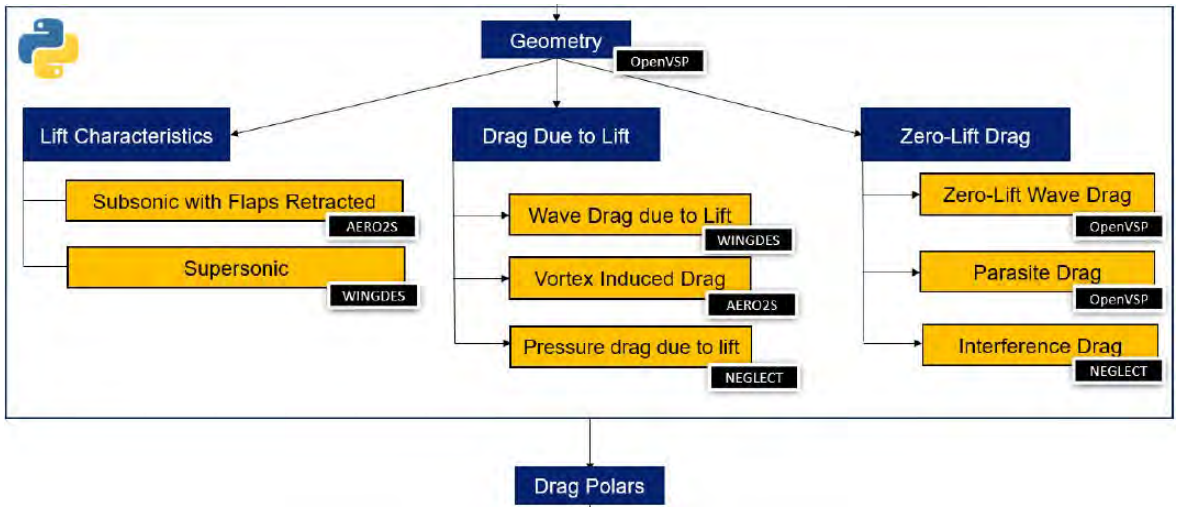

Figure 42. Subsonic drag polar generation. Wave drag effects are neglected in subsonic aerodynamics.

Another major difference between EDS and FASST is the iteration required between aerodynamic and propulsion modules. For subsonic vehicles, as the aircraft drag increases or decreases during the synthesis and sizing process, the engine can be scaled by using mass flow, and the only drag impact is the engine profile and parasitic drag due to the engine nacelle being sized up and down. For supersonic aerodynamics, the size of the engine affects the entire vehicle drag and lift characteristics because the engine is much more integrated into the airframe. Therefore, as the thrust requirements change during the sizing process, the aerodynamics characteristics must also be updated. A potential approach to solve this dilemma is to generate supersonic drag polars as a function of key aircraft parameters. After the aerodynamics, propulsion, and mission analysis (i.e., synthesis and sizing) modules converge, the resulting vehicle and engine are then used to predict LTO noise, emissions, and boom levels. If any of the last three analysis results are unacceptable, the aircraft and engine design will need to be changed, and the entire convergence loop is repeated until all metrics are satisfied. Currently, FASST is not envisioned to incorporate an optimizer to find the optimal configuration. It is envisioned as a framework to perform design space exploration to determine whether there is a feasible space that satisfies fuel burn, emission, LTO noise, and potentially boom.

The subsequent section of the report describes the propulsion and airframe modeling performed during the period of performance, for both the medium SST and business jet SST, in more detail.

Medium SST

The medium SST was sized to cruise at Mach 2.2, carrying 55 passengers at 4,500 nmi with no subsonic mission segments.

Propulsion system modeling

Most subsonic aircraft use a high bypass ratio separate flow turbofan (SFTF), to move a greater amount of air rather than produce a high jet velocity, for high propulsive efficiency, thus resulting in low TSFC. The lower jet velocity is also desirable from a noise perspective. However, these engines have the drawback of large lapse rates in thrust with altitude, thus making them less desirable for supersonic aircraft, which are required to fly at much higher altitudes. To address this issue, a mixed flow turbofan (MFTF) architecture is chosen for this study. The MFTF is a simple modification of the SFTF accomplished by mixing the bypass and core flow before exiting through a single exhaust nozzle. The mixing of the two streams offers some efficiency gains and high specific thrust, which reduces the thrust lapse problem (Hartmann, 1967; Pearson, 1962). Although more advanced architectures exist that may provide even greater benefits, the MFTF was chosen because of its simplicity relative to an adaptive or variable cycle architecture (Welge et al., 2010).

Classical cycle analysis sizes the engine (i.e., determines the airflow requirement to meet a certain requirement, such as thrust) for a single flight condition, such as takeoff. However, the engine must operate over a wide range of conditions, and thus the engine determined at the design flight condition may not meet requirements under other flight conditions. This classical method called “single design point” requires an iterative procedure whereby the design is updated and then

reevaluated under other flight conditions. Multi-design point (MDP) is a technique developed by the Aerospace Systems Design Laboratory to size an engine to simultaneously ensure that requirements are met at multiple flight conditions (Schutte, 2009). This is enabled by the object-oriented structure of NPSS, which allows for copies of the design engine to be simulated at the same time as the design case. A system of equations can then be set up such that the independent design variables may be set by a numerical solver to meet specified targets for different flight conditions.

Modeling method and assumptions

A schematic is included in Figure 43, depicting the components in the engine model and their connectivity. This model inherited much of its structure from previous supersonic work done by Georgia Tech (Welge et al., 2010) with some changes. A different inlet map was used to parametrically model recovery as well as installation drag due to spillage, bypass, and bleed flow. The map was obtained from a library of maps in the PIPSI method (Kowalski & Atkins Jr., 1979) and models a 2D, four-ramp variable geometry inlet. The fan and high-pressure compressor (HPC) maps are generated with the NASA tool CMPGEN within the FASST environment to avoid the need for map scaling. The turbine maps are notional maps that are scaled, because the FASST environment does not currently include a routine for developing turbine maps. Turbine cooling flows are determined from the CoolIt subroutine developed at NASA, which models the required cooling flow as a function of metal temperature and the cooling effectiveness parameter $\left(\phi = \frac{T_{gas} - T_{metal}}{T_{gas} - T_{cool}}\right)$. A mixer gain term was used (0% for unmixed and 100% for perfectly mixed) to model how well the two streams mixed before expanding through the nozzle, to establish a loss of thrust due to imperfect mixing. The nozzle was modeled with discharge coefficient and gross thrust coefficient curves as a function of the pressure ratio from the previous supersonic work (Welge et al., 2010). This curve assumes a fixed geometry and therefore suffers from overexpansion and under expansion losses at any nozzle pressure ratio other than the peak. Consequently, the gross thrust coefficient was much lower under critical flight conditions, such as cruise, than would be expected from the literature (Kowalski & Atkins Jr., 1979). A preliminary method to address this used a 2% adder on the curve, which would not put the peak above 100% and would put the gross thrust coefficient for cruise around 97%. For preliminary estimates, 100 HP is extracted from the high-speed shaft. A fuel temperature of 700 $°R$ was used to be more representative of heat loads on the aircraft on any preheating of the fuel before combustion.

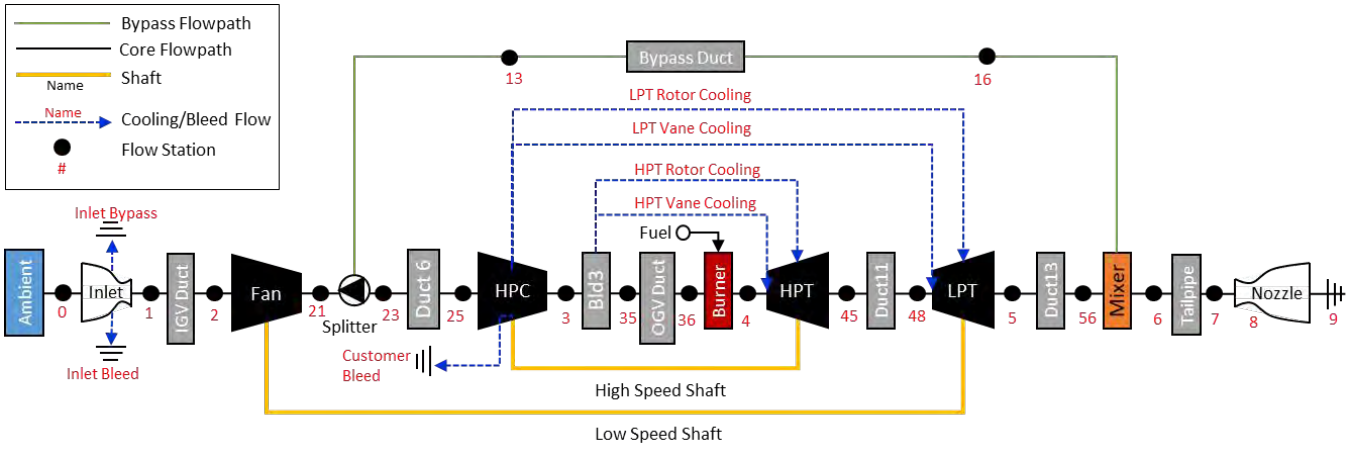

Figure 43. Engine schematic of clean sheet design for medium SST.

MDP cycle setup

As mentioned above, MDP allows for requirements under multiple flight conditions to be met simultaneously. To that end, several flight conditions of interest were determined along with relevant requirements for each of them. The flight conditions chosen are listed in Table 11. The Aerodynamic Design Point (ADP) is the sizing point of the engine and a reference point for defining the turbomachinery component performance. It was selected in this study to be a transonic acceleration point at which having enough thrust to get through without afterburners or the need to dive is critical. The top of climb (TOC) point is typically a critical point at which adequate thrust for a required rate of climb must be ensured. Additionally, this point is part of the supersonic cruise segment, and thus efficiency is of critical concern. The takeoff point ensures enough thrust at aircraft rotation. The takeoff and SLS points are typical points of interest for certification and to ensure sufficient thrust for takeoff. The NPSS solver was then used to determine a cycle that would meet the specified design targets listed in

Table 12. Extraction ratios were set near 1.0 to avoid excessive mixing losses. Turbine inlet temperatures were set at a lower limit of 2800 $°R$ to minimize cooling flow requirements. Fan specific flow was set at 49 $\frac{lbm}{s\,ft^2}$ to aid in fitting the fan inside the capture area, which corresponds to the nacelle dimensions. TOC thrust was set according to the drag data provided by the aerodynamic analysis and assumed weight from historical and other study data and a 300-fpm rate of climb. The takeoff and SLS thrust were set by assuming lapse rates from TOC to takeoff and takeoff to SLS.

Table 11. Cycle design points for a medium SST engine.

Flight Condition	Mach	Altitude	ΔT
ADP	1.2	39,000	0
TOC	2.2	55,000	0
Takeoff	0.25	0	27
SLS	0	0	0

Table 12. NPSS cycle solver targets.

Dependents	Target
Turbine First Vane Temperature, °R	T4max
Extraction Ratio at ADP	0.97
Extraction Ratio at TOC	1.00
Compressor Discharge Temperature, °R	2,800
Inlet Capture Area Ratio at TOC	0.97
Fan Specific Flow, lbm/s/ft²	49.0
Net Thrust at TOC, lbf	16,575.7
Net Thrust at Takeoff, lbf	27,269.7
Net Thrust at SLS, lbf	32,082.0

Off-design power management

The off-design power management scheme for this engine was set up to determine fuel flow such that, starting from SLS, the engine would attempt to maintain the same thrust as the Mach number and altitude are increased, until 100% fan speed is reached. Then the fuel flow would be set to ensure 100% corrected fan speed until a turbine inlet temperature (T41) limit or maximum compressor exit temperature (T3) limit was encountered.

Flow-path development and weight

The flow path and weight model for the engine was developed with WATE++ during a previous supersonic study in which Georgia Tech was involved (Welge et al., 2010).

Results

The engine cycle presented is as of August 23 2019. Table 13 and Table 14 show the efficiencies, pressure losses, bleeds, and modeling assumptions used in the model at each of the design points for the MDP analysis of the current design. Table 15 shows the cycle parameters and performance metrics at each of the design points of the current design. *At the time of writing of this annual report, these propulsion results are still preliminary and have not been completely matched to aircraft performance.*

Table 13. Cycle modeling assumptions for a medium SST engine.

Component	ADP	TOC	TO	SLS
Inlet Recovery	97.8%	91.2%	99.8%	90.0%
Fan Adiabatic Efficiency	87.1%	89.3%	90.3%	89.8%
HPC Adiabatic Efficiency	88.8%	89.3%	89.8%	89.5%
HPT Adiabatic Efficiency	92.0%	92.2%	92.5%	92.5%
LPT Adiabatic Efficiency	93.0%	92.5%	92.9%	93.3%
Nozzle Gross Thrust Coefficient	98.5%	97.1%	93.5%	92.9%
Imperfect Mixing Coefficient	99.5%	99.5%	99.6%	99.6%
Nozzle Discharge Coefficient	96.4%	96.3%	96.7%	97.3%

Table 14. Cycle modeling assumptions for a medium SST engine (cont'd).

Component	ADP	TOC	TO	SLS
IGV Duct Pressure Loss	1.00%			
Duct 6 Pressure Loss	1.00%			
OGV Duct	1.50%			
Fuel LHV, BTU/lbm	18,580			
Fuel Temperature, °R	700			
Burner Efficiency	99.70%			
Burner Pressure Drop	4.00%			
Duct 11 Pressure Loss	0.00%			
Duct 13 Pressure Loss	3.00%			
Mixer Gain	70.00%			
Tailpipe Pressure Loss	2.00%			
Bypass Duct Pressure Loss	4.00%			
Customer Bleed, lbm/s	2.5			

Table 15. Cycle variables and performance metrics.

	ADP	TOC	TO	SLS
Mach	1.2	2.2	0.25	0
Altitude [kft]	39	55	0	0
$\Delta T + ISA$	0	0	27	0
FPR	2.50	2.01	1.98	2.17
BPR	0.649	0.768	0.794	0.740
OPR	24.75	17.76	17.59	20.25
Extraction Ratio	0.97	1.00	1.01	0.995
T41 [R]	2,188.9	2,800.0	2,046.3	2,046.6
T3 [R]	1,349.1	1,790.0	1,320.0	1,298.8
Installed Net thrust [lbf]	13,238	16,576	27,270	32,082
Installed TSFC [lbm/(hr × lbf)]	0.944	1.180	0.661	0.574

Airframe modeling

This section details the process of modeling the airframe including the cabin, vertical tail, area ruling, and aero shaping of the vehicle.

Cabin sizing

The passenger cabin was sized on the basis of the desired seat width and pitch, aisle width, and FAA requirements of emergency exits and the number of flight attendants for a 55-passenger vehicle. Research was performed on the current seat width/pitch of first-class seats in long domestic flights (e.g., JFK to LAX, approximately 6.5 h). The seat pitch, in general, was found to range from 32 in to 38 in. The seat width, in general, ranges from 18 in to 23.3 in. The values chosen for each class of the vehicle are as follows:

Table 16. Seat pitch and width for medium SST cabin.

Class	Seat Pitch (in)	Seat Width (in)
First Class	32	21
VIP	45	24

The arm rests were chosen to be 3.0 in for the single seat in first class and the non-shared arm rest of the double seats in first class. The shared arm rest in first class and the arm rest in the VIP class were set to 3.5 in. The fuselage thickness was assumed to be 6 in, and the cabin cross-section was a circle of 10 ft diameter. Two exits in each side of the fuselage and two steward's seats were added to fulfill the FAA requirements listed in 14 CFR 25.807 and 14 CFR 121.391. Two type I exits were used. One of increased width, equal to 36 in, and another with a width of 24 in, the minimum size set by regulations.

The final cabin layout also contained two lavatories and two galleys. The final cabin length was 80 ft. The following figures show the cabin layout and the first-class cross-section.

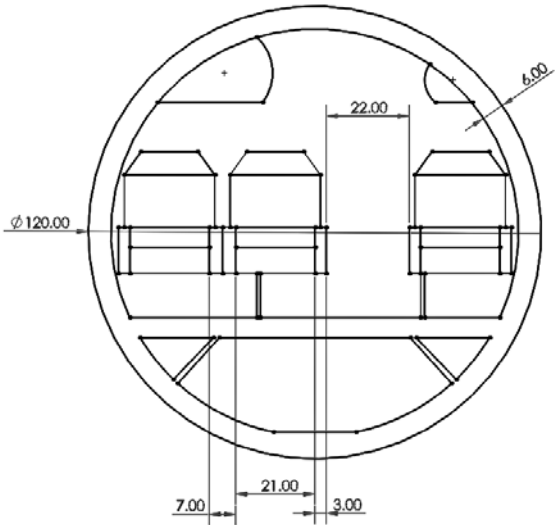

Figure 44. Cross section of first-class cabin layout.

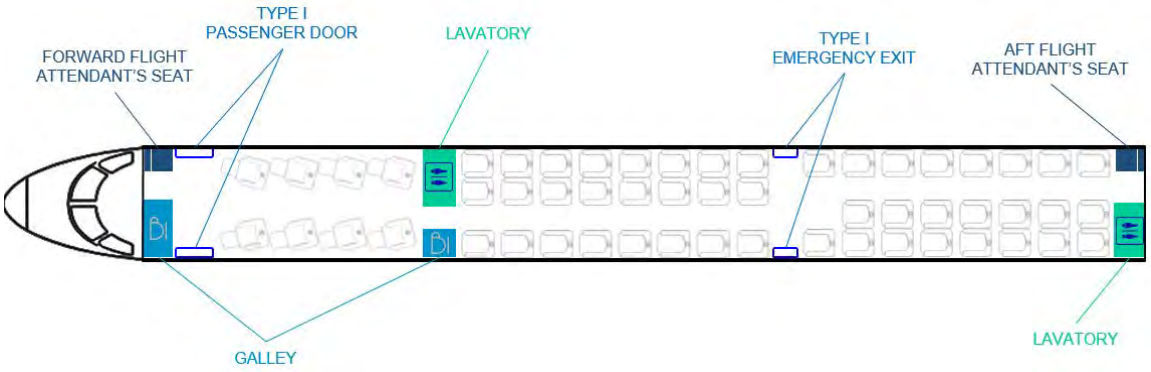

Figure 45. Cabin layout for medium SST.

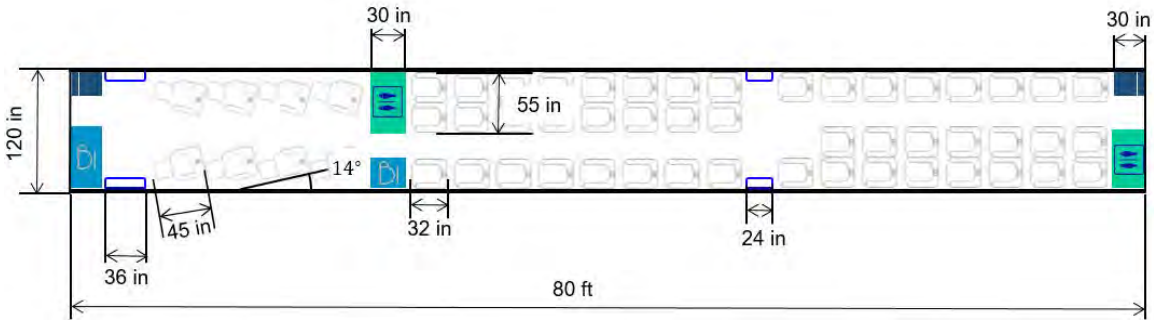

Figure 46. Dimensions of cabin layout for medium SST.

Vertical tail sizing

The vertical tail minimum area was determined by assuming a momentum imbalance due one engine out. It was assumed that the tail of the aircraft has no rudder and that the aircraft will fly at sideslip angle, β, equal to $15°$, as specified in 14 CFR Part 25.147.

The tail minimum area, S_{tail}, is defined by:

$$S_{tail} = \frac{Td}{\frac{1}{2}\rho V^2 C_L|_{\beta=15°}\Delta X}$$

where:

- T is the thrust provided by the inoperative engine.
- d is the distance between the center of the inoperative engine and the aircraft longitudinal axis.
- ρ is the air density at sea level.
- V is $1.3V_{SR1}$ (as required by 14 CFR 25.147).
    - V_{SR1} corresponds to the reference stall speed at maximum landing weight with flaps in the approach position and the landing gear retracted.
- $C_L|_{\beta=15°}$ is the lift coefficient of the tail airfoil at a 15° angle with the free stream velocity.
- ΔX is the distance between the center of gravity (CG) of the vehicle and the aerodynamic center of the tail. The CG of the aircraft was estimated by using a component buildup based on the geometry of the vehicle

This analysis assumes that the aircraft is symmetric with respect to its longitudinal axis. The values used for the medium SST configuration were as follows:

Table 17. Parameters used for vertical tail definition.

Parameters	Value
$\boldsymbol{T}$ (lb)	27,429.7
$\boldsymbol{d}$ (ft)	21.875
$\boldsymbol{\rho}$ (slug/ft³)	0.002377
$\boldsymbol{V_{SR1}}$(ft/s)	228.3
$\boldsymbol{C_L|_{\beta=15°}}$	0.8
$\boldsymbol{\Delta X}$ (ft)	24.8

The minimum area for the tail was found to be 288.2 ft^2. If the assumption that a rudder deflection can increase $C_L|_{\beta=15°}$ to 1 is made, the minimum tail area would be 230.5 ft^2.

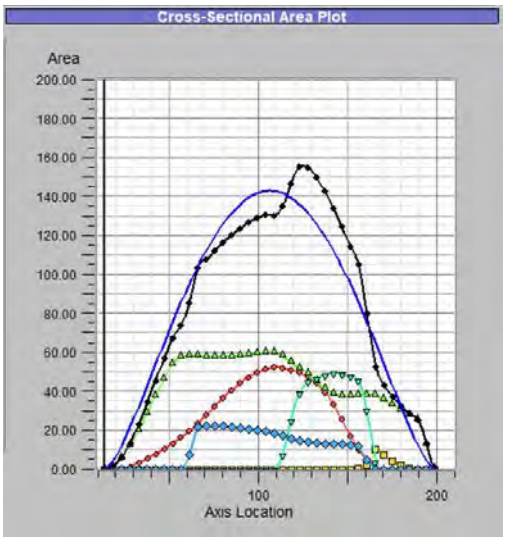

Figure 47. Area ruling distribution plot.

Area ruling

With a cruise Mach of 2.2, the medium SST must minimize wave drag to increase efficiency. One way to decrease wave drag is to area rule an aircraft. Area ruling involves reducing area jumps along the length of the fuselage of the aircraft. To minimize these area jumps, the wing and engines were strategically placed along the length of the aircraft. The nose is very sharp leading to the body, the wing is moved forward, and as the wing ends, the rear engine and vertical tail prevent the area distribution from drastically changing. An area ruling plot corresponding to the configuration shown in Figure 51 is shown in Figure 47. In this figure, the smooth blue line represents an ideal Sears-Haack body, a shape demonstrated to minimize wave drag for supersonic flight, and the black line shows the total area distribution of the aircraft at the cruise Mach number. The other colored lines represent the area contributions of the separate aircraft components, such as the wing, fuselage, and engines. To minimize wave drag, the total area distribution should follow the Sears-Haack body curve as closely as possible.

Aero shaping

In the supersonic regime, small geometric aspects can have major effects on cruise efficiency. To address any of these performance-decreasing sections, we used inviscid computational fluid dynamics (CART3D) to analyze the supersonic performance of the aircraft. By visualizing the pressure distribution across the body of the aircraft, we identified areas of very high or low pressure, and these areas were smoothed or changed to prevent the pressure buildup. The major areas investigated were the cockpit-to-body angle and the diffusers mating the wing engines to the wings. Initially, the angle between the cockpit and body slowed the flow, thus creating a high-pressure region across the cockpit windscreen area. This slowed flow was then expanded drastically beyond Mach 1 aft of the cockpit, thus creating a large low-pressure region. These regions are shown in Figure 48.

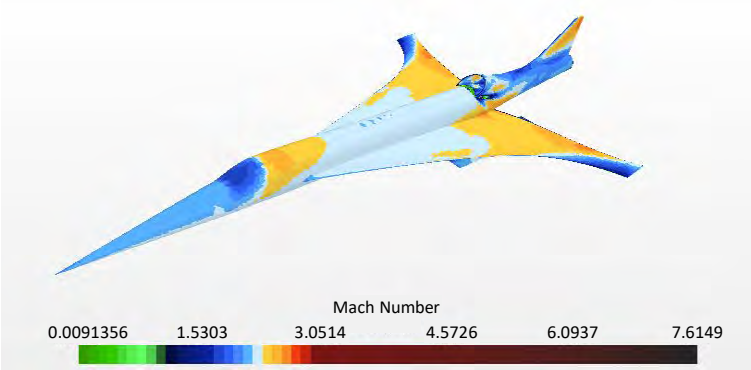

Figure 48. Mach distribution across initial design.

The cockpit angle was reduced to smooth out this localized pressure. Although this leads to poor pilot visibility, the aircraft is assumed to use an advanced vision system similar to the system integrated on the X-59 QueSST aircraft. Figure 49 shows the new cockpit-to-fuselage angle without the presence of the localized pressure. As can be seen in the figure, the top surface of the aircraft has much less variation in pressure and Mach number.

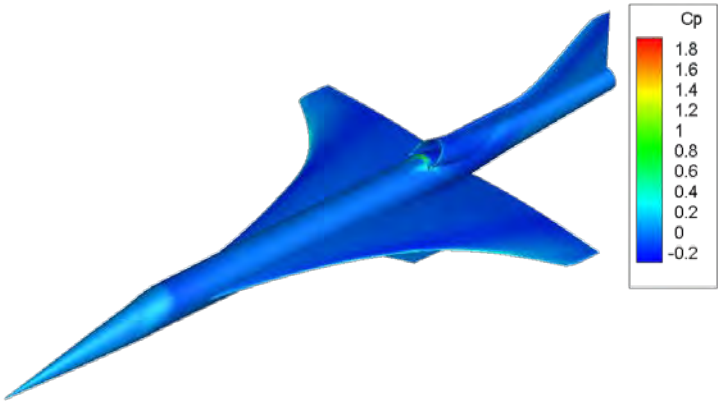

Figure 49. Updated cockpit and fuselage configuration.

The next area investigated was the diverters between the wing engines and the wings. This area generated very high pressures because of the airflow slowing when entering the junction between the nacelle and the wing. To fix this issue, diverters were included between the nacelle and the wing. A diverter starts at the leading edge of the nacelle and curves outward, matching the width of the nacelle by the time the engine mates with the wing. This geometry encourages the flow to move out of the engine-wing junction and prevents as much of a high-pressure region.

Airframe–engine integration

Many engine locations were considered before the two wing engines and single-tail engine were selected. The following figures show examples of engine locations considered. A three-engine configuration was chosen, with the rear engine being embedded into the top of the fuselage. This embedded engine allows for a better area distribution than some of the other configurations. It also allows for some fan noise shielding.

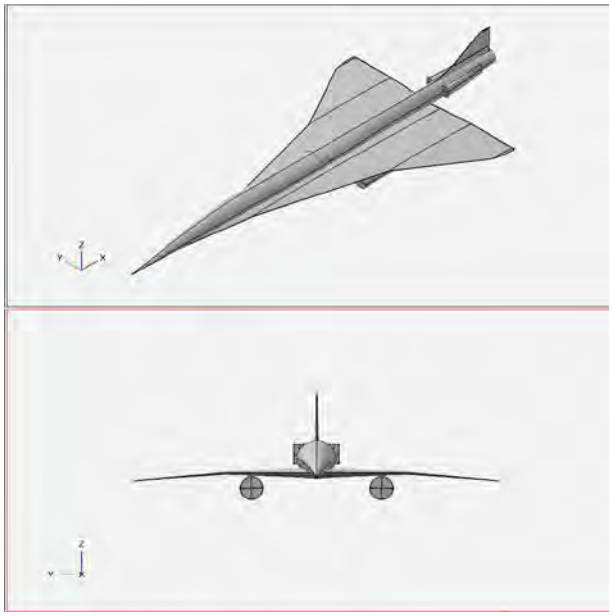

Figure 50. Three-engine rear cheeks.

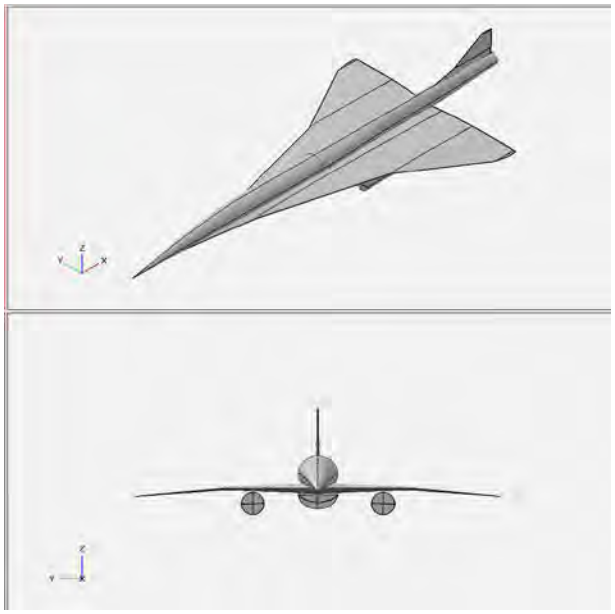

Figure 51. Three-engine belly.

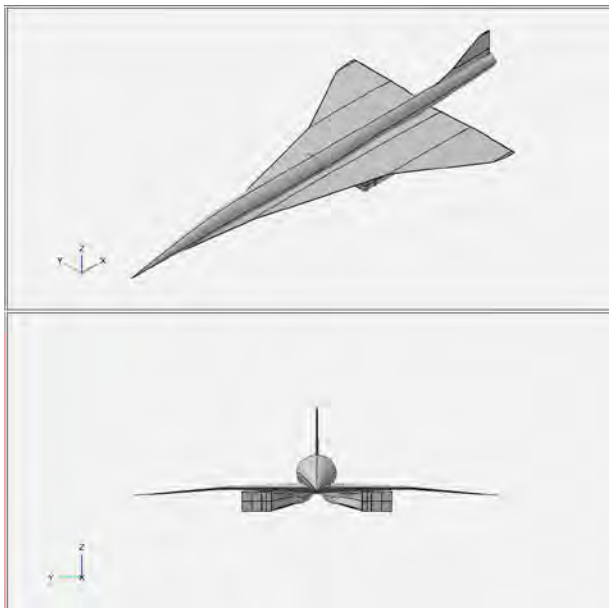

Figure 52. Two-engine S duct.

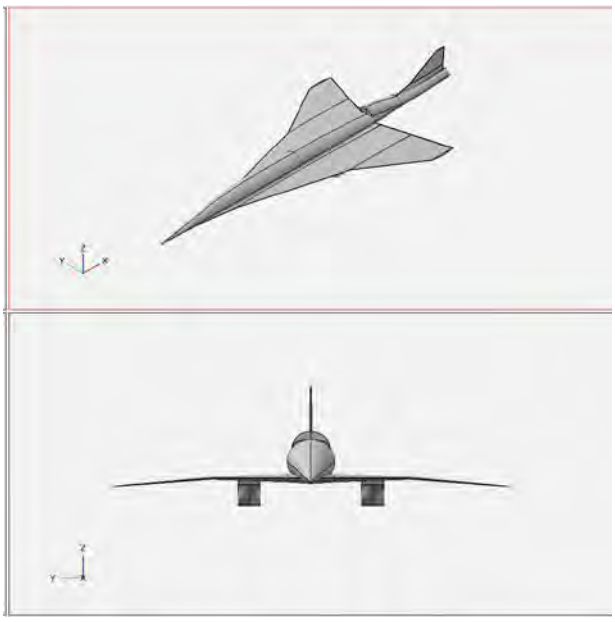

Figure 53. Three-engine integrated nozzle.

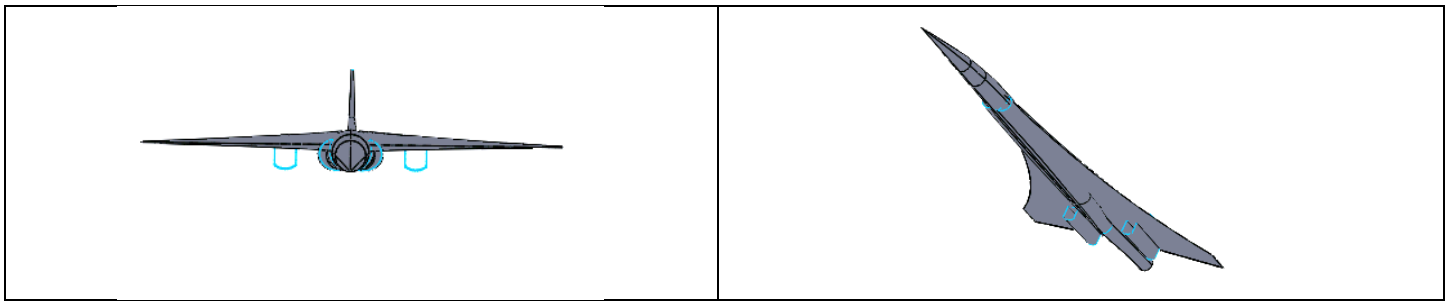

Figure 54. Three-engine cheeks.

A challenge in matching the engine and airframe is consistency in engine size. The drag polar developed by the aerodynamic analysis assumes a particular engine size in defining the airframe geometry. The resultant drag from this analysis determines the thrust requirements for the propulsion system. However, after the propulsion system is sized for the required thrust, the physical engine size may not match the size assumed for generating the drag polar, thus resulting in an iterative procedure between the aerodynamic and propulsion analysis to ensure consistency in engine size. To aid in this procedure, the Georgia Tech researchers decided to fix the engine inlet capture area (i.e., nacelle area) for both propulsion and aerodynamic analysis. The propulsion analysis would then attempt to find a cycle that would meet thrust requirements while maintaining a fixed inlet capture area. A challenge in this procedure was in determining how to size the engine. Normally, the engine would be sized for a thrust requirement; however, because the capture area was fixed, it became desirable to size the engine for a fixed capture area ratio (A_0/A_C) to minimize the installation effects.

Mission analysis

This section presents the preliminarily chosen thrust-to-weight ratio and wing loading along with the mission profile and vehicle sizing results from the sizing tool FLOPS.

Design point

The thrust-to-weight ratio and the wing loading were defined with a constraint analysis tool built in the previous work for the project, by using the mission profile above. The thrust-to-weight ratio was set to 0.42, and the wing loading was set to 106.0 lb/ft^2. These values were chosen with the help of the preliminary tool developed in Task 2. This is designed to be able to fulfil the required mission and simultaneously minimize wing size and engine thrust to achieve a good design.

Mission profile

The vehicle was sized for a mission with a total range (excluding reserve mission) of 4500 nmi. The chosen mission profile was as follows:

- Takeoff: Mach = 0–0.30 at altitude of 0 ft
- Subsonic climb: M = 0.30–0.95; altitude changing from 0 ft to 35,000 ft
- Supersonic climb: M = 0.95–2.20; altitude changing from 35,000 ft to 55,000 ft
- Cruise: constant Mach number and altitude; M = 2.25 and altitude of 55,000 ft
- Descent: deceleration from M = 2.25–0.30; altitude decreasing from 55,000 ft to 0 ft

The reserve mission was defined as follows:

- Reserve fuel available: equal to 10% of total fuel used in main mission
- Total hold time: 30 min
- Climb: from 0 to 10,000 ft, with M increasing up to 0.35
- Cruise: 10,000 ft at M = 0.35

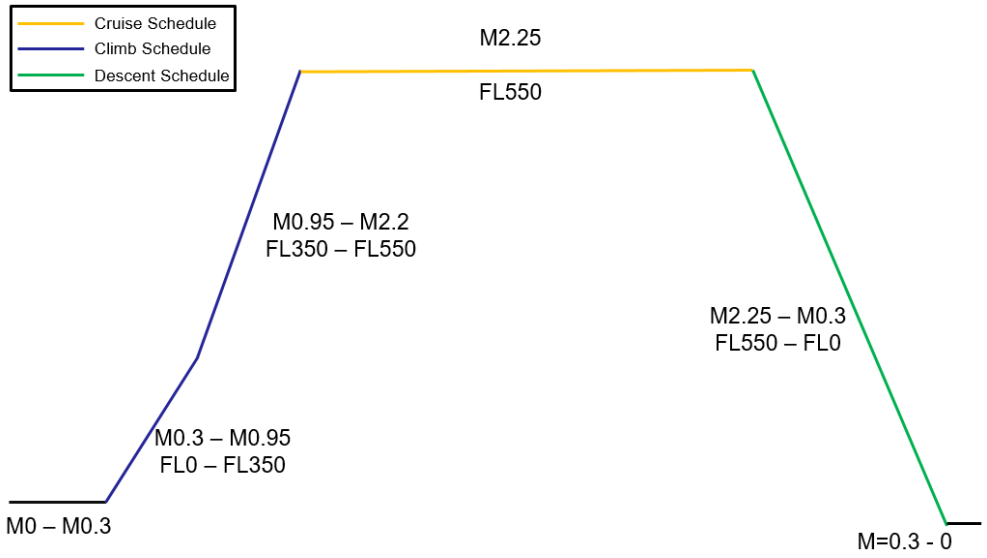

Figure 55. Mission profile for medium SST.

Vehicle sizing

The vehicle sizing loop was performed with FLOPS. The vehicle was defined by using the aerodynamic and propulsion information defined in this report along with the mission profile discussed above. The preliminary vehicle characteristics results are shown in Table 18 and Table 19. *Again, these results are preliminary at the writing of this annual report.*

Table 18. Key metrics for medium SST (preliminary).

Key Metric	Value
Takeoff Gross Weight, lbs	29,389
Design Cruise Mach	2.2
Wing Reference Area (ft^2)	2,777.3
Design Range (nmi)	4,500
Cruise L/D	6.35

Table 19. Weight breakdown of medium SST (preliminary).

Component	Weight (lbs)	% Empty Weight (lbs)		Component (Cont'd)	Weight (lbs)	% Empty Weight (lbs)
Wing	18,111	18.27		Control Surfaces	3,828	3.86
Horizontal Tail	0	0.00		Auxiliary Power	719	0.73
Vertical Tail	665	0.67		Instruments	974	0.98
Fuselage	16,057	16.20		Hydraulics	2,175	2.19
Landing Gear	7,385	7.45		Electricals	2,587	2.61
Nacelle	5,784	5.84		Avionics	1,530	1.54
Structures Total	**48,003**	**48.43**		Air Conditions	3,265	3.29
Engines	31,925	32.21		Anti-icing	237	0.24
Propulsion Miscellaneous	1,370	1.38		**Systems and Equipment Total**	**15315**	**15.45**
Fuel System: Tanks and Plumbing	2,505	2.53		**Weight Empty**	**99118**	**100.00**
Propulsion Total	**35,800**	**36.12**				

Business jet SST

The business jet SST was sized to cruise at Mach 1.4 carrying eight passengers, at 4,500 nmi with no subsonic mission segments.

Propulsion system modeling

An MFTF was also modeled for this aircraft to follow the selected architecture chosen by Aerion (Bogaisky, 2018). Unlike the medium SST commercial vehicle, this engine was not a clean sheet design but instead was a re-fanned derivative of the CFM56. For this work, Georgia Tech remodeled their in-house CFM56 model to be a MFTF.

Modeling method and assumptions

A schematic is included in Figure 56, depicting the components in the engine model and their connectivity. There are a few differences between the model setup for this engine and the one described above for the medium SST engine, owing to the different heritage of each engine. The model for this aircraft was derived from the Georgia Tech in-house CFM56 model for subsonic applications, whereas the medium SST model was a clean sheet design whose model setup was inherited primarily from past supersonic work by Georgia Tech (Welge et al., 2010).

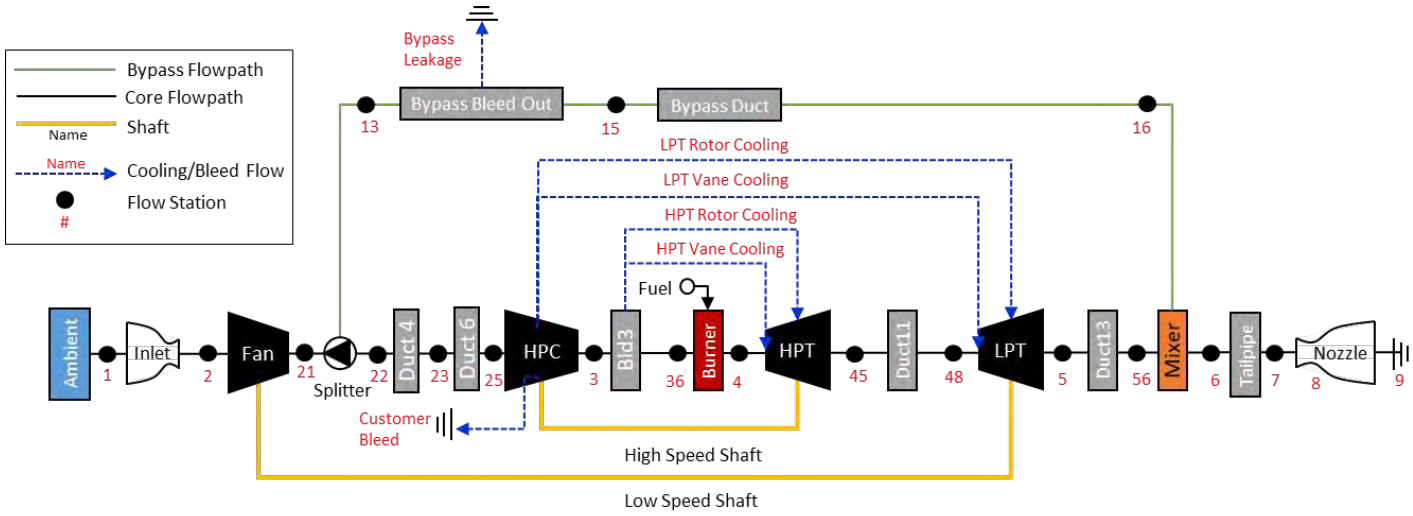

Figure 56. Engine schematic of derivative CFM56.

The main differences are that this model includes a bypass leakage and a different setup of ducts to account for total pressure losses. The sequential duct 4 and duct 6 could have been combined into a single pressure loss element but is the result of having removed an additional compressor between duct 4 and duct 6. Because this did not affect the model, it was left to minimize changes to the model. Unlike the medium SST engine, which was developed within the MDP framework described above, this engine was developed by following a classical single design point approach. The engine was sized at a Mach 1.4 and 50,000 ft at standard day conditions. Two other off-design points of SLS and takeoff on a hot day were examined. The flight conditions are summarized in Table 21. The design point modeling assumptions are included in Table 20. The inlet is currently modeled with a specified recovery, and there is no consideration for the installation effects of inlet drag due to spillage, bypass, or bleed. The maps used for the HPC, high-pressure turbine (HPT), and low-pressure turbine (LPT) came from the in-house CFM56 model at Georgia Tech, but a new fan map was developed with the NASA tool CMPGEN. Turbine cooling flows were set by using an in-house-upgraded version of the CoolIt subroutine according to the methods of Young and Wilcock (2002), accounting for more detailed geometry. The nozzle was modeled by using a discharge coefficient from (Thornock & Brown, 1972) for a 15° convergent section and gross thrust coefficient for a 12° divergent section from (Kuchar, 1989), both as functions of the nozzle pressure ratio. A mixer gain term was used (0% for unmixed and 100% for perfectly mixed) to model how well the two streams mixed before expanding through the nozzle to establish a loss of thrust due to imperfect mixing.

Table 20. Design point modeling assumptions.

Component	Value	Component (Cont'd)	Value
Inlet Recovery	99.5%	LPT Adiabatic Efficiency	89.96%
Fan Adiabatic Efficiency	87%	LPT Non-Chargeable Cooling	5.13%
Duct 4 Pressure Loss	0.48%	LPT Chargeable Cooling	2.06%
Duct 6 Pressure Loss	1.01%	Duct 13 Pressure Loss	1.07%
HPC Adiabatic Efficiency	73.13%	Mixer Gain	75%
Fuel LHV	18,580 Btu/lbm	Tailpipe Pressure Loss	0%
Burner Efficiency	98.27%	Nozzle Gross Thrust Coefficient	96.90%
Burner Pressure Drop	5.40%	Nozzle Discharge Coefficient	97.50%
HPT Adiabatic Efficiency	87.07%	Bypass Duct Pressure Loss	1.49%
HPT Non-Chargeable Cooling	6.67%	Customer Bleed	0.00%
HPT Chargeable Cooling	10.09%	Bypass Leakage	0.5%
Duct 11 Pressure Loss	0.51%		

Off-design power management

A simple power management scheme was chosen for this engine such that fuel flow is set to ensure 100% corrected fan speed unless a maximum turbine inlet temperature constraint is reached.

Results

The results as of August 2019 are shown in Table 21 for each of the three flight conditions examined.

Table 21. Refanned CFM56 derivative performance.

	Design	Takeoff	SLS
Mach	1.4	0.25	0.0
Altitude [kft]	50	0	0
$\Delta T + ISA$ [°R]	0	27	27
Net Thrust [lbf]	3,330	12,416	14,543
TSFC [$\mathbf{lbm/(lbf \cdot h)}$]	0.970	0.664	0.543
BPR	2.35	2.37	2.36
$T41$	3,181	3,043	3,020
$T3$	1,607	1,557	1,543
OPR	24.9	22.3	22.4
FPR	2.0	1.89	1.89
HPCPR	12.6	12.0	12.0
Extraction Ratio	1.1	1.11	1.11
NPR	5.85	1.86	1.79

Airframe modeling

This section details the process of modeling the airframe, including the cabin, vertical tail, area ruling, and aero shaping of the vehicle.

Cabin sizing

A notional cabin layout for the business jet SST was made. It was assumed that the fuselage width would be 7.8 ft. The total cabin length was 30 ft.

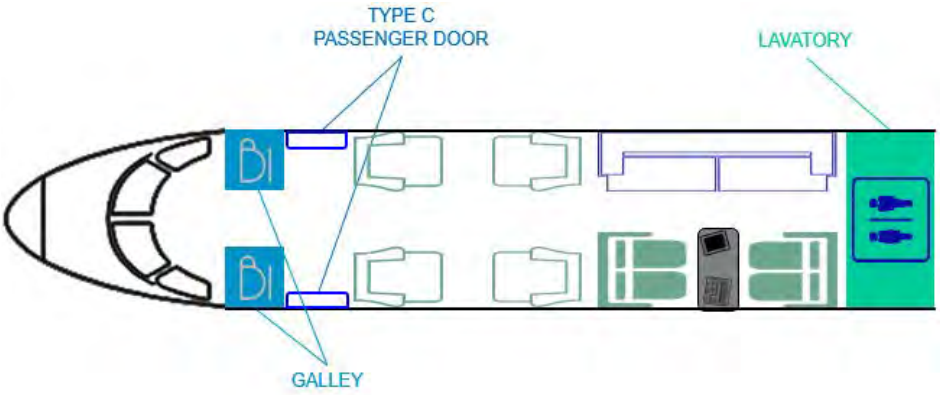

Figure 57. Notional cabin layout for business jet SST.

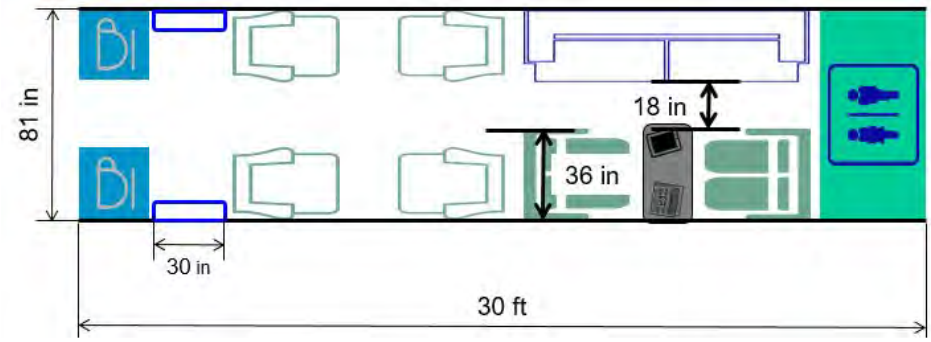

Figure 58. Dimensions of cabin layout for business jet SST.

Vertical tail sizing

The same procedure used to calculate the vertical tail size of the medium SST was used for this configuration. The values used for the business jet SST configuration were as follows:

Table 22. Parameters for vertical tail sizing of business jet SST.

Parameter	Value
T (lbf)	30,000
d (ft)	22.5
ρ (slug/ft^3)	0.002377
V_{SR1}(ft/s)	243.9
$C_L\|_{\beta=15^\circ}$	1.0
ΔX (ft)	97.5

The minimum area for the tail was found to be 108 ft^2.

Area ruling

During the conceptual design, the minimization of wave drag governed the aerodynamic shaping of the aircraft. This drag contribution can be calculated by using slender body theory and supersonic area ruling (Whitcomb, 1966). Because area ruling has been shown to reduce the wave drag, the aircraft design process was shaped by continually checking the cross-sectional area distribution from nose to tail. The design that has the smoothest changes in area is best suited for the supersonic regime. The area distribution was visualized with OpenVSP's Wave Drag tool, a NASA program used for rapid conceptual vehicle design.

Aero shaping

The main design considerations for the business jet SST were number of engines, engine location, wing sweep and planforms, and type of tail.

The initial designs had three engines to reach a compromise between having low takeoff weight and minimizing the impact of engine failure—criteria used during FAA aircraft certification. The engines had a 2D design (Raymer, 2004), which converts kinetic energy into pressure and is adaptable over a wide range of flow conditions, angles of attack and mass flows, but has heavier intakes. Initially, the aircraft had only two engines attached to the fuselage aft of the wings and one engine on top of the fuselage. This design was changed to two engines under the wings and one engine embedded to bottom of the fuselage, because placing the engines at the wing kink minimizes the addition of structural weight and has minimal effects on the generation of lift, and the engine at the root of the tail reduces the total wetted area (Mattingly, 2002). Furthermore, the embedded engine shields forward propagating noise (Crichton et al., 2007) and reduces drag (de la Rosa Blanco, 2007). These advantages outweighed the disadvantage of having embedded engines that take up fuselage space.

The choice of the wing planform shape and location was governed by wave drag. The fundamental objective was to reduce the wave drag, which can be a substantial contribution to the overall drag in the supersonic regime. A double delta wing was selected to be the planform of the vehicle because it is a good compromise between the subsonic and supersonic flight regimes. The high sweep inboard wing is used to keep the wing within the Mach cone when flying in supersonic speeds, and the low seep outboard wing generates more lift in subsonic speeds than a traditional delta wing. If the inboard sweep lies outside the Mach cone, a shockwave forms on the wing, thus leading to inefficiency due to increased drag. By decreasing the sweep outboard, the takeoff and landing performance of the plane is improved, because a pure delta wing would require a very high angle of attack in this low-speed regime. Another benefit of a double delta wing is that it increases the aspect ratio, thus decreasing the induced drag in the subsonic regime. For this reason, the double delta wing was chosen as the planform. Figure 59 presents the original wing, which has sharp changes in the sweep, unlike the smooth wing seen in Figure 60 (right). The design was modified from a sharp wing to a smooth, curved wing because the ogive-like wing has been shown to reduce supersonic drag (Rech & Leyman, 1981).

With the wing planform shape chosen, the next step was to determine the location of the wing on the fuselage. Of the three option—low wing, mid wing, and high wing—the mid-wing was immediately eliminated, because the wing spars would pass through the passenger cabin. A high wing, typically seen on military transports, allows for easier loading and unloading but makes maintenance difficult. A low wing allows for stowing away large landing gear, which facilitates rotation during takeoff, especially for delta wing aircraft with high takeoff angles of attack. Moreover, a low wing combined with under-wing engines allows for easier servicing for both the wing and engines. For this reason, the wing was placed below the fuselage.

A T-tail was used to decrease sonic boom (Li et al., 2008) and because the end plate effect for vertical tail allows for a reduced vertical tail size and minimization of induced drag (Ozgen, 2017). Although the aircraft has a heavier structure and is prone to deep stall for high angles of attack (Scholz, 2017), the decrease in sonic boom was a key advantage. A comparison of the first designs is shown in Figure 59 and Figure 60.

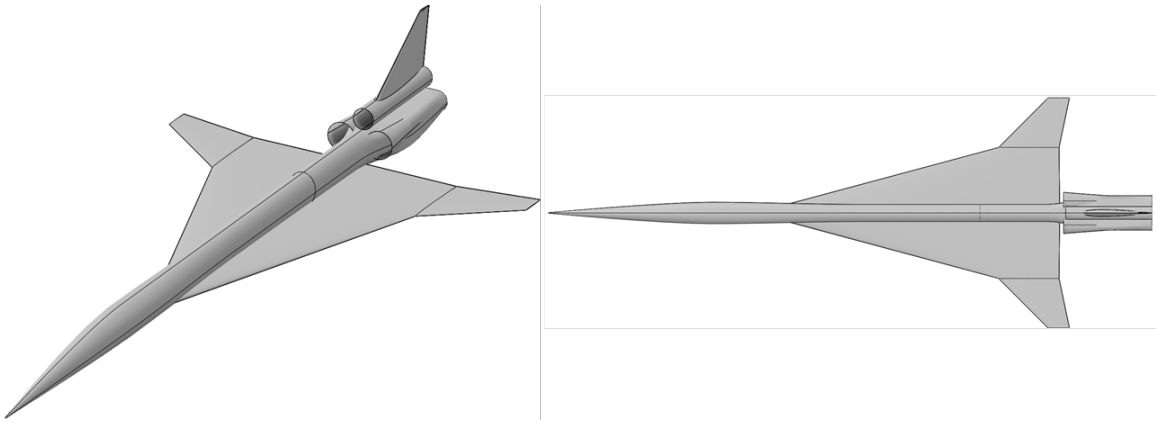

Figure 59. Comparison between iterations for business jet SST – First design: fuselage and tail-mounted engines.

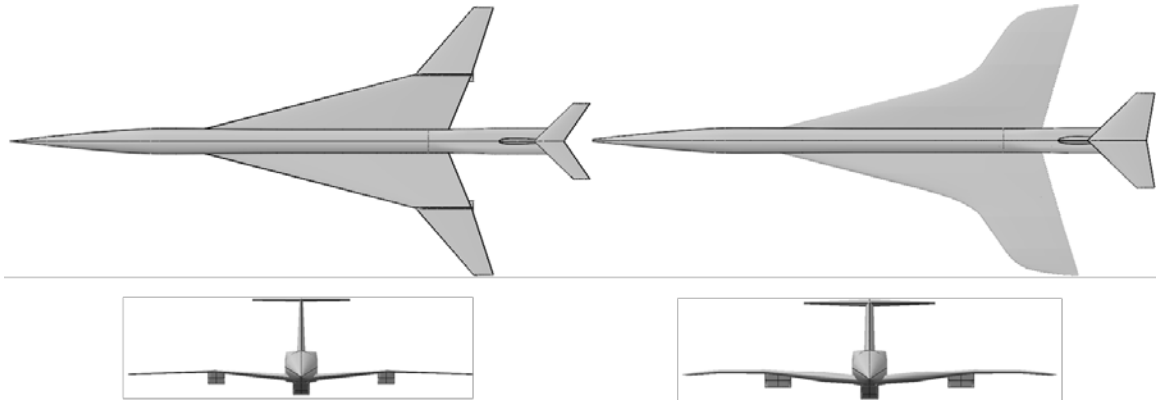

Figure 60. Comparison between design iterations for business jet SST – Later designs: wing mounted and fuselage embedded engines.

Figure 61. Single-swept, two-engine design.

After additional propulsion analysis, a two-engine design was adopted, and the aircraft was redesigned. This design featured two podded engines in the aft of the aircraft to optimize the aircraft for supersonic area ruling. The wing was also changed from a double delta wing to a singular sweep aircraft with a leading edge extension, or strake, because the cruise Mach number proved to be low enough to avoid the additional complexity of the double delta design. This updated design is

shown in Figure 61. As of August 2019, the business jet design was switched to an existing model from NASA at the sponsor's request.

Mission analysis
This section presents the preliminarily chosen thrust-to-weight ratio and wing loading along with the mission profile and vehicle sizing results from the sizing tool FLOPS.

Design point
The thrust-to-weight ratio and the wing loading were defined by using a constraint analysis tool built in the previous work for the project, by using the mission profile above. The thrust-to-weight ratio was set to 0.49, and the wing loading was set to 89 lb/ft^2.

Mission profile
The vehicle was sized for a mission with a total range (excluding reserve mission) of 4,500 nmi. The chosen mission profile was as follows:

- Takeoff: Mach = 0–0.3 at altitude of 0 ft
- Subsonic climb: M = 0.3–0.95; altitude changing from 0 ft to 35,000 ft
- Transonic climb: M = 0.95–1.2; altitude changing from 35,000 ft to 41,000 ft
- Supersonic climb: M = 1.2–1.4; altitude changing from 41,000 ft to 53,683 ft
- Cruise climb: constant Mach number and gradual increase in altitude; M = 1.4 and maximum altitude of 55,000 ft
- Descent: deceleration from M = 1.4–0.3; altitude decreasing from 55,000 ft to 0 ft.

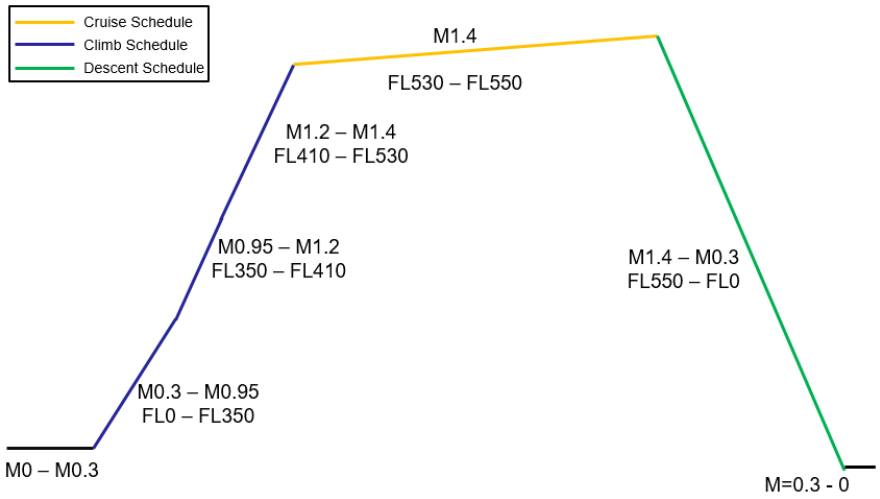

Figure 62. Mission profile for business jet SST.

Vehicle sizing
The vehicle sizing loop was performed by using FLOPS. The vehicle was defined by using the aerodynamic and propulsion information defined in this report along with the mission profile discussed above. The *preliminary* vehicle characteristics results are shown in Table 23 and Table 24. *Again, these results are preliminary at the writing of this annual report.*

Table 23. Key parameters for business jet SST (preliminary).

Key Metric	Value
Takeoff Gross Weight, lbs	140,486
Design Cruise Mach	1.4
Wing Reference Area (ft^2)	1,578.5
Design Range (nmi)	4,000
Cruise L/D	10.0

The *preliminary* weight breakdown for the vehicle is as follows:

Table 24. Weight breakdown of business jet SST (preliminary).

Component	Weight (lbs)	% Empty Weight (lbs)	Component (Cont'd)	Weight (lbs)	% Empty Weight (lbs)
Wing	32,012	40.10	Control Surfaces	2,495	3.13
Horizontal Tail	0	0.00	Instruments	478	0.60
Vertical Tail	804	1.01	Hydraulics	894	1.12
Fuselage	10,438	13.08	Electricals	1,549	1.94
Landing Gear	4,990	6.25	Avionics	1,070	1.34
Nacelle	2,155	2.70	Furnishings and Equipment	2,427	3.04
Structures Total	**50400**	**63.14**	Air Conditions	1,047	1.31
Engines	15,576	19.51	Anti-icing	173	0.22
Thrust Reverser	2,341	0.56	**Systems and Equipment Total**	**10,132**	**12.69**
Propulsion Miscellaneous	449	0.56	**Weight Empty**	**79,823**	**100.00**
Fuel System – Tanks and Plumbing	926	1.16			
Propulsion Total	**19,291**	**24.17**			

Publications

Submitted conference proceedings

Jain, S., Ogunsina, K., Chao, H., Crossley, W. A., & DeLaurentis, D. A. (2020). Predicting routes for, number of operations of, and fleet-level impacts of future commercial supersonic aircraft on routes touching the United States. Abstract submitted to AIAA Aviation Forum for presentation in June 2020.

Outreach Efforts

Multiple interactions with government, industry, and academia have occurred during the course of the project.

ASCENT 10: Aircraft Technology Modeling and Assessment, oral presentation to ASCENT Spring Advisory Committee Meeting, GT, Atlanta GA, April 2019.

Awards

None.

Student Involvement

The Georgia Tech student team consists of seven graduate research assistants (GRA). At the beginning of the project, all seven GRAs engaged in determining supersonic configurations for both the business jet and medium SST, and then the team was divided into geometry, aerodynamics, propulsion, weights, noise, mission analysis, and fleet assessment, with each student taking on multiple topics. GRA leads were identified for each topic. Ms. Taylor Fazzini was the student lead for aerodynamics; Mr. Edan Baltman was the student lead for propulsion; Ms. Barbara Sampaio was the student lead for weights; Mr. Kevyn Tran was the student lead for geometry; Mr. Nikhil Iyengar was the student lead for noise; Mr. Rick Hong was the student lead for mission analysis; and Mr. Thomas Dussage was the student lead for fleet assessment.

The Purdue team includes three graduate students in the effort, all of whom have been conducting tasks in support of the effort. Samarth Jain has just obtained an MS degree and is continuing at Purdue for PhD studies. Kolawole Ogunsina and Hsun Chao are continuing as PhD students.

Plans for Next Period

Georgia Tech

The Georgia Tech team investigated routes that would be capable of carrying enough demand to fill a 50- to 60-seat supersonic aircraft with significant time advantages. It was also demonstrated that an estimate of vehicle demand can be converted to equivalent passenger traffic in GREAT.

The preliminary modeling of supersonic vehicles developed a parametric capability to explore the design constraints for potential future supersonic aircraft design. This is valuable because it allows users to explore specific aircraft capabilities or mission requirements and their influences on the engine and aerodynamic efficiency of the aircraft, as well as a simplified mission performance and weight analysis that results in preliminary estimates of fuel efficiency for a potential aircraft. This results in multipliers of several new aircraft concepts relative to a reference subsonic aircraft type. The resulting fuel intensity of these new types is in the several multiples of a standard single aisle reference aircraft.

This phase of the effort investigated the ability of AEDT to model supersonic aircraft, which it can do but is not well supported. The results obtained from existing or other aircraft developed for other research efforts show specific modeling gaps that influence the accuracy of any potential supersonic aircraft model in AEDT. These modeling gaps resulted in specific recommendations for improving the future modeling capabilities of AEDT.

The fleet analysis tools were expanded to specifically include a separate category for supersonic aircraft. The results for the fleet analysis obtained from GREAT/IDEA, which include several of the supersonic concept aircraft for the first time, are the first attempts at incorporating potential supersonic aircraft into the fleet analysis frameworks. The range of the results shows a relatively modest impact of CO_2 emissions for only a few daily flights on a very limited number of routes. However, following some prior market assessments of a potential demand of more than 1,000 supersonic aircraft over a 10-year period, the results show a potentially very significant increase in CO_2 emissions of aviation.

Future work—shown in the second-year proposal for the current supersonic effort—will focus on reducing the modeling uncertainty in the demand for supersonic aircraft as well as expanding the estimates for supersonic aircraft in the KEIs. The team will also work with the AEDT developers to improve the modeling of supersonic aircraft and enable their accurate representation in the software. Additionally, the fleet-level modeling of supersonic aircraft will focus on expanding the environmental metrics as well as incorporating new models. Finally, the team will develop high-fidelity EDS models of two potential supersonic aircraft that will allow much higher fidelity of the environmental performance of these aircraft. This also will allow investigations into the optimum design and operation of these potential new aircraft.

Purdue

The Purdue team successfully demonstrated FLEET's capabilities for modeling and analyzing the introduction of commercial supersonic aircraft to an existing all-subsonic airline fleet model. This demonstration has shown that FLEET is capable of adjusting scenarios developed by ASCENT 10 Project partners (in the first phase of the ASCENT 10 project) to accommodate for the availability of supersonic aircraft in the airline fleet and, as such, provides some unique features that benefit the FAA in tackling challenging fleet-level emissions forecasting problems.

The preliminary results from FLEET by using the placeholder supersonic aircraft model indicate an increase in the fleet-level total fuel burn for the subsonic-only fleet mix compared with a mix including supersonic aircraft along with subsonic aircraft. In the fleet-mix scheme in which supersonic aircraft become available, the future total fuel burn exceeds that predicted for the subsonic-only fleet by an amount larger than would be expected for the number of supersonic aircraft operated by the airline. When the allocation approach first satisfies passenger demand for business class and above with supersonic aircraft and subsequently satisfies remaining demand with the subsonic fleet, the results indicate a different use, retirement, and acquisition of the subsonic fleet from that predicted in the subsonic-only fleet mix scheme. These changes lead to the increased fleet-level fuel burn trend observed in the preliminary results. At this time, the results still rely on Purdue's simplistic placeholder model for the A10 notional medium SST aircraft, and therefore, the predicted values for fuel burn should not be viewed with high support; the ability to find these trends via FLEET is the more important conclusion at this point in the effort.

The FLEET results—using the placeholder supersonic aircraft model and the simplistic route deviation approach—provide first estimates of which routes in the FLEET network will have supersonic aircraft service, how many round trips the supersonic aircraft would perform on those routes, and the number of passengers carried on these supersonic flights.

Future work (elucidated in detail in the third-year proposal for the current supersonic effort) will include repeating the various studies by using the recently available A10 notional medium SST aircraft model from the Georgia Tech research team. Additionally, the Purdue team will continue to coordinate with the Georgia Tech team to have consistent supersonic aircraft routing, so FLEET will use flight distances based on Georgia Tech's supersonic aircraft route optimization algorithm.

The Purdue team plans to develop a passenger choice model that can replace the supersonic passenger demand assumption of 5% of the total passenger demand. The current idea for this model will combine both the value of travel time to help monetize time savings, which will be a major contributor, and a relationship between trip duration and volume per passenger to help address considerations of comfort, which will be a minor contributor.

The preliminary results presented in this report are based on the allocation approach, which satisfies travel demand first by using supersonic aircraft and next by using subsonic aircraft. In the near term, the Purdue team intends to replace this "supersonic-first" allocation approach with a "simultaneous" allocation approach wherein the supersonic and subsonic aircraft are allocated together on the basis of supersonic and subsonic passenger demand.

Future work will also include assessing the fleet-level advantage of having different types and sizes of supersonic aircraft, defined by certain operational specifications (e.g., Mach cutoff over land) and passenger capacity (e.g., 100-seat supersonic aircraft), available to the FLEET airline.

Table 25 shows the expected objectives and contributions developed among Georgia Tech, Purdue, and FAA. It shows the expected contributions by task and university. This table highlights the plans for the next research period for Georgia Tech. Full details on these plans can be found in the third-year proposal submitted earlier in the summer. Table 26 shows the anticipated list of Milestones for the Georgia Tech portion:

Table 25. University contributions for year 3.

Objectives		Georgia Tech	Purdue
1	Fleet Assumptions and Demand Assessment	Expand airline cost model: Capture vehicle performance sensitivities (passenger capacity, cruise Mach number); evaluate which size vehicle is most likely to be able to close the business case	Fleet assumption, ticket price, and demand model
2	Fleet Analysis	Develop assumptions for supersonic scenarios relative to 12 previously developed subsonic focused fleet scenarios; perform fleet analysis with the gradual introduction of SST vehicles into the fleet.	Fleet impact assessment
3	AEDT Vehicle Definition	Develop methods to model supersonic flights in AEDT	N/A
4	Support CAEP Supersonic Exploratory Study	FASST vehicle modeling: Develop an additional SST class for 100 passengers Develop an AEDT coefficient generation algorithm for the BADA3 supersonic coefficient Perform trade studies to support the CAEP Supersonic Exploratory Study Assess interdependencies for SST	FLOPS or similar; Integrate FASST results; Develop supersonic noise model for FLEET

5	BADA4 Coefficient Generation	Develop, implement, and test BADA4 coefficient generation algorithms; identify gaps and needs for BADA4 coefficient generation for SST	N/A
6	Coordination	Coordinate with entities involved in the CAEP Supersonic Exploratory Study Coordinate with the clean sheet supersonic engine design project	Coordinate with entities involved in the CAEP Supersonic Exploratory Study

Table 26. List of anticipated milestones for the next research period (Georgia Tech).

Milestone	Planned Due Date
1. Fleet Assumptions and Demand Analysis	August 31, 2020
2. Fleet Analysis	August 31, 2020
3. Cruise NOx Emissions Prediction	February 28, 2020
4. AEDT Supersonic Modeling (All but 3.6)	August 31, 2020
5. 100-Passenger SST Vehicle Definition	April 30, 2020
6. Initial CAEP Exploratory Study Results	August 31, 2020
7. BADA4 Coefficient Generation Algorithm	April 30, 2020
8. Subset of EDS BADA4 Coefficient Generated	August 31, 2020

Table 27 highlights the plans for the next research period for Purdue. Full details on these plans can be found in the second-year proposal submitted earlier in the summer.

Table 27. List of anticipated milestones for the next research period (Purdue).

Milestone	Planned Due Date
• Update the baseline year for route network topology, passenger demand distribution, and initial fleet composition to 2015 • Develop and test passenger choice model based on the "effective cost" metric	January 2020
• Provide updated supersonic demand scenario information based on updated baseline year and network topology • Investigate effect of supersonic aircraft operations on subsonic aircraft operations and pricing • Update the aircraft retirement and acquisition models in FLEET • Develop "textbook" models for 55-seat, 10-seat, and 100-seat supersonic aircraft to support FLEET	April 2020
• Integrate type 1, type 2, and type 3 supersonic aircraft models for different seat capacities in FLEET • Identify airport/certification noise metrics for all aircraft, including supersonic, and implement airport noise area constraint approach in FLEET	June 2020
• Develop a separate FLEET-like tool to assess business jet operations and their subsequent impacts on fleet allocation • Use aircraft representations from Georgia Tech teammates into FLEET, and provide FLEET results with these models	July 2020
• Coordinate with colleagues at Georgia Tech to provide a project report summarizing this third phase of work, studying the introduction of supersonic aircraft	August 2020

References

Annual Energy Outlook 2011. (2011). U.S. Energy Information Administration

Bachman, J. (2016). "Supersonic is coming back. Will the airlines buy it?" Bloomberg

Blake, M., Smith, J., Wright, K., Mediavilla, R., Kirby, M., Pfaender, H., Clark, J.P., Volovoi, V., Dorbian, C., Ashok, A. (2010). "Advanced Vehicle concepts and implications for NextGen." NASA CR-2010-216397

Bogaisky, J. (2018). "GE reveals engine that could make Aerion's ambitious supersonic business jet take flight." Forbes

The Concorde Flying Manual Volume II. (1976). British Airways Overseas Division with later amendments.

Crichton, D., de la Rosa Blanco, E., Law, T., & Hileman, J. (2007). "Design and operation for ultra low noise take-off," AIAA 45th Aerospace Sciences Meeting and Exhibit, January 8-11, 2007.

de la Rosa Blanco, E., Hall, C., & Crichton, D. (2007). "Challenges in the silent aircraft engine design," AIAA 45th Aerospace Sciences Meeting and Exhibit, January 8-11, 2007.

Dubois, D. & Paynter, G.C. (2006), "Fuel flow method 2 for estimating aircraft emissions," SAE Transactions Vol. 115, pp. 1-14, Section 1: Journal of Aerospace

Hartmann, A. (1967). "Theory and test of flow mixing for turbofan engines," AIAA 3rd Propulsion Joint Specialist Conference, Vol. 5, No. 6, pp. 522–527. DOI:10.2514/3.43978

Kowalski, E.J. & Atkins Jr., R.A. (1979). "A computer code for estimating installed performance of aircraft gas turbine engines." Advanced Airplane Branch Boeing Military Airplane Company, Vol. I - Final Report

Kuchar, A.P. (1989). "Variable convergent-divergent exhaust nozzle. General Electric Company Aircraft Engine Group", AIAA Education Series, 1989, Chapter 5 of Aircraft Propulsion Systems Technology and Design.

Li, W., Shields, E., & Le, D. (2008). "Interactive inverse design optimization of fuselage shape for low-boom supersonic concepts." Journal of Aircraft, Vol. 45, No. 4, July–August 2008.

Mattingly, J. (2002). Aircraft engine design, AIAA Education Series.

Ozgen, S. (2017). AE 451 aeronautical engineering design I. Middle East Technical University

Pearson, H. (1962). "Mixing of exhaust bypass flow in bypass engine," Journal of The Royal Aeronautical Society, Vol. 66, No. 620, pp. 528–530.

Raymer, D. (2004). Aircraft design: A conceptual approach. AIAA 1992

Rech, J. & Leyman, C.S. (1981). A case study by Aerospatiale and British aerospace on the Concorde. AIAA Professional Study Series

Scholz, E. (2017). Aircraft design – an open educational resource. Hamburg Open Online University

Schutte, J.S. (2009). "Simultaneous multi-design point approach to gas turbine on-design cycle analysis for aircraft engines," Ph.D. Thesis, Georgia Institute of Technology, May 2009.

Thornock, R.L. & Brown, E.F. (1972). "An experimental study of compressible flow through convergent-conical nozzles, including a comparison with theoretical results," Journal of Basic Engineering, pp.926-930.

Welge, H.R., Bonet, J., Magee, T., Chen, D., Hollowell, S. Kutzmann, A., Mortlock, A., Stengle, J., Nelson, C., Adamson, E., Baughcum, S., Britt, R., Miller, G., Tai, J. (2010). "N+2 supersonic concept development and systems integration," NASA-CR-2010-216842.

Whitcomb, R.T. (1966). "Some consideration regarding the application of the supersonic area rule to the design of airplane fuselages,' NACA Research Memorandum, National Advisory Committee for Aeronautics, Washington, July 1966.

Young, J.B. & Wilcock, R.C. (2002). "Modeling the air-cooled gas turbine part 2-coolant flows and losses," Journal of Turbomachinery, 124(2): pp. 214-221.

Appendix: Scenarios

The final set of scenarios developed in the previous phase of this project, with settings for each, is detailed in Table A1 to Table A3.

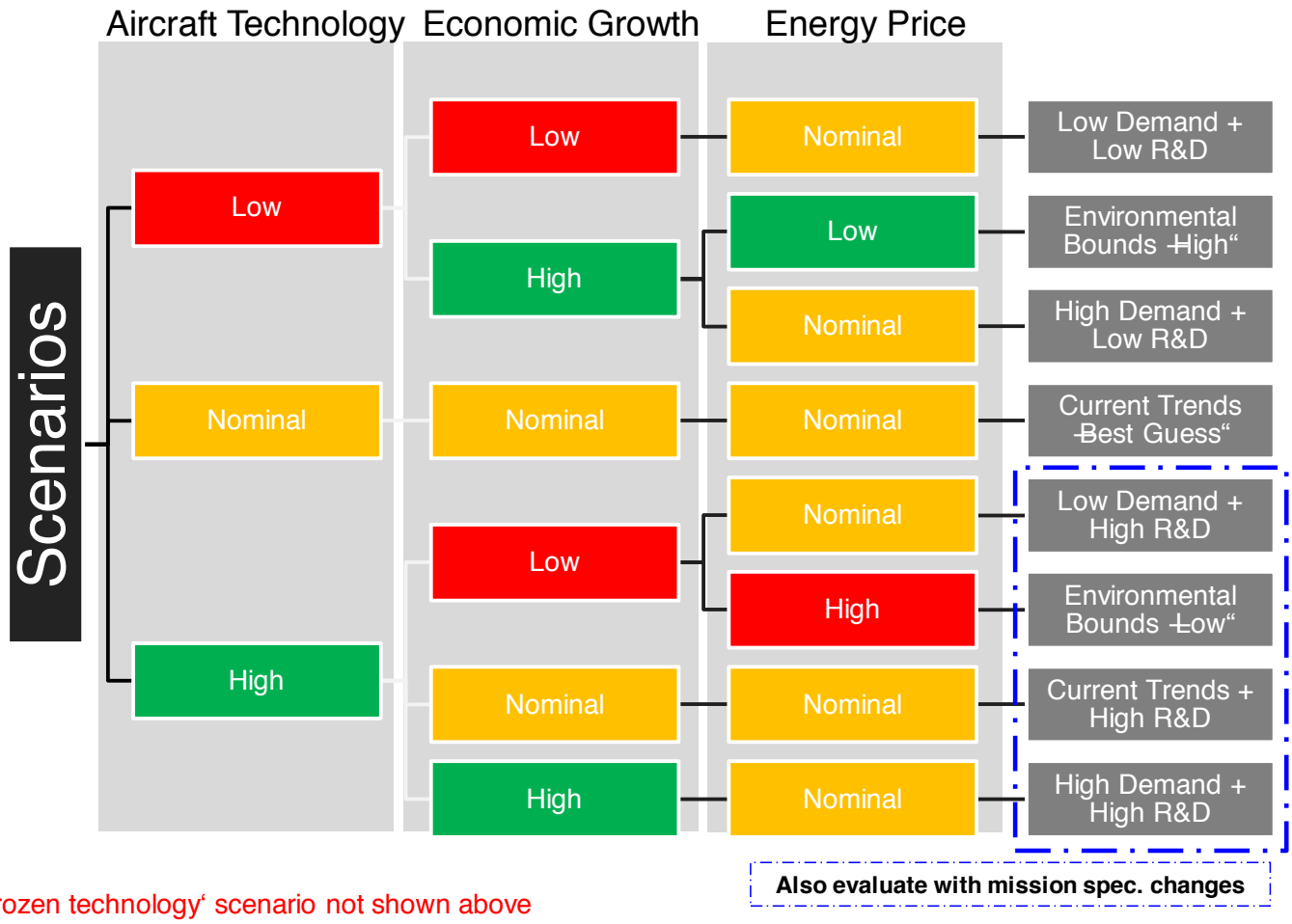

Figure A1. Scenario tree overview.

Table A1 to Table A3 show the final matrix of scenarios. The scenarios are listed by row, whereas the columns list the final worldview descriptors with specific settings for each scenario. Each cell is colored from low to nominal to high settings.

Table A1. Matrix of scenarios and demand and economic model factors.

	GDP Growth (%/year)	Energy Price ($/bbl)	Population Growth (%/year)	International Trade (%/year Asia)	Industry Competetiveness (cent/ASM)	Airport Noise Limitations (% airports noise limited in future)	Cost of CO2 Emissions ($/MT)
Current Trends "Best Guess"	2.8	77	0.58	4.3	12	25	21
Current Trends + High R&D	2.8	77	0.58	4.3	12	25	21
Current Trends + High R&D + Mission Spec.	2.8	77	0.58	4.3	12	25	21
Current Trends Frozen Tech - In-Production Only	2.8	77	0.58	4.3	12	25	21
Environmental "Bounds" - Low	1.8	181	0.45	3.3	12	95	85
Environmental "Bounds" - High	4	41	0.68	5.9	12	4	0
High Demand (Including Global) + High R&D	4	77	0.58	5.9	12	25	21
High Demand (Including Global) + Low R&D	4	77	0.58	5.9	12	25	21
Low Demand (Including Global) + High R&D	1.8	77	0.58	3.3	12	25	21
Low Demand (Including Global) + Low R&D	1.8	77	0.58	3.3	12	25	21
Very High Demand with Noise Limits - Low R&D	4	41	0.68	5.9	12	95	0
Very High Demand with Noise Limits - High R&D	4	41	0.68	5.9	12	95	0

High
Nominal
Low

Table A2. Matrix of scenarios and fleet evolution model factors.

	Fleet Evolution Schedule	Aircraft Retirement	Production Capacity
Current Trends "Best Guess"	Nominal - Twin Aisle First in 2020s	Nominal	No Limits
Current Trends + High R&D	Nominal - Twin Aisle First in 2020s; Adjusted sequence if necessary for first application of new configuration/ architecture/ mission spec. change	Nominal	No Limits
Current Trends + High R&D + Mission Spec.	Nominal - Twin Aisle First in 2020s; Adjusted sequence if necessary for first application of new configuration/ architecture/ mission spec. change	Nominal	No Limits
Current Trends Frozen Tech - In-Production Only	Nominal - Twin Aisle First in 2020s	Nominal	No Limits
Environmental "Bounds" - Low	Nominal - Single Aisle First in 2020s	Early (relative to historical data)	No Limits
Environmental "Bounds" - High	Nominal - Twin Aisle First in 2020s	Late (relative to historical data)	Limits
High Demand (Including Global) + High R&D	Nominal - Twin Aisle First in 2020s	Nominal	No Limits
High Demand (Including Global) + Low R&D	Nominal - Twin Aisle First in 2020s	Nominal	No Limits
Low Demand (Including Global) + High R&D	Nominal - Twin Aisle First in 2020s	Nominal	No Limits
Low Demand (Including Global) + Low R&D	Nominal - Twin Aisle First in 2020s	Nominal	No Limits
Very High Demand with Noise Limits - Low R&D	Nominal - Twin Aisle First in 2020s	Late (relative to historical data)	Limits
Very High Demand with Noise Limits - High R&D	Nominal - Twin Aisle First in 2020s	Late (relative to historical data)	Limits

Table A3. Matrix of scenarios and aircraft technology model factors.

	Amount and Speed of Technology R&D Investment (relative)	TRL 9 Dates	Benefit Levels	Aircraft Configurations	Engine Architectures	Mission Specification Changes
Current Trends "Best Guess"	1.02	Medium	Medium	"Gen 1" Advanced High AR Wing Type 2035+ (check median gen 1 TRL 9 date response)	"Gen 1" as expected; "Gen 2" Open Rotor Type Benefits 2035+	None
Current Trends + High R&D	1.71	Early - Emphasis over benefit level	High	All 3 generations as responded in surveys, Gen 1 2025+, Gen 2/3 2035+	All 3 generations as responded in surveys, Gen 2/3 2035+	None
Current Trends + High R&D + Mission Spec.	1.71	Early - Emphasis over benefit level	High	All 3 generations as responded in surveys, Gen 1 2025+, Gen 2/3 2035+	All 3 generations as responded in surveys, Gen 2/3 2035+	3 generations. 2nd gen redesign for cruise speed reduction. Include range variants
Current Trends Frozen Tech - In-Production Only	0	N/A	N/A	None	None	None
Environmental "Bounds" - Low	1.71	Early - Emphasis over benefit level	High	All 3 generations as responded in surveys, Gen 1 2025+, Gen 2/3 2035+	All 3 generations as responded in surveys, Gen 2/3 2035+	3 generations. 2nd gen redesign for cruise speed reduction. Include range variants?
Environmental "Bounds" - High	0.52	Late	Low	None	None	None
High Demand (Including Global) + High R&D	1.71	Early - Emphasis over benefit level	High	All 3 generations as responded in surveys, Gen 1 2025+, Gen 2/3 2035+	All 3 generations as responded in surveys, Gen 2/3 2035+	3 generations. 2nd gen redesign for cruise speed reduction. Include range variants
High Demand (Including Global) + Low R&D	0.52	Late	Low	None	None	None
Low Demand (Including Global) + High R&D	1.71	Early - Emphasis over benefit level	High	All 3 generations as responded in surveys, Gen 1 2025+, Gen 2/3 2035+	All 3 generations as responded in surveys, Gen 2/3 2035+	3 generations. 2nd gen redesign for cruise speed reduction. Include range variants
Low Demand (Including Global) + Low R&D	0.52	Late	Low	None	None	None
Very High Demand with Noise Limits - Low R&D	0.52	Late	Low	None	None	None
Very High Demand with Noise Limits - High R&D	1.71	Early - Emphasis over benefit level	High	All 3 generations as responded in surveys, Gen 1 2025+, Gen 2/3 2035+	All 3 generations as responded in surveys, Gen 2/3 2035+	3 generations. 2nd gen redesign for cruise speed reduction. Include range variants

Project 017 Pilot Study on Aircraft Noise and Sleep Disturbance

University of Pennsylvania

Project Lead Investigator

Mathias Basner, MD, PhD, MSc
Associate Professor of Sleep and Chronobiology
Department of Psychiatry
University of Pennsylvania
1019 Blockley Hall, 423 Guardian Dr.
Philadelphia, PA 19104-6021
215-573-5866
basner@pennmedicine.upenn.edu

University Participants

University of Pennsylvania

- PI(s): Mathias Basner, associate professor
- FAA Award Number: 13-C-AJE-UPENN-011
- Period of Performance: October 01, 2018, to September 30, 2019
- Task(s):
  - Atlanta (ATL) pilot sleep study: Data analysis

Project Funding Level

This period is a no-cost extension. The funding balance at the start of this period (October 1, 2018) was $45,298. The cost-sharing requirement for this project was fully met by our international collaborators at the German Aerospace Center (DLR) during the original project period ending September 30, 2018.

Investigation Team

- PI(s): Mathias Basner (University of Pennsylvania): study design, data acquisition, data analysis
- Postdoctoral researcher: Michael Smith (University of Pennsylvania): data analysis
- Research assistants: Katharine Casario and Sarah Rocha (both University of Pennsylvania): data acquisition (Sarah Rocha), data analysis (both)

Project Overview

The long-term goal of this line of research is to derive exposure–response relationships for aircraft noise-induced sleep disturbance that are representative of the exposed U.S. population. Studies will have to investigate samples around multiple airports; therefore, it will not be possible to use polysomnography [i.e., simultaneous recording of the electroencephalogram (EEG), electromyogram, and electrooculogram] to monitor sleep because this would require trained personnel at the measurement site in the evening and morning, which would be too costly. An alternative method of using a single-channel electrocardiogram (ECG) and actigraphy to monitor sleep has been examined. This would allow investigation of a greater number of subject samples at lower cost because individuals can be taught how to apply the electrodes themselves. Also, in contrast to polysomnography, awakenings can be identified automatically. Awakenings are defined as brain activations (so-called EEG arousals) that last 15 s or longer. As part of previous research, we refined an algorithm for identifying EEG arousals (Basner et al., 2007) based on increases in heart rate to identify only those arousals ≥15 s in duration, which is the most agreed upon indicator of noise-induced sleep disturbance. High agreement was obtained between arousals scored visually from the EEG and those identified using the refined ECG-based algorithm. The method of using ECG and actigraphy to monitor sleep has been implemented in two pilot field studies to evaluate the quality of data that can be obtained for

unattended physiological and noise measurements. Based on lessons learned, the study protocol is being refined to inform the design and cost of a potential multi-airport study on the effects of noise on sleep.

Task 1 - Data Analysis

University of Pennsylvania

Objective(s)

1. Finish analysis of physiological data received during Philadelphia International airport (PHL) study
2. Finish analysis of acoustical, physiological, and self-reported data of the Atlanta airport (ATL) study
3. Refine and, to the extent possible, automatize the methodology to identify aircraft noise events and maximum sound pressure levels in complex acoustical signals
4. Inform the design of a potential large-scale field study on the effects of aircraft noise on sleep around multiple U.S. airports based on lessons learned from the current field studies
5. Continue our collaboration with colleagues at the DLR to compare, combine, and publish findings from U.S. and German field studies

Research Approach

Based on lessons learned in the PHL sleep study, the methodology was refined and a second pilot study was conducted to evaluate its feasibility on a national scale. ATL airport was was selected for this study in consultation with the FAA and had relevant amounts of nighttime air traffic and a sufficient population from which to sample. To determine the sample regions around the airport, night noise level (L_{night}) contours were provided by the FAA. Additionally, we calculated L_{night} contours for 84 weekdays based on flight track data. For the study, we had 10 sampling regions, 5 east and 5 west of the airport, in the following noise categories: <40 dB (control region), 40<45 dB, 45<50 dB, 50<55 dB, and ≥55 dB L_{night}.

To recruit participants for the study, brief surveys were mailed to randomly selected households within each of the 10 sampling regions. The primary purpose of the survey was to determine the eligibility of individuals to take part in an in-home sleep study. The survey contained questions on the individual's health, sleep, and noise sensitivity. To increase the response rate to the recruitment survey, different incentives, such as a promised gift card or a pre-paid $2.00, were examined. Additionally, survey length and the number of follow-up surveys were varied to determine their effect on response rate. The target number of completed surveys was 200 per 5-dB noise category, for a total of 1000 surveys.

In the survey, participants indicated their interest in taking part in the in-home sleep study, which consisted of 5 nights of unattended ECG and actigraphy measurements and indoor sound recordings. The equipment was mailed to participants' homes, and instruction manuals and videos on how to set up and use the equipment were provided. Mailing the equipment eliminated the need for staff in the field, which significantly reduced the study cost. In addition, mailing the equipment may have increased the response rate because staff did not need to enter participants' homes. For enrolling in the in-home sleep study, participants received varying amounts of compensation. For survey mailing rounds 1 to 5, participants received $20 per night for which measurements were completed. Compensation was increased to $30 per night for mailing rounds 6 to 9, and to $40 per night for rounds 10 to 17. The purpose of increasing the compensation was to evaluate how the response rate changed as compensation increased. This helped us determine a cost-effective compensation for a future multiple airport study. The outcomes for this study were to determine the response rates to both the mail survey and in-home study, assess the feasibility of mailing equipment, and evaluate the quality of data that can be obtained.

Milestone(s)

The following milestones were achieved during the past 12 months:

1. Analysis of the postal survey data in the ATL study was refined and published.
2. Analysis of physiologic and morning questionnaire data in the ATL field study was refined and completed.
3. The physiologic measurement and analysis methodology was refined.
4. The final report for the ATL study was completed and sent to the FAA for review.

Major Accomplishments

Statistical analysis of postal questionnaire data for the pilot study around ATL was refined and finalized (effective sample size $n = 268$). Calculated L_{night} was significantly associated with lower sleep quality [poor or fair; odds ratio (OR) = 1.04 per decibel (dB); $p < .05$], trouble falling asleep within 30 min ≥1/week (OR = 1.06 per dB; $p < .01$), and trouble sleeping due to

awakenings ≥1/week (OR = 1.04 per dB; $p < .05$). L_{night} was also associated with increased prevalence of being highly sleep disturbed (OR = 1.15 per dB; $p < .0001$) and highly annoyed (OR = 1.17 per dB; $p < .0001$) by aircraft noise. Furthermore, L_{night} was associated with several coping behaviors. Residents were more likely to report often or always closing their windows (OR = 1.05 per dB; $p < .01$), consuming alcohol (OR = 1.10 per dB; $p < .05$), using television (OR = 1.05 per dB; $p < .05$), and using music (OR = 1.07 per dB; $p < .05$) as sleep aids. We found no significant relationship between L_{night} and self-reported general health or likelihood of self-reported diagnosis of sleep disorders, heart disease, hypertension, or diabetes.

Analysis of physiologic and morning questionnaire data in the ATL field study was completed. Self-reported awakenings increased as a function of the highest maximum aircraft noise level occurring during the sleep period. Event-related physiologic awakenings increased as a function of the maximum noise level of individual aircraft noise events, although this effect was not significant ($p = .057$), likely because of the low sample size of this pilot study. A larger-scale study among a representative population around multiple airports should be performed, and the approach used in the presented pilot study has been demonstrated to be feasible for this purpose.

We experimentally identified time drift between physiologic and noise measurement equipment and developed synchronization software. We measured the internal device time on the noise recorders and ECG devices relative to actual time determined by Network Time Protocol Internet servers. With our collaborator Uwe Müller at DLR, we developed software to synchronize the timelines of the acoustic and physiologic data. In this time adaptation software, body movements manually identified by auditory examination of the acoustic data were paired against movements detected in the physiologic actigraphy data. Based on the observations of linear drift during recording, we fitted a linear regression to the acoustically and actigraphically scored movements to determine the time drift between data streams within each study night.

The methodology for analyzing event-related awakenings was finalized. A 50-s analysis period will be used, from 5 s before the scored start of an aircraft noise event to 45 s after the start of that same aircraft noise event. This screening window was derived empirically from data collected at four airports—PHL, ATL, Frankfurt (FRA), and Cologne Bonn (CGN)— which maximized slope estimates for the maximum sound pressure level.

A final report on the ATL study was completed. After review by the FAA, changes were implemented and this report was resubmitted in July 2019.

Publications

Peer Reviewed Journal Publications

Basner, M., Witte, M., & McGuire, S. (2019). Aircraft noise effects on sleep – Results of a pilot study near Philadelphia International Airport. International Journal of Environmental Research and Public Health, 16(17): 3178.

Rocha, S., Smith, M., Witte, M., & Basner, M. (2019). Survey results of a pilot sleep study near Atlanta International Airport. International Journal of Environmental Research and Public Health, 16(22): 432.

Smith, M., Rocha, S., Witte, M., & Basner, M. (2020). On the feasibility of measuring physiologic and self-reported sleep disturbance by aircraft noise on a national scale: A pilot study around Atlanta airport. Science of the Total Environment, 718: 137368

Smith, M., Witte, M., Rocha, S., & Basner, M. (2019). Effectiveness of incentives and follow-up on increasing survey response rates and participation in field studies. BMC Medical Research Methodology, 19: 230.

Published Conference Proceedings

Basner, M., Smith, M., Rocha, S., & Witte, M. (2019). Pilot field study on the effects of aircraft noise on sleep around Atlanta International Airport. Presentation and conference paper 23rd International Congress on Acoustics, Aachen, Germany.

Outreach Efforts

Basner, M., Smith, M., Rocha, S., & Witte, M. (2019). Pilot field study on the effects of aircraft noise on sleep around Atlanta International Airport. Oral presentation at 23rd International Congress on Acoustics, Aachen, Germany.

Smith, M., Rocha, S., Witte, M., & Basner, M. (2019) Self-reported sleep disturbance by aircraft noise around Atlanta airport. Poster presentation at SLEEP 2019, San Antonio, TX.

Awards

None.

Student Involvement

None.

Plans for Next Period

We will finalize and publish the final project report. We will continue to disseminate the findings in peer-reviewed journals. We will continue our collaboration with colleagues at DLR to compare findings from U.S. and German field studies and to prepare joint publications.

References

Basner, M., Griefahn, B., Müller, U., Plath, G., & Samel, A. (2007). An ECG-based algorithm for the automatic identification of autonomic activations associated with cortical arousal. Sleep, 30(10):1349-61.

Project 018 Community Measurements of Aviation Emissions Contribution to Ambient Air Quality

Boston University School of Public Health

Project Lead Investigator

Kevin J. Lane
Assistant Professor
Department of Environmental Health
Boston University School of Public Health
715 Albany St. T4W
Boston, MA 02118
617-414-8457
klane@bu.edu

Jonathan I. Levy (through 9/30/17)
Interim Chair and Professor
Department of Environmental Health
Boston University School of Public Health
715 Albany St. T4W
Boston, MA 02118
617-358-2460
jonlevy@bu.edu

University Participants

Boston University School of Public Health

- PI(s): Kevin J. Lane, Assistant Professor; and Jonathan I. Levy, Professor and Associate Chair
- FAA Award Number: 13-C-AJFE-BU, Amendment 7
- Period of Performance: October 1, 2018 to September 30, 2019
- Task(s):
    1. Construct regression models to determine the contributions of aircraft arrivals to ultrafine particulate matter (UFP) and black carbon (BC) concentrations measured during our 2017 monitoring campaign
    2. Conduct site selection for our 2018 monitoring campaign by analyzing our 2017 measurements and by considering optimal sites to determine multiple types of aviation source contributions (**completed in 2017–2018)**
    3. Measure UFP and other air pollutants at sites near Boston Logan International Airport, as selected in Task 2
    4. Develop platforms that will enable comparisons among atmospheric dispersion models implemented by collaborators on ASCENT Project 19 and monitored pollutant concentrations obtained from Project 18 (**completed in 2017–2018)**

Project Funding Level

This project did not receive funding from the FAA during FY2019.

Investigation Team

- ASCENT BUSPH Director and Project 18 Co-Investigator: Jonathan I. Levy, ScD (Professor of Environmental Health, Chair of the Department of Environmental Health, Boston University School of Public Health). Dr. Levy is the Boston University PI of ASCENT. He initiated ASCENT Project 18 and serves the director of BUSPH ASCENT research.
- ASCENT Project 18 Principal Investigator: Kevin J. Lane, PhD (Assistant Professor of Environmental Health, Department of Environmental Health, Boston University School of Public Health). Dr. Lane joined the Project 18 team

in July 2017. Dr. Lane has expertise in the assessment of UFP exposure, geographic information systems, statistical modeling of large datasets, and cardiovascular health outcomes associated with air pollution exposure. He has contributed to study design and data analysis strategies and, as of 10/1/17, has taken over the primary responsibility for project execution; Dr. Lane also contributes to the manuscripts and reports produced.

- Post-Doctoral Researcher: Matthew Simon, PhD. Dr. Simon joined the Project 18 team in September 2017 and is involved in data analysis, field study design and implementation, and scientific manuscript preparation.
- Graduate Student: Chloe Kim, MPH. Ms. Kim is a doctoral student in the Department of Environmental Health at BUSPH. She has taken the lead on organizing and implementing the air pollution monitoring study and will be responsible for the design and execution of related statistical analyses.
- Graduate Student: Bethany Haley. Ms. Haley is a doctoral student in the Department of Environmental Health at BUSPH. She has taken the lead on field monitoring and in processing the air pollution monitoring study and descriptive statistics.

Project Overview

The primary goal of this project was to conduct new air pollution monitoring beneath flight paths to and from Boston Logan International Airport, using a protocol specifically designed to determine the magnitude and spatial distribution of UFP in the vicinity of arrival flight paths. Data were collected to assess whether aircraft emissions, particularly arrival emissions, significantly contribute to UFP concentrations at appreciable distances from the airport. Task 1 was an extension of the ongoing air pollution monitoring and statistical analysis work performed under the current ASCENT Project 18. Tasks 2 and 3 leverage the infrastructure developed for our field campaign and enable measurements that address a broader set of research questions than those evaluated under Task 1, with additional data collection for UFP size distributions and a new air pollutant (NO/NO_2). These tasks provide a strong foundation for Task 4, which increases the potential for future collaborative efforts with Project 19, in which we interpret and apply the collected measurements to inform ongoing modeling efforts at UNC.

A summary of 2017 project methods and data collection is included below to describe the continued application of Project 18 data, including bivariate statistical analysis and multiple regression model development conducted under Task 1 to inform new site selection for Task 2.

Project 18 Task 1 for the 2016–2017 funding cycle focused on designing and implementing an air pollution monitoring study that would allow us to determine contributions from arriving aircraft to ambient air pollution in a near-airport setting. The objective of this task was to assess whether aircraft emissions, particularly arrival emissions, significantly contribute to UFP concentrations at appreciable distances from an airport.

An air pollution monitoring campaign was conducted at six sites located at varying distances from the airport and the arrival flight path to runway 4R (Figure 1). Near-Airport Site 1 (N1): Office of Department of Conservation and Recreation (DCR), Boston, MA; Near-Airport Site 2 (N2): University of Massachusetts (UMASS) Boston campus; Intermediate-Distance Airport Site 1 (I1): Boston Community Development Corporation (CDC) office; Intermediate-Distance Airport Site 2 (I2): Community member residence; Background Site 1 (F1): Fonte Bonne Academy; Background Site 2 (F2): Blue Hills. Sites were selected through a systematic process, considering varying distances from the airport and lateral distances from the 4R flight path and excluding locations close to major roadways or other significant sources of combustion. These sites were specifically chosen to isolate the contributions of arrival aircraft on runway 4R, which is important for the flight activity source attribution task.

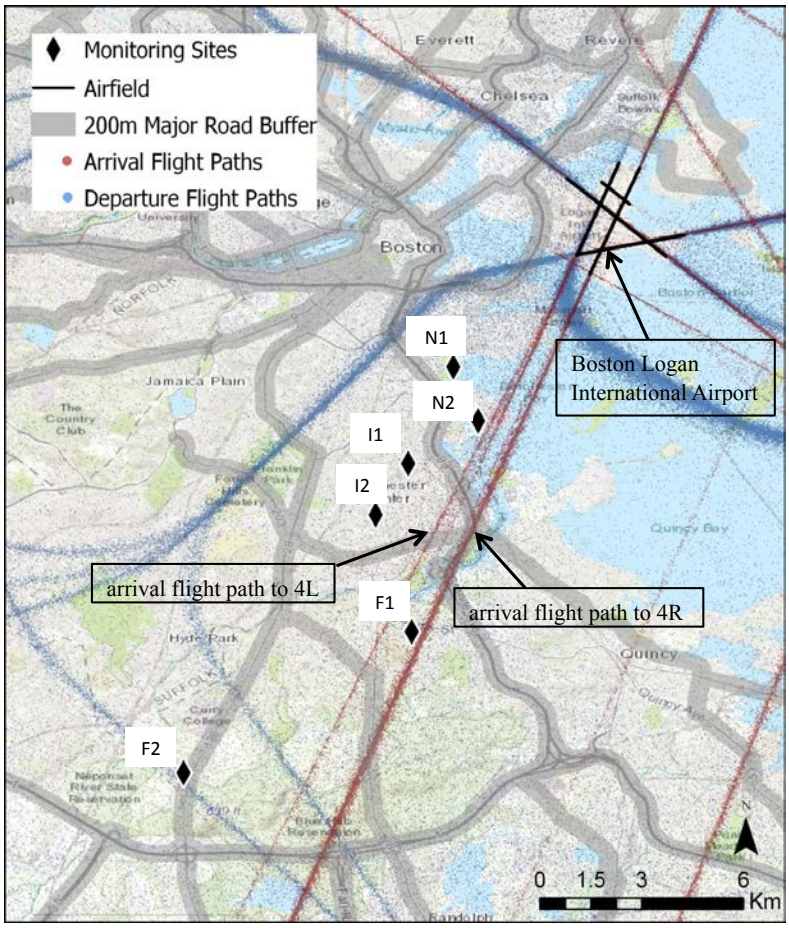

Figure 1. Monitoring sites and runway 4R flight path.

Table 1 presents the characteristics for each monitoring site.

Table 1. Characteristics of each monitoring site.

Site	Distance to flight path 4R (km)	Distance to airport (km)	Average altitudes of arrival aircraft (m)	Monitoring configuration
N1	1	3	210	Indoor*: second-floor office space facing the ocean
N2	< 0.5	4	300	Outdoor: open shed on a boat dock
I1	2	7	400	Indoor*: first-floor restroom facing a small parking area
I2	2	9	460	Outdoor: open shed in the backyard in a residential area
F1	< 0.5	12	610	Indoor*: second-floor classroom
F2	4	17	850	Outdoor: greenhouse at a farm

* For indoor deployment cases, the monitor was placed indoors with tubing running outside to measure ambient concentrations.

Task 1 - Construct Regression Models to Determine the Contributions of Aircraft Arrivals to UFP and BC Concentrations Measured During our 2017 Monitoring Campaign

Boston University School of Public Health

Objective(s)

Under Task 1, we developed regression models to examine contributions from arriving aircraft to ambient air pollution in a near-airport setting. The objective of this task was to determine whether aircraft emissions, particularly in-flight arrival and departure emissions, significantly contribute to ground-level UFP concentrations at appreciable distances from the airport.

Research Approach

Utilizing the air pollution data collected during the 2017 monitoring campaign, we examined average UFP concentrations for days in which the 4R runway was or was not in use under all wind conditions, with the aim of determining the overall impact of arrival aircraft on ambient UFP concentrations at the study sites. We also examined the correlations of UFPs measured simultaneously at multiple study sites to examine the similarities and variations in aircraft impact at different monitoring sites under varying meteorological conditions and flight activity levels. Prior to constructing regression models, we examined space–time plots of our data to identify distinct patterns of plume movement and potential time lag differences between the sites under specific meteorological conditions. Results from these descriptive analyses were used to inform the regression model development process.

For the regression models, we developed multivariate regression models to examine the predicted UFP patterns, using covariates such as meteorology, flight activity, and other ground source contributions such as localized traffic. Each study site was modeled individually to investigate the location-specific impact of aircraft arrivals in addition to meteorological and other local environmental conditions. We also explored novel statistical approaches, i.e., elastic nets and random forest modeling, to elucidate the importance of key covariates at different temporal and distributional scales of analysis.

Milestone(s)

The core milestones for Task 1 included complete regression modeling of UFP and associated manuscript development.

The regression model development is being finalized, and manuscripts are being prepared for submission to peer-reviewed journals.

Major Accomplishments

Descriptive maps and PNC wind rose plots

The statistical analysis for Project 18 was expanded to improve our understanding of the effect of wind direction, wind speed, flight activity, and aircraft engine type on ground-based particle number concentration (PNC) measures. The following figures present the patterns observed over the 2017 data sampling period. Figure 2 displays boxplots of hourly PNCs when the 4R runway had high flight activity, defined as more than 30 flights per hour, compared with no flight activity. In general, the PNC was higher during high flight activity compared with no flight activity. During high flight activity, sites N1 and N2 had higher PNCs compared with the intermediate and background sites. These findings support the hypothesis generation for regression modeling, as they indicate the importance of timing and flight activity.

Additional analysis is being conducted to examine PNCs at different temporal resolutions below 1 hr. Previous studies have focused on analyzing the median or mean hourly concentrations, but due to the intermittent nature of flights, it may be important to examine more finely resolved data, with resolutions below 1 hr, and potential peak exposures in the 95th and 99th percentiles. We have started to plot and analyze 1-s PNC data with corresponding meteorological conditions to investigate the simultaneous relationships among wind direction, wind speed, flight activity, and PNC at each monitoring site. With this aim in mind, we created wind rose PNC plots to identify hotspots under different meteorological conditions at each site (Figure 3). Wind direction is based on the weather station at the airport. Ideal wind conditions (15–45 degrees) exhibited higher concentrations at near-source sites compared with cases in which the monitors were upwind of the arriving aircraft (45–145 degrees). Wind direction had a weaker impact on background site concentrations. We are also further exploring relative wind direction and subcategorization of the operational flight activity to identify periods during which arrivals into 4L were occurring instead of 4R for the nonoperational time periods. These results highlight potential site-specific interactions that may occur between meteorological conditions and flight activity to inform ground-level PNC source attribution.

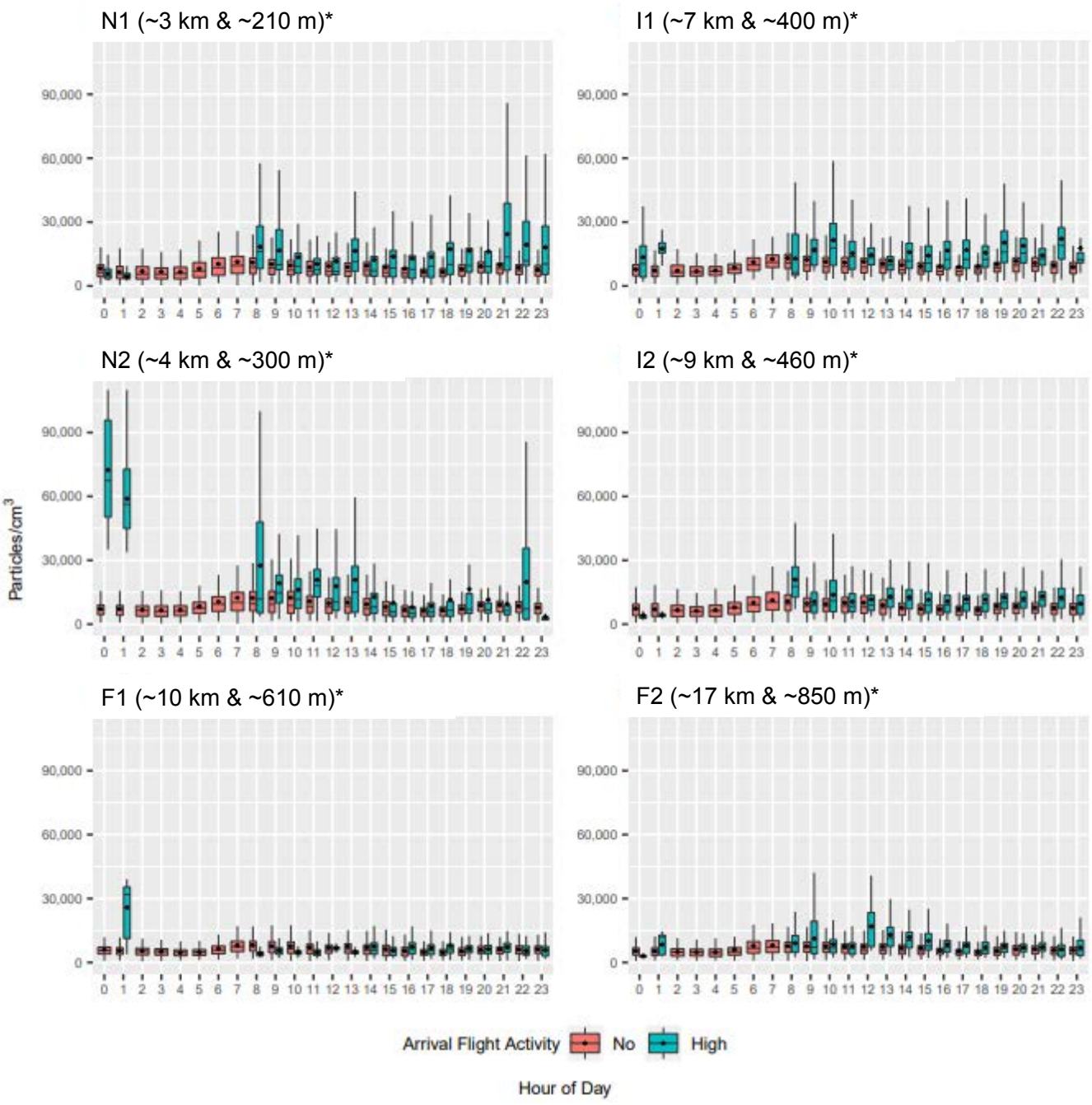

* distance to the airport and average altitudes of arrival aircraft over the site

Figure 2. Diurnal pattern of particle number concentrations (PNCs) under high vs. no arrival aircraft activity conditions.

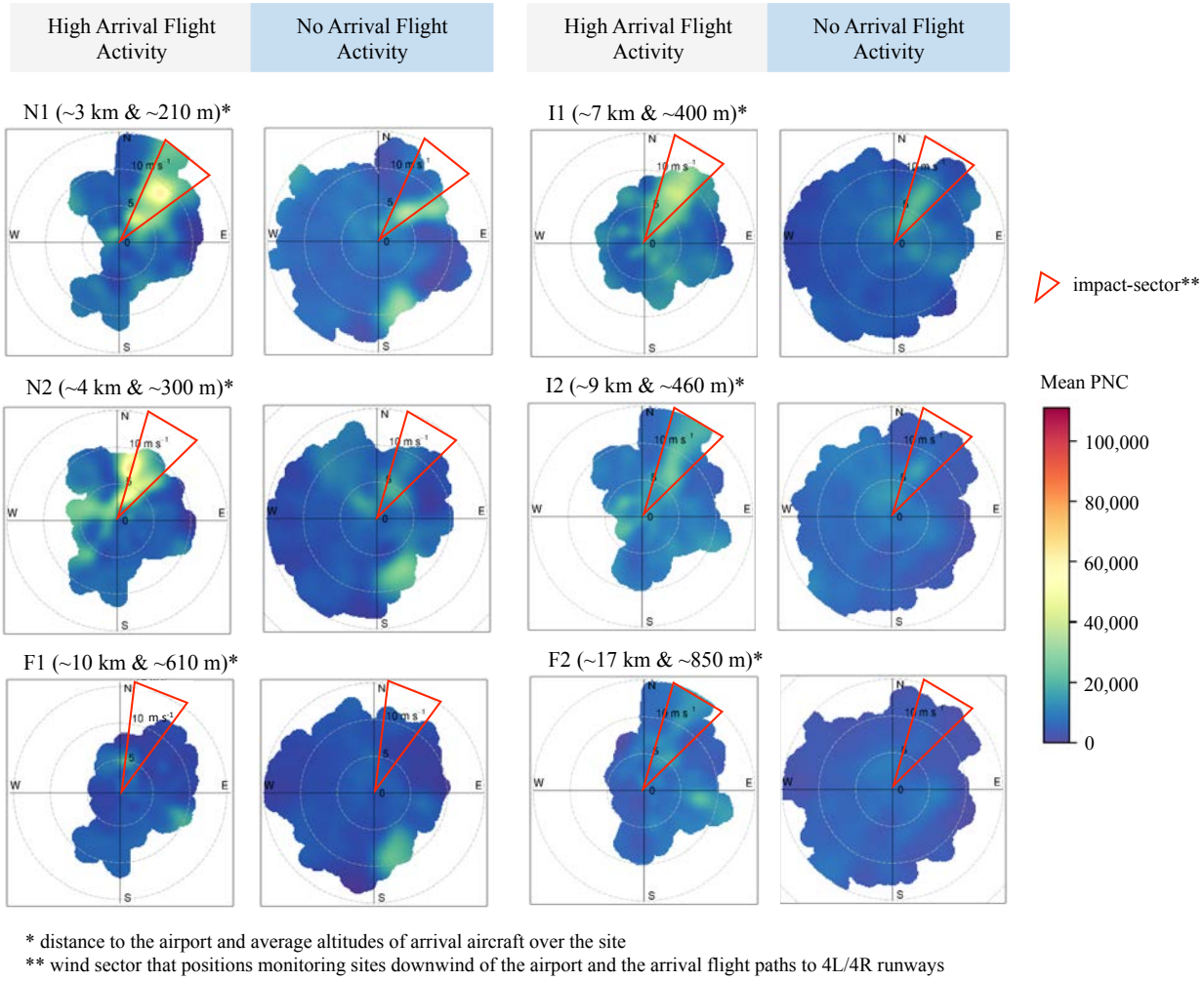

* distance to the airport and average altitudes of arrival aircraft over the site
** wind sector that positions monitoring sites downwind of the airport and the arrival flight paths to 4L/4R runways

Figure 3. Particle number concentration (PNC) wind rose plots for each monitoring site by flight activity on 4R and 4L during high and no flight activity periods. The monitoring sites correspond to map in Figure 1.

Each plot above presents monitoring data for each site-specific wind rose, centered at each monitor geophysical positioning system (GPS) location, with the airport located northeast of each site. Each quadrant represents the direction in which the wind is blowing from, while the circular dashed lines indicate the wind speed in miles per hour. The color represents the PNC range. From the plots, several key points can be inferred and applied for further exploration:

- When flights are occurring, PNC levels are higher than when no flights are occurring.
- Closer sites have elevated PNC hotspots; specifically, DCR (N1) and UMASS (N2), which are closer to the airport, have higher levels than the other sites.
- Hotspots of higher PNC are more pronounced when the wind comes from the airport direction at DCR (N1) and UMASS (N2) during flight activity compared with no flight activity.
- Background sites F1 and F2 have more PNC hotspots during flight activity compared with no flight activity.

Overall, PNC levels are higher when wind comes from the airport direction and when aircraft are flying at lower altitudes, such as at the N1 and N2 sites. For an aircraft arriving into Logan overhead a monitoring site location further away, similar detectable PNC levels are not produced at our background sites under ideal wind conditions, potentially because these aircrafts are at a higher altitude.

PNC regression modeling

The descriptive analyses above informed regression modeling efforts, as presented below. The PNC has a non-normal distribution and is commonly examined as the natural log (LN). Covariates included in this regression model have been found to have a significant univariate relationship with LN PNC. The multivariable linear regression model enables an initial examination of the relationship between spatial–temporal meteorological, flight activity, and other potential ground contributions from traffic sources on the association with the hourly LN PNC. Results from this model should be considered as developments to assist in refinement, as the current model is being expanded to include additional covariate contributions and interactions among predictive factors. Initial regression models have been developed for each monitoring site to compare the total model R^2. Additionally, covariates have been held constant for all models to examine the explanatory power of each variable between sites, thus enhancing our understanding of the relative contributions from flight activity, meteorology, and other local contributions, such as traffic, for source attribution of ground-measured PNCs.

In Table 2, we present preliminary regression model results for the hourly LN PNC at two near-source sites 1 and 2 and a background site 3. Each model includes meteorological variables (wind direction, wind speed, and temperature), temporal information (weekend/weekday and time of day), and flight activity on runway 4R/4L (categorized as no flights, low flight activity [1-10 arriving flights/hr], and high flight activity [>10 arriving flights/hr]). The results obtained by modeling the 99th percentile data are not presented, as they are similar to the results for the 95th percentile PNC. Overall, our regression models indicate a significant positive association between 4L/4R arrival aircraft frequency and measured PNC. In general, the hourly regression models showed a larger increase in PNC associated with 4L/4R arrival activity than the 10-min average regression models (with the exception of the 95th percentile model for site N1), and the 95th percentile models had a larger increase in PNC than the mean models. Because the models have different intercepts, the exponentiated coefficients from different models are not directly comparable, but we can still compare the absolute contributions of 4L/4R activity across the sites by considering both the intercept and the relative 4L/4R arrival aircraft contribution, while holding all other variables constant. For example, at I1, the estimated percent change in the measured 95th percentile 10-min PNC for one additional 4L/4R arrival aircraft was 1.1%, compared with 0.3% for the mean model, with a larger intercept for the 95th percentile PNC model. In other words, the estimated absolute contribution of 4L/4R arrival aircraft on PNC at I1 is larger in the 95th percentile model than in the mean model. In contrast, the impacts of all other aircraft activity at all sites were fairly similar between the mean and 95th percentile models. The coefficients for aircraft activity, including both the 4L/4R arrival aircraft and all other aircraft activity, were lower at the far site (F1) compared with the near and intermediate sites (N1 and I1).

Table 2. Multivariable regression model results for hourly and 10-min mean particle number concentration (PNC) at multiple monitoring sites, accounting for autocorrelation. The monitoring sites correspond to map in Figure 1.

	Mean PNC			
	Hourly		10-Min	
	Exponentiated Regression Coefficients	95% Confidence Interval (CI)	Exponentiated Regression Coefficients	95% Confidence Interval (CI)
	N1			
Intercept	15,100	(9,800, 23,100)	9,500	(6,500, 13,900)
4L/4R runway arrival aircraft frequency	1.016	(1.013, 1.020)	1.008	(1.001, 1.015)
All other aircraft activity frequency	1.007	(1.006, 1.009)	1.002	(0.999, 1.005)
Temperature (Celsius)	0.982	(0.969, 0.994)	0.989	(0.976, 1.001)
Relative humidity (%)	0.993	(0.990, 0.997)	1.000	(0.997, 1.002)
Wind speed (m/s)	0.934	(0.910, 0.959)	0.983	(0.971, 0.995)
Mixing height (m)	1.000	(1.000, 1.000)	1.000	(1.000, 1.000)
Atmospheric pressure (mbar)	0.986	(0.976, 0.997)	1.011	(0.998, 1.025)
Precipitation (mm/hr)	0.966	(0.934, 1.000)	0.989	(0.970, 1.008)
Weekday vs. weekend	1.062	(0.889, 1.267)	1.050	(0.844, 1.306)
Impact sector (yes)	1.119	(0.855, 1.466)	0.941	(0.868, 1.020)
Wind speed (m/s)*Impact sector (yes)	1.114	(1.056, 1.176)	1.031	(1.014, 1.047)

	I1			
Intercept	24,900	(17,600, 35,300)	12,300	(8,900, 17,000)
4L/4R runway arrival aircraft frequency	1.015	(1.012, 1.018)	1.003	(0.997, 1.008)
All other aircraft activity frequency	1.010	(1.009, 1.012)	1.003	(1.000, 1.005)
Temperature (Celsius)	0.964	(0.954, 0.974)	0.989	(0.978, 1.000)
Relative humidity (%)	0.995	(0.993, 0.998)	0.999	(0.997, 1.001)
Wind speed (m/s)	0.913	(0.893, 0.933)	0.986	(0.977, 0.995)
Mixing height (m)	1.000	(1.000, 1.000)	1.000	(1.000, 1.000)
Atmospheric pressure (mbar)	1.003	(0.994, 1.012)	1.012	(1.000, 1.024)
Precipitation (mm/hr)	0.991	(0.963, 1.02)	0.997	(0.983, 1.012)
Weekday vs. weekend	0.904	(0.796, 1.025)	0.996	(0.813, 1.221)
Impact sector (yes)	1.244	(1.021, 1.516)	0.963	(0.908, 1.022)
Wind speed (m/s)*Impact sector (yes)	1.038	(0.997, 1.079)	1.021	(1.007, 1.036)
	F1			
Intercept	20,100	(13,100, 30,8003)	6,100	(4,500, 8,100)
4L/4R runway arrival aircraft frequency	1.010	(1.007, 1.013)	0.999	(0.994, 1.003)
All other aircraft activity frequency	1.004	(1.003, 1.005)	1.001	(0.999, 1.002)
Temperature (Celsius)	0.982	(0.970, 0.994)	1.000	(0.990, 1.010)
Relative humidity (%)	0.990	(0.987, 0.993)	0.999	(0.997, 1.000)
Wind speed (m/s)	0.904	(0.884, 0.925)	0.992	(0.985, 1.000)
Mixing height (m)	1.000	(1.000, 1.000)	1.000	(1.000, 1.000)
Atmospheric pressure (mbar)	0.997	(0.986, 1.007)	1.012	(1.000, 1.023)
Precipitation (mm/hr)	1.024	(0.979, 1.071)	1.004	(0.986, 1.022)
Weekday vs. weekend	1.094	(0.946, 1.266)	1.094	(0.900, 1.330)
Impact sector (yes)	1.079	(0.861, 1.354)	1.016	(0.963, 1.072)
Wind speed (m/s)*Impact sector (yes)	1.023	(0.964, 1.086)	0.995	(0.908, 1.009)

To directly compare the varying contributions of arrival aircraft to the ambient PNC across different models while accounting for other predictors, we calculated PNC estimates using hourly 95th percentile model coefficients under two different arrival aircraft scenarios (zero vs. actual arrival aircraft in 1 hr). While accounting for other predictors in the model, there was a clear contribution of arrival aircraft at all six study sites. The aircraft contribution at N1 was the largest among all sites (Figure 4). For the 27% of 1-hr periods with arrival aircraft on 4L/4R, the estimated arrival aircraft contribution at site N1 had a mean of 11,100 particles/cm^3 (50% of the total PNC). The second and third largest aircraft contributions were observed at I1 and N2, with estimated arrival aircraft contributions of 9,200 and 6,500 particles/cm^3, respectively, during the 1-hr periods with arrival aircraft activity. Both the background-level PNC and aircraft contribution at I2, F1, and F2 were lowest compared with those of the other sites, with aircraft contributions ranging from 2,300 to 5,000 particles/cm^3. Across all hours (not restricting the data to hours with 4L/4R arrival aircraft activity), the mean predicted arrival aircraft contributions ranged from 7% to 26%, with the highest value observed at N1 and the lowest value at F1.

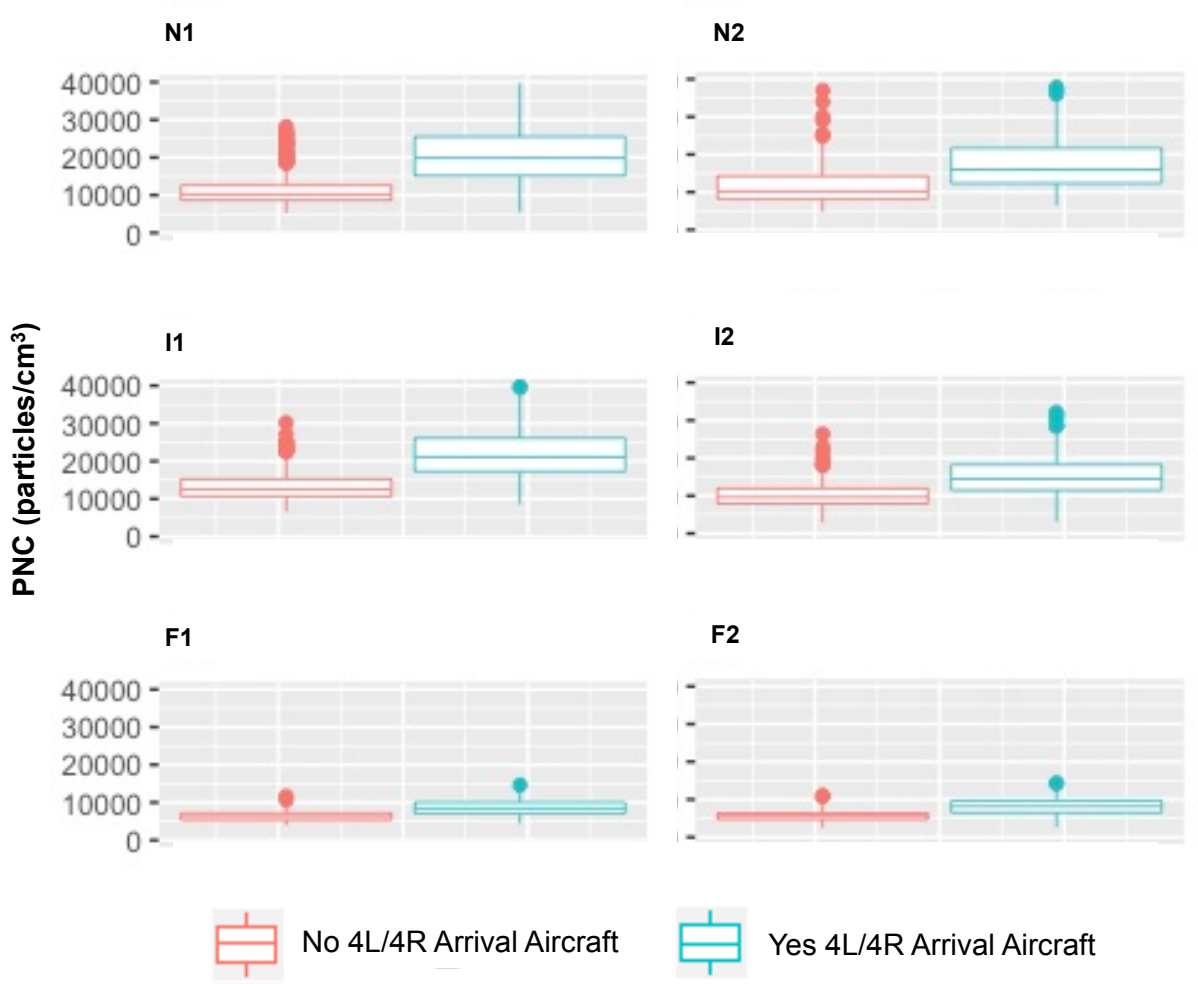

Figure 4. Boxplots displaying 4L/4R arrival aircraft contributions to the estimated ambient particle number concentration (PNC) (95th percentile, 1-hr average) using multivariable regression model predictions for actual arrival activity and no arrival aircraft, restricted to time periods with nonzero 4L/4R arrival aircraft activity.

In addition to linear regression modeling, we explored the use of machine learning regression approaches to identify key covariates and to optimize hourly PNC predictions at each site. This research focused on applications to the UMASS site using a random forest approach, which is a decision-tree-based machine learning algorithm. Each tree is grown by a bootstrap sample, and a random subset of predictors is selected at each split. Predictions are obtained by averaging the results of different trees. Using the random forest model approach, we developed three models to predict the PNC at different hourly scales: hourly median PNC, hourly 95th PNC, and hourly 99th PNC. Figure 5 presents the relative contributions of the covariates to the PNC prediction, measured as the mean square error.

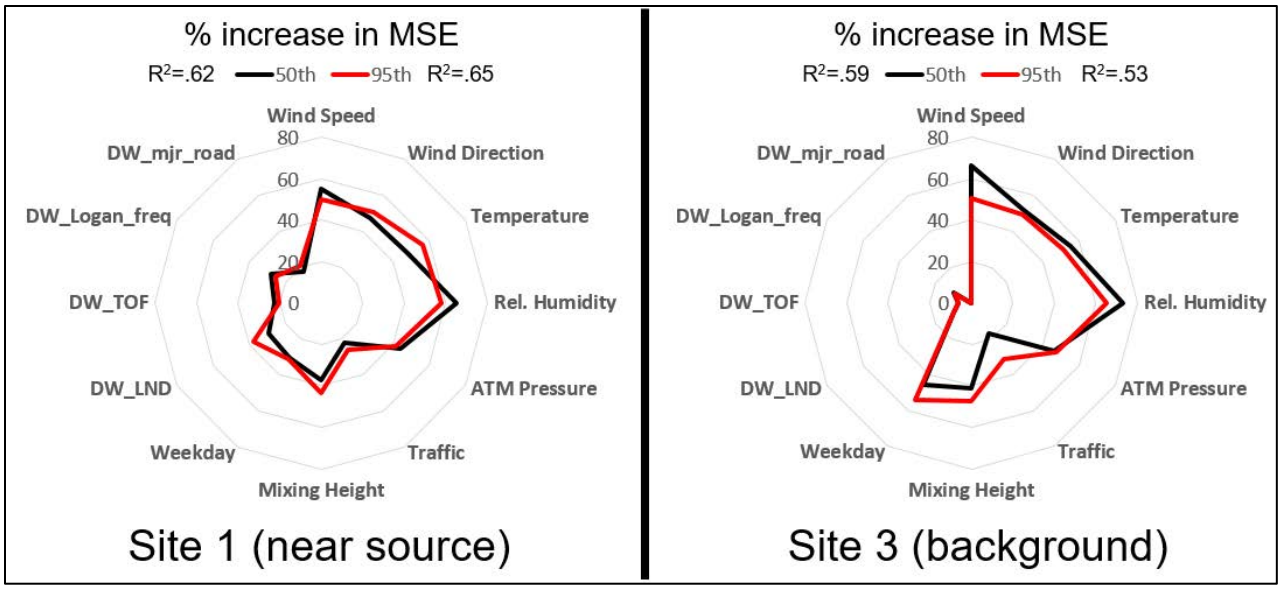

Figure 5. Spider plot showing the importance of each variable in the random forest model based on the mean decrease in model accuracy (as measured by the mean square error).

The mean model regression performance measured as R^2 improved by more than 20% when the random forest approach was applied (R^2 = 0.56). Flight frequency (DW_Logan _Freq) has the largest percent gain in model importance between the median and 95th percentile models (Figure 6). Additionally, the overall random forest model performance had a higher variance for the 50th percentile model compared with that of the 95th percentile model. The random forest modeling approach is being combined with generalized linear regression modeling to identify the best PNC prediction for each site, while also providing interpretable results.

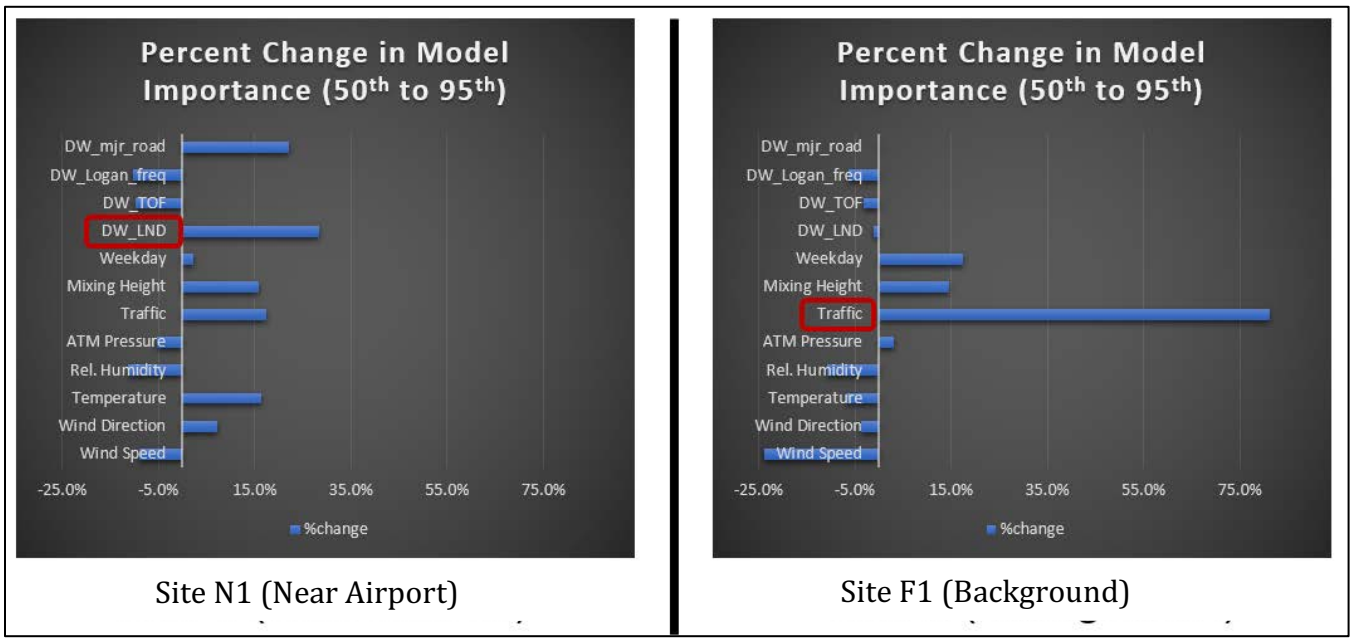

Figure 6. Relative change in the importance of each variable in the random forest model between the median (50th percentile) and the 95th percentile model.

Publications
N/A

Outreach Efforts
- Dr. Jonathan Levy presented and sat on a panel on "Modeling aviation-related ultrafine particles from background concentrations" at the Aviation Emissions Characterization Meeting, National Academy of Sciences, DC, U.S., 2019.
- Dr. Kevin Lane presented and sat on a panel on "Modeling aviation-related ultrafine particles from background concentrations" at the Aviation Emissions Characterization Meeting, National Academy of Sciences, DC, U.S., 2019.
- Dr. Matthew Simon presented an oral presentation entitled "A Machine Learning Approach to Model Community-Level Ultrafine Particle Emissions from Arriving Aircraft" at the International Society for Environmental Epidemiology annual meeting in August 2019.
- Doctoral student Chloe Seyoung Kim presented an oral presentation on a portion of the major accomplishments of Project 18 at the International Society for Exposure Science annual meeting in October 2017.

Awards
None.

Student Involvement
Chloe Seyoung Kim, a doctoral student at BUSPH, was involved in the descriptive analysis and regression modeling of 2017 PNC data. Dr. Kim graduated in December 2020 and has joined the Electric Power research Institute as a research scientist. Bethany Haley, a master's student at BUSPH, has been involved in the descriptive analysis of 2018 sampling data.

Plans for Next Period
Task(s) proposed over the next study period (10/1/18–9/30/19):
Finalize manuscripts for submission to articles.

Task 2 - Conduct Site Selection for our 2018 Monitoring Campaign by Analyzing our 2017 Measurements and by Considering Optimal Sites to Determine Multiple Types of Aviation Source Contributions
Boston University School of Public Health

Objective(s)
Task 2 for the 2017–2018 funding cycle focused on designing and implementing an air pollution monitoring study that would allow us to determine contributions from arriving aircraft to ambient air pollution in a near-airport setting. The objective of this task was to determine whether aircraft emissions, particularly in-flight arrival and departure emissions, can significantly contribute to ground-level UFP concentrations at appreciable distances from the airport.

Research Approach
An air pollution monitoring campaign was conducted at five sites located at varying distances from the airport and arrival/departure flight paths for Boston Logan Airport (Figure 7). Sites were selected through a systematic process, considering varying distances from the airport and laterally from each flight path and excluding locations close to major roadways or other significant sources of combustion. These sites were specifically chosen to isolate the contributions of in-flight aircraft, which is important for the flight activity source attribution task.

PNC (a proxy for UFP) monitoring instruments were established at each monitoring site in a preselected scheme to allow for multiple levels of comparison (e.g., sites beneath vs. not beneath flight paths given prevailing winds, sites at varying distances from the airport, sites at varying lateral distances beneath flight paths). The PNC was measured using TSI condensation particle counters (model 3783). In addition, BC was measured using AethLabs microaethalometers (model AE51), and meteorological data at each site were collected using Davis Vantage Pro2 weather stations.

Figure 7. Monitoring sites for the 2017–2018 sampling campaign around Boston Logan Airport. The site list corresponds to Table 3.

Milestone(s)

This task was placed on hold during FY2019 due to a delay in funding.

Major Accomplishments

Mobile monitoring tasks were placed on hold during FY2019 due to a delay in the release of FAA funding.

Publications

N/A

Outreach Efforts

N/A

Awards
None.

Student Involvement
None.

Plans for Next Period
Task(s) proposed over the next study period (10/1/19–9/30/20): no new tasks are currently planned.

Task 3 - Measure UFP and Other Air Pollutants at Sites Near Boston Logan International Airport, as Selected Under Task 2
Boston University School of Public Health

Objective(s)
Given the sites chosen under Task 2, we conducted a monitoring campaign in 2018 to inform an aviation source attribution analysis as an expansion of the Task 1 regression model development. Our instrumentation and protocol were similar to that of the 2017 monitoring campaign, but with some key enhancements to improve insights regarding aviation source contributions.

Research Approach
At the sites chosen under Task 2, we conducted a monitoring campaign in 2018 to inform ground contributions from in-flight aviation sources beneath multiple landing and take-off runways at various distances from the airport and flight path. The instrumentation and protocol used were the same as the 2017 monitoring campaign, but with some key enhancements to improve insights regarding aviation source contributions to NO/NO_2. The monitoring instruments included the TSI model 3783 water-based CPC for UFP, our primary measure of interest, which was used in the 2017 monitoring campaign. The 3783 model is intended for long-term deployment and can record 1-s average concentrations, which is a valuable time resolution for capturing short-term concentration spikes. Of note, because the model 3783 CPC is temperature-sensitive, we developed and deployed instrumentation in a temperature-conditioned space to protect against extreme heat and cold, allowing for long-term deployment.

In addition, the AethLabs model AE51 microaethalometer was used to measure BC. We also deployed the Alphasense NO/NO_2 sensor, which gives high-fidelity outputs and can be used in future studies with simultaneous real-time measurements at numerous sites. This approach provides an additional pollutant for future comparisons with atmospheric dispersion model outputs, which can help isolate factors that influence predictions of particulate matter vs. gas-phase pollutants. Local Davis Vantage Pro2 weather stations were used to capture real-time wind speed/direction and other meteorological parameters at each sampling site.

Similar to the 2017 campaign, obtaining flight activity data from the FAA for the sampling time periods is essential for future regression model development, which will include the location of each flight as well as basic aircraft characteristics, which can be linked using the AEDT to determine aircraft-specific attributes that may be predictive of emissions and corresponding concentrations.

Milestone(s)
- Obtained permission to resample and/or sample new locations and developed a sampling schedule
- Obtained new monitoring equipment and completed annual manufacturer cleaning and calibration of CPCs
- Implemented air pollution monitoring protocols, including measurements of meteorological parameters

Major Accomplishments
As described above, the air pollution field monitoring campaign was conducted from November 2017 to September 2019 at sites located at varying distances from the airport under multiple arrival and take-off flight paths into Logan Airport (Figure 7). The monitoring was stopped due to a funding delay, but site boxes have been maintained without monitors to allow for redeployment if new funding is obtained. All targets have been met for sample size and data capture, providing a strong foundation for future statistical analyses.

Table 3. Particle number concentration (PNC) distribution at five monitoring sites.

	UMASS	Chelsea	East Boston	South Boston	Winthrop
Sample Size (days)	264	250	167	123	43
Location	Ground Level	Roof 4th Floor	2nd Floor Window	Roof 5th Floor	Ground Level
Other Samplers	BC, meteorology, NO, NO2	BC, meteorology, NO, NO2	BC, NO, NO2	BC, meteorology, NO, NO2	BC, meteorology
0.1st percentile	169	863	172	471	521
1st percentile	379	1750	904	1160	676
5th percentile	975	3270	2020	2610	1400
50th percentile	7440	11900	10800	8260	8680
95th percentile	24500	43700	65000	36300	47000
99th percentile	47200	87800	124000	66300	70300
99.9th percentile	76900	152000	229000	100000	111000

The summary statistics presented in Table 3 cannot provide definitive insights regarding the aviation contributions to the measured PNC, but are helpful for hypothesis generation and for informing future modeling efforts. For example, Chelsea and East Boston have the highest concentrations for the 95th and 99th percentiles of the distribution, which is expected because these sites are closest to the airport and are affected by planes at a lower elevation compared with farther locations such as UMASS. This trend suggests that there may be a more rapid decline in PNC with increasing distance from the airport compared with that observed in the 2017 sampling campaign, which focused on only a single arrival pathway. Consistent seasonal patterns were observed at three monitor sites with data from winter, spring, and summer.

Table 4. Seasonal particle number concentration (PNC) distribution at three monitoring sites.

	UMASS			Chelsea			East Boston		
Sample Size (days)	80	79	93	64	75	105	20	85	54
Season	Winter	Spring	Summer	Winter	Spring	Summer	Winter	Spring	Summer
0.1st percentile	493	309	139	1460	1090	552	879	137	862
1st percentile	1040	496	262	2460	1660	1610	1260	564	1300
5th percentile	3250	1640	547	4350	3210	2950	3290	1810	2230
50th percentile	10100	5970	6390	14100	11200	11100	13800	10600	9920
95th percentile	28600	20200	22800	42200	42100	46000	60100	65400	66100
99th percentile	50500	44800	45300	79900	92200	90300	172000	127000	113000

The median PNC levels were consistently elevated during winter at all three sites, with greater variation at the 95th and 99th percentile. It should be noted that East Boston did not have the same number of sampling days over the winter season. As shown in Table 4, East Boston and Chelsea exhibit an elevated PNC at the median and 95th percentile compared with the UMASS sites across all seasons. Additionally, lower PNC levels were observed during the summer compared with the winter and spring across all three sites.

Table 5. Multi-year seasonal particle number concentration (PNC) distribution at UMASS long-term monitoring site.

	Summer 2017–18	Winter 2017–18	Spring 2018	Summer 2018	Fall 2018	Winter 2018–19	Spring 2019
Dates	6/1/18–8/31/18	12/1/17–2/28/18	3/1/18–5/31/18	6/1/18–8/31/18	9/1/218–11/30/18	12/1/18–2/28/19	3/1/19–5/30/19
Total Days	90	90	80	87	76	42	86
Number of Readings	7,537,890	7,654,161	6,160,559	6,446,895	5,871,405	3,515,138	6,609,864
0.1st percentile	500	1,000	700	300	600	1,200	800
1st percentile	1,300	2,300	1,000	500	1,400	2,000	2,100
5th percentile	2,400	7,200	3,400	1,100	2,800	5,100	3,700
50th percentile	7,500	22,900	14,300	10,100	15,900	22,400	14,700
95th percentile	28,000	55,000	49,000	33,000	53,000	57,000	52,000
99th percentile	58,000	93,000	91,000	67,000	100,000	102,000	96,000
99.9th percentile	110,000	132,000	132,000	140,000	145,000	14,800	144,000

Table 5 provides the PNC distribution by season, ranging from summer 2017 to spring 2019 at the UMASS (N2) monitoring site. Seasonal consistency is observed in the PNC distributions over these two years at the median and higher exposure percentiles. The lowest PNC levels were observed for summer at both the median and higher 95th and 99th percentiles compared with winter and spring.

Publications
N/A

Outreach Efforts
N/A

Awards
None.

Student Involvement
Bethany Haley, a doctoral student at BUSPH, has been involved with field monitoring of the 2018–19 sampling data, data cleaning, and calculations of descriptive statistics.

Plans for Next Period
Task(s) proposed over the next study period (10/1/18–9/30/19): no new tasks are planned during the NCE period.

Task 4 - Develop Platforms that Will Enable Comparisons Between Atmospheric Dispersion Models Implemented by Collaborators on ASCENT Project 19 and Monitored Pollutant Concentrations Obtained from Project 18

Boston University School of Public Health

Objective(s)

While the primary objective of Tasks 1–3 informed aviation source attribution using ambient pollution measurements, insights from the monitoring data and models can be combined with atmospheric dispersion models applied at the same location and dates. Within Project 19, UNC researchers are implementing SCICHEM to examine air quality impacts due to the emission of various air pollutants from aviation, with a current focus on UFP modeling. If Project 19 applies atmospheric dispersion modeling tools focused on locations near Boston Logan International Airport in the future, comparative analyses (modelling and monitoring) could be performed. The purpose of this task is to develop data processing systems that will enable these comparative analyses.

Research Approach

To aid the efforts of Project 19, we developed two output files under Task 4. First, the UFP measurements collected during the 2017 monitoring campaign were processed and provided in the format requested by Project 19. These measurements reflect contributions from both aviation and other sources and are being directly compared with all-source dispersion models such as SCICHEM. In the second phase, regression models are being developed under Task 1, an analogous database with aviation-attributable UFP concentrations has been processed, and outputs are being compared with dispersion model results.

Milestone(s)

The core milestones for Task 4 include the development of an analytical dataset estimating aviation source contributions from the 2017 monitoring campaign, which has been shared with UNC to inform potential collaborative manuscripts.

Major Accomplishments

UFP data from the Project 18 2017 field campaign were cleaned, combined with flight activity and meteorology information, and shared with Project 19. During this time, we collaborated through teleconferences on dispersion modeling efforts conducted by Project 19, resulting in an abstract that has been accepted to the CMAS conference on PNC modeling.

Publications

N/A

Outreach Efforts

Dr. Moniruzzaman Chowdury from Project 19 presented “An integrated modeled and measurement-based assessment of particle number concentrations from a major US airport” at the CMAS conference.

Awards

None.

Student Involvement

Chloe Seyoung Kim, a doctoral student at BUSPH, was involved in the preparation of data to be shared with Project 19 and in the comparison of regression model and dispersion model outputs. Dr. Chloe Kim graduated in December 2020 and is currently working for the Electric Power Research Institute as a research scientist.

Plans for Next Period

No new tasks are planned for this task during the no-cost extension period.

Project 019 Development of Aviation Air Quality Tools for Airshed-Specific Impact Assessment: Air Quality Modeling

University of North Carolina at Chapel Hill

Project Lead Investigator

Saravanan Arunachalam, Ph.D.
Research Professor
Institute for the Environment
University of North Carolina at Chapel Hill
100 Europa Drive, Suite 490
Chapel Hill, NC 27517
919-966-2126
sarav@email.unc.edu

University Participants

University of North Carolina at Chapel Hill

- PI: Saravanan Arunachalam, Research Professor and Deputy Director
- FAA Award Number: 13-C-AJFE-UNC Amendments 1-9
- Period of Performance: October 1, 2018 to September 30, 2019
- Tasks:
    1. Create Boston Logan airport emission inventories.
    2. Create a weather research forecast (WRF)-sparse matrix operator kernel emissions (SMOKE)-community multiscale air quality (CMAQ) modeling application.
    3. Perform a model-monitoring intercomparison at Logan airport.
    4. Develop a framework for a new dispersion model for aircraft sources.

Project Funding Level

$300,000 from the FAA. Matching cost-share was provided by the Los Angeles World Airports (LAWA).

Investigation Team

Prof. Saravanan Arunachalam (UNC) (Principal Investigator) [Tasks 1, 2, 3]
Dr. Chowdhury Moniruzzaman (UNC) (Co-Investigator) [Task 4]
Mr. Calvin Arter (UNC) (Graduate Research Assistant) [Tasks 1, 4]
Dr. Akula Venkatram (UC Riverside) (Consultant) [Task 4]

Project Overview

Aviation is predicted to grow steadily in upcoming years;[1] thus, a variety of aviation environmental policies will be required to meet emission reduction goals in aviation-related air quality and health impacts. Tools are needed to rapidly assess the implications of alternative policies for an evolving population and atmosphere. In the context of the International Civil Aviation Organization (ICAO)'s Committee on Aviation Environmental Protection (CAEP), additional approaches are required to determine the implications of global aviation emissions.

The overall objective of this project is to continue the development and implementation of tools, both domestically and internationally, to allow for an assessment of year-to-year changes in significant health outcomes. These tools must be acceptable to the FAA (in the context of Destination 2025) and/or other decision-makers. The developed methods must

[1] Boeing Commercial Airplane Market Analysis, 2010.

also rapidly provide output in order to support a variety of "what if" analyses and other investigations. While the tools for use within and outside the U.S. need not be identical, a number of goals are desirable for both cases:

- Enable the assessment of premature mortality and morbidity risks due to aviation-attributable particulate matter (PM) having diameter up to 2.5-μm ($PM_{2.5}$), ozone, and other pollutants known to exert significant health impacts;
- Capture airport-specific health impacts at regional and local scales;
- Account for the impact of landing/take-off (LTO) versus non-LTO emissions, including a separation of effects;
- Allow for an assessment of a wide range of aircraft emission scenarios, including differential growth rates and emission indices;
- Account for changes in non-aviation emissions
- Allow for assessments of sensitivity to meteorology;
- Provide domestic and global results;
- Include quantified uncertainties and differences with respect to Environmental Protection Agency (EPA) practices, which are to be minimized when scientifically appropriate;
- Be computationally efficient such that tools can be used in time-sensitive rapid turnaround contexts and for uncertainty quantification.

The overall scope of this work is being conducted at three collaborating universities: Boston University (BU), Massachusetts Institute of Technology (MIT), and the University of North Carolina (UNC) at Chapel Hill. The project is being performed as a coordinated effort with extensive interactions among the three institutions and will be described in reports on three separate projects (ASCENT 18, 19, and 20) by each collaborating university.

The components led by the UNC at Chapel Hill's Institute for the Environment (UNC-IE) include detailed modeling of air quality using the CMAQ model. UNC-IE is collaborating with BU to develop health risk estimates on a national scale using CMAQ outputs. UNC-IE is also collaborating with MIT to perform an intercomparison against nested Goddard Earth Observing System (GEOS)-Chem model applications within the U.S. and to further compare and contrast forward sensitivity and inverse sensitivity (such as adjoint) techniques for source attribution. This project builds on previous efforts within Project 16 of PARTNER, including detailed air quality modeling and analyses using CMAQ at various scales for multiple current and future scenarios as well as health risk projections that successfully characterize the influence of time-varying emissions, background concentrations, and population patterns on the public health impacts of aviation emissions under a national future emission scenario for 2025. Under Project 16, we initiated the development of a new state-of-the-art base year modeling platform for the U.S., using the latest model versions (CMAQ, WRF, SMOKE), emission datasets (Aviation Environmental Design Tool [AEDT], National Emissions Inventories [NEI]), and tools (Modern-Era Retrospective Analysis for Research and Applications [MERRA]-2-WRF, Community Atmospheric Model CAM-2-CMAQ) to downscale initial and boundary condition data from the general circulation models (GCMs) used in the Aviation Climate Change Research Initiative (ACCRI). We are continuing to adapt and refine the tools developed from this platform as part of the ongoing work in this phase of the project.

During this period of performance, the UNC-IE team was expected to perform research on multiple fronts, as described below. However, the FAA has requested that Tasks 1–3 be placed on hold because the collaborative project ASCENT-18 at BU did not receive funding from the FAA during FY2019. Thus, our report is limited to our progress on Task 4.

1. Create Boston Logan airport emission inventories.
2. Create a WRF-SMOKE-CMAQ modeling application.
3. Perform a model–monitoring intercomparison at Logan airport.
4. Develop a framework for a new dispersion model for aircraft sources.

Task 1 - Create Boston Logan Airport Emission Inventories

UNC at Chapel Hill

Objectives

Working with the ASCENT-18 team, identify and obtain (from the FAA) an appropriate aircraft activity data set (e.g., radar data from the Performance Data Analysis and Reporting System [PDARS]) that includes the aircraft type and engine type, along with aircraft space/time coordinates for the chosen modeling period. We will obtain and use the FAA's AEDT 2d to create an aircraft emission inventory for Boston Logan airport for 2017.

Research Approach
N/A

Milestone
This task was placed on hold during FY2019 due to a delay in funding.

Major Accomplishments
This task was placed on hold during FY2019 due to a delay in the release of FAA funding.

Publications
N/A

Outreach Efforts
N/A

Awards
None.

Student Involvement
Calvin Arter and Praful Dodda, current Ph.D. students, performed a review of the AEDT model and attended the AEDT training offered by the Volpe Center at Cambridge, MA.

Plans for Next Period
Start the task, if authorized by the FAA.

Task 2 - Create a WRF-SMOKE-CMAQ Modeling Application
UNC at Chapel Hill

Objectives
In this task, we will create a 12/4/1-km nested application of the WRF–SMOKE–CMAQ modeling system for two seasons (summer and winter) and will simulate two emission scenarios:

- Background emissions from all sources except the Boston Logan airport
- Background emissions and Boston Logan airport emissions during LTO cycles

Next, we will perform multiple sensitivity simulations with the CMAQ v5.2 base and CMAQ v5.2 augmented with the new nucleation mode described by Murphy et al. (2017). Specifically, this study includes a third mode, in addition to the Aitken and accumulation modes that have been used in all CMAQ applications to date.
The emission inventories for non-aviation sectors for this application will rely on the EPA's NEI for the year 2017 (if available) or on projections from the NEI-2014.
The meteorological fields will be downscaled from the National Aeronautics and Space Administration (NASA) MERRA v2 (Reinecker et al., 2011).
The base CMAQ model application will be configured as follows:

a) Aircraft emissions from AEDT processed by AEDTProc;
b) Background emissions from NEI processed by SMOKE v3.6;
c) Meteorology from MERRA downscaled with WRF v3.8;
d) Lightning NO_x;
e) Inline photolysis;
f) Latest version of CMAQ (v5.2), enhanced with the new aircraft-specific emission module described by Huang et al. (2017).

The initial and boundary conditions will be downscaled from a global model such as GEOS-Chem or the Model for Ozone and Related Chemical Tracers (MOZART).

Research Approach
N/A

Milestone
This task was placed on hold during FY2019 due to a delay in funding.

Major Accomplishments
This task was placed on hold during FY2019 due to a delay in the release of FAA funding.

Publications
N/A

Outreach Efforts
N/A

Awards
None.

Student Involvement
None.

Plans for Next Period
Start the task, if authorized by the FAA.

Task 3 - Perform a Model–Monitoring Intercomparison at Boston Logan Airport
UNC at Chapel Hill

Objectives
In this task, UNC will obtain 2017–2018 field observations from the ASCENT-18 team at BU and perform model–measurement comparisons. Thus far, BU has acquired measurements at five fixed-site locations on the arrival path of aircraft at Boston Logan airport. We will collaborate with BU on this task and compare regression and dispersion model-based assessments of ultrafine particles (UFPs) from Boston Logan airport.
As described above, this project is a collaborative effort with the ASCENT-18 investigators and will require a constant exchange of information and results throughout the period of performance. This task will lead to an integrated measurement- and modeling-based assessment of UFPs due to aircraft emissions at Boston Logan airport. In the final phase of this project, during the period of 2019–2020, we will upgrade the modeling application to use new fixed and mobile measurement platforms in the integrated assessment. Our intercomparison will rely on the methods described by Penn et al. (2015) and will be enhanced to use CMAQ-based predictions instead of the AMS/EPA Regulatory Model (AERMOD)-based approach used at the Los Angeles international airport (LAX).

Research Approach
N/A

Milestone
This task was placed on hold during FY2019 due to a delay in funding.

Major Accomplishments
This task was placed on hold during FY2019 due to a delay in the release of FAA funding.

Publications
N/A

Outreach Efforts
N/A

Awards
None.

Student Involvement
None.

Plans for Next Period
Start the task, if authorized by the FAA.

Task 4 - Develop a Framework for a New Dispersion Model for Aircraft Sources
UNC at Chapel Hill

Objectives

The FAA's AEDT is currently coupled with the U.S. EPA's AERMOD dispersion model for aircraft sources and is the required regulatory model in the U.S. for modeling airport-level aircraft operations during LTO cycles.
Recent studies have shown several limitations in the use of AERMOD for modeling aircraft sources. The Airport Modeling Advisory Committee (AMAC) developed a series of recommendations in 2011 to improve the modeling of jet exhaust. Subsequently, the Airport Cooperative Research Program (ACRP) project 02-08 developed guidelines for airport operators in conducting measurements and modeling air quality at airports, which were published in ACRP Report 70 (Kim et al., 2012). In this work, a measurement and modeling study was conducted at Washington Dulles international airport (IAD). More recently, ACRP project 02-58 developed a final report, ACRP Report 171 (Arunachalam et al., 2017), providing dispersion modeling guidance for airport operators with regard to local air quality and health. This study applied four dispersion models, i.e., AERMOD, CALPUFF, SCICHEM, and the U.K.'s Atmospheric Dispersion Modeling System (ADMS)-Airport, to LAX and compared model predictions with high-resolution measurements acquired during the Los Angeles Air Quality Source Apportionment Study (AQSAS). This study had some limitations, including a lack of secondary PM formation modeling and a lack of improved NO_x-to-NO_2 prediction models for aircraft sources. These three reports (AMAC, Kim et al, 2012 and Arunachalam et al, 2017) identified several limitations for AERMOD and presented a series of recommendations for improved dispersion modeling of aircraft emissions for airport-level air quality. Similar to other airport dispersion modeling tools such as AERMOD, the Lagrangian simulation of aerosol transport (LASAT) for airports (LASPORT), and ADMS, C-AIRPORT, a line-source-based dispersion model for aircraft sources based on the C-LINE modeling system (Barzyk et al., 2015), is currently being developed by UNC. This tool can potentially be used for airport modeling in the future.
As part of the proposed ASCENT research under Task 4, we propose the following subtasks:

- Subtask 4a: Perform a comprehensive review of the AEDT/AERMOD approach for modeling aircraft sources. This review will include current known applications of the AEDT/AERMOD modeling system, with a specific focus on how the emission inventories are built to capture aircraft activity and how AEDT/AERMOD treats aircraft sources during various modes of aircraft operation.
- Subtask 4b: Perform a comprehensive review of various approaches for modeling aircraft sources. These approaches will include, but are not limited to, various air quality models within and outside the U.S., including CALPUFF, SCICHEM, C-AIRPORT, ADMS-Airport, LASPORT, etc., and Gaussian, Lagrangian, or other hybrid approaches.
- Subtask 4c: Develop a comprehensive plan or modeling framework that addresses the limitations identified in the above tasks and propose the most suitable and viable approach for modeling pollutants from aircraft sources. The primary objective of this plan is to demonstrate that a robust, improved pollutant dispersion model for aircraft can be developed for U.S. regulatory compliance purposes. The proposed model shall model the dispersion of

pollutants from aircraft sources in a more technically and scientifically advanced manner (compared with current AERMOD capabilities), with the ultimate goal of becoming a potential U.S. regulatory compliance tool, based on future discussions between the FAA and EPA. This plan will include an itemized list of known limitations and a corresponding proposed developmental approach to address these limitations. We will then share the proposed plan with the FAA for the next phase of this task.

Research Approach

In this research, we plan to conduct a comprehensive review of dispersion models for airports and will then formulate a plan to develop an improved model that overcomes some of the shortcomings identified in the review discussed herein.

1. Introduction and Objectives

1.1 Approaches to dispersion modeling

Steady-state plume models are often applied beyond the appropriate range of applicability, with the justification that the concentration at the receptor is representative of the plume that eventually reaches the receptor. In principle, dispersion under unsteady and spatially varying conditions can be treated by puff or particle models, which attempt to model the dispersion of puffs or particles as an unsteady wind field carries them along their trajectories.

1.2 Aircraft emissions

Figure 1 shows an idealized movement pattern for aircraft at a typical airport, separated into four modes. These modes include the approach, taxiing (including idling), takeoff, and climb-out. The greatest potential impact on ground-level concentrations arises during taxiing and takeoff, when emissions occur close to the ground.

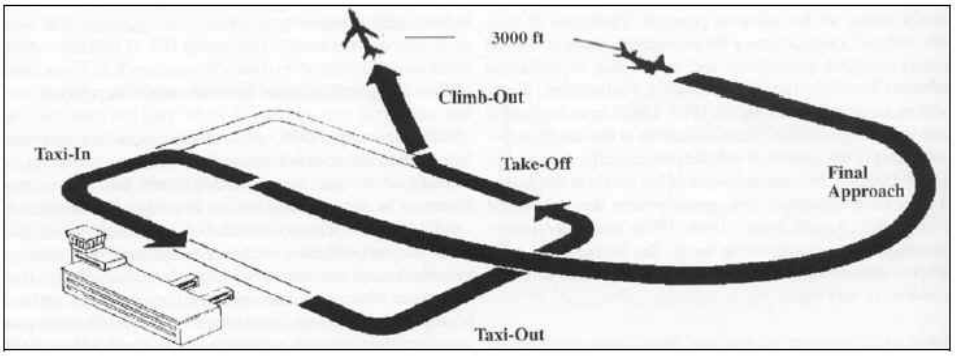

Figure 1. Aircraft modes at an airport (source: ICAO).

2 Literature Review of Dispersion Modeling Studies for Airports

A summary count of the different dispersion models applied in published papers, reports, and conference presentations focused on dispersion modeling for airport-level studies is shown in Figure 2. Dispersion modeling papers for airports, Air Force (AF) bases, and Navy bases have been compiled and reviewed, as shown in chronological order in Table A1 in Appendix A. Based on a review of simulations of pollutant dispersion at airports since the early 1970s utilizing different dispersion models, the most widely used model is found to be AERMOD (Cimorelli et al., 2004), as shown in in Figure 2 and Table A1 in Appendix A. The most widely studied airports are LAX and the London Heathrow (LHR) airport. The most widely simulated pollutant is NO_x, as shown in Table A1 in Appendix A. Several studies have shown that NO_x has been overpredicted at airports.

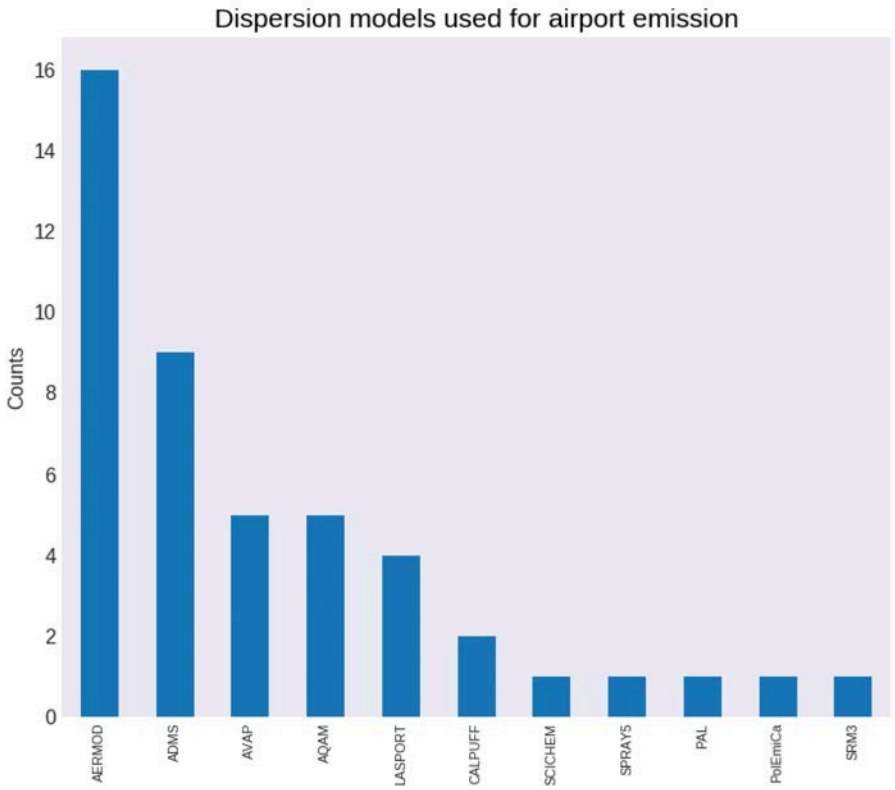

Figure 2. The frequency of papers and reports presenting dispersion modeling results of pollutant dispersion from airports since 1977.

3 Fundamentals of Micrometeorology

We developed a primer that presents the physics of atmospheric boundary layers, which is required to understand the transport and dispersion of pollutants associated with airport emissions. This primer is included in the draft report submitted to the FAA (Arunachalam et al., 2019a).

4 Source Characterization and Emission Model for Airport Dispersion Modeling

In this section, the characterization of aircraft emission sources is discussed for three recent, widely used emission models of airport dispersion (shown in Table A1 in Appendix A): AEDT (Ahearn et al., 2017), ADMS-Airport (CERC, 2017a), and LASPORT (Janicke et al., 2011).

4.1 Source characterization by the AEDT

The AEDT distributes each aircraft's segment emissions into the spatially fixed emission sources required by AERMOD through its built-in emission dispersion module (EDM). For each modeling hour, all flights whose segments cross a given rectangular AERMOD area source (spatially defined by the user for a given domain) are summed for that individual area source. The area sources, composed of all emissions from individual flight segments crossing each area, are used as hourly emission rates in the AERMOD dispersion model.

4.2 Source characterization by ADMS-Airport

A single ADMS-Airport run can simultaneously model a full range of explicit source types, including a single grid source containing up to 3,000 cells, 500 aircraft jet sources, 3,000 road sources, and 1,500 industrial point, line, area, and volume sources (CERC, 2017a). Accelerating jet sources for individual aircraft source are modeled to simulate the near-field plume rise. The jet source has the same aircraft speed, thrust, and emission rate of a moving aircraft following a line segment. An aircraft jet source in this line segment includes the aircraft speed at the start and end of the line segment, the emission rates in g/m^3-s, and the number of interpolation points.

4.3 Source characterization by LASPORT

LASPORT (Janicke et al., 2011) is a Lagrangian dispersion modeling system for airport emissions, with LASAT (LASAT, 2017) as the primary dispersion model. The aircraft emission treatment consists of aircraft traffic (LTO cycles), which is treated as a stationary line source (in "scenario calculations") and a moving line source (in "monitor calculations"), followed by auxiliary power units (APUs), ground power units (GPUs), ground support equipment (GSE), motor traffic (airside and landside), and other sources, which are treated as point, line, and volume sources. These sources are treated as a Lagrangian particle model, which calculates the trajectories of a representative sample of particles using stochastic processes, in contrast to the deterministic approach used by the other reviewed models. The characterized emissions from aircraft sources can be specified according to individual aircraft performance model calculations, designated as monitor calculations in LASPORT, or according to assumptions regarding general fleet makeup and movement, designated as scenario assessments.

5 Review of Dispersion Models Used in Airport Dispersion Modeling Studies

The major components of the 11 dispersion models used in airport dispersion modeling studies since 1970, shown in Figure 2 and listed in Table A2 in Appendix A, are described in the draft report (Arunachalam et al., 2019a) submitted to the FAA. These 11 models are listed below:

1) Airport Vicinity Air Pollution (AVAP) model (Wang et al., 1975),
2) Air Quality Assessment Model (AQAM) (Rote & Wangen, 1975; R. J. Yamartino et al., 1980),
3) Point, Area, and Line (PAL) model (Peterson, 1978),
4) AERMOD model (Cimorelli et al., 2018, 2004),
5) Atmospheric Dispersion Modeling System (ADMS) (Carruthers et al., 1994; CERC, 2016), the ADMS-Urban model (CERC, 2017b), a customized sub-version of the ADMS model, and the ADMS-Airport model (CERC, 2017a), a customized sub-version of the ADMS model for airport dispersion modeling,
6) LASPORT model (Janicke et al., 2011),
7) CALPUFF (California Puff) model (Scire et al., 2000),
8) SCICHEM (SCIPUFF with CHEMistry) model (Chowdhury et al., 2015; Knipping, 2019),
9) Pollution and Emission Calculation (PolEmiCa) model (Synylo & Zaporozhets, 2017; Zaporozhets & Synylo, 2019),
10) SRM3 model (InfoMil, 1998), and
11) SPRAY5 model (Tinarelli et al., 1994)

6 Dispersion Model for Airport Emissions

An airport is a small urban area with a wide range of source types and road and building configurations that can affect the dispersion of pollutants. In principle, any of the commonly used dispersion models, such as AERMOD, CALPUFF, SCICHEM, or ADMS, can be used to model the impact of most emission sources at an airport.

6.1 Modeling dispersion of LTO emissions

It is important to note that the major emission source at an airport, the aircraft, is a moving source that emits pollutants in short bursts during LTO operations. Dispersion from this transient source differs substantially from that associated with continuous sources, which have been well-characterized by field studies and modeling over the past 50 years. Plume dispersion parameters for continuous sources have also been characterized relatively well and have been incorporated in models such as AERMOD. In contrast, empirical knowledge on the dispersion of short releases is limited. Carslaw et al. (2006, 2008) demonstrated that hourly averaged NO_x concentrations at a position 180 m north of a northern runway showed little variation with wind speed at LHR, indicating the significant role of the jet plume buoyancy in governing ground-level concentrations.

6.2 Modeling key physical dispersion processes for airports

Airport dispersion models must account for the following: 1) the impact of structures, such as near-road sound barriers and buildings, on dispersion, 2) chemical reactions, and 3) non-buoyant airport sources near the ground under low wind speeds, which give rise to the highest concentrations. While most models reproduce non-buoyant behavior, they tend to overestimate concentrations under low wind speeds, especially under stable conditions (Arunachalam et al., 2017a).

7 Key Challenges in Dispersion Modeling for Airports

We identified several challenges that arise in modeling the dispersion of pollutants at an airport, as discussed below.

7.1 Source characterization

7.1.1 Area sources

Aircraft operation sources (idling, taxiing, take-off, climbing, and landing) are modeled as area sources in the AEDT/AERMOD. Modeling an aircraft source as an area source is advantageous because no stack parameter data are required for the AEDT

area segment; however, area source modeling for aircraft also has some disadvantages, particularly the plume rise and downwash, caused by building obstacles, cannot be modeled in the area source treatment in AERMOD.

7.1.2 Point sources

One of the greatest challenges in modeling an aircraft source as a point source is the assumption of stack parameters (stack diameter, stack temperature, and stack velocity). If aircraft emission sources can be modeled as point sources, some of the existing limitations, such as the plume rise and building downwash, for airport pollutant dispersion in the AERMOD area source model can be solved, as AERMOD has a plume rise and building downwash modeling option for point source modeling.

7.1.3 Line sources

Aircraft emission sources can be modeled as stationary or moving line sources in a dispersion model. The current AERMOD version has a line source option for onroad sources as a beta (non-regulatory) option. A recent study presented an aircraft emission model in which an individual aircraft is modeled as a line source based on multiple data sources, such as AEDT data, airport flight data, and ICAO engine emission data. Dispersion modeling using this line source model is currently in progress (Arunachalam et al., 2019b).

7.1.4 Jet sources

Aircraft emission sources can be well modeled as jet sources. Aircraft sources can be modeled in two ways: 1) stationary aircraft sources are modeled as an area, volume, line, or point source and 2) moving aircraft sources are modeled as a jet source by tracking an individual jet. The aircraft emission sources are modeled as jet sources in pollutant dispersion modeling for airports by the ADMS-Airport model (Carruthers, 2006; Carruthers et al., 2007; Elie et al., 2008; Sarrat et al., 2012) and PolEmiCa model (Synylo and Zaporozhets, 2017). Jet source modeling has been found to be particularly important for modeling take-off emissions (Elie et al., 2008). However, jet source modeling also has challenges, as high-time-resolution aircraft flight data, including flight trajectories, are required.

7.2 Plume rise

Modeling the plume rise from aircraft exhaust in a dispersion model has remained a challenge in airport dispersion modeling studies over the past four decades (Arunachalam et al., 2017; Daley & Naugle, 1979). In the AEDT modeling system, the primary challenge is associated with the typical assumption of an aircraft emission source as an area source. The plume rise can be easily modeled as either a point source or a jet source in the dispersion model. A detailed proposal for modeling the plume rise of aircraft emissions is given in the ACRP report (Arunachalam et al., 2017).

7.3 Downwash low-height emission source such as aircraft at the gate or terminal

At an airport, a wake vortex can occur around the tarmac, and the Plume RIse Model Enhancements (PRIME) algorithm (Schulman et al., 2000) for downwash in AERMOD may not be feasible, as the emission height for aircrafts at the surface is lower than the building height. The concentration at the wake vortex area near the building, created by the 2 L-shaped walls of the terminal building, may be higher than that at the non-vortex area of the terminal. For a point or area emission whose height is smaller than the building height, a new model may be required.

7.4 Number of air sources

The AEDT generates too many emission segments as individual emission sources as LTO path spans a long distance (>10 km). This higher number of emission sources (a significant fraction of which are in the atmosphere in the LTO path, which has little effect on the surface air quality) increases the computational cost of the Lagrangian SCICHEM model (Arunachalam et al., 2017), an open-source model and the only dispersion model that includes detailed gas-phase and aerosol chemistry.

7.5 Aircraft engine exhaust dynamics

Exhaust dynamics, such as high-speed exhaust during take-off, wing-tip vortices, and plume rises, can be better modeled if individual aircraft engines are modeled as point or jet sources. Because high-speed exhaust and wing-tip vortices arise for individual aircraft (or aircraft engines) and because individual aircraft engines can be easily modeled as a horizontal point source rather than an area or volume source, point source modeling of individual aircraft enables the modeling of these two dynamic exhaust phenomena. As the existing plume rise models, such as the PRIME algorithm (Schulman et al., 2000), are designed for point sources, treating individual aircraft engines as horizontal point sources will also be helpful for modeling plume rises.

8. Framework for an Airport Dispersion Model

The AEDT framework should allow for alternate treatment of sources and corresponding model formulations of governing processes, as in CMAQ (Byun & Schere, 2006). We present a brief summary of the desired framework here.

8.1 Dispersion and plume rise during the LTO cycle

A line thermal model, as shown in Figure 3, assumes a continuous release from an infinitely long line source along the runway, but can be readily adapted for a finite-length line puff whose length is approximately the length of the runway, using an approximation suggested by Venkatram and Horst (2006).

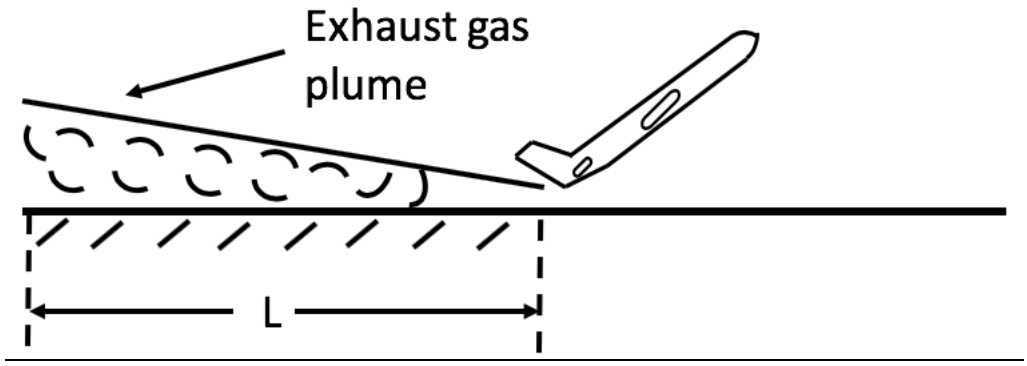

Figure 3. Exhaust gas plume created along the runway during take-off.

8.2 Building effects

The dimensions of the volume sources are governed by buildings adjacent to the sources, where the initial vertical spread corresponds to the building height. Schulte et al. (2015), Amini et al. (2016), and Heist et al. (2013) suggested methods for incorporating building effects in line source models. Omitting the building effects is likely to result in overestimated impacts of airport emissions close to the airport.

8.3 Modeling chemical transformation

NO_x emissions from aircraft and vehicles are converted into NO_2, which is a regulated pollutant. The AEDT framework should include options for different methods of treating NO_x. The new AEDT should also include options for treating the formation of secondary sulfate, nitrate, and organic aerosols from aircraft emissions. One option is a computationally efficient method that separates the transport and chemistry to model the formation of these aerosols, as described by Venkatram et al. (1998).

8.4 Accounting for shoreline meteorology in AERMET

Several of the largest airports in the U.S. are located on a coastline. AERMET, AERMOD's meteorological processor, is based on a one-dimensional boundary layer model that, in principle, cannot be applied to shorelines, where surface properties vary sharply across the water–land interface. Thus, AERMET need to be modified to account for the thermal internal boundary layer (TIBL) that develops during onshore flows, when cold stable air flows from water onto warmer land.

8.5 Effects of aircraft wing-induced flows

The pressure difference across an aircraft wind can drive flow from under the wing to above the wing at the tips, resulting in wing-tip vortices. These relatively long-lived structures can affect the dispersion of aircraft engine emissions. The wing also pushes the air downward to generate lift of the aircraft. In principle, this "downwash" can push emissions down, partially counteracting the effects of the plume rise, particularly when the aircraft is climbing. These effects needs to be incorporated in the proposed model.

8.6. Dispersion at low wind speeds

An evaluation of several dispersion models using data collected at LAX (Arunachalam et al, 2017) showed that the concentrations are overestimated when wind speeds are low. Furthermore, the highest concentrations occurred under light winds (1–2 m/s at 10 m) for both stable and unstable conditions, suggesting the need for better treatment of dispersion under low wind speeds.

9 Evaluation with Data from Field Studies

A diagnostic evaluation of the AEDT will require a new field study with the following elements:

1. Stationary monitors at several locations within an airport, including near runways, to measure the concentrations of relevant pollutants.
2. Mobile monitors to identify hotspots that might be missed by stationary monitors.
3. Stationary monitors downwind of the airport to collect the data required to evaluate model components that are sensitive to boundary layer variables rather than source characteristics.

4. Lidar measurements of exhaust plumes to evaluate model estimates of plumes that rise and spread along the runway during the takeoff roll.
5. Tracer release from an aircraft engine to evaluate the accuracy of the line source approximation. The release could be sampled by several monitors downwind of the runway.
6. Sonic anemometers at several locations to provide micrometeorological inputs for the dispersion model.
7. Sonic Detection and Ranging (Sodar) measurements to provide vertical profiles of horizontal velocity and turbulent velocity, which are needed to evaluate the model with respect to emission dispersion during climb-out in the boundary layer and downwind of the airport.
8. Details of aircraft types and activity during the field study to evaluate the emission model component of the AEDT.

Milestone

We submitted a draft of the framework to the FAA, and a revised version incorporating feedback from the FAA will be submitted.

Major Accomplishments

- Extensive literature review of both dispersion models and local air quality studies at airports across the world.
- Identification of limitations in existing models.
- Initial conceptual approach for modeling aircraft sources to assess local air quality at airports.

Publications

N/A

Outreach Efforts

Presentation at semi-annual ASCENT stakeholder meetings in the spring (Atlanta, GA) and fall of 2019 at Alexandria, VA. Presentation and collaborative discussion during monthly meetings with the ASCENT-18 team at BU.

Awards

None.

Student Involvement

Calvin Arter, a current graduate student, assisted in reviewing the characterization of aircraft sources for the AEDT and ADMS-Airport.

Plans for Next Period

Finalize the framework document for the FAA and begin developing the model.

References

ACI. (2010). Effects of Air Traffic on Air Quality in the Vicinity of European Airports. Airpt. Counc. Int. Eur. Environ. Strateg. Comm.

Ahearn, M., Boeker, E., Gorshkov, S., Hansen, A., Hwang, S., Koopmann, J., Malwitz, A., Noel, G., Reherman, C., Senzig, D., Solman, G.B., Tosa, Y., Wilson, A., Zubrow, A., Dipardo, J., Majeed, M., Bernal, J., Biederman, A., Dinges, E., Rickel, D., Yaworski, M. (2017). Aviation Environmental Design Tool (AEDT) Technical Manual, Version 2d. USDOT-FAA Report no: DOT-VNTSC-FAA-17-16.

Amini, S., Ahangar, F.E., Schulte, N., Venkatram, A. (2016). Using models to interpret the impact of roadside barriers on near-road air quality. Atmos. Environ. 138, 55–64. doi:10.1016/j.atmosenv.2016.05.001

Arunachalam, S., C. Arter, C. Moniruzzaman, and A. Venkatram. (2019a). Framework for Dispersion Model Development for Airport Sources, Draft Report prepared by the University of North Carolina at Chapel Hill for the Federal Aviation Administration, December 2019.

Arunachalam, S., Blanchard, C., Henry, R., Tombach, I. (2013). LAX Air Quality and Source Apportionment Study Volume 1. Executive Summary. Los Angeles World Airports, Environ. Serv. Div.

Arunachalam, S., Naess, B., Seppanen, C., Valencia, A., Brandmeyer, J.E., et al. (2019b). A new bottom-up emissions estimation approach for aircraft sources in support of air quality modelling for community-scale assessments around airports Akula Venkatram Jeffrey Weil Vlad Isakov and Timothy Barzyk. Int. J. Environ. Pollut. 65, 43–58. doi:10.1504/IJEP.2019.101832

Arunachalam, S., Valencia, A., Woody, M.C., Snyder, M.G., Huang, J., Weil, J., Soucacos, P., Webb, S. (2017). Dispersion Modeling Guidance for Airports Addressing Local Air Quality Health Concerns. ACRP Res. Rep. 179, Natl. Acad. Sci. Eng. Med. Transp. Res. Board Natl. Acad. Washington, D.C. doi:10.17226/24881

BAC. (2007). Aircraft Air Emissions D6, New Parallel Runway Draft EIS/MDP, Supplementary Report. Brisbane Airpt. Corp. Rep. Report no: ABN 54 076 870 650.

Barrett, S.R.H., Britter, R.E. (2008). Development of algorithms and approximations for rapid operational air quality modelling. Atmos. Environ. 42, 8105–8111. doi:10.1016/J.ATMOSENV.2008.06.020

Barrett, S.R.H., Britter, R.E. (2009). Algorithms and analytical solutions for rapidly approximating long-term dispersion from line and area sources. Atmos. Environ. 43, 3249–3258. doi:10.1016/j.atmosenv.2009.03.032

Byun, D., Schere, K.L. (2006). Review of the Governing Equations, Computational Algorithms, and Other Components of the Models-3 Community Multiscale Air Quality (CMAQ) Modeling System. Appl. Mech. Rev. 59, 51. doi:10.1115/1.2128636

Carr, E., Lee, M., Marin, K., Holder, C., Hoyer, M., Pedde, M., Cook, R., Touma, J. (2011). Development and evaluation of an air quality modeling approach to assess near-field impacts of lead emissions from piston-engine aircraft operating on leaded aviation gasoline. Atmos. Environ. 45, 5795–5804. doi:10.1016/J.ATMOSENV.2011.07.017

Carruthers, D. (2006). Intercomparison of five modelling methods p g including ADMS-Airport and EDMS for predicting air quality at London Heathrow predicting air quality at London Heathrow Airport presented by, in: AWMA Speciality Conference Guideline on Air Quality Models. Denver, USA.

Carruthers, D., Mchugh, C., Church, S., Jackson, M. (2008). ADMS-Airport : Model Inter-Comparisons and Model Validation, in: 12th International Conference on HarmonisationCERC within Atmospheric Dispersion Modelling for Regulatory Purposes 6th-9th October 2008, Cavtat, Croatia. Cavtat, Croatia.

Carruthers, D., Mchugh, C., Jackson, M., K, J. (2007). Developments in ADMS-Airport to Take Account of Near Field Dispersion and Applications to Heathrow Airport, in: Proceedings of the 11th International Conference on Harmonisation within Atmospheric Dispersion Modelling for Regulatory Purposes. Cambridge, UK, pp. 346–350.

Carruthers, D., Mchugh, C., Jackson, M., K, J. (2011). Developments in ADMS-Airport to take account of near field dispersion and applications to Heathrow Airport. Int. J. Environ. Pollut. 44, 332–341. doi:10.1504/IJEP.2011.038434

Carruthers, D.J., Holroyd, R.J., Hunt, J.C.R., Weng, W.S., Robins, A.G., Apsley, D.D., Thompson, D.J., Smith, F.B. (1994). UK-ADMS: A new approach to modelling dispersion in the earth's atmospheric boundary layer. J. Wind Eng. Ind. Aerodyn. 52, 139–153. doi:10.1016/0167-6105(94)90044-2

Carslaw, D.C., Beevers, S.D., Ropkins, K., Bell, M.C. (2006). Detecting and quantifying aircraft and other on-airport contributions to ambient nitrogen oxides in the vicinity of a large international airport. Atmos. Environ. 40, 5424–5434. doi:10.1016/j.atmosenv.2006.04.062

Carslaw, D.C., Ropkins, K., Laxen, D., Moorcroft, S., Marner, B., Williams, M.L. (2008). Near-field commercial aircraft contribution to nitrogen oxides by engine, aircraft type, and airline by individual plume sampling. Environ. Sci. Technol. 42, 1871–1876. doi:10.1021/es071926a

CERC. (2016). ADMS 5 Atmospheric Dispersion Modelling System User Guide. Cambridge, UK.

CERC. (2017a). ADMS-Airport, Airport Air Quality Management System. Cambridge, UK.

CERC. (2017b). ADMS-Urban, Urban Air Quality Management System. Cambridge, UK.

Chowdhury, B., Karamchandani, P.K., Sykes, R.I., Henn, D.S., Knipping, E. (2015). Reactive puff model SCICHEM: Model enhancements and performance studies. Atmos. Environ. 117, 242–258. doi:10.1016/j.atmosenv.2015.07.012

Cimorelli, A.J., Perry, S.G., Venkatram, A., Weil, J.C., Paine, R.J., Wilson, R.B., Lee, R.F., Peters, W.D., Brode, R.W., Paumier, J.O., Thurman, J. (2018). AERMOD Model Formulation and Evaluation. US EPA EPA Report: Epa-454/ R-18-003. doi:https://www3.epa.gov/ttn/scram/models/aermod/aermod_mfed.pdf

Cimorelli, A.J., Perry, S.G., Venkatram, A., Weil, J.C., Paine, R.J., Wilson, R.B., Peters, W.D., Brode, R.W. (2004). AERMOD: Description of Model Formulation.

Daley, P.S., Naugle, D.F. (1979). Measurement and Analysis of Airport Emissions. J. Air Pollut. Control Assoc. 29, 623. doi:10.1080/00022470.1979.10470763

Den, A. (2010). Final Results from EPA's Lead Modeling Study at the Santa Monica Airport.

DOIRD. (2015). Western Sydney Airport EIS-Local Air Quality and Greenhouse Gas Assesment. West. Sydney Airpt. Draft Environ. Impact Statement 4, Document Control No : AQU-NSW_001_9417B.

Duchene, N., Peeters, S. (2007). ALAQS-AERMOD Dispersion Modelling Verification.

Elie, A., Kervarc, R., Dubot, T., Bourrely, J. (2008). IESTA : a modular distributed simulation platform for the evaluation of air transport systems, in: MASCOT08-IMACS/ISGG Workshop. pp. 1–10.

Farias, F., ApSimon, H. (2006). Relative contributions from traffic and aircraft NOx emissions to exposure in West London. Environ. Model. Softw. 21, 477–485. doi:10.1016/J.ENVSOFT.2004.07.010

Fleuti, E., Hofman, P. (2005). Airport Local Air Quality Studies, ALAQS Case Study: Zurich Airport 2004, a comparison of modelled and measured air quality. EUROCONTROL Exp. Cent. EEC/SEE/20, Report no : EEC/SEE/2005/017.

Fleuti, E., Maraini, S. (2012). Air Quality Assessment Sensitivities, Zurich Airport Case Study. Zurich Airpt.

Heist, D., Isakov, V., Perry, S., Snyder, M., Venkatram, A., Hood, C., Stocker, J., Carruthers, D., Arunachalam, S., Owen, R.C. (2013). Estimating near-road pollutant dispersion: A model inter-comparison. Transp. Res. Part D Transp. Environ. 25. doi:10.1016/j.trd.2013.09.003

InfoMil. (1998). The New National Model (NNM): Model for the Dispersion of Air Pollutants from Sources at Short Distances. Rijkswaterstaat Environ. Minist. Infrastructure Water Manag. Netherl. TNO-Report R98/306.

Janicke, U., Fleuti, E., Fuller, I. (2011). LASPORT—A Model System for Airport-Related Source Systems Based on a Lagrangian Particle Model, in: Proceedings of the 11th International Conference on Harmonisation within Atmospheric Dispersion Modelling for Regulatory Purposes.

Keuken, M.P., Moerman, M., Zandveld, P., Henzing, J.S., Hoek, G. (2015). Total and size-resolved particle number and black carbon concentrations in urban areas near Schiphol airport (the Netherlands). Atmos. Environ. 104, 132–142. doi:10.1016/J.ATMOSENV.2015.01.015

Kim, B., Rachami, J., Robinson, D., Robinette, B., Wyle, K.N., Arunachalam, S., Davis, N., Baek, B.H., Shankar, U., Talgo, K., Yang, D., Hanna, A.F., Wayson, R.L., Noel, G., Gliff, S.S., Zhao, Y., Hopke, P.K., Kumar, P. (2012). Guidance for Quantifying the Contribution of Airport Emissions to Local Air Quality. ACRP Res. Rep. 71, Natl. Acad. Sci. Eng. Med. Transp. Res. Board Natl. Acad. Washington, D.C. doi:10.17226/22757

Knipping, E. (2019). SCICHEM Version 3.2, Technical Documentation. Electr. Power Res. Inst. (EPRI), Palo Alto, Ca Document no : 3002016526.

Kuzu, S.L. (2018). Estimation and dispersion modeling of landing and take-off (LTO) cycle emissions from Atatürk International Airport. Air Qual. Atmos. Heal. 11, 153–161. doi:10.1007/s11869-017-0525-5

LASAT. (2017). LASAT: A program system for the calculation of pollutant dispersion in the atmosphere. Janicke Consult. Environ. Phys.

Lee, G. (2012). Development of techniques for rapidly assessing the local air quality impacts of airports. MIT MS Thesis, Dep. Aeronaut. Astronaut.

McHugh, C., Williams, M., Price, C., Lad, C. (2007). Air Quality Studies for Heathrow: Base Case, Segregated Mode, Mixed Mode and Third Runway Scenarios modelled using ADMS-Airport. Dep. Transp. UK Report no : FM699/R23_Final/07.

Naugle, D.F., Grems, B.C., Daley, P.S. (1978). Air Quality Impact of Aircraft at Ten U.S. Air Force Bases. J. Air Pollut. Control Assoc. 28, 370–373. doi:10.1080/00022470.1978.10470613

Netzer, D.W. (1978). AQAM for Naval Air Operations, in: Sundararaman, N. (Ed.), Air Quality and Aviation, An International Conference. USDOT, FAA, Reston, Virginia, pp. 165 (Report no : FAA-EE-78-26).

Peace, H., Maughan, J., Owen, B., Raper, D. (2006). Identifying the contribution of different airport related sources to local urban air quality. Environ. Model. Softw. 21, 532–538. doi:10.1016/J.ENVSOFT.2004.07.014

Pecorari, E., Mantovani, A., Franceschini, C., Bassano, D., Palmeri, L., Rampazzo, G. (2016). Analysis of the effects of meteorology on aircraft exhaust dispersion and deposition using a Lagrangian particle model. Sci. Total Environ. 541, 839–856. doi:10.1016/J.SCITOTENV.2015.08.147

Penn, S.L., Arunachalam, S., Tripodis, Y., Heiger-Bernays, W., Levy, J.I. (2015). A comparison between monitoring and dispersion modeling approaches to assess the impact of aviation on concentrations of black carbon and nitrogen oxides at Los Angeles International Airport. Sci. Total Environ. 527–528, 47–55. doi:10.1016/J.SCITOTENV.2015.03.147

Peterson, W.B. (1978). User Guide for PAL, A Gaussian-Plume Algorithm for Point, Area and Line sources. US EPA Report no : EPA-600/4-78-013.

Rote, D.M., Wangen, L.E. (1975). A Generalized Air Quality Assesment Model for Air Force operations. US Air Force USAF Report : AFWL-TR-74-304; AD-A006807.

Sabatino, S. Di, Solazzo, E., Britter, R. (2011). The sustainable development of Heathrow Airport: model inter-comparison study. Int. J. Environ. Pollut. 44, 351. doi:10.1504/IJEP.2011.038436

Sarrat, C., Aubry, S., Chaboud, T. (2012). Modelling Air Traffic Impact on Local Air Quality With IESTA and ADMS-Airport : Validation Using Field Measurements on a Regional Airport, in: 28th International Congress of the Aeronautical Sciences. Brisbane, Australia.

Schewe, G.J., Budney, L.J., Jordan, B.C. (1978). CO Impact of General Aviation Aircraft, in: Sundararaman, N. (Ed.), Air Quality and Aviation, An International Conference. USDOT, FAA, Reston, Virginia, pp. 147 (Report no : FAA-EE-78-26).

Schulman, L.L., Strimaitis, D.G., Scire, J.S. (2000). Development and evaluation of the prime plume rise and building downwash model. J. Air Waste Manag. Assoc. 50, 378–390. doi:10.1080/10473289.2000.10464017

Schulte, N., Tan, S., Venkatram, A. (2015). The ratio of effective building height to street width governs dispersion of local vehicle emissions. Atmos. Environ. 112, 54–63. doi:10.1016/j.atmosenv.2015.03.061

Scire, J.S., Strimaitis, D.G., Yamartino, R.J. (2000). A User's Guide for the CALPUFF Dispersion Model, Version 5. Earth Tech, Inc 521.

Segal, H., Yamartino, R. (1981). The influence of aircraft operations on air quality at airports. J. Air Pollut. Control Assoc. 31, 846–850. doi:10.1080/00022470.1981.10465285

Shellar, E. (1978). Air Quality Characteristics at Dulles International Airport for 1976, 1980, 1985 and 1995, in: Sundararaman, N. (Ed.), Air Quality and Aviation, An International Conference. USDOT, FAA, Reston, Virginia, pp. 165 (Report no : FAA-EE-78–26).

Simonetti, I., Maltagliati, S., Manfrida, G. (2015). Air quality impact of a middle size airport within an urban context through EDMS simulation. Transp. Res. Part D Transp. Environ. 40, 144–154. doi:10.1016/J.TRD.2015.07.008

Smith, D.G., Yamartino, R.J., Benkley, C., Isaacs, R., Lee, J., Chang, D. (1977). Concorde air quality monitoring and analysis program at Dulles International Airport. US DOT, FAA U.S. DOT Report No. FAA-AEQ-77-14.

Steib, R., Labancz, K., Ferenczi, Z., Alföldy, B. (2008). Airport (Budapest Ferihegy – Hungary) air quality analysis using the EDMS modeling system. Part I. Model development and testing. Q. J. Hungarian Meteorol. Serv. 112, 99–112.

Synylo, K., Zaporozhets, O. (2017). PolEmiCa model for local air quality assessment in airports, in: 16th Annual CMAS Conference, Chapel Hill, NC, October 23-25, 2017. Chapel Hill, NC, pp. 1–6.

Tinarelli, G., Anfossi, D., Brusasca, G., Ferrero, E., Giostra, U., Morselli, M.G., Moussafir, J., Tampieri, F., F., T. (1994). Lagrangian particle simulation of tracer dispersion in the lee of a schematic two-dimensional hill. J. Appl. Meteorol. 33, 744–756.

Venkatram, A., Du, S., Hariharan, R., Carter, W., Goldstein, R. (1998). The concept of species age in photochemical modeling. Atmos. Environ. 32. doi:10.1016/S1352-2310(98)00032-6

Venkatram, A., Horst, T.W. (2006). Approximating dispersion from a finite line source. Atmos. Environ. 40. doi:10.1016/j.atmosenv.2005.12.014

Wang, I.T., Conley, L.A., Rote, D.M. (1975). Airport Vicinity Air Pollution Model User Guide. FAA, US DOT Report no: FAA-RD-75-230.

Wayson, R.L., Fleming, G.G., Garrity, N.E., Macdonald, J., Lau, M. (2003). Validation of FAA ' s Emissions and Dispersion Modeling System (EDMS): Carbon Monoxide Study, in: 96th Annual Meeting of the Air and Waste Management Association. San Diego, CA.

Yamartino, R. J., Conley, L.A., Rote, D.M. (1980). Analysis for the Accuracy Defination of the Air Quality Assesment Model (AQAM) at Williams Air Force Base, Arizona, V1. Technical Discussion. US Air Force USAF Report : ESL-TR-80-19.

Yamartino, R.J., Rote, D.M. (1978). Updated Model Assesment of Pollution at Major U.S. Airports, in: Sundararaman, N. (Ed.), Air Quality and Aviation, An International Conference. Reston, Virginia, pp. 170 (Report no : FAA-EE-78–26).

Yamartino, R.J., Rote, D.M. (1979). Updated Model Assessment of Pollution at Major U.S. Airports. J. Air Pollut. Control Assoc. 2, 128–132. doi:10.1080/00022470.1979.10470767

Yamartino, R J, Smith, D.G., Bremer, S.A., Heinold, D., Lamich, D., Tailor, B. (1980). Impact of Aircraft Emissions on Air Quality in the Vicinity of Airports. FAA, US DOT 0, Report no: FAA EE-80-098.

Zaporozhets, O., Synylo, K. (2019). Modeling of Air Pollution at Airports. Environ. Impact Aviat. Sustain. Solut. doi:http://dx.doi.org/10.5772/intechopen.84172

Zhou, Y., Levy, J.I. (2009. Between-airport heterogeneity in air toxics emissions associated with individual cancer risk thresholds and population risks. Environ. Heal. 8, 22. doi:10.1186/1476-069X-8-22

Appendix A

Table A1. Dispersion modeling studies on airport/aircraft emissions performed since 1977.

Year	Airport	Model	Emission Model	Meteorology	Species	Ref.
1977	Washington Dulles (IAD), USA	AVAP			CO, NO_2, THC	(Smith et al., 1977)
1978	Washington Dulles (IAD), USA	AQAM			CO	(Shellar, 1978)
1978	Van Nuys (VNY), USA	PAL			CO	(Schewe et al., 1978)
1978	Miramar Naval Air Station	AQAM			CO	(Netzer, 1978)
1978	10 USAF Bases	AQAM			CO, RHC, NO_2, TSP, SO_2	(Naugle et al., 1978)
1978	Los Angeles International (LAX), USA	AVAP			CO	(Yamartino and Rote, 1978)
1979	Los Angeles International (LAX), USA	AVAP			CO, THC, NO_x	(Yamartino and Rote, 1979)
1979	Nellis AF Base	AQAM			NO_x	(Daley and Naugle, 1979)
1980	William AF Base	AQAM			CO, NMHC, NO_x	(Yamartino et al., 1980)
1980	Los Angeles International (LAX), John F. Kennedy International (JFK), Chicago O'Hare International (ORD), USA	AVAP				(Yamartino et al., 1980)
1981	Los Angeles International (LAX), Chicago O'Hare International (ORD), John F. Kennedy International (JFK), USA	AVAP			CO, NO_x, THC	(Segal and Yamartino, 1981)
2003	Washington Dulles (IAD), USA	AERMOD-EDMS	EDMS		CO	(Wayson et al., 2003)
2005	Zurich (ZRH), Switzerland	LASPORT	LASPORT-LASAT		NO_2	(Fleuti and Hofman, 2005)

Year	Airport	Model	Emission Model	Meteorology	Species	Ref.
2006	Manchester (MAN), UK	ADMS-Urban	Manual, ICAO		NO_x	(Peace et al., 2006)
2006	London Heathrow (LHR), UK	ADMS-Urban	Manual, ICAO	U.K. Met Office	NO_x	(Farias and ApSimon, 2006)
2006	London Heathrow (LHR), UK	ADMS-Airport			NO_x, NO_2, O_3	(Carruthers, 2006)
2007	Zurich (ZRH), Switzerland	AERMOD, LASAT	ALAQS-AV	AIRMET	NO_x	(Duchene and Peeters, 2007)
2007	London Heathrow (LHR), UK	ADMS-Airport			NO_x, NO_2	(McHugh et al., 2007)
2007	London Heathrow (LHR), UK	ADMS-Airport	Arbitrary		NO_x, NO_2	(Carruthers et al., 2007)
2007	Brisbane (BNE), Australia	CALPUFF		CALMET	CO, NO_x (NO_2), SO_2, TSP, HC	(BAC, 2007)
2008	London Heathrow (LHR), UK	AERMOD			NO_x	(Barrett and Britter, 2008)
2008	Budapest (BUD), Hungary	AERMOD-EDMS	EDMS		NO_x, CO	(Steib et al., 2008)
2008	London Heathrow (LHR), UK, CAEPort (mock airport)	ADMS-Airport			NO_x	(Carruthers et al., 2008)
2009	32 U.S. airports	AERMOD	EDMS		Benzene, 1,3-butadiene, and benzo[a]pyrene (BaP)	(Zhou and Levy, 2009)
2009	London Heathrow (LHR), UK	AERMOD			NO_x	(Barrett and Britter, 2009)
2010	SMO), USA	AERMOD			Pb	(Den, 2010)
2010	Budapest (BUD) Hungary, Zurich (ZRH), Switzerland, Frankfurt (FRA) Germany	AERMOD, LASPORT	EDMS		NO_2, NO_x	(ACI, 2010)
2011	Santa Monica (SMO), USA	AERMOD			Pb	(Carr et al., 2011)
2011	London Heathrow (LHR), UK	ADMS-Airport	Arbitrary		NO_x, NO_2	(Carruthers et al., 2011)
2011	London Heathrow (LHR), UK	AERMOD	EDMS		NO_x, NO_2	(Sabatino et al., 2011)
2012	Pittsburgh International	AERMOD	Manual, ICAO		$PM_{2.5}$	(Lee, 2012)

Year	Airport	Model	Emission Model	Meteorology	Species	Ref.
	(PIT), Asheville Regional (AVL), USA					
2012	A regional French airport	ADMS-Airport	IESTA		NO_x	(Sarrat et al., 2012)
2012	Zurich (ZRH), Switzerland	LASPORT-LASAT			NO_2	(Fleuti and Maraini, 2012)
2012	Washington Dulles (IAD), USA	AERMOD	EDMS		CO, THC, NMHC, VOC, TOG, NO_x, SO_x, PM_{10}, $PM_{2.5}$, various HAP compounds	(Kim et al., 2012)
2013	Los Angeles International (LAX), USA	AERMOD	EDMS		CO, NO_x, $PM_{2.5}$, SO_2	(Arunachalam et al., 2013)
2015	Amsterdam Schiphol (AMS), Netherlands	SRM3		Stations	EC, PNC	(Keuken et al., 2015)
2015	Florence (FLR), Italy	AERMOD-EDMS	EDMS	Stations	CO, NO_x, SO_x, PM_{10}	(Simonetti et al., 2015)
2015	Los Angeles International (LAX), USA	AERMOD-EDMS	EDMS	Stations	EC, NO_x	(Penn et al., 2015)
2015	Western Sydney (SWZ), Australia	AERMOD-EDMS	EDMS		NO_2, $PM_{2.5}$, PM_{10}, CO, SO_2, benzene, toluene, xylene, formaldehyde	(DOIRD, 2015)
2016	Venice Marco Polo (VCE), Italy	SPRAY5	Manual, ICAO	SWIFT model	NO_x, CO, HC	(Pecorari et al., 2016)
2017	Los Angeles International (LAX), USA	AERMOD-EDMS, CALPUFF, SCICHEM, ADMS-Airport		AIRMET, NWS, CALMET, MMIF,	CO_2, H_2O, CO, VOC, NO_2, NO_x, SO_x, PM_{10}, $PM_{2.5}$	(Arunachalam et al., 2017)
2017	CAEPport (mock airport)	PolEmiCa			NO_x	(Synylo and Zaporozhets, 2017) CMAS
2018	Istanbul Ataturk (ISL), Turkey	AERMOD	Manual, ICAO	AIRMET	HC, CO, NO_x	(Kuzu, 2018)

Table A2. Major components of eight dispersion models used in airport dispersion modeling studies.

Model	AERMOD	ADMS-Airport	LASPORT	SCICHEM	CALPUFF	AQAM	AVAP	PolEmiCa
Reference	(Cimorelli et al., 2004)	(Carruthers et al., 1994; CERC, 2016)	(Janicke et al., 2011)	(Chowdhury et al., 2015)	(Scire et al., 2000)	(Rote and Wangen, 1975)	(Wang et al., 1975)	(Synylo and Zaporozhets, 2017; Zaporozhets and Synylo, 2019)
Sponsor	U.S. EPA	EA and HSE of U.K.	German Airport Association	EPRI	CARB	USAF	FAA	
Developed by	AERMIC	CERC, U.K.	Janicke Consulting	Ramboll	Sigma Research Corporation	ANL	ANL	NAU, Kyiv, Ukraine
Is designed for airports	No	Yes	Yes	No	No	Yes, for military bases and airports	Yes, for civil airports	Yes
Type	Gaussian plume	Gaussian plume	Lagrangian particle	Lagrangian puff	Lagrangian puff, non-steady-state puff	Gaussian plume	Gaussian plume	Gaussian plume
Components	Meteorology, emission, terrain, dispersion	Emission, GIS, dispersion	Dispersion	Meteorology, terrain, dispersion, GUI		Source inventory, short term, long term, and		Engine emissions, jet transport, dispersion

Model	AERMOD	ADMS-Airport	LASPORT	SCICHEM	CALPUFF	AQAM	AVAP	PolEmiCa
						meteorological data		
Is emission processor included	No	Yes	Yes	No	No	Yes	Yes	Yes
Emission source type	Point, area, volume	Road traffic, point, area, volume, grid, jet	Point, line, volume, area, grid	Point, area, volume	Point, line, area, volume	Point, area, line	Point, area, line	Jet
Chemistry	NO-NO_2 (OLM, PVMRM)	NO, NO_2, O_3, sulfate from SO_2	NO, NO_2	Detailed, cb05, cb06	Multi-species			
Plume rise	Yes	Yes	Yes	Yes	Yes	No		Yes
Moving jet model	No	Yes	Yes					Yes
Wake vortex surface effects	No	Yes						Yes
Effects of exhaust speed and exhaust dynamics		Yes	Yes					Yes
Downwash	Yes	Yes	Yes	Yes	Yes			
Wet and dry deposition	Yes	Yes	Yes	Yes	Yes			
Time step used	No	No	Yes	Yes, adaptive time				

Model	AERMOD	ADMS-Airport	LASPORT	SCICHEM	CALPUFF	AQAM	AVAP	PolEmiCa
				steps				
GUI soft visualization	No	Yes, ADMS mapper	Yes	Yes, SCIPUFgui				
Purpose for development	Dispersion for point, area, and volume source	Dispersion for airport	Dispersion for airport			Dispersion for military base and airport	Dispersion for civil airport	Exhaust dynamics
Proprietary	No, free	Yes	Yes	No, free	No, free	NA	NA	NA
Operating system	Windows, Linux	Windows	Windows, Linux for LASAT	Windows, Linux	Windows, Linux			NA
Computation time	Low	Medium		High	Low			

Project 020 Development of NAS-Wide and Global Rapid Aviation Air Quality Tools

Massachusetts Institute of Technology (MIT)

Project Lead Investigator

Professor Steven R.H. Barrett
Raymond L. Bisplinghoff Professor of Aeronautics and Astronautics
Department of Aeronautics & Astronautics
Massachusetts Institute of Technology
77 Massachusetts Ave.
Cambridge, MA 02139
(617) 452-2550
sbarrett@mit.edu

University Participants

Massachusetts Institute of Technology

- PI(s): Steven R. H. Barrett
- FAA Award Number: 13-C-AJFE-MIT, Amendment Nos. 007, 018, 025, 032, and 041
- Period of Performance: August 19, 2014, to August 31, 2020 (via no-cost extension)
- Tasks for current period (September 1, 2018, to August 31, 2020):
  No additional funding was provided for the project for this reporting period. The work therefore covers finalization of tasks from previous years only and was funded during the period September 1, 2018, to November 30, 2018:
  - Provide surface air quality analysis and quantify the effects of aviation on surface air quality
  - Continue work on development of nested domains and provide tool validation
  - Incorporate the nested domains into a single user-friendly framework
  - Support and assist the non-volatile particulate matter (nvPM) standard team on consistency checking of input data and interpreting results
  - Finalize and project uncertainty in ammonia emissions onto aviation impact sensitivities
  - Perform scoping of work for developing a multi-scale adjoint tool

Project Funding Level

$800,000 FAA funding + $50,000 Transport Canada funding = $850,000 total sponsored funds, of which only the FAA-funded portion requires matching funds. Sources of match are that same $50,000 Transport Canada funding (it constitutes both matching funds itself and sponsored funds that do not need to be matched), plus approximately $215,000 from MIT, and third-party in-kind contributions of $114,000 from Byogy Renewables Inc. and $421,000 from Oliver Wyman Group.

Investigation Team

- PI: Professor Steven Barrett, MIT: Tasks 1 and 2
- Co-PI: Dr. Raymond L. Speth, MIT: Task 2
- Co-investigator: Dr. Florian Allroggen, MIT: Task 2
- Research scientist: Dr. Sebastian Eastham, MIT: Tasks 1 and 2
- Postdoctoral associate: Dr. Irene Dedoussi, MIT: Tasks 1 and 2
- Graduate student: Guillaume Chossière, MIT: Task 1

Project Overview

The aim of this project is to develop tools that enable the rapid assessment of the health impacts of aviation emissions. The focus of the project is aviation-attributable particulate matter ≤2.5 μm ($PM_{2.5}$) and ozone on the National Airspace System

(NAS)-wide and global scales. These tools allow for rapid policy analysis and scenario comparison. The adjoint method on which these tools are based provides a computationally efficient way of calculating sensitivities of an objective function with respect to multiple model inputs. The project enhances existing tools in terms of the domains and impacts covered, and in terms of uncertainty quantification. The enhanced tools support the FAA in its strategic vision to reduce the health impacts of aviation emissions and allow for detailed and quantified policy analyses.

Project work for AY2018–2019 was covered under a no-cost extension. Therefore, the tasks that were listed for the previous period of performance (AY2017–2018) and that were worked on during the September 1, 2018, to November 30, 2018, period are reformulated as:

- Task 1: Continue work on the development of nested domains and provide tool validation.
- Task 2: Operationalize the rapid assessment tool for internal use by the FAA.

Task 1 - Nested Domains and Tool Validation

Massachusetts Institute of Technology

Objective(s)

The objective of this task is to continue to work on the development of nested domains and provide tool validation. This includes code development and testing to develop a high-resolution simulation for Europe. This task was completed during the previous period of performance with additional progress during the no-cost extension.

Research Approach

As documented in previous reports, the central tool for this project is the GEOS-Chem adjoint. This reporting period has been dedicated to applying the operationalized tools for quantification of the air quality impacts of aviation in two projects. The first, relevant to this task, was to quantify impacts of aviation in Asia and compare them to impacts from other, non-aviation sectors. Using tools developed under ASCENT 20, the impacts of landing and take-off emissions on Asian air quality in 2015 were quantified as part of a project to determine changes in sources of air quality-related mortality across Asia. This project separated impacts by country, sector, and year, isolating the effects of policy change in various Asian countries on air quality across the region.

Milestone

The task has been completed and a paper published.

Major Accomplishments

We found that aviation was responsible for <0.3% of all air quality-related impacts associated with regional emissions (see Table 1), which is less than half the total impacts from railroad emissions in 2015. This finding was published in Dasadhikari et al. (2019). This work also included validation of the capability of the GEOS-Chem nested tool to reproduce observed surface-level $PM_{2.5}$ concentrations (see Figure 1).

Table 1. Total regional deaths attributed to each sector in 2015; results are truncated to two significant figures.

Aviation	Agriculture	Energy	Fuel Processing	Industry	Residential	Rail Transport.	Road Transport.	Shipping
4,600	580,000	290,000	57,000	440,000	490,000	10,000	69,000	30,000

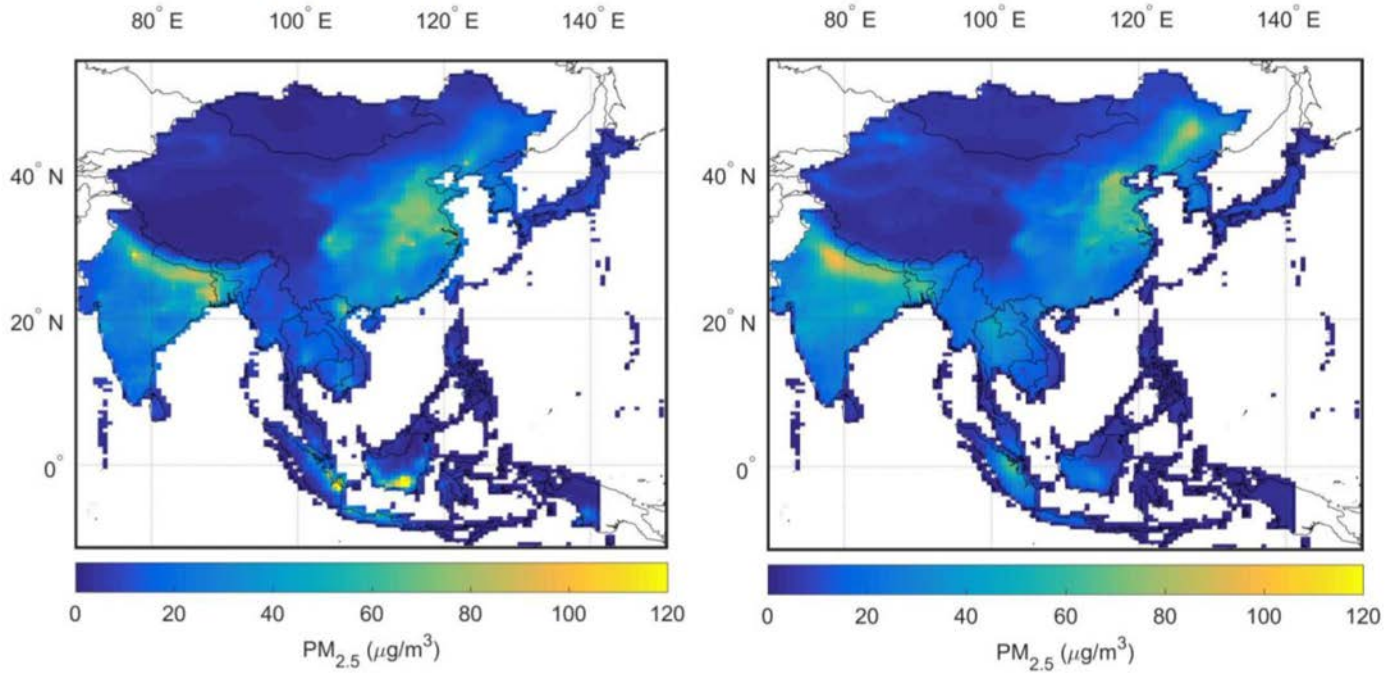

Figure 1. Simulated (left) versus "observed" (right) surface-level concentrations of particulate matter ≤2.5 μm ($PM_{2.5}$) in 2015; the observed values are from a machine learning–based reconstruction that incorporated MODIS satellite observation data.

Publications

Peer-reviewed journal publications:

Dasadhikari, K., Eastham, S. D., Allroggen, F., Speth, R. L., & Barrett, S. R. H. (2019). Evolution of sectoral emissions and contributions to mortality from particulate matter exposure in the Asia-Pacific region between 2010 and 2015. Atmospheric Environment, 116916.

Outreach Efforts

N/A

Student Involvement

Guillaume Chossière, then and currently a PhD candidate in the Department of Aeronautics and Astronautics at MIT, was involved in this study.

Plans for Next Period

This task is complete and no additional funding has been provided.

Task 2 - Operationalization of the Rapid Assessment Tool

Massachusetts Institute of Technology

Objective

The objective is to apply the tools developed under ASCENT 20 to quantify the surface air quality impacts of aviation. This task was completed during the no-cost extension.

Research Approach

The second subproject completed during the no-cost extension was to produce metrics of the marginal air quality costs of aviation. This provide a set of metrics which can be used directly to perform rapid policy assessment. Previous MIT research found that aviation emissions result in ~16,000 premature deaths annually due to impaired air quality (Eastham & Barrett, 2016; Yim et al., 2015). When aiming to reduce these impacts and those from climate change, decision makers often face trade-offs between different emission species or impacts in different times and locations. To inform rational decision-making, the sensitivity data computed for ASCENT 20 were applied to compute aviation's marginal air quality impacts per tonne of species emitted, while accounting for the altitude and chemical composition of the emissions. Uncertainty in chemistry transport modeling was incorporated using scaling factors based on prior literature. Uncertainty in climate, health impact, and economic factors was also quantified.

Milestone

The task has been completed and a paper published.

Major Accomplishments

We found that air quality impacts accounted for 64% of combined climate and air quality impacts, based on fuel burn in 2015, and that the majority of these impacts were associated with cruise-level NO_x emissions. A sensitivity study was conducted to find the contribution of each of the uncertain Monte Carlo input variables to the observed output variance. We found uncertainty in climate sensitivity and the DICE (Dynamic Integrated Climate-Economy model) damage function to be the largest drivers of total output uncertainty.

A detailed description of the research approach and results can be found in a paper which was published as a result of work under both ASCENT 20 and 21 (Grobler et al., 2019).

Publications

Peer-reviewed journal publications:

Grobler, C., Wolfe, P.J., Dasadhikari, K., Dedoussi, I.C., Allroggen, F., Speth, R.L., Eastham, S.D., Agarwal, A., Staples, M.D., Sabnis, J. & Barrett, S.R.H. (2019). Marginal climate and air quality costs of aviation emissions. Environmental Research Letters, 14 114031, https://doi.org/10.1088/1748-9326/ab4942

Outreach Efforts

Results were presented to the FAA.

Student Involvement

N/A

Plans for Next Period

This task is complete and no additional funding has been provided.

References

Eastham, S. D. & Barrett, S. R. H. (2016). Aviation-attributable ozone as a driver for changes in mortality related to air quality and skin cancer. Atmospheric Environment, doi:10.1016/j.atmosenv.2016.08.040.

Grobler, C., Wolfe, P. J., Dasadhikari, K., Dedoussi, I. C., Allroggen, F., Speth, R. L., Eastham, S. D., Agarwal, A., Staples, Sabnis, J., & Barrett, S. R. H. (2019). Marginal climate and air quality costs of aviation emissions. Environmental Research Letters, 14 114031, https://doi.org/10.1088/1748-9326/ab4942.

Yim, S. H. L., Lee, G. L., Lee, I. W., Allroggen, F., Ashok, A., Caiazzo, F., Eastham, S. D., Malina, R. & Barrett, S. R. H. (2015). Global, regional and local health impacts of civil aviation emissions. Environmental Research Letters, 10 034001.

Project 021 Improving Climate Policy Analysis Tools

Massachusetts Institute of Technology

Project Lead Investigator

PI: Steven R. H. Barrett
Raymond L. Bisplinghoff Professor of Aeronautics and Astronautics
Department of Aeronautics and Astronautics
Massachusetts Institute of Technology
77 Massachusetts Avenue, 33-316
Cambridge, MA 02139
+1 (617) 452-2550
sbarrett@mit.edu

Co-PI: Dr. Florian Allroggen
Research Scientist
Department of Aeronautics and Astronautics
Massachusetts Institute of Technology
77 Massachusetts Avenue, 33-115A
Cambridge, MA 02139
+1 (617) 715-4472
fallrogg@mit.edu

University Participants

Massachusetts Institute of Technology

- PI(s): Steven R. H. Barrett, Florian Allroggen (co-PI)
- FAA Award Number: 13-C-AJFE-MIT, Amendment Nos. 004, 017, 024, 037, and 042
- Period of Performance: August 1, 2014, to August 31, 2020 (via no-cost extension)
- Tasks for current period (September 1, 2018, to August 31, 2020):
  No additional funding was provided for the project for this reporting period. The tasks, therefore, cover finalization of tasks from previous years only and were funded during the period from September 1, 2018, to October 31, 2018:
  1. Conceptualize a version of Aviation environmental Portfolio Management Tool - Impacts Climate (APMT-IC) that regionalizes the climate physical impacts and computes the costs thereof
  2. Derive and publish marginal climate costs per unit of aviation emissions for rapid assessments of emissions interventions
  3. Support knowledge transfer

Project Funding Level

$600,000 in FAA funding and $600,000 in matching funds. Sources of match are approximately $162,000 from Massachusetts Institute of Technology (MIT), plus third-party, in-kind contributions of $114,000 from Byogy Renewables Inc. and $324,000 from Oliver Wyman Group.

Investigation Team

- Prof. Steven R. H. Barrett, PI, MIT (Tasks 1, 2, and 3)
- Dr. Florian Allroggen, co-PI, MIT (Tasks 1, 2, and 3)
- Dr. Raymond Speth, co-investigator, MIT (Tasks 1, 2, and 3)
- Dr. Mark Staples, co-investigator, MIT (Tasks 1, 2, and 3)
- Dr. Sebastian Eastham, MIT (Tasks 1, 2, and 3)
- Carla Grobler (PhD student), MIT (Tasks 1, 2, and 3)

Project Overview

The objective of ASCENT Project 21 is to facilitate continued development of climate policy analysis tools that will enable impact assessments for different policy scenarios at the global, zonal, and regional scales and will enable FAA to address its strategic vision on sustainable aviation growth. Following this overall objective, the particular objectives of ASCENT 21 are (1) to continue the development of a reduced-order climate model for policy analysis consistent with the latest scientific understanding; and (2) to support FAA analyses of national and global policies as they relate to long-term atmospheric and environmental impacts.

For the current reporting period, no additional funding was provided. The project team subsequently focused on finalizing tasks from previous years under a no-cost extension. These tasks included (1) conceptualizing how regional heterogeneous aviation growth can be captured more accurately in APMT-IC; (2) deriving and publishing marginal climate costs per unit of aviation emissions; and (3) facilitating knowledge transfer to the FAA Office of Environment and Energy (FAA-AEE) and other researchers.

Task 1 - Conceptualization of Regional Physical Impacts in APMT-IC

Massachusetts Institute of Technology

Objective(s)

The objective of this task is to conceptualize a potential approach for increasing the spatial resolution of estimating radiative forcing (RF) impacts associated with aviation emissions in APMT-IC. Because APMT-IC is currently set up as a global model, global emissions are used as inputs and globally averaged results are the main output. Although this approach leads to reliable results for current-year assessments, it potentially biases results for future scenarios that assume significantly changed aircraft technologies and/or traffic patterns. More specifically, biases due to changing traffic patterns can result from heterogeneities in atmospheric sensitivities. For example, NO_x emissions are estimated to result in 4 to 5 times more tropospheric ozone formation per unit of NO_x over the Pacific compared with a unit of NO_x emissions over Europe or North America (Gilmore et al., 2013).

In this reporting period, we built on the work completed during the previous reporting period, where we investigated the literature on regionalized emissions-to-impacts pathways. We identified two studies with potentially relevant results. First, Fuglestvedt et al. (2010) presented a review of regionalized physical impacts and found little agreement between the regionalized temperature responses. Second, Lund et al. (2017) analyzed regionalized global warming potential and regionalized temperature potential of aviation emissions. They found that global warming and global temperature potentials varied by a factor of 2 to 4 between different source regions.

During the current reporting period, the objective is to conceptualize a regionalized version of APMT-IC based on the research of Lund et al. (2017).

Research Approach

The current structure of APMT-IC is presented in Figure 1. As inputs, the model requires global fuel burn, CO_2 emissions, and NO_x emissions. Subsequently, global CO_2 radiative impacts are calculated by using impulse response functions and a radiative transfer function included in the Intergovernmental Panel on Climate Change (IPCC) 5th Assessment report (Myhre et al., 2013). The global radiative impacts of the short-lived climate forcers are calculated by scaling the radiative impacts from the aviation climate change research initiative (ACCRI) phase two report (Brasseur et al., 2016) to the global fuel burn of the emission scenario. RF is linked to temperature change through a two-box temperature model based on Berntsen and Fuglestvedt (2008). Finally, global temperature change is linked to damages using the Dynamic Integrated model of Climate and the Economy (DICE) damage function (Nordhaus, 2017).

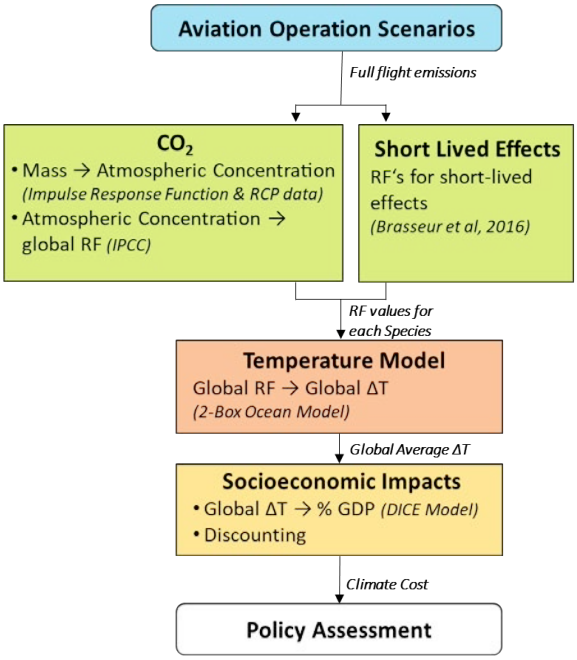

Figure 1. Outline of structure of current version of Aviation environmental Portfolio Management Tool - Impacts Climate (APMT-IC) for one Monte Carlo member. RF, radiative forcing; ΔT, temperature change; GDP, gross domestic product; DICE, Dynamic Integrated model of Climate and the Economy; RCP, representative concentration pathways,

In this task, potential changes to APMT-IC that enable capturing the impacts of regional heterogeneous growth are discussed. Because there is no evidence pointing toward regional heterogeneities of the RF impacts associated with CO_2 emissions, these changes are centered around the modeling of short-lived climate forcers. Changes are not proposed to the damage function. This is because previous work by the project team could not identify consensus on the reduced-order modeling of regionalized damages from regionalized temperature change (Nordhaus, 2017). Therefore, the proposed changes are constrained to linking regional emissions to global mean temperature change, which can subsequently be linked to global damages.

Milestone(s)

The literature study was completed during the previous reporting period, and the proposed concept was completed during this reporting period.

Major Accomplishments

During the current reporting period, the aim of this task of conceptualizing how the impact of different emissions regions can be accounted for in APMT-IC was completed. The proposed structural updates are presented in Figure 2. Most importantly, the proposed modeling structure will require APMT-IC to accept precursor emissions of short-lived forcers broken down by region, where the regions are defined according Lund et al. (2017). The specified local emissions will be linked to local RF in four latitude bands by scaling the local radiative impacts to the local emissions presented by Lund et al. (2017). In turn, these local RF values will be linked to temperature change using the temperature change function and the matrix of regionalized climate sensitivities presented in Lund et al. (2017). Finally, these local temperature changes are converted to a global mean temperature change using an area-weighted average. These steps will be taken individually for each short-lived forcer pathway. Uncertainty estimates for these parameters are presented in Lund et al. (2017) and will also be incorporated into the Monte Carlo simulation.

As a result of these changes, we expect a 17-fold increase in the number of Monte Carlo variables for each short-lived forcer. This will lead to increased run times and memory requirements. Furthermore, the current version of APMT-IC saves results from all Monte Carlo members as output, so further changes might be necessary to reduce the size of the output storage.

Another potential challenge is either a loss of backward compatibility between APMT-IC versions or significant additional implementation costs and loss of flexibility in the current implementation, which result from the fundamentally different architectures. Finally, we note a potential caveat to the proposed approach results from Lund et al. (2017), who calculated their results for year-2006 emissions patterns. The proposed model will subsequently not be capable of capturing the impact of any sub-regional-scale changes in emissions, such as changes in landing and take-off (LTO) and cruise emissions fractions.

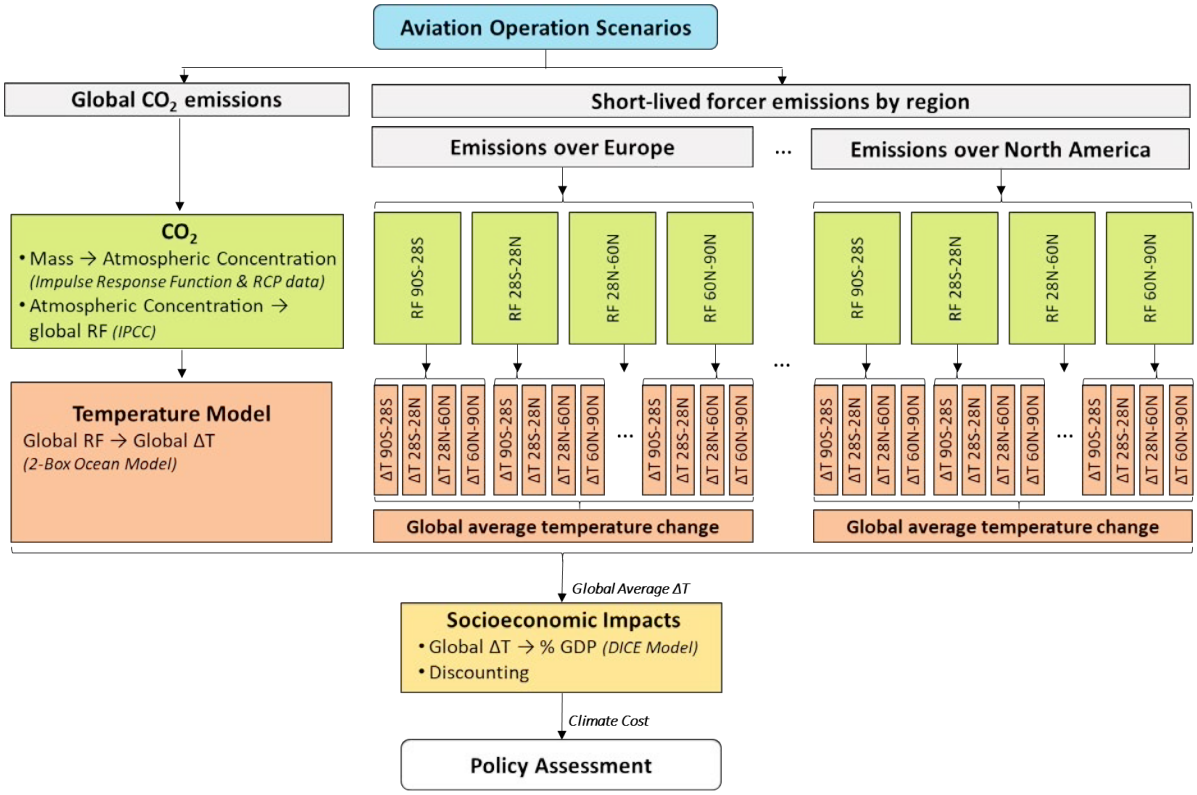

Figure 2. Conceptualization of structure for Aviation environmental Portfolio Management Tool - Impacts Climate (APMT-IC) using regionalized results from Lund et al. (2017) for one Monte Carlo member. RF, radiative forcing; ΔT, temperature change; GDP, gross domestic product; DICE, Dynamic Integrated model of Climate and the Economy.

Publications
N/A

Outreach Efforts
N/A

Student Involvement
The literature study and conceptualization of methods were prepared by Carla Grobler (PhD student, MIT).

Plans for Next Period
N/A

References
Berntsen, T.K. & Fuglestvedt, J.S. (2008). Global temperature responses to current emissions from the transport sectors. Proceedings of the National Academy of Sciences of the United States of America, 105 19154–9 Online: http://www.ncbi.nlm.nih.gov/pubmed/19047640

Brasseur, G.P., Gupta, M., Anderson, B.E., Balasubramanian, S., Barrett, S., Duda, D., Fleming, G., Forster, P.M., Fuglestvedt, J., Gettelman, A. & Halthore, R.N. (2016). Impact of aviation on climate: FAA's aviation climate change research initiative (ACCRI) phase ii. Bulletin of the American Meteorological Society, 97(4), pp.561-583

Fuglestvedt, J. S., Shine, K. P., Berntsen, T., Cook, J., Lee, D. S., Stenke, A., Waitz, I. A (2010). Transport impacts on atmosphere and climate: Metrics. Atmospheric Environment, 44(37), pp. 4648–4677. doi: 10.1016/j.atmosenv.2009.04.044

Gilmore, C.K., Barrett, S.R.H., Koo, J., & Wang, Q. (2013) Temporal and spatial variability in the aviation NO_x-related O_3 impact. Environmental Research Letters, 8 034027

Lund, M. T., Aamaas, B., Berntsen, T. K., Bock, L., Burkhardt, U., Fuglestvedt, J. S. and Shine, K. P. (2017). Emission metrics for quantifying regional climate impacts of aviation. Earth System Dynamics, 8(3), pp. 547–563. doi: 10.5194/esd-8-547-2017

Myhre, G., Shindell, D., Bréon, F., Collins, W., Fuglestvedt, J., Huang, J., Koch, D., Lamarque, J., Lee, D., Mendoza, B., Nakajima, T., Robock, A., Stephens, G., Takemura, T., Zhang, H. (2013). Anthropogenic and natural radiative forcing. Contribution of Working Group I Climate Change 2013: The Physical Science Basis. Contribution of Working Group I to the Fifth Assessment Report of the Intergovernmental Panel on Climate Change [Stocker, T.F., Qin, D., Plattner, G.K., Tignor, M., Allen, S.K., Boschung, J., Nauels, A., Xia, Y., Bex, V., & Midgley, P.M. (eds.). Cambridge, United Kingdom and New York, NY, USA: Cambridge University Press] https://www.ipcc.ch/pdf/assessment-report/ar5/wg1/WG1AR5_Chapter08_FINAL.pdf.

Nordhaus, W.D. (2017). Revisiting the social cost of carbon Proceedings of the National Academy of Sciences of the United States of America, 114 1518–23 http://www.pnas.org/lookup/doi/10.1073/pnas.1609244114

Task 2 - Derivation of Marginal Climate Costs Per Unit Aviation Emissions

Massachusetts Institute of Technology

Objective(s)

Aviation emissions have been found to cause 5% of global anthropogenic RF and ~16,000 premature deaths annually due to impaired air quality (Eastham & Barrett, 2016; Lee et al., 2009; Yim et al., 2015). When aiming to reduce these impacts, decision makers often face trade-offs between different emission species or impacts in different times and locations. To inform rational decision-making, the objective of this task is to compute aviation's marginal climate and air quality impacts per tonne of species emitted during different flight stages and by emission location. This task has been completed in collaboration with the ASCENT 20 project.

Research Approach

The research approach involves applying APMT-IC to calculate costs for full flight emissions by running APMT-IC for an emissions pulse in 2015. Impacts per unit of precursor emissions are derived by normalizing each of the short-lived forcers by its respective precursor emissions.

Full flight results are derived using the APMT-IC model, and LTO and cruise impacts are derived by modifying the LTO and cruise RF per unit of fuel burn. LTO RF results are based on the global warming potential values for ground emissions from the IPCC report (Myhre et al., 2013), whereas cruise radiative impacts are calculated as the difference between the ACCRI (Brasseur et al., 2016) full flight radiative impacts and the LTO results. Climate results are derived for discount rates ranging from 2% to 7%.

A detailed description of the research approach can be found in the publication (see below).

Milestone(s)

Results were derived as described above. The journal paper was prepared and submitted to *Environmental Research Letters*, where it was reviewed, accepted, and published (Grobler et al., 2019).

Major Accomplishments

Results were successfully derived using APMT-IC. Our results indicate that three components are responsible for 97% of climate and air quality damages per unit fuel burn, with individual contributions of NO_x at 58%, CO_2 at 25%, and contrails at 14%. Air quality impacts account for 64% of total impacts. A sensitivity study was conducted to find the contribution of each

of the uncertain Monte Carlo input variables to the observed output variance. We found uncertainty in the climate sensitivity and the DICE damage function to be the largest drivers in the output uncertainty. Furthermore, this work was submitted and published in *Environmental Research Letters*.

Publications

Peer-reviewed journal publications:

Grobler, C., Wolfe, P.J., Dasadhikari, K., Dedoussi, I.C., Allroggen, F., Speth, R.L., Eastham, S.D., Agarwal, A., Staples, M.D., Sabnis, J. & Barrett, S.R.H. (2019). Marginal climate and air quality costs of aviation emissions. Environmental Research Letters, 14 114031, https://doi.org/10.1088/1748-9326/ab4942

Outreach Efforts

A summary of the paper approach and results were presented to the FAA.

Student Involvement

The derivation of the climate metrics, validation, and paper drafting were completed by Carla Grobler (PhD student, MIT).

Plans for Next Period

N/A

References

Brasseur, G.P., Gupta, M., Anderson, B.E., Balasubramanian, S., Barrett, S., Duda, D., Fleming, G., Forster, P.M., Fuglestvedt, J., Gettelman, A. & Halthore, R.N. (2016). Impact of aviation on climate: FAA's aviation climate change research initiative (ACCRI) phase ii. Bulletin of the American Meteorological Society. 97(4), pp.561-583

Eastham, S.D. & Barrett, S.R.H. (2016). Aviation-attributable ozone as a driver for changes in mortality related to air quality and skin cancer. Atmospheric Environment. 144 17–23

Lee, D.S., Fahey, D.W., Forster, P.M., Newton, P.J., Wit, R.C.N., Lim, L.L., Owen, B., & Sausen, R. (2009). Aviation and global climate change in the 21st century. Atmospheric Environment, 43 3520–37, http://dx.doi.org/10.1016/j.atmosenv.2009.04.024

Myhre, G., Shindell, D., Bréon, F., Collins, W., Fuglestvedt, J., Huang, J., Koch, D., Lamarque, J., Lee, D., Mendoza, B., Nakajima, T., Robock, A., Stephens, G., Takemura, T., & Zhang, H. (2013). Anthropogenic and natural radiative forcing. Contribution of Working Group I Climate Change 2013: The Physical Science Basis. Contribution of Working Group I to the Fifth Assessment Report of the Intergovernmental Panel on Climate Change [Stocker, T.F., Qin, D., Plattner, G.K., Tignor, M., Allen, S.K., Boschung, J., Nauels, A., Xia, Y., Bex, V., & Midgley, P.M. (eds.). Cambridge, United Kingdom and New York, NY, USA: Cambridge University Press] https://www.ipcc.ch/pdf/assessment-report/ar5/wg1/WG1AR5_Chapter08_FINAL.pdf.

Yim, S.H.L., Lee, G.L., Lee, I.H., Allroggen, F., Ashok, A., Caiazzo, F., Eastham, S.D., Malina, R. & Barrett, S.R.H. (2015). Global, regional and local health impacts of civil aviation emissions. Environmental Research Letters, 10 034001

Task 3 - Support Knowledge Transfer

Massachusetts Institute of Technology

Objective(s)

The objective of this task is to support FAA analyses of national and global policies as they relate to long-term atmospheric impacts. APMT-IC version 24 builds upon the tool that was used to assess international aircraft and engine stringencies at Committee on Aviation Environmental Protection (CAEP) 8, 9, and 10. Under ASCENT 21 (together with its predecessor, PARTNER 46), the ASCENT 21 team was directly involved in the analysis of all three standards. A further objective of this task is to ensure results are made available to a wider audience.

Research Approach

During this reporting period, a publication was prepared and published in *Environmental Research Letters* (Grobler et al., 2019). This publication includes a model description of APMT-IC version 24b. The research was also summarized and presented to the FAA.

Milestone
Research results were published, and a summary of the publication was presented to the FAA.

Accomplishments
Knowledge transfer was supported through our reporting and communication activities.

Publications
Peer-reviewed journal publications:

Grobler, C., Wolfe, P.J., Dasadhikari, K., Dedoussi, I.C., Allroggen, F., Speth, R.L., Eastham, S.D., Agarwal, A., Staples, M.D., Sabnis, J. & Barrett, S.R.H. (2019). Marginal climate and air quality costs of aviation emissions. Environmental Research Letters, 14 114031, https://doi.org/10.1088/1748-9326/ab4942

Student Involvement
Carla Grobler (PhD student, MIT), who was responsible for updating APMT-IC to version 24 during the previous reporting period, co-authored the publication and compiled the summarized briefing of the publication presented to the FAA.

Plans for Next Period
N/A

Project 022 Evaluation of FAA Climate Tools: APMT

University of Illinois at Urbana-Champaign

Project Lead Investigator

Dr. Donald Wuebbles
Dept. of Atmospheric Sciences
University of Illinois
105 S. Gregory Street
Urbana, IL 61801
Tel: 217-244-1568
Fax: 217-244-4393
Email: wuebbles@illinois.edu

University Participants

University of Illinois at Urbana-Champaign
P.I.(s): Dr. Donald Wuebbles

- Period of Performance: October 16, 2017 to September 27, 2019
- Task(s):
    1. Evaluate version 24 of APMT
    2. Using the CESM global chemistry-climate model, update our earlier analyses of regional effects from aviation based on latitude bands and regions

Project Funding Level

This project did not receive funding from FAA during FY2019 and was operating under a no-cost extension.

Investigation Team

Dr. Donald Wuebbles: project oversight
Jun Zhang (graduate student): analyses of APMT and 3-D atmospheric climate-chemistry modeling analyses

Project Overview

The primary objective of this project was to evaluate the capabilities of the APMT-I model, particularly the Climate module, to ensure this FAA policy analysis tool uses the current state of climate science. Regional climate impacts of aviation were also evaluated using the 3D atmospheric climate-chemistry model. Findings from these studies were reported at several meetings and in special reports to the FAA.

Task 1- APMT-I Climate Evaluation and Review of Requirements Document

University of Illinois at Urbana-Champaign

Objective(s)

In this project, we act as a resource to FAA for analyses relating to metrics and to model development and evaluation of FAA modeling tools and datasets, with special emphasis on testing the Aviation Environmental Portfolio Tool (APMT) model and the further development and evaluation of its climate component to ensure that the underlying physics of the model is addressed properly. A specific focus of this project is on analyses of zonal and regional effects of aviation on climate and testing the resulting incorporation of such effects within APMT. As such, we want to make sure the APMT linking of aviation emissions with climate impacts and the representation of the various components of the cause-effect chain (i.e., from emissions to climate effect) properly represents the state-of-the-science.

Task 2- Three-dimensional Atmospheric Climate-Chemistry Modeling Studies for Aviation Regional Effects on Climate

University of Illinois at Urbana-Champaign

Objective(s)

The aim in this work was to have a better understanding of the climate impacts from aviation emissions on a zonal and regional basis. Since the aviation emissions have significant spatial variability in the sign and magnitude of response, the strength of regional effects is highly likely hidden due to the global averaging of climate change. Thus, it can be important to look at the impact of aviation emission on climate on a regional scale as well as on the global scale. We continue to use a state-of-the-art three-dimensional chemistry-climate model to further our understanding of the chemistry and climate effects from aviation emissions and to do our regional analysis and compare our results with the earlier findings. As part of this effort, we used CAM5-Chem and will now be using the new CAM6-Chem model, the atmospheric component of the Community Earth System Model (CESM). We plan to conduct a series of studies to evaluate aviation impact on climate both in 2006 and 2050. The ultimate goal of this project is to estimate the temperature change over specific regions of interest (e.g., the United States, Europe, and East Asia) resulting from aircraft emissions in 2006 and 2050.

Research Approach

These tasks were on hold during FY2019 due to delay in funding.

Milestone(s)

These tasks were on hold during FY2019 due to delay in funding.

Major Accomplishments

These tasks were on hold during FY2019 due to delay in release of FAA funding.

Publications

N/A

Outreach Efforts

N/A

Awards

N/A

Student Involvement

N/A

Plans for Next Period

- Complete evaluation of 2020 generation modeling capabilities and findings relative to the studies of SSTs done in the 2000 time period.
- Begin studies for new SST scenarios being developed for FAA.
- Evaluate APMT updates, as needed.
- For the regional analyses, reestablish where the project was two years ago when funding was suspended.

Project 023 Analytical Approach for Quantifying Noise from Advanced Operational Procedures

Massachusetts Institute of Technology

Project Lead Investigator

R. John Hansman
T. Wilson Professor of Aeronautics & Astronautics
Department of Aeronautics & Astronautics
Massachusetts Institute of Technology
Room 33-303
77 Massachusetts Ave
Cambridge, MA 02139
617-253-2271
rjhans@mit.edu

University Participants

Massachusetts Institute of Technology

- PI: R. John Hansman
- FAA Award Number: 13-C-AJFE-MIT, Amendment Nos. 008, 015, 022, 031, 046, and 051
- Period of Performance: October 28, 2014, to March 28, 2020
- Task(s):
    1. Evaluate the noise impacts of flight track concentration or dispersion associated with performance-based navigation (PBN) arrival and departure procedures
    2. Identify the key constraints and opportunities for procedure design and implementation of noise-minimizing advanced operational procedures
    3. Develop concepts for arrival and departure procedures that consider noise impacts in addition to operational feasibility constraints
    4. Analyze location-specific approach and departure design procedures in partnership with affected industry stakeholders

Project Funding Level

$860,000 in FAA funding and $860,000 matching funds. Sources of match are approximately $80,000 from Massachusetts Institute of Technology (MIT) and $780,000 from Massachusetts Port Authority (Massport).

Investigation Team

- Professor R. John Hansman (PI)
- Jacqueline Thomas (graduate student)
- Clement Li (graduate student)
- Sandro Salgueiro (graduate student)
- Rachel Price (graduate student)
- Annick Dewald (graduate student)
- Alison Yu (graduate student)

Project Overview

This project will evaluate the noise reduction potential from advanced operational procedures in the terminal (arrival and departure) phases of flight. The noise impact from these procedures is not well understood or modeled in current environmental analysis tools, presenting an opportunity for further research to facilitate air traffic management (ATM) system modernization. This project will leverage a noise analysis framework developed at MIT under ASCENT Project 23 to evaluate a variety of sample procedures. In conjunction, the project will contribute to the memorandum of understanding between the FAA and Massport to identify, analyze, and recommend procedure modifications at Boston Logan Airport.

Task 1 - Evaluate the Noise Impacts of Flight Track Concentration or Dispersion Associated with Performance-Based Navigation (PBN) Arrival and Departure Procedures

Massachusetts Institute of Technology

Objective(s)

This task evaluates the impact of flight track concentration arising from PBN procedure implementation and the potential noise mitigation impact of track dispersion. The effects of track concentration due to PBN procedure implementation have not been fully explored. Although the potential benefits of PBN for flight efficiency and predictability are well understood, the resulting environmental impact has caused increased community awareness and concern over the procedure design process. Current methods and noise metrics do not provide adequate information to inform policy decisions relating to noise concentration or dispersion due to PBN implementation.

In this task, models were used to evaluate noise concentration scenarios using a variety of metrics and procedure design techniques. Noise data from Massport were used to support the simulation effort. The impact of track dispersion was compared with potential community noise reduction through noise-optimal required navigation performance procedure designs that avoid noise-sensitive areas and use background noise masking where possible.

Research Approach

- Evaluate the impact of noise dispersion directly through modeling of a dispersed set of flight tracks in the Aviation Environmental Design Tool (AEDT)
- Analyze population exposure impact using multiple metrics, including day-night average sound level (DNL) and N_{above}
- Validate which metrics best capture the impacts of noise concentration and dispersion

Major Accomplishments

- Determined best metrics for analyzing noise impacts due to dispersion by evaluating which metrics best capture at least 80% of noise complaints from multiple airports and runways
- Completed dispersion modeling method for multiple flight tracks from a single centerline route
- Modeled and evaluated the impacts of dispersion for several departure and arrival scenario examples at Boston Logan Airport using the identified metrics that best captured noise complaints
- Determined the impacts of dispersion concepts recommended by communities after demonstration of initial dispersion concepts
- Refined modeling methods to more accurately model which aircraft realistically fly which tracks based on performance in dispersion simulations

Task 2 - Identify the Key Constraints and Opportunities for Procedure Design and Implementation of Noise-Minimizing Advanced Operational Procedures

Massachusetts Institute of Technology

Objective(s)

Arrival and departure procedure design is subject to physical, regulatory, and workload constraints. Procedures must be flyable by transport-category aircraft using normal, stabilized maneuvers and avionics. The procedures must comply with Terminal Instrument Procedures (TERPS) guidelines for obstacle clearance, climb gradients, and other limitations. The procedures must be chartable and work within the limitations of current flight management systems. Advanced operational procedures must also be compatible with airport and air traffic control operations, avoiding workload saturation for air traffic controllers and pilots.

This task involved evaluating the key constraints affecting advanced operational procedures and opportunities to improve noise performance, identifying those that may affect design and implementation. This process involved collaboration with pilots, air traffic controllers (ATC), procedure designers, and community members. The task also considered current research and evidence on physical, psychological, and social impacts of aircraft noise as well as emerging issues such as community perceptions of equity and the effect of overflight frequency on noise perception.

Research Approach

- Meet with key stakeholders in the implementation pathway to understand procedure development processes, timeline, and constraints
- Research documentation on regulations and operational standards influencing new flight procedure development
- Consult with stakeholders during candidate advanced operational procedure development to identify potential implementation obstacles

Major Accomplishments

- Met with airport operators and airline technical pilots to discuss potential concepts for advanced operational procedures
- Conducted follow-up meetings with ATC, Massport, FAA representatives, communities, and airline technical pilots to discuss initial procedure concepts
- When preparing for phase two of the project, used lessons learned from Block 1 FAA 7100.41 PBN meeting in Block 2 procedure design, incorporating feedback from airline procedure designers

Task 3 - Develop Concepts for Arrival and Departure Procedures that Consider Noise Impacts in Addition to Operational Feasibility Constraints

Massachusetts Institute of Technology

Objective(s)

This task applied the findings from Task 2 to identify a set of generic constraints and procedures for designing feasible and flyable advanced operational procedures to minimize noise perception as measured by traditional metrics (e.g., 65 dB DNL) and alternative metrics that address noise concentration concerns introduced by PBN procedures and emerging equity issues. Given an understanding of technology capabilities and operational constraints, in this task, we developed potential operational concepts and identified potential implementation pathways for both specific locations and generalizable operational concepts. Some of the approaches considered were

- Lateral track management approaches (e.g., dispersion, parallel offsets, equivalent lateral spacing operations, multiple transition points, vectoring, high background noise tracks, critical point avoidance tracks)
- Vertical/speed thrust approaches (e.g., thrust tailoring, steep approaches, delayed deceleration approaches)

In addition, procedures were identified and categorized for the noise reduction effort at Boston Logan Airport. These included “Block 1” procedures, which were characterized by clear predicted noise benefits, limited operational/technical barriers, and

a lack of equity issues, and "Block 2" procedures, which exhibited greater complexity due to potential operational and technical barriers, as well as equity issues (defined as noise redistribution between communities).

Research Approach

- Use feedback from Task 2 to identify procedures with noise reduction potential
- Model procedures using AEDT and the Aircraft Noise Prediction Program (ANOPP) for generic runways to evaluate noise impacts for candidate procedures on a single-event or integrated basis
- Determine noise impacts based on multiple metrics that are location-agnostic (i.e., contour area) as well as location-specific (i.e., population exposure at specific runways)

Major Accomplishments

- Developed a set of generic approach and departure modifications using PBN and other techniques to take advantage of noise benefits from advanced procedures
- Identified key constraints for lateral, vertical, and speed profile redesign based on ATC operational guidelines and FAA procedure design criteria
- Modeled and showed the impacts of candidate vertical/speed thrust approaches that were within FAA procedure design criteria
- Identified and made recommendations for Block 1 procedures for assessment by the FAA for implementation at Boston Logan Airport
- Identified candidate Block 2 procedures for noise reduction at Boston Logan Airport

Task 4 - Analyze Location-Specific Approach and Departure Design Procedures in Partnership with Affected Industry Stakeholders

Massachusetts Institute of Technology

Objective(s)

Advanced operational procedures may be particularly applicable for specific airports based on local geography, population density, operational characteristics, fleet mix, and local support for procedure modernization (among other factors). Specific procedures will be evaluated at a series of representative airports around the United States. It is anticipated that this task will involve collaboration with multiple airports and air carriers on potential opportunities at locations that would benefit from advanced PBN procedures.

For the Boston Logan Airport noise reduction project, this task also involves collaboration with the FAA 7100.41 PBN working group, which is the initial operation evaluation group for new procedure design concepts.

Research Approach

- Coordinate with a specific airport operator to evaluate procedure design opportunities with noise reduction potential
- Work closely and communicate with affected stakeholders throughout the procedure evaluation, design, and analysis process to ensure that key constraints and objectives are appropriate for the selected location on a procedure-by-procedure basis

Major Accomplishments

- Continued regular meetings and collaboration with Massport to finalize Block 1 procedure recommendations and to develop Block 2 arrival and departure procedures for analysis at Boston Logan Airport
- Performed detailed noise analysis for Block 1 and preliminary Block 2 arrival and departure procedure concepts that addressed community concerns, including population impact estimation based on 2010 census data and regridding methodology developed for this research
- Assisted with community outreach meetings about noise in the Boston area
- Presented at and collaborated with stakeholders during the FAA 7100.41 PBN working group meeting for evaluation of the Block 1 procedure concepts at Boston Logan Airport
- Reconsidered select Block 1 procedures not accepted by FAA 7100.41 PBN working group and revised proposed procedures based on feedback to be recommended in Block 2

- Modeled noise impacts of Block 1 procedures re-recommended for Block 2

Publications

- "Block 1 Procedure Recommendations for Logan Airport Community Noise Reduction," 2017. Link: http://hdl.handle.net/1721.1/114038
- Thomas, J; Hansman, J. "Framework for Analyzing Aircraft Community Noise Impacts of Advanced Operational Flight Procedures," *Journal of Aircraft*, Volume 6, Issue 4, 2019. https://doi.org/10.2514/1.C035100
- Thomas, J., Yu, A., Li, C., Toscano, P., and Hansman, R.J. "Advanced Operational Procedure Design Concepts for Noise Abatement" *In Thirteenth USA/Europe Air Traffic Management Research and Development Seminar*, Vienna, 2019.
- Yu, A., and Hansman, R.J. "Approach for Representing the Aircraft Noise Impacts of Concentrated Flight Tracks" *AIAA Aviation Forum 2019*, Dallas Texas, 2019.

Outreach Efforts

- September 27, 2017: Poster to ASCENT Advisory Board
- December 5, 2017: Call with Boeing to discuss procedure noise impact validity
- March 16, 2018: Discussion with Minneapolis-St. Paul (MSP) Airport about metrics
- April 4, 2018: Poster to ASCENT Advisory Board
- May 7, 2018: Presentation to FAA 7100.41 PBN Working Group
- June 24, 2018: Discussion with air traffic controllers about dispersion concepts
- July 23, 2018: Briefing to FAA Joint University Program research update meeting
- October 9, 2018: Poster to ASCENT Advisory Board
- November 8, 2018: Presentation to Airline Industry Consortium
- March 3, 2019: Presentation to the Aviation Noise and Emissions Symposium
- October 15, 2019: Presentation to the ASCENT Advisory Board
- November 12, 2019: Presentation to Airline Industry Consortium
- Numerous community meetings
- Numerous briefings to politicians representing eastern Massachusetts (local, state, and federal)
- Briefing to FAA Management Advisory Council
- In-person outreach and collaboration with Massport, operator of Boston Logan Airport and ASCENT Advisory Board member

Awards

2018 Dept of Transportation/FAA COE Outstanding Student of the Year Award to Jacqueline Thomas

Student Involvement

Graduate students have been involved in all aspects of this research in terms of analysis, documentation, and presentation.

Plans for Next Period

The next phase of this project will involve continued outreach to stakeholders affected by implementation of advanced operational procedures, including airlines, airports, ATC, the FAA, and communities. The next phase will include finalization of Block 2 procedures for recommendation. Operational challenges of specific noise reduction procedures, such as the delayed deceleration approach and dispersion concepts, will be identified. This procedure evaluation process is expected to inform recommendations to airport operators, airlines, and the FAA to develop noise-mitigating advanced operational procedures at specified locations in the National Airspace System.

Project 025 Shock Tube Studies of the Kinetics of Jet Fuels

Stanford University

Project Lead Investigator

Ronald K. Hanson
Woodard Professor
Mechanical Engineering Department
Stanford University
452 Escondido Mall
650-723-6850
rkhanson@stanford.edu

University Participants

Stanford University

- PI(s): Prof. Ronald K. Hanson
- FAA Award Number: 13-C-AJFE-SU-017
- Period of Performance: October 1, 2018, to September 30, 2019
- Task(s):
    1. Area #1: Chemical kinetics combustion experiments

Project Funding Level

$110,000 from FAA with 1:1 matching funding of $110,000 from Stanford University.

Investigation Team

- Prof. Ronald K Hanson, principal investigator, research direction
- Dr. David F Davidson, senior research engineer, research management
- Jiankun Shao, graduate student, research assistant
- Yu Wang, graduate student, research assistant
- Nicolas Pinkowski, graduate student, research assistant
- Alison Ferris, graduate student, research assistant

Project Overview

The fifth year of this program aims to continue building a fundamental kinetics database to describe the combustion behavior of modern jet fuels. To this end, the program focused on two project areas: shock tube/laser absorption kinetics measurements to characterize Shell IH2 fuels (now referred to as Shell CPK-0), and the correlation of chemical and physical fuel properties with infrared (IR) spectral features. The results will be used to provide unique input constraints for the development of hybrid-chemistry (HyChem) models and to reveal the sensitivity of combustion properties to fuel composition, with the ultimate goal of simplifying the alternative fuel certification process.

Task 1 - Chemical Kinetics Combustion Experiments

Stanford University

Objective(s)

This work aims to use shock tube/laser absorption experiments to characterize Shell IH2 fuel and extend the fundamental kinetics database built over the past four years; shock tube measurements include ignition delay time (IDT) measurements

under conditions comparable to those used to characterize previous FAA fuels and species time-history measurements during fuel pyrolysis. A second area of research is the development of fuel prescreening tools, based on IR absorption ratio measurements of jet fuels. Finally, this multi-year research program aims to culminate in the completion of American Institute of Aeronautics and Astronautics (AIAA) book chapters describing the research progress of the past four years.

IDT and species time-history measurements conducted in shock tubes provide valuable fundamental kinetics data for FAA fuels. These data are a critical input for Area #2, which seeks to develop a new hybrid and detailed kinetics model for jet fuels (HyChem). The data provided will also ensure that the combustion models developed in Area #4 (combustion model development and validation) to model the extinction and ignition processes controlling lean blowout, cold ignition, and high altitude relight are chemically accurate.

Research Approach

The development, refinement, and validation of detailed reaction mechanisms describing the pyrolysis and oxidation of fuels require experimental data as targets for kinetics models. Experimentally, the best way to provide these targets at high temperatures and pressures is with shock tube/laser absorption experiments, conducted over a wide range of pressures, temperatures, and fuel and oxidizer compositions.

Reflected shock wave experiments provide a test environment that does not introduce additional fluid mechanics, turbulence, or heat transfer effects to the target phenomena. This allows isolation of the target phenomena (IDTs and species concentration time-histories) in a quiescent high-temperature, high-pressure environment that is very well characterized and hence amenable to modeling. Recent work in our laboratory to develop the constrained reaction volume (CRV) methodology provides an additional tool to provide shock tube data under constant-pressure constraints when needed, to significantly simplify the gasdynamic/thermodynamic models needed to properly simulate reactive reflected shock wave data.

The strength in the Stanford shock tube approach comes with the implementation of laser diagnostics that enable the simultaneous measurement of species time-histories. Using laser absorption, we are able to provide quantitative time-histories during fuel pyrolysis and oxidation of the fuel, including transient radicals (e.g., OH, CH_3), stable intermediates (e.g., CH_4, C_2H_4, isobutene, CH_2O, and aromatics), combustion products (including CO, CO_2, and H_2O), and temperature. Furthermore, measurements of the pyrolysis and oxidation systems of real fuels, rather than of surrogates or solvent surrogates, provide a direct link to actual fuel behavior.

An important goal of the current research is to investigate the possibility of characterizing jet fuel composition and combustion behavior based on the fuel's IR absorption (Fourier transform IR, FTIR) spectrum. As the shock tube/spectroscopic research has progressed under FAA support, a large database of kinetic and spectroscopic measurements for a variety of jet fuels has been acquired. Using this database, we have developed correlations between the spectroscopic properties of neat jet fuel with fuel composition and with important combustion parameters such as derived cetane number (DCN), lean blowout, and C_2H_4 pyrolysis yields.

Shock tube experiments: methods and results

Stanford has one of the largest and best-equipped shock tube laboratories in the United States, perhaps in the world, with five shock tubes: three large-diameter [12, 14, and 15 cm internal diameter (I.D.)] high-purity shock tubes; one heated, large-diameter, high-purity shock tube (14 cm I.D., see Figure 1a); and one heated high-pressure shock tube (5 cm I.D., capable of achieving >500 atm). Additionally, we have unique capability for species measurements using laser absorption diagnostics (see Figure 1b) developed over the past 30 years. In these experiments, temperatures from <500 to >3000 K, and pressures from sub-atmospheric (0.2 atm) to >500 atm can be achieved in different carrier gases, such as argon or air, with demonstrated test times up to and exceeding 50 ms at low temperatures.

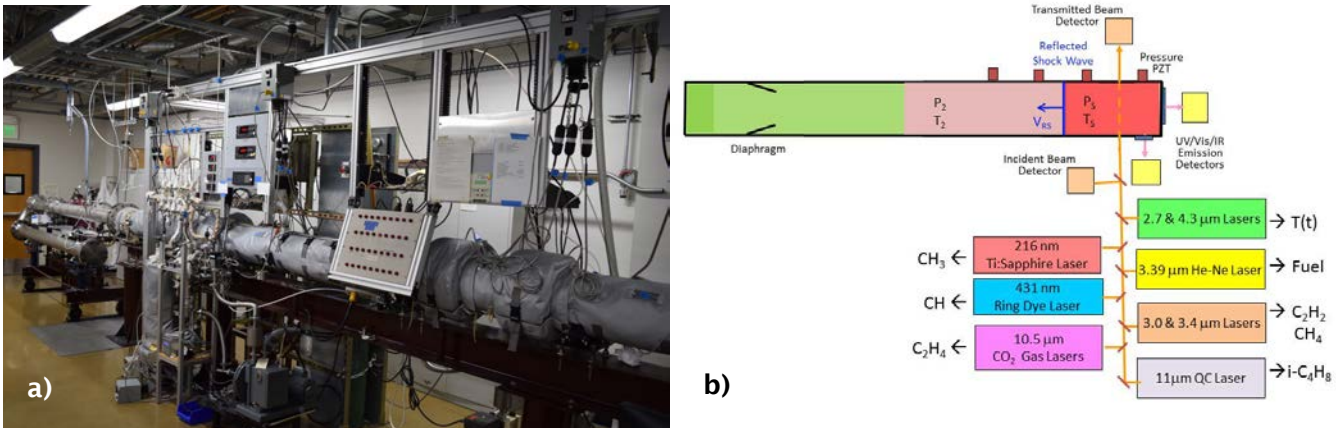

Figure 1. (a) Stanford 14-cm-diameter shock tube; and (b) schematic of shock tube/laser absorption setup. Simultaneous measurement of multiple species time-histories and temperature with microsecond time resolution are enabled using this arrangement (only a partial list of accessible species is indicated).

Two types of shock tube experiments have been performed to characterize the IH2 fuel: IDT experiments and pyrolysis species time-history experiments. Figures 2a and 2b show the IDT results at high and low temperatures, respectively, at 12–13 atm, for the IH2 fuel, a 50/50 blend of IH2 and Jet A, and Jet A; a comparison with Jet A IDT results recorded in the previous year of the project (2018) is also included.

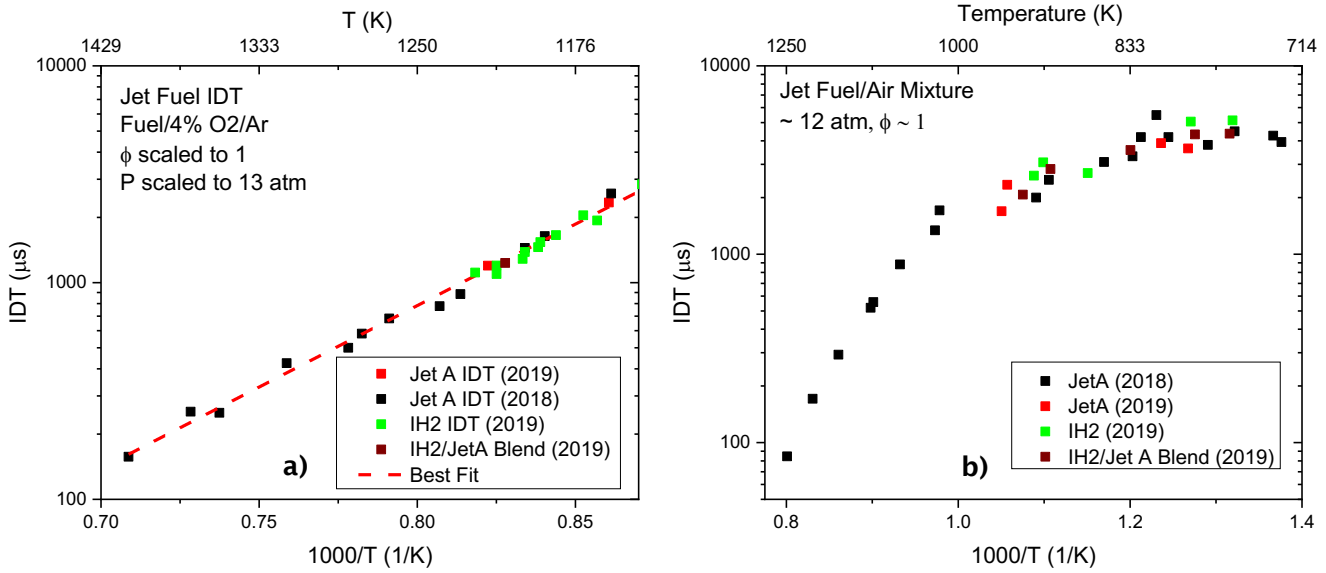

Figure 2. (a) High-temperature jet fuel (IH2 and Jet A) ignition delay time (IDT) results; and (b) low-temperature jet fuel IDT results.

Overall, similar IDTs are observed for Jet A, IH2, and the IH2/Jet A blend at high temperatures; a weak difference in IDT is observed between the three fuel types below 1000 K. Notably, below 800 K, IH2 IDTs are consistently longer than Jet A IDTs, and IH2/Jet A blend IDTs tend to fall between the two.

In addition to the IDT measurements, the first multi-wavelength laser absorption/shock tube speciation experiments for the Shell IH2 fuel were conducted. Fuel, methane, ethylene, and propene were measured at 1300 K and ~3.5 atm using

absorption diagnostics at 3.41, 3.175, 10.532, and 10.958 μm, respectively. Representative data acquired using six simultaneous wavelengths are shown in Figure 3a, and the corresponding mole fraction measurements for the same experiment are shown in Figure 3b. The ultimate goal of this work is to measure fuel, methane, acetylene, ethylene, ethane, propene, isobutene, 1-butene, and aromatics at 1200–1500 K and 3–4 atm using nine absorption diagnostics at 3.41, 3.175, 2.998, 10.532, 3.35, 10.958, 11.345, 10.675, and 3.28 μm, respectively.

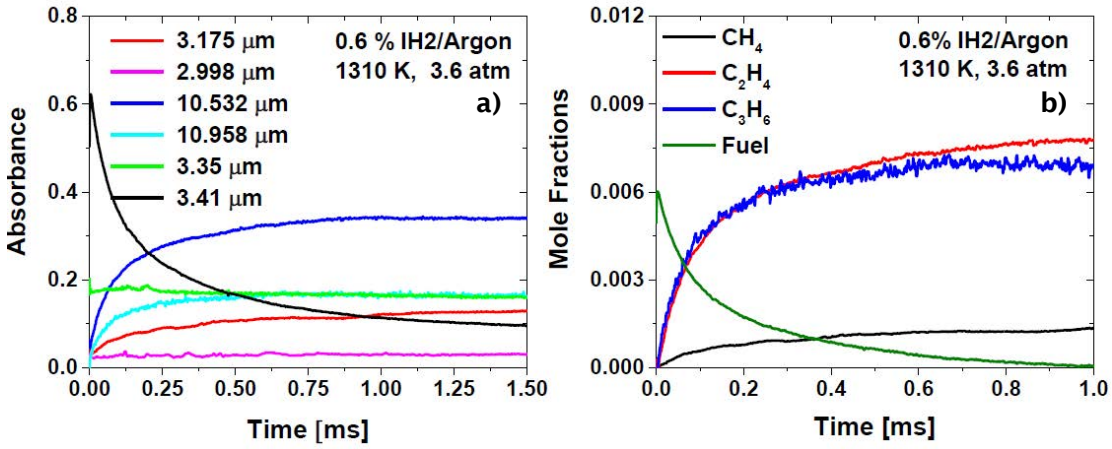

Figure 3. (a) Six-wavelength laser absorption measurements for an IH2/Ar pyrolysis reflected-shock experiment; (b) species mole fraction measurements (methane, ethylene, propene) for the same pyrolysis experiment depicted in Figure 3a.

The IDT and species time-history measurements acquired for the IH2 fuel and its blend with Jet A are directly applicable to the development of the HyChem jet fuel model.

IR spectrum analysis: results

FTIR spectra of Jet A, Shell IH2, and a 50/50 blend of IH2/Jet A were used to characterize their respective fuel compositions by decomposing each spectrum using the major molecular class FTIR spectral database set, developed through prior work done in this program. Figure 4 shows the mid-IR spectra of Jet A, IH2, and the 50/50 blend.

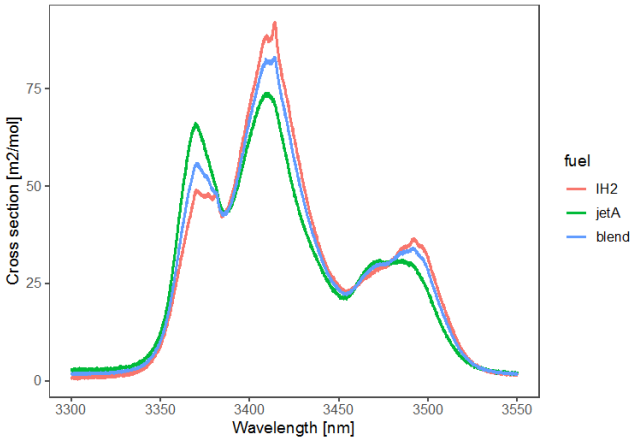

Figure 4. Fourier transform infrared (FTIR) spectra for Jet A, IH2, and a 50/50 blend. A strong absorption feature is seen in all fuels at the *n*-alkane peak near 3.41 μm.

The corresponding fuel properties predicted by the IR analysis of the fuels are shown in Table 1, together with values obtained via traditional measurement methods.

Table 1. Comparison of Jet A and 50/50 IH2/Jet A blend fuel properties estimated using infrared (IR) analysis and corresponding values measured using conventional means. DCN, derived cetane number; IBP, initial boiling point; Vis., viscosity; NHC, net heat of combustion.

Jet A	Measured	IR Estimate	% Variation
DCN	49	46	-6%
Flash pt.	48	45	-6%
IBP	155	156	1%
Kinematic Vis.	4.6	4.7	2%
NHC	43	43	0%
Density	0.80	0.80	0%
Blend	**Measured**	**IR Estimate**	**% Variation**
DCN	44	46	5%
Flash pt.	42	52	24%
IBP	150	166	11%
Kinematic Vis.	4.4	4.6	5%
NHC	43	43	0%
Density	0.82	0.84	2%

The IR analysis results show good agreement with measured property results, suggesting that IR analysis is a promising technique for prescreening potential next-generation jet fuels. The greater variation in flash point and initial boiling point (IBP) results is likely due to insufficient cycloalkane data, which is necessary to fine-tune the IR spectral analysis for fuels such as IH2 that have significant cycloalkane content.

Milestone(s)

Major milestones included regular reporting of experimental results and analysis at monthly meetings for both the Kinetics Working Group and the Steering Working Group, as well as reporting at FAA Quarterly and ASCENT annual meetings.

Major Accomplishments

During the fifth year of this program, major advances were made in several areas:

- IDT measurements were acquired for the Shell IH2 fuel and a 50/50 blend of IH2/Jet A from 750 to 1200 K, at 13 to 14 atm.
- Shell IH2 pyrolysis speciation measurements of fuel, methane, ethylene, and propene were begun, with the ultimate goal of measuring methane, acetylene, ethylene, ethane, propene, isobutene, 1-butene, and aromatics at nine laser absorption wavelengths from 1200 to 1500 K at 3–4 atm.
- FTIR spectra of Jet A and IH2 fuels were used to successfully estimate the fuels' properties, including DCN, flash point, IBP, kinematic viscosity, net heat of combustion (NHC), and density.
- The C4 HyChem model was revised and finalized using data collected during Year 4 of this program
- The kinetics and HyChem section of the AIAA volume titled *Fuel Effects on Operability of Aircraft Gas Turbine Combustors* was completed.

Publications

Peer-reviewed journal publications

Ding, Y., Wang, S., & Hanson, R.K. (2019). Sensitive and interference-immune formaldehyde diagnostic for high-temperature reacting gases using two-color laser absorption near 5.6 μm. Combustion and Flame 213, 194-201. https://doi.org/10.1016/j.combustflame.2019.11.042

Pinkowski, N.H., Cassady, S.J., Davidson, D.F., & Hanson, R.K. (2019). Multi-wavelength speciation of high-temperature 1-butene pyrolysis. Fuel 244, 269-281. https://doi.org/10.1016/j.fuel.2019.01.154
Pinkowski, N.H., Ding, Y., Johnson, S.E., Wang, Y., Parise, T.C., Davidson, D.F., & Hanson, R.K. (2019). A multi-wavelength speciation framework for high-temperature hydrocarbon pyrolysis. Journal of Quantitative Spectroscopy and Radiative Transfer 225, 180-205. https://doi.org/10.1016/j.jqsrt.2018.12.038
Pinkowski, N.H., Wang, Y., Cassady, S.J., Davidson, D.F., & Hanson, R.K. (2019). A streamlined approach to hybrid-chemistry modeling for a low cetane-number alternative jet fuel. Combustion and Flame 208, 15-26. https://doi.org/10.1016/j.combustflame.2019.06.024
Shao, J., Ferris, A.M., Choudhary, R., Davidson, D.F., & Hanson, R.K. (2020). A shock tube study of natural gas pyrolysis and ignition at elevated pressures and temperatures. Submitted, Proceedings of the Combustion Institute (38th International Symposium on Combustion).
Shao, J., Wei, W., Choudhary, R., Davidson, D.F., & Hanson, R.K. (2019). Shock tube measurement of the CH3+C2H6→ CH4+C2H5 rate constant. The Journal of Physical Chemistry A. 123, 42, 9096-9101 https://doi.org/10.1021/acs.jpca.9b07691
Shao, J., Zhu, Y., Wang, S., Davidson, D.F., & Hanson, R.K. (2018). A shock tube study of jet fuel pyrolysis and ignition at elevated pressures and temperatures. Fuel 226 338-344. https://doi.org/10.1016/j.fuel.2018.04.028
Wang, K., Xu, R., Parise, T., Shao, J., Movaghar, A., Lee, D.J., Part, J., Gao, Y., Lu, T., Egolfopoulos, F., Davidson, D.F., Hanson, R.K., Bowman, C.T., & Wang, H. (2018). A physics-based approach to modeling real-fuel combustion chemistry – IV. HyChem modeling of combustion kinetics of a bio-derived jet fuel and its blends with a conventional jet a. Combustion and Flame 198, 477-489. https://doi.org/10.1016/j.combustflame.2018.07.012
Wang, Y., Davidson, D.F., & Hanson, R.K. (2019). A new method of predicting derived cetane number for hydrocarbon fuels. Fuel 241 319-326. https://doi.org/10.1016/j.fuel.2018.12.027
Wang, Y., Ding, Y., Wei, W., Cao, Y., Davidson, D.F., & Hanson, R.K. (2019). On estimating physical and chemical properties of hydrocarbon fuels using mid-infrared FTIR spectra and regularized linear models. Fuel 255, 115715. https://doi.org/10.1016/j.fuel.2019.115715

Published conference proceedings

Pinkowski, N., Davidson, D.F., & Hanson, R.K. (2019). Multi-wavelength speciation of high-temperature alternative and conventional jet fuel pyrolysis. Paper 2019-1769, AIAA SciTech Forum, San Diego, CA. https://arc.aiaa.org/doi/pdf/10.2514/6.2019-1769
Wang, Y., Cao, Y., Davidson, D.F., & Hanson, R.K. (2019). Ignition delay time measurements for distillate and synthetic jet fuels. Paper 2019-2248, AIAA SciTech Forum, San Diego, CA. https://arc.aiaa.org/doi/pdf/10.2514/6.2019-2248

Outreach Efforts

Multi-wavelength speciation measurements of various jet fuels were presented by Nico Pinkowski at the AIAA SciTech Forum in San Diego, CA, in January 2019 ("Multi-wavelength speciation of high-temperature alternative and conventional jet fuel pyrolysis"). At the same AIAA SciTech Forum, Yu Wang presented jet-fuel IDT measurements ("Ignition Delay Time Measurements for Distillate and Synthetic Jet Fuels").

Awards

None.

Student Involvement

Graduate students are actively involved in the acquisition and analysis of all experimental data. Nicolas Pinkowski (current graduate student) performed the multi-wavelength speciation experiments and presented the results at the AIAA SciTech Forum in San Diego in January 2019. Yu Wang (current graduate student) performed the IR spectral analysis/fuel prescreening work and presented the results at the AIAA SciTech Forum in San Diego in January 2019. Jiankun Shao successfully defended his PhD thesis, which was based in part on work performed under this contract. Rui Xu also successfully defended his PhD thesis on the HyChem modeling approach, which was refined using work performed under this contract. Both Dr. Jiankun Shao and Dr. Rui Xu are currently employed as postdoctoral fellows at Stanford University. Alison Ferris (current graduate student) has additionally contributed to the project through compilation of experimental results and report writing.

Plans for Next Period

In the next period, we plan to:

- Complete time-resolved, Shell IH2 pyrolysis speciation measurements of methane, acetylene, ethylene, ethane, propene, isobutene, 1-butene, and aromatics using nine laser absorption wavelengths from 1200 to 1500 K at 3–4 atm
- Acquire aldehyde (CH_2O) species time-histories in low-temperature oxidation experiments to further refine HyChem performance at low temperatures
- Develop and validate a HyChem model for the pyrolysis and oxidation of the Shell IH2 fuel
- Apply FTIR analysis to the characterization of neat IH2 fuel (obtain additional cycloparaffin property data; e.g., flash point, DCN)

Project 027 Advanced Combustion (Area #3)

Georgia Institute of Technology
Oregon State University

Project Lead Investigator

Tim Lieuwen
Professor
Aerospace Engineering
Georgia Institute of Technology
270 Ferst Drive, G3363 (M/C 0150)
Atlanta, GA 30332-0150
404-894-3041
tim.lieuwen@ae.gatech.edu

University Participants

Georgia Institute of Technology

- PI(s):
  - Prof. Tim Lieuwen
  - Prof. Jerry Seitzman
  - Prof. Wenting Sun
- FAA Award Number: 13-C-AJFE-GIT-008
- Period of Performance: December 1, 2018 to November 30, 2019
- Task(s):
  1. Lean Blowout. In this task, the lean blowout characteristics of alternative jet fuels are measured and compared to those of Jet A fuel.
  2. Ignition. In this task, the ignition probabilities of alternative jet fuels are measured and compared to those of Jet A fuel.

Oregon State University

- PI(s): David Blunck
- FAA Award Number: 13-C-AJFE-OSU-02
- Period of Performance: December 1, 2018 to November 30, 2019
- Tasks:
  1. Turbulent Flame Speed. In this task, the turbulent flame speeds of alternative jet fuels are measured and compared to those of Jet A fuel.

Project Funding Level

Georgia Institute of Technology
FAA Funding: $30,000
Cost Share: $30,000 provided by Georgia Institute of Technology

Oregon State University
During the reporting period, the remaining funds were spent, and an additional $4,441 was provided by OSU to complete the project.

Investigation Team

- Tim Lieuwen (Georgia Institute of Technology): Principal Investigator. Prof. Lieuwen is the PI overseeing all tasks and is the manager of Task 1. Lean Blowout.
- Jerry Seitzman (Georgia Institute of Technology): Co-Principal Investigator. Prof. Seitzman is the manager of Task 2. Ignition.
- David Blunck (Oregon State University): Co-Principal Investigator. Prof. Blunck is the manager of Task 3. Turbulent Flame Speed.
- Wenting Sun (Georgia Institute of Technology): Co-Principal Investigator. Prof. Sun is acting as an internal expert consultant on kinetic mechanisms.
- Tonghun Lee (University of Illinois Champaign): Co-Principal Investigator. Prof. Lee is the lead diagnostic expert.
- Benjamin Emerson (Georgia Institute of Technology): Research Engineer. Dr. Emerson is responsible for the design and maintenance of experimental facilities, experimental operations, and the management and safety of graduate students. He is also acting as the administrative coordinator for all three tasks.
- David Wu (Georgia Institute of Technology): Research Engineer. Mr. Wu is responsible for the design and maintenance of experimental facilities, experimental operations, and the management and safety of graduate students.
- Glenda Duncan (Georgia Institute of Technology): Administrative Staff. Mrs. Duncan provides administrative support.
- Tiwanna Williams (Georgia Institute of Technology): Administrative Staff. Mrs. Williams provides administrative support.
- Seth Hutchins (Georgia Institute of Technology): Lab Coordinator. Mr. Hutchins maintains the core lab facilities and provides technician services.
- Machine Shop Staff (Georgia Institute of Technology): The Aerospace Engineering machine shop provides machining services for experimental facility maintenance/construction.
- Nick Rock (Georgia Institute of Technology): Graduate Student. Mr. Rock is leading the lean blowout task.
- Hanna Ek (Georgia Institute of Technology): Graduate Student. Ms. Ek is the lead data analyst for the lean blowout task.
- Sheng Wei (Georgia Institute of Technology): Graduate Student. Mr. Wei currently leads the ignition task.
- Jonathan Bonebrake (Oregon State University): Graduate Student. Mr. Bonebrake was the lead graduate student experimentalist on the turbulent flame speed task.
- Nathan Schorn (Oregon State University): Graduate Student. Mr. Schorn recently started and has transitioned to leading the effort to operate the burner and to collect and analyze data.

Project Overview

The objective of this project was to conduct advanced combustion testing of alternative jet fuels, with the aim of accomplishing two goals. The first goal was to rank the lean blowout boundaries, ignition probabilities, and turbulent flame speeds of alternative fuels relative to conventional Jet A fuel. The second goal was to produce data that could support the modeling and simulation tasks of other teams. For the second goal, data were measured as needed and as requested by other teams. These data typically consisted of velocity field measurements, high-speed flame images, and test rig boundary conditions.

During this program, we tested a total of 20 fuel mixtures. Sixteen of these fuels were pure (unblended) fuels, designated as A1, A2, A3, C1, C2, C3, C4, C5, S1, S2, S3, high TSI, C7, C8, C9, and n-dodecane. The A1, A2, and A3 fuels represent the range of conventional Jet A fuels. The other fuels have different physical and/or chemical properties. We also tested three sets of blends: A2/C1 blends, A2/C5 blends, a C1/n-heptane blend, and a C1/n-dodecane blend. These fuels have been tested under three tasks, which are summarized below. The details of these tasks are given in the remainder of this report.

1. Lean blowout measurements. The highest-priority lean blowout measurement was fuel screening, in which the blowout boundaries of various fuels were compared to that of Jet A fuel. This task also included measurements of the combustor velocity field, the spatiotemporal evolution of the flame position, and several thermodynamic rig boundary conditions, such as the air flow rate, surface temperature, gas temperature, and gas pressure.
2. Forced ignition measurements. Similar to the blowout task, the highest-priority forced ignition measurement was fuel screening. In the forced ignition task, the fuel screening activity indicated the ignition probabilities of various fuels, which were then compared with the ignition probability of Jet A fuel. The ignition probability is a common measure of combustor ignitability and was measured by sparking the igniter hundreds of times and measuring the

fraction of spark events that successfully ignited the combustor. This task included a modeling component, which has begun to exhibit the capability for ignition probability prediction. Such a predictive capability would take combustor conditions (pressure, temperature, and fuel–air ratio) in addition to key fuel properties (vaporization and chemical kinetic properties) as inputs and would produce an ignition probability as the output. To support this modeling effort, measurements of detailed ignition physics were acquired, including images of the fuel spray, ignition kernel, and flame.

3. Turbulent flame speed measurements. Similar to the other two tasks, the high-priority measurement for Task 3 was fuel screening, in which the turbulent flame speeds of various fuels were compared with that of Jet A fuel. This task also had a significant rig development aspect, which provided subatmospheric pressure capability.

This report covers the 5th year of a 5.5-year program. The following sections provide a summary of the most important results from all five years for each of the three tasks. The first and third tasks were funded during the fifth year; thus, new results are included relative to the fourth-year report. The second task was not funded during the fifth year, and hence, its results are repeated from the fourth-year report.

Task 1– Lean Blowout

Georgia Institute of Technology

Objective(s)

The objective of this task was to obtain two types of measurements, i.e., fuel screening and detailed diagnostics, in a combustor rig operating near lean blowout. Fuel screening was performed in order to rank the blowout boundaries of each fuel relative to Jet A fuel. Detailed diagnostics were conducted to produce data that could support the modeling teams by providing physical insight and important simulation boundary conditions.

Research Approach

This task was performed with a combustor rig, as shown in Figure 3. The rig was a high-pressure, swirl-stabilized spray combustor with original equipment manufacturer (OEM)-relevant hardware. The combustor was configured similarly to the referee rig at the Air Force Research Lab, although the dome and liner cooling arrangements of the referee rig differ. The referee rig has a higher level of complexity for these components, providing a closer simulation of a real combustor. However, the reduced complexity of the Georgia Tech rig enables a greater rate of data generation and allows laser-based diagnostics that are not possible in the referee rig.

This research project consisted of four major activities. First, the test conditions were collaboratively selected by the LBO working group. The test condition selection included input from the OEMS as well as other stakeholders, such as the referee rig team and modeling teams. Together, these teams selected one combustor pressure and three air preheat temperatures for lean blowout testing. These parameters were designed to simulate idle and altitude conditions at which lean blowout poses the greatest risk. The selected combustor pressure was 3 atm, and the selected air preheat temperatures were 300, 450, and 550 K.

Second, screening data were acquired by outfitting the combustor test rig with an advanced fuel cart. The fuel cart had ten fuel tanks, each of which could hold a different fuel. The cart could rapidly switch between these fuels, which enabled the lean blowout testing of ten fuels in a single session; this capability is advantageous because it promotes repeatability by eliminating the potential for uncontrolled variations in test conditions between test days. Fuel screening was conducted by igniting the combustor and intentionally leaning it to the lean blowout limit. The conditions under which the combustor blew out were recorded, and the process was repeated until the first fuel tank was empty. This repetitive process typically produced 20–30 blowout points for a single fuel. This procedure was then repeated for the fuels in the other nine tanks. Figure 1 shows screening data measured during the third year of the project. Correlations between the cetane number and the blowout equivalence ratio at elevated temperatures first became evident in this third-year data set. For example, Figure 1 shows a stronger correlation between the blowout equivalence ratio and cetane number at the two higher inlet temperatures (450 and 550 K) vs. the lower inlet temperature (300 K).

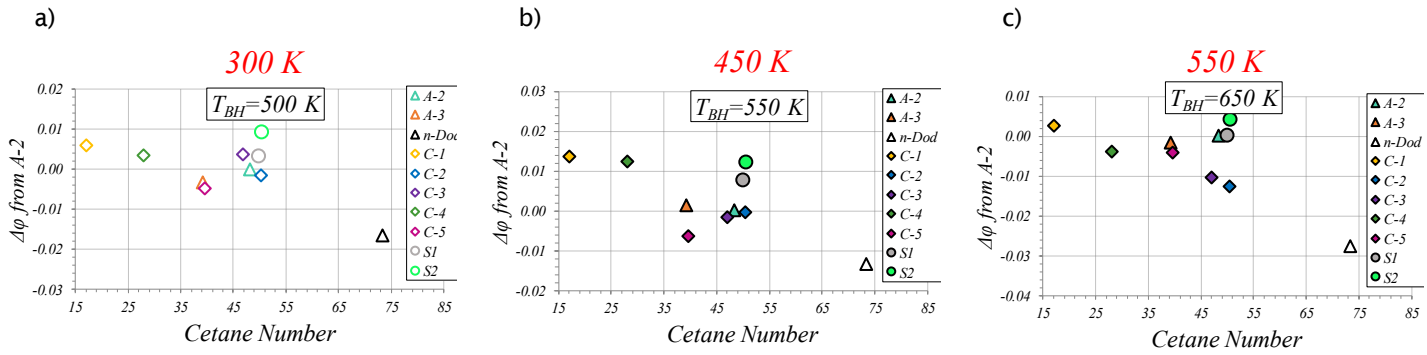

Figure 1. Sample of third-year screening data for three preheat temperatures and three bulkhead temperatures, demonstrating a strong correlation between lean blowout and cetane number. The correlation coefficients for the blowout equivalence ratio and cetane number are -0.21 at 300 K, -0.79 at 450 K, and -0.76 at 550 K.

Third, detailed data were acquired to support the modeling groups and to improve the team's understanding of the physics of lean blowouts. The lean blowout team performed detailed laser-based measurements, which were provided to the modeling groups to help them refine and validate their simulations. The measurements incorporated several laser-based techniques that were synchronized at 5,000 frames per second, including the following:

- Stereoscopic particle image velocimetry (s-PIV) to obtain planar measurements of the three-component velocity field
- Planar laser-induced fluorescence of the OH molecule (OH PLIF) to obtain measurements of the flame position
- Planar laser-induced fluorescence of the liquid fuel (fuel PLIF) to obtain measurements of the liquid fuel spray location

High-speed chemiluminescence images were also acquired during the third step. Figure **2** presents a representative chemiluminescence image. These measurements can be more easily acquired and analyzed than the laser-based diagnostics outlined above; thus, chemiluminescence imaging has the advantage of rapid implementation. Due to this advantage, chemiluminescence imaging was applied for more fuels and test conditions than the laser-based techniques. The chemiluminescence images also helped reveal the qualitative burning characteristics near lean blowout and assisted the team in determining the roles of ignition and extinction in the lean blowout process. Area 3 and Area 7 are both currently analyzing these data in order to make such a determination. In addition to these optical measurements, the third activity also produced measurements of combustor boundary conditions, including air flow rate, air and fuel temperature, combustor pressure, and surface temperature.

Figure 2. Sample chemiluminescence image of a flame burning n-dodecane at an air preheat temperature of 300 K.

Fourth, data analysis was performed to convert the raw measured data into useful data. In data screening, the combustor operation data were analyzed to identify lean blowout events and associated operating points. Uncertainty analysis was also performed in order to determine the statistical significance of the results. In some cases, the uncertainty analysis results motivated the lean blowout group to acquire additional data in order to reduce the uncertainty. The detailed data were analyzed in two steps: pre-processing and post-processing. Pre-processing was applied to the velocity field measurements and consisted of an intensive cross-correlation algorithm to convert raw images into velocity fields. This step was extremely time-consuming and difficult. Post-processing was conducted to produce time-averaged velocity fields, to produce the root mean square velocity field, and to extract key vortical flow features. These post-processed data were then provided to the modeling teams.

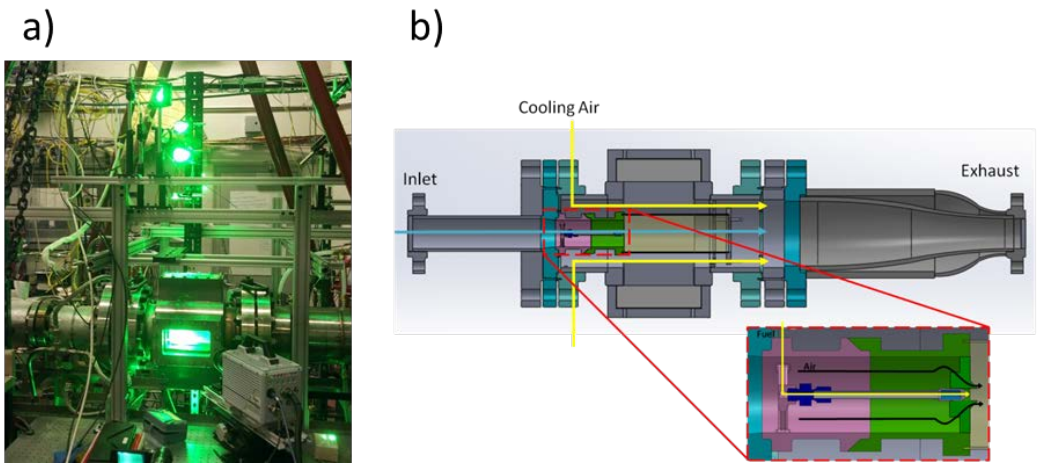

Figure 3. High-shear swirl combustor. a) Pressure vessel instrumented for high-speed stereo particle image velocimetry (PIV) and planar laser-induced fluorescence (PLIF) of OH. b) Cross-section of a generic swirler holder/injector.

A supervised machine learning regression technique was applied to the fuel screening data during the fifth year, with the aim of identifying cause-and-effect relationships between the fuel properties and blowout characteristics. These cause-and-effect relationships are difficult to identify via classical statistics because the fuel properties are strongly intercorrelated, which can lead to inaccurate interpretations.

The regression procedure consisted of a hierarchical non-negative garrote with a two-step approach. First, important groups of variables or parameters, such as “physical properties” or “chemical properties”, are identified. This step requires a physical understanding of the system. Second, a series of regressions are applied to the data based on the groups and the variables within the groups. The groupings used in this study are shown in Table 1.

Table 1. Hierarchical non-negative garrote groupings.

Group 1	Group 2	Group 3	Group 4	Group 5	Group 6	Group 7
T_{10}	ν (mm^2/s) 313 (K)	T_{50}	% iso-Paraffins	H/C	% Aromatics	DCN
MW	ρ (kg/m^3) 288 K	T_{90}	σ (mN/m) 300 K	LHV (MJ/kg)	Smoke Point (mm)	Ri

The regression model consists of tuning parameters determined from a cross-validation procedure. During cross-validation, a subset of the data (the training data set) and the regression are tested against the remaining data (the validation data set). This process is repeated with different portions of the data serving as the training data set until all data have served as training data. The cross-validation procedure is illustrated in Figure 4.

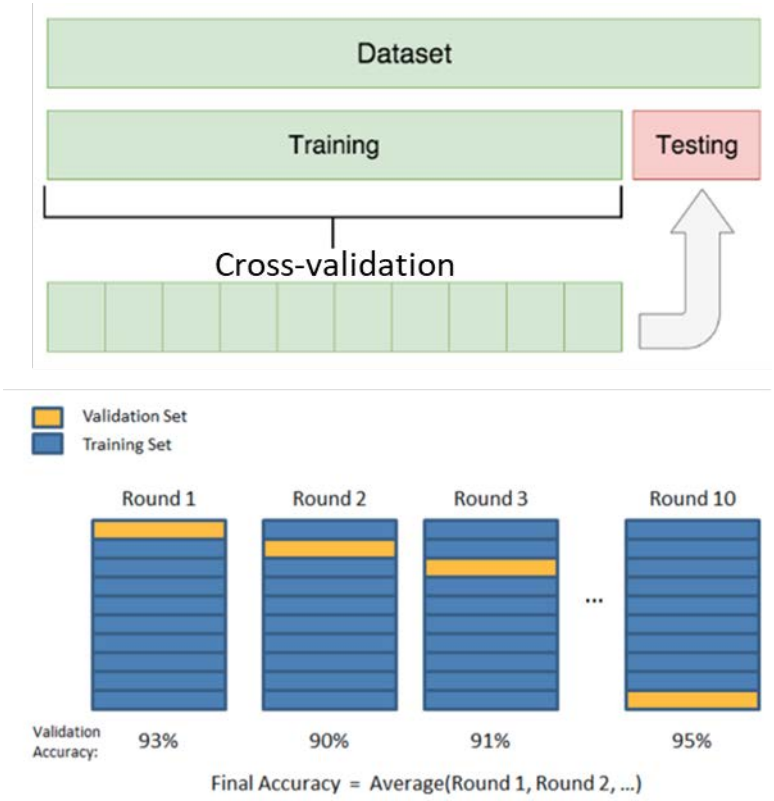

Figure 4. Illustration of the cross-validation procedure.

The results of this analysis indicated that different parameters influence the blowout at different combustor inlet temperatures. These results are shown graphically in Figure 5, which presents the regression coefficients that relate the LBO equivalence ratio to the fuel properties. At low combustor inlet temperatures, the 90% boiling point has the strongest influence on LBO characteristics (see the right-most blue bar in Figure 5). However, at higher combustor inlet temperatures, the derived cetane number (DCN) has the strongest influence on LBO characteristics (see the left-most yellow and orange bars in Figure 5). This result strongly supports the hypothesis from UDRI that physical properties are important for LBO at low temperatures and that autoignition properties are important for LBO at high temperatures. In addition, these results identify the most important individual parameters. Finally, we note that the regression model exhibited the best performance when we adjusted the DCN for the 20% most volatile fuel constituents, which supports the preferential vaporization hypothesis proposed by other teams.

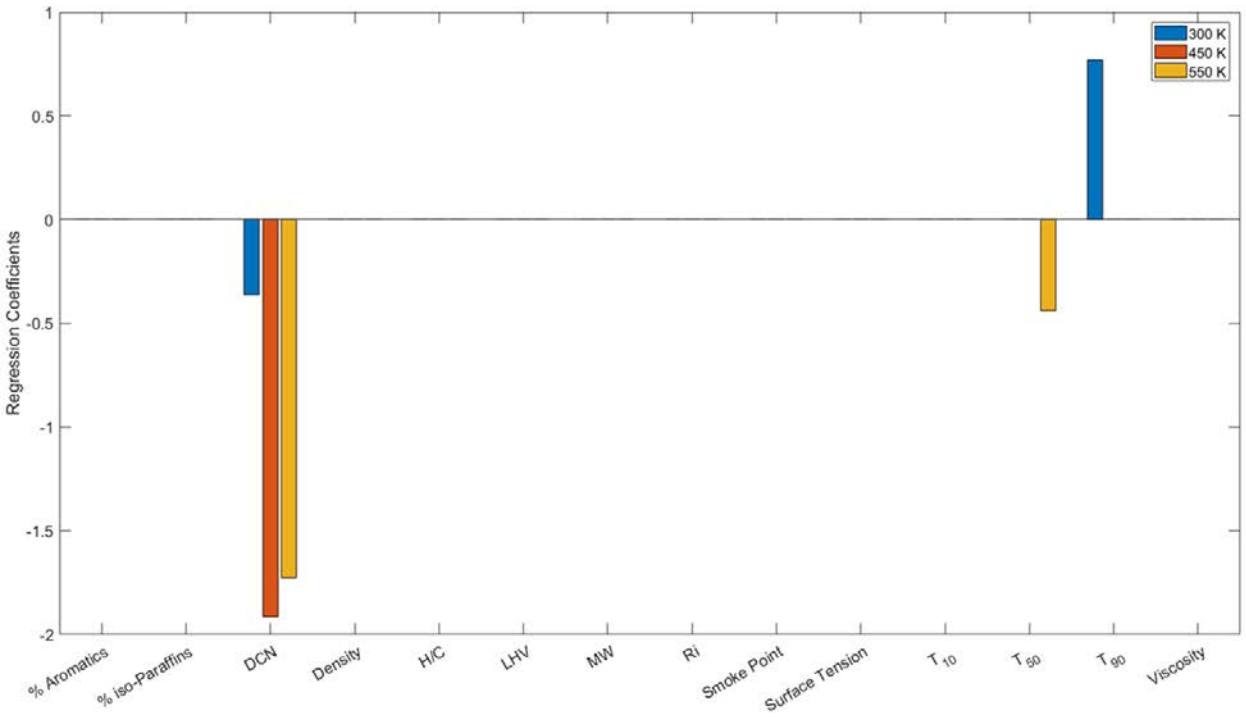

Figure 5. Results of the hierarchical non-negative garrote for three combustor inlet temperatures.

Milestone(s)

- Boundary condition measurements. This step was completed during years 1 and 2.
- Detailed diagnostic measurements. This step was completed during years 1 and 2.
- Data screening. This step was completed during year 4.
- Analysis. This step was completed during year 5.

Major Accomplishments

1. We have developed a data analysis framework that explains the sensitivity of lean blowout to different fuel characteristics. This framework is robust against intercorrelated parameters, and the analysis results support several hypotheses that have been presented by various NJFCP team members.
2. We supported the LBO chapter of the AIAA book during year 5.

Publications

Peer-reviewed journal publications

Emerson, B., and Ozogul, H. 2020. Experimental Characterization of Liquid-gas Slip in High Pressure, Swirl Stabilized, Liquid-fueled Combustors. Accepted for publication in *Experiments in Fluids*.

Rock, N., Emerson, B., Seitzman, J. and Lieuwen, T., 2020. Near-lean blowoff dynamics in a liquid fueled combustor. Combustion and Flame, 212, pp.53-66.

Won, S.H., Rock, N., Lim, S.J., Nates, S., Carpenter, D., Emerson, B., Lieuwen, T., Edwards, T. and Dryer, F.L., 2019. Preferential vaporization impacts on lean blow-out of liquid fueled combustors. Combustion and Flame, 205, pp.295-304.

Wei, S., Sforzo, B. and Seitzman, J., 2018. High-Speed Imaging of Forced Ignition Kernels in Nonuniform Jet Fuel/Air Mixtures. Journal of Engineering for Gas Turbines and Power, 140(7), p.071503.

Chterev, I., Rock, N., Ek, H., Emerson, B., Seitzman, J., Jiang, N., Roy, S., Lee, T., Gord, J. and Lieuwen, T., 2017. Simultaneous imaging of fuel, OH, and three component velocity fields in high pressure, liquid fueled, swirl stabilized flames at 5 kHz. Combustion and Flame, 186, pp.150-165.

Won, S. H., Rock, N., Lim, S. J., Nates, S., Carpenter, D., Emerson, B., Lieuwen, T., Edwards, T., Dryer, F. Preferential Vaporization Impacts on Lean Blow-Out of Liquid Fueled Combustors.

Published conference proceedings

Rock, N., Chterev, I., Emerson, B., Won, S.H., Seitzman, J. and Lieuwen, T., 2019. Liquid fuel property effects on lean blowout in an aircraft relevant combustor. Journal of Engineering for Gas Turbines and Power, 141(7).

Rock, N., Emerson, B.L., Seitzman, J. and Lieuwen, T., 2019. Dynamics of Spray Flames under Near-Lean Blowoff Conditions. In AIAA Scitech 2019 Forum (p. 1433).

Ek H., Chterev I., Rock N., Emerson B., Seitzman J., Jiang N., Proscia W., Lieuwen T., "Feature Extraction from Time Resolved Reacting Flow Data Sets", Proceedings of the ASME Turbo Expo, Paper #GT2018-77051, 2018.

Emerson, B., and Ozogul, H. 2018. Experimental Characterization of Liquid-gas Slip in High Pressure, Swirl Stabilized, Liquid-fueled Combustors, in Western States Section of the Combustion Institute – Spring 2018 Meeting.

Rock, N., Chterev, I., Emerson, B., Seitzman, J. and Lieuwen, T., 2017, June. Blowout Sensitivities in a Liquid Fueled Combustor: Fuel Composition and Preheat Temperature Effects. In ASME Turbo Expo 2017: Turbomachinery Technical Conference and Exposition (pp. V04AT04A022-V04AT04A022). American Society of Mechanical Engineers.

Chterev, I., Rock, N., Ek, H., Emerson, B.L., Seitzman, J.M., Lieuwen, T.C., Noble, D.R., Mayhew, E. and Lee, T., 2017. Simultaneous High Speed (5 kHz) Fuel-PLIE, OH-PLIF and Stereo PIV Imaging of Pressurized Swirl-Stabilized Flames using Liquid Fuels. In 55th AIAA Aerospace Sciences Meeting (p. 0152).

Rock, N., Chterev, I., Smith, T., Ek, H., Emerson, B., Noble, D., Seitzman, J., Lieuwen, T. "Rreacting Pressureized Spray Combustor Dynamics, Part 1. Fuel Sensitivities and Blowoff Characterization" Proceedings of the ASME Turbo Expo 2016, Seoul, South Korea, 2016, GT2016-56346

Chterev, I., Rock, N., Ek, H., Smith, T., Emerson, B., Noble, D., E. Mayhew, T. Lee, N. Jiang, S. Roy, Seitzman, J., Lieuwen, T. "Rreacting Pressureized Spray Combustor Dynamics, Part 2. High Speed Planar Measurements" *Proceedings of the ASME Turbo Expo 2016, Seoul, South Korea*, **2016**, *GT2016-56345*

Dissertations

Chterev, I. Flow Characterization of Lifted Flames in Swirling, Reacting Flows. Ianko Chterev. August, 2017. PhD Dissertation. Georgia Institute of Technology.

Outreach Efforts

This program provided research opportunities to multiple undergraduate students and one high school student. In addition, one graduate student presented his work on this project at the 2019 AIAA SciTech conference, and one graduate student complete his PhD based on the work conducted under this program.

Awards

Graduate student Nick Rock was awarded ASCENT Student of the Year in April 2017.

Student Involvement

Dr. Nick Rock was actively involved in the lean blowout experimental effort for all five years. As a PhD student, Dr. Rock was responsible for operating the experimental facility. He led the screening measurements, operated the facility for the detailed diagnostic efforts, and analyzed the screening data. Dr. Rock has completed his PhD and now works for Spectral Energies in Dayton, OH.

Hanna Ek has been involved in the lean blowout effort as a data analysist. Ms. Ek has been responsible for processing and analyzing the large volume of detailed data produced by the PIV, PLIF, and Mie scattering measurements.

Dr. Ianko Chterev was actively involved in the lean blowout experimental effort. His primary responsibility was the design of experimental procedures and support of detailed diagnostic measurements. Dr. Chterev has completed his PhD and now works as a postdoctoral researcher for the German Aerospace Center (DLR) in Stuttgart, Germany.

Dr. Eric Mayhew visited Georgia Tech from the University of Illinois at Urbana-Champaign and helped lead the execution of the laser and optical diagnostics. Dr. Mayhew has completed his Ph.D. and now works as a postdoctoral Fellow at the U.S. Army Research Laboratory.

Plans for Next Period

We completely expended our budget during the fifth year. We plan to continue to author and present papers from this work, and we will continue to support the LBO chapter of the AIAA book that is being produced from this program.

Task 2- Ignition

Performance site: Georgia Institute of Technology

Objective(s)

This year's ignition task had four objectives. The first objective was to expand the database of room-temperature ignition probability measurements, and the second objective was to acquire and analyze ignition probabilities for chilled fuels. The third objective was to characterize the droplet size distribution for a liquid spray, and the fourth objective was to couple liquid droplet heating and vaporization physics to the previously developed perfectly stirred reactor (PSR) model. This enhanced model simulates the spark kernel development process to elucidate the relative effects of chemical reactions, dilution cooling, and droplet heating and vaporization on the ignition process.

Research Approach

The first activity in the ignition task for 2018 was the testing of ignition probabilities for liquid sprays of room-temperature and chilled fuels. This task began with modification of the test facility. The fuel delivery system was modified to provide liquid sprays rather than prevaporized fuels. The most important fuel system modifications include the installation of a solid cone pressure atomizer (fuel injector) near the entrance of the test section and the addition of a fuel chiller. Moreover, the splitter plate was removed from the test rig to provide a single pure air stream. The fuel injector location was selected to produce ignition probabilities in the range of 1%–10% and was fine-tuned to prevent fuel droplet impingement on the igniter. Scattering of a HeNe laser from the liquid droplets was measured to monitor the fuel spray trajectory. A schematic of the fuel delivery system is shown in Figure 6.

As the second activity, liquid fuel testing was conducted with a cross-flow air velocity of 10 m/s, an equivalence ratio of φ = 0.55, a cross-flow air temperature of 80 ˚F, and a pressure of 1 atm. For room-temperature fuel sprays, ignition probabilities were measured for A2, A3, C1, C2, C3, C5, C7, C8, and C9. For chilled fuel, ignition probabilities were measured for A1, A2, A3, C1, C3, C4, C5, C7, and C8. Some fuels could not be chilled in this system, as they would freeze. The ignition probabilities of each fuel relative to A2 are shown in Figure 7. For comparison, the results from previous assessments of prevaporized fuels are also displayed. There are several noteworthy differences between the ignition probabilities of liquid vs. prevaporized fuels; for example, the rankings of the ignition probabilities differ. The ignition probabilities of A3, C2, and C3 are reduced relative to the other fuels when tested as liquid sprays. As another noteworthy difference, the range of probabilities is larger for chilled fuel sprays than for room-temperature fuel sprays.

The differences in the ignition probabilities of liquid sprays vs. prevaporized fuels provide some important insights. For example, the rate-limiting properties of prevaporized fuels should be the chemical properties, because the physical properties govern the vaporization process, which has been bypassed by prevaporization. However, the rate-limiting properties for liquid sprays may include both physical and chemical properties. Therefore, the differences in ignition probability demonstrate the important role of physical properties (such as viscosity, boiling point, etc.) in the ignition of liquid fuel sprays, whereas special attention has been paid to properties that govern vaporization (recovery temperature, vapor pressure) and atomization (viscosity). The correlations between the viscosities and the 10% recovery temperatures for the fuel sprays are shown in Figure 8 and Figure 9.

For the third activity in the ignition task, the droplet distribution was measured via PDPA. In aviation gas turbine combustors, jet fuels are injected as liquid sprays. These liquid sprays transition to gaseous fuel vapors before they burn. The droplet size can play an important role in the phase transition process by affecting the droplet heat transfer process. Therefore, PDPA measurements of droplet size and velocity distribution for an array of fuels were performed. Normalized size distribution data for fuel C3 (high viscosity), A2 (intermediate viscosity), and C5 (low viscosity) at approximately 5 mm above the igniter center are presented in Figure 10. Significant differences in droplet size distributions were observed; for example, the C3 fuel has more droplets in the larger size range (above 30 μm), while the C5 fuel has only a small percentage of droplets in that size range. Thus, the PDPA data can be used for more advanced CFD simulations.

Finally, a reduced-order model was enhanced to study the physics of forced ignition in a liquid fuel spray. The conceptual model construction is shown in Figure 11. In an example case study, forced ignition is simulated in a spray of 5-μm single droplets uniformly distributed with an equivalence ratio of 1. The heat release, dilution cooing, and droplet heating and vaporization rates are shown in Figure 12. The initial results show that the energy required to heat and vaporize a droplet is 10 times smaller than the heat release rate and dilution cooling, and therefore, the droplet is not expected to substantially affect the ignition kernel's temperature during ignition heating. Consequently, the time delay observed before the chemical heat release is likely due to heating of the droplets. If this delay is too long, the kernel will be significantly cooled by dilution, and ignition will not occur.

Milestone(s)

- Produced high-quality, reproducible ignition probability data for room-temperature liquid fuel sprays
- Produced high-quality, reproducible ignition probability data for chilled liquid fuel sprays
- Acquired droplet size and velocity distribution data for several fuels
- Enhanced a reduced-order ignition model that includes droplet heating and vaporization processes

Major Accomplishments

- Fuel spray ignition probabilities correlate to properties that control droplet size and vaporization.
- The acquired droplet distribution data could be useful for CFD models.
- The reduced-order ignition model shows that the magnitude of the droplet cooling effect is small compared to those of the chemical heat release and dilution cooling.

Publications

Peer-reviewed journal publications

Wei, S., Sforzo, B. and Seitzman, J., 2018. High-Speed Imaging of Forced Ignition Kernels in Nonuniform Jet Fuel/Air Mixtures. Journal of Engineering for Gas Turbines and Power, 140(7), p.071503.

Sforzo, B., Dao, H., Wei, S. and Seitzman, J., 2017. Liquid fuel composition effects on forced, nonpremixed ignition. Journal of Engineering for Gas Turbines and Power, 139(3), p.031509.

Published conference proceedings

S. Wei, B. Sforzo and J. Seitzman, "Fuel Composition Effects on Forced Ignition of Liquid Fuel Sprays," GT2018-77196 Proceedings of the ASME/IGTI Turbo Expo 2018, June 11-14, 2018 Oslo Norway.

Y. Tang, M. Hassanaly, V. Raman, B. Sforzo, S. Wei and J. Seitzman, "Simulation of Gas Turbine Ignition Using Large Eddy Simulation Approach," GT2018-76216 Proceedings of the ASME/IGTI Turbo Expo 2018, June 11-14, 2018 Oslo Norway.

Ek H., Chterev I., Rock N., Emerson B., Seitzman J., Jiang N., Proscia W., Lieuwen T., "Feature Extraction from Time Resolved Reacting Flow Data Sets", Proceedings of the ASME Turbo Expo, Paper #GT2018-77051, 2018.

Sforzo, B., Wei, S. and Seitzman, J.M., 2017. Non-premixed Ignition of Alternative Jet Fuels. In 55th AIAA Aerospace Sciences Meeting (p. 0147).

Sforzo, B., Dao, H., Wei, S. & Seitzman, J. "Liquid Fuel Composition Effects on Forced, Non-Premixed Ignition" *Proceedings of the ASME Turbo Expo 2016, Seoul, South Korea*, **2016**, *GT2016-56163*

Outreach Efforts
Conference presentation at ASME Turbo Expo 2018, Oslo, Norway

Awards
None.

Student Involvement
Sheng Wei was the lead student on all of the ignition task objectives. Daniel Cox was involved in data analysis. Sabrina Noor aided in data analysis for prevaporized ignition simulation. Vedant Mehta conducted a parametric study on droplet ignition. John Ryu helped with the multisize droplet ignition study. Sheng Wei graduated with a PhD.

Plans for Next Period
N/A

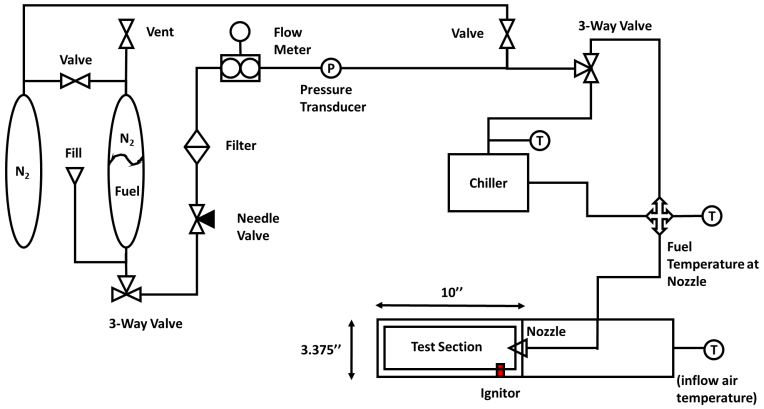

Figure 6. Schematic of the liquid fuel delivery system.

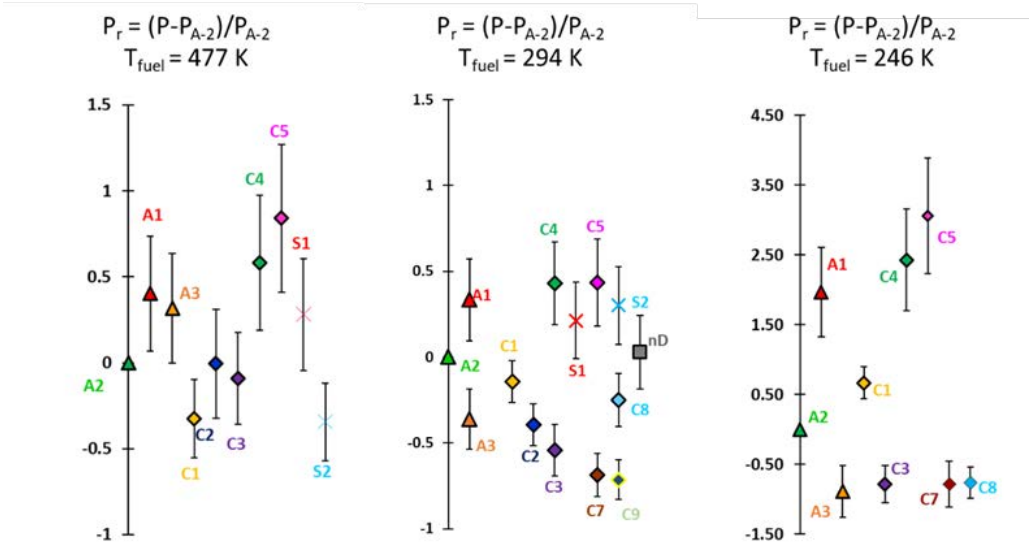

Figure 7. Ignition probability rankings, scaled with respect to the A2 probability. Error bars show 68% uncertainty. Left: prevaporized fuel/air mixture; middle: room-temperature liquid fuel spray; right: chilled liquid fuel spray.

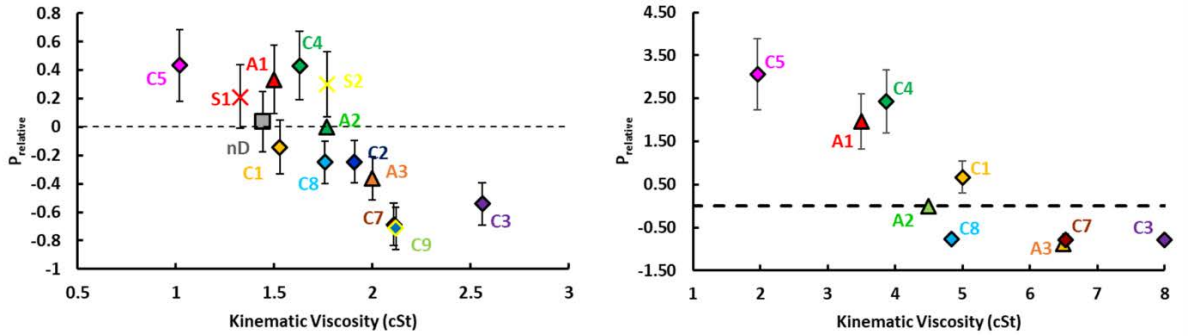

Figure 8. Relative probabilities vs. relative viscosity for room-temperature fuel. Left: probability results for room-temperature fuel spray; right: probability results for chilled fuel spray.

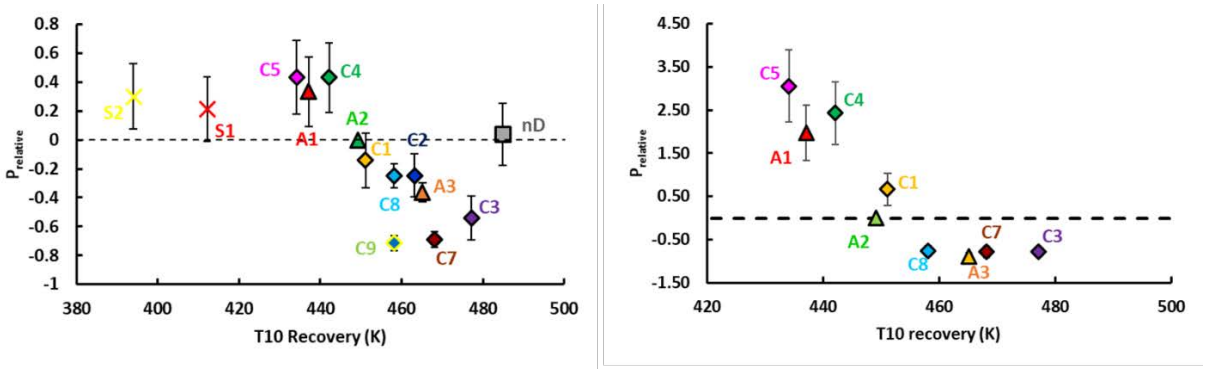

Figure 9. Relative probabilities vs. 10% recovery temperature. Left: probability results for room-temperature fuel spray; right: probability results for chilled fuel spray.

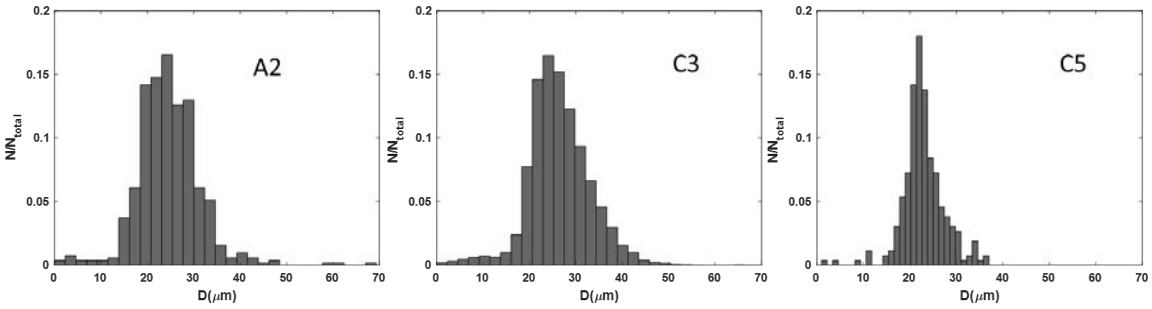

Figure 10. Normalized size distribution at 5 mm above the igniter center.

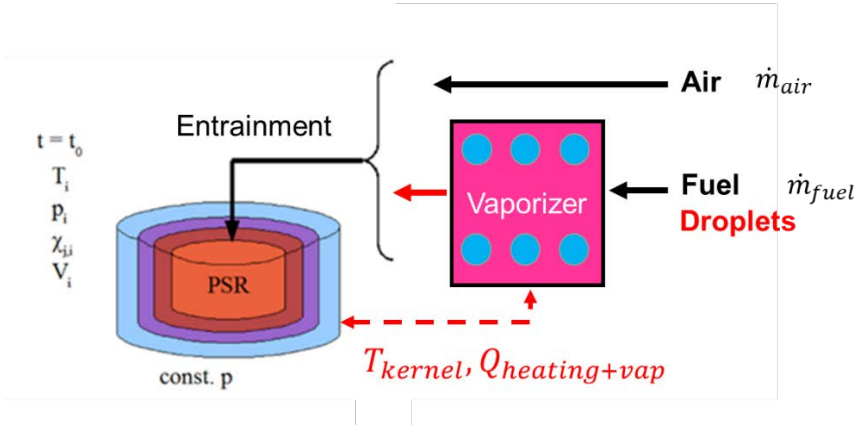

Figure 11. Conceptual perfectly stirred reactor (PSR) model with droplet vaporization.

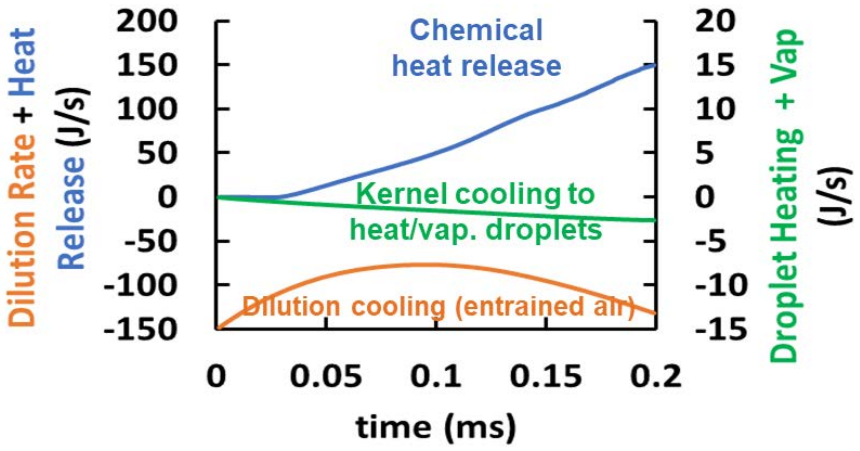

Figure 12. Chemical heat release, dilution cooling, and droplet heating/vaporization rates for a successful ignition of 5-μm droplets at an equivalence ratio of 1.

Task 3- Turbulent Flame Speed

Oregon State University

Objective(s)

This task had three objectives. The first objective was to measure and identify the sensitivity of the turbulent flame speed to fuel composition, for a range of jet fuels and test conditions (including atmospheric and subatmospheric pressures). The second objective was to build a database of turbulent flame speeds for prevaporized jet fuels. This year, we initiated a collaboration with Suresh Menon (GT), who is performing simulations of turbulent flames anchored to a burner. The third objective was to measure the sensitivity of turbulent flames to local extinction.

Research Approach

Testing was conducted using a laboratory test rig that produced turbulent flames. The rig featured a prevaporizer based on designs developed by the Air Force Research Laboratory and a burner based on designs developed by Lieuwen and colleagues. The experimental arrangement consisted of fuel- and air-metering systems that delivered prevaporized jet fuel

and air to the burner. The fuel was vaporized using a series of heaters, reaching a temperature near 200 ºC. The air/fuel mixture flowed through an adjustable turbulence generator, which produced turbulence intensities (TIs) ranging from 10% to 20% of the bulk flow velocity, independent of the bulk flow velocity. A premixed methane pilot flame was used for ignition and stabilization of the Bunsen burner flame.

Data were collected for three fuels (A2, C1, and C5), and test conditions included two pressures (1 and 0.7 atm), Reynolds numbers near 10,000, a range of equivalence ratios ($0.75 \leq \Phi \leq 1.0$), and TIs near 20%. Chemiluminescence imaging was performed under all conditions, and high-speed imaging was conducted for a subset of the tests. Chemiluminescence imaging was conducted using a 16-bit intensified charge-coupled device camera with a 1024 x 1024 pixel resolution and a 25 mm f/4.0 UV camera lens. For each flow condition (Re, Φ, and TI), data were typically collected over a 3-min period at 2 Hz.

The most important accomplishment of this activity was subatmospheric pressure testing (i.e., objective 1), which is important for relight conditions in engines at high altitudes. Figure **13** shows a photograph of a burner operating under subatmospheric conditions. Figure **14** shows measured turbulent consumption speeds for C1, C5, and A2 at 1 and 0.7 atm (left panel) and normalized turbulent consumption speeds (right panel). Note that the flame speeds increase as the pressure decreases, and a fuel sensitivity is observed between C1, C5, and A2. This trend indicates that the relight characteristics for C1, C5, and A2 may differ when an aircraft is at altitude. Further testing of practical systems is required to verify this postulate. It is also noted that although the turbulent consumption speed increases with decreasing pressure, the mass consumption rate of the fuel decreases with decreasing pressure (see Figure **15**), which is consistent with the literature.

The second objective was partially addressed by initiating a collaboration with Suresh Menon (GT). His team has simulated cold-flow conditions for a burner and plans to simulate the reacting flow. This collaboration is anticipated to serve as a baseline for evaluating the chemistry models created as part of the NJFCP program.

In the third activity (addressing objective 3), we evaluated a methodology for detecting the onset of local extinction events in the flame brush. Previously in this program, a fuel sensitivity to the onset of flame instability was detected based on large changes in the apparent turbulent flame speed. However, this flame evaluation technique is highly time-consuming, and it is difficult to relate the physics of flame speed measurements to local extinction. During this year, efforts were made to develop a better method to more readily determine breaks in the flame front. High-speed flame images were acquired, and analysis tools were developed to quantify the turbulent statistics of emissions from the flames. Figure 16 provides a representative image of a turbulent statistical parameter (i.e., integral length scale) that was evaluated as a potential metric of the onset of breaks in the flame front. We are currently using the shape of the radial intensity distribution as a marker of flame tip opening. Further testing is required to verify the validity of this approach.

During the fifth year, this task had very modest funding. Hence, we focused on completing data collection and analysis and on reporting and distributing the results. The completed and pending publications resulting from this period and work are shown below. The student funded by this project (Nathan Schorn) completed and defended his thesis.

Milestone(s)

- Nathan Schorn successfully defended his MS thesis.
- Three publications were prepared: two from Mr. Schorn's work and one from research performed by a previous student (Aaron Fillo).
- The experimental arrangement was used to support research for two undergraduate honors theses. One project focused on the manner in which fuel preheating alters flame speeds. The second project focused on measurements of the fraction of radiative heat released by a Bunsen flame with and without dilution.

Major Accomplishments

- Turbulent flame speeds were measured under atmospheric and subatmospheric conditions, exhibiting an evident fuel sensitivity.
- The flame extinction was found to be sensitive to fuel composition. This finding may be important for the program's lean blowout tasks, which aim to understand how ignition and extinction influence the lean blowout process.
- It was found that the surrogate fuel (S1) has flame speeds similar to that of Jet A fuel.

Figure 13. Photograph of a flame in a pressure vessel under subatmospheric conditions.

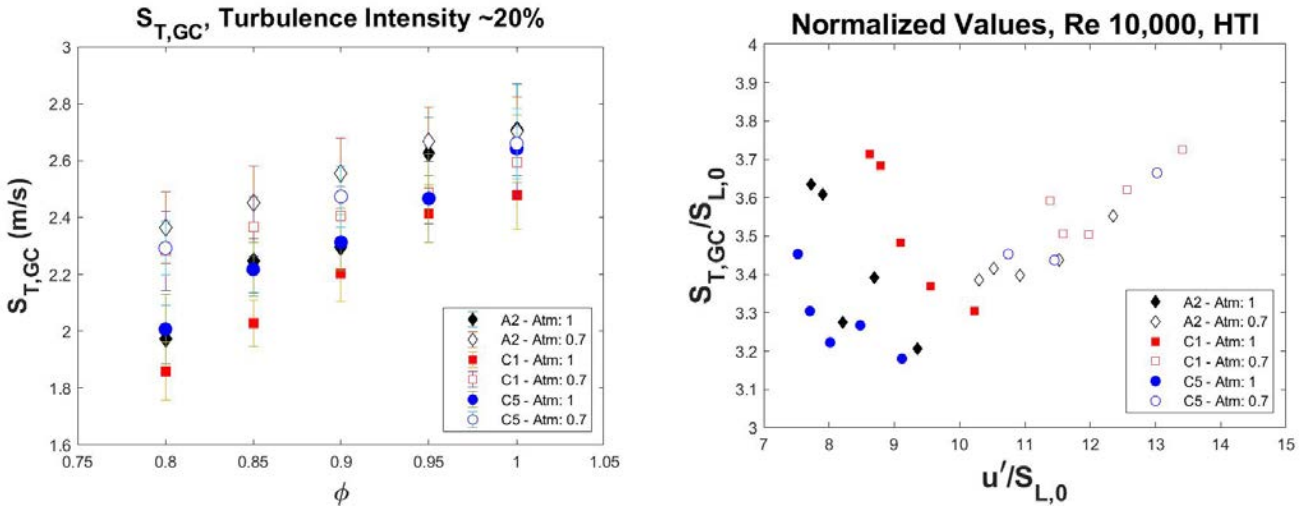

Figure 14. Turbulent consumption speeds (left) and normalized turbulent consumption speeds (right) for A2, C1, and C5 at 1 and 0.7 atm.

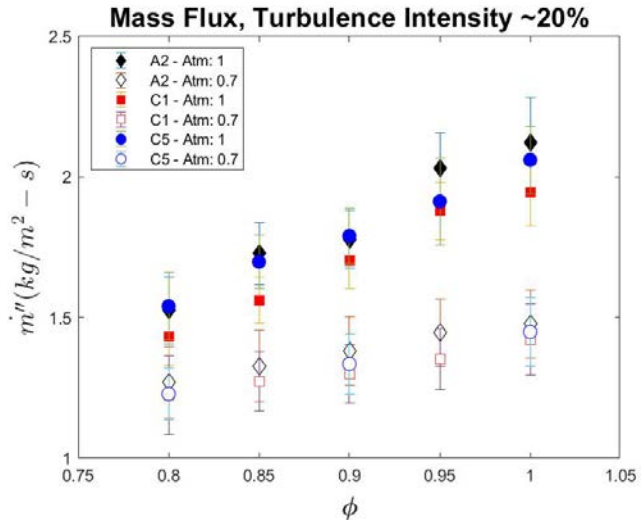

Figure 15. Mass consumption speeds of jet fuels at 1 and 0.7 atm.

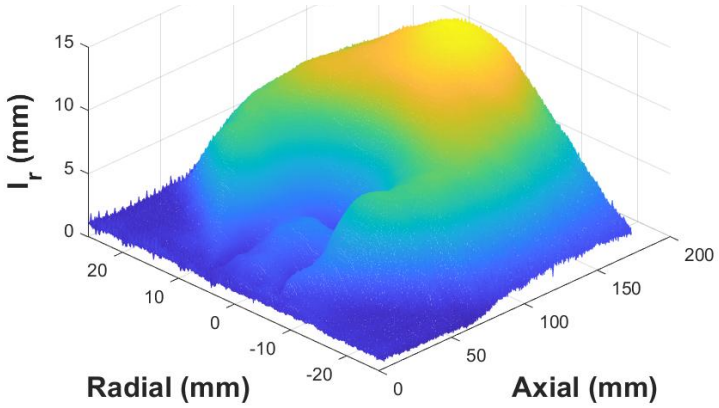

Figure 16. Radial integral length scale of visible light emissions from a turbulent Bunsen burner flame with A2 fuel. Such statistics have been considered as potential markers of the onset of openings in the flame brush.

Publications

Published conference proceedings

Schorn, N., Bonebrake, J., Pendergrass, B., Fillo, A., & Blunck, D. (2019). Turbulent consumption speed of large hydrocarbon fuels at sub-atmospheric conditions. AIAA Science and Technology Forum and Exposition 2019, San Diego, CA

Schorn, N., Blunck, D. "Flame Stability of Turbulent Premixed Jet Flames of Large Hydrocarbon Fuels," Western States Section Meeting of the Combustion Institute, (2017).

Fillo, A., Bonebrake, J., Blunck, D. "Impact of Fuel Chemistry and Stretch Rate on the Global Consumption Speed of Large Hydrocarbon Fuel/Air Flames," Western States Section Meeting of the Combustion Institute, (2017).

Fillo, A., Blunck, D., "Effects of Fuel Chemistry and Turbulence Intensity on Turbulent Consumption Speed for Large Hydrocarbon Fuels," Western States Section of the Combustion Institute, Fall 2015.

J. Bonebrake, A. Fillo, D. Blunck, "Effect of Turbulent Fluctuations on Radiation Emissions from a Premixed Flame," Western States Section Meeting of the Combustion Institute, Provo, UT (2015).

E. Zeuthen, D. Blunck, "Radiation emissions from Turbulent Diffusion Flames Burning Large Hydrocarbon Fuels," Western States Section Meeting of the Combustion Institute, Provo, UT (2015).

E. Zeuthen, D. Blunck, "Radiation Characteristics of Turbulent Diffusion Flames Burning Alternative Aviation Fuels," 9th US Combustion Meeting, Cincinnati, OH (2015).

Dissertations

Fillo, A.J., 2016. The Global Consumption Speeds of Premixed Large-Hydrocarbon Fuel/Air Turbulent Bunsen Flames.

Outreach Efforts

N/A

Awards

Fillo, A. (2016). The global consumption speeds of premixed large-hydrocarbon fuel/air turbulent Bunsen flames. Oregon State University, received a 2017 OSU Distinguished Master's Thesis Award.

Student Involvement

Jonathan Bonebrake, a PhD student, has helped to collect and analyze data. He also designed and built the subatmospheric pressure vessel and vacuum system.

Aaron Fillo, a PhD student, has worked tangentially on this project to analyze results and further investigate scientific phenomena.

Nathan Schorn, an MS student, has collected and analyzed data.

Multiple undergraduate students, including under-represented students, have worked with graduate students to operate the burner and to collect data, providing a significant opportunity for undergraduates to engage in research.

Plans for Next Period

The team from OSU will provide two remaining contributions. First, we will complete the publication process. One paper is currently under peer review, a second paper will be submitted by the end of December, and a third paper will be revised and resubmitted for peer review. As our second contribution, we will support the LBO book chapter as needed. Our team has previously provided content for the introduction to the LBO section, and we will gladly help to revise the introduction or provide new content as requested.

Project 029(A) National Jet Fuel Combustion Program – Area #5: Atomization Test and Models

Purdue University

Project Lead Investigator

Robert P. Lucht
Ralph and Bettye Bailey Distinguished Professor of Combustion
School of Mechanical Engineering
Purdue University
West Lafayette, IN 47907-2088
765-714-6020 (Cell)
Lucht@purdue.edu

University Participants

Purdue University

- PI(s): Robert P. Lucht, Jay P. Gore, Paul E. Sojka, and Scott E. Meyer
- FAA Award Number: COE-2014-29A, 401321
- Period of Performance: October 1, 2018 to September 30, 2019
- Tasks:
    1. Obtain phase Doppler anemometry (PDA) data across one plane in the variable ambient pressure spray (VAPS) test rig operated with the referee rig nozzle for numerous fuels under near-lean blowout (LBO) conditions and under cold fuel/cold air flow conditions approximating ground light-off (GLO) and high-altitude relight (HAR) conditions
    2. Extend PDA measurements to obtain data across multiple planes for an evaluation of detailed combustor simulations by Suresh Menon, Vaidya Sankaran, and Matthias Ihme
    3. Obtain PDA and/or Malvern measurements for selected operating conditions in the VAPS test rig to provide data for the spray correlation analysis of Nader Rizk
    4. Perform PDA measurements for fuel blends, including Fuel X and/or another blend designed for testing differences in atomization characteristics, to examine the sensitivity of correlations and computations to changes in fuel properties
    5. Ensure data quality through repeated tests at Purdue and through comparisons of spray measurements at Pratt and Whitney, the University of Dayton Research Institute/Air Force Research Laboratory, and the University of Illinois at Urbana/Champaign.

Project Funding Level

The funding level from the FAA was $120,000 for year 5. Purdue University provided cost-sharing funds in the amount of $120,000.

Investigation Team

- PI Dr. Robert Lucht, Bailey Distinguished Professor of Mechanical Engineering is responsible for overseeing the project at Purdue University. He is also responsible for mentoring one of the graduate students, coordinating activities with Stanford, working with all parties for appropriate results, and reporting results as required.
- Co-PI Dr. Jay Gore, Reilly Professor of Mechanical Engineering works closely with the PI and oversees the work performed by one of the graduate students. He is also responsible for interacting with the CFD groups to suggest comparisons with experiments and with results of an adaptive grid solver.
- Co-PI Dr. Paul Sojka, Professor of Mechanical Engineering is mentoring one of the graduate students and is responsible for supervising the spray measurements.

- Co-PI Scott Meyer, Managing Director of Maurice J. Zucrow Laboratories is responsible for coordinating facility upgrades and for performing facility design reviews.
- Graduate student Daniel Shin is responsible for performing the PDA measurements and for modifying the VAPS test rig for operation under near-LBO and cold start conditions. Graduate student Hasti Veeraraghava Raju has conducted simulations with an adaptive grid solver and has performed comparisons with experimental results and results from the other CFD groups. Graduate student Neil Rodrigues contributes to the project by providing advice for the PDA measurements and technical editing.

Project Overview

The objectives of this task, as stated in the Invitation for ASCENT COE Notice of Intent (COE-2014-29), are to "measure the spray characteristics of the nozzles used in the Referee Combustor used in Area 6 tests and to develop models for characterizing the atomization and vaporization of the reference fuels." We are conducting experiments within the joint experimental and modeling effort. The experimental tasks are being performed at Purdue University, and the modeling tasks are being performed by Prof. Matthias Ihme's group at Stanford University, Prof. Suresh Menon's group at Georgia Tech, and Vaidya Sankaran's group at United Technologies Research Center (UTRC). Nader Rizk is developing spray correlations based on the measurements.

Purdue University has highly capable test facilities for measuring spray characteristics over wide ranges of pressure, air temperature, and fuel temperature. The experimental diagnostics applied in this project include PDA and high-frame-rate shadowgraphy. The atomization and spray dynamics for multiple reference and candidate alternative fuels have been characterized for the referee rig nozzle operating under near-LBO conditions. In the future, measurements will be performed for these fuels under operating conditions characteristic of HAR. A new fuel, IH2 (Shell CPK-0), has been added to the test matrix and is being investigated under LBO and cold start conditions.

Task 1 - Measurement of Spray Characteristics under Near-Lean-Blowout and Chilled Fuel Conditions

Purdue University

Objective(s)

The objectives of this task are to visualize and measure the characteristics, including drop size distributions and axial velocity components, of sprays generated by a nozzle in the referee combustor in the Area 6 tests. The resulting data are being applied by Nader Rizk to develop spray correlations and by Matthias Ihme (Stanford University), Suresh Menon (Georgia Tech), and Vaidya Sankaran (UTRC) to develop a submodel for detailed computer simulations. The spray data are being shared with the FAA National Jet Fuel Characterization Program (FAA-NJFCP) team members for their interpretation and for the development of modeling, simulation, and engineering correlation-based tools.

An upgraded VAPS test rig at Purdue University is utilized to measure spray characteristics over a range of pressures, atomizing gas temperatures, and fuel temperatures. Our work has led to the identification of challenges associated with performing reliable and reproducible spray measurements while keeping the windows of the apparatus clean. PDA has emerged as the technique of choice for obtaining drop size distribution and axial and radial velocity data for comparison with numerical simulations. The VAPS facility was upgraded to support experiments over the entire range of fuel and air temperatures and pressures of interest. We have compared reacting and nonreacting spray data by collaborating with the UIUC/UDRI/AFRL Area 6 team.

The experimental data have supported the continued development and evaluation of engineering spray correlations, including the dependence of the Sauter mean diameter, spray cone angle, and particle number density per unit volume on the fuel properties at the fuel and air temperatures of interest. The experimental data provide detailed statistical measurements for comparison with high-fidelity numerical simulations of mixing and combustion processes. The predicted spatial distribution of the liquid fuel and of the resulting vapor and breakdown components from the liquid fuels critically affects the ignition, flame stabilization, and pollutant formation processes.

The project objectives are summarized as follows:

1. Obtain PDA data across different planes in the VAPS test rig operating with the referee rig nozzle for numerous fuels under near-LBO conditions and under cold fuel/cold air flow conditions approximating GLO and HAR conditions
2. Provide data to the research groups of Suresh Menon, Vaidya Sankaran, Matthias Ihme, and Jay Gore for simulations
3. Conduct PDA measurements for selected operating conditions in the VAPS test rig to provide data for the spray correlation analysis of Nader Rizk
4. Perform PDA measurements for fuel blends, including Fuel X and/or another blend designed for testing differences in atomization characteristics, to examine the sensitivity of correlations and computations to changes in fuel properties
5. Ensure data quality through repeated tests at Purdue and through comparisons with spray measurements at P&W, UDRI/AFRL, and UIUC

Research Approach

The Purdue University VAPS test rig facility is designed to measure spray characteristics over wide ranges of pressure, atomizing gas temperature, and fuel temperature. Liquid fuels can be supplied to the test rigs by multiple systems. A facility-integrated system draws fuel from one of two certified flame-shield fuel containments to test standard aviation fuels as well as alternative blends. A mobile fuel system, developed under the combustion rules and tools (CRATCAF) program and redeployed during the first year of the NJFCP program, is being utilized for further control of additional injector circuits and for supplying alternative fuel blends. Both systems were designed with two independently controlled and metered circuits to supply fuel to the pilot and main injector channels of the test injector. The mass flow rates of both fuel supplies are measured with Micro Motion Elite® Coriolis flow meters. A nitrogen sparge and blanket ullage system is used to reduce the dissolved oxygen content of the fuel, which is monitored by a sensor immediately upstream of the fuel control circuits. High-pressure gear pumps provide fuel at rates of up to 30 kg/hr, which is supplied to the control circuits at a regulated line pressure of 10 MPa. The mobile fuel system was built with two onboard heat exchangers, and a chilling unit controls the fuel temperature over a range of 193–263 K (-80 ºC to -10 ºC).

Milestone(s)

The tasks performed in FY2019 are listed below:

Quarter 1

1. The VAPS test rig and PDA system were moved to the new High-Pressure Combustion Laboratory.
2. A new stand for the VAPS test rig was designed and fabricated.
3. A new exhaust pipe line for the VAPS test rig was designed for installation in the new test cell.
4. Modifications and insulation were applied to the major facility nitrogen lines for the pressure vessel and airbox flows.
5. The expansion of the data acquisition and control system (DACS) in the new test cell was initiated.
6. The chapter on spray measurements for the American Institute of Aeronautics and Astronautics (AIAA) NJFCP book was edited and revised.
7. Daniel Shin published an AIAA SciTech 2019 paper on the cold start spray measurements and presented this work at the SciTech conference in San Diego on January 10, 2019.
8. Fuel sensitivity in LBO trends was successfully demonstrated with a flamelet-based combustion model, and the computational time was reduced by 60% compared with detailed chemistry simulations.
9. “LBO simulations and flame structure analysis with detailed chemistry and FGM model” was presented orally at the NJFCP review meeting in Cleveland, Ohio.
10. The need for detailed flow and combustion measurements was identified for computational model evaluations and was discussed in detail at the NJFCP review meeting.

Quarter 2

1. Modifications and improvements of the DACS for the VAPS test rig in the new test cell were completed.
2. The chapter on spray measurements for the AIAA NJFCP book was edited and revised.
3. Manuscripts describing the results of LBO and cold start measurements were prepared for submission to the *AIAA Journal of Propulsion and Power* and the *AIAA Journal*, respectively.
4. Domain sensitivity analyses were initiated in CFD calculations.
5. Further detailed analysis of the flame structure were performed using the flamelet-generated manifold (FGM) combustion model.

Quarter 3

1. A new design for vessel window port orientation (90-degree angle between windows) was proposed for planar laser-induced florescence (PLIF), structured laser illumination planar imaging (SLIPI), and PIV imaging measurements.
2. A manuscript on LBO measurements was submitted to the *AIAA Journal of Propulsion and Power*.
3. The chapter on spray measurements for the AIAA NJFCP book was edited and revised.
4. A CFD model for simulating the actual size of the test rig plenum was developed.
5. The finite-rate chemistry (FRC) model employed for LBO simulations was validated using CARS measurements for temperature and species and using PIV measurements for velocity in a laboratory turbulent jet flame.
6. A manuscript was prepared and submitted to the *Journal of the Energy Institute* on FRC model validation.
7. Chemical pathway analyses were initiated for flames under turbulent conditions.

Quarter 4

1. A new vessel window design was implemented to enable PLIF, SLIPI, and PIV measurements of the spray structure and dynamics.
2. A manuscript for LBO measurement was accepted by the *AIAA Journal of Propulsion and Power* and is currently in press.
3. A manuscript on the cold start measurements was prepared for submission to the *AIAA Journal*.
4. The AIAA book chapter was revised.
5. LES simulations were performed for the domain sensitivity.
6. The manuscript on FRC simulations was revised based on feedback from the reviewers, and a revised version was then submitted to the *Journal of the Energy Institute*.
7. A methodology for constructing quantitative reaction pathways was established to study the chemical pathways under turbulent conditions using the atmospheric jet flame LES results.

Major Accomplishments

Experimental contributions

The work described in this section is part of the Purdue contribution to a larger FAA-funded effort, NJFCP. The major objective of the work at Purdue was to measure spray properties (droplet size, droplet velocity, spray cone angle) for a variety of jet fuels and candidate jet fuels under a wide range of conditions, including LBO and GLO conditions. These measurements were successfully performed last year using PDA, which provided single-point measurements of the spray. For a more detailed investigation of the spray using two-dimensional (2D) planar imaging, PLIF and SLIPI were proposed, which required a significant modification of the test rig. The remainder of this section presents the process of the test rig modification for the new High-Pressure Combustion Laboratory test cell at Purdue.

Experimental systems

The Purdue VAPS test rig comprises two major components: the airbox assembly and the pressure vessel. The airbox assembly is a length of pipe in which the hybrid air-blast pressure-swirl atomizer is mounted. The airbox is placed within the pressure vessel, which allows a pressurized atomizing gaseous flow through the airbox to be isolated from the vessel to create a pressure difference across the gas swirler. The pressure vessel is rated to withstand 4.14 MPa (600 psi) at 650 ˚C (1200 ˚F). The vessel originally had four windows in a single horizontal plane, which allowed laser diagnostic measurements to be performed within the test section. Figure 1 shows schematic diagrams of the previous window system and the new window system. The original window system included two diametrically opposed 114-mm window ports and two 64-mm window ports at a 60˚ angle with respect to one of the 114-mm ports. This window system was modified to include three 114-mm window ports, with one port oriented at a 90˚ angle with respect to the diametrically opposed 114-mm window ports, and one of the 63.5-mm window ports was removed. This new window system allows PLIF and SLIPI measurements, which can provide a 2D representation of the spray rather than the point measurements produced by PDA.

A mobile fuel system was used to supply pressurized fuel to the injector mounted on the airbox. The mobile fuel system had a chiller unit with two heat exchangers to chill the fuel to the desired temperature. This mobile fuel system was redesigned and integrated with the new stand for the VAPS test rig, as shown in Figure 2. The fuel control and supply system panels were reproduced from the mobile fuel system and were integrated into the VAPS test rig stand. Additionally, the chiller unit and two heat exchangers were removed from the test cell and reinstalled outside the test cell.

Figure 3 shows a photograph of the integrated VAPS test rig. The window purge manifolds are attached, and the flow lines for the airbox and vessel nitrogen flows are connected to the VAPS rig. The DACS box is also attached to the stand for measurement sensors, such as pressure transducers and thermocouples.

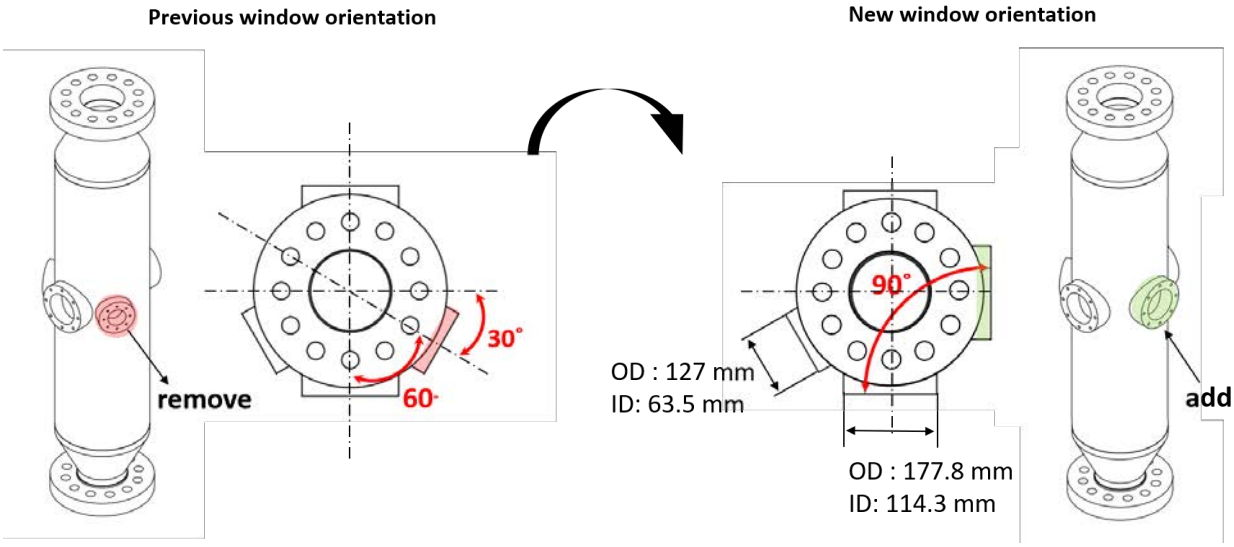

Figure 1. Schematic diagrams of the previous and modified window systems in the variable ambient pressure spray (VAPS) test rig.

Figure 2. Photographs of the modified fuel supply system integrated into the variable ambient pressure spray (VAPS) test rig stand.

Figure 3. Photograph of the variable ambient pressure spray (VAPS) test rig.

Proposed PLIF and PDA configuration

PLIF was proposed to provide 2D spray visualization and more qualitative measurements of the liquid volume distribution. PLIF is a powerful measurement technique and is widely used in spray and combustion applications requiring knowledge of the liquid and vapor phase concentrations and 2D representations of the flame and spray. In PLIF, a laser sheet illuminates the flow and excites the ground-state fluid molecules to a higher electronic energy state. The excited molecules then de-excite and emit light at a longer wavelength. A tracer species, such as a florescent dye, may be added to the fluid or may naturally be present in the fuel, such as aromatic hydrocarbon in fuels. The population of tracer species in a unit volume of the fluid is directly proportional to the fluorescence signal, which allows us to measure the concentration or mass distribution of the spray. The spray cone angle can also be measured from the 2D spray image. Time-resolved imaging of the spray measurement is possible with high laser pulse rates (10 kHz or higher), which enables an investigation of the time dependence of the spray regime characteristics. Figure 4 shows the proposed PLIF and PDA systems installed near the VAPS test rig. Each measurement will be performed separately under LBO conditions for the A2 fuel.

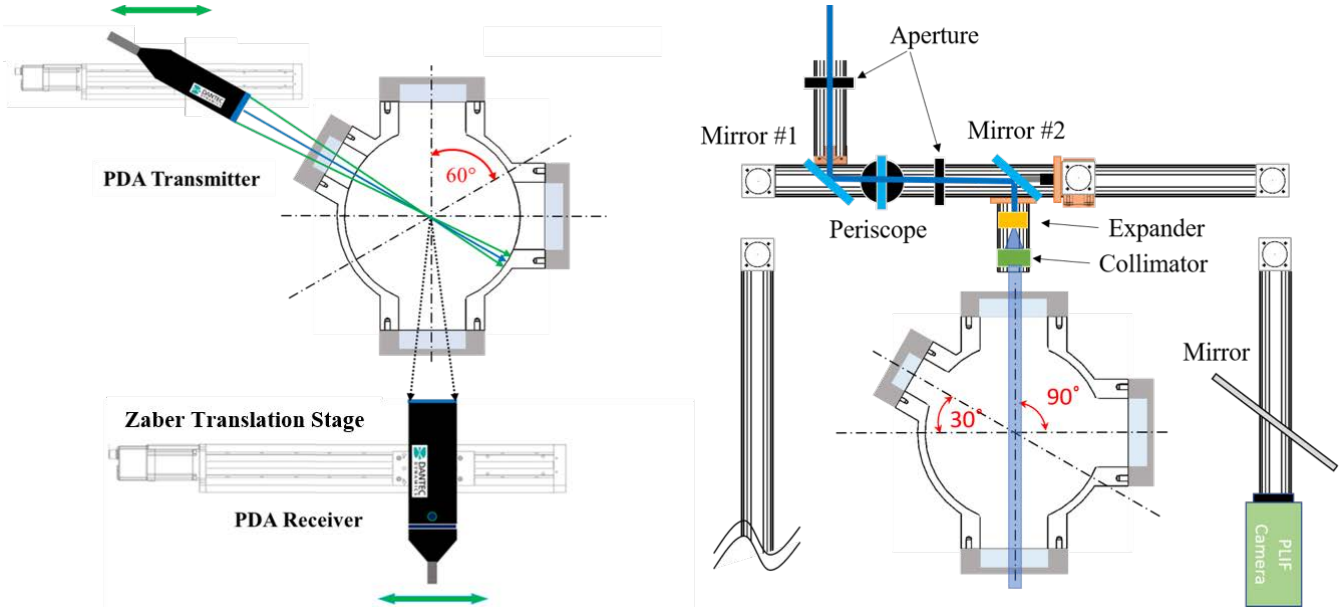

Figure 4. Proposed phase Doppler anemometry (PDA) and fuel planar laser-induced fluorescence (PLIF) measurement system for the variable ambient pressure spray (VAPS) rig.

Computational contributions

The following section describes the computational efforts in predicting the fuel sensitivity of LBO in the referee combustor. The CFD model developed for LBO calculations is illustrated in Figure 5. The flow through all passages, including minute effusion holes on the liners, is resolved in this CFD model. The computational grid for flow simulations with all passages open is shown in Figure 6. The grid is locally refined in the regions with the steepest gradients and is relatively coarse in sections with weaker gradients, based on adaptive mesh refinement (AMR).

Reacting LES simulations were performed for the referee combustor using the finite volume-based compressible CFD solver CONVERGE (Convergent Science Inc., 2017). The gas-phase equations are described with a Eulerian approach, and the liquid spray is modeled with discrete injections of droplets using a Lagrangian approach. The subgrid stress tensor terms in the momentum equations are modeled using a non-viscosity-based one-equation model to obtain closure (Pomraning & Rutland, C.J., 2002). The combustion process is modeled using the FGM method, which has been successfully employed to predict phenomena such as flame extinction and reignition in spray flames (El-Asrag et al., 2016; Elasrag & Li, 2018; Ihme et al., 2005; Ihme & Pitsch, 2008; Ma et al., 2019; van Oijen et al., 2016). A compact kinetic mechanism based on fuel surrogates is used to represent chemical reactions (Hasti et al., 2018). The FGM model accounts for the effects of turbulence on the reaction rates via a joint PDF of the mixture fraction, the mixture fraction variance, and a reaction progress variable. A fully automated on-the-fly meshing strategy combined with the cut-cell Cartesian method and AMR was employed, and the mesh parameters were selected based on a previous grid sensitivity study (Hasti et al., 2018). Additional mesh evaluation studies for the present reacting flow conditions demonstrated that more than 90% of the turbulent kinetic energy is resolved. Additional details on the boundary conditions and the spray can be found in reports by Hasti et al. (2018; 2018).

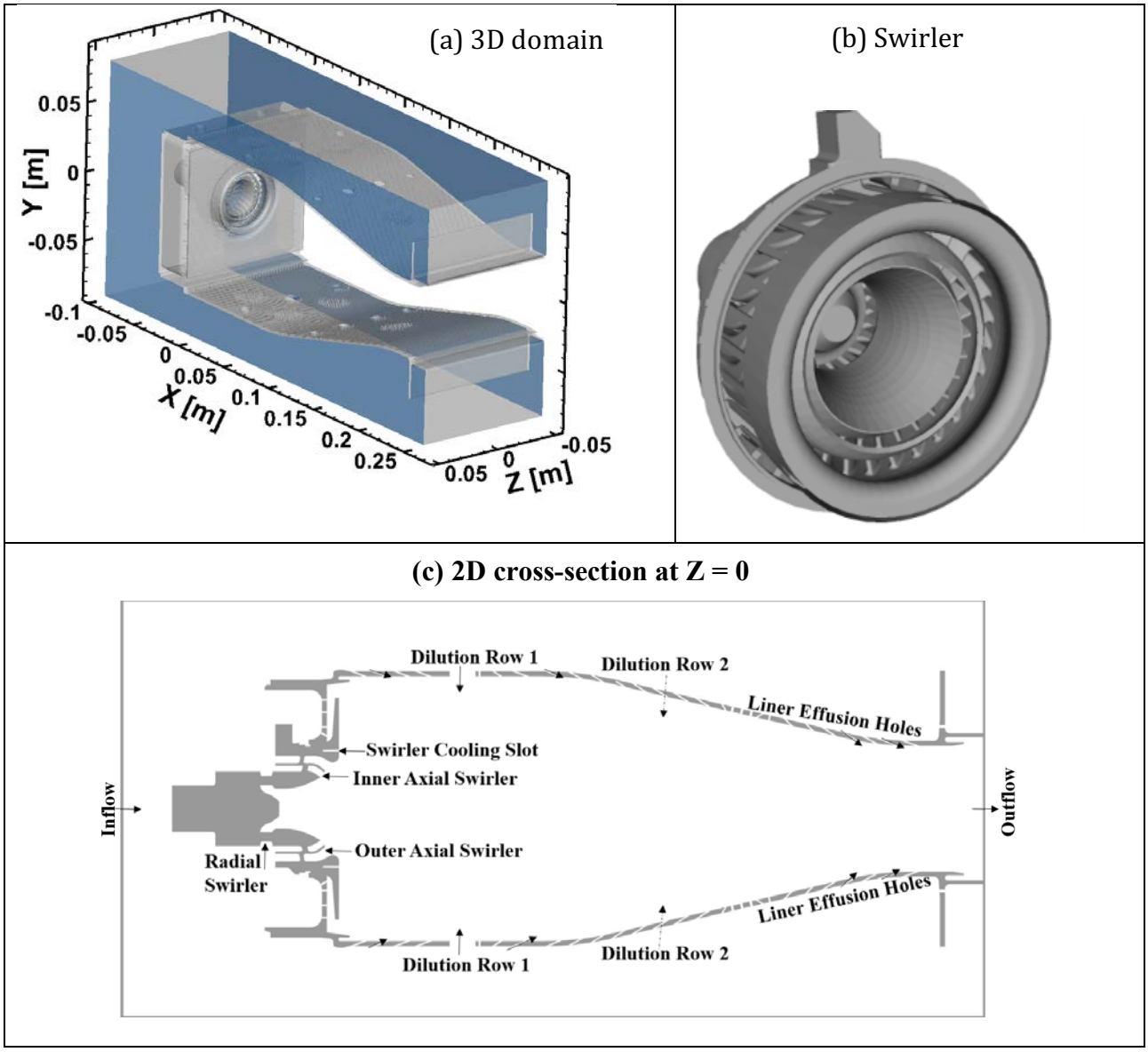

Figure 5. (a) 3D computational domain, (b) magnified view of the 3D swirler, and (c) magnified view of the 2D cross-section at Z = 0 (mid-plane).

The spray is represented by an ensemble of six ring injectors, each with prescribed cumulative distribution functions for the droplet diameter, average velocity, cone angle, mass flow rate, and parcel number. The spray boundary conditions (droplet diameter, average velocity, and cone angle) at 2 mm from the nozzle exit are obtained from the PDA measurements (see measurement details in our experimental contribution section) at 25.4 mm from the deflector plate (Bokhart et al., 2017; Bokhart et al., 2018). An ensemble of six ring injectors, each with its own droplet size and velocity distribution, represents the nozzle. Taylor analogy secondary breakup and dynamic drag models are employed to estimate the secondary breakup and resulting spray droplet dynamics. A droplet dispersion model is used to include the effects of the sub-grid-scale flow field on the discrete parcels. The droplet evaporation rates are calculated using the Frossling correlation based on the laminar mass diffusivity of the fuel vapor, mass transfer number, and Sherwood number. The prescribed fuel properties are set as those determined for the A2 and C1 fuels.

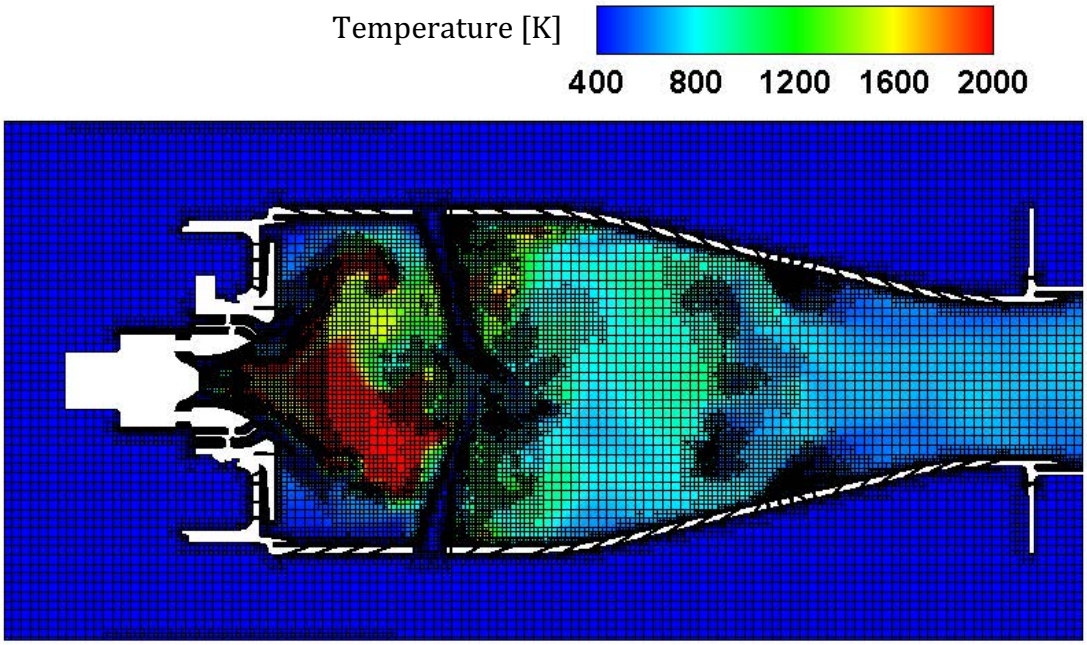

Figure 6. Computational grid with adaptive mesh refinement (AMR) on the mid-plane (Z = 0) of the referee combustor for a reacting case with the flamelet-generated manifold (FGM) combustion model, with colored temperature [K] contours.

LES simulations were performed for a global equivalence ratio of 0.096, which was experimentally found to produce stable combustion. From this condition, the fuel flow rate is reduced in a gradual stepwise manner; larger time steps are initially applied, and the flow rate steps are progressively reduced as impending blowout behavior is observed, as shown in Figure 7. The simulations are run with a fixed global equivalence ratio for at least two flow-through durations, estimated as approximately 30 ms. The fixed equivalence ratio is maintained beyond 30 ms if a quasisteady heat release rate is not reached within either of those limits. The heat release rate is used as a criterion for identifying the LBO. The global equivalence ratio steps resulting from this process are plotted in Figure 7 as a function of time for fuel A2 (left) and C1 (right). The experimental data shown by red filled circles indicate that the C1 fuel (right) blows out at a higher equivalence ratio than the A1 fuel (left).

Reacting spray comparison under near-LBO conditions

Spray statistics were collected via LES calculations at a stable operating point over a period of two flow-through durations. The averaging process over two flow-through durations is started after the flame and heat release rate reach a quasisteady state. Figure 8 shows the experimental (Mayhew et al., 2017) and predicted droplet statistics as a function of radial distance for the FRC and FGM combustion models at four axial stations. The fuel spray exhibits a pattern, with smaller-diameter droplets near the hollow cone surface 10 mm downstream of the nozzle exit. This distribution widens in the radial direction toward the downstream locations, with larger droplets towards the center and smaller droplets in the outer regions. The two combustion models satisfactorily capture this trend for both fuels, and better agreement with the experiments is observed for the downstream locations. The axial and radial velocities increase away from the center and decrease with increasing spray cone angle. These trends are accurately captured for the near-nozzle regions as well as in the downstream regions for both fuels. Overall, the Lagrangian spray setup can accurately capture the spray breakup and evaporation.

Flame shape comparison

OH* chemiluminescence data from the UIUC experiments (Mayhew et al., 2017) were utilized to compare the line-of-sight average OH mass fraction from LES simulations for four kinetic mechanisms and two combustion models. The results for detailed, skeletal, reduced, and compact mechanisms are displayed in Figure 9 alongside the experimentally observed OH* chemiluminescence. The results from the detailed, skeletal, and reduced mechanisms are qualitatively similar, and the

experimental data (OH* chemiluminescence) and detailed mechanism calculations (OH) show similar spreads in the radial and axial directions. However, it must be noted that these comparisons are qualitative in nature. The experimental images are based on false color and do not indicate a quantitative measurement of the OH field. The horizontal position of 0 mm corresponds to the deflector plate. OH formation marks the high-temperature heat release region, which extends 50 mm downstream of the deflector plate and also corresponds to the downstream location of the first row of dilution holes. This area is the stable region of the swirl-stabilized flame and exhibits a truncated cone shape, with regions of high OH/heat release corresponding to the cone angle of the hollow spray cone. This trend indicates strong burning and heat release near the spray cone surface downstream of the swirl cup. The A2 fuel exhibits a higher degree of asymmetry in OH* for this configuration and measurement. These regions of intense heat release are qualitatively captured by all four chemistry mechanisms. The flame shape computed for the FGM combustion model shows a stronger and larger reaction zone compared with the FRC model.

LBO approach

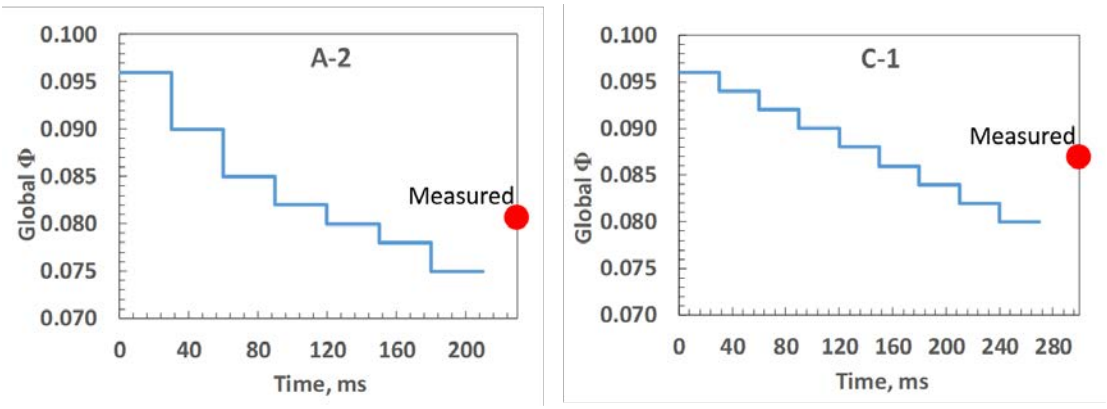

Figure 7. Staged fuel ramp-down approach for lean blowout (LBO) prediction. The red dot represents the measured LBO global equivalence ratio.

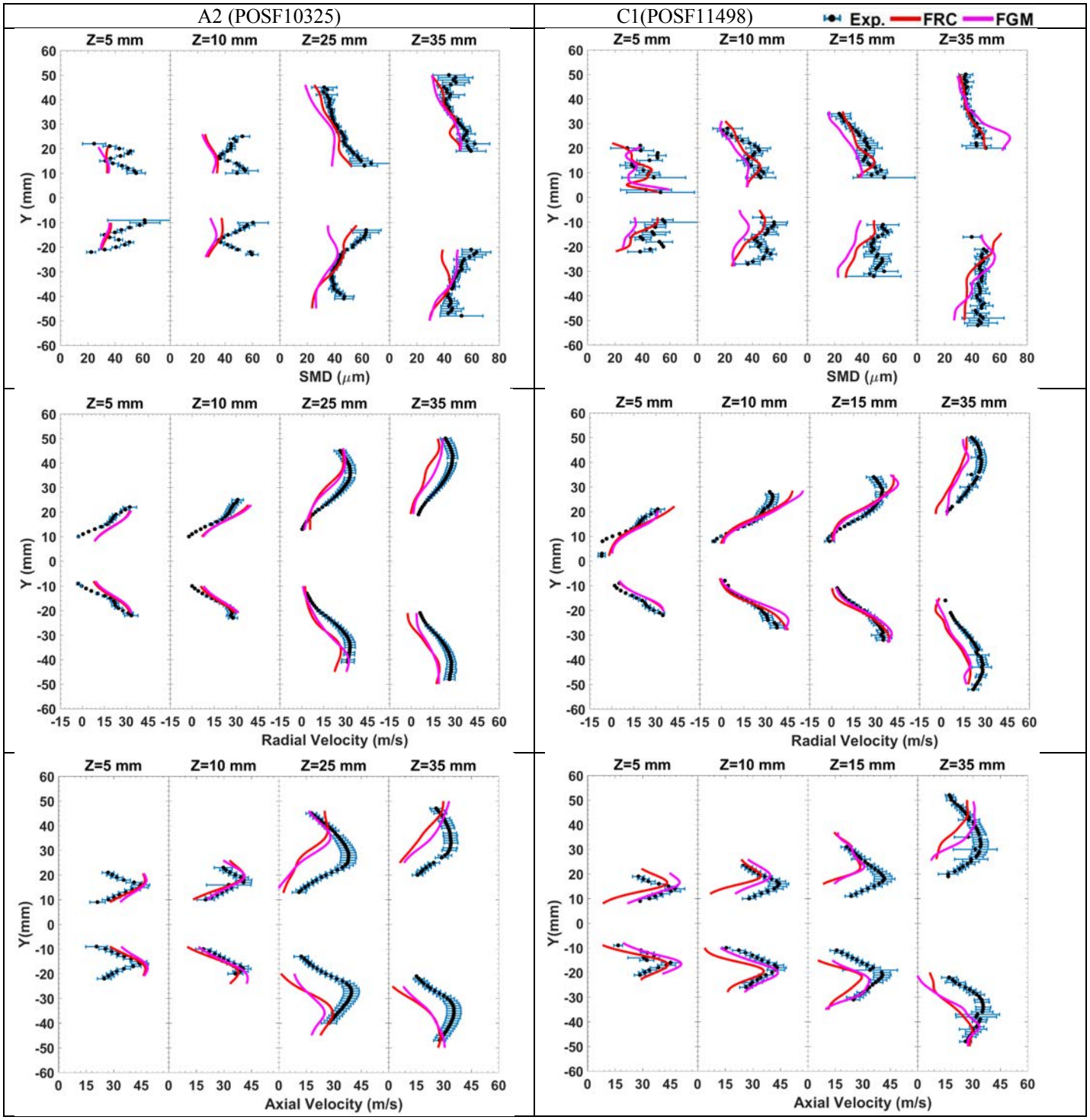

Figure 8. Comparison of spray statistics and phase Doppler anemometry (PDA) data (Mayhew et al., 2017) for a stable flame at $\phi = 0.096$.

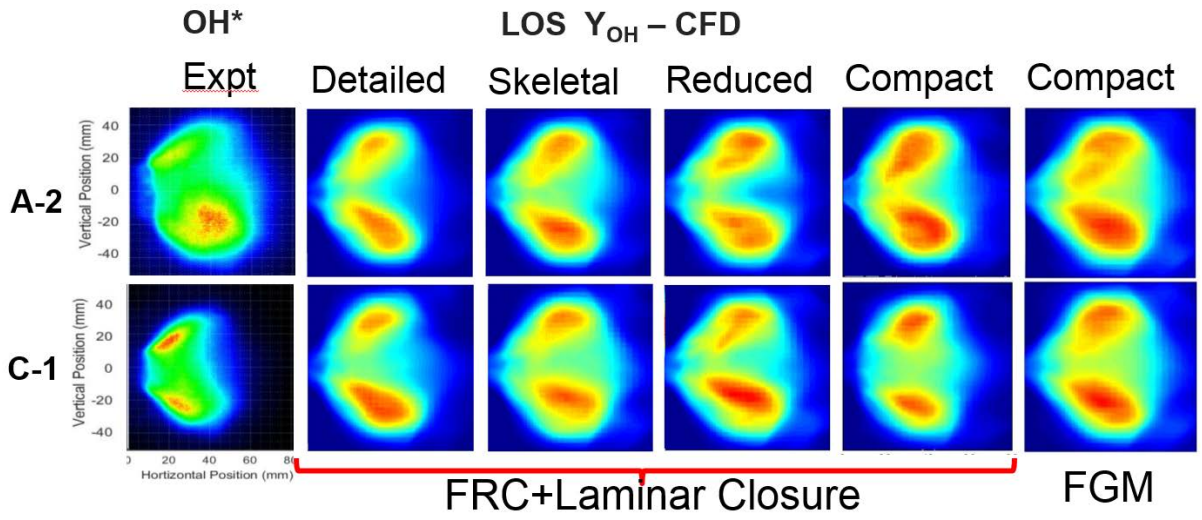

Figure 9. Line-of-sight average OH mass fraction obtained from LES compared with experimental OH* obtained from chemiluminescence.

The computed velocity, temperature, and mean OH mass fraction contours are compared for the FRC and FGM combustion models in Figure 10. The results for the FRC model show a pointed flame root and a smaller reaction zone, whereas the FGM model results show a stronger flame root and a much larger reaction zone. However, experimental validation data would be highly beneficial to verify the computational model results and to guide further enhancements in the model.

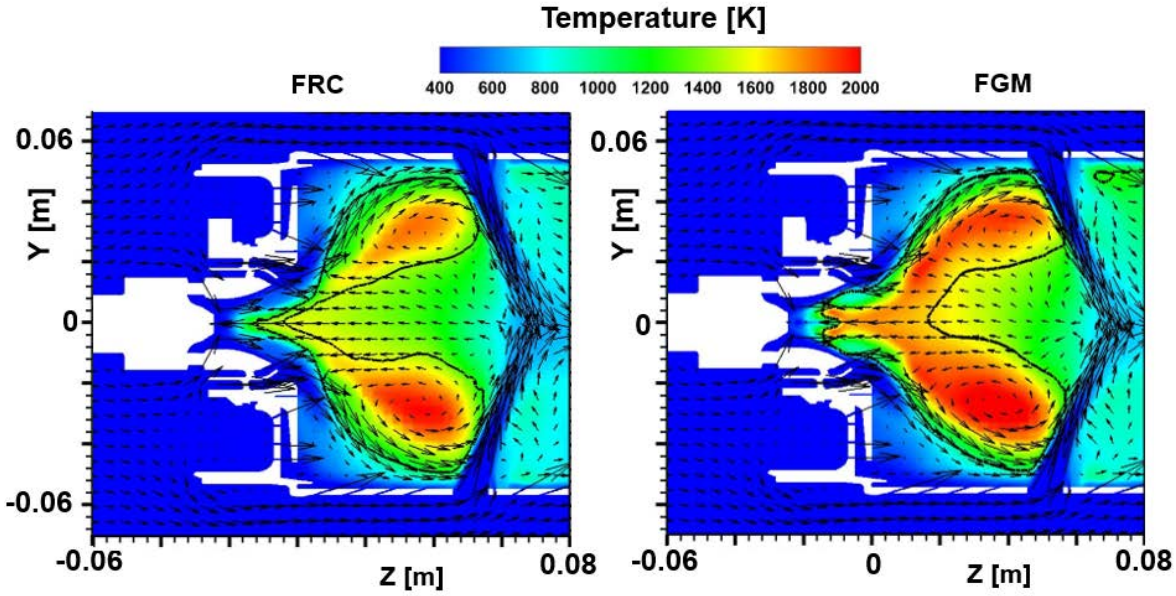

Figure 10. Comparison of temperature (filled contours), velocity (vectors), and an isocontour for a mean OH mass fraction of 5e-04 (black line) for C1 fuel.

Heat release rate

The evolutions of the heat release rate for varying equivalence ratios and for two fuels under the FGM combustion model are shown in Figure 11. The flame is initially stable; subsequently, a steady decrease followed by a sharp reduction in the heat release rate is observed for both the A2 and C1 fuels. The heat release rates are allowed to reach a steady state prior to the next step. In this figure, the dotted black line shows the mean heat release rate, and the dotted pink line shows the ideal heat release rate.

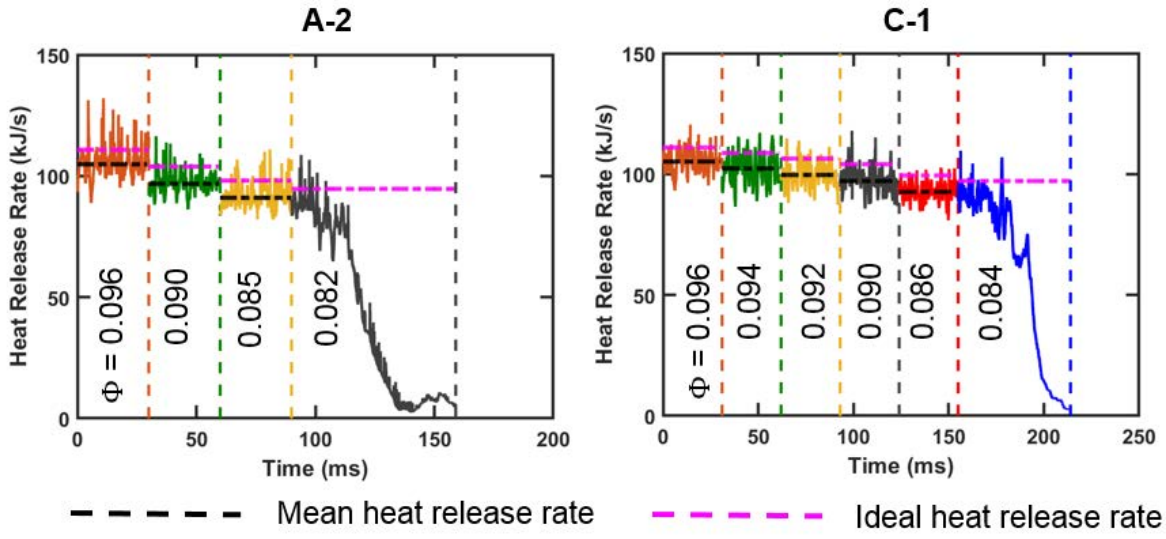

Figure 11. Heat release rate under the flamelet-generated manifold (FGM) combustion model.

LBO equivalence ratio comparison

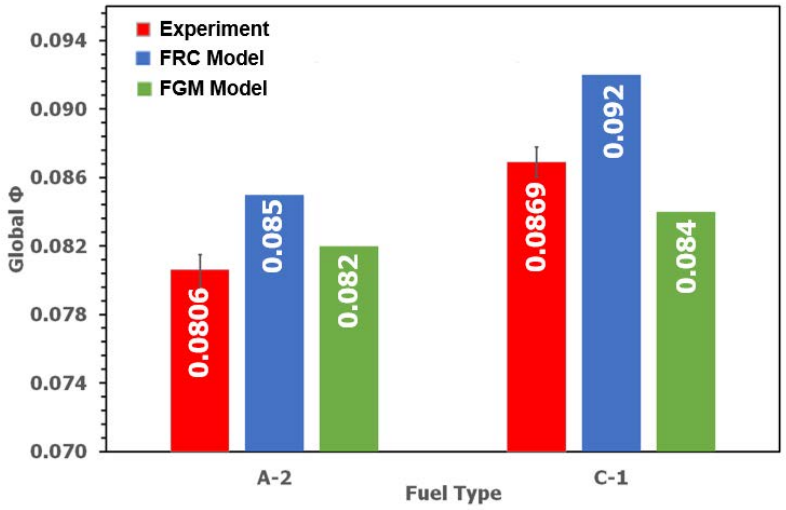

Figure 12. Comparison of lean blowout (LBO) equivalence ratios from experiments and LES, including results from detailed chemistry and the flamelet-generated manifold (FGM) combustion model.

The LBO trends for both fuels are compared with experimental results in Figure 12. The C1 fuel blows out at a higher equivalence ratio compared to A2 in the experiments. This LBO dependence on the fuel's physical and chemical properties is very complex. The simulations with the FRC and FGM combustion models can qualitatively capture the LBO trend and relative behaviors for each fuel. However, the FGM model predicts that LBO will occur at a lower equivalence ratio compared to the FRC model due to the stronger flame root and larger reaction zone, as shown in Figures 9 and 10.

Analysis of scalars in the primary zone

As shown in Figure 13, a control volume within the primary zone of the combustor was chosen for scalar analysis in an effort to understand the LBO mechanism and to identify the precursors for early detection of incipient LBO conditions. The volume-averaged equivalence ratio, temperature, and mass fractions of OH and CH_2O (HCHO) are shown in Figure 14. Under near-stable flame conditions, all variables decrease with time. During LBO, as the equivalence ratio decreases, the temperature and OH decrease, but the CH_2O concentration increases due to partial oxidation. A similar trend towards the onset of LBO has been observed experimentally at Cambridge for a swirl-stabilized laboratory combustor (Giusti & Mastorakos, 2017).

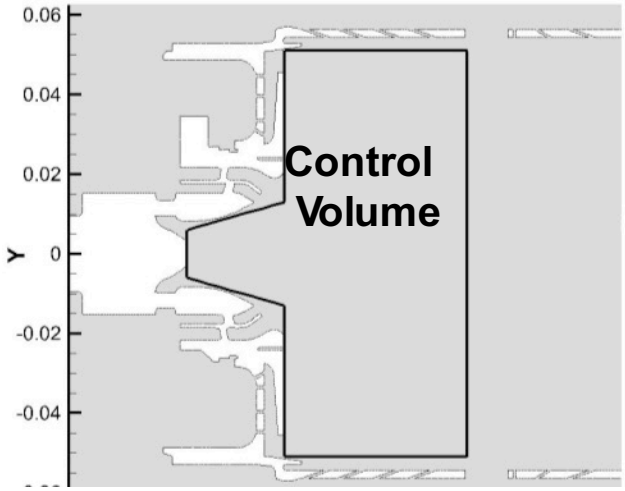

Figure 13. Sampling region within the primary zone for investigating the combustion process during lean blowout (LBO).

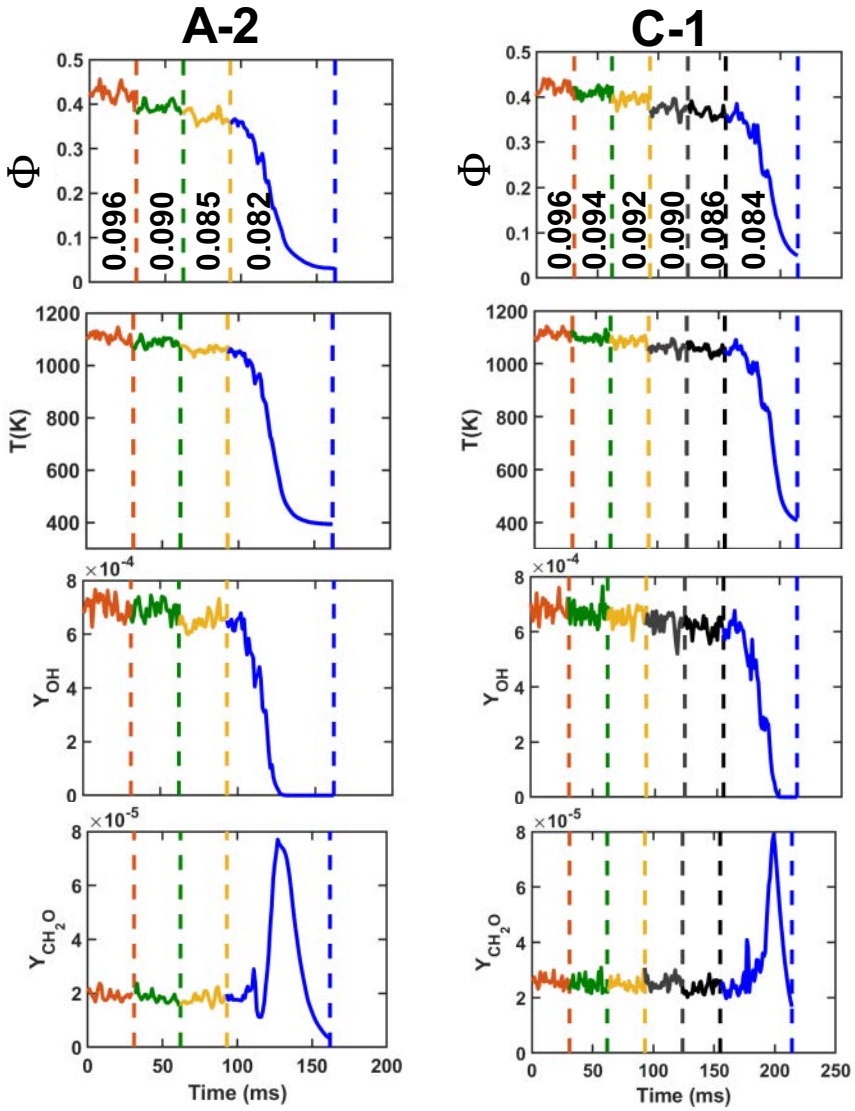

Figure 14. Comparison of lean blowout (LBO) equivalence ratios obtained from experiments and LES, including detailed chemistry and the flamelet-generated manifold (FGM) combustion model.

Domain sensitivity study

The previous LES simulations were performed with a reduced plenum size and excluded bypass air passages near the combustor exit. The air flow rate at the domain inlet was also reduced to account for these excluded bypass passages. However, it would be beneficial to clarify the effect of plenum size on the air flow splits and the resulting combustor flow field. During 2019, we initiated efforts to model the actual size of the plenum in the rig hardware and included all bypass air passages near the combustor exit. Computational modeling of the actual plenum size with all combustor passages has been completed, and these new simulations will be applied with the actual rig inlet air flow rate of 391.4 g/s at the computational domain inlet. The reduced and actual plenum domains are compared in Figure 15. A domain sensitivity study was performed under nonreacting conditions, and LES simulations were completed during the 4th quarter of 2019. These results will be analyzed during the 1st quarter of 2020. Reacting LES simulations and LBO computations will be performed based on the domain impact on the flow splits and combustor flow field.

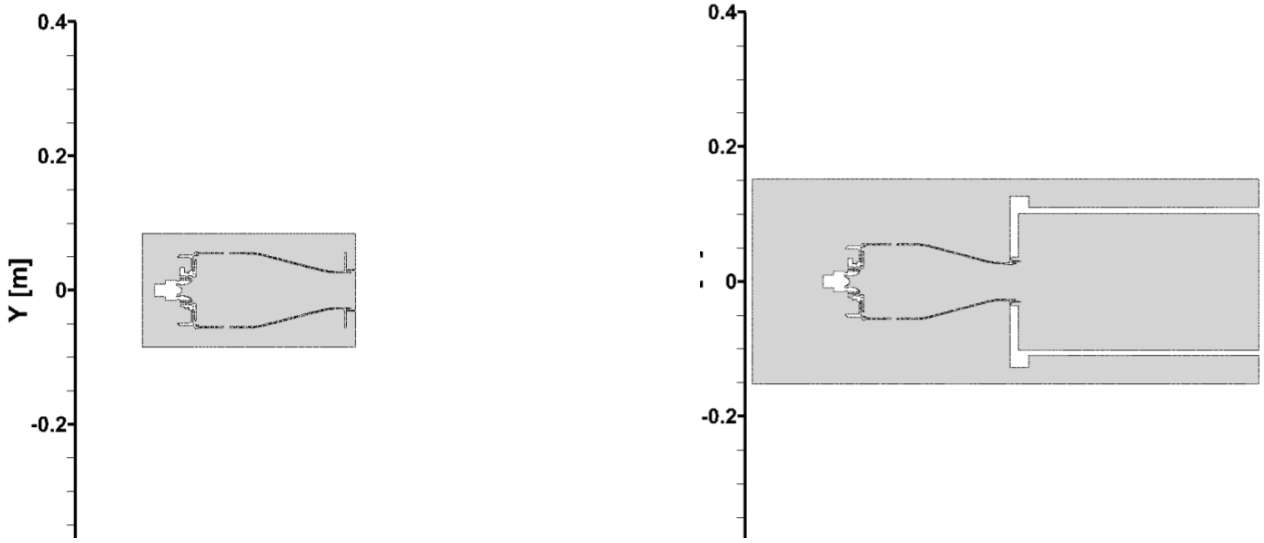

Figure 15. Comparison of computational domains with the reduced (left) and actual plenum (right) size.

Publications

Peer-reviewed journal publications

Feyz, M., Hasti, V.R., Gore, J.P., Chowdhury, A., & Nalim, R. (2019). Scalar predictors of premixed gas ignition by a suddenly-starting hot jet. International Journal of Hydrogen Energy, Volume 44, Issue 42, Pp:23793-23806, https://doi.org/10.1016/j.ijhydene.2019.07.066

Feyz, M., Hasti, V.R., Gore, J.P., & Nalim, R. Analytical and numerical approach to near-field ignition of H2/air by injection of hot gas. Submitted to Combustion and Flame, 2019.

Feyz, M., Hasti, V.R., Gore, J.P., & Nalim, R. (2019). Large eddy simulation of hot jet ignition in moderate and high-reactivity mixtures. Computers and Fluids, 183, pp:28–37, https://doi.org/10.1016/j.compfluid.2019.03.014

Feyz, M., Nalim, R., Hasti, V.R., & Gore, J.P. (2019). Modeling and analytical solution of the near-field entrainment in starting turbulent jets. AIAA Journal, pp: 1-8, https://doi.org/10.2514/1.J057612

Feyz, M., Nalim, R., Hasti, V.R., & Gore, J.P. (2019). Statistical analysis of scalars for ignition via transient hot jet. 11th US National Combustion Meeting, Pasadena, CA 91101 USA

Hasti, V.R., Lucht, R.P., & Gore, J.P. (2019). Large eddy simulation of hydrogen piloted CH4/air premixed combustion with CO_2 dilution. Journal of the Energy Institute, https://doi.org/10.1016/j.joei.2019.10.004.

Hasti, V.R., Navarkar, A., & Gore, J.P. Optimal sensor location for early detection of incipient lean blowout condition in a realistic gas turbine engine using support vector machine. Submitted to the Proceedings of the Combustion Institute, 2019 (38th International Symposium on Combustion).

Hasti, V.R., Navarkar, A., & Gore, J.P. A hybrid convolutional autoencoder – support vector machine model for early detection of lean blowout onset in a realistic gas turbine combustor. Manuscript under preparation for submission to Energy Conversion and Management. 2020

Shin, D., Bokhart, J.A., Rodrigues, N.S., Sojka, P., Gore, J.P., & Lucht, R.P. (2019). Non-reacting spray characteristics for alternative aviation fuels at near lean blowout conditions. AIAA Journal of Propulsion and Power. Accepted for publication.

Published conference proceedings

Bokhart, J.A., Shin, D., Gejji, R., Buschhagen, T., Naik, S.V., Lucht, R.P., Gore, J.P., Sojka, P.E., & Meyer, S.E. (2017). Spray measurements at elevated pressures and temperatures using phase doppler anemometry. Presented at the 2017 AIAA SciTech Meeting, Grapevine, TX. Paper Number AIAA-2017-0828.

Buschhagen, T., Zhang, R.Z., Naik, S.V., Slabaugh, C.D., Meyer, S.E., Gore, J.P., & Lucht, R.P. (2016). Effect of aviation fuel type and fuel injection conditions on non-reacting spray characteristics of hybrid air blast fuel injector. Presented at 2016 AIAA SciTech Meeting, San Diego, CA. Paper Number AIAA 2016-1154.

Feyz, M., Nalim, R., Hasti, V.R., & Gore, J.P. (2019). Statistical analysis of scalars for ignition via transient hot jet. 11th US National Combustion Meeting, Pasadena, CA 91101 USA

Goyal, V., Hasti, V.R., Gore, J.P., & Mongia, H.C. (2015). Detached eddy simulation of turbulent swirl-stabilized flame. 9th U.S. National Combustion Meeting, Central States Section of the Combustion Institute. Cincinnati, Ohio, USA

Goya1, V., Roncancio, R., Kim, J., Navarkar, A., Hasti, V.R., & Gore, J.P. (2019). Effect of initial fuel temperature on flame spread rate of alternative aviation fuels. 11th US National Combustion Meeting, Pasadena, CA 91101 USA

Goya1, V., Tursyn, Y., Hasti, V.R., & Gore, J.P. (2019). Experimental investigation of hot surface ignition temperatures for aviation fuels. 11th US National Combustion Meeting, Pasadena, CA 91101 USA

Han, D., Hasti, V.R., Gore, J.P., & Lucht, R.P. An experimental and computational study of turbulent lean premixed flames. Propellants and Combustion Session, AIAA Propulsion and Energy 2015 Conference, Orlando, Florida, USA

Hasti, V.R., Kumar, G., Liu, S., Lucht, R.P., & Gore, J.P. (2018). A computational study on H2 piloted turbulent methane / air premixed flame with CO_2 dilution. 2018 Spring Technical Meeting, Central States Section of the Combustion Institute, Minneapolis, MN 55455 USA

Hasti, V.R., Kumar, G., Liu, S., Lucht, R.P., & Gore, J.P. (2018). Large eddy simulation of pilot stabilized turbulent premixed CH_4+air jet flames. 2018 AIAA Aerospace Sciences Meeting, AIAA SciTech Forum, (AIAA 2018-0675)

Hasti, V.R., Liu, S., Kumar, G., & Gore, J.P. (2018). Comparison of premixed flamelet generated manifold model and thickened flame model for bluff body stabilized turbulent premixed flame. 2018 AIAA Aerospace Sciences Meeting, AIAA SciTech Forum, (AIAA 2018-0150)

Hasti, V.R., Kundu, P., Kumar, G., Drennan, S.A., Som, S., & Gore, J.P. (2018). A numerical study of flame characteristics during lean blow-out in a gas turbine combustor. 2018 Joint Propulsion Conference, AIAA Propulsion and Energy Forum, (AIAA 2018-4955)

Hasti, V.R., Kundu, P., Kumar, G., Drennan, S.A., Som, S., & Gore, J.P. (2018). Numerical simulation of flow distribution in a realistic gas turbine combustor. 2018 Joint Propulsion Conference, AIAA Propulsion and Energy Forum, (AIAA 2018-4956)

Hasti, V.R., Kundu, P., Kumar, G., Drennan, S.A., Som, S., Won, S.H., Dryer, F.L., & Gore, J.P. (2018). Lean blow-out (LBO) computations in a gas turbine combustor. 2018 Joint Propulsion Conference, AIAA Propulsion and Energy Forum, (AIAA 2018-4958)

May, P.C., Nik, M.B., Carbajal, S.E., Naik, S., Gore, J.P., Lucht, R.P., & Ihme, M. (2016). Large-eddy simulations of fuel injection and atomization of a hybrid air-blast atomizer. Presented at the 2016 AIAA SciTech Meeting, San Diego, CA. Paper Number AIAA 2016-1393.

Roncancio, R., Navarkar, A., Hasti, V.R., Goyal, V., & Gore, J.P. (2019). Effect of carbon nanotubes addition on the flame spread rate over a jet a pool. 11th US National Combustion Meeting, Pasadena, CA 91101 USA

Shin, D., Bokhart, J.A., Rodrigues, N.S., Lucht, R.P., Gore, J.P., Sojka, P.E., & Meyer, S.E. (2018). Spray characteristics at lean blowout and cold start conditions using phase doppler anemometry. Presented at the 2018 AIAA SciTech Meeting, Kissimmee, Florida.

Shin, D., Bokhart, J.A., Rodrigues, N.S., Naik, S.V., Lucht, R.P., Gore, J.P., Sojka, P.E., & Meyer, S.E. (2018). Spray characteristics of a hybrid airblast pressure-swirl atomizer at cold start conditions using phase doppler anemometry. Presented at ICLASS 2018 14th Triennial International Conference on Liquid Atomization and Spray Systems, Chicago, Illinois.

Shin, D., Bokhart, J.A., Rodrigues, N.S., Sojka, P., Gore, J.P., & Lucht, R.P. (2019). Experimental study of spray characteristics at cold start and elevated ambient pressure using hybrid airblast pressure-swirl atomizer. Presented at 2019 AIAA SciTech Meeting, San Diego, CA. Paper Number AIAA 2019-1737.

Outreach Efforts

N/A

Awards

- Veeraraghava Raju Hasti received the Gordon C. Oates Air Breathing Propulsion Graduate Award - 2019 from the AIAA Foundation. The AIAA Foundation presents this award to a graduate student performing excellent research in air and space science.
- Veeraraghava Raju Hasti received the Computational Interdisciplinary Graduate Program's Bilsland Dissertation Fellowship from Purdue University in 2019.

- Veeraraghava Raju Hasti received the Outstanding Graduate Student Mentor award from Purdue University in May 2019.
- Veeraraghava Raju Hasti received the Outstanding Service award from the College of Engineering, Purdue University in May 2019.
- Veeraraghava Raju Hasti won 1st prize (best poster) under the 100 Years Category in the Sustainable Economy and Planet Poster Competition for PhD Students, Ideas Festival, 150 Years Celebrations at Purdue University for his poster presentation entitled "Quantum Computers on Artificial Intelligence: Automatic and Adaptive Solutions," given February 6, 2019.
- Veeraraghava Raju Hasti delivered an invited talk entitled "Computational methodology for biofuel performance assessment" at the Spring CIGP Symposium, Purdue University, April 17, 2019.
- Veeraraghava Raju Hasti and Jay P. Gore delivered a keynote speech entitled "Computational Study of Fuel Effects on Lean Blow-Out in a Realistic Gas Turbine Combustor" at the Modeling and Simulation of Turbulent Mixing and Reaction: For Power, Energy and Flight, April 12–13, 2019.
- Veeraraghava Raju Hasti was elected as Chair for the Membership Committee of the Gas Turbine Engines Technical Committee (GTE TC), AIAA, August 2019.
- Veeraraghava Raju Hasti delivered an invited talk entitled "Computational Methodology for Biofuel Performance Prediction" at the Academic Research Colloquium, University of Dayton, September 10–12, 2019.
- Veeraraghava Raju Hasti successfully defended his PhD dissertation on October 30, 2019.
- Veeraraghava Raju Hasti served as a Global Ambassador following selection by the Purdue Graduate School for interactions with prospective international students on November 8, 2019.
- Veeraraghava Raju Hasti represented Purdue University at the Big Ten Grad Expo on September 22, 2019, following selection by the Office of Interdisciplinary Graduate Programs and Computational Interdisciplinary Graduate Programs. Hasti also served on a Panel at the Big Ten Grad Expo on September 22, 2019.
- Veeraraghava Raju Hasti was invited by the College of Engineering to serve on the Graduate Students Panel on May 21, 2019 to interact with global undergraduate summer interns through the Purdue Undergraduate Research Experience (PURE).
- Veeraraghava Raju Hasti delivered a presentation on computational research opportunities in combustion and energy at the Mechanical Engineering Visitation Program for prospective graduate students on February 14, 2019 at Purdue University.
- Jay P. Gore delivered an invited talk entitled "Radiation Heat Transfer in High Pressure Gas Turbine Combustors" at the United Technologies Research Center (UTRC) Workshop on Combustor–Turbine Wall Heat Transfer Modeling and Prediction, East Hartford, CT, March 11, 2019.
- Jay P. Gore delivered an invited talk entitled "Radiation and Soot Measurements in High Pressure Gas Turbine Combustors" at the United Technologies Research Center (UTRC) Follow-up Meeting for Combustor–Turbine Wall Heat Transfer at the ASME IGTI Conference, Phoenix, AZ, June 16, 2019.

Student Involvement

PhD student Daniel Shin is primarily responsible for performing PDA measurements under LBO and HAR/GLO conditions and for upgrading the VAPS test rig in a new test cell. PhD student Neil Rodrigues and postdoctoral research associate Rohan Gejji assist with the project when their expertise is required. PhD student Veeraraghava Raju Hasti is primarily responsible for developing and performing the LES simulations. Veeraraghava Raju Hasti has graduated and is currently a Research Assistant Professor in the School of Mechanical Engineering at Purdue.

Plans for Next Period

The proposed deliverables and tasks for FY2020 are listed below.

Year-5 deliverables

The year-5 deliverables for Area 5, Project 29A are as follows:

Experimental

1. Complete the VAPS test rig integration and prepare the rig for operation
2. Begin PLIF measurements of A2 fuel under LBO and elevated ambient pressure conditions
3. Perform PDA measurements of C3 fuel under near-LBO conditions
4. Continue revisions and complete the spray section in the AIAA book chapter
5. Continue interactions with the three CFD groups (Ihme, Vaidya, and Menon)

Computational

1. Contribute to writing of the CFD book chapter
2. Complete the domain sensitivity analysis under nonreacting conditions
3. Perform reacting LES simulations with the partially stirred reactor (PaSR) combustion model and LBO computations for the actual plenum computational domain if the plenum size has a significant impact on the flow splits and combustor flow field
4. Compare results from completed FRC simulations, including any simulation results without zonal chemistry being applied during the simulation, using HyChem detailed, skeletal, and reduced mechanisms to determine why inaccurate trends are obtained for the detailed and reduced mechanisms
5. Analyze reaction pathways to identify the key chemical pathways responsible for LBO and compare these pathways for A2 and C1 fuels
6. Conduct new simulations based on tasks 9 and 10 to understand or improve consistency among the HyChem detailed, skeletal, and reduced mechanisms
7. Publish journal papers on computational efforts

The tasks to be performed for FY2020 are listed below:

Quarter 1 FY2020

1. Complete the upgraded VAPS test rig integration and prepare the rig for operation
2. Conduct PLIF measurements for the A2 fuel
3. Publish a manuscript describing the cold start measurements in the *AIAA Journal*
4. Continue work on the spray section of the AIAA book chapter
5. Share boundary, initial, and operating conditions and resulting experimental data with the correlations and modeling teams (Rizk, Ihme, Menon, and Sankaran)
6. Contribute to writing of the CFD book chapter
7. Complete the domain sensitivity analysis under nonreacting conditions

Quarter 2 FY2020

1. Collaborate with Area 4 and Area 6 members and with the spray subcommittee to develop an experimental test matrix for year 5
2. Conduct further PLIF measurements for the PhD thesis work of graduate student Daniel Shin
3. Share boundary, initial, and operating conditions and resulting experimental data with the correlations and modeling teams (Rizk, Ihme, Menon, and Sankaran)
4. Continue work on the CFD book chapter
5. Perform reacting LES simulations with the PaSR combustion model and LBO computations for the actual plenum computational domain if the plenum size has a significant impact on the flow splits and combustor flow field
6. Compare results from completed FRC simulations, including any simulation results without zonal chemistry being applied during the simulation, using the HyChem detailed, skeletal, and reduced mechanisms to determine why inaccurate trends are produced for the detailed and reduced mechanisms

Quarter 3 FY2020

1. Prepare a journal paper on the elevated ambient pressure measurements
2. Share boundary, initial, and operating conditions and resulting experimental data with the correlations and modeling teams (Rizk, Ihme, Menon, and Sankaran)
3. Continue work on the CFD book chapter
4. Analyze reaction pathways to identify the key chemical pathways responsible for LBO and compare these pathways for A2 and C1 fuels
5. Prepare journal manuscripts based on the reaction pathway analysis

Quarter 4 FY2020

1. Share boundary, initial, and operating conditions and resulting experimental data with the correlations and modeling teams (Rizk, Ihme, Menon, and Sankaran)
2. Conduct new simulations if required to understand or improve consistency among the HyChem detailed, skeletal, and reduced mechanisms

References

Bokhart, A., Shin, D., Gejji, R.M., Sojka, P., Gore, J.P., Lucht, R. P., Naik, S. V., and Buschhagen, T. (2017). Spray measurements at elevated pressures and temperatures using phase doppler anemometry. 55th AIAA Aerospace Sciences Meeting. American Institute of Aeronautics and Astronautics.

Bokhart, A., Shin, D., Rodrigues, N.S., Sojka, P., Gore, J.P., & Lucht, R.P. (2018). Spray characteristics of a hybrid airblast pressure-swirl atomizer at near lean blowout conditions using phase doppler anemometry. American Institute of Aeronautics and Astronautics.

Convergent Science, Inc. (2017). CONVERGE CFD, Version 2.4,. Madison, WI

El-Asrag, H.A., Braun, M., & Masri, A.R. (2016). Large eddy simulations of partially premixed ethanol dilute spray flames using the flamelet generated manifold model. Combustion Theory and Modelling Vol. 20, No. 4, pp. 567-591. doi: 10.1080/13647830.2016.1159732

Elasrag, H. & Li, S. (2018). Investigation of extinction and reignition events using the flamelet generated manifold model. ASME Turbo Expo 2018: Turbomachinery Technical Conference and Exposition. Vol. Volume 4A: Combustion, Fuels, and Emissions.

Giusti, A. & Mastorakos, E. (2017). Detailed chemistry LES/CMC simulation of a swirling ethanol spray flame approaching blow-off. Proceedings of the Combustion Institute Vol. 36, No. 2, pp. 2625-2632. https://doi.org/10.1016/j.proci.2016.06.035

Hasti, V.R., Kundu, P., Kumar, G., Drennan, S.A., Som, S., & Gore, J.P. (2018). A numerical study of flame characteristics during lean blow-out in a gas turbine combustor. 2018 Joint Propulsion Conference, No. AIAA 2018-4955. doi: doi:10.2514/6.2018-4955

Hasti, V.R., Kundu, P., Kumar, G., Drennan, S.A., Som, S., & Gore, J.P. (2018). Numerical simulation of flow distribution in a realistic gas turbine combustor. 2018 Joint Propulsion Conference, No. AIAA 2018-4956. doi: doi:10.2514/6.2018-4956

Hasti, V.R., Kundu, P., Kumar, G., Drennan, S.A., Som, S., Won, S.H., Dryer, F.L., & Gore, J.P. (2018). Lean blow-out (LBO) computations in a gas turbine combustor. 2018 Joint Propulsion Conference, No. AIAA 2018-4958. doi:10.2514/6.2018-4958

Ihme, M., Cha, C.M., & Pitsch, H. (2005). Prediction of local extinction and re-ignition effects in non-premixed turbulent combustion using a flamelet/progress variable approach. Proceedings of the Combustion Institute Vol. 30, No. 1, pp. 793-800. doi: https://doi.org/10.1016/j.proci.2004.08.260

Ihme, M. & Pitsch, H. (2008). Prediction of extinction and reignition in nonpremixed turbulent flames using a flamelet/progress variable model: 1. A priori study and presumed PDF closure. Combustion and Flame Vol. 155, No. 1, pp. 70-89. doi: https://doi.org/10.1016/j.combustflame.2008.04.001

Ma, P.C., Wu, H., Labahn, J.W., Jaravel, T., & Ihme, M. (2019). Analysis of transient blow-out dynamics in a swirl-stabilized combustor using large-eddy simulations. Proceedings of the Combustion Institute Vol. 37, No. 4, pp. 5073-5082. doi: https://doi.org/10.1016/j.proci.2018.06.066

Mayhew, E., Mitsingas, C.M., McGann, B., Hendershott, T., Stouffer, S., Wrzesinski, P., Caswell, A.W., & Lee, T. (2017). Spray characteristics and flame structure of jet a and alternative jet fuels. 55th AIAA Aerospace Sciences Meeting. doi: 10.2514/6.2017-0148

Pomraning, E. & Rutland, C.J. (2002). Dynamic one-equation nonviscosity large-eddy simulation model. AIAA Journal Vol. 40, No. 4, pp. 689-701. doi: 10.2514/2.1701

van Oijen, J.A., Donini, A., Bastiaans, R.J.M., ten Thije Boonkkamp, J.H.M., & de Goey, L.P.H. (2016). State-of-the-art in premixed combustion modeling using flamelet generated manifolds. Progress in Energy and Combustion Science Vol. 57, pp. 30-74. doi: 10.1016/j.pecs.2016.07.001

Project 31(A) Alternative Jet Fuel Test and Evaluation

University of Dayton Research Institute

Project Lead Investigator

Steven Zabarnick, PhD
Division Head
Fuels and Combustion Division
University of Dayton Research Institute
300 College Park
Dayton, OH 45469-0043
937-255-3549
Steven.Zabarnick@udri.udayton.edu

University Participants

University of Dayton Research Institute

- PI(s): Steven Zabarnick, Division Head
- FAA Award Number: 13-C-AJFE-UD
- Overall Period of Performance: April 8, 2015 to September 9, 2020
- Task(s):
  - Period of Performance: April 8, 2015 to March 14, 2016 – Amendment No. 006
    1. Evaluate the performance of candidate alternative fuels via the ASTM D4054 approval process
  - Period of Performance: August 13, 2015 to August 31, 2016 – Amendment No. 007
    2. Evaluate the performance of candidate alternative fuels via the ASTM D4054 approval process
  - Period of Performance: August 5, 2016 to August 31, 2017 – Amendment No. 012
    3. Manage the evaluation and testing of candidate alternative fuels
  - Period of Performance: July 31, 2017 to August 31, 2019 – Amendment No. 016
    4. Manage the evaluation and testing of candidate alternative fuels
  - Period of Performance: August 30, 2018 to August 31, 2019 – Amendment No. 021
    5. Manage the evaluation and testing of candidate alternative fuels
  - Period of Performance: Extended period of performance end from September 10, 2019 to September 9, 2020 – Amendment No. 023

Project Funding Level

Amendment No. 006	$309,885
Amendment No. 007	$ 99,739
Amendment No. 012	$693,928
Amendment No. 016	$999,512
Amendment No. 021	$199,966

In-kind cost sharing has been obtained from:

LanzaTech	$ 55,801 (2015)
LanzaTech	$ 381,451 (2016)
UDRI	$ 43,672 (2016)
Neste	$ 327,000 (2017)
Boeing	$2,365,338 (2017)
Shell	$ 280,000 (2019)
IHI	$1,150,328 (2019)

Investigation Team

- Steven Zabarnick, PI, New candidate fuel qualification and certification
- Richard Striebich, Researcher, Fuel chemical analysis and composition
- Linda Shafer, Researcher, Fuel chemical analysis and composition
- John Graham, Researcher, Fuel seal swell and material compatibility
- Zachary West, Researcher, Fuel property evaluation
- Rhonda Cook, Technician, Fuel property testing
- Sam Tanner, Technician, Fuel sampling and shipping
- Carlie Anderson, Researcher, Fuel chemical analysis
- Tak Yamada, Researcher, Fuel chemical analysis
- Amanda Arts, Co-Op Student, University of Kentucky, Fuel property evaluation

Project Overview

Alternative jet fuels offer the potential benefits of reduced global environmental impacts, increased national energy security, and stabilized fuel costs for the aviation industry. The FAA is committed to the advancement of "drop-in" alternative fuels. The successful adoption of alternative fuels requires approval for use by the aviation community, followed by large-scale production of a fuel that is cost-competitive and that meets the safety standards of conventional jet fuel. Alternative jet fuels must undergo rigorous testing to become qualified for use and be incorporated into ASTM International specifications.

Cost-effective, coordinated performance testing capability (in accordance with ASTM D4054) is needed to support the evaluation of promising alternative jet fuels. The objective of this project is to provide the necessary capability to support either (a) the evaluation of to-be-determined alternative fuel(s) selected in coordination with the FAA or (b) a fuel test and evaluation project with a specific alternative fuel(s) in mind.

The proposed program should provide the following capabilities:

- Identify alternative jet fuels, including blends with conventional jet fuel, with the potential to be economically viable and to support FAA's NextGen environmental goals for testing
- Perform engine, component, rig, or laboratory tests or any combination thereof to evaluate the performance of alternative jet fuels in accordance with ASTM International standard practice D4054
- Identify and conduct unique testing, beyond that defined in ASTM International standard practice D4054, to support the evaluation of alternative jet fuels for inclusion in ASTM International jet fuel specifications
- Obtain baseline and alternative jet fuel data to assess any effects of an alternative jet fuel on aircraft performance, maintenance requirements, and reliability
- Coordinate efforts with activities sponsored by the Department of Defense and/or other government parties that may be supporting relevant work
- Report relevant performance data for the alternative fuels tested, including quantified effects of the alternative fuel on aircraft and/or engine performance and on air quality emissions relative to conventional jet fuel. Reported data will be shared with the FAA (NJFCP), the broader community (e.g., ASTM International), and the ASCENT COE Program 33 "Alternative Fuels Test Database Library."

Tasks 1 and 2 - Evaluate the Performance of Candidate Alternative Fuels via the ASTM D4054 Approval Process and Manage the Evaluation and Testing of Candidate Alternative Fuels

University of Dayton Research Institute

Objective

Cost-effective, coordinated performance testing capability (in accordance with ASTM D4054) is needed to support the evaluation of promising alternative jet fuels. The objective of this project is to provide the capability necessary to support either a) the evaluation of to-be-determined alternative fuel(s) selected in coordination with the FAA or b) a fuel test and evaluation project with a specific alternative fuel(s) in mind.

Research Approach

The intent of this program is to provide the capability needed to perform specification and fit-for-purpose evaluations of candidate alternative fuels, with the aim of providing a pathway forward through the ASTM D4054 approval process. The UDRI team is capable of performing a large number of these evaluations, and we are prepared to work with other organizations, such as SwRI and engine OEMs, with unique test capabilities, as needed. These assessments include additional engine, APU, component, and rig evaluations. The UDRI testing capabilities include efforts at the laboratories of the Fuels Branch of AFRL and at our campus laboratory facilities.

The following lists provide examples of the evaluations that can be provided by UDRI:

Tier I

1. Thermal stability (quartz crystal microbalance)
2. Freeze point (ASTM D5972)
3. Distillation (ASTM D86)
4. Hydrocarbon range (ASTM D6379 & D2425)
5. Heat of combustion (ASTM D4809)
6. Density, API gravity (ASTM D4052)
7. Flash point (ASTM D93)
8. Aromatics (ASTM D1319)

Tier II

1. Color, saybolt (ASTM D156 or D6045)
2. Total acid number (ASTM D3242)
3. Aromatics (ASTM D1319 & D6379)
4. Sulfur (ASTM D2622)
5. Sulfur mercaptan (ASTM D3227)
6. Distillation temperature (ASTM D86)
7. Flash point (ASTM D56, D93, or D3828)
8. Density (ASTM D1298 or D4052)
9. Freezing point (ASTM D2386, D5972, D7153, or D7154)
10. Viscosity at -20˚C (ASTM D445)
11. Net heat of combustion (ASTM D4809)
12. Hydrogen content (ASTM D3343 or D3701)
13. Smoke point (ASTM D1322)
14. Naphthalenes (ASTM D1840)
15. Calculated cetane index (ASTM D976 or D4737)
16. Copper strip corrosion (ASTM D130)
17. Existent gum (ASTM D381)
18. Particulate matter (ASTM D2276 or D5452)
19. Filtration time (MIL-DTL-83133F Appendix B)
20. Water reaction interface rating (ASTM D1094)
21. Electrical conductivity (ASTM D624)
22. Thermal oxidation stability (ASTM D3241)

Extended physical and chemical characterization

1. Lubricity evaluation: BOCLE test (ASTM D5001)
2. Evaluation of low-temperature properties: scanning Brookfield viscosity
3. Detection, quantification, and/or identification of polar species: as necessary
4. Detection, quantification, and/or identification of dissolved metals: as necessary
5. Initial material compatibility evaluation: optical dilatometry and partition coefficient measurements to determine the fuel-effected swell and fuel solvency in three O-ring materials (nitrile, fluorosilicone, and fluorocarbon) and up to two additional fuel system materials
6. Experimental thermal stability evaluation: quartz crystal microbalance to measure thermal deposit tendencies and oxidation profiles at elevated temperatures
7. Evaluation of viscosity vs. temperature: ASTM D445 to determine the fuel viscosity at 40˚C and -40˚C to assess the viscosity variation with temperature

In addition to the above physical and chemical fuel evaluation capabilities, UDRI has extensive experience in the evaluation of microbial growth in petroleum-derived and alternative fuels. These evaluations include standard lab culturing and colony counting methods and advanced techniques such as quantitative polymerase chain reaction (QPCR) and metagenomic sequencing. These methods enable quantitative measurements of microbial growth rates in candidate alternative fuels for comparison with petroleum fuels.

UDRI also has extensive experience in the evaluation of elastomer degradation upon exposure to candidate alternative fuels. Various methods are used to evaluate seal swell and O-ring fixture leakage, including optical dilatometry, sealing pressure measurements, fuel partitioning into the elastomer, and the use of a pressurized temperature-controlled O-ring test device.

Moreover, UDRI can perform fuel–material compatibility testing using the D4054 procedures for fuel soak testing, postexposure nonmetallic and metallic material testing, and surface and microstructural evaluation. The 68 "short-list" materials and the 255 materials on the complete list can be tested.

Milestone(s)

The schedule for this project is dependent upon the receipt of alternative fuel candidates for testing. As candidate fuels are received, a testing schedule will be established via coordination with the FAA and collaborators. Our existing relationships with these organizations will help expedite this process.

Major Accomplishments

Shell IH2 testing

Discussions with Shell on their IH2 fuel and process (hydropyrolysis and hydrotreating of woody biomass, MSW, and Ag residue) began in 2017 and proceeded through 2018. In January 2019, samples of their CPK-0 (zero aromatics) fuel were received by the Clearinghouse for testing. Testing proceeded at UDRI and SwRI through the spring of 2019, with a draft research report produced in the summer. In October 2019, initial warm LBO testing of the CPK-0 fuel blends was performed in the referee combustor. We await the production of larger quantities of IH2 fuel for additional cold LBO and ignition studies in the referee rig. In addition, a Phase 1 research report will be presented to the OEM committee in the spring of 2020, with the anticipation of OEM APU and engine combustor sector testing during late 2020 or early 2021. The unusually high cycloparaffin content (>95%) of this fuel will dictate the need for additional tier 3 testing, with the extent of testing potentially being limited by the fuel's excellent performance in the referee rig.

IHI Bb-Oil SPK testing

Discussions with IHI of Japan on their Bb-oil fuel and process (algae cultivation with hydrocarbon and oil extraction) began in 2018, with initial fuel samples received in January 2019. Testing proceeded during the winter and spring of 2019, with a resulting Fast Track research report being submitted for balloting in June 2019. This fuel consists of approximately 40% cycloparaffins and thus has a higher density than that specified in the Fast Track guidelines. The OEM review was completed in August 2019, and we are in the process of completing additional testing on another production sample to address OEM questions.

Fischer–Tropsch coprocessing

Fulcrum Bioenergy is interested in adding Fischer–Tropsch (FT) coprocessing to the D1655 fuel specification to permit small quantities (<10%) of FT waxes to be used as feed to petroleum refinery hydrocracking reactors. This change would allow the use of FT waxes produced from the gasification of municipal solid wastes in petroleum refinery operations, enabling jet fuel to be produced without operation modifications. To support this effort, this project received vacuum gas oil (VGO)-produced jet fuel and fuel produced from a co-feed of VGO and FT wax product. We assessed the D1655 Table 1 properties, JFTOT thermal stability, trace metals, GCxGC hydrocarbon type, GCxGC polars, lubricity additive responses, and conductivity additive responses. A research report was produced, and FT coprocessing was balloted in an ASTM October 2019 ballot.

Publications

Written reports

ASTM Ballot. (2019). Modification of ASTM D1655: Co-processing of Fischer-Tropsch feedstocks with petroleum hydrocarbons for jet production using hydrotreating & hydrocracking.

D4054 Fast Track Research Report. (2019). Evaluation of synthesized paraffinic kerosene from algal oil extracted from *botryococcus braunii* (ihi bb-spk).

Outreach Efforts

Presentations on Project 31a activities were given at the April (Atlanta) and October (Alexandria) 2019 ASCENT meetings and the December 2018 CAAFI Biennial General Meeting & Integrated ASCENT Symposium in Washington, DC. Meetings were held with the OEM team, FAA, fuel producers, and others at the December 2018 ASTM D02 Committee Meeting in Atlanta, the June 2019 ASTM D02 Committee Meeting in Denver, and the March 2019 UK MoD Aviation Fuels Committee meeting in London, UK.

Awards

None.

Student Involvement

None.

Plans for Next Period

We are awaiting the receipt of larger quantities of the Shell IH2 fuel for further evaluation, including cold LBO testing, ignition testing, APU cold start and ignition evaluation, and engine OEM sector evaluation. We expect the Shell IH2 phase 1 research report to be completed and submitted to the OEM committee in the first quarter of 2020. We intend to perform additional testing of the IHI Bb-SPK and Fulcrum Bioenergy FT coprocessing after feedback is received from the submitted ASTM ballots. We will continue discussions with new fuel producers and expect new candidates to enter the process in the coming months.

Tasks 3 and 4 - Manage the Evaluation and Testing of Candidate Alternative Fuels

University of Dayton Research Institute

Objective

The objective of this work is to manage the evaluation and testing of candidate alternative jet fuels in accordance with ASTM International standard practice D4054 (see Figure 1).

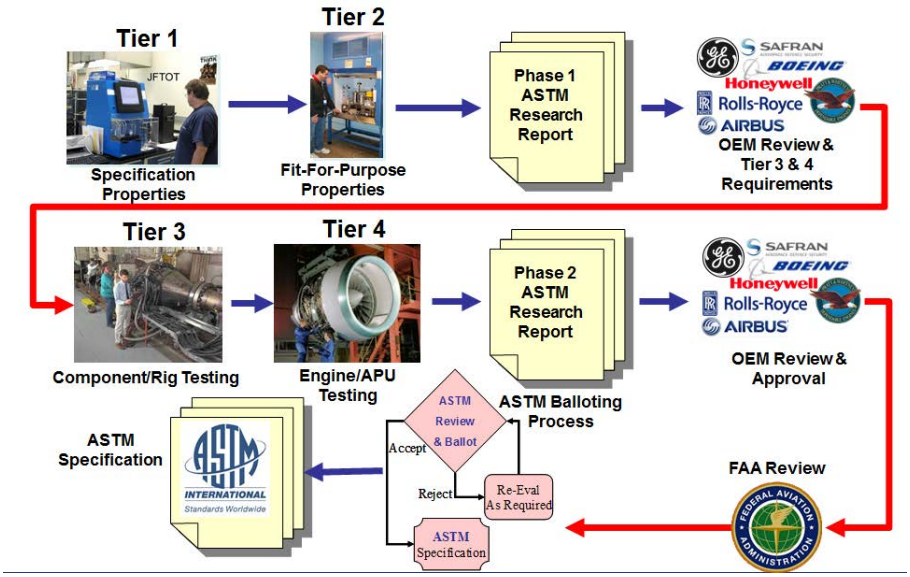

Figure 1. ASTM D4054 qualification process.

Research Approach

UDRI will subcontract with other research organizations, test laboratories, and/or OEMs to conduct the following tasks in support of the evaluation and ASTM specification development for alternative jet fuels. The purpose of this project is to manage and coordinate the D4054 evaluation process illustrated in Figure 2 in order to facilitate the transition of alternative fuels to commercial use.

Subtask 1: General support

- Develop and make available a D4054 process guide that describes logistical procedures for the handling of test fuels, documentation requirements, test report issuance and delivery, and contact information. This guide is intended to provide clear instructions to candidate fuel producers for entering the ASTM D4054 process.

Subtask 2: Phase 1 support

- Coordinate the handling of phase 1 candidate test fuel samples for tier 1 and 2 testing
- Review process descriptions provided by the fuel producer to determine acceptability for incorporation into the phase 1 research report
- Review test data from tier 1 and 2 testing to determine acceptability for incorporation into the phase 1 research report
- Issue and deliver a phase 1 research report to OEMs
- In conjunction with the fuel producer, review and respond to comments regarding the phase 1 research report, as submitted by the OEMs
- Conduct additional tier 1 or 2 testing in response to OEM comments as required
- Review and consolidate OEM requirements for D4054 tier 3 and 4 testing, as submitted by the OEMs
- Deliver consolidated D4054 tier 3 and 4 testing requirements to the fuel producer

Subtask 3: Phase 2 support

- Coordinate the funding and scheduling of D4054 tier 3 and 4 testing with OEMs and other test facilities
- Coordinate the handling of phase 2 candidate test fuel samples for tier 3 and 4 testing
- Review test data from tier 3 and 4 testing to determine acceptability for incorporation into the phase 2 research report
- Issue and deliver the phase 2 research report to OEMs

- In conjunction with the fuel producer, review and respond to comments submitted by OEMs regarding the phase 2 research report
- Conduct additional tier 3 or 4 testing in response to OEM comments as required
- Issue and deliver phase 2 research report addendums reporting the additional tier 3 or 4 test results as required

Subtask 4: OEM review meetings

- Schedule periodic OEM meetings to review the testing status and the research report evaluations
- Identify suitable meeting venues and support equipment
- Develop agendas and coordinate with attendees for participation in these meetings
- Record meeting minutes, including agreements, commitments, and other action items
- Issue and distribute meeting minutes to all attendees

Subtask 5: Single-laboratory GCxGC method documentation

- Document UDRI GCxGC methodology for hydrocarbon type analysis
- Develop reference materials for the creation of GCxGC hydrocarbon type templates
- Measure single-laboratory precision of the GCxGC methods

Subtask 6: Multi-laboratory GCxGC method documentation

- Validate the precision of GCxGC methods over multiple laboratories
- Identify alternative GCxGC methods, including column selection and order, and modulation techniques
- Perform a correlation study to determine the agreement among laboratories, methods, and hardware choices

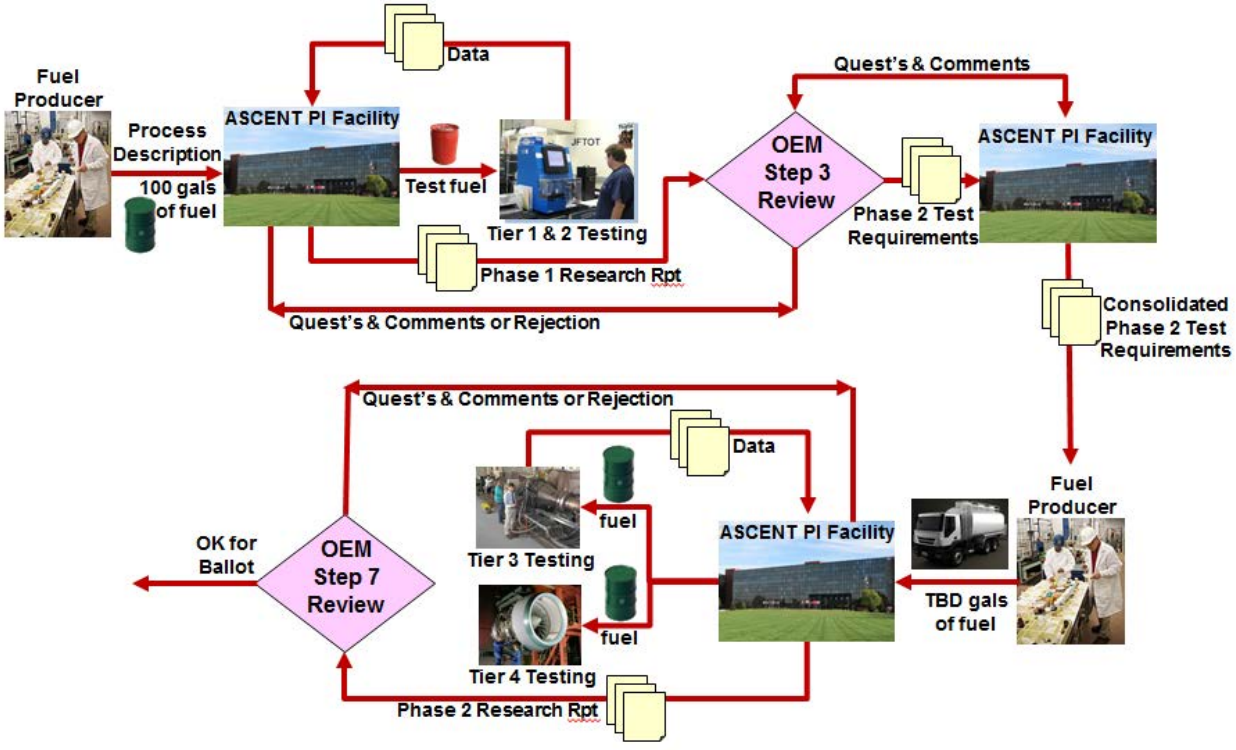

Figure 2. D4054 evaluation process.

Milestone(s)

The schedule for this project is dependent upon the receipt of alternative fuel candidates for testing. As candidate fuels are received, a testing schedule will be established via coordination with the FAA and collaborators. Our existing relationships

with these organizations will help expedite this process. Figure 3 shows a Gantt chart schedule for the testing and approval of candidate fuels that are currently under evaluation or that will soon enter the evaluation process.

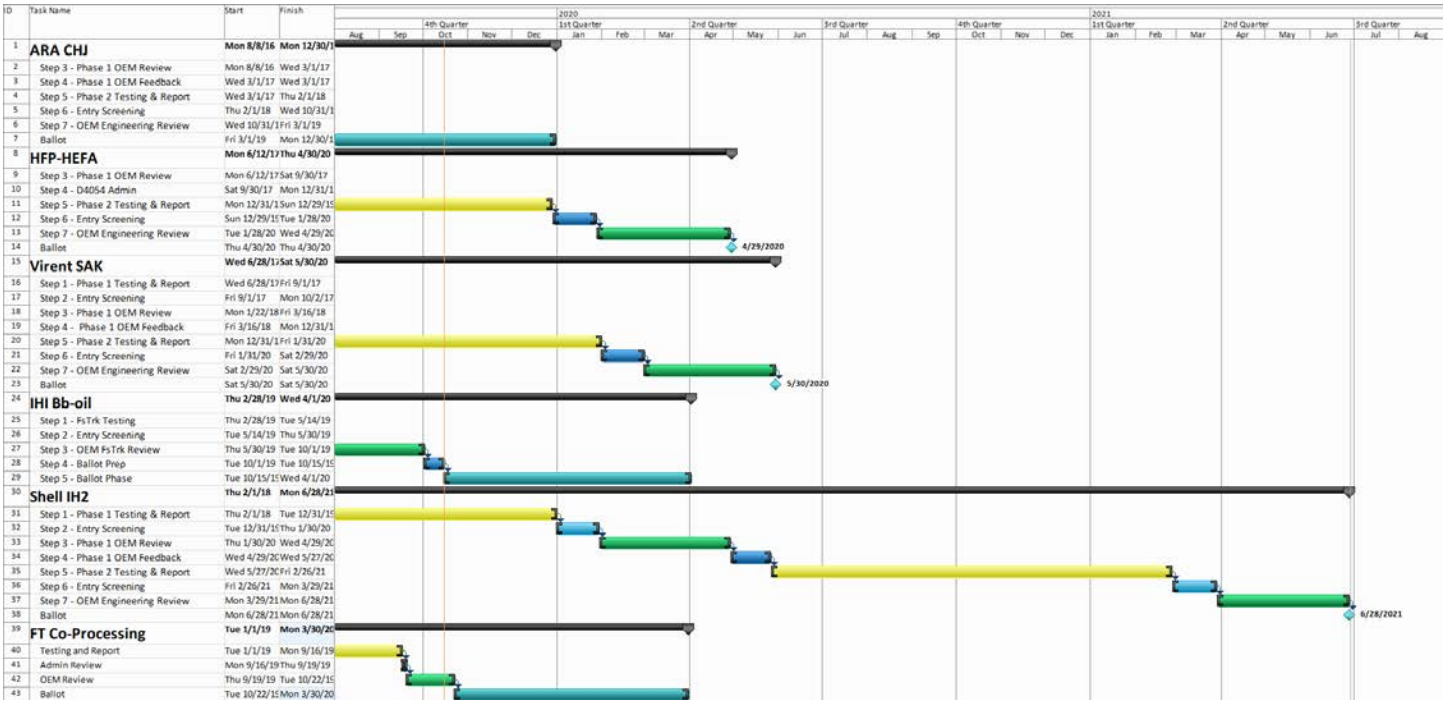

Figure 3. Schedule for fuel evaluations.

Major Accomplishments

Fast track annex development

A D7566 Generic Annex concept was originally presented to the OEM committee, in which a set of highly stringent property requirements would be used to create a D7566 annex without the feedstock or process being defined. This annex would enable the rapid approval of a wide variety of fuels that closely resemble already approved fuels with regard to composition and physical properties. However, the OEM committee was concerned about the lack of an OEM review for each fuel approved through this process. Thus, the Generic Annex pathway was abandoned in the spring/summer of 2018. In response to OEM concerns, a Fast Track Annex to D4054 was proposed in the winter of 2018/19, which included a list of stringent properties and chemical composition requirements. This Fast Track Annex would require an identification of the feedstock and processing, along with a required OEM review of the research report results. The goal would be an allowed 10% blend limit with a much more rapid approval pathway. Fast Track approval would result in the creation of a D7566 annex for each approved fuel. Ultimately, the Fast Track Annex was balloted in the spring of 2019 and approved in April 2019.

GCxGC method documentation

Two GCxGC method reports were completed and made available to the fuel community (UDRI Method FC-M-101 Flow Modulation GCxGC for Hydrocarbon Type Analysis of Conventional and Alternative Aviation Fuels; UDRI Method FC-M-102 Identification and Quantitation of Polar Species in Conventional and Alternative Aviation Fuels Using SPE-GCxGC). The first report documents the UDRI/AFRL hydrocarbon type analysis method based on flow modulation GCxGC and “normal phase” column order (nonpolar followed by polar columns). The second report documents the UDRI/AFRL polar analysis, which uses a solid-phase extraction pre-separation technique to separate and concentrate trace polar species. After pre-separation, the fuel polars are analyzed by GCxGC separation. These reports are being made available to any parties that express interest. These documents are now included in the ASTM D4054 Fast Track Annex A4 (ASTM D4054 Annex A4. Fast Track OEM Qualification and Approval Process for New Aviation Turbine Fuels). These methods provide the fuel community with new

tools to enable accurate fuel composition analysis and improved techniques for evaluating and qualifying new candidate alternative fuels.

GCxGC precision – intra- and interlab comparisons
To investigate the precision of GCxGC hydrocarbon type analyses, we assessed a single fuel over a number of years using a single instrument (intralab comparison). We also compared two different GCxGC systems, i.e., flow modulation with a nonpolar initial column and a polar secondary column vs. thermal modulation with a polar initial column and a nonpolar secondary column. We also compared measurements between two labs (UDRI/AFRL vs. NASA Glenn) for a number of fuels using the same instrument type and column configuration. We are in the process of compiling data for interlaboratory comparisons with multiple external laboratories that use a variety of GCxGC configurations and instruments.

OEM committee coordination
The ongoing effort of ASTM OEM committee coordination continued during this period. This effort involves coordinating the engine and airframer OEM meetings, which have occurred in concert with the biannual ASTM D02 sessions and at the annual UK MoD AFC meeting in London. Southwest Research Institute continues to receive funding to aid in coordinating the OEM meetings and in communicating with the OEMs for discussions and research report reviews of new candidate alternative jet fuels. In addition, a Gantt schedule is updated monthly; this schedule shows a queue of candidate fuels and the completed and expected schedule as these fuels move through the ASTM D4054 process of testing, review, balloting, and approval. A recent version of this schedule is shown in Figure 3. In support of the ongoing OEM committee coordination, subcontracts were extended to our ASCENT grant end date of 31 August 2020 with Boeing, GE Aviation, Honeywell, Rolls Royce, Pratt & Whitney, and Southwest Research Institute.

Publications

Written reports

UDRI Method FC-M-101. Flow modulation GCxGC for hydrocarbon type analysis of conventional and alternative aviation fuels. UDR-TR-2018-40.

UDRI Method FC-M-102. Identification and quantification of polar species in conventional and alternative aviation fuel using SPE-GCxGC. UDR-TR-2018-41.

Outreach Efforts

Presentations on Project 31a were given at the April (Boston) and October (Alexandria) 2018 ASCENT meetings. Meetings were held with the OEM team, FAA, and others at the December 2017 ASTM D02 Committee Meeting in Houston, TX and the March 2018 UK MoD Aviation Fuels Committee meeting in London, UK. Monthly meetings were held in Dayton with IHI, a Japanese company interested in entering their algae fuel in the D4054 process. We also continue to have biweekly teleconferences with Shell on their soon-to-be-submitted IH2 fuel.

Awards

None.

Student Involvement

Amanda Arts, Co-Op Student, University of Kentucky, to graduate in May 2020.

Plans for Next Period

We plan to perform and complete GCxGC interlaboratory precision studies and continue coordination of the OEM committee reviews. We held an OEM committee meeting at the December 2019 ASTM D02 meeting in New Orleans and will hold OEM committee meetings at the UK MoD AFC March 2020 meeting in London and the June and December 2020 ASTM meetings.

Project 033 Alternative Fuels Test Database Library (Year V)

University of Illinois Urbana-Champaign

Project Lead Investigator

Tonghun Lee
Professor
Mechanical Science & Engineering
University of Illinois at Urbana-Champaign
1206 W. Green St.
Urbana, IL 61801
517-290-8005
tonghun@illinois.edu

University Participants

University of Illinois at Urbana-Champaign

- PI(s): Tonghun Lee, Professor
- FAA Award Number: 13-C-AJFE-UI-026
- Period of Performance: August 15, 2018 to August 14, 2019
- Task(s):
    1. Launch of generation II online database
    2. Preliminary efforts to link the database with JETSCREEN

Project Funding Level

Funding Level: $130,000
Cost Share: Software license support from Reaction Design (ANSYS)

Investigation Team

- Tonghun Lee (Professor, University of Illinois at Urbana-Champaign): Overall research supervision
- Anna Oldani (Graduate Student, University of Illinois at Urbana-Champaign): Compilation of fuel test data and database development

Project Overview

This study seeks to develop a comprehensive and foundational database of current and emerging alternative jet fuels by integrating relevant pre-existing jet fuel data into a common archive that can support scientific research, enhance operational safety, and provide guidelines for the design and certification of new jet fuels. In previous years of this project, efforts were focused on the integration and analysis of pre-existing jet fuel data from various government agencies and individual research groups. Over the last year, we have started to convert all of the compiled data to a new nonstructured query language (NoSQL) format using a JavaScript object notation (JSON) schema, thus allowing the data to be analyzed in a flexible manner using various programming languages. To this end, we have launched the second generation of our online database, which utilizes a new nonrelational database structure. This version will provide interactive analysis functions for users and flexible methods for plotting and downloading data. We have also made significant progress in integrating our database with a similar database in the European JETSCREEN program. Through this process, we have identified new goals, including the need to collect and archive data from fuels used on flights. With these future developments, we hope that the database will one day not only serve as a comprehensive and centralized knowledge base utilized by the aviation community but will also be a resource that can enhance operation efficiency and safety. With the prolific diversification of new jet fuels expected in

the near future, particularly of alternative jet fuels, the ability to track critical fuel properties and test data from both research and operation perspectives is expected to be highly valuable for the future of commercial aviation.

Task 1 – Launch of the Generation II Online Database

University of Illinois Urbana-Champaign

Objective(s)

The main objective of this task is to design and launch the generation II Alternative Jet Fuels Test Database online. The goals that guided the first-generation database, namely, establishing a foundational repository of current and emerging information on alternative jet fuels and fuel blends, would be continued in this version. However, the generation II database would exceed our original goal and would be designed using a completely new architecture that allows for flexible analysis and scaling in the future. The new database would utilize a NoSQL format that would be sufficiently flexible to accommodate various data types and that could be easily accessed by any common programming language. This database would also allow large-scale analysis of alternative jet fuel data using advanced algorithms, such as machine learning, and would potentially be linked with other similar databases in the future. The specific goals of this task are as follows:

- Design a nonrelational database and schema for fuel properties and test data
- Convert the entire dataset to the nonrelational JSON (Schema) format
- Build a new generation II database and launch this database online
- Provide interactive analysis capabilities for users

Research Approach

Strategy for the converting the generation II database to NoSQL

The significant task of selecting a database structure and conversion process was completed last year. Currently, the database has grown significantly to house over 25,000 separate fuel records, as shown in the top panel of Figure 1.

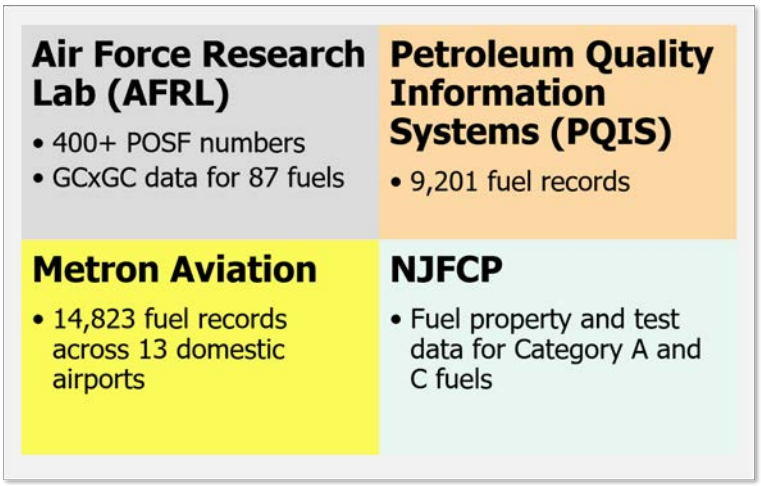

Figure 1. Overview of data records in the current database and comparison of relational and nonrelational databases.

The catalogue of data currently available in the database was primarily assembled from four separate sources. The fuels with POSF (AFRL fuel database code) number designations were added from the internal database at the Air Force Research Laboratory (Wright Patterson Air Force Base), which we carefully parsed to identify important data. The second dataset was

obtained from the PQIS reports of the Naval Air Systems Command (NAVAIR) and corresponds to a compilation of fuel data geared primarily towards military use. The third set was provided by Metron Aviation, who compiled fuel properties from samples collected at airports through a previous ASCENT project. The dataset resulting from this study proved valuable by providing a landscape of fuels currently used in commercial aviation and guided our future efforts focused on capturing this type of data in real time, as will be discussed below for Task 2. The final dataset was obtained from the National Jet Fuel Combustion Program within ASCENT; for this set, we moved all of the testing data from the KSN to the current database.

Conversion to a NoSQL schema

The database initially housed a large collection of information in many different formats. In year IV, we decided to convert the entire database to a NoSQL structure, primarily because the fuel documents and reports had different formats and varying amounts of data. For example, a dataset for one fuel may include viscosity, density, and heat of combustion measurements, while a dataset for another fuel may only include density. Furthermore, multiple tests may be performed for a single fuel property. A flexible schema would provide a means for storing and retrieving data in a flexible manner and would allow analysis via various programming languages. This change would also enable the incorporation of new information types in the database without major changes to the existing dataset. As an additional benefit of this conversion, the database could be integrated with other similar databases. An effort to perform this type of integration with the European JETSCREEN database will be described in the next section.

After the NoSQL format had been chosen, the selection of a NoSQL service was required. We chose DynamoDB, which is operated by Amazon Web Services (AWS) and has an ongoing contract with the University of Illinois. However, the data would be stored in a nonrelational schema termed JSON, which is language-independent and can be easily interfaced with any other platform should we choose to move away from AWS in the future. The next step involved converting our entire dataset to the JSON format. The JSON format stores data using value pairs, of which the first is a string denoted as a key. However, values can also act as keys pointing to other values, resulting in a complex schema with nested keys. To access data, these specific keys are retrieved through the programming language. This complexity allows for a flexible representation of multiple data types. In this process, we developed an individual JSON format for each test and then wrote automated scripts using Python to convert the data into the nonrelational format. An example of a JSON schema for one of the most complex datasets (GCxGC) is shown in Figure 2.

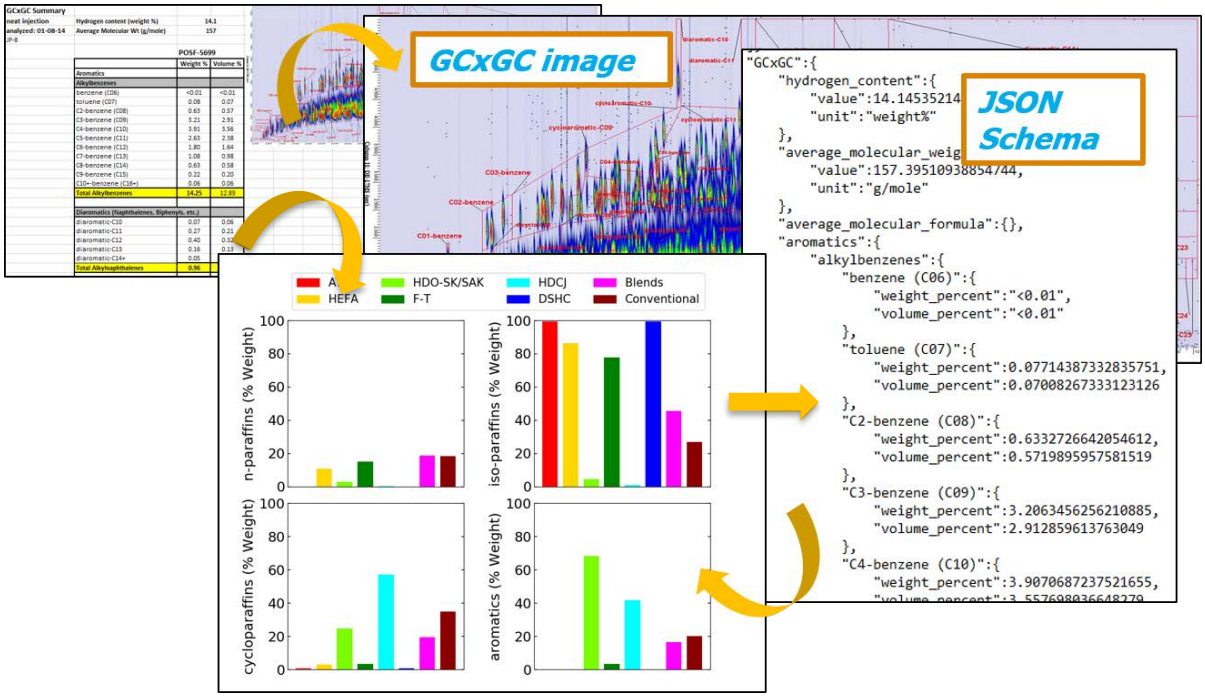

Figure 2. Conversion of GCxGC information to a dedicated JavaScript object notation (JSON) file using a Python script.

Currently, all of the data in the database have been converted into a JSON schema and can be analyzed in a flexible manner using Python scripts. An example of the analysis flexibility provided by the JSON schema (showing the fuel chemical composition) is presented in the lower right inset of Figure 2.

Generation II online database (summer 2019)

A beta version of the generation II database was launched online in the summer of 2019. The websites for both the generation I and generation II databases are shown in Figure 3. As data conversion to the JSON schema was nearing completion, we aimed to develop an online interface that could accommodate the new database format. The web version of the database has a three-tiered structure. On the outermost layer is an HTML-based web interface, as shown on the right side of Figure 3. All of the functionality of the previous database is maintained, and the security login features have been migrated from the previous version. The generation II database uses an interface that will also work with mobile and handheld devices. The inner layer houses the metadata, similar to the first database, and supports search functions for the user. The folder structure that was applied to organize the data in the first database was also retained in this version, allowing the user to access the data in this manner. The inner core contains the AWS database, which houses the JSON files, where the fuel data are stored. Duplicate data are saved on both the AWS and our department servers for security. File upload and comment functions for users have been carried over from the original version, and security oversight will be performed by the IT department at the University of Illinois.

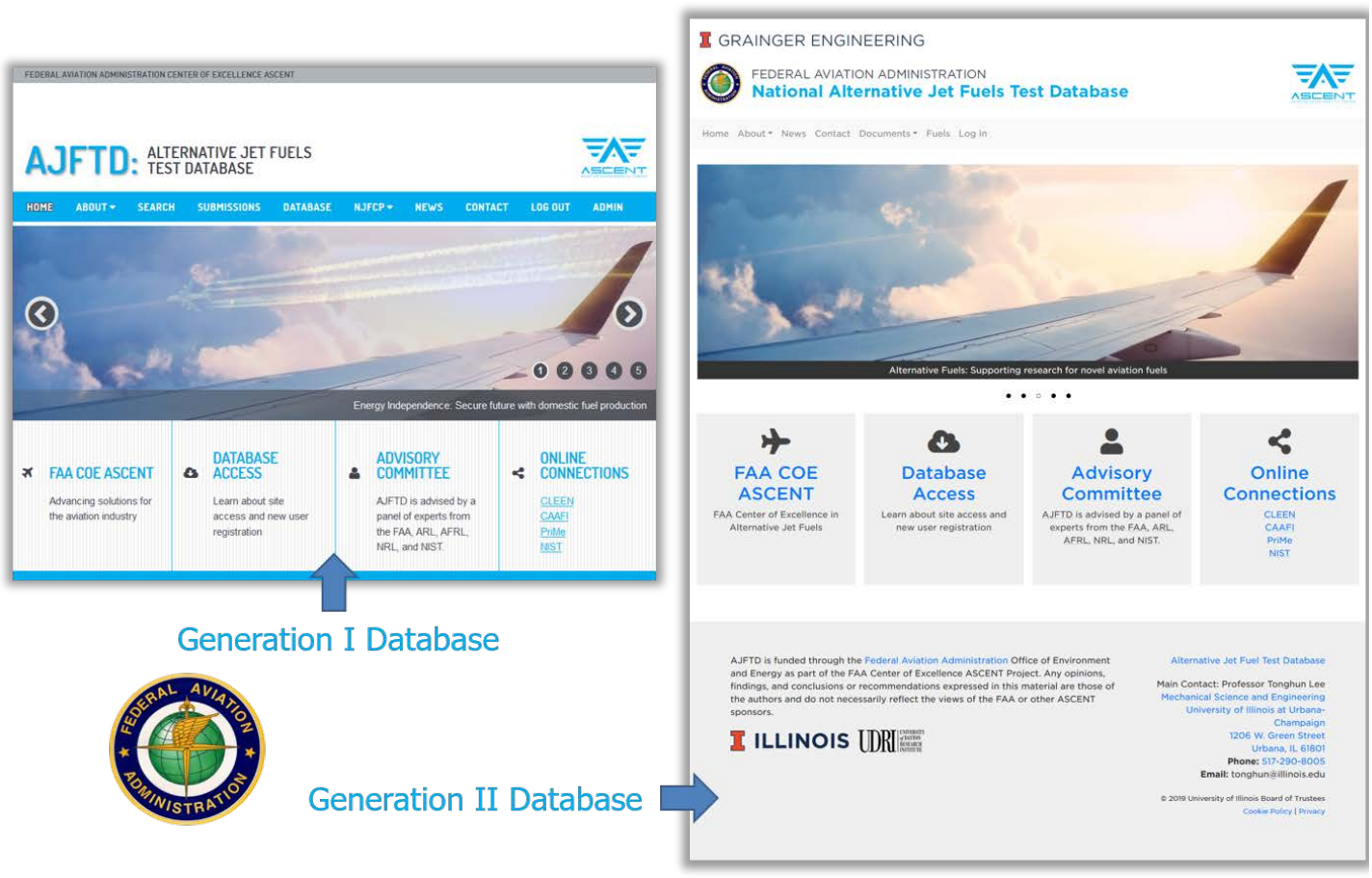

Figure 3. Generation I (left) and generation II (right) databases. URL: https://altjetfuels.illinois.edu/

As the entire dataset has now been converted to a nonrelational JSON format, we can apply a flexible range of analysis routines, as stated in the previous section. As a key aspect of the new database, we will provide a range of sophisticated

analysis routines with which the user can directly interface on the website. The program for interfacing with the data files allows flexible analysis routines to be executed and easily modified. The first analysis routine to be built into the web interface will be a fuel comparison module. For example, a user can compare a specific property for a given fuel to the distribution for a subset of fuels in the database. An example of this routine is shown in Figure 4, where the flash point and kinematic viscosity of a specific fuel are plotted against those in the database. The user can also choose different subsets of fuels in the database to apply in the comparison. As shown in Figure 4, this analysis can be graphically presented through the website, and the user can download the actual data.

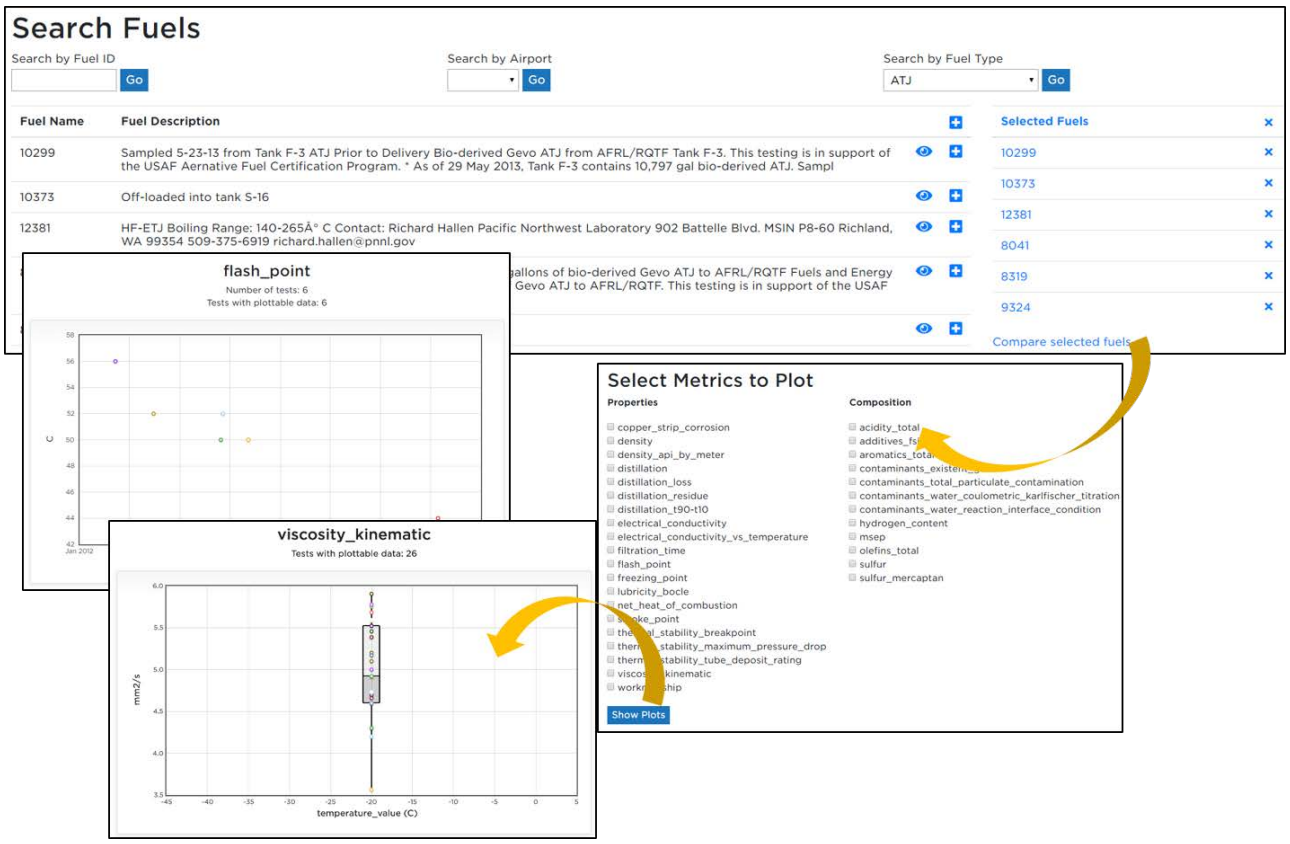

Figure 4. Interactive data analysis interface in the generation II online database.

In the future, we will expand the analysis capabilities of the database. We also envision applying more advanced correlation techniques based on machine learning to examine the correlations among different properties and their impact on the overall fuel performance. We have previously generated basic correlation factors for key properties using standard regression techniques. The application of machine learning may open the door to an extensive study of correlation factors that cover the entire property space of fuels in the database.

Milestone(s)

3 months

At the 3-month mark, we determined specific analysis routines for the database and decided to convert the data to a nonrelational data format in collaboration with the JETSCREEN program in Europe. The design of the generation II database was initiated, and the AWS database, which uses the DynamoDB infrastructure, was established at the University of Illinois. All of the Python scripts that were developed and used to facilitate the transition were documented.

6 months

At the 6-month mark, data conversion to the JSON format was fully completed and vetted. A preliminary analysis of the new

nonrelational data was initiated, based on an examination of fuel property variations in our dataset. An internal beta test version of the database was completed, user testing commenced, and bugs in the web interface were identified. A technical and strategic roadmap for database integration with JETSCREEN was established.

9 months
At the 9-month mark, a fully working version of the generation II database was launched at https://altjetfuels.illinois.edu/. All data from the previous database were migrated onto the new system, and a secure online login was activated for all previous users. A vision of the joint JETSCREEN database integration was presented at the CRC meeting. The database analysis was extended to include Metron data from airports and GCxGC data.

12 months
At the 12-month mark, a preliminary online analysis tool was integrated with the database and made available to a general audience. This tool provides a graphical output of fuel property variations. Plans for expanding the online analysis capabilities and data download methods were drafted. A new data plotting and download function for users was added for fuel property comparisons.

Major Accomplishments

Conversion of data to JSON format (nonrelational digital format)
More than 25,000 fuel records have been converted to the JSON format, which can be easily accessed by most programming languages. GCxGC data have been obtained for >100 AFRL fuels and added to the JSON schema, and Metron data from airports (~14,000) have also been added. This step is the first toward establishing a foundational fuel database that will enable researchers to better analyze statistical correlations and compare property variations for alternative jet fuels. This format will also allow us to link the database with others, including JETSCREEN.

Launching of the generation II database website
We have launched a new version of the online database website at https://altjetfuels.illinois.edu/. The new website has enhanced capabilities, including (a) AWS DynamoDB integration using a nonrelational data structure, (b) online analysis tools for fuel property distribution visualization, (c) compatibility for small and handheld devices, and (d) flexible data upload and download capabilities.

Preliminary analysis
Using the new JSON schema, a fuel data analysis was performed to demonstrate the efficacy of the database for visualizing property distributions and identifying erroneous data and outliers. Composition graphs and distillation plots for alternative and conventional fuels were also produced as a starting point for the analysis. As more fuel data are obtained and added to the database, more meaningful and statistically significant analyses will be possible, including those based on machine learning methods.

Publications
N/A

Outreach Efforts
N/A

Awards
Anna Oldani (Graduate Student): DOT Student of the Year Award
Anna Oldani (Graduate Student): Society of Women in Engineering Award for Research Excellence

Student Involvement
This project was primarily conducted by one graduate student (Anna Oldani).

Plans for Next Period
In the next period, we intend to integrate online analysis tools based on 'big data' analysis. We will modify part of the database to be stored in the cloud for integration with the JETSCREEN program, which will provide a starting point for an international database. More details can be found in Task 2.

Task 2 – Preliminary Efforts to Link the Database with JETSCREEN

University of Illinois Urbana-Champaign

Objective(s)

The main objective of this task was to develop methods for integrating the current database with a similar system in the European JETSCREEN program. This effort was established through a series of discussions with the JETSCREEN team, where the benefits of such an endeavor were clearly identified. While the primary aim of this collaborative effort is to provide scientific data to support the approval process of alternative fuels, new directions, such as creating a foundational platform that can be used to integrate real-time fuel property data from flights, were also identified for future efforts. The major goals of this task are as follows:

- Identify benefits for integrating the database with JETSCREEN
- Converge on a single JSON schema for database integration
- Determine guidelines for comparing fuel properties for certification studies
- Determine the structure of a joint database and user interface protocols
- Determine specific near-term and long-term goals for database integration

Research Approach

Database integration with JETSCREEN

JETSCREEN is a European program spearheaded by the German Aerospace Center (DLR) and the University of Birmingham in the UK dedicated to providing fuel producers, air framers, and aeroengine and fuel system OEMs with knowledge and screening tools to streamline the alternative jet fuel approval process. The key objectives of JETSCREEN include (1) assessing the compatibility of fuels with respect to fuel and combustion systems, (2) quantifying the added value of alternative jet fuels, and (3) supporting research for optimizing fuel formulation to attain the full environmental potential of synthetic and conventional fuels.

Since the inception of the JETSCREEN program, we have communicated with the JETSCREEN leadership regarding approaches in which we can benefit from each other, as many of the goals of ASCENT align well with those of JETSCREEN. A timeline of milestones in our joint effort is presented in Figure 5. As the most important aspect of this specific project, JETSCREEN is establishing a database much like the system discussed herein. In the later stages of 2017, we concluded that it would be mutually beneficial to integrate parts of the two databases into one system and to establish a foundation that could, in the future, encompass additional database links around the globe. In December 2018, at the annual JETSCREEN meeting, we presented specific goals, both technical and strategic, regarding this integration process. From a technical perspective, we put forth a common nonrelational JSON schema and other details regarding the database structure, interface, analysis routines, etc. It was also determined that while the data location would be common for our database and JETSCREEN, the interface and analysis routines would be different and customized to suit the needs of either party. Both our database and JETSCREEN would develop separate online portals for accessing the data. From a strategic perspective, we plan to gear the database towards two critical goals: (1) fuel certification analysis and (2) inclusion of fuel properties from airports (described in more detail below). These goals were presented at both the CRC and IASH meetings in 2019.

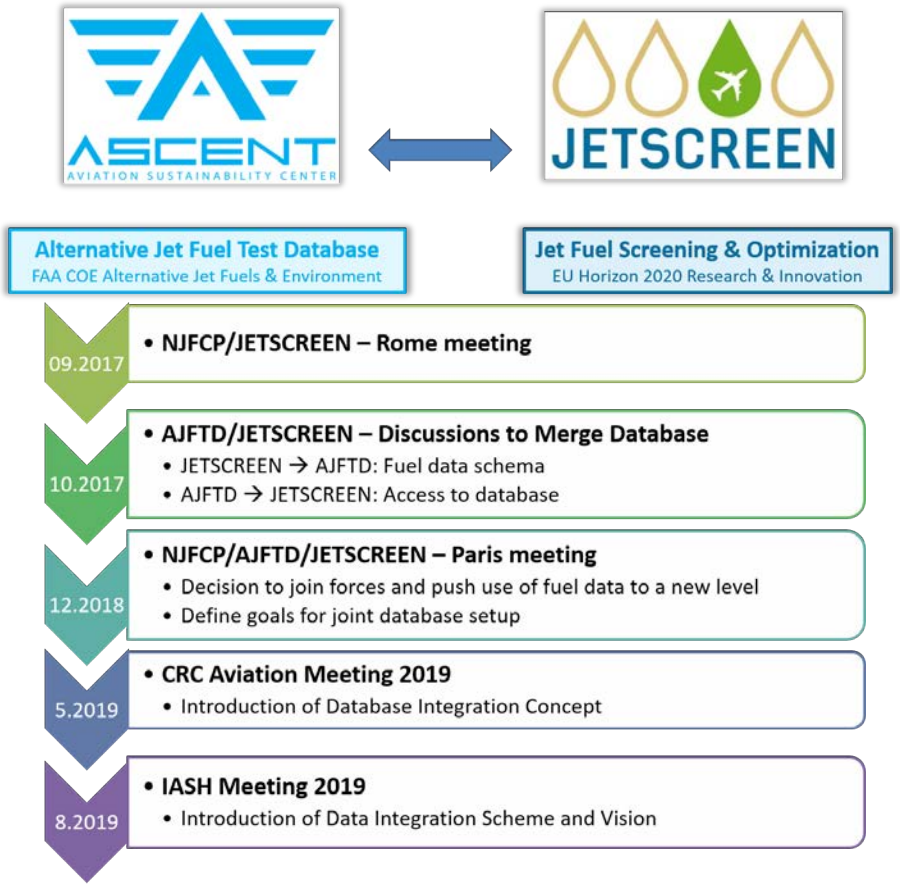

Figure 5. Timeline of milestones relevant to the integration of our database with JETSCREEN.

Fuel property analysis to support certification

This database makes a critical contribution by providing a measure for comparing new fuels to current fuels in the database. A combination of whisker plots and data points was chosen for optimal visualization of this comparison, as illustrated in Figure 6. Here, properties from a specific new fuel blend are compared with those for a subset of fuels in the database. The center point of the box shows the median, and the interquartile ranges are shown as the edges of the box (left and right). The solid whiskers show the distribution of fuels from the database while the dotted whiskers show the limits of the specification. The green data points designate properties that are within the range of fuel properties in the dataset, while the yellow points show properties that are outside the range of the database but still within the specification guidelines. The red points fall outside of the specification entirely. Both our database (generation II) and the JETSCREEN online interface will utilize this comparison method, where users can choose to compare a selected fuel with our entire database or a subset of fuels.

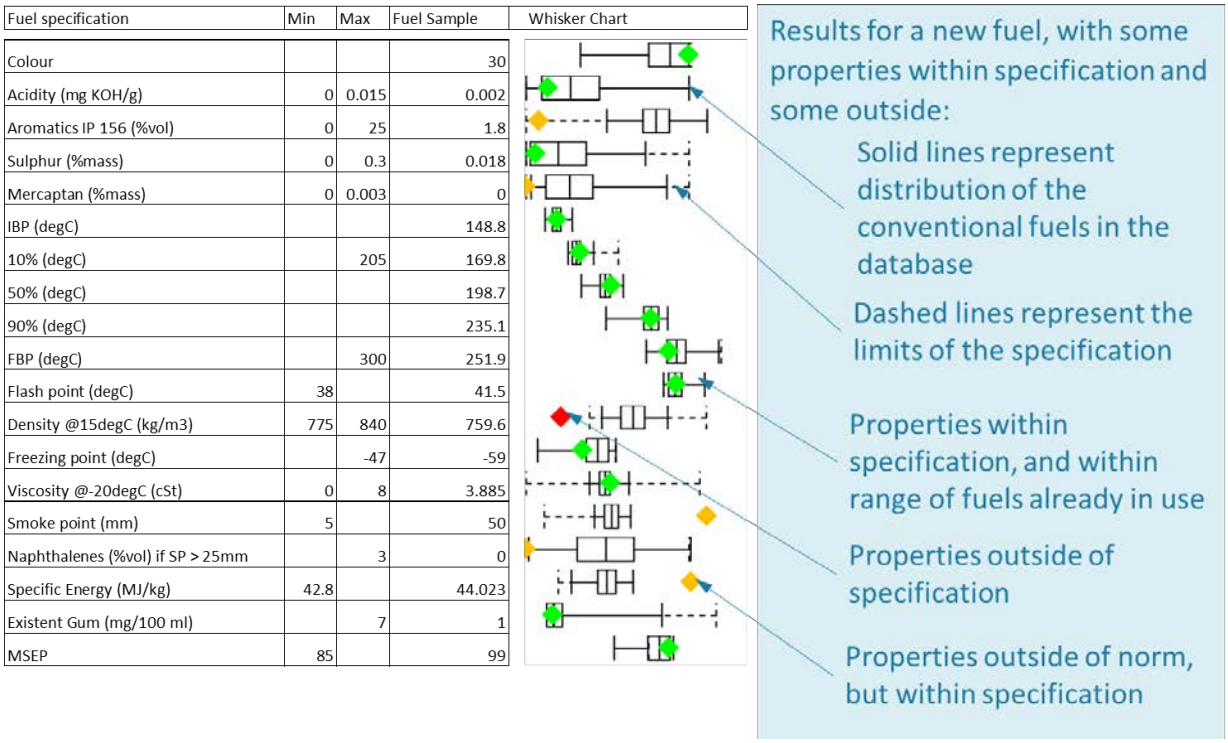

Fuel specification	Min	Max	Fuel Sample
Colour			30
Acidity (mg KOH/g)	0	0.015	0.002
Aromatics IP 156 (%vol)	0	25	1.8
Sulphur (%mass)	0	0.3	0.018
Mercaptan (%mass)	0	0.003	0
IBP (degC)			148.8
10% (degC)		205	169.8
50% (degC)			198.7
90% (degC)			235.1
FBP (degC)		300	251.9
Flash point (degC)	38		41.5
Density @15degC (kg/m3)	775	840	759.6
Freezing point (degC)		-47	-59
Viscosity @-20degC (cSt)	0	8	3.885
Smoke point (mm)	5		50
Naphthalenes (%vol) if SP > 25mm		3	0
Specific Energy (MJ/kg)	42.8		44.023
Existent Gum (mg/100 ml)		7	1
MSEP	85		99

Figure 6. Comparison of fuel properties with those in the database and ASTM specifications. The red data point indicates a value that is outside the specifications.

In addition to the fuel property analysis shown in Figure 6, the nonrelational schema utilized for the database allows us to deploy a range of advanced analysis methods, including machine learning algorithms, that can seek different correlation factors between properties and fuel performance. Even a general correlation between properties may reduce the tests required for the approval process, and an analysis of GCxGC data could shed light on the relationship between fuel performance and fuel blend chemical composition. To this end, JETSCREEN and our team will launch a machine learning exercise to identify critical correlations between properties that have not yet been determined through previous methods.

Figure 7. Impact of integrating real-time data from airports regarding fuels used in actual flights.

Integration of actual fuels used at airports

A new direction was identified during the early stages of discussion with JETSCREEN: to seek a method for compiling data on fuels utilized in commercial flights. This direction was motivated by two aspects. First, in the process of compiling the database, we came across airport data collected by Metron Aviation through an earlier ASCENT project. It became apparent that this type of data was very valuable, providing a roadmap for tracking real fuels being deployed in the field. We were surprised to find that as the data were being generated, no standard archiving method was applied, and the data were being discarded after quality control of the fuel had been performed. Second, as we identified the long-term impact of this database (sample shown in Figure 7), the need for data on fuel that was actually being used, both in real time and compiled over the long term, became increasingly evident. Such data would not only provide a means for assessing the quality and variation of fuels currently in use but, over time, would also provide an archive of changes in overall chemical compositions and physical properties. This type of data can greatly aid in the analysis of the environmental impact of fuels over time.

Milestone(s)

Throughout this year, we have worked with the JETSCREEN team to develop a plan for merging a portion of the database. We envision that this step will establish the foundation for an international platform, where various nations can both upload fuel data and utilize data from other nations. We have set forth several motivations and strategies to complete this task and have established firm guidelines for use in this collaboration. We plan to present these plans and acquire reviews from the academic community in the next year and will then make the necessary modifications.

Major Accomplishments

JETSCREEN integration vision

We have established a technical and strategic vision to integrate our database with the JETSCREEN database. The new database will not only provide support for the integration of alternative fuel blends, but will also provide a foundation that can integrate data for fuels used in commercial flights. In this manner, the system will amass data that can optimize both operational efficiency and safety in the future.

Publications

Oldani, Anna. (2019). Alternative jet fuel variation and certification considerations. In progress.

Outreach Efforts
N/A

Awards
Anna Oldani (Graduate Student): DOT Student of the Year Award
Anna Oldani (Graduate Student): Society of Women in Engineering Award for Research Excellence

Student Involvement
This project was primarily conducted by one graduate student (Anna Oldani). Oldani surveyed the data, interacted with the data sources, and created strategies to integrate the data into the database. Oldani also developed a web-based portal for implementation of the web interface and analyzed the available data to evaluate the property variance. Oldani presented these results at conferences and FAA ASCENT meetings. Anna Oldani completed her PhD in April 2019 and began working at the FAA Office of Environment and Energy in September 2019.

Plans for Next Period
Database integration and capture of real-time fuel use data
In year VI of the database project, we will implement fully extended data evaluation activities using the new nonrelational structure and will integrate the database with JETSCREEN. Additionally, we will engage with airports to evaluate the potential for integrating real-time data. New advanced analysis methods will be made available online.

- Evaluation and analysis of all data, including GCxGC, Metron, and PQIS data
- Utilization of machine learning algorithms for data analysis (property correlations)
- Integration of a common database with JETSCREEN, with separate user interfaces
- Interaction with airports to assess pathways for capturing data on fuels in use
- Inclusion of additional data and continued integration of fuel data from all sources

Project 034 National Jet Fuels Combustion Program – Area #7: Overall Program Integration and Analysis

University of Dayton

Project Lead Investigator

Joshua Heyne
Assistant Professor
Mechanical Engineering
University of Dayton
300 College Park
Dayton, OH 45458
937 229-5319
Jheyne1@udayton.edu

University Participants

University of Dayton

- PI(s): Joshua Heyne
- FAA Award Number: 13-C-AJFE-UD (Amendment Nos. 9, 10, 13, 17, and 18)
- Period of Performance: September 18, 2015, to December 31, 2019
- Task(s):
    1. Overall National Jet Fuels Combustion Program (NJFCP) integration and coordination
    2. Development of operability surrogate fuels

Project Funding Level

Amendment No. 9: $134,999.00 (September 18, 2015, to February 28, 2017)
Amendment No. 10: $249,330.00 (July 7, 2016, to December 31, 2017)
Amendment No. 13: $386,035.00 (August 30, 2016, to December 31, 2017)
Amendment No. 17: $192,997.00 (August 3, 2017, to September 30, 2018)
Amendment No. 18: $374,978.00 (December 7, 2017, to December 31, 2018)

Investigation Team

- Joshua Heyne (University of Dayton) is the project lead investigator for coordinating all NJFCP teams (both ASCENT and non-ASCENT efforts).
- Robert Stachler (University of Dayton) is a PhD student conducting the lean blowout (LBO) and emissions measurements in the well-stirred reactor.
- Erin Peiffer (University of Dayton) is a master's student linking experimental results across ASCENT and non-ASCENT teams.
- Katherine Opacich (University of Dayton) is an undergraduate research assistant working to document NJFCP activities and analyze ignition data across NJFCP teams.
- Shane Kosir (University of Dayton) is an undergraduate research assistant working to analyze LBO data.
- Zhibin Yang (University of Dayton) is a graduate student research assistant working to develop physical surrogates.
- Jen Colborn (University of Dayton) is an undergraduate research student assistant aiding in the testing of fuels on the Referee Rig.

Project Overview

The NJFCP is composed of more than two dozen member institutions contributing information and data, including expert advice from gas turbine original equipment manufacturers (OEMs), federal agencies, other ASCENT universities, and

corroborating experiments at the German Aerospace Center (DLR Germany), National Research Council Canada, and other international partners. The project is tasked to coordinate and integrate research among these diverse program stakeholders and academic PIs; cross-analyze results from other NJFCP areas; collect data for modeling and fuel comparison purposes in a well-stirred reactor; conduct large eddy simulations of sprays for the Area 3 high-shear rig; procure additional swirler geometries for the NJFCP areas and allied partners while developing an interface of NJFCP modeling capabilities with OEM requirements. Work under this program consists of, but is not limited to:

- conducting meetings with member institutions to facilitate the consistency of testing and modeling
- coordinating timely completion of program milestones
- documenting results and procedures
- creating documents critical for program process (e.g., fuel down selection criteria)
- soliciting and incorporate program feedback from OEMs
- reporting and presenting on behalf of the NJFCP at meetings and technical conferences
- integrating state-of-the-art combustion and spray models into user-defined-functions (UDFs)
- advising the program steering committee

Task 1 - Integration and Coordination of NJFCP Teams

University of Dayton

Objective

The objective of this task is to integrate and coordinate all ASCENT and non-ASCENT team efforts by facilitating meetings, summarizing results, presenting results external to the NJFCP, communicating regularly with the steering committee, and other related activities.

Research Approach

The NJFCP is integrated and coordinated by two main techniques: (1) the structural combining of various teams into six topic areas; and (2) routine meetings and discussion both internal and external to individual topic areas. The topic areas are distinguished by the dominant physics associated with them (topics I and IV), the culmination of all relevant combustion physics (topics II, III, V), and wrapping all work into a singular OEM graphical user interface package (topic VI). These six topic areas are as follows:

Topic I. Chemical kinetics: Foundational to any combustion model is a chemical kinetic model and the validation data anchoring modeling predictions.
Topic II. LBO: This topic covers data, screening, and validation under relevant conditions to statistically and theoretically anticipate fuel property effects on this figure of merit (FOM).
Topic III. Ignition: Similar to the LBO topic, the focus here is experimental screening and validation data for statistical and theoretical predictions.
Topic IV. Sprays: Historically, the dominant effect of fuel FOM behavior has been the spray character of the fuel relative to others. Experimentalists in this topic area focus on measuring effects of fuel property on spray behavior. Analogous to topic I, spray behavior is not an FOM like topics II and III, although it is critical to bound the physical property effects on combustion behavior relative to other processes (i.e., chemical kinetics).
Topic V. Computational fluid dynamics (CFD) modeling. Complementary to the empirical topics II, III, and IV, the CFD modeling topic focuses on the theoretical prediction of measured data and facilitates the development of theoretical modeling approaches.
Topic VI. UDF development: Once the theoretical modeling approaches matured in topic V are validated, UDFs are developed for OEM evaluation of fuel performance in proprietary rigs.

These topic area teams meet and coordinate regularly. At minimum, NJFCP-wide meetings are held monthly and topic area meetings occur typically every 2 to 3 weeks.

Milestone

NJFCP Year 4 Meeting 2019

Major Accomplishments

- Book editing and coordination.

- Developing and publishing a Civil Aviation Alternative Fuels Initiative (CAAFI) R&D prescreening document to aid novel companies and producers in the refinement and development of fuels that can most easily eclipse the Tier 3 and 4 testing.

Publications

Peer-reviewed journal publications

Peiffer, E.E., Heyne, J.S., & Colket, M. (2019). Sustainable aviation fuels approval streamlining: auxiliary power unit lean blowout testing. AIAA Journal, pg. 1-9, https://doi.org/10.2514/1.J058348.

Ruan, H., Qin, Y., Heyne, J., Gieleciak, R., Feng, M., & Yang, B. (2019). Chemical compositions and properties of lignin-based jet fuel range hydrocarbons. Fuel 256 115947, https://doi.org/10.1016/j.fuel.2019.115947

Published conference proceedings

Heyne, J., Opacich, K., Peiffer, E., & Colket, M. (2019). The effect of chemical and physical fuel properties on the approval and evaluation of alternative jet fuels. 11th U.S. National Combustion Meeting, Pasadena, CA

Opacich, K.C., Heyne, J.S., Peiffer, E., & Stouffer, S.D. (2019). Analyzing the relative impact of spray and volatile fuel properties on gas turbine combustor ignition in multiple rig geometries. AIAA SciTech, AIAA 2019-1434, San Diego, CA

Written reports

CAAFI R&D Committee. (2019). Prescreening of synthesized hydrocarbons intended for candidates as blending components for aviation turbine fuels. Commercial Alternative Aviation Fuel Initiative (CAAFI), CAAFI R&D Committee Publication

Outreach Efforts

Invited talks

Colket, M. & Heyne, J. (2018). Early evaluation of alternative jet fuels based on NJFCP results. Advanced Bioeconomy Leadership Conference (ABLC), San Francisco, CA

Colket, M. & Heyne, J. (2019). Major results from the National Jet fuels and Combustion Program. ASME TurboExpo, Phoenix, AZ

Colket, M., Heyne, J., & Lee, T. (2018). An overview of ASCENT research efforts to improve our understanding of how fuel composition and characteristics determine performance. CAAFI Biennial General Meeting

Colket, M., Heyne, J., & Lee, T. (2018). NJFCP update: Properties and modeling to FOM predictions. JetScreen Meeting, Paris, FR

Edwards, T. & Heyne, J. (2019). Towards the minimization of ASTM D4054 tier 3 & 4 AJF approvals. 2019 CRC Aviation Committee Meetings, San Juan, PR

Heyne, J. (2019). Drop-in high-performance fuels: From molecule selection to mission benefits. NREL IBRF Lab, Golden, CO

Heyne, J. (2019). The approval and evaluation NJFCP learnings and high-performance fuels for operability and mission benefits. Rolls-Royce, Indianapolis, IN

Conference presentations

Opacich, K., Heyne, J.S., Peiffer, E., & Stouffer, S.D. (2018). Analyzing the relative impact of spray and volatile fuel properties on gas turbine combustor ignition. DESS2018-019, 14th Dayton Engineering Sciences Symposium, Wright State University

Stachler, R., Heyne, J., Peiffer, E., Stouffer, S., & Miller, J. (2018). Assessment of lean blowoff in a toroidal jet stirred reactor. Dess2018-055, 14th Dayton Engineering Sciences Symposium, Wright State University

Articles/press

Heyne, J., Wang, H., & Kalman, J. (2018). Safely improving jet, rocket fuels. Aerospace America, 2018 Year in Review, Propellants and Combustion Technical, Committee Contribution

Funded program review presentations

Heyne, J. & Colket, M. (2019). AIAA Book and year 5 - next steps and action item review. NJFCP 2019 Review Meeting, OAI, Cleveland, OH

Heyne, J. & Colket, M. (2019). Highlights of NJFCP achievements - overall impact of program tiers and HPF. NJFCP 2019 Review Meeting, OAI, Cleveland, OH

Heyne, J., Colket, M., Moder, J., & Shaw, C. (2018). NJFCP status update. FAA ASCENT, Alexandria, VA
Heyne, J., Emerson, B., Lieuwen, T., Stouffer, S., Blunck, D., Corporan, E., Mastorakas, N., & de Oliveira, P. (2019). LBO WG update and 4 year summary. NJFCP 2019 Review Meeting, OAI, Cleveland, OH
Stouffer, S., Heyne, J., Boehm, R., Mayhew, E., Lee, T., & Canteenwalla, P. (2019). Ignition WG update and 4 year summary. NJFCP 2019 Review Meeting. OAI, Cleveland, OH

Awards

Joshua Heyne:
- University of Dayton Nominee, Blavatnik National Awards for Young Scientists, 2019.
- Outstanding Service Award, ASME Dayton Section, 2018.

Shane Kosir:
- Ohio Space Grant Consortium Master's Fellowship, 2019
- Class of 1902 Award of Excellence for Outstanding Mechanical Engineering Achievement, 2019

Katherine Opacich:
- Ohio Space Grant Consortium Master's Fellowship, 2019
- The Martin C. Kuntz, 1912, Award of Excellence to the Outstanding Junior in Mechanical Engineering, 2018

Student Involvement

Erin Peiffer, graduate research assistant, June 2017 to December 2018. Erin is a master's student linking experimental results across ASCENT and non-ASCENT teams.
Zhibin Yang, graduate research assistant, August 2018 to present. Zhibin is a graduate student research assistant working to develop physical surrogates.
Katherine Opacich, undergraduate research assistant, November 2017 to present. Katherine is an undergraduate research assistant working to document NJFCP activities and analyze ignition data across NJFCP teams.
Shane Kosir, undergraduate research assistant, January 2018 to present. Shane is research assistant working to analyze LBO data.
Jen Colborn, undergraduate research assistant, January 2017 to December 2018. Jen is an undergraduate research student assistant aiding in the testing of fuels on the Referee Rig.

Plans for Next Period

Continue to perform all relevant coordination- and integration-related tasks.

Task 2 - Overall NJFCP Summary Coordination

University of Dayton

Objective

Research Approach

Introduction

Anthropogenic carbon emissions are increasingly being tied to deleterious environmental effects. To this end, various regulatory bodies are focusing on methods to minimize emissions of carbon in the transportation sector. The International Civil Aviation Organization (ICAO), for example, has established a Carbon Offsetting and Reduction Scheme for International Aviation (CORSIA), which sets voluntary carbon reduction standards during Phase 1 (through 2026) and mandatory standards during Phase 2 (2027 and beyond) (IATA, 2018). Sustainable aviation fuel (SAF) consumption will need to increase to >10% of total jet fuel consumption by 2040 to meet ICAO commitments. On a global basis, this is more than the total volume of jet fuel consumed currently.

The key to the success of these goals is minimizing the barriers that inhibit the commercialization of novel SAFs to market. One of these critical barriers is the approval and evaluation process that SAFs must pass before commercialization. The approval of an SAF is contingent upon many factors, including bulk and trace fuel properties (ASTM D4054, Tiers 1 and 2) and the effect the fuel has on operability limits (ASTM D4054, Tiers 3 and 4). These later tests (Tiers 3 and 4) involve much larger fuel volumes and focus on testing three so-called FOMs. These FOMs, in turn, correspond to the most critical safety criteria required of fuel: the ability to stably hold a flame and to ignite under severe conditions.

Explicitly, the ability of a fuel to hold a flame stably is called the LBO limit of a fuel and it represents the lower operability limit of the stability loop. The other two key FOM behaviors are determined by the ease with which a fuel can ignite under cold atmospheric conditions (cold start) and cold-altitude conditions (altitude relight).

Over the last four years, the NJFCP has pursued advancements in understanding that could streamline the process of approving new alternative jet fuels for use in the aviation industry. Specifically, the program is focused on critical combustion-related safety aspects associated with the utilization of new fuels. The NJFCP is a joint effort among government, universities, engine manufacturers, and international partners. The program objectives have been described in detail (Colket et al., 2017), summaries of progress have been presented annually (Heyne et al., 2017; Heyne et al., 2018), and selective individual accomplishments have recently been presented or published (Bokhart et al., 2017; Hasti et al., 2018; Ma et al., 2019; Panchal et al., 2018; Rock et al., 2019; Wang et al., 2019). Major results have been in the areas of understanding the dependence of fuel properties on limits of LBO and of cold start and altitude relight. To explore these phenomena, new facilities and test procedures have been created, and science/technology related to fuel dependence (vaporized and spray) on chemical kinetics, spray phenomena, CFD simulations, ignition, and LBO have been tested both in controlled laboratory rigs and in engine-like hardware under realistic flow conditions.

One major and new conclusion of the program thus far is that LBO can depend *both* on the chemical nature and the physical properties of the fuel, based on hardware design and flow conditions of the rig and the fuel nozzle/swirler. The dependence on physical properties of the fuel has been known for decades (Lefebvre, 1983; Lefebvre & Ballal, 2010). However, the demonstration that LBO can be dependent on the derived cetane number (DCN), especially for combustors of modern design with new fuel injectors and intense fuel/air mixing is a relatively new observation and has been strongly validated under this program (Chtev et al., 2017; Stachler et al., 2017). A second major conclusion is the confirmation that ignition and altitude relight are most strongly correlated with fuel physical properties, in particular, density, volatility, viscosity, and surface tension. The relative dependency on each of these parameters and how they change with operating conditions and hardware is still under investigation.

Here, we report on the most recent cross-area analysis for two key FOM evaluation criteria as part of the approval and evaluation process for alternative jet fuel. Moreover, these cross-area analyses are articulated as a means to test a fuel formally as part of the ASTM D4054 approval process, informally as a prescreening process for potential jet fuel candidates, and for the prediction of deleterious operability. Combined, these tests and tools could facilitate the reduction of expensive and volume-intensive approval tests, enabling additional fuels to meet CORSIA requirements and faster approval and lower investment costs.

Methods/experiments

The NJFCP comprises multiple working groups each tasked with addressing specific problems. Combined, these working groups complement other aspects of the program by providing a greater level of experimental resolution on specific physics or adding a modeling accompaniment. The working groups include Kinetics, Sprays, LBO, Ignition, CFD, and Common Format Routine. This report focuses on combining and analyzing data from several teams within the LBO and Ignition working groups that have focused on quantifying fundamental FOM behavior under conditions identified by the NJFCP engine company advisory committee. The detailed methods used in these cross-area analyses have been documented previously (Heyne et al., 2018). Here, we report only the combined results from these works as well as the implications for ASTM approval and prescreening, while documenting fuels tested as well as recognizing key institutions and facilities.

Fuels

The fuels tested under the NJFCP have been documented extensively in previous publications (Edwards, 2017; Heyne et al., 2018). These fuels span properties associated with the range of conventional (Category A) fuels, and a wide breadth of alternative and "test" fuels that stress the drop-in requirements; for example, Category C fuels. The operability sensitivity to conventional fuels is defined by the variance in the three Category A, or petroleum, fuels. The sensitivity to fuel effects from alternative fuels, then, is loosely bounded by the variance from the Category C fuels. Although the Category C fuel variance does not represent all possible alternative fuel property effects, the variance still captures many of the possible major contributions for fuel operability effects. Additional Category C fuels (C-7, C-8, and C-9) have been added to the NJFCP as new needs have developed. Table 1 and Figure 1 describe and illuminate the associated fuel property and compositional variance for the 12 NJFCP fuels.

Table 1. NJFCP Category A and C fuels. The Category A fuels represent the range of petroleum-derived fuels currently in use today; Category C fuels represent alternative jet fuels that have "extreme" properties that could affect figure of merit (FOM) operability limits.

Fuel	POSF Number	Composition, % volume	Description
A-1	10264	Petroleum JP-8 (w/high flash point and low viscosity and aromatics)	Low flash, viscosity, and aromatics
A-2	10325	Petroleum Jet A	Nominal jet fuel
A-3	10289	Petroleum JP-5	High flash, viscosity, and aromatics
C-1	11498, 12368, 12384	Gevo ATJ, Highly branched C12 and C16 alkanes	Low DCN, unusual boiling range
C-2	11813, 12223	16% *tri*-methylbenzene + 84% C14 *iso*-alkanes	Chemically asymmetric boiling range
C-3	12341, 12363	64% A-3 + 36% farnesane	High viscosity fuel, at viscosity limit for jet fuel at −20˚C
C-4	12344, 12489	60% C9-12 *iso*-alkanes, 40% C-1	Low DCN, conventional, wide boiling range
C-5	12345, 12713, 12789, 12816	73% C10 *iso*-alkanes, 17% *tri*methylbenzene	Flat boiling range
C-6		High *cyclo*-alkane content	High *cyclo*-alkanes
C-7	12925	75% RP-2, 23% A-3, 2% decalin	High *cyclo*-alkanes
C-8	12923	Jet A + Exxon aromatic blend	High (maximum allowable) aromatics
C-9	12933	80% R-8 HEFA, 20% *n*-C12	High DCN

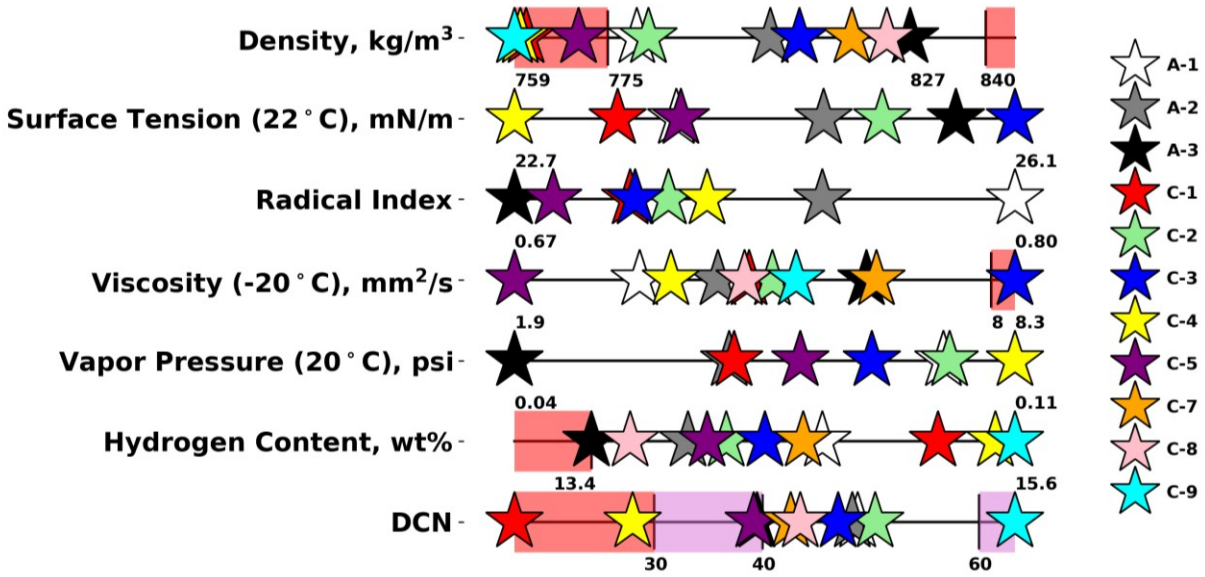

Figure 1. Category A and C range of fuel properties. Red regions represent established limits and purple areas represent proposed limits or areas to explore further. Category A fuels set the bounds of what is currently being used compared with the alternative jet fuel property ranges represented by the Category C fuels.

Institutions and experimental facilities

The NJFCP is composed of several working groups, each of which focuses on a given technical area relevant to the testing, evaluation, and modeling of an SAF. The focus of this paper is to highlight several key experimental facilities and their results as they directly relate to the SAF approval and evaluation process (ASTM D4054). The two most critical working groups evaluating operability limit sensitivity due to SAFs are the Ignition and LBO working groups. These groups have the most direct testing outcomes toward reducing the cost and time intensity of SAF approvals, because these are the two tests targeted in the high-volume Tier 3 and 4 tests. These working groups are composed of approximately 5 to 7 smaller research groups each. The details of many of these individual research groups can be found in dedicated papers, so we focus here on the most developed analyses and impactful results.

The major results from the LBO working group can be summarized via the variance observed in the data from an auxiliary power unit (APU) operated by Honeywell, a Tay combustor rig at the University of Sheffield, and the Referee Rig and toroidal jet-stirred reactor (TJSR), both at the Air Force Research Laboratory (AFRL)/University of Dayton Research Institute (UDRI). Combined, these groups span extremes in combustor geometries and test conditions, in terms of mixedness, atomization, and swirl stabilization. The Honeywell APU engine is characterized as being dominated by fuel physical properties for fuel operability limits and is one extreme of spray-atomization break-up dominance (Culbertson & Williams, 2017). The TJSR, being prevaporized and premixed, is at the other end of the spray-atomization break-up spectrum (Stachler et al., 2018). It has no spray character and, as a result, is dominated entirely by fuel chemical effects. The remaining rigs, the Referee Rig and the Tay combustor, could be dominated by either spray or chemical effects depending on thermodynamic and aerodynamic conditions (Khandelwal & Ahmed, 2017; Stouffer et al., 2017); both rigs utilize a pressure atomizer with an external co-axial swirler. The Ignition working group's major results will be highlighted only through results from one rig, the Honeywell APU (Culbertson & Williams, 2017). This rig is the only one with fully public results on ignition, although all other rigs show similar qualitative behavior.

Results and discussion

LBO

The LBO of a rig is contingent upon the competition of chemical, distillate, and physical properties in the determination of the limit. Under advantageous spray conditions, chemical properties will dominate the limit, whereas at lower temperatures

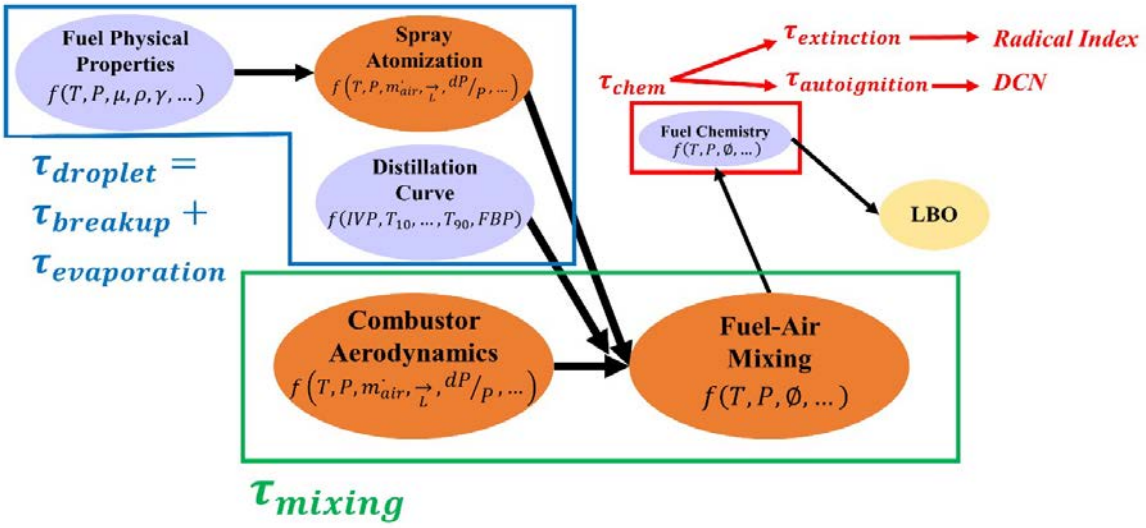

Figure 2. Generic physical phenomena controlling lean burnout (LBO) limits. Right-ward objects are dependent upon left-ward objects. Thus, spray properties can hinder later chemical reactions on the right side of the diagram. Purple objects correspond to fuel properties that can lead to engine operability sensitivity. The three bulk operability timescales identified are droplet, mixing, and chemical timescales. DCN, derived cetane number.

Figure 2 illustrates the dependency of cascading processes on the eventual global flame extinction at LBO. Moreover, any one of the three bulk properties associated with fuels can become the eventual bottleneck.

Figure 3 illustrates the relative sensitivity of these three bulk properties on LBO for previously reported NJFCP fuels. Sensitivities reported in Figure 3 were determined by random selection of orthogonal variables that could lead to LBO or represent the three fuel physical processes leading to LBO. For example, the 10%, 20%, or 50% distilled temperatures could all be representative of a fuel's distillate character. These temperatures are varied many times across the data regressions in parallel with other properties that could be important to other key processes, such as viscosity, surface tension, and density in the case of droplet break-up.

Results corroborate the physical and intuitive understanding of how each rig works. Physical and distillate properties dominate in the rig that has the least aggressive spray break-up mechanisms; see Figure 3a). Conversely, chemical properties dominate in the TJSR rig, as this rig is entirely premixed and prevaporized. The two rigs with swirlers exhibit some dependency on multiple properties. The Referee Rig, as before, is most directly influenced by the autoignition propensity of a fuel; that is, the DCN (Stouffer et al., 2017).

Combined, this analysis is carried out over hundreds of experimental observations, four rigs, and more than 11 fuels. The R^2 value was, at worst, 0.88 for one combination of properties in one rig, for which preferential vaporization has been discussed extensively (Bell et al., 2018). The implication, then, is that with this reduced-order regression, potential deleterious effects that might be discovered during Tier 3 and 4 testing can be mitigated by bounding properties similar to specification sheets. Fortunately, the properties used in this analysis are measured at earlier stages of fuel production scaling and Tier 1 and 2.

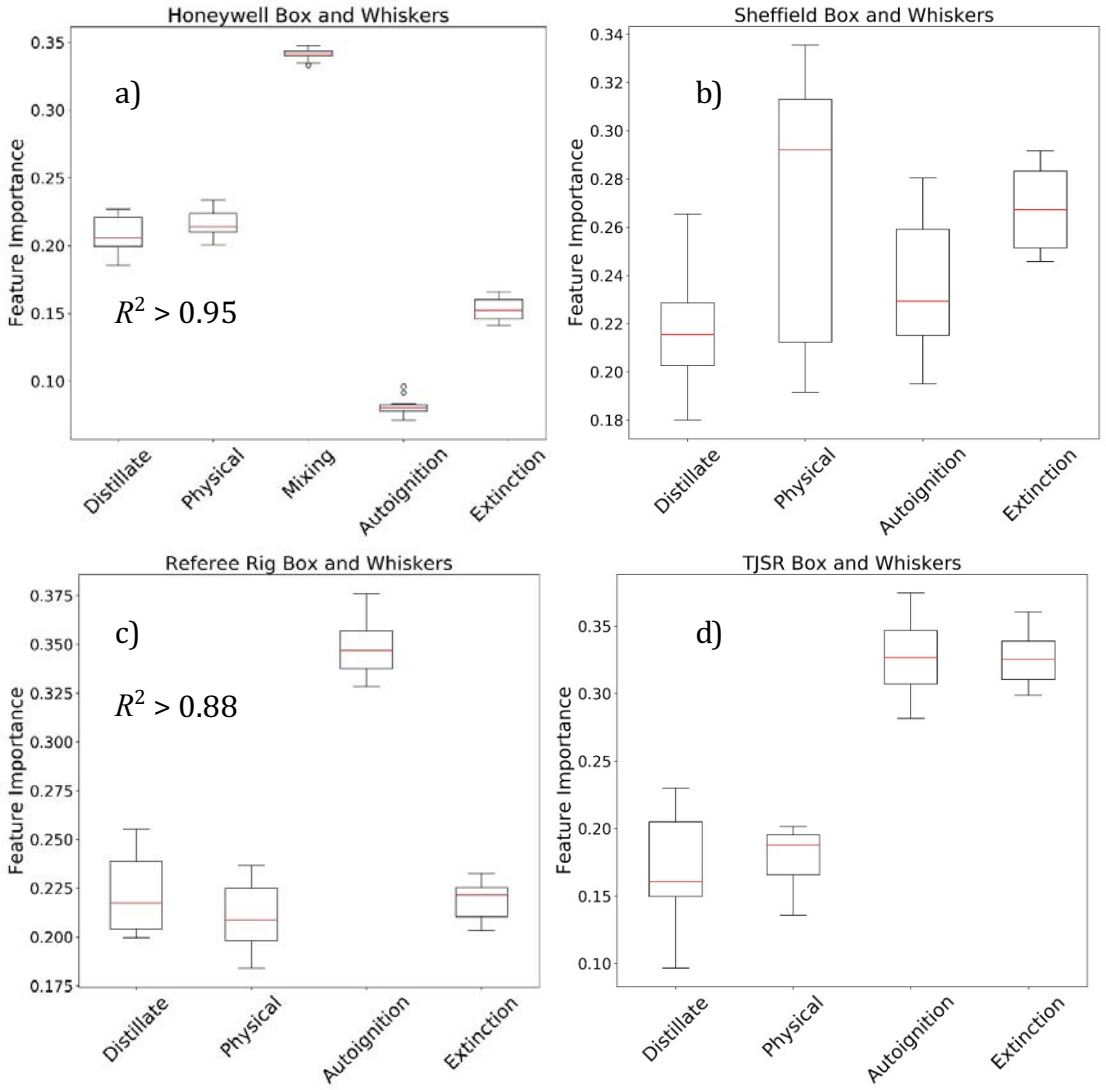

Figure 3. Box and whisker plots summarizing the analysis for the major contributions considered to lead to lean burnout (LBO) in four rigs of diverse architecture and conditions. Physical and distillate properties dominate the fuel effects in the Honeywell auxiliary power unit (APU; a) and the Sheffield rig (b). Chemical properties (autoignition and extinction) are strongly correlated with combustion phenomena in the Referee Rig (c) and the toroidal jet-stirred reactor (TJSR; d).

Ignition

Similar to the LBO flow path, the progression to ignition is illustrated in Figure 4. The critical fuel properties affecting successful ignition probability are shown in light purple; other ovals represent important categorical processes that are not directly tied to fuel effects. Thus far in the NJFCP, the effect of chemical properties is minimal for practical ignition probabilities. Sparse chemical effects have been reported in prevaporized, partially premixed combustion experiments.

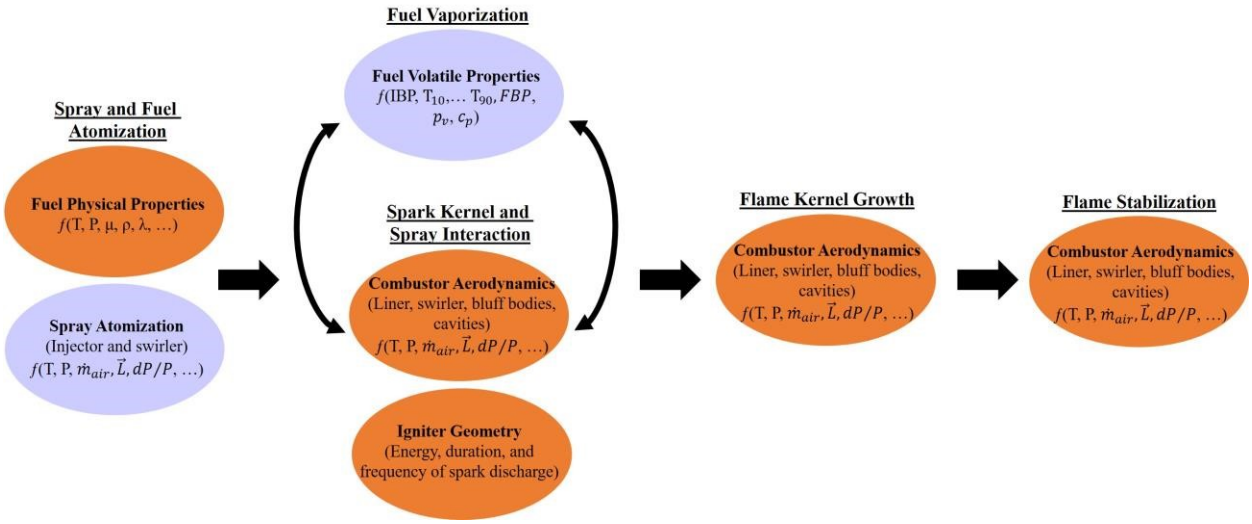

Figure 4. General flow diagram of physical processes for a stabilized flame from the injection of a plasma spark. Two of the five outlined processes involve potential fuel effects, and both of these fuel effects are common to the lean burnout (LBO) process outlined in Figure 2.

Ignition experiments analyzed here based on the data reported by Culbertson and Williams at Honeywell (Culbertson & Williams, 2017). This study (Culbertson & Williams, 2017) tested only 6 of the 11 NJFCP fuels. Previous analysis on these data showed competitive importance of surface tension and viscosity, depending upon the condition of the fuels (Opacich et al., 2019). Figures 5 and 6 report updated analyses for these data, with the updated analysis considering potential droplet temperature variance for chilled and heated fuels. This droplet temperature variance is intended to account for the potential droplet heat inductance due to spark kernel–droplet interactions. Thus, at higher levels of heat transfer to the droplet, surface temperatures and, in turn, vapor pressures will be higher.

Figure 5 illustrates the random forest regression analysis (RFRA) for the fuel property variables outlined in Figure 4. The RFRA is evaluated for fuel physical properties at the conditions reported (Culbertson & Williams, 2017). However, fuel vapor pressure for the RFRA is evaluated at the temperatures reported on the x-axis. This analysis is then repeated 100 times every 1˚C. The apparent scatter in feature importance for each of the properties represents the randomness associated with each RFRA evaluation. These RFRA evaluations involved randomness introduced at both the variable and data set level. Figure 5 suggests that the ignition probability of a fuel is most directly related to the density and surface tension of a fuel. Variance in the viscosity is also strongly correlated with ignition probability. At 50˚C, the feature importance of vapor pressure increases significantly, coincident with the inversion in the vapor pressure of A-1 and C-1 (Opacich et al., 2019).

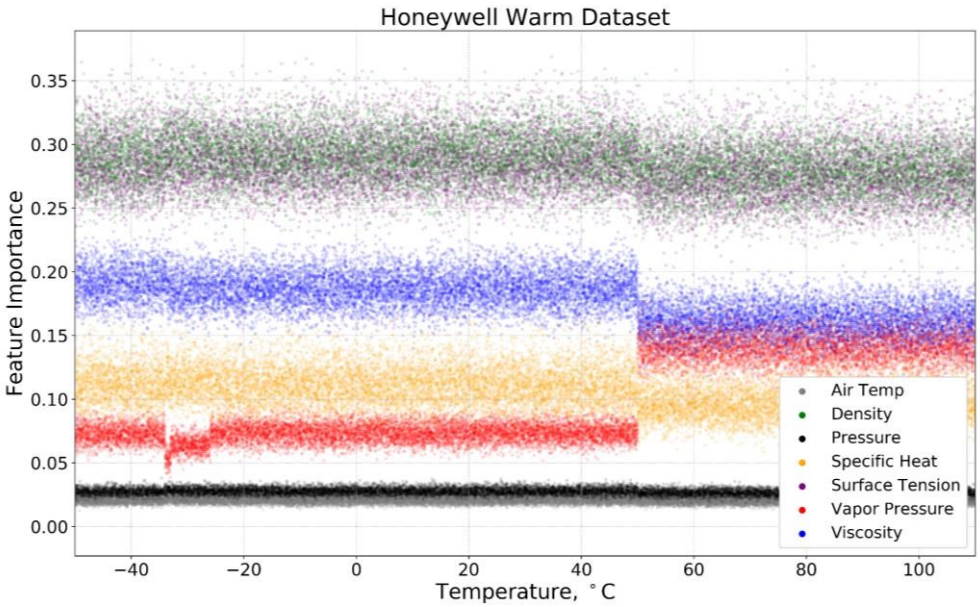

Figure 5. Feature importance concerning varying the droplet temperature for warm fuel tests in a Honeywell auxiliary power unit (APU). Vapor pressure has negligible importance for low temperatures but greater importance at high temperatures. The step change in the importance of vapor pressure represents the temperature at which C-1 has a higher vapor pressure than A-1. The noise in the plots represents the variance introduced by random selection of variables and subsets of data.

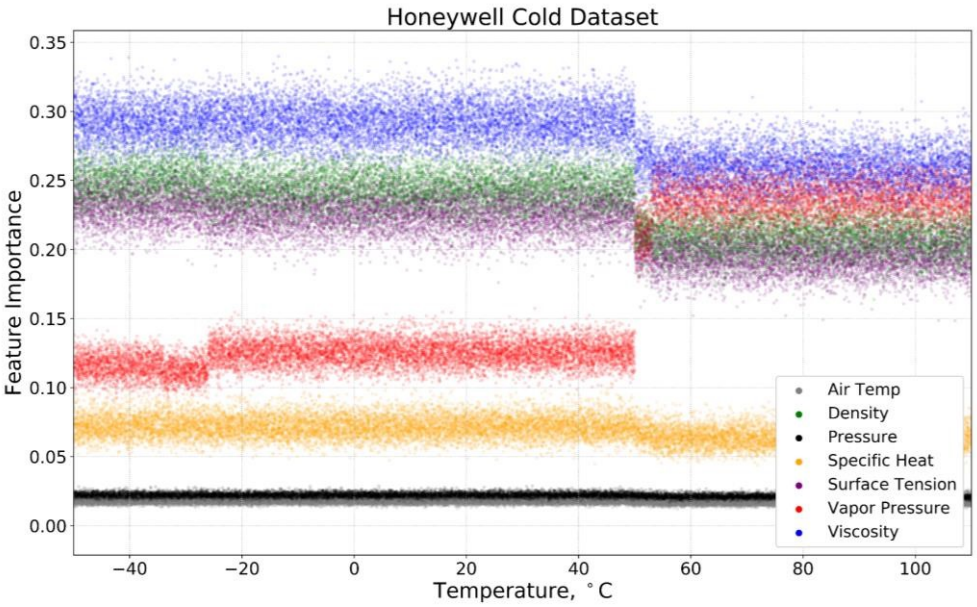

Figure 6. Feature importance for several critical properties in the ignition of a fuel. The cold fuel data analyzed here have more sensitivity to the viscosity of the fuel, which increases exponentially with decreasing temperature. Dependence of surface tension and density are nearly indistinguishable because of their nominal collinearity. The dramatic increase in the importance of the vapor pressure coincides with the inversion of the C-1 and A-1 vapor pressure curves.

Figure 6 shows a similar RFRA as that in Figure 5 for the cold fuel data of Culbertson and Williams. These analyses suggest that ignition probabilities are first affected by the viscosity of a fuel and second by the surface tension and density of a fuel at low droplet temperatures. However, as droplet temperature exceeds 50°C, the vapor pressure of the fuel eclipses the feature importance of surface tension and density. Note that only at temperatures above 50°C are vapor pressures high enough to support combustion.

The feature importance effects between the warm and cold fuel cases appear counterintuitive. The cold fuel data are more sensitive to droplet temperature exceeding 50°C, and the probability of this occurring under the −37 to −19°C cold fuel condition is low compared with that under warm ambient fuel conditions. Although this observation is not conclusive, it is suggestive that additional analysis is needed.

Conclusions

LBO and ignition probability data from the four rigs were analyzed using orthogonal fuel properties and RFRA methods. LBO data from hundreds of data points, 11 fuels, many operating conditions, and four very different rigs and fuel injection approaches were analyzed. The results accounted for more than 89% of all variance. Fuel-dependent LBO effects depend on the chemical, physical, and distillate properties of a fuel, thermodynamic conditions, and geometrical bias of an experiment. DCN is an effective marker for autoignition reactivity of a fuel near LBO. Physical properties dominate cold ignition behavior and LBO in configurations with less intensive mixing-swirl stabilization and aggressive atomization methods. Distillate properties can affect evaporative timescales. Deleterious fuel effects are particularly apparent when chemical and distillate property effects are coupled in the case of preferential vaporization.

Combined, our observations offer an opportunity to not only screen fuels early in the approval process, before Tier 3, but also illuminate paths for prescreening of fuel properties. Prescreening fuel properties, as part of (or prior to) ASTM D4054 Tier 1 and 2 testing, would involve the evaluation or prediction of the properties listed above. Preliminary analysis suggests that with as little as several liters, most properties critical to LBO and cold ignition/altitude relight could be evaluated. These prescreening tests could also be done using predictive, low-volume fuel testing methods such as two-dimensional gas chromatography (GCxGC), nuclear magnetic resonance, and Fourier transform infrared spectroscopy.

Milestone

NJFCP Year 4 Meeting 2019

Major Accomplishments

- Book editing and coordination.
- Developing and publishing a Civil Aviation Alternative Fuels Initiative (CAAFI) R&D prescreening document to aid novel companies and producers in the refinement and development of fuels that can most easily eclipse the Tier 3 and 4 testing.
- Experimental results from testing surrogate fuels can illustrate the maximum FOM sensitivity, aiding in the prescreening and formal evaluation of novel SAFs

Publications

Peer-reviewed journal publications

Peiffer, E.E., Heyne, J.S., & Colket, M. (2019). Sustainable aviation fuels approval streamlining: Auxiliary power unit lean blowout testing. AIAA Journal, pg. 1-9, https://doi.org/10.2514/1.J058348

Ruan, H., Qin, Y., Heyne, J., Gieleciak, R., Feng, M., & Yang, B. (2019). Chemical compositions and properties of lignin-based jet fuel range hydrocarbons. Fuel 256 115947, https://doi.org/10.1016/j.fuel.2019.115947

Published conference proceedings

Heyne, J., Opacich, K., Peiffer, E., & Colket, M. (2019). The effect of chemical and physical fuel properties on the approval and evaluation of alternative jet fuels. 11th U.S. National Combustion Meeting, Pasadena, CA

Opacich, K.C., Heyne, J.S., Peiffer, E., & Stouffer, S.D. (2019). Analyzing the relative impact of spray and volatile fuel properties on gas turbine combustor ignition in multiple rig geometries. AIAA SciTech, AIAA 2019-1434, San Diego, CA

Written reports

CAAFI R&D Committee. (2019). Prescreening of synthesized hydrocarbons intended for candidates as blending components for aviation turbine fuels. Commercial Alternative Aviation Fuel Initiative (CAAFI), CAAFI R&D Committee Publication

Outreach Efforts

Invited talks

Colket, M. & Heyne, J. (2018). Early evaluation of alternative jet fuels based on NJFCP results. Advanced Bioeconomy Leadership Conference (ABLC), San Francisco, CA

Colket, M. & Heyne, J. (2019). Major results from the National Jet fuels and Combustion Program. ASME TurboExpo, Phoenix, AZ

Colket, M., Heyne, J., & Lee, T. (2018). An overview of ASCENT research efforts to improve our understanding of how fuel composition and characteristics determine performance. CAAFI Biennial General Meeting

Colket, M., Heyne, J., & Lee, T. (2018). NJFCP update: Properties and modeling to FOM predictions. JetScreen Meeting, Paris, FR

Edwards, T. & Heyne, J. (2019). Towards the minimization of ASTM D4054 tier 3 & 4 AJF approvals. 2019 CRC Aviation Committee Meetings, San Juan, PR

Heyne, J. (2019). Drop-in high-performance fuels: From molecule selection to mission benefits. NREL IBRF Lab, Golden, CO

Heyne, J. (2019). The approval and evaluation NJFCP learnings and high-performance fuels for operability and mission benefits. Rolls-Royce, Indianapolis, IN

Conference presentations

Opacich, K., Heyne, J.S., Peiffer, E., & Stouffer, S.D. (2018). Analyzing the relative impact of spray and volatile fuel properties on gas turbine combustor ignition. DESS2018-019, 14th Dayton Engineering Sciences Symposium, Wright State University

Stachler, R., Heyne, J., Peiffer, E., Stouffer, S., & Miller, J. (2018). Assessment of lean blowoff in a toroidal jet stirred reactor. Dess2018-055, 14th Dayton Engineering Sciences Symposium, Wright State University

Articles/press

Heyne, J., Wang, H., & Kalman, J. (2018). Safely improving jet, rocket fuels. Aerospace America, 2018 Year in Review, Propellants and Combustion Technical, Committee Contribution

Funded program review presentations

Heyne, J. & Colket, M. (2019). AIAA Book and year 5 - next steps and action item review. NJFCP 2019 Review Meeting, OAI, Cleveland, OH

Heyne, J. & Colket, M. (2019). Highlights of NJFCP achievements - overall impact of program tiers and HPF. NJFCP 2019 Review Meeting, OAI, Cleveland, OH

Heyne, J., Colket, M., Moder, J., & Shaw, C. (2018). NJFCP status update. FAA ASCENT, Alexandria, VA

Heyne, J., Emerson, B., Lieuwen, T., Stouffer, S., Blunck, D., Corporan, E., Mastorakas, N., & de Oliveira, P. (2019). LBO WG update and 4 year summary. NJFCP 2019 Review Meeting, OAI, Cleveland, OH

Stouffer, S., Heyne, J., Boehm, R., Mayhew, E., Lee, T., & Canteenwalla, P. (2019). Ignition WG update and 4 year summary. NJFCP 2019 Review Meeting. OAI, Cleveland, OH

Awards

Joshua Heyne:

- University of Dayton Nominee, Blavatnik National Awards for Young Scientists, 2019.
- Outstanding Service Award, ASME Dayton Section, 2018.

Shane Kosir:

- Ohio Space Grant Consortium Master's Fellowship, 2019
- Class of 1902 Award of Excellence for Outstanding Mechanical Engineering Achievement, 2019

Katherine Opacich:

- Ohio Space Grant Consortium Master's Fellowship, 2019
- The Martin C. Kuntz, 1912, Award of Excellence to the Outstanding Junior in Mechanical Engineering, 2018

Student Involvement

Erin Peiffer, graduate research assistant, June 2017 to December 2018. Erin is a master's student linking experimental results across ASCENT and non-ASCENT teams.
Zhibin Yang, graduate research assistant, August 2018 to present. Zhibin is a graduate student research assistant working to develop physical surrogates.
Katherine Opacich, undergraduate research assistant, November 2017 to present. Katherine is an undergraduate research assistant working to document NJFCP activities and analyze ignition data across NJFCP teams.
Shane Kosir, undergraduate research assistant, January 2018 to present. Shane is research assistant working to analyze LBO data.
Jen Colborn, undergraduate research assistant, January 2017 to December 2018. Jen is an undergraduate research student assistant aiding in the testing of fuels on the Referee Rig.

References

Bell, D.C., Heyne, J.S., Won, S.H., & Dryer, F.L. (2018). The impact of preferential vaporization on lean blowout in a referee combustor at figure of merit conditions. ASME Power Conference.

Bokhart, A.J., Dongyun, S., Gejji, R., Buschhahen, T., Naik, S.V., Lucht, R.P., Gore, J.P., Sojka, P.E., & Meyer. S.E. (2017). AIAA Aerospace Sciences Meeting

Chtev, I., Rock, N., Ek, H., Emerson, B.L., Seitzman, J.M., Lieuwen, T.C., Noble, D.R., Mayhew, E., & Lee, T. (2017). Simultaneous high speed (5 kHz) Fuel-PLIE, OH-PLIF and stereo PIV imaging of pressurized swirl-stabilized flames using liquid fuels. 55th AIAA Aerospace Sciences Meeting

Colket, M.B., Heyne, J., Rumizen, M., Gupta, M., Edwards, T., & Roquemore, W.M. et al. (2017). An overview of the national jet fuels combustion program. AIAA J

Culbertson, B. & Williams, R. (2017). AFRL-RQ-WP-TR-2017-0047

Edwards, T. (2017). Reference jet fuels for combustion testing. 55th AIAA Aerospace Sciences Meeting. 1–58

Hasti, V.R., Kumar, G., Liu, S. Lucht, R.P., & Gore, J.P. (2018). Large eddy simulation of pilot stabilized turbulent premixed CH4+air jet flames. 2018 AIAA Aerospace Sciences Meeting

Heyne, J.S., Colket, M.B., Gupta, M., Jardines, A., Moder, J.P., & Edwards, J.T. et al. (2017). Year 2 of the national jet fuels combustion program: Towards a streamlined alternative jet fuels certification process. 55th AIAA Aerospace Science Meeting, 1– 13

Heyne, J.S., Peiffer, E., Colket, M.B., Jardines, A., Shaw, C., & Moder, J.P. et al. (2018). Year 3 of the National Jet Fuels Combustion Program: Practical and scientific impacts of alternative jet fuel research. 56th AIAA Aerospace Science Meeting

IATA. (2018). Carbon Offsetting and Reduction Scheme for International Aviation (CORSIA): Fact sheet.

Lefebvre, A.H. (1983). Fuel effects on gas turbine combustion. Dayton, OH

Lefebvre, A. & Ballal, D. (2010). Gas turbine combustion alternative fuels and emissions. 3rd ed. Boca Raton: Taylor and Francis Group

Khandelwal, B. & Ahmed, I. (2017). Research report on lean blowout limit the university of Sheffield Department of Mechanical Engineering.

Ma, P.C., Wu, H., Labahn, J.W., Jaravel, T., & Ihme, M. (2019). Analysis of transient blow-out dynamics in a swirl-stabilized combustor using large-eddy simulations. Proceedings of the Combustion Institute. 37 5073–5082

Opacich, K.C., Heyne, J.S., Peiffer, E., & Stouffer, S.D. (2019). Analyzing the relative impact of spray and volatile fuel properties on gas turbine combustor ignition in multiple rig geometries. AIAA Scitech 2019 Forum

Panchal, A., Ranjan, R., & Menon, S. (2018). Effect of chemistry modeling on flame stabilization of a swirl spray combustor. 2018 Joint Propulsion Conference

Rock, N., Chterev, I., Emerson, B., Won, S.H., Seitzman, J., & Lieuwen, T. (2019). Liquid fuel property effects on lean blowout in an aircraft relevant combustor. J. Eng. Gas Turbines Power 141 71005–71013

Stachler, R.D., Heyne, J.S., Stouffer, J.S., Miller, J.D., & Roquemore, W.M. (2017). AIAA SciTech forum. 55th AIAA Aerospace Science Meeting

Stachler, R.D., Peiffer, E., Kosir, S.T., Heyne, J.S., Stouffer, S.D., & Miller, J.D. (2018). Lean blowoff and emissions of alternative and conventional fuels using a toroidal jet stirred reactor. AIAAJ. (in submission).

Stouffer, S.D., Hendershott, T.H., Monfort, J.R., Diemer, J., Corporan, E., Wrzesinski, P., & Caswell, A.W. (2017). Lean blowout and ignition characteristics of conventional and surrogate fuels measured in a swirl stabilized combustor. 55th AIAA Aerospace Science Meeting, 1–14

Wang, Y., Cao, Y., Wei, W., Davidson, D.F., & Hanson, R.K. (2019). A new method of estimating derived cetane number for hydrocarbon fuels. Fuel 241 319–326.

Task 3 - Development of Operability Surrogate Fuels

University of Dayton

Objective

The objective was the development of surrogate fuels for operability testing.

Research Approach

Introduction

Increases in global ambient temperature and mean sea level have had negative effects on marine ecosystems, fish productivity, agriculture, and the human population on coastal zones. These factors, paired with the increase in natural disasters, have led to increased volatility of the environment indicative of climate change due to anthropogenic carbon emissions (Neumann et al., 2015). The reduction of these carbon emissions has great potential in the transportation sector, where aviation contributes approximately 9% of these emissions (Office of Transportation and Air Quality, 2019). Commercial aviation must significantly reduce its greenhouse gas (GHG) impact to continue to support global mobility and commerce as NASA is predicting a 2-fold increase in passenger flights in the next decade (NASA, 2018). Through the ICAO, the commercial aviation industry has adopted and defined a method to reduce the global environmental impact of air travel through CORSIA, which sets the voluntary standards to reduce carbon emissions during Phase 1 (through 2026) and mandatory standards during Phase 2 (2027 and beyond) (IATA, 2018). By the year 2050, under a CORSIA-type domestic emission policy, the demand for SAF will need to increase to more than 10% of total jet fuel consumption (Chao et al., 2019).

Any commercial deployment of SAF relies on the approval and evaluation of the fuel via ASTM D4054. This specification ensures the safe usage, fungibility, performance, and compatibility of the SAF under standard usage and severe operability conditions. Specifically, Tier 3 engine operability tests focus on fuel effects under the so-called FOM limit phenomena; namely, LBO, high-altitude relight, and cold-start ignition (Lefebvre, 1983; Rock et al., 2019; Stachler et al., 2017). Because of the broad range of potential physical and chemical properties of a new SAF, extensive combustor testing is typically needed to eclipse uncertainty and ensure safety for FOM operability issues. Estimations for the direct testing for a candidate SAF in cost and volume are said to be in the range of $5 million and 28,000 to 115,000 gallons (Ruzimen, 2018). This estimate does not include overhead costs for all parties involved in the process or the cost of supplying large quantities of potentially expensive test fuel (Colket et al., 2017). Because of the nature of this costly and volume-intensive testing process, the NJFCP's mission is to streamline the SAF approval process and, in turn, reduce the carbon intensity of aviation transportation by ensuring a broad and diverse portfolio of SAF fuels, feedstock, and processing technologies (Colket et al., 2017; Heyne et al., 2017; Heyne et al., 2018).

Recent work on LBO of SAFs in four combustor rigs showed that DCN is the most significant feature importance using RFRA in both the Referee Rig and TJSR, and the second most significant feature importance in the Sheffield rig (Peiffer & Heyne, n.d.; Peiffer et al., n.d.). These three rigs show dominance of chemical timescales near LBO, where chemical timescales are a function of the fuel's chemical properties and accompanying thermodynamic conditions. However, experiments using the Honeywell APU show no sign of DCN affecting LBO (Peiffer et al., 2019). Lack of a swirler and presence of a small pressure atomizer attribute to this difference and enhance the dominance of evaporative timescales near LBO, where evaporative timescales are a function of fuel physical properties and distillate properties.

Recent efforts into gas turbine combustor ignition and the relative impact of spray and volatile fuel properties indicate that the down-selected properties of viscosity, density, surface tension, vapor pressure, and specific heat capacity nearly capture the variance in ignition probability (Opacich et al., 2019). Ignition probability, a metric to determine successful ignitions, is used in gas turbine combustion where turbulence and stochasticity exist. Furthermore, viscosity, density, and surface tension have a larger impact than vapor pressure and specific heat capacity on ignition behavior for both the Referee Rig and Honeywell APU (Opacich et al., 2019). At higher fuel temperatures, surface tension is the most important property to predict relative ignitability in the Honeywell APU. The current certification process for SAF via ASTM D4054 has no specification limit for surface tension. However, surface tension is strongly and positively correlated with density, and there is a specification limit for density in all Category A fuels (Heyne et al., 2017; Heyne et al., 2018).

Historically, surrogates have been used for the manipulation or prescription of fuel properties to mimic the properties of target fuels. Surrogates have been used to mimic autoignition, ignition delay, extinction strain rate, and emissions. The usage of surrogate formulation to understand combustion phenomenon has been explored by Dooley et al. (2010) and Kim et al. (2014; 2017). Dooley *et al.* outlined a method for fuel-specific surrogate formulation through empirical correlation. The surrogates were designed to emulate chemical kinetic behavior of a target real fuel. Kim *et al.* developed two surrogates with empirical correlations to emulate chemical and physical properties that affect spray and ignition within the diesel combustion process. While these surrogate studies have transformed, confirmed, and in some cases transcended fundamental understandings, combustion theory and SAF approvals could benefit from the manipulation, instead of mimicking, of properties to illustrate complex physical competitions between properties at limit points; namely, LBO and ignition.

This work combines the work of Bell et al. (2017) with recent surface tension and NJFCP reference fuels to report fuels with orthogonal spray break-up properties to illuminate these spray break-up physics via scalable surrogates, which can stress limit theory and competitions between density, surface tension, and viscosity. Here, we report a method and specific orthogonal surrogate compositions on an *N*-dimensional Pareto front concerning the total property space. These compositions and properties represent a near-maximum variance that can be associated with hydrocarbon molecules in the jet fuel distillation range. No previous works have reported results of comparable fuel properties, number of fuels, and the broader implication of their results at once. Moreover, we report the maximum variance in key properties relative to the subset of fuels used here. This fuel property variance, in turn, facilitates both practical and theoretical efforts. Practically, experimental results can illustrate the maximum FOM sensitivity, aiding in the prescreening and formal evaluation of novel SAFs (Colket et al., 2017; Peiffer et al., 2019; Raun, 2019). Theoretically, tests of these fuels can be used to confirm or reject hypotheses regarding the competition of spray break-up, fluid dynamics, chemistry, and heat-mass transfer, elevating both theory and computational fluid dynamics validation test data.

Materials and methods

Materials

Thirteen fuels were used as the basis for maximizing fuel property variance. Three conventional, or Category A, fuels representing a “best” (A-1, POSF 10264), “average” (A-2, POSF 10325), and “worst” (A-3, POSF 10289) were used. Ten fuels composed of blends or neat alternative fuels were available with the relevant properties under the desired condition. The fuels utilized here were the basis of the NJFCP to investigate a wide range of chemical and physical fuel characteristics. Edwards (2013; Edwards et al., 2017) contains explanations of the specified reference fuels. Table S1 of the supplemental information contains property information about the fuels. In Figure 7, a plot presents the fuels used in this work with normalized key properties, revealing the variance of these properties among these neat blend components.

Blending rule

The blending rules used to predict the properties of the optimized SAF blends were molecular weight (MW), atomic hydrogen-to-carbon ratio (H/C), DCN, density (ρ) at −30˚C, kinematic viscosity (μ) at −30˚C, distillation curve (T10, T50, T90), and surface tension (σ) at −30˚C. Blending rules were incorporated from the efforts of Bell et al. (2017) from the general surrogate calculator. Validation methods were additionally performed in the work of Bell et al. to ensure proper usage (Bell et al., 2017). However, a surface tension blending rule was seldom considered and never included in the surrogate calculator. Therefore, for this effort, a surface tension blending rule will be integrated into the surrogate calculator.

Surface tension

The surface tension of the fuel blends was calculated using the Macleod-Sugden correlation as indicated in Equation (1) (Poling et al., 2000). In the equation, σ_m is the surface tension of the mixture, where ρ_{Lm} and ρ_{Vm} are the liquid and vapor mixture density, respectively. $[P_{Lm}]$ and $[P_{Vm}]$ are the parachor of the liquid and vapor mixture. At low pressures, the term P_{Vm} involving vapor density could be neglected (Poling et al., 2000). For this study, all jet fuels were blended at ambient conditions; thus, P_{Vm} is neglected. With this simplification to Equation (1), the equation can be rewritten as shown in Equation (2). Equations (3) and (4) are used to calculate the parachor of the liquid. $[P_{ij}]$ is the parachor of the mixture, where $[P_i]$ and $[P_j]$ are the parachor of pure component *i* and *j*. λ_{ij} is the binary interaction coefficient determined from experimental data; in the absence of experimental data, λ_{ij} could be set to be 1.

$$\sigma_m = \left[[P_{Lm}]\rho_{Lm} - [P_{Vm}]\rho_{Vm}\right]^n \quad (1)$$

$$\sigma_m = \left[[P_{Lm}]\rho_{Lm}\right]^n \quad (2)$$

$$[P_{Lm}] = \sum_i \sum_j x_i x_j [P_{ij}] \tag{3}$$

$$[P_{ij}] = \lambda_{ij} \frac{[P_i] + [P_j]}{2} \tag{4}$$

When *n* in Equation (2) is set to 4, the equation can be reduced to the Weinaug-Katz equation (Weinaug & Katz, 1943). In this study, λ_{ij} in Equation (4) is given a value of one with supporting experimental material provided in the Figure 8. Although previous application of this blending rule were used for pure component mixing, here it was used for complex jet fuels mixtures with supporting material provided in Figure 8.

Jet fuel blend optimizer

The Bell *et al.* general surrogate calculator (Bell et al., 2017) is shown to be effective with the current blending methods, where it only minimizes overall error rather than reducing the error of each property relative to their targets individually. The jet fuel blend optimizer (JudO) can optimize user-defined properties at an *N*-dimensional scale. The goal of this optimization is to keep other user-specified properties constant and stress certain properties to create orthogonal surrogate fuels. Blending rules are integrated into objective functions to achieve desired property values.

Figure 9 presents a schematic of the optimization approach, which is based on the framework of JudO (Kosir et al., 2019; Flora et al., 2018). JudO uses mole fractions of the fuel set as inputs to the optimization. All initial guesses are randomly generated, where each fuel has a chance to be assigned a value for mole fractions between 0 and 1. This strategy aids in the optimization technique to investigate a wide range of potential compositions with accompanying potential local minima, rendering a "unbiased" optimization final solution.

Once the initial guess is determined, a Mixed Integer Distributed Ant Colony Optimization (MIDACO) solver (Schlueter et al., 2013) will start to optimize the mole fractions based on the given random initial guess with supplied objective and constraint functions. The objective functions were evaluated on the l^2 norm and normalized to A-2 values. MIDACO is a commercially available numerical high-performance solver that uses ant colony optimization with multiple objective functions to obtain a near-global optimum solution. An advantage to using this solver is the derivative-free, evolutionary hybrid algorithm that treats the objective and constraint functions as a "black-box which may contain critical function properties like non-linearity, non-convexity, discontinuities or even stochastic noise" solver (Schlueter et al., 2013).

When the optimization is complete with the supplied compositions, functions, and thus, fuel mixture properties, JudO will output possible best mole fractions, enabling a Pareto solution. Those possible best solutions are then compiled to form the cumulative Pareto front, which is a combination of all the solutions obtained from the initial guesses; 10,000 initial guesses were used for each run in this study. Orthogonal surrogate fuels are then determined via down selection from the compiled solutions presented in the cumulative Pareto front. Orthogonality in this study was focused only on the three properties of interest (surface tension, density, viscosity). Additionally, other objective functions were added to increase the variance in values of the three interesting properties during down selection to obtain the largest variance in results during the combustor FOM testing.

Results and discussion

Fuel blending optimization is performed over four scenarios involving three variables (surface tension, viscosity, density) and two levels for each variable (larger than A-2 value, smaller than A-2 value). Orthogonal array testing is then generated for the four scenarios in Table 2, according to the appropriate variable and level. Orthogonal array testing was then used to maximize variance across several critical properties for combustor testing and minimize the number of tests (Tsui, 1992).

With each scenario, 10,000 random initial compositional guesses to unbiased solutions and the corresponding Pareto solutions were used to generate the cumulative Pareto front. Figures 10, 11, 12, and 13 consists of scatterplots and histograms of Pareto front solutions, illustrating converged probability densities and relative opportunities for property variance. Each scatterplot consists of calculated properties. Each dot on a scatterplot represents one of the possible best solutions found by JudO. The purple dashed line represents the properties of A-2. Using orthogonal array testing, a surrogate was selected and represented by the orange star. The surrogates were selected to minimize or maximize the properties of density, viscosity, and surface tension, relative to A-2, according to the four scenarios. Other properties were intended to be as close to the A-2 values as possible using the other objective functions in this optimization. The properties considered here were MW, H/C, DCN, σ, μ, and ρ. Although the selected surrogate might not have the absolute minimum values of the

solution space, the multi-dimensionality concerning all properties suggests the largest variance happens at that point. Down-selected surrogate fuels and their respective properties for each of the scenarios are presented in Table 3, and Figures 10, 11, 12, and 13 identify the mole fractions and volume fractions of each surrogate. Four surrogate fuels were then blended and measured at −30˚C for viscosity and density. There was no error between measured and calculated density at −30˚C for the four surrogate fuels. Viscosity measurements also showed good results with reasonable error. This could be due to viscosity having an exponential relationship with temperature, whereas density has a linear relationship with temperature.

Figure 10 displays the total of 3,047,039 results of scenario 1, where the intention of surrogate 1 was to have the lowest surface tension, viscosity, and density; surrogate 1 consists primarily of 68% A-1 and 28% C-4, where A-1 is the "best" jet fuel, with all three properties lower than that of A-2, and C-4 has the second-lowest surface tension and relatively low viscosity and density. C-1 has the lowest surface tension; however, with relatively high viscosity, it was not considered in the solution of surrogate 1. Figure 12 illustrates scenario 2, which minimizes surface tension and maximizes viscosity and density. Each of the 3,336,938 possible best solutions is shown on the scatterplots. The orange star represents surrogate 2, which was the best solution for this scenario. This mixture consists of 29% A-1 and 68% C-3, where C-3 has the highest viscosity and relatively high density. Figure 13 shows 2,201,505 solutions for scenario 3, and, like the previous figures, indicates the best solution for surrogate 3 by the orange star. The goal of surrogate 3 was to minimize viscosity and maximize surface tension and density. Surrogate 3 consists of 53% A-1 and 46% A-2, where A-2 is the target fuel of this study. Figure 14 reports 3,937,813 solutions for scenario 4, and the objective for surrogate 4 was to minimize density and maximize surface tension and viscosity. The selected surrogate consisted of a six-component mixture, much different from the other solutions: 3% A-2, 2% C-4, 59% C-7, 5% C-9, 5% Syntroleum S-8, and 21% Camelina HEFA. Minimizing density while maximizing surface tension was difficult with the fuels selected for this work. Because the majority of the fuels selected here had positive correlations between surface tension and density, it was challenging to minimize density while maximizing surface tension. If larger variance needs to be achieved, then more novel fuels, solvents, and neat molecules need to be integrated into JudO. This is also a limitation of JudO; the surrogate properties can only be as high or low as the highest or lowest fuel used in JudO. After generation of these four surrogates, ignition probability can be further characterized on a fuel basis by the three variables in the orthogonal array testing (Opacich et al., 2019).

Conclusion

Previous efforts from the NJFCP program have shown that certain fuel properties (σ, μ, and ρ) have the most on predicting ignition probabilities (Heyne et al., 2019; Opacich et al., 2019; Peiffer et al., 2019). Current ASTM D4054 and D1655 specifications set bounds on viscosity and density; however, surface tension does not have a bound on any values at any given temperature. Surface tension has been validated and incorporated into JudO, a fuel blending optimization tool. These fuel properties, along with other pertinent properties important in combustion testing of novel fuels, were then integrated into JudO as objective functions to create surrogate fuels to further understand the effect on key properties relative to ignition probability. With these enhancements to JudO, more surrogates can be designed based on key properties of other combustor FOMs and accompanying hypotheses on performance parameters. In this work, four orthogonal surrogate fuels were created using JudO and orthogonal array testing to maximize variance in the specified fuel properties above. This work and supporting experimental evidence could lower the barrier for SAF approval and facilitate the achievement of the carbon reduction goals. In future research, more properties need to be added to JudO to cover more FOMs, and more novel fuels, solvents, and neat molecules need to be considered for integration in this tool to achieve greater variance in properties than currently estimated.

Table 2. Orthogonal array testing.

Scenarios	σ(-30°C), mN/m	μ(-30°C), cSt	ρ(-30°C), kg/L	Surrogate
Reference	30.0	6.1	0.837	A-2
1	⬇	⬇	⬇	1
2	⬇	⬆	⬆	2
3	⬆	⬇	⬆	3
4	⬆	⬆	⬇	4

Table 3. Properties of orthogonal fuels for all scenarios.

Property	A-2 Reference	Scenario Surrogate 1 min(σ, μ, ρ)	Surrogate 2 min(σ),max(μ, ρ)	Surrogate 3 min(μ),max(σ, ρ)	Surrogate 4 min(ρ),max(σ, μ)
MW, g/mol	159	156	172	156	169
σ (−30˚C), mN/m	30.0	26.7	28.1	28.5	29.4
ρ (−30˚C), kg/L	0.837	0.806	0.832	0.824	0.827
ν (−30˚C), cSt	6.1	4.8	9.1	5.3	8.9
DCN	48	41	48	48	48
H/C	1.91	2.04	1.98	1.95	2.05
T10, ˚C	160	151	175	154	173
T50, ˚C	209	186	231	201	218
T90, ˚C	260	241	254	254	262
ρ (−30˚C),* kg/L	[redacted]	0.806	0.832	0.824	0.826
ρ % error	[redacted]	0%	0%	0%	0%
ν (−30˚C),* cSt	[redacted]	4.5	10.3	5.2	8.5
ν % error	[redacted]	-6%	13%	2%	5%

*Properties are measured at −30˚C.

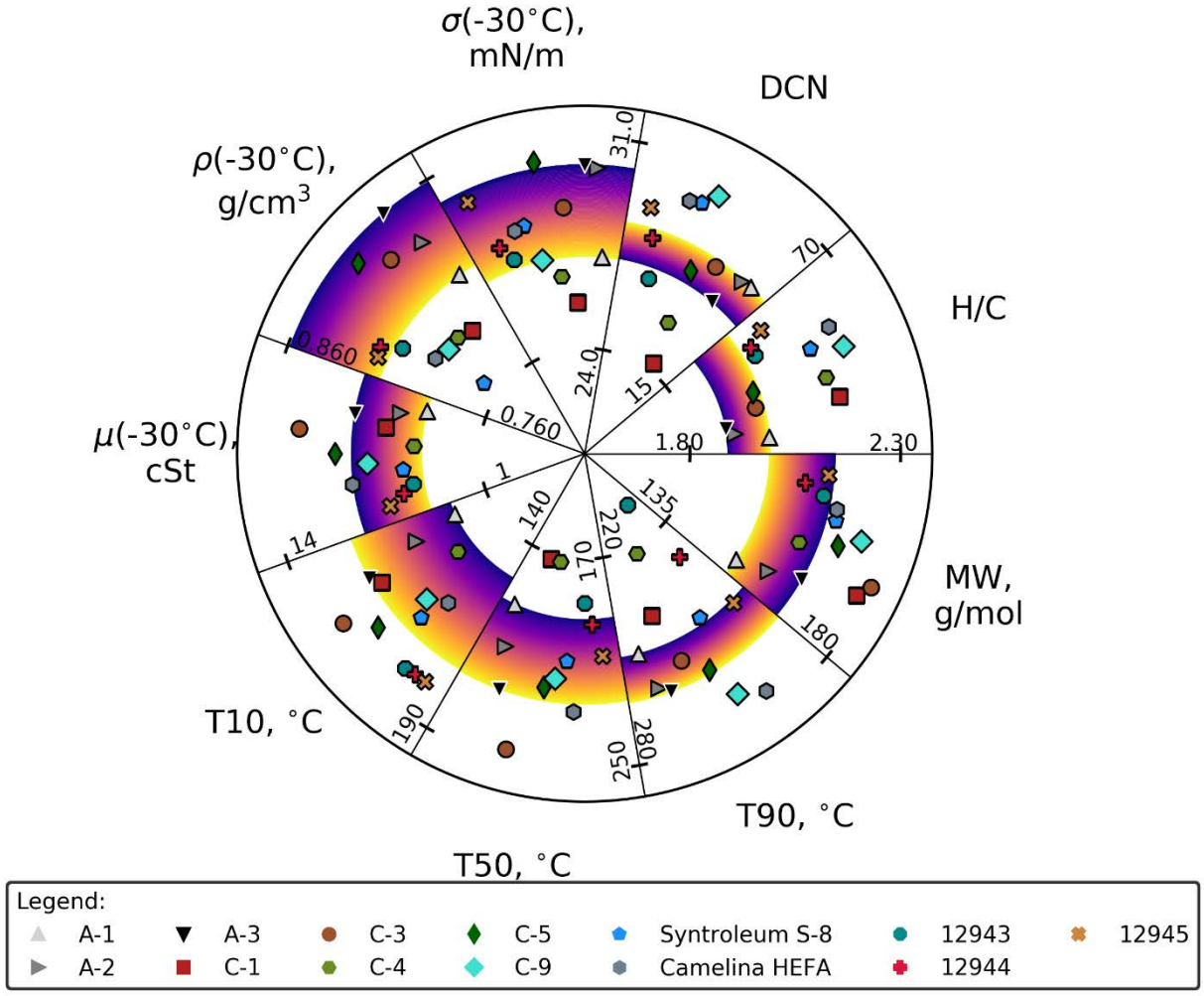

Figure 7. A plot of the 13 fuels and their respective normalized properties. Category A fuels are shown in the color gradient on the map, where yellow is the "best" case and purple is the "worst" case for each property. The rest of the fuels are plotted according to their normalized properties and respective to their marker.

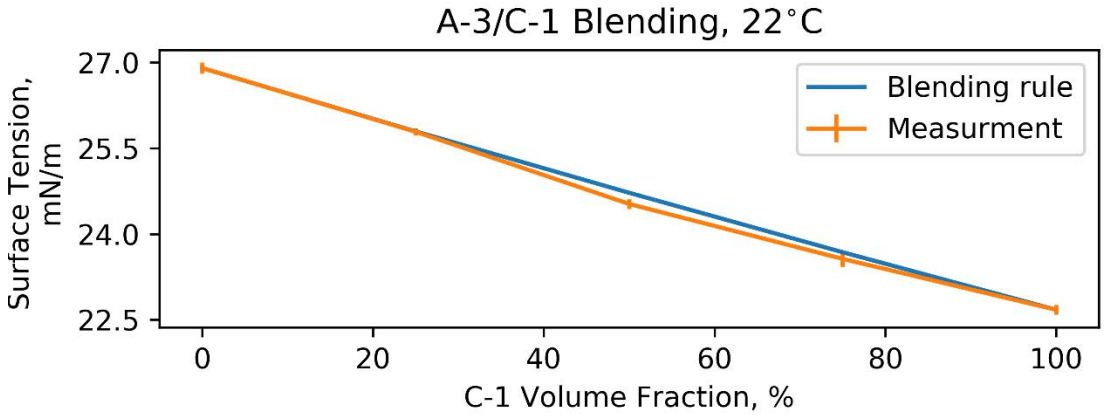

Figure 8. Surface tension blending rule validation. Error bar represent 95% confidence interval.

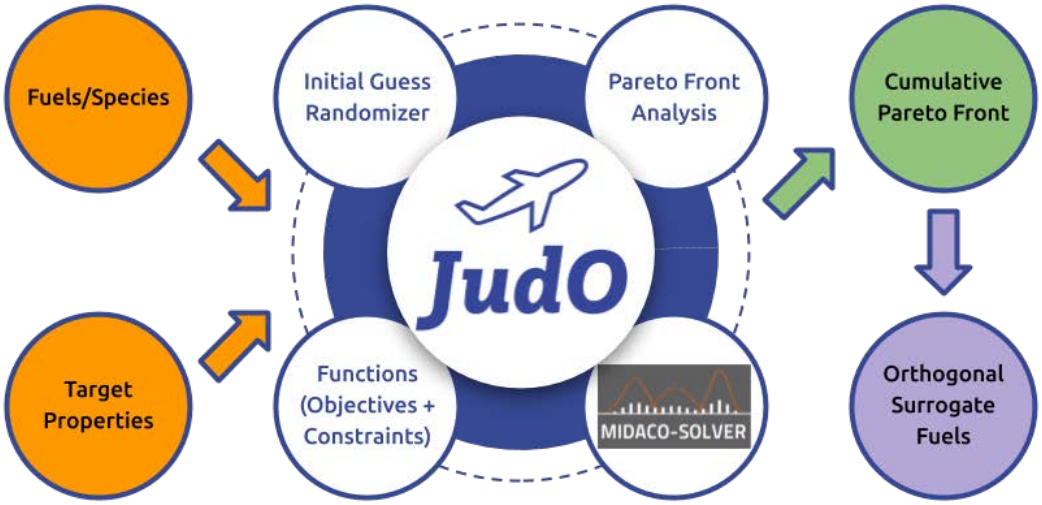

Figure 9. Schematic of the jet fuel blending optimization tool JudO, a suite centered around a computational tool called Mixed Integer Distributed Ant Colony Optimization (MIDACO) (Schlueter et al., 2013), which is implemented to optimize a user-specified fuel set (conventional and alternative jet fuels) of varying properties with specific design parameters and target properties (MW, H/C, DCN, density, kinematic viscosity, distillation curve, and surface tension) to illuminate Pareto front compromises for the fuels considered here.

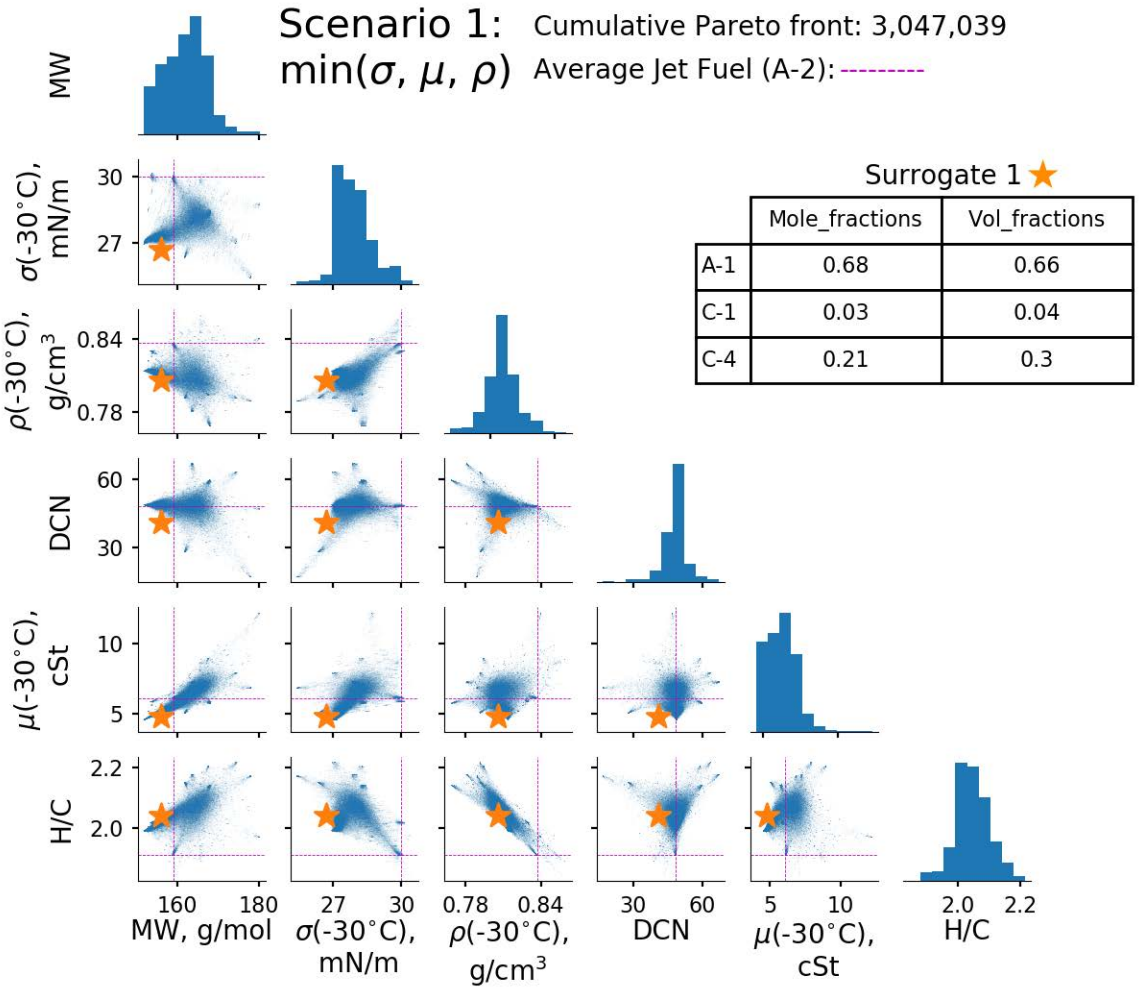

	Mole_fractions	Vol_fractions
A-1	0.68	0.66
C-1	0.03	0.04
C-4	0.21	0.3

Figure 10. Cumulative Pareto solutions for scenario 1 with combinations of optimized properties on histograms and scatterplots with other properties. Scatterplots consist of calculated properties with respect to each other. Each dot on a scatterplot represents one of the possible best solutions found using the jet fuel blending optimization tool JudO. The dashed line indicates the properties of A-2, and the orange star represents the properties of surrogate 1 with respect to the cumulative Pareto solutions.

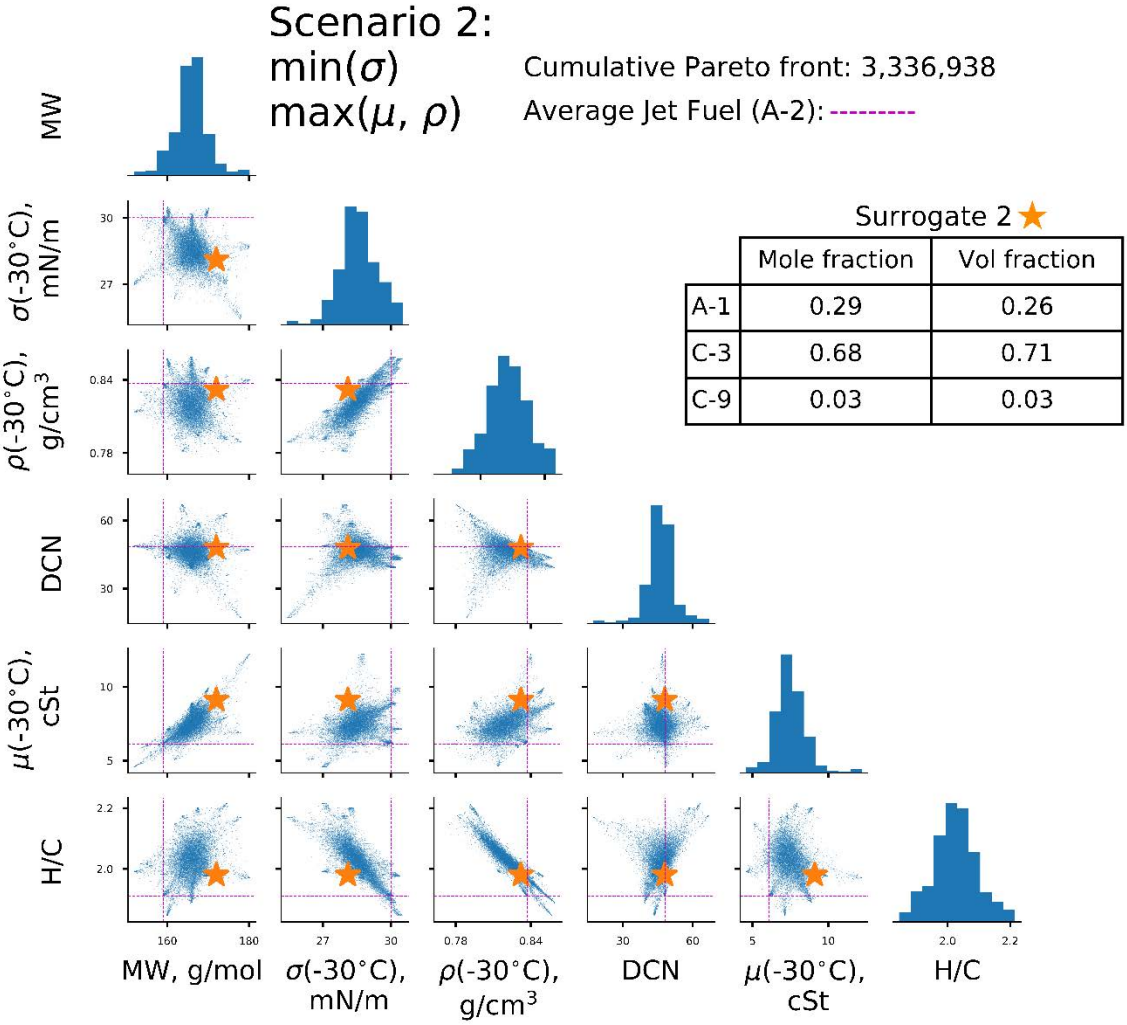

Figure 11. Cumulative Pareto solutions for scenario 2. Scatterplots consist of calculated properties with respect to each other. Each dot on a scatterplot represents one of the possible best solutions found using the jet fuel blending optimization tool JudO. The dashed line indicates the properties of A-2, and the orange star represents the properties of surrogate 2 with respect to the cumulative Pareto solutions.

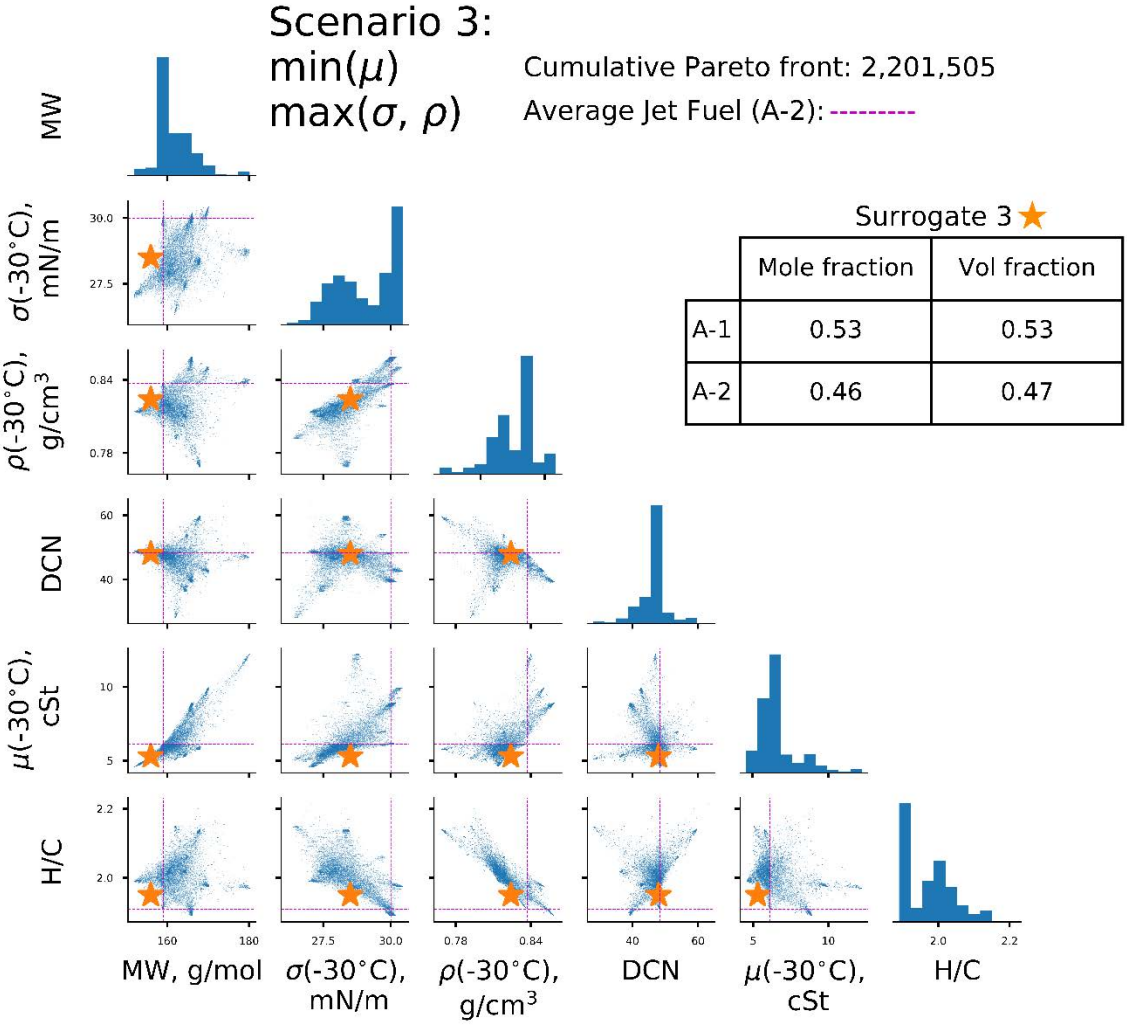

Figure 12. Cumulative Pareto solutions for scenario 3. Scatterplots consist of calculated properties with respect to each other. Each dot on a scatterplot represents one of the possible best solutions found using the jet fuel blending optimization tool JudO. The dashed line indicates the properties of A-2, and the orange star represents the properties of surrogate 3 with respect to the cumulative Pareto solutions.

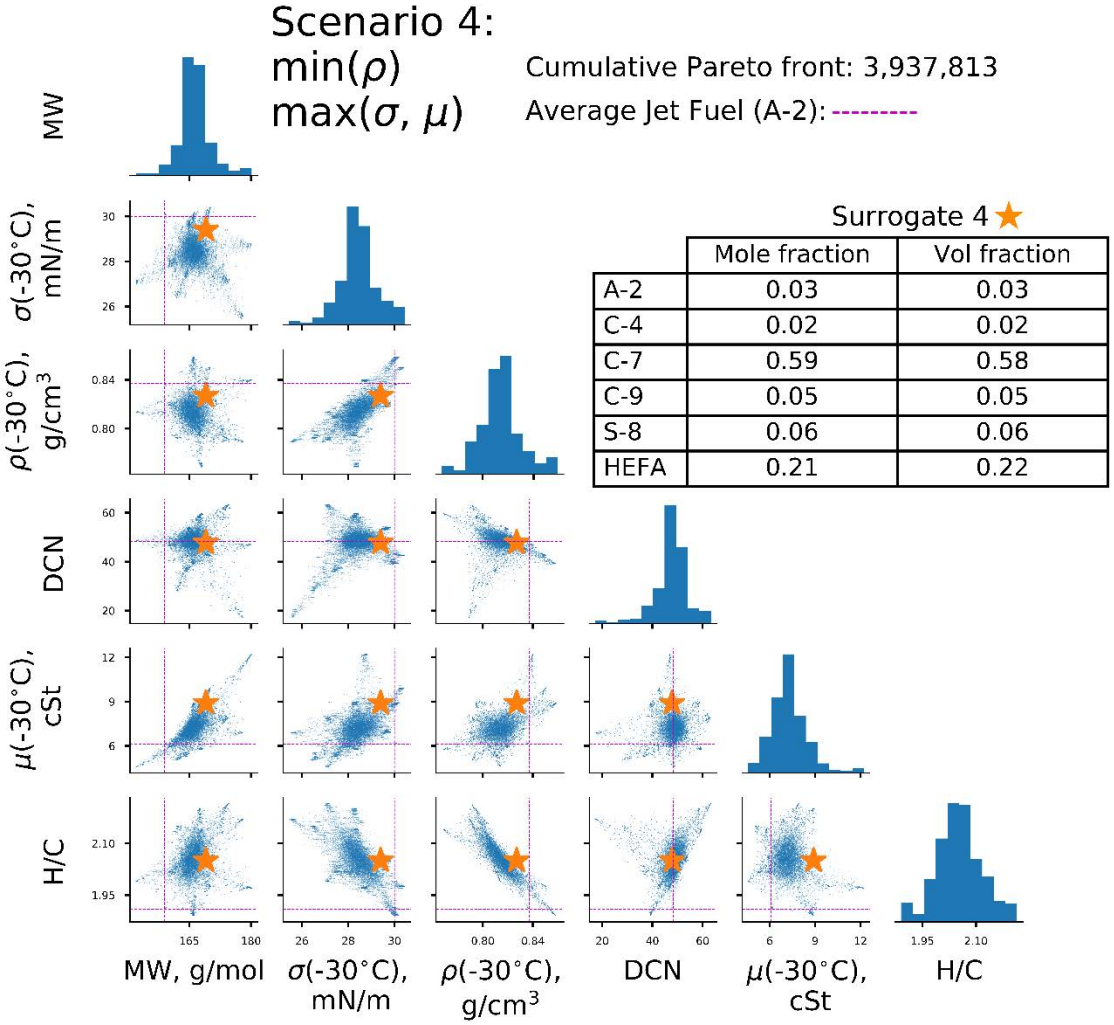

	Mole fraction	Vol fraction
A-2	0.03	0.03
C-4	0.02	0.02
C-7	0.59	0.58
C-9	0.05	0.05
S-8	0.06	0.06
HEFA	0.21	0.22

Figure 13. Cumulative Pareto solutions for scenario 4. Scatterplots consist of calculated properties with respect to each other. Each dot on a scatterplot represents one of the possible best solutions found using the jet fuel blending optimization tool JudO. The dashed line indicates the properties of A-2, and the orange star represents the properties of surrogate 4 with respect to the cumulative Pareto solutions.

Milestone(s)

- Surrogate fuels were formulated to exacerbate or ameliorate properties of a given fuel, rather than to mimic the properties.
- Orthogonal reference surrogate fuels were generated to identify the effect of specific properties on combustor operability testing.
- Surface tension blending was incorporated into a currently used fuel blending optimization tool, where this property was not previously considered.

Major Accomplishments

Reporting operability surrogate fuels.
Fuel blending optimization tool updated with surface tension and incorporation of NJFCP fuels.
Experimental results from testing surrogate fuels can illustrate the maximum FOM sensitivity, aiding in the prescreening and formal evaluation of novel SAFs.

Publications

Peer-reviewed publications
Orthogonal Reference Surrogate Fuels for Operability Testing (publication is in preparation).

Outreach Efforts

Presentation at 15th Dayton Engineering Sciences Symposium

Awards

None.

Student Involvement

Zhibin Yang, graduate research assistant. Zhibin is working to develop physical surrogates.
Robert Stachler, PhD student. Robert is helping with surrogate fuel formation.

Plans for Next Period

Plans for the next period include finalizing the publication in progress and Zhibin Yang finishing his master's degree.

References

Bell, D., Heyne, J.S., Won, S.H., Dryer, F., Haas, F.M., & Dooley, S. (2017). On the development of general surrogate composition calculations for chemical and physical properties. 55th AIAA Aerospace Sciences Meeting, 1–5. doi:10.2514/6.2017-0609

Chao, H., Buyung, D., Delaurentis, D., & Stechel, E.B. (2019). Carbon off setting and reduction scheme with sustainable aviation fuel options: Fleet-level carbon emissions impacts for U. S. airlines. Transportation Research Part D: Transport and Environment, 2020;75:42–56. doi:10.1016/j.trd.2019.08.015

Colket, M.B., Heyne, J., Rumizen, M., Gupta, M., Edwards, T., & Roquemore, W.M. et al. (2017). An overview of the national jet fuels combustion program. AIAA J.

Dooley, S., Won, S.H., Chaos, M., Heyne, J., Ju, Y., & Dryer, F.L. et al. (2010). A jet fuel surrogate formulated by real fuel properties. Combustion and Flame, 157:2333–9. doi:10.1016/j.combustflame.2010.07.001

Edwards, T. (2017). Reference jet fuels for combustion testing. 55th AIAA Aerospace Sciences Meeting, 1–58

Edwards, J.T., Shafer, L.M., & Klein, J.K. (2013). U.S. Air Force hydroprocessed renewable jet (HRJ) fuel research

Flora, G., Kosir, S., Heyne, J., Zabarnik, S., & Grupta, M. (2018). Properties calculator and optimization for drop-in alternative jet fuel blends. AIAA, 1–14. doi:10.2514/6.2019-2368

Heyne, J.S., Colket, M.B., Gupta, M., Jardines, A., Moder, J.P., & Edwards, J.T. et al. (2017). Year 2 of the national jet fuels combustion program: Towards a streamlined alternative jet fuels certification process. 55th AIAA Aerospace Science Meeting, 1–13

Heyne, J.S., Peiffer, E., Colket, M.B., Jardines, A., Shaw, C., Moder, J.P., et al. (2018). Year 3 of the National Jet Fuels Combustion Program: Practical and scientific impacts of alternative jet fuel research. 56th AIAA Aerospace Science Meeting

Heyne, J.S., Opacich, K.C., Peiffer, E.E., & Colket, M. (2019). The effect of chemical and physical fuel properties on the approval and evaluation of alternative jet fuels. 11th U.S. National Combustion Meeting, p. 1–10

IATA. (2018). Carbon Offsetting and Reduction Scheme for International Aviation (CORSIA): Fact sheet
Kim, D., Martz, J., Abdul-Nour, A., Yu, X., Jansons, M., & Violi, A. (2017). A six-component surrogate for emulating the physical and chemical characteristics of conventional and alternative jet fuels and their blends. Combustion and Flame, 179:86–94. doi:10.1016/j.combustflame.2017.01.025
Kim, D., Martz, J., & Violi, A. (2014). A surrogate for emulating the physical and chemical properties of conventional jet fuel. Combustion and Flame, 161:1489–98. doi:10.1016/j.combustflame.2013.12.015
Kosir, S.T., Behnke, L., Heyne, J.S., Zabarnick, S., Flora, G., & Denney, R.K. et al. (2019). Improvement in jet aircraft operation with the use of high-performance alternative drop-in fuels in conventional fuels. AIAA SciTech Forum 2019:1–27
Lefebvre, A.H. (1983). Fuel effects on gas turbine combustion. Wright-Patterson AFB, Dayton, OH
NASA. (2018). NASA update FAA ASCENT meeting 2018
Neumann, B., Vafeidis, A.T., Zimmermann, J., & Nicholls, R.J. (2015). Future coastal population growth and exposure to sea-level rise and coastal flooding - a global assessment. PLOS ONE 2015; doi:10.1371/journal.pone.0118571
Office of Transportation and Air Quality. (2019). Fast facts U.S. Transportation sector greenhouse gas emissions 1990-2017
Opacich, K.C., Heyne, J.S., Peiffer, E., & Stouffer, S.D. (2019). Analyzing the relative impact of spray and volatile fuel properties on gas turbine combustor ignition in multiple rig geometries. AIAA Scitech 2019 Forum
Peiffer, E.E. & Heyne, J.S. (n.d.). Characteristic timescales for lean blowout of alternative jet fuels in four combustor rigs.
Peiffer, E.E., Heyne, J.S., & Colket, M. (2019). Sustainable aviation fuels approval streamlining: Auxiliary power unit lean blowout testing. AIAAJ, 1–9. doi:10.2514/1.J058348.
Poling, B., Prausnitz, J., & O'Connell, J. (2000). The properties of gases and gas mixtures. doi:10.1036/0070116822
Rock, N., Emerson, B., Seitzman, J., & Lieuwen, T. (2019). Liquid fuel property effects on lean blowout in an aircraft relevant combustor.141. doi:10.1115/1.4042010.
Ruan. H., Qin, Y., Heyne, J., Gieleciak, R., Feng, M., & Yang, B. (2019). Chemical compositions and properties of lignin-based jet fuel range hydrocarbons. Fuel, 256:115947. doi:10.1016/j.fuel.2019.115947
Rumizen, M. (2018). D4054 Clearinghouse. (Personal communication)
Schlueter, M., Erb, S.O., Gerdts, M., & Kemble, S. (2013). MIDACO on MINLP Space Applications, 1–25.
Stachler, R.D., Heyne, J.S., Stouffer, S.D., Division, E.E., Miller, J.D., & Roquemore, W.M. et al. (2017). Investigation of combustion emissions from conventional and alternative aviation fuels in a well-stirred reactor. 1–28. doi:10.2514/6.2017-0382.
Tsui, K.L. (1992). An overview of Taguchi method and newly developed statistical methods for robust design. IIE Transactions, 24:44–57. doi:10.1080/07408179208964244.
Weinaug, C.F. & Katz, D.L. (1943). Surface tensions of methane-propane mixtures. Industrial Engineering Chemistry, 35:239–46. doi:10.1021/ie50398a028

Project 036 Parametric Uncertainty Assessment for the Aviation Environmental Design Tool (AEDT)

Georgia Institute of Technology

Project Lead Investigator

Principal Investigator:
Professor Dimitri N. Mavris
Director, Aerospace Systems Design Laboratory
School of Aerospace Engineering
Georgia Institute of Technology
Phone: (404) 894-1557
Fax: (404) 894-6596
Email: dimitri.mavris@ae.gatech.edu

Co-Principal Investigator:
Dr. Yongchang Li
Chief, Aviation Environmental Policy Branch
Aerospace Systems Design Laboratory
School of Aerospace Engineering
Georgia Institute of Technology
Phone: (404) 385-2776
Fax: (404) 894-6596
Email: yongchang.li@ae.gatech.edu

University Participants

Georgia Institute of Technology

- FAA Award Number: 13-C-AJFE-GIT, Amendment 019, 29, 30, 40, and 49
- Period of Performance: September 1, 2018 to August 31, 2019
- Task(s): Parametric Uncertainty Quantification for BADA4

Project Funding Level

The current funding for this project is based on amendments 30, 40, and 49 for a total of $300,000 from May 31, 2019 to May 30, 2020. The Georgia Institute of Technology has agreed to a total of $300,000 in matching funds.

Investigation Team

- Prof. Dimitri Mavris (PI) oversees the entire project.
- Dr. Yongchang Li (Co-PI, project lead) leads the research team in performing capability demonstrations and tests and in validating various functionalities of different AEDT versions.
- Dr. Michelle Kirby (Co-PI) oversees the entire project and supports all of the research activities.
- Dr. Dongwook Lim (research staff) conducts capability demonstrations, verifications, and validations of new AEDT features and functionalities.
- Zhenyu Gao (graduate student) conducts parametric uncertainty quantification analyses for the BADA4 model, created the AEDT study, and performed a sensitivity analysis for this study.
- Yee Chan Jin (graduate student) developed a BADA4 calculator in the form of a spreadsheet using BADA4 equations to quantify aircraft performance.
- Ameya Behere (graduate student) supports the system testing of AEDT features.
- Dr. Holger Pfaender (research staff) provides consultation and support.

Project Overview

The FAA's Office of Environment and Energy (AEE) has developed a comprehensive suite of software tools that allow for a thorough assessment of the environmental effects of aviation, particularly for assessments of interdependencies among aviation-related noise, emissions, performance, and cost. As the heart of this tool suite, the high-fidelity AEDT is a software system that models aircraft performance in space and time to estimate fuel consumption, emissions, noise, and air quality impacts. This software has been developed by the FAA AEE for public release as the next-generation FAA environmental consequence tool. AEDT enables evaluations of interdependencies among aircraft-related fuel consumption, emissions, and noise. AEDT 2 was released in four phases. The first version, AEDT 2a, was released in March 2012 (US FAA, AEDT 2a UQ Report, 2014; US FAA, AEDT 2a SP2 UQ Supplemental Report, 2014) and the second version, AEDT 2b, was released in May 2015 (US FAA, AEDT 2b UQ Report, 2016). The third and fourth versions, AEDT 2c and AEDT 2d, respectively, were released in September 2016 and September 2017. A new version, AEDT 3b, was released in September 2019, with major updates, including the inclusion of the BADA4 performance model for fuel consumption, emissions, and noise and the implementation of reduced thrust and alternative weight profiles for departure operations.

The uncertainty quantification applied in this project comprehensively assesses the accuracy, functionality, and capabilities of AEDT during the development process. The major purposes of this effort are as follows:

- Contribute to the external understanding of AEDT
- Demonstrate and evaluate AEDT's capability and fidelity (ability to represent reality)
- Help AEDT users to understand the sensitivities of output responses to variations in input parameters/assumptions
- Identify gaps in functionality
- Identify high-priority areas for further research and development

The uncertainty quantification consists of verification and validation, capability demonstrations, and parametric uncertainty/sensitivity analysis.

Task 1- Parametric Uncertainty Quantification for BADA4

Georgia Institute of Technology

Objective(s)

The implementation of BADA4 in the new series of AEDT 3 created additional needs for model verification and validation, as well as uncertainty analysis. For aircraft trajectory simulation and performance modeling within air traffic management, the BADA4 model is an important update of its precedent version, BADA Family 3. The BADA4 model consists of more complex performance models with significantly more performance parameters. By identifying and quantifying how the key AEDT outputs respond to variations in BADA4 performance parameters, we can better identify the primary contributors to AEDT output uncertainties under BADA4 for future tool development and enhancement and can inform users regarding the expected variation in AEDT outputs.

Research Approach

To perform a system-level parametric uncertainty analysis on BADA4 parameters and to gain insights for future AEDT improvements, a four-step uncertainty quantification process has been applied, including uncertainty characterization, sensitivity analysis, uncertainty propagation, and global sensitivity analysis (Lim et al., 2018). As the first step, uncertainty characterization identifies and mathematically represents the uncertainty sources that may impact key AEDT outputs. Second, the sensitivity analysis quantifies the influence of each uncertainty source on the outputs of interest by varying each input parameter within a reasonable range. The third step, uncertainty propagation, is applied to propagate uncertainties across all uncertainty sources through a system model to obtain nondeterministic distributions of the outputs. Finally, the global sensitivity analysis quantifies the contribution of variance in each output. Table 1 lists the key methods used in the four-step uncertainty quantification process, and the following subsections provide details on the current progress of the BADA4 parametric uncertainty quantification.

Uncertainty Characterization

Uncertain BADA4 parameters

Uncertainty characterization is the first step in performing uncertainty quantification for a complex model. The uncertainty characterization step in this work includes three components: (1) a list of BADA4 input parameters that may have a significant

impact on key AEDT outputs, such as fuel burn, emission, and noise metrics; (2) a mapping and understanding of how the BADA4 parameters are applied to calculate key performance metrics, leading to a tool for rapid BADA4 analysis; and (3) a list of uncertain physical factors in real-world operations, such as uncertainties in weather, weight, or takeoff profile, that may influence the outputs of interest and their uncertainty ranges.

BADA4 coefficients are stored in different tables of the FLEET database, and a summary of the BADA4 parameters is provided in section 7.2 of the BADA4 user manual (Eurocontrol Experimental Centre). In this study, we focus on aircraft with turbofan engines, with a total of eight BADA4 parameter categories. Detailed information of the eight BADA4 parameter categories and subcategories is given in Table 2.

Table 1. Four steps of the uncertainty quantification process and key methods.

Step	Methods
Step 1 Uncertainty Characterization	**Mapping** of key Aviation Environmental Design Tool (AEDT) inputs to key environmental metrics based on literature reviews and expert knowledge Analysis of AEDT Fleet DB to **quantify the variability** in AEDT input parameters **Correlation analysis** of AEDT input parameters
Step 2 Sensitivity Analysis	**One-factor-at-a-time (OFAT) design of experiments**, in which each input parameter is varied one at a time while the other parameters are held constant at baseline values
Step 3 Uncertainty Propagation	**Screening test** to reduce the number of variables for surrogate models; screening test with 5,000 cases using the Latin hypercube sampling technique; use of an ANOVA test and a regression model to yield a Pareto plot **Surrogate modeling** using an artificial neural network **Monte Carlo simulation** **Copulas theory** to capture correlations between input parameters
Step 4 Global Sensitivity Analysis	Assessment of the impact of input parameters on the outputs **Total sensitivity index** to measure the relative impact of each input parameter

Table 2. Summary of BADA4 parameter categories.

Category	Subcategory
Aerodynamic Forces and Configuration Model (AFCM)	Clean drag model coefficients (D)
	Nonclean drag model coefficients (D_NC)
	Other performance parameters
Propulsive Forces Model (PFM)	Other performance parameters
Turbofan Model (TFM)	Turbofan idle rating thrust coefficients (TI)
	Turbofan idle rating fuel coefficients (FI)
	Turbofan non-idle rating thrust coefficients (A)
	Turbofan non-idle rating fuel coefficients (F)
	Turbofan flat-rated area throttle coefficients (Bn)
	Turbofan temperature-rated area throttle coefficients (Cn)
Kinematic Limitations Model (KLM)	Other performance parameters
Geometric Limitations Model (GLM)	Other performance parameters
Buffet Limitations Model (BLM)	Maximum lift clean configuration buffet coefficients (BF)
	Maximum lift nonclean configuration buffet coefficients (CL_MAX)
	Other performance parameters
Dynamic Limitations Model (DLM)	Other performance parameters
Airline Procedure Model (ARPM)	Other performance parameters

Each aircraft with turbofan engines has BADA4 coefficients from all eight categories. The exact number of BADA4 coefficients in each category depends on the aircraft model and is typically within the range of 200–300. In addition to BADA4 coefficients, in this uncertainty quantification work, aircraft noise and performance (ANP) and airport weather parameters were also studied, as these parameters have a strong impact on AEDT outputs produced by the BADA4 model. The BADA4 uncertainty quantification task deals with a much larger number of parameters than the uncertainty quantification task conducted for BADA3. Taking the Boeing 737-700 as an example, the total number of parameters changed from 16 to 193 between the BADA3 and BADA4 models. With an increased number of input parameters, the expected computational cost and complexity for the entire uncertainty quantification process also grow.

Uncertain physical parameters

In the last step of the uncertainty characterization process, the physical parameters in real-world operations are identified and quantified. The two major sources of such uncertainties are airport weather parameters and departure profiles. Among airport weather parameters, six key parameters are used in AEDT performance calculations: temperature, sea-level pressure, station pressure, dew point, relative humidity, and wind speed. These weather parameters can change significantly over a one-year period and can even vary significantly from morning to evening, depending on the airport location. In addition, the reduced thrust and alternative weight departure profiles developed under ASCENT project 45 reflect actual operation-level uncertainties during departure. In the characterization of physical uncertainty sources, both components are included and quantified. Taking Atlanta International Airport (KATL) as an example, a list of uncertain physical parameters and their uncertainty ranges are given in Table 3.

Table 3. Uncertain physical parameters at Atlanta International Airport (KATL).

Item	Baseline Value	Upper Bound	Lower Bound
Temperature @ KATL	62	94	25
Sea-level Pressure @ KATL	1018.02	1032	1004
Station Pressure @ KATL	980.61	993	968
Dew Point @ KATL	50.86	74	9
Relative Humidity @ KATL	67.65	100	20
Wind Speed @ KATL	7.03	24	0
Alternative Weight	Baseline Weight	Alternative Weight	
Takeoff Thrust	100%	Three Reduced Thrust Levels: -5%, -10%, -15%	

The upper and lower bounds of the six weather parameters at KATL, as shown in Table 3, were developed based on historical data. In this process, a histogram of data for each parameter over the past 40 years was created, with the upper and lower bounds given as the upper and lower boundaries of the 95% confidence interval, respectively. The alternative weight and takeoff thrust uncertainties are represented by the previously defined alternative weight and reduced thrust profiles.

Sensitivity analysis procedure

Because the uncertainty quantification process for AEDT and BADA4 involves manipulating the input parameters and running a number of cases with the updated parameter values, an automated, replicable process is needed for effectively conducting the analysis. Such an automated process was initially developed to perform a one-factor-at-a-time (OFAT) computer experiment. The OFAT design of experiment (DoE) is a type of computer experiment in which only one input parameter is varied at a time, while the remaining input parameters are maintained at their baseline values. By implementing the OFAT DoE, one can assess how each individual input influences the outputs. More specifically, the results of an OFAT experiment can provide insight into how variations in inputs impact the variations in outputs with respect to direction and magnitude. In this study, an automated process was developed to facilitate the computer experiment, as shown in Figure 1. In this automated process, a Python script was created to integrate different tools, including the SQL server management studio, AEDT, and batch report, and to automatically process each case sequentially.

The process depicted in Figure 1 can be applied for an OFAT DoE study for both BADA4 coefficients and physical parameters. This process consists of three main steps:

1. Create a table storing the input parameters of interest, their variation ranges, and the location of the parameters in the STUDY database. The parameter location is normally denoted by the name of the table in the STUDY database and row/column identifiers, which can uniquely identify the parameter. Quantification of the variation range for each parameter is a crucial step in uncertainty quantification analysis, which typically uses two methods for different analysis steps. In the sensitivity analysis step, lower and upper bounds with a uniform percentage variation (e.g., ±10%, based on engineering judgment or subject-matter-expert [SME] opinions) are given for each parameter. If the objective is to study the propagation of uncertainty through a system model to precisely quantify the variation in outputs due to variations in inputs, the variation range and probability distribution of each parameter must be determined through a data analysis process.
2. Run the Python script to automatically process all of the cases and to generate performance, emissions, and noise reports for each case.
    1. The Python script reads the information regarding the first parameter from the table created in Step 1 and uses the information to generate SQL queries for manipulating the parameter value in the STUDY database.
    2. The Python script executes the SQL queries and edits the parameter value in the STUDY database.
    3. The Python script calls AEDT to run the case with the updated parameter value.
    4. The Python script calls the AEDT report run tool to generate the performance, emission, and noise reports.

5. The Python script calls the SQL script to reset the parameter to the baseline value.
6. Steps 2.1–2.5 are then repeated for the next parameter.

3. After all of the cases have been run, implement a developed MATALAB script to postprocess all of the sensitivity analysis results.

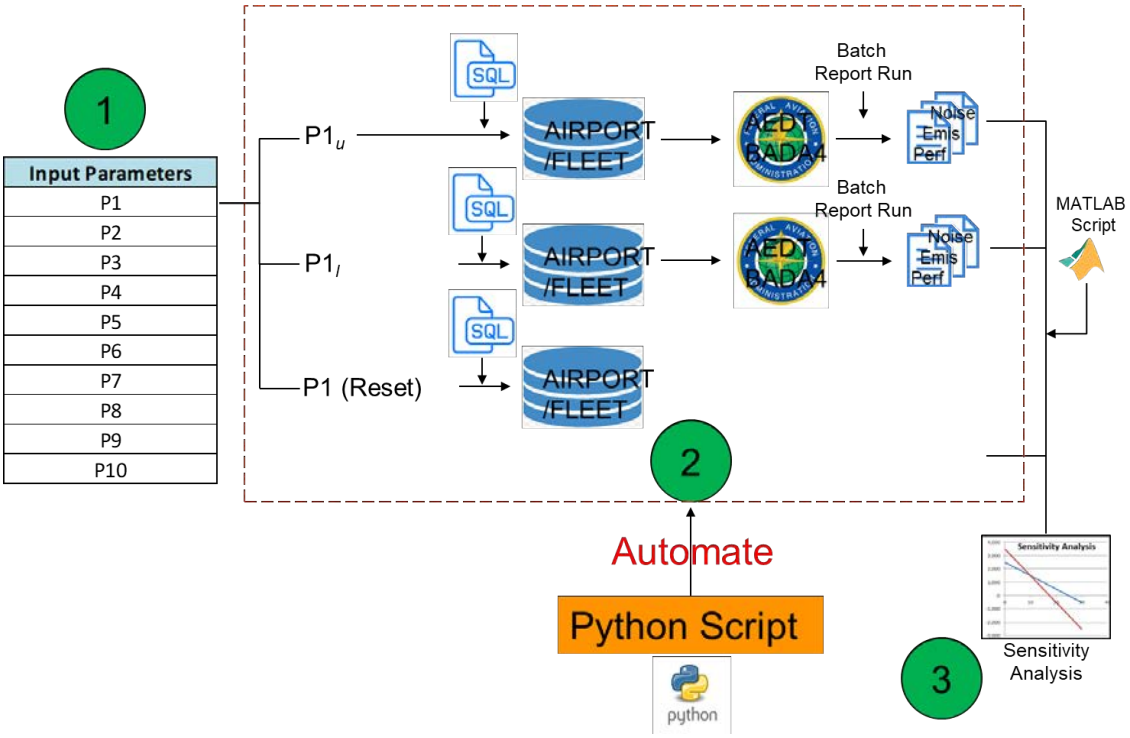

Figure 1. Automated one-factor-at-a-time (OFAT) experiment process.

Sensitivity analysis results for physical parameters

The automated process described above can conduct a complete computer experiment by repeating the analysis for each case according to the DoE table. Using this process, we conducted an OFAT DoE study for the parameters defined in Table 3. To conduct a sensitivity analysis on the outputs, an AEDT study must be designed using these parameters. Table 4 shows the basic information regarding the AEDT study created for sensitivity analysis. This study includes two aircraft with both departure and arrival operations, operating at runway 08 of KATL. For the outputs, both full-flight performance metrics and departure/arrival-level metrics were analyzed to provide more insight.

Table 4. Information provided for sensitivity analysis.

Aircraft	Airbus A320-200 and Boeing 737-800
Airport	Atlanta International Airport (KATL), runway 08
Operations	Arrival and departure
Number of Outputs (21)	Fuel burn (6): overall + fuel burn at five segments
	NOx emission (6): overall + NOx emission at five segments
	Noise (9): contour area, length, and width at 70, 75, and 80 dB for arrival and at 75, 80, and 85 dB for departure
Parameter Range	Airport weather and operation uncertainties
Number of Cases	Departure: 8 parameters, 16 cases; Arrival: 6 parameters, 12 cases
Experiment Type	One-factor-at-a-time (OFAT) design of experiment (DoE)

The results of the case runs were processed and analyzed by a MATLAB script. For each case, the analysis script first obtains the performance output values directly from the performance reports, and the noise output values are obtained by plotting the noise contours and calculating the contour characteristics. Subsequently, the output values for each case are compared to output values for the baseline case, based on percentage changes in the outputs. Because there are four aircraft and operation combinations, four result tables were generated.

The sensitivity analysis results are summarized in Table 5 - Table 8. Due to space limitations, only the full-flight fuel burn and NOx emission results are shown in the tables, with the omission of segment-level results. Each table presents results for a specific aircraft and operation combination. Some general observations are made based on the sensitivity analysis results:

1. Among weather parameters, temperature, sea-level pressure, and wind speed have observable impacts on all outputs, including fuel burn, NOx emission, and noise, for both departure and arrival operations.
2. Relative humidity does not influence fuel burn, but does impact NOx emission and noise.
3. Dew point and station pressure do not impact any of the outputs of interest.
4. Alternative weight and reduced thrust profiles influence the outputs in departure, with significant influences on the noise contours, particularly at higher noise levels.

Table 5. Sensitivity analysis results: B737-800 arrival.

Case No.	Parameter Name	Bounds	Fuel Burn	NOx Emission	70 dB: Area	70 dB: Length	70 dB: Width	75 dB: Area	75 dB: Length	75 dB: Width	80 dB: Area	80 dB: Length	80 dB: Width
1	TEMPERATURE (F)	94	-0.6%	-25.1%	-35.6%	-16.0%	-22.6%	-28.7%	-8.0%	-25.0%	-34.0%	-18.2%	-19.0%
2		25	0.9%	11.9%	-6.5%	-4.2%	-1.3%	-7.8%	-3.2%	-6.6%	-14.5%	-6.8%	-8.1%
3	SLP_PR (mb)	1032	0.7%	1.6%	1.1%	0.5%	0.5%	0.9%	0.6%	0.6%	1.5%	0.8%	0.8%
4		1004	-0.7%	-1.6%	-1.2%	-0.5%	-0.5%	-0.9%	-0.6%	-0.6%	-1.5%	-0.7%	-0.8%
5	ST_PR (mb)	993	0.0%	0.0%	0.0%	0.0%	0.0%	0.0%	0.0%	0.0%	0.0%	0.0%	0.0%
6		968	0.0%	0.0%	0.0%	0.0%	0.0%	0.0%	0.0%	0.0%	0.0%	0.0%	0.0%
7	DEW_P (F)	74	0.0%	0.0%	0.0%	0.0%	0.0%	0.0%	0.0%	0.0%	0.0%	0.0%	0.0%
8		9	0.0%	0.0%	0.0%	0.0%	0.0%	0.0%	0.0%	0.0%	0.0%	0.0%	0.0%
9	REL_HUM (%)	100	0.0%	-6.5%	-2.1%	-0.7%	-1.6%	-1.2%	-0.4%	-1.4%	0.1%	0.0%	0.2%
10		20	0.0%	10.3%	-27.2%	-12.9%	-16.6%	-23.4%	-7.0%	-20.4%	-32.3%	-17.2%	-18.2%
11	WND_SPD (Knots)	24	10.7%	15.5%	7.7%	2.2%	7.7%	10.9%	3.9%	9.6%	19.7%	9.2%	9.9%
12		0	-3.7%	-5.3%	-2.9%	-0.7%	-2.7%	-4.1%	-1.3%	-3.9%	-6.4%	-3.2%	-3.3%

Table 6. Sensitivity analysis results: A320-200 arrival.

Case No.	Parameter Name	Bounds	Fuel Burn	NOx Emission	70 dB: Area	70 dB: Length	70 dB: Width	75 dB: Area	75 dB: Length	75 dB: Width	80 dB: Area	80 dB: Length	80 dB: Width
1	TEMPERATURE (F)	94	-0.7%	-19.3%	-32.1%	-16.2%	-17.2%	-28.3%	-13.0%	-19.3%	-28.7%	-12.2%	-17.1%
2		25	0.8%	12.1%	-2.9%	-1.7%	0.1%	-7.7%	-3.1%	-4.2%	-13.3%	-4.1%	-8.3%
3	SLP_PR (mb)	1032	0.7%	1.3%	1.5%	0.5%	0.7%	1.5%	0.8%	0.8%	1.5%	0.7%	0.9%
4		1004	-0.7%	-1.3%	-1.5%	-0.5%	-0.7%	-1.5%	-0.7%	-0.9%	-1.5%	-0.6%	-0.9%
5	ST_PR (mb)	993	0.0%	0.0%	0.0%	0.0%	0.0%	0.0%	0.0%	0.0%	0.0%	0.0%	0.0%
6		968	0.0%	0.0%	0.0%	0.0%	0.0%	0.0%	0.0%	0.0%	0.0%	0.0%	0.0%
7	DEW_P (F)	74	0.0%	0.0%	0.0%	0.0%	0.0%	0.0%	0.0%	0.0%	0.0%	0.0%	0.0%
8		9	0.0%	0.0%	0.0%	0.0%	0.0%	0.0%	0.0%	0.0%	0.0%	0.0%	0.0%
9	REL_HUM (%)	100	0.0%	-6.8%	-0.6%	-0.2%	-0.4%	0.4%	0.2%	0.0%	1.9%	0.7%	1.2%
10		20	0.0%	10.7%	-25.5%	-13.0%	-12.8%	-25.2%	-10.9%	-16.6%	-30.8%	-13.0%	-18.7%
11	WND_SPD (Knots)	24	8.9%	15.8%	7.0%	1.7%	5.7%	10.2%	4.4%	7.5%	13.7%	4.3%	8.7%
12		0	-3.1%	-5.4%	-2.7%	-0.8%	-2.2%	-3.7%	-1.2%	-2.8%	-5.2%	-1.7%	-3.3%

Table 7. Sensitivity analysis results: B737-800 departure.

Case No.	Parameter Name	Bounds	Fuel Burn	NOx Emission	75 dB: Area	75 dB: Length	75 dB: Width	80 dB: Area	80 dB: Length	80 dB: Width	85 dB: Area	85 dB: Length	85 dB: Width
1	TEMPERATURE (F)	94	6.3%	-21.2%	-17.2%	12.6%	-15.5%	-43.8%	-23.1%	-19.7%	-46.5%	-27.1%	-25.2%
2		25	-3.5%	10.3%	20.4%	-2.2%	25.0%	24.1%	5.1%	11.2%	7.9%	2.5%	5.9%
3	SLP_PR (mb)	1032	-0.2%	0.6%	-1.7%	-1.6%	0.0%	-1.6%	-1.5%	0.0%	-1.6%	-1.4%	0.0%
4		1004	0.2%	-0.6%	1.8%	1.6%	0.0%	1.6%	1.6%	-0.1%	1.6%	1.5%	-0.1%
5	ST_PR (mb)	993	0.0%	0.0%	0.0%	0.0%	0.0%	0.0%	0.0%	0.0%	0.0%	0.0%	0.0%
6		968	0.0%	0.0%	0.0%	0.0%	0.0%	0.0%	0.0%	0.0%	0.0%	0.0%	0.0%
7	DEW_P (F)	74	0.0%	0.0%	0.0%	0.0%	0.0%	0.0%	0.0%	0.0%	0.0%	0.0%	0.0%
8		9	0.0%	0.0%	0.0%	0.0%	0.0%	0.0%	0.0%	0.0%	0.0%	0.0%	0.0%
9	REL_HUM (%)	100	0.0%	-5.5%	3.5%	0.2%	2.1%	1.7%	0.8%	0.6%	-1.0%	-0.5%	-0.3%
10		20	0.0%	8.7%	-9.5%	-2.1%	-5.8%	-19.7%	-10.4%	-7.6%	-25.5%	-16.1%	-10.3%
11	WND_SPD (Knots)	24	-1.2%	-1.5%	-4.0%	-5.6%	2.0%	-3.2%	-5.0%	2.2%	-3.5%	-5.9%	2.5%
12		0	0.5%	0.6%	1.7%	2.4%	-0.8%	1.4%	2.1%	-0.9%	1.5%	2.5%	-1.0%
13	ALT WEIGHT	-	1.7%	2.3%	2.6%	2.6%	-0.6%	2.5%	2.7%	-0.7%	2.3%	2.6%	-0.8%
14	REDUCED THRUST	-5%	0.0%	0.0%	-1.7%	0.3%	-3.4%	-2.0%	0.6%	-7.7%	-4.2%	1.4%	-9.6%
15	REDUCED THRUST	-10%	1.6%	2.2%	-5.2%	10.5%	-13.4%	-19.7%	-5.1%	-15.3%	-23.1%	-7.1%	-18.5%
16	REDUCED THRUST	-15%	1.7%	2.2%	-6.1%	11.2%	-14.0%	-21.0%	-4.1%	-19.7%	-25.2%	-4.7%	-25.4%

Table 8. Sensitivity analysis results: A320-200 departure.

Case No.	Parameter Name	Bounds	Fuel Burn	NOx Emission	75 dB: Area	75 dB: Length	75 dB: Width	80 dB: Area	80 dB: Length	80 dB: Width	85 dB: Area	85 dB: Length	85 dB: Width
1	TEMPERATURE (F)	94	7.0%	-16.4%	-35.8%	-18.6%	-9.1%	-39.6%	-25.6%	-13.1%	-32.0%	-26.3%	-16.3%
2		25	-3.3%	-3.6%	15.0%	8.3%	6.3%	-5.1%	-4.3%	1.5%	-14.9%	-12.0%	-3.3%
3	SLP_PR (mb)	1032	-0.3%	0.1%	-1.6%	-1.3%	-0.4%	-1.8%	-1.4%	-0.4%	-2.1%	-1.7%	-0.3%
4		1004	0.3%	-0.1%	1.6%	1.4%	0.4%	1.8%	1.4%	0.3%	2.1%	1.8%	0.3%
5	ST_PR (mb)	993	0.0%	0.0%	0.0%	0.0%	0.0%	0.0%	0.0%	0.0%	0.0%	0.0%	0.0%
6		968	0.0%	0.0%	0.0%	0.0%	0.0%	0.0%	0.0%	0.0%	0.0%	0.0%	0.0%
7	DEW_P (F)	74	0.0%	0.0%	0.0%	0.0%	0.0%	0.0%	0.0%	0.0%	0.0%	0.0%	0.0%
8		9	0.0%	0.0%	0.0%	0.0%	0.0%	0.0%	0.0%	0.0%	0.0%	0.0%	0.0%
9	REL_HUM (%)	100	0.0%	-5.5%	2.5%	1.5%	1.1%	1.1%	0.5%	0.5%	1.6%	1.3%	0.5%
10		20	0.0%	8.6%	-19.3%	-11.1%	-7.2%	-25.6%	-15.6%	-10.1%	-28.2%	-20.7%	-13.6%
11	WND_SPD (Knots)	24	-1.1%	-1.6%	-3.9%	-5.4%	1.7%	-4.6%	-6.8%	2.2%	-4.5%	-6.5%	2.8%
12		0	0.4%	0.7%	1.6%	2.4%	-0.7%	1.9%	2.8%	-0.9%	1.9%	2.5%	-1.1%
13	ALT WEIGHT	-	1.6%	2.2%	2.4%	2.6%	-0.6%	2.2%	2.7%	-0.7%	1.9%	3.0%	-0.7%
14	REDUCED THRUST	-5%	-0.1%	-0.1%	-0.9%	0.9%	-5.4%	-1.3%	1.7%	-6.0%	-1.8%	3.4%	-6.4%
15	REDUCED THRUST	-10%	2.2%	-2.2%	-14.8%	-2.8%	-10.7%	-14.4%	-2.2%	-11.6%	-14.6%	-6.2%	-12.5%
16	REDUCED THRUST	-15%	2.3%	-2.0%	-15.7%	-1.5%	-16.2%	-15.7%	0.2%	-17.8%	-16.7%	-2.1%	-19.2%

Overall, it was observed that uncertainties in temperature, relative humidity, and wind speed can cause variations in the estimated outputs. Therefore, to accurately model the performance and noise metrics for departure and arrival, it is important to take such uncertainty sources into account. To illustrate the influences of weather parameters and other physical factors, we plotted noise contours at all noise levels for all cases, as shown in Figure 2, for each aircraft and operation combination. In each plot, the purple, green, and yellow lines represent the lowest, middle, and highest noise contour levels,

respectively. It can be seen that for a given noise level, the noise contour can vary significantly from case to case, resulting in differences of up to 50% in contour area, length, and width compared with the baseline weather and operation values.

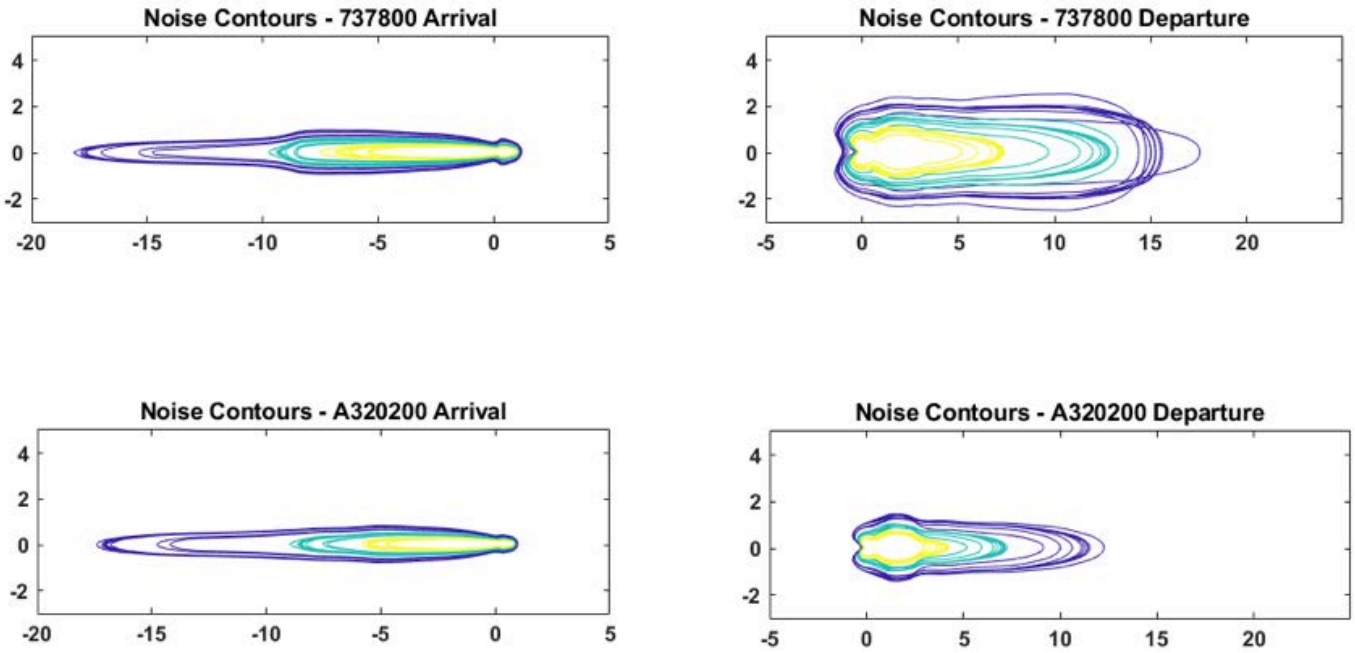

Figure 2. Noise contour variations under weather and operation uncertainties.

In addition, it was observed that different weather parameters influence the noise contours in various ways. Taking the 75-dB departure noise contours for aircraft B737-800 as an example, the noise contour changes caused by temperature, sea-level pressure, relative humidity, and wind speed are shown in Figure 3. In each plot, the red, black, and blue lines represent the noise contour for the upper bound, baseline value, and lower bound of the parameter studied.

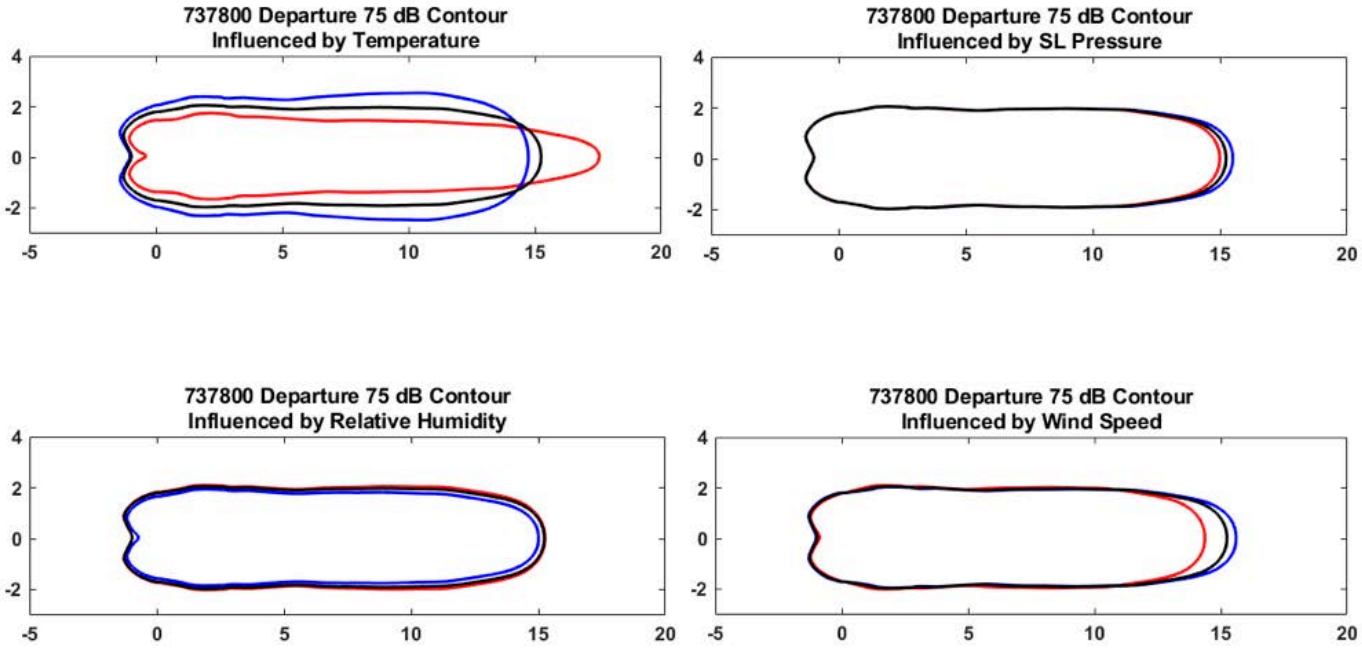

Figure 3. Noise contour changes for B737-800 departure at 75 dB.

The panel in the upper left of Figure 3 shows that under high-temperature conditions, the contour area decreased (17.2% smaller than at the baseline temperature), and the contour shape changed significantly. Compared to the baseline case, the contour length under high-temperature conditions increased by 12.6%, and the contour width decreased by 15.5%. In contrast, for the low-temperature case, the contour variation shows the opposite trend. The contour shape has a lower aspect ratio, and the contour length and width change by -2.2% and +25.0%, respectively. Moreover, when the relative humidity varied, the contour area, length, and width changed in the same direction. That is, all three contour metrics increased at higher relative humidity and decreased at lower relative humidity. Although the influences of sea-level pressure and wind speed are not as significant as those for temperature and relative humidity, these factors also exhibit a pattern. They primarily influence the contour area due to a change in contour length, with little to no impact on contour width.

Uncertainty propagation

After the uncertainty characterization and sensitivity analysis, uncertainty propagation analysis is performed. In uncertainty propagation, the uncertainty is mapped from uncertain inputs to the output through a system model. Subsequently, a statistical analysis of the nondeterministic output results can be conducted for further decision-making. A typical uncertainty propagation process is illustrated in Figure 4.

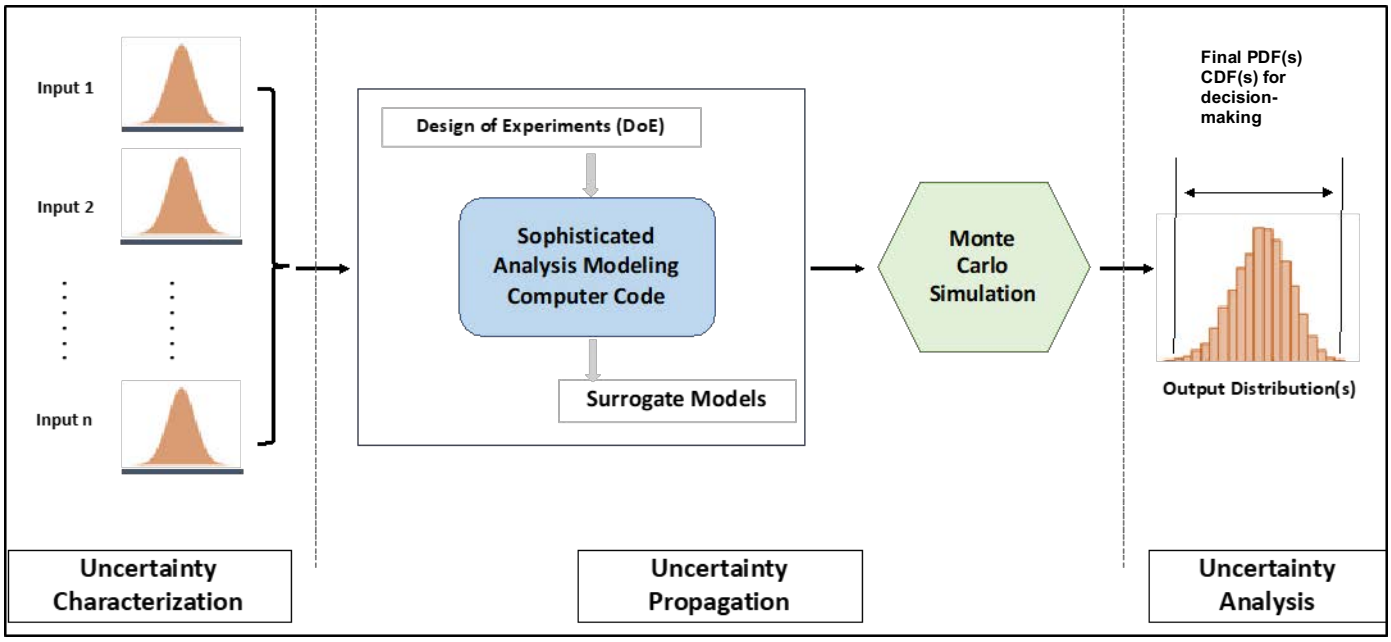

Figure 4. Uncertainty propagation analysis process.

The uncertainty propagation analysis shown in Figure 4 is implemented through three primary steps. Before the uncertainty propagation can be conducted, the uncertainty of each parameter must be represented mathematically. This representation is typically obtained through data analysis, computer experiments, and SME opinions, with the objective of assigning a probability distribution to represent the uncertainty of each input parameter. Unlike the OFAT sensitivity analysis, in which the uncertainty bounds for all parameters are set to $\pm 10\%$, the goal of this step is to ensure that the uncertainty representation of each parameter reflects their real-world behavior as much as possible. In the second step of uncertainty propagation analysis, the uncertainties of the input parameters are propagated to the outputs through the AEDT and BADA4 models. Because these models are complex and the processes are computationally expensive, further experimental design and surrogate modeling can be used to facilitate this process. Monte Carlo simulations provide an effective means for conducting uncertainty propagation in this case because these simulations can handle a large number of probabilistic inputs, various distribution types, and highly nonlinear models. Finally, an uncertainty analysis is conducted based on the uncertainty propagation results, which are expected to reflect the uncertainty in the output of interest. This uncertainty propagation step, together with the global sensitivity analysis described in the next section, are expected to be conducted in the next stage of the project.

Global sensitivity analysis

Global sensitivity analysis is another future avenue of this work. In contrast to the OFAT sensitivity analysis, a sensitivity analysis is considered to be global if all input parameters are simultaneously varied over their entire uncertainty ranges. This approach is used to decompose the total uncertainty of each output and attribute it to different input parameters. This step provides insight into how strongly each input parameter affects and contributes to the total uncertainty of an output. The key metrics used in this step include the total sensitivity index, which measures the relative impact of each input parameter.

Milestone(s)

Milestone	Due Date	Estimated Date of Completion	Actual Completion Date	Status	Comments (Problems & Brief Resolution Plan)
A36 Kickoff Meeting	5/3/2016	5/3/2016	5/3/2016	Completed	
Quarterly Report (Aug)	7/31/2016	7/31/2016	7/31/2016	Completed	
ASCENT Meeting	9/27-28/2016	9/27-28/2016	9/27-28/2016	Completed	
Quarterly Report (Nov)	10/31/2016	10/31/2016	10/31/2016	Completed	
Annual Report	1/18/2017	1/18/2017	1/13/2017	Completed	
Quarterly Report (Jan)	1/31/2017	1/31/2017	1/27/2017	Completed	
Quarterly Report (Mar)	3/31/2017	3/31/2017	3/31/2017	Completed	
ASCENT Meeting	4/18/2017	4/18/2017	4/18/2017	Completed	
Quarterly Report (Jun)	6/30/2017	6/30/2017	6/30/2017	Completed	
ASCENT Meeting	9/26/2017	9/26/2017	9/26/2017	Completed	
Quarterly Report (Oct)	10/30/2017	10/30/2017	10/30/2017	Completed	
Annual Report	11/30/2017	11/30/2017	11/30/2017	Completed	
Quarterly Report (Jan)	1/31/2018	1/31/2018	1/31/2018	Completed	
Quarterly Report (Mar)	3/31/2018	3/31/2018	3/31/2018	Completed	
ASCENT Meeting	4/3-4/2018	4/3-4/2018	4/3-4/2018	Completed	
Quarterly Report (Jun)	6/30/2018	6/30/2018	6/30/2018	Completed	
ASCENT Meeting	10/9-10/2018	10/9-10/2018	10/9-10/2018	Completed	
Quarterly Report (Oct)	10/30/2018	10/30/2018	10/30/2018	Completed	
Annual Report	11/30/2018	11/30/2018	11/30/2018	Completed	
Quarterly Report (Jan)	1/31/2019	1/31/2019	1/31/2019	Completed	
ASCENT Meeting	4/18-19/2019	4/18-19/2019	4/18-19/2019	Completed	
Quarterly Report (Apr)	4/30/2019	4/30/2019	4/30/2019	Completed	
Quarterly Report (Jul)	7/31/2019	7/31/2019	7/31/2019	Completed	
ASCENT Meeting	10/22-23/2019	10/22-23/2019	10/22-23/2019	Completed	
Quarterly Report (Oct)	10/31/2019	10/31/2019	10/31/2019	Completed	
Annual Report	11/30/2019	11/30/2019	11/30/2019	In Progress	

Major Accomplishments

As of December 2018, all new AEDT Sprint releases, including Sprints 112-129, have been tested. Eighteen AEDT Sprints have been tested, focusing on new features and added capabilities. Some of the new features/capabilities were minor updates to the GUI, bug fixes, or data updates. Major updates included track control, NO_2 emissions dispersion modeling, and a user-defined profile editor. To understand the background of new AEDT features, all relevant documents were reviewed, including software requirement documents, database design documents, AEDT Sprint release notes, updated technical manuals, user manuals, and research papers/reports. Basic tests of all new AEDT versions were completed to confirm their functionality, and issues were reported to the FAA and the development team via biweekly ASCENT project teleconferences and weekly AEDT development-lead calls. Identified issues and follow-up actions taken by the developers were documented and shared through the Team Foundation Server (TFS) online system. The TFS also allows for reporting of any potential areas of improvements in AEDT algorithms and user friendliness.

Finally, a sensitivity analysis was conducted to investigate how variations in input parameters impact the variations in output parameters in the AEDT BADA4 model. Physical parameters, including weather parameters, takeoff weight, and thrust, were identified as input parameters for the sensitivity analysis. An automated process was developed to automatically call AEDT to run each case with updated parameter values and to generate performance, emissions, and noise reports. The sensitivity results provide insights into how the input parameters impact the AEDT outputs with the BADA4 model in terms of magnitude and direction.

Publications

Written reports

ASCENT quarterly reports (Jan. 2019; Apr. 2019; Jul. 2019, Oct. 2019)
ASCENT annual report (Nov. 2018)

Peer-reviewed journal publications

Gao, Z., Behere, A., Li, Y., Lim, D., Kirby, M., & Mavris, D.M. Quantitative assessment of the new departure profiles with improved weight and thrust modeling. To be submitted to Journal of Aircraft.

Outreach Efforts

N/A

Awards

None.

Student Involvement

Zhenyu Gao is a third-year PhD student who started in fall 2016. Mr. Gao has conducted a literature review on uncertainty quantification methods and has performed tests of newly released AEDT features. Mr. Gao is being trained on related tools such as INM, AEDT Tester, AEDT 2e, and AEDT 3b.

Ameya Behere is a third-year PhD student who started in fall 2016. Mr. Behere has conducted a literature review on uncertainty quantification methods and has performed tests of newly released AEDT features. Mr. Behere is being trained on related tools such as INM, AEDT Tester, AEDT 2e, and AEDT 3b.

Yee Chan Jin is a second-year Master student who started in fall 2018. Mr. Jin has conducted a literature review on uncertainty quantification methods and has performed tests of newly released AEDT features. Mr. Jin is being trained on related tools such as INM, AEDT Tester, AEDT 2e, and AEDT 3b. Mr. Jin graduated in Dec. 2019 and is currently employed by Southwest Airlines.

Plans for Next Period

This project officially ended on August 31, 2019; however, some of the tasks performed by GT will be continued under the new ASCENT project 54. GT will perform the system testing, validation, and verification tasks for the new versions of AEDT 3c and beyond to identify any issues that should be addressed by the development team. The detailed tasks will be discussed with FAA project managers.

References

Eurocontrol Experimental Centre. (Mar. 2016) User manual for the base of aircraft data (bada) family 4.
Lim, D., Li, Y., LeVine, M.J., Kirby, M., & Mavris, D.M. (2018). Parametric uncertainty quantification of aviation environmental design tool. 2018 Multidisciplinary Analysis and Optimization Conference, AIAA AVIATION Forum, (AIAA 2018-3101)
US FAA, AEDT 2a UQ Report, 2014
US FAA, AEDT 2a SP2 UQ Supplemental Report, 2014
US FAA, AEDT 2b UQ Report, 2016

Project 037 Continuous Lower Energy, Emissions, and Noise (CLEEN) II System-Level Assessment

Georgia Institute of Technology

Project Lead Investigator

Dimitri Mavris (PI)
Regents Professor
School of Aerospace Engineering
Georgia Institute of Technology
Mail Stop 0150
Atlanta, GA 30332-0150
Phone: 404-894-1557
Email: dimitri.mavris@ae.gatech.edu

University Participants

Georgia Institute of Technology

- PI(s): Dr. Dimitri Mavris (PI), Dr. Jimmy Tai (Co-PI)
- FAA Award Number: 13-C-AJFE-GIT-013
- Period of Performance: August 31, 2018 to August 31, 2019
- Task(s): Technology Modeling and Assessment

Project Funding Level

FAA funding was distributed at the following levels.

- Georgia Institute of Technology ($170,000)

The Georgia Institute of Technology (GT) has agreed to a total of $170,000 in matching funds. This total includes salaries for the project director, research engineers, and graduate research assistants and computing, financial, and administrative support, including meeting arrangements. The institute has also agreed to provide tuition remission for any students whose tuition is paid via state funds.

Investigation Team

- Dimitri Mavris, Principal Investigator, Georgia Institute of Technology
- Jimmy Tai, Co-Investigator, Georgia Institute of Technology
- Holger Pfaender, Technology Modeling and Assessment, Georgia Institute of Technology
- Chris Perullo, Technology Modeling and Assessment, Georgia Institute of Technology

Project Overview

The objective of this research project is to support the FAA by independently modeling and assessing the technologies that are being advanced under the Continuous Lower Energy, Emissions, and Noise (CLEEN) II program. This task involves direct coordination and data sharing in order to accurately model the environmental benefits of their developments at the vehicle and fleet levels. The long-term goals of this project include vehicle- and fleet-level assessments of fuel burn, emission, and noise benefits for CLEEN II aircraft and engine advancements. GT will create vehicle- and fleet-level Environmental Design Space (EDS) models using a combination of both CLEEN II and other public domain N+1 (next generation) and N+2 (two generations out) technologies. The outcomes of the technology and fleet assumptions from workshops conducted under the previous ASCENT Project 10 will be heavily leveraged for this effort. The ASCENT Project 10 was conducted in conjunction with industry, government, and academia to establish a standardized set of scenarios and assumptions regarding future demand and operations growth. These scenarios can be used to assess the impact of advanced

technologies, such as those being developed under CLEEN II, on aviation-related fuel burn, emissions, and noise generation. Other technologies expected to enter service in the analysis time period will also be included to ensure that the predicted impacts are relevant and accurate.

Task 1 – Technology Modeling and Assessments

Georgia Institute of Technology

Objective

The objective of this task is to support the FAA by independently modeling and assessing the technologies that are being developed under the CLEEN II program. This task will involve direct coordination and data sharing with CLEEN II companies in order to accurately model the environmental benefits of these technologies at the vehicle and fleet levels.

Research Approach

The objective of this research project is to support the FAA by independently modeling and assessing technologies developed under the CLEEN II program. This effort involves direct coordination and data sharing with companies developing technologies under CLEEN II, with the aim of accurately modeling the environmental benefits of these technologies at the vehicle and fleet levels.

GT was previously selected to perform all system-level assessments for the CLEEN program under PARTNER Project 36 and ASCENT Project 10. As a result, GT has a unique position from both a technical and programmatic standpoint to continue system-level assessments for CLEEN II. From a technical perspective, GT has significantly enhanced the EDS over the last five years to incorporate advanced, adaptive, and operational technologies targeting fuel burn, noise, and emissions. The EDS was successfully applied to all CLEEN I contractor technologies, including GE open rotors, twin-annular premixing swirler (TAPS) II combustors, flight management system (FMS) engines and airframes, Pratt & Whitney geared fans, Boeing adaptive trailing edge and ceramic matrix composite (CMC) nozzles, Honeywell hot section cooling and materials, and Rolls-Royce turbine cooling technologies. GT also gained significant experience in communicating system-level modeling requirements to industry engineers and translating the impacts to fleet-level fuel burn, noise, and emission assessments. This broad technical knowledge base covering both detailed aircraft and engine design and high-level benefit assessments puts GT in a unique position to assess CLEEN II technologies.

As the ultimate goal of this work is to conduct fleet-level assessments for aircraft representatives of future “in-service” systems, GT must create system-level EDS models using a combination of both CLEEN II and other public domain N+1 and N+2 technologies. The outcomes of technology and fleet assumption-setting workshops conducted under ASCENT Project 10 will be heavily leveraged for this effort. The consideration of non-CLEEN II technologies and potential future fleet scenarios will help to bound the impact of CLEEN II on future fleet fuel burn, emissions, and noise. During our first year, nondisclosure agreements were signed with all CLEEN II contractors.

Because the FAA will also be performing a portion of the EDS technology modeling work, EDS training was provided to the FAA in 2016 under ASCENT Project 10. This training provided the FAA with the skill set required to use EDS.

In the previous year of this project, GT initiated modeling activities with Aurora, Pratt & Whitney, and GE. This modeling process included validations of underlying EDS models, the information and data exchange necessary to model the individual technologies, and related EDS modeling activities. In addition, GT has assisted the FAA with in-house modeling of Delta/MDS and GE combustion technologies. This process has increased the FAA’s use of FAA personnel for EDS system-level assessment modeling.

Moving towards the end of the project, this year’s work will focus on completing vehicle- and fleet-level assessments for CLEEN II. This step includes final technology modeling details for each vehicle-level assessment of fuel burn, emissions, and noise generated by CLEEN II industry contractors in comparison to current best-in-class results, along with fleet-level estimates of fuel burn, emissions, and noise, including community noise impact estimates for multiple relevant airports. By quantifying this impact, we will quantify the number of increased operations per day that CLEEN II technologies can enable without increasing noise exposure to the surrounding community. While airports in the U.S. are generally not noise-constrained, some European airports have limited capacities to meet noise constraints. Understanding the impact of

technologies on the future U.S. fleet is critical to quantifying interactions between economic growth (i.e., increased flight operations at a given airport) and community noise impacts.

GT has completed most of the technology modeling thus far. Remaining items include updates of technology models using the most recent data from contractors and a final fleet assessment. The table in the next section shows the current status of technology modeling. Where work remains, a brief description is provided after the table.

Milestone(s)

Milestone	Planned Due Date
Complete Modeling of Chosen Contractor's Technologies	08/2018
Preliminary Fleet Assessment	02/2019

Major Accomplishments

- GT has signed nondisclosure agreements with all CLEEN II contractors.
- The Delta/MDS modeling is complete.
- The Aurora modeling is complete.
- Modeling for GE FMS is complete, pending further updates to technology.
- Modeling for GE TAPS III is complete.
- The modeling framework for GE MESTANG is complete.
- Modeling for the Boeing compact nacelle is complete.
- Data exchange and assumptions for the Honeywell blade outer air seal and combustor have been defined.
- Modeling for the Boeing structurally efficient wing is complete.
- Modeling for the GE FMS is 80% complete, and the approach has been finalized.
- The modeling approach for the Collins slim nacelle has been finalized, and data and assumptions are being reviewed with Collins and PW.
- Ongoing efforts are being made to model UTAS zoned liner technology.
- The fleet analysis for CLEEN I is currently being repeated with the updated EDS version and preliminary CLEEN II estimates.
- An approach for modeling Pratt & Whitney technologies has been determined, and the modeling is 75% complete.

Contractor	Technology / Model Impact Area	Initial Modeling Discussions Held with Contractor	Modeling Underway	Percentage Complete	May Require Update
Aurora (technologies listed are subparts of double-bubble fuselage)	D8 Configuration	✓	✓	100%	No
Boeing	Structurally Efficient Wing	✓	✓	100%	No
	Compact Nacelle	✓	✓	100%	No
Delta/MDS/America's Phenix	Leading Edge Protective Fan Blade Coating	✓	✓	100%	No

Contractor	Technology / Model Impact Area	Initial Modeling Discussions Held with Contractor	Modeling Underway	Percentage Complete	May Require Update
GE	Twin-Annular Premixing Swirler (TAPS) III Low NOx Combustor	✓	✓	100%	No
	More Electric Systems and Technologies for Aircraft in the Next Generation (MESTANG)	✓	✓	90%	Yes
	Flight Management System (FMS)	✓	✓	100%	Yes
	Low-Pressure-Ratio Advanced Acoustic	✓		0%	
Honeywell	Compact Combustor	✓	✓	75%	Yes
	Turbine Blade Outer Air Seal	✓	✓	75%	No
Pratt & Whitney	Compressor and Turbine Aeroefficiency Technologies	✓	✓	65%	Yes
Collins/Rohr/UTAS	Slim Nacelle	✓	✓	75%	Yes
	Noise Liner Technologies	✓	✓	50%	Yes
Rolls-Royce	Advanced Rich Quench Lean Low NOx Combustor	✓		25%	

Remaining modeling work

- GE MESTANG
  - Received revised flight profiles from GE for baselining technology benefit; need to update EDS model and reconfirm benefit numbers with GE
- GE Low-Pressure-Ratio Advanced Acoustic
  - Waiting on information from GE; modeling not yet started
- Honeywell Compact Combustor
  - Received preliminary combustor correlation estimates from Honeywell
  - Will update correlations and finalize model when Honeywell completes high-pressure testing at NASA facility; only minor modeling changes required
- Honeywell Turbine Blade Outer Air Seal
  - Have received modeling impacts from Honeywell; have modeled similar technology for CLEEN I from Honeywell; will implement and confirm at the same time as the compact combustor validation

- Pratt & Whitney Compressor and Turbine Aeroefficiency Technologies
  - Have held several working meetings with Pratt & Whitney; have agreed upon a modeling approach; have received the required modeling data from Pratt & Whitney; will run sensitivity studies and verify trends with PW
- Collins Slim Nacelle
  - Iteration with PW almost complete (one meeting left) for sensitivity of the low-pressure drop bypass duct to engine performance, based on Collins' request
  - Have determined modeling approach for noise impacts; difficulty in capturing higher-fidelity noise attenuation effects; iterations on approach continuing with Collins
- Rolls-Royce Advanced Rich Quench Lean Low NOx Combustor
  - Will use the same modeling approach applied for Honeywell when Rolls-Royce completes testing, but with an empirical NOx model specific to Rolls-Royce

Publications
N/A

Outreach Efforts
CLEEN Consortium

Awards
None.

Student Involvement
Siyuan Wu is a graduate student who has been assisting with modeling of UTAS noise technologies. Wu has graduated and is currently working in industry.

Plans for Next Period
Future work will focus on completing the technology modeling and conducting fleet analysis assessments for presentation at the May 2020 Consortium.

This work will also support attendance at CLEEN Consortium meetings and preliminary and detailed contractor design reviews to identify any updates required for previously developed technology models.

Project 038 Rotorcraft Noise Abatement Procedure Development

The Pennsylvania State University, Continuum Dynamics, Inc.

Project Lead Investigator

Kenneth S. Brentner
Professor of Aerospace Engineering
Department of Aerospace Engineering
The Pennsylvania State University
233 Hammond Building
University Park, PA
(814) 865-6433
ksbrentner@psu.edu

University Participants

The Pennsylvania State University

- PI: Kenneth S. Brentner, Professor of Aerospace Engineering
- FAA Award Number: 13-C_AJFE-PSU-038, Amendment No. 41
- Period of Performance: September 2018 to August 2019
- Task(s) (during this period):
  1. Continue evaluating flight test data to determine the effectiveness of noise abatement procedures
  2. Evaluate and refine noise abatement procedure development strategy
  3. Demonstrate the potential of refined noise abatement procedures

Project Funding Level

FAA: $150,000; In-Kind Matching (Continuum Dynamics, Inc.): $150,000

Investigation Team

- Kenneth S. Brentner, PI, The Pennsylvania State University; acoustic prediction lead on all tasks.
- Joseph F. Horn, Co-PI, The Pennsylvania State University; flight simulation lead supporting all tasks.
- Daniel A. Wachspress, Co-PI, Continuum Dynamics, Inc.; responsible for rotor loads, wake integration, and Comprehensive Hierarchical Aeromechanics Rotorcraft Model (CHARM) coupling.
- Mrunali Botre, Graduate Research Assistant, The Pennsylvania State University; primarily responsible for establishing new aircraft models, developing simulations for new helicopter types, performing acoustic predictions, and developing flight abatement procedures; involved in all tasks.

Project Overview

Rotorcraft noise consists of several components, including rotor noise, engine noise, gearbox and transmission noise, etc. Rotor noise is typically the dominant component of rotorcraft noise to which the community is exposed upon takeoff and landing and along the flight path of the helicopter. Rotor noise consists of multiple noise sources, including thickness noise and loading noise (typically combined as rotational noise), blade-vortex-interaction (BVI) noise, high-speed-impulsive (HSI) noise, and broadband noise. Each noise source has a own unique directivity pattern around the helicopter. Furthermore, aerodynamic interactions among rotors, interactions between the airframe wake and a rotor, and unsteady time-dependent loading generated during maneuvers typically result in significant increases in loading noise. The combination of all potential rotor noise sources renders the prediction of rotorcraft noise highly complex, even though not all noise sources are present at any given time in the flight (e.g., BVI noise usually occurs during the descent, and HSI noise only occurs during high-speed forward flight).

In ASCENT Project 6, "Rotorcraft Noise Abatement Operating Conditions Modeling," the project team coupled a MATLAB-based flight simulation code with CHARM and PSU-WOPWOP to perform rotorcraft noise prediction. This noise prediction system was used to develop noise abatement procedures through computational and analytical modeling. Although this noise prediction system cannot predict engine noise or HSI noise, it was thoroughly validated via a comparison between predicted noise levels for a Bell 430 aircraft and flight test data (Ref. 19) for several observer positions and operating conditions.

In previous work for ASCENT Project 38, representative helicopters were recommended for noise abatement procedure development. These helicopters were selected to enable a determination of whether noise abatement procedures could be developed for various categories of helicopters, (i.e., 2-blade light, 4-blade light, 2-blade medium, etc.) or whether aircraft-specific design considerations would be required. Aircraft models were established for the following aircraft: Bell 430, Sikorsky S-76C+ and S-76D, Bell 407 and 206L, Airbus EC130 and AS350, and Robinson R66 and R44. Predictions were made before the 2017 FAA/NASA noise abatement flight test to provide guidance for the flight test. After the flight test, a comparison of L_A time histories and sound exposure level (SEL) contour plots revealed a problem in the broadband noise prediction, which was subsequently corrected. Initial validation comparisons demonstrated that the simulations were within a few dBA of the flight test data; however, some discrepancies in the simulations (simplifications) remained, requiring a detailed examination.

The objective of this continuing project is to utilize computational and analytical modeling to develop noise abatement procedures for various helicopters in different phases of flight. The extension of this project also includes predictions aiming to analyze various flight procedures to determine their effectiveness in noise reduction. Comparisons of predictions and flight test data provide further validation of the noise prediction system and allow a deeper understanding of the impact of noise abatement procedures on noise directivity and amplitude. Emphasis is given to more complicated flight procedures (turns with deceleration or descending turns) and validation of the noise prediction system for these complex procedures. The predictions help to explain the details of the noise generated in various procedures, which will aid in the design of refined noise abatement flight procedures.

Task 11 - Continue Evaluating Flight Test Data to Determine the Effectiveness of Noise Abatement Procedures

The Pennsylvania State University

Objective(s)

The objective of this task is to provide continued assistance in the evaluation of flight test data and the effectiveness of various noise abatement procedures. Our goal is to understand the interactions among various noise sources, to determine which sources are predominantly changed by a given flight procedure, and to identify the governing mechanisms. Special emphasis was given to turns and more complicated procedures during the second half of this year.

Research Approach

The noise prediction system developed in ASCENT Projects 6 and 38 will be used and updated as necessary. The PSU-WOPWOP code will be used for noise prediction and will be coupled with a MATLAB flight simulator and CHARM to form a rotorcraft noise prediction system. The flight test data will be examined, and the measured and predicted results will be compared to help explain any significant but unexpected details of the noise measurements. This evaluation can also identify the primary and secondary noise sources involved in a given flight procedure and can clarify how the noise abatement was achieved (which can lead a generalized procedure for other helicopter categories, weights, etc.).

Milestone(s)

The milestones for this task include (a) analysis of noise predictions and flight data for straight flight profiles, (b) analysis of simulated and measured noise for level turns (without deceleration), and (c) analysis of noise from complex flight profiles (decelerating turns and descending turns). This task will examine various predicted noise sources and will investigate which sources are important in the flight test data (for several different microphones).

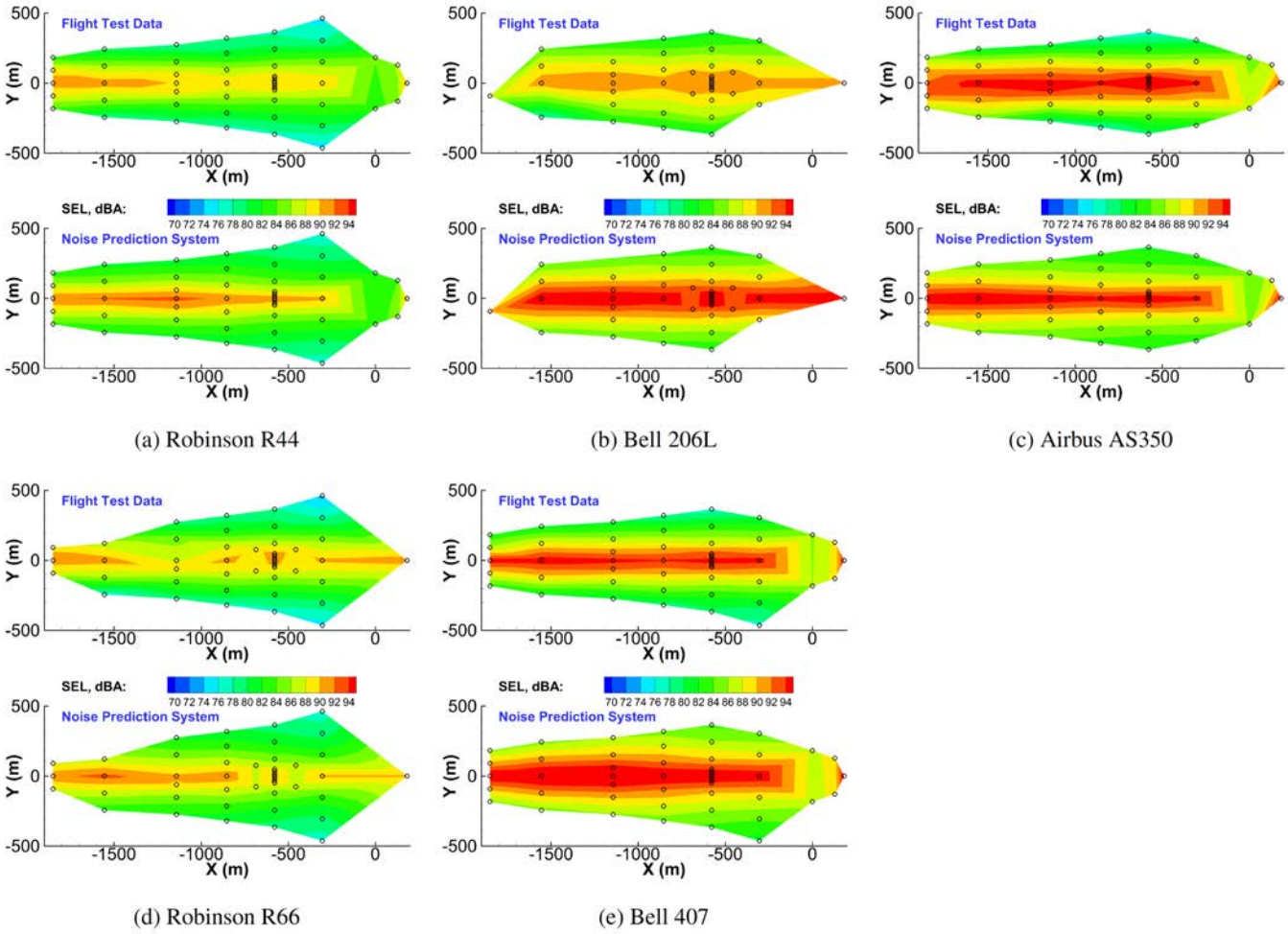

Figure 1. Total sound exposure level (SEL, dBA) for an 80-kts level flight. For each subfigure, top: flight test data; bottom: prediction.

Major Accomplishments

Noise predictions were made for five aircraft flown in the 2017 FAA/NASA noise abatement flight test. SEL contours from the simulations were compared to the flight test data. Straight flight conditions (level flight [shown in Figure 1] and 6° descent) were considered first. Individual noise components were considered (not shown here), and it was found that thickness noise is dominant as the helicopter approaches while loading and broadband noise is dominant overhead during the peak and after the helicopter passes. The main rotor is the primary source of low-frequency noise (OASPL) while the tail rotor is the primary contributor for L_A. The predicted SEL contours were slightly higher than the flight test data, except for Airbus AS350, because the thickness noise for a level flight was overpredicted. As determined in Task 12, it is important to match the small transients in the time-dependent aircraft position and attitude in the flight test to obtain the best agreement. Hence, the aircraft motion was included in the simulation, and the results were improved. For the straight cases, a comparison of the nominal flight path and attitude (both constants) with the actual flight variables resulted in a significantly better correlation, even though the changes were small.

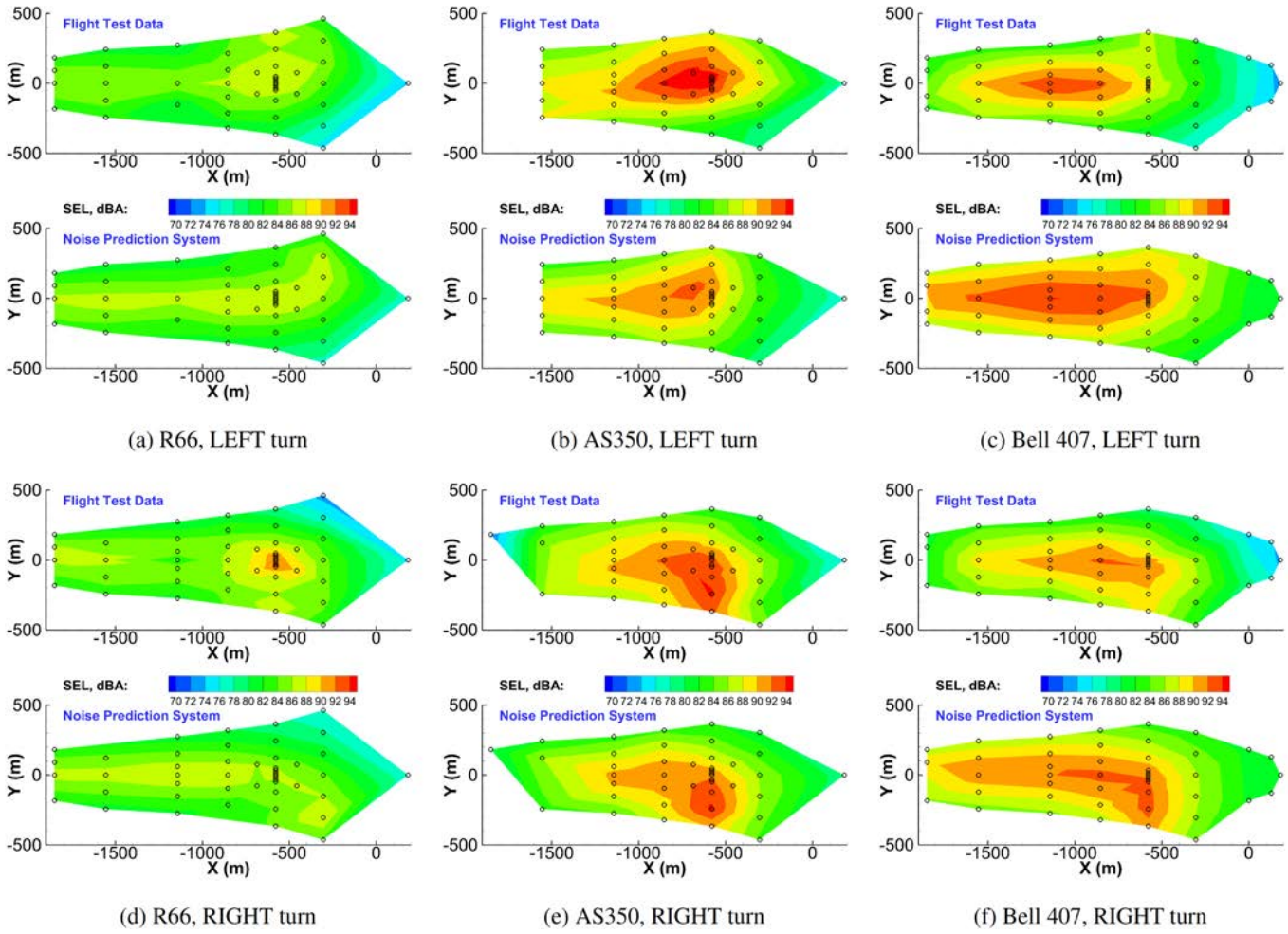

Figure 2. Total sound exposure level (SEL, dBA) for a level decelerating turn. The final roll angle is 25˚ for all turns. For each subfigure, top: flight test data; bottom: prediction.

Next, we considered level right and left turns (see Figure 2). For these maneuvers, it was discovered that the broadband noise was based only on the first timestep in the simulation, remaining constant throughout the turns. This phenomenon limited the accuracy of the predictions; thus, the PSU-WOPWOP code was modified to read in a time history of the input parameters for the Pegg loading model for each window time. This modification has been incorporated in all results shown in this report. It was observed that the SELs during level flight are normally higher than those during left and right level turns. This trend most likely occurs because the L_A peak has a shorter duration when the aircraft is turning. Thus, each microphone location will measure lower SEL levels.

Results for the most complex cases, i.e., decelerating or descending turns, are shown in Figures 3 and 4. These maneuvers are more complex and difficult, although not overwhelming, for the pilot to execute. Both decelerating turns and descending turns had generally higher SEL values compared with the level turn case. The lighter Robinson aircraft had lower noise levels due to their lower weight. Interestingly, although the flight test and simulations exhibited different SEL values, the agreements between the flight test and prediction data are roughly constant for all flight conditions and aircraft types.

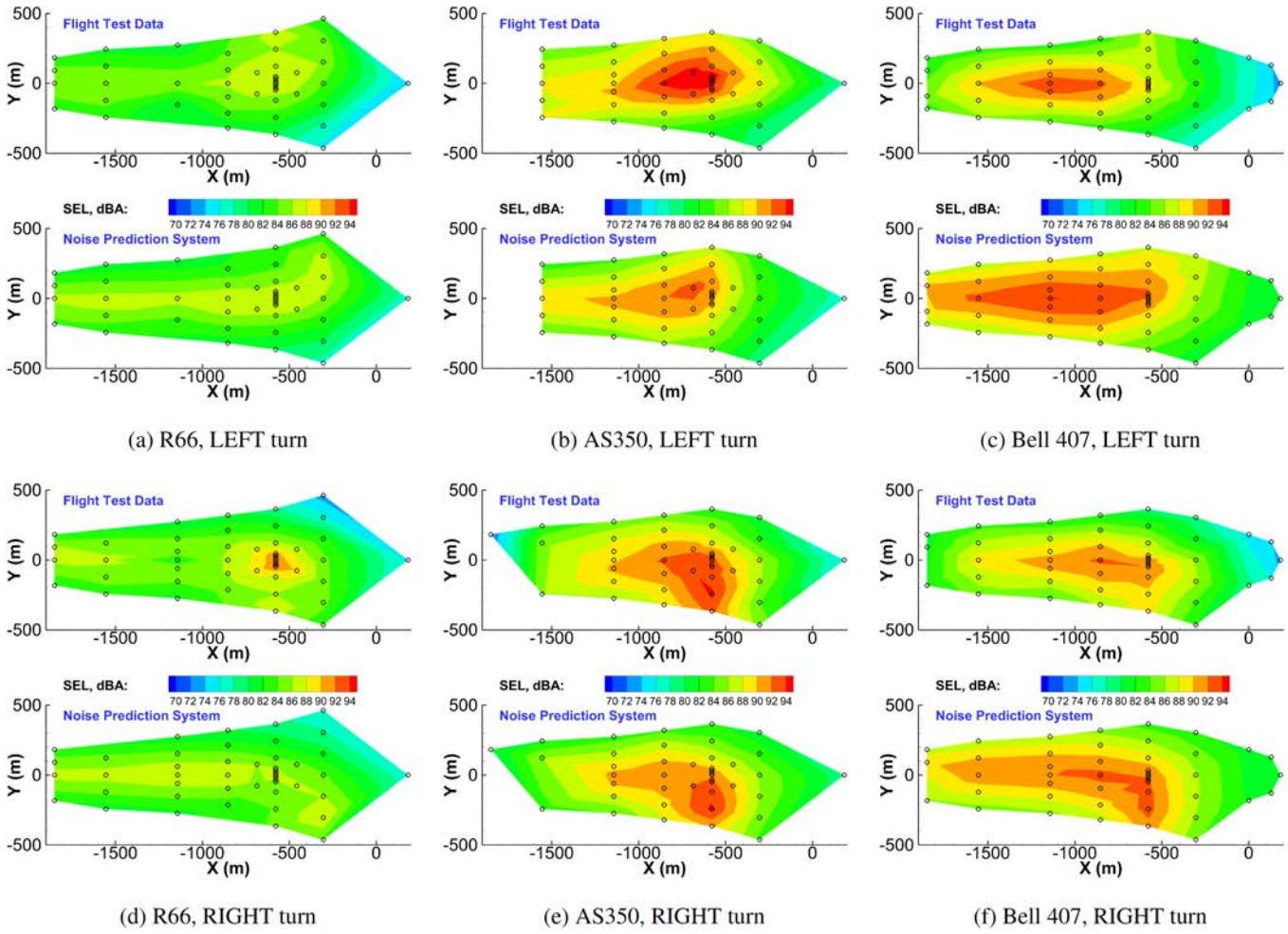

Figure 3. Total sound exposure level (SEL, dBA) for a level decelerating turn. The final roll angle is 35˚, with a deceleration from 80 kts at 2 kts/s. For each subfigure, top: flight test data; bottom: prediction.

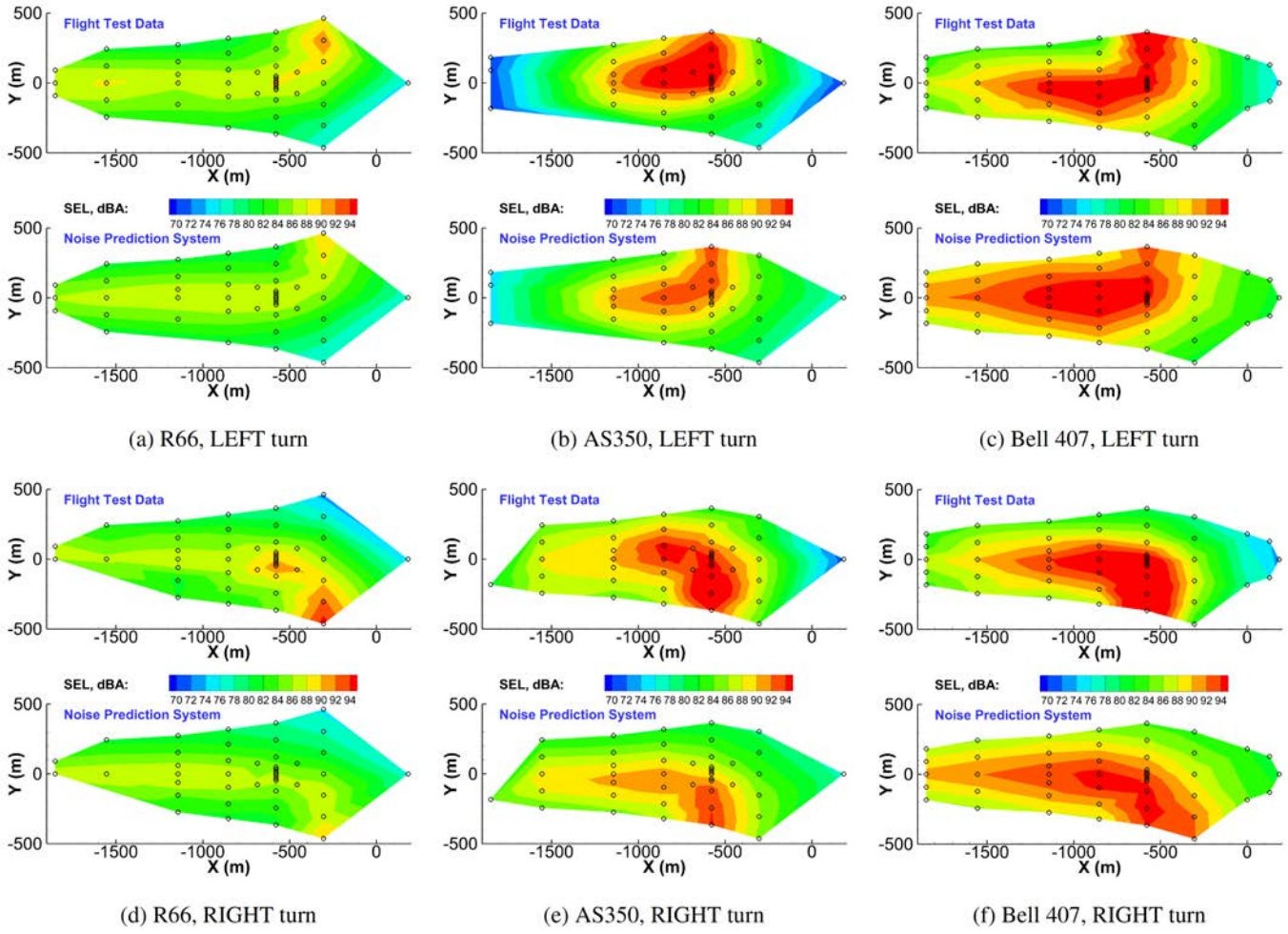

Figure 4. Total sound exposure level (SEL, dBA) for an 80-kts descending turn, with a flight path angle of 6˚ and a final roll angle of 35˚. For each subfigure, top: flight test data; bottom: prediction.

Publications

Published conference proceedings

Botre, M., Brentner, K.S., Horn, J.F., & Wachspress, D.A. (2019). Developing a comprehensive noise prediction system for generating noise abatement procedures. 25th AIAA/CEAS Aeroacoustics Conference, Delft, The Netherlands, https://doi.org/10.2514/6.2019-2617

Botre, M., Brentner, K.S., Horn, J.F., & Wachspress, D.A. (2019). Validation of helicopter noise prediction system with flight data. VFS 75th Annual Forum, Philadelphia, PA.

Outreach Efforts

N/A

Awards

None.

Student Involvement
Mrunali Botre, a graduate assistant currently working toward her PhD at Penn State, performed the acoustic predictions and assisted in developing and implementing the broadband noise reflection capability in PSU-WOPWOP.

Plans for Next Period
During the next period, helicopter models representing the aircraft in the 2019 FAA/NASA flight test will be developed from publicly available sources. Several of the noise abatement procedures executed during the flight test will be simulated with the noise prediction system. Based on both the noise predictions and measured data, the noise abatement procedures will be analyzed. The effectiveness of these procedures for the heavier helicopters in the 2019 test will be compared to that for the lighter helicopters in the 2017 test, which will indicate the feasibility of classifying helicopter noise based on the helicopter size, type, and weight.

Task 12 - Evaluate and Refine Noise Abatement Procedure Development Strategy
The Pennsylvania State University

Objective
The objective of this task is to assess the development of noise abatement procedures and the data needed for this activity.

Research Approach
For this effort, the noise prediction system developed in ASCENT Projects 6 and 38 will be used to perform noise predictions and to process the acoustic pressure data from the 2017 FAA/NASA noise abatement flight test. This comparison will have two primary goals: (a) to determine the importance of tracking the helicopter position and attitude in a precise manner, which will also provide guidance on the execution of noise abatement procedures, and (b) to evaluate and verify the effectiveness of noise abatement flight procedures by evaluating both flight test data and simulated noise for various maneuvers and a range of helicopter types. Incidentally, it will also be important to determine whether the limited helicopter information that is currently available (i.e., incomplete data complemented by engineering judgement) is sufficient for obtaining an agreement with flight test data and for developing noise abatement procedures.

Milestone(s)
The milestones for this task are (1) analysis and validation of the predicted noise through a comparison with flight test data with different precision levels for tracking the flight test aircraft state as a function of time and (2) comparison of complex procedures to determine whether a given procedure results in noise abatement.

Major Accomplishments
Noise predictions were made for comparison with the 2017 FAA/NASA noise abatement flight test. In the evaluation of flight test data, it was discovered that the simulation must include aircraft position and attitude deviations from the nominal flight path (which was used in the initial predictions). When the simulation matched the aircraft position and attitude, it provided reasonable results. However, the results were not perfect, and the errors associated with deviations in the flight path and time-dependent aircraft attitude were not quantified. Thus, it was determined that the position and state of the aircraft must match the flight test data as closely as possible to validate the predictions.

In this task, to determine the sensitivity of the noise predictions to relatively small changes in flight path and attitude, we developed an improved flight controller that incorporated more information and that more closely matched the flight test data for each aircraft. Figure 5 shows the position and attitude time history for the two controllers in comparison to the flight test data. The conditions for Figure 5 correspond to a steady level flight, and the nominal flight condition (steady flight path) is shown for the original controller (left column). The original controller allows the aircraft to drift in the y-direction by approximately 50 ft over the 60-s flight period. The original controller also encountered difficulty in following the roll of the flight test. In contrast, the improved flight controller can track the flight test aircraft position and attitude much more closely. The roll angle still exhibits a slight deviation (right column of Figure 5), but the angle is tracked reasonably well over time. Although this example corresponds to steady level flight conditions, similar improvements were observed for more complex maneuvers.

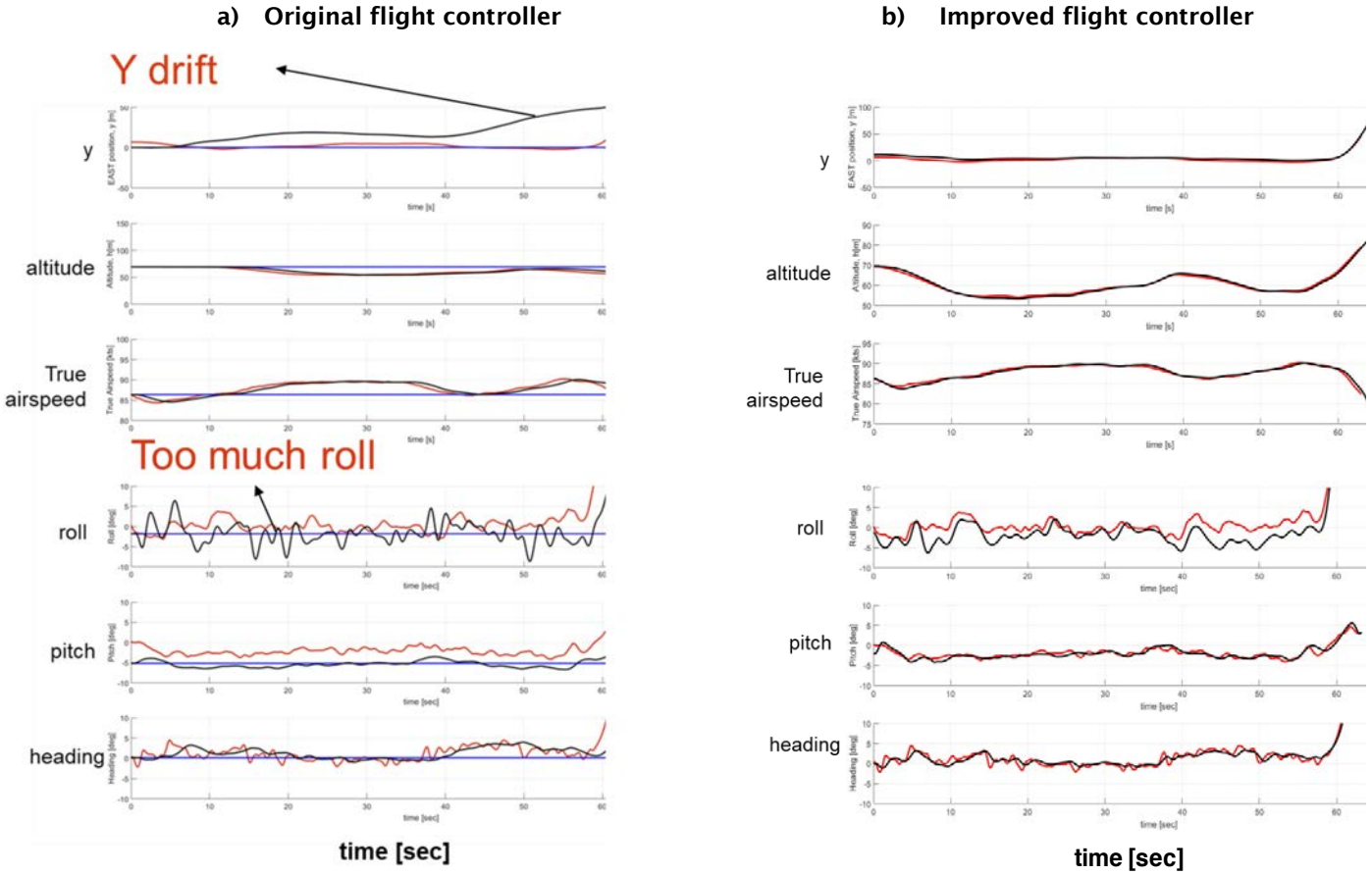

Figure 5. Comparison of flight trajectory and attitude between the original and improved flight controllers for the Robinson R44 under 80-kts steady level flight conditions. —— flight test; —— steady flight path; —— simulated flight trajectory.

To demonstrate the improved noise prediction attained by the new flight controller, results for a descending left turn are shown in Figure 6 for the Bell 407 aircraft. For this complicated maneuver, the results for the improved flight controller show better agreement with the flight test data. Although the SEL contours for the improved controller do not exhibit a perfect agreement, the increased noise that occurs as the helicopter leaves the turn (rolls back to level flight) is captured by the improved controller (see the higher SEL levels as the flight path leaves the contour grid in the right figures). There is some discrepancy (overprediction) as the aircraft enters the turn, but overall, the SEL contours are improved by using the new flight controller. These examples were chosen to demonstrate that relatively small changes in the flight path and, more importantly, in the time-dependent aircraft attitude can be influential in the noise validation and the development of noise abatement flight procedures. Numerous other examples are documented in Mrunali Botre's PhD dissertation.

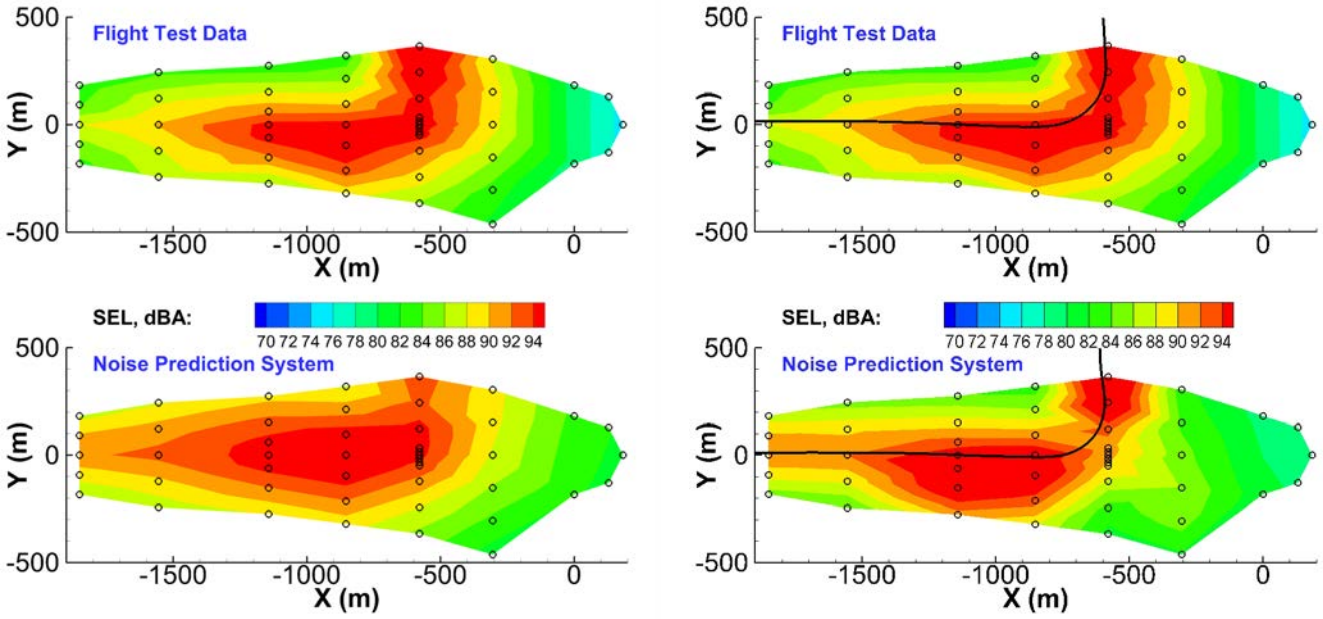

a) Original flight controller

b) Improved flight controller

Figure 6. Comparison of measured and predicted sound exposure level (SEL) contours from two flight controller models for a descending left turn of the Bell 407 aircraft. Top: flight test data; bottom: predicted SEL.

Publications

Published conference proceedings

Botre, M., Brentner, K.S., Horn, J.F., & Wachspress, D.A. (2019). Developing a comprehensive noise prediction system for generating noise abatement procedures. 25th AIAA/CEAS Aeroacoustics Conference, Delft, The Netherlands, https://doi.org/10.2514/6.2019-2617

Botre, M., Brentner, K.S., Horn, J.F., & Wachspress, D.A. (2019). Validation of helicopter noise prediction system with flight data. VFS 75th Annual Forum, Philadelphia, PA.

Outreach Efforts

N/A

Awards

None.

Student Involvement

Mrunali Botre, a graduate assistant currently working toward her PhD at Penn State, performed the acoustic predictions for this task. She also postprocessed the flight test data for the comparison.

Plans for Next Period

During the next period, we expect to begin working on the validation with and analysis of the 2019 FAA/NASA flight test data, which include results for four larger aircraft. This analysis will enable a comparison of noise abatement procedures for different "classes" of vehicles (different size and weight classes). The validation aspect of this task will compare various noise prediction models and their accuracy for the different sizes and weights included in the 2017 and 2019 flight tests. It is expected that some of the simpler models (i.e., Pegg's broadband noise model) may not perform as well for heavier, larger helicopters.

Task 13 - Demonstrate the Potential of Refined Noise Abatement Procedures

The Pennsylvania State University

Objective

The objective of this task is to demonstrate the potential of refined noise abatement procedures by simulating the flight procedures executed in the 2017 FAA/NASA acoustic flight test and ultimately comparing these procedures to new simulated procedures.

Research Approach

In this task, predictions of noise abatement procedures executed in the flight test will be simulated and compared to the optimal procedures developed under the new strategy. The process will be thoroughly documented (details are provided in Mrunali Botre's PhD dissertation, which is currently under review, and in the publication list for this task) and will provide the basis for future low-noise operational guideline development. Both linear flight profiles and turns will be considered, along with more complex procedures. These demonstrations will consider flight conditions both with and without BVI noise.

Milestone

The noise abatement flight procedures executed in the 2017 FAA/NASA flight tests will be compared to simulations, including future simulations of potentially improved noise abatement procedures. The first milestone will be a comparison between flight test data and the most refined predictions of simple and complex maneuvers for several aircraft.

Major Accomplishments

SEL noise contour predictions were made for five of the six aircraft in the 2017 flight test for linear (non-turning) flight procedures. Three of the six aircraft were simulated for level turns (Figure 7), decelerating turns (Figure 8), and descending turns (Figure 9). (Note: the most refined and updated figures, as of this report, are shown in this task.) The agreement was generally good, usually within 2 dBA. These conditions were analyzed in detail by examining the different noise components separately: thickness, loading, and broadband noise; main rotor and tail rotor noise (including the breakdown of noise components for each rotor). OASPL and L_A time histories were evaluated for several microphone locations. It was found that although the simulated SEL contours showed good agreement, discrepancies arose in the time history data. For example, the thickness noise was often overpredicted as the helicopter approached the observer, but this overprediction was still below the 10-dB down points included in the SEL calculation. Similarly, it was often found that the loading and broadband noise were overpredicted after the peak value in the time history. The main rotor is generally the dominant contributor to the OASPL, while the tail rotor is dominant in the L_A plots (as might be expected). Although there are only a limited number of flight procedures, many results were determined once the rotor noise components were analyzed separately. The details of these findings are documented in Mrunali Botre's PhD dissertation (currently under review).

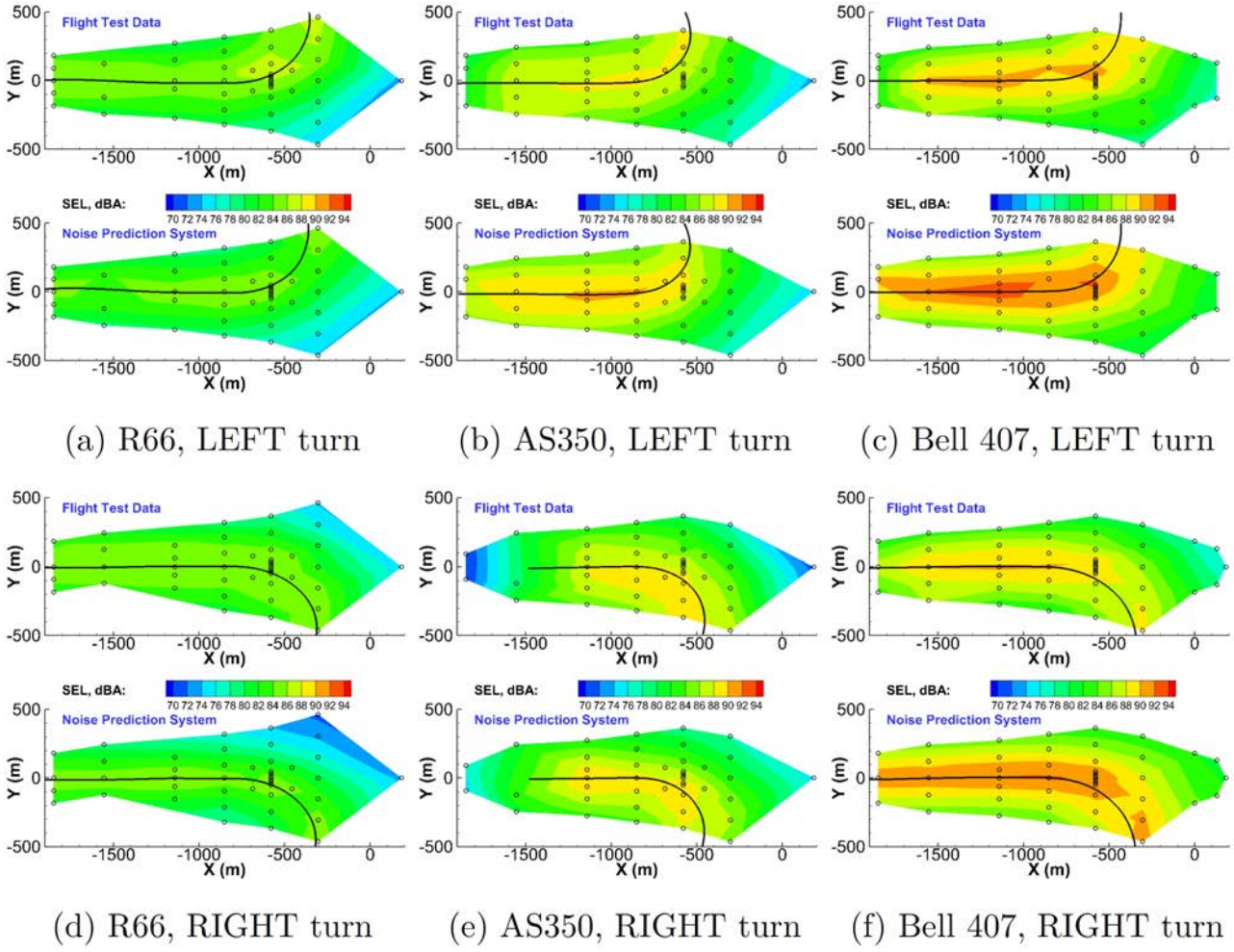

Figure 7. Total sound exposure level (SEL, dBA) for 80-kts level turns with a final roll angle of 25˚. For each subfigure, top: flight test data; bottom: prediction.

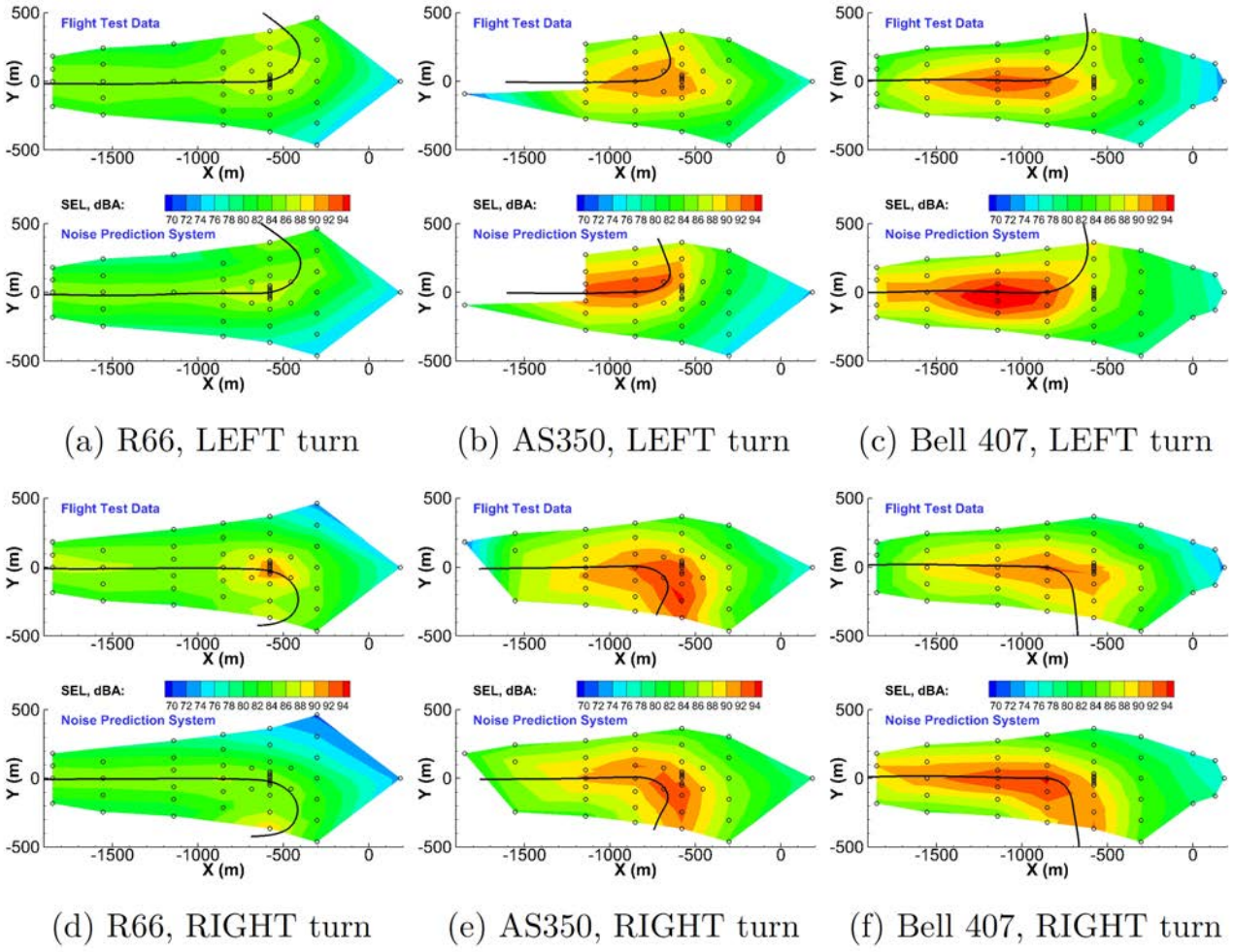

Figure 8. Total sound exposure level (SEL, dBA) for level decelerating turns, with a final roll angle of 35˚ and deceleration from 80 kts at 2 kts/s. For each subfigure, top: flight test data; bottom: prediction.

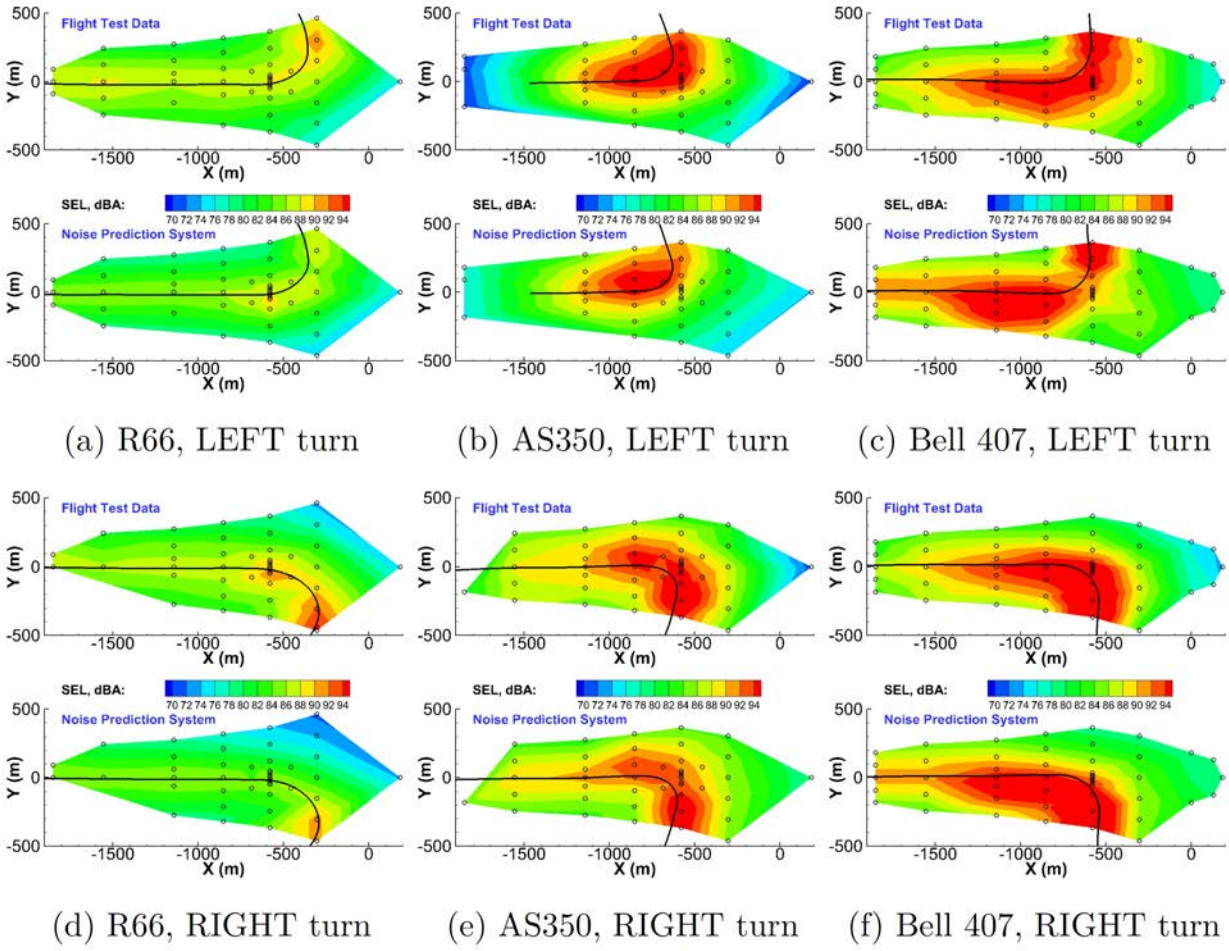

Figure 9. Total sound exposure level (SEL, dBA) for 80-kts descending turn with a flight path descent angle of 6˚ and a final roll angle of 35˚. For each subfigure, top: flight test data; bottom: prediction.

Publications

Published conference proceedings

Botre, M., Brentner, K.S., Horn, J.F., & Wachspress, D.A. (2019). Developing a comprehensive noise prediction system for generating noise abatement procedures. 25th AIAA/CEAS Aeroacoustics Conference, Delft, The Netherlands, https://doi.org/10.2514/6.2019-2617

Botre, M., Brentner, K.S., Horn, J.F., & Wachspress, D.A. (2019). Validation of helicopter noise prediction system with flight data. VFS 75th Annual Forum, Philadelphia, PA.

Outreach Efforts

N/A

Awards

None.

Student Involvement

Mrunali Botre, a graduate assistant currently working toward her PhD at Penn State, performed the acoustic predictions and worked with Volpe to provide the needed predictions and any explanations regarding the results.

Plans for Next Period

More attention will be given to the noise abatement procedures executed in the 2017 and 2019 flight tests. Evaluations of the procedures and the generated noise (compared to a baseline procedure) will be aided by the availability of noise components in the simulations. This step will provide information regarding which noise sources, rotors, and frequency ranges are important.

Project 039 Naphthalene Removal Assessment

Massachusetts Institute of Technology

Project Lead Investigator

Prof. Steven R. H. Barrett
Leonardo Associate Professor of Aeronautics and Astronautics
Department of Aeronautics and Astronautics
Massachusetts Institute of Technology
77 Massachusetts Avenue – Bldg. 33-316
Cambridge, MA 02139
(617)-452-2550
sbarrett@mit.edu

University Participants

Massachusetts Institute of Technology

- PI(s): Prof. Steven R. H. Barrett and Dr. Raymond Speth (Co-PI)
- FAA Award Number: 13-C-AJFE-MIT, Amendment Nos. 026, 034, 043, and 053
- Period of Performance: July 8, 2016 to August 31, 2020 (with the exception of funding and cost share information, this report covers the period from October 1, 2018 to September 30, 2019)
- Task(s):
    1. Explore relationship between polycyclic aromatic hydrocarbon (PAH) formation and aircraft particulate matter (PM) emissions
    2. Calculate air quality and climate impacts of naphthalene removal
    3. Conduct integrated cost-benefit analysis of impacts of naphthalene removal in the United States

Project Funding Level

The funding comprises $840,000 in FAA funding and $840,000 in matching funds. Sources of match are approximately $233,000 from Massachusetts Institute of Technology (MIT), plus third-party in-kind contributions of $361,000 from Oliver Wyman Group and $246,000 from Byogy Renewables, Inc.

Investigation Team

- Prof. Steven Barrett (MIT) serves as PI for the A39 project as head of the Laboratory for Aviation and the Environment. Prof. Barrett both coordinates internal research efforts and maintains communication among investigators in the various MIT research teams mentioned below.
- Dr. Raymond Speth (MIT) serves as co-PI for the A39 project. Dr. Speth directly advises students performing research in the Laboratory for Aviation and the Environment, with a focus on assessment of naphthalene removal refinery options; climate and air quality modeling; and fuel alteration life-cycle analysis. Dr. Speth also coordinates communication with FAA counterparts.
- Prof. William Green (MIT) serves as a co-investigator for the A39 project, as head of the Green Research Group. Prof. Green advises students on work in the Green Research Group focused on computer-aided chemical kinetic modeling of PAH formation.
- Mr. Randall Field (MIT) is the Executive Director of the MIT Energy Initiative and a co-investigator of the A39 project. Drawing upon his experiences as a business consulting director at Aspen Technology Inc., Mr. Randall provides mentorship to student researchers in the selection and assessment of naphthalene removal refining options and process engineering at large.
- Mr. Drew Weibel (MIT) is a graduate student researcher in the Laboratory for Aviation and the Environment. Mr. Weibel is responsible for conducting selection and assessment of naphthalene removal refining options; calculation of refinery process requirements and fuel composition effects from selected processes; estimation of

capital and operating costs of naphthalene removal processes; air quality and climate modeling; and integrated cost-benefit analysis.
- Mr. Lukas Brink (MIT) is a graduate student researcher in the Laboratory for Aviation and the Environment. Mr. Brink is responsible for the development of a combustor model quantifying the effect of naphthalene removal on soot emissions, the modeling of air quality and climate impacts, and integrated cost-benefit analysis.
- Mr. Max Liu (MIT) is a Ph.D. candidate in the Green Research Group. Mr. Liu is responsible for development and analysis of a chemical kinetic model of PAH formation with fuel-composition effects.
- Dr. Mica Smith (MIT) is a postdoctoral associate in the Green Research Group. Ms. Smith is responsible for the experimental measurements being used for the validation of the chemical kinetic mechanisms.
- Dr. Agnes Jocher (MIT) is a postdoctoral associate in the Green Research Group. Ms. Jocher is responsible for evaluating microphysical models that link the presence of PAH molecules to the formation of soot particles and for providing modeling expertise in combining these models with the kinetic models being developed.

Project Overview

Aircraft emissions impact the environment by perturbing the climate and reducing air quality, thus leading to adverse health impacts, including increased risk of premature mortality. As a result, understanding how different fuel components can influence pollutant emissions, as well as the resulting impacts and damage to human health and the environment, is important in guiding future research aims and policy. Recent emissions measurements have shown that removal of naphthalenes while keeping the total aromatic content unchanged can dramatically decrease emissions of particulate matter (Brem et al., 2015; Moore et al., 2015). The objective of this research is to determine the benefits, costs, and feasibility of removing naphthalenes from jet fuel, with regard to the refiner, the public, air quality, and the environment. Specific goals of this research include:

- Assessment and selection of candidate refining processes for the removal of naphthalenes from conventional jet fuel, including details of required technology, steady-state public cost, and changing life-cycle emissions impacts at the refinery
- Development of a chemical kinetics model to better understand the link between fuel aromatic composition and the resulting PM emissions due to jet fuel combustion
- Assessment of the climate and air quality impacts associated with naphthalene reduction and/or removal from jet fuel
- Development of a life-cycle analysis of the relative costs of removing naphthalene from jet fuel and the associated benefits due to avoided premature mortalities and climate damage for a range of possible scenarios

References

Brem, B.T., Durdina, L., Siegerist, F., Beyerle, P., Bruderer, K., Rindlisbacher, T., Rocci-Denis, S., Andac, M.G., Zelina, J., Penanhoat, O., & Wang, J. (2015). Effects of fuel aromatic content on nonvolatile particulate emissions of an in-production aircraft gas turbine. Environmental Science and Technology 49 13149–57

Moore, R.H., Shook, M., Beyersdorf, A., Corr, C., Herndon, S., Knighton, W.B., Miake-Lye, R., Thornhill, K.L., Winstead, E.L., Yu, Z., Ziemba, L.D. & Anderson, B.E. (2015). Influence of jet fuel composition on aircraft engine emissions: A synthesis of aerosol emissions data from the NASA APEX, AAFEX, and ACCESS missions. Energy Fuels 29 2591–600

Task 1 - Explore Relationship Between PAH Formation and Aircraft PM Emissions

Massachusetts Institute of Technology

Objective

The formation of black carbon (soot) from hydrocarbon fuels can be considered to take place in two stages. First, fuel components and combustion intermediates react and form PAHs. Large PAHs then act as soot nuclei, which grow as they absorb both PAH and other species, coagulate through collisions with other soot particles, carbonize, and partially oxidize (Richter & Howard, 2000). The details of the fuel composition mainly affect the first step of this process: the formation of PAHs. The objective of this task is to develop a combustor model that includes the formation of PAH species from different fuel components and the conversion of these PAH species to soot particles or non-volatile PM (nvPM) emissions, to enable evaluation of the sensitivity of soot emissions to fuel composition.

Research Approach

The Reaction Mechanism Generator (RMG) was used to develop a detailed chemical kinetic mechanism for jet fuel combustion that includes the formation of PAH (Gao et al., 2016). As part of this task, we have extended RMG to include recently discovered PAH growth pathways, such as the phenyl addition pathway, cyclization via carbenes, and an aromatic-catalyzed intramolecular H-transfer mechanism. We then used this improved version of RMG to generate a higher-fidelity chemical kinetic model for the formation of PAHs in naphthalene-containing flames. This approach is being utilized to produce a chemical kinetic mechanism describing the first stage of soot particle production.

These mechanisms are then utilized within Cantera (Goodwin et al., 2013), a combustion modeling framework. A combustor model, as schematically shown in Figure 1, is developed to evaluate emissions for varying fuel compositions and flight conditions. The model consists of two main parts: the primary zone and the secondary zone. In the primary zone, upstream air is mixed with fuel and reacts with a certain characteristic residence time. Then, in the secondary zone, the resulting air-fuel mixture is mixed with both secondary and dilution air.

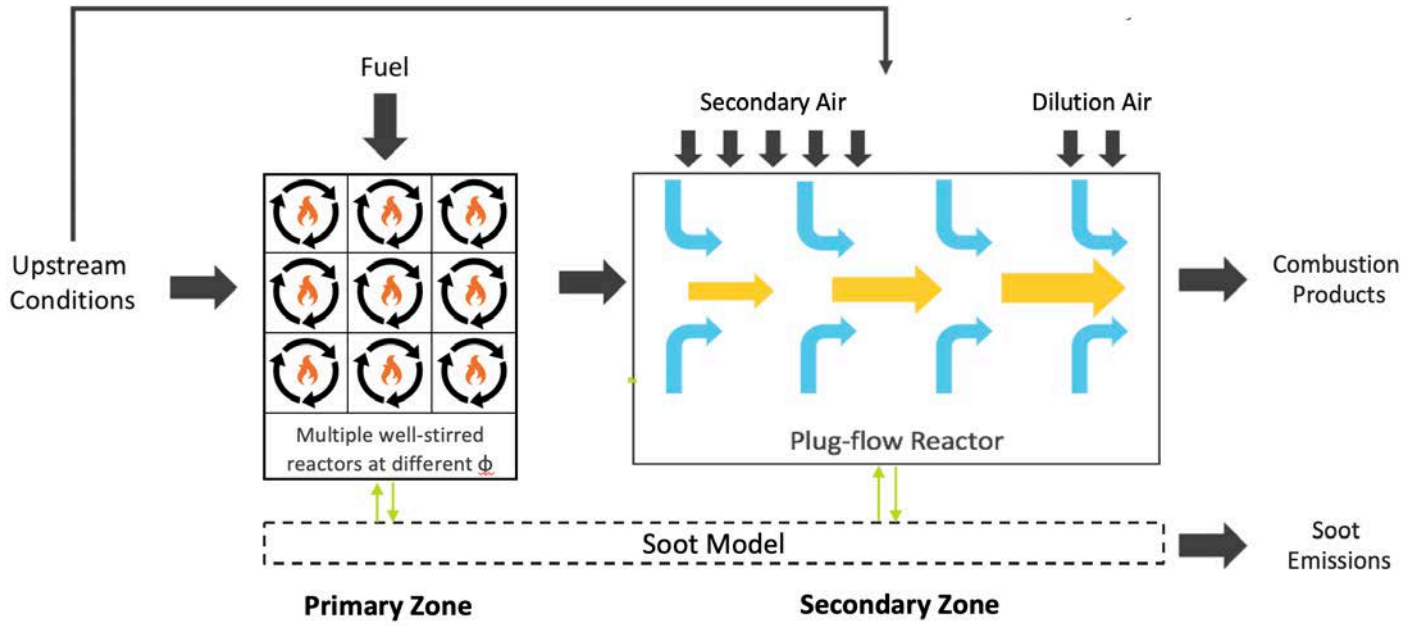

Figure 1. Schematic of the gas turbine combustor model including a soot model.

The primary zone consists of a set of *N* well-stirred reactors at different equivalence ratios, to account for mixture inhomogeneity. The secondary zone is modeled as a plug-flow reactor and is shown in more detail in Figure 2. After the flow exits the *N* primary zone reactors, it is mixed again and split into an outer and core part upon entering the secondary zone. This latter split is used to model the incomplete mixing that occurs in the second part of the combustor. The fraction of the air-fuel mixture that enters the secondary-zone core is a model variable, as are the location along the secondary zone where both streams become fully mixed and the pattern in which the mixing takes place. Other design variables in the secondary zone include the division between secondary and dilution air, the starting location of both, and the length over which they are injected.

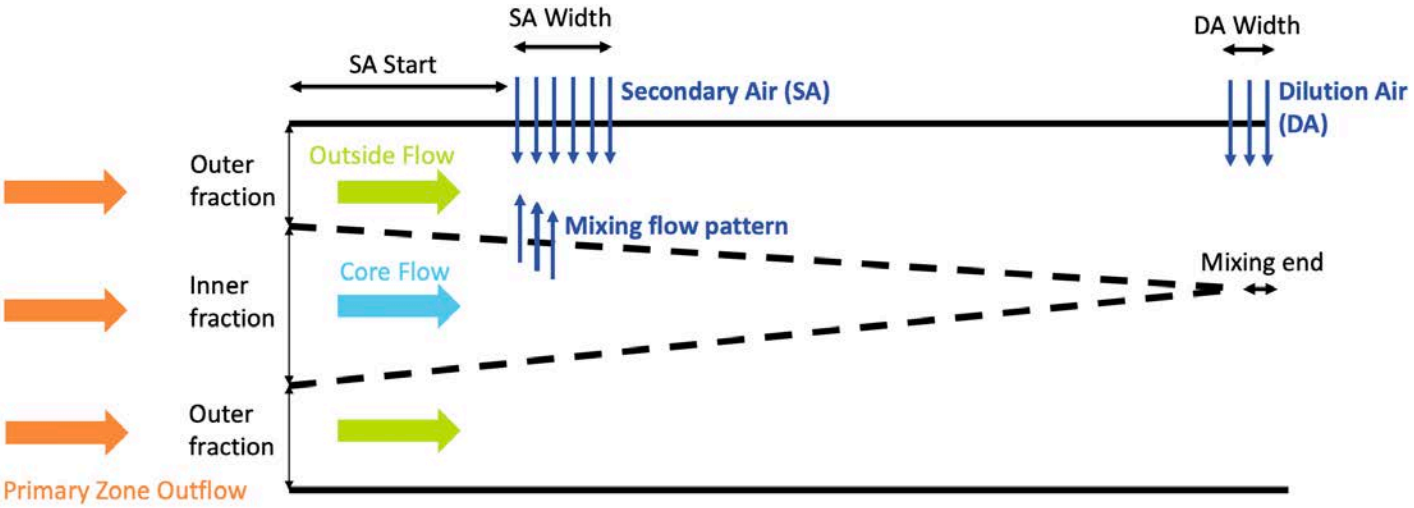

Figure 2. Overview of the combustor model secondary zone.

As shown in Figure 1, the primary and secondary zones are both coupled with a soot model. This soot model consists of four stages: nucleation (nuc), coagulation (coag), surface growth (sg), and oxidation (ox). For each of the four stages, multiple mechanisms from the literature are implemented, and the corresponding effects on the soot number (*N*) and mass (*M*) density are computed. Using multiple mechanisms provides confidence that the obtained results are robust even though the individual mechanisms from the literature may vary. This is especially important, because all mechanisms are simplifications of a complex problem, and caution is thus warranted when they are used outside the specific cases and conditions for which they were originally developed and tested.

Equation 1 shows the dependency of the number density on the four stages of the soot formation process. Because surface growth does not affect the total number of particles, no surface growth term is present.

$$\frac{dN}{dt} = \left(\frac{dN}{dt}\right)_{nuc} + \left(\frac{dN}{dt}\right)_{coag} + \left(\frac{dN}{dt}\right)_{ox} \tag{1}$$

The mass density development is shown in Equation 2. No coagulation term is present here because coagulation through collisions of soot particles is not expected to decrease the overall soot mass.

$$\frac{dM}{dt} = \left(\frac{dM}{dt}\right)_{nuc} + \left(\frac{dM}{dt}\right)_{sg} + \left(\frac{dM}{dt}\right)_{ox} \tag{2}$$

The implemented nucleation mechanisms can be divided into three categories, depending on the main precursor species used. The most extensive methods first model the dimer formation from PAH species and then use the dimer concentration to calculate the nucleation rates. The second set of methods directly considers the PAH species and their collision rates. Third, a set of methods is implemented by using the C_2H_2 concentration, which is assumed to be directly correlated with PAH concentrations (Schiener & Lindstedt, 2018).

For coagulation, two main mechanisms are considered. The first, from Kazakov and Frenklach (1998), splits coagulation into a pure coagulation part and an aggregation part, and considers collision frequencies in the free, transition, and continuum regimes. In the more straightforward second method, the coagulation rate is computed on the basis of a single collision frequency rather than multiple frequencies in different regimes (Wen et al., 2003).

Similarly to coagulation, the surface growth mechanisms can also be divided into two categories. The first category consists of methods modeling surface growth as being a first-order reaction with acetylene (C_2H_2) and being proportional to the total soot surface area. The second category combines surface growth and oxidation by using the Hydrogen Abstraction C_2H_2 Addition (HACA) mechanism (Frenklach & Wang, 1991). This mechanism considers six main reactions and uses them to compute the active radical carbon site number density, which then determines the soot surface growth and oxidation rates.

Beyond the HACA mechanism oxidation method, a second group of implemented oxidation methods directly considers the concentrations of O_2, OH, and O as well as the total soot surface area in computing the change in soot mass density. In order to calculate the effect of oxidation on the soot number density, a log-normal particle size distribution (Zhao et al., 2003) is assumed, relating the decrease in soot mass density to a decrease in soot number density.

The formation of soot adds extra complexity to the overall combustor model, because in addition to the previously existing gas phase, an additional solid (soot) phase is present. Because Cantera solely covers the former, the interactions between both phases must be accounted for manually. This process is shown in more detail in Figure 3. During nucleation and surface growth, carbon and hydrogen from the gas phase to the solid phase in the form of PAH species and C_2H_2. However, oxidation causes carbon and hydrogen to shift back from the solid phase to the gas phase in the form of CO_2, CO, and H.

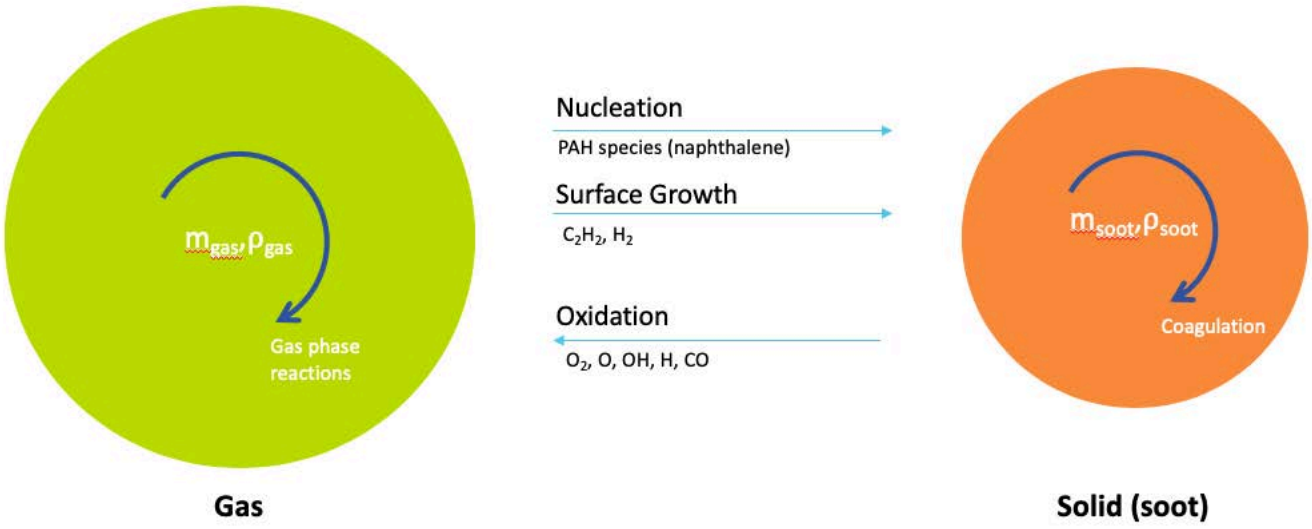

Figure 3. Interactions between the gas phase and the solid (soot) phase in the combustor model.

Emission data from the ICAO Aircraft Engine Emissions Databank (EASA, 2019) are used to optimize the primary and secondary zone design parameters to accurately match NO_x and CO emissions for take-off, climb, idle, and approach flight conditions. Sweeps using different combinations of soot mechanisms as well as fuel compositions are performed next to generate data on the sensitivity of soot emissions to varying naphthalene concentrations.

Milestone(s)

Both the primary and secondary zone of the combustor model were completed, and the different soot mechanisms were implemented.

Major Accomplishments

The chemical kinetic mechanism and combustor model were used to calculate formation rates of PAH species over a range of engine-relevant conditions. Figure 4 shows the evolution of several key aromatic species as the engine thrust setting is varied from near-idle to full power conditions for a representative surrogate fuel.

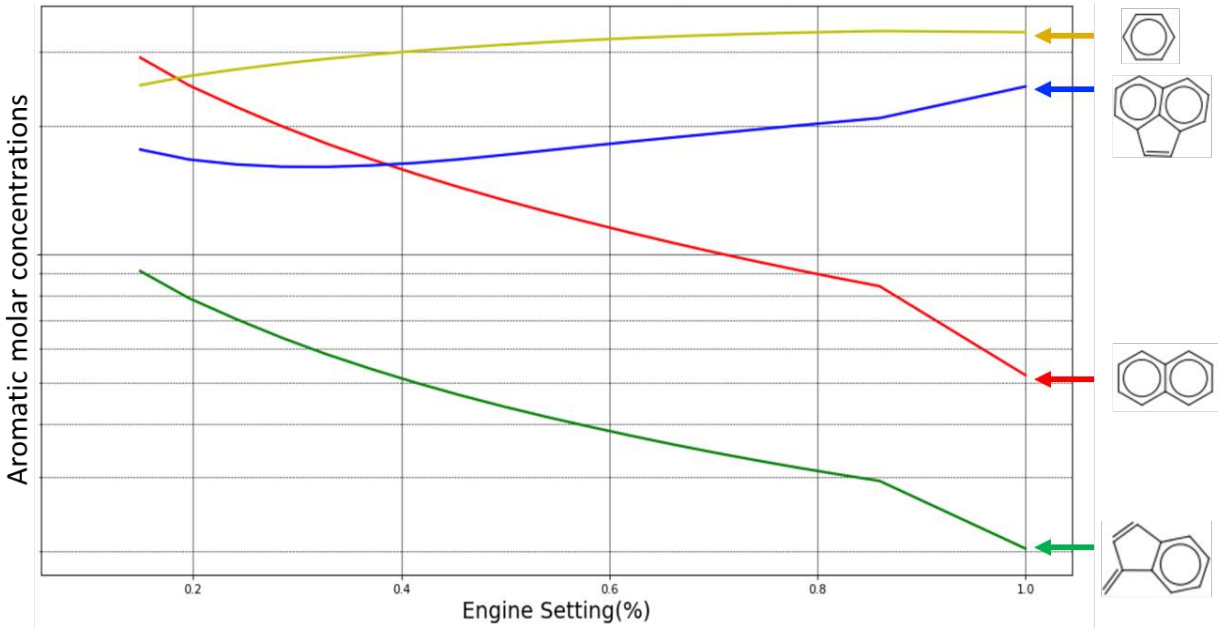

Figure 4. Evolution of selected aromatic species concentrations in the combustor primary zone as a function of engine setting.

Publications
N/A

Outreach Efforts
N/A

Awards
None.

Student Involvement
This task was conducted primarily by Drew Weibel and Lukas Brink, working directly with Prof. Steven Barrett and Dr. Raymond Speth. Mr. Weibel graduated with a Master of Science in 2018.

Plans for Next Period
The next step for this task is to optimize the primary and secondary zone design parameters to match emission data. After this optimization is performed, naphthalene concentrations in the fuel can be varied, and data from the various soot mechanisms on the effects of different fuel compositions on soot emissions will be collected.

References
EASA. (2019). ICAO Aircraft Engine Emissions Databank, version 26A. Online: https://www.easa.europa.eu/easa-and-you/environment/icao-aircraft-engine-emissions-databank

Frenklach, M. & Wang, H. (1991). Detailed modeling of soot particle nucleation and growth. Symposium (International) on Combustion, 23 1559–66

Gao, C.W., Allen, J.W., Green, W.H., & West, R.H. (2016). Reaction mechanism generator: Automatic construction of chemical kinetic mechanisms. Computer Physics Communications, 203 212–225

Goodwin, D.G., Moffat, H.K., & Speth, R.L. (2013). Cantera: An object-oriented software toolkit for chemical kinetics, thermodynamics, and transport processes. (http://www.cantera.org)

Kazakov, A. & Frenklach, M. (1998). Dynamic modeling of soot particle coagulation and aggregation: Implementation with the method of moments and application to high-pressure laminar premixed flames. Combustion and Flame, 114 484–501
Richter, H. & Howard, J.B. (2000). Formation of polycyclic aromatic hydrocarbons and their growth to soot—A review of chemical reaction pathways. Progress in Energy and Combustion Science 26 565–608
Schiener, M.A. & Lindstedt, R.P. (2018). Joint-scalar transported PDF modelling of soot in a turbulent non-premixed natural gas flame. Combustion Theory and Modelling 22 1134–75
Wen, Z., Yun, S., Thomson, M.J., & Lightstone, M.F. (2003). Modeling soot formation in turbulent kerosene/air jet diffusion flames. Combustion and Flame, 135 323–40
Zhao, B., Yang, Z., Johnston, M.V., Wang, H., Wexler, A.S., Balthasar, M., & Kraft, M. (2003). Measurement and numerical simulation of soot particle size distribution functions in a laminar premixed ethylene-oxygen-argon flame. Combustion and Flame, 133 173–88

Task 2 - Calculate Air Quality and Climate Impacts of Naphthalene Removal

Massachusetts Institute of Technology

Objective

The objective of this task is to calculate the air quality and climate impacts of a policy in which naphthalene is removed from jet fuel used in the United States.

Research Approach

The air quality effects of changes in aircraft PM emissions are evaluated by using the GEOS-Chem adjoint model, which we have previously used for assessing health impacts of emissions (Dedoussi & Barrett, 2014). The use of an adjoint model, which is a computationally efficient approach to calculating the sensitivity of an aggregate objective function (e.g., population exposure to $PM_{2.5}$), enables evaluation of a range of scenarios in a single run, thus allowing for incorporation of upstream uncertainty in the emissions indices for different species. The PM exposure calculated by using GEOS-Chem includes both the effects of changes in black carbon emissions and changes due to sulfur reductions that accompany the removal of naphthalenes (in the case in which hydrotreating is used to remove naphthalenes). The spatial pattern of emissions of nvPM, and sulfur compounds is taken from the 2015 inventory from the Aviation Environmental Design Tool (AEDT).

Climate impacts of naphthalene removal include contributions at both the fuel production and fuel consumption stages.

The additional refinery processing required to reduce or remove naphthalene requires process fuel, steam, electricity, and, in the case of hydrotreating, hydrogen production. The greenhouse gas (GHG) emissions associated with each of these processes increase life-cycle jet fuel GHG emissions. Using the results calculated as part of the refinery modeling work conducted in the previous project year, we found the GHG emissions associated with naphthalene removal to be 135 g CO_2e per kg fuel for hydrotreating and 144 g CO_2e per kg fuel for extractive distillation.

Consumption of reduced-naphthalene fuel decreases radiative forcing (RF) from aviation black carbon, and reductions in sulfur decrease the cooling effect of sulfates (Mahashabde et al., 2011). Contrail impacts are estimated according to studies on the impact of reducing the number of ice nuclei available for contrail formation. Caiazzo et al. (2017) have found that decreasing ice nuclei by 67% (an amount representative of a fully paraffinic biofuel) reduces contrail RF by <13%. Burkhardt et al. (2018) found that reducing ice nuclei by 50% reduces contrail RF by ~20%. Here, the reductions in contrail RF found in these studies are scaled by the estimated reduction in nvPM emissions from naphthalene removal.

The combined climate impacts of these effects are evaluated by using the APMT-Impacts Climate model, a policy-oriented rapid assessment tool that provides probabilistic estimates of climate impacts.

Milestone

The work completed for this task was presented in an Information Paper prepared for the CAEP/12-WG3/2 meeting and presented on October 7, 2019.

Major Accomplishments

On the basis of a literature review of nvPM emissions measurements from engines using fuels with varying levels of naphthalene (Brem et al., 2015; DeWitt et al., 2008), the potential range of reduction in nvPM emissions associated with 95% naphthalene removal was estimated to be 15–40%, or 5.0–12.5 mg nvPM per kg fuel. Monetized climate impacts for the different climate forcing pathways are summarized in Table 1, presented on a cents-per-gallon basis with both median values and a range indicating the 90% confidence interval. Monetized air quality impacts of naphthalene removal are similarly summarized in Table 2.

Table 1. Monetized climate benefits of naphthalene removal.

Impact Pathway	Impact (¢/gallon)
Black carbon radiative forcing (15% nvPM reduction)	0.09 (90% CI: 0.01 – 0.23)
Black carbon radiative forcing (40% nvPM reduction)	0.23 (90% CI: 0.04 – 0.61)
Contrail radiative forcing (15% nvPM reduction)	1.06 (90% CI: 0.30 – 2.59)
Contrail radiative forcing (40% nvPM reduction)	2.77 (90% CI: 0.77 – 6.89)
Hydrotreating CO_2 emissions	-1.82 (90% CI: -0.30 – -4.70)
Extractive distillation CO_2 emissions	-1.89 (90% CI: -0.31 – -5.01)
Sulfate aerosol (hydrotreating only)	-4.17 (90% CI: -0.61 – -11.23)

Table 2. Monetized air quality benefits of naphthalene removal.

Impact Pathway	Impact (¢/gallon)
nvPM emissions (15% nvPM reduction)	0.04 (90% CI: 0.02 – 0.06)
nvPM emissions (40% nvPM reduction)	0.11 (90% CI: 0.06 – 0.16)
Sulfur emissions (hydrotreating only)	1.92 (90% CI: 1.04 – 2.76)

Publications

N/A

Outreach Efforts

N/A

Awards

None.

Student Involvement

This task was conducted primarily by Drew Weibel, working directly with Prof. Steven Barrett and Dr. Raymond Speth.

Plans for Next Period

Additional work has been planned to estimate changes in contrail radiative forcing associated with the use of naphthalene-depleted fuels by using the Contrail Evolution and Radiation Model (Caiazzo et al., 2017). In addition, current air quality results are based on a regional atmospheric model, simulated at a resolution of 0.5° × 0.667°, whereas nvPM impacts have been shown to be underestimated with lower-resolution models (Punger & West, 2013). Additional work has been planned to provide better estimates of these impacts through higher-resolution local modeling approaches.

References

Brem, B.T., Durdina, L., Siegerist, F., Beyerle, P., Bruderer, K., Rindlisbacher, T., Rocci-Denis, S., Andac, M.G., Zelina, J., Penanhoat, O., & Wang, J. (2015). Effects of fuel aromatic content on nonvolatile particulate emissions of an in-production aircraft gas turbine. Environmental Science & Technology, 49 13149–57

Burkhardt, U., Bock, L., & Bier, A. (2018). Mitigating the contrail cirrus climate impact by reducing aircraft soot number emissions. Climate and Atmospheric Science, 1 37
Caiazzo, F., Agarwal, A., Speth, R.L., & Barrett, S.R.H. (2017). Impact of biofuels on contrail warming. Environ. Res. Lett., 12 114013
Dedoussi, I.C. & Barrett, S.R.H. (2014). Air pollution and early deaths in the United States. Part II: Attribution of PM2.5 exposure to emissions species, time, location and sector. Atmospheric Environment, 99 610-7
DeWitt, M.J., Corporan, E., Graham, J. & Minus, D. (2008). Effects of aromatic type and concentration in fischer-tropsch fuel on emissions production and material compatibility. Energy Fuels, 22 2411-8
Mahashabde, A., Wolfe, P., Ashok, A., Dorbian, C., He, Q., Fan, A., Lukachko, S., Mozdzanowska, A., Wollersheim, C., Barrett, S.R.H., Locke, M., & Waitz, I.A. (2011). Assessing the environmental impacts of aircraft noise and emissions. Progress in Aerospace Sciences, 47 15-52
Punger, E.M. & West, J.J. (2013). The effect of grid resolution on estimates of the burden of ozone and fine particulate matter on premature mortality in the USA. Air Quality, Atmosphere & Health, 6 563-73

Task 3 - Conduct Integrated Cost-Benefit Analysis of Impacts of Naphthalene Removal in the United States

Massachusetts Institute of Technology

Objective

The objective of this task is to produce an integrated cost-benefit analysis of naphthalene removal in the United States, accounting for the additional refining cost as well as the air quality and climate impacts.

Research Approach

The overall cost-benefit assessment of naphthalene removal includes fuel production costs, air quality benefits, and climate impacts from fuel production and fuel consumption. These effects are placed on a common monetized basis to compare different naphthalene removal scenarios. We consider uncertainties in the assessment of each component and use these uncertainties to compute the likelihood of a net benefit for different scenarios.

Milestone

The work completed for this task was presented in an Information Paper prepared for the CAEP/12-WG3/2 meeting and presented on October 7, 2019.

Major Accomplishments

The processing costs, air quality benefits, and climate impacts of naphthalene removal are converted to a common basis of cents per gallon, as presented in Table 3. The totals shown exclude contrail effects, which have not yet been quantified. In the absence of large impacts on contrail net radiative forcing, the current results suggest that the benefits of widespread naphthalene removal are outweighed by the costs of processing the fuel and the CO_2 emissions associated with that processing.

Table 3. Costs (positive) and benefits (negative) of naphthalene removal.

	Component	Hydrotreatment (¢/gallon)		Extractive Distillation (¢/gallon)	
Processing	Refinery	9.1	(8.7 – 9.5)	6.4	(6.1 – 6.8)
Air quality	nvPM	-0.1	(-0.02 – -0.16)	-0.1	(-0.02 – -0.16)
	Fuel sulfur	-1.9	(-1.0 – -2.7)	0	
Climate	nvPM	-0.2	(-0.02 – -0.6)	-0.2	(-0.02 – -0.6)
	Fuel sulfur	3.9	(0.6 – 10.5)	0	
	Contrails	-1.7	(-0.4 – -5.3)	-1.7	(-0.4 – -5.3)
	Refinery CO_2	1.8	(0.3 – 4.5)	1.8	(0.3 – 4.8)
Total		**10.9**	**(5.8 – 16.8)**	**6.3**	**(2.4 – 9.3)**

For both naphthalene removal processes, the climate impacts of the refinery CO_2 emissions exceed the air quality and climate benefits of naphthalene removal, neglecting the potential for significant contrail effects. In addition, in the case of hydrotreatment, the net present value of the climate warming associated with sulfur removal is greater than the NPV of the reduced air-quality-related damages. In addition to these environmental costs are the costs associated with processing jet fuel in the refinery. These results suggest that, in the absence of a strong contrail effect, naphthalene removal on a nationwide basis would unlikely to be cost beneficial. However, naphthalene removal may still be beneficial under certain circumstances, e.g., if applied to fuels used at airports with particular air quality concerns.

Publications
N/A

Outreach Efforts
The results of this work were presented to CAEP Working Group 3 at a meeting in Garching, Germany on October 7, 2019.

Awards
None.

Student Involvement
This task was conducted primarily by Drew Weibel, working directly with Prof. Steven Barrett and Dr. Raymond Speth. Mr. Weibel graduated with a Master of Science in 2018.

Plans for Next Period
Future work for this task consists of incorporating updated climate and air quality impacts, as well as evaluating scenarios in which naphthalene is removed only at certain places or times to maximize the benefit, e.g., targeting fuel used at specific airports.

Project 040 Quantifying Uncertainties in Predicting Aircraft Noise in Real-world Scenarios

The Pennsylvania State University
Purdue University

Project Lead Investigator

Victor W. Sparrow
Director and United Technologies Corporation Professor of Acoustics
Graduate Program in Acoustics
The Pennsylvania State University
201 Applied Science Bldg.
University Park, PA 16802
+1 (814) 865-6364
vws1@psu.edu

University Participants

Pennsylvania State University

- PI(s): Victor W. Sparrow, United Technologies Corporation Professor of Acoustics
- Co-PI: Philip J. Morris, Boeing/A.D. Welliver Professor of Aerospace Engineering
- FAA Award Number: 13-C-AJFE-PSU, Amendment 49
- Period of Performance: May 31, 2019 to October 31, 2020
- Task(s):
  1. Assess uncertainty in aircraft noise events, examining the BANOERAC and similar data sets
  2. Assess uncertainty in realistic noise source models in ANOPP

Purdue University

- PI(s): Kai Ming Li, Professor of Mechanical Engineering
- FAA Award Number: 13-C-AJFE-PU, Amendment 31
- Period of Performance: May 31, 2019 to May 31, 2020
- Task:
  3. Validate the noise model capabilities of the FAA Aviation Environmental Design Tool (AEDT) by comparing numerical results with field data and quantify uncertainties of both model prediction and measurement in trying to predict aircraft noise (or pattern of change) in the real world

Project Funding Level

FAA funding to Penn State in 2019–2020 is $170K. FAA funding to Purdue in 2019–2020 is $85K.

Airbus has committed in-kind cost share for both Penn State and Purdue regarding the SILENCE(R) data set, and this in-kind cost share is currently in process, awaiting a non-disclosure agreement. The point of contact for this cost sharing is Pierre Lempereur, pierre.lempereur@airbus.com.

Investigation Team

Pennsylvania State University

Victor W. Sparrow (PI), Task 1
Philip J. Morris (co-PI), Task 2
Graduate research assistant Harshal P. Patankar, Task 1

Purdue University
Kai Ming Li (PI), Task 3
Graduate research assistant Yiming Wang, Task 3

Special Acknowledgments

European Union Aviation Safety Agency
Illimar Bilas, Section Manager
Willem Franken
ANOTEC Engineering S.L.
Nico van Oosten

The BANOERAC (background noise level and noise levels from en route aircraft) data were provided to Penn State and Purdue by the European Union Aviation Safety Agency via a special licensing agreement, with the assistance of ANOTEC Engineering S.L. This in-kind data contribution is greatly appreciated.

Project Overview

The ASCENT R&D portfolio is designed to assist the Federal Aviation Authority (FAA) in meeting the overarching environmental performance goal for the Next Generation Transportation System (NextGen) to attain environmental protection that allows sustained aviation growth. This task is part of the aviation modeling and analysis task of the ASCENT R&D portfolio, with the goal to improve the accuracy of the FAA's environmental modeling tools. This project is providing data and methods to improve aircraft weight and take-off thrust modeling capabilities within the FAA Aviation Environmental Design Tool (AEDT). Furthermore, atmospheric conditions and ground properties have significant impacts on accurate predictions of aircraft noise. The accuracy of these inputs is critical for the predictions. The research performed by Penn State and Purdue through FAA ASCENT Center research grants has informed FAA regarding the limitations of existing noise tools and helped advance the state of the art in aircraft noise modeling. Appropriate models were developed and enhanced to account for the effects of meteorological conditions, atmospheric absorption, and the Doppler effect due to source motions on the propagation of aircraft noise. The purpose of this project is to understand and quantify uncertainty in the prediction of noise propagation of aircraft.

ASCENT Project 40 is developing numerical methods that could later be used in FAA tools to predict aircraft noise. The current proposal addresses an improved approach to extend the uncertainty quantification methods of Wilson et al. (2014) and other algorithms. Realistic aircraft trajectories and meteorology in the atmosphere are being used to predict aircraft flyover noise levels. The results will be compared with field data already acquired in DISCOVER-AQ Acoustics, the Vancouver Airport Authority, BANOERAC, and SILENCE(R) databases. In addition, uncertainties on geometric locations of source and receivers, effective surface impedance and ground topography, and source motion have been incorporated in this year of effort.

If successful, the outcomes of ASCENT Project 40 will lead to the development of improved methodologies that could be implemented in FAA tools to predict aircraft noise in the presence of real-world weather. By having faster predictions and predictions verified with field data, the project will help to improve confidence when making decisions regarding aircraft noise, such as choosing sites for new runways and implementing new landing approach and take-off patterns over populated areas. The project team has identified key drivers for quantifying uncertainties in predicting aircraft noise. To assess these uncertainties, an integrated approach will be used to understand uncertainties in (a) the aircraft state and resulting noise levels and directivity (source); (b) the atmospheric and meteorological conditions (propagation); and (c) the ground impedance and terrain model (receiver). This integrated approach will include all predominant uncertainties between the source and receiver. One of the main motivations of the current project is to guide these recent advancements to reach a research readiness level that leads to possible implementation in AEDT in the future.

This research will enhance the accuracy of AEDT through improved aircraft noise propagation modeling. This improvement is needed to support the evaluation and development of aircraft flight routes and procedures that could reduce community noise. These improvements will also facilitate the implementation of NextGen by improved characterization of the efficiency benefits it would deliver. If this research is not performed, the accuracy of the noise prediction tool may not be representative of real-world operations and would thus affect studies used by airport authorities.

Also, in 2019, a collaborative initiative with National Aviation University of Ukraine was continued and close cooperation with Georgia Tech on ASCENT Project 43 was initiated.

Task 1 - Assess Uncertainty in Aircraft Noise Events, Examining the BANOERAC and Similar Data Sets

Pennsylvania State University

Task 2 - Assess Uncertainty in Realistic Noise Source Models in ANOPP

Pennsylvania State University

Objectives

The research will (1) review and analyze available field measurement data for patterns that are influenced by the (change of) meteorological conditions; (2) identify sets of field data for specific scenarios that contain proper parameters/quality input values to validate the enhanced modeling capabilities; (3) use the enhanced modeling capabilities to understand the patterns identified in the field measurement data that are influenced by the (change of) meteorological conditions and (4) quantify uncertainties in predicting aircraft noise in real-world situations.

Research Approach

Overview of the BANOERAC data

BANOERAC was a project initiated by the European Union Aviation Safety Agency in 2009 (ANOTEC Consulting S.L., 2009). The project had two main goals, the first of which was to prepare maps for Europe showing background noise levels. The calculation method relied on the population density to determine background noise levels, based on earlier work by Stiftelsen for industriell og teknisk forskning (SINTEF; Trondheim, Norway). The measurements of background noise and en route aircraft noise were conducted in Spain (see Figure 1). The first part of the BANOERAC study focused on correcting the SINTEF model for extremely low population density areas by taking background noise measurements (this is not the focus of the analysis presented here). The second part of the study involved measurements of en route aircraft noise, which were conducted from February to July 2009 (covering both winter and summer seasons). Data collection was spread over 20 days in the six-month period. The measured data included time histories of aircraft tracking data and noise measurement data (third-octave levels) from two microphones (one placed 1.2 m above the ground, the second inverted and placed on a flat plate on the ground). The locations of the noise monitors can be seen in Figure 1. Meteorological data from a ground meteorological station (time synchronized with the noise monitors) and seven distant sounding stations (seven Spanish airports shown by blue circles in Figure 1) are also provided.

Limitations of the available meteorological data

The data from the ground meteorological system (placed on a 1.8-m-high mast at the noise measurement site) consist of temperature, relative humidity, wind speed, wind direction, and atmospheric pressure. Although the data are synchronized in time with noise measurement data, they provide information at only one physical location (i.e., not along a vertical profile).

The data from the seven meteorological sounding stations do provide vertical profiles of the meteorological variable but the data are available for every 12 hr (and not synchronized with the noise events). In addition, the sounding stations are far away from the noise measurement sites, making the former unusable for inclusion in the acoustic propagation calculations.

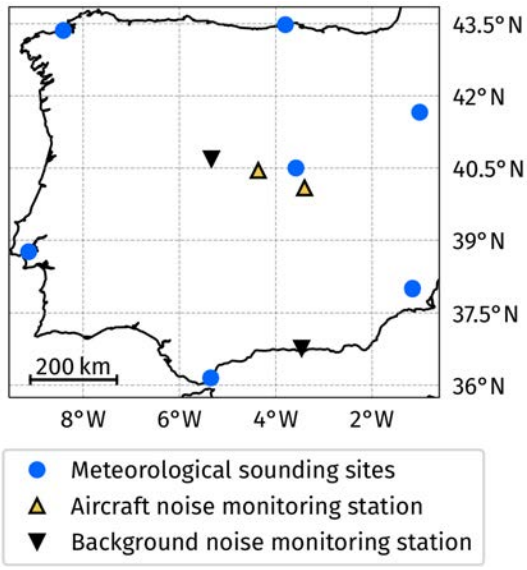

Figure 1. Map of Spain showing locations of measurement sites.

A brief overview of the data handling process

In total, the dataset included 1,056 aircraft events. Events that were reported to be contaminated (by noise from helicopters, general aviation, motorized vehicles, wind, birds, and other natural sources) were removed, and only events that had audible commercial aircraft noise were selected. This reduced the number of events to 537. To this point, only the information reported in the BANOERAC report (ANOTEC Consulting S.L., 2009) was utilized for the data filtering process. All data from the 537 events were visualized to inspect the quality, the results of which are summarized in Table 1. The aim of this exercise was to understand the fleet mix of the usable data. Table 1 shows that the types of aircraft commonly found in U.S. airports are well represented. As can be seen in the last row, of 537 events that were considered uncontaminated (i.e., that only included noise from commercial aircrafts), only 68 events were useful for validating existing noise modeling capabilities.

Table 1. Number of aircraft events not contaminated by nonaircraft noise sources according to the BANOERAC report (shown in black) and number of aircraft events possibly useful for validation (based on a preliminary visual inspection performed by Penn State and subject to change) (shown in blue).

Aircraft class	Aircraft model	Cruise	Descent	Climb	Total
Business jet	Beech 390	0 (0)	1 (0)	0 (0)	1 (0)
Long-range quad	747-400	2 (0)	1 (1)	0 (0)	3 (1)
	A-340-300	0 (0)	6 (1)	27 (7)	33 (8)
	A-340-500	2 (0)	0 (0)	0 (0)	2 (0)
	A-340-600	0 (0)	5 (1)	8 (1)	13 (2)
Long-range twin	757-200	7 (1)	4 (1)	0 (0)	11 (2)
	757-300	2 (0)	0 (0)	0 (0)	2 (0)
	767-200	0 (0)	2 (1)	0 (0)	2 (1)
	767-300	1 (0)	1 (1)	0 (0)	2 (1)
	767-400	0 (0)	1 (1)	0 (0)	1 (1)
	777-200	1 (0)	8 (3)	0 (0)	9 (3)
	A-330-200	2 (1)	10 (3)	3 (1)	15 (5)
	A-330-300	9 (2)	1 (0)	1 (0)	11 (2)
	A300F4 BELUGA	0 (0)	1 (1)	0 (0)	1 (1)
Medium-range (Gen 2)	737-300	19 (1)	0 (0)	0 (0)	19 (1)
	737-400	4 (0)	1 (0)	0 (0)	5 (0)
	737-700	30 (3)	1 (0)	0 (0)	31 (3)
	737-800	68 (7)	15 (3)	11 (4)	94 (14)
	A-318	4 (0)	0 (0)	0 (0)	4 (0)
	A-319	54 (4)	15 (2)	22 (0)	91 (6)
	A-320	57 (4)	38 (5)	40 (5)	135 (14)
	A-321	27 (1)	10 (1)	7 (1)	44 (3)
Regional jet (Gen 1)	F100	6 (0)	0 (0)	2 (0)	8 (0)
Total events		**295 (24)**	**121 (25)**	**121 (19)**	**537 (68)**

Visualization of a candidate event

After carefully reviewing the 68 selected events, we chose one event that had the least amount of nonaircraft noise for the preliminary investigation. The data for this event were recorded on the morning of March 10, 2009, and involved a Boeing 757-200 aircraft. The aircraft trajectory (Figure 2), the altitude time history (solid black line in Figure 4), and the noise monitor location were used to calculate the distance between the aircraft and the noise monitor (dashed blue line in Figure 4). Figure 3 shows the time history of third-octave band sound pressure levels (SPL) visualized with a colormap and the overall SPL (OASPL) with red lines. The BANOERAC project report mentions instances of contamination of noise data by insect noise (above 1 kHz). Hence, the OASPL is shown for 25 to 1000 Hz (dotted red line in Figure 3) and 25 to 4000 Hz (solid red line in Figure 3). For the event under consideration, there was virtually no difference between the two lines, implying that the dominant part of the sound energy is in frequency bands below the 1000-Hz third-octave band. Interference patterns (because of direct and ground-reflected sound energy) show up in the data measured by the microphone placed 1.2 m above the ground. Figure 5 shows the time history of the aircraft ground speed (aircraft slowing by about 190 km/hr) and a constant heading angle (which can be corroborated with the aircraft trajectory shown in Figure 2).

Next, the time history of the distance between the aircraft and the noise monitor was combined with the time history of third-octave SPLs, and the results are shown in Figure 6 (SPL vs. distance). For the 25- to 1600-Hz third-octave bands, the SPLs were lower when the aircraft was approaching the noise monitor than when it was going away from the noise monitor (for the same distance). For this event, the maximum geometric distance was about 12 km and the duration of the event was less than 90 s. This implies that changes in meteorological conditions (over the distance and duration involved) probably play an insignificant role when explaining the difference in levels for the same geometric distance. The two likely explanations are convective amplification and aircraft noise directivity.

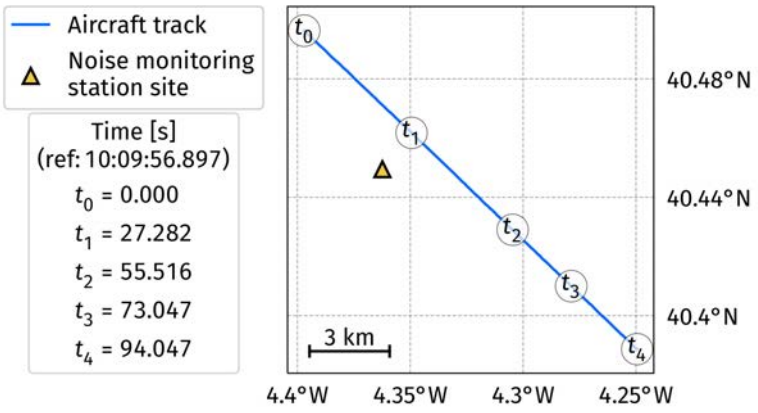

Figure 2. Time history of the aircraft trajectory.

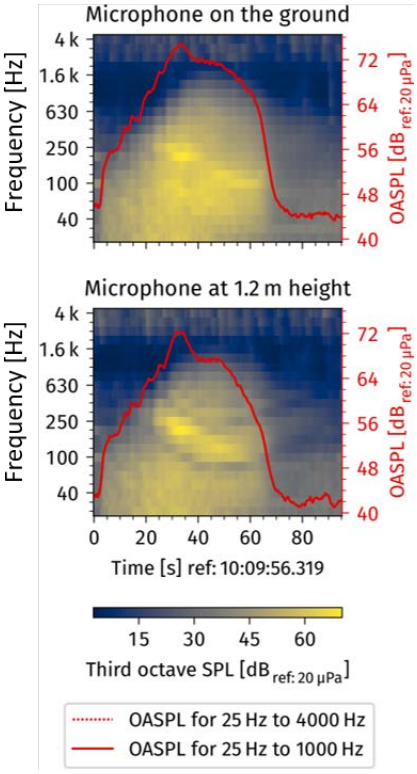

Figure 3. Time history of third-octave SPLs and OASPL for microphone on the ground and microphone at 1.2 m height.

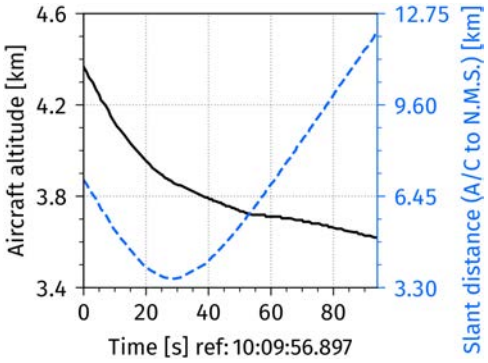

Figure 4. Time history of aircraft altitude and the slant distance between the aircraft (A/C) and the noise monitoring station (N.M.S.).

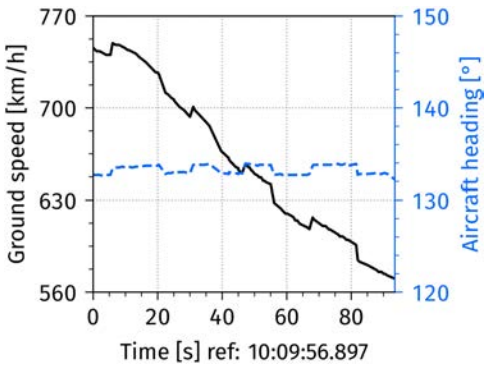

Figure 5. Time history of aircraft ground speed and aircraft heading angle.

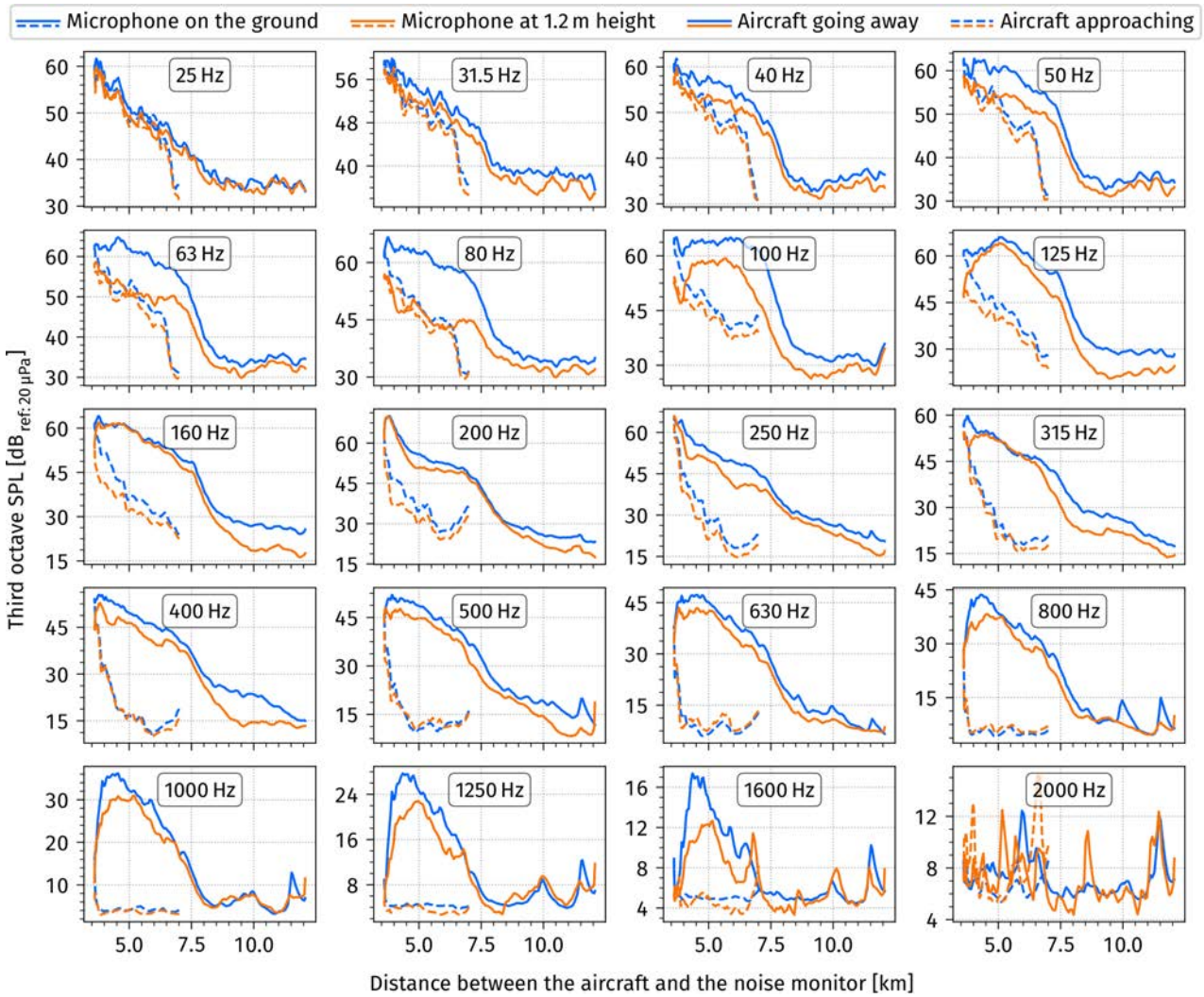

Figure 6. Dependence of the third-octave SPL on the distance between the aircraft and the noise monitor.

Convective amplification

For a moving source, the effect of convection on the received SPL depends on the Mach number, M, and the emission angle (as shown in Figure 7). This effect can be calculated using Equation (40.1), where $n = 1$ for a monopole or dipole source and $n = 2$ for a quadrupole source (Ruijgrok, 1994). In general, aircraft noise can be represented using multipole expansion (i.e., as a combination of a monopole, a dipole, a quadrupole, and higher-order sources). For now, we will treat the aircraft as a monopole source.

$$\text{Convective amplification} = -20(n+1)\log\left(1 - M\cos\theta_{\text{emission}}\right) \tag{40.1}$$

The Mach number needs to be calculated using the airspeed of the aircraft, but the available data are only for ground speed. The flight altitude for the event under consideration was about 4 km, where typical wind velocity could be as high as 100 km/hr. Because wind speed and wind direction information were not available, we considered three scenarios (i.e., no wind, aircraft flying downwind, and aircraft flying upwind) to assess the effect of wind on convective amplification. The results are shown in Figure 8. As can be seen, if wind speed and direction are not known, then the uncertainty in predicting convective amplification can be as high as 6 dB.

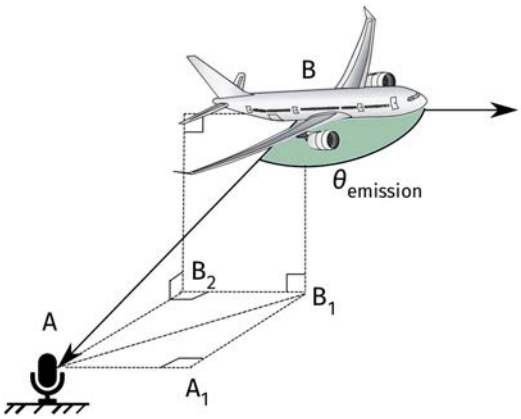

Figure 7. A schematic showing the emission angle and its relation to the aircraft and the receiver location.

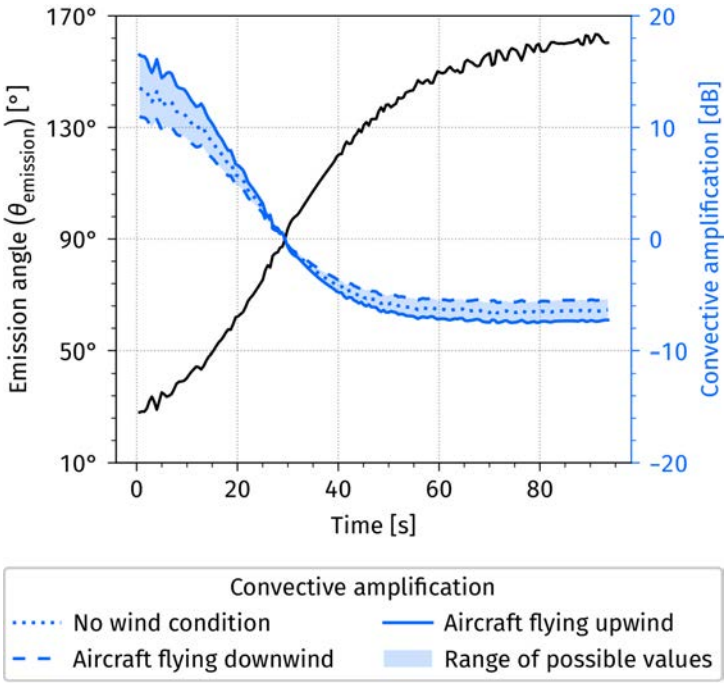

Figure 8. Time history of the emission angle and convective amplification for three wind conditions.

Aircraft directivity

The main sources of aircraft noise are jet noise, fan and turbine noise, combustion chamber noise, and airframe noise (Zaporozhets et al., 2011). The overall directivity of aircraft noise depends on the relative strengths and directivities of each of these sources (which, in turn, can be functions of aircraft configuration, aircraft state, and engine power). For the event under consideration, as a first attempt at including aircraft directivity, we assumed that jet noise would be the dominant source; hence, the overall noise directivity would closely resemble jet noise directivity. The polar directivity pattern shown in Figure 10 was assumed to represent the overall aircraft noise directivity (ANOPP documentation, NASA).

For the event under consideration, the time history of the polar angle was calculated using the geometry shown in Figure 9.

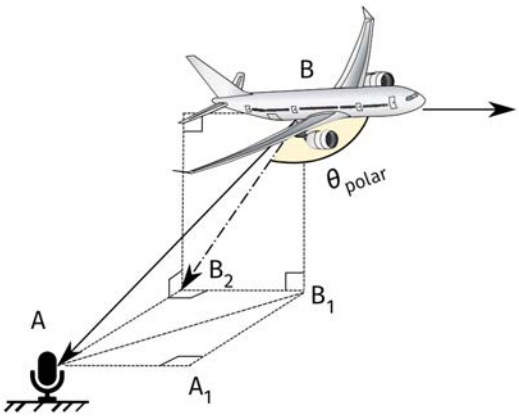

Figure 9. A schematic showing the polar angle and its relation to the aircraft and the receiver location.

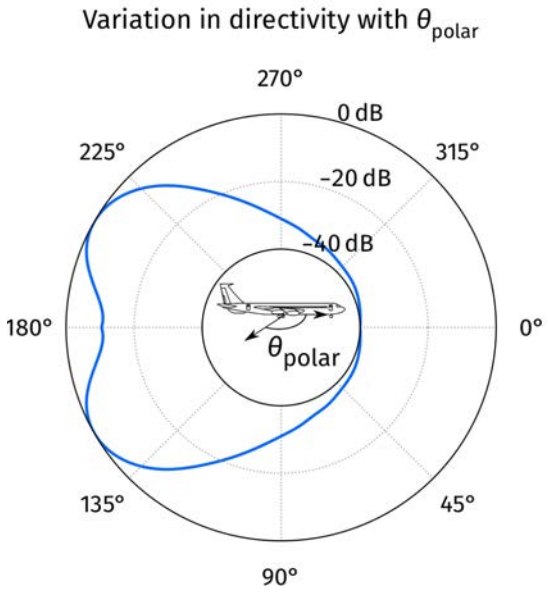

Figure 10. A typical directivity pattern associated with jet noise.

Results and discussion

In our first attempt at comparing measured data (Figure 6) with predictions, the 500-Hz third-octave band was chosen as a representative case. To calculate the acoustic absorption for the 500-Hz third-octave band (using ISO 9613-1and SAE-ARP-5534), we assumed a temperature of 13 ˚C and relative humidity of 30% (these values are based on data measured at the ground meteorological station). Figure 11 shows the predicted normalized SPL and the three contributing factors: acoustic propagation and absorption, convective amplification, and jet noise directivity. The dashed and solid lines in Figure 11 correspond to the duration of the event when the aircraft is approaching and going away from the noise monitor, respectively. The effect of acoustic propagation in both cases is the same for the same distance (irrespective of whether the aircraft is approaching or going away). Convective amplification and jet noise directivity appear to be competing factors; that is, convective amplification results in higher levels when the aircraft is approaching the noise monitor and the contribution from jet noise directivity is lower for that part of the event (and vice versa when the aircraft is going away from the noise monitor). It is evident that the combined effect of the three factors results in qualitative agreement with the measured data (Figure 6).

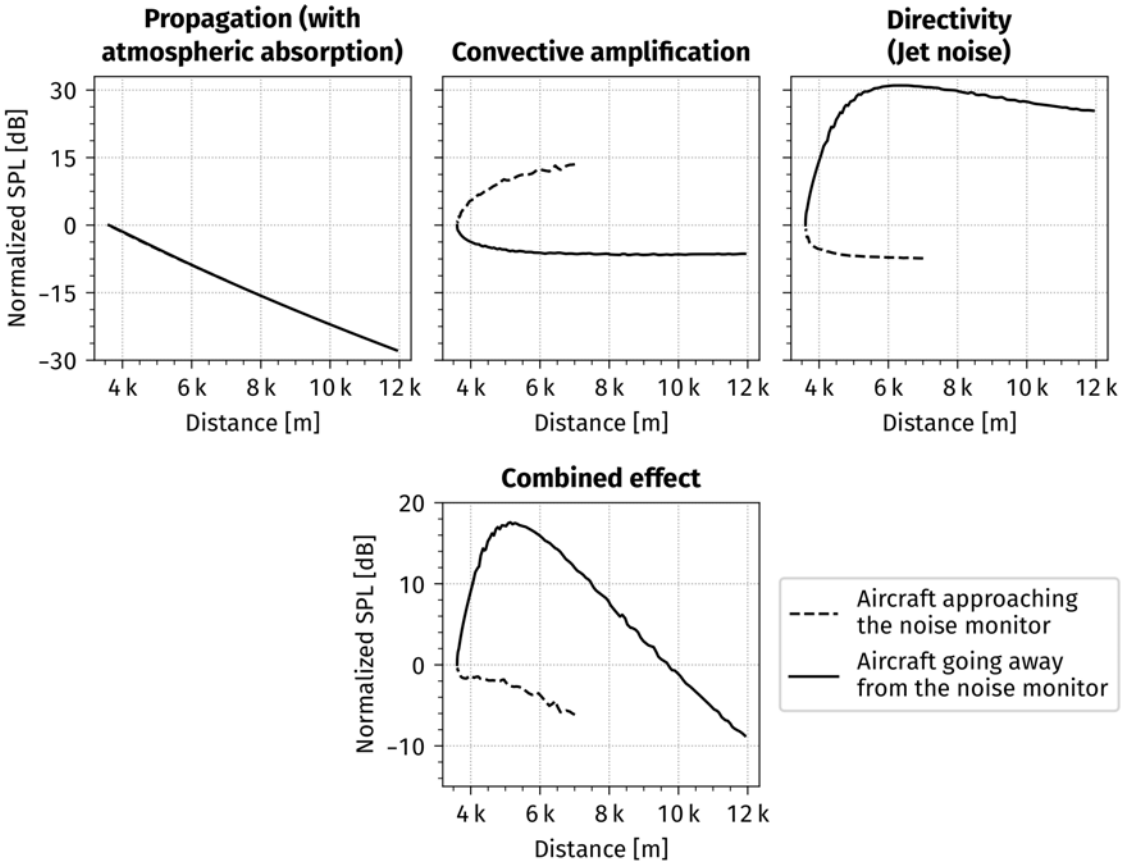

Figure 11. Normalized SPL as a combination of acoustic propagation, convective amplification, and jet noise directivity.

Based on the preliminary analysis shown in this work, the following conclusions can be drawn:

1. To accurately predict aircraft noise, it is necessary to account for both convective amplification and aircraft directivity.
2. Source levels and directivity as a function of frequency are needed to explain the details of the received noise levels across all third-octave bands of interest.
3. Detailed information about aircraft state is required to predict the absolute source levels and the overall directivity.
4. Vertical profiles of meteorological variables are needed to correctly predict acoustic propagation and absorption effects.

Initial efforts on Aircraft Noise Prediction Program (ANOPP) prediction for source models

Preliminary noise propagation predictions have shown the importance of using a realistic noise source directivity when interpreting the ground-based measurements. To provide such a noise source description, the NASA Aircraft Noise Prediction Program (ANOPP2) is being used. Selected information from the BANOERAC dataset is being used to identify the aircraft and engine type and the flight conditions. An example is shown in Table 2. In this case, the aircraft is descending. Based on the aircraft location and the rate of descent, a reasonable estimate can be made of the aircraft's destination, flap settings, and weight (information that is not included in the dataset). The information in the table was provided to colleagues at Georgia Tech, who provided an initial input script for ANOPP2. This script enables the aircraft noise source to be characterized and the information is provided to the propagation prediction team. The basic script is also used to make noise predictions at the observer location for comparison with those determined when a realistic atmosphere is included. In addition, the variation in the noise source calculation caused by changes to the assumed aircraft state can be quantified.

Table 2. Example flight information from BANOERAC dataset.

Event type	Descent
Aircraft model	Boeing 737-800
Engine model	(2x) CFMI CFM56-7B26
Mean ground speed (ft/s)	562.1
Mean rate of descent (ft/s)	26.3
Mean altitude (ft)	17,448
Weight at event time (lbs)	139,205

Milestone(s)

The raw data from the BANOERAC dataset has been parsed and visualized to identify aircraft noise events that might be useful to validate existing noise modeling capabilities. Preliminary analysis of a candidate event has been completed to guide future efforts.

Major Accomplishments

For accurate aircraft noise predictions, we have demonstrated the importance of high-speed source motion (convective amplification) and source directivity. Qualitative agreement has been achieved between predicted and measured aircraft noise from a real-world database.

Publications

N/A

Outreach Efforts

N/A

Awards

None.

Student Involvement

Graduate research assistant Harshal P. Patankar has been the primary person working on this task. An undergraduate student, Stephen Willoughby, has also been contributing. Neither student has graduated at this time.

Plans for Next Period

1. Penn State plans to look closely at the effects of aircraft state (to predict source levels and directivity) and propagation on the received noise levels.
2. Penn State previously showed that the overall approach of Wilson et al. (2014) could be adapted to the aircraft noise prediction problem (Patankar & Sparrow, 2018; Patankar & Sparrow, 2019). This approach will be extended by using a 2-dimensional ray tracing model to comment on the uncertainty in predictions caused by the lack of or insufficient meteorological conditions.

References

Lopes, L.V. & Burley, C.L. (2016). ANOPP2 User's Manual documentation, NASA/TM-2016-219342.

ANOTEC Consulting S. L. (2009). BANOERAC Project final report, Document ID PA074-5-0.

Aspuuru, I. & van Oosten, N. (2009). ANOTEC Consulting S. L. Delivery of flight trajectory data of BANOERAC project (Document Number: PAT001-1)

Patankar, H. & Sparrow, V. (2018). Quantifying the effect of uncertainty in meteorological conditions on aircraft noise propagation. Proc. of Internoise, Chicago, IL

Patankar, H. & Sparrow, V. (2019). Effect of uncertainty in meteorological conditions on aircraft noise levels. Journal of the Acoustical Society of America 145(3, Pt. 2): 1885

Ruijgrok, G.J. J. (2007). Elements of aviation acoustics, 2nd Ed. VSSD, Delft, The Netherlands.

Wilson, D.K., Pettit C.L., Ostashev, V. & Vecherin, S. (2014). Description and quantification of uncertainty in outdoor sound propagation calculations. Journal of the Acoustical Society of America 136(3): 1013-1028
Zaporozhets, O., Tokarev, V., & Attenborough, K. (2011). Aircraft noise: Assessment, prediction, and control, Spon Press.

Task 3 - Validate the Noise Model Capabilities of AEDT by Comparing Numerical Results with Field Data and Quantify Uncertainties of Both Model Prediction and Measurement in Trying to Predict Aircraft Noise (or Pattern of Change) in the Real World

Objectives

To assess the uncertainties in aircraft noise prediction, an integrated approach will be used to understand uncertainties in the aircraft state and resulting noise levels due to source motion (source), the atmospheric and meteorological conditions (propagation), and ground impedance and the terrain model (receiver). This approach will include all predominant uncertainties between the source and receiver.

Research Approach

Background

The Purdue research team has been working extensively on the DISCOVER-AQ dataset in the past two years. The full details of the scope of the DISCOVER-AQ acoustic research effort and its measured results can be found in Boeker et al. (2015). In summary, NASA conducted a series of acoustic measurements near Houston, Texas, in September 2013. The aim of these acoustic measurements was to measure in situ acoustic level data from two aircraft operating with controlled flight paths, in which the corresponding acoustic, meteorological, aircraft position, and performance data were recorded. This combined dataset was designed to provide a comprehensive validation of various modeling of noise levels from a flyover aircraft. The receivers were located in areas with relatively low ambient noise levels and minimal outside transportation noise sources and at a variety of distances and elevation angles from the nominal aircraft flight paths.

After an initial study, the Purdue team identified that the maneuvers of the Lockheed P-3B Orion (see Figure 12) contained the most relevant acoustic datasets for detail investigations. The Lockheed P-3B Orion is a four-engine turboprop aircraft with a maximum gross take-off weight of 135,000 lbs. The propeller blades were manufactured by Hamilton Standard. Each of the propeller blades was driven by an Allison T56-A-14 turboprop engine delivering 4,100 shp.

Figure 12. Lockheed P-3B Orion four-engine turboprop aircraft used in the experiment.

Accomplishments in the past two years (2016–2018) of Project 40 at Purdue University

A typical source spectrum of the noise radiated by the Lockheed P-3B Orion is shown in Figure 13a. For this type of turboprop aircraft, the low-frequency tonal components (below 200 Hz) dominate the sound fields, which is quite different from the noise spectrum of the Boeing 747-100 jet engine aircraft (Ahearn et al., 2017) shown in Figure 13b (see Figure 18b for the Lockheed F-22 jet engine noise spectrum). The low-frequency components are usually much lower for the noise radiated from jet engines. Hence, jet noise cannot propagate long range in the atmosphere because of high air absorption at mid- to high-frequency regimes. Compared with that of jet engines, noise radiated from turboprop engines can travel a

relatively longer distance to the ground because the rate of atmospheric absorption of sound is typically much smaller in this low-frequency regime. For ground-based receivers, the en route noise from a turboprop aircraft is likely more noticeable than that of a jet-driven aircraft.

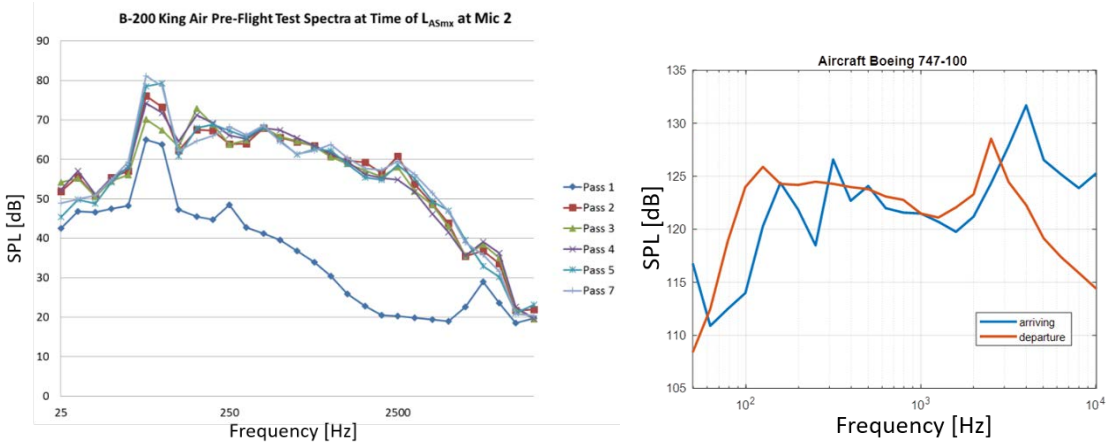

(a) (b)

Figure 13. Typical noise spectra of two types of aircraft engines: (a) Lockheed P-3B Orion turboprop engine; and (b) Boeing 747-100 jet engine.

Using the available information, we could identify the flight trajectory of the test aircraft and the atmospheric sound speed profiles during the flight trials. With onboard noise monitoring equipment and ground-based microphones, we were able to extract the measured data and compare them with the predictions due to a flyover aircraft. According to the results, the assumption that the test aircraft can be modeled as an omnidirectional source is satisfactory only at higher frequencies (over about 300 Hz); use of the omnidirectional source model has become increasingly inadequate for source frequencies below 125 Hz.

The Purdue team has developed an empirical model to estimate the directivity patterns of the test aircraft. Figure 14 compares the predicted and measured time histories of a typical set of measured data with a source frequency of 63 Hz. The agreement between the measured results and predictions is reasonably good.

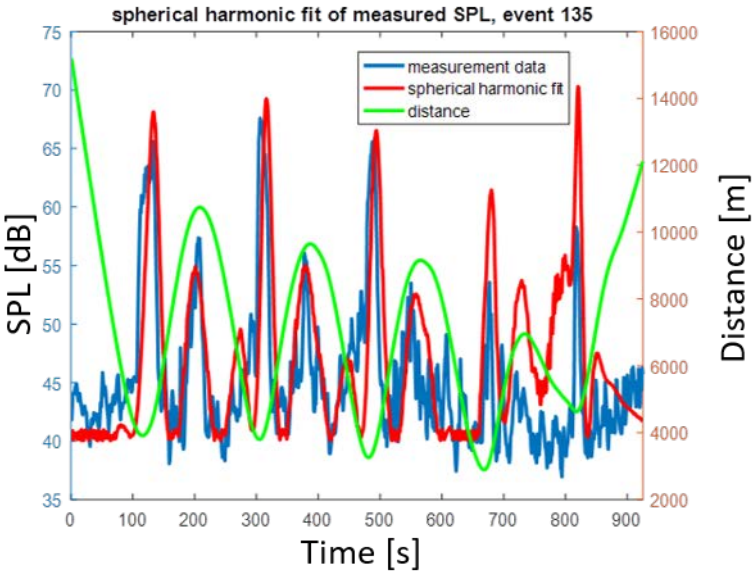

Figure 14. Comparison of measured and predicted time histories of A-weighted SPL of the test aircraft at a frequency of 63 Hz.

According to AEDT (Ahearn et al., 2017), attenuation (*Att*) due to an "acoustically soft" ground can be modeled using the following empirical formula:

$$Att\left(l_{seg}\right)=\begin{cases}11.83\times\left[1-e^{-0.00274 l_{seg}}\right] & 0\le l_{seg}\le 3000\text{ ft}\\ 10.86 & l_{seg}>3000\text{ ft}\end{cases},$$

where l_{seg} is the horizontal sideline distance measured from the aircraft flight path. The Purdue team has examined the uncertainties in the prediction of aircraft noise due to the ground effect according to the empirical formula. The ground effect of the predicted/measured sound fields is caused by interference of direct and reflected waves arriving at the receivers. The intrinsic variability in the predictions depends on a number of factors, including the source/receiver geometry, source frequency, atmospheric turbulence, acoustic characteristics of the ground surface, and terrain profile (Attenborough et al., 2007).

Figure 15 compares the predicted attenuation due to the ground effects for source frequencies of 250 and 500 Hz. The predicted attenuation according to the AEDT model is shown by the gold line. The predicted attenuation at different sideline distances is shown for snow-covered (blue) and grass-covered (red) ground with frequencies at 250 Hz (solid line) and 500 Hz (dashed line). The Delany-Bazley (D-B) model (Attenborough et al., 2007) was used to predict the effective impedance of the ground surface in Figure 15. In the D-B model, a single parameter known as "effective flow resistivity" is used to characterize the impedance of the ground surface. Parametric values of 20 and 250 kPa m·s^{-2} were used to model snow-covered ground and grassland. The source and receiver heights were 100 and 0 m above the ground, respectively, in the simulations shown in Figure 15. The total sound fields were computed by summing the direct and reflected waves coherently. We can see that the discrepancy in predicting attenuation can be as high as 6 dB between the AEDT and D-B models.

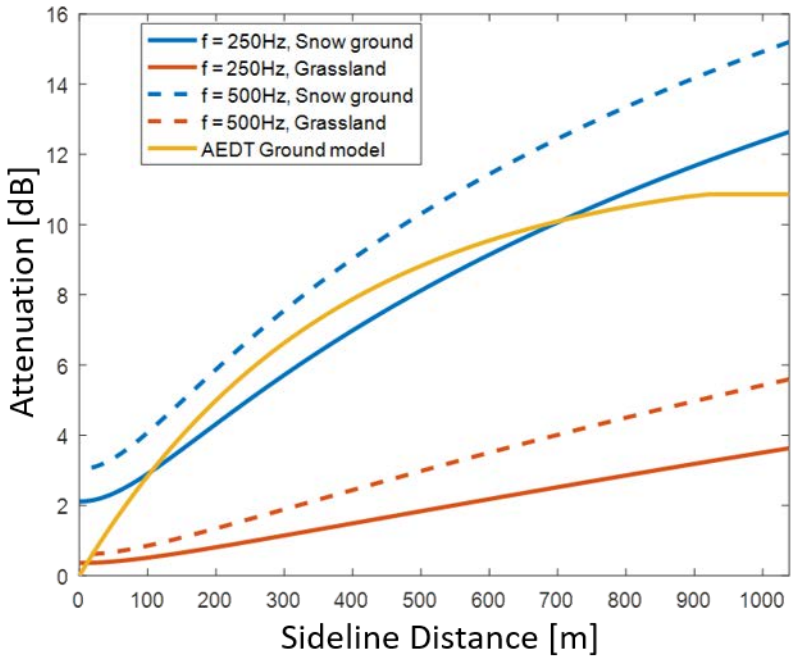

Figure 15. Comparison of AEDT ground model with a more precise ground impedance model.

The Purdue team has conducted a detailed analysis on the overall uncertainties on the DISCOVER-AQ dataset. Figure 16 shows the improvement in prediction of the A-weighted SPL. The agreement between the field data and our current prediction scheme using an improved spherical directivity pattern (gold) was much better than that using the monopole model (red); that is, noise due to an omnidirectional source. The agreement was especially good in the location of the first peak.

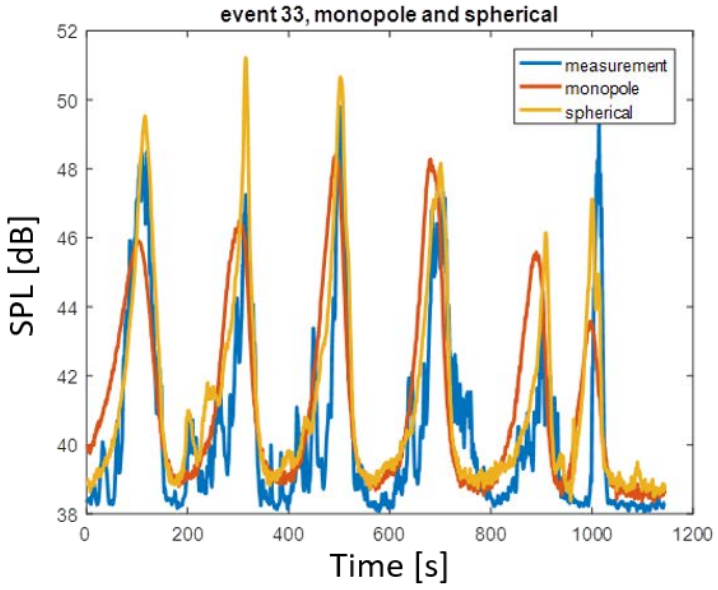

Figure 16. Comparison of predicted and field data for the A-weighted SPL of a typical event.

Figure 17 shows that the prediction "errors" with the use of the source directivity model have been reduced. However, larger error still exists when the distance is short and the elevation angle small. Future work should focus on the analysis of ground effects because most measurement sites are located in the vicinities of forested grounds, which would change the measured sound and many aircraft paths are above water-covered regions.

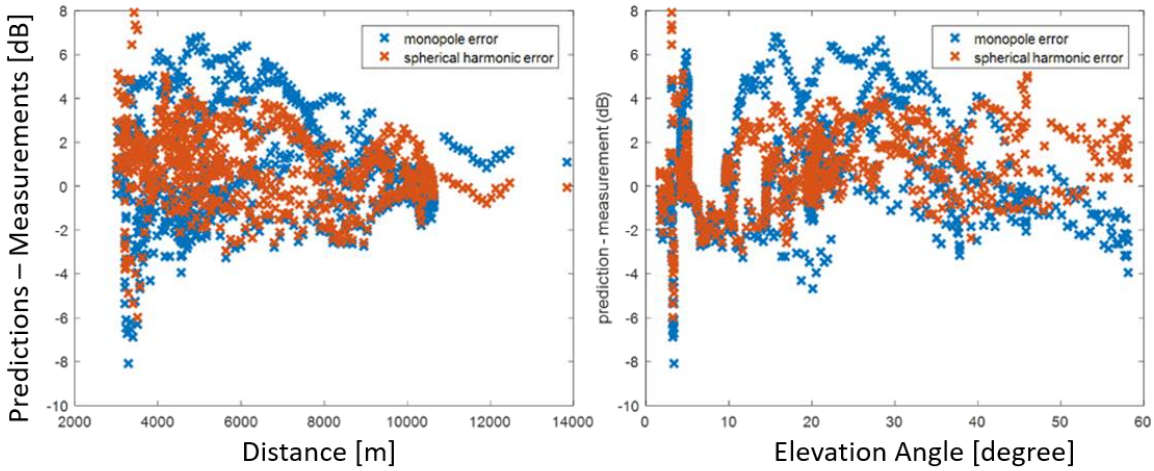

Figure 17. Discrepancies between measurement data and predictions for a selected event.

In the past year, the Purdue team has also studied the effect of source motion on predicting the A-weighted noise levels of flyover aircraft. Again, the DISCOVER-AQ dataset was used for comparison with predicted results. Figure 18 shows that the A-weighted SPL due to the test aircraft (driven by turboprop engines) showed higher sensitivity to the Doppler effect than aircraft driven by jet engines.

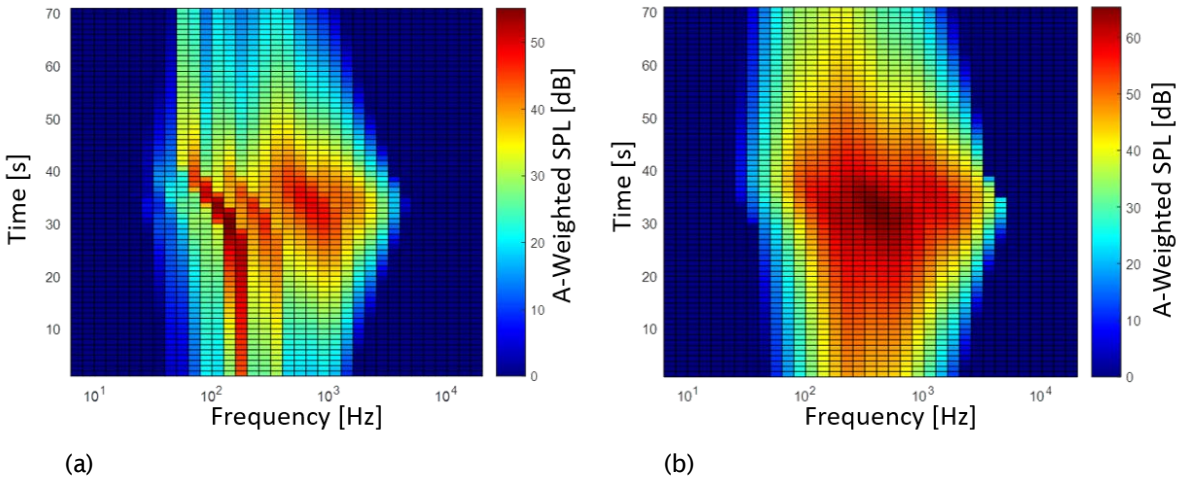

(a) (b)

Figure 18. Measured A-weighted SPL at different times of a flyover aircraft: (a) P3-B Orion (turboprop engines), and (b) F-22 (jet engine).

We also showed that predictions without the inclusion of Doppler effects usually underestimate the maximum A-weighted SPL for P-3B Orion test aircraft.

Milestones and Major Accomplishments

To complete the tasks for the current year, we launched an initial study to identify a set of relevant data in the DISCOVER-AQ report. Figure 19 shows detailed receiver locations and a three-dimensional view for a flight event near the airport of Conroe, Texas. There is one set of data for the level flight path before the spiral section and one set after the spiral maneuver. The measured noise data for the level flight before the spiral path had better signal-to-noise ratios because the flyover aircraft was operated at a lower elevation and, therefore, was much closer to the microphones mounted on the ground near the forest about 10 miles from Conroe airport. Hence, this set of data will be used in our work for the coming year. There are 11 groups of similar level flight tests with noise levels recorded by four to six receivers. Atmospheric profiles recorded by weather balloon will be used for comparisons with various numeric models.

Figure 19. Flight path and receiver locations for level flight (events 279–284) in DISCOVER-AQ measurement results.

Publications

Wang, Y. (2019). "Propagation of en-route aircraft noise." PhD. Thesis, School of Mechanical Engineering, Purdue University

Wang, Y., & Li, K.-M. (2019). Doppler's shift on aircraft noise propagation in modern aircraft noise prediction tools. Journal of the Acoustical Society of America 148(4, Pt. 2): 2824.

Outreach Efforts

N/A

Awards

Graduate research assistant Yiming Wang received the Institute of Noise Control Engineering (INCE) Best Graduate Student Award, 2018.

Student Involvement

Graduate research assistant Yiming Wang has been the primary person working on this task.

Plans for Next Period

The Purdue team plans four tasks:

1. Assess the DISCOVER-AQ Acoustics datasets for use in validating noise tools (propagation).
2. Assess the influence of source (aircraft) motion on the accuracy in predicting en route aircraft noise (source).
3. Assess the impacts of geometric locations of source and receiver, the effective surface impedance, and the ground topography on the accurate prediction of aircraft noise (receiver).
4. Assess the overall uncertainty in the noise prediction (propagation + source + receiver) of flyover aircraft.

Three of these four tasks are being conducted in coordination with the Penn State team. The Purdue team will also focus on the use of DISCOVER-AQ datasets to investigate the influence of ground effects on predicting aircraft noise (Task C). Other Purdue efforts include the investigation of the Doppler effect on measured noise contents (for the shift in frequency and change in noise levels) for approaching and receding aircraft.

References

Ahearn, M., et al. (2017). Aviation Environmental Design Tool (AEDT) technical manual, Version 2d., Report DOT-VNTSC-FAA-17-16

Attenborough, K., Li, K.M., & Horoshenkov, K. (2007). Predicting outdoor sound. Taylor & Francis.

Boeker, E., et al. (2015). DISCOVER-AQ acoustics measurement and data report, DOT-VNTSC-FAA-15-09.

Cheng, M. (2016). Vancouver Airport Authority [Private Communication].

SILENCE(R) Consortium; a description of this research program can be found here: http://www.xnoise.eu/index.php?id=85 (Last Accessed 7/15/2017). The research program is under the administration of X-Noise, which is a collaborative network in the European Union specializing in aeroacoustics.

Project 041 Identification of Noise Acceptance Onset for Noise Certification Standards of Supersonic Airplanes

The Pennsylvania State University

Project Lead Investigator

Victor W. Sparrow
Director and United Technologies Corporation Professor of Acoustics
Graduate Program in Acoustics
The Pennsylvania State University
201 Applied Science Bldg.
University Park, PA 16802
+1 (814) 865-6364
vws1@psu.edu

University Participants

The Pennsylvania State University

- PI(s): Vic Sparrow, United Technologies Corporation Professor and Director, Graduate Program in Acoustics
- FAA Award Number: 13-C-AJFE-PSU Amendment 45
- Period of Performance: March 29, 2019 to August 29, 2020
- Tasks:
  1. Obtaining confidence in signatures, assessing metrics sensitivity, and adjusting for reference day conditions
  2. Assessing secondary sonic boom propagation

Queensborough Community College, City University of New York

- Co-Investigator: Kimberly A. Riegel, subrecipient to The Pennsylvania State University (Penn State)

Project Funding Level

This project supports the identification of noise acceptance onset for noise certification standards of supersonic airplanes through research conducted on multiple tasks at the Penn State University. The FAA funding to Penn State in 2019–2020 is $390,000. Matching funds are expected to meet cost share on both Tasks. Boom Supersonic has pledged $300,000, and Gulfstream has pledged $100,00.

Investigation Team

For 2019–2020, the investigation team includes:

- Victor W. Sparrow, PI (Task 1 and 2), The Pennsylvania State University
- Trevor Stout, postdoctoral scholar (Task 2), The Pennsylvania State University
- Lucas Wade, graduate research assistant (Task 1), The Pennsylvania State University
- Joshua Kapscos, graduate research assistant (Task 1), The Pennsylvania State University
- Juliet Page, coinvestigator, subrecipient to Penn State, Volpe – The National Transportation Systems Center
- Kimberly A. Riegel, coinvestigator, subrecipient to Penn State, Queensborough Community College, City University of New York
- Steve Ogg, et al., Boom Supersonic [industrial partner]
- Robbie Cowart, Joe Salamone, et al., Gulfstream [industrial partner]

Project Overview

FAA participation continues in International Civil Aviation Organization, Committee on Aviation Environmental Protection (ICAO CAEP) efforts to formulate a new civil, supersonic aircraft sonic boom (noise) certification standard. This research

investigates elements related to the potential approval of supersonic flight over land for low boom aircraft. The efforts include investigating certification standards, assessing community noise impact, and developing methods to assess the public acceptability of low boom signatures. The proposed research will support NASA in the collaborative planning and execution of human response studies that gather the data to correlate human annoyance with low-level sonic boom noise. As the research progresses, this may involve the support of testing, data acquisition and analyses, field demonstrations, laboratory experiments, or theoretical studies, for example, see Maglieri et al. (2014).

Task 1 - Obtaining Confidence in Signatures, Assessing Metrics Sensitivity, and Adjusting for Reference Day Conditions

The Pennsylvania State University

Objective

As national aviation authorities move forward in developing noise certification standards for low-boom supersonic airplanes, several research gaps exist in areas including signature fidelity, metrics, metrics sensitivity to real-world atmospheric effects, and adjustments for reference conditions. Research support is needed by FAA and international partners in these areas to progress toward standards.

The objective of this activity is to continue research at Penn State in the ASCENT Center of Excellence to complement the ongoing development of sonic boom standards within the Committee for Aviation Environmental Protection's (CAEP) Working Group 1 (Noise Technical), Supersonics Standards Task Group (SSTG). This research will ensure that the behavior of the sonic boom metrics considered in the SSTG discussions is well understood and will account for sonic boom variability effects, to move forward with sonic boom noise certification standard development and consideration of subsequent rulemaking.

Task 1 in ASCENT Project 41 focuses on several, but not all, research initiatives needed to move toward the development of a low-boom supersonic en-route noise certification standard.

Research Approach

Background

An ongoing effort of ASCENT Project 41 is determining the variability in sonic boom loudness level at the ground as a result of various atmospheric effects. Last year's report outlined a study of the effects of turbulence on sonic boom signatures, particularly how these effects might be isolated and removed from the signatures. Because turbulence is stochastic in nature, this is an important step in finding a more consistent baseline level for the purpose of supersonic aircraft certification.

Although turbulence is strongest in the lowest few kilometers of the atmosphere, heterogeneities in other atmospheric variables, including ambient pressure, temperature, relative humidity, and wind can have a significant impact on the level of the sonic boom over its entire propagation path. These quantities are thus of primary importance in the certification effort. Therefore, the focus of Project 41 Task 1 in 2018–2019 was to study the change in boom level that fluctuations in these quantities induce while also exercising the PCBoom sonic boom propagation software. According to the "reference day" certification method being explored by CAEP Working Group 1, all atmospheric variations were produced by altering a standard reference atmosphere.

The reference atmosphere in question uses mean temperature and pressure profiles taken from ICAO standard 7488/3 (or ISO 2533). Relative humidity is calculated from an equation given in Annex C of ISO 9613. No winds are present in the reference atmosphere. Plots of the pressures, temperatures, and relative humidities associated with the reference atmosphere are given below up to an altitude of 200 kft.

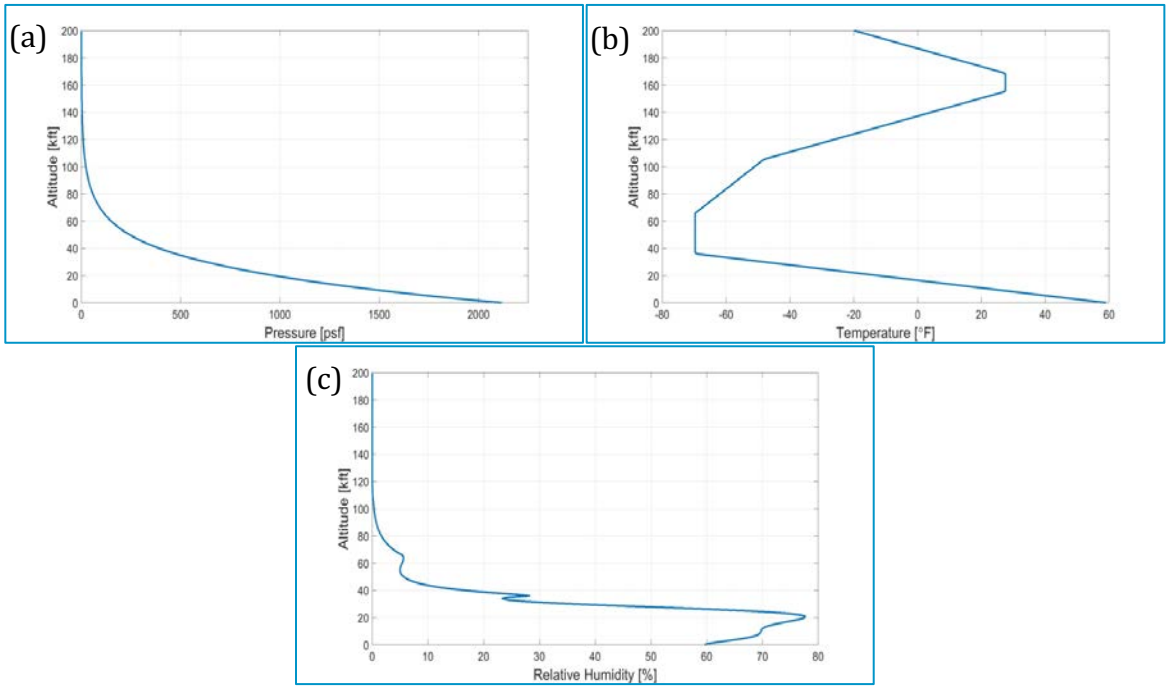

Figure 1. Plots of the reference atmosphere pressure in psf (a), temperature in °F (b), and relative humidity (c) up to 200 kft.

PCBoom 6.7b vs. 6.7.1.1

The work undertaken in 2018–2019 required heavy use of sonic boom propagation software. The chosen software, PCBoom, was developed by kbrWyle and is maintained in part by NASA. The latest version available to the public at the start of this work was 6.7b, which relied on a split-step pseudospectral numerical solution of an augmented Burgers' equation. An updated version, 6.7.1, was provided to Penn State in July of 2019, and a further revision, 6.7.1.1, was supplied in August 2019 (Lonzaga, 2019). The updated version involved a complete restructuring of the Burgers' solver and incorporated wind effects such as Doppler shift and convective amplification. Cases without winds did not change significantly, but any results for which wind was present needed to be redone after the update. The two versions are compared for a particular set of propagation cases in the "Linear Wind Profile" section below. All cases used as input a computational fluid dynamics simulated pressure signature for a Lockheed Martin LM-1021 concept low boom aircraft, which was a configuration provided in the 2nd AIAA Sonic Boom Prediction Workshop as well as the 6.7b installation of PCBoom as an example case. Only undertrack levels are reported.

Temperature smoothing

One of the first cases studied was a smoothing of the temperature profile in Figure 1. The justification for doing so is twofold. First, a real atmosphere will generally not have such a clear distinction (slope discontinuity) between the linear temperature lapse of the troposphere and the isothermal portion of the lower stratosphere. Instead, a real atmosphere will fluctuate about this idealized profile and have a smoother transition between the two regions. Therefore, it was of interest to determine how much of a change in sonic boom level this sort of smoothing would produce. Second, slope discontinuities can cause instability in some numerical methods. Thus, it was important to verify that PCBoom could properly handle such a discontinuity. The smoothed profile could be used as a comparative tool, because the two profiles would not be expected to produce wildly different results unless numerical instability were present. Of note, relative humidity is partially dependent on temperature, and therefore its profile needed to be altered appropriately. The smoothed case is plotted for both temperature and relative humidity in Figure 2 below.

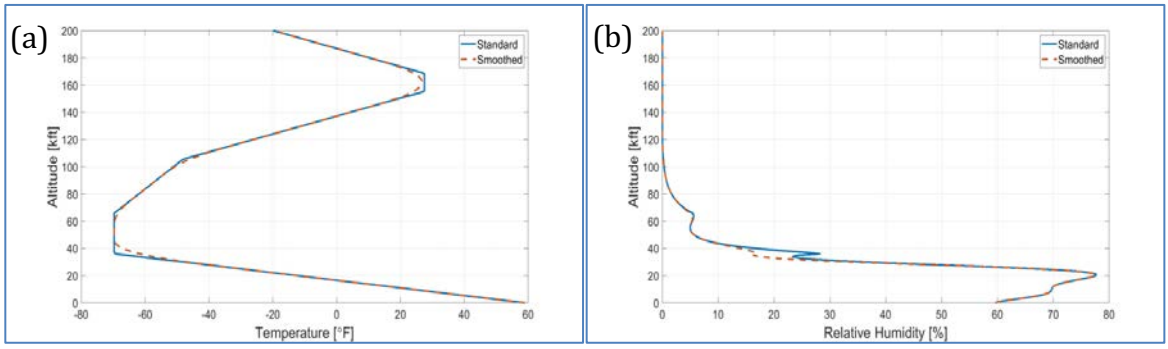

Figure 2. Smoothed temperature profile (a) and resulting relative humidity profile (b).

After propagation of the sonic booms to the ground in PCBoom, two key sonic boom metrics were computed, among others. Both the Steven's Mark VII Perceived Level (PL) and the Indoor Sonic Boom Annoyance Predictor (ISBAP) were calculated and are utilized below. The change in sonic boom level due to the smoothing was seen to be approximately 0.04 PLdB/0.04 dB ISBAP, thus confirming that PCBoom does not have any difficulty in processing the discontinuity, and small fluctuations about the mean profile produce correspondingly small fluctuations in boom level.

Shifts in molar concentrations of water vapor

Water vapor concentration is a key component in determining the extent of atmospheric absorption due to molecular relaxation. Because absorption limits waveform steepening and hastens amplitude decay, it is an important factor in determining overall boom loudness. Thus, the research team sought to observe the quantitative impact of water vapor concentration (or, loosely, relative humidity) on boom level. To do so, the molar concentration of water vapor was increased and then decreased by 25% relative to the reference profile, and the corresponding relative humidity was computed. The resulting curves are plotted in Figure 3.

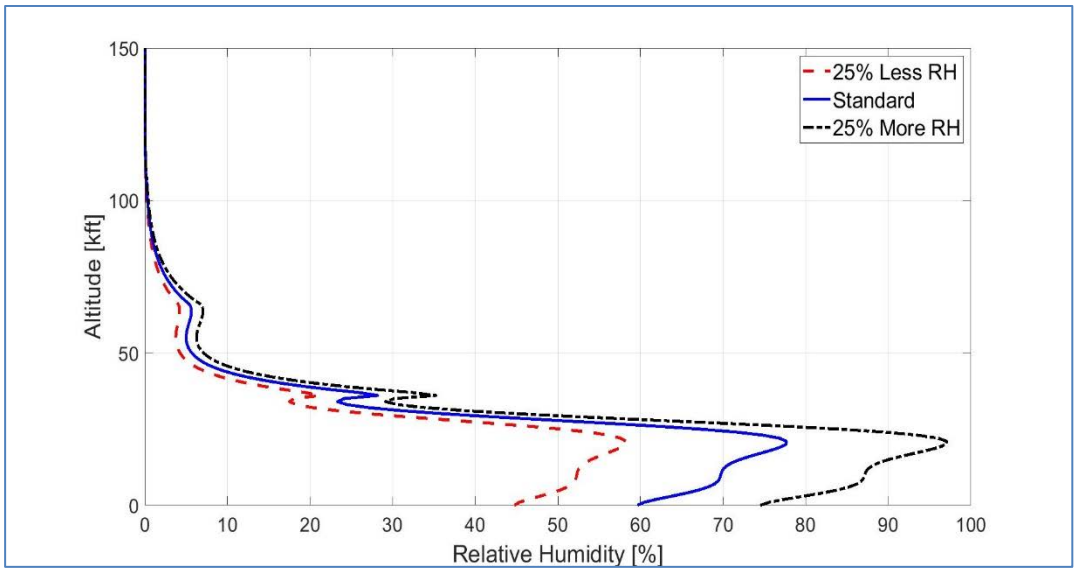

Figure 3. Relative humidity profile after increasing or decreasing the molar concentration of water vapor by ±25%.

Unexpectedly, this rather dramatic shift in water vapor concentration induced a maximum decrease (due to -25% shift) in PL of only approximately 0.9 dB and 0.6 dB for ISBAP, and a maximum increase (due to +25% shift) of only 0.5 PLdB and 0.35 dB ISBAP.

Linear wind profile

Because wind convects sound, it can have a marked impact on the propagation path of sonic booms and therefore their loudness. It may either increase or decrease the boom level depending on its direction relative to the nominal propagation direction of the sonic boom. In this study, a set of basic linear wind profiles was added to the otherwise unchanged reference atmosphere. Although these profiles are not realistic, they are helpful in understanding the effect that wind has on loudness in general. Ground wind speeds were taken to be zero to satisfy the no-slip condition, whereas peak wind speeds at the simulated flight altitude of 55,000 ft ranged from an 80 ft/s headwind to an 80 ft/s tailwind in increments of 10 ft/s. Changes in both PL and ISBAP relative to the windless reference atmosphere were determined. The result from PCBoom 6.7b is shown below, with the updated 6.7.1.1 result following shortly after.

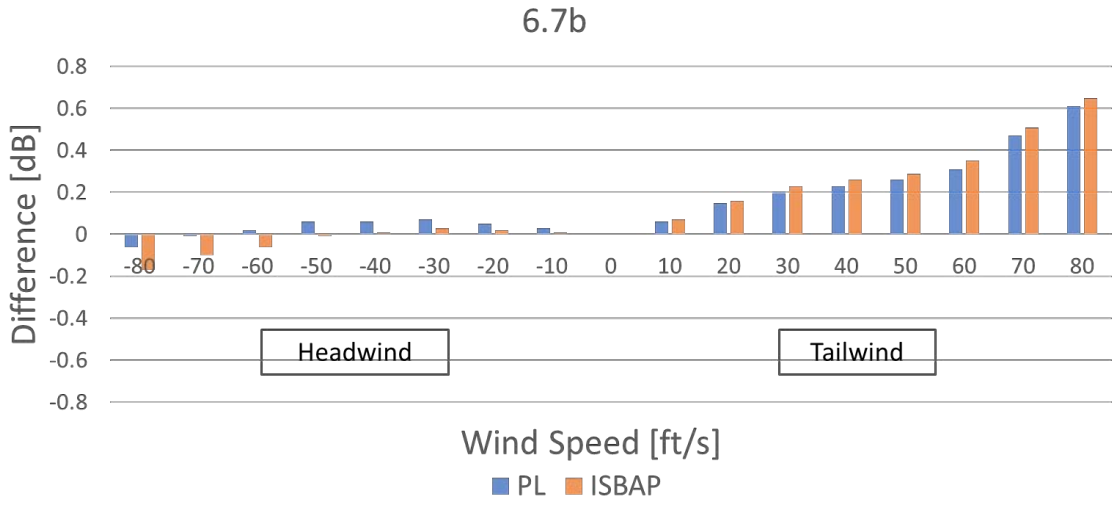

Figure 4. Difference in boom level due to linear wind gradient, as computed in PCBoom 6.7b.

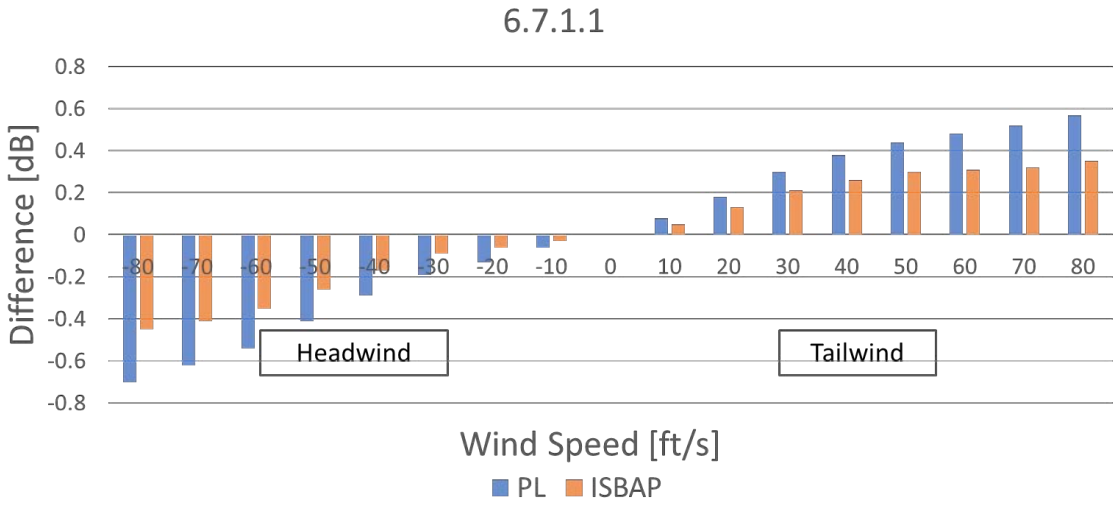

Figure 5. Difference in boom level due to linear wind gradient, as computed in PCBoom 6.7.1.1.

The trend of version 6.7b seen in Figure 4 was a source of confusion when the chart was produced, because increasing the tailwind with all other parameters held fixed would be expected to invariably increase boom level. However, with wind effects properly accounted for (Lonzaga, 2019), as in PCBoom 6.7.1.1 (Fig. 5), this trend is indeed recovered. As shown in Figure 5,

the difference in the PL metric in dB can vary as much as 0.7 dB because of the wind effects, and a similar effect is observed for ISBAP, the indoor sonic boom annoyance predictor metric.

Milestone

The impacts of various perturbations of a reference atmosphere on sonic boom levels were assessed in two different versions of the PCBoom propagation software.

Major Accomplishments

ASCENT Project 41 Task 1 has determined potential variability in sonic boom PL/ISBAP due to various atmospheric perturbations, which may prove useful in sonic boom noise certification of supersonic aircraft.

Publications

Published Conference Abstract

Wade, L. & Sparrow, V. (2019). Effects of perturbing a reference atmosphere on sonic boom propagation metrics. Journal of the Acoustical Society of America. **145**(3, Pt. 2) 1903.

Outreach Efforts

N/A

Awards

None.

Student Involvement

Luke Wade was the Penn State graduate research assistant who worked on ASCENT Project 41 during the 2018–2019 academic year. In addition to the work outlined above, he provided support within CAEP Working Group 1 and submitted cases for the 3rd AIAA Sonic Boom Prediction Workshop to be held in January 2020. He has since received a Fellowship from NASA for conducting further research in the area of sonic booms. Graduate research assistant Joshua Kapcsos is currently learning the PCBoom software and will be taking over from Luke in future Project 41 tasks.

Plans for Next Period

Further work on the study of atmospheric perturbations may be carried out, including the study of more realistic wind profiles, crosswinds, and statistical analysis of boom level variability due to changes in the atmosphere.

References

Lonzaga, J.B. (2019). Recent enhancements to NASA's PCBoom sonic boom propagation code. AIAA Aviation Forum, Dallas, Texas, USA.

Maglieri, D., Bobbitt, P., Plotkin, K. Shepherd, K., Coen, P., & Richwine, D. (2014). Sonic boom: Six decades of research. NASA SP-2014-622.

Task 2 - Assessing Secondary Sonic Boom Propagation

The Pennsylvania State University
Queensborough Community College, City University of New York

Objective

Because both normal boom and low-boom supersonic aircraft are getting closer to implementation, assessing all aspects of the sonic boom noise that reaches the ground is important. This includes the need to more comprehensively understand secondary sonic booms, when and why they occur, and the resulting signatures.

Research Approach

Background

Most of the research in the United States to understand the regular occurrence of secondary sonic booms observed on the northeast coast as a result of the Concorde was completed in 1980. There are two main types of secondary sonic booms. Type I is the ground boom resulting from shock waves emanating off the top of the aircraft that refract downward for certain atmospheric conditions. Type II is the boom that bounces off the ground or water surface and is bent in the atmosphere, then returns to the ground. To better predict the conditions that result from these secondary sonic booms, the variance in the atmospheric conditions, type of aircraft and trajectory should be examined.

The primary focus of the initial work in Task 2 of ASCENT Project 41 in 2019 was the re-creation of the original 1980 work by Rickley and Pierce by using the PCBoom modeling software (Plotkin et al., 2007). The 2019 research was primarily undertaken by postdoctoral scholar Trevor Stout. After his departure from Penn State, the work was continued by Dr. Kimberly Riegel of Queensborough Community College and the project PI Dr. Victor Sparrow.

Original FAA results

The original FAA report number ADA088160, authored by Ed Rickley and Allan Pierce, measured and simulated the sonic booms that were being heard in New England because of the Concorde. At the time, supersonic flight over land was already banned by the FAA, so the sonic booms that were impinging on land near the coast were not from the undertrack boom. The authors measured the signatures in several places where secondary sonic booms were perceived, including Malden, MA, and Applebachsville, PA. Using measured atmospheric data at the locations where sonic booms were being heard, the authors also predicted where the type I and type II secondary sonic booms would be heard for a Concorde aircraft flying into New York City and Washington, DC. Figure 44 from the report shows their predicted focus lines for both type I and type II and the primary boom carpet edge that would be created on a flight into New York. The original figure has been reproduced here as Figure 6 for reference.

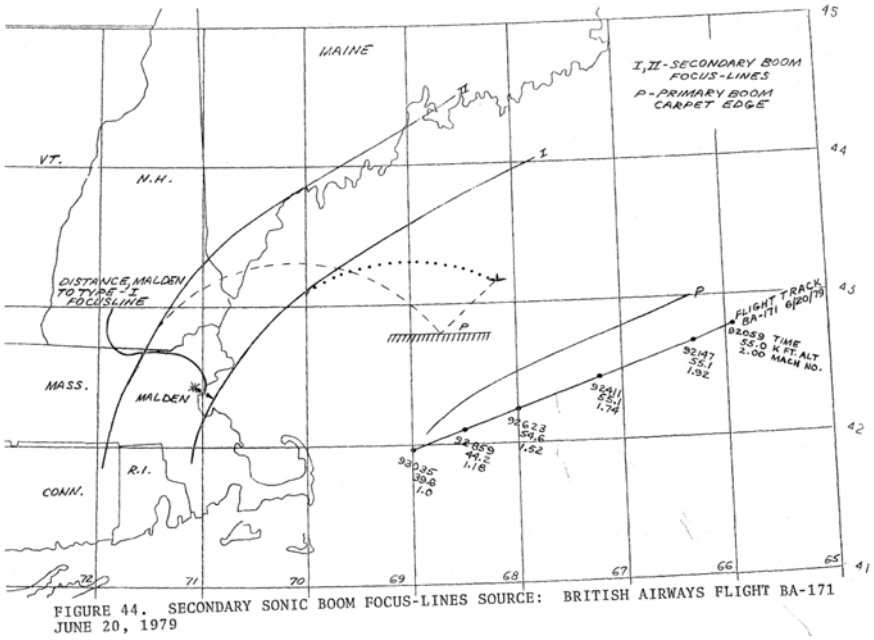

Figure 6. The predicted sonic boom type I and type II focus lines for a Concorde Aircraft approaching New York City, as produced in the original 1980 FAA report by Rickley and Pierce.

Re-creation of results with PCBoom

To determine the agreement between the results from the PCBoom software version 6.7b and the original predictions, we used the same atmospheric conditions outlined in the report and the same flight trajectory and signature from the Concorde

as inputs into the PCBoom software. Originally, a flat earth was assumed. Figure 7 shows the ray trajectories for the first run of PCBoom. The black ray trajectories do not hit the ground, whereas the blue ray trajectories bounce off the ground. After the rays that intersected with the ground were identified, the propagated rays were then refined so that only the rays that intersected with the ground would be calculated. PCBoom was run again with the refined set of rays. This process resulted in a set of rays where the ray/ground intersection could be identified, and a plot of the locations where secondary sonic booms would have reached the ground was created. Figure 8 shows the resulting secondary carpet and compares the results to the original predictions from the 1980 Rickley and Pierce report. The flat earth model shows good agreement with the original data and increases the confidence that PCBoom is accurately modeling the secondary sonic booms.

However, Figure 7 shows that these secondary sonic booms can travel distances of 600 km. At these distances, the flat earth approximation may not be the most accurate representation. PCBoom has the option to include a spherical earth or an ellipsoidal earth approximation. Therefore, both simulations were performed, and the results were compared to the original predicted 1980 report simulations. The agreement for the spherical earth is still reasonable. However, there are some differences, primarily in the type II ground intersection locations as well as some differences in all the ray trajectories directly in front of the aircraft. Figure 9 shows the spherical earth results, and Figure 10 shows the ellipsoidal earth results. Although there are substantial differences between the flat earth approximation and the other simulations, the differences between the spherical and the ellipsoidal earth are very small.

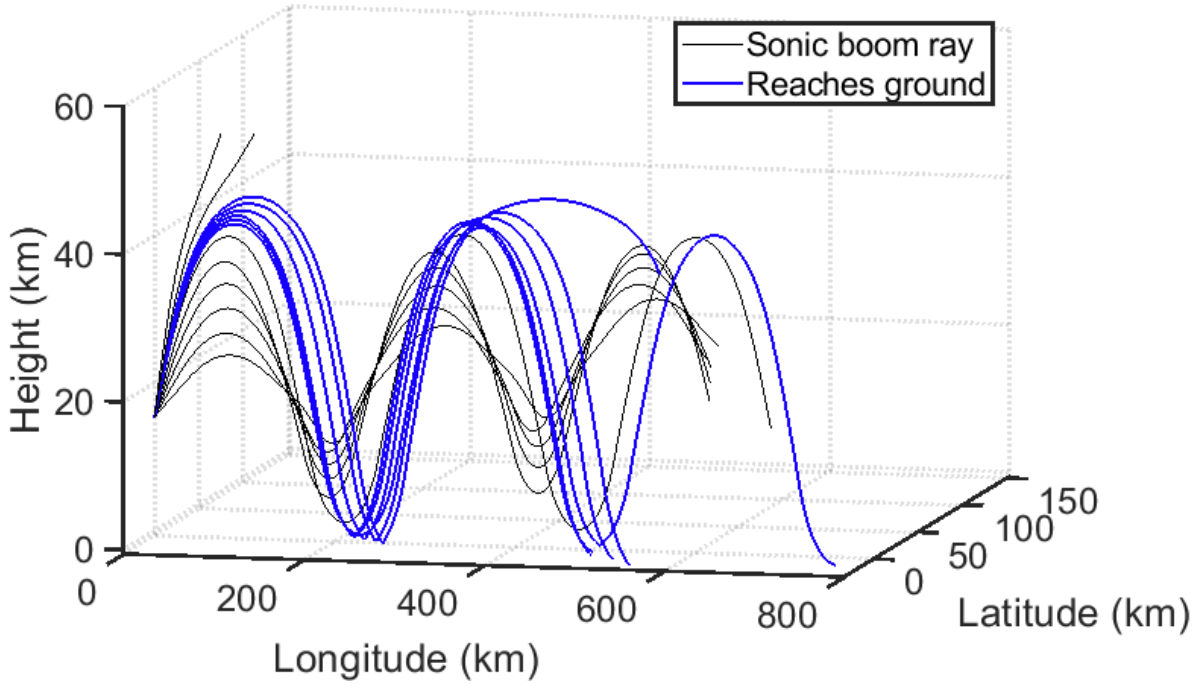

Figure 7. The ray trajectories of the propagated sonic boom rays, with the rays that reach the ground highlighted in blue.

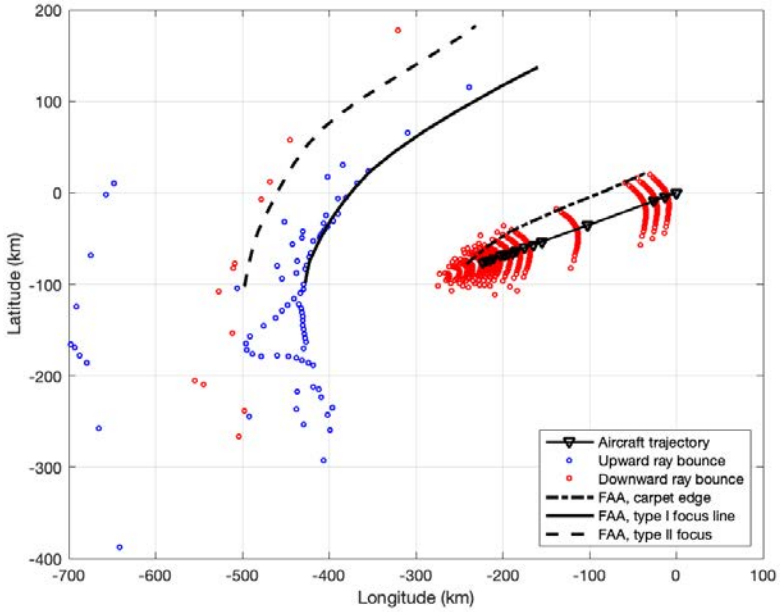

Figure 8. The secondary boom carpet for a flat earth approximation is shown with type I secondary sonic booms shown in blue and type II shown in red. The original focus lines from the 1980 Rickley and Pierce report area are shown in the figure as solid and dashed black lines.

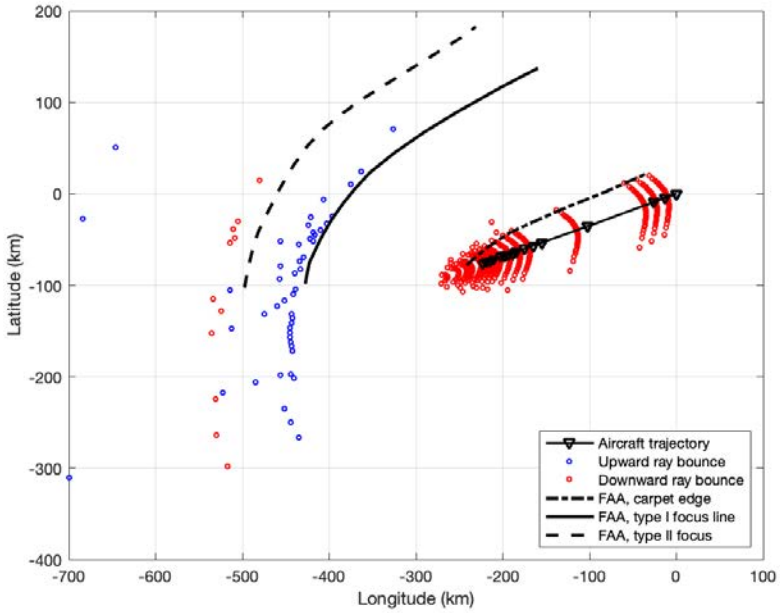

Figure 9. The secondary boom carpet with a spherical earth is shown with type I secondary sonic booms shown in blue and type II shown in red. The original focus lines from the 1980 Rickley and Pierce report area are shown in the figure as the solid and dashed black lines.

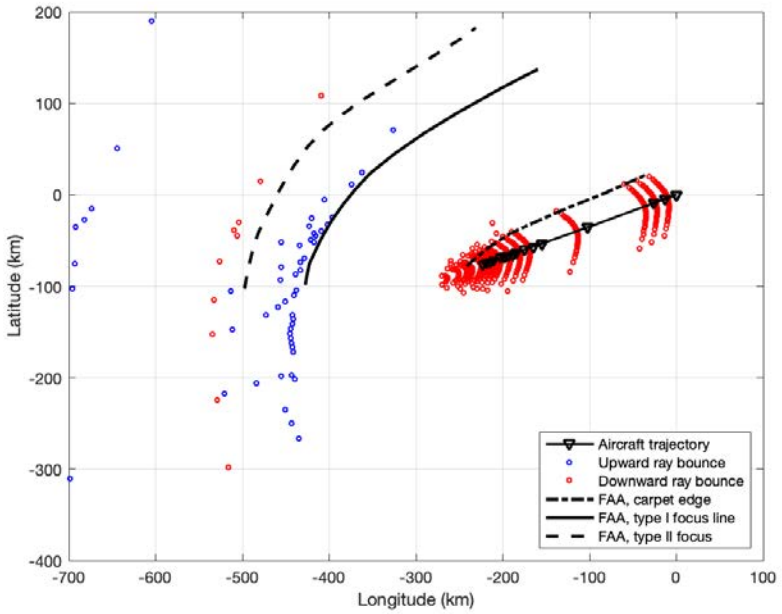

Figure 10. The secondary boom carpet with an ellipsoidal earth is shown with type I secondary sonic booms shown in blue and type II shown in red. The original focus lines from the 1980 Rickley and Pierce report area are shown in the figure as the solid and dashed black lines.

Milestone
The project is now underway.

Major Accomplishments
ASCENT Project 41 Task 2 has now successfully re-created the simulations performed by Rickley and Pierce in 1980 by using the PCBoom modeling software, and the new results show good agreement with the 1980 work.

Publications
Published Conference Abstract

Riegel, K., Sparrow, V., & Stout, T. (2019). Preliminary analysis of the PCboom software for calculating secondary sonic booms. Journal of the Acoustical Society of America. **146**(4) 2782.

Outreach Efforts
N/A

Awards
None.

Student Involvement
None.

Plans for Next Period
The project team will investigate the influence of upper atmospheric winds on the distribution of secondary sonic booms. The pressure signatures of the received secondary sonic booms will be predicted. If time allows, different aircraft will be used to determine differences in the received secondary sonic boom levels.

References

Plotkin, K., Page, J., & Haering, E. (2007). Extension of PCBoom to over-the-top booms, ellipsoidal earth, and full 3-D ray tracing. AIAA 2007-3677, 13th AIAA/CEAS Aeroacoustics Conference

Rickley, E. & Pierce, A. (1980). Detection and assessment of secondary sonic booms in New England. FAA-AEE-80-22, accessible as ADA088160

Project 042 Acoustical Model of Mach Cutoff Flight

The Pennsylvania State University

Project Lead Investigator

Victor W. Sparrow
Director and United Technologies Corporation Professor of Acoustics
Graduate Program in Acoustics
The Pennsylvania State University
201 Applied Science Bldg.
University Park, PA 16802
+1 (814) 865-6364
vws1@psu.edu

University Participants

The Pennsylvania State University

- PI(s): Dr. Victor W. Sparrow (PI), Dr. Michelle C. Vigeant (Co-PI)
- FAA Award Number: 13-C-AJFE-PSU, Amendments 20, 33, and 42
- Period of Performance: June 28, 2016 to December 31, 2019
- Task(s):
    1. Propagation modeling with enhanced ray-tracing capabilities
    2. Study of human perception of Mach cutoff sounds

Project Funding Level

$170,000 for 2018–2019, The Pennsylvania State University

Aerion Corporation is providing cost-share in-kind matching funds to The Pennsylvania State University (Penn State). Our point of contact at Aerion is Gene Holloway, gholloway@aerioncorp.com. Aerion is providing the necessary near-field computational fluid dynamics data and other relevant information to help guide the project team in making accurate predictions of the Mach cutoff sonic boom signatures that may be produced by Aerion's future supersonic aircraft.

Investigation Team

- Principal Investigator: Victor W. Sparrow, The Pennsylvania State University, Task 1
- Co-Investigator: Michelle C. Vigeant, The Pennsylvania State University, Task 2
- Graduate Research Assistant: Zhendong Huang (assessment and extension of Mach cutoff models), The Pennsylvania State University, Task 1
- Graduate Research Assistants: Nick Ortega and Jonathan Broyles (human perception of Mach cutoff sounds), The Pennsylvania State University, Task 2

Project Overview

ASCENT Project 42 brings together resources to provide preliminary information to the FAA regarding the noise exposure of supersonic aircraft flying under Mach cutoff conditions. Studies in the 1970s showed that Mach cutoff supersonic flight was possible, but there are currently no data establishing the frequency and extent of noise exposures or guidelines for managing such exposures. Penn State is shedding light on the Mach cutoff phenomena.

Aerion Corporation and many others believe that Mach cutoff supersonic flight is both viable (Plotkin, et al., 2008) and very likely to be acceptable to the public, but there is a lack of data to back up this assertion. Thus, research must be conducted to provide a technical basis for rulemaking regarding Mach cutoff operations.

The basic concept of Mach cutoff relies on the ambient temperature being substantially colder at flight altitudes than on the ground. Hence, the speed of sound is substantially slower at flight altitudes than at the ground. As illustrated in Figure 1, it is possible to fly in a range of Mach numbers (perhaps between Mach 1.0 and Mach 1.15) while having the sonic boom noise refract (bend) upward such that the rays never reach the ground. However, this picture is over-simplified, because the temperature profile in the atmosphere is never a smooth, linear function as depicted here. For higher Mach numbers, the sonic boom will impact the ground before refracting upward.

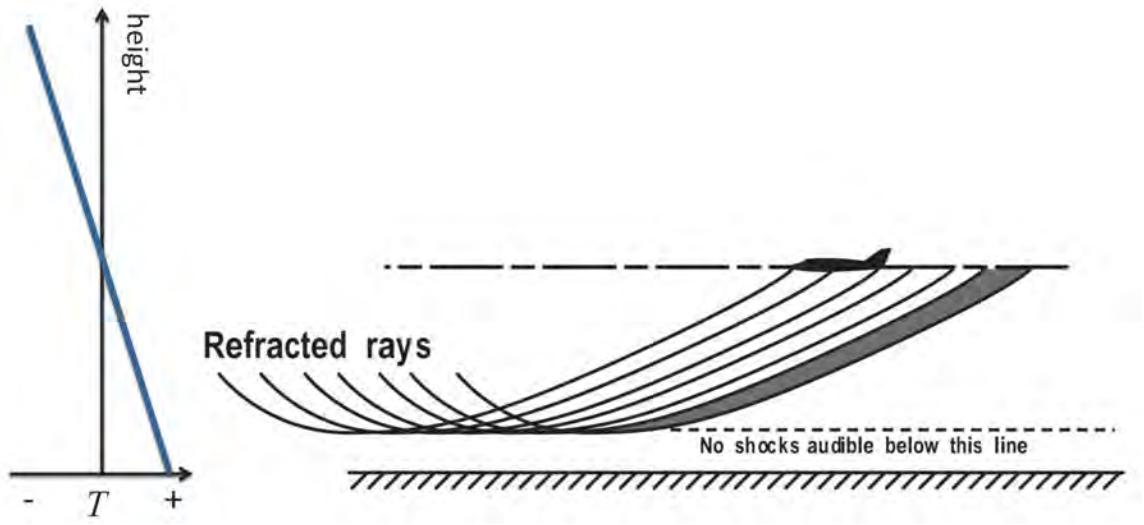

Figure 1. Simplified view of the Mach cutoff in which sonic boom noise does not reach the ground surface. Left: ambient temperature versus height (Sparrow). Right: aircraft and ray diagram showing refraction of sonic boom (NASA).

Little is known about the noise impact of Mach cutoff operations for future supersonic aircraft. The concept of Mach cutoff was introduced by Lockheed engineers in the mid-1960s (Shurcliff, 1970). NASA conducted some field experiments in the early 1970s, focusing on other speed regimes of flight and validating some of the Mach cutoff theory for some of the sound field. This research was conducted in Nevada with a 466 m (1,529 ft) tower (Haglund & Kane, 1973). Then to more directly address the Mach cutoff issue, a theoretical and experimental study was conducted in the mid-1970s with FAA support. The studies estimated altitudes and Mach number regimes to ensure that the focus boom does not reach the ground. That field campaign used fighter jets flying out of Langley Air Force Base to a test area in the Atlantic Ocean off Wallops Island, Virginia (Perley, 1977). Using the available instrumentation, the study concluded that Mach cutoff flight was feasible.

None of those studies made any recordings of sufficient quality to assess human response to the Mach cutoff noise. The theoretical studies estimating the altitude and Mach number restrictions for focus boom avoidance assumed a simple atmospheric model (linear sound speed profile), and it did not include real-world atmospheric effects. Hence the 1960s–1970s work was very good but represents only a start toward determining appropriate flight conditions for routine Mach cutoff supersonic flights over the continental United States.

Task 1 - Propagation Modeling with Enhanced Ray-Tracing Capabilities

The Pennsylvania State University

Objective

Research will be conducted to understand Mach cutoff operations and how often people would hear the unique Mach cutoff sounds. This includes estimating the flight altitude and Mach number restrictions for focus boom avoidance, including real-world atmospheric effects and assessments of practical Mach cutoff flight.

Research Approach

Methodology

Mach cutoff depends on the upward refraction of the sound in the atmosphere due to the temperature and wind speed gradients. To examine this phenomenon, the original propagation theory (Nichols, 1971) and the analysis of caustic phenomena observed during the threshold Mach number flights (Haglund & Kane, 1973) were retraced for extensibility. Nichols' theory and Haglund and Kane's criteria were used in the 1970s to assess Mach cutoff. In Nichols' theory, the atmosphere is assumed to have only vertical variations in temperature and horizontal wind. On the basis of one form of the refraction law specifying the normal direction of a wavefront, it was argued that for upward sound refraction, a direct sonic boom noise would not reach the ground as long as the acoustic wavefront normal becomes parallel to the ground. The cutoff Mach number, corresponding aircraft ground speed, and distance between sonic boom caustic and the ground can then be determined. In agreement with Nichols' theory, Haglund and Kane's analysis led to a criterion for Mach cutoff flight, in which "in order for shock wave cutoff above the ground from a supersonic airplane, the airplane ground speed must be less than the maximum speed of propagation of the shock wave beneath the airplane."

One limitation of earlier Mach cutoff theories (including Nicholls' and Haglund and Kane's) and existing tools (e.g., PCBoom) is that vertical winds are not included. In a realistic atmosphere, however, a noticeable vertical wind can sometimes exist. A sea breeze is one example in which a wind is blowing from sea to land, which normally occurs along coasts during daytime, and involves ascending and descending motion of the air. As the vertical wind becomes non-negligible, both the launch angle of sound rays away from the aircraft and the altitude of the caustic will be affected, as shown in Figure 2. Thus, clarifying the difference between the refraction law for a sound ray and that for the normal to a wavefront in a moving atmosphere is important (Ostashev et al., 2001).

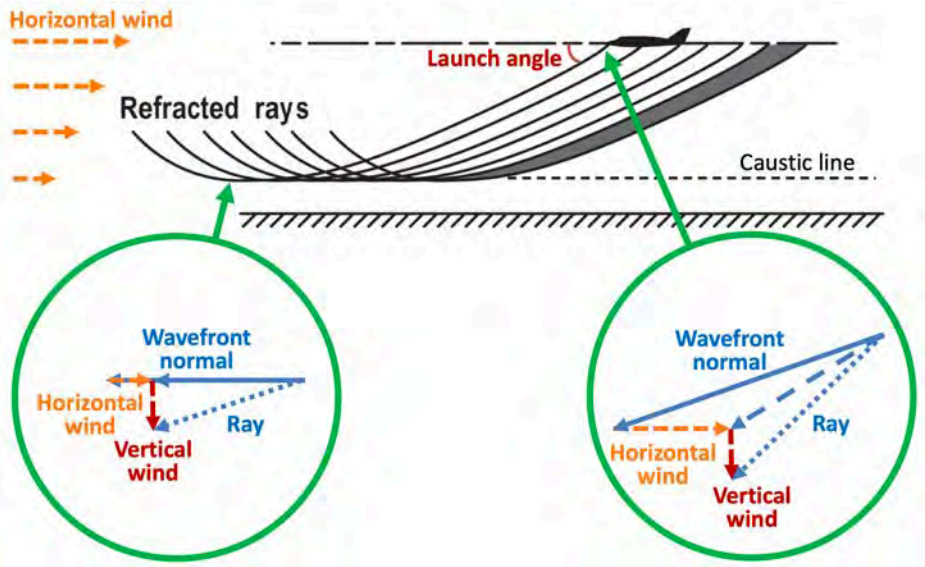

Figure 2. Contributions of a vertical wind to the difference between the wavefront normal and ray directions. Diagram courtesy NASA; adapted from Maglieri et al. (1971).

Another limitation in both Nicholls' theory and Haglund and Kane's analysis is that, by calculating the cutoff Mach number on the basis of the atmospheric conditions only at the flight and ground levels, the impact of realistic vertical atmospheric profiles in between those two levels on the sound propagation is not included. For sonic boom propagation over a long horizontal distance, horizontal variations in the atmosphere can also be important for Mach cutoff.

To produce an acoustical model that can lead to more accurate estimates of the safe cutoff altitude, the flight Mach number and ground speed for Mach cutoff flight, three-dimensional (3-D) ray-tracing equations have been examined (Pierce, 1989). On this basis, a 3-D fourth-order Runge–Kutta integration ray-tracing scheme has been developed, which can read in realistic atmospheric data including the arbitrary speed of sound variations as well as arbitrary 3-D winds including longitudinal, lateral and vertical wind components. It can be used to simulate sonic boom propagation through the 3-D atmosphere.

The data from High-Resolution Rapid Refresh (HRRR) were used for the atmosphere (Benjamin et al., 2016). HRRR is a numerical weather model developed by the National Oceanic and Atmospheric Administration Earth System Research Laboratory. It is the highest spatial and temporal resolution forecast system that is run operationally every hour by the National Centers for Environmental Prediction's Environmental Modeling Center. The previous operational version, HRRRv2, generates hourly analyses and forecasts for 18 to 36 hours over the contiguous United States. This model has a horizontal resolution of 3 km, with 40 pressure levels up to an altitude of approximately 20 km. This dataset includes surface and upper-level pressure fields of temperature, u- and v-components of winds, and vertical wind, among other variables used. Although an official HRRR archive does not exist, unofficial copies are available from other sources (Blaylock et al., 2017).

As shown in Figure 3, the HRRR model provides data over the contiguous United States. The Lambert Conformal Conic Projection is used by the National Oceanic and Atmospheric Administration for the HRRR data grid, and thus the projected x and y axes, are not always aligned with the true east and north directions. HRRR has a 3-km horizontal resolution; as shown in this figure, only 1 out of every 50 HRRR grid points along each axis is shown on the map. Typically, sonic boom noise can propagate horizontally for 40–100 km before reaching a cutoff point. Hence, the HRRR grid point resolution is capable of capturing the horizontal variation in the atmosphere on this local ray-tracing scale. Thus, the atmosphere is not assumed to be vertically stratified in the computational domain of the simulation. For each simulation, after the instantaneous location of the cruising aircraft along the flight path has been specified, a 200 km × 200 km horizontal region can then be selected as the corresponding computational domain, and the atmospheric variables at those HRRR grid points within this area can be mapped into the computational domain, along with a natural neighbor interpolation to represent the local atmospheric profile.

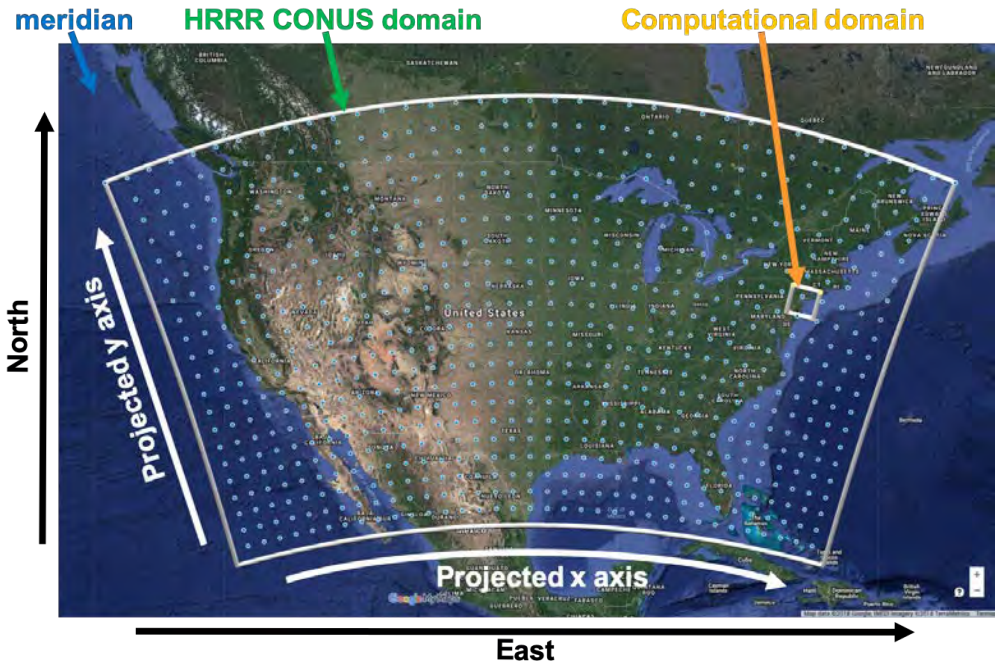

Figure 3. Map of the contiguous United States with grid points of the HRRR data.

With the input atmospheric data, the next step is to incorporate the Mach cutoff operational parameters proposed by Aerion Corporation. For this study, both a lower flight altitude of 12.5 km (41,010 ft) and a higher one of 15.24 km (50,000 ft) were adopted. The flight direction was inferred according to the location of the aircraft along the flight path.

When an aircraft is flying under the Mach cutoff condition, a focused boom is formed at the cutoff altitude, which corresponds to loud sound energy. Below that cutoff altitude, there is an evanescent wave decaying rapidly toward the ground, which typically covers a distance of a few hundred feet. To ensure that the caustic never intercepts the ground, an adequate safety margin must be allowed (Plotkin et al., 2008). To date, the cutoff Mach number has been determined as the largest Mach number possible (0.01 resolution in Mach number) with at least a 500 m clearance of a caustic on the ground. In each simulation, sound rays with different azimuthal angles are plotted to verify the clearance of a caustic. A ray diagram example for an eastbound flight over New York John F. Kennedy International Airport (JFK), cruising at the cutoff Mach number, is shown in Figure 4. The ground elevation plotted below the sound rays that is obtained from HRRR matches the one showing on GoogleMyMaps. The corresponding true air speed, aircraft ground speed, and vertical distance between the caustic and ground were calculated, as shown in Table 1. This method was used to assess the viability of Mach cutoff operations for the three busiest air routes in the United States in the year of 2017.

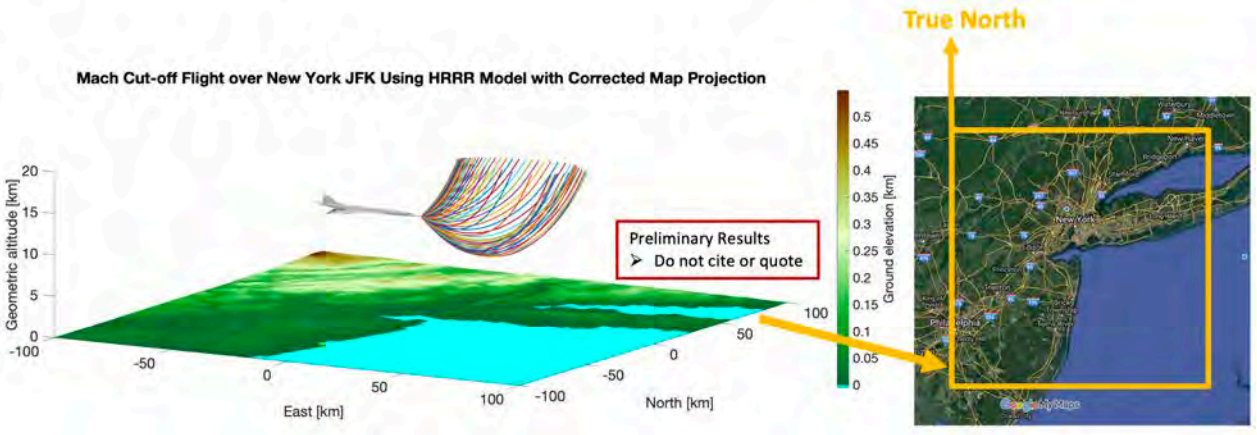

Figure 4. Ray diagram for an eastbound flight over New York JFK, cruising at the cutoff Mach number.

Table 1. Flight and atmospheric conditions obtained from a ray-tracing simulation for a Mach cutoff flight.

Atmospheric & flight variables	HRRR
Cut-off Mach number	1.06
Temperature @ aircraft	219.38 K
True air speed	704.08 mph
Longitudinal wind @ aircraft	120.76 mph
Crosswind @ aircraft	-22.14 mph
Aircraft ground speed	825.14 mph
Maximum sound speed (below aircraft)	754.58 mph (@ 0.04 km)
Maximum effective sound speed (below aircraft)	845.72 mph (@ 8.50 km)
Altitude of caustic	8.57 km
Ground elevation (below caustic)	0.00 km
Caustic to ground distance	8.57 km

Results

To investigate the accuracy of Haglund and Kane's theory in predicting the threshold Mach number, as an example, we ran ray-tracing simulations by using HRRR data for an aircraft flying over New York City at an altitude of 12.5 km (41,010 ft) at 2 p.m. EDT on January 1, 2017, with a flight direction of 0.294 degree north of east. In this case, if the aircraft was flying at Mach 1.0654, the threshold Mach number predicted by Haglund and Kane's theory, a direct sonic boom would have reached the ground (Figure 5). Ray-tracing simulation further showed that the aircraft should be able to fly only at Mach 1.05 in order to have a 500 m clearance of a caustic on the ground (Figure 6).

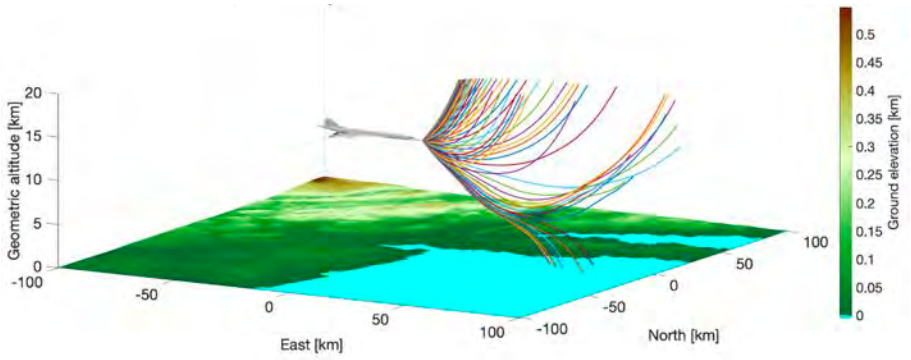

Figure 5. Supersonic flight at Mach 1.0654 over New York JFK. Note the rays reaching the ground.

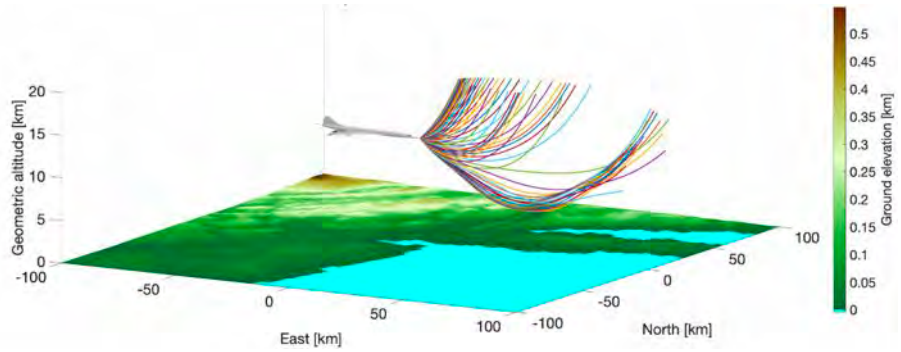

Figure 6. Mach cutoff flight at Mach 1.05 over New York JFK. Note that no rays impact the ground.

In another example, a hypothetical round-trip flight between Los Angeles and New York City at an altitude of 50,000 ft departing at 2 p.m. EDT on January 1, 2017 was examined. As shown in Figure 7, Haglund and Kane's theory overpredicts the cutoff Mach number and ground speed along the route, as compared with the values obtained from ray-tracing simulations. The eastbound case is shown to the left, and the westbound case is shown to the right in Figure 7. For the westbound case, this difference in the predicted cutoff Mach number can be as large as 0.06 of a Mach. Simultaneously, by increasing the resolution of the cutoff Mach number calculation from 0.01 to 0.005, the variations in both the cutoff Mach number and ground speed become smoother.

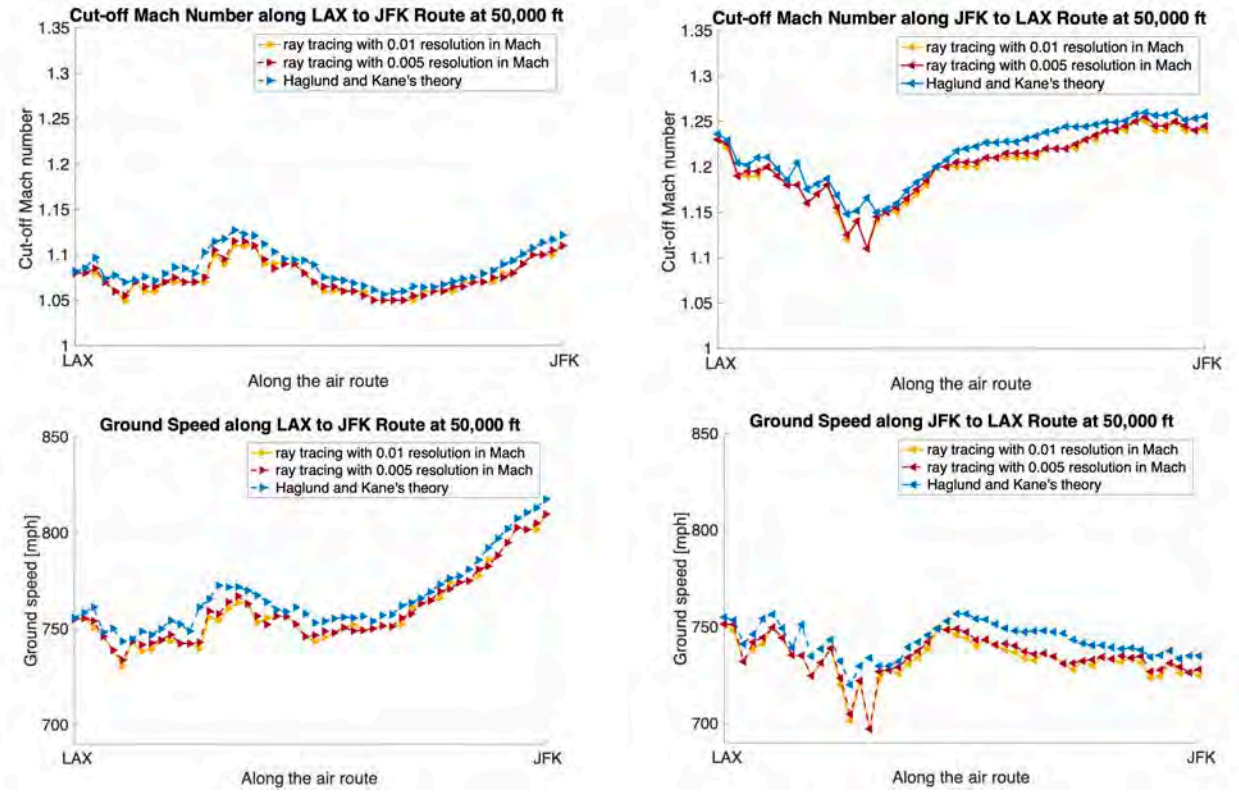

Figure 7. Variation in cutoff Mach number (top) and ground speed (bottom) along a route predicted from ray-tracing simulation vs. from Haglund and Kane's theory. Eastbound is shown to the left, and westbound is shown to the right.

To provide statistical prediction of the viability of Mach cutoff flight due to the atmosphere, ray-tracing simulations were run by using corresponding HRRR data for the three busiest air routes, two flight altitudes and 16 realistic atmospheric profiles in parallel at ICS-ACI, a cloud computing service at Penn State. The cases included in the Mach cutoff study are shown in Table 2, and Figure 8 shows a map of the air routes that were selected. All simulations used a resolution of 0.01 in Mach number, and the caustic was assumed to need to be at least 500 m above the ground. The atmosphere was further assumed to be stationary at each location along a route, so that the HRRR data produced at the takeoff time were used to represent the atmosphere along the route. For each location along those three routes, the minimum, maximum, and mean of the cutoff Mach numbers and ground speeds over 16 weather situations were calculated for eastbound and westbound flights at two flight altitudes (Figures 9–14).

Table 2. Cases in Mach cutoff study.

	Cases
Times per day in UTC	12AM, 6AM, 12PM, 6PM
Days in 2017	Jan 1, Apr 1, Jul 1, Oct 1
Flight altitudes	41,000 ft, 50,000 ft
Locations per air route	50
Air routes	LAX–JFK, SFO–MIA, DFW–JFK
Round-trip	eastbound, westbound

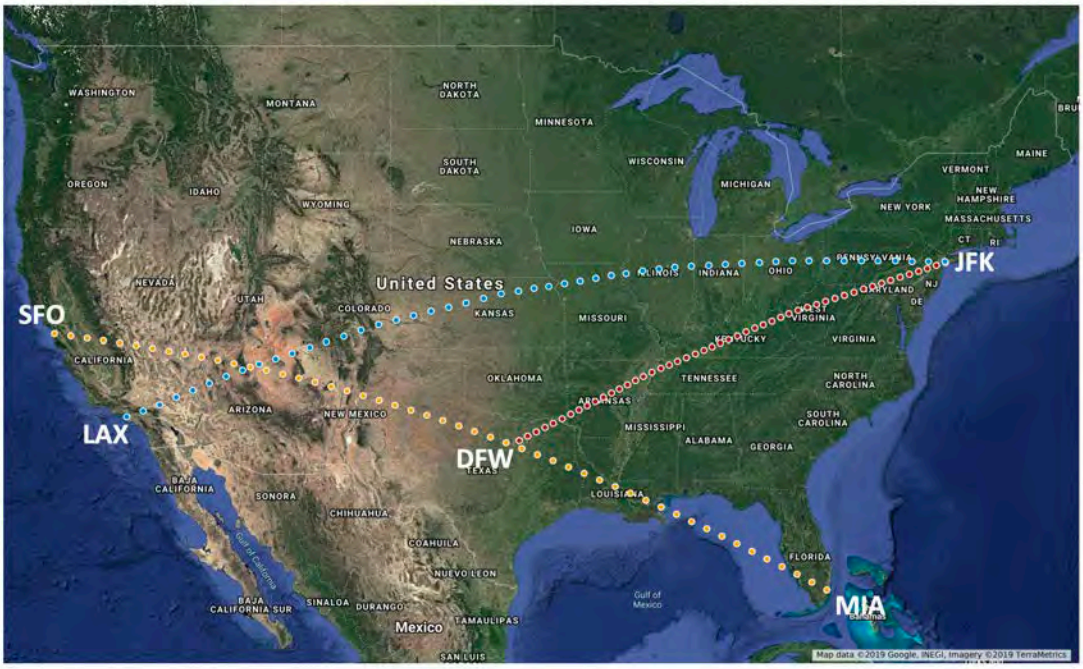

Figure 8. Three busiest air routes in the United States, selected for this study.

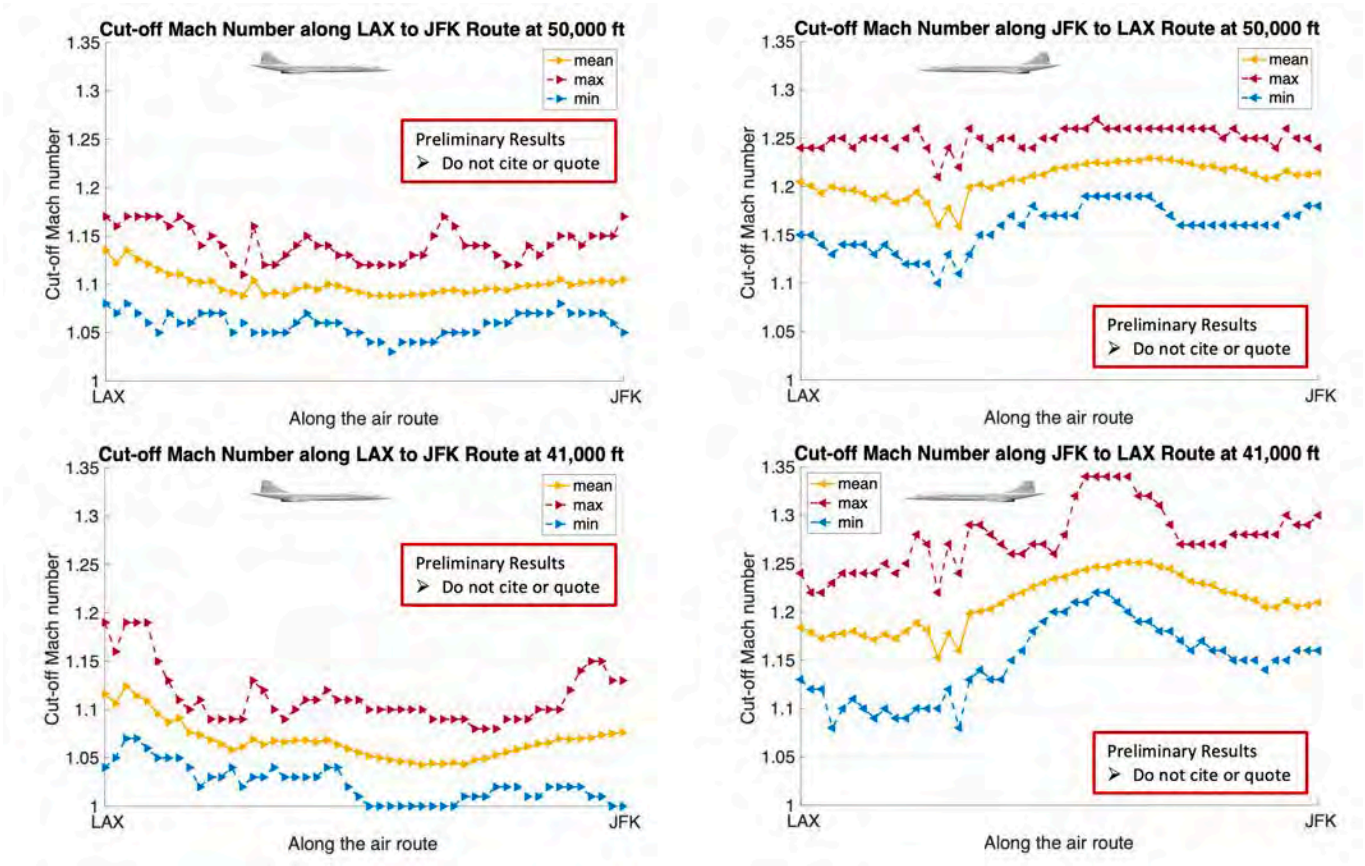

Figure 9. Variation in cutoff Mach number along the Los Angeles International Airport (LAX)–JFK route at 41,000 ft and 50,000 ft. Again, eastbound is shown to the left, and westbound is shown to the right.

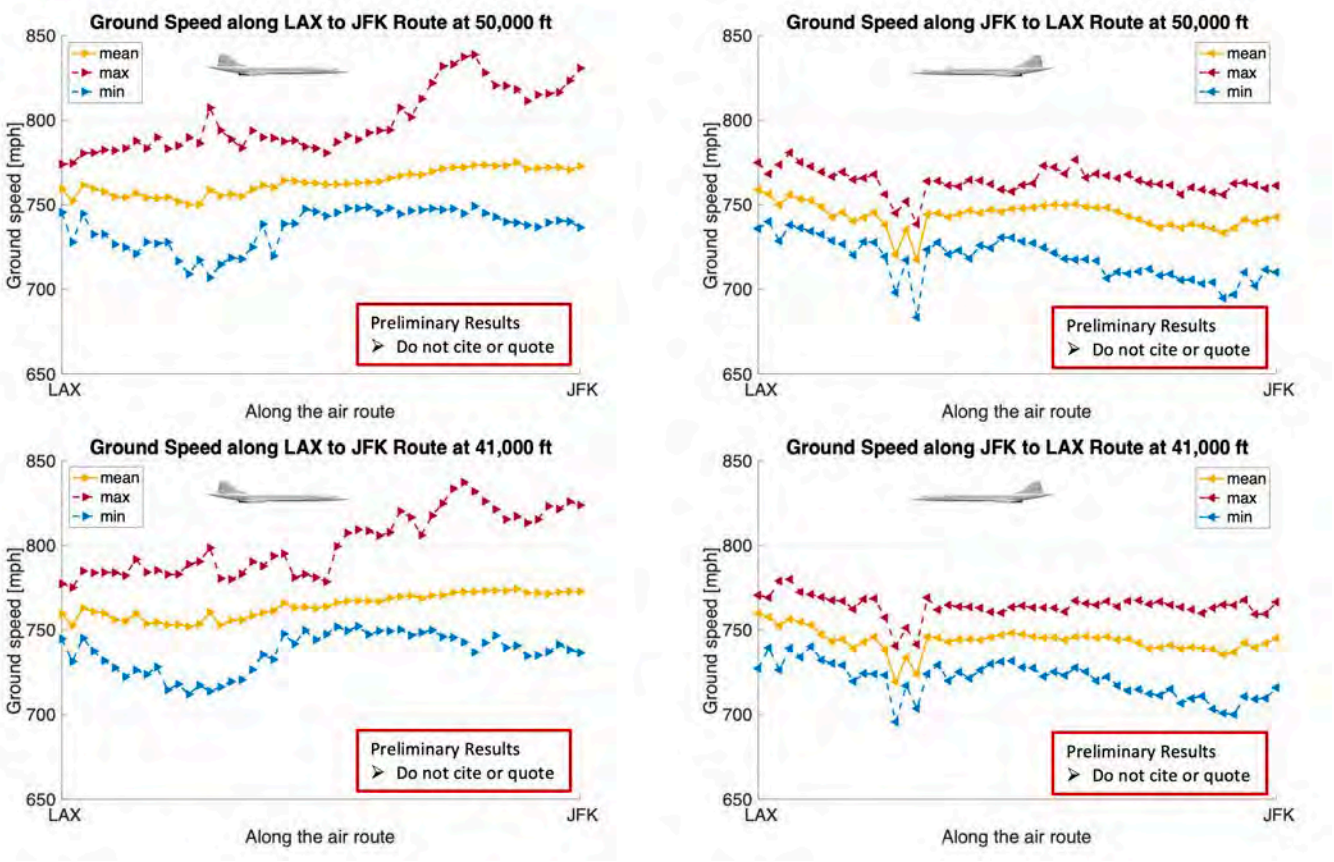

Figure 10. Variation in ground speed along the LAX–JFK route at 41,000 ft and 50,000 ft. Again, eastbound is shown to the left, and westbound is shown to the right.

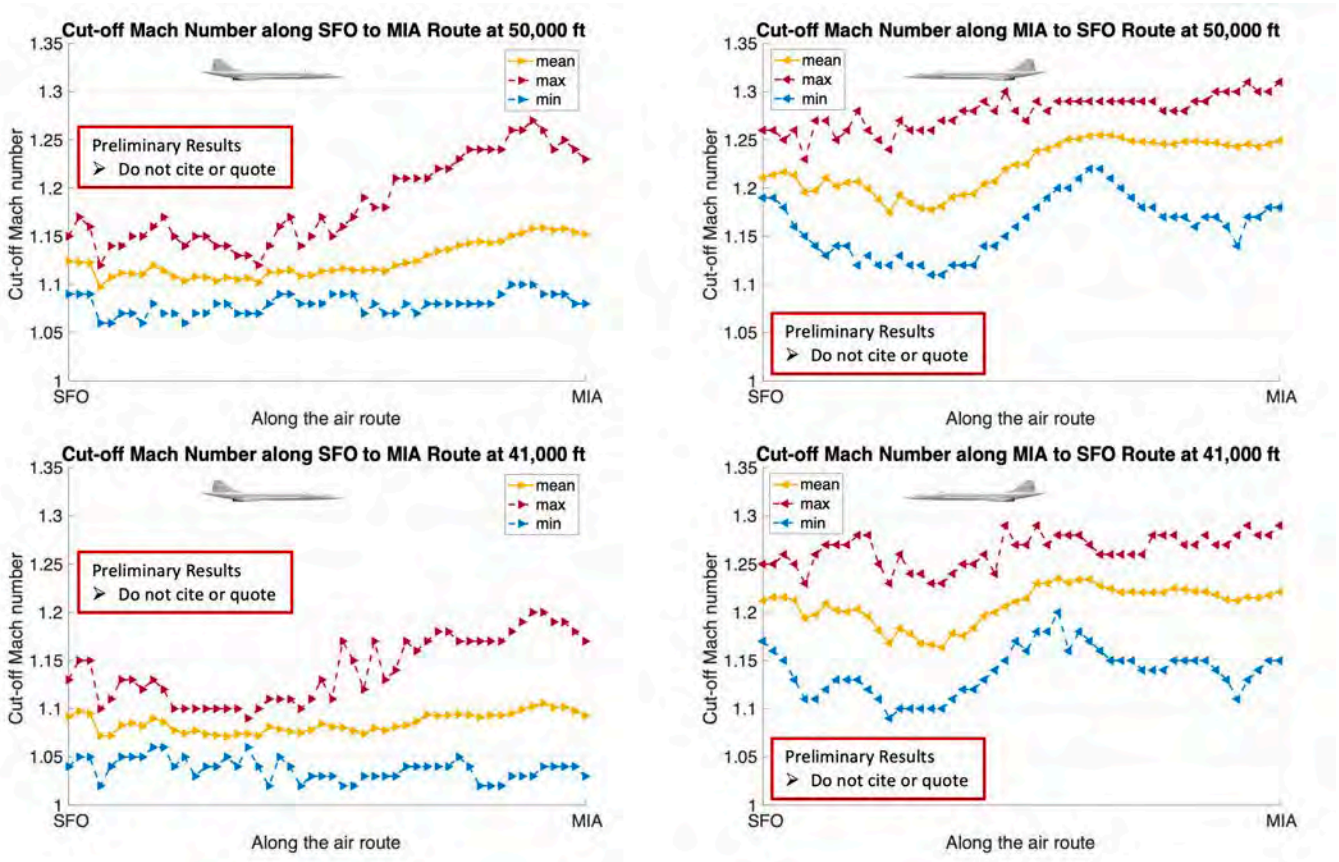

Figure 11. Variation in cutoff Mach number along the San Francisco International Airport (SFO)–Miami International Airport (MIA) route at 41,000 ft and 50,000 ft. Again, eastbound is shown to the left, and westbound is shown to the right.

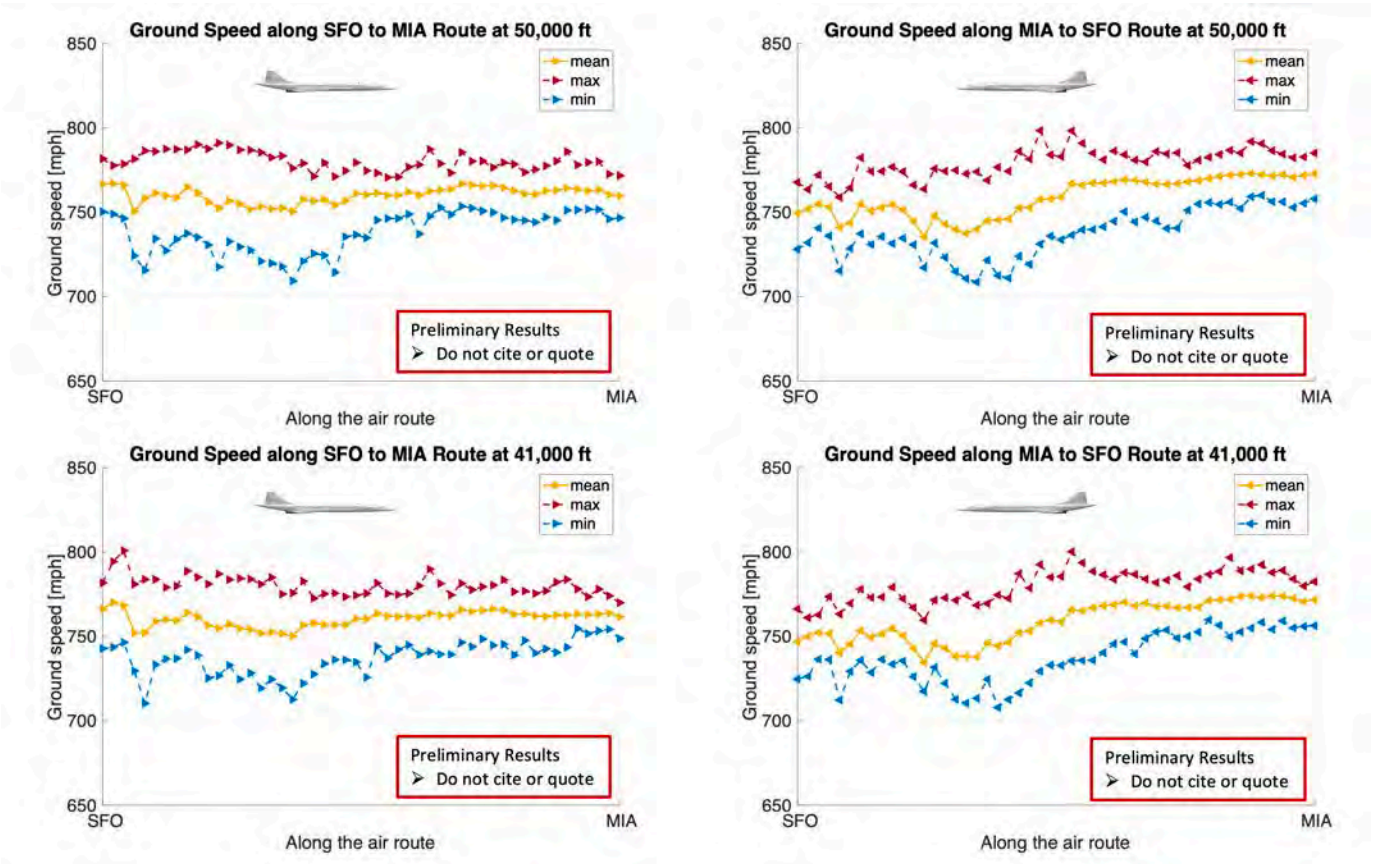

Figure 12. Variation in ground speed along the SFO–MIA route at 41,000 ft and 50,000 ft. Again, eastbound is shown to the left, and westbound is shown to the right.

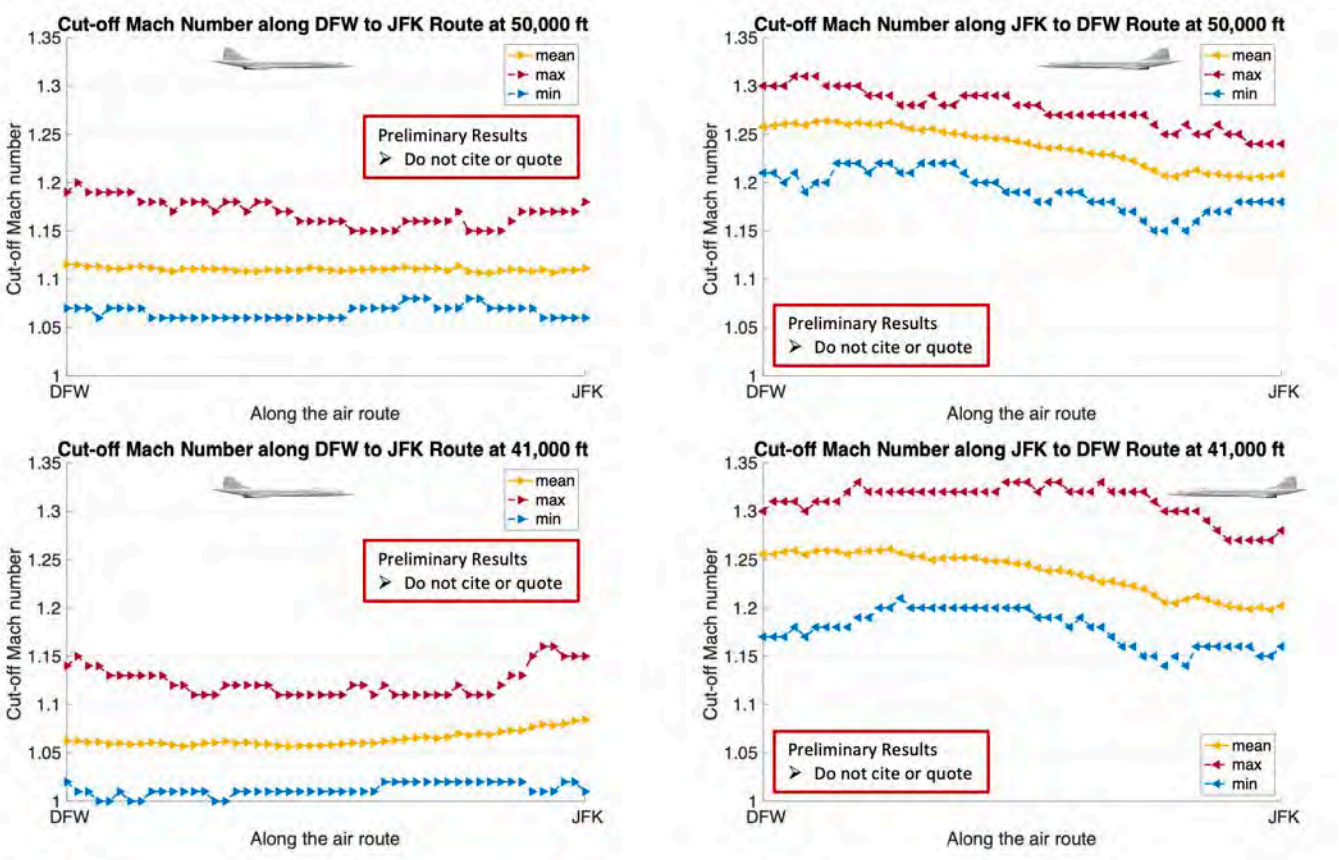

Figure 13. Variation in the cutoff Mach number along the Dallas/Fort Worth International Airport (DFW)–JFK route at 41,000 ft and 50,000 ft. Again, eastbound is shown to the left, and westbound is shown to the right.

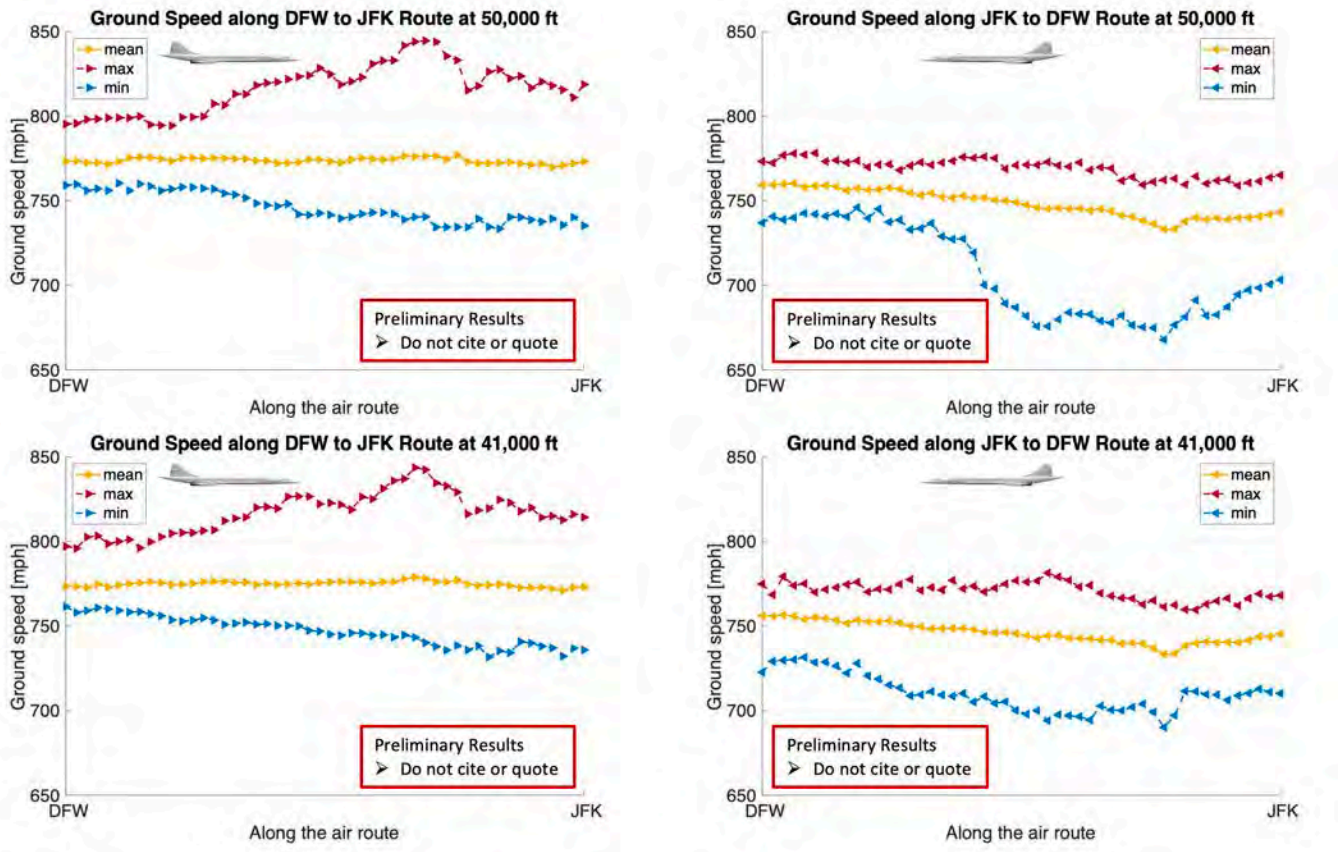

Figure 14. Variation in ground speed along the DFW–JFK route at 41,000 ft and 50,000 ft. Again, eastbound is shown to the left, and westbound is shown to the right.

As shown in Figures 9–14, Mach cutoff operations will very often work, and sometimes the aircraft can fly as fast as Mach 1.34 under Mach cutoff. However, at least for a segment of the LAX–JFK eastbound route, enabling Mach cutoff it is difficult at a flight altitude of 41,000 ft, but increasing the flight altitude can alleviate the issue in this case. Implementing Mach cutoff is easier for a westbound flight than for an eastbound flight whenever the wind is mainly blowing eastward, as seems to be relatively common. In other words, implementing Mach cutoff is easier when flying into a headwind than with a tailwind. When flying with a tailwind is inevitable, one should try to fly at an altitude at which the local longitudinal wind speed is smaller, so that the local effective sound speed can be smaller; this may help to achieve a higher Mach number that is well above Mach 1.0 if the temperature is not varying significantly in that region, although by doing so one may not be able to increase the aircraft ground speed.

In addition, in some cases, a larger cutoff Mach number can be achieved by increasing the flight altitude. However, this is not always the case. For example, in Figure 9 for a westbound flight from JFK to LAX, flying at a higher altitude did not necessarily contribute to a higher cutoff Mach number. This is primarily because, in certain cases, the dominant eastward wind speed is decreasing with increasing altitude at higher altitudes below the flight levels so that in the same region, the effective sound speed (thermodynamic speed of sound plus wind speed) increases with increasing altitude. Thus, in this particular case, a higher cutoff Mach number can be achieved by flying at an altitude at which the local effective sound speed is at a minimum. Although the flight altitude can affect the cutoff Mach number, it seems to have only a small impact on the maximum aircraft ground speed, because according to Haglund and Kane's theory, the maximum aircraft ground speed is related to the maximum speed of propagation of the shock wave beneath the airplane.

Finally, the minimum and maximum curves of both the cutoff Mach number and ground speed seem to always be separated, thus implying that either the seasonal or the daily variation in the atmosphere may significantly affect how fast an aircraft can fly under Mach cutoff. This finding led to the question of whether the temporal variation in the atmosphere at a given location during the time of the flight should be considered. To illuminate this, one example has been investigated in which the LAX–JFK eastbound route was selected, which has a travel distance of 2,469 miles. This one-way trip lasts approximately 5.5 hours for a subsonic flight. If the stationary atmosphere assumption is made so that the same atmosphere is used all the way, the simulation showed that an average ground speed of 767.5 mph could be achieved for a Mach cutoff flight, and accordingly a Mach cutoff flight departing at 12 p.m. UTC on Jan 1, 2017 from LAX to reach JFK lasts 3.2 hours. If the temporal variation in the atmosphere is included, then an hourly or a 20-minute-interpolated atmosphere can be used for the simulation, as shown in Figure 15.

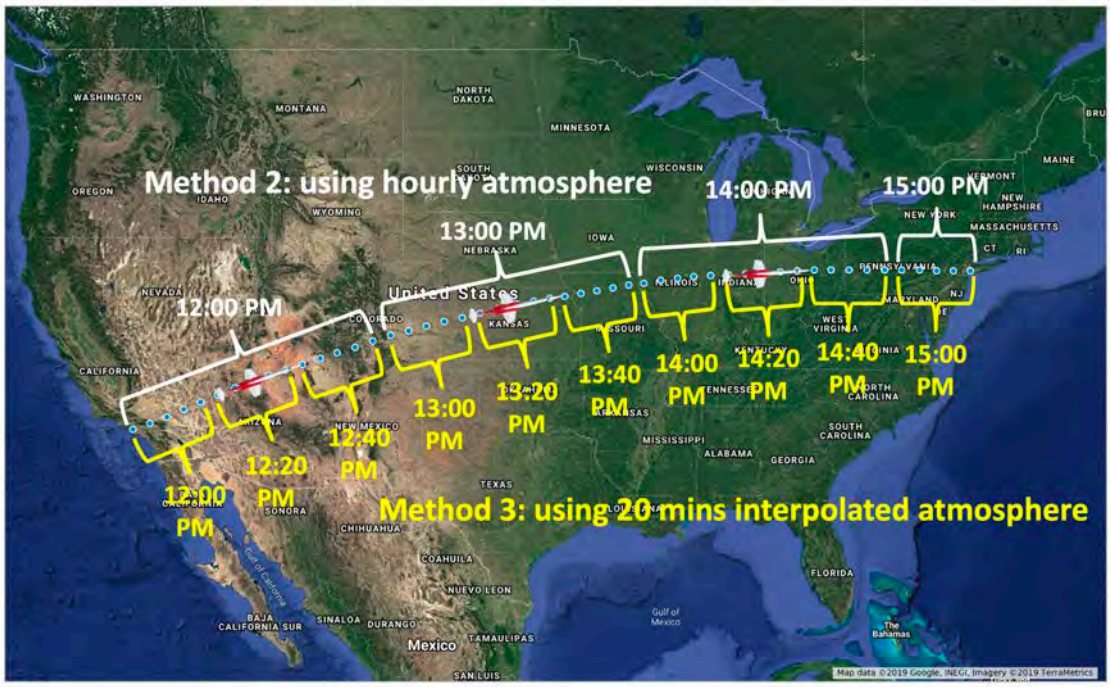

Figure 15. Considering the time variation in the atmosphere for the LAX–JFK eastbound route. Method 2 shows the atmosphere being updated hourly, and Method 3 shows the atmosphere being updated every 20 minutes.

Figure 16 shows that, when the aircraft is approaching the destination, the temporal variation in the atmosphere can accumulate, so that there is a noticeable difference in the ground speed prediction by the time the flight reaches its destination. Thus, including a time-varying atmosphere may be useful for more accurate modeling of the Mach cutoff. A preliminary conclusion based on a limited number of simulations is that the atmosphere must be updated at least hourly to accurately predict the ground speed.

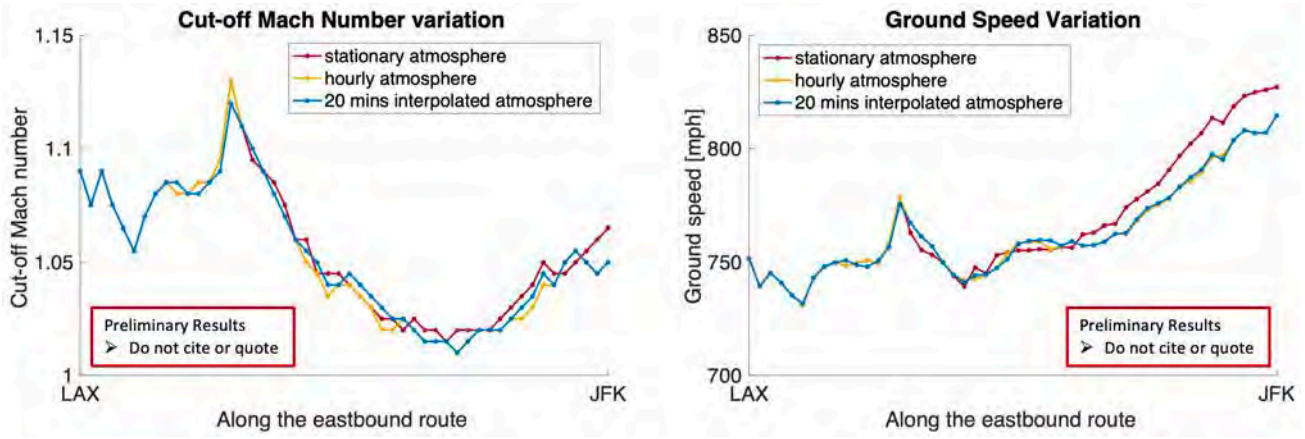

Figure 16. Impact of temporal variation in the atmosphere on the cutoff Mach number and ground speed for the LAX–JFK eastbound route taking off at 12 p.m. UTC on Jan 1, 2017 with a flight altitude of 12.5 km. There is no clear trend in the cutoff Mach number, but the ground speed accumulates a difference in ground speed upon approach to JFK.

Milestone(s)

Milestone	Date
A 3-D ray-tracing algorithm had been developed to read in HRRR data that can include a local horizontal variation in the atmosphere.	February 28, 2019
A parallelized version of the ray-tracing algorithm had been developed that can run by using the Penn State cloud computing service.	April 30, 2019
A preliminary statistical analysis of the viability of Mach cutoff flight due to atmosphere was performed.	August 31, 2019

Major Accomplishments

In this research, a 3-D ray-tracing algorithm has been developed for the acoustical model of Mach cutoff flight, which can read in realistic atmospheric data including arbitrary speed of sound variations as well as arbitrary 3-D winds. It shows that ray-tracing simulation can be more accurate than Haglund and Kane's theory in predicting the viability of Mach cutoff flight. Ray-tracing simulations were then run by using HRRR data combined with three busiest air routes, two flight altitudes, and 16 realistic atmospheric profiles in the year of 2017, to enable statistical prediction of the viability of Mach cutoff flight. This research shows that Mach cutoff operations will very often work if the atmosphere is sufficiently well known. Enabling Mach cutoff is easier for a westbound flight than an eastbound flight. In some cases, a larger cutoff Mach number can be achieved by increasing the flight altitude, which is not always true. Although the flight altitude can affect the cutoff Mach number, it seems to have only a small impact on the maximum aircraft ground speed. Either the seasonal or daily variation in the atmosphere may significantly affect how fast an aircraft can fly under Mach cutoff. For accurate modeling, the time variation in the atmosphere during the flight should be included.

Publications

Published conference abstract

Huang, Z. & Sparrow, V. (2019). Predicting the statistical occurrence of Mach cutoff using a 3-D ray tracing model and high-resolution weather data. Journal of the Acoustical Society of America. 146(4, Pt. 2) 2781

Outreach Efforts

N/A

Awards
None.

Student Involvement
Zhendong Huang is the graduate research assistant supported by Project 42 at Penn State on this task. He is pursuing his Ph.D. in the Penn State Graduate Program in Acoustics.

Plans for Next Period
N/A

References
Benjamin, S.G., Weygandt, S.S., Brown, J.M., Hu, M., Alexander, C.R., Smirnova, T.G., & Lin, H. (2016). A North American hourly assimilation and model forecast cycle: The rapid refresh. Monthly Weather Review. 144(4) 1669-1694

Blaylock, B.K., Horel, J.D., & Liston, S.T. (2017). Cloud archiving and data mining of High-Resolution Rapid Refresh forecast model output. Computers & Geosciences. 109 43-50

Haglund, G. & Kane, E. (1973). Flight test measurements and analysis of sonic boom phenomena near the shock wave extremity. NASA Report CR-2167

Maglieri, D.J., Hilton, D., Huckel, V., Henderson, H., & McLeod, N. (1971). Measurements of sonic boom signatures from flights at cutoff Mach number. NASA SP-255

Nichols, J. (1971). A note on the calculation of 'cut-off' Mach number. Meteorological Mag. 100 33-46

Ostashev, V.E., Hohenwarter, D., Attenborough, K., Blanc-Benon, P., Juvé, D., & Goedecke, G.H. (2001). On the refraction law for a sound ray in a moving medium. Acta Acustica united with Acustica. 87(3) 303-306

Perley, R. (1977). Design and demonstration of a system for routine, boomless, supersonic flights. FAA Report No. FAA-RD-77-72

Pierce, A.D. (1989). Acoustics: An introduction to its physical principles and applications. (1989 Ed.) Woodbury, N.Y: Acoustical Society of America

Plotkin, K., Matisheck, J., & Tracy, R. (2008). Sonic boom cutoff across the United States. In 14th AIAA/CEAS Aeroacoustics Conference (29th AIAA Aeroacoustics Conference), AIAA Paper 3033

Shurcliff, W. (1970). S/S/T and sonic boom handbook. Ballantine, p. 63

Task 2 - Subjective Study on Annoyance, Metrics, and Descriptors
The Pennsylvania State University

Objective(s)
- Identify the key perceptual attributes of Mach cutoff ground signatures
- Determine how these attributes are correlated with the annoyance ratings of these signals
- Identify a metric appropriate for predicting annoyance due to Mach cutoff ground signatures
- Assess the relative annoyance of Mach cutoff ground signatures compared with road, rail, and subsonic aircraft traffic noise

Research Approach
Introduction
This research will provide the first major contribution to the body of literature on the perception of Mach cutoff. The ultimate goal of this work is to identify a metric that can be used to predict annoyance due to Mach cutoff flights. Subjective testing data will inform metric selection and corresponding values to use for certification. Because Mach cutoff ground signatures are unique sounds that have not been part of the public's day-to-day experience, the impact on community annoyance is difficult to predict. In addition, these signatures are perceptually different from N-shaped sonic booms. As such, new subjective tests are necessary to assess perception of these sounds and ultimately predict annoyance in communities.

The task is subdivided into three studies: (a) descriptor study, (b) annoyance factor study, and (c) absolute annoyance study. At the end of the last period, Study 1, the descriptor study, was completed, identifying descriptors for sounds heard on the ground during Mach cutoff operations. Study 2, the annoyance factor study, has now been completed, including

investigation of the relationships among perceptual qualities, metrics, and perceived annoyance. The third study, the degree of annoyance study, which was in development last period, is now complete. The purpose of this study was to obtain the absolute annoyance ratings and the relative preference for the signatures relative to other common transportation noises, i.e., road, rail, and subsonic aircraft noise, and to further evaluate the proposed metrics from the second study to predict community annoyance response to Mach cutoff ground signatures.

These perceptual studies were approved for human subjective testing by the Institutional Review Board of The Pennsylvania State University (Penn State IRB).

Perceptual study 1: Descriptor study (summary)

Introduction

Study 1 was designed as an exploratory study to investigate terms, or descriptors, used by laypersons to describe what is heard during Mach cutoff operations. The primary objectives were to identify perceptual attributes of Mach cutoff ground signatures and to identify the descriptors associated with these attributes. A secondary objective was to characterize stimuli from NASA's "Farfield Investigation of No-boom Thresholds" (FaINT) (Cliatt et al., 2016) to aid in stimulus selection in Study 2.

This study was introduced in the Y1 (2016–2017) report and described in detail in last year's Project 42 Y2 (2017–2018) annual report. This section will give an overview of the study design and results for completeness and to provide a background for the other perceptual studies.

Study design

Free Choice Profiling (Williams & Langron, 1984) was selected as the subjective testing method for Study 1. First, subjects listened to a set of 12 stimuli and provided (by typing into a text box) their own terms to describe the stimuli. Second, subjects completed a short interview process to select three to five terms from their lists that they believed to represent the most important features of the stimuli. Third, subjects rated each of a set of 24 stimuli on the refined set of three to five terms that the subjects selected. All stimuli in both sets were selected from the FaINT database. A total of 28 subjects participated, ranging in age from 18 to 38 years (median 22 years), with 14 males and 14 females.

Generalized Procrustes Analysis (GPA) (Gower, 1974) was used to generate a "consensus space" to unify the various ratings of each subject for each of their respective descriptors. Individual ratings of each stimulus are transformed into this consensus space, such that each subject's ratings become directly comparable. In this space, traditional analyses, e.g., linear regression and analysis of variance (ANOVA), can be conducted.

Results

GPA produced a consensus space with three principal components or factors, as many as three of which could be deemed significant. Factor 1 explained 82.2%, factor 2 explained 6.3%, and factor 3 explained 5.0% of the variance. Average transformed ratings, or factor scores, of the stimuli were calculated, thus allowing for comparisons and analyses across the various subjects' datasets. The factor scores were used to calculate correlations, or factor loadings, between the factors and each of the subjects' descriptors, and the descriptors were placed in the perceptual space, as shown in Figure 17. The placement of the descriptors in the perceptual space allowed for interpretation of the factors themselves. The positive end of factor 1 included terms related to loud sounds, such as "explosive," "powerful," and "thunderous," whereas terms related to quiet sound were located opposite. On the positive end of factor 2 were terms related to sounds with broad frequency content, such as "white noise" and "whistling," whereas terms related to sounds dominated by low frequencies, such as "rumbly" and "bass-heavy," were located opposite. According to this analysis, factor 1 is associated with loudness, and factor 2 is associated with frequency content.

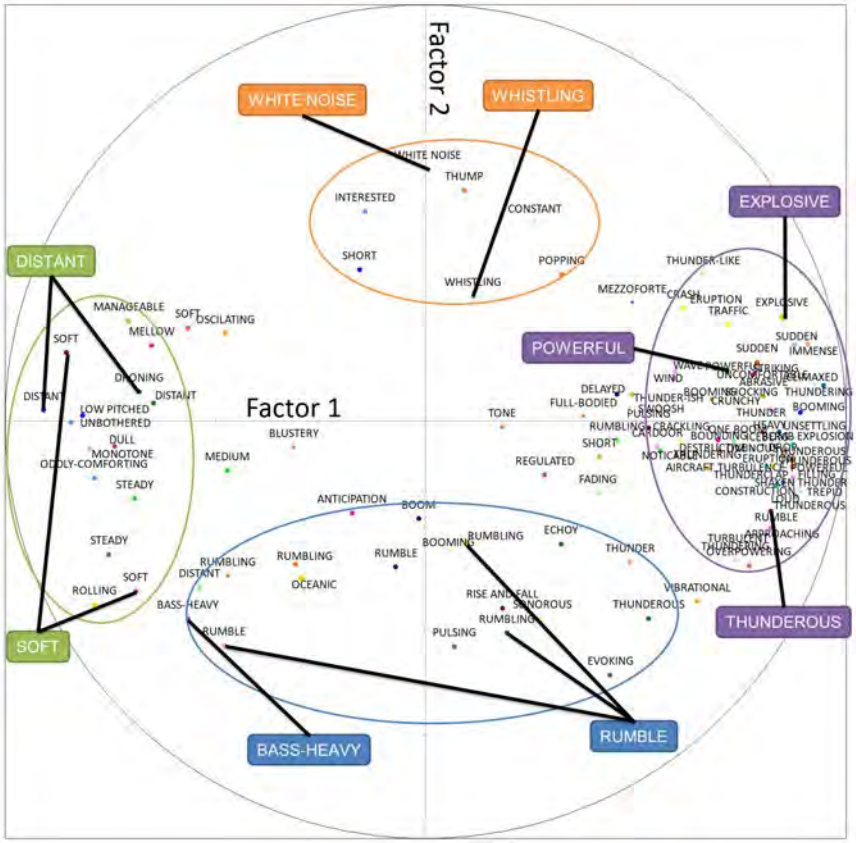

Figure 17. Descriptors placed in the consensus space. Clusters of loudness-related terms appear on the left and right, and clusters of frequency-related terms appear on the top and bottom (reproduced from the 2017–2018 annual report).

The stimuli themselves were also analyzed in the consensus space, thus enabling characterization and grouping of the stimuli for use in Study 2. Average factor scores of the stimuli were used and are plotted against the first two principal components in Figure 18. In addition, *k*-means clustering (Gaëtan, 2005) was used to group the stimuli into three clusters, which were also labeled. According to the descriptor analysis, the stimulus clusters could be described as follows: cluster 1 consisted of softer stimuli; cluster 2 had louder, more rumbly stimuli; and cluster 3 included stimuli with more high-frequency content.

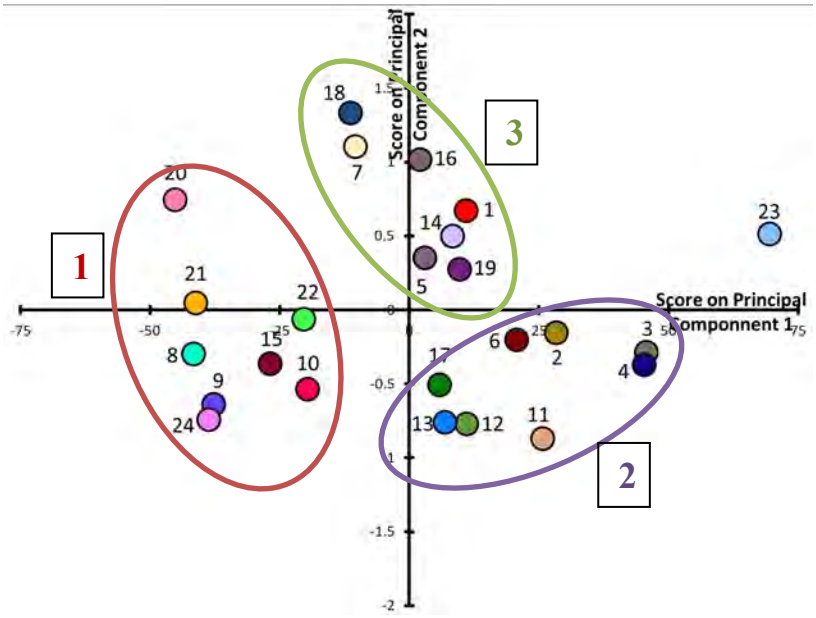

Figure 18. Average stimulus locations plotted on principal component axes. Three clusters of stimuli are highlighted: cluster 1 – soft, cluster 2 – loud, and cluster 3 – high (reproduced from the 2017–2018 annual report).

Perceptual study 2: Annoyance factor study

Study design

As described in the Y2 (2017–2018) annual report, Study 2 investigates relative perceptual differences between recorded and simulated signatures of overhead Mach cutoff flight. The key objectives in this study were to assess the relationship between perceived qualities and annoyance, to identify potential metrics for predicting perception, particularly annoyance, and to assess the impact of changing the initial portion of the Mach cutoff ground signature on annoyance. Secondary objectives included identifying any effects of demographics on the various perceptual ratings and investigating relationships among demographics, hearing thresholds, and noise sensitivity.

Two sets of stimuli were used in the study: a set of six recordings and a set of nine stimuli containing the same six recordings with three additional stimuli described below. The six recordings used in all rating sets were selected from the FaINT database (Cliatt et al., 2016) according to the results from Study 1. As mentioned above, the 24 stimuli used in Study 1 fell into three clusters (with one outlier). Two stimuli were selected from each of the three clusters to form the set of six. The six stimuli are plotted in Figure 19 and are arranged such that stimuli from the same cluster are in the same column.

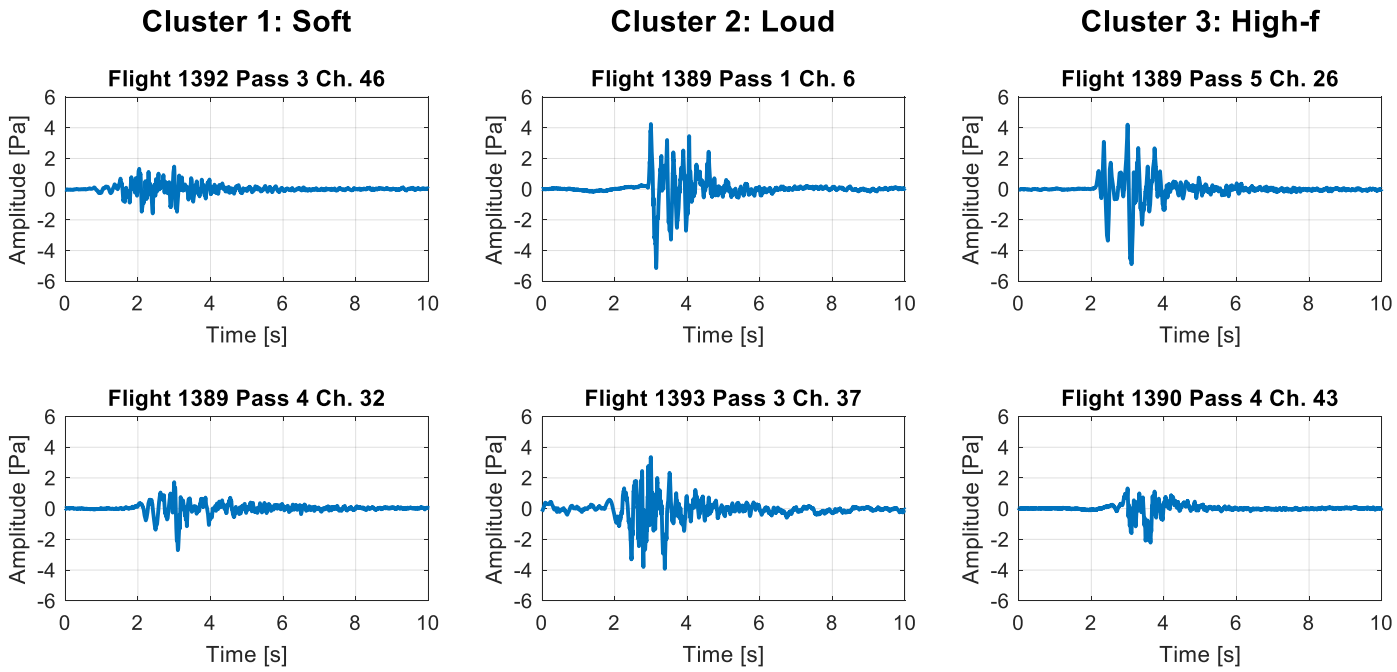

Figure 19. The six recordings selected from the FaINT dataset (ASHRAE, 2019), used as stimuli in all four rating sets in Study 2. Stimuli are grouped in columns according to the three clusters found in Study 1.

The second stimulus set consisting of nine stimuli was designed to investigate the effect of the initial decayed shock portion of Mach cutoff signatures. For traditional sonic booms, the initial shock wave dominates perception, and the post-boom noise is rarely considered. However, in Mach cutoff operations, the initial shock decays to such an extent before arriving at the ground that the post-boom noise may be more perceptually significant. The extent of this effect has not been evaluated experimentally. Therefore, additional stimuli were added to the annoyance set and were intended to separate the effect of post-boom noise from the effect of the initial decayed shock.

Three simulated shocks were generated, starting from two recordings of typical N-shaped booms. Both recordings were numerically propagated past the caustic to one diffraction-boundary-layer thickness below the caustic. The third (quietest) shock came from the louder of the two recordings propagated two diffraction-boundary-layer thicknesses below the caustic. A broadband gain was applied to decrease the amplitude of all three shocks, on the basis of the limitations of the reproduction facility. The three simulated shocks were then added to one of the six stimuli selected to not have any audible shock, thus creating three new stimuli. The simulated shocks were generated by Zhendong Huang in Task 1 of this project. The three new composite stimuli containing the three synthesized shocks can be seen along with the original recorded stimulus in Figure 20. The detailed plot on the right shows that the synthesized waveforms varied in both amplitude and steepness. The three stimuli containing simulated shocks were added to the set of six to form a set of nine stimuli used in rating annoyance.

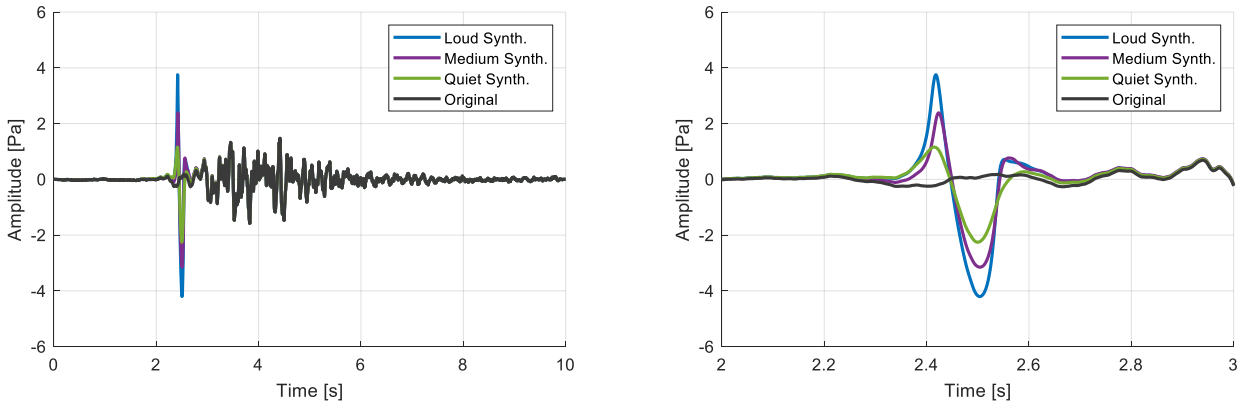

Figure 20. The three additional stimuli included in the annoyance rating set, plotted along with the original FaINT recording. The full waveforms are shown on left, with a detailed view of the synthesized shocks on the right. Note: the four stimuli differ only where the synthesized shock was added, so they look like one waveform before 2 seconds and after 3 seconds, respectively.

The method of paired comparisons with a rating scale (Parizet et al., 2005) was selected as the listening test method for this study. In this method, each stimulus is compared directly to every other stimulus. For each possible pairing of stimuli, subjects determine which of the stimuli falls higher on a given comparative scale and rates how much higher the stimulus should sit on the scale. Subjects listened to the set of six recordings and rated them on three comparative scales: thunder (how "thunderous" is the stimulus?), rumble (how "rumbly" is the stimulus?), and swoosh (how "swooshing" is the stimulus?), the three factors resulting from Study 1. Subjects rated the set of nine stimuli on a comparative annoyance scale (how "annoying" is the stimulus?).

Data collection

Subjective testing and stimulus reproduction took place in the "Auralization and Reproduction of Acoustic Sound-Fields" (AURAS) facility (Neal, 2015) on Penn State campus (Figure 21). The facility consists of 32 loudspeakers housed in an anechoic chamber; 30 mid- to high-frequency speakers are arranged in an approximately spherical arrangement surrounding a single listening position. This arrangement of loudspeakers allows for reproduction by using third-order Ambisonics, a technique for reproducing spatial characteristics of a sound-field (Gerzon, 1973). Two 18-inch-driver subwoofers were used to produce characteristics of the stimuli below 80 Hz. For Study 2, all stimuli were processed spatially to appear to come from in front of the listener, 30° above the horizontal, to be representative of an aircraft flying in the distance.

Figure 21. The AURAS facility at Penn State. The photo on the left shows the anechoic chamber as set up for testing. The center image shows the subwoofers with a two-way loudspeaker included for scale. The final image on the right shows a schematic of the arrangement of the loudspeaker positions around the central listening point.

Paired comparison with a rating scale was implemented with the testing interface shown in Figure 22. For each pair of stimuli, subjects used the testing interface to compare the two stimuli. Subjects were instructed to listen to each stimulus at least once by using the "play A" and "play B" buttons. The subject then rated the difference on a continuous scale in terms of how much better the given attribute described one or the other stimulus. For the set in which the attribute was annoyance, A rating of -2 = "A is much more annoying than B" and a rating at the opposite end of the scale, and a rating of +2 = "B is much more annoying" than A."

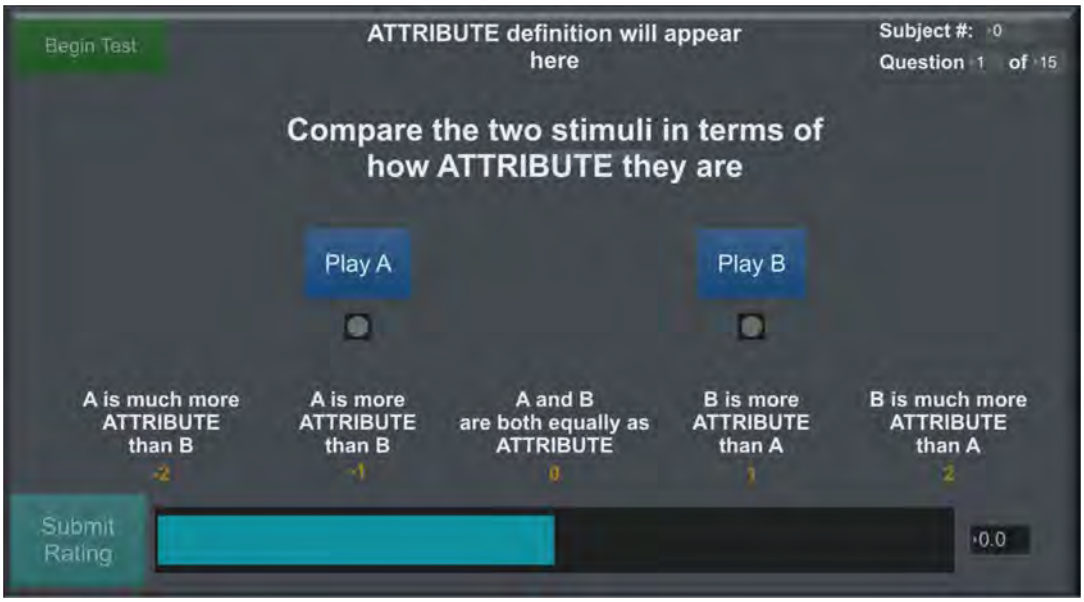

Figure 22. Study 2 subjective testing interface. Subjects clicked on the "play A" and "play B" buttons, decided which stimulus had more of the given attribute, i.e., "annoying," "thunderous," "rumbly," or "swooshing," and rated how large that difference was by using the slider bar (reproduced from the 2017–2018 annual report).

A total of 42 subjects (18 male) ranging from 18 to 60 years of age participated in the study, with a mean age of 36.9 and a standard deviation of 13.1 years. Subjects were required to have hearing thresholds of a 25 dB hearing level (HL) or lower in the 250–4000 Hz octave bands. Hearing thresholds were measured at the time of testing both to ensure that the criteria were met and to allow for post-hoc analyses of demographic effects. Noise sensitivity was also measured with the Weinstein Noise Sensitivity Survey (Weinstein, 1978). Specific age and gender demographics are shown in Figure 23. There were fewer subjects in the higher age groups, but overall the subjects' ages were well distributed. The gender ratio was skewed slightly, with a 4:3 female-to-male ratio. The potential effects of demographics are explored in the analysis, but it will be shown that the demographics did not affect the other results of this study.

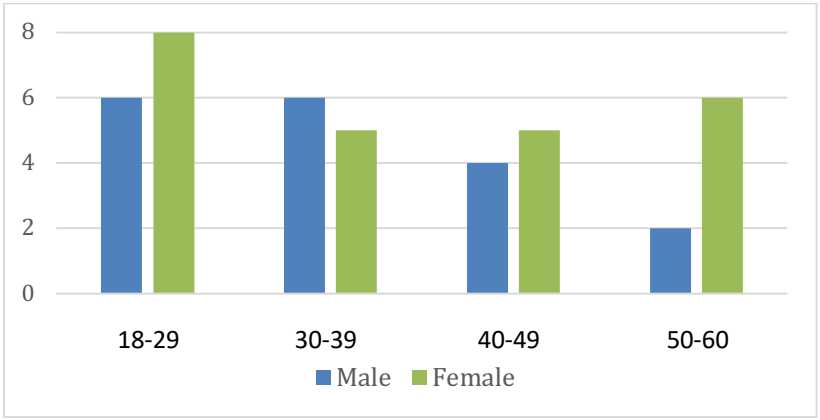

Figure 23. Demographic breakdown of Study 2 participants. The number of participants decreased with age; more females participated than males.

Data analysis methods

Before any analyses were conducted, the individual comparison ratings were transformed into a single rating for each stimulus. The conversion of the comparison ratings to a single rating for each stimulus was achieved by summing across all ratings for a given stimulus. If a stimulus was rated higher in a given comparison, the absolute value of the comparison rating was added to the stimulus rating. Otherwise, nothing was added. Thus, for each comparison, only one of the two stimuli being compared would have its stimulus rating increased. This procedure was performed separately for each perceptual scale and each subject, thus resulting in one rating from each subject for each stimulus on each scale.

Analyses were targeted to answer five separate questions:

1. How are the perceptual attributes of thunder, rumble, and swoosh related to annoyance?

   This question investigates the relationship between the annoyance ratings and the other perceptual attributes. However, analysis for this question was complicated by covariance (interdependent relationships) among the thunder, rumble, and swoosh ratings. Typical linear regressions assume that the input variables are independent of one another, but the results obtained tended to increase and decrease together. It was therefore necessary to find a new factor space in which traditional analysis could be run. In Study 1, the ratings were transformed by using GPR (Gower, 1974), which was able to handle the differences in rating scales across subjects. In this study, all subjects used the same rating scale, so principal component analysis (PCA) and Varimax rotation were used to make this necessary perceptual space. PCA (Johnson & Wichern, 2013) created three orthogonal factors out of the three rating scales, which, according to the definition of orthogonality, have zero covariance. The factors were then rotated with a Varimax rotation (Johnson & Wichern, 2013) to create three new orthogonal factors, each closely related to the ratings on one of the three perceptual scales. (The Varimax rotation process leads to a set of orthogonal regressors, which is assumed in linear regression.) Each factor was treated as a new perceptual scale similar to but separate from the original attribute ratings. Linear regression was used to model the effects of these factors on the annoyance ratings. Additionally, linear regression was used to model the effects of the principal components on the annoyance ratings.

2. Which metrics form the best model for predicting each perceptual factor?

   As a first pass, correlation testing was used to compare the predictive power of each metric individually for each perceptual attribute. For more detailed analysis allowing for a linear combination of multiple metrics, a stepwise regression (Kushner et al., 2004) was used to select which metrics formed the best set for predicting ratings. This procedure was carried out on the rating data for each perceptual attribute (annoyance, thunder, rumble, and swoosh). Metrics that were investigated as possible candidates to predict the perceptual ratings were the following: sound exposure level (SEL), weighted by B, C, and E (SEL_X); perceived loudness (PL) (Stevens, 1972); perceived sound exposure level (PL_{SEL}) (Cliatt et al., 2016); average sharpness (S_{av}) (Zwicker & Fastl, 1990); and three exploratory metrics based on RC Mark II (ASHRAE, 2019). After stepwise regression identified the metrics for the

model, linear regression was run to model the ratings by using the metrics. Finally, correlation data were processed to determine whether other metrics were statistically comparable in terms of predictive power.

3. How does the addition of a synthesized decayed shock to a Mach cutoff stimulus influence annoyance?

   This question was explored to determine whether the perception of the decayed shock had a strong influence on the annoyance ratings and thus would need to be studied in more detail. ANOVA modeled the effect of modifying the decayed shock on annoyance ratings. For this analysis, annoyance ratings were calculated in two separate ways, differing in which of the comparisons were summed across. The first set of ratings was calculated by using only the comparisons between the four stimuli of interest, namely the original recording and the three modified stimuli (three comparisons per stimulus). This set of ratings allowed for the detection of differences in annoyance ratings when stimuli with different decayed shock signals (or the absence of a decayed shock in the case of the original recording) were directly compared. The second set of ratings was calculated by using only the comparisons to the other stimuli and not direct comparisons between the stimuli of interest (five comparisons per stimulus, one for each of the other five recordings). This set enabled investigation of whether inclusion of different decayed shock signatures change annoyance ratings relative to other more general Mach cutoff stimuli. ANOVA was then run twice, and each rating set was modeled on the categorical effect of the stimulus number.

4. Do the demographics of the participants affect the ratings?

   This question was asked to ensure that the results of this study obtained by using the sample of subjects would represent general trends in the broad population rather than being influenced by the sample. Ratings were analyzed with multivariate analysis of covariance (MANCOVA) (Johnson & Wichern, 2013)**Error! Reference source not found.**, modeling the ratings on each stimulus as a linear combination of demographics, including age, gender, noise sensitivity score, and hearing threshold. Specifically, age was divided into four categories: 18–29, 30–39, 40–49, and 50–60 years of age. Noise sensitivity scores were assessed with Weinstein's Noise Sensitivity Scale (Weinstein, 1978). Hearing thresholds were divided into low, mid, and high frequencies by averaging across the 125- and 250-; 500- and 1000-; and 2000-, 4000-, and 8000-Hz octave bands, respectively. Interaction effects between demographics and stimulus number were also included. Including these interaction effects was essential, because any non-interaction effect would reasonably be zero. Non-interaction effects would average across stimuli, and the averages of the comparisons were always zero.

5. How are demographic factors, hearing thresholds, and noise sensitivity related?

   This question was explored as a point of interest. Analysis of covariance (ANCOVA) was used to examine the effects of the other demographics on noise sensitivity, and multivariate analysis of variance (MANOVA) was used to analyze the effects of demographics on the hearing thresholds (without noise sensitivity included). The inputs to the ANCOVA were the same demographics detailed above except for noise sensitivity, and the inputs to the MANOVA were also the same demographics, except with the average low-, mid-, and high-frequency hearing thresholds removed.

Results part 1 – Factor analysis of attribute ratings

Orthogonal factors were used to identify which of the three perceptual attributes considered (thunder, rumble, and swoosh) was most strongly linked with annoyance. Three orthogonal factors were formed with a PCA followed by a Varimax rotation, each primarily correlated with one of the three rating scales. Correlation between the Varimax factors and the original rating scales is provided in Table 3. As can be seen, factor 1 is primarily associated with thunder ratings, factor 2 is primarily associated with rumble, and factor 3 is primarily associated with swoosh. Because of these strong correlations, further analyses can be interpreted by assuming that the factor scores approximate the original attributes. A linear regression was run, modeling average annoyance ratings as a linear combination of the average Varimax factor scores. This model accounted for 99.4% of the variance of average annoyance ratings. Factor 1 (associated with thunder) had the largest effect on annoyance ratings, as shown in Table 4, though all effects were significant.

Table 3. Correlations between Varimax factors and original ratings. From the correlation values, factor 1 is associated with thunder ratings, factor 2 is associated with rumble, and factor 3 is associated with swoosh.

Attribute	Factor 1	Factor 2	Factor 3
Thunder	0.940	0.192	0.281
Rumble	0.172	0.961	0.0923
Swoosh	0.267	0.096	0.959

Table 4. Annoyance modeled as a linear combination of Varimax factor scores. Factors are listed along with their associated perceptual attributes, the regression coefficient, and the *P* values. Thunder ratings had the largest regression coefficient, indicating the strongest link to annoyance.

Factor	Related Rating	Coefficient	*P* value
Factor 1	Thunder	0.415	0.0211
Factor 2	Rumble	0.356	0.0302
Factor 3	Swoosh	0.318	0.0564

From the PCA, a single component was identified as the primary factor that best predicted perceived annoyance. PCA of the three perceptual attributes (excluding annoyance) resulted in three principal components, the first of which accounted for 59% of the total variance (across thunder, rumble, and swoosh ratings), the second of which accounted for 26%, and the third of which accounted for 15%. The first principal component was also highly correlated with annoyance ratings, with an r^2 value of 0.989. This result indicates that one common component (split among the three Varimax factors above and common to the original three rating sets) controlled the perceived annoyance.

Results part 2 – Analysis of attribute ratings and noise metrics

In a first step, each factor was tested for correlation with the entire set of metrics, which included B-, C-, and E-weighted SEL, PL, PL_{SEL}, S_{av} (Neal, 2015), and three RC-based metrics ($RC_{xx\text{-}xx}$). Weighted SEL involved application of a frequency-based weighting to the stimulus to calculate a weighted SEL. PL was calculated with Steven's Mark VII frequency and loudness weighting (Stevens, 1972). PL_{SEL} was developed by the FaINT research team at NASA. For S_{av}, the Zwicker method was used to calculate sharpness and then averages across the stimulus.

The RC-based metrics are exploratory and were developed for this study. They are based on Room Criteria Mark II (ASHRAE, 2019), a background noise room acoustics metric that includes a quality indicator for "rumble." The RC-based metric is calculated as follows. First, the sound being analyzed is filtered into octave bands, and decibel levels are calculated in each octave band. The average mid-frequency decibel level is used to set a baseline contour that is flat below 31 Hz and has a -5 dB/octave slope above 31 Hz. The contour is adjusted to cross through the average mid-frequency rating. Decibel deviations from the contour are averaged across the 8-, 16-, 31-, and 63-Hz octave bands, and the result is the value of the experimental metric. Three metrics were calculated by using different frequency ranges to select the baseline contour: $RC_{.25\text{-}.5k}$ uses the 250- and 500-Hz octave bands, $RC_{.5\text{-}1k}$ uses the 500- and 1000-Hz octave bands, and $RC_{.25\text{-}1k}$ uses the 250-, 500-, and 1000-Hz octave bands.

For each perceptual attribute, the same procedure was used to analyze the data. First, correlation coefficients between the attribute and each of the metrics considered were calculated. The correlation analysis also indicated which metrics' correlations were statistically the same. Metrics were then input into a stepwise regression, which was used to select one or more metrics as the best model for the perceptual attribute. According to the correlation values, alternate models were then also run by using the metrics that statistically had a similar correlation coefficient.

For annoyance, the correlation analysis identified SEL_B and SEL_E as the metrics most highly correlated with annoyance ratings (Figure 24). They were identified to not have statistically different correlations. Stepwise regression identified SEL_B as the best candidate metric for predicting annoyance. Regression was therefore run for modeling annoyance with SEL_B and SEL_E, as shown in Table 5. The two regressions produced similar results, and whereas SEL_B had a lower *P* value, the two were not statistically different in terms of predictive power. Both trend lines were calculated and plotted in Figure 25.

These analyses indicate that annoyance is best modeled with only one metric, in agreement with the factor analysis suggesting that one underlying component predicts annoyance. From the metrics selected to predict annoyance, the underlying perceptual attribute is likely to be loudness.

Table 5. Annoyance predicted with SEL_B and SEL_E. Both metrics predict annoyance well, with similar results.

Attribute	Metric	Coefficient	Standard Error	*P* value	Model r^2
Annoyance	SEL_B	0.169	0.0162	< 0.0001	0.304
Annoyance	SEL_E	0.146	0.0150	< 0.0001	0.276

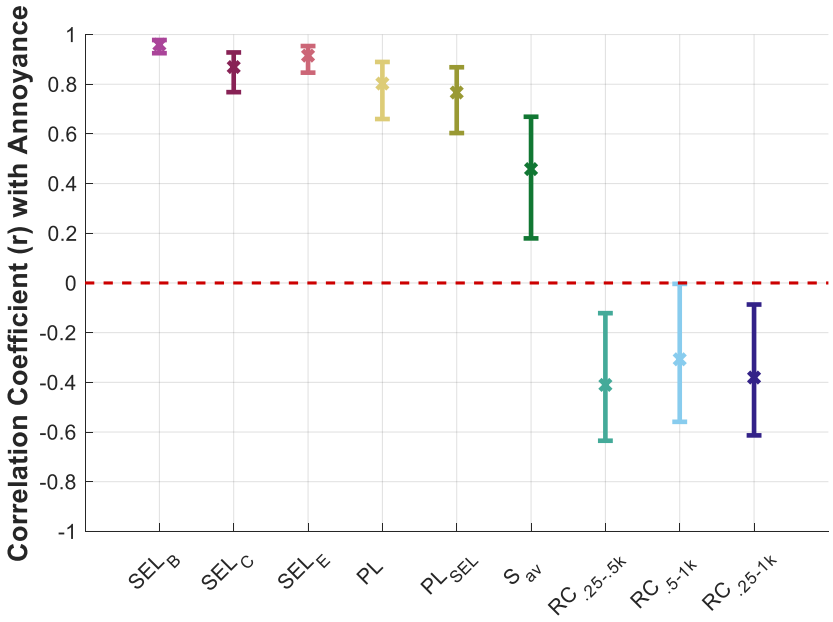

Figure 24. Correlation between annoyance ratings and each of the nine considered metrics. For each metric, the sample correlation is plotted with 95% confidence intervals also indicated. SEL_B and SEL_E had the strongest correlation with annoyance.

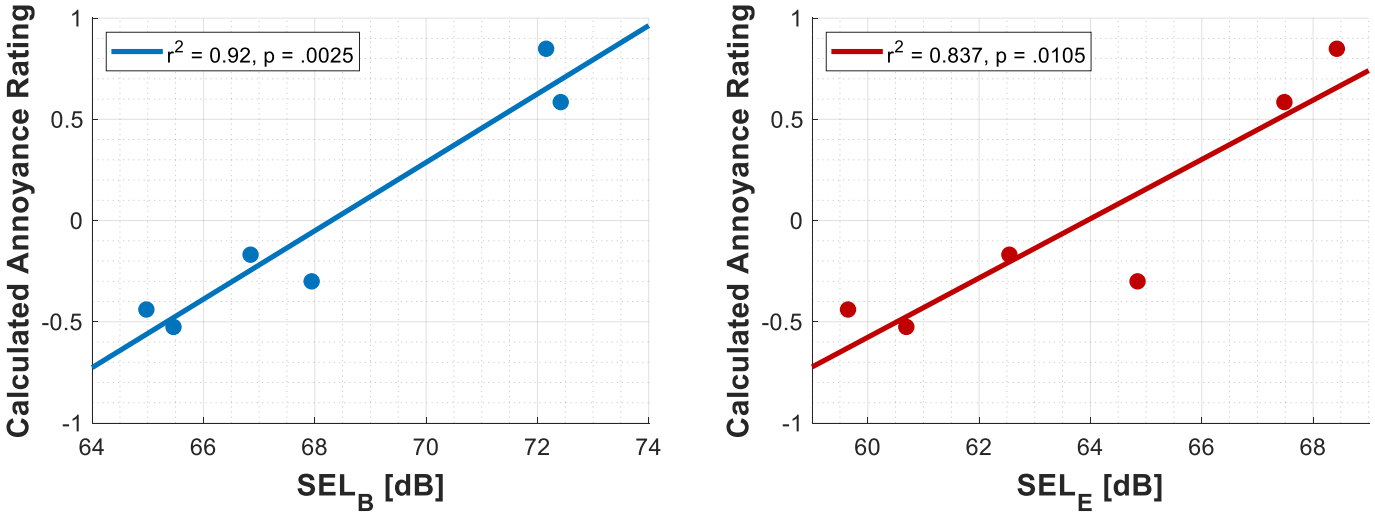

Figure 25. Regression curves (trend lines) for annoyance ratings, with average annoyance ratings of each stimulus on the *y* axis and calculated metric levels along the *x* axis. Coefficients of determination (r^2) and *P* values are also indicated, as based on the average stimulus ratings.

For thunder, the correlation analysis identified SEL_B and SEL_E as the metrics most highly correlated with thunder ratings (Figure 26). They were identified to not have statistically different correlations. In addition, all three RC-based metrics were identified as having statistically significant coefficients with thunder ratings but in this case were found to be negatively correlated. The correlations for each of the RC-based metrics were not statistically different. Stepwise regression identified SEL_B and $RC_{.5\text{-}1k}$ as the best set of metrics for predicting thunder ratings. Regression was therefore run six times, by modeling thunder with each of SEL_B and SEL_E as the first metric, with each of the three RC-based metrics as the second metric (Table 6). Because thunder was strongly correlated with annoyance, it follows that the same SEL metrics would predict thunder ratings well. The RC-based metrics with negative regression coefficients indicated that stimuli rated high on the thunder scale had higher mid- to low-frequency energy ratios, possibly because louder stimuli would have decayed less, and atmospheric decay acts more quickly on higher frequencies. In addition, the perceptual attribute of "thunder" was defined as the "sharp crack of thunder," which should be more related to higher than lower frequencies. Thus, a negative correlation with the RC-based metrics, which are measures of low-frequency content, seems appropriate.

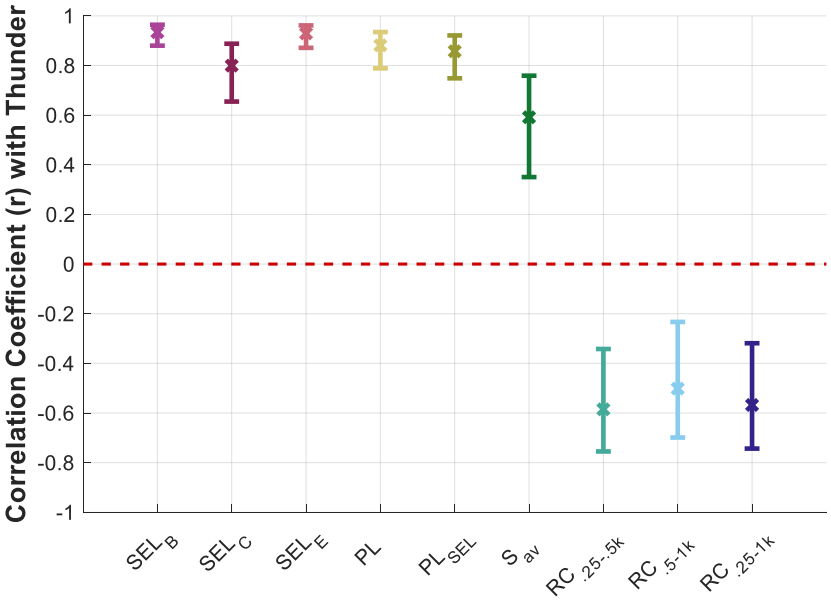

Figure 26. Correlation between thunder ratings and metrics. For each metric, the sample correlation is plotted with 95% confidence intervals also indicated. SEL_B and SEL_E had the strongest correlation with thunder. All three RC-based metrics did not have statistically different correlation coefficients.

Table 6. Thunder predicted with various metrics. All metric sets predict thunder well, although using SEL_B leads to a somewhat stronger result.

Attribute	Metric	Coefficient	Standard Error	*P* value	Model m^2
Thunder	SEL_B	0.218	0.0118	< 0.0001	0.677
	$RC_{.5\text{-}1k}$	-0.0476	0.00790	< 0.0001	
Thunder	SEL_B	0.218	0.0118	< 0.0001	0.677
	$RC_{.25\text{-}1k}$	-0.0476	0.00790	< 0.0001	
Thunder	SEL_B	0.217	0.0120	< 0.0001	0.673
	$RC_{.25\text{-}.5k}$	-0.0461	0.00800	< 0.0001	
Thunder	SEL_E	0.208	0.0120	< 0.0001	0.630
	$RC_{.5\text{-}1k}$	-0.0180	0.00834	0.0314	
Thunder	SEL_E	0.204	0.0124	< 0.0001	0.633
	$RC_{.25\text{-}1k}$	-0.0231	0.00914	0.0120	
Thunder	SEL_E	0.203	0.0125	< 0.0001	0.634
	$RC_{.25\text{-}.5k}$	-0.0244	0.00915	0.0082	

For rumble, the correlation analysis identified SEL_C as the metric most highly correlated with rumble ratings (Figure 27). Stepwise regression identified SEL_C and $RC_{.25\text{-}.5k}$ as the best set of metrics for predicting rumble ratings. Regression was therefore run by modeling rumble with SEL_C as the first metric and each of the three RC-based metrics as the second metric (Table 7). Whereas the RC-based metrics were not significantly correlated with rumble ratings, after SEL_C accounted for

some of the variance, the RC-based metrics became significant. This result indicates that the perception of rumble was correlated with the perception of loudness, but the timbral aspects isolated by the RC-based metrics were still significant.

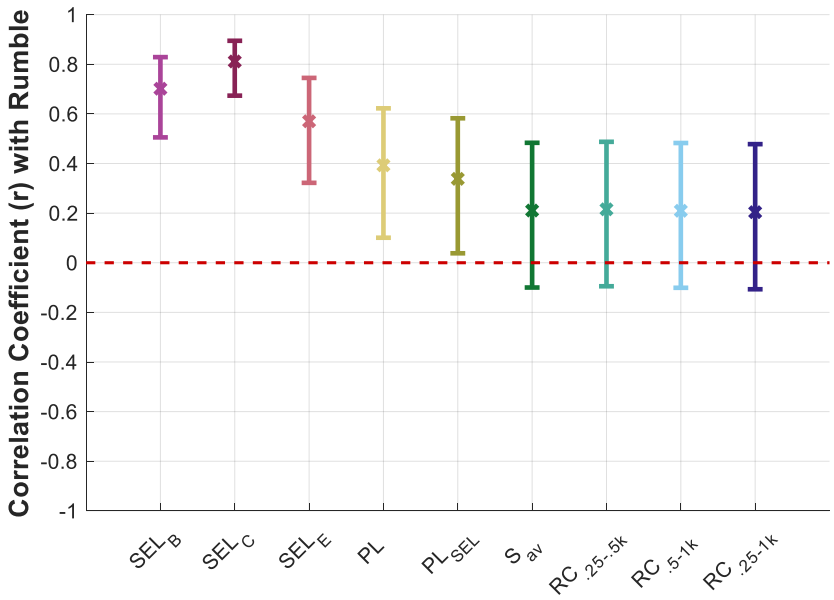

Figure 27. Correlation between rumble ratings and metrics. For each metric, the sample correlation is plotted (*x*), with 95% confidence intervals also indicated. SEL_C had the strongest correlation with rumble. All three RC-based metrics did not have statistically different correlation coefficients.

Table 7. Rumble predicted with various metrics. Any of the RC-based metrics may be used with SEL_C to predict rumble.

Attribute	Metric	Coefficient	Standard Error	*P* value	Model r^2
Rumble	SEL_C	0.163	0.0182	< 0.0001	0.255
	$RC_{.25\text{-}.5k}$	0.0349	0.0112	0.0021	
Rumble	SEL_C	0.163	0.0183	< 0.0001	0.253
	$RC_{.25\text{-}1k}$	0.0338	0.0113	0.0030	
Rumble	SEL_C	0.161	0.0183	< 0.0001	0.249
	$RC_{.5\text{-}1k}$	0.0297	0.0107	0.0058	

For swoosh, the correlation analysis also identified SEL_B and SEL_E as the metrics most highly correlated with thunder ratings (Figure 28). They were identified to not have statistically different correlations. Stepwise regression identified SEL_B and SEL_C as the best set of metrics for predicting swoosh ratings. Regression was therefore run by modeling swoosh with SEL_B or SEL_E as the first metric, and SEL_C as the second metric (Table 6). With two loudness metrics involved in predicting swoosh ratings, the stimuli rated higher on the swoosh scale were likely to have some timbral quality. The differences in frequency weightings for different SEL metrics were able to isolate that timbral quality.

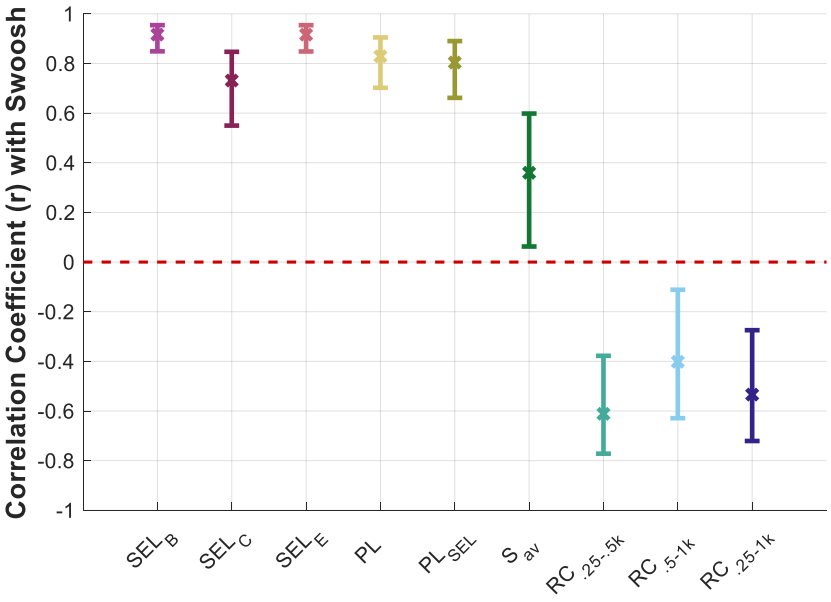

Figure 28. Correlation between swoosh ratings and metrics. For each metric, the sample correlation is plotted (*x*) with 95% confidence intervals also indicated. SEL_B and SEL_E had the strongest correlations with swoosh.

Table 8. Swoosh predicted with various metrics. Both models produced similar results, although SEL_B produced a statistically better model.

Attribute	Metric	Coefficient	Standard Error	*P* value	Model r^2
Swoosh	SEL_B	0.392	0.0415	< 0.0001	0.443
	SEL_C	-0.235	0.0451	< 0.0001	
Swoosh	SEL_E	0.247	0.0307	< 0.0001	0.400
	SEL_C	-0.100	0.0366	0.0068	

In summary, loudness-based metrics best predicted ratings on all four perceptual scales. SEL_B and SEL_E were the single best metrics for predicting annoyance, thunder, and swoosh, whereas SEL_C was effective in predicting perception of rumble. For thunder and rumble, RC-based metrics were statistically significant predictors after accounting for loudness. Swoosh ratings were bet predicted with a combination of two loudness metrics, SEL_B and SEL_C. The models with the highest coefficients of determination are summarized in Table 9.

Table 9. Summary of strongest regression models. For each attribute, one of the weighted sound exposure level metrics was the strongest predictor of perception.

Attribute	Metric	Coefficient	Standard Error	*P* value	Model r^2
Annoyance	SEL_B	0.169	0.0162	< 0.0001	0.304
Thunder	SEL_B	0.218	0.0118	< 0.0001	0.677
	$RC_{.5\text{-}1k}$	-0.0476	0.00790	< 0.0001	
Rumble	SEL_C	0.163	0.0182	< 0.0001	0.255
	$RC_{.25\text{-}.5k}$	0.0349	0.0112	0.0021	
Swoosh	SEL_B	0.392	0.0415	< 0.0001	0.443
	SEL_C	-0.235	0.0451	< 0.0001	

Results part 3 – ANOVA of synthesized shock stimuli
Additional analyses were conducted to investigate the effect of including a simulated decayed shock wave with a representative Mach cutoff signature. ANOVA was run for both methods of calculating annoyance ratings, and the results showed no statistical difference in mean ratings across the four stimuli. The lack of difference is illustrated by the overlapping 95% confidence intervals in Figure 29. The lack of this effect indicates that, for the cases tested in this study, the longer "post-shock" noise has a larger effect on annoyance than the initial shock.

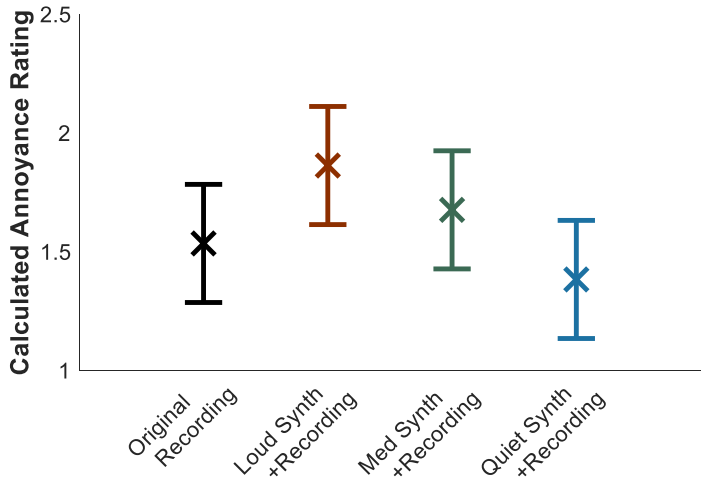

Figure 29: Annoyance ratings for the modified stimuli (synthesized boom added plus original). The mean annoyance ratings of the four related stimuli are indicated with an X along with the 95% confidence intervals. The clear overlap demonstrates the lack of statistical evidence for an effect of adding a synthesized boom on the annoyance ratings.

Results part 4 – Demographic investigations
Aside from low-frequency hearing thresholds, demographics were not found to have a significant effect on the perceptual ratings. The results of the MANCOVA testing for the effects of demographics on ratings are summarized in Table 10, with effects significant at the $P = 0.05$ level marked in bold. As expected, the stimulus had a statistically significant effect on ratings for all variables. The only demographic factor analyzed that had a significant effect was the average low-frequency hearing threshold. For this type of analysis in which a number of effects are assessed, the *P* value at which the results are considered significant must be adjusted with Bonferroni correction, which yielded $P < 0.0073$ as the threshold for significance.

Table 10. Demographic effects on rating data. Other than the stimulus, only low-frequency hearing had a significant effect on ratings (with Bonferroni correction, a result is considered significant at $P < 0.0073$).

Effect	*P* value
Stimulus	< 0.0001
Age	0.334
Gender	0.0263
Low-Frequency	< 0.0001
Mid-Frequency	0.909
High-Frequency	0.0081
Noise Sensitivity	0.567

To further investigate the effect of the low-frequency hearing threshold, we ran an individual ANOVA, modeling perceptual ratings by using the low-frequency hearing threshold as described previously. This analysis is summarized in Table 11, in which significant effects are again marked in bold. The analysis indicates that a low-frequency hearing threshold had a significant effect on thunder ratings ($P < 0.0125$). The lack of gender and age effects is illustrated in Figure 30, which shows the means and 95% confidence intervals for the annoyance ratings of the different demographic groups considered. Of note, the significant overlap in confidence intervals provides a visual confirmation of this finding that the demographics did not influence the rating data.

Table 11. Effects of low-frequency hearing threshold on each rating variable. A significant effect of low-frequency hearing threshold was found for thunder ratings only. That is, low-frequency hearing thresholds affect the perception of the thunderous aspects of the stimuli.

Effect	Variable	*P* value
Low-frequency hearing threshold	Thunder	< 0.0001
	Rumble	0.0278
	Swoosh	0.855
	Annoying	0.418

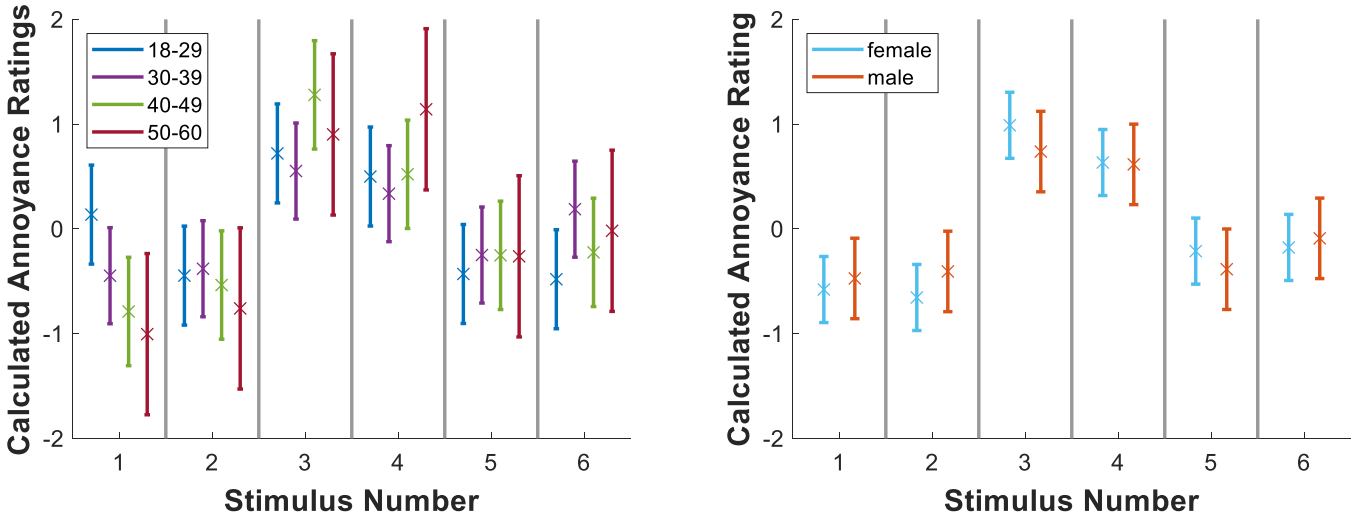

Figure 30. Demographics vs. annoyance ratings, with Figure a (left) divided by age category and Figure b (right) divided by gender. The overlapping intervals indicate that ratings were not statistically different across the demographic groups. For both plots, average annoyance rating and 95% confidence interval are plotted.

Relationships among demographic factors were investigated through ANCOVA and MANOVA. Effects of demographics on noise sensitivity were investigated through ANCOVA, as summarized in Table 12. The analysis indicated a significant relationship between average mid-frequency hearing thresholds and noise sensitivity, but the effect is weak (r^2= 0.0092). Analysis of demographic effects on hearing thresholds matched that reported in the literature, showing increased hearing thresholds with increased age, more pronounced at higher frequencies (Patterson et al., 1982) (Table 13).

Table 12. Investigations of the effects of demographic factors on noise sensitivity. Mid-frequency hearing thresholds had some relationship with the noise sensitivity score.

Effect	***P* value**
Age	0.0237
Gender	0.510
Low-Frequency	0.148
Mid-Frequency	0.0078
High-Frequency	0.735

Table 13. Effects of demographics on average hearing thresholds. Age was found to have a significant effect on mid- and high-frequency hearing thresholds.

Effect	Variable	*P* value
Gender	Low-Frequency	0.0221
	Mid-Frequency	0.0540
	High-Frequency	0.0568
Age	Low-Frequency	0.104
	Mid-Frequency	0.0000
	High-Frequency	0.0000

Summary

The primary finding in this study is that loudness controls the perception of annoyance due to Mach cutoff ground signatures. Loudness-related metrics, especially B- and E-weighted SEL, were most effective in modeling annoyance and other perceptual ratings. Although each perceptual attribute tested was related to annoyance, one underlying principal component explained most of that relationship. The addition of a synthesized shock to the Mach cutoff stimuli did not have a significant effect on annoyance ratings. In general, demographic effects were not significant. A more detailed summary of the findings separated according to the five questions of interest is provided in Table 14 on the following page.

Table 14. Analysis methods and results summary. For each of the five questions listed in the "Data Analysis Methods" section, the question, analysis methods, explanation of the analysis methods, and key findings are included.

Question	Method(s)	Explanation of Statistical Analysis	Key Findings
How are the perceptual attributes of thunder, rumble, and swoosh related to annoyance?	Factor analysis and linear regression (univariate)	Factor analysis was used to obtain orthogonal factors from all perceptual ratings and to find principal components. Two linear regressions were run, modeling annoyance by using the factors of components.	Annoyance is related to both thunder and swoosh ratings. One underlying factor (first principal component) captures the effect of both.
Which metrics form the best model best for predicting each perceptual factor?	Stepwise regression (univariate) and correlation testing	For each perceptual rating variable, metrics were selectively added into the regression model to best explain the overall variance with the fewest metrics. Correlation tests indicated significant differences between metrics.	Annoyance and thunder ratings are predicted well with sound exposure level metrics (SEL_B or SEL_E). Swoosh ratings are predicted by using SEL_C and SEL_E combined. Rumble ratings are predicted well by SEL_C and $RC_{.25\text{-}1k}$.
How does the addition of a synthesized decayed shock to a Mach cutoff stimulus influence annoyance?	ANOVA	Annoyance ratings were modeled as combinations of stimulus and subject ID effects (ANOVA). Only the ratings on the modified stimuli were used. Ratings were calculated in two ways.	The addition of the synthesized booms did not have a statistically significant effect on annoyance ratings.
Do the demographics of the participants affect the ratings?	MANCOVA	Using continuous and categorical predictors requires the general linear model, which is analyzed with MANCOVA. All rating sets were modeled by using the interactions between demographic effects and stimulus number.	Demographics did not have a statistically significant effect on subjective ratings. Low-frequency hearing thresholds did have a statistically significant effect on ratings of thunder.
How are demographics, hearing thresholds, and noise sensitivity related?	ANCOVA and MANOVA	Hearing thresholds were modeled with age category and gender as independent variables (MANOVA). Noise sensitivity was modeled with hearing thresholds, age, and gender as independent variables (ANCOVA). Interaction effects were also investigated.	Age did have a statistically significant effect on mid- and high-frequency hearing thresholds. Mid-frequency hearing thresholds did have a statistically significant, albeit weak, effect on noise sensitivity.

Study 3: Degree of annoyance study

Study design

The purpose of Study 3 was to determine the degree of annoyance caused by Mach cutoff signatures relative to road, rail, and subsonic air traffic noise. These three transportation types were selected because most of the population is familiar with these sounds (Wesler, 1973). A secondary purpose of this study was to obtain additional data to further investigate a possible metric to predict annoyance due to Mach cutoff signatures and compare these findings to the results of Study 2.

Stimuli details

The stimuli used in this study were recordings of the four transportation modes, in which the Mach cutoff signatures were a subset of those used in the second study. For the remaining three types of traffic noise, field recordings were made in the state of Pennsylvania. Road traffic recordings were obtained from two interstates in proximity to State College, rail recordings were obtained from three different locations within an approximately 50-mile radius, and subsonic aircraft recordings were obtained at the local airport, University Park Airport (SCE), and Philadelphia International Airport (PHL). The road traffic recordings were made on interstates I-80 and I-99. On I-80, two microphones were set up in the shoulder closest to the median, 5 feet from the closest travel lane, for eastbound traffic at mile marker 152. On I-99, the same two

microphones were set up at the same distance from the closest travel lane (5 feet) for northbound traffic at mile marker 67. Recordings were taken on the morning of Monday, December 3. This time was selected because of high average annual daily traffic obtained from the Pennsylvania Department of Transportation. Approximately 45 minutes of continuous recordings were obtained at each location.

The rail recordings were taken at three local rail lines in the towns of Bellefonte, Lewistown, and Tyrone, Pennsylvania. Recordings were taken at multiple locations to obtain samples of different types of rail traffic. In Bellefonte, an old diesel engine train, moving at a constant speed of 15 mph was recorded. In Lewistown, a recording was taken of the westbound Amtrak passenger train as it passed by and decelerated to a train stop. In Tyrone, multiple freight trains were recorded with various numbers of attached freight cars. These train passes had much higher sound pressure levels and more complex acoustic signatures than the other three types of trains. For all recordings, train horns were sounded, and in most cases brake squeal was also recorded. The duration of the recordings at each location ranged from 10 minutes to a few hours depending on the location.

The subsonic aircraft stimuli were obtained from two Pennsylvania airports, SCE and PHL. Multiple locations were used in obtaining the recordings at both airports, and most of the locations were near the runways. Different flight operations were recorded including takeoff, landing, and a plane flyover pass. The orientation in which the microphones recorded the planes also differed depending on whether the plane flew overhead or perpendicularly to the microphones. Several hours of recording time were collected at both airports. The aircraft at SCE were small regional jets, whereas the aircraft at PHL were medium to large jets. For further stimuli variety, recordings were obtained from Dr. Patricia Davies at Purdue University.

After all recordings were obtained, four 10-second segments were selected for each transportation mode. The stimuli duration of 10 seconds was based on the typical duration of NASA's recorded Mach cutoff signatures. This duration was sufficiently long to allow for a complete subsonic aircraft signature, whereas for road and rail, 10-second segments were selected from the longer recordings. The signatures for the road and rail transportation modes varied in vehicular density (i.e., one vehicular pass to multiple vehicular passes, with and without semitrailer trucks) and in noise characteristics (i.e., train horn vs. train brake). Two additional recordings, one Mach cutoff and one subsonic aircraft, were also included as reference stimuli, which was needed for one of the two testing methods used. (More details about the test methods are provided in the next section.) One Mach cutoff stimulus and one subsonic aircraft stimulus were selected as the reference stimuli because of the emphasis on aircraft noise in the study. The stimuli were selected because the signatures had similar loudness, sharpness, and SEL_8 weightings to the other stimuli in the transportation modes.

To quantitatively compare the selected stimuli for each transportation mode to assess whether a suitable variety of stimuli were selected, loudness (phons) and sharpness (acum) were calculated for each stimulus (FastI, 2006), as shown in Figure 31. In general, within the sets of four stimuli for each of the transportation modes, a range of loudness and sharpness values was observed, with the exception of Mach cutoff and sharpness for the road stimuli. Loudness in phons represents equal loudness at mid-frequency, whereas sharpness in acum is an acoustic metric that accounts for high-frequency content of a sound. Given the similarity of the mid- to high-frequency content in the Mach cutoff signatures, we did not expect to observe much variation. Road stimuli have a wide range of spectral energy in the low- and mid-frequency ranges, but not in high frequencies, thus explaining the uniform sharpness values.

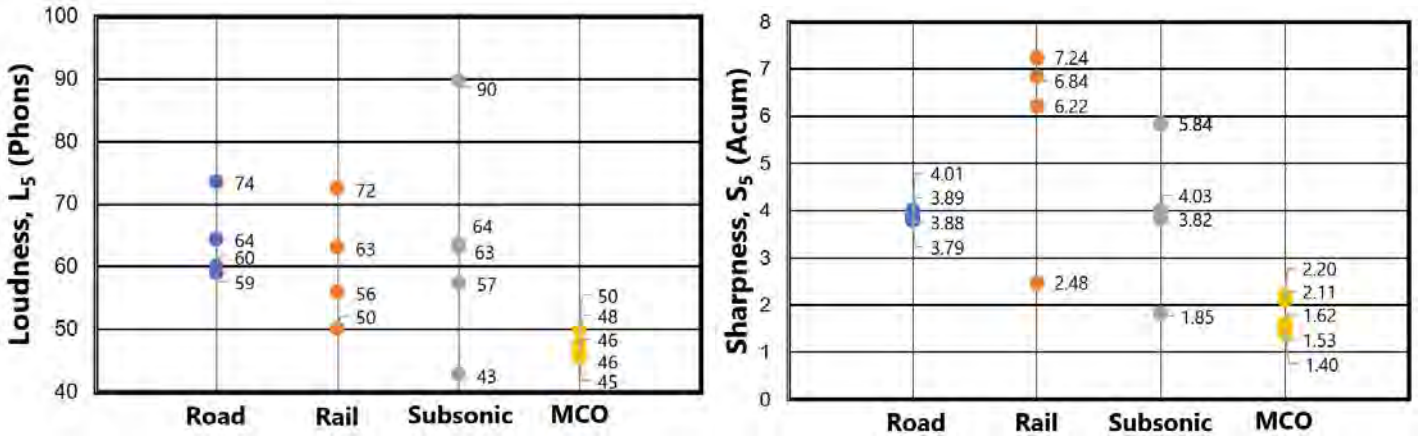

Figure 31. The loudness, L_S in phons and the sharpness, S_S in acum of the stimuli are shown in the left and right plots, respectively. In general, a range of values were observed for all transportation types, with the exception of Mach cutoff (MCO) and sharpness in road.

The study was designed to include three different listening conditions: (a) traffic noise as experienced outdoors at a residence in proximity to a traffic source ("outdoor condition"), (b) traffic noise as experienced indoors in a typical residential construction at the same location as the first condition ("indoor condition"), and (c) a condition wherein all of the stimuli were normalized to have the same PL ("equalized condition"). The first two conditions were included to provide two realistic listening scenarios for the subjects (e.g., envisioning that they are outdoors or indoors, and the last condition served as a check for the findings of the first two conditions while controlling for loudness. In other words, the equalized condition was included to evaluate whether the differences in ratings across transportation modes were primarily due to differences in overall sound pressure levels and less influenced by differences in temporal and frequency characteristics.

For the outdoor condition, the obtained recordings needed to be attenuated to be representative of a typical closest resident distance to the transportation source, because the recordings were collected near the sound sources. To determine an appropriate "typical" closest distance of a residence to a major roadway, rail line, and airport, several locations within four major U.S. cities, Atlanta, Chicago, Houston, and New York City, were reviewed. Representative examples are shown in Figure 32. According to this informal survey of a number of residences near to major transportation types, the following distances were selected as the typical closest distance or worst-case conditions: 300 feet for both major roadways and rail lines, and 1,500 ft to major airports. The latter was selected as the closest distance for Mach cutoff traffic as well.

Figure 32. Examples of the researched closest residential distances to interstates, rail lines, and airports.

For the indoor condition, a typical residential construction with an exterior wall of 2 × 6 wood studs (Bradley & Birta, 2001) was used to further attenuate the outdoor recordings. The transmission loss (TL) data for this construction are shown as the purple curve in Figure 33. The composite TL was calculated for a home with this exterior wall construction, in which the total area was subdivided such that approximately one-third were windows, approximately one-twentieth was a door, and the remainder was the 2 × 6 wood stud construction, represented as the pink curve in Fig. 33. These percentages were obtained by researching common residential homes in these transportation noise worst cases. Because this calculation assumes that all openings are perfectly sealed, a field TL measurement of an apartment in proximity to I-99 was obtained (yellow curve) and, as shown, is significantly lower than the theoretical composite wall. Although the construction of the apartment exterior wall and windows is not identical to the theoretical base wall, the overall attenuation levels due to non-ideal installation conditions were considered representative of actual facades. As a result, the overall TL applied to the outdoor signals generally followed the shape of the theoretical base wall but was significantly attenuated further to be comparable to the in-situ measurements (black curve). On average, across all frequencies, the attenuation was approximately 20 dB. The final selection of the applied TL to the signatures was made in combination with listening to the signals and subjectively determining whether they sounded representative of how traffic noise would sound inside a residence close to the transportation mode location. As a point of comparison, the exterior wall used by NASA (Page et al., 2014) is included in the same plot (green curve).

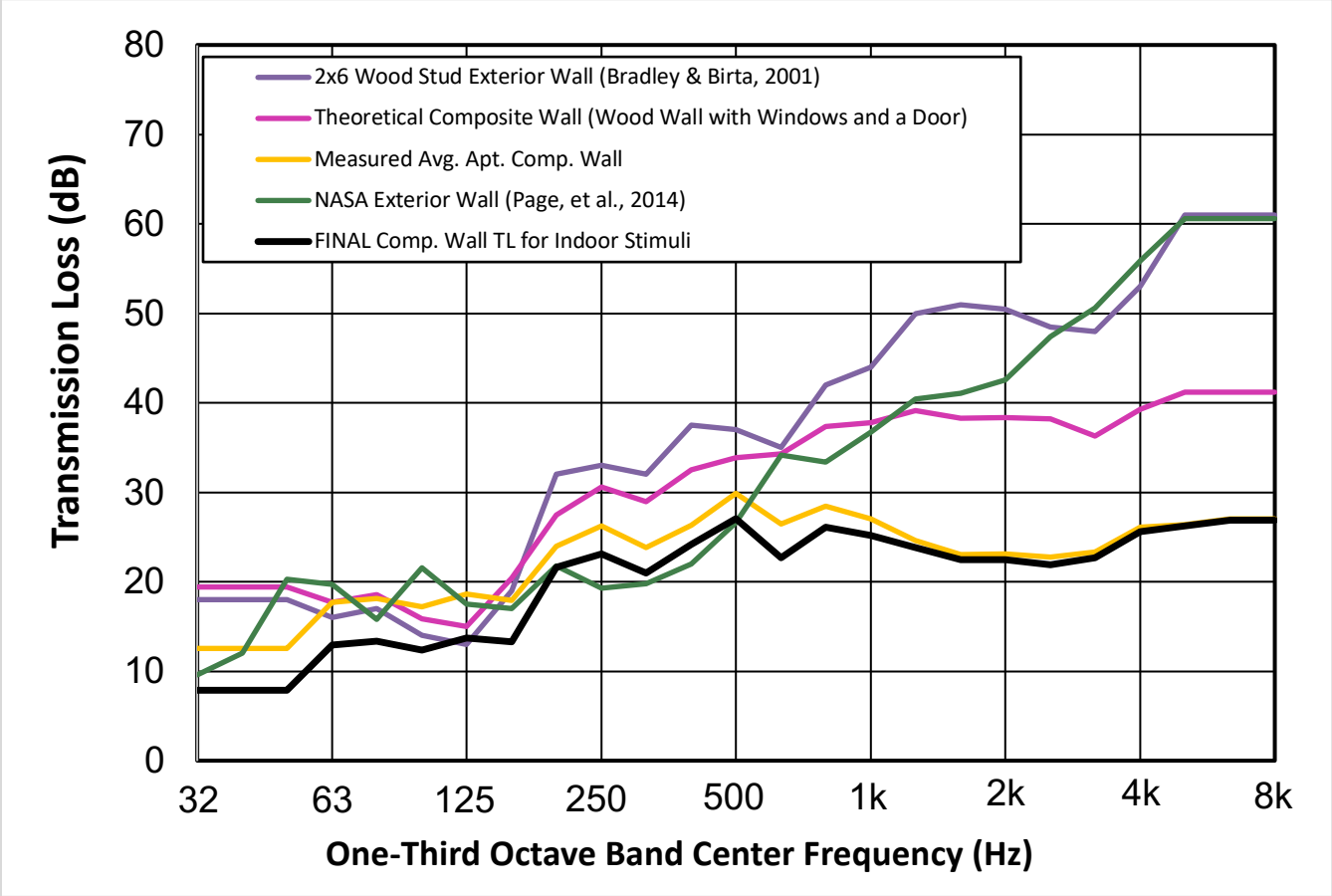

Figure 33. The finalized indoor filter transmission loss (black curve) is applied to the outdoor stimuli to generate the indoor stimuli. Additional curves are included for reference as described in the text.

Finally, the equalized condition was created by applying SEL B- and E-weightings to the stimuli to normalize the PL for the stimuli both within and across transportation types. The applied weighting networks are shown in Figure 34, and the final SEL_B and SEL_E levels of all stimuli are shown in Figure 35. B- and E-weightings were selected on the basis of the findings of Study 2, wherein both of these metrics were found to best predict annoyance and thunder. SEL_B was used to equalize the aircraft stimuli, whereas SEL_E was used for road and rail. Two different metrics were used for the equalization because the selected metrics were found to be more effective at equalizing the levels of the stimuli within a transportation mode. The target was a value of 60 dB for all stimuli. As shown in Figure 35, this target was generally achieved for all stimuli, with the exception of the Mach cutoff stimuli, which were played back approximately at a level of SEL_E = 40 dB. A 20-dB gain was not applied the Mach cutoff stimuli to bring these signals to 60 dB, because listening to all of the stimuli indicated that the PL of these stimuli was very similar to that of all other stimuli. The difference in actual playback levels was due to how humans perceive the very low-frequency content of these signals. If the Mach cutoff signals were raised by 20 dB, then the subjects would hear an unrealistic mid- and high-frequency content sound, because the little mid- and high-frequency content would be much higher while the low-frequency content would be heavily attenuated, thus distorting the stimuli's noise characteristics.

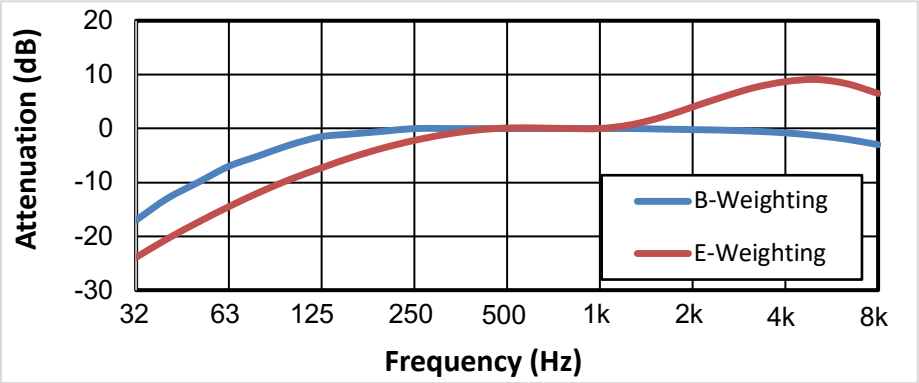

Figure 34. The attenuation across whole-octave frequency for SEL B- and E- weighting. SEL_B was applied to the subsonic aircraft and Mach cutoff stimuli, and SEL_E was applied to the road and rail stimuli.

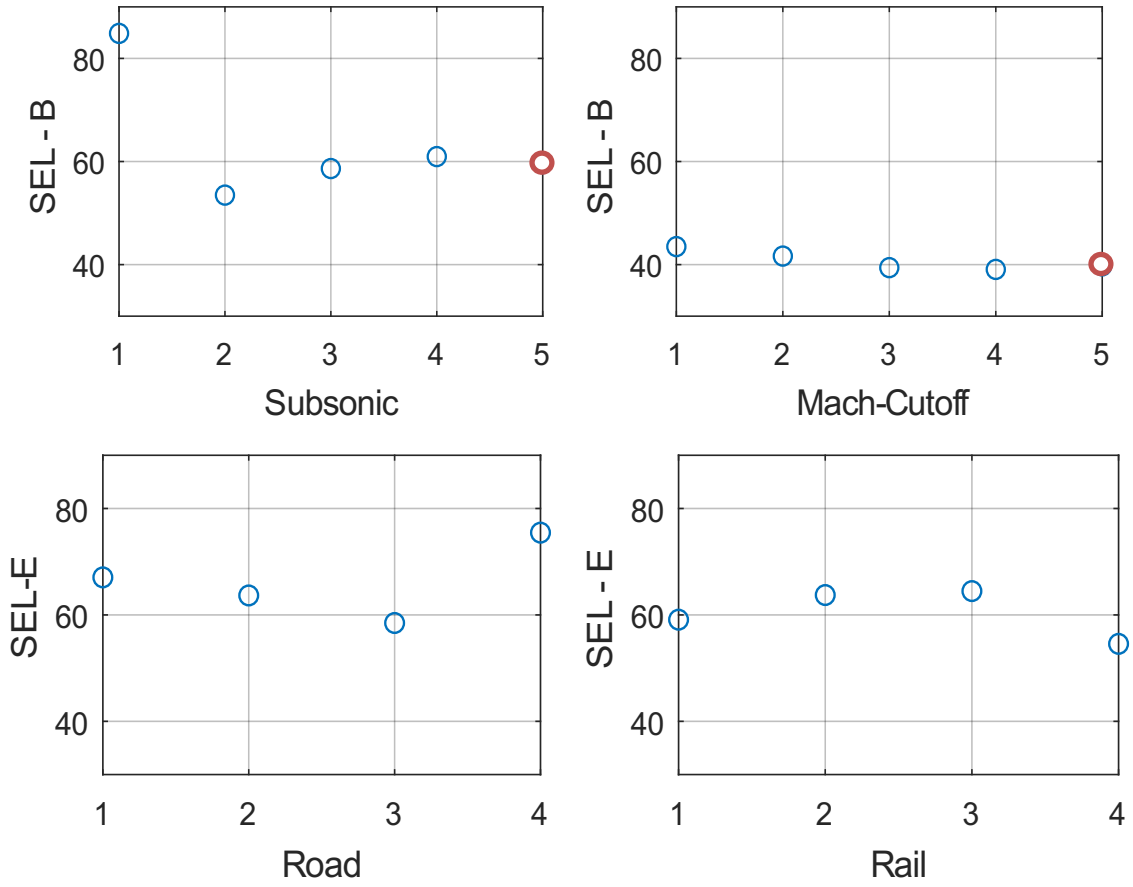

Figure 35. SEL B- and E-weightings were applied to each transportation mode. These weightings equalized the loudness for the stimuli in every transportation mode. SEL_B was applied to subsonic aircraft and Mach cutoff, and SEL_E was applied to road and rail stimuli. The red circles represent the two additional reference stimuli used in the Preference method.

Subjective testing methods

To investigate the perception of Mach cutoff signatures relative to common transportation modes, we used two different subjective listening test methods: method 1, termed the "degree of annoyance" method, required participants to give absolute ratings of each stimulus one at a time, and method 2, termed the "transportation mode relative preference" method, required participants to rate their relative preference for each stimulus relative to five other presented stimuli (multi-stimuli comparison method). All participants were required to provide responses by using both methods for all three conditions. More details about the individual test sets are provided in the "Data Collection" section. Participants completed a training set before the actual test sets, which included the loudest and softest stimuli from the outdoor and indoor conditions, respectively. Each training set had the same number of questions as their respective testing method: annoyance rating had 16 questions per condition, and transportation mode preference had four questions per condition.

Method 1, the degree of annoyance method, was designed so that each stimulus was presented individually. The testing interface is shown in Figure 36. The subject was asked to play the sound and then rate the sound on an absolute scale from 1 to 5 where the numbers were labeled with the following word anchors: 1 = "not at all annoying," 3 = "moderately annoying," and 5 = "highly annoying." The selected descriptions of the anchors were the same as used by Page in 2014. The rating scale was continuous, and the participants moved a slider along the length of the scale to provide their ratings. There were 16 stimuli used in this method—four stimuli from each transportation mode—and all 16 stimuli for one of the three conditions were included within a given series of questions in random order.

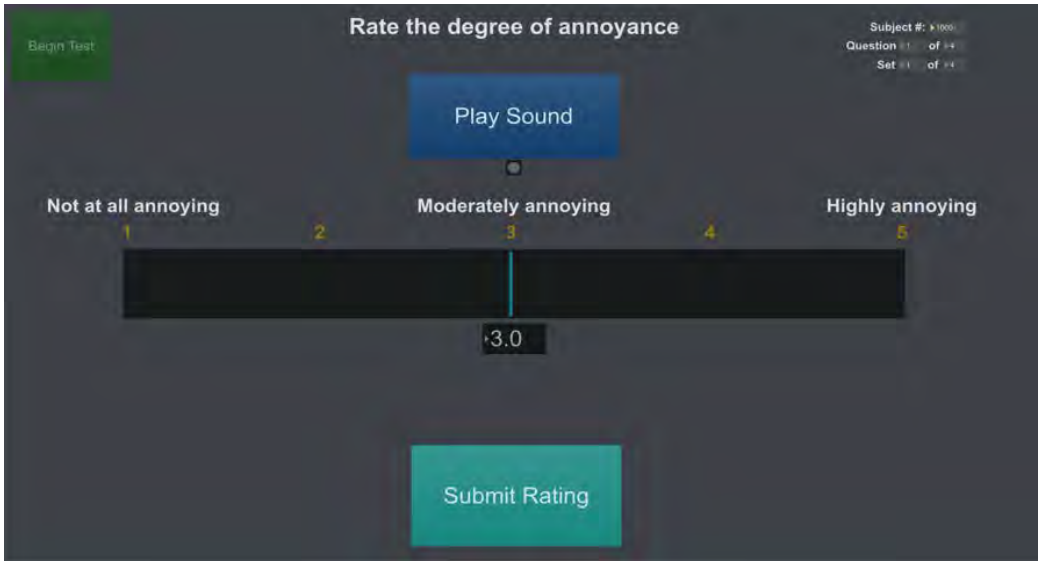

Figure 36. The subjective testing interface for method 1, the degree of annoyance method. One stimulus was presented per question, and participants were required to rate the degree of annoyance in response to each stimulus. The rating scale ranged between 1 = not at annoying and 5 = highly annoying.

Method 2, the relative transportation mode preference, was designed to provide a series of four questions with multiple stimuli at a time and required participants to rate their preference of each signal relative to the others in the set. The testing interface is shown in Figure 37. The rating scale used in this method ranged from -50 to +50 with the word anchors: -50 = "I do not like it" and +50 = "I like it." This method was adapted from reference (Torija et al., 2019), which used the method to investigate participants' relative preference for different types of aircraft engine noise. To compare the ratings across the questions, we included two reference stimuli in all four questions. The reference stimuli were selected to be one additional Mach cutoff signature and one additional subsonic aircraft signature. These same two reference stimuli were included in all questions to normalize the ratings and allow for comparison of the results across the series of four questions for each condition. In addition to the two reference stimuli, one of the four stimuli from the four transportation modes was randomly included in question. That is, for a given condition, participants received a series of four questions, each including one of the four stimuli for each of the transportation modes from method 1, along with the two reference stimuli (six signals in total per question). Over the series of four questions, all 16 of the stimuli from method 1 were

included without repetition and were randomly assigned to each question for each participant. Within each question, the order of presentation of the stimuli, i.e., A, B, C, etc., was also randomized.

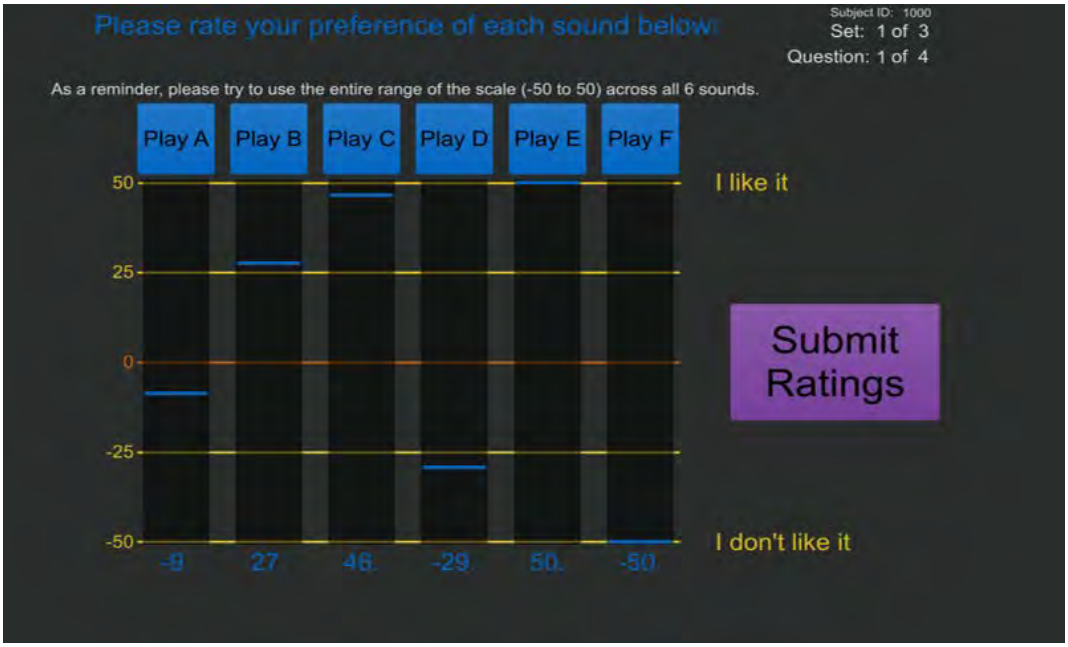

Figure 37. The subjective testing interface for Method 2, the transportation mode relative preference method. Multiple stimuli were presented for each question, in which one stimulus of each of the four transportation modes represented four of the six stimuli, and the remaining two stimuli were reference stimuli that were included in all sets (one additional subsonic aircraft signature and one additional Mach cutoff signature).

Data collection

The testing procedure for each subject was as follows. First, the subject read, asked any questions, and signed the informed consent form. Second, a hearing screening was administered to ensure that the subject had maximum hearing thresholds of 35 dB HL in the whole-octave frequency bands from 250 Hz to 8000 Hz, where the threshold is the lowest sound pressure level that a person can detect. A 0-dB threshold was considered the baseline hearing without any loss. In other words, any threshold value exceeding 0 dB indicates some degree of hearing loss. However, thresholds between 0 and 25 dB HL are considered to be within the normal hearing range. Thresholds between 25 and 35 dB HL are classified as mild hearing loss. Prior work has shown that participants with hearing in the 0- to 15-dB portion of the normal range provide more reliable data. However, to ensure a more representative sample from the population was included in this study, the hearing threshold requirements were relaxed to 35 dB HL, because in general, as people age, their hearing thresholds increase.

An overview of the question sets is provided in Table 15. Participants completed a total of three sets with multiple parts within each set. All participants began with the indoor condition for their first set (set 1) and were randomly assigned one of the two test methods. The indoor condition was presented first to promote participants to use a broader range of the rating scale than they might otherwise have used if they were first presented with either the outdoor or equalized condition, because the stimuli in those conditions were presented at higher sound pressure levels. To improve the reliability of the data, we required participants to review a set of tutorial slides and complete a series of practice questions before the collection of actual test data for both methods. As a result, there were four parts in set 1, as shown in the table. After set 1, participants were given a break of several minutes before sets 2 and 3, which each contained two parts. The last two sets were for the remaining two conditions, outdoors and equalized, which were presented in random order. Within these sets, participants were required to rate the stimuli by using both test methods, which were also presented in random order independently of the orders in the other sets. The question order within each set was randomized for all

participants. Afterward, demographic and other information was collected through online questionnaires. The average duration for the entire session was approximately 90 minutes.

Table 15. Summary of subjective listening test method. All participants completed all sets, and a training set was administered before actual test data collection for each method, as shown in set 1. The stimuli for the indoor condition were presented first to all participants to encourage use of the full range of the rating scales. The test method within each set was randomized across sets for all subjects.

	Set 1 - Indoor Condition				Set 2 - Outdoor or Equalized		Set 3 - Outdoor or Equalized	
Q Type	**Part A**	**Part B**	**Parc C**	**Part D**	**Part A**	**Part B**	**Part A**	**Part B**
Training	Method 1* (16 Q)	N/A	Method 2^ (4 Q)	N/A	N/A		N/A	
Actual Test	N/A	Method 1 (16 Q)	N/A	Method 2 (4 Q)	Method 1 or 2	Alternate method	Method 1 or 2	Alternate method
Training	Method 2 (4 Q)	N/A	Method 1 (16 Q)	N/A	N/A		N/A	
Actual Test	N/A	Method 2 (4 Q)	N/A	Method 1 (16 Q)	Method 1 or 2	Alternate method	Method 1 or 2	Alternate method

*Method 1: *Degree of Annoyance Method* - individual stimulus rating method, 16 Questions

^Method 2: *Transportation Mode Relative Preference Method* - multi-stimuli comparison method, 4 Questions

Study 3 included 38 participants. The age and gender demographics are summarized in Figure 38. The goal was to obtain approximately even numbers of participants within the five age categories shown in the figure and approximately even numbers of each gender within these age subdivisions. Extensive efforts were made over a period of 4 months to recruit participants to achieve this goal. Recruitment efforts included posting flyers at locations that older participants might frequent, newspaper advertisements, and a Facebook advertisement. Despite these efforts, most of the participants were in the first two age categories (n = 24) and only a single male participant was in the upper three age categories. As will be discussed, additional statistical analyses were conducted to determine whether this unevenly distributed sample affected the overall findings.

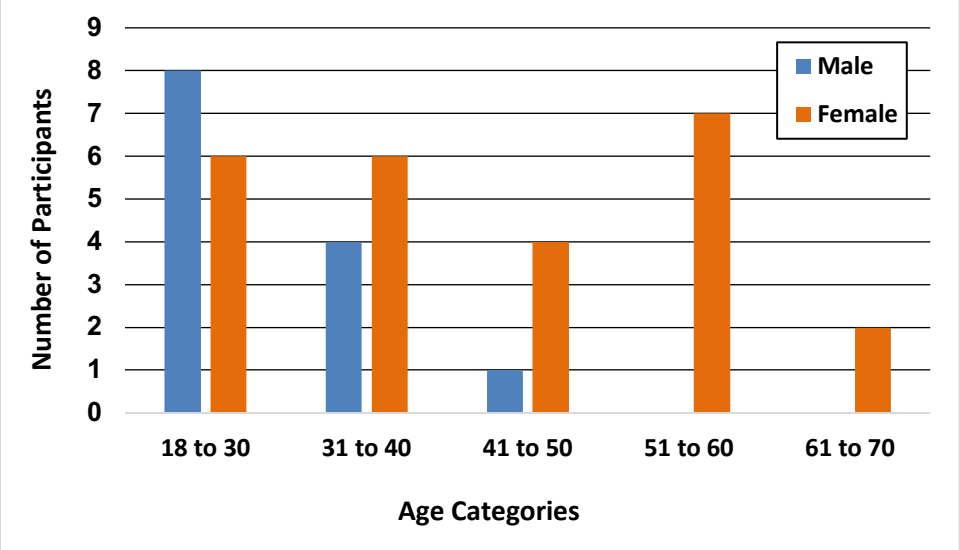

Figure 38. Participant demographics. Fewer individuals in the upper three age categories (n = 14) participated than in the first two categories (n = 24). Nearly twice as many females (n = 25) participated than males (n = 13).

Data analysis

For all analyses for both the degree of annoyance and transportation mode preference method, the subjects provided numerical ratings for stimuli on absolute and relative scales, respectively. The rating for each transportation mode was averaged for each method in relation to interaction variables including gender and age. This process resulted in four rating values, one for each transportation mode, that could be used for further analysis. Linear regression and both linear and univariate and multivariate analysis of variance statistical analyses were conducted (ANOVA and MANOVA, respectively).

The first statistical analysis was to determine the average degree of annoyance and transportation mode preference across all ages. This was conducted by using a univariate ANOVA on the ratings across the four transportation modes, and transportation modes was found to have a significant effect on both annoyance (F = 102.8, P < 0.001) and relative preference ratings (F =148.7, P < 0.001). As shown in Figure 39, Mach cutoff was perceived as the least annoying and had the highest relative preference ratings. No significant differences in ratings were found among the three other transportation modes.

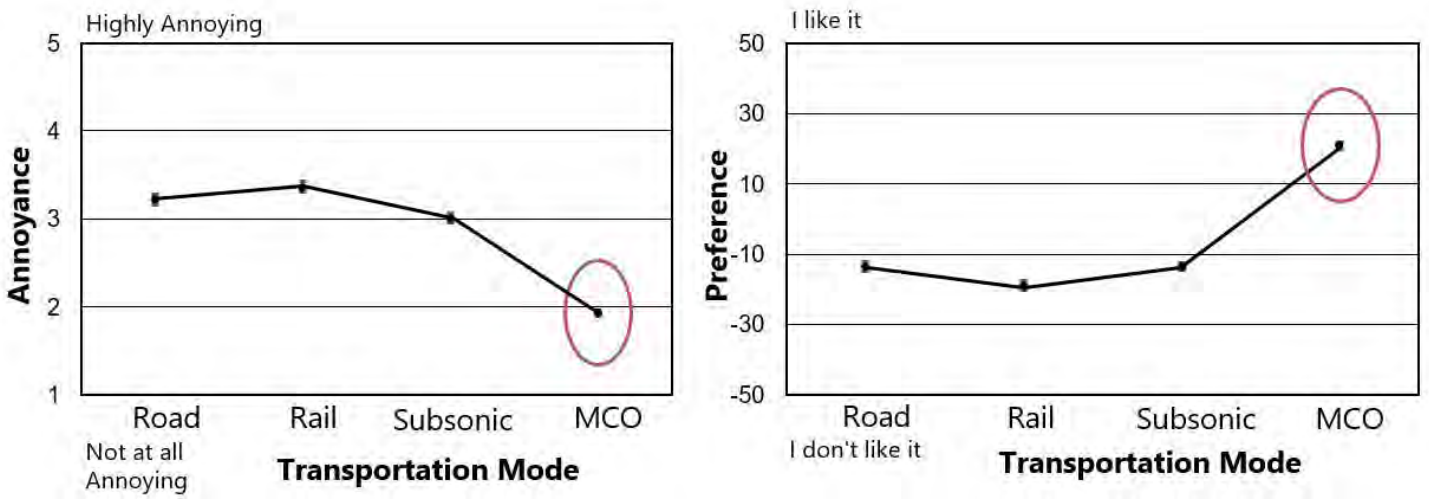

Figure 39. The results of methods 1 and 2. Degree of annoyance and relative transportation preference ratings, are shown at left and right, respectively. The same overall conclusion can be drawn from the resutls of these two very different test methods: Mach cutoff signatures are the least objectionable, as compared with the other three transportation modes. Note: The error bars represent the standard error of the mean and are so small because each data point represents 456 ratings: for each transportation mode type, participants rated four stimuli for three conditions, so 38 × 4 × 3 ratings per data point are shown in each plot. All remaining plots include error bars, which are similarly very small because each data point shown represents a large number of ratings.

To investigate whether there was an effect of condition (outdoors, indoors, and equalized) on the ratings of each transportation, we performed a MANOVA test on the conditions (Figure 40). In Method 1, the annoyance ratings of the stimuli in the indoors condition were significantly lower than those in the other two conditions, but the same trend is observed across all three conditions as in the overall average results shown in the previous figure, i.e., that Mach cutoff signatures are the least annoying, and no significant differences in ratings were observed across the other transportation types.

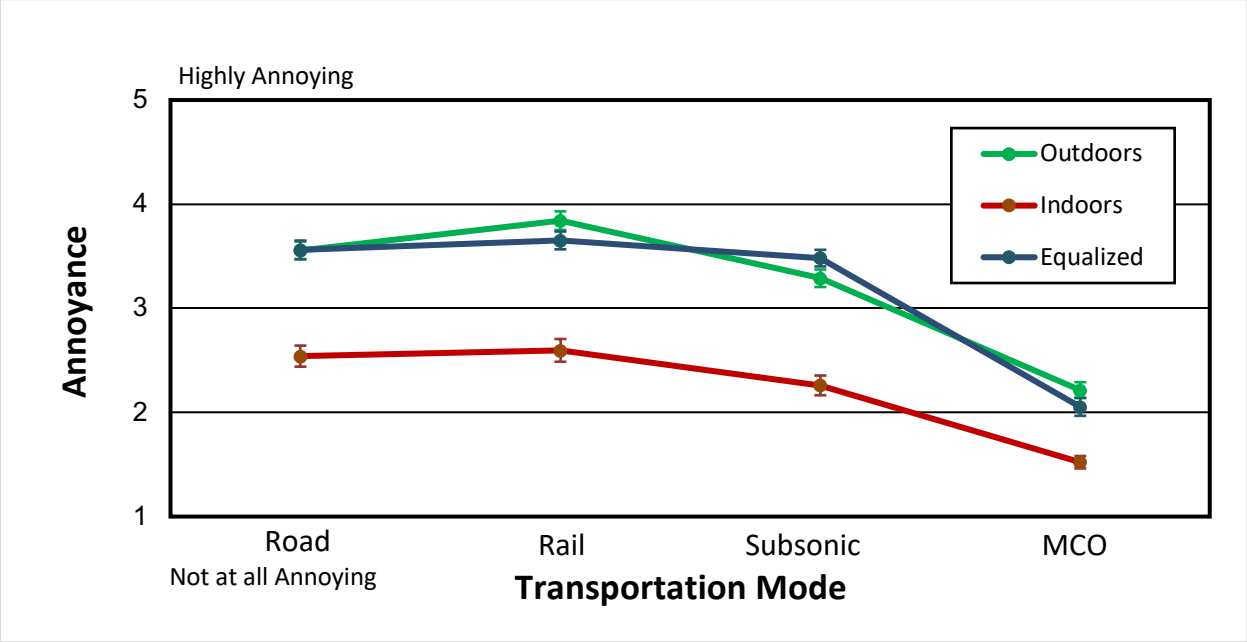

Figure 40. Method 1 results: the average annoyance ratings of each transportation mode separated by condition. For all conditions, Mach cutoff signatures had the lowest annoyance ratings.

For method 2, the results are more consistent across condition, probably because of the inclusion of the two reference stimuli in each question, as shown in Figure 41. The average preference was found for each condition. In this method, the indoor condition was not as statistically different as the annoyance rating method. This result may suggest that transportation mode preference is a more robust rating method. It can also be seen that Mach cutoff is the most preferable transportation mode across all conditions.

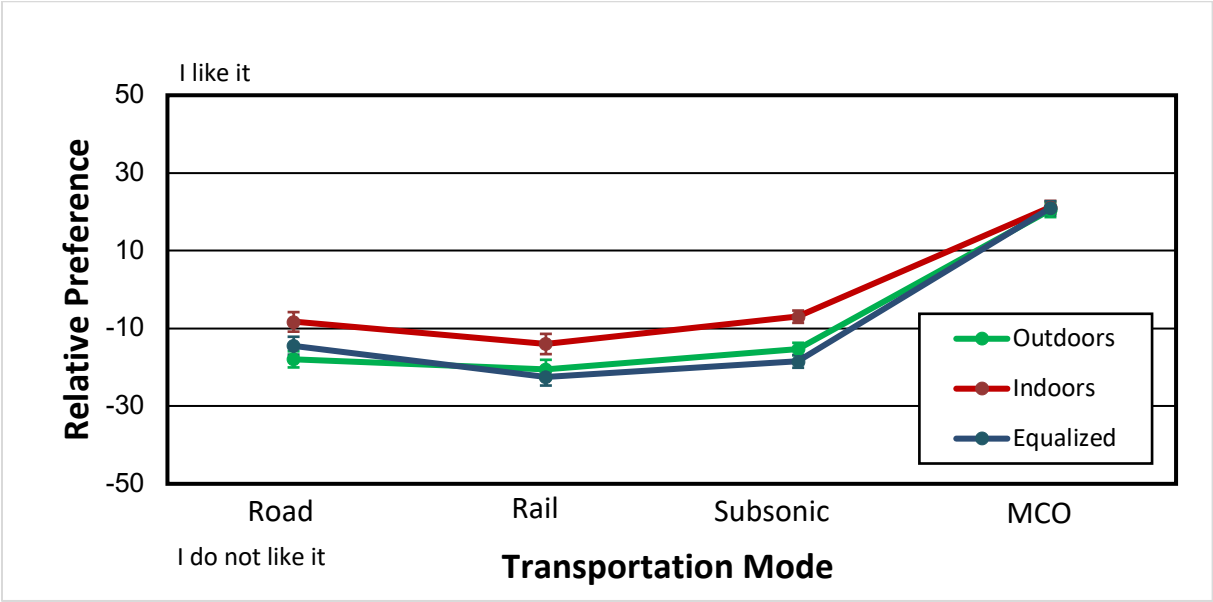

Figure 41. Method 2 results: the average preference for each condition. The indoor condition was not statistically different from the other transportation modes, as it was for method 1.

The effect of gender on the results was investigated and was found to be significant ($F = 5.853$, $P = 0.001$); see Figure 42. Male subjects gave higher annoyance ratings for the road, rail, and subsonic aircraft signatures than female subjects. This finding differs from those of prior work reported in the literature, which generally show that females are generally more noise sensitive than males (Harris, 1991). Annoyance ratings of Mach cutoff were not found to be statistically different across gender.

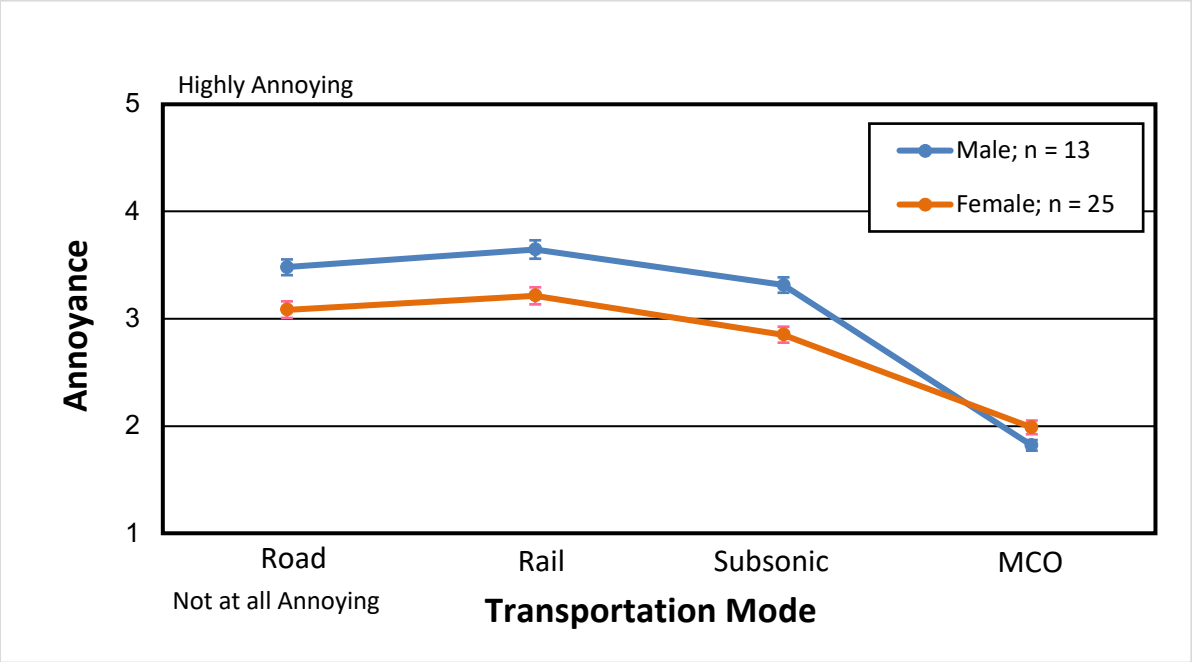

Figure 42. Annoyance ratings separated by gender for the entire dataset of individuals 18–70 years old (n = 38). Males rated road, rail, and subsonic aircraft traffic signatures as being significantly more annoying than females. No significant differences were found between the annoyance ratings of Mach cutoff signatures.

To investigate whether these findings are biased because of the disproportionate ratio of males to females in the sample, we evaluated only the results from the participants in the lowest two age categories, 18–30 and 31–40 years old, because an even number of male and female subjects participated (Figure 43). A significant interaction effect of transportation mode and gender was also found with the equal gender model (F = 2.709, P = 0.044). The findings are consistent with the previous findings that included ratings from all of the participants. That is, even though the participant sample obtained does not have an even number of male and female participants, the results are not skewed by the much higher number of female participants.

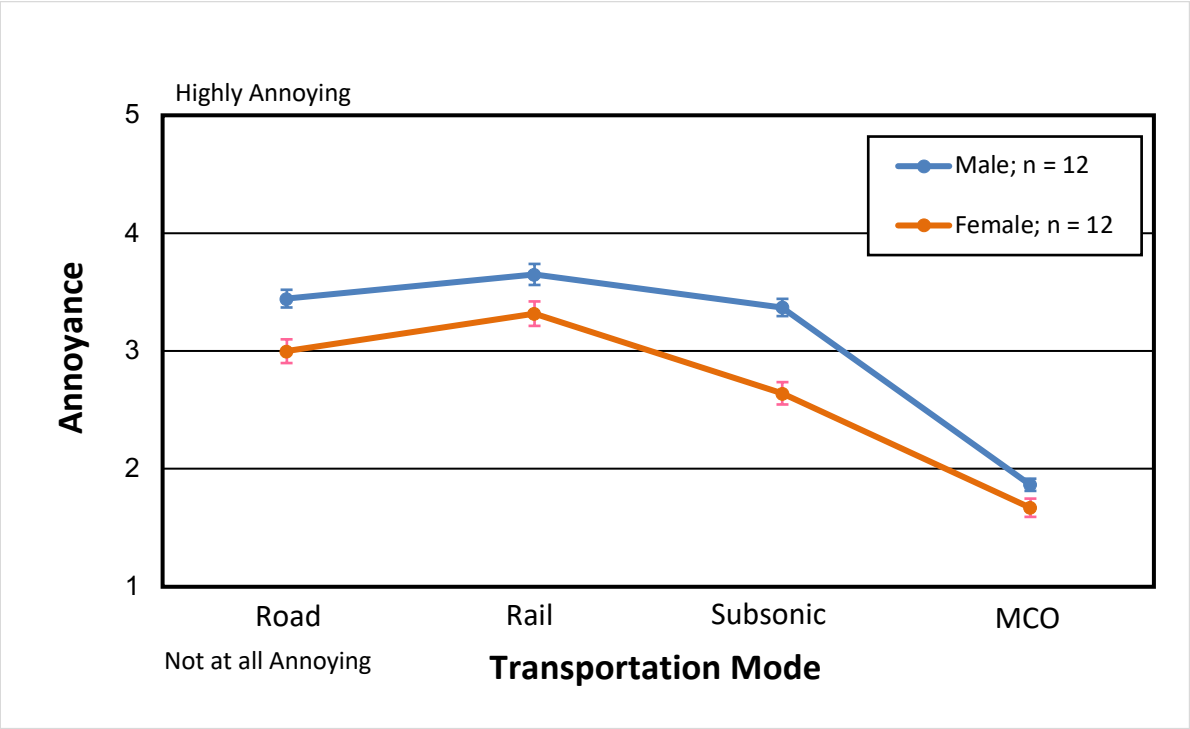

Figure 43. Annoyance ratings separated by gender for the subset of participants 18–40 years old only (n = 24), to analyze a dataset with an equal number of participants of each gender. The results of this equal gender model show that the trends are similar to those when the data from all participants are included, therefore showing that the overall results do not seem to be biased by the unequal numbers of each gender in the participant sample tested.

The effect of age on ratings was also analyzed by dividing the participants into two age groups: 18–50 and 51–70. The interaction between transportation modes and age was found to be significant (F = 15.380, P < 0.001). No significant differences were found between the age groups for road traffic and subsonic stimuli. However, differences were found for the two other transportation modes. The younger age group rated rail as significantly more annoying than did the older group, whereas the opposite result was found for Mach cutoff (Figure 44). We hypothesized that the older participants might have positive associations or nostalgia associated with rail sounds, as reported informally at the conclusion of the test session. For the case of Mach cutoff, the older participants may have had worse hearing thresholds at the higher frequencies, which would cause the low-frequency content to be perceived as louder than the loudness perceived by individuals with lower high-frequency thresholds. The finding that the older participants found Mach cutoff to be more annoying is consistent with findings reported by Foraster (2016) suggesting that older individuals tend to be more noise sensitive than younger individuals.

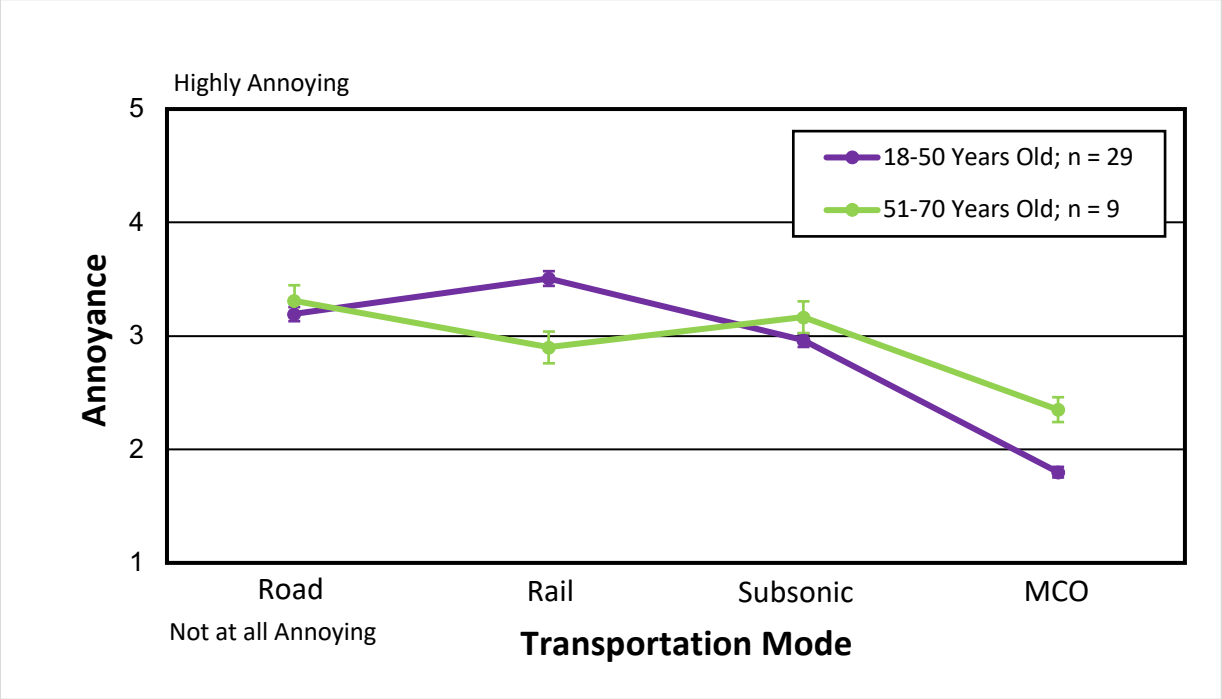

Figure 44. Annoyance ratings separated by two age groups: participants 18–50 years old (n = 29) and participants 51–70 years old (n = 9). No significant differences in annoyance ratings were found between the age groups for the road and subsonic aircraft stimuli. The participants 18–50 years old rated rail as significantly less annoying and Mach cutoff as significantly more annoying than those 51–70 years old.

The effect of age on ratings was also evaluated by comparing participants from the two lowest age categories (Figure 45), because the number of participants in each was relatively similar, unlike the division of participants above and below 50 years old (Figure 38). Significant differences in ratings were found for three of the four transportation modes considered, again with a significant interaction effect of transportation mode and age (F = 28.110, P < 0.001). Participants 18–30 years old rated both road and rail as significantly more annoying than those 31–40 years old, whereas the lowest age category rated Mach cutoff as significantly more annoying than the next age category.

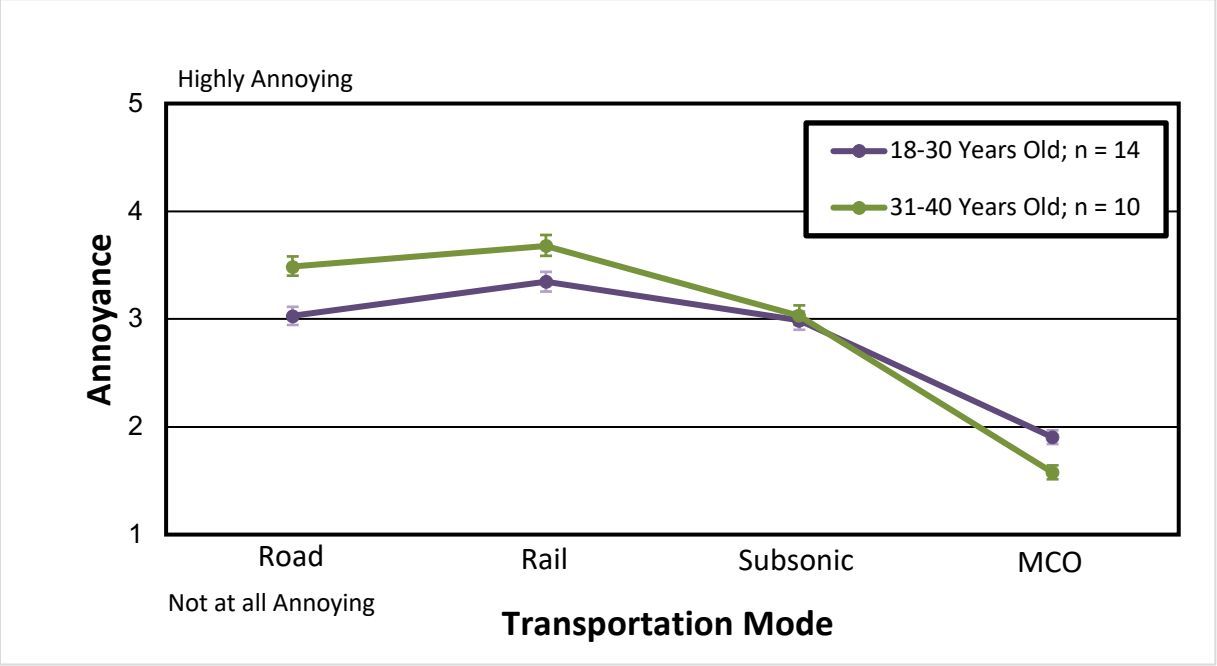

Figure 45. Average annoyance for the age ranges of 18–30 and 31–40 years. The annoyance ratings show similar trends, and there is no major difference in rail annoyance ratings.

Finally, the effect of test method order was also investigated and was found to be significant for the annoyance ratings (F = 11.249, P < 0.001), as shown in Figure 46. Subjects who took the transportation mode relative preference method first found the stimuli to be more annoying than subjects who took the annoyance rating method first. However, the trends for both test method orders are nearly identical. In addition, Mach cutoff is perceived to be the least annoying transportation mode regardless of order, thus suggesting that the conclusions stated above are still valid.

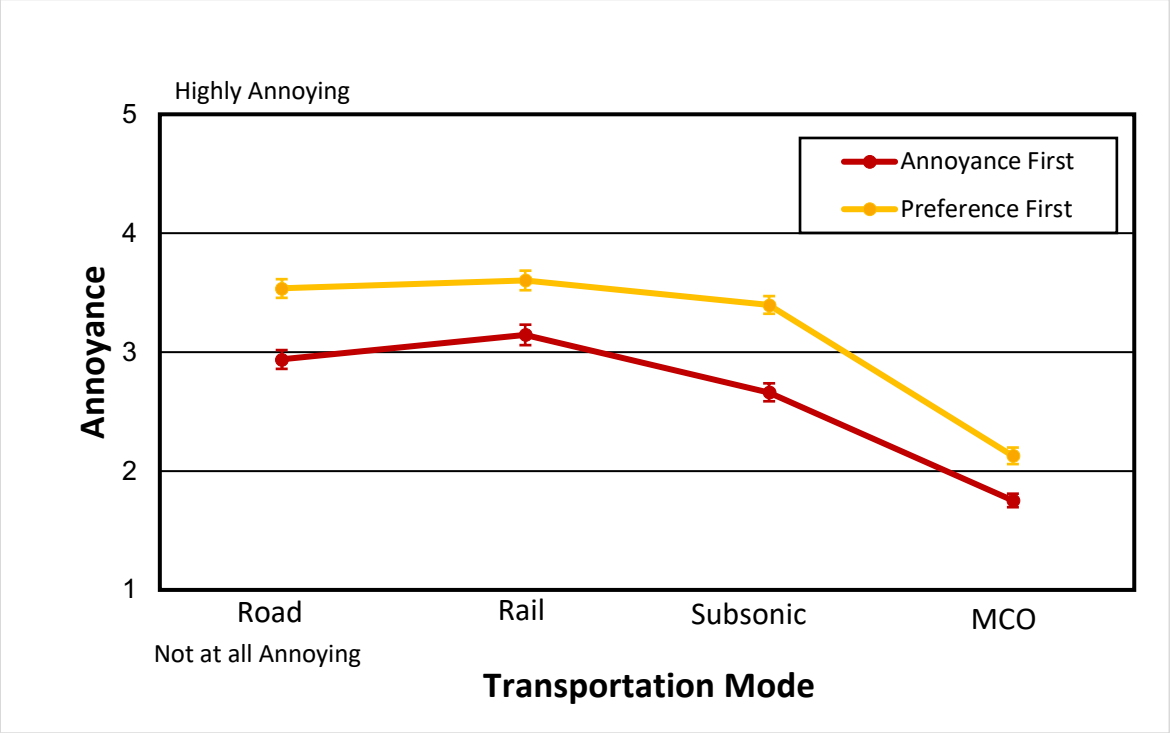

Figure 46. Method 1, average annoyance ratings separated by test method order. When subjects were given method 2 first (relative preference method), stimuli were rated as significantly more annoying than when those who completed method 1 (annoyance rating method) first.

The effect of test order on the ratings obtained in method 2 for preference was significant for only the Mach cutoff ratings (Figure 47). No significant effects were found for the relative preference ratings of the other three transportation modes. This finding may be a result of the relative preference method's use of reference stimuli, which allows for the ratings to be normalized.

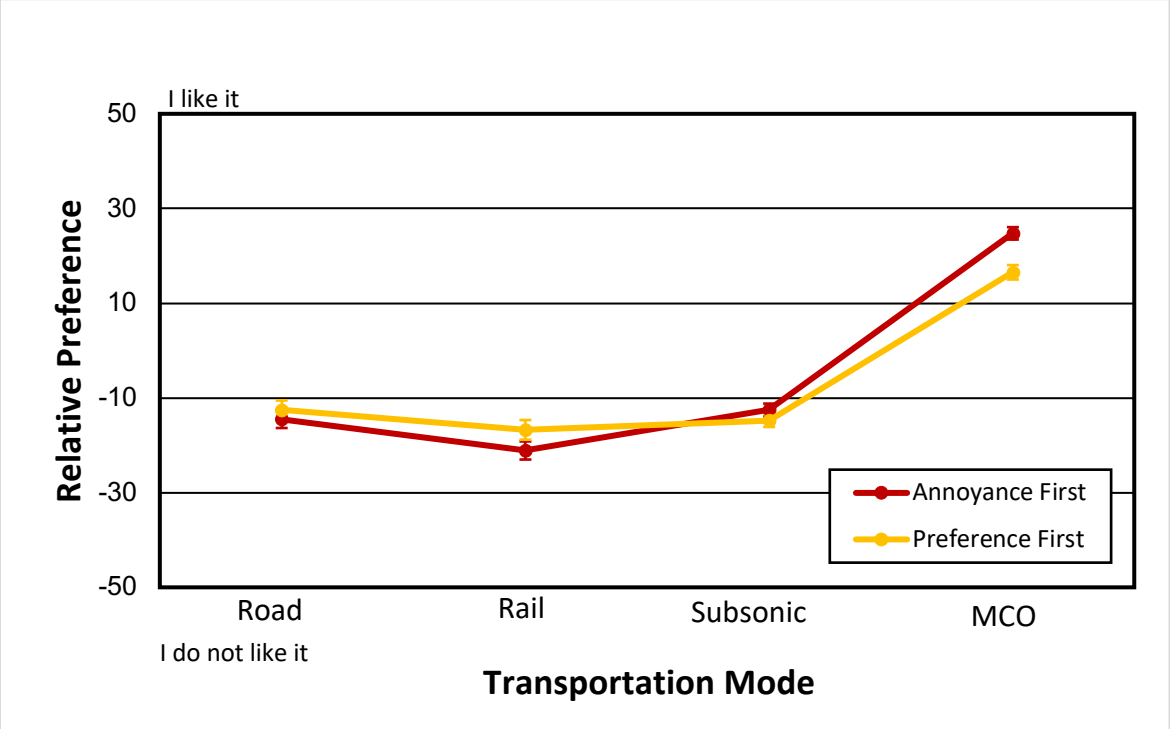

Figure 47. Method 2, average relative preference separated by test method order. No significant differences in relative preference ratings of the road, rail, and subsonic stimuli as a function of test method order were found. However, for Mach cutoff signatures, participants who completed the annoyance rating method first, the preference ratings of the Mach cutoff stimuli were significantly higher than those of participants who completed method 2 first.

Finally, the metrics considered as candidates to predict annoyance ratings in Study 2 were again considered in the analysis of the annoyance ratings from Study 3. Correlations between the annoyance ratings and five acoustic metrics; loudness (L_5), (phons), sharpness (S_5), and SEL with B- and E- weighting were found. These values are shown in Table 16. Values in bold correspond to a *P* value less than 0.005. As can be seen from the results, SEL_B and SEL_E have the statistically highest significance. This suggests that SEL_B and SEL_E are possible predictors of civilian annoyance due to Mach cutoff.

Table 16. Correlation between Mach cutoff annoyance and acoustical metrics.

Metric	Outdoors	Indoors	Equalized
Loudness (L_5)	*R* = 0.421, *P* = 0.104 (ns)	*R* = 0.432, *P* = 0.095 (ns)	*R* = 0.375, *P* = 0.152 (ns)
Loudness (Phons)	*R* = 0.799, *P* < 0.001	*R* = 0.714, *P* = 0.002	*R* = 0.762, *P* = 0.001
Sharpness (S_5)	*R* = 0.834, *P* < 0.001	*R* = 0.735, *P* = 0.001	*R* = 0.768, *P* = 0.001
SEL_B	*R* = 0.698, *P* = 0.003	*R* = 0.636, *P* = 0.008	*R* = 0.551, *P* = 0.027

Summary
Study 3 incorporated three transportation modes (road, rail, and subsonic aircraft) to provide context to Mach cutoff signatures. The recordings were obtained on-site at regional locations that captured various noise characteristics of each transportation mode. The study used two methods to investigate how Mach cutoff is perceived, as compared with other common transportation modes. The first method was an annoyance rating, which used an absolute scale to determine the perceived degree of annoyance for that stimulus. The second method was a transportation mode relative preference method, which used a relative rating to compare the transportation mode stimuli against each other. The two methods were tested in three condition sets: an indoor condition, an outdoor condition, and an equalized condition. The primary objective of the study was to determine how Mach cutoff signatures are perceived in terms of annoyance and relative preference to the three common transportation modes of road, rail, and subsonic aircraft travel. The specific questions considered and a summary of the findings are provided in Table 17.

Table 17. Analysis methods and results summary. The question, analysis methods, explanation of the analysis methods, and key findings are included.

Question	Method(s)	Explanation of Statistical Analysis	Key Findings
How do the annoyance ratings of Mach cutoff signatures compare to the ratings of road, rail, and subsonic aircraft noise?	ANOVA	ANOVA was used to investigate whether transportation mode had a significant effect on the annoyance ratings. Interactions of transportation mode with stimuli condition (indoor, outdoor, and equalized), age, and gender were also analyzed.	Mach cutoff was found to have significantly lower annoyance ratings than the other three transportation modes. No statistically significant differences were found between the ratings of the other three modes.
What is the relative preference of Mach cutoff signatures compared with the other three transportation modes?	ANOVA	ANOVA was used to investigate whether transportation mode had a significant effect on the relative preference ratings. Interactions of transportation mode with stimuli condition (indoor, outdoor, and equalized), age, and gender were also analyzed.	Mach cutoff was found to have significantly higher relative preference ratings than the other three transportation modes. Significant interaction effects were also found, which in some cases resulted in significantly different preference ratings between the other transportation modes.
Did the demographics of age and gender have a significant effect on the annoyance and relative preference ratings?	MANOVA	MANOVA was used to investigate the significant interaction effects found in both the annoyance rating method and relative preference method results.	No significant differences in Mach cutoff ratings were found across gender; however, age was found to be significant, with the older participants rating Mach cutoff as more annoying/less preferable than the younger participants.
Were the same metrics from Study 2 that were found to best predict annoyance to Mach cutoff also found to be the most appropriate metrics to predict the annoyance ratings of all four transportation modes?	Linear regression	Linear regression was used to investigate whether the five acoustical metrics considered were predictive of the annoyance ratings of the four transportation modes. Correlation tests indicated significant differences between metrics.	SEL_B and SEL_E were found to be potential candidates to predict civilian annoyance of Mach cutoff signatures.

Milestone(s)

Milestone (Proposal)	Comments	Planned Due Date	Status
The hybrid simulated and measured stimuli will be developed; experimental design for the first subjective study will be completed. ASCENT Adv. Committee presentation.	According to the results of Study 2, there was no need to further investigate hybrid stimuli. Instead, the purpose of study 3 was revised to investigate the perception of annoyance of Mach cutoff signatures relative to road, rail, and subsonic aircraft traffic sounds.	November 1, 2018	Complete
Study 2 will be completed, and a single metric will be proposed.	SEL_B and SEL_E were found to be the best predictors of annoyance. Either metric may be appropriate for predicting annoyance due to Mach cutoff operations.	February 1, 2019	Complete
Study 3 using the indoor stimuli will be completed, and the results will yield a predicted percentage highly annoyed curve due to Mach cutoff signatures heard indoors.	In addition to indoor stimuli, Study 3 included outdoor and equalized stimuli. The results of this study confirmed the findings of Study 2 for the recommended metrics. The modification to the experimental design does mean that a percentage highly annoyed curve was not obtained.	July 31, 2018	Complete
Final reporting.	(No change)	November 22, 2019	Complete

Major Accomplishments

- Study 2 factor analysis was completed, and the factors correlating with annoyance were identified.
- Study 2 metric analysis was completed: metrics appropriate for predicting each perceptual attribute, including annoyance, were identified.
- Study 2 analysis of the inclusion of simulated shocks with NASA recordings was completed: no significant effect of adding simulated shock was found on the annoyance ratings.
- Study 2 demographic investigations were completed: the relationships between demographics and perceptual data were evaluated, and relationships among demographic factors were investigated.
- All Study 3 stimuli were obtained from local interstates, railways, and airports.
- The degree of annoyance study (Study 3) was designed; two methods were used (annoyance rating and transportation mode preference).
- Study 3 data collection was completed; 38 subjects participated in the study.
- Statistical analyses were conducted on the collected data with linear regression and ANOVA.
- Interactions among variables such as the transportation mode, gender, age, and condition were found for the annoyance ratings and transportation mode preference.

Publications

Published conference abstracts

Broyles, J., Vigeant, M.C., & Sparrow, V.W. (2019). Perceived annoyance of Mach cutoff flight ground signatures compared to common transportation sounds. Journal of the Acoustical Society of America **146**(4, Pt. 2) 2782.
Ortega, N.D., Vigeant, M.C., & Sparrow, V.W. (2019). Identifying metrics to predict annoyance due to Mach cutoff flight ground signatures. Journal of the Acoustical Society of America. **145**(3, Pt. 2) 1899.

Outreach Efforts

N/A

Awards

Jonathan Broyles, National Council of Acoustical Consultants (NCAC) Student Travel Award (October 2019) to support participation in ASA San Diego.

Student Involvement

Nicholas Ortega was primarily responsible for test design, stimulus selection, test preparation, statistical analyses, and presentation preparation for the first two studies. Ortega presented the results of Study 2 at ASA Louisville in Spring 2019.

Jonathan Broyles was primarily responsible for the test design, stimulus recordings (road, rail, and subsonic transportation modes), stimulus selection, test preparation, statistical analyses, and presentation preparation for the third study. He will present a talk on this study at ASA San Diego in December 2019.

Plans for Next Period

None. This report will serve as the final report, because the project will not be continuing in 2019–2020. (The PI will work with the graduate students who worked on this project, Nick Ortega and Jonathan Broyles, to publish peer-reviewed journal articles on the worked completed under the support of P42 in the coming year. All manuscripts will be sent to the project manager for review before submission to a journal.)

References

ASHRAE. (2019). ASHRAE handbook: HVAC applications. American Society of Heating, Refrigerating, and Air-Conditioning Engineers, Atlanta.

Bradley, J. & Birta, J. (2001). On the sound insulation of wood stud exterior walls. Journal of the Acoustical Society of America 110(6) 3086-3096.

Cliatt II, L.J., Hill, M.A., & Haering Jr., E.A. (2016). Mach cutoff analysis and results from NASA's Farfield investigation of no-boom thresholds. 22nd AIAA/CEAS Aeroacoustics Conference, AIAA 2016-3011.

Fastl, H. (2006). Psychoacoustic basis of sound quality evaluation and sound engineering. The Thirteenth International Congress on Sound and Vibration; Austria.

Gaëtan, L. (2005). Individual vocabulary profiling of spatial enhancement systems for stereo headphone reproduction. Audio Engineering Society Convention 119, paper 6629.

Gerzon, M. (1973). Periphony: With-height sound reproduction. Journal of the Audio Engineering Society 21(1) 2-10

Gower, J.C. (1974). Generalized procrustes analysis. Psychometrika 40(1) 33-51.

Foraster, M., Eze, I., Vienneau, D., Brink, M., Cajochen, C., Caviezel, S., Heritier, H., Schaffner, E., Schindler, C., Wanner, M., Wunderli, J.M., Roosli, M., & Probst-Hensch, N. (2016). Long-term transportation noise annoyance is associated with subsequent lower levels of physical activity. Environmental International, 91 341-349.

Harris, C.M. (1991). Handbook of acoustical measurements and noise control (3rd ed., Ch. 23). McGraw-Hill.

Johnson, R. & Wichern, D. (2013). Applied multivariate statistical analysis. Pearson.

Kutner, M.H., Nachtsheim, C.J., & Neter, J. (2004). Applied linear regression models (4th ed). McGraw-Hill.

Neal, M.T. (2015). Investigating the sense of listener envelopment in concert halls using third-order ambisonic reproduction over a loudspeaker array and a hybrid room acoustics simulation method. M.S. Thesis, The Pennsylvania State University.

Page, J.A., Hodgdon, K., Krecker, P., Cowart, R., Hobbs, C., Wilmer, C., Koening, C., Holmes, T., Gaugler, T., Shumway, D., Rosenberger, J., & Philips, D. (2014). Waveforms and sonic boom perception and response (WSPR): Low-boom community response program pilot test design, execution, and analysis. NASA/CR-2014-218180.

Parizet, E., Hamzaoui, N., & Sabatié, G. (2005). Comparison of some listening test methods: A case study. Acta Acustica united with Acustica. 91(2) 356-364.

Patterson, R.D., Nimmo-Smith, I., Weber, D.L., & Milroy, R. (1982). The deterioration of hearing with age: Frequency selectivity, the critical ratio, the audiogram, and speech threshold. Journal of the Acoustical Society of America 72(6) 1788-1803.

Penn State IRB. STUDY00005018. Acoustical model of Mach cutoff flight.

Stevens, S.S. (1972). Perceived level of noise by mark VII and decibels (E). Journal of the Acoustical Society of America 51(2, Pt. 2) 575-601.

Torija, A., Roberts, S., Woodward, R., Flindell, I., McKenzie, A., & Self, R. (2019). On the assessment of subjective response to tonal content of contemporary aircraft noise. Applied Acoustics, 146 190-203.

Weinstein, N.D. (1978). Individual differences in reactions to noise: A longitudinal study in a college dormitory. Journal of Applied Psychology. 63(4) 458-466.

Wesler, J.E. (1973). Surface transportation noise and its control. Journal of the Air Pollution Control Association. 23(8) 701-703.
Williams, A.A. & Langron, S.P. (1984). The use of free-choice profiling for the evaluation of commercial ports. Journal of the Science of Food and Agriculture. 35 558-568
Zwicker, E. & Fastl, H. (1990). Psychoacoustics. Berlin: Springer-Verlag.

Appendix: Perceptual Study 2 Additional Figures

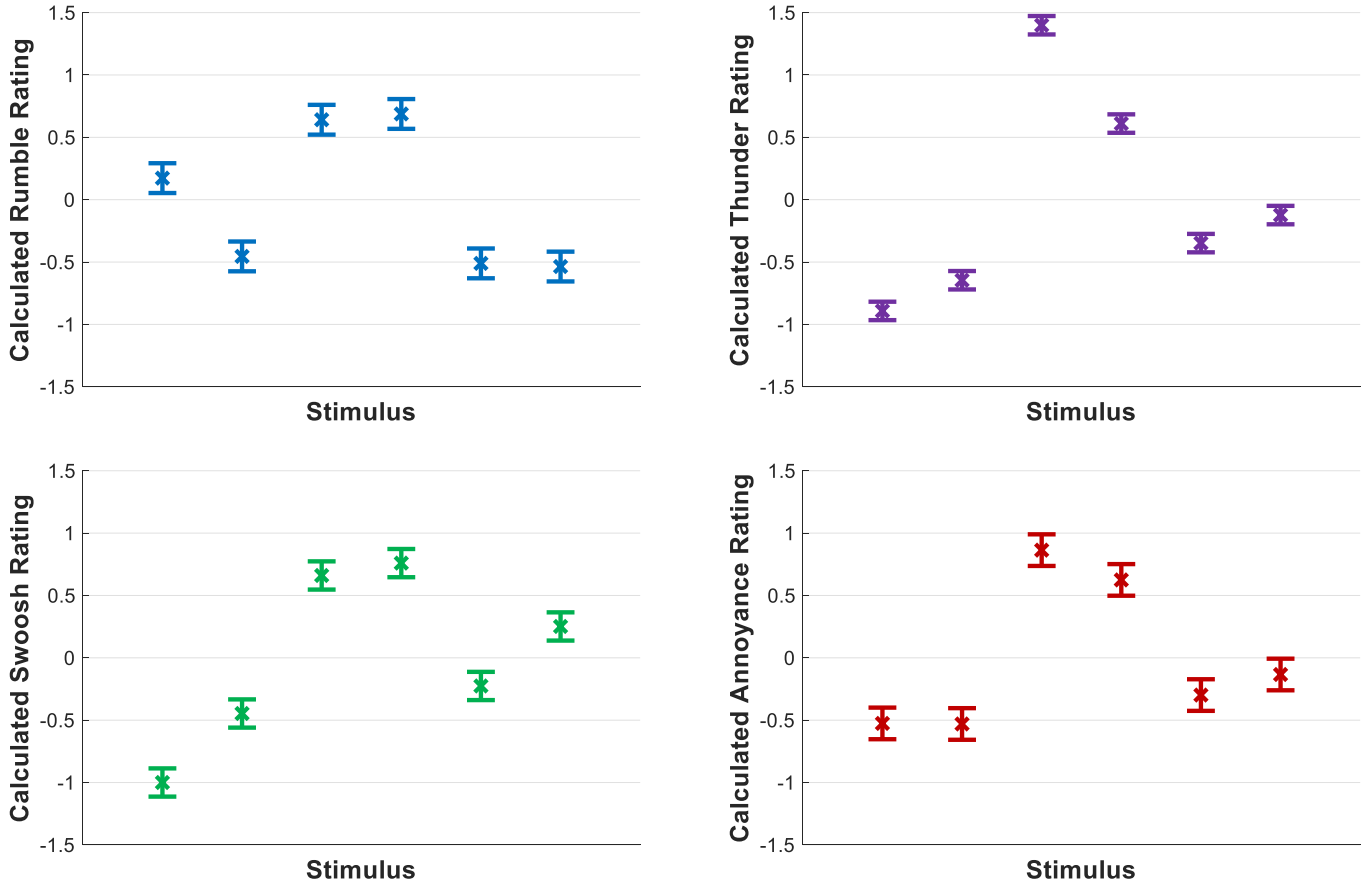

Figure A1. Rating data on all scales for each stimulus. Averages are plotted with the "X" symbol, and error bars indicate 95% confidence intervals for the mean value.

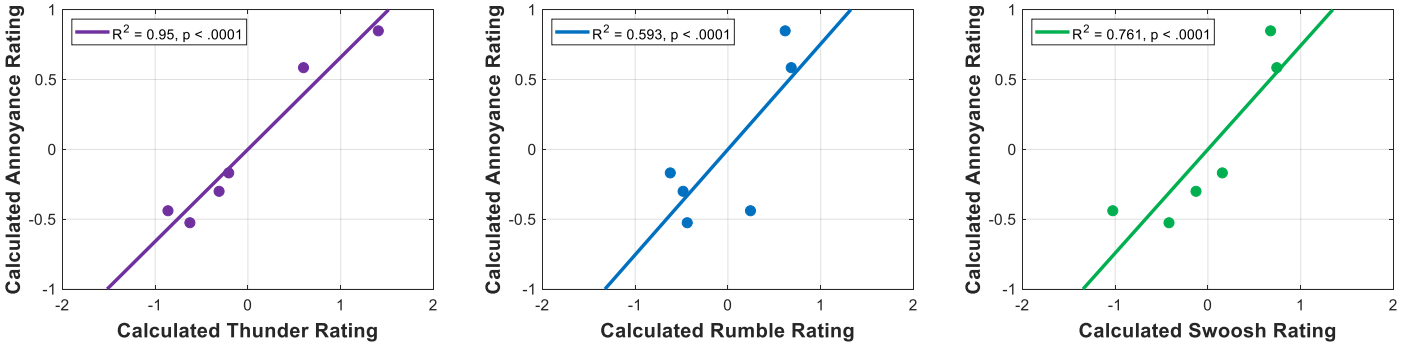

Figure A2. Trend lines showing relationships between "annoying" ratings and all other ratings. Only average ratings are plotted. Correlations values are calculated between average ratings, but *P* values are calculated on the basis of the entire dataset.

Project 043 Noise Power Distance Re-Evaluation

Georgia Institute of Technology

Project Lead Investigator

Dimitri Mavris (PI)
Regents Professor
School of Aerospace Engineering
Georgia Institute of Technology
Mail Stop 0150
Atlanta, GA 30332-0150
Phone: 404-894-1557
Email: dimitri.mavris@ae.gatech.edu

University Participants

Georgia Institute of Technology

- PI(s): Dr. Dimitri Mavris (PI), Mr. Christopher Perullo (Co-PI), Dr. Michelle Kirby (Co-PI)
- FAA Award Number: 13-C-AJFE-GIT-048
- Period of Performance: June 28, 2016 to March 28, 2020
- Task(s):
    1. Investigate the impact of frequency content on standard NPD curves through a sensitivity study of weather effects in AEDT
    2. Investigate the impact of frequency content on NPD+C data by utilizing NASA's ANOPP tool
    3. Perform a validation with noise data in AEDT

Project Funding Level

This project is funded at the following levels: Georgia Institute of Technology ($220,000). The Georgia Institute of Technology has agreed to a total of $220,000 in matching funds. This total includes salaries for the project director, research engineers, and graduate research assistants and for computing, financial, and administrative support, including meeting arrangements. The institute has also agreed to provide tuition remission for students whose tuition is paid via state funds.

Investigation Team

- Dimitri Mavris, Principal Investigator, Georgia Institute of Technology
- Michelle Kirby, Co-Investigator, Georgia Institute of Technology
- Tejas Puranik, Research Faculty, Georgia Institute of Technology
- Yongchang Li, Research Faculty, Georgia Institute of Technology
- Christopher Perullo, Research Faculty, Georgia Institute of Technology
- Ameya Behere, graduate student, Georgia Institute of Technology
- Sarah Malak, graduate student, Georgia Institute of Technology
- Shilpa Ravoory, graduate student, Georgia Institute of Technology
- Wenxin Zhang, graduate student, Georgia Institute of Technology
- Seulki Kim, graduate student, Georgia Institute of Technology
- Andrew Van Zwieten, graduate student, Georgia Institute of Technology

Project Overview

The standard technique for evaluating fleet noise is to estimate flight procedure source noise using noise power distance (NPD) curves. Noise calculations within the Aviation Environmental Design Tool (AEDT) rely on NPD curves provided by aircraft manufacturers. This dataset reflects representative aircraft categories at set power levels and aircraft configurations. Noise levels are obtained as a function of slant distance via spherical spreading through a standard atmosphere, and other

correction factors are applied to obtain the desired sound field metrics at the location of the receiver. The current NPD model does not consider the aircraft configuration (e.g., flap settings) or alternative flight procedures being implemented. These factors are important, as the noise characteristics of an aircraft depend on thrust, aircraft speed, and airframe configuration, among other contributing factors such as ambient conditions. The outcome of this research is an approach based on the suggested NPD + configuration (NPD+C) format, which will enable more accurate noise predictions due to its inclusion of aircraft configuration and speed changes.

This project is currently in its third year, which started late due to funding issues. As a result, the work is not yet complete, and a brief description of the current work status is provided in the following sections. During the third year (this year), this work has focused on two main topics. First, prior work will be extended to examine the impact of NPD spectral (frequency) content on NPD+C curves. In this work, the impact of the NPD+C approach is investigated while the trajectories and spectral data are held constant in order to isolate the effect of the appropriate NPDs. This first focus is divided into two aspects: (a) the manner in which the spectral data are used within AEDT while all other parameters are held constant and 2) the manner in which the noise contours change when utilizing spectral data generated from the Environmental Design Space (EDS) in a fashion similar to that of the NPD+C approach. Second, the NPD+C approach will be validated using available aircraft operation and airport noise monitoring data. A brief description of the prior work is provided for reference.

In year 1, Georgia Tech leveraged domain expertise in aircraft and engine design and performed an analysis to evaluate gaps in the current NPD curve generation and subsequent prediction process with respect to fleet noise prediction changes arising from aircraft configuration and approach speed. The team applied EDS physics-based modeling capabilities to conduct a sensitivity analysis to identify additional parameters to be included in the NPD+C format. In year 2, we focused on providing recommendations on potential additional data required for AEDT and developing correction models for existing NPD curves within AEDT to mimic the NPD+C estimations. The results showed that correction models for existing AEDT NPD curves can be created to morph the baseline NPD curves into data that match an NPD+C dataset created through a physical modeling tool. This process was developed and tested for three aircraft sizes (50-, 150-, and 300-passenger aircraft), but a full development of correction functions is beyond the scope of this work. The development of a full set of correction functions has been proposed, but has not yet been funded.

The prior work primarily focused on determining which aspects of aircraft configuration and speed are the primary drivers of community noise. The results indicate that the impact of aircraft speed on component (engine, flap) source noise and flap angle are the major parameters to include in any NPD approach, including one based on configuration. To focus on understanding these complex results, the prior work did not examine the impact of configuration or speed changes on the spectral (frequency) content of the NPD data. In theory, an NPD dataset containing different noise levels for different configuration and speed settings should also have different frequency contents for each configuration and speed setting, which will impact noise predictions for nonstandard day conditions. The current work will investigate this impact.

Task 1- Investigate the Impact of Frequency Content on Standard NPD Curves

Georgia Institute of Technology

Objective(s)

AEDT currently uses a single spectral dataset that is assumed to be consistent with an observer directly beneath the flight path. The spectral data are used to correct noise attenuation as the atmosphere is shifted from a standard day. Incorrect spectral data can lead to substantial over- or underestimations of the community noise contour. As more detailed aircraft configuration data are included in the NPD dataset, the spectral data will change, which leads to more fundamental questions regarding the accuracy of using a single spectral dataset for the entire NPD curve. To investigate the impact of these assumptions, Georgia Tech will use NASA's ANOPP noise prediction tool to generate a unique spectral dataset for each combination of thrust and distance for standard approach and departure NPD curves. Once generated, an XML format must be created to allow this information to be used with a modified version of AEDT, which was developed during year 1 of this project. This modified AEDT version enables a unique NPD dataset to be used for each flight segment (instead of a common NPD dataset, as is currently used). Additional modifications to the source code will be made to input unique spectral information, generated by ANOPP, for use in each AEDT flight segment.

Once modifications are made to AEDT, a sensitivity study will be performed to examine the impact of the inclusion of unique spectral data for each thrust–distance combination. The 80-dB sound exposure level (SEL) contour will be examined for multiple aircraft sizes, including the regional jet, single-aisle, and twin-aisle classes. The 80-dB SEL contour will be examined first because it trends well with the resulting 65-dB DNL contour; however, complete grids will be generated, enabling examinations of any contour noise level. Other contour areas will be examined if further insight is required. This information will be used to inform the FAA of any possible prediction errors in the current AEDT approach.

The objective of Task 1 is to investigate the impact of frequency content on the standard NPD curves in AEDT. To conduct this investigation, the following questions will be considered:

1. How are spectral data utilized in AEDT?
2. Which parameters should be varied and what should the variation ranges be?
3. What are the major drivers behind the impact?

Task 1 establishes a baseline for comparison in Task 2. Both tasks are focused on quantifying the potential benefit derived from including spectral information for each NPD+C aircraft configuration and speed and on determining whether a single spectral parameter for approach and departure is sufficient. Task 1 will use baseline AEDT NPD and spectral data information for a given aircraft under varying weather conditions to establish the impact of spectral content. It should be noted that the spectral data are used for nonstandard day conditions, which has motivated a sensitivity test for varying weather conditions. Determining the sensitivity to different weather conditions enables an examination of the impact of spectral content for NPD and NPD+C data. Subsequently, Task 2 will use NPD+C data generated for a single spectral class per vehicle (NPD+C and single spectrum for each NPD+C curve per vehicle) and multiple spectral classes per vehicle (unique to each speed and aircraft configuration). The results can then be compared to evaluate whether the NPD+C approach should use a single spectral class per vehicle or whether configuration- and speed-dependent spectra are warranted. Because this task is ongoing, the establishment of a baseline for comparison is described.

Research Approach

Weather variation and test case generation

To assess the effect of weather parameters on noise and emissions, a quantitative sensitivity analysis must be performed. However, prior to any simulations, the weather parameters and relevant variation ranges were identified. The airports included in the sensitivity study were selected based on the variation in airport altitude. Once the airports were selected, the weather parameters for these airports were studied over a 20-year time frame. Data were obtained from Iowa State University's Iowa Environmental Mesonet database, which contains an archive of automated airport weather observations at various locations. The results of a sample analysis of temperature variations at the Atlanta airport over a period of ten years are shown in Figure 1. The variable indicating the hourly temperature is defined as 'tmpf' in this figure. By performing these analyses, suitable variation ranges were identified for the airports.

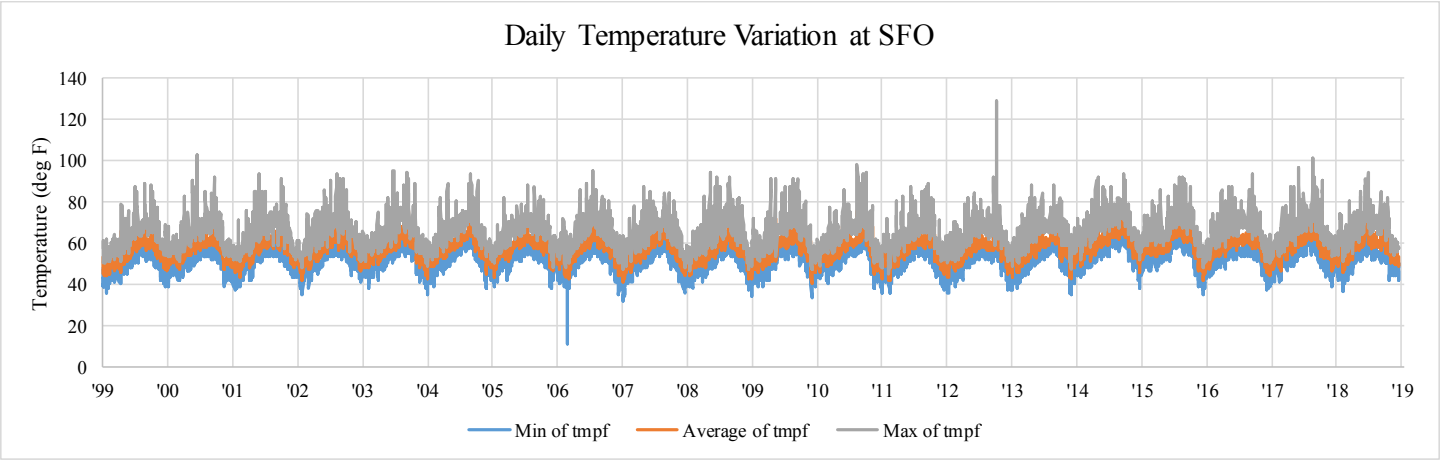

Figure 1. Daily temperature variation at the SFO airport over 20 years.

Once suitable ranges for weather parameters were identified, the parameters were modeled in AEDT through the airport weather definition. In AEDT, an airport weather definition consists of six parameters: temperature, dew point, relative humidity, station pressure, sea-level pressure, and wind speed. Wind speed is defined as a scalar value and thus represents only the magnitude. The wind is always assumed to act as a headwind for all operations at the airport (regardless of runway assignments), and there is no option to specify the wind direction. The remaining five parameters are correlated and cannot be varied independently. For example, for the group of temperature, relative humidity, and dew point, the values of any two parameters can be used to calculate the third value. Sea-level pressure and station pressure are also correlated, and additionally, pressure values affect humidity calculations. To model weather variations in AEDT, it is important to ensure internal consistency among the weather parameters. Hence, the sea-level pressure and dew point were not varied independently in the weather design of experiment (DOE) study; instead, these parameters were calculated as dependent on the other four parameters.

For an initial sensitivity study, a one-factor-at-a-time (OFAT) DOE approach was chosen. In such a DOE study, only one parameter is varied while all others are set to their baseline value. Temperature and wind speed were varied at two levels, denoted Min and Max. Because the humidity has a nonlinear effect on noise and emissions, more levels of relative humidity were modeled. The complete DOE is shown in Table 1.

Table 1. Design of experiment (DOE) of test scenarios for initial weather sensitivity analysis.

Test Scenario	Temperature (deg F)	Sea-level Pressure (mb)	Station Pressure (mb)	Dew Point (deg F)	Relative Humidity (%)	Wind Speed (knots)
Baseline	62	1018.02	980.61	50.86	67.65	7.03
Temperature	40	1018.02	980.61	30.00	67.65	7.03
Wind Speed	62	1018.02	980.61	50.86	67.65	0.00 30.00
Humidity	62	1018.02	980.61	-40.03 20.44 37.40 47.96 55.76 62.00	1 20 40 60 80 100	7.03

Relative and absolute humidity

There are several methods for modeling atmospheric humidity. While approaches based on the relative humidity and dew point may be more common, both values are dependent on ambient temperature. There are also dependencies on ambient pressure; however, in the context of weather, the appropriate standard atmospheric pressure at a given altitude is assumed. These dependencies arise because the intrinsic capacity of the ambient air to hold water vapor is dependent on its temperature and pressure. The maximum water vapor content of air under saturated conditions increases with temperature and decreases with pressure. For example, a 50% relative humidity at 70 ˚F and 1 bar corresponds to a higher water content than 50% relative humidity at 50 ˚F and 1 bar, but a lower water content than 50% relative humidity at 70 ˚F and 0.99 bar.

This approach is problematic because changes in relative humidity values may not reflect the desired changes in the water content in air (absolute humidity). However, in an OFAT type analysis, the use of a linear relative humidity variation is justified when the temperature and pressure are set to baseline conditions.. The actual water vapor content was calculated for all conditions, as shown in Figure 2. This figure shows that a linear variation in relative humidity leads to a linear variation in absolute humidity for the baseline temperature and pressure. It must be noted that when multiple parameters are varied across test scenarios, it may be desirable to assume a linear variation in absolute humidity when calculating the relative humidity. This approach may lead to a more accurate modeling of humidity variation than modeling based on a linear variation in relative humidity.

AEDT modeling of OFAT weather sensitivity analysis

After the DOE was constructed, the different test scenarios were simulated in AEDT. For the initial study, a single aircraft and airport combination (Boeing 737800, KATL) was used. Initial simulations were performed using the STANDARD stage length standard 3 (SL3) departure procedure. However, after our initial analysis, it was found that the weather parameters affect

both aircraft performance and noise/emission models. For example, the effect of temperature on aircraft performance is shown in Figure 3.

For this task, it was desirable to isolate the weather sensitivity of the noise/emission models rather than the performance. Hence, later simulations were performed using a fixed-point profile instead of a procedural profile. A fixed-point profile allows the entire AEDT performance model to be bypassed. To model a fixed-point profile, the performance output of the STANDARD SL3 procedural profile was simply reformatted and imported as a fixed-point profile in AEDT. The results shown below are based on fixed-point profile simulations.

Temperature sensitivity

The effect of ambient temperature on the noise and emissions is summarized in this section. This sensitivity analysis was performed by comparing results for the baseline temperature (62 ˚F) with a low-temperature case (40 ˚F) and a high-temperature case (100 ˚F). The effects on the SEL noise metric are shown in Figure 4 and Table 2. For the high-temperature case, it is observed that the contour decreases in both length and area, while the opposite effect is observed at low temperature. This trend was observed consistently across different dB levels, although the magnitude of the change differs.

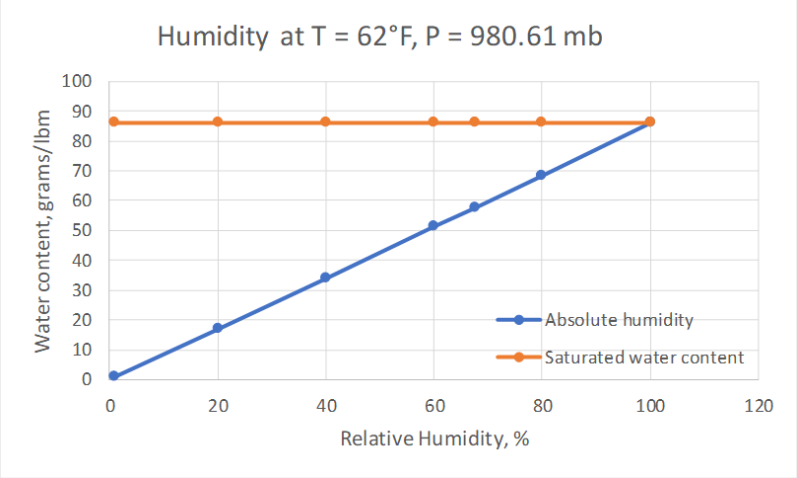

Figure 2. Absolute vs. relative humidity under baseline temperature and pressure conditions.

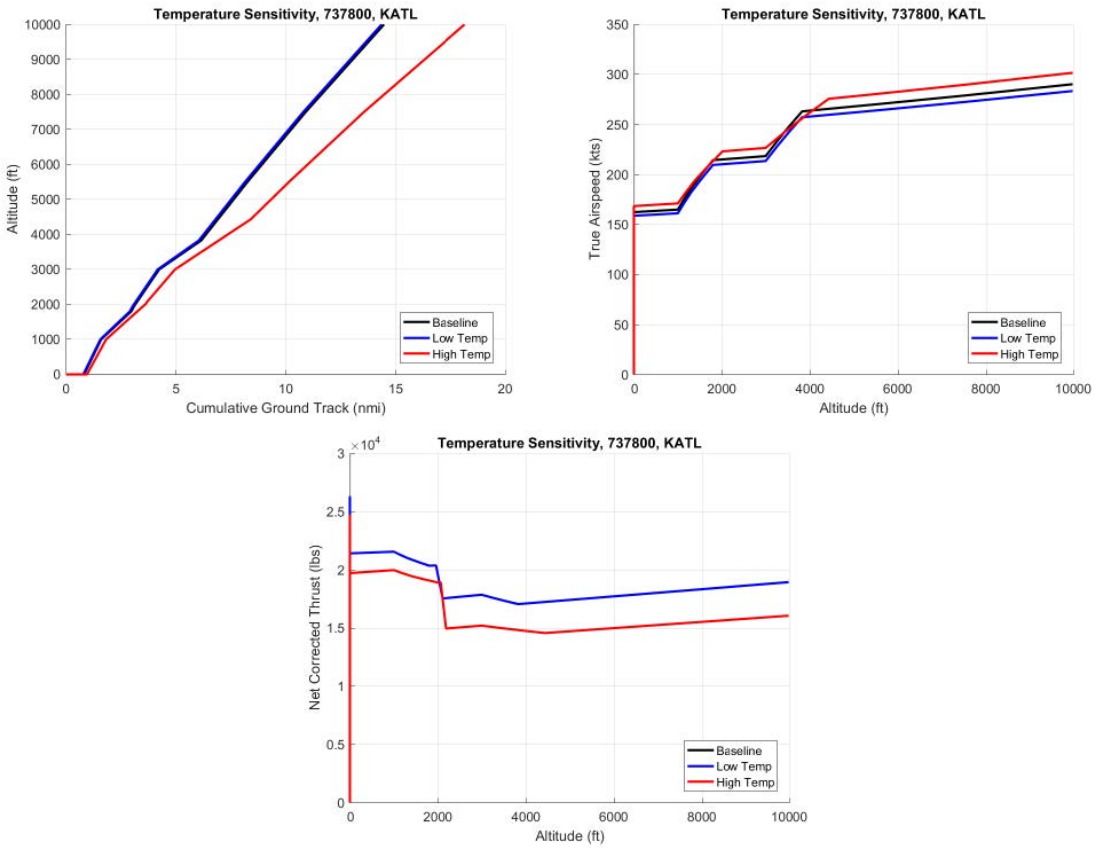

Figure 3. Effect of temperature on aircraft performance.

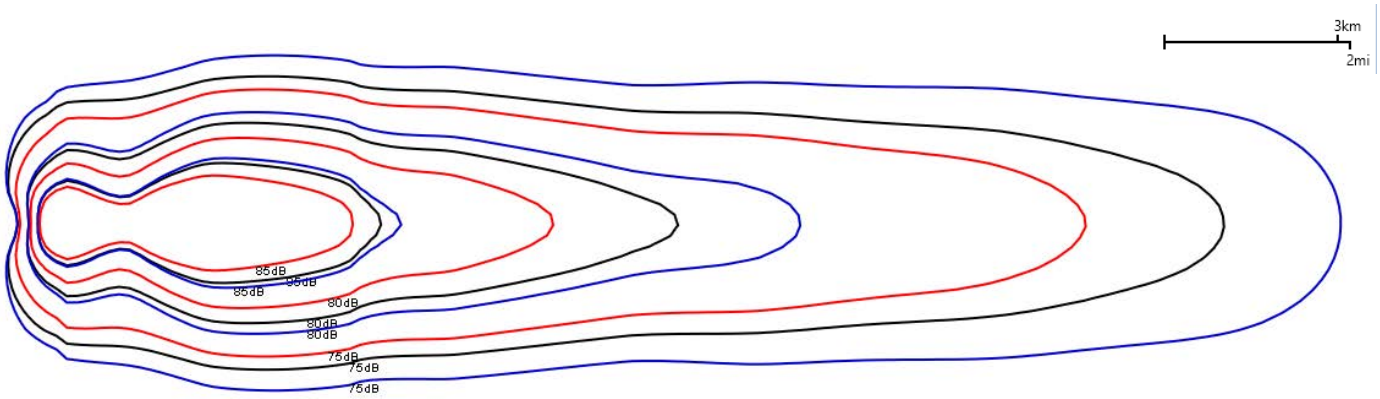

Figure 4. Effect of ambient temperature on sound exposure level (SEL, dB) contours.

Table 2. Effect of temperature on contour attributes.

Contour (dB)	Baseline		Low Temperature				High Temperature			
	Length (km)	Area (km^2)	Length (km)		Area (km^2)		Length (km)		Area (km^2)	
75	47.37	82.63	53.04	11.98%	112.50	36.15%	41.53	-12.32%	63.25	-23.45%
80	25.72	28.03	30.39	18.14%	36.12	28.87%	20.91	-18.69%	19.02	-32.13%
85	14.19	9.25	14.95	5.32%	10.26	10.91%	12.74	-10.21%	6.59	-28.71%

The effect of temperature on fuel burn and NO_x emissions is shown in Figure 5. A slight variation is observed in fuel burn under a lower ambient temperature, leading to a lower fuel consumption. A higher sensitivity is observed for NO_x emissions, with an inverse correlation between the temperature and NO_x emissions. For temperatures beyond the engine's flat rating, the high-temperature thrust model is used by AEDT. In this thrust model, the combustor temperature is held constant at its maximum value and does not change with increasing ambient temperature. Moreover, a higher ambient temperature for a given relative humidity implies a higher absolute humidity, in terms of the mass fraction of water vapor to dry air. The absolute humidity has an inverse correlation to NO_x production, as shown in detail in Figure 10. Therefore, the NO_x generation inside the combustor, given as a fraction of the fuel flow rate, decreases due to the constant maximum combustor temperature and increased water content. Although the overall fuel consumption increases marginally for the high-temperature case, the NO_x production rate is much lower than the baseline case, thereby leading to a lower total NO_x production.

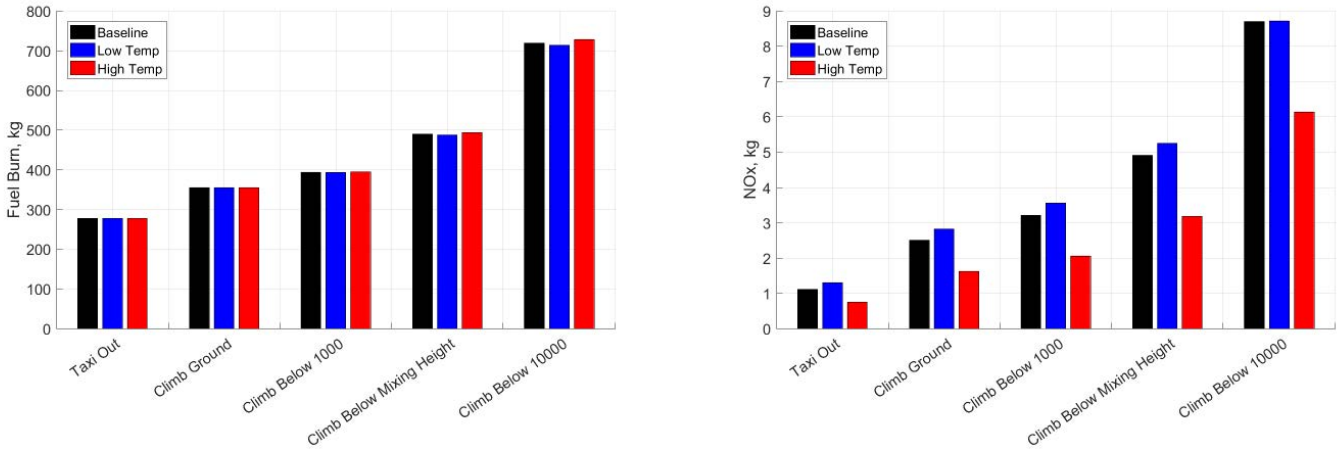

Figure 5. Effect of ambient temperature on fuel burn and NO_x emissions.

Sensitivity to wind speed

The effect of wind on noise and emissions is summarized in this section. This sensitivity analysis was performed by comparing the results for the baseline wind (7.03 kts) with a no-wind case and a high-wind case (30 kts). It should be noted that AEDT Aircraft Performance Module applies all winds as a headwind, regardless of the aircraft flight orientation. Additionally, AEDT's Aviation Acoustic Module does not model the effect of wind on noise propagation, i.e., the sound is not "carried" by the wind. Therefore, any effects on the noise grid are expected to arise from changes in aircraft performance. Because a fixed-point profile is used in this study, no effect of wind on the SEL dB noise grid was observed, as shown in Figure 6.

Although there is no change in the noise results, the fuel burn and emissions are affected by the wind, as displayed in Figure 7. This influence arises because the wind impacts the aircraft's fuel flow rates due to changes in drag. A positive correlation is observed with higher winds, leading to a higher fuel consumption as well as higher NO_x emissions.

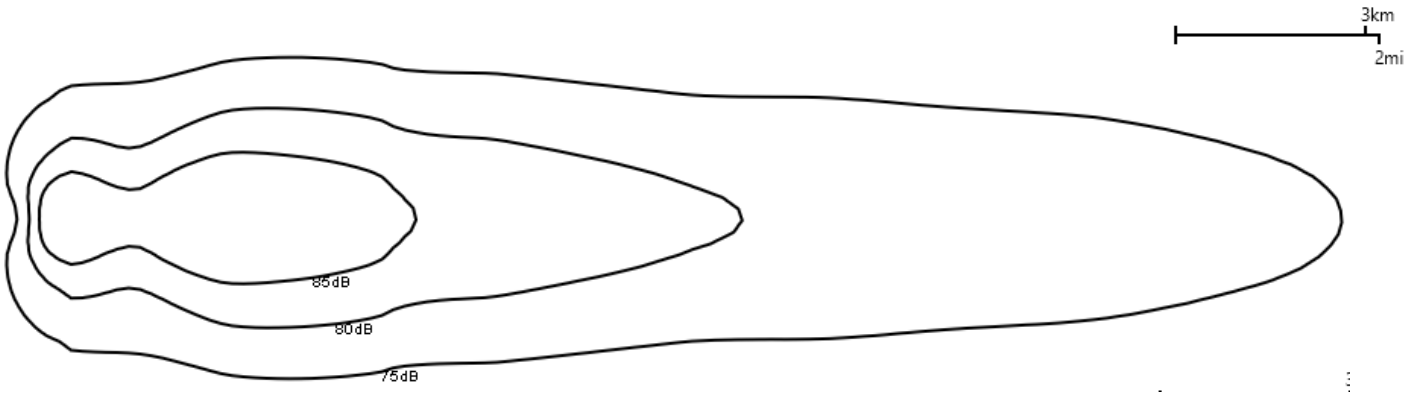

Figure 6. Effect of wind speed on sound exposure level (SEL, dB) contours.

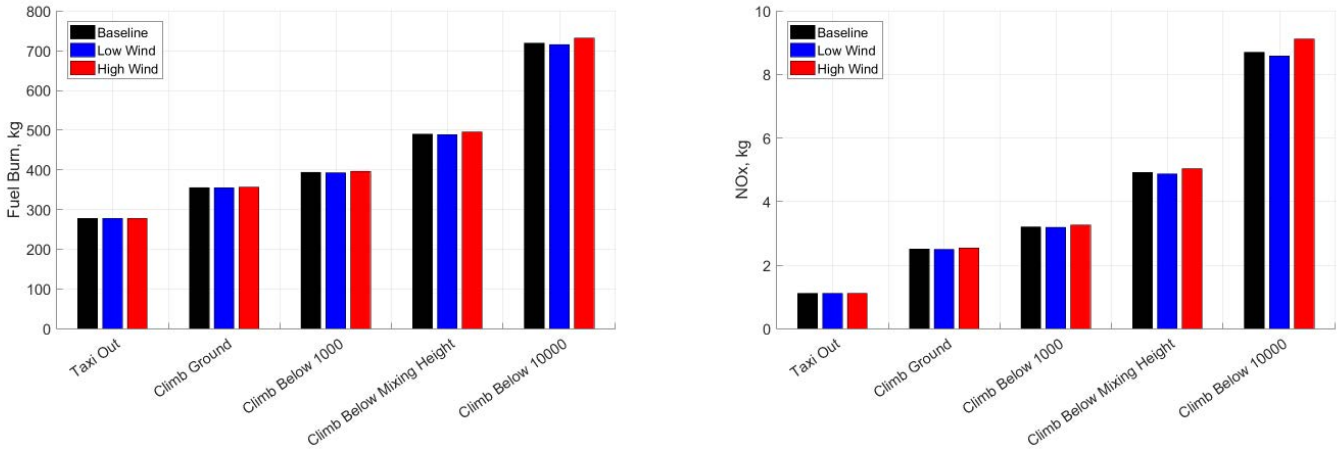

Figure 7. Effect of wind speed on fuel burn and NO_x emissions.

Sensitivity to humidity

The effect of humidity on noise and emissions is summarized in this section. To visualize the nonlinear effect of humidity, additional test points were included, as previously described. The effect of humidity on the SEL dB noise metric is shown in Figure 8. A minimal effect on noise is observed for humidity values of 40%–80%. A slight increase is observed for the 100% humidity case, and a large decrease is observed for the 1% and 20% humidity cases. The observed nonlinearity is displayed in Figure 9. Although these figures appear to suggest a "break point" of 40%, it is likely that this value arises from the choice of humidity values for the simulations. A higher-resolution sensitivity analysis in the range of 1%–40% is required to identify more accurate trends.

In addition to effects on noise, the impact of humidity on fuel burn and emissions is shown in Figure 10. The NO_x emissions are inversely correlated with humidity; in contrast, the fuel burn is unaffected by humidity, as humidity has no impact on aircraft performance in AEDT.

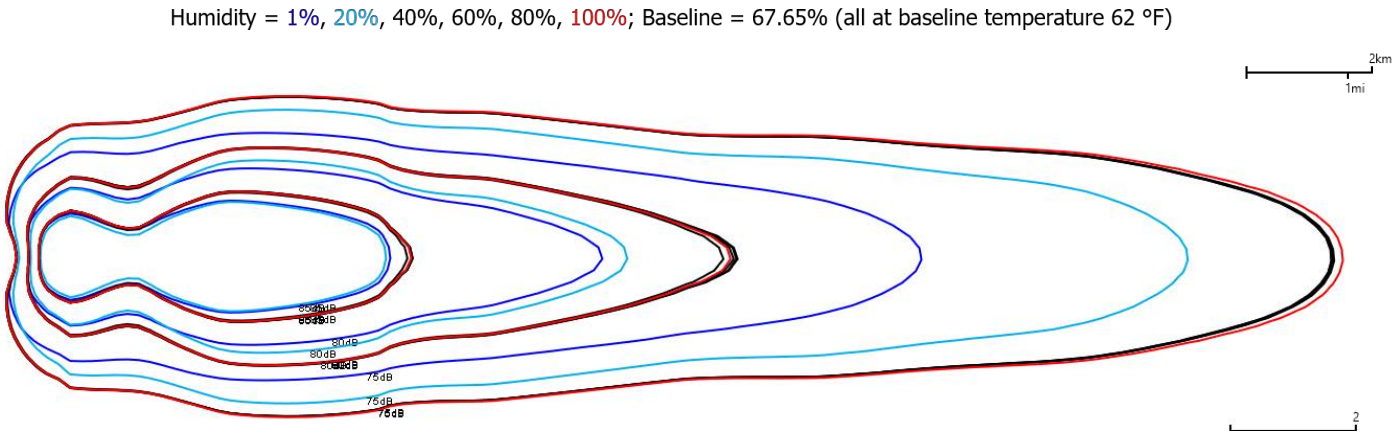

Figure 8. Effect of ambient air humidity on sound exposure level (SEL, dB) contours.

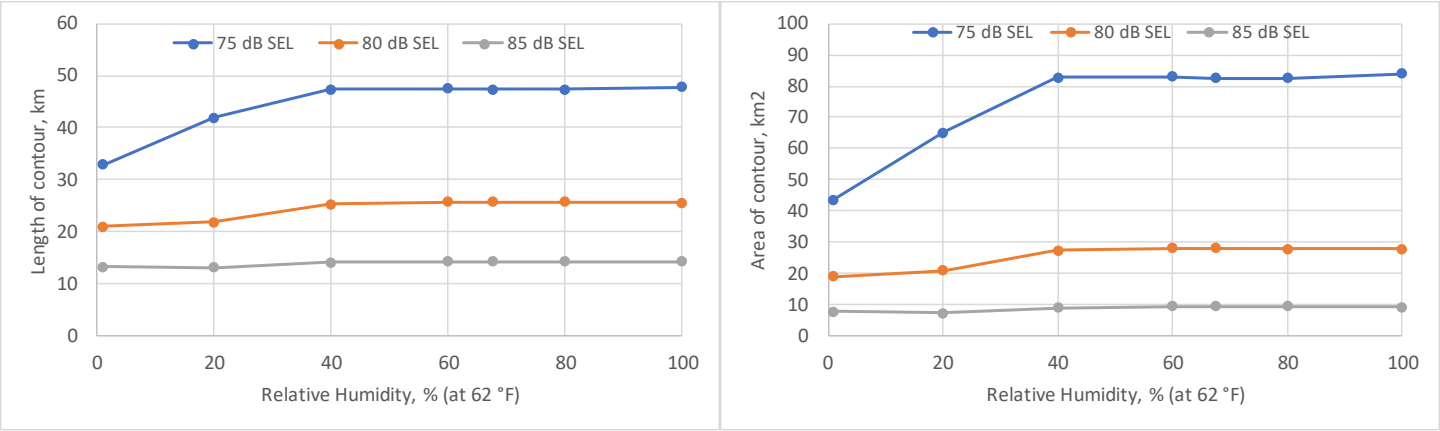

Figure 9. Nonlinear sensitivity of noise contour attributes to ambient air humidity.

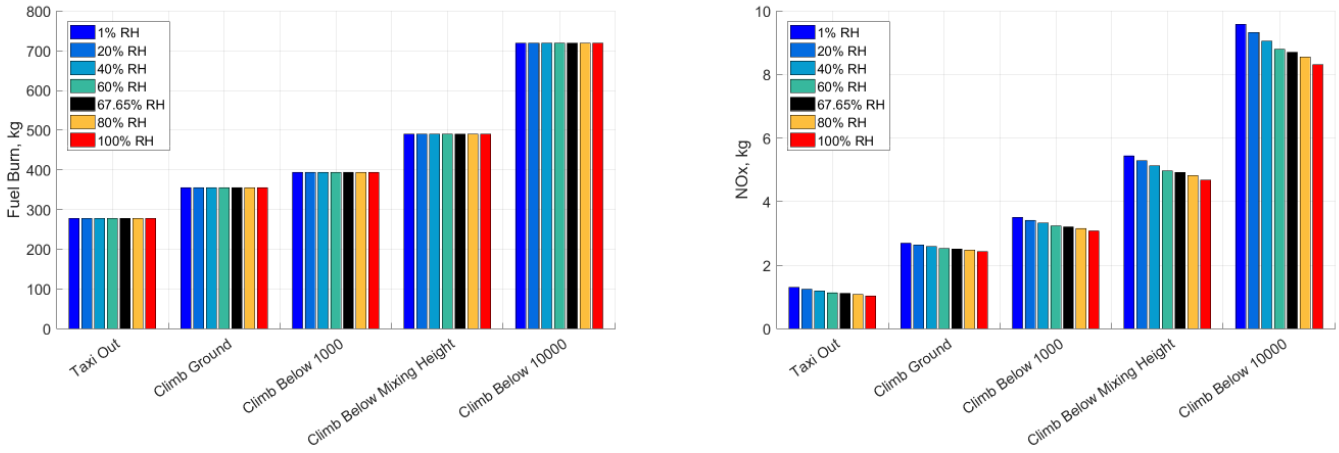

Figure 10. Effect of humidity on fuel burn and emissions.

Milestone

The objective of this task is to understand how spectral data are utilized within the AEDT and to evaluate the variability in the environmental metrics of interest.

Major Accomplishments

- Gathered 20-year historical weather data for four airports to determine the atmospheric variability and developed an automated process to perform a DOE study evaluating how the spectral data affect noise metrics
- Performed sensitivity analyses of ambient temperature, humidity, wind speed, and pressure for noise and emission metrics of interest

Publications

N/A

Outreach Efforts

Bi-weekly telephone meetings with the FAA, Volpe, and ATAC.
Bi-annual ASCENT meetings.

Awards
None.

Student Involvement
Graduate research assistant Ameya Behere participated in this work and conducted the research for this task.

Plans for Next Period
The next steps for Task 1 include several measures to improve the quality of the weather sensitivity analysis, including the following:

1. Extend the terminal altitude of departure profiles to 15,000 ft AFE.
2. Add station pressure as a variable in the sensitivity analysis.
3. Repeat the study for multiple aircraft types: CRJ 900, B767-300ER, and B777-200ER with GE engines.
4. Repeat the study for multiple airports: SFO, DEN, and MEX.

Task 2- Investigate the Impact of Frequency Content on NPD+C Data
Georgia Institute of Technology

Objective(s)
Task 1 will be re-executed using NPD+C data with spectral content to include configuration information (flight speed and flap setting). The AEDT sensitivity study will be repeated, and the results will be compared to those obtained using the standard NPD approach. Changes in contour area will be analyzed to determine whether the increased complexity due to the inclusion of configuration-dependent spectral data is outweighed by the increased fidelity of community noise predictions for typical weather at the airport. Similar to Task 1, we selected airports with variations in altitude and temperature. In addition to understanding the fidelity of the frequency content required for the NPD+C approach, this work will inform the FAA of any frequency-specific issues associated with the use of speed and configuration information in community airport noise prediction.

Research Approach
Five aircraft with varying parameters, including flap angle, aircraft airspeed, and gear setting, were assessed in ANOPP/EDS in order to generate spectral data and SELs as a function of thrust at various distances. Table 3 lists these aircraft and their configurations.

Table 3. Spectral and noise power distance (NPD) sensitivity analysis matrix.

Aircraft Size	EDS Representative Aircraft	Speed (kts)	Flap Angle	Gear Setting
50pax	CJR900	130, 142, 150, 154, 160, 166, 178, 190, 220	0°, 5°, 10°, 15°, 25°, 30°, 40°	Up, Down
100pax	737-700	130, 142, 150, 154, 160, 166, 178, 190, 220	0°, 5°, 10°, 15°, 25°, 30°, 40°	Up, Down
150pax	737-800	130, 142, 150, 154, 160, 166, 178, 190, 220	0°, 5°, 10°, 15°, 25°, 30°, 40°	Up, Down
210pax	767-300ER	130, 142, 150, 154, 160, 166, 178, 190, 220	0°, 5°, 10°, 15°, 25°, 30°, 40°	Up, Down
300pax	777-200ER	130, 142, 150, 154, 160, 166, 178, 190, 220	0°, 5°, 10°, 15°, 25°, 30°, 40°	Up, Down

Milestone(s)
The objective of this task is to utilize NASA's ANOPP tool to replace the current spectral data in AEDT with speed- and configuration-specific spectral data and to assess the variability among the environmental metrics of interest.

Major Accomplishments

- Prepared NPD+C and spectral data to be input into AEDT for specified aircraft.

The spectral data for the 150pax aircraft are graphically shown in the figures below. Figure 11 presents spectral data for approaches at 130 kts and 190 kts, for both the up and down gear settings. It is evident from these graphs that there is little variation in noise level beyond 1000 Hz with respect to the aircraft configuration at lower speeds; however, at higher speeds, there is more variation at higher frequencies with respect to the aircraft configuration. In contrast, during departure, the aircraft configuration does not greatly influence the noise level, as shown in Figure 12. This result is expected because the overall noise primarily arises from the engine thrust, and thus, little variation occurs with changes in configuration. The relationships between the SEL and thrust for both approaches and departures were also analyzed. During the approach, the SEL is fairly constant, exhibiting little change with the different thrust levels, as shown in Figure 13,. This effect is particularly pronounced at higher speeds, such as 220 kts. However, during departure, the lower SELs change significantly as the thrust increases, as shown in Figure 14.

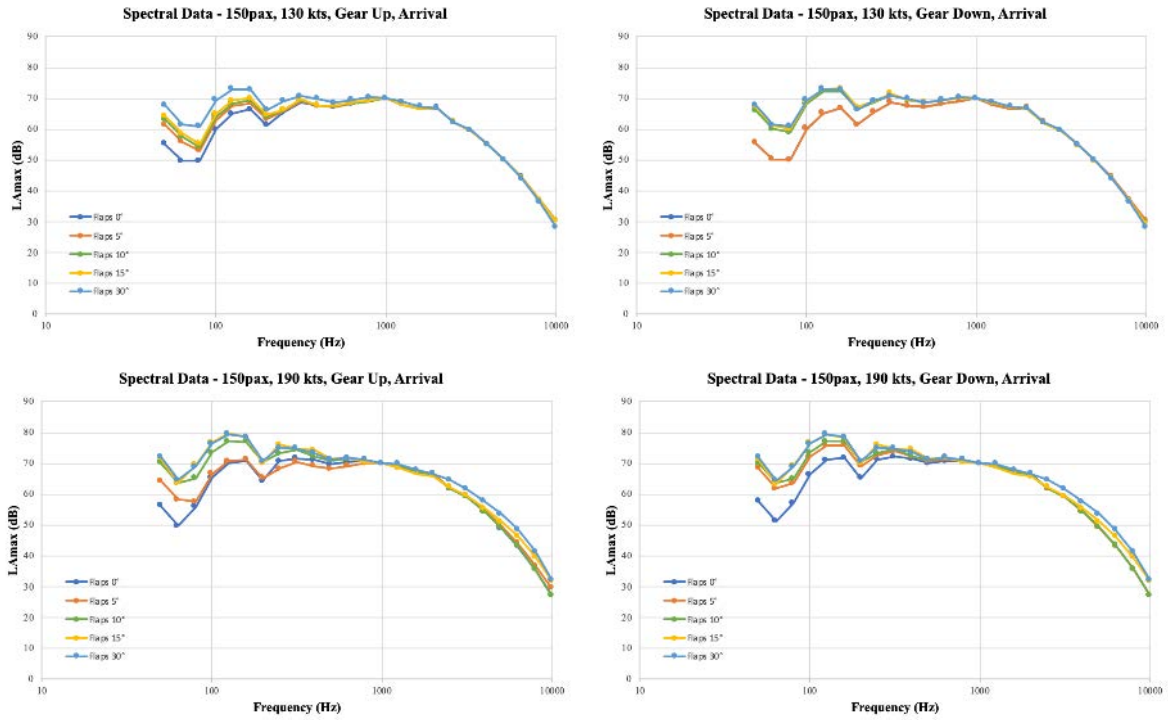

Figure 11. Spectral data for 150pax aircraft during arrival.

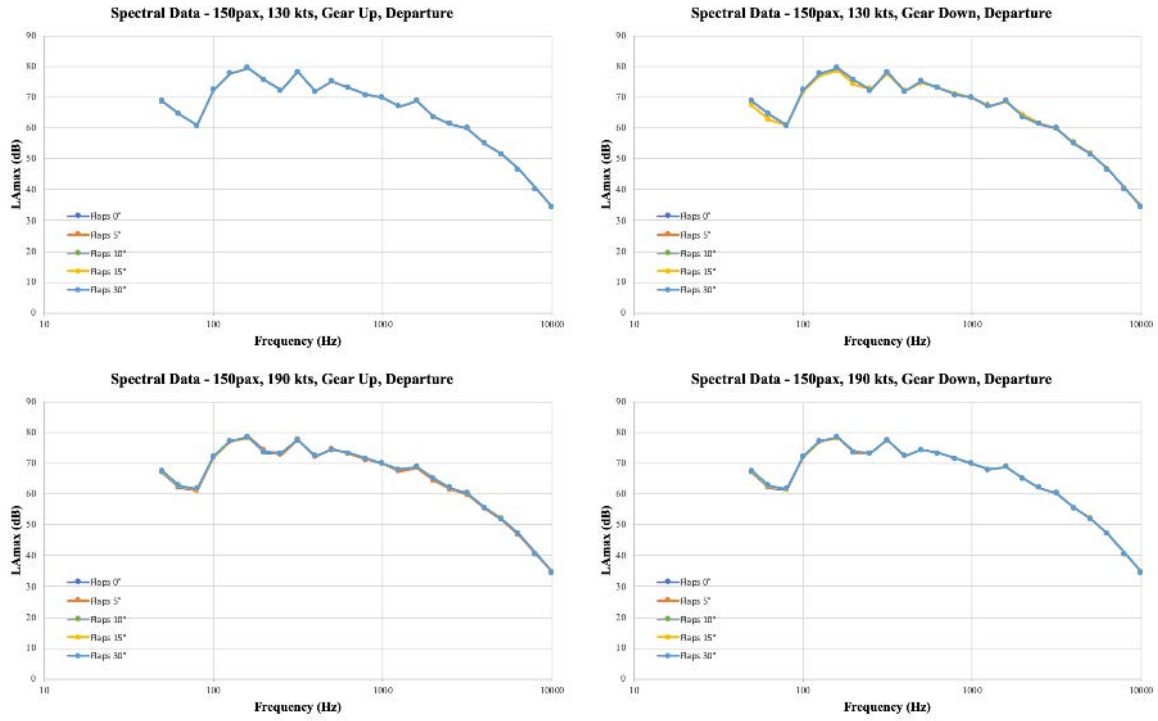

Figure 12. Spectral data for 150pax aircraft during departure.

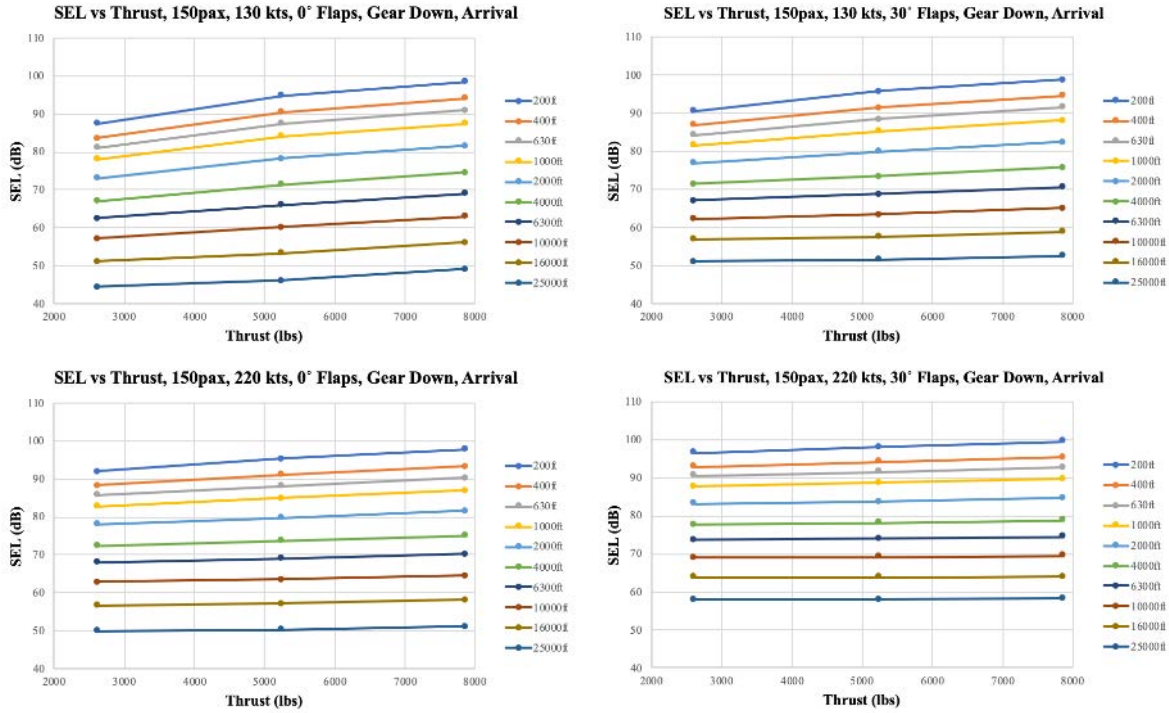

Figure 13. Sound exposure level (SEL) vs. thrust for 150pax aircraft during arrival.

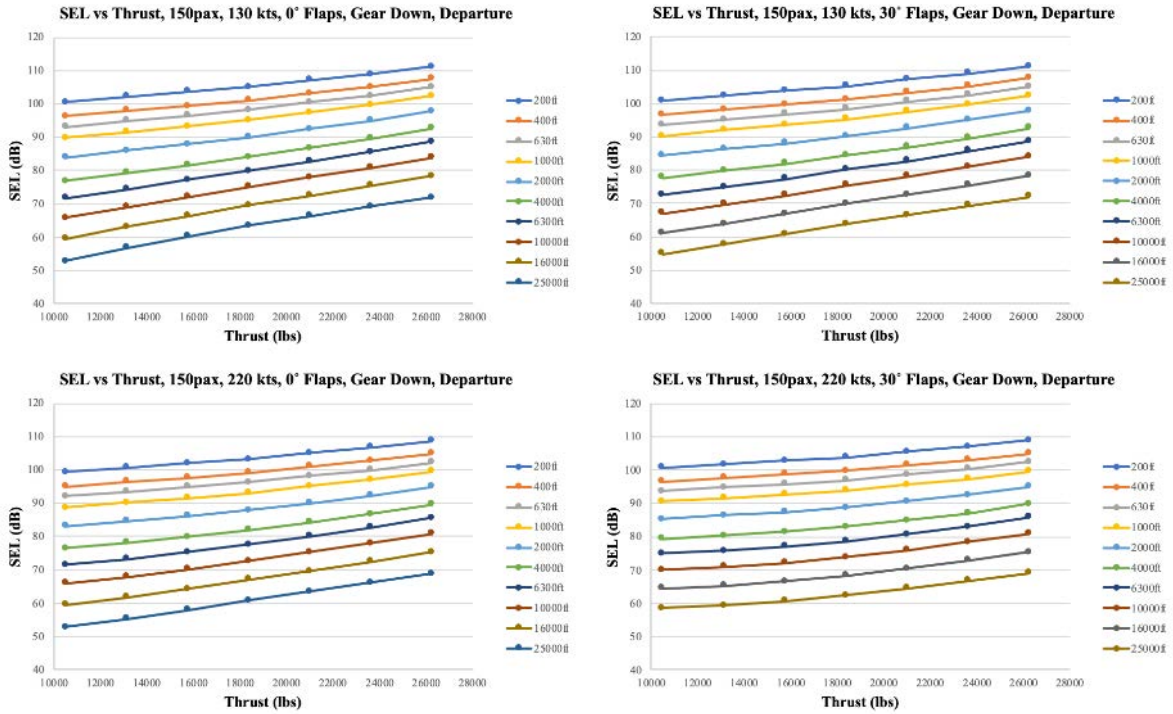

Figure 14. Sound exposure level (SEL) vs. thrust for 150pax aircraft during departure.

Publications
None.

Outreach Efforts
Bi-weekly telephone meetings with the FAA, Volpe, and ATAC.
Bi-annual ASCENT meetings.

Awards
None.

Student Involvement
Graduate research assistants Sarah Malak, Shilpa Ravoory, and Wenxin Zhang participated in this work and conducted the research for this task.

Plans for Next Period
Our team is currently analyzing the adapted AEDT code in order to include multiple spectral datasets to the departure/approach procedure for different airports and to ultimately modify the AEDT source code to utilize flight-segment-specific spectra.

Task 3- Validation with Noise Data in AEDT

Georgia Institute of Technology

Objective(s)

The main objective of this task is to validate the AEDT noise calculations using real-world operation data obtained from a commercial airline and noise monitoring data from a partner airport. The second objective of this task is to support the main objective of modeling real-world airline data (such as radar or flight operation quality assurance [FOQA]) in AEDT using profile points in an automated manner.

Research Approach

This task will use actual operational aircraft data and noise monitor data to determine whether the increased complexity resulting from the NPD+C approach is accompanied by an increased accuracy relative to community noise prediction. Georgia Tech has worked with a major airline and a U.S. airport to obtain the necessary data. The next step is to identify a subset of flights for performing a validation. Once an appropriate subset is identified, Georgia Tech will create or use existing EDS models for the selected aircraft. In creating the EDS model to generate the NPD+C curves, Georgia Tech will also estimate the aircraft state from available trajectory and airline operational data. This process requires estimates of aircraft configuration (i.e., flaps and slat setting), aircraft orientation (i.e., climb angle), and engine state (i.e., power setting).

Georgia Tech will use the EDS models and state estimates to generate NPD+C curves for selected aircraft using NASA's ANOPP2. It is expected that an increased accuracy will be obtained for aircraft modeled with NPD+C curves under this approach; however, a full comparison will be made with respect to the baseline case to examine where the accuracy is improved. Currently, Georgia Tech is also developing a technique to correct existing baseline NPD data within AEDT to account for low-speed configurations and low speeds, without the need to construct ANOPP2 or other physics-based models for each aircraft. The accuracy of this correction method relative to the baseline case and ANOPP2-generated NPD+C curves will also be assessed in terms of SEL and LAmax differences at the measurement points. The resulting trajectories will be implemented with ANOPP to generate NPD+C information, which will then be compared with the existing AEDT NPD predictions and measured data. For this task, Georgia Tech will use the standard propagation models available within AEDT. This task will enhance our understanding of improved noise predictions for airports using the regular NPD and NPD+C approaches for selected operations.

The steps of our research approach are outlined in Figure 15. To complete these steps, the team conducted a literature review of prior validation efforts and identified the requirements for a data collection plan.

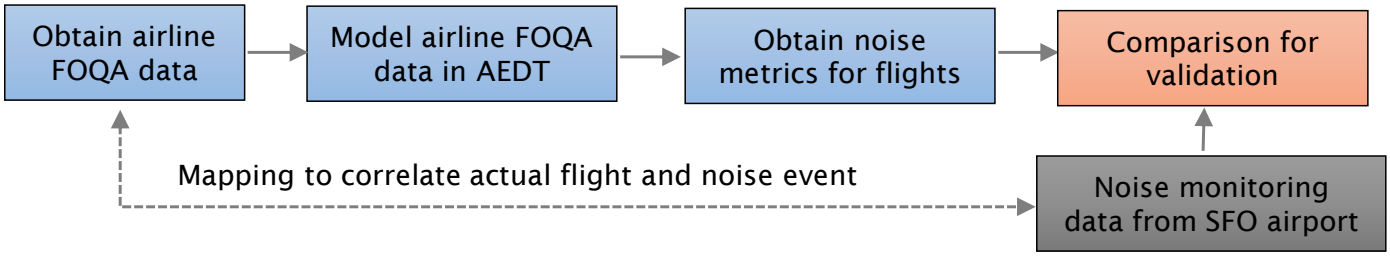

Figure 15. Overall steps of the validation methodology.

The first part of this task was a literature review in which the team investigated various sources of previous validation efforts, including prior studies in which single-event noise levels were compared with measurements obtained from airport noise monitoring systems (Page et al., 2000; Plotkin et al., 2013). From these studies, our team identified various methods for validating noise models and typical corresponding metrics.

In the next part of this task, the data requirements were determined, and data collection for the validation task was performed. In this step, knowledge obtained from our review of previous validation studies was used to identify data that would be useful for noise model validation. For this validation effort, the truth value for noise will be obtained from airport noise monitoring stations (in this case, San Francisco International Airport). In addition, to validate the noise models, data

from real-world operations must be acquired, and these operations must be modeled in AEDT. In prior validation work, radar data were typically used, which lack certain important parameters, such as the actual throttle setting (thrust) or configuration. Therefore, the team focused on acquiring higher-fidelity FOQA data from an airline partner. Because of their properties and parameters, FOQA datasets are the perfect candidate for validation efforts.

Following the data requirement analysis, the Georgia Tech team acquired high-fidelity FOQA data from an airline partner for operations at the SFO airport. These data correspond to approximately 800 flights from three different airframes over the past two years. For each flight, over 600 parameters are sampled at a frequency of 1 Hz. The flight data contain parameters that are useful for flight modeling in AEDT, including but not limited to the following:

- Height above take-off/touchdown
- Speed (true, ground, etc.)
- Latitude, longitude
- Configuration parameters such as the status of flaps, slats, landing gear, and spoilers
- Gross weight
- Thrust (left, right engine)

The team developed scripts to automatically process FOQA data to identify the appropriate number of segments for AEDT modeling. In this iterative process, the FOQA data are sequentially sampled at an increasing number of points in order to reduce the discrepancy between the AEDT modeled outputs and the actual FOQA data. The aim is to achieve the best match with as few profile points as possible. The process illustrated in Figure 16 is used to create a fixed-profile point study to model the performance of FOQA flights in AEDT. Using this process, our team modeled various FOQA flights in AEDT and obtained corresponding noise metrics.

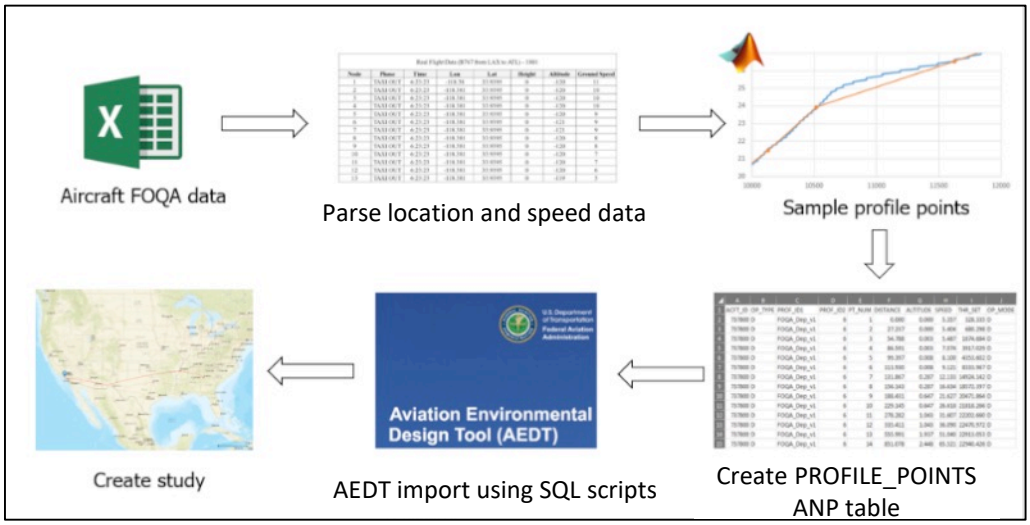

Figure 16. Steps for creating fixed-point profiles in AEDT for FOQA flights.

As the final step in this research approach, the modeled noise performance is compared with the actual noise measured at the airport. For this step, the Georgia Tech team is leveraging their relationship with the San Francisco International Airport noise office. The data are obtained in the form of a comma-separated variable (CSV) file or Excel document and contain information such as the start date and time of the event, the location of the noise monitoring station, noise metrics (SEL, LAmax), event duration, and event class. Figure 17 shows an example of noise event data obtained by the SFO international airport from one of their noise monitoring locations. The Georgia Tech team is currently obtaining similar data for all 800 FOQA flights from a partner airline.

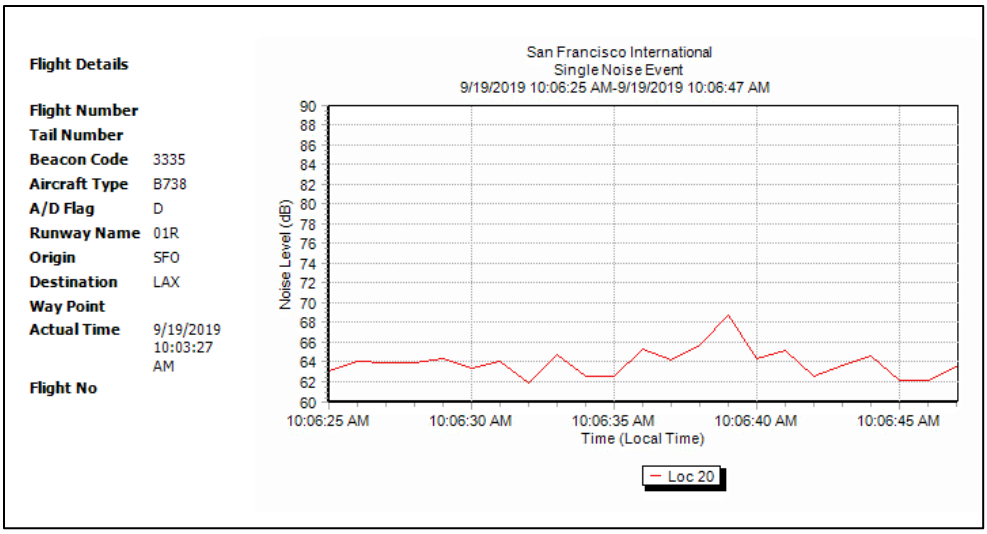

Figure 17. An example of noise monitoring data expected for all flight datasets from the SFO international airport.

Milestone

The objective of this task is to conduct a validation of AEDT's noise predictive capability using real-world noise monitoring data.

Major Accomplishments

- Obtained real-world FOQA performance data from an airline partner for 13 airframes
- Established a process for sampling FOQA data for modeling in AEDT
- Compared a FOQA profile with an AEDT default profile to assess the impacts of all assumptions in AEDT APM
- Created visualization dashboards and statistical analysis codes to extract common departure modes based on FOQA data

Publications

Conference proceedings

Perullo, C., Santa-Ruiz, A., Kirby, M., Mavris, D., & Lim, D. (2019). Investigation of aircraft configuration and speed on traditional noise-power-distance curves. Noise-Con 2019, NC19-192.

Outreach Efforts

Meetings with the ASCENT team were scheduled for subsequent work. Presentations were given at SAE A-21 meetings and NoiseCon 2019, and biweekly FAA tool team presentations were given as appropriate.

Awards

None.

Student Involvement

Graduate research assistants Ameya Behere, Dylan Monteiro, and Andrew Van Zwieten (graduated August 2019) participated in this work and conducted the research for this task.

Plans for Next Period

With some of the important modeling steps completed, the team is currently obtaining noise monitoring and noise event data for approximately 800 flight data records from the San Francisco International Airport noise office. Additionally, the team will obtain noise monitoring locations and will model this information in AEDT. Once obtained, these data will be

compared with AEDT noise calculations for the same flight data records, and validation metrics will be quantified for these flights.

References

AEDT. (2016). Aircraft Environmental Design Tool, version 2.c. FAA, Washington, DC

ANOPP. (1998). Aircraft noise prediction program, version 1.0. NASA, Langley, VA. Ref. LAR-16809-GS

Aratani, L. (August 9, 2018) D.C. residents suffer major setback in fight over plane noise from National Airport. The Washington Post

Federal Aviation Administration (FAA). (Retrieved December 2019) Aircraft noise issues. United States Department of Transportation

John A. Volpe National Transportation Systems. (2008). Integrated Noise Model (INM) version 7.0 technical manual. FAA-AEE-08-01

Page, J.A., Hobbs, C.M., Plotkin, K.J., Stusnick, E., & Shepherd, K.P. (2000). Validation of aircraft noise prediction models at low levels of exposure. NASA technical report number: CR-2000-210112.

Plotkin, K.J., Page, J.A., Gurovich, Y., & Hobbs, C.M. (2013). Detailed weather and terrain analysis for aircraft noise modeling (No. Wyle Report 13-01). John A. Volpe National Transportation Systems Center (US)

Raymer, D.P. (2006). Aircraft design: A conceptual approach. 4th ed., AIAA Education Series, Reston, Virginia, pp. 197

U.S. DOT Volpe Center. (2017). Aviation Environmental Design Tool (AEDT) technical manual, version 2d. FAA, ATAC Corp, CSSI, Inc, Metron Aviation DOT-VNTSC-FAA-17-16

U.S. FAA. (2016). Aviation Environmental Design Tool (AEDT) technical manual version 2c. DOT-VNTSC-FAA-16-11

Project 044 Aircraft Noise Abatement Procedure Modeling and Validation

Massachusetts Institute of Technology

Project Lead Investigator

R. John Hansman
T. Wilson Professor of Aeronautics & Astronautics
Department of Aeronautics & Astronautics
Massachusetts Institute of Technology
Room 33-303
77 Massachusetts Ave
Cambridge, MA 02139
617-253-2271
rjhans@mit.edu

University Participants

Massachusetts Institute of Technology

- PI(s): R. John Hansman
- FAA Award Number: 13-C-AJFE-MIT, Amendment Nos. 050 and 057
- Period of Performance: September 1, 2018 to August 31, 2020 (via no-cost extension)
- Task(s):
    1. Evaluate general approaches to aircraft noise validation
    2. Develop validation approach options
    3. Develop detailed flight test plans
    4. Perform initial experimental runs on targets of opportunity
    5. Evaluate experimental results and implications for ANOPP and AEDT and low-noise procedures

Project Funding Level

Project Funding Level: $350,000 FAA funding and $350,000 matching funds. Sources of match are approximately $79,000 from Massachusetts Institute of Technology (MIT) and $271,000 from the Massachusetts Port Authority.

Investigation Team

- Prof R. John Hansman (PI)
- Jacqueline Thomas (graduate student)
- Clement Li (graduate student)
- Sandro Salgueiro (graduate student)
- Rachel Price (graduate student)
- Annick Dewald (graduate student)
- Alison Yu (graduate student)

Project Overview

This project will develop an approach to validating advanced operational flight procedures that incorporate modified configurations and speeds. Noise analysis developed at MIT under ASCENT Project 23 shows opportunities to reduce community noise under flight tracks through configuration and speed changes. Analysis results indicate that flight speed can significantly impact noise population exposure. There is a question as to whether one of the models used for these results—the FINK airframe noise model from ANOPP, which was developed from flight tests in the 1970s—might still be valid for modern aircraft. Thus, this project will utilize discussions with industry experts to determine the validity of the

modeled noise impacts of advanced operational procedure concepts. This project will also evaluate potential opportunities for aircraft noise validation.

Task 1 - Evaluate General Approaches to Aircraft Noise Validation

Massachusetts Institute of Technology

Objective(s)

This task will be to evaluate the different options for improved validation of the ANOPP source component models as well as confirmation of any noise reductions from proposed low-noise procedures. Approaches to experimental design will be considered, including dedicated engineering flight trials, which would include parametric sweeps of velocity and aircraft configuration at various power conditions potentially including engine shutdown or more likely idle thrust. Another approach would be to monitor preliminary operational trials of reduced speed departures. This process would involve collaborating with airline operators, who would need to be willing to fly trials of procedures, and ATC, who would have to approve the procedures. A ground measurement system would need to be in place under the departure tracks.

Potential monitoring approaches will also be considered, including distributed microphone arrays or single microphone installations as well as potential phased-array microphone configurations. The most effective microphone configuration will depend on the experimental approach. For example, the phased array microphones may provide benefits in isolating aerodynamic noise from engine noise if the engine shutdown condition is not feasible (as is likely to be the case). A distributed array much further out on the departure trajectory than traditional noise monitoring locations may be effective for monitoring climb noise variations with speed and configuration.

This task will use a systems approach and will explore options with potential collaborators on experimental opportunities to identify options for experimental validation. This will include consulting experts who have previously performed noise measurement campaigns or experts in noise monitoring to understand options and best practices.

Research Approach

- Evaluate the different options for improved validation of the ANOPP source component models as well as confirmation of any noise reductions from proposed procedures
- Collaborate with industry and operators to determine who would be willing to fly procedures
- Evaluate potential challenges associated with flight testing and taking measurements

Major Accomplishments

- Communication was established between the team and ANOPP noise experts at NASA to determine whether data might already exist on the airframe noise of modern aircraft and might be used to determine the noise impacts of reduced speed departure concepts.
- We examined flight procedure data from simulator and flight demonstrations to validate flight procedure modeling methods and the feasibility of the flight procedure.
- We modeled the possible noise variations as a result of atmospheric changes throughout a standard year to show what amount of variation in monitored noise would be expected if flight trials were conducted to determine the noise impacts of procedures with speed and configuration variations.

Task 2 - Develop Validation Approach Options

Massachusetts Institute of Technology

Objective(s)

On the basis of the results of Task 1 and initial discussions with potential collaborators (measurement experts, model developers, manufacturers, operators, and test locations), one or more validation options will be identified. Targets of opportunity will be explored in which noise measurements may supplement other planned flight trials. For each option, the potential advantages and disadvantages will be identified, and preliminary flight test plans will be developed in coordination with the identified collaborators and in consultation with subject matter experts such as NASA. Potential advantages include the willingness of operators or collaborators to participate and provide test resources including aircraft

and measurement systems. Other factors include measurement system resolution and discrimination of noise sources. Timing and location may also be considered. On the basis of this analysis, recommendations for next steps will be made.

Research Approach

- Explore targets of opportunity for noise measurements or flight testing
- Identify sources of data that can be used for validation from industry or other entities

Major Accomplishments

- Several meetings and discussions with ANOPP noise experts at NASA were held to determine the validity of ANOPP airframe noise models for modern aircraft.
- We worked with industry to uncover data on clean airframe noise of modern aircraft.
- We worked with a research team at Stanford to identify noise monitor data of high-lift devices that could be used to validate noise of flight procedures with significant airframe noise contributors.
- We identified a target of opportunity to fly a low-noise approach procedure via industry sponsored tests.

Task 3 - Develop Detailed Flight Test Plans

Massachusetts Institute of Technology

Objective(s)

For the recommended validation options identified in Task 2, detailed flight test plans will be developed. Flight test plans for dedicated engineering flights would involve detailed planning of the speed, configuration, and thrust of each trial. Test plans for flight trails in collaboration with airline operators would focus more heavily on documenting the flown profiles to analyze the associated data measurements. Opportunity exists in both of these types of trials to validate not only the expected effects of aircraft speed versus noise in the analysis models but also the expected noise impacts of procedures including delayed deceleration approaches, steeper approaches, and continuous approaches.

Research Approach

- Develop flight test plans for validation of operations and low-noise procedures
- Collaborate with airline operators and industry to determine appropriate data collection for trail flight tests

Major Accomplishments

- We assisted in flight plan design for the delayed deceleration approach procedure and how to communicate the approach to pilots.
- We developed assessment methods to examine which noise benefits of the procedure were attributed to which portions of the procedure.

Task 4 - Initial Experimental Runs on Targets of Opportunity

Massachusetts Institute of Technology

Objective

If targets of opportunity are identified in Task 2 that would occur within the period of performance of this proposed research, initial experimental runs would be conducted after consultation with AEE and other relevant parties.

Research Approach

- Document procedure recommendations thoroughly and unambiguously so that simulator or flight trials are possible
- Meet with airline technical pilots and representatives from aircraft manufacturers to discuss operational constraints and test opportunities
- Develop test plans and protocols for potential flight trials
- Develop test plans and protocols for potential noise measurement campaigns
    - Specific flight test locations
    - Operational field measurements

Major Accomplishments

- The delayed deceleration approach concept was identified as a noise abatement flight procedure as a candidate for flight test demonstration.
- Potential delayed deceleration approaches combined with steeper approaches were assessed for feasibility and noise reduction impacts between the MIT team and the industry team.
- Weekly meetings and discussions with industry were held to determine the feasibility of delayed deceleration approaches and steeper approaches.
- Simulator flight tests were conducted for the proposed delayed deceleration and steeper approach concept.
- A delayed deceleration approach procedure was flight tested for operational demonstration.

Task 5 - Evaluate Experimental Results and Implications for ANOPP and AEDT and Low-Noise Procedures

Massachusetts Institute of Technology

Objective(s)

Contingent on data availability from Task 4 or other data identified as part of the experimental approach and discussions with collaborators, this task in coordination with NASA will:

- Evaluate the ANOPP correlations relative to experimental results,
- Identify discrepancies that need to be corrected, and
- Determine whether the results and data are sufficient to improve discrepancies or whether continued validation and testing are required.

The implications for AEDT from the data will be evaluated. The results of the flight tests and ASCENT Project 44 may create opportunities to continue to improve the noise-power-distance and configuration curves in AEDT. Validating the noise component modules in ANOPP would also allow for potential component corrections within the noise models of AEDT. The implications for AEDT will allow future research teams to continue to develop the AEDT noise models upon the results of the flight tests from this project.

Implications for the development of low-noise procedures will also be evaluated. Validation and improvement of the noise models ANOPP and AEDT will allow for higher-fidelity development of low-noise procedures. Validation of procedures such as delayed deceleration approaches will also create opportunity for the development of further low-noise procedures.

Research Approach

- Evaluate implications for modeling low-noise procedures with ANOPP and AEDT
- Evaluate implications for the development of low-noise procedures.

Milestone

The delayed deceleration approach was flown as an operational flight demonstration on the Boeing EcoDemonstrator at Atlantic City Airport in November of 2019.

Major Accomplishments

- Noise analysis was performed on simulated flight tests to show the impacts of different decisions made for actual flight test implementation, such as when and where the delayed deceleration would occur.
- Noise results were compared with data provided by Stanford on configuration noise.

Publications

Jensen, L. & Hansman, R.J. (2018) Data-driven flight procedure simulation and noise analysis in a large-scale air MIT

Jensen, L., O'Neill, G., Thomas, J., Yu, A., & Hansman, R.J. (2018). Block 1 procedure recommendations for Logan Airport community noise reduction. MIT ICAT Report

Jensen, L., Thomas, J., Brooks, C., Brenner, M., & Hansman, R.J. (2017). Analytical approach for quantifying noise from advanced operational procedures. European Air Traffic Management Research and .Development Seminar

Reynolds, T., Sandberg, M., Thomas, J., & Hansman, R.J. (2016). Delayed deceleration approach noise assessment. 16th AIAA Aviation Technology, Integration, and Operations Conference.

Thomas, J. & Hansman, R.J. (2020). Evaluation of the impact of transport jet aircraft approach and departure speed on community noise. MIT ICAT Report
Thomas, J. & Hansman, R.J. (2020). Modeling and assessment of delayed deceleration approaches for community noise reduction. AIAA Aviation
Thomas, J. & Hansman, R.J. (2019). Framework for analyzing aircraft community noise impacts of advanced operational flight procedures. Journal of Aircraft, Volume 6, Issue 4. https://doi.org/10.2514/1.C035100
Thomas, J. & Hansman, R.J. (2017). Modeling performance and noise of advanced operational procedures for current and future aircraft. MIT International Center for Air Transportation
Thomas, J., Jensen, l., Brooks, C., Brenner, M., & Hansman, R.J. (2017). Investigation of aircraft approach and departure velocity profiles on community noise. AIAA Aviation Forum, p. 1-12
Thomas, J., Yu, A., Li, C., Toscano, P., & Hansman, R.J. (2019). Advanced operational procedure design concepts for noise abatement. In Thirteenth USA/Europe Air Traffic Management Research and Development Seminar, Vienna.
Thomas, J., Yu, A., Li., C., Maddens Toscano, P., & Hansman, R.J. (2019). Advanced operational procedure design concepts for noise abatement. USA/Europe ATM R&D Seminar
Yu, A. & Hansman, R.J. (2019). Aircraft noise modeling of dispersed flight tracks and metrics for assessing impacts. MIT ICAT Report
Yu, A. & Hansman, R.J. (2019). Approach for representing the aircraft noise impacts of concentrated flight tracks. AIAA Aviation Forum 2019, Dallas, Texas. https://doi.org/10.2514/6.2019-3186

Outreach Efforts

- October 15,2019: Presentation to the ASCENT Advisory Board
- November 8, 2019: Presentation to NASA
- November 12, 2019: Presentation to Airline Industry Consortium
- Weekly meetings with industry
- Biweekly teleconferences and meetings with FAA Technical Monitors
- In-person outreach and collaboration with Massport, operator of Boston Logan Airport and ASCENT Advisory Board member

Awards

2018 Department of Transportation/FAA COE Outstanding Student of the Year Award to Jacqueline Thomas

Student Involvement

Graduate students have been involved in all aspects of this research in terms of analysis, documentation, and presentation.

Plans for Next Period

The next phase of this project will involve continued work with industry on finalizing the delayed deceleration approach noise according to the data from the flight procedure demonstration. The team will continue to evaluate additional airframe noise measurement opportunities for modeled noise validation. Discussions with the pilots from the flight demonstration of the delayed deceleration approach will be conducted to collect lessons learned that will be necessary to perform this procedure in future operations. Additional operational implications and strategies for overcoming challenges associated with the flight procedures will be researched. Implications for modeling low-noise procedures with AEDT and ANOPP will be determined.

Project 045 Takeoff/Climb Analysis to Support AEDT APM Development

Georgia Institute of Technology

Project Lead Investigator

Professor Dimitri N. Mavris
Director
Aerospace Systems Design Laboratory
School of Aerospace Engineering
Georgia Institute of Technology
Phone: (404) 894-1557
Fax: (404) 894-6596
Email: dimitri.mavris@ae.gatech.edu

Dr. Michelle R. Kirby, Co-PI
Chief, Civil Aviation Research Division
Aerospace Systems Design Laboratory
School of Aerospace Engineering
Georgia Institute of Technology
Phone: (404) 385-2780
Fax: (404) 894-6596
Email: michelle.kirby@ae.gatech.edu

University Participants

Georgia Institute of Technology (GT)

- PI(s): Prof. Dimitri Mavris, Dr. Michelle R. Kirby (Co-PI)
- FAA Award Number: 13-C-AJFE-GIT, Amendment 020,035, 43, and 46
- Period of Performance: August 15, 2016 to March 28, 2019
- Tasks:
  - Task 1: NADP library investigation
  - Task 2: Arrival profile modeling
  - Task 3: Integrated impact assessment of inaccuracies from thrust, weight, procedures, and NPD curves

Project Funding Level

The project is funded at the following levels: GT ($175,000). Cost-share details are below:

GT has agreed to a total of $175,000 in matching funds. This total includes salaries for the project director; research engineers; graduate research assistants; and computing, financial and administrative support, including meeting arrangements. The institute has also agreed to provide tuition remission for the students, paid for by state funds.

Investigation Team

- Prof. Dimitri Mavris, Principal Investigator, Georgia Institute of Technology
- Dr. Michelle Kirby, Co-Investigator, Georgia Institute of Technology
- Dr. Yongchang Li, Research Faculty, Georgia Institute of Technology
- Dr. Tejas Puranik, Research Faculty, Georgia Institute of Technology
- Dr. Don Lim, Research Faculty, Georgia Institute of Technology
- Ameya Behere, Graduate Student, Georgia Institute of Technology

- Zhenyu Gao, Graduate Student, Georgia Institute of Technology (Task 2)
- Yee Chan Jin, Graduate Student, Georgia Institute of Technology (Task 1)
- Dylan Monteiro, Graduate Student, Georgia Institute of Technology (Task 3)
- Ana Gabrielian, Graduate Student, Georgia Institute of Technology (Task 2)
- Loren Isakson, Graduate Student, Georgia Institute of Technology (Task 1)

Project Overview

Accurate modeling of aircraft performance is a key factor in estimating aircraft noise, emissions, and fuel burn. Within the Aviation Environmental Design Tool (AEDT), many assumptions are made for aircraft performance modeling with respect to aircraft weight and departure procedure, coupled with aircraft departure typically being modeled by assuming that full rated takeoff power/thrust is used. As operations around airports continue to evolve, there is a need to examine those assumptions and to improve the modeling accuracy with flight data. In recent years, flight data are increasingly being used to enhance models and bring model estimation even closer to reality. Research is needed to build on prior work with a view to develop a robust set of recommendations for improved estimation processes for takeoff weight, reduced thrust takeoffs, and departure profiles within AEDT.

Task 1 - NADP Library Investigation

Georgia Institute of Technology

Objective(s)

Previous research efforts under Project 45 led to the development of the NADP Library, a set of noise abatement departure profiles (NADPs) that are defined as procedural profiles in AEDT. The library is generic and can be applied to any aircraft or airport. Each such profile is based on the combination of three parameters: thrust cutback, initial acceleration, and final acceleration. The complete flowchart is described in Figure **1**. The distinction between the two NADP-2 profile types comes from the thrust cutback initiation. Profiles following the “before” track use climb thrust to accelerate through the flap schedule, and those following the “after” track use takeoff thrust instead, NADP-1 profiles differ from “before” NADP-2 profiles because of the use of a constant speed climb step between the cutback and initiation of acceleration.

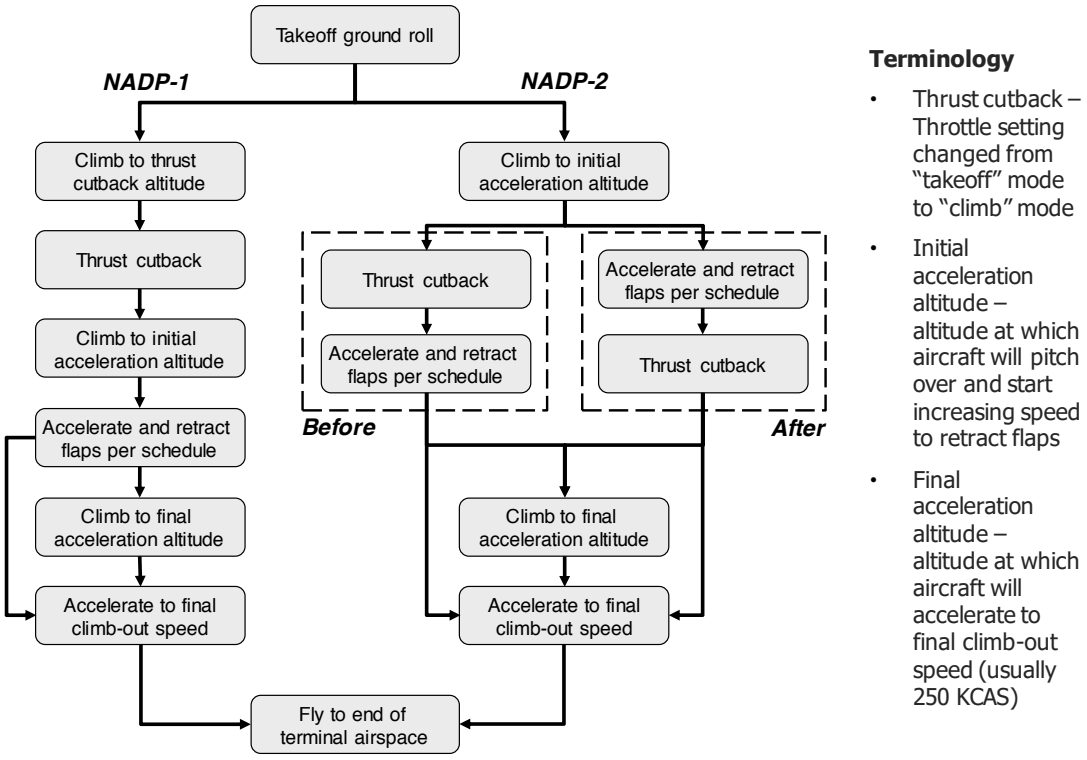

Figure 1. Description of generic NADP within NADP Library.

Research Approach

There are 6 NADP-1 profiles and 13 NADP-2 defined in the library. Even more modeling options are possible when the possibilities of alternate weight and reduced thrust are considered. Including such a high number of profiles as modeling options in future versions of AEDT is undesirable. Therefore, a grouping of profiles within NADP Library is required so that a subset of these 19 profiles can be selected. A single profile within each group can then be chosen to represent the all other profiles within the group.

Any grouping must reproduce the high variability in modeling options present in the original library, while simultaneously minimizing the error arising from the substitution of profiles within a group. Such a process requires clustering algorithms that can be applied to different comparison metrics. Because the similarity between profiles is to be judged between their environmental impacts, the following comparison metrics were identified for preliminary analysis:

1. Performance-based comparison metrics
    a. Trajectory root mean square (RMS)
    b. Speed RMS
    c. Thrust RMS
2. Noise-based comparison metrics
    a. RMS of sound exposure level (SEL) grid difference
    b. Differences in contour area, length, and width
3. Emissions-based comparison metrics
    a. Difference in fuel burn up to 1,000 ft, 3,000 ft and the complete profile
    b. Difference in NOx emissions up to 1,000 ft, 3,000 ft and the complete profile

All comparison metrics are calculated pairwise for all profiles. The 6 NADP-1 and 13 NADP-2 profiles are not compared to one another. Thus, for the complete set of 19 NADP profiles, a 6×6 and 13×13 matrix of each calculated similarity metric is obtained. The computation process for calculating the performance-based comparison metrics is outlined below.

The performance data and trajectories of different profiles are compared with an RMS-based methodology. The performance results from an AEDT simulation consist of a table, with each row representing a particular point in space-time reported by altitude, cumulative distance traveled, speed, and thrust, among other parameters. Because different profiles result in different performance data, the points in these tables are not expected to match in any parameter. For the calculation of comparison metrics, it is desirable for a single parameter to be specified for consistent sampling. To solve this problem, an independent set of data points is generated by using linear interpolation on each NADP profile. The interpolated profiles shown in Figure **2** are similar to the raw profiles except the interpolated profile points that define the curve share the same altitudes.

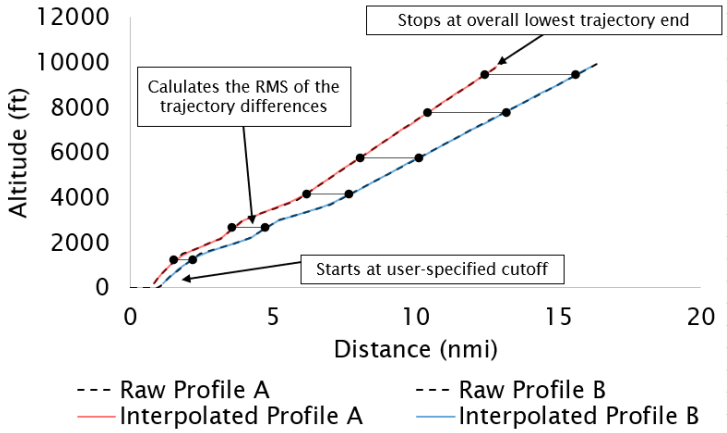

Figure 2. Trajectory comparison method visualization.

Given that the interpolated profiles are the same size and share the same step size, the differences between distance, speed, and thrust may be calculated. In Figure **2**, these differences are represented by horizontal lines linked at discrete points along the red and blue lines. Samples are represented by filled black circles. Sampling currently takes place every 200 feet, starting at a user-specified point and ending at the lowest altitude between the two profiles.

The set of differences is then squared and summed, as shown in equation 1, where n represents the number of samples in the set. The variable x represents the trajectory state being analyzed (e.g., cumulative distance traveled). The calculated result provides an overall measure of discrepancy between the two profiles in terms of distance.

$$x_{rms} = \sqrt{\frac{x_1^2 + x_2^2 + \cdots + x_n^2}{n}} \tag{1}$$

For example, if x_{rms} equals 2.07 nmi, on average, profiles A and B are approximately 2.07 nmi apart. The average value is calculated in the sense of RMS. Many alternative methods exist to calculate averages, such as taking a simple mean of the absolute value of differences. If more than two profiles are being analyzed, this methodology is used with each possible pair, constructing a matrix of resulting combinatory RMS values. Given the sheer volume of information, results are better visualized with conditional formatting, creating a heat map matrix, as listed in Table **1**, Table **2**, and Table **3** for the same NADP1 profile set in terms of velocity, distance, and thrust, respectively.

Table 1. Sample RMS heat map matrix comparing profile velocities.

RMS Speed(kts)	NADP1_1-3	NADP1_2-3	NADP1_3-3	NADP1_4-3	NADP1_6-3	NADP1_7-3
NADP1_1-3	0.00	13.81	20.92	13.81	20.93	20.93
NADP1_2-3	13.81	0.00	10.78	0.00	10.78	10.78
NADP1_3-3	20.92	10.78	0.00	10.78	0.00	0.01
NADP1_4-3	13.81	0.00	10.78	0.00	10.78	10.78
NADP1_6-3	20.93	Symmetric		10.78	0.00	0.01
NADP1_7-3	20.93	10.78	0.01	10.78	0.01	0.00

Table 2. Sample RMS heat map matrix comparing profile cumulative distance.

RMS Distance(nmi)	NADP1_1-3	NADP1_2-3	NADP1_3-3	NADP1_4-3	NADP1_6-3	NADP1_7-3
NADP1_1-3	0.00	0.27	0.43	0.29	0.46	0.52
NADP1_2-3	0.27	0.00	0.23	0.04	0.26	0.32
NADP1_3-3	0.43	0.23	0.00	0.22	0.04	0.13
NADP1_4-3	0.29	0.04	0.22	0.00	0.23	0.29
NADP1_6-3	0.46	Symmetric		0.23	0.00	0.09
NADP1_7-3	0.52	0.32	0.13	0.29	0.09	0.00

Table 3. Sample RMS heat map matrix comparing profile total thrust.

RMS Thrust(lb)	NADP1_1-3	NADP1_2-3	NADP1_3-3	NADP1_4-3	NADP1_6-3	NADP1_7-3
NADP1_1-3	0.00	354.42	532.81	545.74	675.09	938.66
NADP1_2-3	354.42	0.00	273.88	415.61	497.53	820.54
NADP1_3-3	532.81	273.88	0.00	497.75	415.39	774.04
NADP1_4-3	545.74	415.61	497.75	0.00	273.85	690.14
NADP1_6-3	675.09	Symmetric		273.85	0.00	633.88
NADP1_7-3	938.66	820.54	774.04	690.14	633.88	0.00

The last number in the NADP profile label represents the stage length. In Table **1**, the stage length is 3. Of note, the matrix shown is symmetric, because directionality does not matter. To read Table **1**, start at a row containing the profile of interest, and then move right until encountering the column of the second profile of interest. The number presented is the RMS value comparing these two profiles.

Noise is compared by using RMS in a different manner, as shown in Table 4. In this case, *n* in equation 1 represents the total number of grid points in one profile. As long as the number of grid points and the latitude/longitude coordinates match between two profiles, then the difference in noise at every grid point is calculated and root-mean-squared. This procedure provides a single metric to assess the overall discrepancy between two profiles. Of note, the noise contours in Table 4 are taken at sea level in this particular case.

Table 4. Sample RMS heat map matrix comparing profile noise.

RMS Sound(db)	NADP1_1-3	NADP1_2-3	NADP1_3-3	NADP1_4-3	NADP1_6-3	NADP1_7-3
NADP1_1-3	0.00	0.35	0.57	0.36	0.58	0.66
NADP1_2-3	0.35	0.00	0.25	0.09	0.26	0.40
NADP1_3-3	0.57	0.25	0.00	0.27	0.09	0.31
NADP1_4-3	0.36	0.09	0.27	0.00	0.25	0.33
NADP1_6-3	0.58	Symmetric		0.25	0.00	0.23
NADP1_7-3	0.66	0.40	0.31	0.33	0.23	0.00

For example, NADP1_1-3 and NADP1_7-3 differ on average by 0.66 dB in the upper-right-hand corner. Notably, NADP1_1-3 has the least in common with the rest of the profiles in terms of overall average noise level. Further analysis on the actual shape of the noise contours is required to determine why.

Emissions analysis presents an exception to the rule. Instead of calculating an RMS value between profiles, a simple difference in total fuel burn and NO_x emissions is calculated between two profiles. The results are organized into a heat map matrix for easy visualization in Table **5**. NOx emissions are shown for the climb up to mixing height, which is 3,000 ft above field elevation in this situation. For example, between NADP1_3-3 and NADP1_4-3, total NO_x emissions differ by 0.107 kilograms. The sign of the difference is removed for the entire matrix, so which profile results in greater NO_x emission cannot be inferred.

Table 5. Sample RMS heat map matrix comparing profile NOx emissions up to 3,000 ft mixing height.

Diff NOx(kg)	NADP1_1-3	NADP1_2-3	NADP1_3-3	NADP1_4-3	NADP1_6-3	NADP1_7-3
NADP1_1-3	0.000	0.099	0.416	0.089	0.407	0.381
NADP1_2-3	0.099	0.000	0.318	0.010	0.308	0.283
NADP1_3-3	0.416	0.318	0.000	0.328	0.010	0.035
NADP1_4-3	0.089	0.010	0.328	0.000	0.318	0.293
NADP1_6-3	0.407	Symmetric		0.318	0.000	0.025
NADP1_7-3	0.381	0.283	0.035	0.293	0.025	0.000

Various clustering methods can be used to transform heat maps into clusters. However, at this stage, there are multiple comparison metrics to consider without any relative priority scaling. Moreover, the comparison metrics have different units and ranges of typical values, thus further adding complexity to the clustering process. Therefore, a normalization scheme is needed that can compute each comparison metric on the same relative scale, thus enabling relative comparison. Several normalization schemes will be considered:

1. Performing RMS over relative differences instead of absolute differences
2. RMS scaled by mean of values
3. RMS scaled by range of values
4. RMS scaled by standard deviation
5. RMS scaled by interquartile range

The complete flowchart of the grouping process is shown in Figure **3**. The objective of the grouping process is to start with the complete NADP Library and end with a Reduced NADP Library that contains fewer profile definitions while retaining the variability of the original profile set. Any grouping must hold true across different operating conditions, thus necessitating the involvement of different test conditions in the grouping process. The currently identified parameters are aircraft size, airport altitude, and stage length. The selected airports correspond to a large variation in airport altitude and aid in assessing the effects of airport altitude on the profiles, and are also synergistic with Project 43 research. After a combination of these parameters has been compiled into a test matrix, a set of automation tools are used to generate results for each test case. The results relevant to grouping are the performance, noise, and emissions. Next, comparison metrics are computed between

results for profile pairs, as previously described in detail. The comparison metrics are stored as heat map matrices, which will be used as inputs to the final step of clustering/grouping. In this step, heat maps are converted into clusters by using techniques that preserve variability with a minimum number of groups/clusters. Different techniques are being explored, and the most suitable will be implemented. After the grouping is complete, the Reduced NADP Library will be obtained.

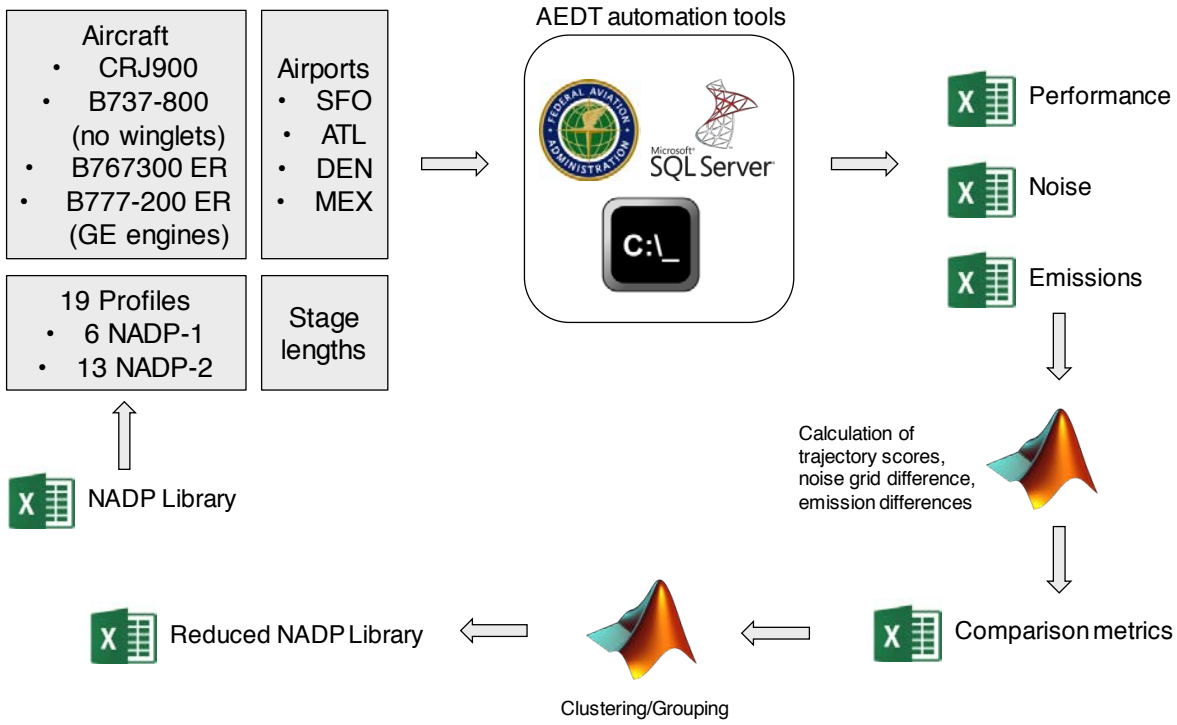

Figure 3. Process of NADP Library grouping.

Milestone

The objective of this task is to provide recommendations for the implementation of NADPs in AEDT. To accomplish this, the NADP Library is being analyzed to shortlist three to five different profiles that are representative of the variability among NADPs.

Major Accomplishments

- Development and implementation of metrics to numerically compare NADP library profiles by using MATLAB scripts
- Automation of processes to enable analysis of numerous combinations of aircraft, airports, profiles, and takeoff weights

Publications

N/A

Outreach Efforts

Bi-weekly calls with the FAA, Volpe, and ATAC. Bi-annual ASCENT meetings.

Awards

None.

Student Involvement

Ameya Behere and Loren Isakson, Graduate Research Assistants, Georgia Institute of Technology

Plans for Next Period

- Implement normalization techniques for same scale assessment of comparison metrics
- Implement clustering algorithms for grouping of NADP library profiles
- Develop the reduced NADP library as options for future implementation into AEDT
- Compare the reduced NADP library to real-world flight data to inform the selection process for implementation into AEDT

Task 2 - NextGen Arrival Profile Modeling

Georgia Institute of Technology

Objective(s)

Previous research has extensively investigated the difference between departure procedures in AEDT and the actual departure procedures observed by using data types such as radar data, Flight Operational Quality Assurance (FOQA) data, and airline and airport documentation, thus resulting in a library of departure procedures. A similar study is to take place for arrival procedures. The use of FOQA data from one airline will be utilized to assess the accuracy of AEDT arrival procedures for 14 airframes. The FOQA data will be used to find different arrival characteristics such as level off altitude, velocity, gear setting and flap setting. These different characteristics will then be compared to what is currently prescribed in AEDT. If a significant difference is found, new arrival profiles will be proposed.

Research Approach

Recent research conducted under ACRP 02-55 has developed methods to model advanced NextGen profiles in AEDT. The project is now complete, and the final deliverables included a report and technical guidance for selecting appropriate aircraft approach and departure profiles, which are available to the public. The GT team has conducted a thorough review of the work conducted in ACRP 02-55 and has created an actionable plan to incorporate the findings.

The ACRP 02-55 objective was to capture and represent arrival procedures used in the real world. This was done by creating additional standard or default procedures that are not currently within AEDT. The researchers working on this study had access to Performance Data Analysis and Reporting System (PDARS) data for more than 274,000 arrival procedures. The data was taken from 30 airports throughout the United States for 68 different aircraft types. From this, the flights were grouped according to the level off length, level off altitude and aircraft class. An example of this grouping would be "A-LJ-1-3000-40to49-5to14." This signifies an approach operation for a large jet with a stage length of 1, which has a level off at 3,000 ft, for a distance between 40 and 49 nmi, ending with 5 to 14 nmi from the airport. The flights were then modeled to fly out of one airport, KATL, to make the trajectories comparable. Level off "bins" for flights were created every 1,000 ft.

An averaged trajectory for these grouped flights was then created and compared to their analogous baseline trajectories, which were STANDARD AEDT approach procedures found in AEDT2a service pack 2. The method used to average the flights was not explicitly defined within the airport. A trajectory score was computed for the average trajectories of the different groups with the following formula:

$$TrajScore = \frac{\sum_{i=1}^{N} \left| H_{avg,i} - H_{BL,i} \right|}{N}$$

where H_{avg} is the altitude from the averaged trajectory, and H_{BL} is the altitude of the baseline from AEDT. These were then normalized to the number of samples taken. Samples were taken every 1 nautical mile in ground track distance. After the grouping process and the calculation of trajectory scores, the worst six profiles for six aircraft classes were chosen to create AEDT procedures by using AEDT's altitude controls functionality. Then 36 approach profiles were generated for six different aircraft classes.

This document was helpful in providing a method to group different flight trajectories. The GT team will create their own algorithm for averaging a particular group of flights according to characteristics that will be discussed later. The averaging

and grouping findings will then be compared to the findings in the ACRP 02-55 document to assess whether there is a correlation between the two.

A similar study will be conducted by the GT team with a new set of airline data acquired from one airline. FOQA data from 21,146 flights and 14 airframes will be used to assemble trajectories into groups. The data include information about altitude, ground track distance, thrust, velocity, gear position, flap position, etc.; the data are more thorough than the PDARS data that the ACRP 02-55 research used. Popular arrival settings for each of the previously described parameters will be heavily inspected to find common departure modes.

A systematic parsing of the data must first be conducted, because these data include the entire flight trajectory from taxi and takeoff to landing and taxi again. For the purposes of this task, the GT team will be investigating only the altitude from 6,000 ft until touchdown, because this is the same altitude range that AEDT uses in its definition of approach. The data will then be entered into visualization software. This software allows users to easily manipulate the data to see trends; an example of this software is shown in Figure 4. This dashboard allows users to see popular modes of flight for approach. The parameters that will be investigated are altitude, ground track distance, thrust, velocity, gear position, and flap position, because these are the parameters that most affect the noise generated by the aircraft. A demonstrational study with 100 flights of data is shown below. This will be expanded to include all the flights for all the airframes.

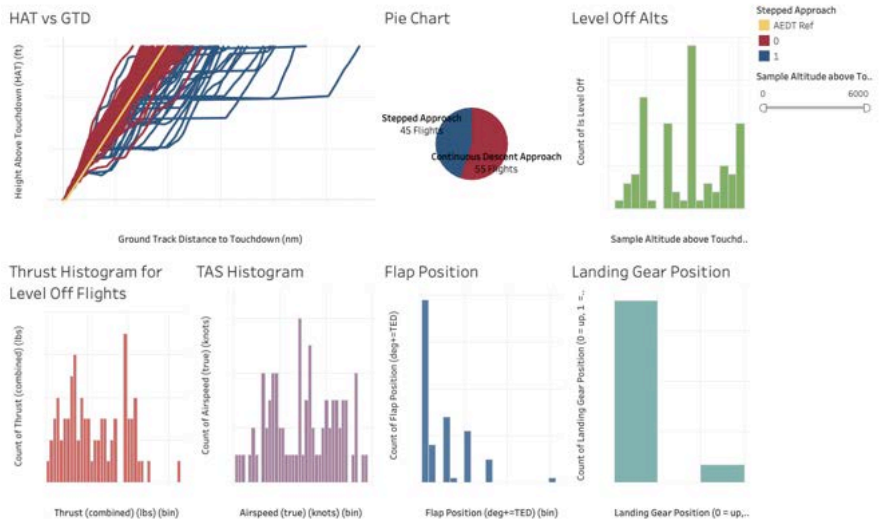

Figure 4. Dashboard with key flight characteristics during arrival for a single-aisle passenger aircraft.

Trends are already observable in the level off altitude, thrust setting, airspeed, flap setting, and landing gear position in the data from 100 flights alone. For example, approximately half the flights have level off segments, which can be seen in the pie chart and the color coding of the plotted flight trajectories. Of these flights categorized as level off, there is an obvious popular altitude for level offs, which can be seen in the "Level Off Alts" chart.

Approach profile and performance variation from the STANDARD AEDT procedure has the potential to change the noise and emissions outputted from an aircraft during this operation. To accurately capture these products, the AEDT procedures must be representative of real aircraft operations. The above approach will allow our team to make proper comparisons and suggestions for improvement to current AEDT procedures. This research will continue into the next period, with examination of different airports and aircraft types with a comparison to the AEDT approach profiles. Initial assessments of real-world flight data indicate differences with respect to the AEDT profile that are dependent on the airport of choice.

Milestone

The objective of this task is to provide insight into how accurately the current AEDT approach profile represents how real-world flight trajectories are performed and, if it does not, to propose new profiles for use.

Major Accomplishments

- Obtained real-world FOQA performance data from airline partner for 13 airframes
- Created a parsing algorithm that observes only the approach phase of flight
- Created an algorithm that detects level segments during the approach phase
- Used this algorithm to create a detailed statistical analysis of the FOQA data to observe common approach procedural patterns

Publications

N/A

Outreach Efforts

Bi-weekly calls with the FAA, Volpe, and ATAC. Bi-annual ASCENT meetings.

Awards

None.

Student Involvement

Ameya Behere and Loren Isakson, Graduate Research Assistants, Georgia Institute of Technology

Plans for Next Period

- Analyze the results of this algorithm and compare the characteristics of real approach procedures to that prescribed in AEDT, to suggest better methods of modeling arrival procedures

Task 3 - Integrated Impact Assessment of Inaccuracies from Thrust, Weight, Procedures, and NPD Curves

Georgia Institute of Technology

Objective

Assess the total impact of proposed improvement in accuracy in modeling assumptions from thrust, weight, procedures, and noise-power-distance (NPD) curves in AEDT vs. real-world settings. The final comparisons will be among standard baseline AEDT modeling assumptions, improved AEDT modeling assumptions (based on real-world data), and actual real-world noise contours.

Research Approach

The research approach is presented in Figure **5**. The initial focus of this task was the departure phase of flight.

Process FOQA data

The objective of this step was to obtain the FOQA data and extract relevant phases of flight and parameters. Approximately 21,000 flights from 14 different airframes were obtained. For the initial iteration to test the methodology presented in Figure **5**, the analysis focused on a single-aisle passenger aircraft, for which there were approximately 4,500 flight records. Scripts were created to automate the data extraction from the raw FOQA files, such that only the relevant segments and parameters were extracted. For this analysis, the departure segment was defined as the start of ground roll until 15,000 ft above runway elevation. The extracted parameters were airspeed (true), airspeed (calibrated), thrust, landing gear position, flap position, gross weight, altitude, ground track distance, and time.

Determine departure modes

The primary focus of this step was to determine common departure modes flown by real-world aircraft by using the extracted FOQA data. Departure modes refer to combinations of airspeed, thrust, and configuration (flap and landing gear) for a given aircraft and stage length. There are two main ways in which this will be accomplished: a visualization dashboard and statistical analysis. For the visualization, dashboards were created in Tableau to visualize the parameter distributions at certain altitudes (Figure **6**) and statistical box plots of specific parameters for a range of altitudes (Figure **7**). These dashboards help users find common departure modes for the relevant parameters at key altitudes. For the statistical analysis,

a script was created that calculates statistical quantities (e.g., mode, median, mean, and standard deviation) for all parameters of interest at different altitude and stage length combinations. Thus, users can easily identify statistically representative values for parameters and create common departure modes. This stage of the approach is currently in progress.

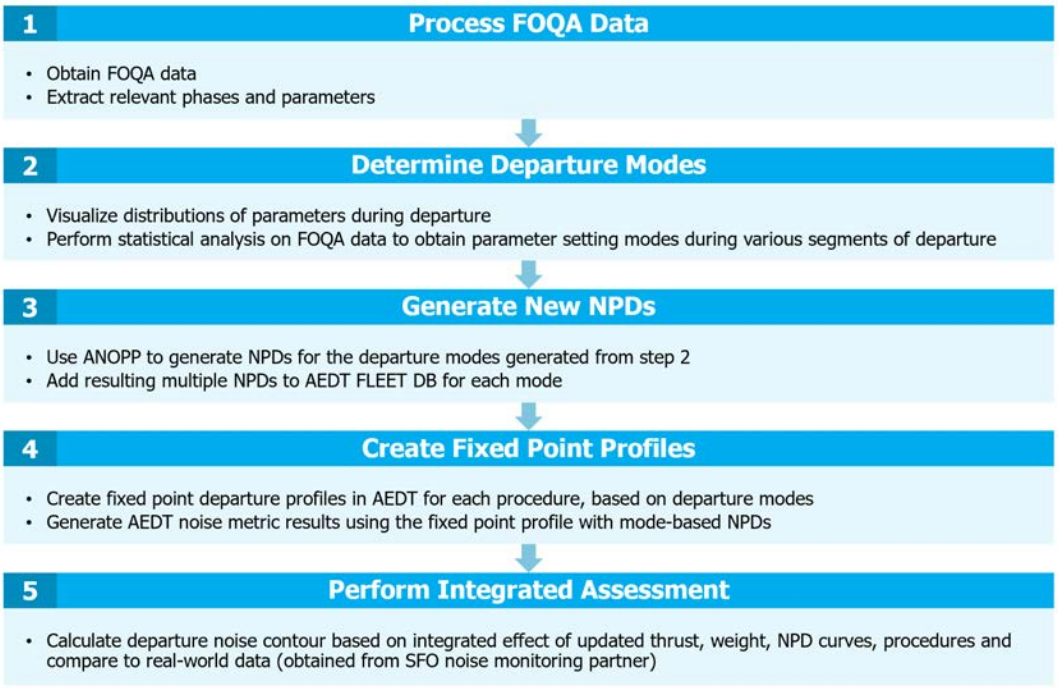

Figure 5. Task 3 research approach.

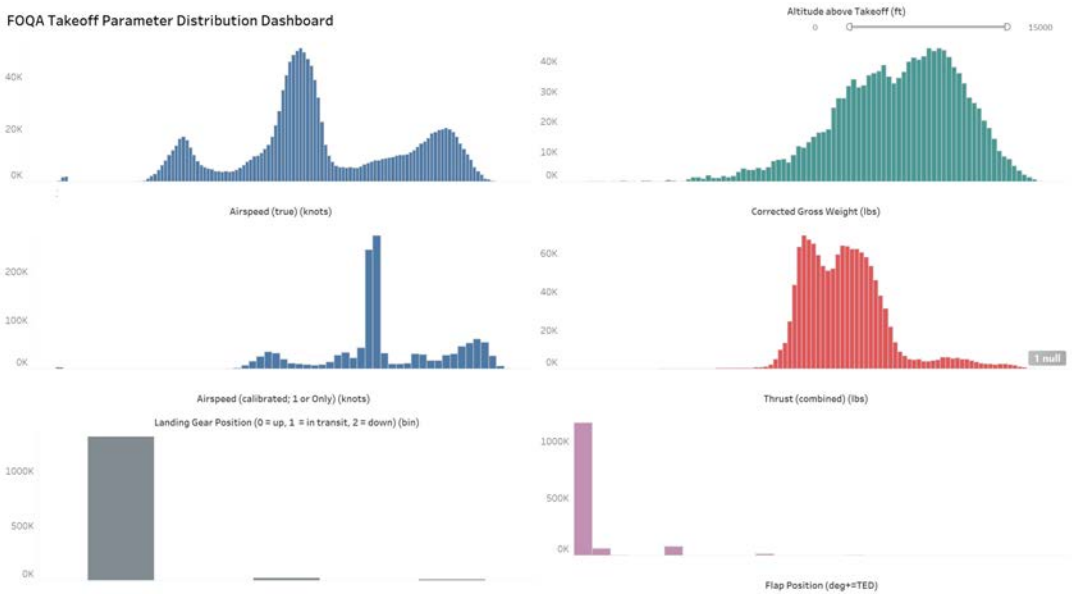

Figure 6. Representative FOQA parameter distribution dashboard.

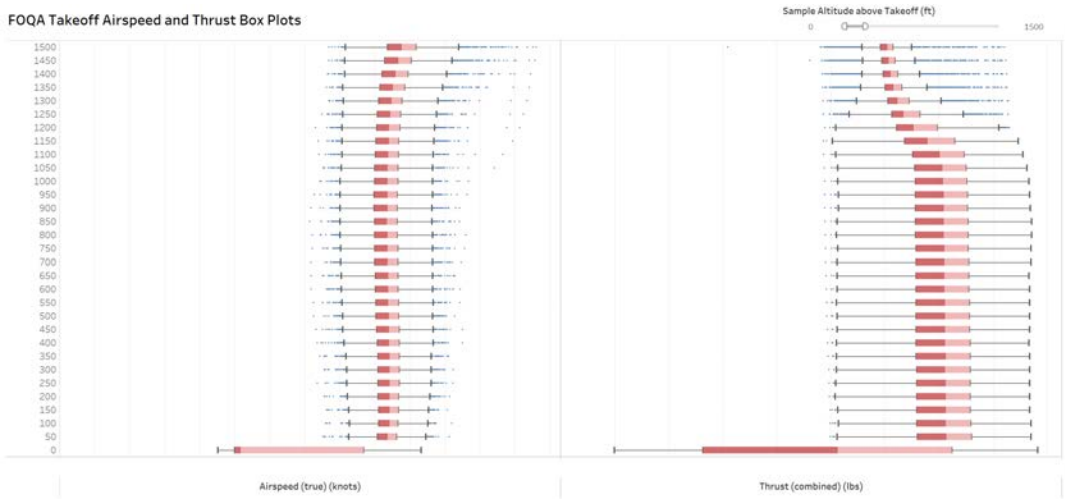

Figure 7. Representative FOQA parameter box plot analysis dashboard.

Generate new NPDs
The departure modes generated from the FOQA analysis will be used to generate a set of new NPD curves for the fleet. The tool used to generate the NPDs will be Aircraft Noise Prediction Program (ANOPP), a noise calculation tool developed by NASA. These new NPDs will have characteristics of real-world flights and are expected to separately consider the noise from the engine and the airframe, which are configuration dependent. Because these NPDs are mode based, multiple NPDs could exist for the same thrust setting, owing to different flap and landing gear configurations. Therefore, a substantial portion of the research will be focused on incorporating multiple NPDs for the same thrust setting into the AEDT fleet database. This work is not the primary focus of this project; instead, the work from ASCENT Project 43 will be leveraged as much as possible to aid in this specific subtask. This phase of the research approach is still in progress.

Create fixed point profiles
The focus of this step is to generate fixed point profiles in AEDT for the aircraft in this study. Fixed point profiles will be used because the thrust setting is already known for the departure modes based on the FOQA data. This phase of the research is still in progress.

Perform integrated assessment
The final step is performing integrated assessment by calculating departure noise contours based on the integrated effect of updated thrust, weight, NPD curves, and procedures. The resulting contours will be compared to real-world noise contours. The comparisons will be across standard AEDT contours, new AEDT contours with updated modeling assumptions and departure modes, and real-world noise contours. This phase of the research is still in progress.

Representative results – departure modes
This section presents preliminary results for departure modes for a single-aisle passenger aircraft, according to the analysis from Step 2 of the approach in Figure **5**. The results are shown for an altitude above takeoff of 1,000 ft. The statistical analysis code was applied to the 4,500 flights for this airframe, and the results are presented in Table 6.

Table 6. Statistical analysis results of select parameters for a single-aisle passenger departures at 1,000 ft above takeoff.

Stage Length	Corrected Gross Weight (lb)		Thrust (combined) (lb)		Airspeed (true) (knots)		Flap Position (degrees)	Landing Gear Position (0 = up, 1 = in transit, 2 = down)
	Mean	Standard Deviation	Mean	Standard Deviation	Mean	Standard Deviation	Mode	Mode
1	148,324	8,962	31,796	3,076	186.7	11.6	1	0
2	154,937	7,789	33,857	3,209	182.9	10.7	5	0
3	165,394	6,395	36,132	2,360	186.5	9.2	5	0
4	172,123	6,457	37,467	2,476	189.7	9.0	5	0
All	162,051	11,373	35,263	3,414	186.6	10.2	5	0

This statistical analysis was supplemented with visualization of the parameters by using the dashboard created to confirm the shapes of the distributions and gain additional insights. Consider the results for stage length 1 as an example. The parameter distribution for stage length 1 at 1,000 ft above takeoff is shown in
Figure **8**. The distribution for true airspeed is reasonably normally distributed, and a mean of 187 knots seems appropriate. The distribution for the corrected gross weight has a mean of 148,324 lb, and the figure shows that it is negatively skewed; i.e., the median is greater than the mean (the median corrected gross weight is 150,300 lb). The distribution for the combined thrust has a mean of 31,796 lb with a slight positive skew; i.e., the median is less than the mean (the median combined thrust is 31,234 lb). However, there is no evidence of any multi-modal distributions for these continuous parameters, thus suggesting that the mean values from the statistical analysis are appropriate to describe the parameter states at this altitude. Additionally, the figure confirms the mode value of 0 for landing gear position; in fact, all flights had the landing gear up by 1,000 ft. The figure also confirms the mode value of 1˚ for flap position. However, a flap position of 5˚ is also fairly common for these flights.

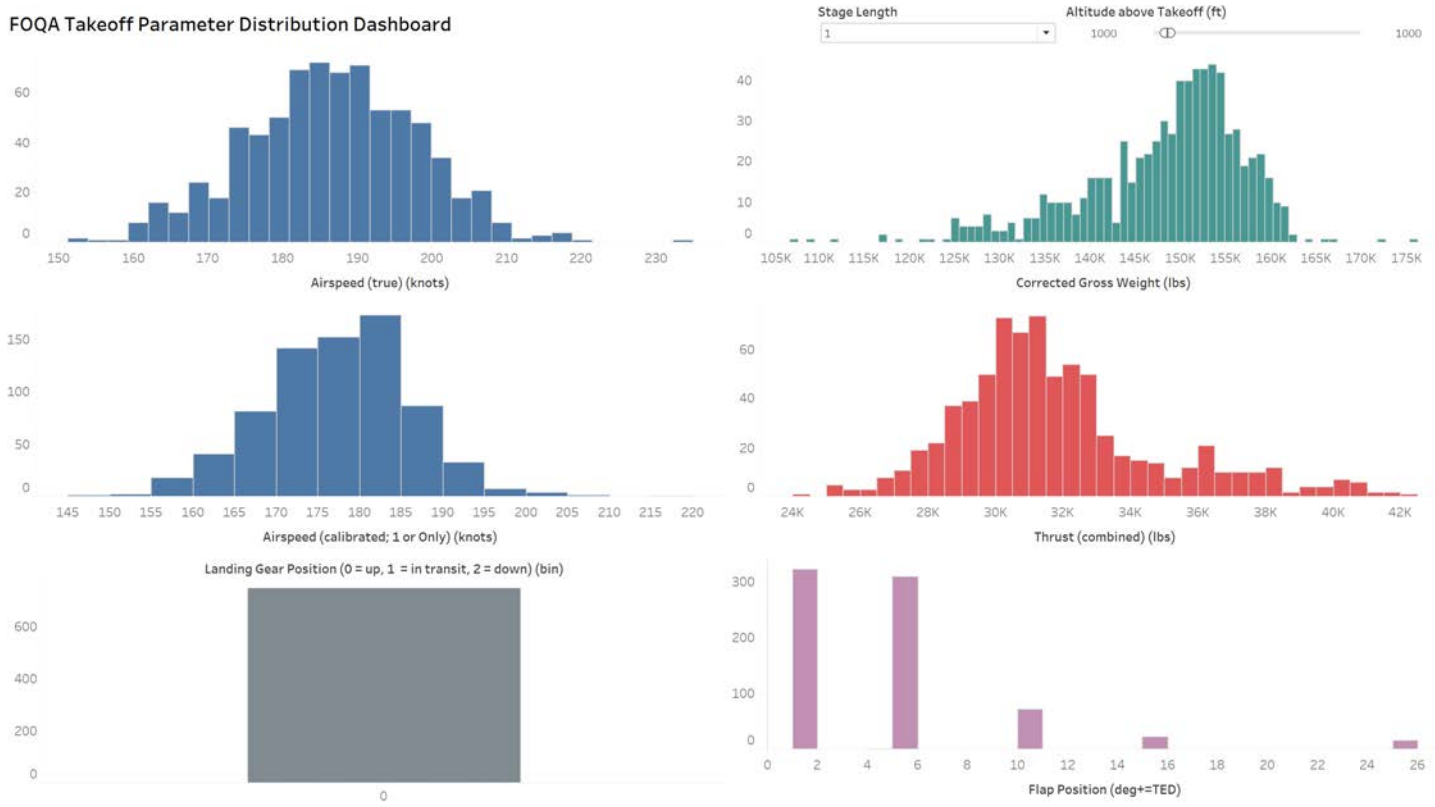

Figure 8. FOQA parameter dashboard result for stage length 1 at 1,000 ft above takeoff.

The combined statistical analysis and visualization dashboard led to the creation of representative departure modes for this aircraft, which are presented in Table 7. These modes are to be used to generate NPD curves for the aircraft.

Table 7. Representative departure modes.

Stage Length	Corrected Gross Weight (lb)	Airspeed (true) (knots)	Thrust (combined) (lb)	Flap Position (degrees)	Landing Gear Position (0 = up, 1 = in transit, 2 = down)
1	148,300	187	31,800	1	0
2	154,900	183	33,900	5	0
3	165,400	186	36,100	5	0
4	172,100	190	37,500	5	0

Milestone(s)

The main objective of this task is to quantify the impact of using each takeoff assumption improvement on the noise predicted by AEDT and compare with real-world noise monitoring data.

Major Accomplishments

- Obtained real-world FOQA performance data from airline partner for 13 airframes
- Identified a process for sampling of FOQA data for modeling in AEDT
- Compared an FOQA profile with the AEDT default profile for assessment of impacts from all assumptions in AEDT APM
- Created visualization dashboards and statistical analysis codes to extract common departure modes based on FOQA data
- Exploring a mode-based methodology for incorporating multiple NPDs for the same thrust setting into the AEDT fleet database

Publications

None.

Outreach Efforts

Bi-weekly calls with the FAA, Volpe, and ATAC. Bi-annual ASCENT meetings.

Awards

N/A

Student Involvement

Dylan Monteiro, Graduate Research Assistant, Georgia Institute of Technology

Plans for Next Period

The primary focus for the next period will be:

- Generate a library of departure modes on the basis of FOQA data, and use these modes to generate NPDs
- Explore different techniques to incorporate multiple NPDs for the same thrust setting into the AEDT fleet database
- Perform integrated assessment to quantify the total impact of inaccuracies from thrust, weight, procedures, and NPD curves

Project 046 Surface Analysis to Support AEDT Aircraft Performance Model (APM) Development

Massachusetts Institute of Technology and Massachusetts Institute of Technology Lincoln Laboratory

Project Lead Investigator

Hamsa Balakrishnan
Associate Professor
Aeronautics and Astronautics
Massachusetts Institute of Technology
77 Massachusetts Ave., 33-207
Cambridge, MA 02139
617-253-6101
hamsa@mit.edu

University Participants

Massachusetts Institute of Technology (MIT) and MIT Lincoln Laboratory

- PI(s): Hamsa Balakrishnan
- FAA Award Number: 13-C-AJFE-MIT, Amendment Nos. 021and 035
- Period of Performance: September 1, 2018, to August 31, 2019
- Task(s):
    - 1.A Extend analysis to broader range of aircraft types that serve U.S. domestic operations
    - 1.B Extend analysis on airport-specific differences that significantly affect surface fuel burn to more U.S. airports
    - 1.C Identify AEDT surface APM enhancements to support emissions and noise inventories
    - 1.D Recommend AEDT APM enhancements and coordinate with AEDT APM developers
    - 2.A Undertake more detailed studies to extend AEDT capabilities to model surface noise and emissions impacts
    - 2.B Identify representative application scenarios and estimate the impact of improved surface movement modeling capability
    - 2.C Develop implementation plan to transition appropriate surface modeling enhancements into the operational AEDT product

Project Funding Level

$75,000 in FAA funding and $75,000 in matching funds. Source of match is approximately $75,000, all from Massachusetts Institute of Technology (MIT).

Investigation Team

- Prof. Hamsa Balakrishnan, co-PI (MIT)
- Dr. Tom Reynolds, co-PI (MIT Lincoln Laboratory, via $75,000 separate contract)
- Sandeep Badrinath (graduate student)
- Emily Joback (MIT Lincoln Laboratory staff)

Project Overview

The current taxi phase models in the AEDT make a number of simplifying assumptions that reduce the accuracy of their fuel burn and emissions predictions. First, the current AEDT model assumes a constant engine-specific thrust level (and resulting fuel flow rate) during taxi, determined from engine manufacturer certification data (International Civil Aviation Organization (ICAO), n.d.). However, this assumption can be significantly different from actual characteristics during operational conditions for a given aircraft because of factors such as the age of the engine (as the engine gets older, the amount of fuel it burns changes), as well as pilot technique (chosen taxi thrust level or "riding the brakes" instead of throttling down the engines when coming to a stop). Second, default taxi times are often assumed to be consistent with the standard certification landing and take-off (LTO) cycle, which assumes 26 min of taxi time on the airport surface, typically broken into 19 min for taxi-out and 7 min for taxi-in. Clearly, different airports may have very different taxi times depending on topology, configuration, congestion levels, and so on, which can lead to a large range in taxi times. Using empirical data to determine realistic taxi time distributions can be effective, but these distributions need to be updated regularly to capture evolving airport conditions. Finally, the fuel burn contribution in the non-movement area from the gate time, pushback, and engine start events [including engine and auxiliary power unit (APU) contributions] are typically neglected but can be significant. This project addresses these three issues by leveraging empirical data to build statistical and predictive models of fuel flow for a given airport and aircraft type. These analyses are designed to capture "first-order" enhancements to provide recommendations for future development of tools such as AEDT.

References

International Civil Aviation Organization (ICAO). (2014). Aircraft Engine Emissions Databank. Online database

Task 1 - Progress and Plans

Massachusetts Institute of Technology, Massachusetts Institute of Technology Lincoln Laboratory

Objective

The objective of this research project is to identify and evaluate first-order methods to improve taxi performance modeling in AEDT to better reflect actual operations. This objective will be met through analyses using surface surveillance (Airport Surface Detection Equipment, Model X; ASDE-X) and Aviation System Performance Metrics (ASPM) taxi time datasets, in combination with a statistical analysis of flight data recorder (FDR) archives and other operational fuel burn data. Subsequent research phases may address potential higher-order enhancement areas.

Research Approach

This report focuses on the latest accomplishments of the Phase 2 activities.

Task 1.A: Extend Phase 1 analysis to broader range of aircraft types

Phase 1 of ASCENT 46 (July 2016 to August 2017) extended this approach by synthesizing such statistical models with surface traffic models obtained through analysis of ASDE-X data (Dopelheuer & Lecht, 1998). A particular focus of this phase was the analyses needed to identify and extract first-order versus higher-order effects on fuel burn. To do so, we considered fuel consumed in the non-movement area (including gate, pushback, and engine start events that have previously not been studied in detail, as well as accounting for APU fuel during these events), as well as the movement areas, including the relative effects of acceleration events on fuel burn compared with baseline fuel flow rates.

Through a synthesis of prior work in Airport Cooperative Research Program (ACRP) 02-27 (Martin et al., 1996), ACRP 02-45 (Kyprianidis et al., 2015), AEDT documentation, stakeholder input, and data analysis, the following gaps were identified: (1) a need to improve/refresh taxi times at different airports; (2) absence of a surface-specific regression model, even for modeling the baseline fuel burn index; (3) no evaluation of the magnitude of non-movement area, engine startup, or APU fuel burn impacts; and (4) no consideration of acceleration events and the resulting increase in the fuel flow rate. In addition, we noted that existing surface APM models were deterministic in nature and did not evaluate the uncertainty or variability associated with real operations.

Figure 1 shows a typical fuel flow rate profile (post-pushback and engine start) during taxi-out. It can be seen that the fuel flow rate profile (red curve) can be divided into two distinct regions: a baseline region and a fuel flow spike region. The baseline region is characterized by an almost constant (low-variation) fuel flow rate having a low value. The fuel flow spike

region is characterized by spikes in the fuel flow rate with values greater than the baseline fuel flow rate. Therefore, these two fuel flow rate regions need to be modeled separately.

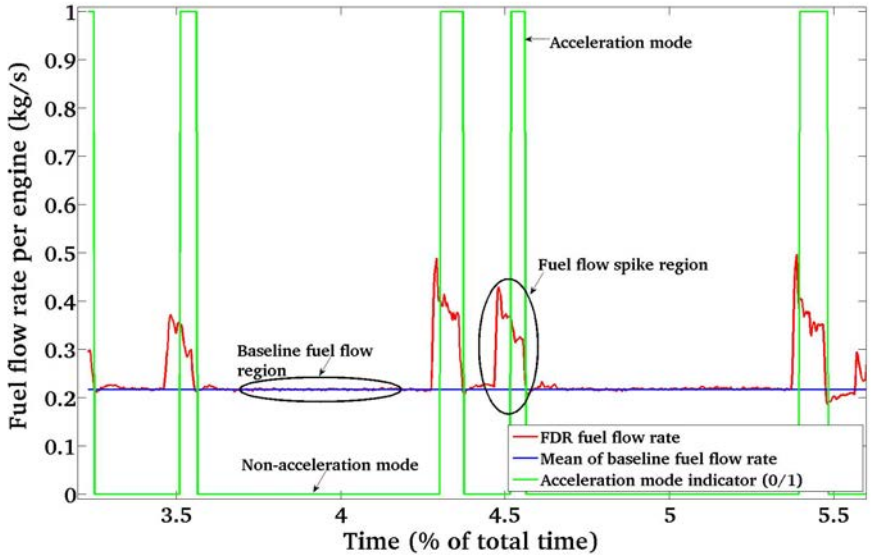

Figure 1. Typical fuel flow rate profile in taxi-out; FDR, flight data recorder.

Phase 1 also analyzed different characteristics of the baseline fuel flow region for two example aircraft types, the A330-343 and the B777-300ER, extracted from operational FDR data and found that, on average, more than 90% of taxi-out fuel consumption occurs during the baseline fuel flow region. Therefore, in the current work, only the baseline fuel flow region was modeled and the fuel flow spikes were neglected. Figure 1 also shows a mean baseline fuel flow rate (in blue) obtained by averaging the baseline fuel flow rates for a particular taxi-out operation.

The values of aircraft acceleration during taxi are generally not explicitly recorded in the trajectory data. Hence, the raw trajectory data are smoothed in order to estimate the variables of interest (such as acceleration mode, shown in green in Figure 1). Finally, the mean baseline fuel flow rate per engine in taxi-out (blue curve in Figure 1) was regressed against the mean values of the selected predictor variables. An ordinary least squares (OLS) regression approach was found to be sufficient to develop this simplistic model (which is based on the same functional form as the current AEDT model). Table 1 shows the OLS-derived equations for modeling the fuel flow rate in taxi-out for six aircraft types.

Table 1. Ordinary least squares (OLS) regression equations to model fuel flow rate per engine during taxi-out, along with the number of observations (flights) in the training dataset. $\dot{m}_{f_{ICAO}}$ is the baseline taxi fuel flow rate from the International Civil Aviation Organization (ICAO) engine emissions databank (International Civil Aviation Organization (ICAO), 2014), and δ and θ are the pressure and temperature ratios relative to standard atmospheric values.

A/C Type	Engine Type	# Training Obs.	OLS Model Equation
A320-214	2 × CFMI CFM56-5B4/2	103	$0.812 \cdot \dot{m}_{f_{ICAO}} \cdot \delta_{\infty}^{-0.123} \cdot \theta_{\infty}^{-0.483}$
A321-111	2 × CFMI CFM56-5B1/2	46	$0.796 \cdot \dot{m}_{f_{ICAO}} \cdot \delta_{\infty} \cdot \theta_{\infty}^{0.209}$
A330-343	2 × RR Trent 772B-60	117	$0.779 \cdot \dot{m}_{f_{ICAO}} \cdot \delta_{\infty} \cdot \theta_{\infty}^{0.350}$
A340-313	4 × CFMI CFM-56 5C4/P	37	$1.019 \cdot \dot{m}_{f_{ICAO}} \cdot \delta_{\infty}^{-6.690} \cdot \theta_{\infty}^{0.597}$
B777-300ER	2 × GE GE90-115BL	81	$0.753 \cdot \dot{m}_{f_{ICAO}} \cdot \delta_{\infty} \cdot \theta_{\infty}^{0.717}$
C Series 100 (RJ)	2 × PW PW1542G	95	$0.966 \cdot \dot{m}_{f_{ICAO}} \cdot \delta_{\infty} \cdot \theta_{\infty}^{0.186}$

We also compared predictions from such baseline fuel flow modeling with the estimates provided by AEDT, which uses the ICAO fuel burn indices in conjunction with the Boeing Fuel Flow Correction. Because the pressure and temperature ratios are approximately 1 for taxi operations, the multiplicative factor in Table 1 is the key differentiator from AEDT, which uses a constant value of 1.1 for all aircraft types. The results are shown in Table 2 and suggest that significant benefits may be achieved through such a data-driven methodology.

Table 2. Performance of the ordinary least squares (OLS)-based baseline fuel flow rate models and the Aviation Environmental Design Tool (AEDT) model to predict fuel flow rates on unseen test data during taxi-out. The number of flights in the test data is also shown.

A/C Type	# Test Observations from FDR	Mean error (%)		Mean absolute error (%)	
		OLS Model	AEDT	OLS Model	AEDT
A320-214	34	1.0	36.3	13.3	39.4
A321-111	14	3.8	47.1	14.9	50.1
A330-343	37	-3.0	36.4	5.8	39.1
A340-313	12	-0.7	7.8	9.1	12.5
B777-300ER	25	-2.2	42.3	3.1	43.1
C Series100 (RJ)	30	0.1	17.7	5.5	19.3

Recently, these results have been extended to include another source of taxi fuel burn data provided by Airlines for America (A4A), which included both A320 and B737 aircraft types. The former allowed us to compare the A320 results from these data compared with the FDR data reported above, and the latter allowed us to develop taxi fuel burn estimates for the B737, which had been a major gap in our analysis to date. Given the prevalence of B737 operations in the United States, this was a critical gap to be filled. In each case, the A4A data provided total fuel burn for a large number of flights, which allowed us to estimate total fuel burn models of the form

Total fuel burn = **[taxi-out fuel flow rate]** × **taxi-out time** + [airborne fuel flow rate] × airTime + [taxi-in fuel flow rate] × taxi-in time + intercept

The bolded term is the one of interest given the objectives of this program. For the A320, the regression model was trained on the A4A data from 2014 (123,995 flights), tested on 2012–2013 + 2015 data (396,334 flights) for A320-232 (includes V2527-A5 and V2527E-A5 engine types). The resulting linear regression model was

Total fuel burn = **21.3** × **taxi-out time** + 94.7 × airTime + 21.5 × taxi-in time + 535.4

The estimated taxi-out fuel flow rate of 21.3 lb/min was compared with the FDR baseline fuel flow rate (with CFM56-5B4/2 engines) of 25.8 lb/min, with the difference being attributed to the different engine types between the FDR and A4A analysis. The 21.3 lb/min estimated fuel flow rate is 63% of the ICAO fuel flow rate (V2527-A5) estimate of 33.9 lb/min.

For the B737, the regression model was trained on A4A data from 2014 (193,727 flights) and tested on 2012–2013 + 2015 data (810,155 flights). Most were B737 with CFM56 engines. The resulting linear regression model was

Total fuel burn = **22.0** × **taxi-out time** + 81.2 × airTime + 23.6 × taxi-in time + 588.3

The estimated taxi-out fuel flow rate of 22.0 lb/min is 76% of the baseline ICAO fuel flow rate (CFM56-7B24 engines) of 28.8 lb/min.

Task 1.B: Extend Phase 1 findings on airport-specific differences that significantly affect surface fuel burn to more U.S. airports

Airport-specific taxi-out times are available in AEDT but are outdated. For this part of the study, taxi times were collected from the FAA's ASPM. This dataset contains flight-specific taxi-out times, available to the nearest minute. ASPM data from flights across 25 major U.S. airports were aggregated for dates between 2011 and 2018 to provide information about changes in taxi times over many years.

Figure 2 shows the taxi-out time statistics for 25 airports for 2017. The red dotted line is the 19-min taxi-out time assumption from the ICAO LTO cycle. For some airports, this is a reasonably good approximation of the median of the distribution, but for others it is not (the red % value gives the error between the median and the 19-min approximation). Sometimes it is beneficial to reduce the number of taxi time distributions to a few clusters that capture the spectrum of differences seen in the taxi-out distributions for all airports. To this end, each of the airport distributions was fitted to a cumulative distribution function and the resulting curves were clustered into 6 groups. For some clusters (such as cluster 1), the 19-min approximation was relatively accurate. However, for other clusters (such as cluster 5), such an estimate would introduce significant error compared with the actual taxi-out time at the airports in this group. It is also interesting to note which airports are paired. For example, JFK and LGA have been identified as airports with similar taxi-out characteristics. Both distributions have a higher spread and higher mean compared with other airports. In contrast, Chicago Midway (MDW) is dissimilar enough from any of the other airports that it is placed in a cluster (6) by itself.

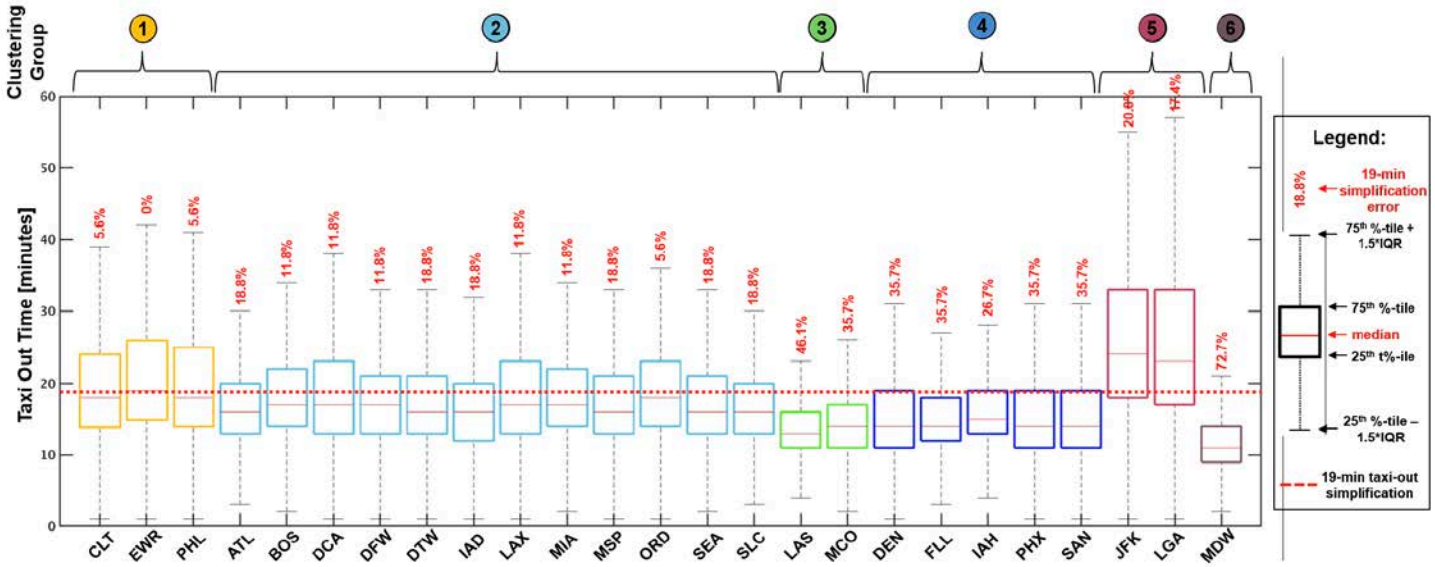

Figure 2. Boxplot of airport distributions by clustering group (outliers removed).

The multiple years of data also allowed us to see how taxi time varied over time as infrastructure changed at the airports, as well as with seasonal, weather (e.g., visual vs. instrumental meteorological conditions), and airport configuration differences. Examples of these are shown in Figures 3 and 4 below. Equivalent figures have been generated for all 25 airports.

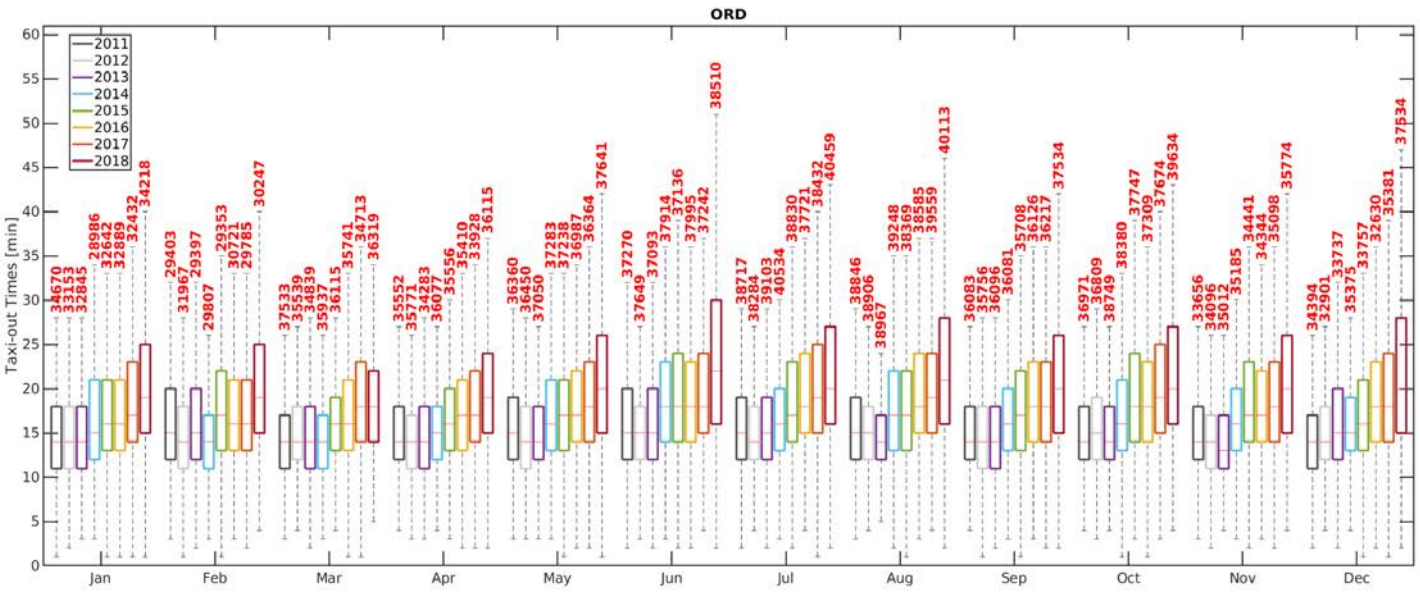

Figure 3. Boxplot of 2011–2018 taxi-out time distributions for Chicago O'Hare Airport (ORD).

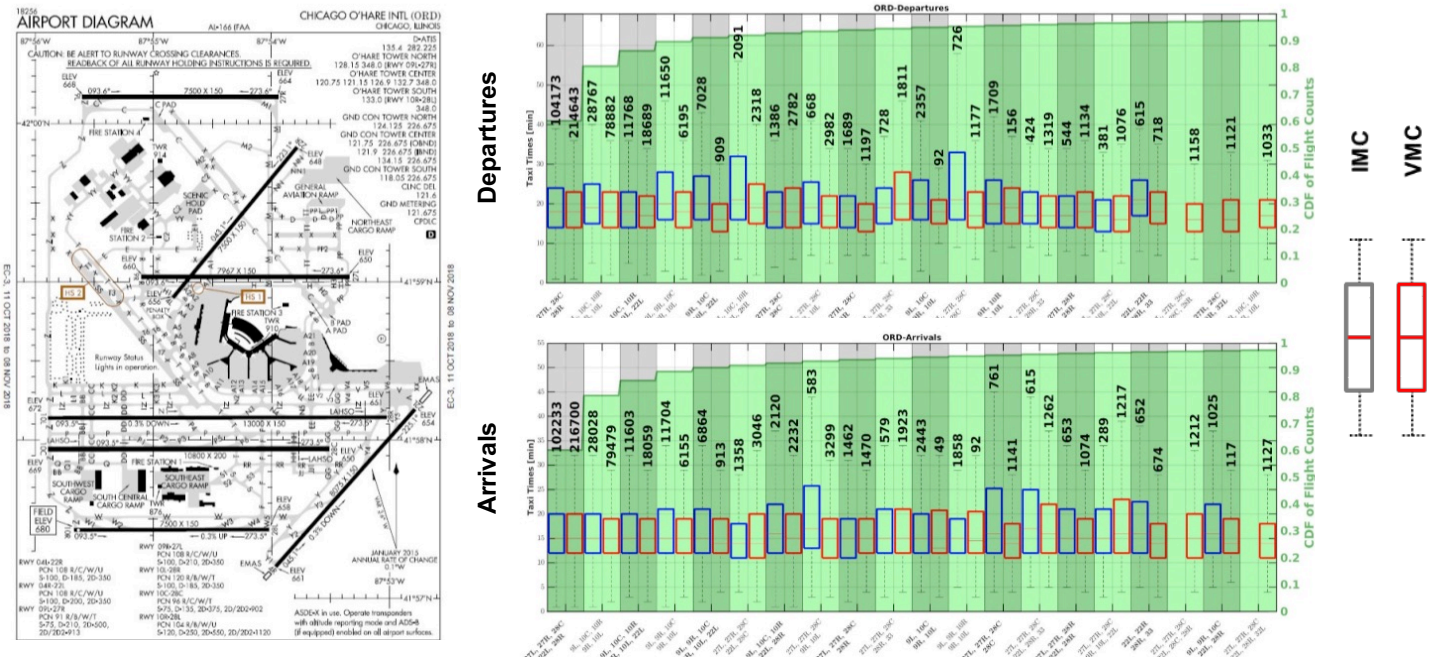

Figure 4. Boxplot of taxi-out time distributions as a function of weather (visual vs. instrumental meteorological conditions, VMC vs. IMC) and runway configurations for Chicago O'Hare Airport (ORD).

Adding gate, pushback, and engine startup fuel estimates

To establish a more accurate model of fuel burn at a given airport, the fuel consumed during engine startup, as well as the APU contribution at the gate, pushback, and engine startup, was also investigated in this study. Differences in fuel burn for

these phases across different airports were found to be negligible; however, fuel burn distributions were found to vary significantly between different aircraft types. For this analysis, data from FDR was available for a European carrier for a selection of aircraft types. This contains a record over time of information specific to a flight, including fuel burn and velocity.

Figure 5 shows the raw FDR data for a sample flight. For this part of the analysis, the flight was broken up into multiple segments, because the gate, pushback, and engine start have different APU and engine fuel burn settings. APU fuel burn rates were obtained from the ACRP 02-25 guidance document (ACRP 02-25, 2012), which groups aircraft into categories (narrow body, wide body, jumbo wide body, regional jet, and turbo prop) and gives the APU settings for the "no load" (gate), "environmental control systems" (pushback), and "main engine start" conditions for each aircraft category. The APU is turned on while at the gate in the "no load" condition, after the aircraft has been disconnected from the gate's electricity. Through discussion with an experienced commercial pilot, we determined that the APU is typically first turned on between 10 and 15 min before pushing back from the gate at large U.S. airports. Therefore, for all aircraft, the gate time was assumed to be 12.5 min, although different assumptions may be appropriate at other airports; for example, where off-gate stands are more common. Pushback was defined from the point at which the aircraft began to move back from the gate to the point when one of the engines began burning fuel. As can be seen in Figure 4, most aircraft start the first engine while still in the process of pushback by the tug from the gate, before halting and completing engine startup with the remaining engines. Engine startup was defined from the end of pushback to when the aircraft begins to move for taxi after all engines have started up and post-engine checklists are complete.

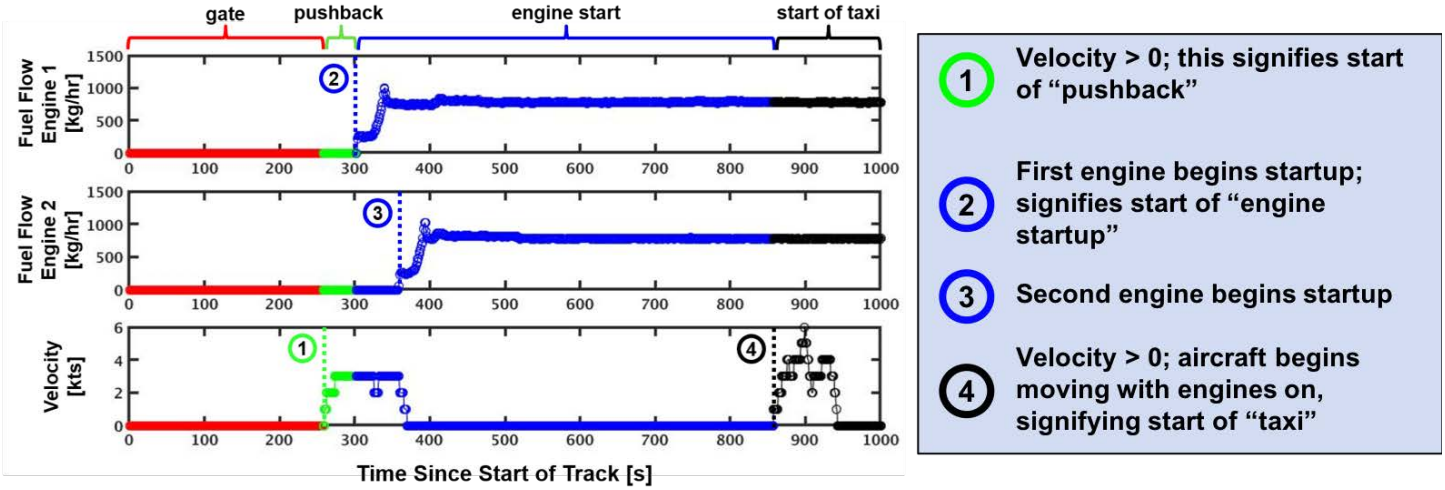

Figure 5. Example flight data recorder (FDR) data for a single flight gate, pushback, and engine start event.

Much of the work incorporated preprocessing the data before performing statistical analysis, because many flights had corrupted data, such as non-zero fuel or velocity at the beginning of the track. Once tracks had been corrected for these issues, the fuel burn totals for the gate/pushback/engine start processes were aggregated over all flights of a given aircraft type available in the FDR data as a statistical approach to building fuel burn histograms from historical data. The resulting fuel burn distributions for the types studied are shown in Figure 6 (left). The relationship between fuel burn and aircraft size was then investigated as a means to predict the fuel burn of flights not within the FDR dataset. The maximum takeoff weight was used for each data type, pulled from the BADA 3.6 dataset (EUROCONTROL, n.d.). The total fuel burned during gate/pushback/engine start is shown in Figure 6 (right) to be linearly related to the weight of the aircraft type; this correlation was used to predict the approximate fuel burn for aircraft types not available in the FDR data set. Estimates for some example types using the observed correlation are presented as dashed lines in Figure 6 (left).

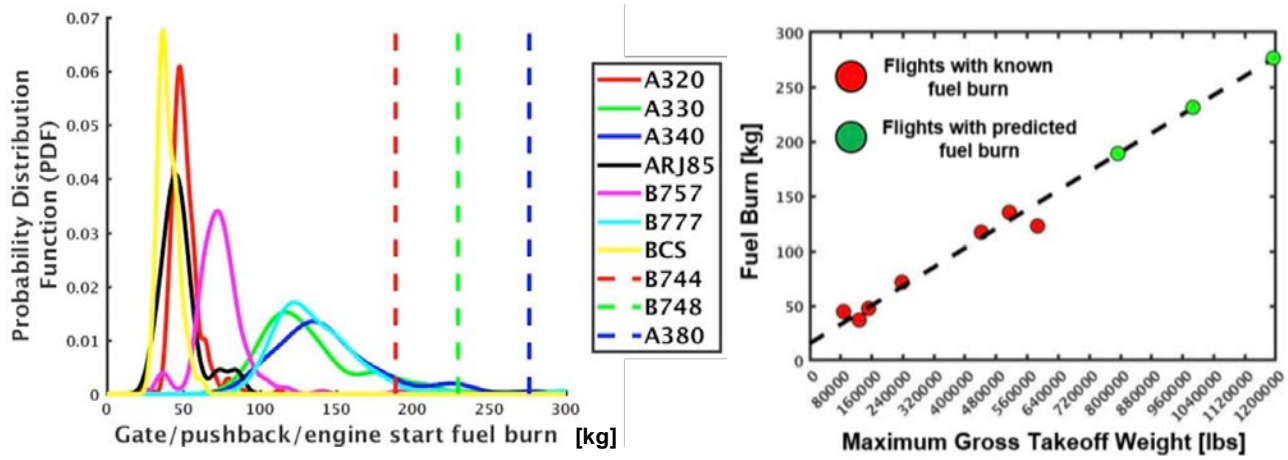

Figure 6. PDF curves for gate, pushback, and engine start fuel burn by aircraft type.

The total fuel burn between the gate up to the point at which an aircraft begins to taxi can be seen to vary significantly between aircraft types and can be a significant fraction of total surface fuel burn. Figure 7 shows the percentage of pre-taxi fuel burn relative to total surface fuel burn from the types analyzed from the FDR data. For narrow body aircraft, this percentage of total fuel burn is higher than that of the larger body aircraft, as seen in the left plot of Figure 6. The right plot of the figure shows that the typical contribution of the pre-taxi fuel compared with the total fuel burned on the aircraft surface is between 10% and 40% on average, reinforcing the need to carefully consider this component of surface fuel burn.

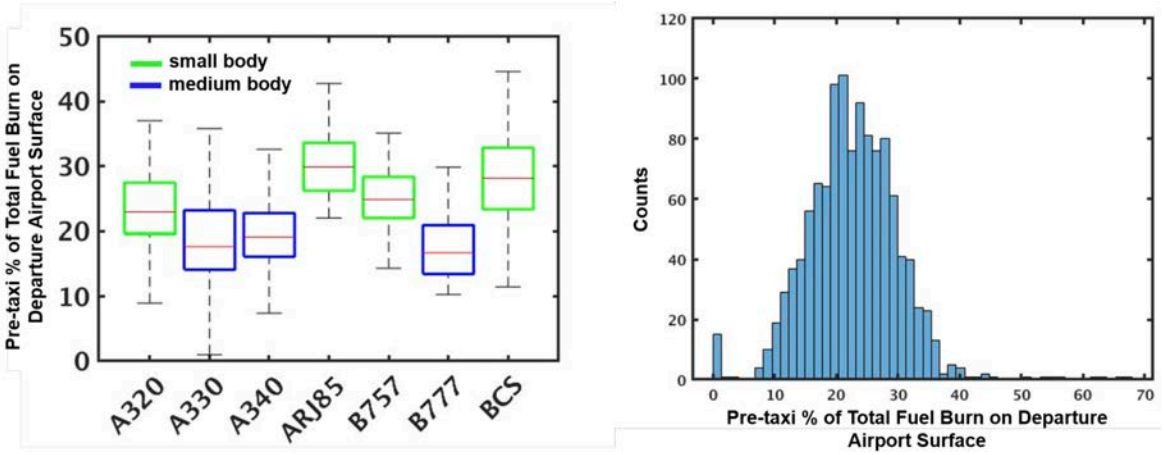

Figure 7. Pre-taxi fuel burn as a percentage of total fuel burned during departure from gate to wheels-off, per aircraft type (left) and as an aggregate distribution (right).

Task 1.C: Identify AEDT surface APM enhancements to support emissions and noise inventories
The work to date has focused on the enhancement of AEDT surface APM to support fuel burn models. We have begun to conduct a preliminary study (based on prior literature) to identify potential first-order effects in the modeling of emissions and noise. Our literature survey for emissions modeling has considered literature on NO_x (e.g., P3-T3 methods), HC, CO, and soot emissions. The references in the bibliography have been the primary sources reviewed for emissions modeling. In ongoing work, we are undertaking a similar exercise on noise modeling, beginning with ACRP 02-27 (2009; 2013).

Task 1.D: Recommend AEDT APM enhancements and coordinate with AEDT APM developers
Based on the modeling enhancements developed from this process, specific targeted recommendations for AEDT APM improvements for the surface domain will be made. Coordination will be required throughout with the primary AEDT APM

developers; that is, Volpe and ATAC, to ensure that the research is practical and will directly inform enhancements to the APM.

Major Accomplishments

The proposed work is expected to have high impact as it will improve the accuracy and expand the capability to model surface fuel, and therefore noise and emissions within AEDT.

Milestone

Tasks 1.A to 1.D were carried out from September 2018 to August 2019. Phase 3 tasks (see below) are planned.

Publications

Published Conference Proceedings

Clemons, E., Reynolds, T.G., Badrinath, S., Chati, Y., & Balakrishnan H. (2018). Enhancing aircraft fuel burn modeling on the airport surface. AIAA Aviation 2018 Conference, Atlanta

Outreach Efforts

Presentation at the American Institute of Aeronautics and Astronautics (AIAA) AVIATION 2018 Conference

Awards

None.

Student Involvement

Graduate students have been involved in all aspects of this research. Dr. Y. S. Chati received his PhD from MIT in 2018, and currently works at Apple Inc. Sandeep Badrinath is currently a PhD candidate at MIT.

Plans for Next Period

Phase 3 tasks are planned next and will commence when the next funding increment is released. Planned tasks are below.

References

ACRP 02-25. (2012). Handbook for evaluating emissions and costs of APUs and alternative systems. Transportation Research Board

ACRP 02-27. (2009). Enhanced modeling of aircraft taxiway noise, volume 1: Scoping. Transportation Research Board

ACRP 02-27. (2013). Enhanced modeling of aircraft taxiway noise, volume 2: Aircraft taxi noise database and development process. Transportation Research Board

ACRP 02-45. (2016). Methodology to improve EDMS/AEDT quantification of aircraft taxi/idle emissions. Transportation Research Board

Ahearn, M. et al. (2016). Aviation Environmental Design Tool (AEDT) technical manual, version 2b, service pack 3. U.S. Department of Transportation John A. Volpe National Transportation Systems Center, Report No. DOT-VNTSC-FAA-16-11

Baughcum, S.L., Tritz, T.G., Henderson, S.C., & Pickett, D.C. (1996). "Scheduled civil aircraft emission inventories for 1992: database development and analysis. NASA Contractor Report 4700, [Appendix D contains the Boeing Method 2 Fuel Flow Methodology Description]

Deidewig, F., Dopelheuer, A., & Lecht., M. (1996). Methods to assess aircraft engine emissions in flight. Congress of the International Council of the Aeronautical Sciences

Dopelheuer, A. (2000). Aircraft emission parameter modelling. Air and Space Europe, Vol. 2, No. 3, pp. 34-37

Dopelheuer, A. & Lecht, M. (1998). Influence of engine performance on emission characteristics. RTO AVT Symposium on Gas Turbine Engine Combustion, Emissions and Alternative Fuels, Lisbon

EUROCONTROL. Base of Aircraft Data (BADA) website. http://www.eurocontrol.int/services/bada.

International Civil Aviation Organization (ICAO). (2014). Aircraft Engine Emissions Databank. Online database

Kim, B. et al. (2005). System for assessing Aviation's Global Emissions (SAGE) Version 1.5, Technical Manual. John A. Volpe National Transportation Systems Center, Massachusetts Institute of Technology, and Logistics Management Institute, Report No. DOT-VNTSC-FAA-05-14

Kim, B. & Rachami, J. (2008). Aircraft emissions modeling under low power conditions. Technical Report, Observatory for Sustainability in Aviation

Kyprianidis, K.G., Nalianda, D., & Dahlquist, E. (2015). A NOx emissions correlation for modern RQL combustors. Energy Procedia, Vol. 00

Martin, R.L., Oncina, C.A., & Zeeben, J.P. (1996). A simplified method for estimating aircraft engine emissions. Appendix C of Scheduled Civil Aircraft Emission Inventories for 1992: Database Development and Analysis

Schaefer, M. & Bartosch, S. (2013). Overview on fuel flow correlation methods for the calculation of NOx , CO, and HC emissions and their implementation into aircraft performance software. DLR Report

Wasiuk, D.K., Lowenberg, M.H., & Shallcross, D.E. (2015). An aircraft performance model implementation for the estimation of global and regional commercial aviation fuel burn and emissions. Transportation Research Part D, Vol. 35, pp. 142-159

Task 2 – Enhancements to AEDT's Dispersion Modeling Capabilities

Massachusetts Institute of Technology, Massachusetts Institute of Technology Lincoln Laboratory

Objective(s)

Research Approach

Task 2.A: Undertake more detailed studies to extend AEDT capabilities to model surface noise and emissions impacts

In the prior phase of the work, relevant literature sources and other modeling approaches were identified and reviewed with respect to surface noise and emissions modeling (e.g., ACRP reports, P3-T3 emissions models). Based on these activities, a roadmap has been developed of how researchers will use the enhanced surface fuel flow models to benefit noise and emissions modeling in AEDT. The current proposal is to map engine power settings for different taxi phases (stops, idle taxi, and accelerations) to noise and emissions effects. By considering the accuracy of resulting noise and emissions effects as a function of location on the airport surface, we can start to understand the potential utility of these proposed enhancements. We are initially using the case of A320 FDR data to illustrate how we can analyze taxi speed profiles to identify acceleration events on the airport surface. These in turn can be used to determine correlations between acceleration events and fuel flow and thrust spikes from the relevant parameters in the FDR data. In this task, similar correlations will be found for other aircraft types contained in our FDR data archive, which can then be used for airports where we do not have FDR data but we do have ASDE-X data from which we can identify acceleration events as a function of time and location. The resulting fuel flow and thrust profiles will be used as input to appropriate noise and emissions analyses for those airports. Sensitivity studies will also be conducted as appropriate.

The main subtasks to be undertaken are as follows:

1. Enhance AEDT's surface performance modeling to improve AEDT's dispersion modeling capabilities for airport air quality analysis. The surface performance model currently available in AEDT is the Delay, Sequence and Queuing Model (DSQM). In its current implementation, DSQM sometimes exhibits congestion on the taxiway network, with long delays resulting in delayed flights, incorrect runway assignments, and errors in the emissions attributed to extended runways (especially in case of heavy aircraft). The research team will assess the current implementation of DSQM and associated issues, will make recommendations on improvements and, if appropriate, will develop a new and improved surface queuing model that would address these issues.
2. Evaluate and refine baseline fuel burn/emissions indices by considering modeling techniques based on analysis of FDR data, and evaluate discrepancies with the ICAO Emissions Databank values by leveraging the A4A fuel burn data.
3. Make initial enhancements to noise models by incorporating location-specific thrust levels during taxi (e.g., ramp area, taxiways, runway queues).

Task 2.B: Identify representative application scenarios and estimate the impact of improved surface movement modeling capability

The main subtasks to be undertaken are as follows:

1. Use AEDT baseline modeling (with improved DSQM and/or newly developed surface performance model as described in Task 1.A) and user-defined input to predict noise, emission, and fuel burn for the scenarios identified.
2. Compare the predictions and evaluate the impact of improved surface movement modeling capability.
3. Identify a few practical scenarios that represent environmental analysis of typical airport settings.

Priorities for extensions will be established through continued engagement with FAA sponsors, AEDT developers, and other appropriate stakeholders.

Task 2.C: Develop implementation plan to transition appropriate surface modeling enhancements into the operational AEDT product

The research team conducts regular analysis status and results review with FAA sponsors and AEDT developers. This will continue in the current tasking, with the intent to identify an implementation plan and schedule to transition specific surface modeling enhancements into appropriate versions of the operational AEDT product given their developmental maturity and programmatic priorities. Further engage with AEDT developers who, in prior phases of the work, identified the need for functionality tailored to different user classes:

1. Basic users wanting the ability to select "canned" options representative of typical operating conditions; for example, based on ASPM-derived empirical distributions. We can also analyze the impact of infrastructure development (e.g., runway construction) that could change airport capacity and traffic flows on the surface and subsequently affect fuel burn, noise, and emissions.
2. Intermediate users wanting the ability to modify behaviors based on appropriate modeled parameters; for example, available in the existing AEDT DSQM and the new surface performance model if proposed.
3. Advanced users wanting complete control over all aspects of aircraft and airport dynamics; for example, based on ASDE-X data.

Major Accomplishments

This work will enable this by maturing enhanced surface fuel, noise and emissions models and then work with AEDT developers and key stakeholders to develop an implementation plan which transitions these enhancements into the operational AEDT product. By tailoring the enhancements to different AEDT user classes, the impacts of the model enhancements will be maximized across the spectrum of AEDT users.

Publications

N/A

Outreach Efforts

N/A

Awards

None.

Student Involvement

Sandeep Badrinath, PhD candidate, MIT

Plans for Next Period

N/A

Project 47 Clean-Sheet Supersonic Aircraft Engine Design and Performance

Massachusetts Institute of Technology

Project Lead Investigator

Prof. Steven R. H. Barrett
Leonardo Associate Professor of Aeronautics and Astronautics
Department of Aeronautics and Astronautics
Massachusetts Institute of Technology
77 Massachusetts Avenue – Building 33-322
(617)-452 2550
sbarrett@mit.edu

University Participants

Massachusetts Institute of Technology

- PI(s): Prof. Steven R. H. Barrett
- FAA Award Number: 13-C-AJFE-MIT, Amendment No. 052
- Period of Performance: March 29, 2019, to March 28, 2020 (with the exception of funding and cost share information, this report covers the period from March 29, 2019, to September 30, 2019)
- Task(s):
    1. Identify mission profiles and operating requirements for propulsion systems
    2. Develop an engine cycle model for a supersonic aircraft propulsion system
    3. Assess environmental footprint of an engine for a supersonic transport aircraft

Project Funding Level

$250,000 FAA funding and $250,000 matching funds. Sources of match are approximately $73,000 from Massachusetts Institute of Technology (MIT), plus third-party, in-kind contributions of $177,000 from Byogy Renewables Inc.

Investigation Team

- Prof. Steven Barrett (MIT) serves as PI for the A47 project as head for the Laboratory for Aviation and the Environment. Prof. Barrett coordinates internal research efforts and maintains communication between investigators in the various MIT research teams.
- Dr. Raymond Speth (MIT) serves as co-investigator for the A47 project. Dr. Speth directly advises student research in the Laboratory for Aviation and the Environment focused on assessment of fuel and propulsion system technologies targeting reduction of aviation's environmental impacts. Dr. Speth also coordinates communication with FAA counterparts.
- Dr. Jayant Sabnis (MIT) serves as co-investigator for the A47 project. Dr. Sabnis co-advises student research in the Laboratory for Aviation and the Environment. His research interests include turbomachinery, propulsion systems, gas turbine engines, and propulsion system–airframe integration.
- Dr. Choon Tan (MIT) serves as co-investigator for the A47 project. Dr. Tan directly advises student research in the Gas Turbine Laboratory focused on unsteady and three-dimensional flow in turbomachinery and propulsive devices, aerodynamic instabilities in aircraft gas turbine engines, and propulsion systems.
- Mr. Prashanth Prakash is a PhD student in the Laboratory for Aviation and the Environment. He is responsible for developing engine models in the Numerical Propulsion System Simulation (NPSS) tool, for developing the combustor reactor network model, and for analyzing the sensitivity of engine emissions to design parameters.
- Mr. Laurens Voet is a graduate student researcher in the Gas Turbine Laboratory. Mr. Voet is responsible for determining propulsion system requirements for supersonic aircraft designs, for relating the noise footprint to the

relevant engine parameters, for estimating the effective perceived noise level (EPNL) for given aircraft trajectories, and for proposing clean-sheet engine design solutions to reduce its noise footprint.

Project Overview

A number of new civil supersonic aircraft designs are currently being pursued by industry in different Mach regimes and for different size classes (e.g., supersonic business jets at low-supersonic Mach numbers and airliners at high-supersonic Mach numbers). Compared with those for subsonic aircraft, engines for supersonic aircraft present unique challenges in terms of their fuel consumption, noise, and emissions impacts because of their unique operating conditions. The propulsion systems currently proposed by the industry are developed around the core (high-pressure compressor, combustor, and high-pressure turbine) of existing subsonic engines, with modifications to the low-pressure spool (fan and low-pressure turbine).

ASCENT Project 47 aims to evaluate the design space of "clean-sheet" engines designed specifically for use on civil supersonic aircraft, and to determine the resulting environmental performance of such engines. Unlike previous commercial supersonic engines, which were adapted from military aircraft, or planned propulsions systems derived from current commercial engines, a clean-sheet engine takes advantage of recent advances in propulsion system technology to significantly improve performance and reduce emissions and noise footprints. This project will quantify these benefits for a range of engine designs relevant to currently proposed civil supersonic aircraft.

Specific goals of this research include:

- Development of a framework for quantifying the noise and emissions footprints of propulsion systems used on civil supersonic aircraft
- Assessment of the difference in environmental footprint between a derived engine and a clean-sheet engine for a civil supersonic aircraft
- Development of a roadmap for technology development, focusing on reducing the environmental footprint associated with engines for civil supersonic aircraft

A summary of accomplishments to date include the following:

- A survey of supersonic transport concepts and existing designs was carried out, and the Stanford University Aerospace Vehicle Environment (SUAVE) was selected to analyze mission profiles and derive propulsion system requirements.
- Multiple engine models were developed in the NPSS tool. The baseline engine chosen for the derivative engine analysis was the CFM56-5B engine.
- A reactor network framework was developed to estimate NO_x emissions. The model was calibrated to the International Civil Aviation Organization (ICAO) data for the CFM56-5B3 engine.
- A framework was set up to estimate the noise footprint (sound pressure level, SPL) of the engine given the relevant engine parameters using a semi-empirical model.

Task 1 - Identify Mission Profiles And Operating Requirements For Propulsion Systems

Massachusetts Institute of Technology

Objective(s)

The first objective of this task is to identify representative mission profiles of commercial supersonic transport aircraft (i.e., characterize stages of the mission by defining parameters such as climb rates and accelerations). A second objective is to use these mission profiles and representative aircraft parameters (e.g., wing area, drag and lift polars) of civil supersonic aircraft operating in different Mach regimes to derive propulsion system requirements for supersonic aircraft.

Research Approach

Survey of the design space

In Figure 1, we present a set of supersonic transport aircraft concepts and existing designs with their respective range and cruise Mach number.

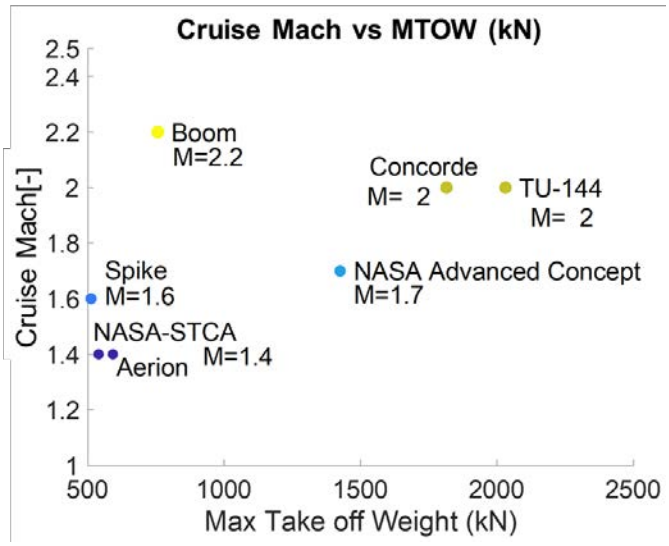

Figure 1. Range versus maximum take-off weight for civil supersonic transport aircraft concepts and existing designs.

Figure 1 shows the variability of different concepts and designs for supersonic transport. The only existing designs are the Anglo-French Concorde and the Russian Tupolev TU-144 in the Mach 2 regime. However, upcoming companies looking to bring supersonic transport back to the market are developing aircraft in different Mach regimes, including low-supersonic (M~1.4), mid-supersonic (M~1.6), and high-supersonic (M~2), and in different weight classes: small business jets and larger airliners.

Mission profiles

The only existing supersonic transport aircraft were the Concorde and Tupolev TU-144. Morisset (1974) compared their performance and shows their mission profiles. A typical mission profile of Concorde is shown in Figure 2. This mission profile is chosen as a case to test the tool to derive propulsion system requirements for a supersonic transport aircraft. The mission profile is modeled in SUAVE (MacDonald et al., 2015). A comparison of the mission profiles can be seen in Figure 2. The descent profile in SUAVE is modeled as a single mission stage because it is assumed that the propulsion requirements during descent will not be critical.

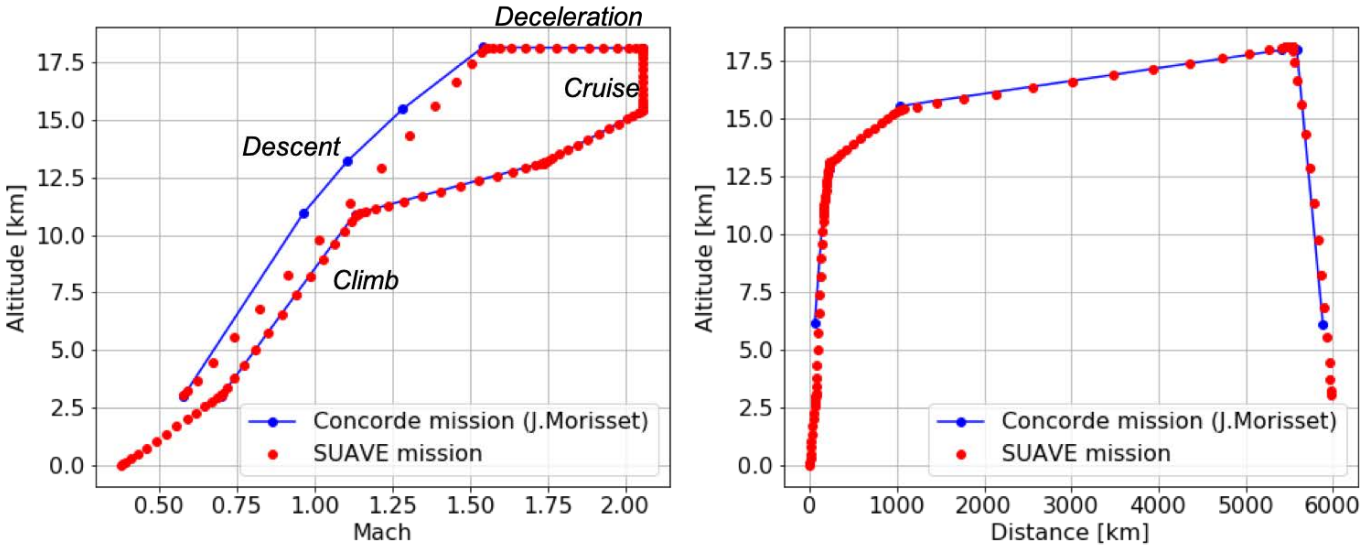

Figure 2. Typical mission profile of Concorde.

Propulsion system requirements

The SUAVE tool is used to estimate propulsion system requirements for the Concorde aircraft based on the Concorde flight reports (Morisset, 1974). The standard aircraft parameters and aerodynamic coefficients of the Concorde aircraft from the SUAVE tool are used. The propulsion system requirements (i.e., thrust) of the Concorde mission are given in the top graph of Figure 3. The variation in the drag coefficient of the aircraft during the mission is given in the bottom graph of Figure 3. The discontinuities in the thrust profile come from jumps in climb rates and in acceleration rates. In Figure 3, the drag coefficient can be seen to sharply increase when crossing the sound barrier. From the thrust profile, the most critical points in the mission can be identified. The engine will need to be able to generate the specified thrust at these points. Therefore, the thrust at these critical points will be a direct input in Task 2 when developing the engine cycle model.

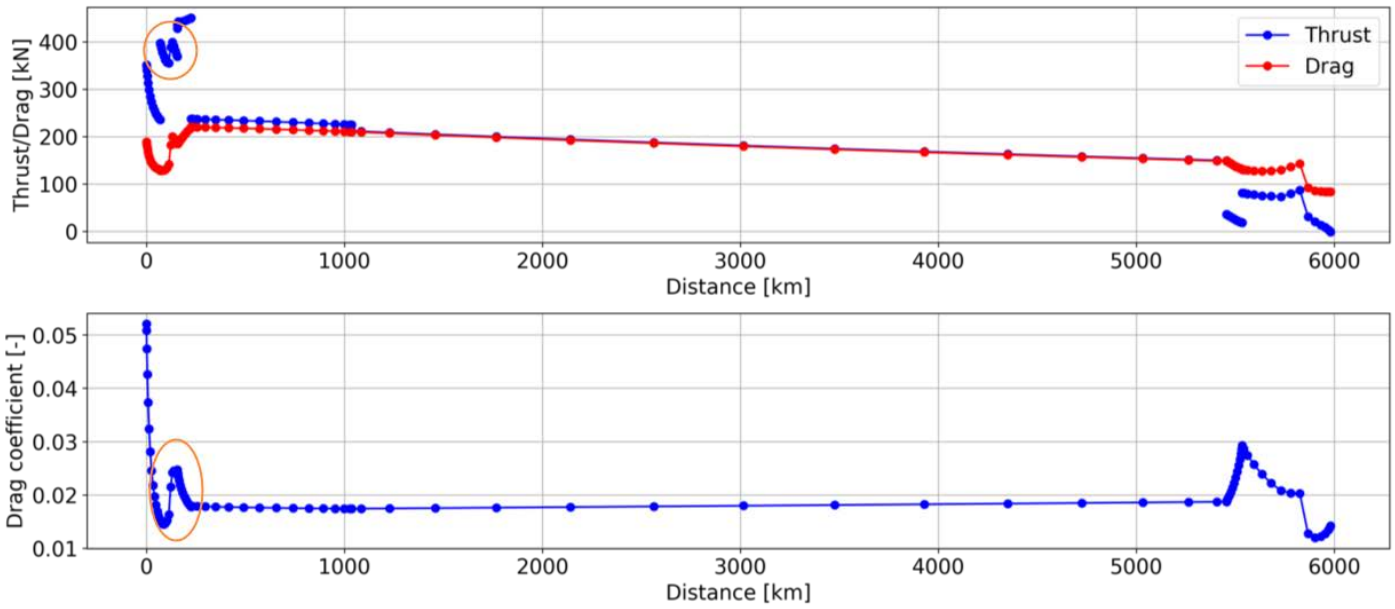

Figure 3. Propulsion system requirements (i.e., thrust and drag) and drag coefficient throughout the mission given in Figure 2. The circled areas indicate the transonic acceleration.

NASA 55-tonne STCA

NASA has designed a 55-tonne Supersonic Transport Concept Aircraft (STCA) with a cruise Mach number of 1.4 (Berton & Geiselhart, 2019). The aircraft configuration of the STCA will be used in future work to derive propulsion system requirements for a small business jet in the low-supersonic Mach regime.

Milestone(s)

A review of the supersonic transport concepts and existing designs was conducted, and the appropriate tools to derive propulsion system requirements for a supersonic transport aircraft flying a specific mission were identified.

Major Accomplishments

Literature review

A survey of supersonic transport concepts and existing designs was conducted. Upcoming players in the supersonic transport market are developing aircraft in different Mach regimes (i.e., low-, mid-, and high-supersonic regimes) and weight classes (i.e., business jet and airliner).

Framework

SUAVE was selected to derive propulsion system requirements for a supersonic aircraft flying a specific mission profile.

Publications
N/A

Outreach Efforts
Our team contacted Boom Supersonic on October 15, 2018, to discuss representative mission profiles and aircraft parameters.

Prof. Steven Barrett gave a presentation titled "Clean-sheet supersonic engine design and performance" at the ASCENT meeting in Atlanta, GA, on April 19, 2019.

Dr. Jayant Sabnis gave a presentation titled "Clean-sheet supersonic engine design and performance" at the ASCENT meeting in Alexandria, VA, on October 22, 2019.

Awards
None.

Student Involvement
This task was conducted primarily by Laurens Voet, a graduate research assistant working under the supervision of Dr. Jayant Sabnis, Dr. Raymond Speth, and Dr. Choon Tan.

Plans for Next Period
1. Apply the framework to derive propulsion system requirements to the NASA 55-tonne STCA (expected completion: February 2020)
2. Define the critical operating point at which the engines are sized for different missions of supersonic transport aircraft (expected completion: April 2020)

References
Berton, J. & Geiselhart, K. (2019). NASA 55 tonne Supersonic Transport Concept Aeroplane (STCA) release package. NASA GRC/NASA LaRC

Lukaczyk, T., Wendorff, A.D., Botero, E., MacDonald, T., Momose, T., Variyar, A., Vegh, M.J., Colonno, M., Economon, T.D., Alonso, J.J., Orra, T.H., and da Silva, C.I. (2015). SUAVE: An open-source environment for multi-fidelity conceptual vehicle design. AIAA Multidisciplinary Analysis and Optimization Conference. AIAA-2015-3087

Morisset, J. (1974). Tupolev 144 and Concorde – The official performances are compared for the first time. NASA Technical Translation TT F15,446.

Task 2 - Develop An Engine Cycle Model For A Supersonic Aircraft Propulsion System
Massachusetts Institute of Technology

Objective
The objective of this task was to develop an engine cycle deck to analyze clean-sheet and derivative propulsion systems for commercial supersonic aircraft.

Research Approach
The NPSS tool is chosen to develop the engine cycle decks for clean-sheet and derivative engines, because it is an industry standard tool that facilitates future collaboration with other users of the tool.

Baseline engine
To develop the derivative engine, a baseline engine is first chosen and modeled. The CFM56-5B engine was chosen for this task because it is the donor engine for the proposed GE Affinity engine. The baseline engine was modeled using published data from Jane's Aero Engines (Gunston, 1996) and data published in the Emissions Databank (EDB) by the European Union Aviation Safety Agency (EASA) (EASA, 2019). The data published by EASA consists of fuel flow and emission indices of several

species at take-off, climb, idle, and approach conditions of various thrust variants of the CFM56-5B engine. The EDB data can be processed based on the serial number of the tested engines to relate multiple entries in the databank to a common engine, as shown in Figure 4.

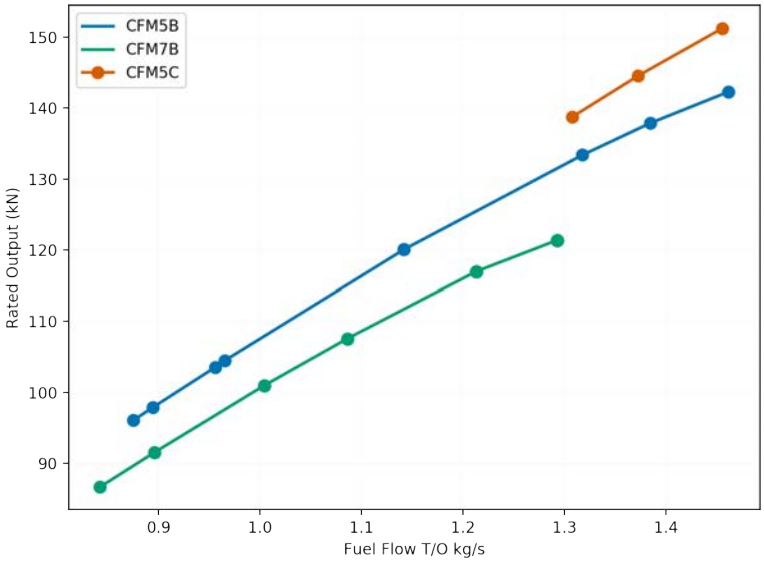

Figure 4. Variants of the CFM56 engine; the CFM56-5B TechInsertion engine is chosen for the baseline engine.

The engine model (see schematic below) consists of an inlet, fan, low-pressure compressor (LPC), high-pressure compressor (HPC), combustor, high-pressure turbine (HPT), low-pressure turbine (LPT), and nozzles for the bypass and core ducts.

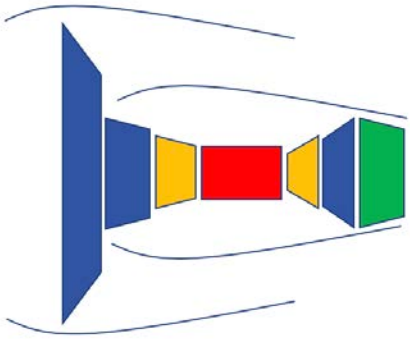

Figure 5. Schematic of the unmixed-turbofan model of the CFM56-5B, showing the low-pressure spool (blue), the high-pressure spool (yellow), combustor (red), and nozzle (yellow).

Component parameters such as efficiencies, pressure ratios, and bleed flows for the engine model were varied at a chosen design point. The point chosen for this was the sea-level static thrust of the highest thrust variant of the engine. Subsequent off-design runs were carried out to evaluate whether the model matched the published data on fuel flow at particular thrust levels.

Furthermore, the CFM56-5B and CFM56-7B engines share the same physical core. This information is used to validate the model representing the core specifically by using the core model calibrated to the CFM56-5B data to represent the CFM56-7B engine, by fixing the core components and varying only the low-spool components.

Derivative engine
The core from the baseline engine is adopted along with a new low spool to meet the take-off thrust requirements of the NASA STCA aircraft. The common core is represented by holding the high-spool component map scaling factors and HPT bleed fractions constant at the CFM56-5B values. The LPC is removed from the CFM56-5B model and a mixer and the convergent nozzle is replaced with a convergent-divergent nozzle.

Work on sizing the derivative engine for the NASA-STCA aircraft is currently ongoing.

Clean-sheet engine
A clean-sheet engine with a new core is modeled by allowing the HPC, combustor, and HPT to be sized at the design point. That is, the high-spool component map scaling factors and the HPT cooling flows are allowed to vary (in contrast to the derivative engine scenario). The design space of the engine therefore grows in the clean-sheet scenario.

Work on sizing the clean-sheet engine for the NASA-STCA aircraft is currently ongoing.

Milestone(s)
Multiple engines were developed in NPSS. The baseline engine modeled was the CFM56-5B engine, and the core from this engine was used to model the CFM56-7B engine. Work on the supersonic derivative engine and clean-sheet engine models developed are ongoing.

Major Accomplishments
Publicly published data are used to build a CFM56-5B3 model in NPSS and calibrate it at sea-level static conditions as shown in Figure 6.

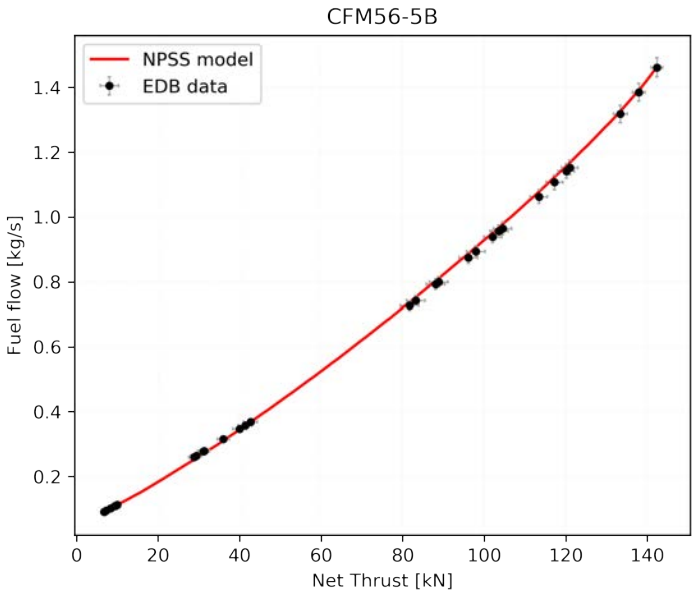

Figure 6. Off-design comparison of the Numerical Propulsion System Simulation (NPSS) model and International Civil Aviation Organization (ICAO) data from the Emissions Databank (EDB) for the CFM56-5B.

The model is compared with the data available in the EDB maintained by EASA on behalf of ICAO. The average root mean square (RMS) error for all the landing and take-off (LTO) data points is approximately 2%, suggesting a successful calibration.

The same core is used in a CFM56-7B engine and compared with EDB data as shown in Figure 7. The average RMS error was approximately 3% in this case (Figure 7).

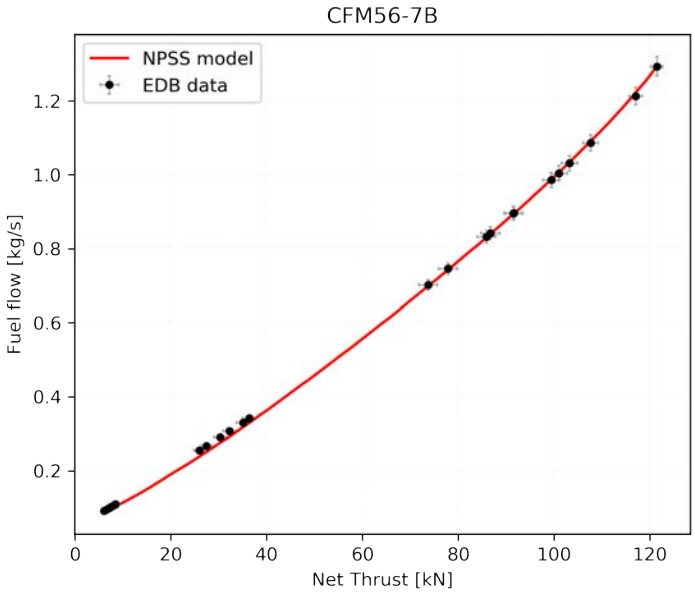

Figure 7. Off-design comparison of the Numerical Propulsion System Simulation (NPSS) model and International Civil Aviation Organization (ICAO) data from the Emissions Databank (EDB) for the CFM56-7B using the common core.

An analysis of a derivative engine based on this core was started and work is currently ongoing. Simultaneously, a model of a clean-sheet engine is being developed.

Publications
N/A

Outreach Efforts
Dr. Jayant Sabnis gave a presentation titled "Noise and emission characteristics of commercial supersonic aircraft propulsion systems" at the Aviation Noise and Emissions Symposium on March 5, 2019.

Awards
None.

Student Involvement
This task was conducted primarily by Prashanth Prakash, a graduate research assistant working under the supervision of Dr. Jayant Sabnis, Dr. Raymond Speth, and Dr. Choon Tan.

Plans for Next Period
Various degrees of derivative engine models are to be developed, ranging from an "off-the-shelf" repurposing of an entire engine to using only the core of an existing engine (expected completion: May 2020).

A clean-sheet approach that ranges from redesigning a core with existing technology (e.g., metallurgy, cooling technology) to using new technology (e.g., advanced materials) and adaptive cycles to meet contrasting requirements at supersonic cruise and sea-level take-off (expected completion: December 2020).

References
EASA (2019). ICAO Aircraft Engine Emissions Databank, version 26A. Online: https://www.easa.europa.eu/easa-and-you/environment/icao-aircraft-engine-emissions-databank

Gunston, B. (1996). Jane's aero-engines. Jane's Information Group, Print.

Task 3 - Assess Environmental Footprint Of An Engine For A Supersonic Transport Aircraft

Massachusetts Institute of Technology

Objective

The objective of this task is to develop models to assess the environmental footprint of a supersonic transport aircraft. Models for both the noise footprint and the emissions footprint will be developed.

Research Approach

Emissions modeling

The outline of our approach to modeling the emissions from the engines designed is shown in Figure 8. The aircraft configuration and mission profile determine the propulsion system requirements that need to be met. Once the engine is sized based on these requirements, temperatures and pressures in the flow path can be determined. The temperature and pressure at the inlet to the combustor (T_3, P_3) along with the mass flow rate of the fuel and air are used in a combustor model to estimate the emissions of NO_x. The emissions of NO_x are particularly sensitive to the inlet temperature and residence time in the combustor.

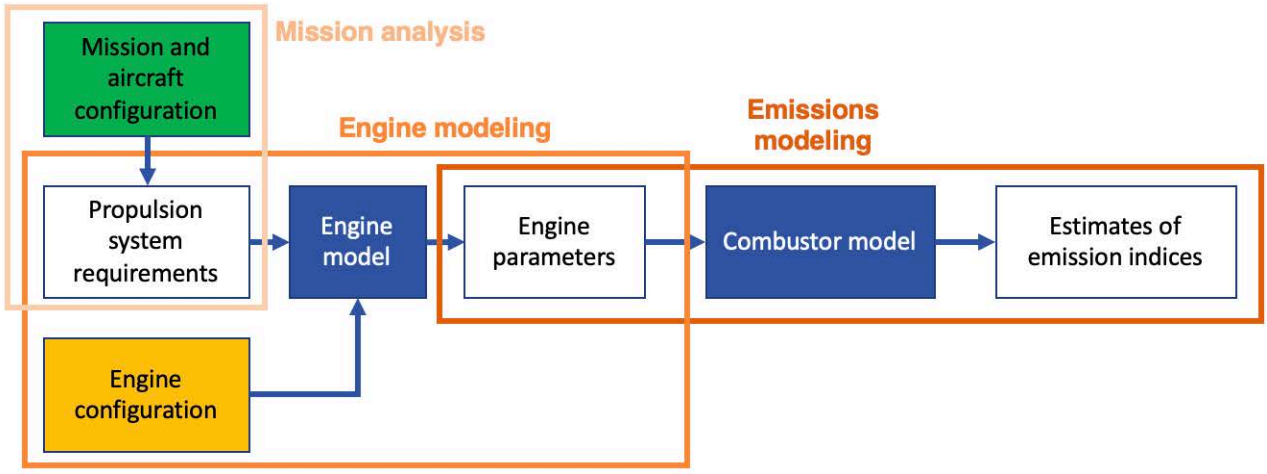

Figure 8. Overview of the emissions modeling framework.

The following values are calculated using the NPSS engine model at the combustor inlet:

- Air mass flow rate
- Fuel mass flow rate
- Temperature
- Pressure

These values are used in a reactor network model as shown in Figure 9.

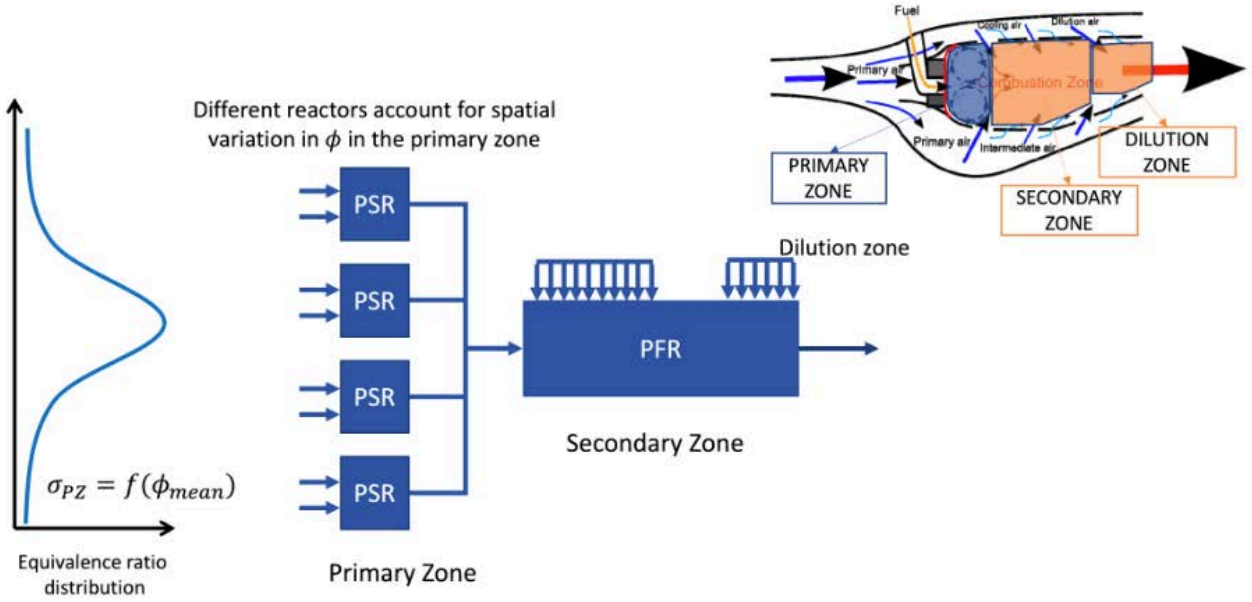

Figure 9. Schematic of the reactor network model to estimate emissions from the combustor. PSR, perfectly stirred reactors; PFR, plug flow reactor; PZ, primary zone; σ, standard deviation; ϕ, equivalence ratio.

The reactor network model consists of an interconnected network of perfectly stirred reactors (PSR) to represent the primary zone and plug flow reactors (PFR) to represent the secondary and dilution zones. The reactor net model is implemented using the Cantera package (Goodwin et al., 2018) in Python. The model parameters are calibrated to the emissions data published in the EDB.

Noise footprint

A flow chart for the noise footprint assessment is given in Figure 10.

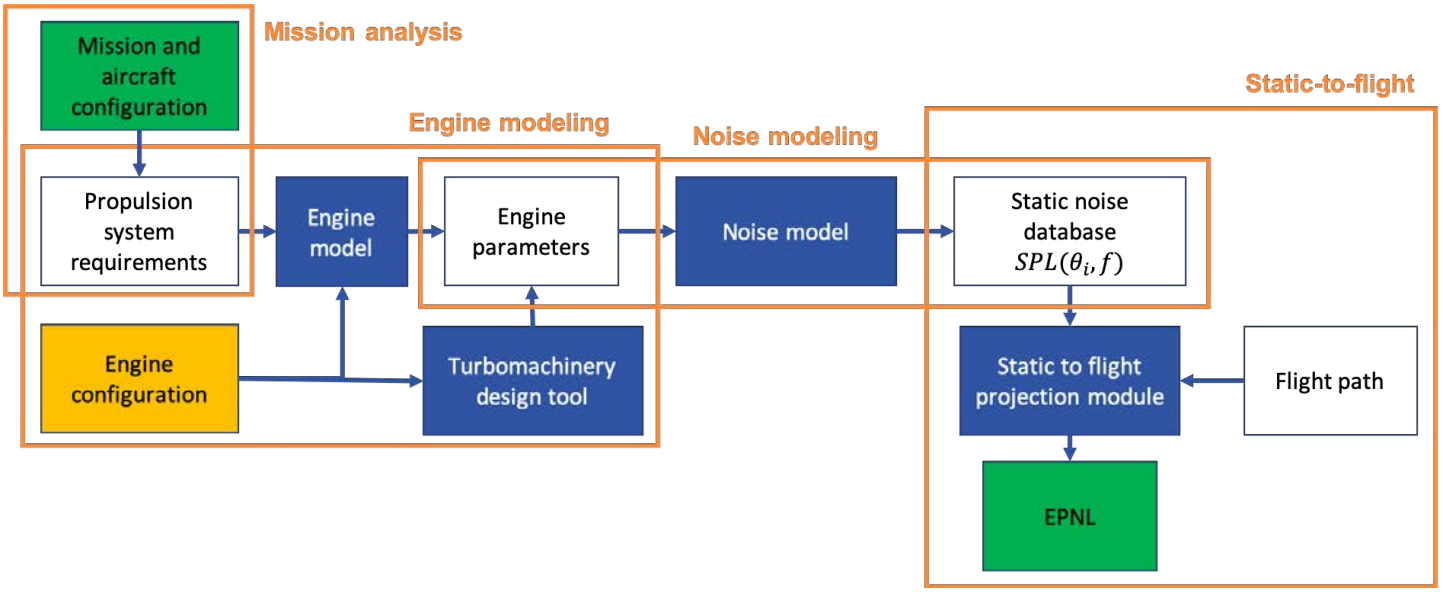

Figure 10. Overview of noise footprint assessment. SPL, sound pressure level; EPNL, effective perceived noise level.

The driving parameter used in the noise certification of aircraft is the EPNL, as defined by ICAO in Annex 16 Environmental Protection Volume I Aircraft Noise (ICAO, 2008). As can be seen from Figure 10, four modules need to be developed to define the link between an aircraft configuration flying a given mission and the resulting EPNL during landing and take-off.

As can be seen in Figure 10, the first module is the mission analysis tool. The objective of the mission analysis tool is to derive the propulsion system requirements for an aircraft configuration flying a specific mission. The mission analysis tool is described in Task 1.

Second, an engine modeling tool has to be developed. The objective of the engine modeling tool is to define the link between the propulsion system requirements and the engine parameters relevant for the noise model. The relevant engine parameters are both thermodynamic (e.g., temperatures, pressures, mass flow rates inside the engine) and geometric (e.g., fan diameter, turbomachinery rotor-stator spacing). The thermodynamic parameters are determined using the NPSS engine cycle deck, as described in Task 2. The geometric parameters are determined using a preliminary turbomachinery design tool. The engine modeling tool depends primarily on a specific engine configuration (e.g., a derived engine, a clean-sheet engine).

Third, a noise modeling tool needs to be developed. The objective of the noise modeling tool is to define the link between relevant engine parameters and a static noise database (i.e., SPL as a function of frequency, polar and azimuthal projection angle). The static noise database is generated by addressing by estimating the SPL from two main different noise sources: the airframe and the engine noise source. Although this work focuses on the engine noise footprint, the airframe will be important when effects such as shielding are considered. The engine noise source is divided into several modules, based on the different components in the engine. The following noise modules are developed, based on the Aircraft Noise Prediction Program (ANOPP) theoretical manual (Zorumski, 1981):

- Jet noise module based on the SAE ARP876 method (Society of Automotive Engineers, 1978)
- Jet noise module based on the Stone method (Stone, 1974; Stone & Montegani, 1980)
- Fan noise module based on the Heidmann method (Heidmann, 1975)
- Turbine noise module based on a method developed by GE (Matta et al., 1977)
- Airframe noise module based on the Fink method (Fink, 1977)

As an example, Figure 11 shows the directivity of the overall SPL and the spectral distribution of the jet mixing SPL using the SAE ARP876 module. The input parameters for the jet mixing noise module are given in Table 1 and are taken from the STCA

Release Package Noise Assessment at t = 0.0 s. The outputs of the model are compared with the outputs of the STCA Release Package in Figure 11.

Table 1. Parameters of the jet mixing noise module.

Variable	Value	Variable	Value
Ambient speed of sound c_O	346.16 m/s	Jet density $\rho^*_{jet} = \rho_{jet} / \rho_0$	0.68421
Ambient density ρ_0	1.183 kg/m³	Jet velocity $V^*_{jet} = V_{jet} / c_0$	1.1859
Number of engines N_e	1	Jet total temperature $T^*_{jet} = T_{jet} / T_0$	1.7352
Flight Mach number M_0	0	Jet area $A^*_{jet} = A_{jet} / A_{ref}$	0.60647
Distance between source and pseudo-observer r_S	0.311 m		
Engine reference area A_e	0.96 m²		

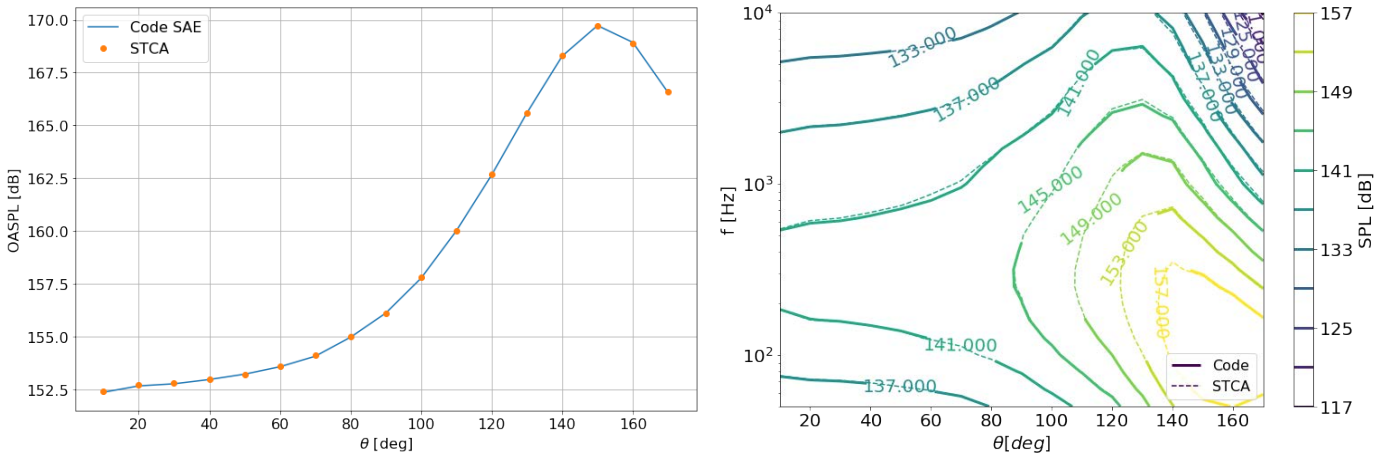

Figure 11. Directivity of overall sound pressure level (OASPL) of the SAE ARP 876 jet mixing module (left), and spectral distribution of the SPL of the SAE ARP 876 jet mixing module (right).

Finally, a static-to-flight projection tool needs to be developed. The objective of the static-to-flight projection tool is to derive the EPNL from the static noise database. A standard take-off procedure, as defined under ICAO Annex 16 (1) Section 3.6.2., and a standard approach procedure, as defined under ICAO Annex 16 (1) Section 3.6.3, will be used to calculate the EPNL. The take-off procedure is given in Figure 12. The static-to-flight projection tool has not been developed yet.

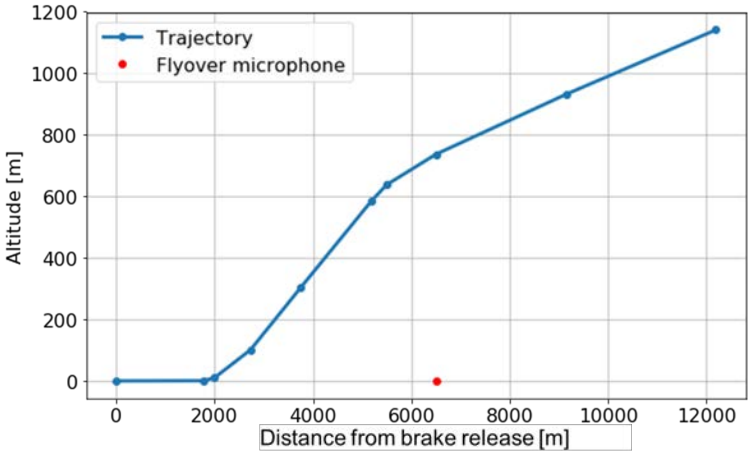

Figure 12. Standard take-off trajectory of the 55-tonne STCA used in the static-to-flight projection. The flyover microphone is indicated at 6500 m after brake release.

Milestone(s)

A model deriving the static noise database from relevant engine parameters was set up. A reactor network–based model was developed and NO_x emissions were calibrated to the EDB data using combustor inlet values obtained from the NPSS model of the CFM56-5B engine.

Major Accomplishments

Emissions model

A framework was developed to estimate the NO_x footprint (emissions index) of the baseline engine, given the relevant engine parameters using a reactor network model. A comparison of the model developed and the EDB data is shown in Figure 13.

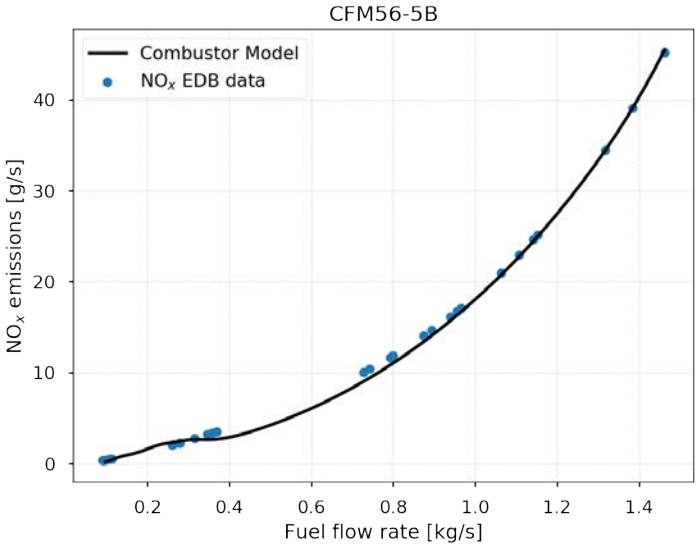

Figure 13. Comparison of NO_x emissions [g/s] at different fuel flows between the combustor model and International Civil Aviation Organization (ICAO) data from the Emissions Databank (EDB).

Noise model

A framework was set up to estimate the noise footprint (SPL) of the engine given the relevant engine parameters using a semi-empirical model.

Publications
N/A

Outreach Efforts
Dr. Jayant Sabnis gave a presentation titled "Noise and emission characteristics of commercial supersonic aircraft propulsion systems" at the Aviation Noise and Emissions Symposium on March 5, 2019.

Prof. Steven Barrett gave a presentation titled "Clean-sheet supersonic engine design and performance" at the ASCENT meeting in Atlanta, GA, on April 19, 2019.

Dr. Jayant Sabnis gave a presentation titled "Clean-sheet supersonic engine design and performance" at the ASCENT meeting in Alexandria, VA, on October 22, 2019.

Awards
None.

Student Involvement
This task was conducted primarily by Prashanth Prakash and Laurens Voet, graduate research assistants working under the supervision of Dr. Jayant Sabnis, Dr. Raymond Speth, and Dr. Choon Tan.

Plans for Next Period
Emission footprint
- Continue work on the combustor model for rich-quench-lean (RQL) and staged combustors
- Continue modeling other emissions species such as CO and soot
- Calibrate combustor models to data available on existing engines
- Expected completion: May 2020

Noise footprint
- Continue the framework development to derive the noise footprint from relevant engine parameters (expected completion: March 2020)
- Start developing a preliminary turbomachinery design tool to derive relevant geometrical engine parameters for an engine configuration (expected completion: August 2020)

References
Fink, M. (1977). Airframe noise prediction method. FAA-RD-77-29

Goodwin, D.G., Speth, R.L., Moffat, H.K., & Weber, B.W. (2018). Cantera: An object-oriented software toolkit for chemical kinetics, thermodynamics, and transport processes. Version 2.4.0. doi:10.5281/zenodo.1174508

Heidmann, M. (1975). Interim prediction method for fan and compressor source noise. NASA TM X-71763

ICAO (2008). Annex 16 environmental protection volume I: Aircraft noise

Matta, R., Sandusky G., & Doyle, V. (1977). GE core engine noise investigation – Low emission engines. FAA-RD-77-4

Society of Automotive Engineers. (1978). Gas turbine jet exhaust noise prediction. ARP876

Stone, J. (1974). Interim prediction method for jet noise. NASA TM X-71618

Stone, J. & Montegani, F. (1980). An improved prediction method for the noise generated in flight by circular jets. NASA TM-81470

Zorumski, W.E. (1981). Aircraft noise prediction theoretical manual. NASA TM-83199 Parts 1 and 2. Currently maintained at NASA LaRC by the ANOPP team in electronic format and provided upon request

Project 048 Analysis to Support the Development of an Engine nvPM Emissions Standard

Massachusetts Institute of Technology

Project Lead Investigator

Steven Barrett
Associate Professor
Department of Aeronautics & Astronautics
Massachusetts Institute of Technology
77 Massachusetts Ave
Building 33-316
Cambridge, MA 02139
617-452-2550
sbarrett@mit.edu

University Participants

Massachusetts Institute of Technology

- PI(s): Prof. Steven Barrett
- Co-PI: Dr. Raymond Speth
- FAA Award Number: 13-C-AJFE-MIT, Amendment Nos. 027, 036, 045, and 054
- Period of Performance: July 8, 2016 to May 31, 2020 (reporting here with the exception of funding level and cost share only for the period October 1, 2018 to September 30, 2019)
- Tasks:
    1. Cost-benefit analysis of non-volatile particulate matter (nvPM) standard options
    2. SCOPE11 method to predict aircraft engine nvPM emissions
    3. Evaluating the retirement of the smoke number (SN) limit

Project Funding Level

$550,000 FAA funding and $550,000 matching funds. Sources of match are approximately $149,000 from Massachusetts Institute of Technology (MIT), plus third-party, in-kind contributions of $87,000 from University College London, $158,000 from Oliver Wyman Group, and $156,000 from Byogy Renewables Inc.

Investigation Team

- Prof. Steven Barrett (MIT) serves as PI for the A48 project as head of the Laboratory for Aviation and the Environment. Prof. Barrett coordinates internal research efforts and maintains communication between investigators in the various MIT research teams.
- Dr. Raymond Speth (MIT) serves as co-PI for the A48 project. Dr. Speth directly advises student research in the Laboratory for Aviation and the Environment focused on assessment of fuel and propulsion system technologies targeting reduction of aviation's environmental impacts. Dr. Speth also coordinates communication with FAA counterparts.
- Dr. Jayant Sabnis (MIT) serves as co-investigator for the A48 project. Dr. Sabnis co-advises student research in the Laboratory for Aviation and the Environment. His research interests include turbomachinery, propulsion systems, gas turbine engines, and propulsion system–airframe integration.
- Akshat Agarwal (MIT) is a graduate student in the Laboratory for Aviation and the Environment. He is responsible for conducting the cost-benefit analysis of the nvPM emissions standard and developing methods for estimating nvPM emissions based on smoke number measurements.

Project Overview

The FAA's Office of Environment and Energy (FAA-AEE) is working with the international community to establish an international aircraft engine nvPM standard for engines of rated thrust greater than 26.7 kN. The proposed nvPM standard will influence the development of future engine technologies, resulting in reduction of nvPM emissions from aircraft engines. A reduction in nvPM emitted by aircraft engines will lead to improved human health and climate impacts of aviation. To this end, the FAA needs to understand and quantify how an nvPM standard might impact the total nvPM emissions for the National Air Space (NAS) as well as the globe, including overall system-wide environmental and monetary costs and benefits.

The objective of this project is to provide support for FAA decision-making related to the nvPM certification standard by analyzing scenarios involving different emission metrics, policy options, and assumptions about technology and fleet evolution. The analyses being conducted include economic, climate, air quality, and noise impact assessments on both global and NAS-wide bases. Activities executed for this project year focus on identifying and evaluating nvPM metrics and policy options, analyzing and developing methods to correct measurements based on fuel properties and ambient conditions, developing emissions inventories based on estimated technological responses to proposed regulations, and conducting cost-benefit analyses of proposed regulations. This research is also contributing to the understanding of how an nvPM standard may influence future engine development, fleet evolution, and associated fleet-wide nvPM emissions.

Task 1 - Cost-Benefit Analysis of non-volatile Particulate Matter (nvPM) Standard Options

Massachusetts Institute of Technology

Objective(s)

The objectives for this task involve estimating the climate and health impacts of the emissions, and the associated uncertainties, caused by each policy option. Results are shared with FAA project managers.

Research Approach

To calculate and monetize the environmental effects of a policy option, we use the APMT-Impacts Climate model, developed under ASCENT Project 21, and the APMT-Impacts Air Quality tool, developed under ASCENT Project 20. The climate model has been continuously improved upon since Marais et al. (2008), with the latest developments described by Grobler et al. (2019). The model allows rapid estimation of the climate impacts due to aviation and can quantify the associated uncertainty. It has previously been used in the Committee on Aviation Environmental Protection (CAEP)/8, CAEP/9, and CAEP/10 cycles. The air quality model uses a computationally efficient adjoint approach to estimate air quality impacts due to a set of emissions, requiring only multiplication of the pre-computed sensitivities with three-dimensional emissions (latitude × longitude × altitude). In all estimates, we quantify the uncertainty attributable to the concentration response functions that relate a change in concentration to a change in premature mortalities. In addition, for full-flight emissions, we estimate the uncertainty due to ammonia emissions. Finally, high-resolution adjoint sensitivities have also been calculated for certain regions (North America and Asia-Pacific), and we use these sensitivities to estimate regional air quality impacts in addition to the global results. Both the climate and global air quality models are able not only to compute the physical impacts (temperature change and premature mortalities, respectively), but also to monetize these impacts for use in a cost-benefit analysis. This aggregate global environmental impact can be combined with estimates of the industry costs to give a net cost-benefit result. If the benefits are greater than the costs, then the regulation is cost-beneficial and vice versa if the costs outweigh the benefits.

To use the climate and air quality tools, the effect of each policy option on emissions is estimated using the Aviation Environmental Design Tool (AEDT). Twelve policy options were modeled, and each option was considered with and without trade-offs with other emissions species (e.g., reducing nvPM could increase NO_x emissions). The change in full-flight nvPM mass and nvPM number emissions relative to baseline business-as-usual emissions for a 2024 policy implementation date are shown in Figure 1. Policy options 7, 8, and 9 are indistinguishable, as are options 10, 11, and 12, so each set is grouped together for the remainder of this section. As expected, nvPM mass emissions decrease for all policy options, with the reduction ranging between 1.5% and 44.8% in 2032 and 1.0% and 74.0% in 2042. Similarly, nvPM number emissions decrease by between 0.35% and 20.9% in 2032 and between 0.32% and 41.6% in 2042. The change in emissions tends to increase over time as engines that meet the standard replace those in the baseline. In addition, the percentage reduction in nvPM mass is consistently greater than the reduction in nvPM number.

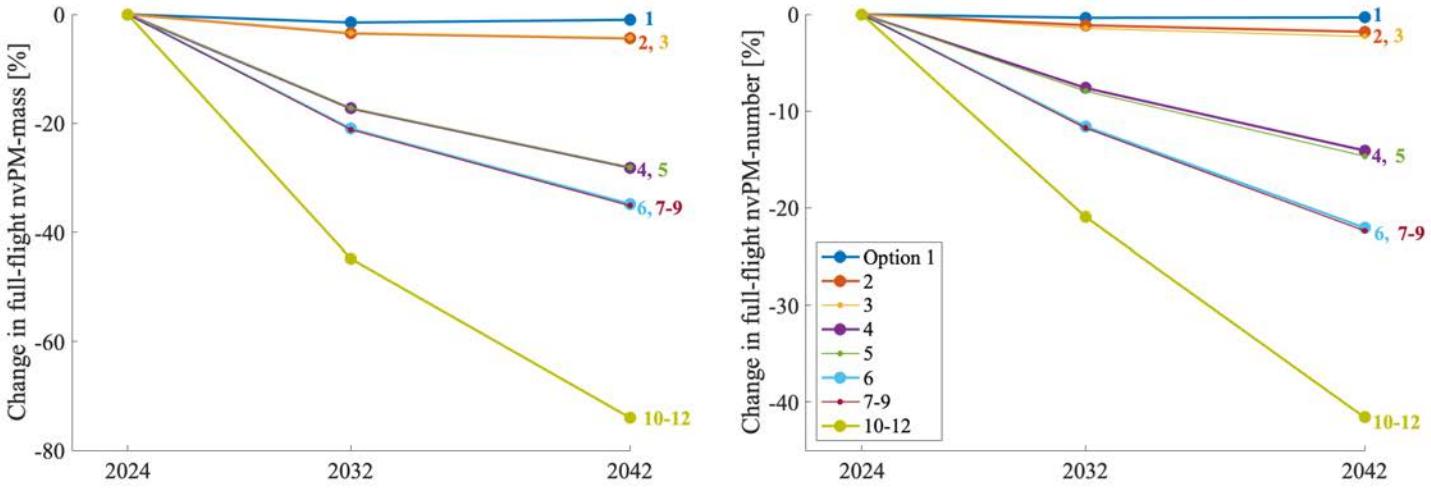

Figure 1. Percentage change in non-volatile particulate matter (nvPM) mass (left) and nvPM number (right) emissions relative to the baseline business-as-usual scenario for full-flight aviation activity, assuming a 2024 implementation date.

Figure 2 uses full-flight emissions to estimate the monetized impact of each policy option when using scenarios with no trade-offs. The air quality model has also been used to estimate monetized health impacts for landing and take-off (LTO) emissions; however, these results are not presented below. In policy options 1 through 9, the climate damages outweigh the air quality health impacts. In addition, industry costs outweigh the combined environmental benefits, leading to a net societal cost. The reverse is true for policy options 10–12, where the air quality impacts outweigh the industry costs, leading to a net societal benefit. Given the large required reduction in nvPM emissions to pass these policy options, certain engines are assumed unable to respond. These engines are substituted with others that have lower NO_x emissions, leading to a reduction in air quality emissions and thus a net societal benefit. Results for scenarios with trade-offs were also considered in this task.

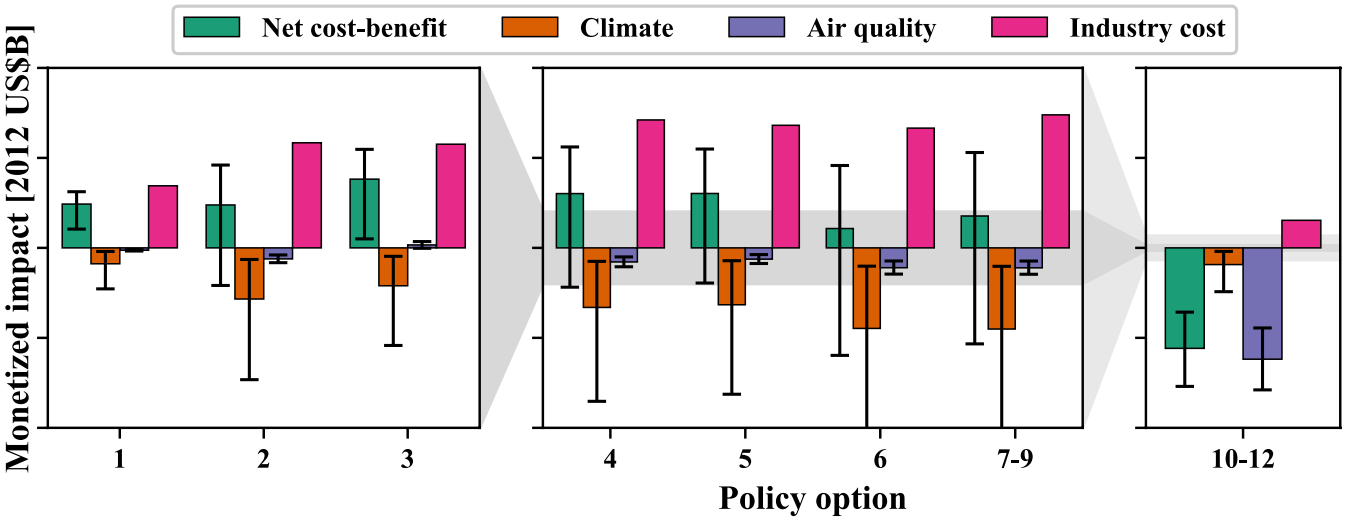

Figure 2. Cost-benefit analysis for the "no trade-offs" scenario using full-flight emissions for air quality impacts. The left panel, showing policy options 1–3, uses a zoomed-in scale equivalent to the gray shaded area of the middle panel. Likewise, the middle panel, showing policy options 4–9, uses a zoomed-in scale equivalent to the gray shaded area of the right panel. Analysis was conducted using the mid environmental lens and a 3% discount rate.

Milestone
The completed cost-benefit analysis was presented to the FAA in a detailed report and presentation in order to inform decision-making related to the CAEP/11 standard.

Major Accomplishments
This work has been completed and the results shared in a series of presentations to FAA-AEE. A detailed report on the results was written and shared with the FAA as well.

Publications
N/A

Outreach Efforts
Our results have been communicated to the FAA in a detailed report and presentation.

Awards
None.

Student Involvement
Graduate student Akshat Agarwal used the APMT-Impacts component models to evaluate climate and air quality costs for each policy option, and developed visualizations to help decision-makers understand the results of the cost-benefit analysis.

Plans for Next Period
N/A

References
Grobler, C., Wolfe, P.J., Dasadhikari, K., Dedoussi, I.C., Allroggen, F., Speth, R.L., Eastham, S.D., Agarwal, A., Staples, M.D., Sabnis, J., & Barrett, S.R.H. (2019). Marginal climate and air quality costs of aviation emissions. Environmental Research Letters 14 (11): 114031. https://doi.org/10.1088/1748-9326/ab4942

Marais, K., Lukachko, S.P., Jun, M., Mahashabde, A., & Waitz, I.A. (2008). Assessing the impact of aviation on climate. Meteorologische Zeitschrift 17 (2): 157–72. https://doi.org/10.1127/0941-2948/2008/0274

Task 2 - SCOPE11 Method To Predict Aircraft Engine nvPM Emissions
Massachusetts Institute of Technology

Objective
The objective for this task was to develop an approach to estimate aircraft engine nvPM-mass and particle number emissions using SN measurements.

Research Approach
The SN has been found to be correlated with nvPM mass concentration over a range of SN values (Stettler et al., 2013; Wayson et al., 2009); however, these approaches either used measurements not taken at the same time and with the same engine or used non-aircraft engine sources of nvPM emissions. In addition, they did not develop approaches to estimate nvPM particle number emissions, which is a crucial emission that can affect the climate impact of contrails (Burkhardt et al., 2018). In addition, the systems used to measure nvPM emissions lead to particle losses that can affect the measurements of mass and particle number (AIR6504, 2017). This work focuses on improving the estimates of nvPM mass emissions using an updated aircraft engine emissions dataset, develops an approach to account for particle losses, and finally develops a method to estimate particle number emissions.

To develop each correlation, we use two complementary datasets. Dataset 1 consists of 1,407 paired instrument-measured nvPM mass concentrations and SN measurements. This is used to develop the correlation between SN and mass concentration. The form of the equation, best-fit values, and the 95% confidence intervals are:

$$C_{\mathrm{nvPM},i} = \frac{k_1 e^{k_2 \mathrm{SN}}}{1 + e^{k_3(\mathrm{SN}+k_4)}}$$
$$k_1 = 648.4 \pm 44.9\ \mu\mathrm{g/m^3}$$
$$k_2 = 0.0766 \pm 0.0038$$
$$k_3 = -1.098 \pm 0.120$$
$$k_4 = -3.064 \pm 0.277$$

where k_i are constants to be fitted and $C_{\mathrm{nvPM},i}$ is the instrument-measured nvPM mass concentration. Dataset 2 consists of 264 simultaneous nvPM mass and particle number emissions measurements. These measurements all used the same certification-compliant measurement system as dataset 1 and also included estimates of particle losses. This dataset was used to estimate measurement losses for nvPM mass emissions using the form, best-fit values, and 95% confidence intervals shown below:

$$k_{slm} = \ln\left(\frac{a_1 \cdot C_{\mathrm{nvPM},i}(1+\beta_{\mathrm{mix}}) + a_2}{C_{\mathrm{nvPM},i}(1+\beta_{\mathrm{mix}}) + a_3}\right)$$
$$a_1 = 3.219 \pm 0.135$$
$$a_2 = 312.5 \pm 119.1\ \mu\mathrm{g/m^3}$$
$$a_3 = 42.6 \pm 19.4\ \mu\mathrm{g/m^3}$$

where a_i are constants to be fitted, β_{mix} is the bypass ratio for mixed engines and 1 otherwise, and k_{slm} is the loss correction for nvPM mass emissions. k_{slm} can be used with the instrument-measured mass concentration to estimate the mass concentration at the exit or exhaust plane of the engine ($C_{\mathrm{nvPM},e}$):

$$C_{\mathrm{nvPM},e} = k_{\mathrm{slm}} \cdot C_{\mathrm{nvPM},i}$$

Finally, to estimate particle number emissions, we assumed emissions to be lognormally distributed. Assuming a geometric standard deviation (GSD) of 1.8 and soot density (ρ) of 1,000 $\mathrm{kg/m^3}$, we can estimate particle number emissions ($C_{N,e}$) using the method of Heintzenberg (1994):

$$C_{N,e} = \frac{6 C_{\mathrm{nvPM},e}}{\pi \rho \mathrm{GMD}^3 e^{4.5(\ln \sigma)^2}}$$

In this equation, the only unknown is the GMD, which represents the geometric mean diameter of the nvPM particles. This can be predicted using an estimate of nvPM mass concentration in the combustor ($C_{\mathrm{nvPM},c}$) as shown below:

$$\mathrm{GMD\ [nm]} = a\ {C_{\mathrm{nvPM},c}}^{b}$$
$$a = 5.08 \pm 0.55\ \mathrm{nm}$$
$$b = 0.185 \pm 0.015$$

To estimate $C_{\mathrm{nvPM},c}$, we used basic gas turbine theory to estimate conditions at the combustor exit and used this to scale $C_{\mathrm{nvPM},e}$. The full details of the method can be found in Agarwal et al. (2019).

Starting with certification SN measurements found in the International Civil Aviation Organization (ICAO) Engine Emissions Data Bank (EDB) (EASA, 2017), we can apply each step of the above method to estimate emissions of nvPM mass at the instrument, mass at the exit plane, and particle number at the exit plane. In Figure 3, we show the prediction compared with measurements from dataset 2. The overall R^2 value in each case is ~0.8, but this value tends to be lower for predictions during taxi operations. This is driven by the wide data spread between SN and mass concentration at low SN.

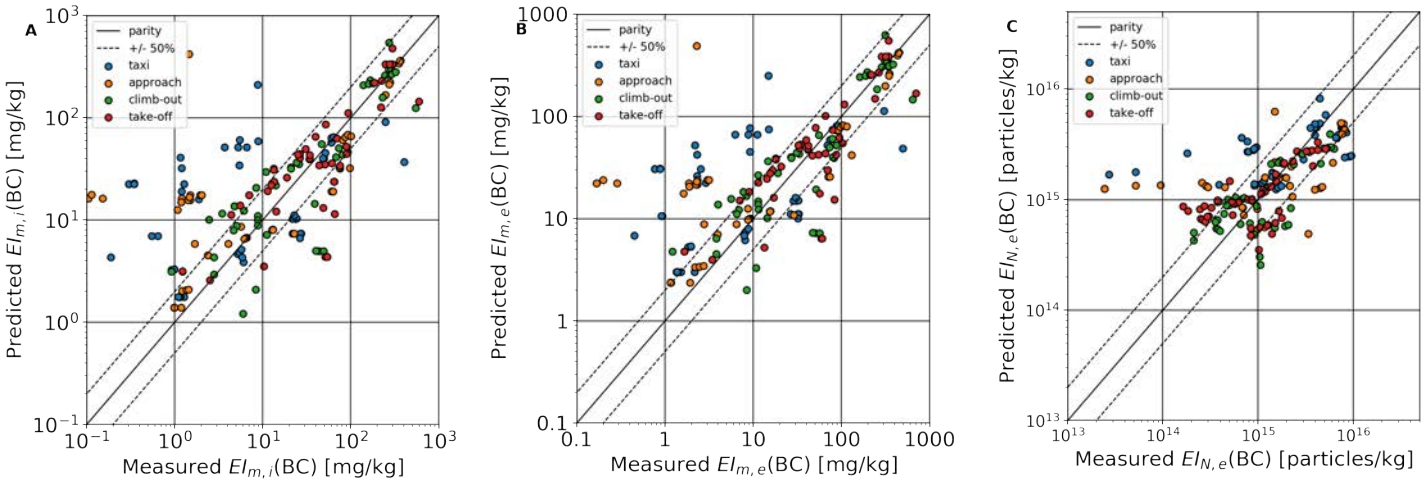

Figure 3. Parity plots of predicted versus measured results for (A) non-volatile particulate matter (nvPM) mass emissions at the instrument, (B) nvPM mass emissions at the exit plane, and (C) nvPM number emissions at the exit plane. $EI_{m,i}(BC)$, black carbon mass emissions index at the instrument; $EI_{m,e}(BC)$, black carbon mass emissions index at the exit plane; $EI_{N,e}(BC)$, black carbon number emissions index at the exit plane.

Milestone
The methods for estimating black carbon mass and number emissions based on smoke number were documented in a white paper which was shared with the FAA and CAEP Working Group 3.

Major Accomplishments
The completion of this work resulted in a peer-reviewed publication in *Environmental Science & Technology* (Agarwal et al., 2019).

Publications
Agarwal, A., Speth, R. L., Fritz, T. M., Jacob, S. D., Rindlisbacher, T., Iovinelli, R., Owen, B., Miake-Lye, R. C., Sabnis, J. S., & Barrett, S. R. H. (2019). SCOPE11 Method for Estimating Aircraft Black Carbon Mass and Particle Number Emissions. Environmental Science & Technology, 53(3), 1364–1373. https://doi.org/10.1021/acs.est.8b04060

Outreach Efforts
Our results were regularly communicated to the FAA and ICAO-CAEP in a detailed report and presentation.

Awards
None.

Student Involvement
Graduate student Akshat Agarwal was responsible for developing the method for estimating particle number emissions based on combustor mass concentration and was the lead author of the paper documenting the method.

Plans for Next Period
N/A

References

Agarwal, A., Speth, R.L., Fritz, T.M., Jacob, S.D., Rindlisbacher, T., Lovinelli, R., Owen, B., Miake-Lye, R.C., Sabnis, J.S., & Barrett, S.R.H. (2019). "SCOPE11 method for estimating aircraft black carbon mass and particle number emissions. Environmental Science & Technology 53 (3): 1364–73. https://doi.org/10.1021/acs.est.8b04060

AIR6504. (2017). Procedure for the calculation of non-volatile particulate matter sampling and measurement system penetration functions and system loss correction factors - SAE aerospace information report 6504 (AIR6504)

Burkhardt, U., Bock, L., & Bier, A. (2018). Mitigating the contrail cirrus climate impact by reducing aircraft soot number emissions. Npj Climate and Atmospheric Science 1 (1): 37. https://doi.org/10.1038/s41612-018-0046-4.

EASA. (2017). ICAO Engine Emissions Databank (EDB) V24

Heintzenberg, J. (1994). Properties of the log-normal particle size distribution. Aerosol Science and Technology 21 (1): 46–48. https://doi.org/10.1080/02786829408959695

Stettler, M.E.J., Swanson, J.J., Barrett, S.R.H., & Boies, A.M. (2013). Updated correlation between aircraft smoke number and black carbon concentration. Aerosol Science and Technology 47 (11): 1205–14 https://doi.org/10.1080/02786826.2013.829908

Wayson, R.L., Fleming, G.G., & Lovinelli, R. (2009). Methodology to estimate particulate matter emissions from certified commercial aircraft engines. Journal of the Air & Waste Management Association 59 (1): 91–100, https://doi.org/10.3155/1047-3289.59.1.91

Task 3 - Evaluating The Retirement of the Smoke Number (SN) Limit

Massachusetts Institute of Technology

Objective

This task aimed to understand the effectiveness of the CAEP/10 maximum mass concentration limit in preventing the visibility of aircraft engines. A limit with this feature would allow regulators to retire the SN limit, which was developed with these goals in mind.

Research Approach

The overall method follows a similar approach to how the SN limit was evaluated (Stockham and Betz, 1971; Champagne, 1971; Munt, 1979). Aerosol optical theory following Bond and Bergstrom (2006) was used to relate the transmissivity of light through black carbon aerosol with the mass concentration, as follows:

$$C_{\mathrm{nvPM,e}} = \frac{\rho_{\mathrm{soot}}\,\lambda \log(1/T)}{K_{\mathrm{e}}\,L}$$

where ρ_{soot} is the soot density, λ is the wavelength of light, T is the transmissivity of light through the soot particles, K_e is the mass-normalized absorption coefficient, and L is the path length of the light through the exhaust plume. A transmissivity of 98% was considered the limit below which the plume becomes visible and was used as the baseline throughout the analysis. As a representation of path length, we used the diameter of the exhaust nozzle, which was estimated using gas turbine theory, following Cumpsty and Heyes (2015). We used rated thrust, overall pressure ratio, bypass ratio, and fuel flow rate values at rated thrust from the EDB and assumed a bypass-to-jet velocity ratio of 0.9 for unmixed turbofan engines. For mixed-flow turbofan engines, this ratio was changed and a matching stagnation pressure at the mixing plane was imposed instead.

Results for turbojets, unmixed turbofans, and mixed-flow turbofans for a range of engines are shown in Figure 4. Engines were chosen to span a wide range of rated thrusts and manufacturers, and the analyses were conducted as if engines are turbojet, unmixed turbofans, or mixed-flow turbofans, respectively. The current CAEP/10 limit is included as well as the same limit if it were not shifted upward by 2 standard deviations. This second line is analogous to the SN limit in mass concentration space. These results show that the SN limit is suitable for turbojet engines, which is the type of engine it was originally developed for. The current CAEP/10 limit seems to be sufficient to prevent the visibility of unmixed turbofan engines; however, neither limit would prevent the visibility of mixed-flow turbofan engines.

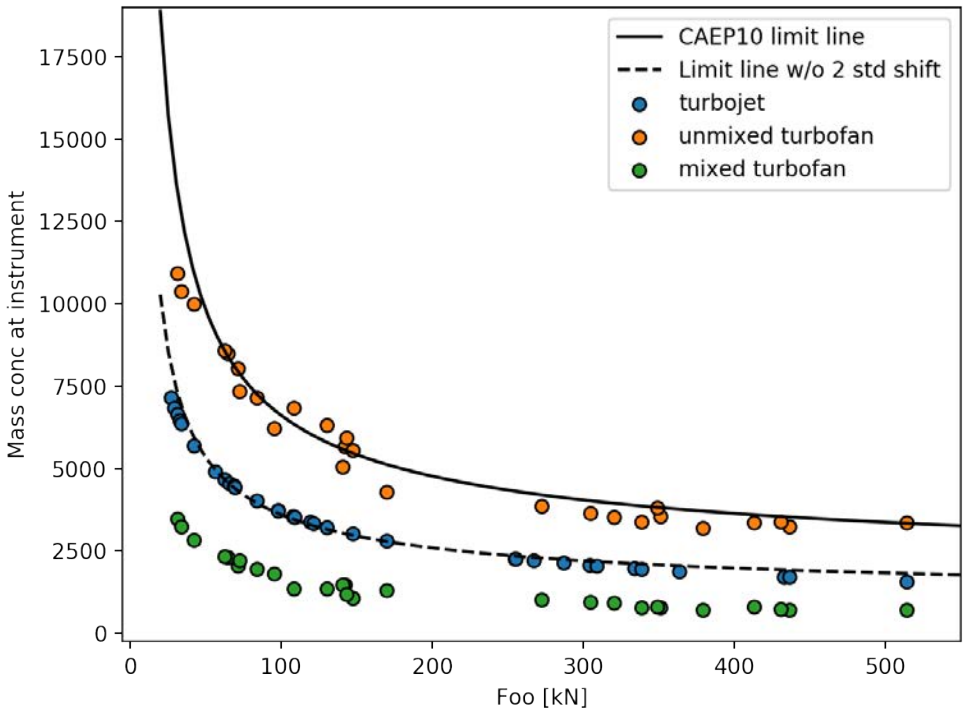

Figure 4. Instrument-measured mass concentration [μg/m^3] versus rated thrust [kN] for turbojet (blue), unmixed turbofans (orange), and mixed-flow turbofans (green) at a transmissivity of 98%. Also shown are the CAEP/10 limit and the limit without a shift of 2 standard deviations (2 std).

Milestone
The analysis of the effectiveness of the SN and CAEP/10 standards at preventing plume visibility was completed.

Major Accomplishments
This work was presented to FAA project managers and ICAO-CAEP members in Working Group 3. In addition, the work culminated with a working paper to the CAEP/11-WG3/10 meeting in Montreal.

Publications
N/A

Outreach Efforts
Our results have been communicated to the FAA and ICAO-CAEP in a detailed report and presentation.

Awards
None.

Student Involvement
Graduate student Akshat Agarwal investigated approaches to estimating plume visibility that have been applied historically and developed an updated analysis based on engine cycle analysis for modern engines.

Plans for Next Period
N/A

References

Bond, T.C. & Bergstrom, R.W. (2006). Light absorption by carbonaceous particles: An investigative review. Aerosol Science and Technology 40 (1): 27–67. https://doi.org/10.1080/02786820500421521

Champagne, D.L. (1971). Standard measurement of aircraft gas turbine engine exhaust smoke. American Society of Mechanical Engineers Digital Collection. https://doi.org/10.1115/71-GT-88

Cumpsty, N. & Heyes, A. (2015). Jet propulsion. Third edition. Cambridge University Press.

Munt, R.W. (1979). Evaluation of aircraft smoke standards for the criterion of invisibility. EPA-AA_SDSB 79-25

Stockham, J. & Betz, H. (1971). Study of visible exhaust smoke from aircraft jet engines. FAA-RD-71-22

Publications Index

Project 001

Twenty-one graduate students and five undergraduate students involved.

Publications

- Impact of co-product selection on techno-economic analyses of alternative jet fuel produced with forest harvest residuals. (2019). In revision, BioFPR
- English, B.C. & Rials, T. (2018). Feedstock viability and potential economic impacts. Paper presented at the CAAFI annual meeting, Washington, D.C.
- Fu. J., Morgan, T., Summers, S., & Turn, S. Fuel properties of Millettia pinnata seeds and pods grown in Hawaii. Draft manuscript
- Galligan, T.R., Staples, M.D., Speth, R.L., & Barrett, S.R.H. Life cycle greenhouse gas emission reduction potential of aviation biofuels in the US. (in preparation)
- Geleynse, S., Jiang, Z., Brandt, K., Garcia-Perez, M., Wolcott, M., & Zhang, X. (2020). Pulp Mill Integration with Alcohol-to-Jet Conversion Technology. Fuel Process Technology, 201, 106338
- Han, Y., Gholizadeh, M., Tran, C.-C., Kaliaguine, S., Li, C.-Z., Olarte, M., & Garcia-Perez, M. (2019). Hydrotreatment of pyrolysis bio-oil: A review. Fuel Processing Technology, 195:106140
- Lewis, K. C., Newest, E. K., Peterson, S. O., Pearlson, M. N., Lawless, E.A., Brandt, K., Camenzind, D. et al. (2019). US alternative jet fuel deployment scenario analyses identifying key drivers and geospatial patterns for the first billion gallons. Biofuels, Bioproducts and Biorefining, 13(3):471-485. doi:10.1002/bbb.1951
- Markel, E., English, B.C., Hellwinckel, C.M., & Menard, J.R. (2019). Potential for Pennycress to support a renewable jet fuel industry. Ecology, Pollution and Environmental Science, SciEnvironm 1:121
- Martinkus, N., Latta, G., Rijkhoff, S.A.M., Mueller, D., Hoard, S., Sasatani, D., Pierobon, F., & Wolcott, M. (2019). A multi-criteria decision support tool for biorefinery siting: Using economic, environmental, and social metrics for a refined siting analysis, Biomass and Bioenergy, 128, 105330
- Morgan, T.M., Youkhana, A., Ogoshi, R., Turn, S., & Garcia-Perez, M. (2019). Review of biomass resources and conversion technologies for alternative jet fuel production in Hawai'i and tropical regions. Energy & Fuels, 2699-2762
- Pires, A.P.P., Arauzo, J., Fonts, I., Domine, M.E., Fernanzed, Arroyo, A., Garcia-Perez, M.E., Montoya, J., Chejne, F., Pfromm, P., & Garcia-Perez, M. (2019). Challenges and opportunities for bio-oil refining: A review. Energy & Fuels, 33(6):4683-4720
- Sharma, B. P., Yu, T.E., English, B.C., Boyer, C., & Larson, J.A. (2019). Impact of government subsidies on a cellulosic biofuel sector with diverse risk preferences toward feedstock uncertainty. (In review). Submitted to Energy Policy
- Sharma, B. P., Yu, T.E., English, B.C., Boyer, C., & Larson, J.A. (2019). Stochastic optimization of cellulosic biofuel supply chain under feedstock yield uncertainty. Energy Procedia, 158: 1009-1014
- Stevens et al. A stochastic techno-economic analysis of aviation biofuel production from pennycress seed oil. Under development.
- Stevens et al. Policy recommendations to expand production of aviation biofuels: Lessons from a techno economic analysis. Under development.
- Taheripour, F., Zhao, X., Horridge, M., Farrokhi, F., & Tyner, W. Modeling Land Use in Computable General Equilibrium Models: Preserving Physical Area of Land. Journal of Global Economic Analyses. (In press)
- Taheripour, F., & Tyner, W. US biofuel production and policy: Implications for land use changes in Malaysia and Indonesia. Biotechnology for Biofuels. (In press)
- Trejo-Pech, C., Larson, J.A., English, B.C., & Yu, T.E. (2019). Cost and profitability analysis of a prospective Pennycress to sustainable aviation fuel supply chain in southern USA. Energies, 12, no. 16: 3055
- Trejo-Pech, C.O., Larson, J., English, B., & Yu, T.E. (2019). Return and risk profile of a potential Pennycress processing facility for the aviation industry. Southern Agricultural Economics Association, 51st Annual Meeting Program, Birmingham, AL
- Wang, Z.J., Staples, M.D., Tyner, W.E., Zhao, X., Malina, R., & Barrett, S.R.H. Quantitative policy analysis for aviation biofuel production technologies. (in preparation)

- Yu, E., Sharma, B.P., English, B.C., & Boyer, C.N. (2019). Economic and environmental analysis of a sustainable jet fuel sector: A game-theoretic perspective. (In review). Submitted to Energy Economics
- Zhao, X., van der Mensbrugghe, D., Keeney, R., & Tyner, W. (2020) Improving the way land use change is handled in economic models. Economic Modeling, 84,13-26. https://doi.org/10.1016/j.econmod.2019.03.003

Reports

- CAEP/12-FTG/02-IP/03: Land Use Change Emission Accounting in GLOBIOM and GTAP-BIO. Montreal, September 2019
- CAEP/12-FTG/02-WP/08: Progress Report from the ILUC Subgroup. Montreal, September 2019
- CAEP/12-FTG/02-WP/15: ILUC Permanence. Montreal, September 2019
- CAEP/12-FTG/02-WP/09: Potential Methodology for the Fuel Production Evaluation Task. Montreal, September 2019
- CAEP/-SG/20191-WP/09: Progress on Development of LCA Values. Johannesburg, December 2019
- Comments on: CAEP-SG/20194-WP Indonesia Observations on Result of LCA. Johannesburg, December 2019
- CAEP/11-WP/44: Core LCA values and methods. Montreal, February 2019
- CAEP/11-WP/45: Technical report outlining the methodology and calculation of default core life cycle emissions values for sustainable alternative fuels under CORSIA. Montreal, February 2019
- CAEP/11-WP/46: Emission credits from the production of CORSIA eligible fuels. Montreal, February 2019
- CAEP/11-WP/50: Summary of the work of the policy task group. Montreal, February 2019
- CAEP/12-FTG/01-WP/06: Discussion on the CAEP/12 workplan for the technology and production subgroup. Montreal, May 2019
- CAEP/12-FTG/01-WP/08: Discussion on the CAEP/12 workplan for the core LCA subgroup. Montreal, May 2019

Presentations

- Boglioli, M., Strauss, S., Hoard, S., Mueller, D., Budowle, R., Beeton, T., & Jensen-Ryan, D. (2019). Searching for culture in 'cultural capital': The case for a mixed-methods approach to production facility siting. CSU Energy
- Choi, Y., Lambert, D., Jensen, K., Clark, C., English, B., & Thomas, M. (2019). Consumer Preferences for Potting Mix Product with Biochar under the IIA assumption. Western Agricultural Economics Association Annual Meeting, Coeur d'Alene, ID
- English, B.C., Menard, J. R., Trejo-Pech, C., Rahmann, U., & Edward Yu, T. (2018). Initial steps to laying the groundwork for a renewable aviation fuel industry in Tennessee: Economic feasibility and economic impact analysis. Poster presented at CAAFI annual meeting, Washington, DC
- English, B.C. & Rials, T. (2018). Feedstock viability and potential economic impacts. Paper presented at CAAFI annual meeting, Washington, DC
- Gaffney, M., Sanders, C., Hoard, S., & Mueller, D. (2018). Community Capitals: Strategic Application of the CAAM. Commercial Aviation Alternative Fuels Initiative (CAAFI) Annual Meeting. Washington, DC
- Gill, M., Jensen, K., Upendram, S., Labbe, N., & English, B.C. (2019). Consumers' Willingness to Pay for Disposable Dinnerware Molded from Wheat Straw. Western Agricultural Economics Association Annual Meeting, Coeur d'Alene, ID
- Gill, M., Jensen, K., Upendram, S., English, B., Labbe, N., Jackson, S., & Lambert, D. (2019). Consumer Preferences for Environmental Attributes in Disposable Dinnerware. Poster presented at Applied and Agricultural Economics Association, Atlanta, GA
- Mueller, D., Hoard, S., Roemer, K., Rijkhoff, S., & Sanders, C. (2018). Quantifying the Community Capitals Framework: Strategic Application of the Community Assets and Attributes Model. Pacific Northwest Political Science Association. Bend, OR
- Sharma, B.P., Yu, T.E., English, B.C., & Boyer, C.N. (2018). Welfare Analysis of Carbon Credits to the Sustainable Aviation Fuel Sector: A Game-Theoretic Perspective. Poster presented at CAAFI annual meeting, Washington, DC
- Staples, M. (2018). Long-term CO2 emissions reduction potential of aviation biofuels in the US. Presentation given at the CAAFI BGM, Washington, DC
- Staples, M. (2018). Life cycle GHG emissions modeling for international policy. Presentation at CAAFI BGM, Washington, DC
- Summers, S. (2019). The results of her work were presented at the Fall 2019 American Chemical Society meeting, San Diego, CA
- Taheripour, F. (2019). Attended CRC meeting and made a presentation on regional land use change values. Argonne National Laboratory, Lemont, IL, October, 15-17

- Taheripour, F. (2019). Presented research outcomes on ILUC values at the National Biodiesel Conference & Expo, San Diego, CA, January 21-24
- Taheripour, F. (2019). Presented research outcomes on ILUC values at the GTAP 22nd Annual Conference on Global Economic Analysis, University of Warsaw, Warsaw, Poland
- Taheripour, F. (2019). Presented research outcomes on ILUC values at the 2019 AAEA Annual Meeting, Atlanta, GA
- Thomas, M., Jensen, K.L., Clark, C.D., Lambert, D., English, B.C., & Walker, F.R. (2019). Tennessee Home Gardener Preferences for Environmental Attributes in Gardening Supplies: A Multiple Indicators Multiple Causation Analysis. Paper presented at SNA
- Trejo-Pech, C.O., Larson, J., English, B., & Yu, T.E. (2019). Return and risk profile of a potential Pennycress processing facility for the aviation industry. Southern Agricultural Economics Association, 51st Annual Meeting Program, Birmingham, AL
- Turn, S. (2019). Results of the fuel sampling, analyses, and equilibrium analyses were presented at the Thermochemical Biomass 2019 Conference, Chicago, Il
- Tyner, W. (2018). Economic availability of feedstock for alternative jet fuels. Presentation at Civil Aviation Alternative Fuels Initiative (CAAFI) Washington, DC
- Wang, J. (2019). Harmonized stochastic techno-economic assessment and policy analysis for alternative fuels. Presentation given for the January 17 CAAFI SOAP-Jet webinar

Project 002

Four undergraduate students involved.

Presentations

Presentations on the data analysis and interpretation to date have been made at:

- ASCENT advisory board meeting, Washington DC, October 2018
- AGU Fall Meeting in session A33K – Improving the Science of Emissions through Inventories, Observations and Models III, 12 December 2018, Washington DC.
- AEC Roadmap Meeting held in Washington DC in May 2019.

Project 003

Four graduate students involved.

Project 008

- Site developed and contents are published at www.noisequest.psu.edu

Project 010

Ten graduate students involved.

Publications

- Jain, S., Ogunsina, K., Chao, H., Crossley, W. A., & DeLaurentis, D. A. (2020). Predicting routes for, number of operations of, and fleet-level impacts of future commercial supersonic aircraft on routes touching the united states. Abstract submitted to AIAA Aviation Forum for presentation in June 2020

Presentations

- Jain, S., Ogunsina, K., Chao, H., Crossley, W. A., & DeLaurentis, D. A. (2020). Predicting routes for, number of operations of, and fleet-level impacts of future commercial supersonic aircraft on routes touching the united states. Abstract submitted to AIAA Aviation Forum for presentation in June 2020

Project 017

Publications

- Basner, M., Witte, M., & McGuire, S. (2019). Aircraft noise effects on sleep – Results of a pilot study near Philadelphia International Airport. International Journal of Environmental Research and Public Health, 16(17): 3178
- Basner, M., Smith, M., Rocha, S., & Witte, M. (2019). Pilot field study on the effects of aircraft noise on sleep around Atlanta International Airport. Conference paper 23rd International Congress on Acoustics, Aachen, Germany
- Rocha, S., Smith, M., Witte, M., & Basner, M. (2019). Survey results of a pilot sleep study near Atlanta International Airport. International Journal of Environmental Research and Public Health, 16(22): 432
- Smith, M., Witte, M., Rocha, S., & Basner, M. Effectiveness of incentives and follow-up on increasing survey response rates and participation in field studies. Manuscript currently under second round of peer review with BMC Medical Research Methodology
- Smith, M., Rocha, S., Witte, M., & Basner, M. On the feasibility of measuring physiologic and self-reported sleep disturbance by aircraft noise on a national scale: A pilot study around Atlanta airport. Finalized manuscript, to be submitted November/December 2019 to Frontiers in Physiology special issue Aerospace health and safety: Today and the future

Presentations

- Basner, M., Smith, M., Rocha, S., & Witte, M. (2019). Pilot field study on the effects of aircraft noise on sleep around Atlanta International Airport. Presentation at 23rd International Congress on Acoustics, Aachen, Germany
- Smith, M., Rocha, S., Witte, M., & Basner, M. (2019) Self-reported sleep disturbance by aircraft noise around Atlanta airport. Poster at SLEEP 2019, San Antonio, TX

Project 018

Two graduate students involved.

Presentations

- Simon, M. (2019). A Machine Learning Approach to Model Community-Level Ultrafine Particle Emissions from Arriving Aircraft. Presented at the International Society for Environmental Epidemiology Annual Meeting, August

Project 019

Two graduate students involved.

Presentations

- Presentation at bi-annual ASCENT stakeholder meetings in Spring and Fall 2019

Project 020

One graduate student involved.

Publications

- Dasadhikari, K., Eastham, S. D., Allroggen, F., Speth, R. L. and Barrett, S. R. H. (2019). Evolution of sectoral emissions and contributions to mortality from particulate matter exposure in the Asia-Pacific region between 2010 and 2015. Atmos. Environ. 116916, doi.org/10.1016/j.atmosenv.2019.116916
- Grobler, C., Wolfe, P.J., Dasadhikari, K., Dedoussi, I.C., Allroggen, F., Speth, R.L., Eastham, S.D., Agarwal, A., Staples, M.D., Sabnis, J. & Barrett, S.R.H. (2019). Marginal climate and air quality costs of aviation emissions. Environ. Res. Lett. 14 114031, https://doi.org/10.1088/1748-9326/ab4942

Project 021

One graduate student involved.

Publications

- Grobler, C., Wolfe, P.J., Dasadhikari, K., Dedoussi, I.C., Allroggen, F., Speth, R.L., Eastham, S.D., Agarwal, A., Staples, M.D., Sabnis, J. & Barrett, S.R.H. (2019). Marginal climate and air quality costs of aviation emissions. Environ. Res. Lett. 14 114031, https://doi.org/10.1088/1748-9326/ab4942

Project 022

One graduate student involved.

Project 023

Six graduate students involved.

Publications

- Thomas, J. & Hansman, J. (2019). Framework for analyzing aircraft community noise impacts of advanced operational flight procedures. Journal of Aircraft, Volume 6, Issue 4. https://doi.org/10.2514/1.C035100
- Thomas, J., Yu, A., Li, C., Toscano, P., & Hansman, R.J. (2019). Advanced operational procedure design concepts for noise abatement. In Thirteenth USA/Europe Air Traffic Management Research and Development Seminar, Vienna
- Yu, A. & Hansman, R.J. (2019). Approach for representing the aircraft noise impacts of concentrated flight tracks. AIAA Aviation Forum 2019, Dallas, TX. https://doi.org/10.2514/6.2019-3186

Presentations

- Thomas, J., Yu, A., Li, C., Toscano, P., & Hansman, R.J. (2019). Advanced operational procedure design concepts for noise abatement. Thirteenth USA/Europe Air Traffic Management Research and Development Seminar, Vienna
- Yu, A. & Hansman, R.J. (2019). Approach for representing the aircraft noise impacts of concentrated flight tracks. AIAA Aviation Forum 2019, Dallas, TX, March

Project 025

Four graduate students involved.

Publications

- Ding, Y., Wang, S., & Hanson, R.K. (2019). Sensitive and interference-immune formaldehyde diagnostic for high-temperature reacting gases using two-color laser absorption near 5.6 μm. Under review, Combustion and Flame
- Pinkowski, N.H., Wang, Y., Cassady, S.J., Davidson, D.F., & Hanson, R.K. (2019). A streamlined approach to hybrid-chemistry modeling for a low cetane-number alternative jet fuel. Combustion and Flame 208, 15-26. https://doi.org/10.1016/j.combustflame.2019.06.024
- Pinkowski, N.H., Cassady, S.J., Davidson, D.F., & Hanson, R.K. (2019). Multi-wavelength speciation of high-temperature 1-butene pyrolysis. Fuel 244, 269-281. https://doi.org/10.1016/j.fuel.2019.01.154
- Pinkowski, N.H., Ding, Y., Johnson, S.E., Wang, Y., Parise, T.C., Davidson, D.F., & Hanson, R.K. (2019). A multi-wavelength speciation framework for high-temperature hydrocarbon pyrolysis. J. Quantitative Spectroscopy and Radiative Transfer 225, 180-205. https://doi.org/10.1016/j.jqsrt.2018.12.038
- Pinkowski, N., Davidson, D.F., & Hanson, R.K. (2019). Multi-wavelength speciation of high-temperature alternative and conventional jet fuel pyrolysis. Paper 2019-1769, AIAA SciTech Forum, San Diego, CA. https://arc.aiaa.org/doi/pdf/10.2514/6.2019-1769

- Shao, J., Wei, W., Choudhary, R., Davidson, D.F., & Hanson, R.K. (2019). Shock tube measurement of the CH3+C2H6→CH4+C2H5 rate constant. J. Phys. Chem. A. 123, 42, 9096-9101 https://doi.org/10.1021/acs.jpca.9b07691
- Shao, J., Zhu, Y., Wang, S., Davidson, D.F., & Hanson, R.K. (2018). A shock tube study of jet fuel pyrolysis and ignition at elevated pressures and temperatures. Fuel 226 338-344. doi:10.1016/j.fuel.2018.04.028
- Shao, J., Ferris, A.M., Choudhary, R., Davidson, D.F., & Hanson, R.K. (2020). A shock tube study of natural gas pyrolysis and ignition at elevated pressures and temperatures. Submitted, Proc. Combust. Inst. (38th International Symposium on Combustion)
- Wang, K., Xu, R., Parise, T., Shao, J., Movaghar, A., Lee, D.J., Part, J., Gao, Y., Lu, T., Egolfopoulos, F., Davidson, D.F., Hanson, R.K., Bowman, C.T., & Wang, H. (2018). A physics-based approach to modeling real-fuel combustion chemistry – IV. HyChem modeling of combustion kinetics of a bio-derived jet fuel and its blends with a conventional jet a. Combustion and Flame 198, 477-489. https://doi.org/10.1016/j.combustflame.2018.07.012
- Wang, Y., Ding, Y., Wei, W., Cao, Y., Davidson, D.F., & Hanson, R.K. (2019). On estimating physical and chemical properties of hydrocarbon fuels using mid-infrared FTIR spectra and regularized linear models. Fuel 255, 115715. https://doi.org/10.1016/j.fuel.2019.115715
- Wang, Y., Davidson, D.F., & Hanson, R.K. (2019). A new method of predicting derived cetane number for hydrocarbon fuels. Fuel 241 319-326. DOI 10.1016/j.fuel.2018.12.027
- Wang, Y., Cao, Y., Davidson, D.F., & Hanson, R.K. (2019). Ignition delay time measurements for distillate and synthetic jet fuels. Paper 2019-2248, AIAA SciTech Forum, San Diego, CA. https://arc.aiaa.org/doi/pdf/10.2514/6.2019-2248

Presentations

- Pinkowski, N., Davidson, D.F., & Hanson, R.K. (2019). Multi-wavelength speciation of high-temperature alternative and conventional jet fuel pyrolysis. AIAA SciTech Forum, San Diego, CA, Jan. 2019.
- Wang, Y., Cao, Y., Davidson, D.F., & Hanson, R.K. (2019). Ignition delay time measurements for distillate and synthetic jet fuels. AIAA SciTech Forum, San Diego, CA, Jan. 2019.

Project 027

Eleven graduate students involved.

Publications

- Schorn, N., Bonebrake, J., Hoter, Z., Fillo, A., & Blunck, D. Pressure effects on the turbulent consumption speed of large hydrocarbon fuels. AIAA Journal, under review
- Schorn, N., Hoter, Z., & Blunck, D. Turbulent combustion behavior of a surrogate jet fuel. In preparation for submission to Fuels
- Schorn, N., Bonebrake, J., Pendergrass, B., Fillo, A., & Blunck, D. (2019). Turbulent consumption speed of large hydrocarbon fuels at sub-atmospheric conditions. AIAA Science and Technology Forum and Exposition 2019, San Diego, CA https://doi.org/10.2514/6.2019-0735
- Schorn, N. (2019). Turbulent Bunsen Burner Analysis. M.S. Thesis, Oregon State University

Presentations

- Schorn, N., Bonebrake, J., Pendergrass, B., Fillo, A., & Blunck, D. (2019). Turbulent consumption speed of large hydrocarbon fuels at sub-atmospheric conditions. AIAA Science and Technology Forum and Exposition 2019, San Diego, CA

Project 029(A)

Three graduate students involved.

Publications

- Feyz, M., Hasti, V.R., Gore, J.P., Chowdhury, A., & Nalim, R. (2019). Scalar predictors of premixed gas ignition by a suddenly-starting hot jet. International Journal of Hydrogen Energy, Volume 44, Issue 42, Pp:23793-23806, https://doi.org/10.1016/j.ijhydene.2019.07.066
- Feyz, M., Hasti, V.R., Gore, J.P., & Nalim, R. (2019). Large eddy simulation of hot jet ignition in moderate and high-reactivity mixtures. Computers and Fluids, 183, pp:28–37, https://doi.org/10.1016/j.compfluid.2019.03.014
- Feyz, M., Nalim, R., Hasti, V.R., & Gore, J.P. (2019). Modeling and analytical solution of the near-field entrainment in starting turbulent jets. AIAA Journal, pp: 1-8, https://doi.org/10.2514/1.J057612
- Feyz, M., Hasti, V.R., Gore, J.P., & Nalim, R. Analytical and numerical approach to near-field ignition of H2/air by injection of hot gas. Submitted to the Combustion and Flame
- Feyz, M., Nalim, R., Hasti, V.R., & Gore, J.P. (2019). Statistical analysis of scalars for ignition via transient hot jet. 11th US National Combustion Meeting, Pasadena, CA 91101 USA
- Goya1, V., Roncancio, R., Kim, J., Navarkar, A., Hasti, V.R., & Gore, J.P. (2019). Effect of initial fuel temperature on flame spread rate of alternative aviation fuels. 11th US National Combustion Meeting, Pasadena, CA 91101 USA
- Goya1, V., Tursyn, Y., Hasti, V.R., & Gore, J.P. (2019). Experimental investigation of hot surface ignition temperatures for aviation fuels. 11th US National Combustion Meeting, Pasadena, CA 91101 USA
- Hasti, V.R., Lucht, R.P., & Gore, J.P. (2019). Large eddy simulation of hydrogen piloted CH4/air premixed combustion with CO_2 dilution. Journal of the Energy Institute, https://doi.org/10.1016/j.joei.2019.10.004
- Hasti, V.R., Navarkar, A., & Gore, J.P. A hybrid convolutional autoencoder – support vector machine model for early detection of lean blowout onset in a realistic gas turbine combustor. Manuscript under preparation for submission to Energy Conversion and Management
- Hasti, V.R., Navarkar, A., & Gore, J.P. Optimal sensor location for early detection of incipient lean blowout condition in a realistic gas turbine engine using support vector machine. Submitted to the Proceedings of the Combustion Institute (38th International Symposium on Combustion)
- Roncancio, R., Navarkar, A., Hasti, V.R., Goyal, V., & Gore, J.P. (2019). Effect of carbon nanotubes addition on the flame spread rate over a jet a pool. 11th US National Combustion Meeting, Pasadena, CA 91101 USA
- Shin, D., Bokhart, J.A., Rodrigues, N.S., Sojka, P., Gore, J.P., & Lucht, R.P. (2019). Non-reacting spray characteristics for alternative aviation fuels at near lean blowout conditions. AIAA Journal of Propulsion and Power. Accepted for publication
- Shin, D., Bokhart, J.A., Rodrigues, N.S., Sojka, P., Gore, J.P., & Lucht, R.P. (2019). Experimental study of spray characteristics at cold start and elevated ambient pressure using hybrid airblast pressure-swirl atomizer. 2019 AIAA SciTech Meeting, San Diego, CA. Paper Number AIAA 2019-1737

Presentations

- Gore, J.P. (2019). Radiation Heat Transfer in High Pressure Gas Turbine Combustors. Invited talk, United Technologies Research Center (UTRC) Workshop on Combustor-Turbine Wall Heat Transfer Modeling and Prediction, East Hartford, CT, 11th March
- Gore, J.P. (2019). Radiation and Soot Measurements in High Pressure Gas Turbine Combustors. Invited talk, United Technologies Research Center (UTRC) Follow-up Meeting for Combustor-Turbine Wall Heat Transfer at the ASME IGTI Conference, Phoenix, AZ, 16th June
- Hasti, V.R. (2019). Quantum Computers on Artificial Intelligence: Automatic and Adaptive Solutions. Ideas Festival, 150 Years Celebrations at Purdue University, poster presentation, February 6
- Hasti, V.R. (2019). Computational methodology for biofuel performance assessment. Invited talk, Spring CIGP Symposium, Purdue University, April 17
- Hasti, V.R., & Gore, J.P. (2019). Computational Study of Fuel Effects on Lean Blow-Out in a Realistic Gas Turbine Combustor. Keynote speech, Modeling and Simulation of Turbulent Mixing and Reaction: For Power, Energy and Flight, April 12-13
- Hasti, V.R. (2019). Computational Methodology for Biofuel Performance Prediction. Invited talk, Academic Research Colloquium, University of Dayton, September 10-12

- Shin, D., Bokhart, J.A., Rodrigues, N.S., Sojka, P., Gore, J.P., & Lucht, R.P. (2019). Experimental study of spray characteristics at cold start and elevated ambient pressure using hybrid airblast pressure-swirl atomizer. Presented at 2019 AIAA SciTech Meeting, San Diego, CA

Project 031(A)

One graduate student involved.

Publications

- ASTM Ballot. (2019). Modification of ASTM D1655: Co-processing of Fischer-Tropsch feedstocks with petroleum hydrocarbons for jet production using hydrotreating & hydrocracking
- D4054 Fast Track Research Report. (2019). Evaluation of synthesized paraffinic kerosene from algal oil extracted from *botryococcus braunii* (ihi bb-spk)

Presentations

- Presentations on Project 31a activities were given at the April (Atlanta) and October (Alexandria) 2019 ASCENT meetings
- Presentation on Project 31a activities was given at the December 2018 CAAFI Biennial General Meeting & Integrated ASCENT Symposium, Washington DC.
- Meetings were held with the OEM team, FAA, fuel producers, and others at the December 2018 ASTM D02 Committee Meeting in Atlanta, the June 2019 ASTM D02 Committee Meeting in Denver, and the March 2019 UK MOD Aviation Fuels Committee meeting in London UK

Project 033

One graduate student involved.

Publications

- Oldani, Anna. (2019). Alternative jet fuel variation and certification considerations. In progress

Project 034

Three graduate students and three undergraduate students involved.

Publications

Peer-reviewed Journal Publications

- Peiffer, E.E., Heyne, J.S., & Colket, M. (2019). Sustainable aviation fuels approval streamlining: Auxiliary power unit lean blowout testing. AIAA Journal, pg. 1-9, https://doi.org/10.2514/1.J058348
- Ruan, H., Qin, Y., Heyne, J., Gieleciak, R., Feng, M., & Yang, B. (2019). Chemical compositions and properties of lignin-based jet fuel range hydrocarbons. Fuel 256 115947, https://doi.org/10.1016/j.fuel.2019.115947

Published Conference Proceedings:

- Heyne, J., Opacich, K., Peiffer, E., & Colket, M. (2019). The effect of chemical and physical fuel properties on the approval and evaluation of alternative jet fuels. 11th U.S. National Combustion Meeting, Pasadena, CA
- Opacich, K.C., Heyne, J.S., Peiffer, E., & Stouffer, S.D. (2019). Analyzing the relative impact of spray and volatile fuel properties on gas turbine combustor ignition in multiple rig geometries. AIAA SciTech, AIAA 2019-1434, San Diego, CA

Written Reports:

- CAAFI R&D Committee. (2019). Prescreening of synthesized hydrocarbons intended for candidates as blending components for aviation turbine fuels. Commercial Alternative Aviation Fuel Initiative (CAAFI), CAAFI R&D Committee Publication

Articles/Press:

- Heyne, J., Wang, H., & Kalman, J. (2018). Safely improving jet, rocket fuels, Aerospace America, 2018 Year in Review, Propellants and Combustion Technical, Committee Contribution, December

Presentations

Invited Talks:

- Colket, M., & Heyne, J. (2018). Early Evaluation of Alternative Jet Fuels Based on NJFCP Results. Advanced Bioeconomy Leadership Conference (ABLC), San Francisco, CA, November
- Colket, M., Heyne, J. & Lee, T. (2018). NJFCP Update: Properties and Modeling to FOM Predictions. JetScreen Meeting, Paris, FR, December
- Colket, M., & Heyne, J. (2019). Major results from the National Jet fuels and Combustion Program. ASME TurboExpo, Pheonix, AZ, June
- Edwards, T., & Heyne, J. (2019). Towards the Minimization of ASTM D4054 Tier 3 & 4 AJF Approvals. 2019 CRC Aviation Committee Meetings, San Juan, PR, May
- Heyne, J., Colket, M., & Lee, T. (2018). An overview of ASCENT research efforts to improve our understanding of how fuel composition and characteristics determine performance. CAAFI Biennial General Meeting, December
- Heyne, J. (2019). The Approval and Evaluation NJFCP Learnings and High-Performance Fuels for Operability and Mission Benefits. Rolls-Royce, Indianapolis, IN, April
- Heyne, J. (2019). Drop-in High-Performance Fuels: From Molecule Selection to Mission Benefits. NREL IBRF Lab, Golden, CO, March

Conference Presentations

- Stachler, R., Heyne, J., Peiffer, E., Stouffer, S., & Miller, J. (2018). Assessment of Lean Blowoff in a Toroidal Jet Stirred Reactor. DESS2018-055, 14th Dayton Engineering Sciences Symposium, Wright State University, November
- Opacich, K., Heyne, J.S., Peiffer, E., & Stouffer, S.D. (2018). Analyzing the Relative Impact of Spray and Volatile Fuel Properties on Gas Turbine Combustor Ignition. DESS2018-019, 14th Dayton Engineering Sciences Symposium, Wright State University, November

Funded Program Review Presentations:

- Heyne, J., Colket, M., Moder, J., & Shaw, C., (2018). NJFCP Status Update. FAA ASCENT, Alexandria, VA, Oct
- Heyne, J., & Colket, M. (2019). AIAA Book and Year 5 - Next Steps and Action Item Review. NJFCP 2019 Review Meeting, OAI, Cleveland, OH, March
- Heyne, J., Emerson, B., Lieuwen, T., Stouffer, S., Blunck, D., Corporan, E., Mastorakas, N., & de Oliveira, P. (2019). LBO WG Update and 4 Year Summary. NJFCP 2019 Review Meeting, OAI, Cleveland, OH, March
- Heyne, J., & Colket, M. (2019). Highlights of NJFCP Achievements - Overall impact of program Tiers and HPF. NJFCP 2019 Review Meeting, OAI, Cleveland, OH, March
- Stouffer, S., Heyne, J., Boehm, R., Mayhew, E., Lee, T., & Canteenwalla, P. (2019). Ignition WG Update and 4 Year Summary. NJFCP 2019 Review Meeting, OAI, Cleveland, OH, March

Project 036

Four graduate students involved

Publications

- Gao, Z., Behere, A., Li, Y., Lim, D., Kirby, M., & Mavris, D.M. Quantitative assessment of the new departure profiles with improved weight and thrust modeling. To be submitted to Journal of Aircraft

Project 37

One graduate student involved.

Project 038

One graduate student involved.

Publications

- Botre, M., Brentner, K.S., Horn, J.F., & Wachspress, D.A. (2019). Developing a comprehensive noise prediction system for generating noise abatement procedures. 25th AIAA/CEAS Aeroacoustics Conference, Delft, The Netherlands, https://doi.org/10.2514/6.2019-2617

Presentations

- Botre, M., Brentner, K.S., Horn, J.F., & Wachspress, D.A. (2019). Developing a comprehensive noise prediction system for generating noise abatement procedures. 25th AIAA/CEAS Aeroacoustics Conference, Delft, The Netherlands
- Botre, M., Brentner, K.S., Horn, J.F., & Wachspress, D.A. (2019). Validation of helicopter noise prediction system with flight data. VFS 75th Annual Forum, Philadelphia, PA

Project 039

Three graduate students involved.

Presentations

- Presented an Information Paper prepared for the CAEP/12-WG3/2 meeting, October 7, 2019.

Project 040

Two graduate students involved and one undergraduate student involved.

Publications

- Wang, Y. (2019). Propagation of enroute aircraft noise. PhD dissertation, Purdue University

Presentations

- Patankar, H. & Sparrow, V. (2019). Effect of uncertainty in meteorological conditions on aircraft noise levels. J. Acoust. Soc. Am. 145(3, Pt. 2) 1885
- Wang, Y. & Li, K.M. (2019). Doppler's shift on aircraft noise propagation in modern aircraft noise prediction tools. J. Acoust. Soc. Am. 146. Oral presentation at the ASA 2019 Fall meeting

Project 041

Two graduate students involved.

Presentations

- Riegel, K., Sparrow, V., & Stout, T. (2019). Preliminary analysis of the PBboom software for calculating secondary sonic booms. J. Acoust. Soc. Am. 146(4) 2782. Acoustical Society of America presentation San Diego, CA, USA
- Wade, L. & V. Sparrow, V. (2019). Effects of perturbing a reference atmosphere on sonic boom propagation metrics. Acoustical Society of America presentation, Louisville, KY, USA

Project 042

Three graduate students involved.

Presentations

- Broyles, J., Vigeant, M.C., & Sparrow, V.W. (2019). Perceived annoyance of Mach-cutoff flight ground signatures compared to common transportation sounds. J. Acoust. Soc. Am 146:2782. Acoustical Society of America (ASA) Fall 2019 Meeting Presentation, San Diego, CA
- Ortega, N.D., Vigeant, M.C., & Sparrow, V.W. (2019). Identifying metrics to predict annoyance due to Mach-cutoff flight ground signatures. J. Acoust. Soc. Am. 145:1899. Acoustical Society of America (ASA) Spring 2019 Meeting Presentation, Louisville, KY

Project 043

Five graduate students involved.

Publications

- Perullo, C., Santa-Ruiz, A., Kirby, M., Mavris, D., & Lim, D. (2019). Investigation of Aircraft Configuration and Speed on Traditional Noise-Power-Distance Curves. Noise-Con 2019, NC19-192

Presentations

- Perullo, C., Santa-Ruiz, A., Kirby, M., Mavris, D., & Lim, D. (2019). Investigation of Aircraft Configuration and Speed on Traditional Noise-Power-Distance Curves. Noise-Con 2019

Project 044

Six graduate students involved.

Publications

- Modeling and Assessment of Delayed Deceleration Approaches for Community Noise Reduction. Extended Abstract Submitted for Review, 2020 AIAA Aviation Conference

Presentations

- Modeling and Assessment of Delayed Deceleration Approaches for Community Noise Reduction. Extended Abstract Submitted for Review, 2020 AIAA Aviation Conference

Project 045

Six graduate students involved.

Publications

- Behere, A., Lim, D., Li, Y., Jin, Y.C., Gao, Z., Kirby, M., & Mavris, D. (2020). Sensitivity analysis of airport level environmental impacts to aircraft thrust, weight, and departure procedures. 2020 AIAA SciTech Conference
- Lim, D., Behere, A., Jin, Y.C., Li, Y., Kirby, M., Gao, Z., & Mavris, D. (2020). Improved noise abatement departure procedure modeling for aviation environmental impact assessment. 2020 AIAA SciTech Conference

Presentations

- Behere, A., Lim, D., Li, Y., Jin, Y.C., Gao, Z., Kirby, M., & Mavris, D. (2020). Sensitivity analysis of airport level environmental impacts to aircraft thrust, weight, and departure procedures. To be presented at 2020 AIAA SciTech Conference
- Lim, D., Behere, A., Jin, Y.C., Li, Y., Kirby, M., Gao, Z., & Mavris, D. (2020). Improved noise abatement departure procedure modeling for aviation environmental impact assessment. To be presented at 2020 AIAA SciTech Conference
- 2019 NoiseCon presentation

Project 046

One graduate student involved.

Project 047

Two graduate students involved.

Presentations

- Sabnis, J. (2019). Noise and Emission Characteristics of Commercial Supersonic Aircraft Propulsion Systems. Aviation Noise and Emissions Symposium, March

Project 048

One graduate student involved.

Publications

- Agarwal, A., Speth, R.L., Fritz, T.M., Jacob, S.D., Rindlisbacher, T., Iovinelli, R., Owen, B., Miake-Lye, R.C., Sabnis, J.S., & Barrett, S.R.H. (2019). SCOPE11 Method for Estimating Aircraft Black Carbon Mass and Particle Number Emissions. Environmental Science & Technology, 53 (3): 1364–73. https://doi.org/10.1021/acs.est.8b04060
- Working paper to the CAEP/11-WG3/10 meeting in Montreal

Project Funding Allocations by Federal Fiscal Year

Breakout by Project

Project		Funding Based on award date						
		2014	2015	2016	2017	2018	2019	Total
001	Alternative Jet Fuel Supply Chain Analysis	$1,599,943	$1,425,000	$1,498,749	$1,855,461	$1,102,865	$1,034,039	$8,516,057
002	Ambient Conditions Corrections for Non-Volatile PM Emissions Measurements	$2,800,000	$750,000	-$147,766	$725,500	-	$1,217,221	$5,344,955
003	Cardiovascular Disease and Aircraft Noise Exposure	$200,000	$200,000	$200,000	$340,000	-	$1,729,286	$2,669,286
004	Estimate of Noise Level Reduction	$150,000	-	-	-	-$8,845	-	$141,155
005	Noise Emission and Propagation Modeling	$212,000	$200,000	-	-	-	-	$412,000
006	Rotorcraft Noise Abatement Operating Conditions Modeling	$250,326	-	-	-	-	-	$250,326
007	Civil, Supersonic Over Flight, Sonic Boom (Noise) Standards Development	$100,000	$200,000	-	-	-	-	$300,000

Project		Funding Based on award date						
		2014	2015	2016	2017	2018	2019	Total
008	Noise Outreach	$ 30,000	$ 50,000	$ 75,000	$ 25,000	-	$ 30,000	$210,000
010	Aircraft Technology Modeling and Assessment	$899,979	$200,000	$310,000	$669,567	$764,185	-	$2,843,731
011	Rapid Fleet-wide Environmental Assessment Capability	$600,000	$270,000	$300,000	-	-	-	$1,170,000
012	Aircraft Design and Performance Assessment Tool Enhancement	$ 90,000	-	-	-	-	-	$90,000
013	Micro-Physical Modeling & Analysis of ACCESS 2 Aviation Exhaust Observations	$200,000	-	-	-	-	-	$200,000
014	Analysis to Support the Development of an Aircraft CO2 Standard	$520,000	-	-	-	-	-	$520,000
017	Pilot Study on Aircraft Noise and Sleep Disturbance	$154,000	$343,498	$266,001	$134,924	-	-	$898,423
018	Health Impacts Quantification for Aviation Air Quality Tools	$150,000	$150,000	$200,000	$270,000	-	-	$770,000

Project		Funding Based on award date						
		2014	2015	2016	2017	2018	2019	Total
019	Development of Aviation Air Quality Tools for Airport-Specific Impact Assessment: Air Quality Modeling	$320,614	$369,996	-	$625,378	-	$300,000	$1,615,988
020	Development of NAS wide and Global Rapid Aviation Air Quality	$150,000	$200,000	$250,000	$250,000	-	-	$850,000
021	Improving Climate Policy Analysis Tools	$150,000	$150,000	$150,000	$150,000	-	-	$600,000
022	Evaluation of FAA Climate Tools	$150,000	$30,000	$ 75,000	$100,000	-	-	$355,000
023	Analytical Approach for Quantifying Noise from Advanced Operational Procedures	-	$296,711	$250,000	$250,000	-	$250,000	$1,046,711
024	Emissions Data Analysis for CLEEN, ACCESS, and Other Recent Tests	$244,975	-	$ 75,000	-	-	-	$319,975
025	National Jet Fuels Combustion Program – Area #1: Chemical Kinetics Combustion Experiments	-	$615,000	$210,000	$200,000	$ 2,556	$110,000	$1,137,556

Project		Funding Based on award date						
		2014	2015	2016	2017	2018	2019	Total
026	National Jet Fuels Combustion Program – Area #2: Chemical Kinetics Model Development and Evaluation	-	$200,000	-	-	-$ 2,556	-	$197,444
027	National Jet Fuels Combustion Program – Area #3: Advanced Combustion Tests	-	$1,010,000	$580,000	$265,000	-	$ 30,000	$1,885,000
028	National Jet Fuels Combustion Program – Area #4: Combustion Model Development and Evaluation	-	$470,000	$ 55,000	-	-	-	$525,000
029	National Jet Fuels Combustion Program – Area #5: Atomization Tests and Models	-	$640,000	$360,000	$150,000	-	$120,000	$1,270,000
030	National Jet Fuels Combustion Program – Area #6: Referee Swirl-Stabilized Combustor Evaluation/Support	-	$349,949	-	-	-	-	$349,949
031	Alternative Jet Fuels Test and Evaluation	-	$489,619	$744,891	$999,512	$183,019	-	$2,417,041

Project		Funding Based on award date						
		2014	2015	2016	2017	2018	2019	Total
032	Worldwide LCA of GHG Emissions from Petroleum Jet Fuel	-	$150,000	-	-	-	-	$150,000
033	Alternative Fuels Test Database Library	-	$199,624	$119,794	$165,000	-	$163,584	$648,002
034	National Jet Fuels Combustion Program – Area #7: Overall Program Integration and Analysis	-	$234,999	$635,365	$192,997	$374,978	-	$1,438,339
035	Airline Flight Data Examination to Improve flight Performance Modeling	-	$150,001	-	-	-	-	$150,001
036	Parametric Uncertainty Assessment for AEDT2b	-	$ 65,000	$175,000	$380,000	-	$300,000	$920,000
037	CLEEN II Technology Modeling and Assessment	-	$200,000	$150,000	$170,000	-	$170,000	$690,000
038	Rotorcraft Noise Abatement Procedures Development	-	$150,000	$150,000	$150,000	$150,000	-	$600,000
039	Naphthalene Removal Assessment	-	-	$200,000	$290,000	-	$350,000	$840,000

Project		Funding Based on award date						
		2014	2015	2016	2017	2018	2019	Total
040	Quantifying Uncertainties in Predicting Aircraft Noise in Real-world Situations	-	-	$218,426	$200,000	-	$255,000	$673,426
041	Identification of Noise Acceptance Onset for Noise Certification Standards of Supersonic Airplane	-	-	$160,000	$221,000	-	$390,000	$771,000
042	Acoustical Model of Mach Cut-off	-	-	$255,000	$150,000	$170,000	-	$575,000
043	Noise Power Distance Re-Evaluation	-	-	$150,000	$ 75,000	-	$220,000	$445,000
044	Aircraft Noise Abatement Procedure Modeling and Validation	-	-	-	-	$350,000	-	$350,000
045	Takeoff/Climb Analysis to Support AEDT APM Development	-	-	$250,000	$ 75,000	$ 8,845	$175,000	$508,845
046	Surface Analysis to Support AEDT APM Development	-	-	$ 75,000	$ 75,000	$ 75,000	-	$225,000
047	Clean Sheet Supersonic Engine Design and Performance	-	-	-	-	-	$250,000	$250,000

Project		Funding Based on award date						
		2014	2015	2016	2017	2018	2019	Total
048	Analysis to Support the Development of an Engine nvPM Emissions Standards	-	-	$150,000	$200,000	-	$200,000	$550,000

Breakout by University*

	Funding Based on award year							
University	**2013**	**2014**	**2015**	**2016**	**2017**	**2018**	**2019**	**Total**
Boston University	$5,000	$350,000	$350,000	$400,000	$610,000	-	$1,729,286	$3,444,286
Georgia Institute of Technology	$5,000	$1,660,000	$1,625,001	$1,435,000	$1,468,500	$650,000	$895,000	$7,738,501
Massachusetts Institute of Technology	$10,000	$1,153,927	$1,179,073	$1,855,000	$1,690,000	$1,000,000	$1,050,000	$7,938,000
Missouri University of Science and Technology	$5,000	$2,800,000	$750,000	-$147,766	$725,500	-	$1,217,221	$5,349,955
Oregon State University	$5,000	-	$160,000	$80,000	$59,000	-	-	$304,000
Pennsylvania State University	$5,000	$862,301	$766,711	$958,426	$890,424	$320,000	$797,623	$4,600,485
Purdue University	$5,000	$389,979	$1,030,000	$763,750	$747,067	$114,185	$605,000	$3,654,981
Stanford University	$5,000	$380,000	$1,155,000	$345,000	$200,000	-	$110,000	$2,195,000
University of Dayton	$5,000	-	$906,196	$1,349,087	$1,192,509	$574,944	-	$4,027,736
University of Hawaii	$10,000	-	$75,000	$100,000	$125,000	-	$200,000	$510,000

	Funding Based on award year							
University	**2013**	**2014**	**2015**	**2016**	**2017**	**2018**	**2019**	**Total**
University of Illinois	$5,000	$349,943	$553,000	$375,000	$265,000	-	$130,000	$1,677,943
University of North Carolina	$5,000	$320,614	$369,996	-	$625,378	-	$300,000	$1,620,988
University of Pennsylvania	$5,000	$154,000	$343,498	$266,001	$134,924	-	-	$903,423
University of Tennessee	$5,000	$200,000	$100,000	$100,000	$225,000	-	$260,000	$890,000
University of Washington	$5,000	$60,000	$29,997	$15,000	-	-	-	$109,997
Washington State University	$20,000	$974,228	$864,968	$725,961	$796,039	$510,918	$390,911	$4,283,025

Breakout by State*

	Funding Based on award year							
State	2013	2014	2015	2016	2017	2018	2019	Total
California	$5,000	$380,000	$1,155,000	$345,000	$200,000	-	$110,000	2,195,000
Georgia	$5,000	$1,660,000	$1,625,001	$1,435,000	$1,468,500	$650,000	$895,000	$7,738,501
Hawaii	$10,000	-	$75,000	$100,000	$125,000	-	$200,000	$510,000
Illinois	$5,000	$349,943	$553,000	$375,000	$265,000	-	$130,000	$1,677,943
Indiana	$5,000	$389,979	$1,030,000	$763,750	$747,067	$114,185	$605,000	$3,654,981
Massachusetts	$15,000	$1,503,927	$1,529,073	$2,255,000	$2,300,000	$1,000,000	$2,779,286	$11,382,286
Missouri	$5,000	$2,800,000	$750,000	-$147,766	$725,500	-	$1,217,221	$5,349,955
North Carolina	$5,000	$320,614	$369,996	-	$625,378	-	$300,000	$1,620,988
Ohio	$5,000	-	$906,196	$1,349,087	$1,192,509	$574,944	-	$4,027,736
Oregon	$5,000	-	$160,000	$80,000	$59,000	-	-	$304,000
Pennsylvania	$10,000	$1,016,301	$1,110,209	$1,224,427	$1,025,348	$320,000	$797,623	$5,503,908
Tennessee	$5,000	$200,000	$100,000	$100,000	$225,000	-	$260,000	$890,000
Washington	$25,000	$1,034,228	$894,965	$740,961	$796,039	$510,918	$390,911	$4,393,022

*Totals include administrative funds not associated with specific NFOs